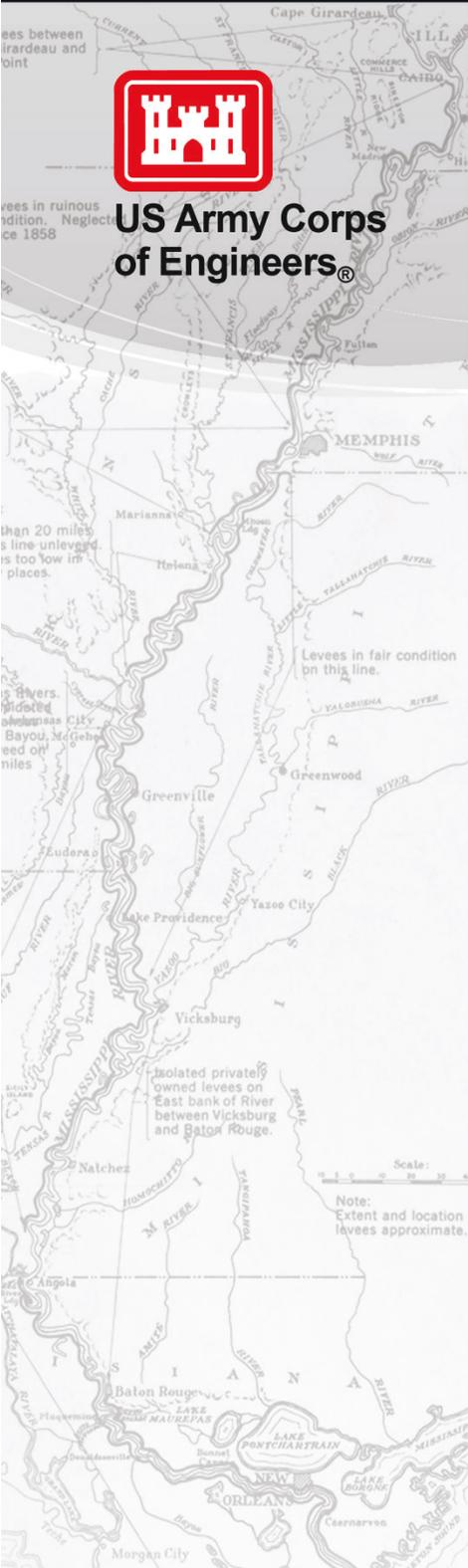


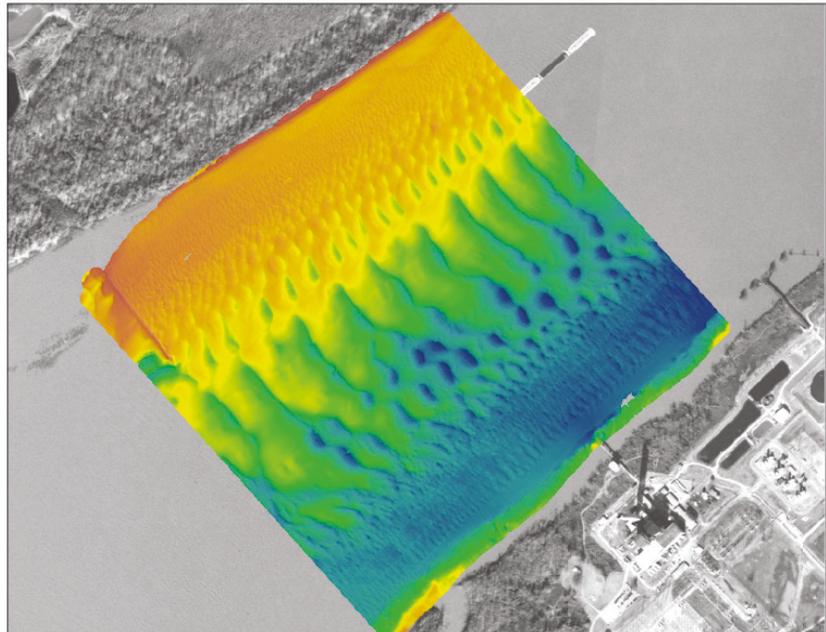


US Army Corps of Engineers®



# Mississippi River Bedform Roughness and Streamflow Conditions near Vicksburg, Mississippi

Data Collection Summary and Analysis  
MRG&P Report No. 22 • October 2018



## MRG&P

Mississippi River  
Geomorphology &  
Potamology Program



# **Mississippi River Bedform Roughness and Streamflow Conditions near Vicksburg, Mississippi**

## **Data Collection Summary and Analysis**

Michael T. Ramirez, S. Jarrell Smith, James W. Lewis,  
and Thad C. Pratt

*Coastal and Hydraulics Laboratory  
U.S. Army Engineer Research and Development Center  
3909 Halls Ferry Road  
Vicksburg, MS 39180-6199*

Final report

Approved for public release; distribution is unlimited.

Prepared for U.S. Army Corps of Engineers, Mississippi Valley Division  
Mississippi River Geomorphology & Potamology Program  
1400 Walnut Street  
Vicksburg, MS 39180

Under Project 127672, "Bed Form Roughness Investigation"

## Abstract

Bedforms are a consequence of flow of sufficient magnitude over a mobile sediment bed. They are a primary component of the drag acting upon a moving stream, yet are infrequently explicitly treated in numerical models of fluvial sediment transport. This study aims to document the collection of bathymetric data in the Mississippi River in an area of persistent and dynamic bedforms over a range of flow conditions, statistically examine bedform geometry, and parameterize results for inclusion in numerical models. Bathymetric data were collected several times to measure rates of bedform transport. Linear profiles of the bedforms were extracted from the bathymetry and analyzed for roughness and dune population statistics. These statistics are compared with the flow conditions under which the bedforms were observed. Bedforms increase in size with discharge and decrease in steepness (height:length ratio). At extremely high discharges, bedforms begin to decrease in size. In comparing results with methods for calculating form drag coefficients, it was observed that the dunes at higher river stages, despite their greater size, may present less resistance to flow due to their reduced steepness and reduced relative heights (dune height:flow depth).

**DISCLAIMER:** The contents of this report are not to be used for advertising, publication, or promotional purposes. Citation of trade names does not constitute an official endorsement or approval of the use of such commercial products. All product names and trademarks cited are the property of their respective owners. The findings of this report are not to be construed as an official Department of the Army position unless so designated by other authorized documents.

**DESTROY THIS REPORT WHEN NO LONGER NEEDED. DO NOT RETURN IT TO THE ORIGINATOR.**

# Contents

<b>Abstract .....</b>	<b>ii</b>
<b>Figures and Tables.....</b>	<b>iv</b>
<b>Preface.....</b>	<b>vi</b>
<b>Unit Conversion Factors .....</b>	<b>vii</b>
<b>1 Introduction.....</b>	<b>1</b>
Background .....	1
Objective .....	1
Approach.....	2
<b>2 Methods .....</b>	<b>3</b>
Field data collection .....	3
Roughness analysis .....	4
Flow characteristics.....	7
<b>3 Results .....</b>	<b>9</b>
Bathymetry.....	9
Roughness .....	9
Streamflow.....	14
<i>River stage and slope records.....</i>	<i>14</i>
<i>Rating curve .....</i>	<i>17</i>
<b>4 Discussion .....</b>	<b>20</b>
Friction factors.....	20
<b>5 Conclusion and Recommendations .....</b>	<b>24</b>
<b>References .....</b>	<b>25</b>
<b>Appendix A: Bathymetry .....</b>	<b>27</b>
<b>Appendix B: Bedform Profiles .....</b>	<b>40</b>
<b>Appendix C: Bedform Roughness Statistics.....</b>	<b>333</b>
<b>Report Documentation Page</b>	

# Figures and Tables

## Figures

Figure 1. Map of the study area, with river bed elevation survey focus area outlined in the dashed box. The complex geometry of the dunes can be observed covering the bed surface and extending upstream and downstream of the survey area. ....	4
Figure 2. Example of bed profile analysis from March 2015. (A) is the raw bed elevation profile, (B) shows the high-pass filtered roughness profile with $R_{ave}$ and $R_{RMS}$ statistics, (C) gives counts of bedforms of different sizes, and (D) is the power spectral density estimate ( $S_z$ ) of the roughness profile.....	6
Figure 3. Selected roughness statistics for study discharges. (A-D) Roughness RMS for survey lines 5, 7, 9, and 11. (E-H) Rugosity for survey lines 5, 7, 9, and 11. (I-L) Average wavelength for survey lines 5, 7, 9, 11. (M-P) Steepness for survey lines 5, 7, 9, and 11. A vertical dashed line is given on each plot at flood stage discharge for Vicksburg.....	11
Figure 4. Average dune heights ( $H_{rms}$ ) compared to average wavelengths ( $\lambda_{ave}$ ) for all roughness profiles analyzed. Colors represent the rating-curve estimated stream discharge at the time of each survey. Included are relations for best-fit and maximum height:length ratios for 1,491 measurements of dune geometry in a variety of environments compiled by Flemming (2000). ....	13
Figure 5. Gaging station records of Mississippi River stage at Greenville (blue), Vicksburg (red), and Natchez (yellow), converted to NAVD88 water surface elevations for the period 2000–2016. ....	14
Figure 6. Water surface slope calculated between Greenville, Vicksburg, and Natchez gaging stations for the period 2000–2016.....	15
Figure 7. Water surface slope calculated compared to water surface elevation for the Greenville-Vicksburg reach and the Vicksburg-Natchez reach daily for the period 2000–2016.....	15
Figure 8. Boat-based water surface elevation profiles in the vicinity of the study area (study area indicated with vertical dashed lines) recorded in May 2011, September 2012, March 2015, April 2015, and May 2015. Each water surface profile was fit with a linear least-squares regression (shown by dashed lines) for the reach downstream of the Vicksburg river gage (at RK701; indicated by black circles at the gage-recorded elevation for each date) to estimate the water surface slope (shown above each profile). ....	16
Figure 9. Comparison of water surface slopes recorded aboard the survey vessel and those calculated based on the stage differences between gaging stations at Greenville, Vicksburg, and Natchez.....	17
Figure 10. Rating curve for stage and discharge data at Vicksburg, MS, over the period 2000–2016. Flood stage is marked with a vertical dashed line at ~26.45 m NAVD88. ....	18
Figure 11. Average flow velocity (calculated from cross-sectional ADCP data) compared to water surface elevation at Vicksburg for the period 2000–2016. Flood stage is marked with a vertical dashed line at elevation ~26.45 m NAVD88. Peak and trough phases were omitted from this figure for clarity; they do not follow any apparent trend. ....	19
Figure 12. Mississippi River discharge at Vicksburg, calculated from the rating curve in Figure 10. ....	19
Figure 13. Average roughness height ( $R_{ave}$ ) and friction factors calculated from the survey and streamflow data. The vertical dashed lines indicate the discharge at flood stage. ....	21

Figure 14. Form drag component of Darcy-Weisbach friction factor $f$ (Darcy-Weisbach $f$ minus van Rijn skin-friction factor $f'$ ) compared to form drag estimates following Vanoni and Hwang (1967; open squares), Engelund (1977; filled circles), and van Rijn (1993; triangles). Point colors represent the river discharge at the time of measurement, and the dashed line represents unity (following Julien et al. [2002]).	23
Figure 15. Bathymetry data from May 15, 2011.	28
Figure 16. Bathymetry data from May 15, 2011, with analyzed lines overlaid.	28
Figure 17. Bathymetry data from May 19, 2011.	29
Figure 18. Bathymetry data from May 19, 2011, with analyzed lines overlaid.	29
Figure 19. Bathymetry data from October 2, 2012.	30
Figure 20. Bathymetry data from October 2, 2012, with analyzed lines overlaid.	30
Figure 21. Bathymetry data from October 3, 2012.	31
Figure 22. Bathymetry data from October 3, 2012, with analyzed lines overlaid.	31
Figure 23. Bathymetry data from April 29, 2013.	32
Figure 24. Bathymetry data from April 29, 2013, with analyzed lines overlaid.	32
Figure 25. Bathymetry data from March 19, 2015.	33
Figure 26. Bathymetry data from March 19, 2015, with analyzed lines overlaid.	33
Figure 27. Bathymetry data from April 30, 2015.	34
Figure 28. Bathymetry data from April 30, 2015, with analyzed lines overlaid.	34
Figure 29. Bathymetry data from May 19, 2015.	35
Figure 30. Bathymetry data from May 19, 2015, with analyzed lines overlaid.	35
Figure 31. Bathymetry data from January 12, 2016.	36
Figure 32. Bathymetry data from January 12, 2016, with analyzed lines overlaid.	36
Figure 33. Bathymetry data from January 15, 2016.	37
Figure 34. Bathymetry data from January 15, 2016, with analyzed lines overlaid.	37
Figure 35. Bathymetry data from January 25, 2016.	38
Figure 36. Bathymetry data from January 25, 2016, with analyzed lines overlaid.	38
Figure 37. Bathymetry data from January 29, 2016.	39
Figure 38. Bathymetry data from January 29, 2016, with analyzed lines overlaid.	39

## Tables

Table 1. List of dates, water discharge, survey vessels, sonar systems, and other data collected during the study period.	3
Table 2. Summary of bedform statistics for each study period. The values here are the average across the entire study area for each day; full statistics are given in Appendix C.	10
Table 3. Calculated roughness statistics.	333

## Preface

The research documented in this report was conducted as part of the Mississippi River Geomorphology & Potamology (MRG&P) Program, Project 127672, “Bed Form Roughness Investigation.” The MRG&P is part of the Mississippi River and Tributaries Program and is managed by the U.S. Army Corps of Engineers (USACE), Mississippi Valley Division (MVD), and Districts. The MRG&P Technical Director was Dr. Ty Wamsley. The MVD Commander was MG Richard G. Kaiser. The MVD Director of Programs was Mr. James A. Bodron.

Mississippi River engineering direction and policy advice were provided by the Mississippi River Commission. The Commission members were MG Kaiser, USACE; the Honorable Sam E. Angel; the Honorable Norma Jean Mattei, PhD; RDML Shepard Smith, National Oceanic and Atmospheric Administration; BG Mark Toy, USACE; and BG Paul E. Owen, USACE.

Direct supervision of the U.S. Army Engineer Research and Development Center (ERDC), Coastal and Hydraulics Laboratory (CHL) aspects of this effort were provided by Dr. Jackie Pettway, Chief of the Navigation Division (CEERD-HN); Dr. Cary Talbot, Chief of the Flood and Storm Protection Division (CEERD-HF); Mr. Thad Pratt, Chief of the Field Data Collection and Analysis Branch (CEERD-HNF); and Mr. Keith Flowers, Chief of the River Engineering Branch (CEERD-HFR). The Acting Director of CHL was Mr. Jeffrey R. Eckstein.

The Commander of ERDC was COL Ivan P. Beckman, and the Director of ERDC was Dr. David W. Pittman.

## Unit Conversion Factors

Multiply	By	To Obtain
cubic feet	0.02831685	cubic meters
cubic inches	1.6387064 E-05	cubic meters
cubic yards	0.7645549	cubic meters
degrees (angle)	0.01745329	radians
degrees Fahrenheit	(F-32)/1.8	degrees Celsius
feet	0.3048	meters
inches	0.0254	meters
miles (nautical)	1,852	meters
miles (U.S. statute)	1,609.347	meters
pounds (mass)	0.45359237	kilograms
square feet	0.09290304	square meters
square inches	6.4516 E-04	square meters
square miles	2.589998 E+06	square meters
square yards	0.8361274	square meters
tons (force)	8,896.443	newtons
tons (2,000 pounds, mass)	907.1847	kilograms
tons (2,000 pounds, mass) per square foot	9,764.856	kilograms per square meter
yards	0.9144	meters



# 1 Introduction

## Background

The history of bedform studies in the Mississippi River likely begins with Johnson's "Sand Wave and Sediment Observations" from the 1879 Army Corps of Engineers Annual Report (Johnson 1879). Johnson measured sand waves by lead line in the Mississippi River near Helena, AR, and documented the important observation that the sand waves increased in size with river stage, and vice versa.

Many authors in the ensuing 140 years have attempted to construct empirical, theoretical, and statistical relations to explain bedform geometries and transport rates not just in the Mississippi River but in a variety of subaqueous and subaerial mobile-bed environments and laboratory studies (e.g., Bagnold 1941; Simons et al. 1965; Nordin and Alget 1966; Hino 1968; Nordin 1971; Robert 1988; Kennedy and Odgaard 1991; Julien and Klaassen 1995; Karim 1999; Flemming 2000; Tjerry and Fredsøe 2005; van der Mark et al. 2008). Within the broad body of literature on this subject, authors have highlighted the morphodynamic feedbacks between bed configuration, flow parameters, and bed material properties. In general, it is evident that bedforms are a natural consequence of the transport of non-cohesive sediment by a moving fluid. Emerging irregularity of form leads to local variability in the flow, which, in most cases, is self-propagating—acceleration of flow over obstacles increases ability of that flow to move the material, further concentrating topography and modifying the flow, etc.

## Objective

In large rivers, this behavior, combined with the naturally unsteady hydrograph, leads to an ever-evolving population of bedforms. These bedforms, along with planform irregularities (which in the particular case of the Mississippi River are largely static) present the primary components of frictional flow resistance. In numerical modeling of fluvial hydraulics, friction is an important determinant of flow characteristics; however, the contribution of individual bedforms to form drag is rarely explicitly calculated. This work seeks to progress towards a methodology for (1) analyzing and characterizing a bedform-covered channel bed and the flow

conditions under which they formed and (2) accurately parameterizing the resistance to flow presented by that population of bedforms.

## **Approach**

Bathymetric data were collected several times over the period 2011–2016 to measure rates of bedform transport using the integrated section surface difference over time version 2 (ISSDOTv2) methodology (Abraham et al., 2011). Linear profiles of the bedforms were extracted from the bathymetry and analyzed for roughness and dune population statistics. Streamflow characteristics during the survey periods were calculated from boat-based and gaging-station data. The roughness statistics were then compared with the flow conditions under which the bedforms were observed.

## 2 Methods

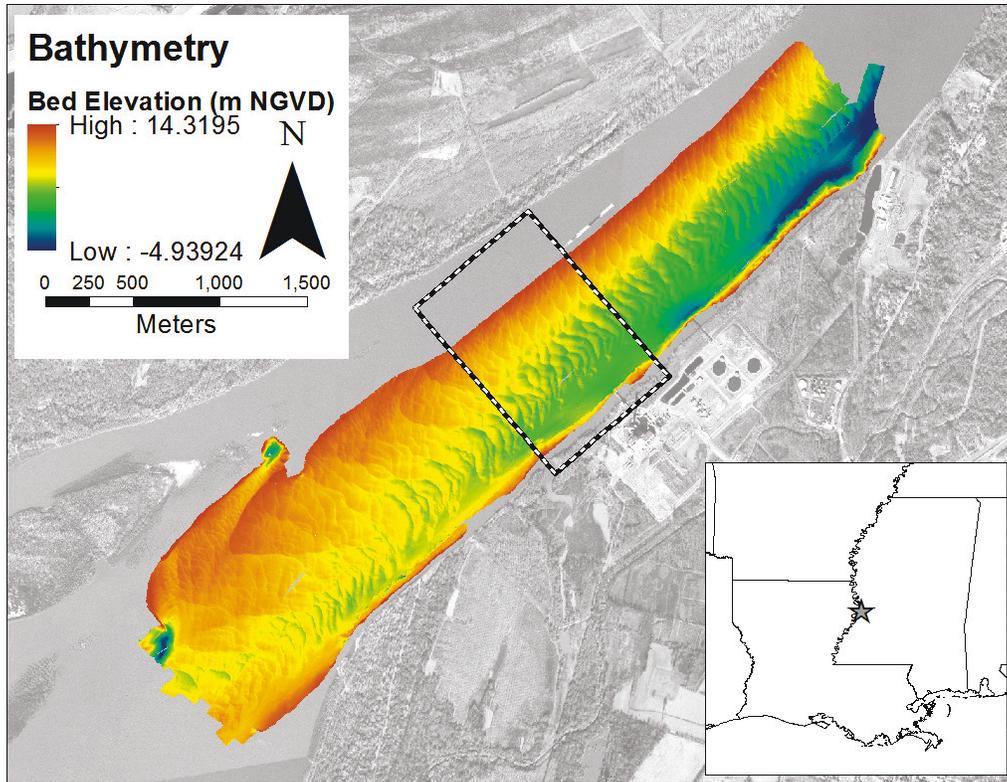
### Field data collection

Multibeam sonar bathymetry data were collected over an area ~1 square kilometer (km<sup>2</sup>) in the Mississippi River (River Mile 432) near Vicksburg, MS (Figure 1), on the dates listed in Table 1 with the survey vessels and sonar systems also referenced in Table 1. Survey data were acquired and post-processed using Hypack® Hydrographic Survey and Processing Software.

**Table 1. List of dates, water discharge, survey vessels, sonar systems, and other data collected during the study period.**

Date	Water Discharge (m <sup>3</sup> /s)	Survey Vessel	Sonar System	Other Data Collected
15 May 2011	62,960	RV <i>SeaArk</i>	GeoSwath 250 kHz	
18 May 2011	64,330	N/A	N/A	Water Surface Profile
19 May 2011	64,400	RV <i>SeaArk</i>	GeoSwath 250 kHz	
4 September 2012	7,135	N/A	N/A	Water Surface Profile
2 October 2012	8,185	RV <i>SeaArk</i>	GeoSwath 250 kHz	
3 October 2012	8,335	RV <i>Gannett</i>	GeoSwath 500 kHz	
29 April 2013	31,870	RV <i>Gannett</i>	GeoSwath 500 kHz	
19 March 2015	31,580	RV <i>T Waller</i>	GeoSwath 250 kHz	Water Surface Profile
30 April 2015	35,960	RV <i>T Waller</i>	GeoSwath 250 kHz	Water Surface Profile
19 May 2015	22,810	RV <i>T Waller</i>	GeoSwath 250 kHz	Water Surface Profile
12 January 2016	47,720	RV <i>T Waller</i>	GeoSwath 250 kHz	ADCP
15 January 2016	49,530	RV <i>T Waller</i>	GeoSwath 250 kHz	ADCP
25 January 2016	43,050	RV <i>T Waller</i>	GeoSwath 250 kHz	ADCP
29 January 2016	36,220	RV <i>T Waller</i>	GeoSwath 250 kHz	ADCP

Figure 1. Map of the study area, with river bed elevation survey focus area outlined in the dashed box. The complex geometry of the dunes can be observed covering the bed surface and extending upstream and downstream of the survey area.



## Roughness analysis

Bathymetric survey lines, labeled 5, 7, 9, and 11, were selected for detailed analysis as these lines were collected while the survey vessel was traveling upstream, and therefore these lines have greater spatial data density (due to the vessel's slower pace traveling upstream compared to downstream). Points along two linear profiles were extracted from each survey line (e.g., 5\_1, 5\_2, 7\_1, 7\_2) to provide 1-dimensional bed elevation profiles for signal analysis. (See Appendix A for profile locations.)

These raw profiles (e.g., Figure 2A) were binned and averaged at 0.3 meter (m) intervals and interpolated to a horizontal precision of 0.1 m using a piecewise cubic Hermite interpolating polynomial algorithm. The profiles were then high-pass filtered, and any remaining Direct Current (DC) offset was removed to provide an Alternating Current (AC) signal for analysis. A DC signal is one which varies about some non-zero value. The mean of the entire profile is the DC offset, and an AC signal is one which has a DC offset of zero. From the resulting signal varying approximately zero

(Figure 2B), roughness statistics rugosity ( $R_{rug}$ ), roughness average ( $R_{ave}$ ), roughness root mean square (RMS) ( $R_{RMS}$ ), skewness ( $R_{ske}$ ), and kurtosis ( $R_{kur}$ ) were calculated according to the following:

$$R_{rug} = \frac{\sqrt{\sum_{x_1}^{x_n} y_x^2 + n}}{n} \quad (1)$$

$$R_{ave} = \frac{1}{n} \sum_{x_1}^{x_n} |y_x| \quad (2)$$

$$R_{RMS} = \sqrt{\frac{1}{n} \sum_{x_1}^{x_n} y_x^2} \quad (3)$$

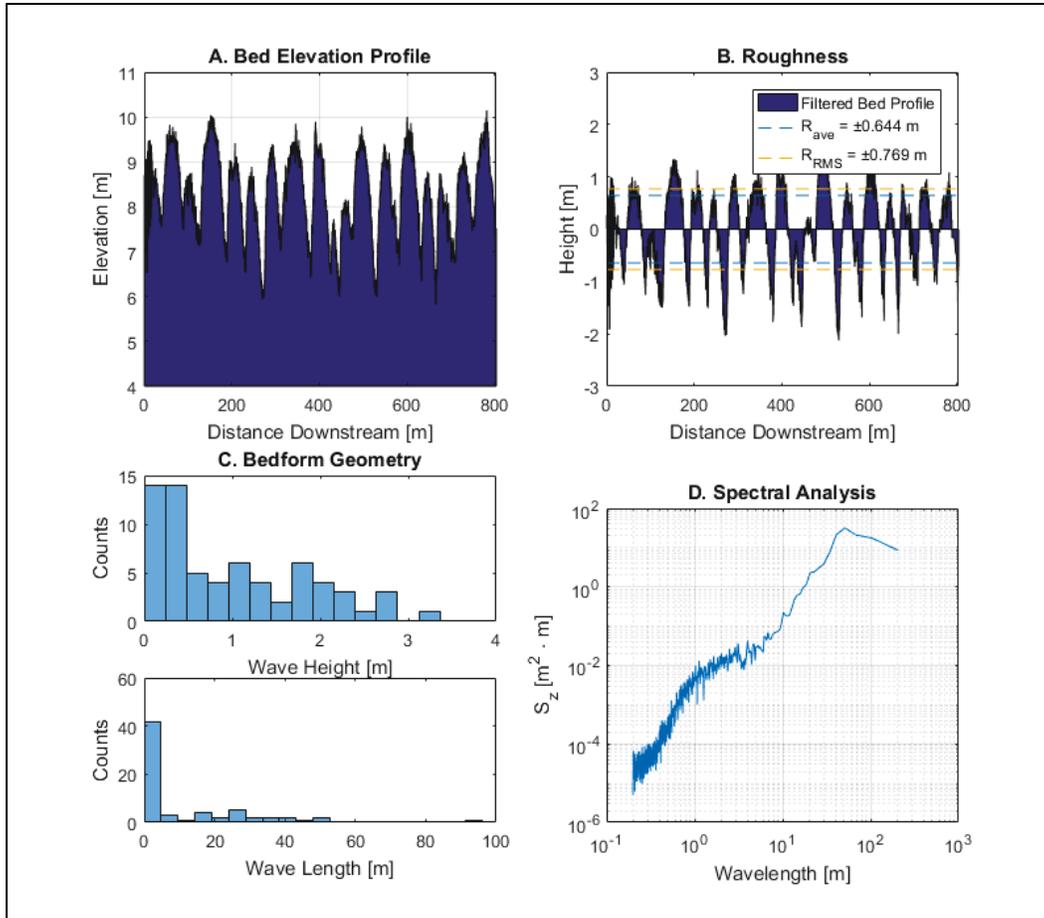
$$R_{ske} = \frac{1}{nR_{RMS}^3} \sum_{x_1}^{x_n} y_x^3 \quad (4)$$

$$R_{kur} = \frac{1}{nR_{RMS}^4} \sum_{x_1}^{x_n} y_x^4 \quad (6)$$

where:

- $n$  = number of nodes along which bed elevation is measured
- $x$  = horizontal distance along bed elevation profile at node  $n$
- $y_x$  = relative elevation above/below mean elevation along profile at distance  $x$ .

Figure 2. Example of bed profile analysis from March 2015. (A) is the raw bed elevation profile, (B) shows the high-pass filtered roughness profile with  $R_{ave}$  and  $R_{RMS}$  statistics, (C) gives counts of bedforms of different sizes, and (D) is the power spectral density estimate ( $S_z$ ) of the roughness profile.



Zero-crossing analysis was performed to define a single bedform as the roughness profile between successive downward origin crossings. Zero-crossing analysis uses the distance between consecutive zero crossings to distinguish individual dunes. A zero crossing is a location where the profile crosses the  $x$  axis at  $y = 0$ . From the population of bedforms (e.g., Figure 2C), significant and RMS heights and mean lengths were calculated ( $H_{sig}$ ,  $H_{RMS}$ ,  $T_{ave}$ ). Significant heights were calculated as the 67th percentiles of the bedform population. The ratio of  $H_{RMS}$  to  $T_{ave}$  is the bedform steepness (from Clifton and Dingler [1984]). Spectral density estimation was performed on each roughness profile using Welch's method (Figure 2D). Note that all dune heights referred to in this study are defined as the vertical distance between consecutive bedform troughs and crests.

## Flow characteristics

Streamflow characteristics during the survey periods were calculated from boat-based and gaging-station data. Boat-based water surface elevations were calculated by real-time kinematic post-processing of the survey vessel's navigation record. Water surface slope was calculated by fitting a linear regression through the water surface elevations overlying the survey area. It was observed that the water surface profile exhibited a concave-up inflection point at the location of the Vicksburg gage (RK701; U.S. Interstate Highway 20 bridge). For this reason, water surface profile slopes were fit to elevations downstream of the bridge over a reach ~10 km centered on the survey area (RK697). These boat-based recordings of river surface elevation were collected on the following dates:

- 18 May 2011 \*
- 4 September 2012 \*
- 19 March 2015
- 30 April 2015
- 19 May 2015.

\* These dates did not correspond with the multibeam surveys but did occur under similar flow conditions as the May 2011 and October 2012 surveys.

Gaging station stage data from the period 2000–2016 were collected from stream gages at Greenville, Vicksburg, and Natchez, MS, maintained by U.S. Army Corps of Engineers (USACE), Vicksburg District (MVK) (data available from [www.rivergages.com](http://www.rivergages.com)). These data were converted to North American Vertical Datum of 1988 (NAVD88) elevations using the linear correction for gage zero height at each station and National Oceanic and Atmospheric Administration, National Geodetic Survey, Vertical Datum Conversion (NOAA NGS VERTCON) software ([https://www.ngs.noaa.gov/cgi-bin/VERTCON/vert\\_con.prl](https://www.ngs.noaa.gov/cgi-bin/VERTCON/vert_con.prl)) for datum shift and were used to calculate daily long-range water surface slopes. Bed shear stress ( $\tau_b$ ) was calculated from the gage data by the depth-slope product:

$$\tau_b = \rho g h S \quad (6)$$

where:

- $\rho$  = fluid density, in kilograms per cubic meter
- $g$  = gravitational acceleration, 9.8 meters per second<sup>2</sup> (m/s<sup>2</sup>)
- $h$  = water depth, in meters
- $S$  = water surface slope.

Vessel-based acoustic Doppler current profiler (ADCP) measurements of water discharge were collected ~weekly (sometimes the data are collected more frequently, e.g., during historic flood events in 2008 and 2011) by the USACE MVK over the interval 2000–2016. These measurements were matched to the daily stage records at Vicksburg gage to construct a stage-discharge rating curve for the study interval.



## 3 Results

### Bathymetry

The bathymetric results show the study area as the medial section of a bank-attached sand bar along the west bank of the Mississippi River near River Mile 432 (~3 km downstream of the U.S. Interstate Highway 20 bridge). The asymmetrical river cross section exhibits a relatively steep slope from its eastern bank down to the channel thalweg and a more gently sloping surface associated with the sand bar on the western margin. The channel thalweg in this reach is within 1 m of NAVD88 datum, so water depth varies with river stage from approximately 15 m at low flow to over 27 m during flood stages. The west bank in this reach has an extensive vegetated batture area, which may be inundated at flood stage. The wetted channel width is dependent on river stage, ranging from 1,100 m at low flow, to 1,500 m prior to overbanking, up to several kilometers after inundation of the batture.

Dunes observed by surveying the sand bar ranged from a few decimeters to several meters in height and ~10 to ~100 m in length. The largest bedforms were observed across the center of the sand bar, near survey lines 5, 7, and 9. Smaller dunes were found towards the margins of the bar, in the shallow water near survey line 3, and the deepest water near survey line 11. These dunes did not often exceed 1 m in height or a few 10s of meters in length. Dune coverage near line 11 was most variable; during some of the surveys, large dunes from the base of the sandbar extended into an otherwise featureless thalweg while other surveys showed the thalweg to be completely mantled by smaller bedforms.

The full results of the bathymetric surveys are presented in detailed maps of each study period and extracted lines in Appendix A.

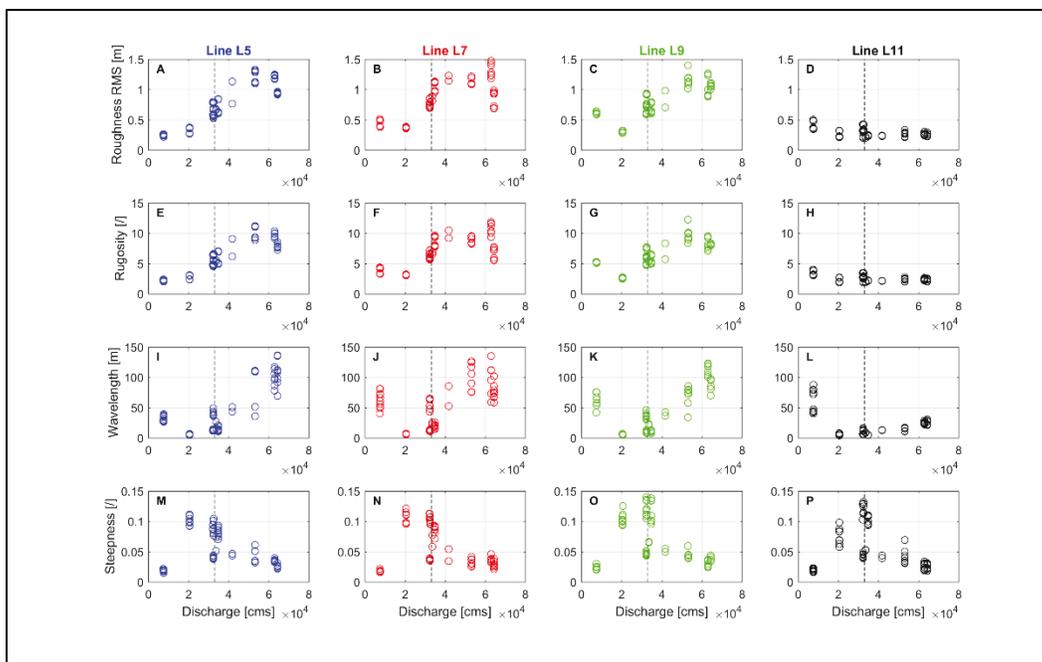
### Roughness

The results of roughness analysis for all bed profiles during each survey period are listed in Table 2, and a subset of the statistics is displayed in Figure 3, categorized by profile line number. All analyzed profiles are shown in Appendix B, and the full set of computed statistics is given in Appendix C (Table 3).

Table 2. Summary of bedform statistics for each study period. The values here are the average across the entire study area for each day; full statistics are given in Appendix C.

Date	Water Disch. ( $Q_w$ , $m^3/s$ )	Roughness Average ( $R_{ave}$ , m)	Roughness RMS ( $R_{RMS}$ , m)	Rugosity ( $R_{rug}$ )	Skewness ( $R_{ske}$ )	Kurtosis ( $R_{kur}$ )	Sig. Wave Height ( $H_{sig}$ , m)	RMS Wave Height ( $H_{RMS}$ , m)	Average Wave-length ( $T_{ave}$ , m)	Steepness
15 May 2011	62,960	0.836	1.051	8.447	-0.559	3.109	4.203	3.035	91.367	0.033
18 May 2011	64,330	0.589	0.748	6.040	-0.508	3.328	3.016	2.084	72.658	0.028
19 May 2011	64,400	0.361	0.441	3.758	0.024	2.745	1.500	1.095	52.124	0.022
4 Sept. 2012	7,135	0.342	0.420	3.579	0.074	2.715	1.468	1.074	55.630	0.019
2 Oct. 2012	8,185	0.467	0.574	4.802	-0.200	2.663	2.036	1.505	37.087	0.042
3 Oct. 2012	8,335	0.538	0.663	5.479	-0.341	2.724	1.733	1.102	10.368	0.109
29 Apr. 2013	31,870	0.553	0.679	5.644	-0.299	2.795	1.705	1.095	11.918	0.097
19 Mar. 2015	31,580	0.249	0.316	2.689	-0.204	3.188	0.813	0.549	5.685	0.097
30 Apr. 2015	35,960	0.796	0.957	8.025	-0.485	2.628	3.199	2.187	44.089	0.054
19 May 2015	22,810	0.763	0.938	7.728	-0.465	2.755	3.517	2.726	79.112	0.036
12 Jan. 2016	47,720	0.656	0.803	6.645	-0.414	2.721	2.923	1.901	41.987	0.046
15 Jan. 2016	49,530	0.475	0.603	4.876	-0.326	3.099	1.820	1.189	18.866	0.062
25 Jan. 2016	43,050	0.836	1.051	8.447	-0.559	3.109	4.203	3.035	91.367	0.033
29 Jan. 2016	36,220	0.589	0.748	6.040	-0.508	3.328	3.016	2.084	72.658	0.028

Figure 3. Selected roughness statistics for study discharges. (A-D) Roughness RMS for survey lines 5, 7, 9, and 11. (E-H) Rugosity for survey lines 5, 7, 9, and 11. (I-L) Average wavelength for survey lines 5, 7, 9, 11. (M-P) Steepness for survey lines 5, 7, 9, and 11. A vertical dashed line is given on each plot at flood stage discharge for Vicksburg.



In general, the dune dimensions (Roughness Average, Roughness RMS, Significant Wave Height, RMS Heights, and Average Wave Period) were observed to increase with water discharge for all of the profile lines except Lines 11.1 and 11.2. Line 11 was in the thalweg of the channel, devoid of bedforms during most of the study periods. When bedforms were present in this area of the channel, they were either very small or were the tips of bedforms extending out from the sand bar area. Profile lines 5, 7, and 9 exhibited these bedform growth trends except at the lowest and highest observed flows. At the lowest observed flows, bedforms in these areas appeared to have greater dimensions than apparently warranted by the current flow conditions (e.g., Figure 3A, B, C, I, J, K; flows below 10,000  $\text{m}^3/\text{s}$ ). These *oversized* dunes are interpreted to be a relict feature of higher river stages prior to the low-flow study periods that had not yet equilibrated to the slower flow conditions. At the other end of the spectrum, bedforms at the highest river discharges did not appear to respond to additional increases in flow; indeed, the bedforms decreased in height at the highest measured discharge on 19 May 2011 (probably most evident in Figure 3B), interpreted to be the result of a transition from bedload transport to suspended transport for the principal bed-material grain sizes. These decreased dune heights (or decrease in the rate of dune height increase with

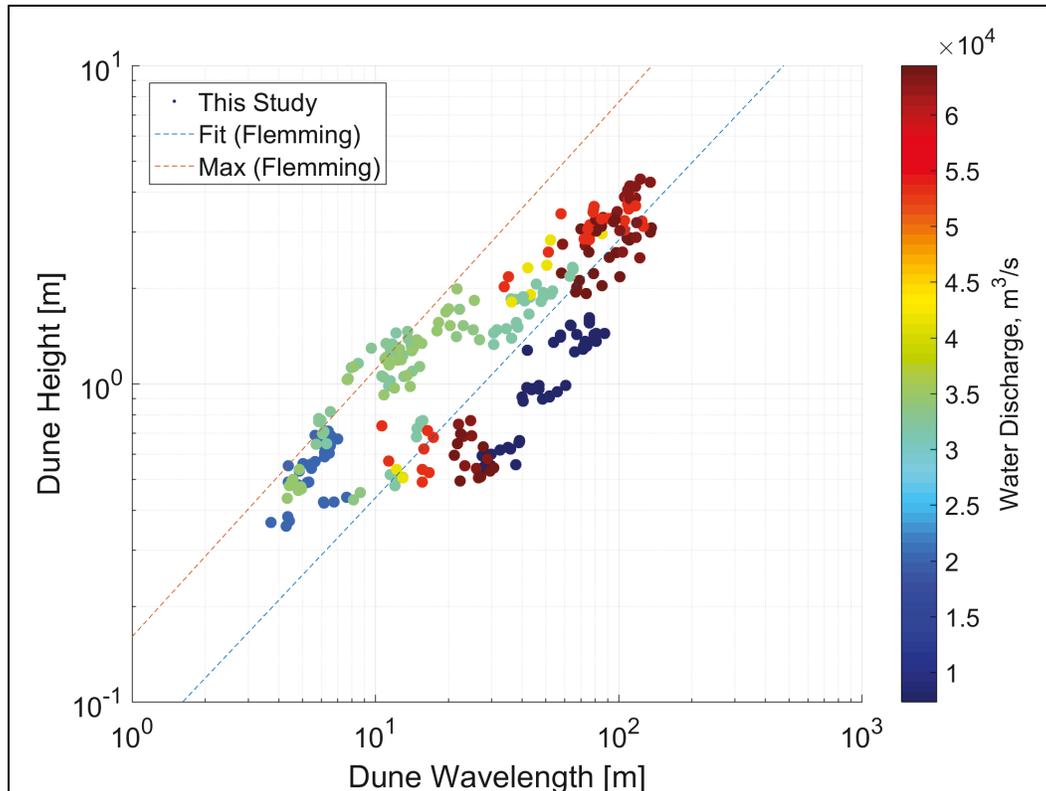
discharge) are accompanied by an elongation of the dune forms: as wavelength increases more rapidly than wave height, the dune steepness (height:length ratio) decreases at the highest discharges (Figure 3M, N, O).

This effect is perhaps best illustrated in Figure 4, which gives the calculated average dune height ( $H_{rms}$ ), wavelength ( $T_{ave}$ ), and water discharge for all of the analyzed profiles. From water discharges of 20,000 m<sup>3</sup>/s to 35,000 m<sup>3</sup>/s, the dunes were observed to grow along a trajectory similar to that of the limit calculated by Flemming (2000). For discharges greater than ~35,000 m<sup>3</sup>/s, increases in dune wavelength outpaced increases in dune height, leading to reduced dune steepness at the highest flows. This limit on dune height is attributed by Flemming (2000) to both a sediment-supply limit in constructing such large bedforms as well as a transition from bedload-dominant transport to suspended-dominant transport when the critical shear velocity for the bed-material grain size is exceeded. This particular effect has been observed elsewhere in the lower Mississippi River by Ramirez and Allison (2013), who found that dunes grew to a maximum size with increasing discharge to a point, but further increases in discharge were accompanied by halted or reduced dune magnitude and steepness.

Some of the smallest dunes observed in this study were measured during the highest discharge event in May 2011 (red and orange points near the bottom of Figure 4). These bedforms were found in the channel thalweg along profile line 11 (see Appendix A for profile line locations). This location was observed in all study periods to have the smallest (or non-existent) bedforms, and bedforms in this location appear to be governed by a different set of geometric constraints than those over the core of the sand bar area. This location—being in the deepest part of the channel—experiences the highest flow velocities and may exhibit the transition to suspension transport earlier than shallower channel areas (Ramirez and Allison 2013).

The trends included in Figure 4 calculated by Flemming (2000) come from a study of 1,491 subaqueous bedform profiles from a variety of environments and geographic locations (including laboratory, river, and marine bedforms). In that work, Flemming observed that bedforms over five orders of magnitude were highly correlated ( $r=0.98$ ) along this trend. The author also found that for any given bedform spacing (wavelength), the maximum bedform steepness, according to Flemming, was not appreciably exceeded (shown as the “Max” line in Figure 4).

Figure 4. Average dune heights ( $H_{rms}$ ) compared to average wavelengths ( $\lambda_{ave}$ ) for all roughness profiles analyzed. Colors represent the rating-curve estimated stream discharge at the time of each survey. Included are relations for best-fit and maximum height:length ratios for 1,491 measurements of dune geometry in a variety of environments compiled by Flemming (2000).



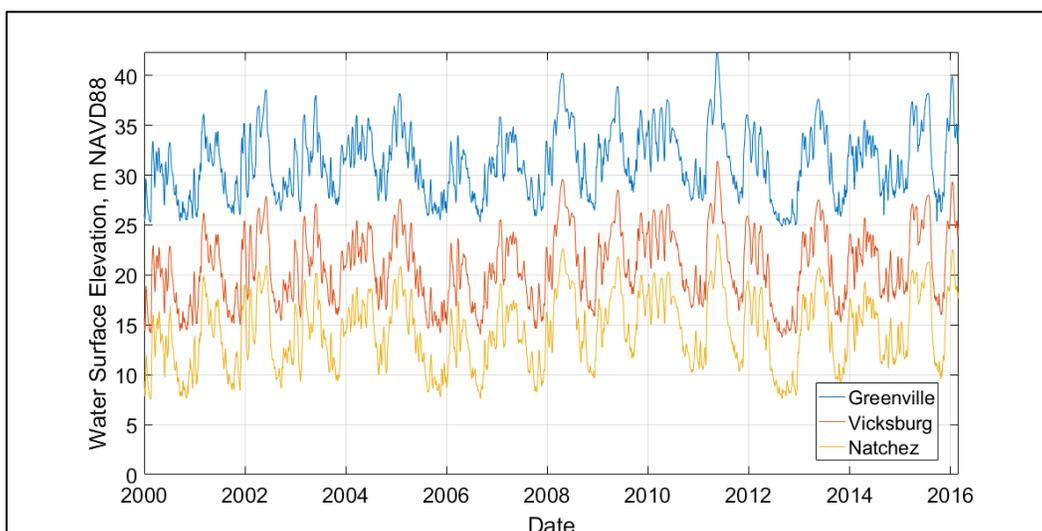
Note that some of the largest (in wavelength) bedforms observed in the present study were observed during the lowest water discharge (dark blue points are from October 2012). This is interpreted to be an anomalous result of dunes that had grown under greater flow conditions prior to the survey period but which had not yet been deconstructed due to the decreased sediment transport capacity under low flow. What is particularly remarkable about this observation is the fact that 2012 did not have any particularly high-flow periods during which these large dunes could be expected to have grown—that year was one of only three in the past decade to have not exceeded *flood stage* at the Vicksburg gage. It is possible that these dunes were relict features of the previous flood in 2011 and that the relatively low flows throughout 2012 did not have enough transport energy to re-equilibrate the bed morphology.

## Streamflow

### River stage and slope records

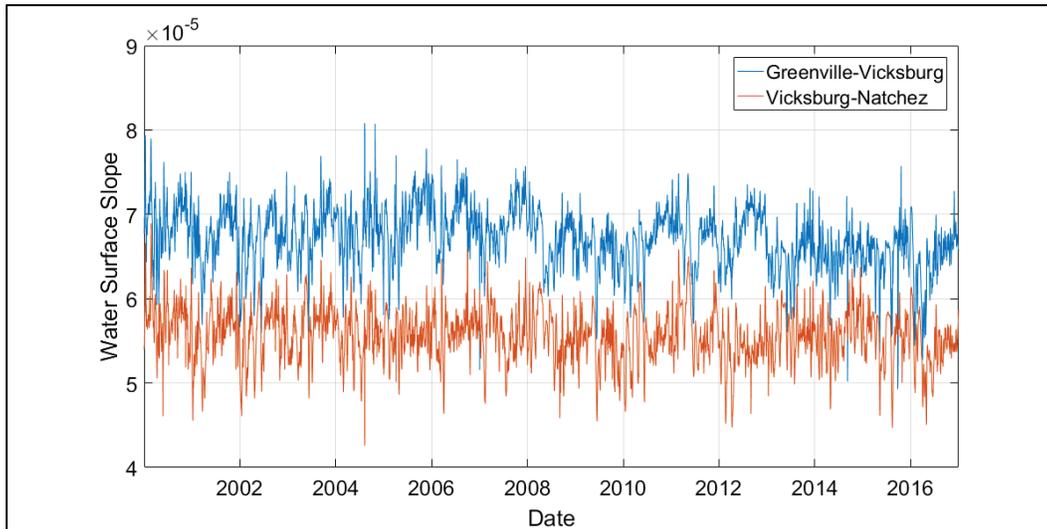
River stage records were analyzed for the Greenville, Vicksburg, and Natchez, MS, gaging stations for the period 2000–2016. These records are displayed in Figure 5. From these records the seasonal flood nature of the hydrograph can be observed as well as the higher-frequency variation of week-to-month-long floods. The flood during 2011 set high-water records in Vicksburg and Natchez.

Figure 5. Gaging station records of Mississippi River stage at Greenville (blue), Vicksburg (red), and Natchez (yellow), converted to NAVD88 water surface elevations for the period 2000–2016.



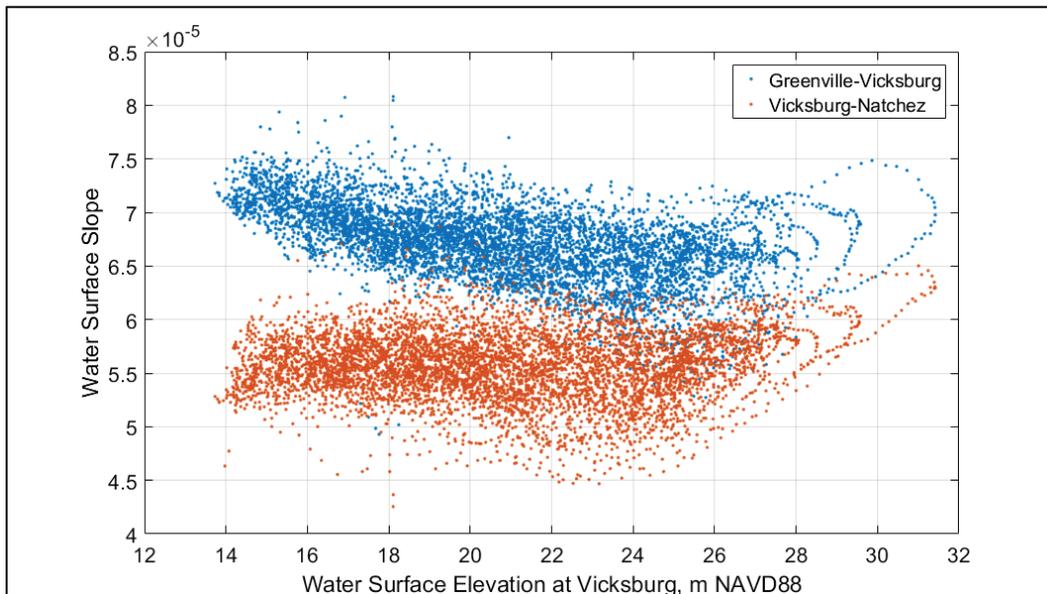
These datum-referenced stage records were used to construct time series of long-range Mississippi River water surface slope using the head differential and river distance between the gaging stations. The slope time series are shown in Figure 6. The slope between Greenville and Vicksburg was almost always greater than the slope between Vicksburg and Natchez throughout the time period measured, indicating an overall concave-up water surface profile for the Greenville to Natchez reach. A long-term (decadal) trend toward lesser water surface slopes over both reaches throughout the period of record may be observed, though this trend has a much lesser magnitude than the annual variability.

Figure 6. Water surface slope calculated between Greenville, Vicksburg, and Natchez gaging stations for the period 2000–2016.



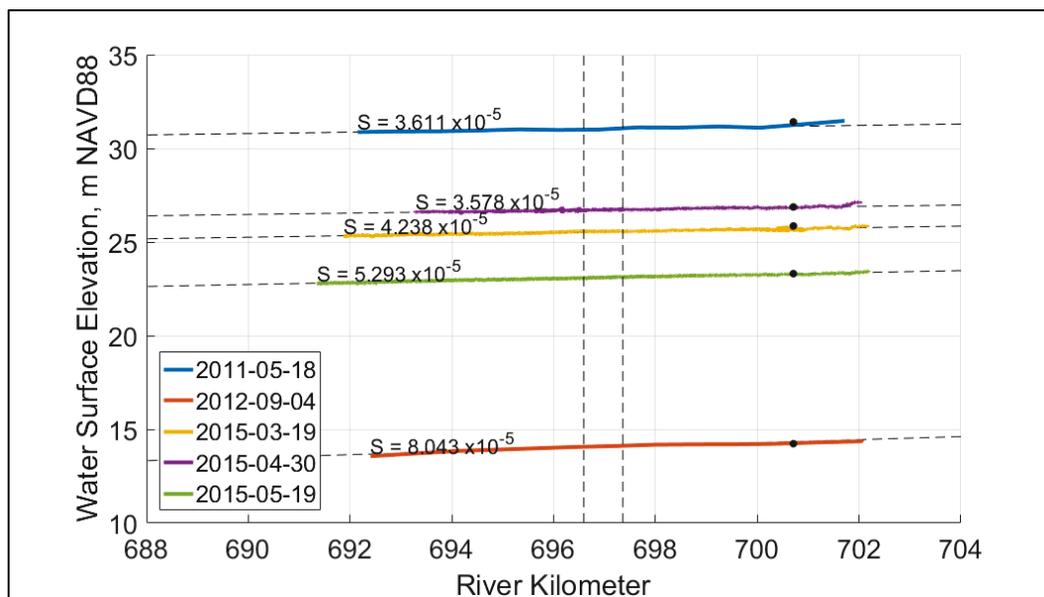
Gage-calculated water surface slopes are compared with water surface elevations for the period 2000–2016 in Figure 7. An inverse relation between water surface elevation and water surface slope was observed for the Greenville-Vicksburg reach, indicating generally lower water surface slopes for higher river stages, though there does appear to be a slight rise in water surface slope for the highest observed river stages. No apparent correlation was observed between water surface elevation and water surface slope for the Vicksburg-Natchez reach.

Figure 7. Water surface slope calculated compared to water surface elevation for the Greenville-Vicksburg reach and the Vicksburg-Natchez reach daily for the period 2000–2016.



The calculated water surface slopes for the study area based on boat-recorded water surface elevation data are shown in Figure 8 along with the gage-recorded water surface elevation at the Vicksburg gage (black circles). The boat-measured water surface elevations were in agreement with those measured at the Vicksburg gaging station. In general, boat-measured water surface slopes appear to decrease with increasing river stage, although the slopes recorded for the two highest measured river stages (May 2011 and April 2015) were nearly equivalent.

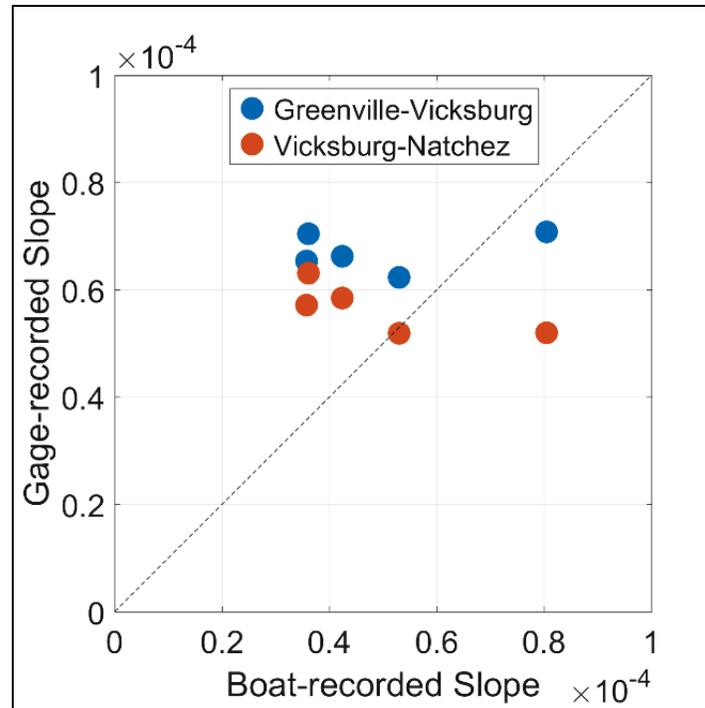
Figure 8. Boat-based water surface elevation profiles in the vicinity of the study area (study area indicated with vertical dashed lines) recorded in May 2011, September 2012, March 2015, April 2015, and May 2015. Each water surface profile was fit with a linear least-squares regression (shown by dashed lines) for the reach downstream of the Vicksburg river gage (at RK701; indicated by black circles at the gage-recorded elevation for each date) to estimate the water surface slope (shown above each profile).



The boat-recorded water surface slopes are compared with the gage-recorded water surface slopes in Figure 9. This figure shows a weak negative correlation between the two methods for estimating water surface slope and indicates that the gage records—while in agreement with the boat-measured water surface elevations—may not be a reliable predictor for the water surface slope in the vicinity of the study area. On the contrary, it is possible that the boat-based measurement of slope, while accurate, may only represent fleeting conditions (these measurements were collected over 10s of minutes); in that case, the gage-calculated slopes may represent a better time- and reach-average of the conditions under which bedforms were built.



Figure 9. Comparison of water surface slopes recorded aboard the survey vessel and those calculated based on the stage differences between gaging stations at Greenville, Vicksburg, and Natchez.



### Rating curve

The relation between water surface elevation at Vicksburg and ~weekly measured river discharge is given in Figure 10. In general, the data follow the relation

$$Q_w = e^{0.128 \cdot h_{ws} + 7.046} \quad (7)$$

where:

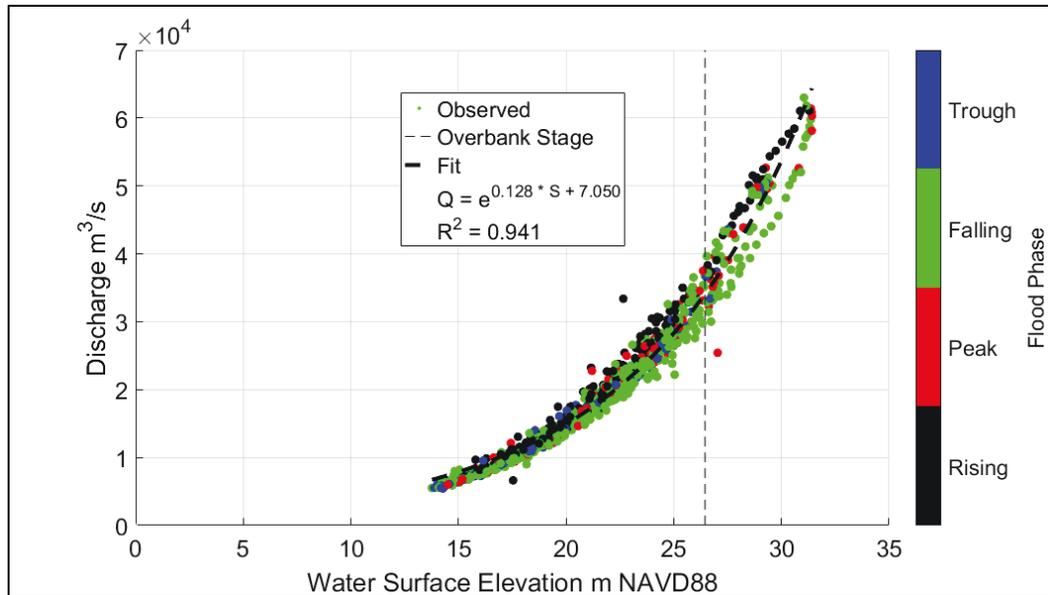
$Q_w$  = water discharge, in cubic meters per second

$h_{ws}$  = water surface elevation, in meters NAVD88.

A pattern was noted during the analysis that the rating curve differed for rising and falling hydrograph intervals. To highlight this, measurements collected during different hydrographic phases are plotted in different colors. Flood phase was determined mathematically using the first derivative of the stage at Vicksburg with respect to time: intervals with positive or negative slopes greater than the median value were marked as rising or falling, respectively. Intervals were marked peak or trough where

the slope was less than the median value and the curvature (second derivative) was negative or positive, respectively. From Figure 10, it can be observed that discharge during a rising hydrograph is often greater than that predicted by the rating curve, and vice versa for falling hydrographs. Peak and trough flood phases do not appear to obey any particular pattern.

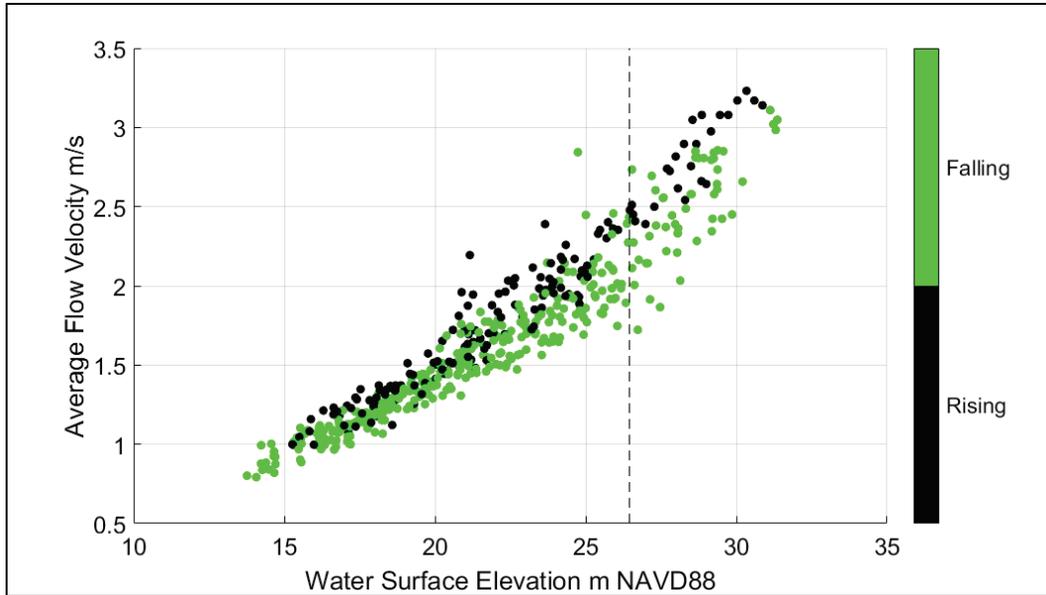
Figure 10. Rating curve for stage and discharge data at Vicksburg, MS, over the period 2000–2016. Flood stage is marked with a vertical dashed line at ~26.45 m NAVD88.



A similar relation can be observed between average measured flow velocity (from the ADCP cross-sectional data) and water surface elevation at different phases of the hydrograph, shown in Figure 11. This hysteresis *loop* has been observed before for this reach of the river, and changes in river bed roughness between rising and falling flow have been suggested as a possible component cause of this phenomenon, along with unsteady flow, temperature variation, and net aggradation/degradation of the river bed<sup>1</sup>. The result of this phenomenon is an ephemeral and mobile backwater effect, where a passing flood wave will increase water surface slopes in front of it and decrease water surface slopes behind it.

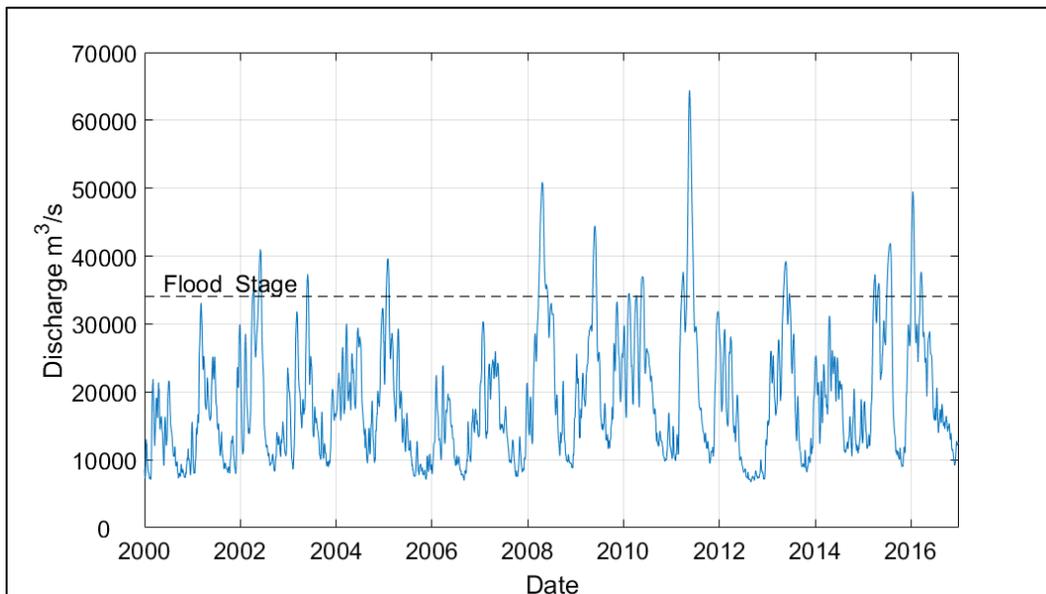
<sup>1</sup> Copeland, R. R. In preparation. *Mississippi River and Tributaries Flowline Assessment: Mississippi River Sedimentation Report*. MRG&P Report. Vicksburg, MS: U.S. Army Engineer Research and Development Center.

Figure 11. Average flow velocity (calculated from cross-sectional ADCP data) compared to water surface elevation at Vicksburg for the period 2000–2016. Flood stage is marked with a vertical dashed line at elevation ~26.45 m NAVD88. Peak and trough phases were omitted from this figure for clarity; they do not follow any apparent trend.



The full time series of rating-curve derived discharge data is shown in Figure 12.

Figure 12. Mississippi River discharge at Vicksburg, calculated from the rating curve in Figure 10.



## 4 Discussion

### Friction factors

In numerical models, friction is often represented using the Manning coefficient  $n$  (USACE 1994). Similarly, Chézy's coefficient  $C$  and the Darcy-Weisbach friction factor  $f$  relate flow velocity, flow depth, and river slope in different ways:

$$f = \frac{8ghS}{V^2} \quad (8)$$

$$n = \frac{1}{V} h^{\frac{2}{3}} S^{\frac{1}{2}} \quad (9)$$

$$C = \frac{V}{h^{\frac{1}{3}} S^{\frac{1}{2}}} \quad (10)$$

where:

$g$  = gravitational acceleration

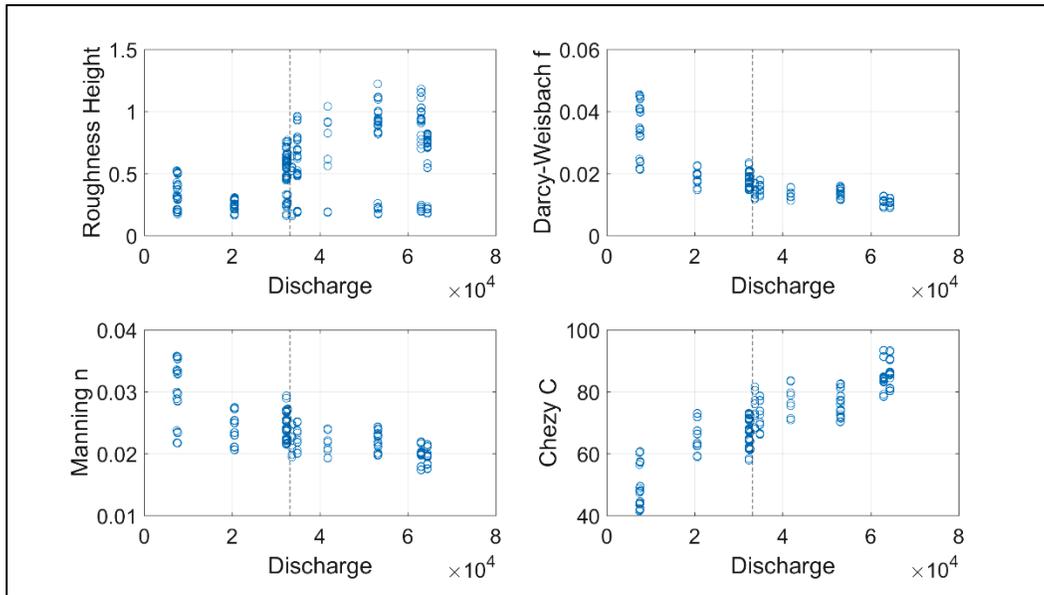
$h$  = local flow depth

$S$  = reach-averaged slope

$V$  = depth-averaged velocity.

Note, Chézy's coefficient varies inversely with flow depth and slope. These values were calculated for the conditions at each of the analyzed roughness profiles using the flow depth at each profile (river stage minus average profile elevation), slopes calculated from the Vicksburg-Natchez gage reach (since boat-measured slopes were only available for a few of the study periods), and cross-section-averaged velocities from the rating curve in Figure 11 (velocities local to the roughness profiles were not available for all study periods; however, ADCP data from the January 2016 study period show depth-averaged velocity to be relatively laterally uniform across the sand bar). The calculated coefficients are shown in Figure 13. From these data it seems evident that frictional resistance to flow decreases with increasing discharge.

Figure 13. Average roughness height ( $R_{ave}$ ) and friction factors calculated from the survey and streamflow data. The vertical dashed lines indicate the discharge at flood stage.



For estimating a friction factor based on the geometry and magnitude of the bedforms, Julien et al. (2002) suggest decomposing the Darcy-Weisbach friction factor  $f$  into its skin-friction and form-drag components following van Rijn (1984), Vanoni and Hwang (1967), and Engelund (1977):

$$f = f' + f'' \quad (11)$$

where:

$f'$  = skin-friction (sediment grain resistance) factor  
 $f''$  = form drag friction factor.

The skin-friction component (sediment grain resistance; van Rijn 1984) depends on the ratio of water depth to sediment grain diameter:

$$f' = \left( 2.03 * \log \left( \frac{12.2h}{d_{90}} \right) \right)^{-2} \quad (12)$$

where:

$d_{90}$  = 90th percentile bed-material grain diameter.

Since only a single estimate for  $d_{90}$  was used in this study (an estimated  $d_{90}$  of 500 microns [ $\mu\text{m}$ ] was used based on the bed samples reported in

Pratt et al.<sup>1</sup>, sediment grain samples were not collected for the present study), this value varies here only with flow depth. Nonetheless, it is considered the minor component of the total friction factor compared to the form drag factor (by greater than one order of magnitude). Calculated values for  $f'$  averaged 0.00148 with a standard deviation of  $9.66 \times 10^{-5}$ .

The Vanoni and Hwang (1967) approach to calculating the form drag factor depends on both the dune steepness and relative height (dune height to water depth ratio):

$$f'' = \left( 3.3 * \log \left( \frac{\lambda h}{\Delta^2} \right) - 2.3 \right)^{-2} \quad (13)$$

where:

$\lambda$  = dune wavelength

$\Delta$  = dune height.

Similarly, the formula of Engelund (1977) uses the same geometric parameters in a different arrangement:

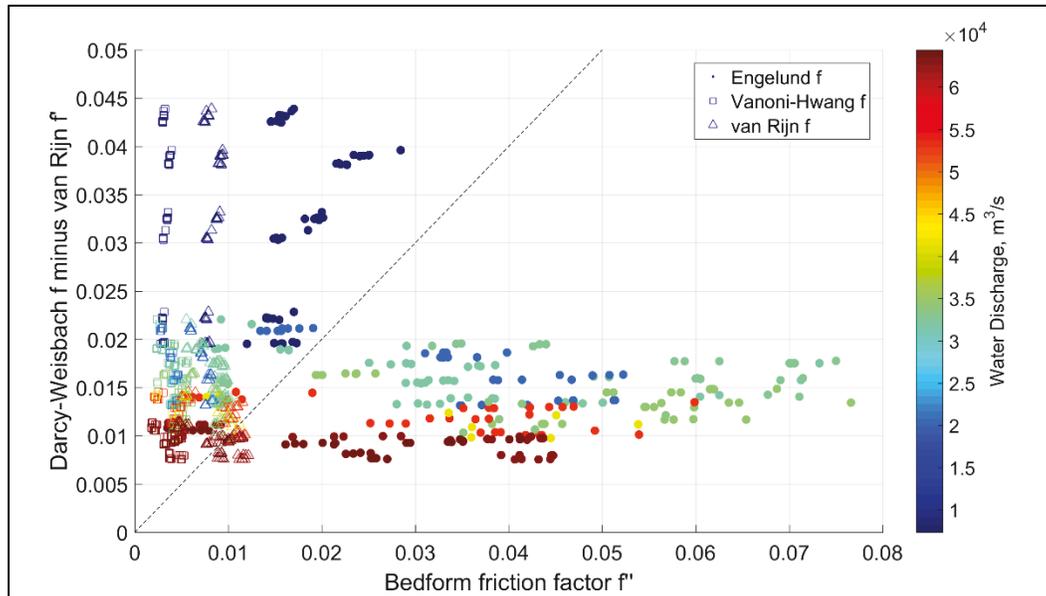
$$f'' = 10 \frac{\Delta^2}{\lambda h} * e^{-2.5 \frac{\Delta}{h}} \quad (14)$$

A value for  $f''$  can also be calculated by subtracting  $f'$  from  $f$ , providing an independent estimate depending only on the flow conditions and sediment particle diameter. This is useful for comparing with the values calculated from the dune geometries, as in Figure 14.

---

<sup>1</sup> Pratt, T. C., N. Ganesh, J. Vaughn, D. Perkey, T. Kirklin, A. Jackson, T. Waller, and W. Butler. In preparation. *Mississippi River Hydrodynamics Study Field Data Collection*. ERDC/CHL Special Report. Vicksburg, MS: U.S. Army Engineer Research and Development Center.

Figure 14. Form drag component of Darcy-Weisbach friction factor  $f$  (Darcy-Weisbach  $f$  minus van Rijn skin-friction factor  $f'$ ) compared to form drag estimates following Vanoni and Hwang (1967; open squares), Engelund (1977; filled circles), and van Rijn (1993; triangles). Point colors represent the river discharge at the time of measurement, and the dashed line represents unity (following Julien et al. [2002]).



There is little agreement in the  $f''$  values calculated from bedform geometries compared to those calculated from the flow conditions, except in the general range of values. The method of Vanoni and Hwang (1967) underpredicts  $f''$  for the conditions observed in the present study, with little variability. While the method of Engelund (1977) generally overpredicts values for  $f''$ , it does apparently group the data into two distinct populations, particularly when considering the river discharge (colors in Figure 14). Values calculated at the lowest measured river discharge fall into a narrow band between  $\sim 0.01$  to  $0.03$ , while values calculated for higher discharges (above  $20,000 \text{ m}^3/\text{s}$ ) tended towards more extreme values for  $f''$ . Notably, the flow conditions observed at the lowest discharges produced greater Darcy-Weisbach-derived  $f''$  values, coinciding with the study periods during which the bedforms are interpreted to be in disequilibrium with the flow conditions (discussed in the Roughness section above). It appears there are two different morphodynamic regimes at work, depending on whether the flow is strong enough to rearrange the dunes. Once this threshold discharge is exceeded, the effect of form drag on the flow is evidently the same regardless of bedform geometry. It is possible that at these higher stages, the drag effects of planform, sand-bar geometry, and friction along the vegetated banks become more important contributors of resistance to flow than the in-channel bedforms.

## 5 Conclusion and Recommendations

Bedform profiles were extracted from the bathymetry measured in the Mississippi River over a range of discharges and analyzed for roughness and dune population statistics. At most locations across the sandbar, the bedforms were observed to increase in size and decrease in steepness (height:length ratio) with discharge. The increase in steepness was largely the result of increasing dune wavelength outpacing increases in dune height. Also notable is a decrease in dune heights at extremely high discharges (as observed in May 2011), which may be associated with increasing proportion of suspension to bedload transport. Punctuating these trends in dune growth is a *step*, or inflection occurring near  $\sim 35,000 \text{ m}^3/\text{s}$  (evident in Figure 3 and Figure 13), corresponding with the bankfull river conditions. The step in dune growth, and resulting friction coefficients at this discharge, may be the result of reconfiguration of the flow following overbanking. The Darcy-Weisbach and Manning friction coefficients calculated for the survey conditions decreased with discharge while the Chezy coefficient increased with discharge. These results suggest that the dunes at higher river stages, despite their generally greater size, may present less resistance to flow due to their reduced steepness and reduced relative heights (dune height:flow depth).

These bathymetric datasets, despite having been collected for the purposes of difference-based bedform transport measurements, are invaluable for observing the morphodynamic response of bedforms to flow conditions. It may prove useful to incorporate these computations in the estimation of bedform transport rates to resolve any possible correlation. While a full range of possible flow conditions are presented here, additional datasets for similar flow conditions will help constrain the range of natural variability as well as elucidate any effects related to the observed dependency of flow velocity on flood phase. Furthermore, it is advised that ADCP measurements of flow be collected each time these data are collected as many of the flow conditions used in this study are estimated from gage records and rating curves. Independent measurements will help with improving rating curve accuracy and distinguishing between local conditions and those averaged over long distances between gage stations.



## References

- Abraham D., R. Kuhnle, and A. J. Odgaard. 2011. "Validation of Bed Load Transport Measurements with Time Sequenced Bathymetric Data." *ASCE Journal of Hydraulic Engineering* 137(7): 723-728.  
[https://ascelibrary.org/doi/abs/10.1061/\(ASCE\)HY.1943-7900.0000357](https://ascelibrary.org/doi/abs/10.1061/(ASCE)HY.1943-7900.0000357).
- Bagnold, R. A. 1941. *The Physics of Blown Sand and Desert Dunes*. London: Methuen.
- Clifton, H. E., and J. R. Dingle. 1984. "Wave-Formed Structures and Paleoenvironmental Reconstruction." *Marine Geology* 60(1-4): 165-198.  
<https://www.sciencedirect.com/science/article/pii/002532278490149X>.
- Engelund, F. 1977. *Hydraulic Resistance for Flow over Dunes*. Progress Report 44. Denmark: Institute of Hydraulics and Hydraulic Engineering, Tech. Univ.
- Flemming, B. W. 2000. "The Role of Grain Size, Water Depth and Flow Velocity as Scaling Factors Controlling the Size of Subaqueous Dunes." *Marine Sandwave Dynamics, Lille, France*, 55-60. <http://www.shom.fr/fileadmin/SHOM/PDF/04-Activites/sedimentologie/marid123/TPflemprem.pdf>.
- Hino, M. 1968. "Equilibrium-Range Spectra of Sand Waves Formed by Flowing Water." *Journal of Fluid Mechanics* 34(3): 565-573.
- Johnson, J. B. 1879. "Results of Sand Wave and Sediment Observations." In *U.S. Army Chief of Engineers Annual Report*, part III, 1,963-1,970.
- Julien, P. Y., and G. J. Klaassen. 1995. "Sand-Dune Geometry of Large Rivers during Floods." *Journal of Hydraulic Engineering* 121(9): 657-663.
- Julien, P. Y., G. J. Klaassen, W. B. M. Ten Brinke, and A. W. E. Wilbers. 2002. "Case Study: Bed Resistance of Rhine River during 1998 Flood." *Journal of Hydraulic Engineering* 128(12). doi: 10.1061/(ASCE)0733-9429(2002)128:12(1042).
- Karim, F. 1999. "Bed-Form Geometry in Sand-Bed Flows." *Journal of Hydraulic Engineering* 125(12): 1253-1261.
- Kennedy, J. F., and A. J. Odgaard. 1991. *Informal Monograph on Riverine Sand Dunes*. CR CERC-91-2. Vicksburg, MS: U.S. Army Engineer Research and Development Center. <https://erdc-library.erdcdren.mil/xmlui/handle/11681/2798>.
- Nordin, C. F. 1971. *Statistical Properties of Dune Profiles*. U.S. Geological Survey Professional Paper 562-F. U.S. Geological Survey.  
<https://pubs.er.usgs.gov/publication/pp562F>.
- Nordin, C. F., and J. H. Algert. 1966. "Spectral Analysis of Sand Waves." *Journal of the Hydraulics Division, Proceedings of the American Society of Civil Engineers*. Issue 5: 95-114.

- Ramirez, M. T., and M. A. Allison. 2013. "Suspension of Bed Material over Sand Bars in the Lower Mississippi River and Its Implications for Mississippi Delta Environmental Restoration." *Journal of Geophysical Research: Earth Surface* 118: 1085–1104. doi:10.1002/jgrf.20075.
- Robert, A. 1988. "Statistical Properties of Sediment Bed Profiles in Alluvial Channels." *Mathematical Geology* 20(3): 205–225.
- Simons, D. B., E. V. Richardson, and C. F. Nordin. 1965. *Bedload Equation for Ripples and Dunes*. U.S. Geological Survey Professional Paper 462-H. U.S. Geological Survey. <https://pubs.er.usgs.gov/publication/pp462H>.
- Tjerry, S., and J. Fredsøe. 2005. "Calculation of Dune Morphology." *Journal of Geophysical Research* 110(F4). doi:10.1029/2004JF000171.
- U.S. Army Corps of Engineers. 1994. *Engineering and Design: Hydraulic Design of Flood Control Channels*. EM 1110-2-1601. Washington, DC: U.S. Army Corps of Engineers.
- van der Mark, C. F., A. Blom, and S. J. M. Hulscher. 2008. "Quantification of Variability in Bedform Geometry." *Journal of Geophysical Research* 113(F3). doi:10.1029/2007JF000940.
- van Rijn, L. C. 1984. "Sediment Transport, Part III: Bed Forms and Alluvial Roughness." *Journal of Hydraulic Engineering* 110(12): 1733–1754. doi: 10.1061/(ASCE)0733-9429(1984)110:12(1733).
- van Rijn, L. C. 1993. *Principles of Sediment Transport in Rivers, Estuaries, and Coastal Seas*. The Netherlands: Aqua Publications.
- Vanoni, V., and L. S. Hwang. 1967. "Relation between Bed Form and Friction in Streams." *Journal of the Hydraulics Division, ASCE* 93:121–144.

## **Appendix A: Bathymetry**

Bathymetric maps from each of the study dates are presented here (Figures 15–38), at 1:8000 scale, rotated 45 compass degrees counterclockwise so that the upstream direction is towards the top of the page. Each survey is displayed twice: once with only the survey bathymetry (in elevation meters NAVD88) as a colored raster and once with the survey data overlaid by the profile lines along which data were extracted for roughness analysis.

Figure 15. Bathymetry data from May 15, 2011.

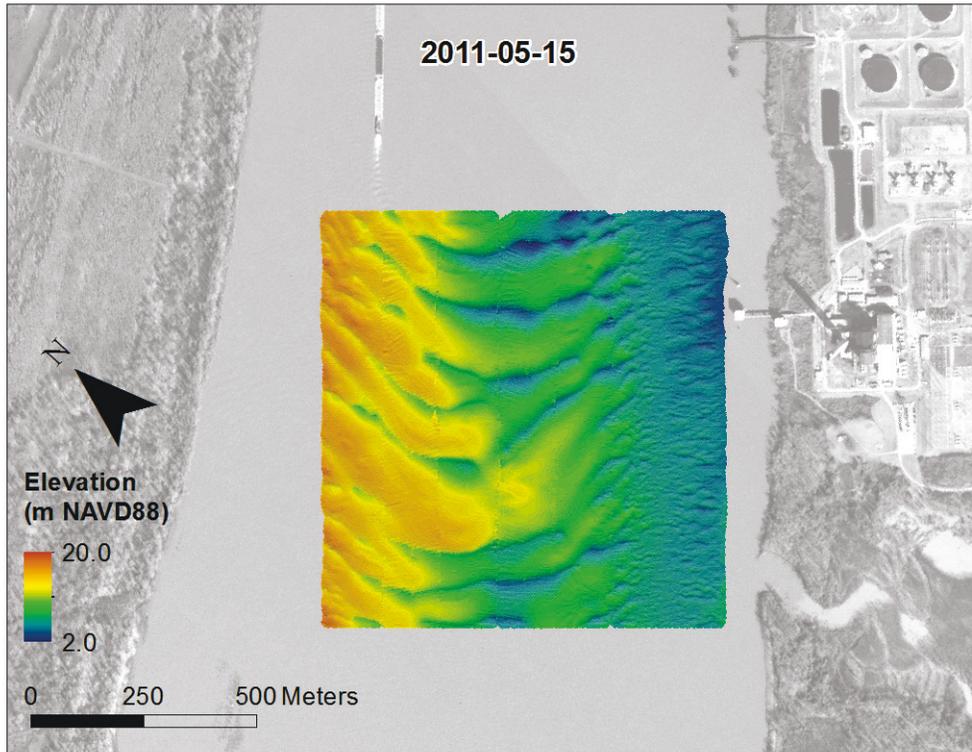


Figure 16. Bathymetry data from May 15, 2011, with analyzed lines overlaid.

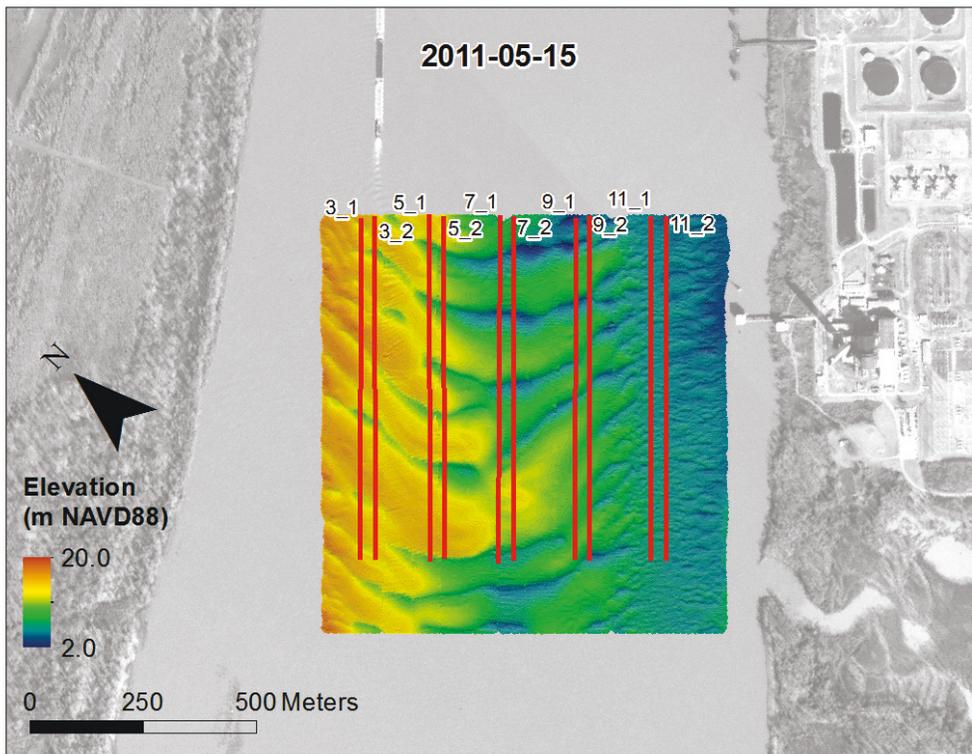


Figure 17. Bathymetry data from May 19, 2011.

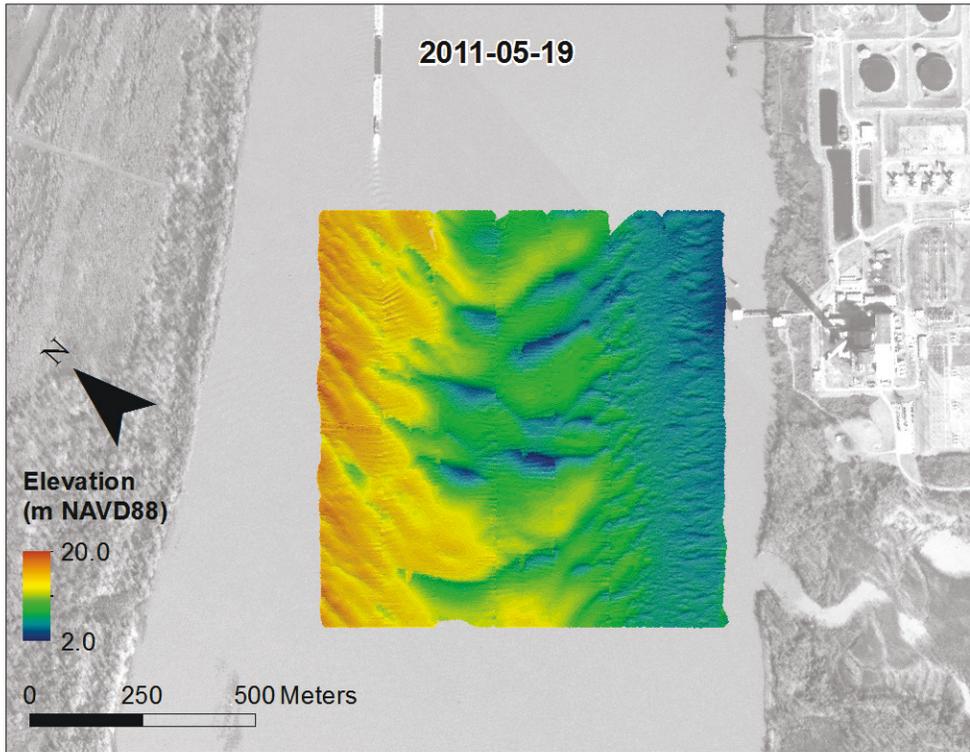


Figure 18. Bathymetry data from May 19, 2011, with analyzed lines overlaid.

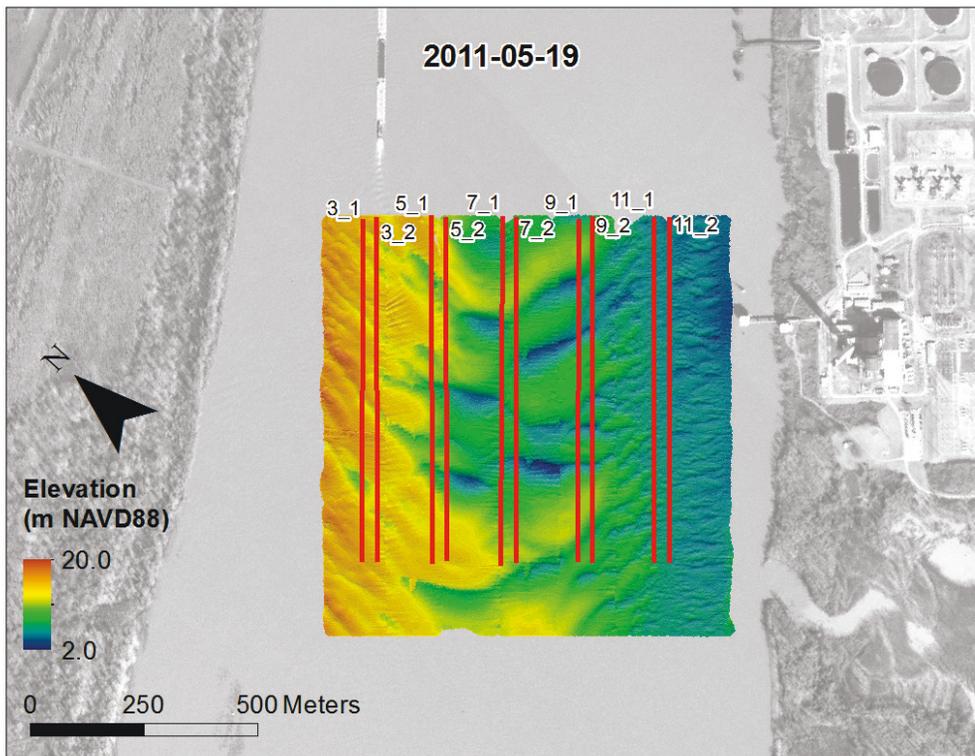


Figure 19. Bathymetry data from October 2, 2012.

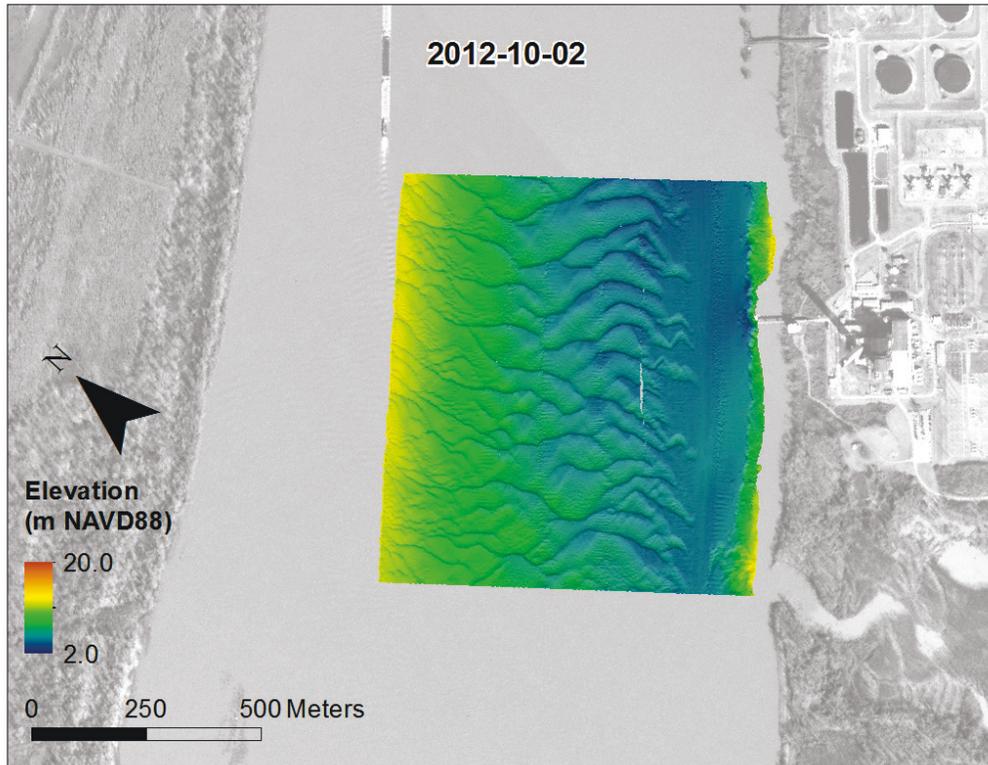


Figure 20. Bathymetry data from October 2, 2012, with analyzed lines overlaid.

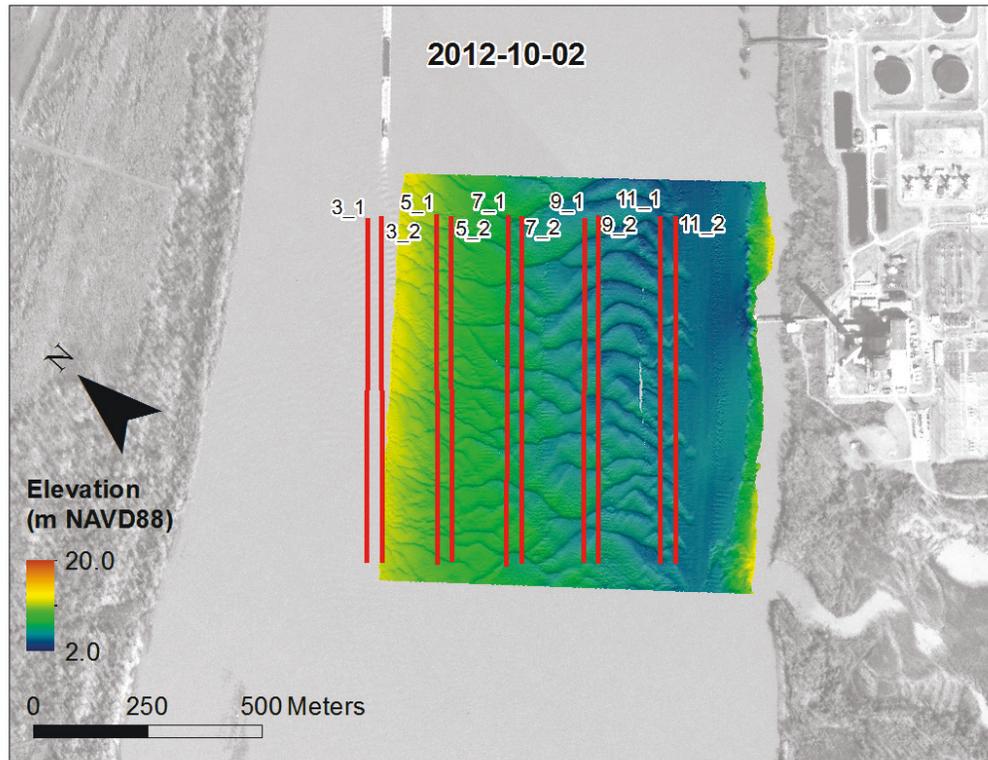


Figure 21. Bathymetry data from October 3, 2012.

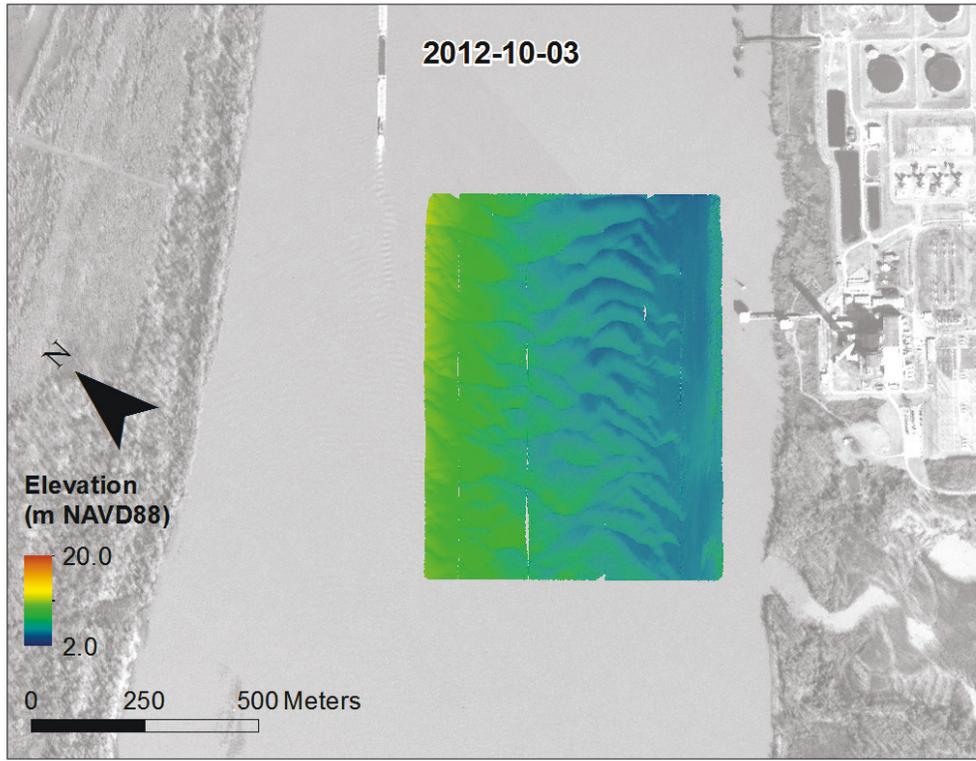


Figure 22. Bathymetry data from October 3, 2012, with analyzed lines overlaid.

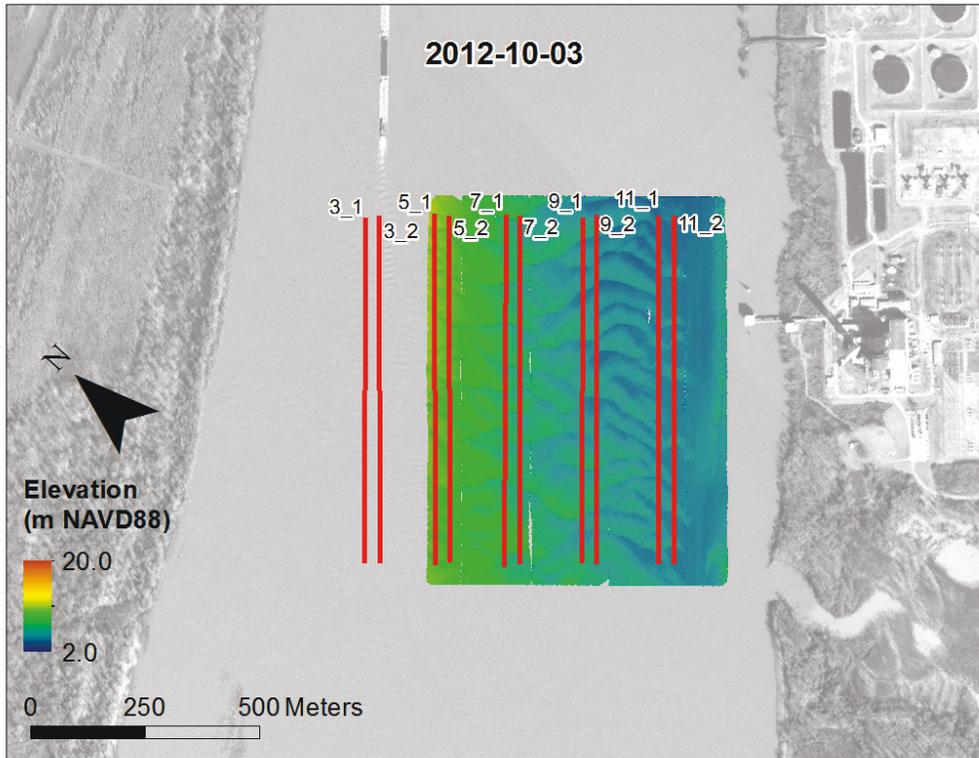


Figure 23. Bathymetry data from April 29, 2013.

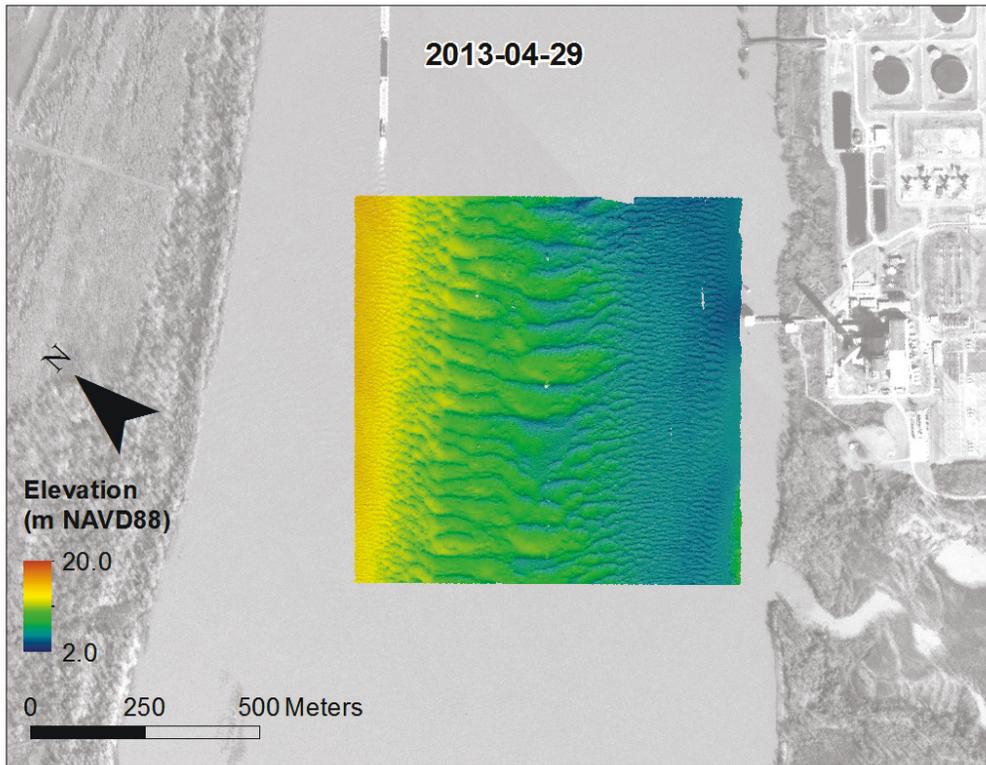


Figure 24. Bathymetry data from April 29, 2013, with analyzed lines overlaid.

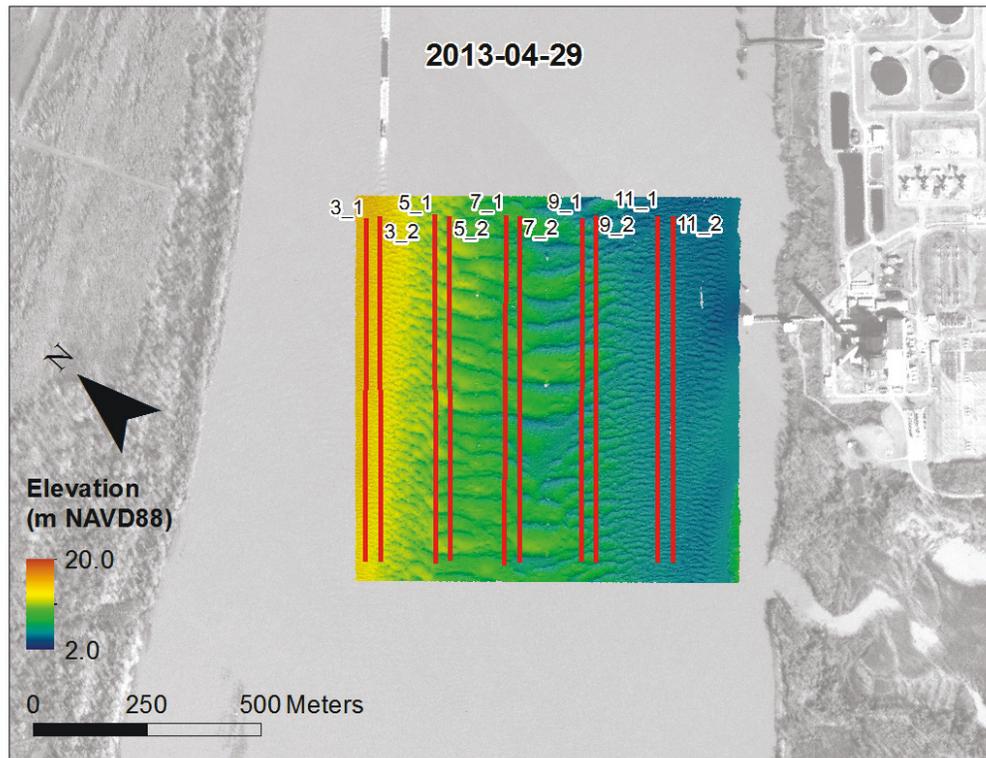




Figure 25. Bathymetry data from March 19, 2015.

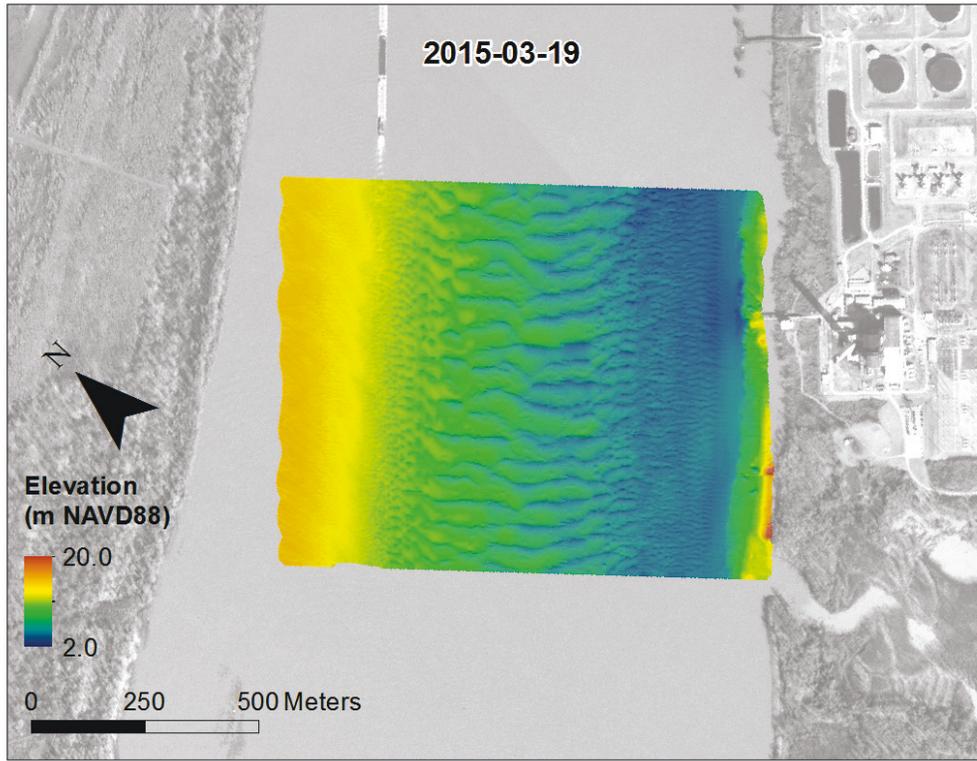


Figure 26. Bathymetry data from March 19, 2015, with analyzed lines overlaid.

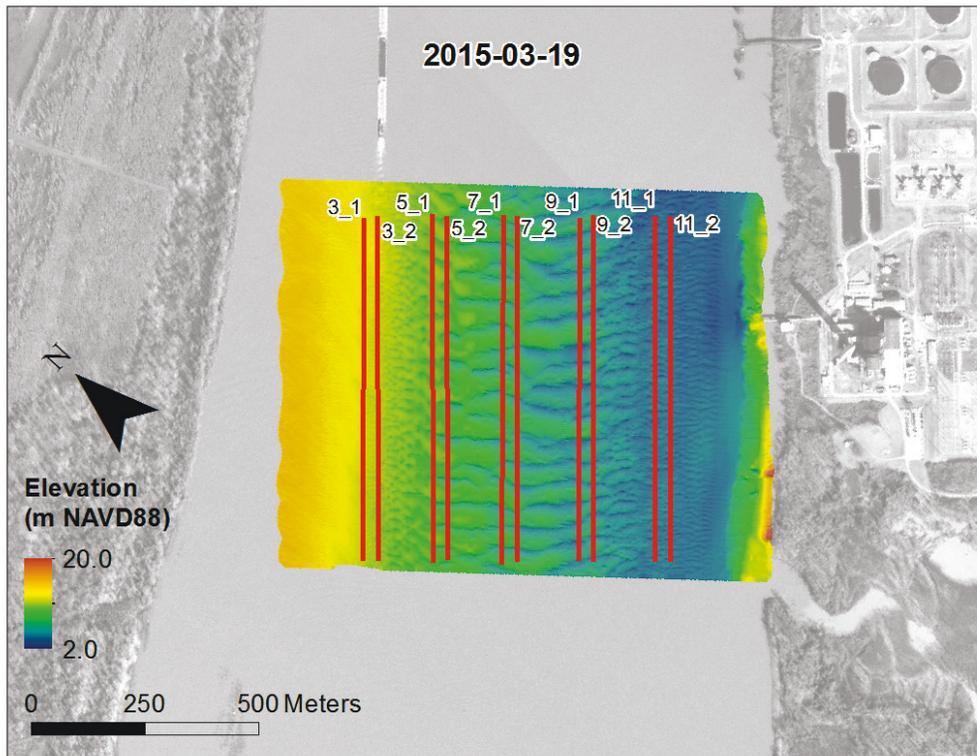


Figure 27. Bathymetry data from April 30, 2015.

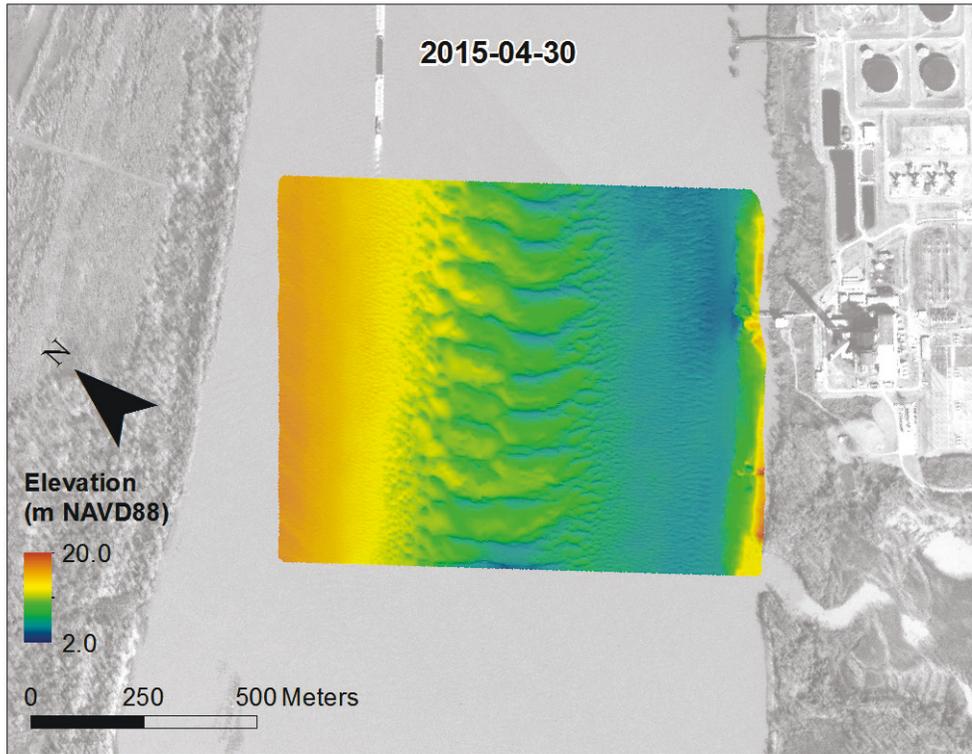


Figure 28. Bathymetry data from April 30, 2015, with analyzed lines overlaid.

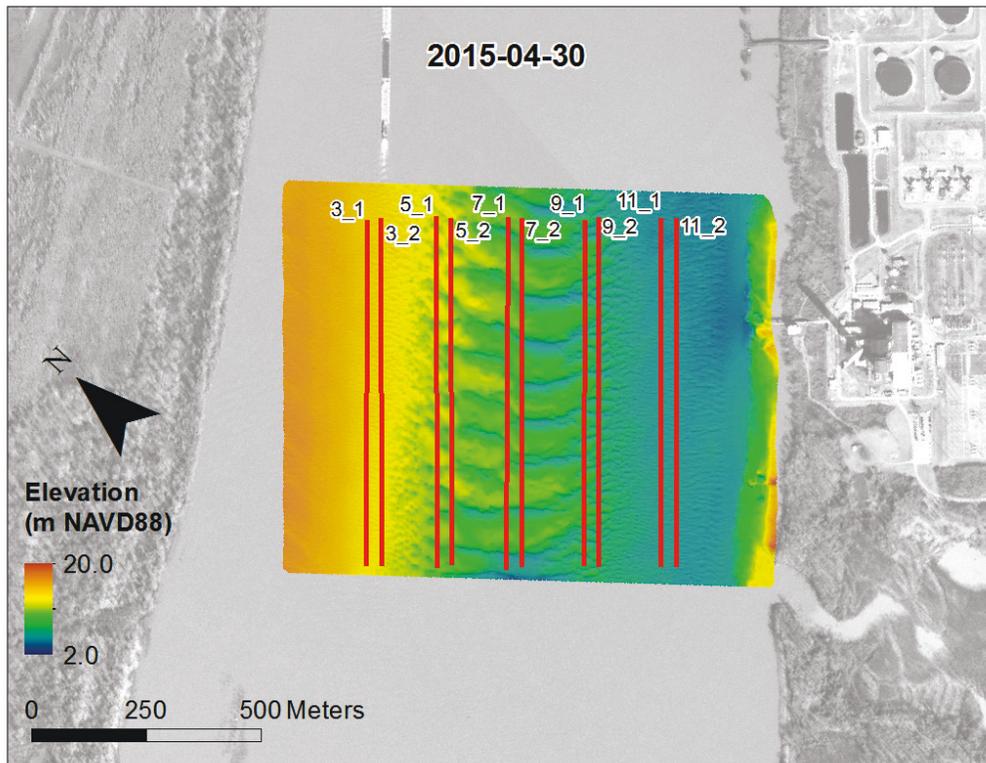


Figure 29. Bathymetry data from May 19, 2015.

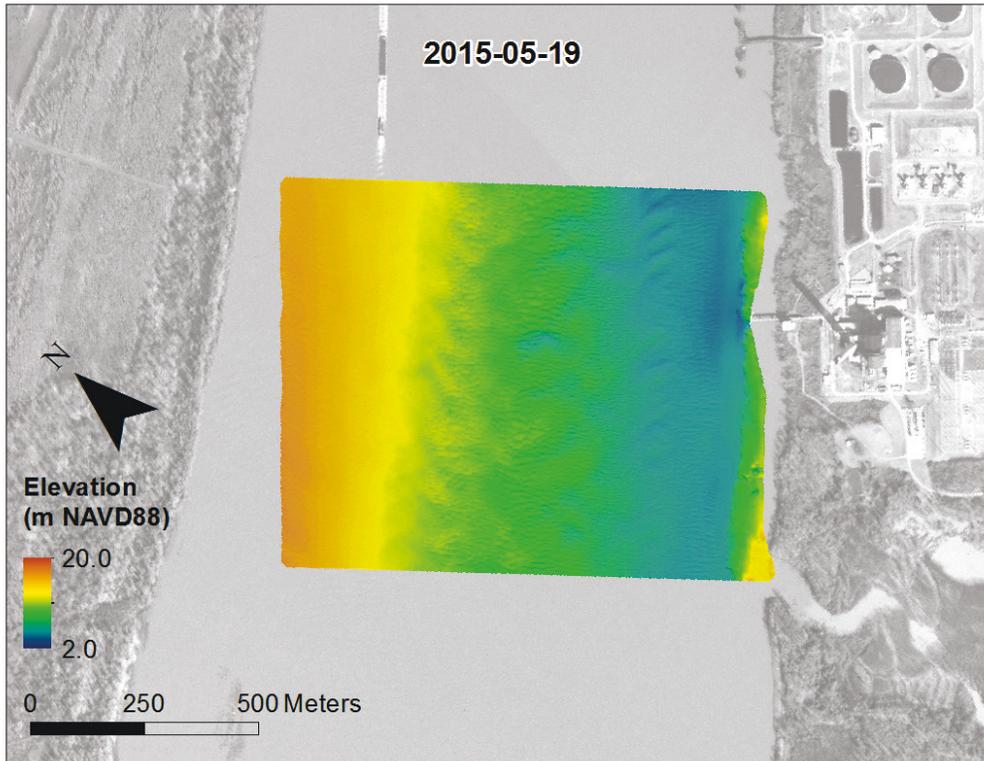


Figure 30. Bathymetry data from May 19, 2015, with analyzed lines overlaid.

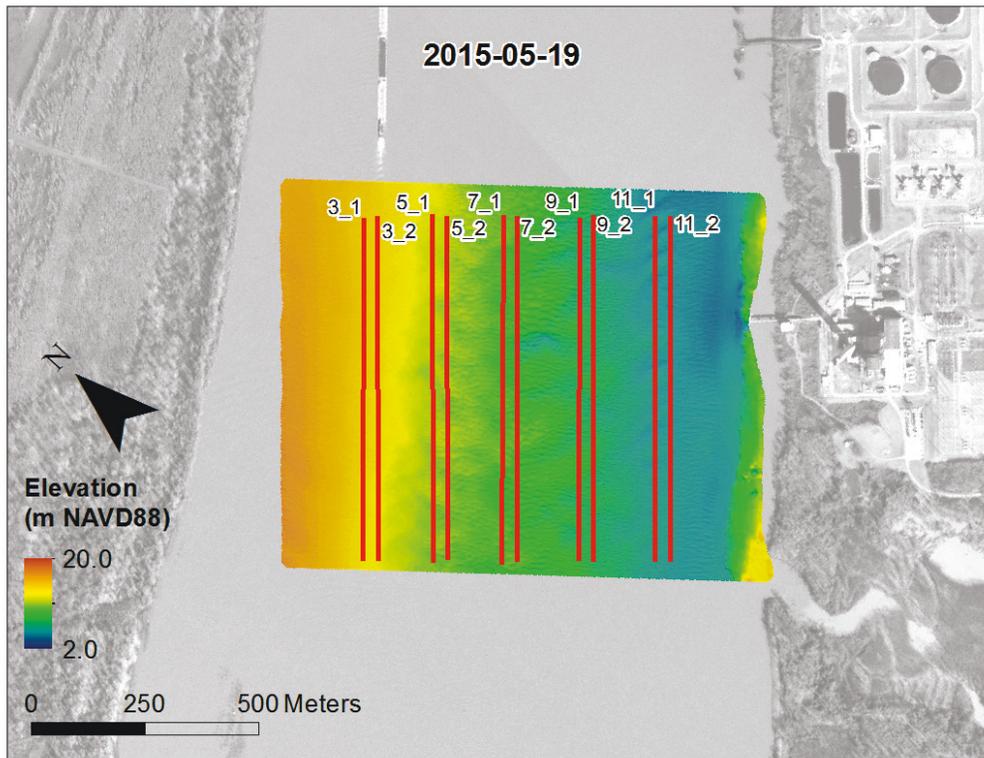


Figure 31. Bathymetry data from January 12, 2016.

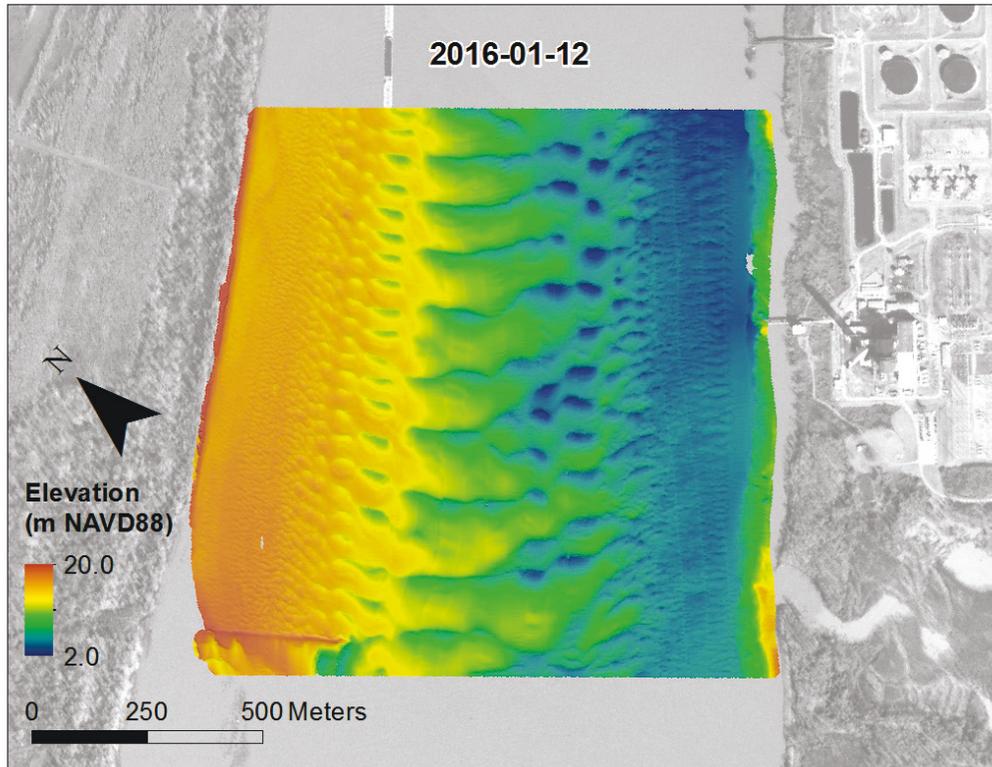


Figure 32. Bathymetry data from January 12, 2016, with analyzed lines overlaid.

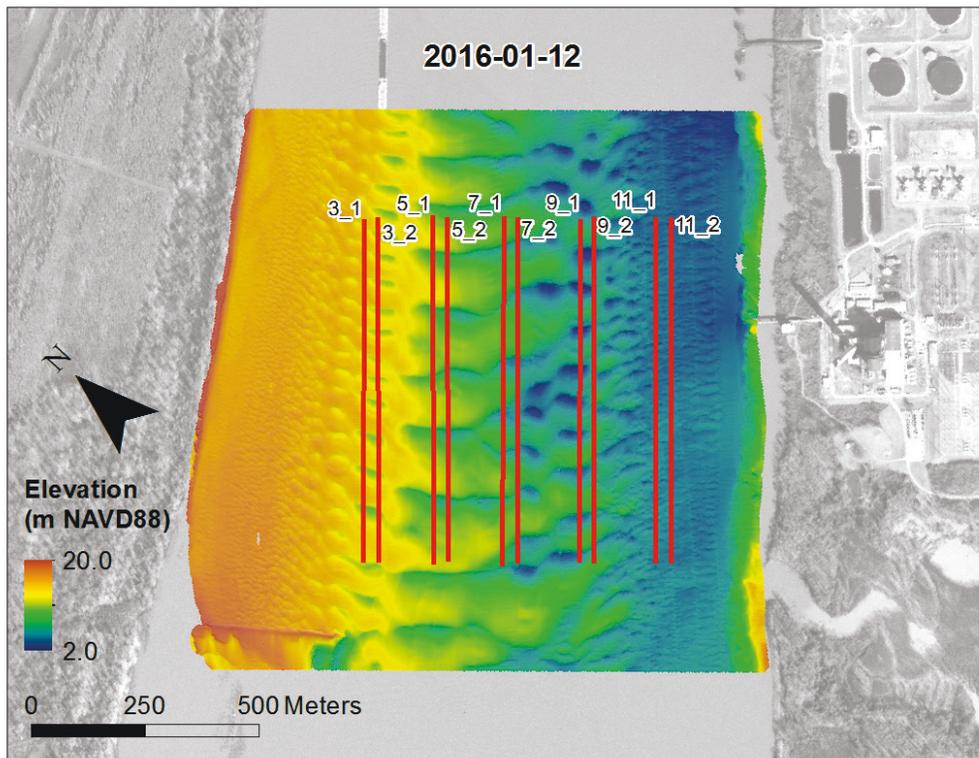


Figure 33. Bathymetry data from January 15, 2016.

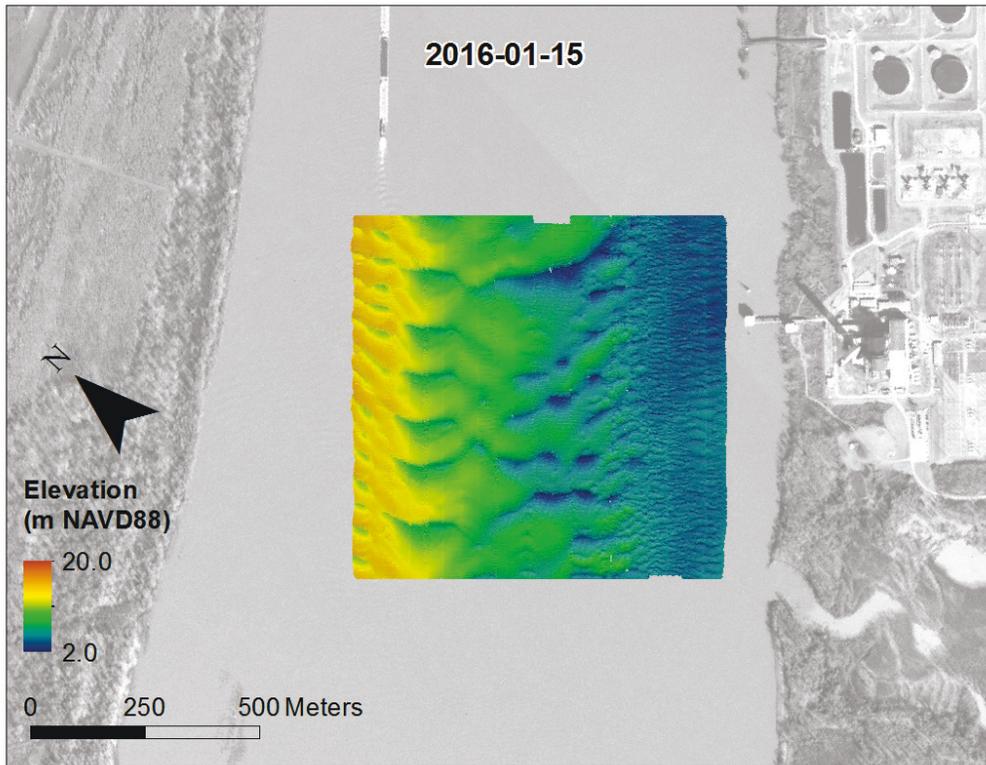


Figure 34. Bathymetry data from January 15, 2016, with analyzed lines overlaid.

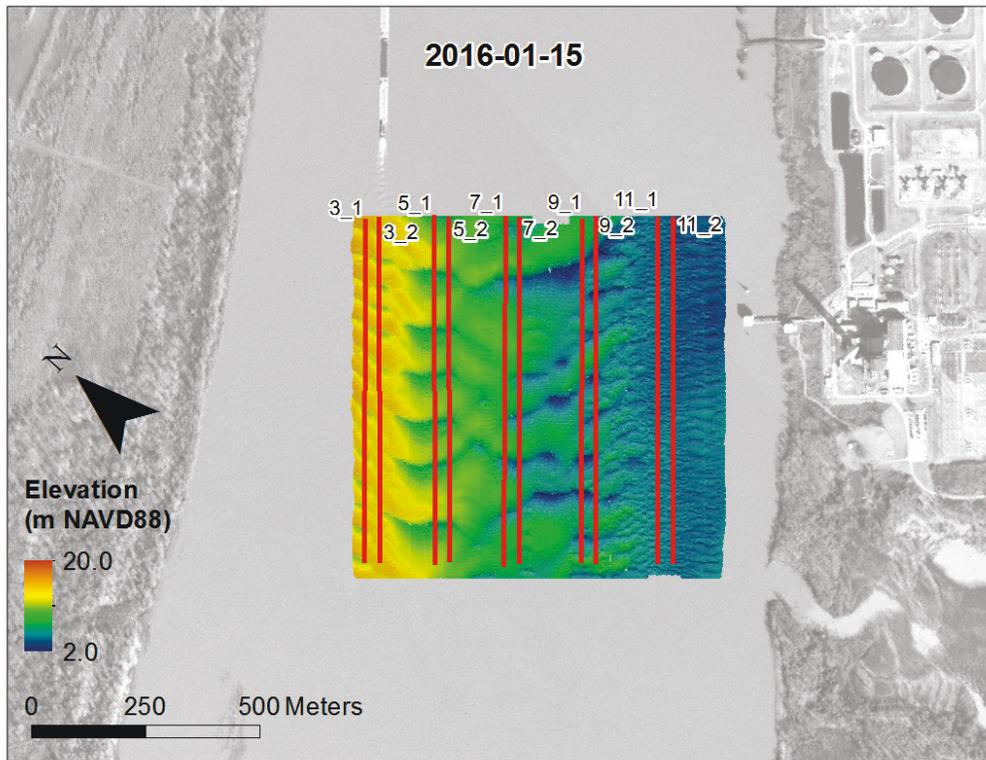


Figure 35. Bathymetry data from January 25, 2016.

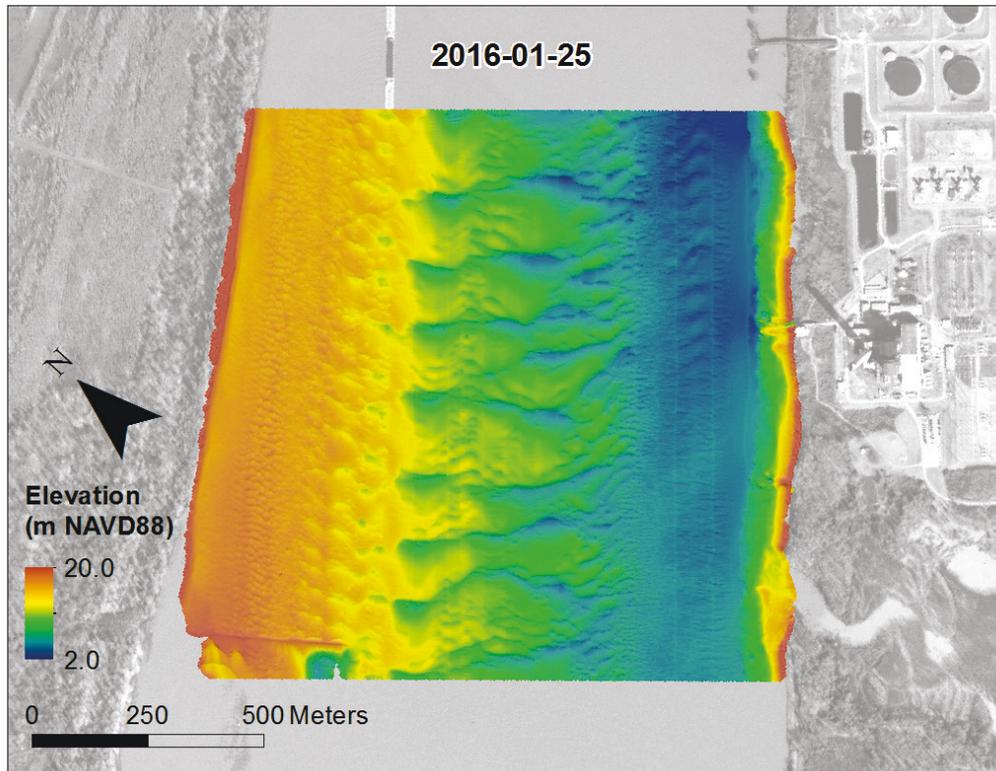


Figure 36. Bathymetry data from January 25, 2016, with analyzed lines overlaid.

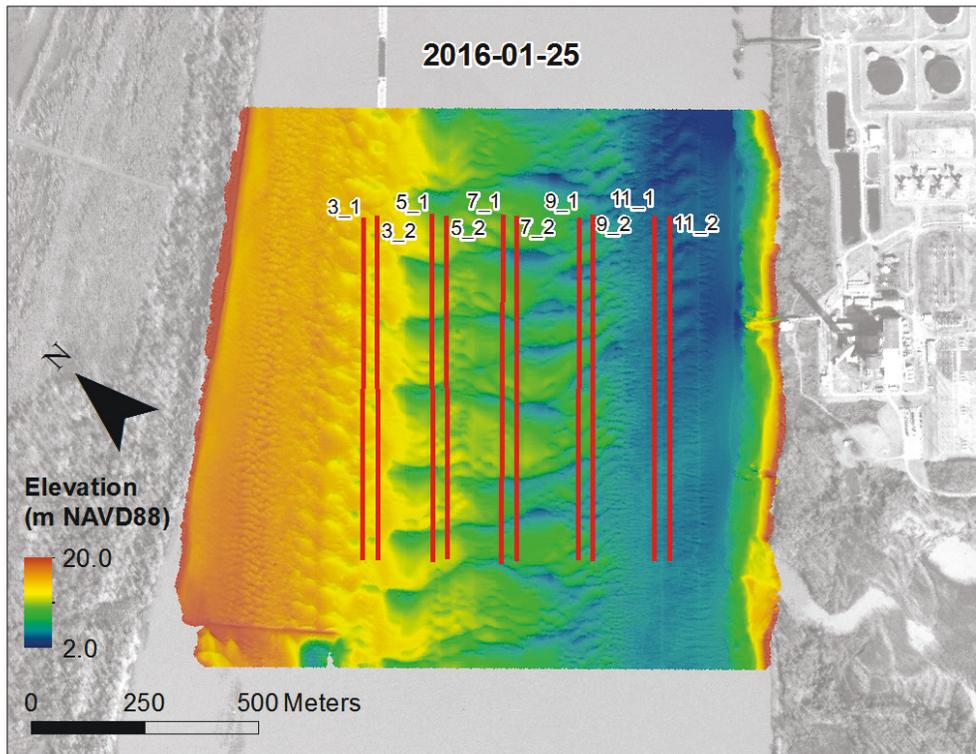


Figure 37. Bathymetry data from January 29, 2016.

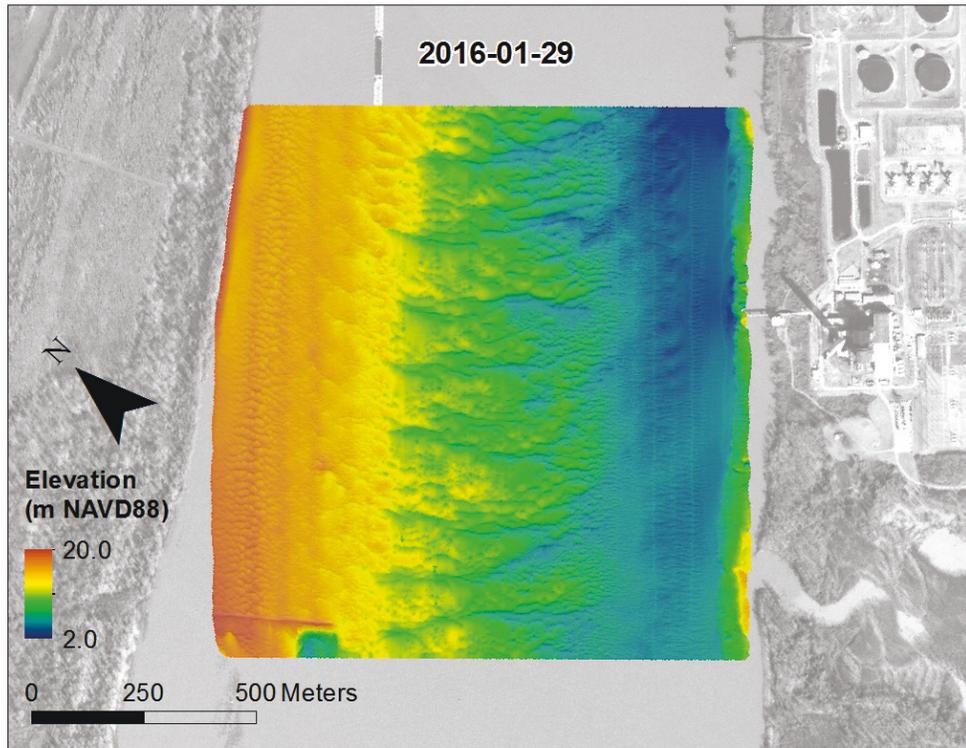
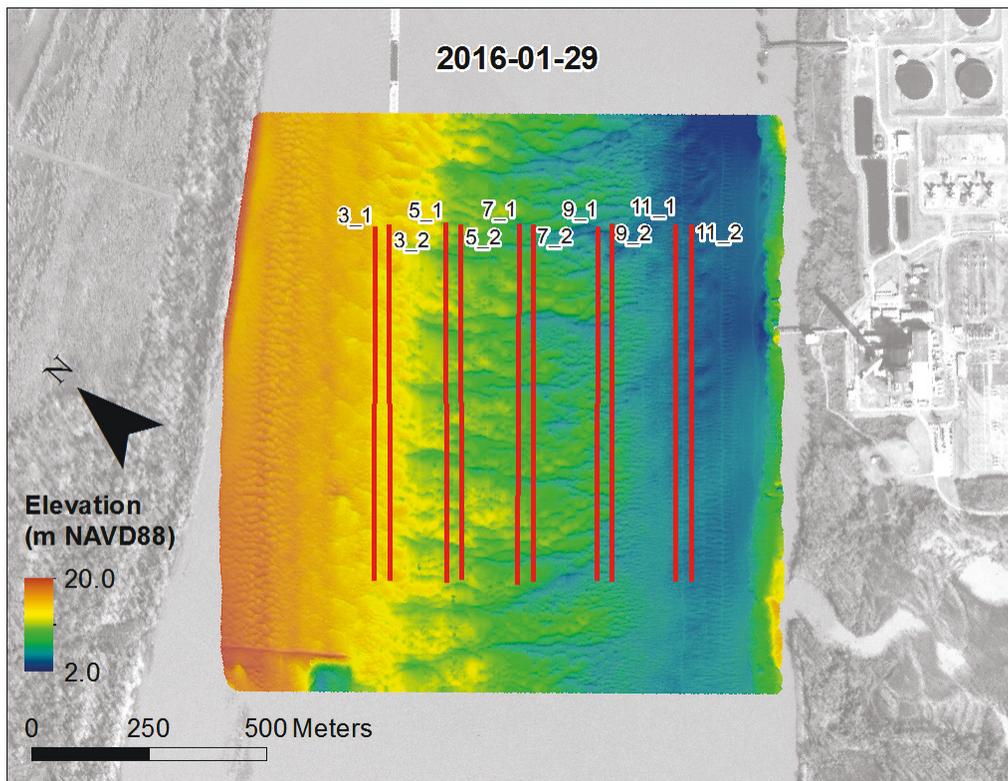


Figure 38. Bathymetry data from January 29, 2016, with analyzed lines overlaid.

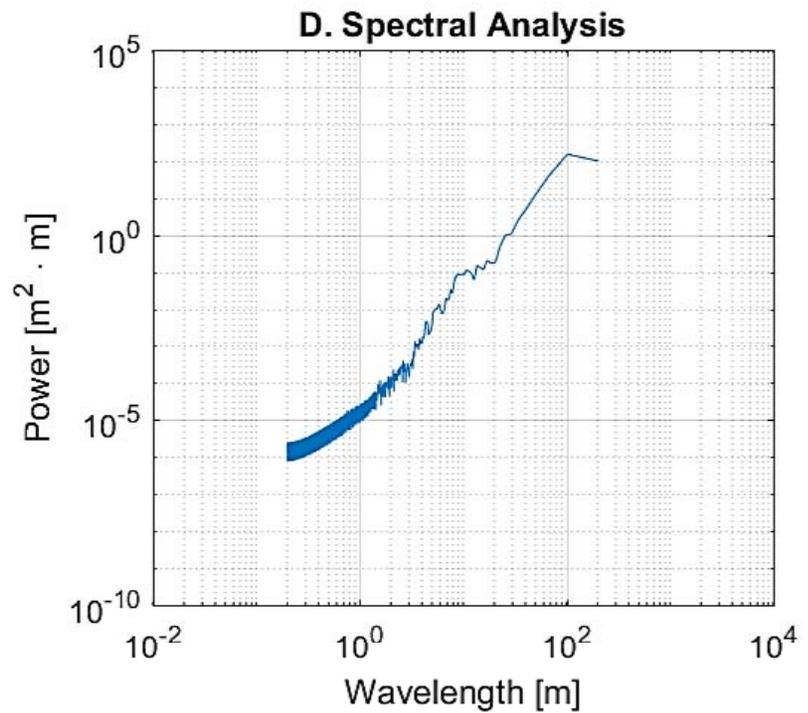
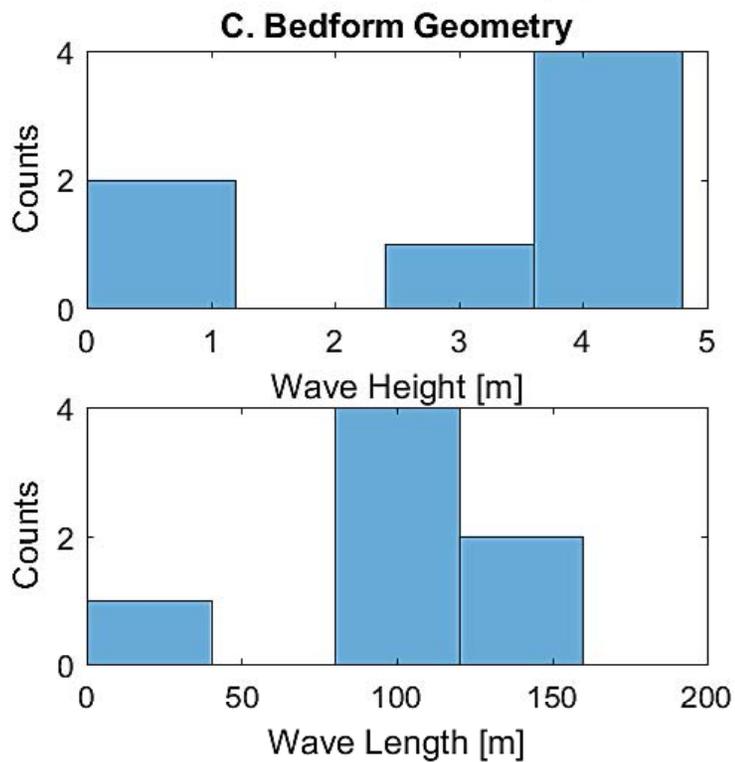
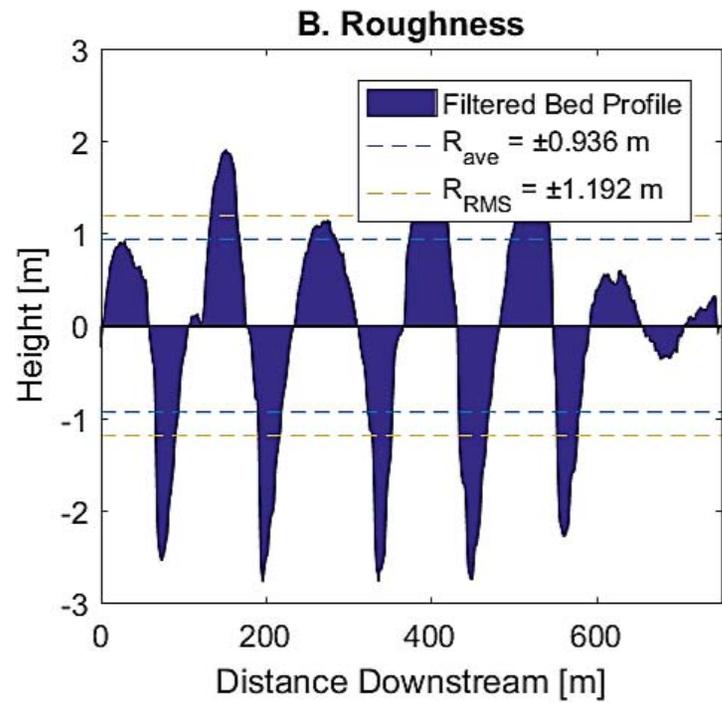
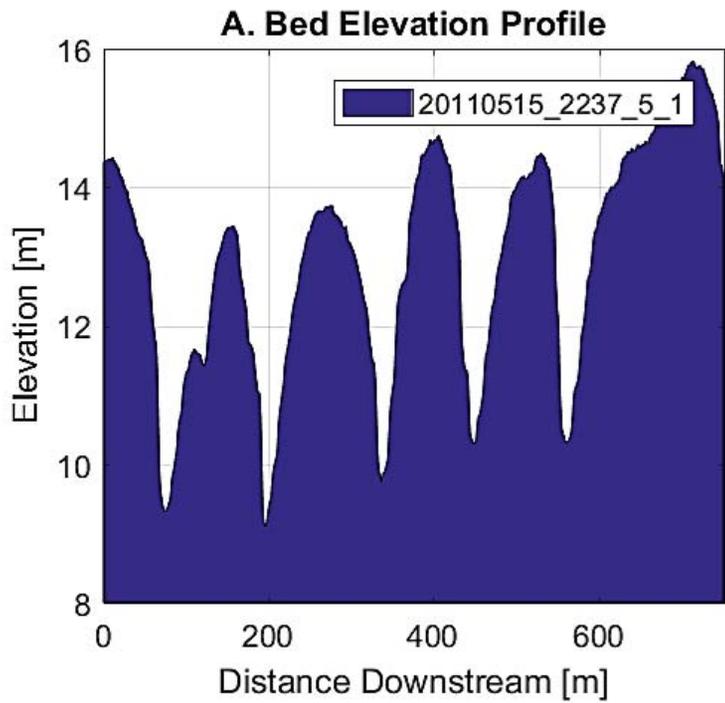


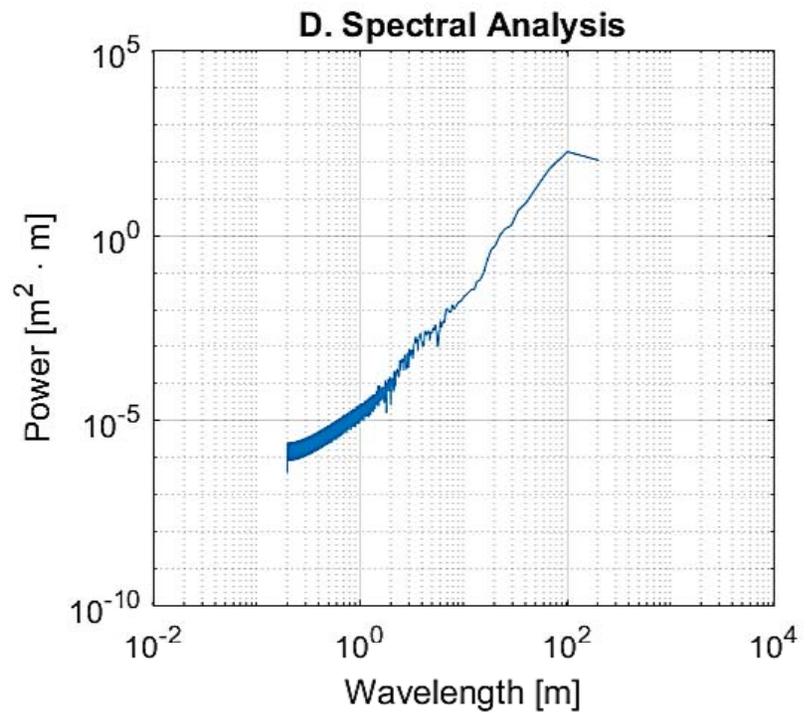
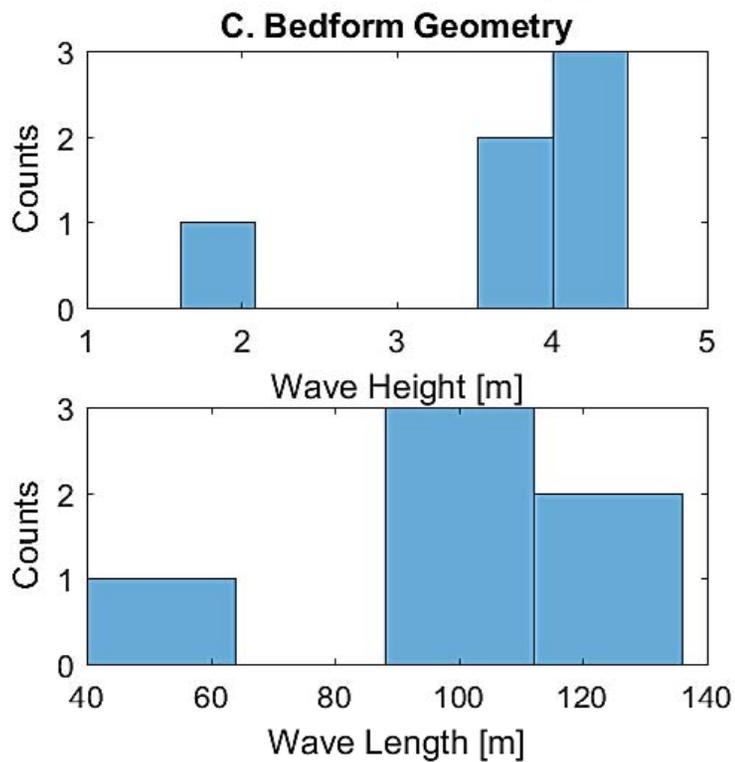
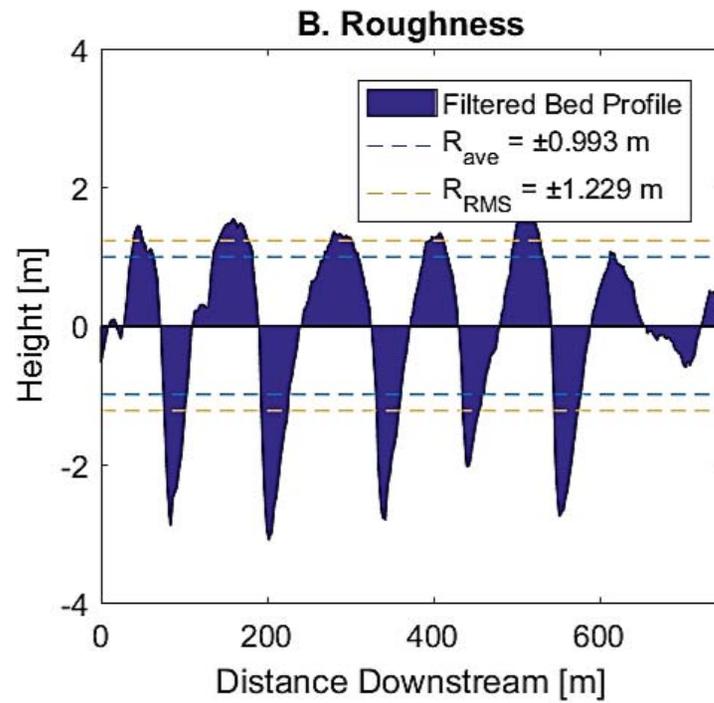
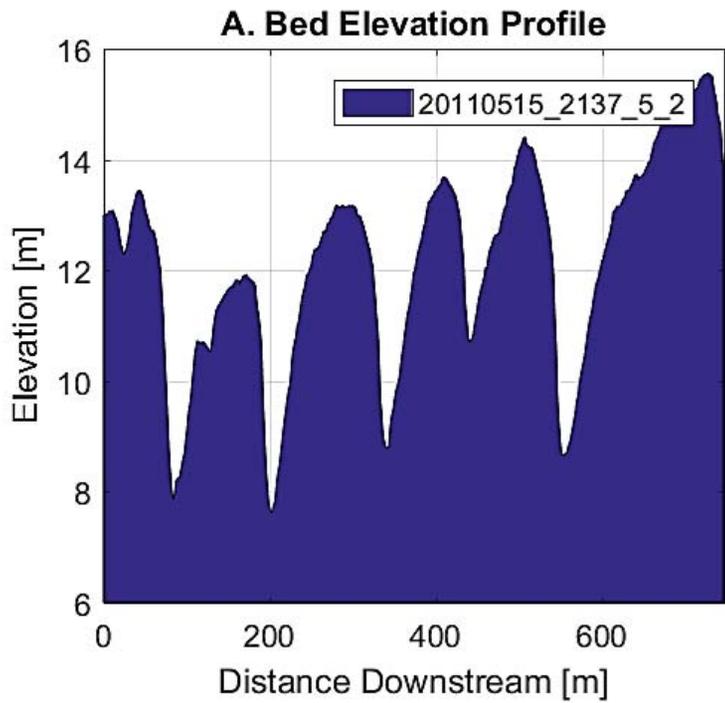
## Appendix B: Bedform Profiles

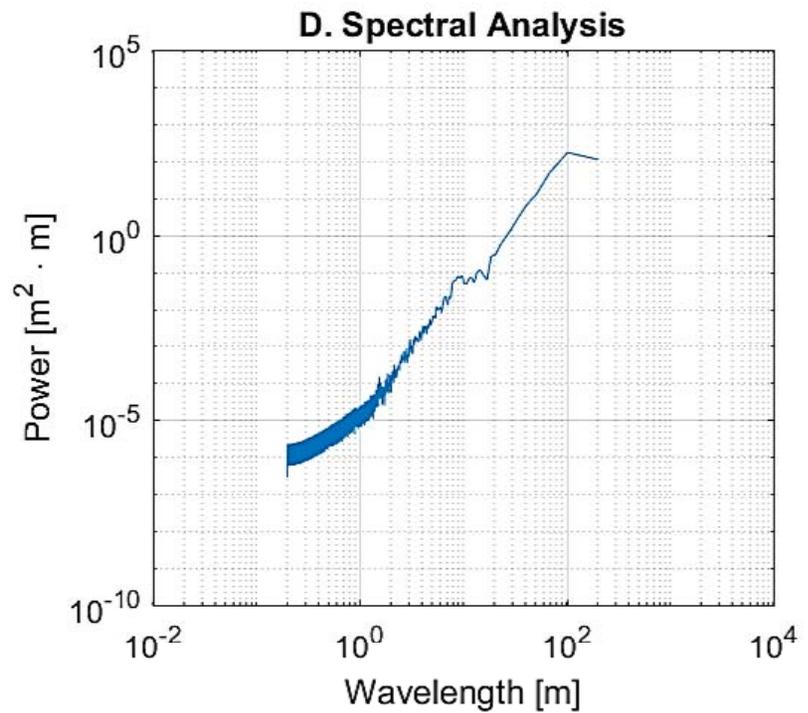
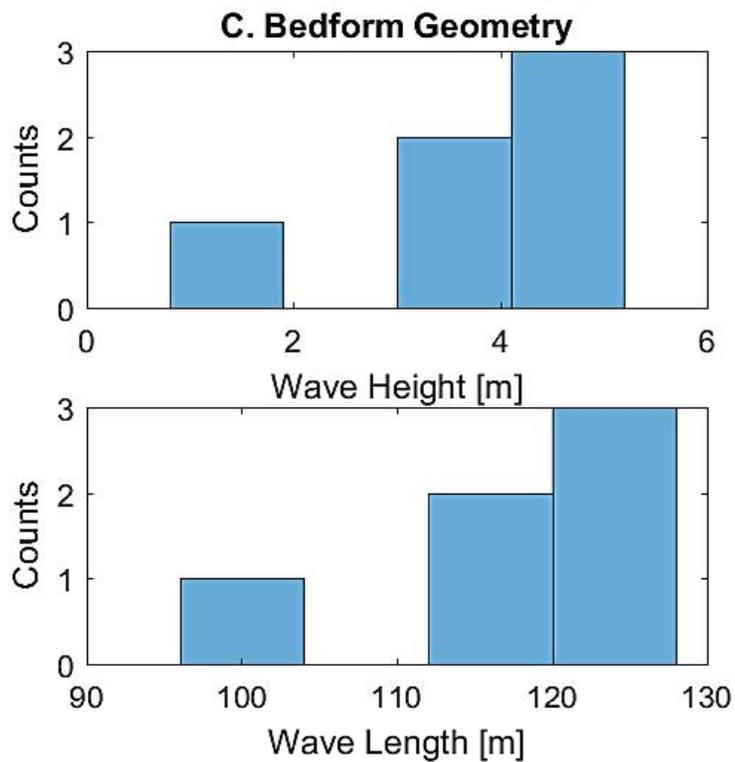
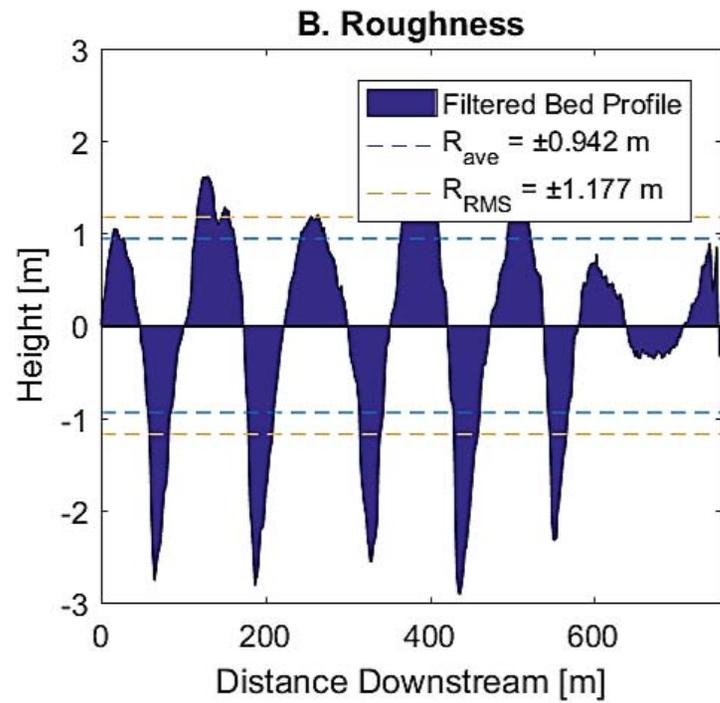
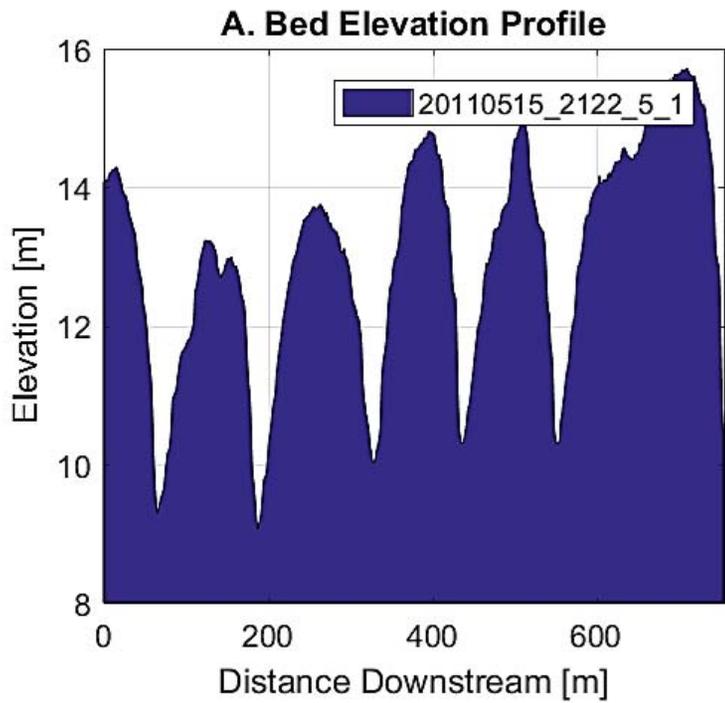
Each page of Appendix B contains a four-part figure (NOTE: For the printed copy of this report, Appendix B is found on the accompanying CD: AppendixB.pdf.):

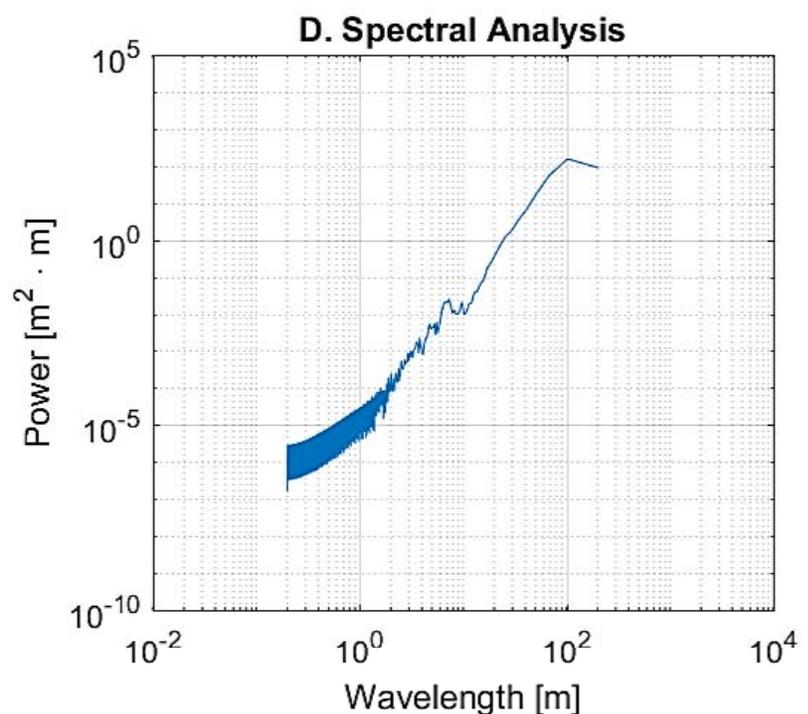
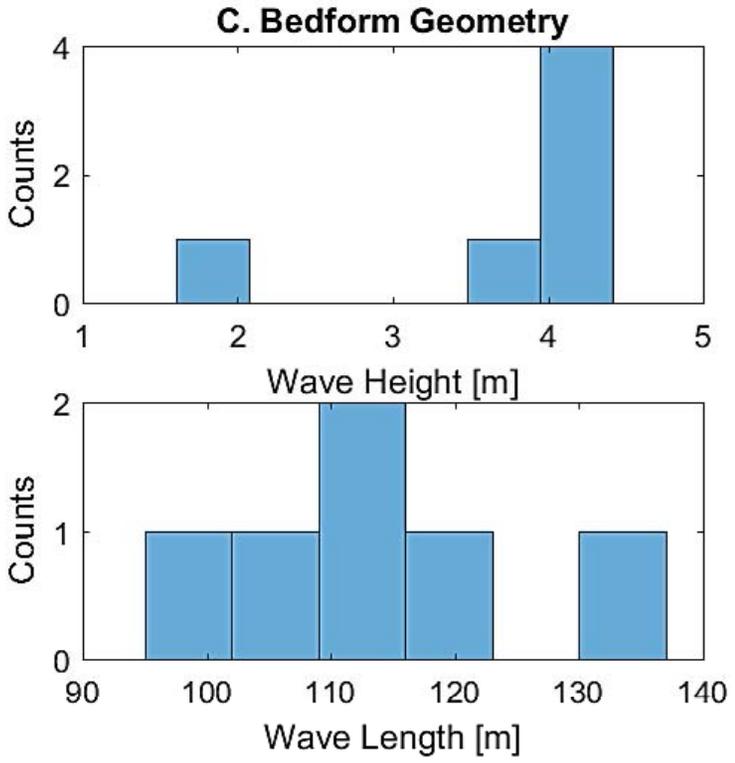
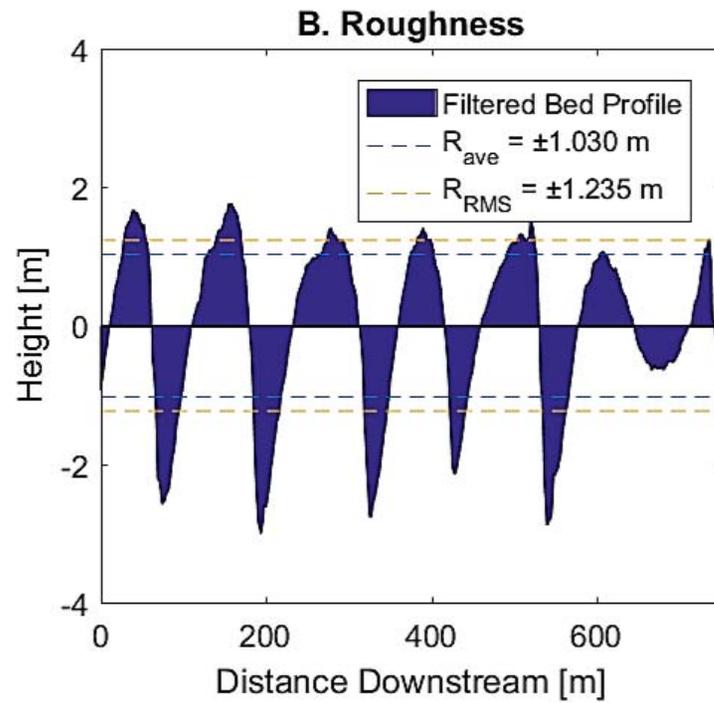
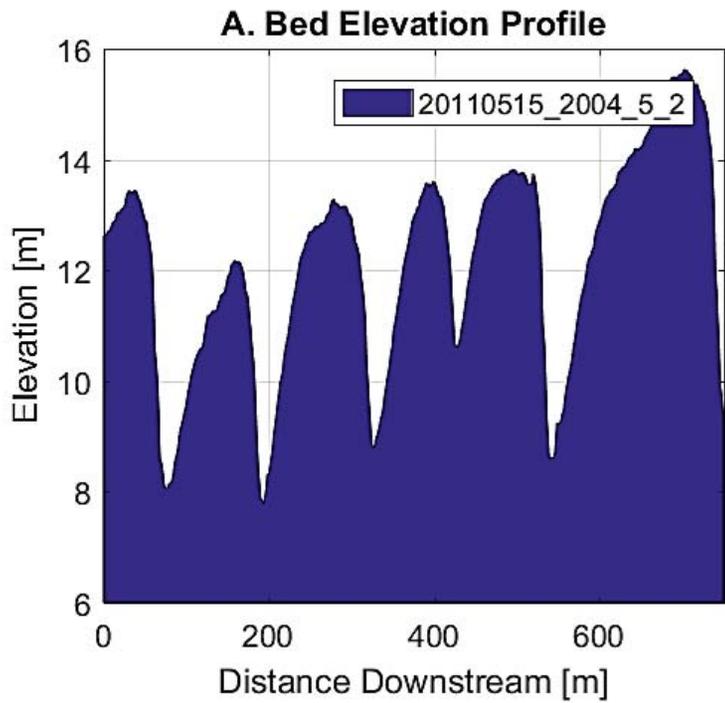
- (A) Shows the bed elevation profile with distance downstream along the profile. The date, time, and line location of the profile are provided in the form YYYYMMDD\_HHMM\_line\_subsection. Line and subsection numbers reference those shown in Appendix A.
- (B) Shows the bed elevation profile after lowpass filtering and DC-offset removal. Also shown are the calculated  $R_{ave}$  and  $R_{RMS}$  heights.
- (C) Shows two histograms of the bedform population, one for bedform heights and one for bedform wavelengths. These were calculated from the population produced by the zero-crossing analysis.
- (D) Is a power spectrum of bedform wavelengths, calculated using the Welch method.

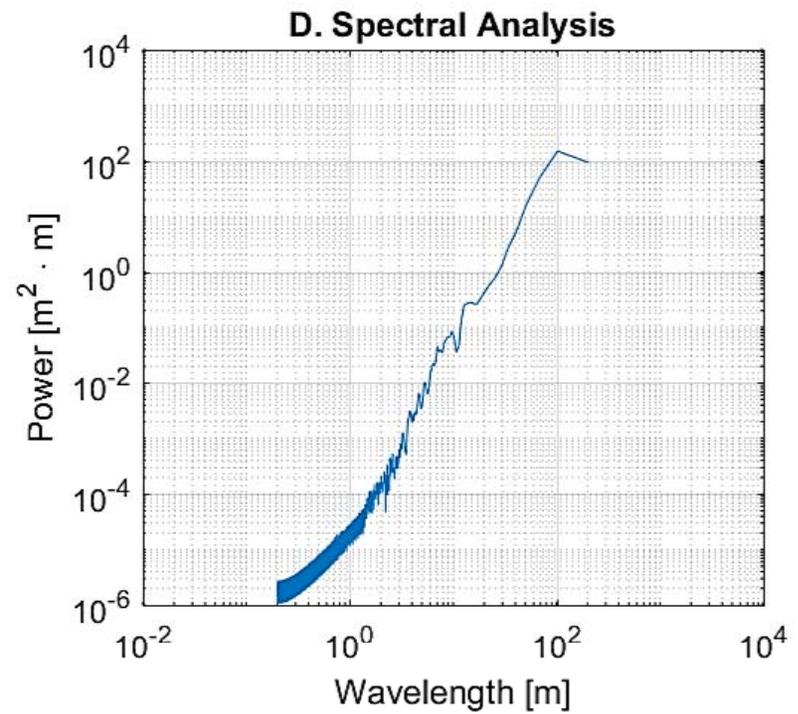
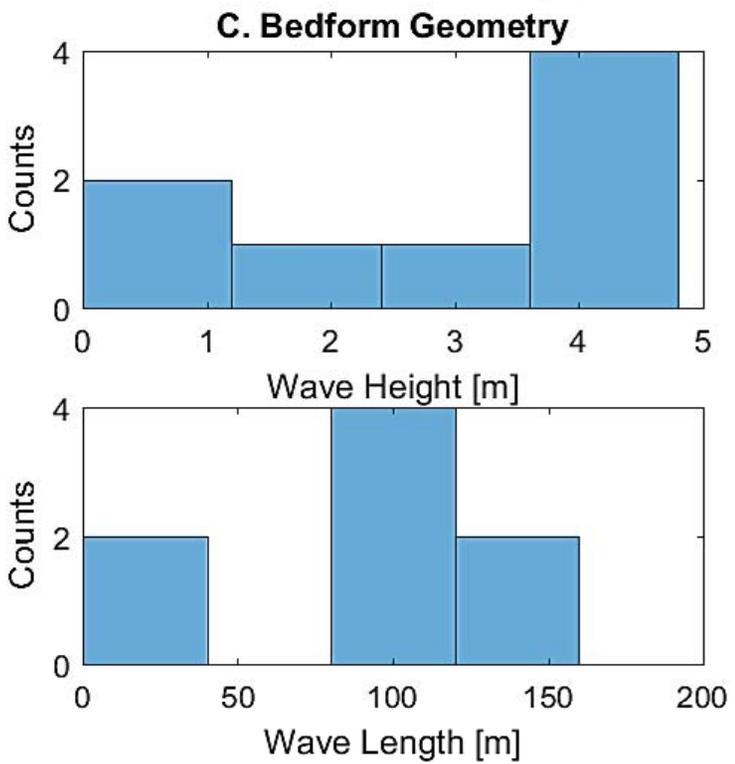
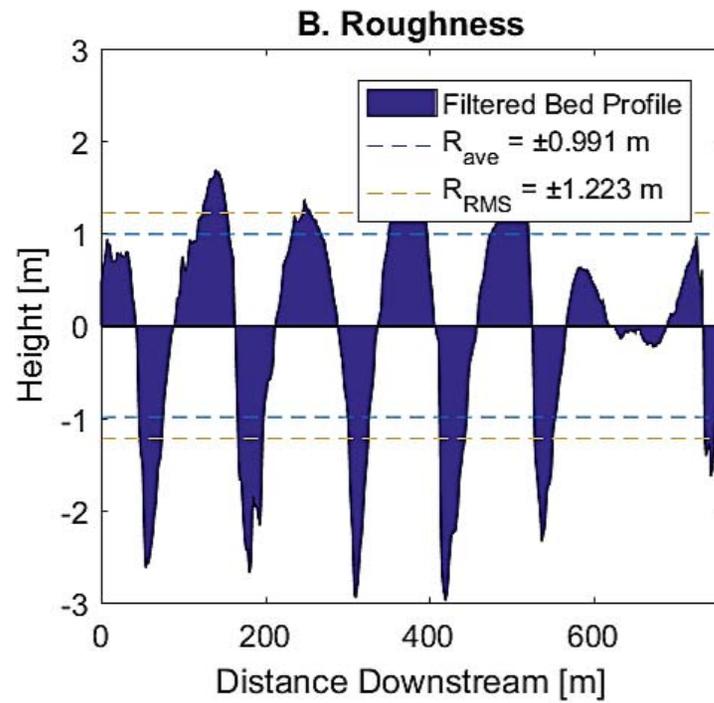
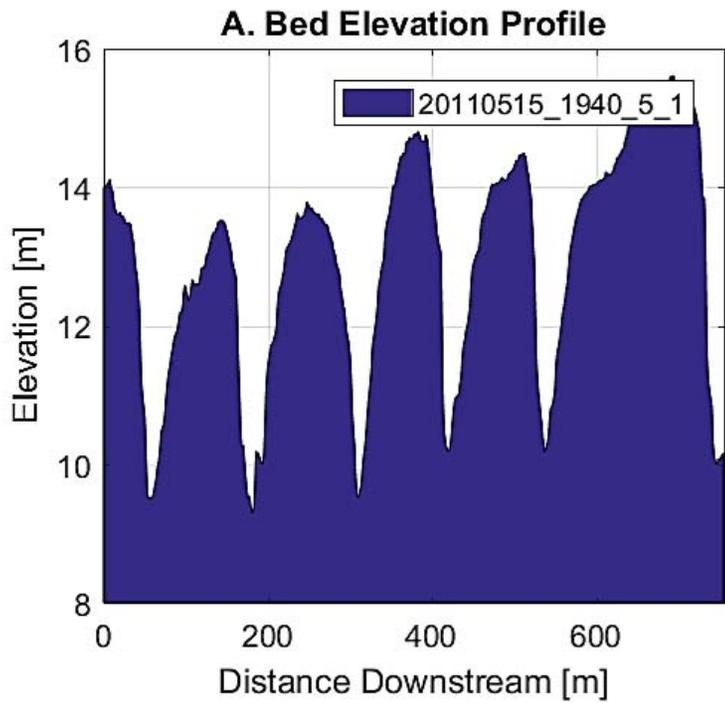


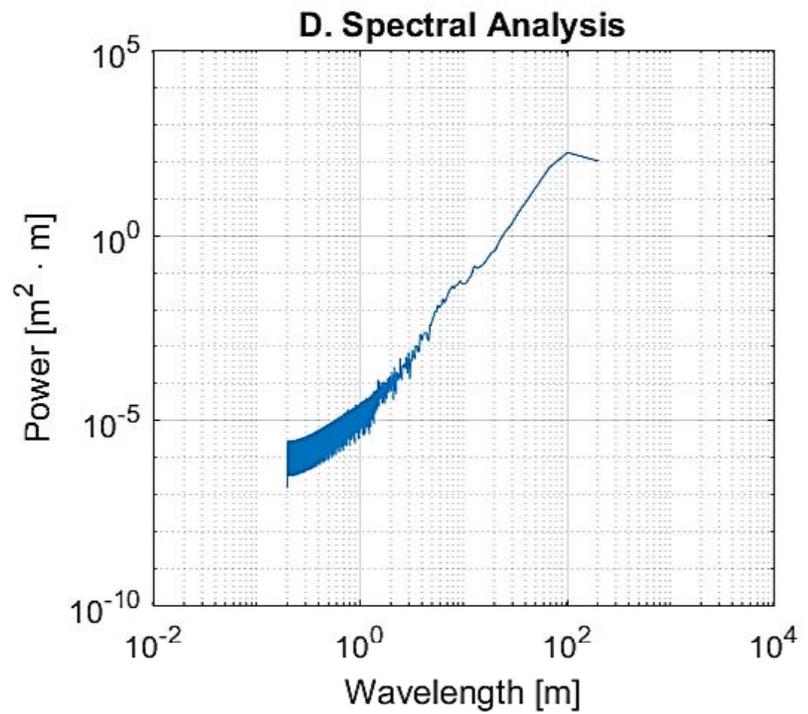
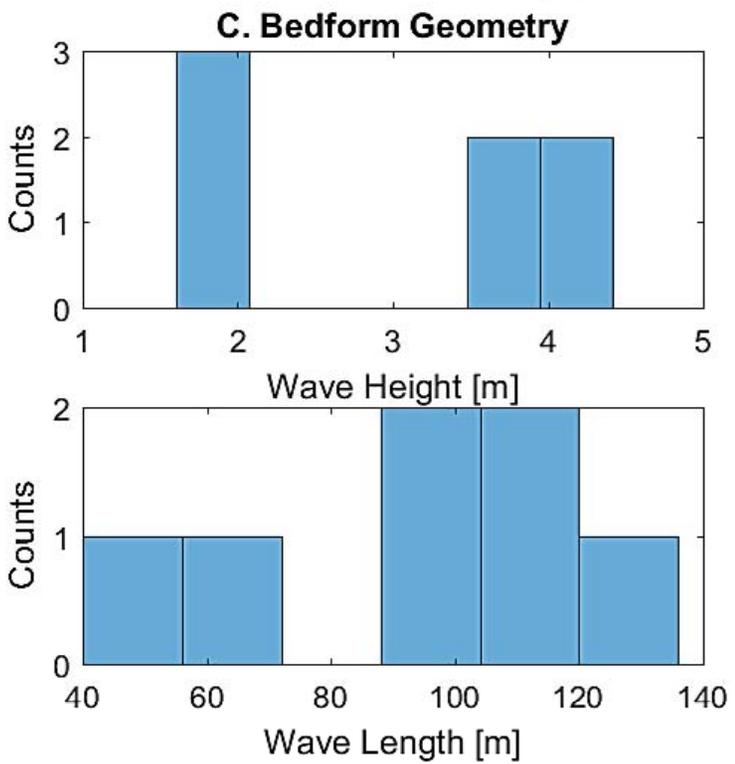
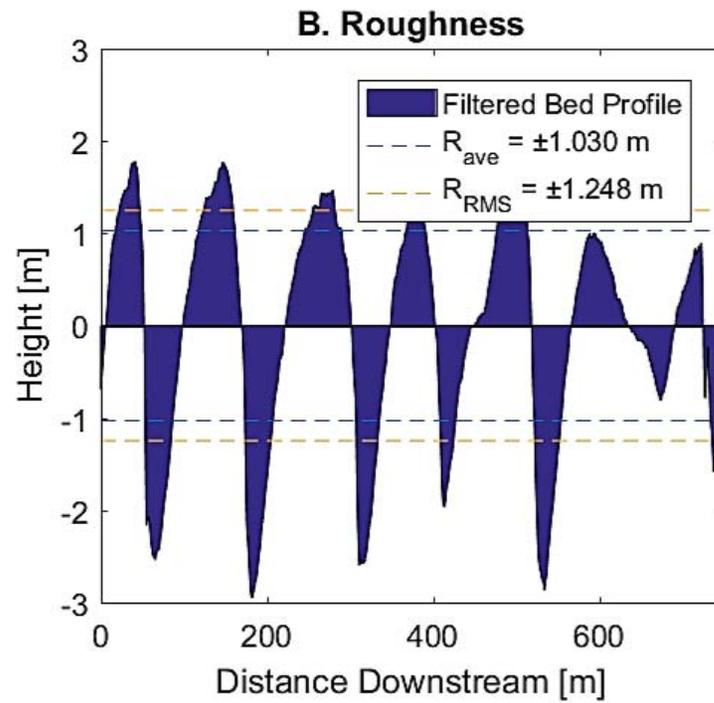
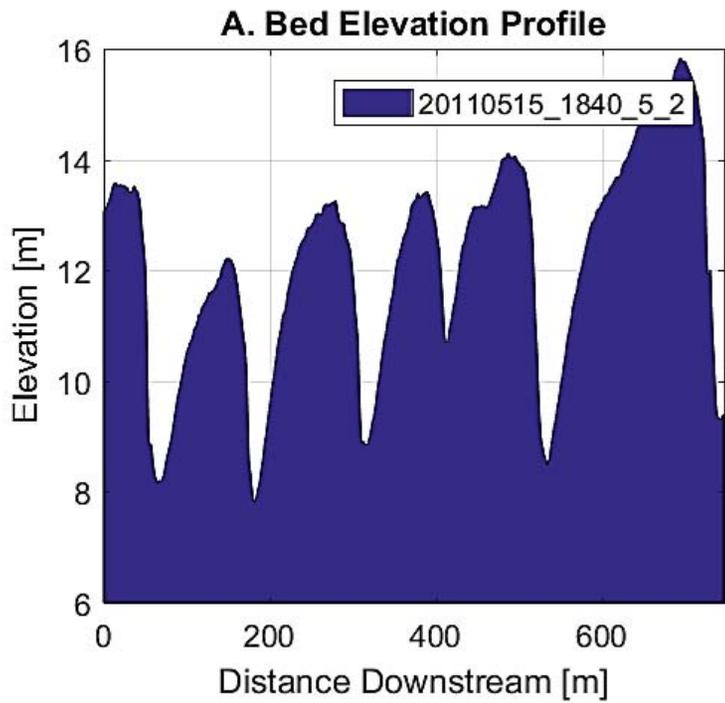


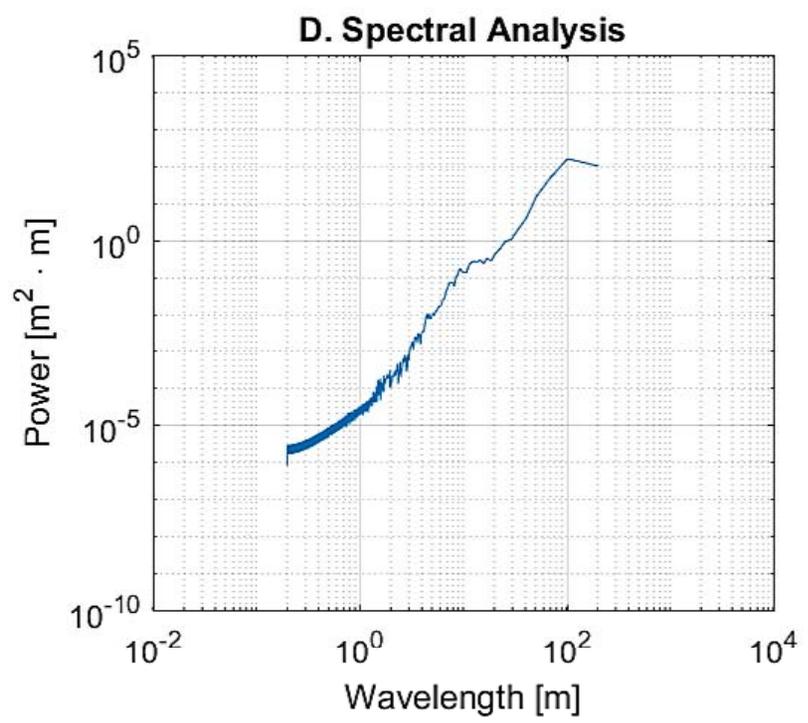
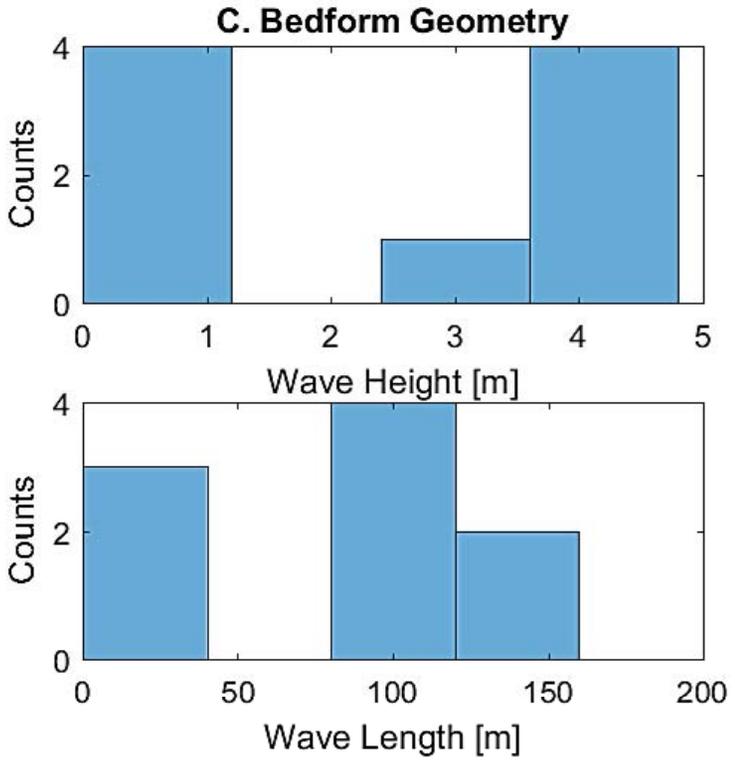
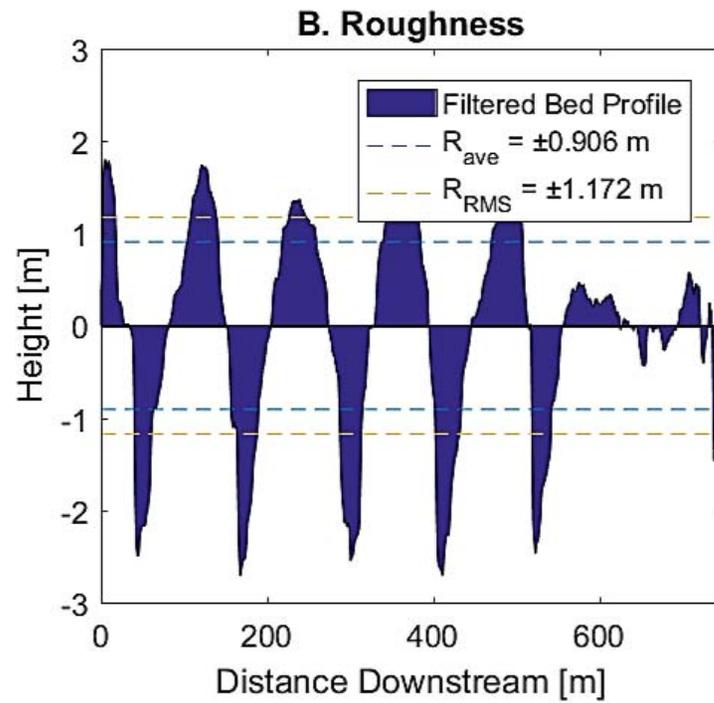
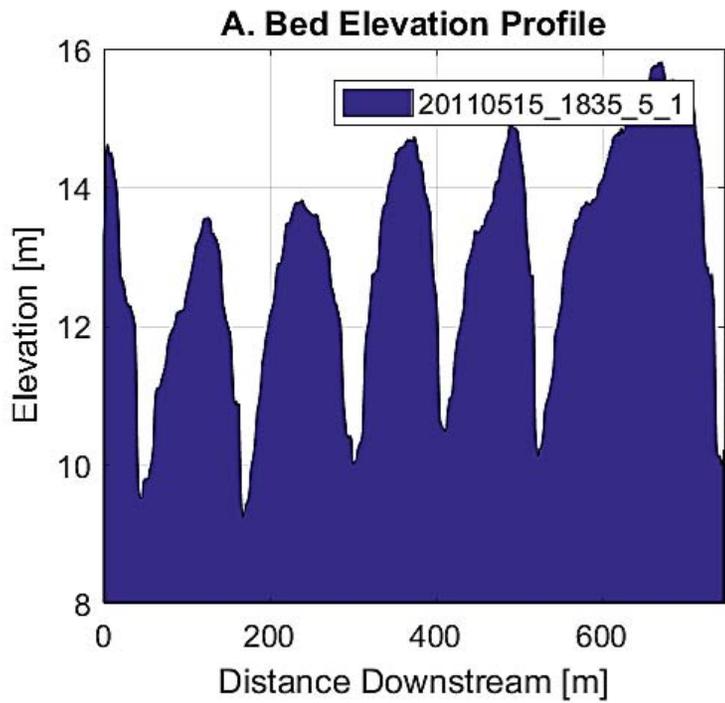




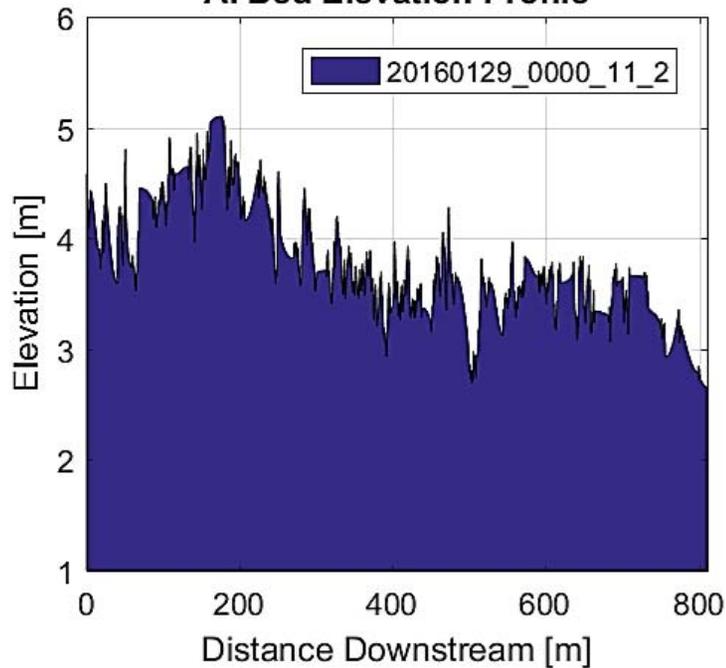




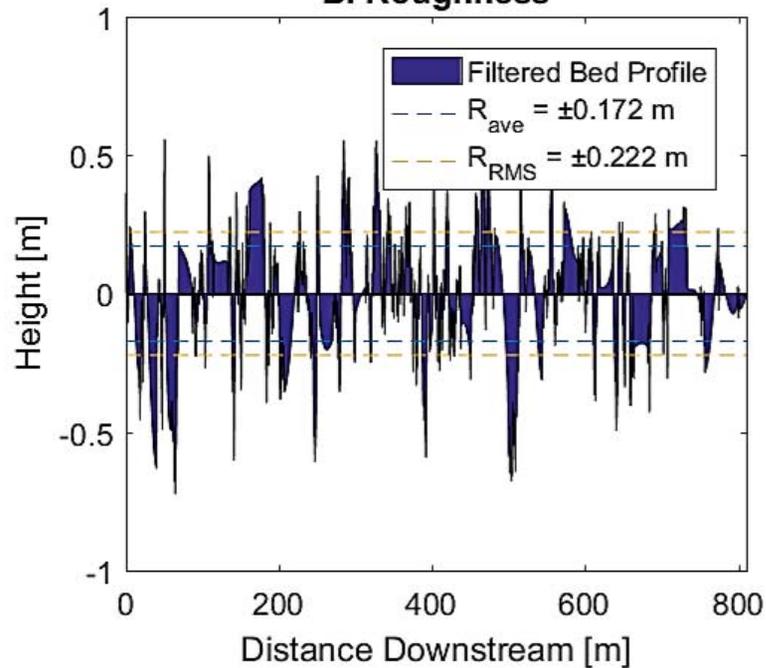




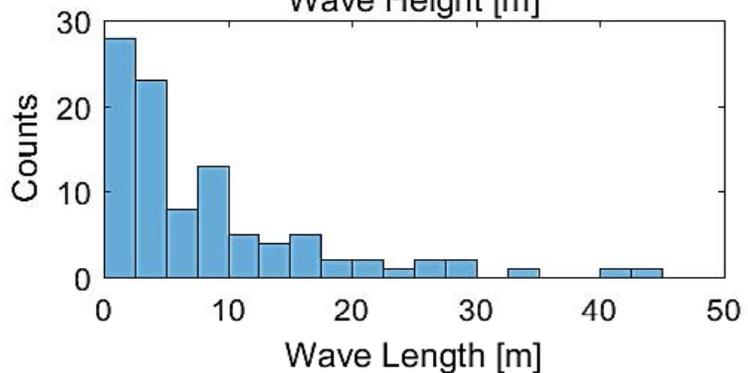
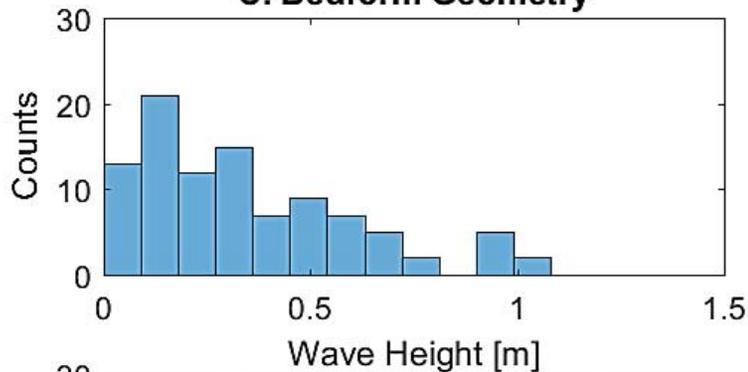
**A. Bed Elevation Profile**



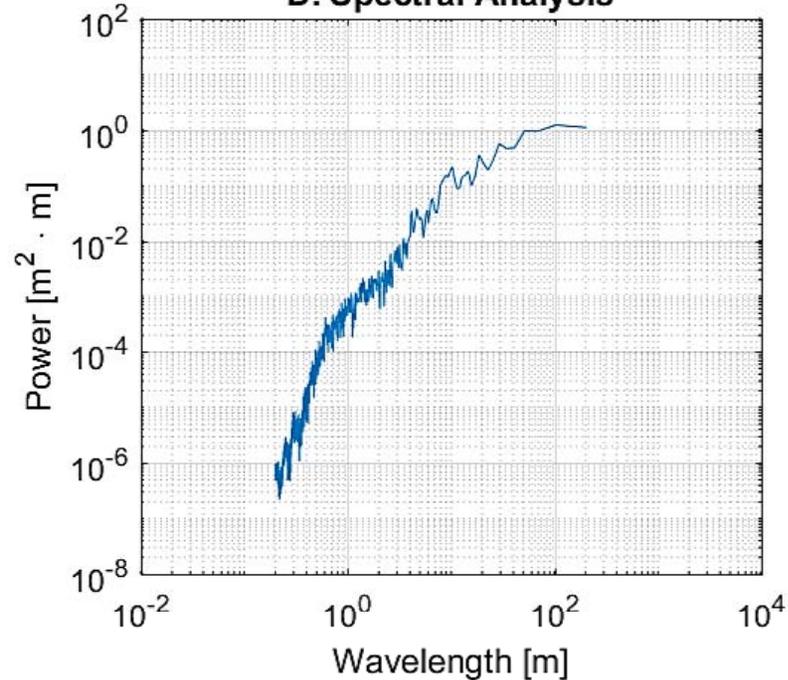
**B. Roughness**



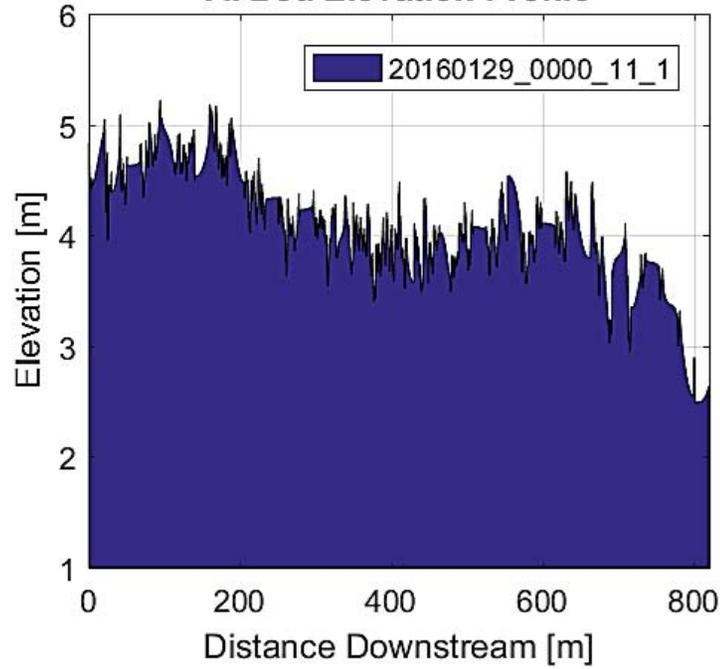
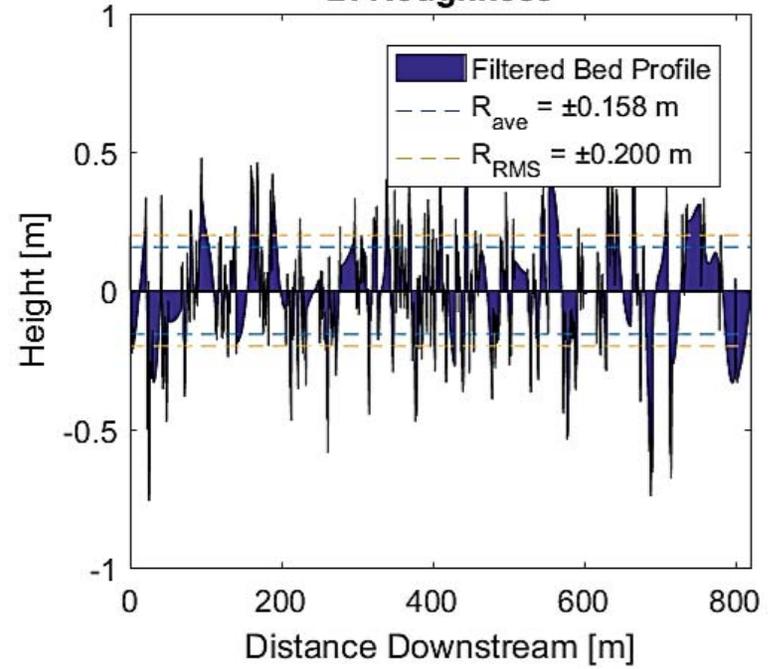
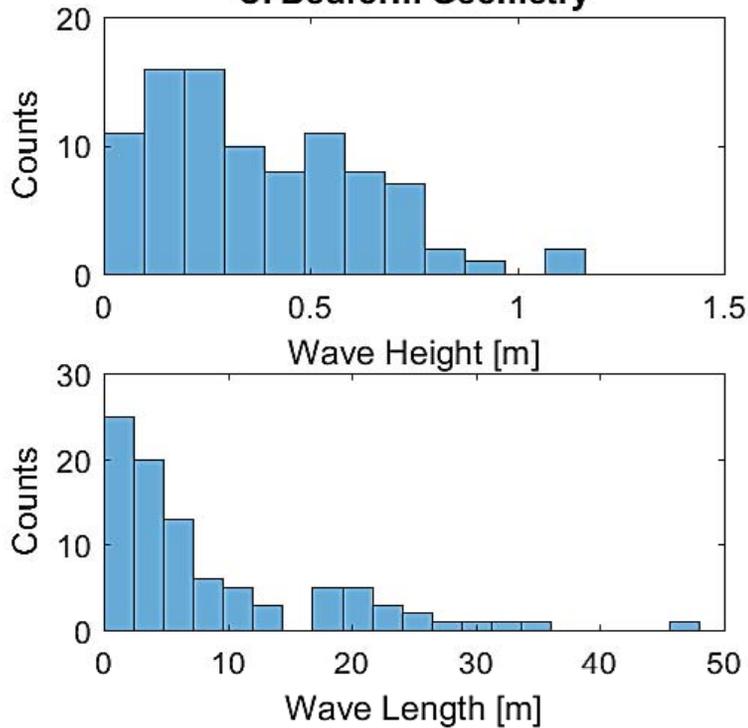
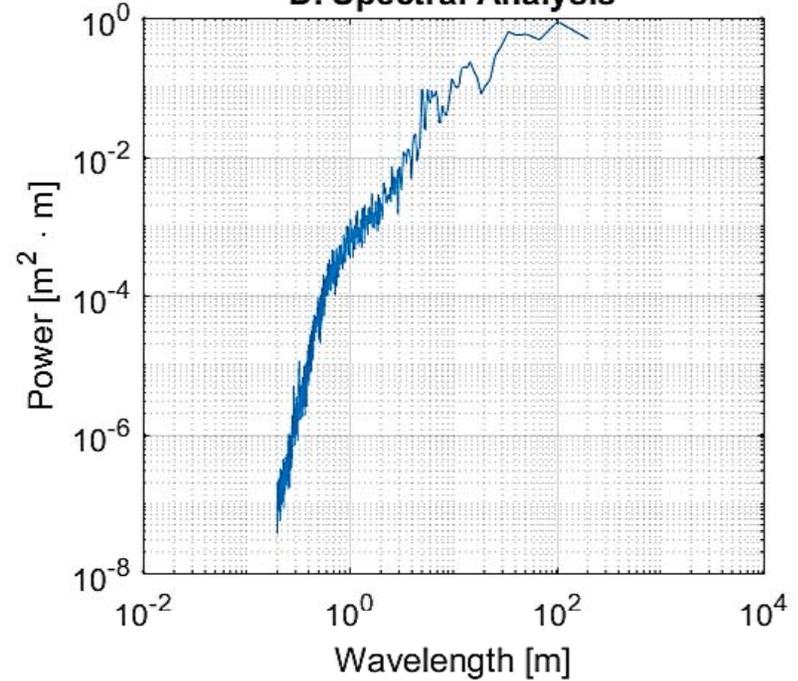
**C. Bedform Geometry**

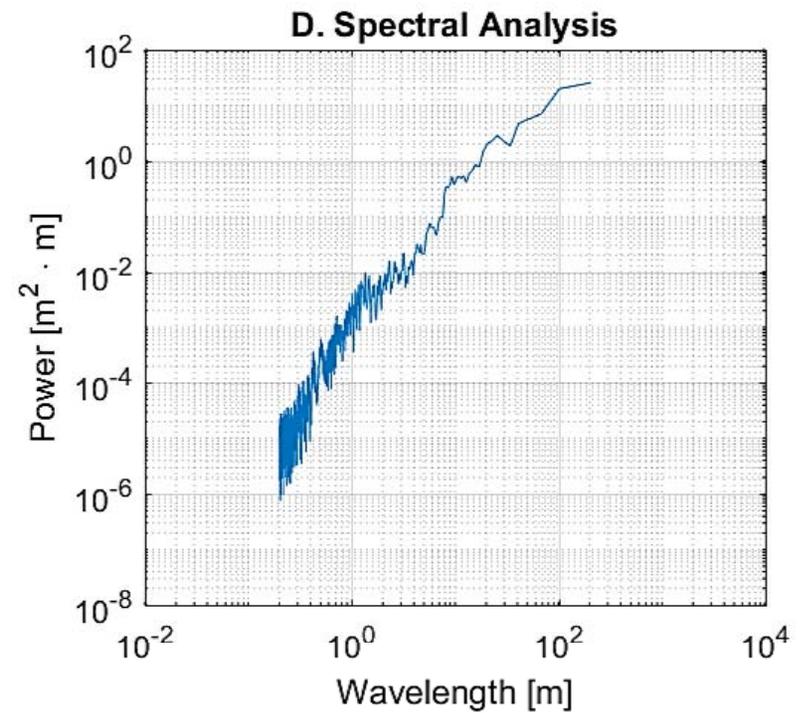
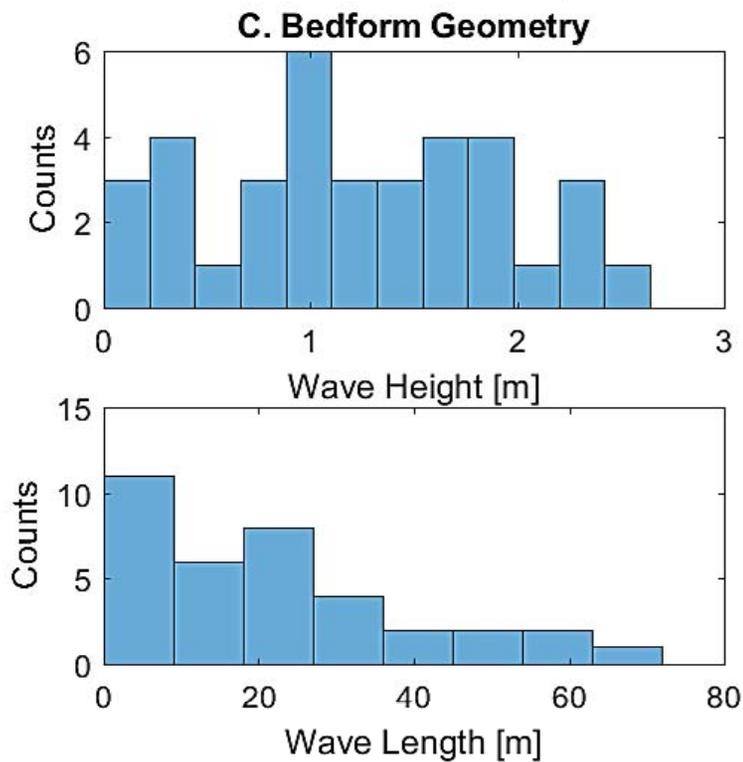
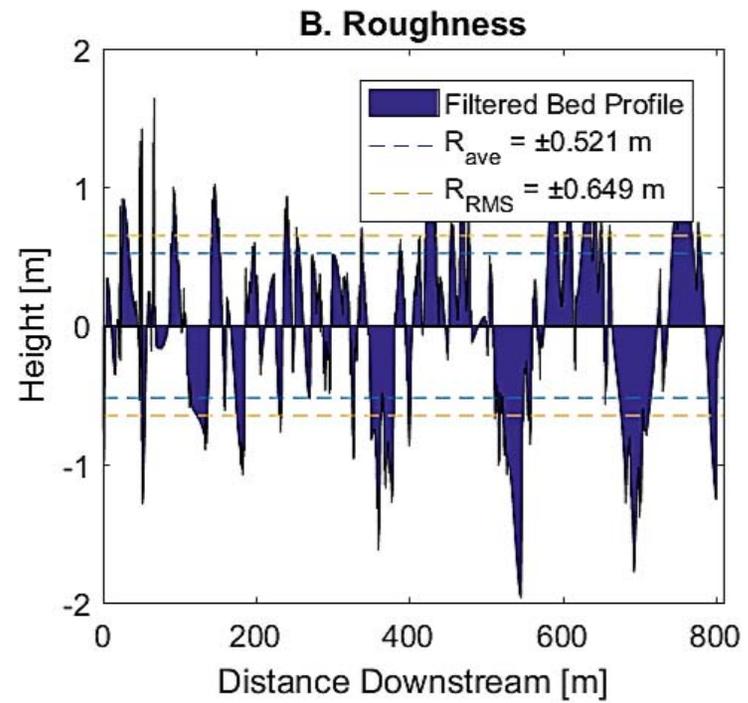
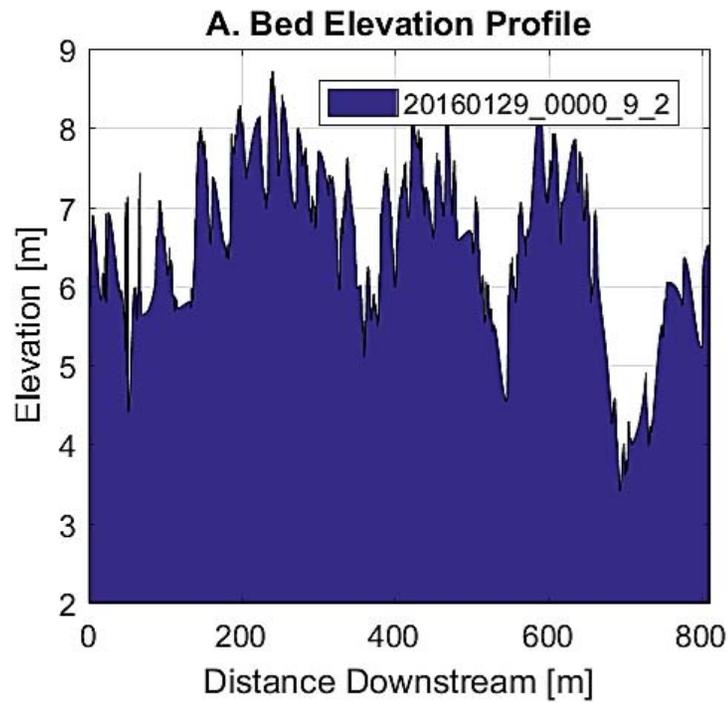


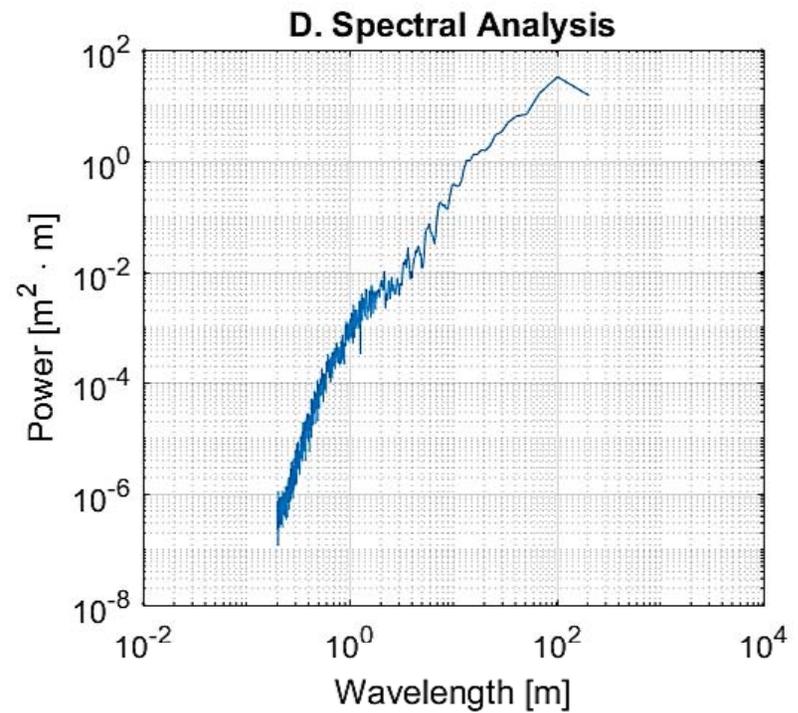
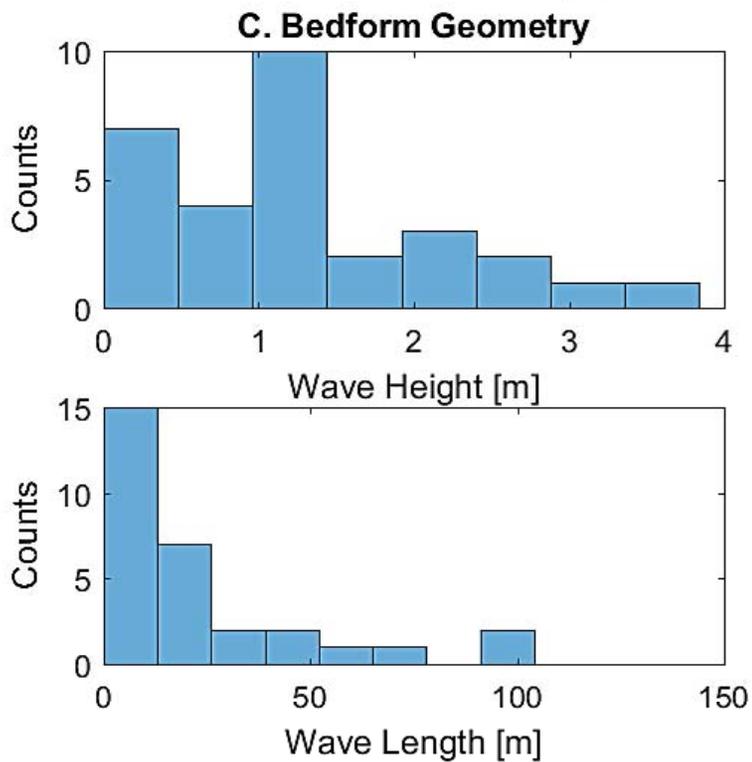
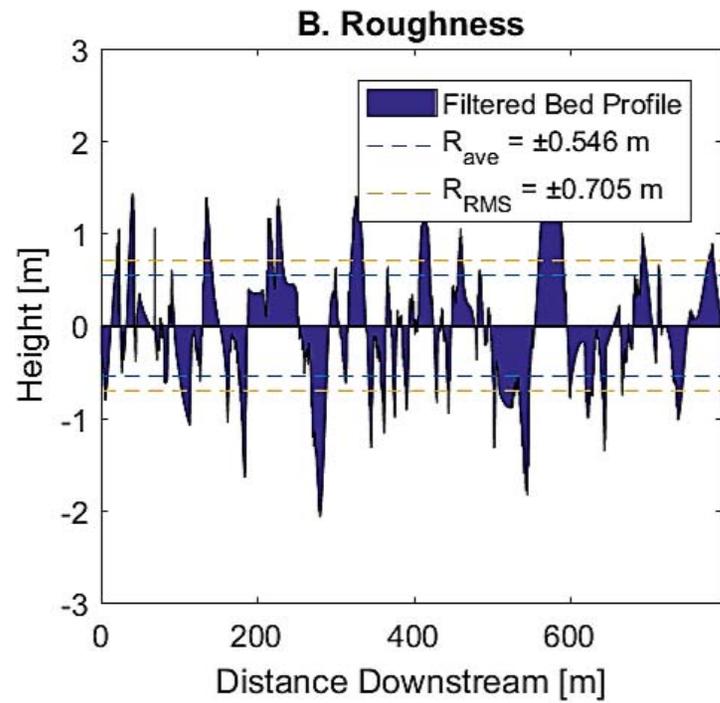
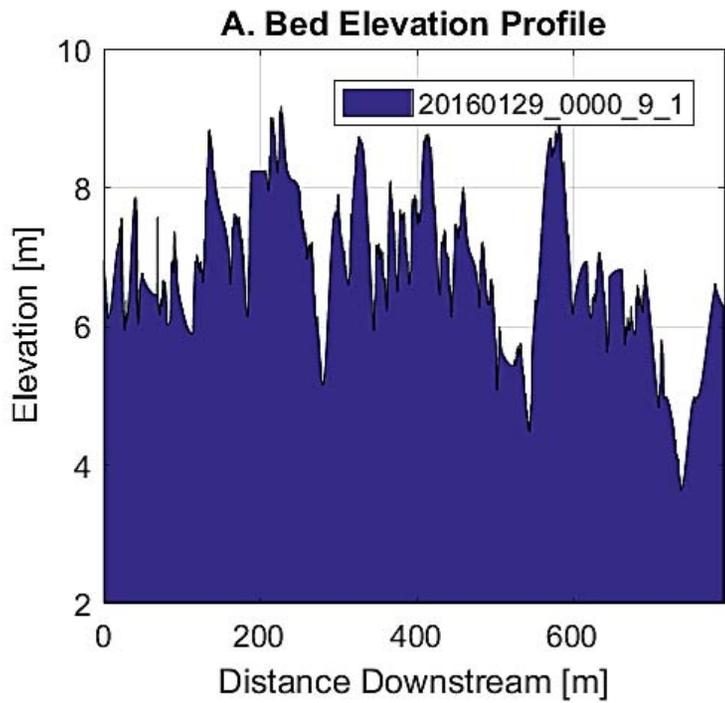
**D. Spectral Analysis**

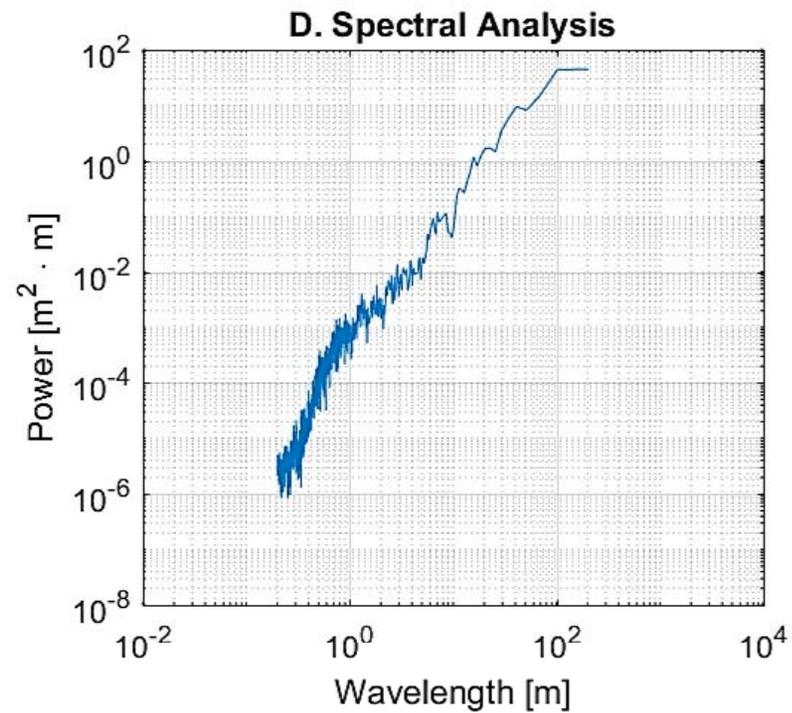
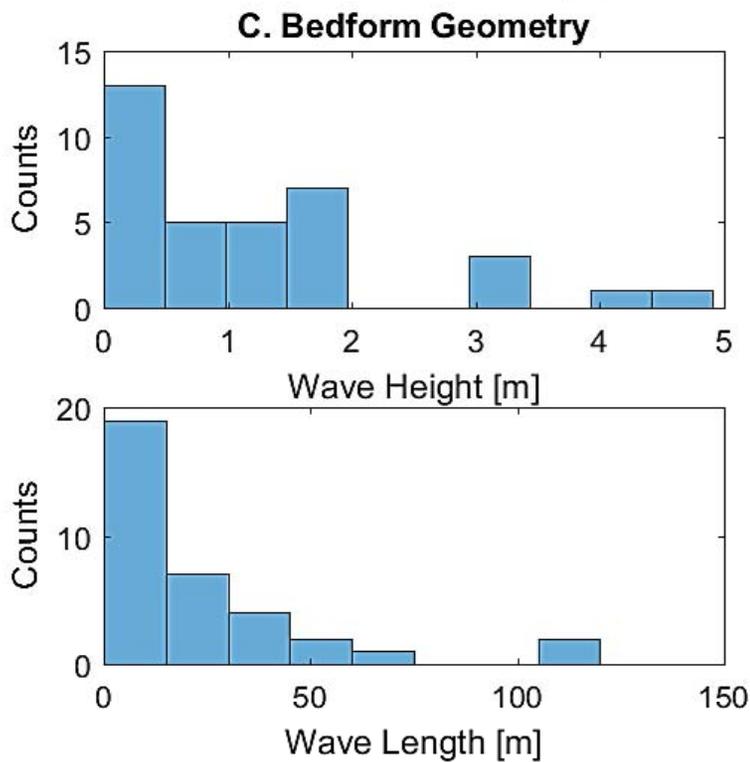
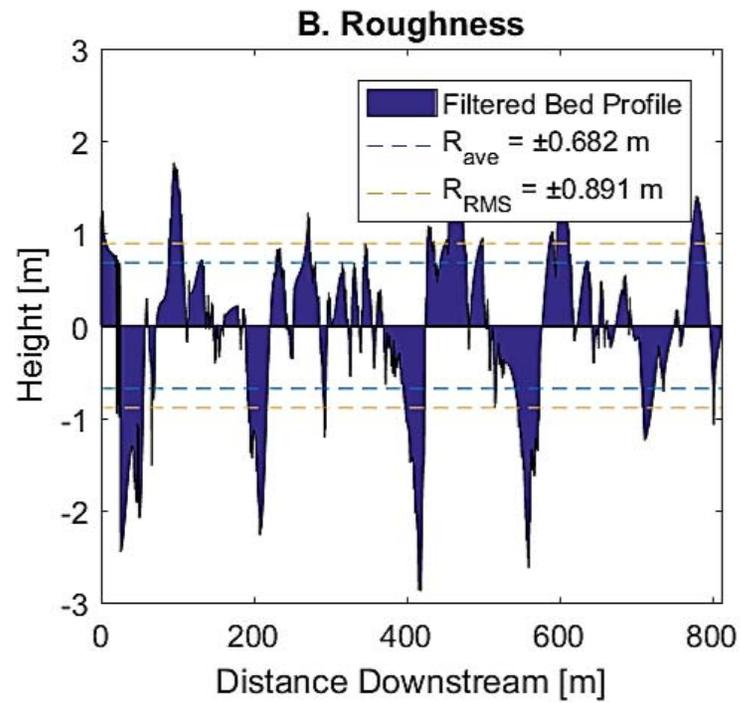
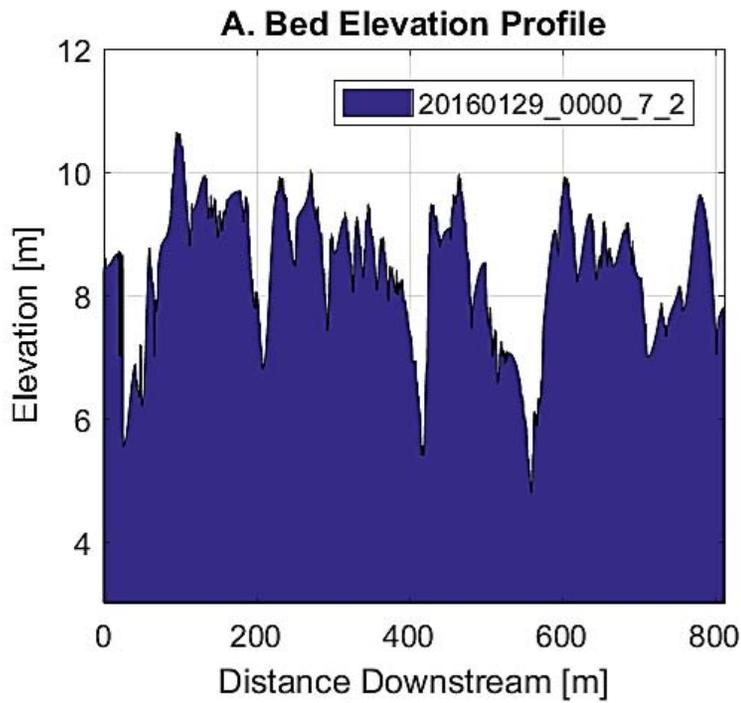


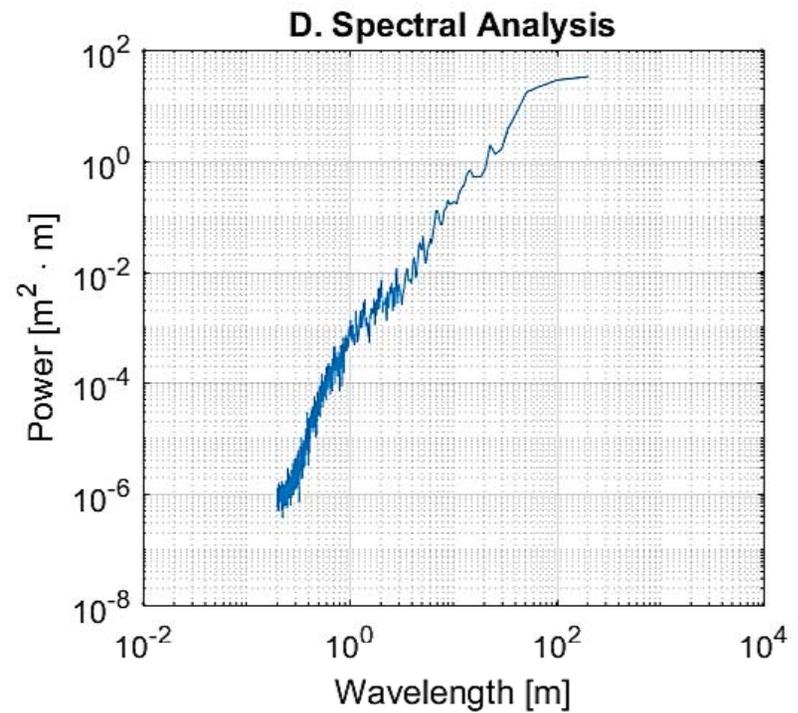
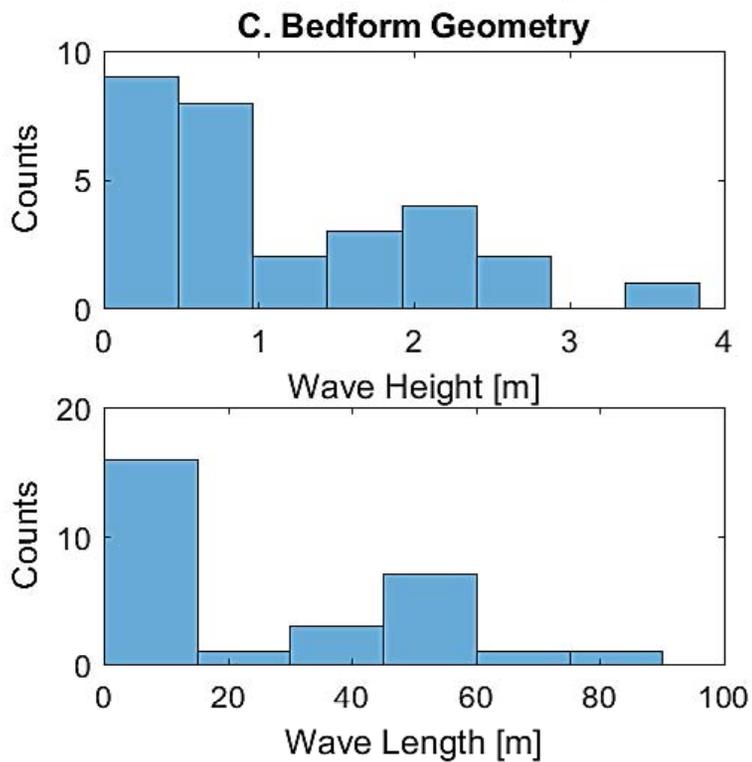
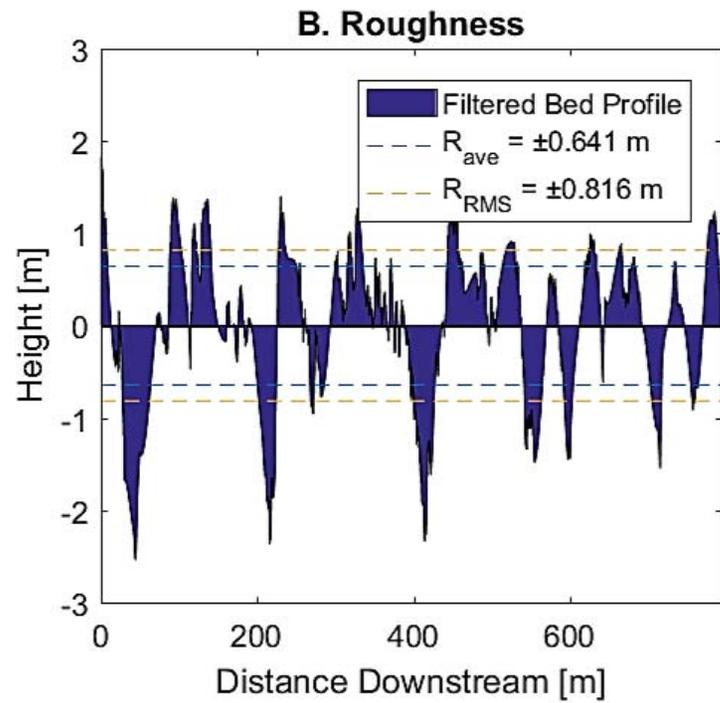
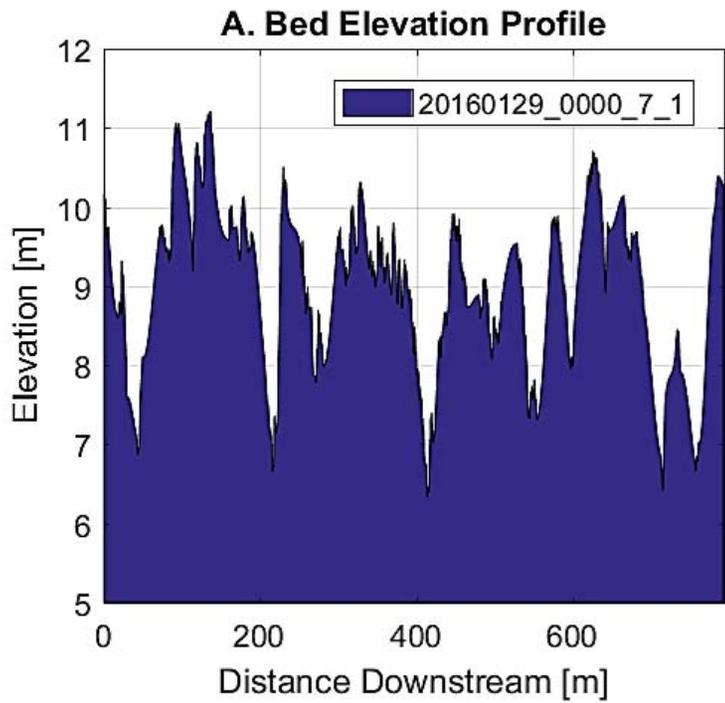


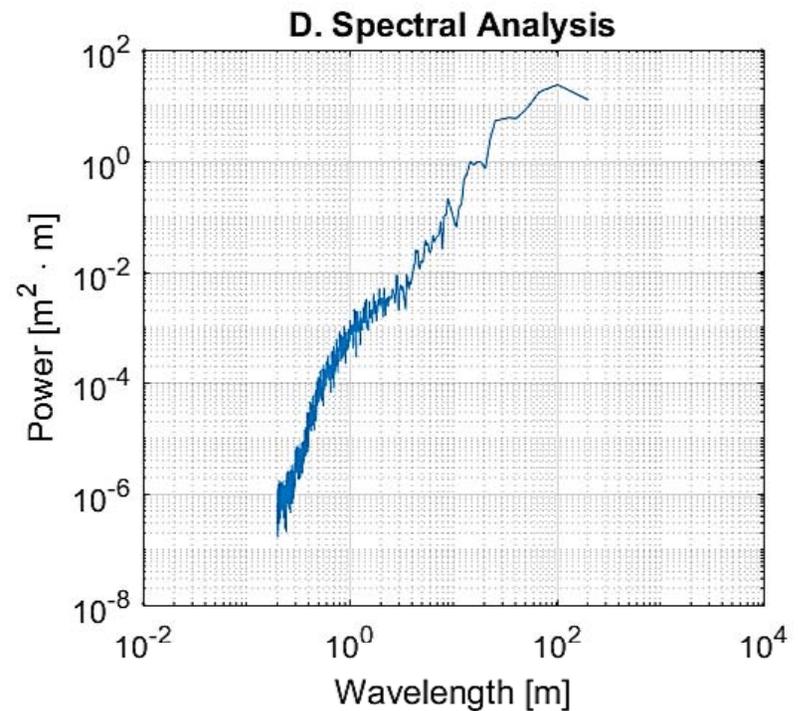
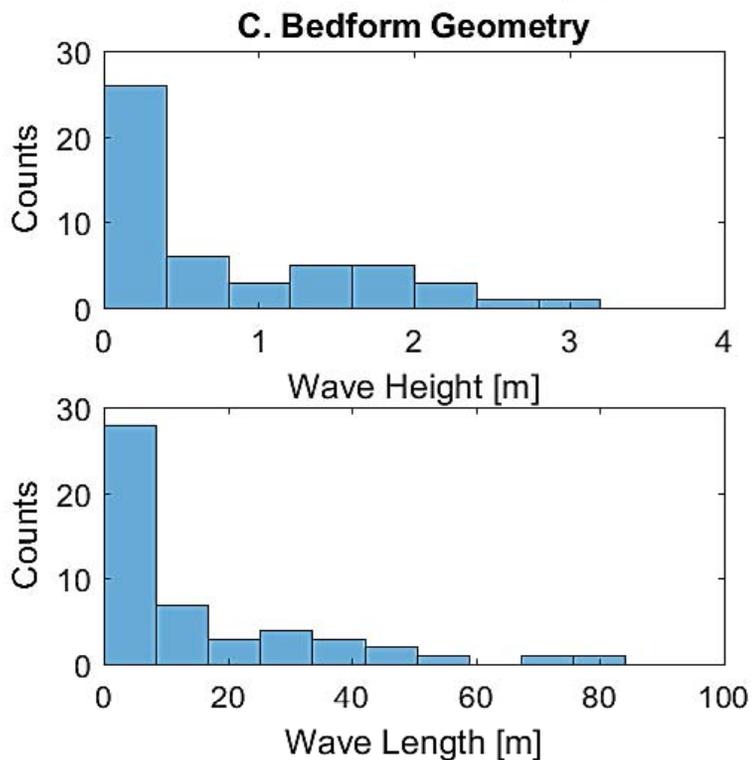
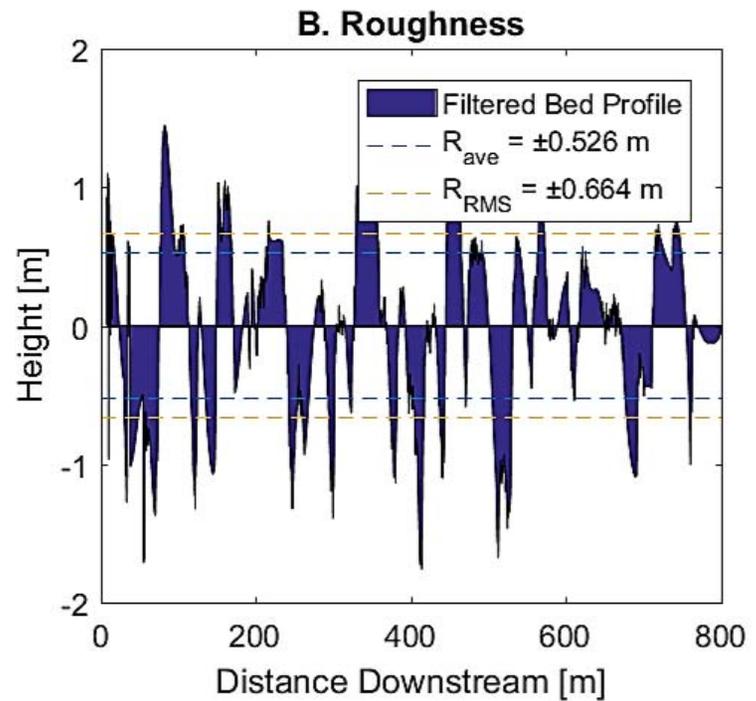
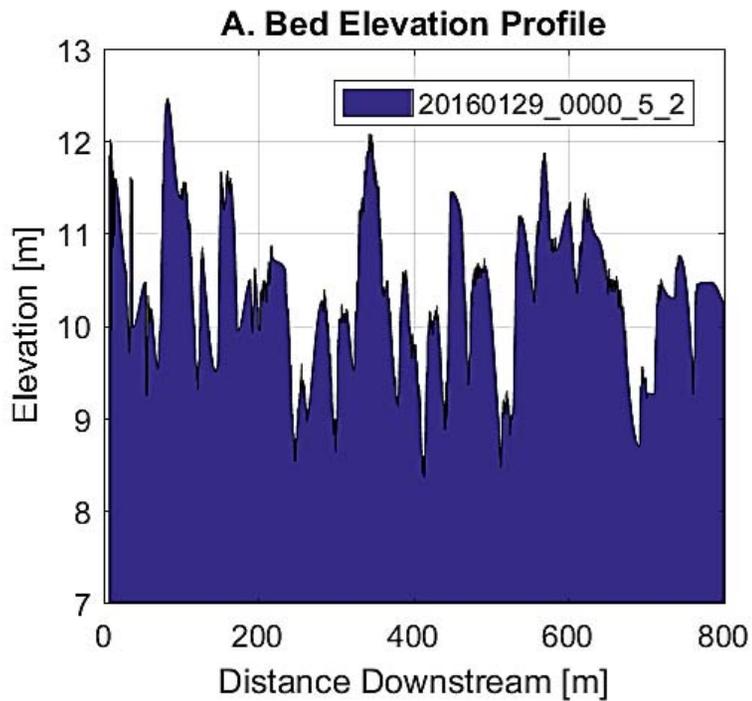
**A. Bed Elevation Profile****B. Roughness****C. Bedform Geometry****D. Spectral Analysis**

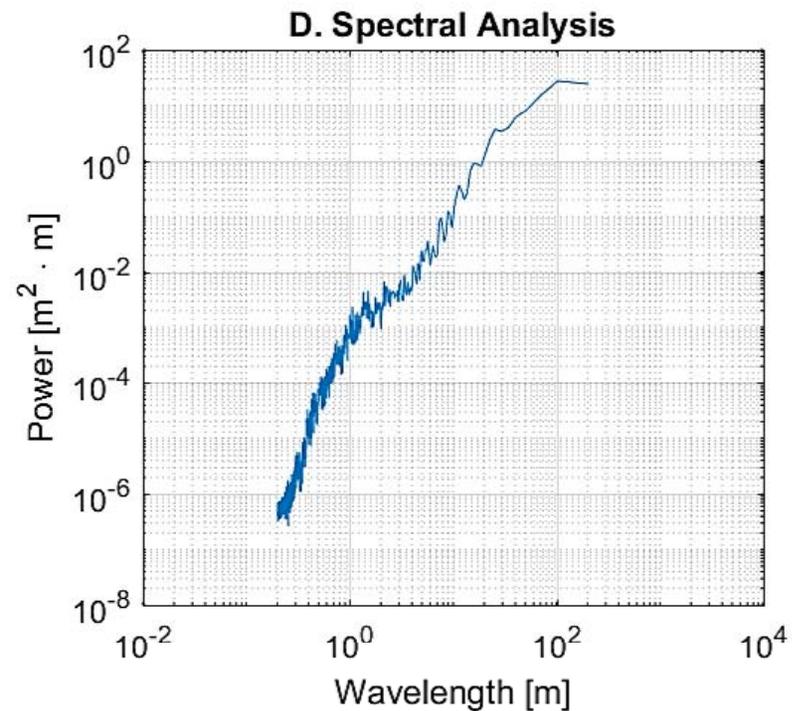
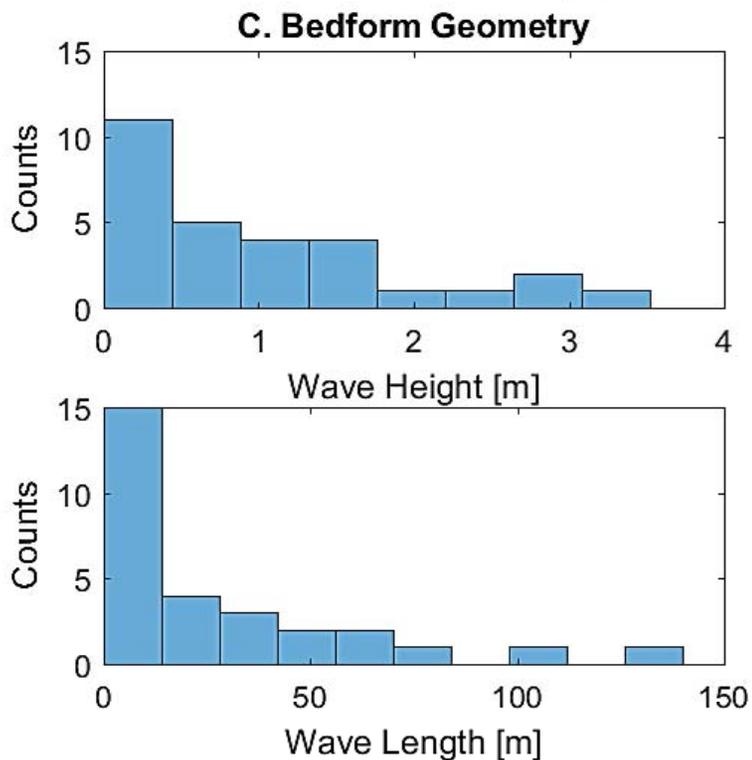
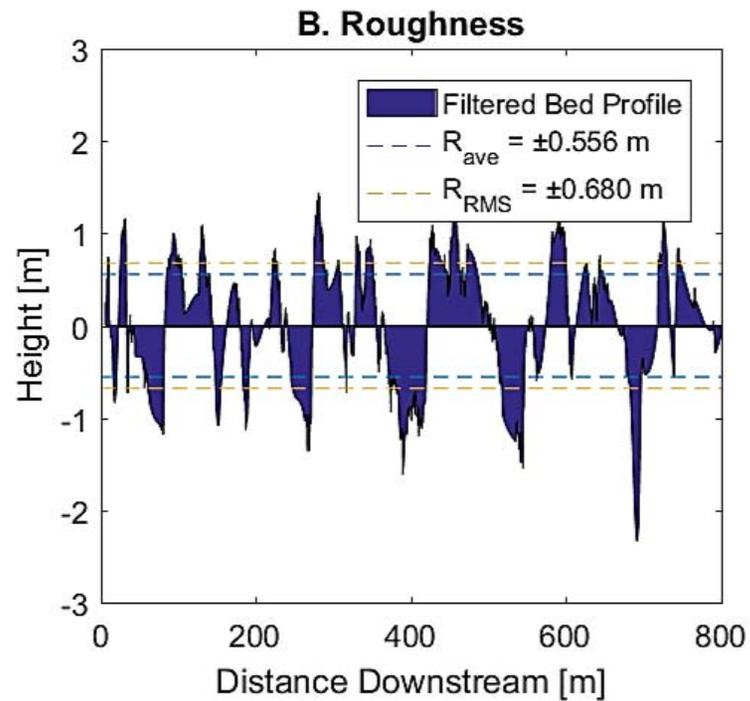
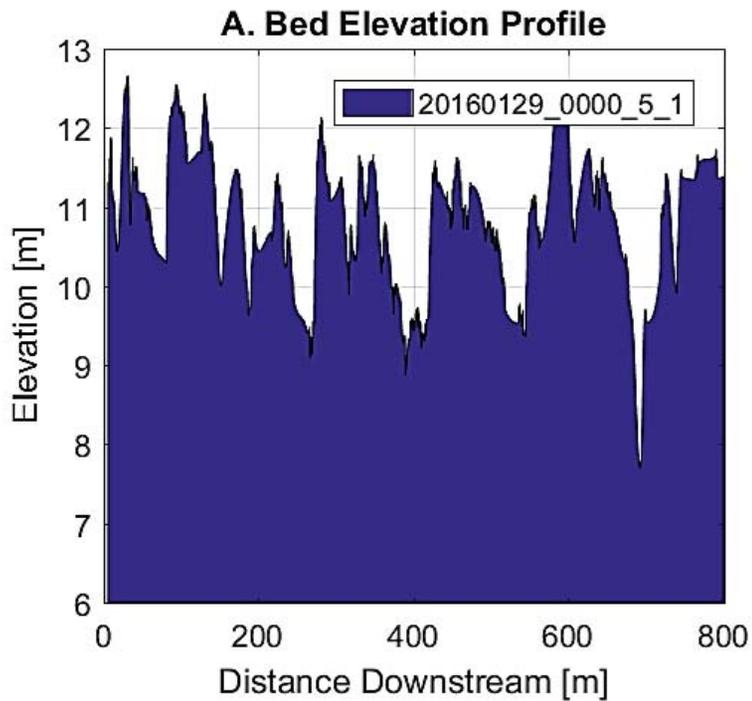


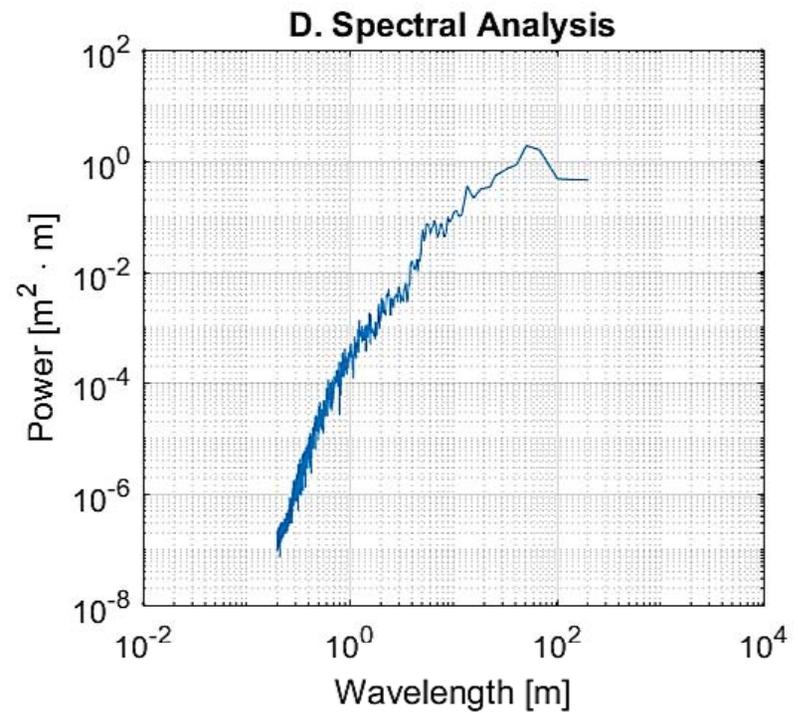
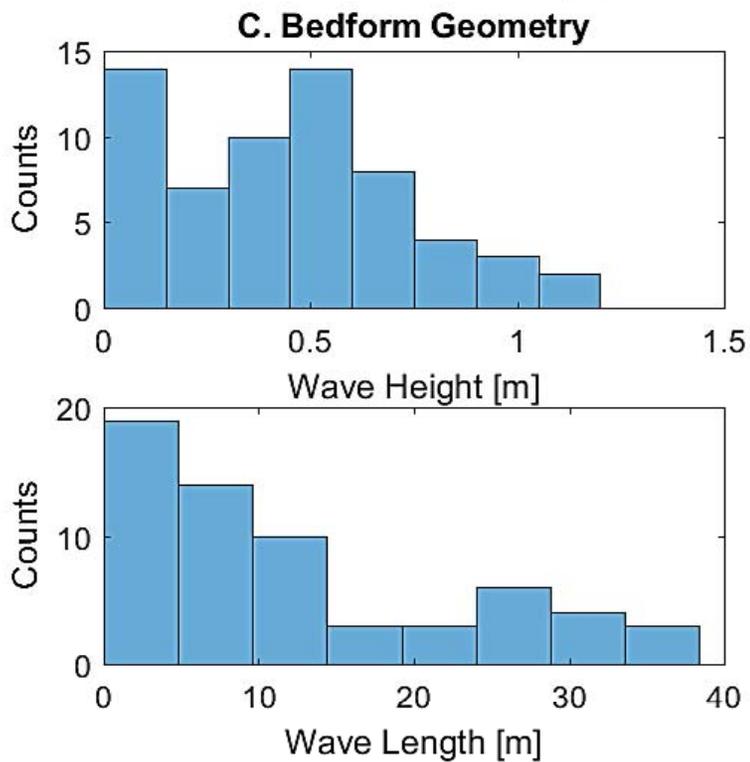
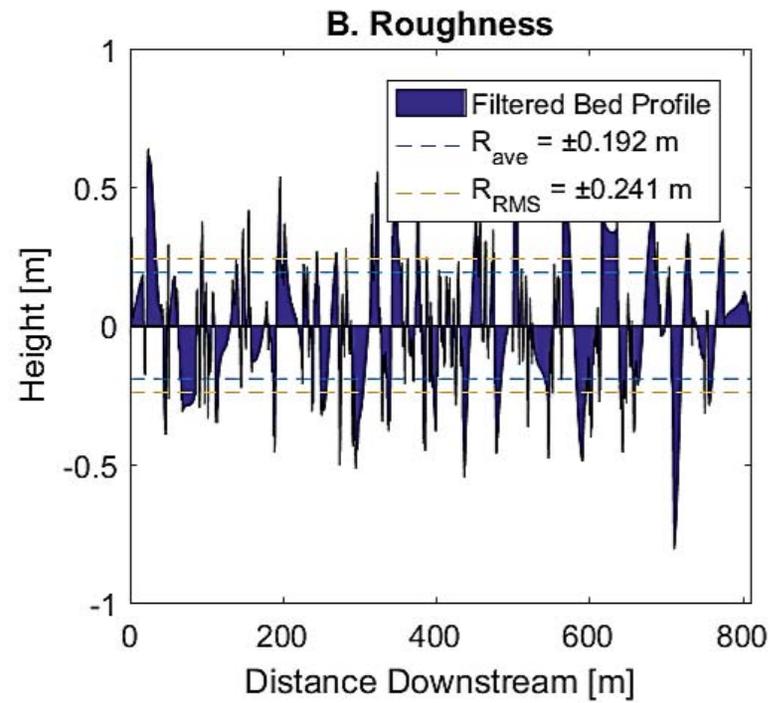
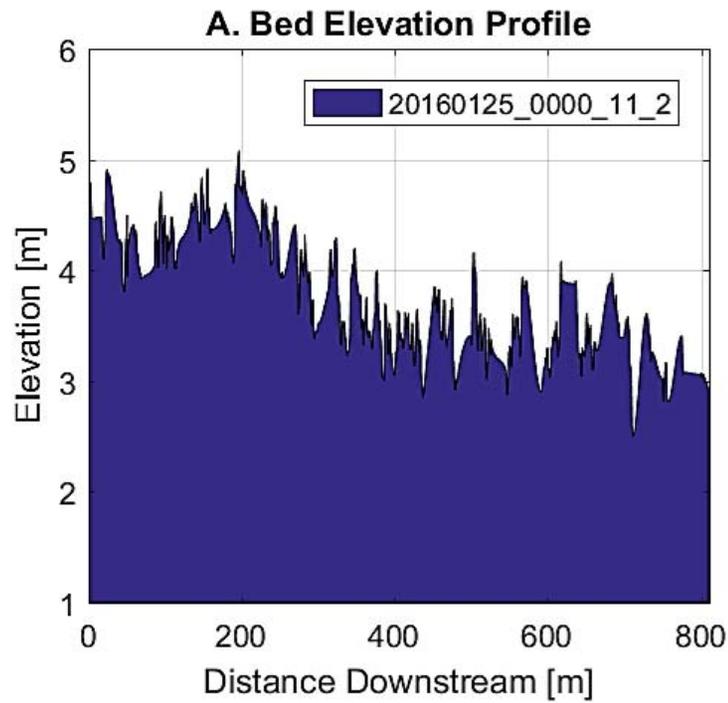




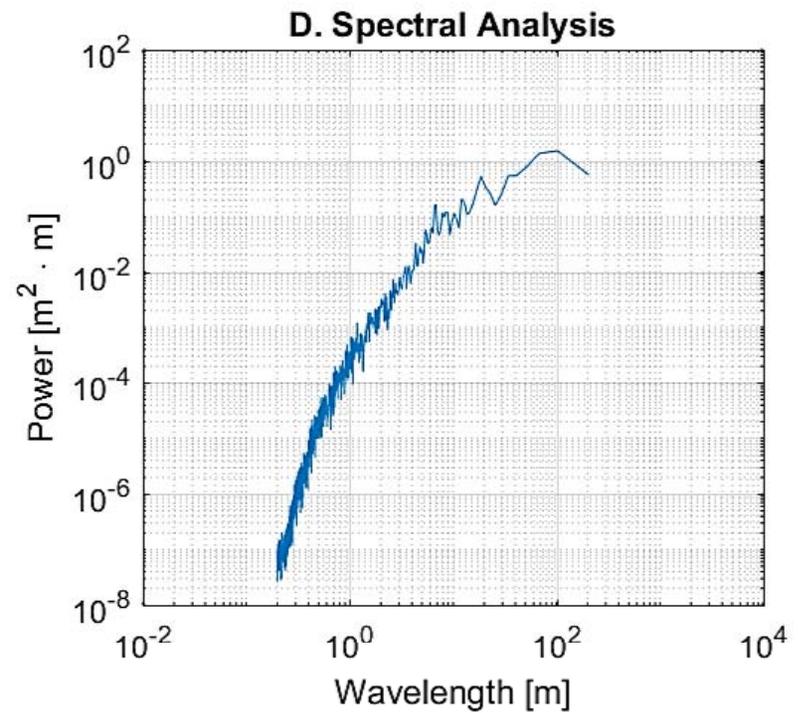
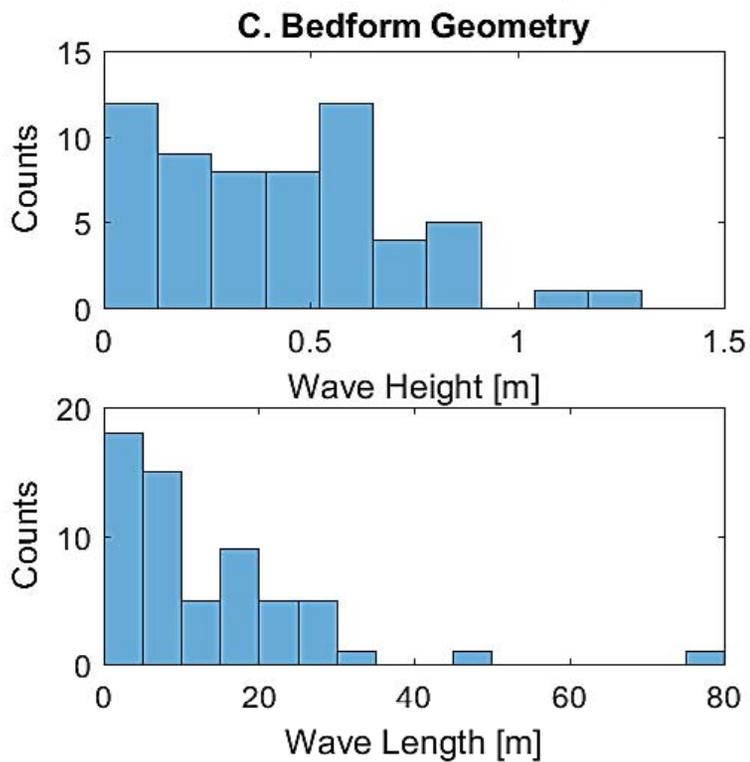
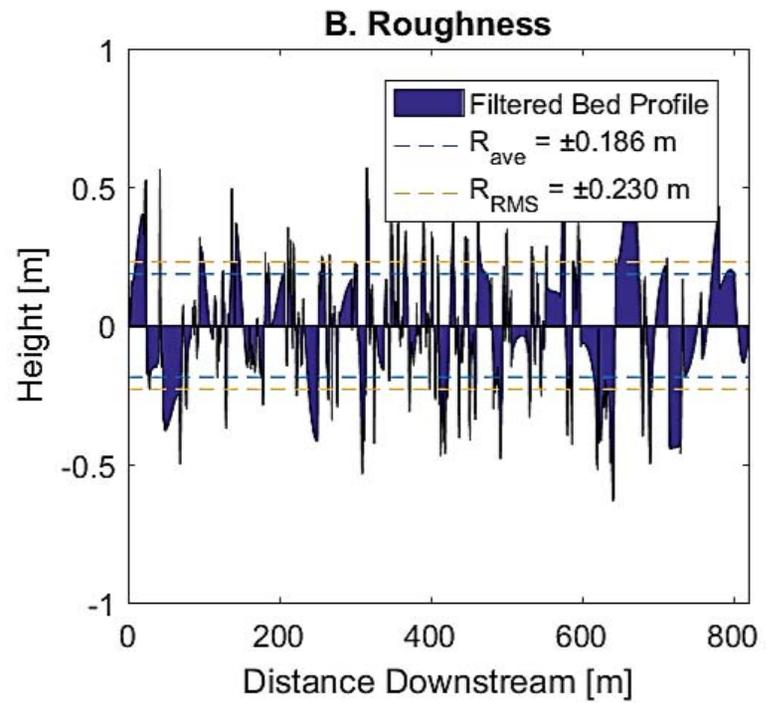
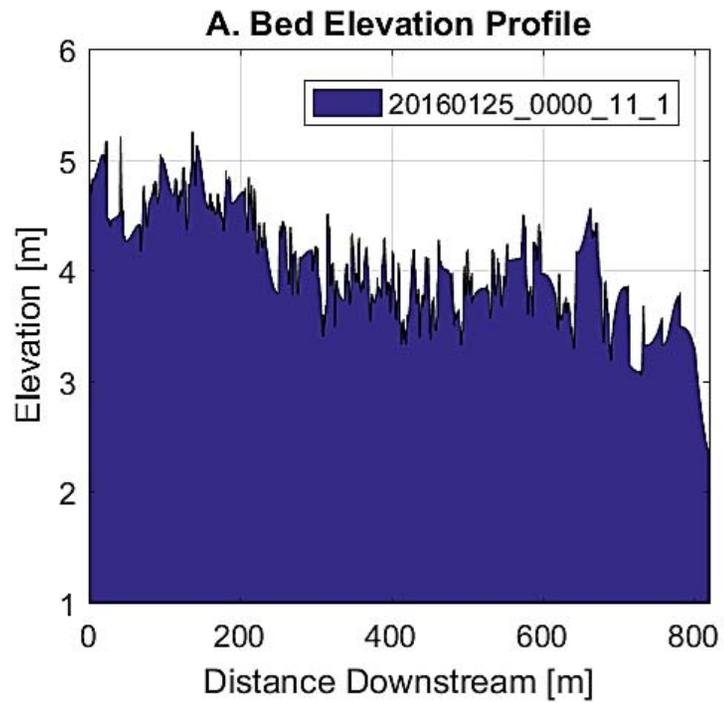


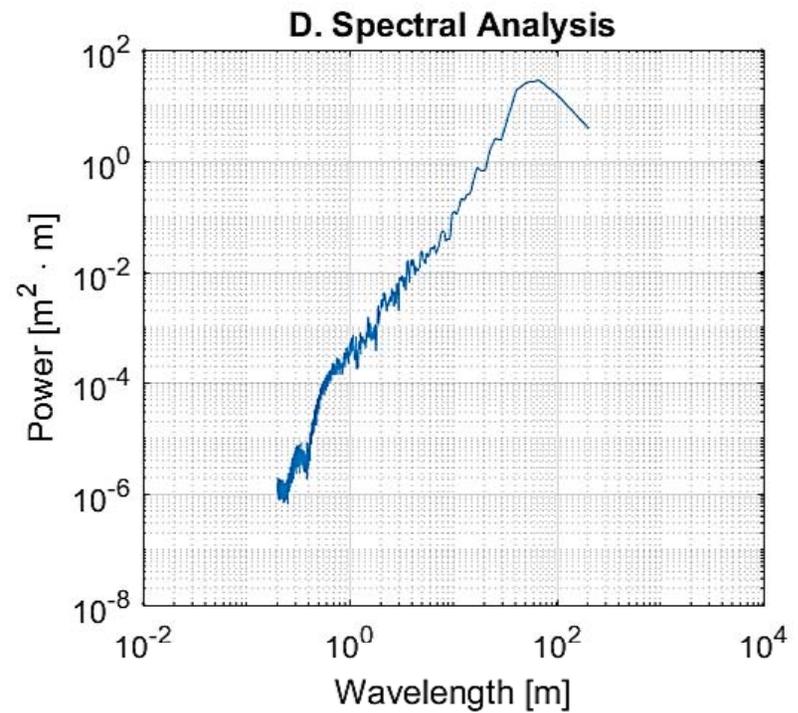
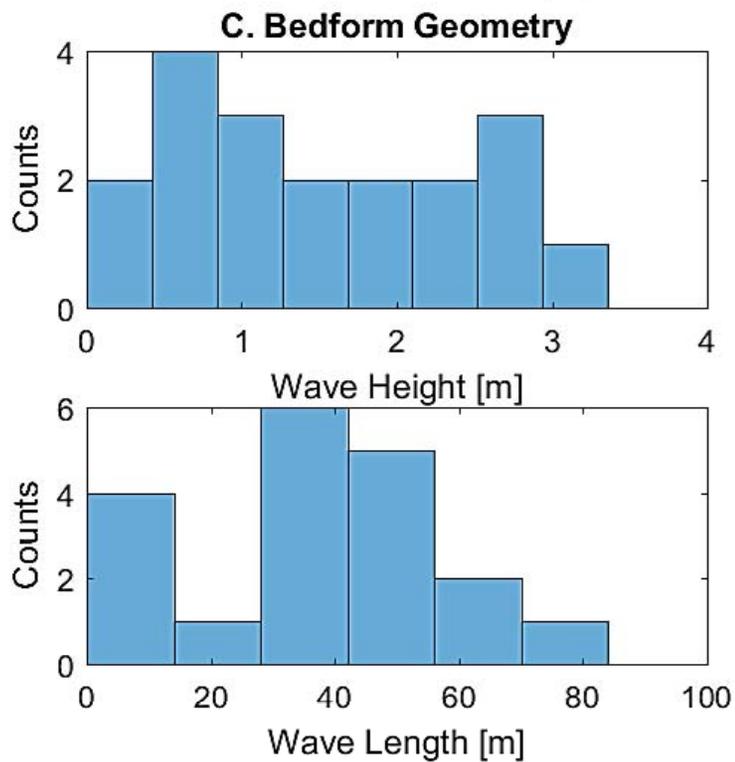
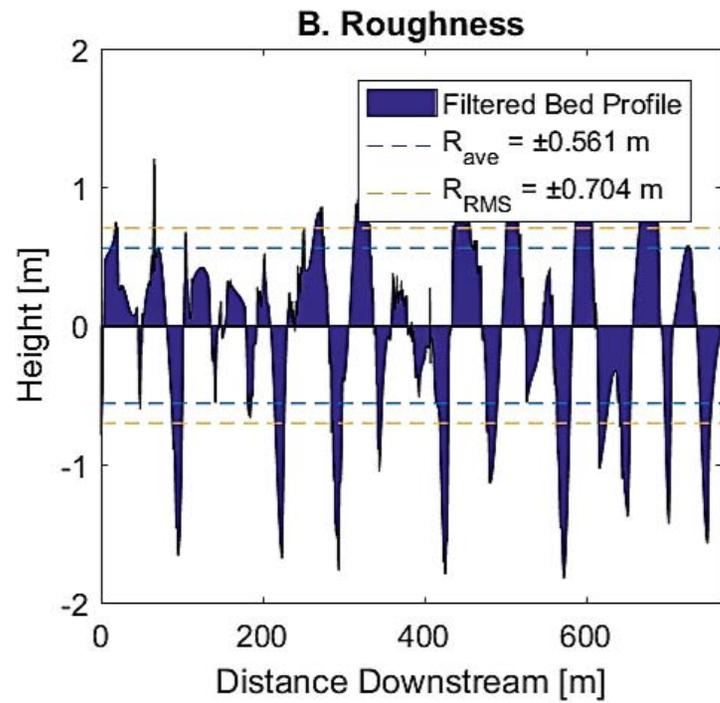
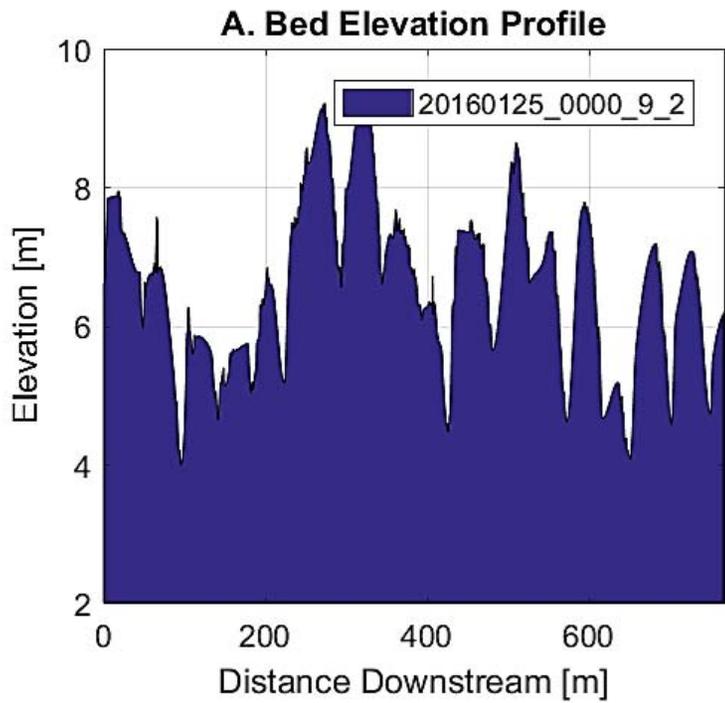


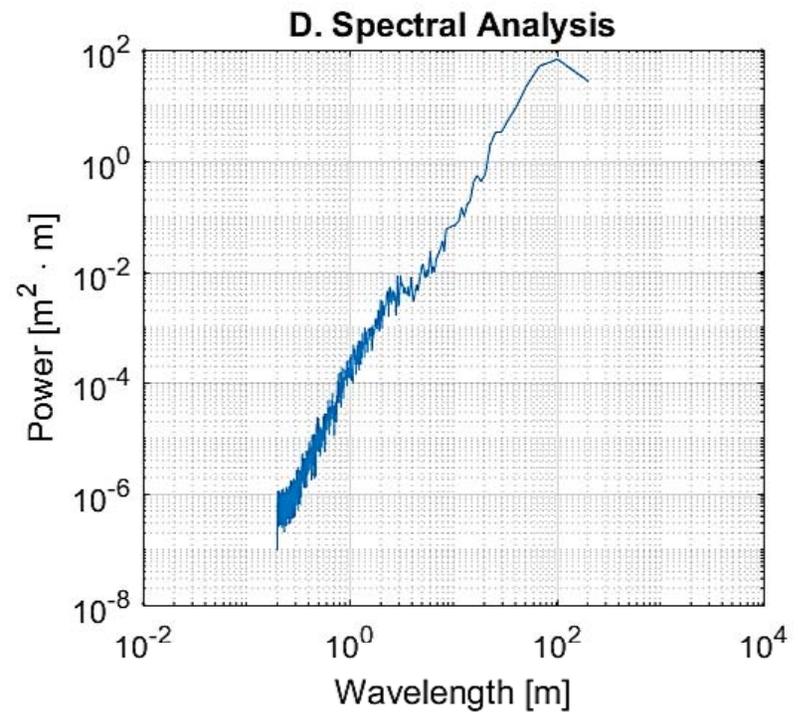
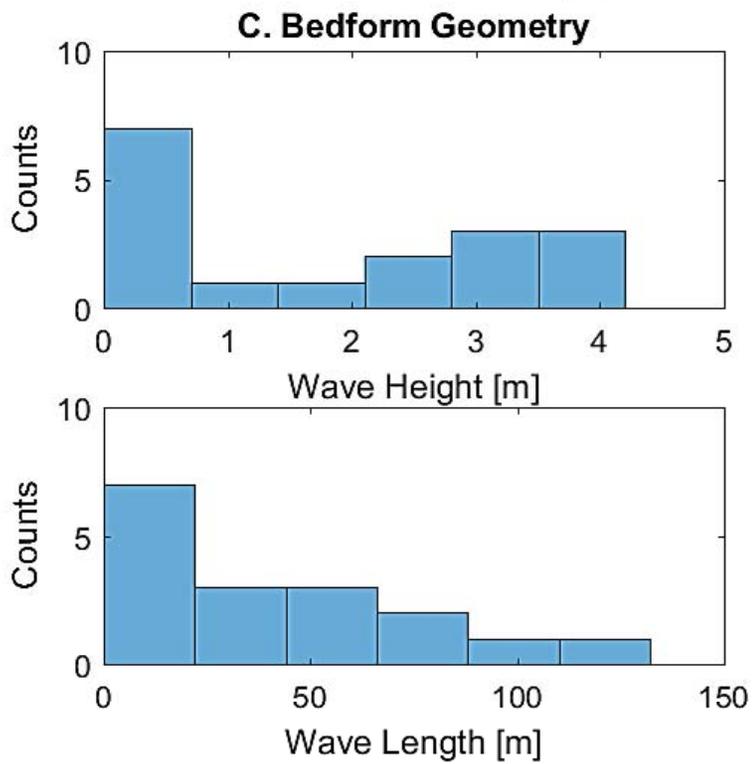
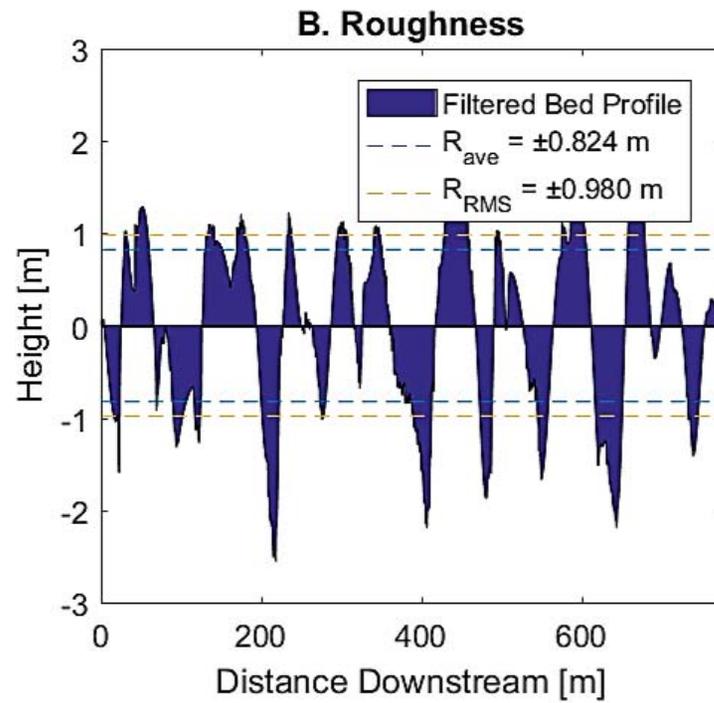
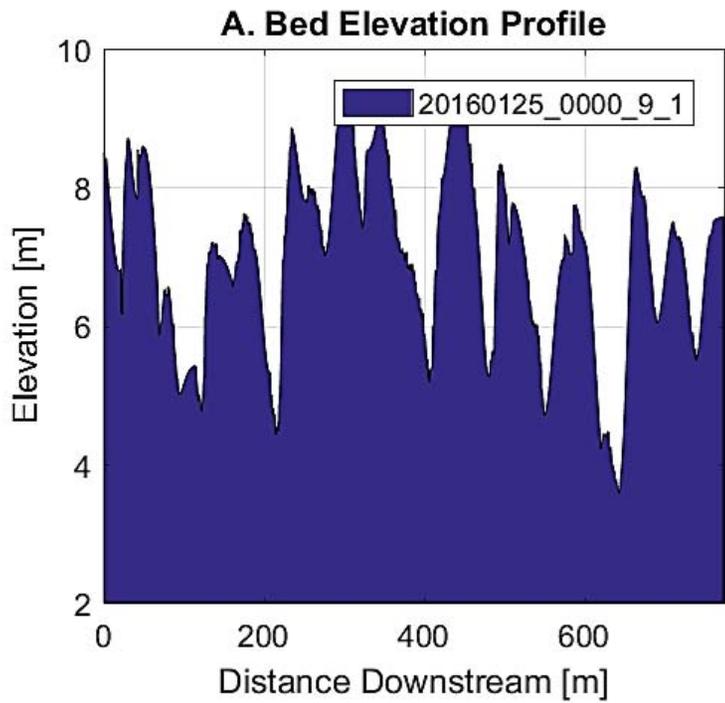


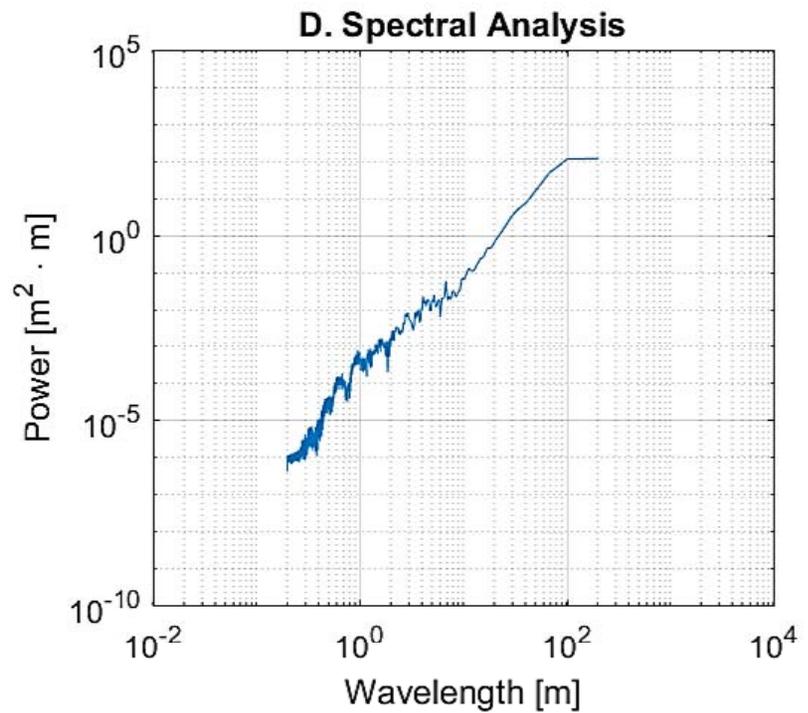
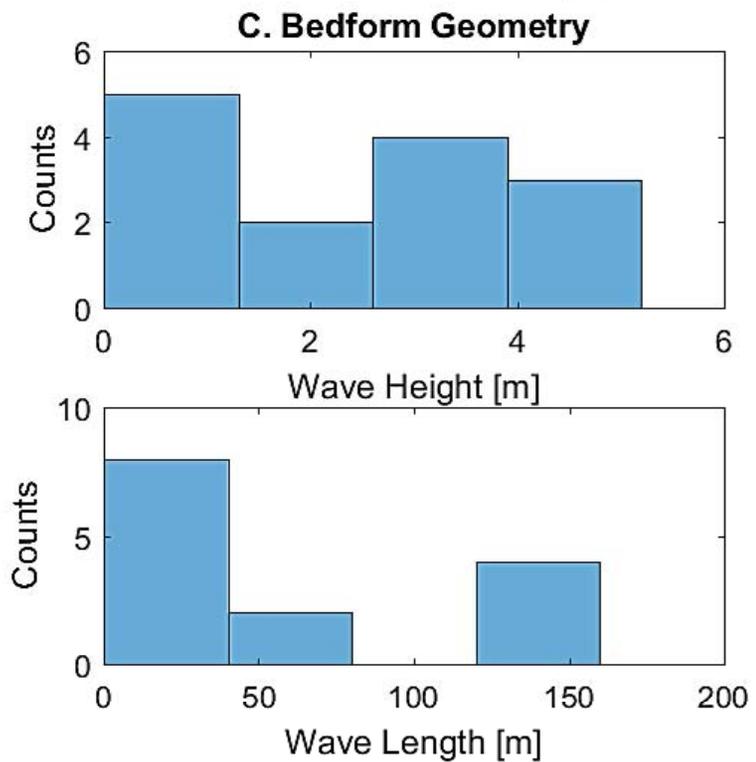
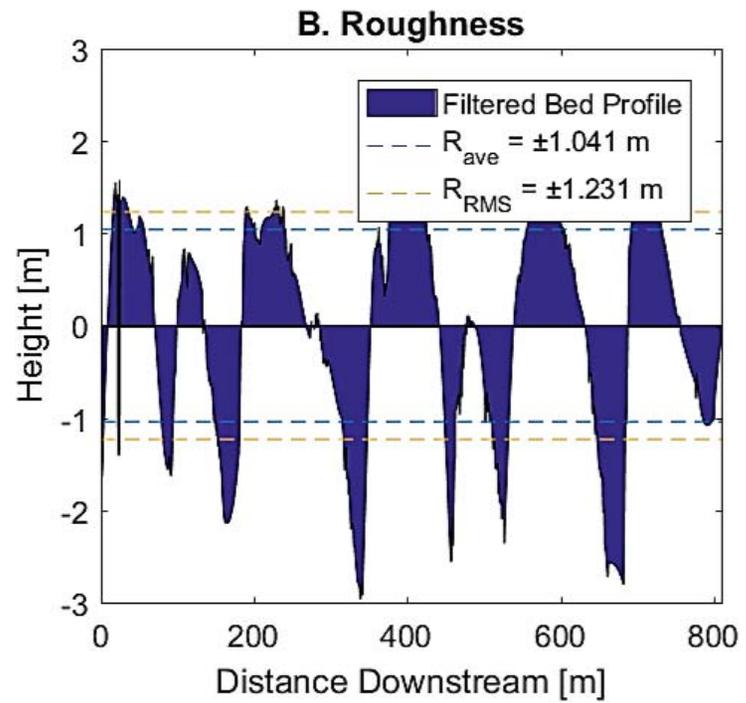
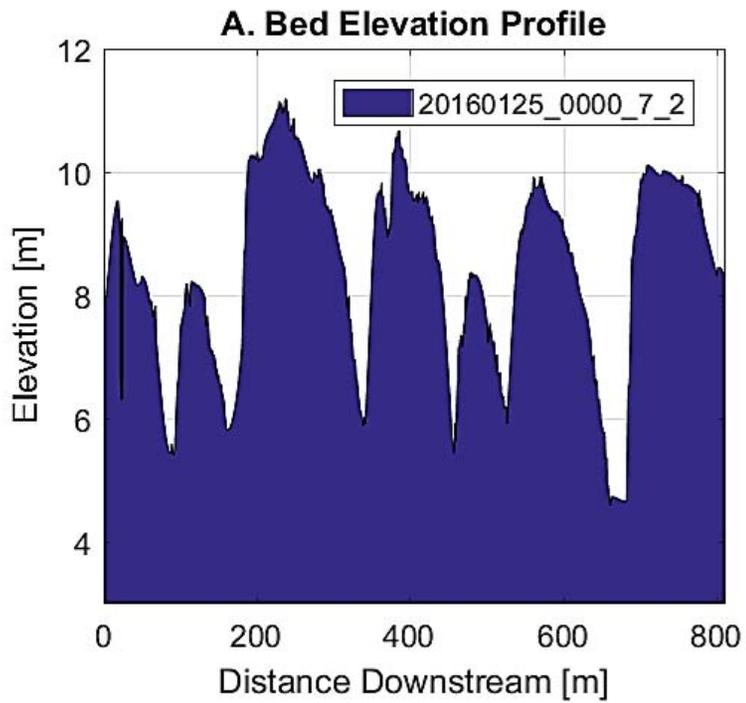


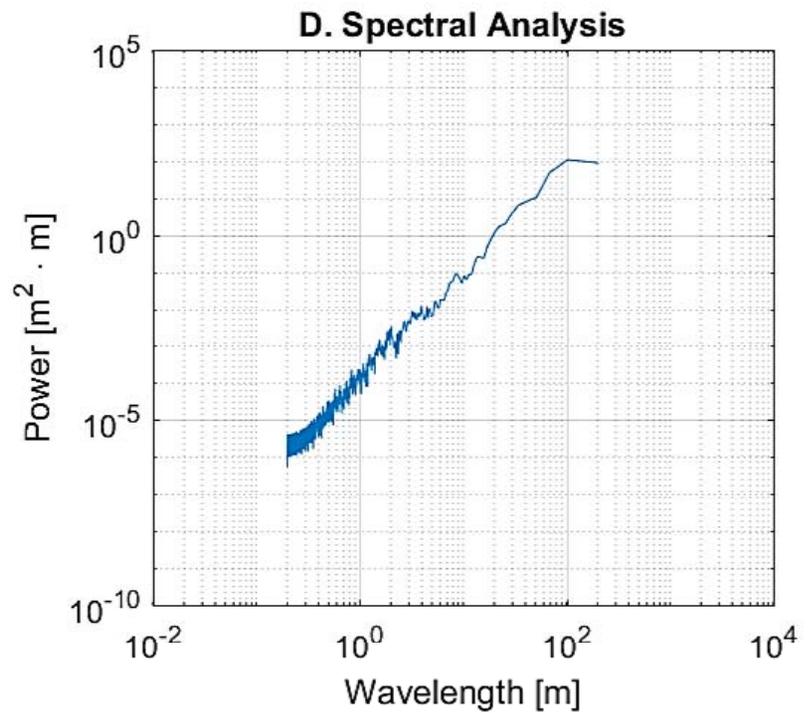
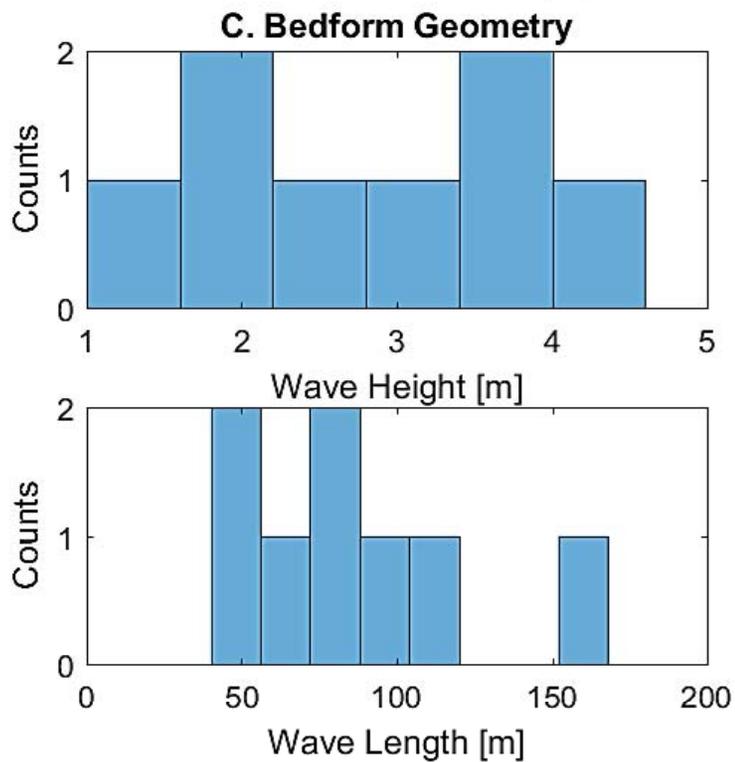
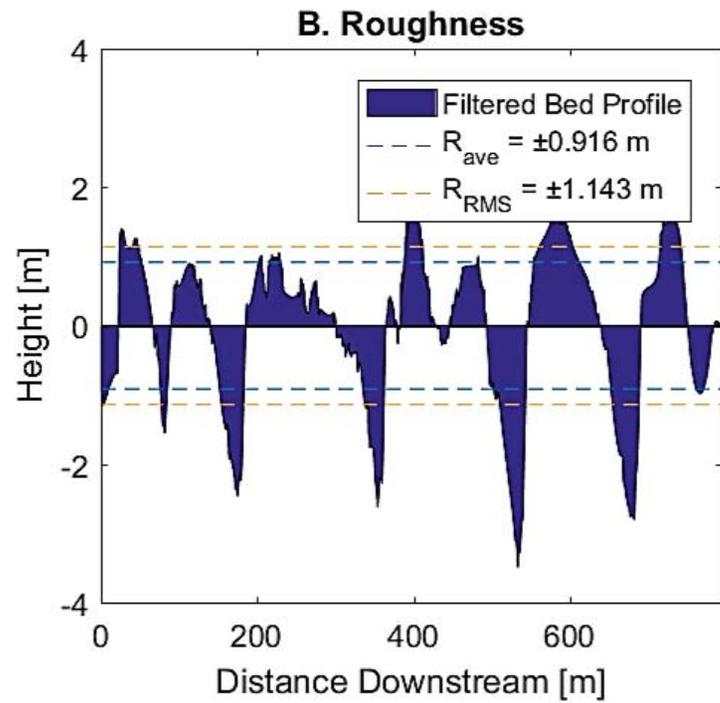
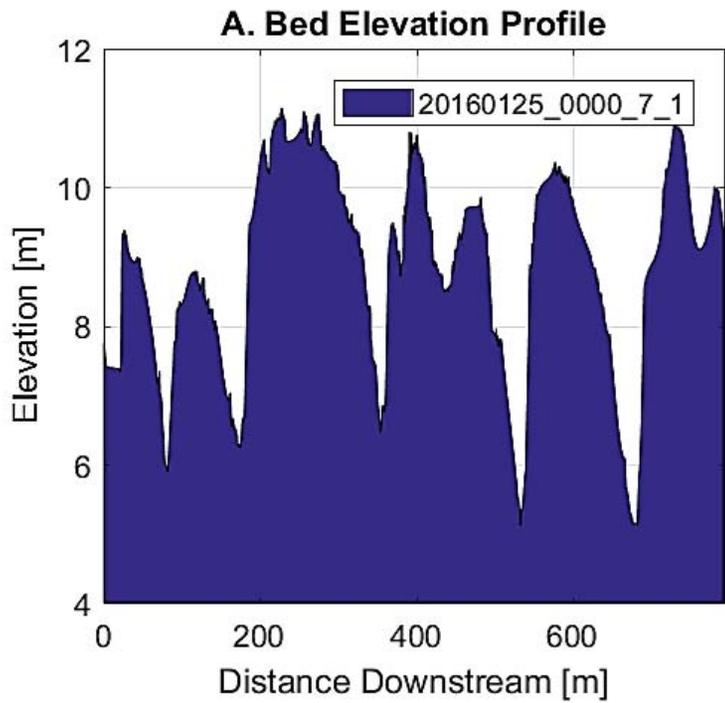


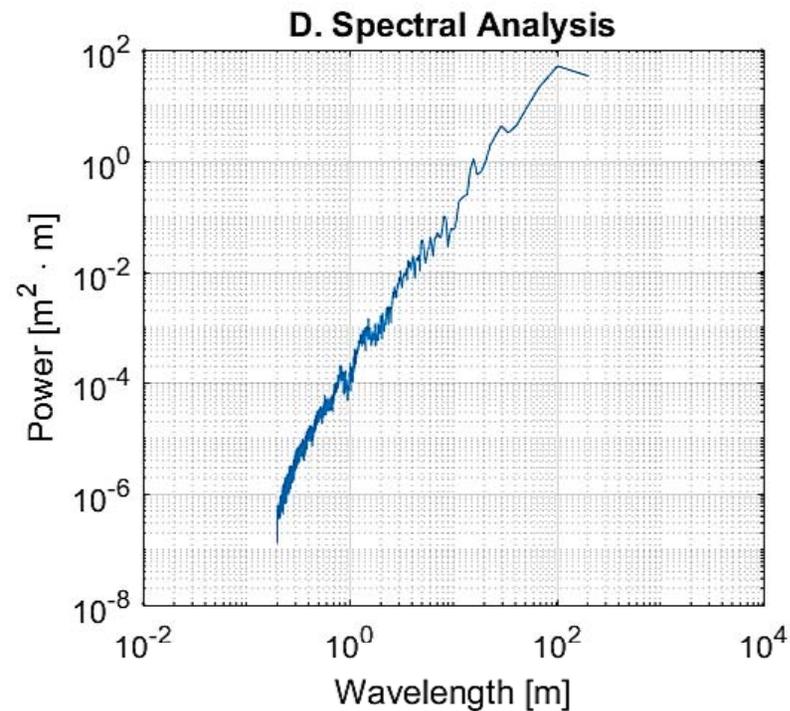
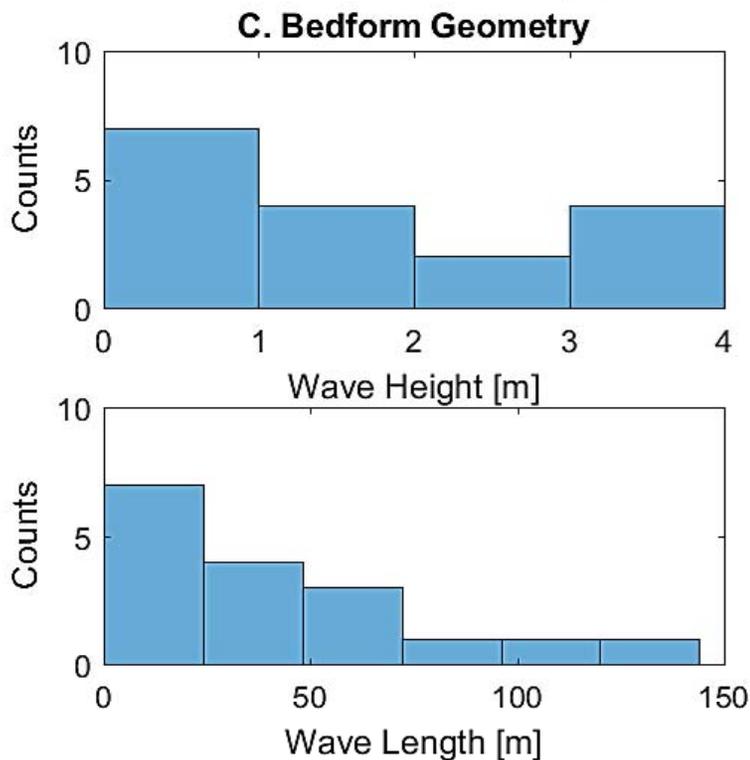
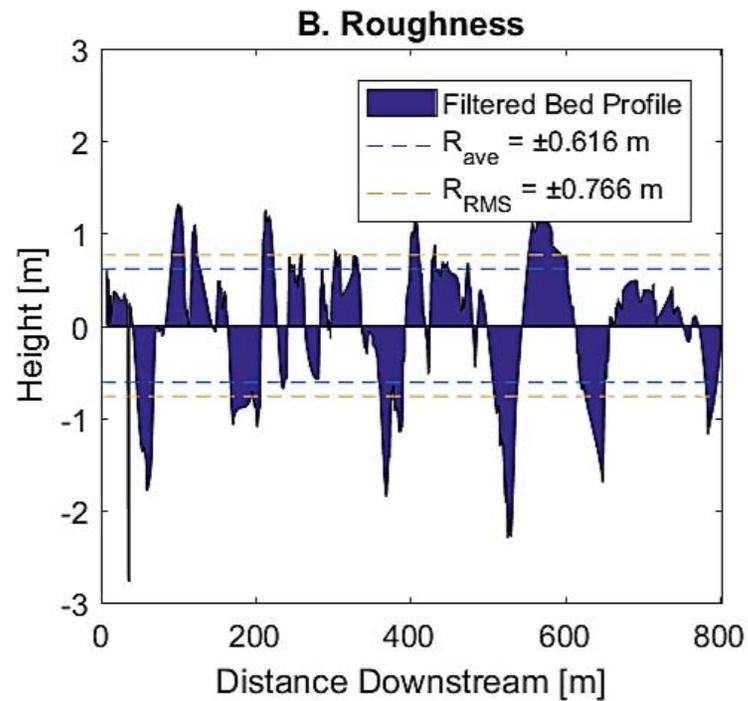
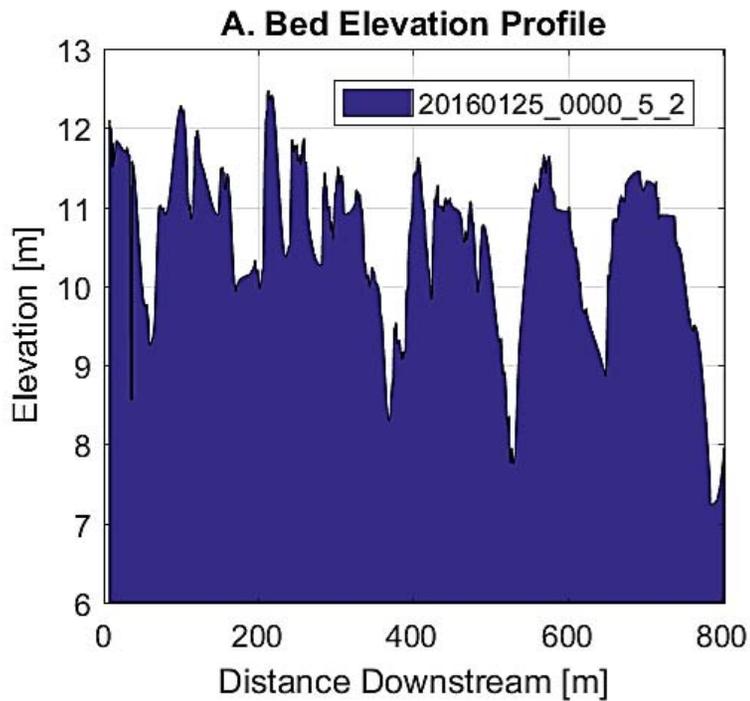


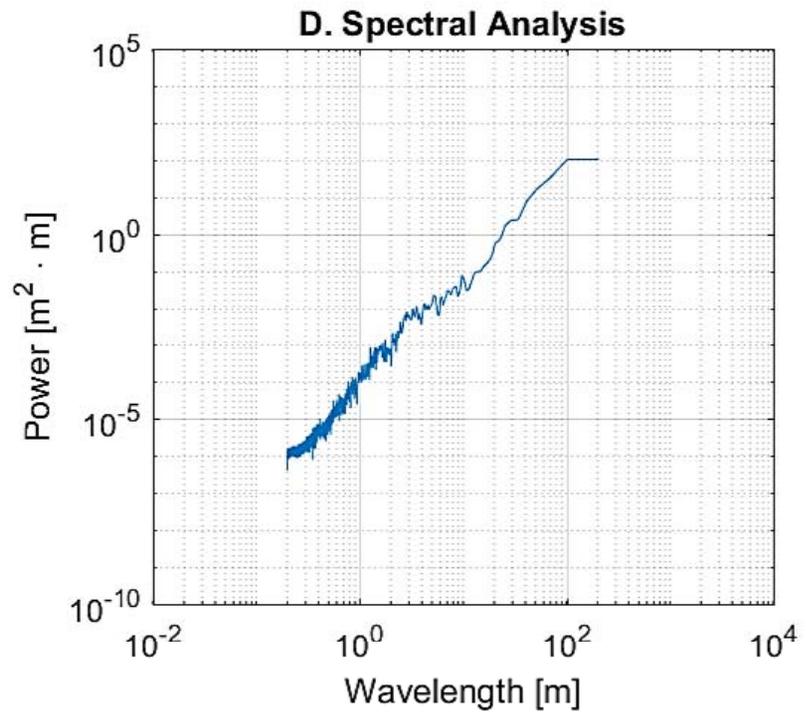
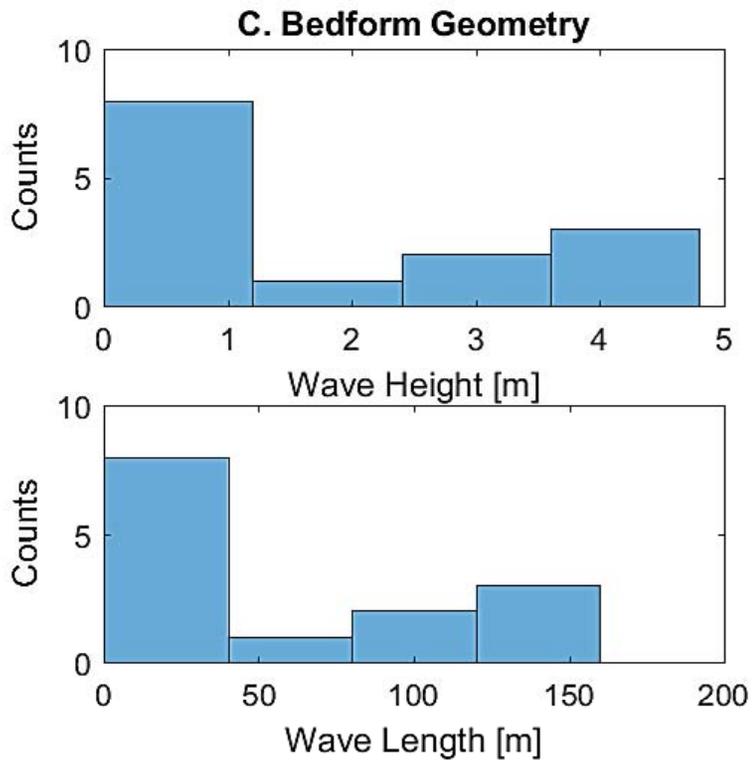
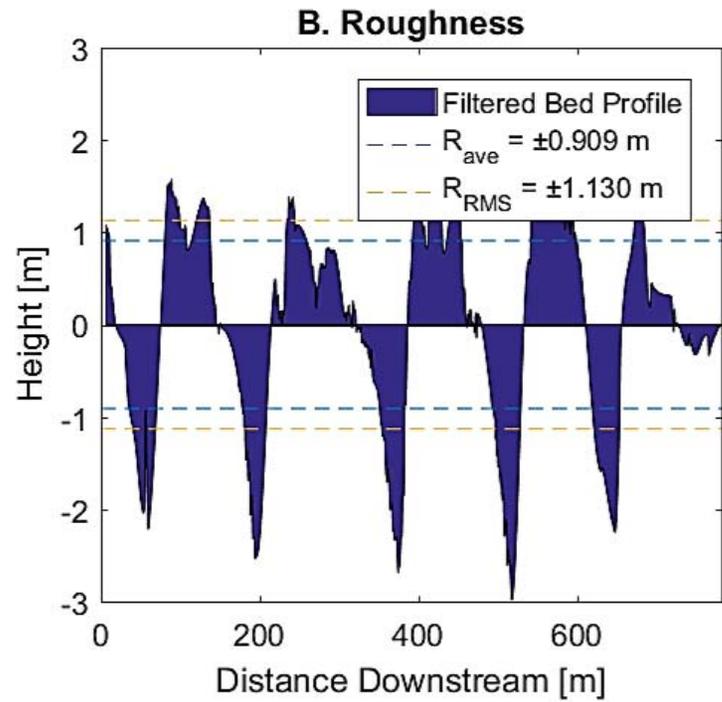
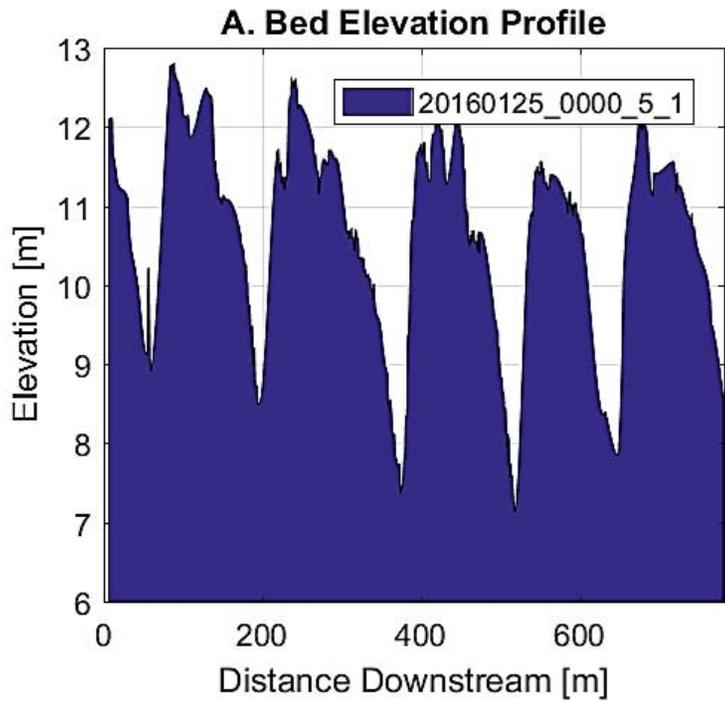




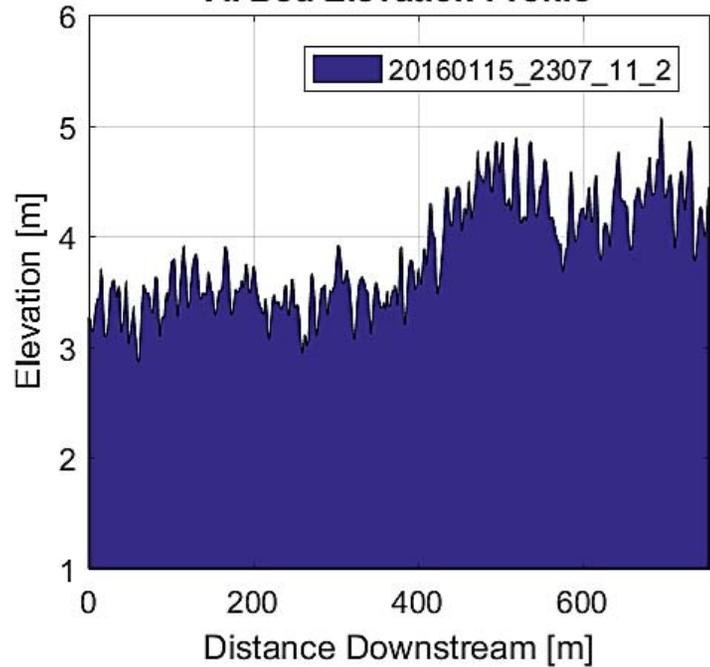




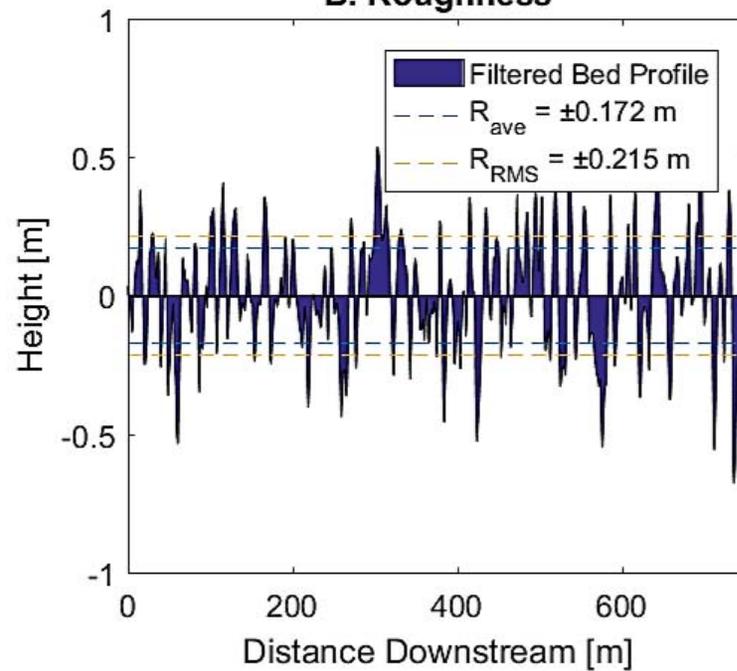




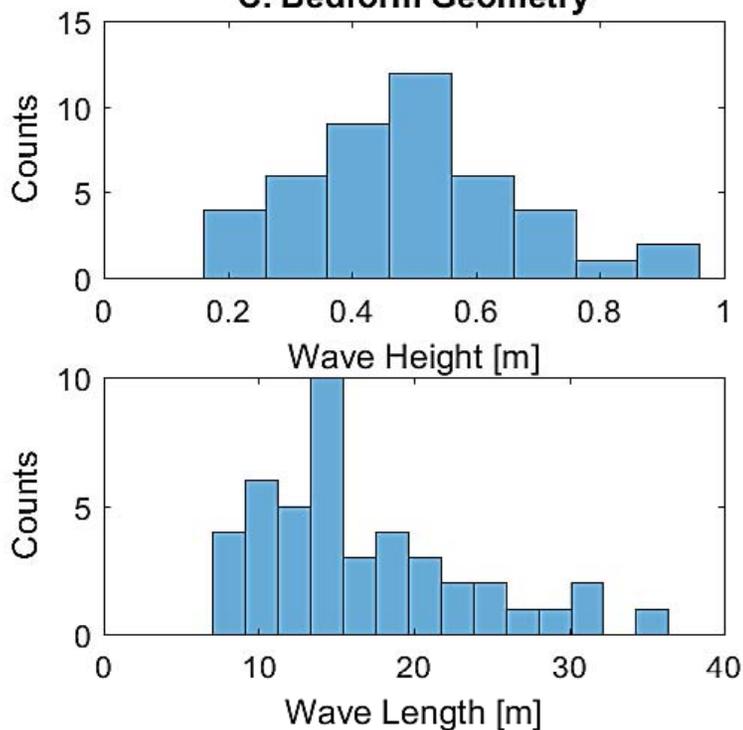
**A. Bed Elevation Profile**



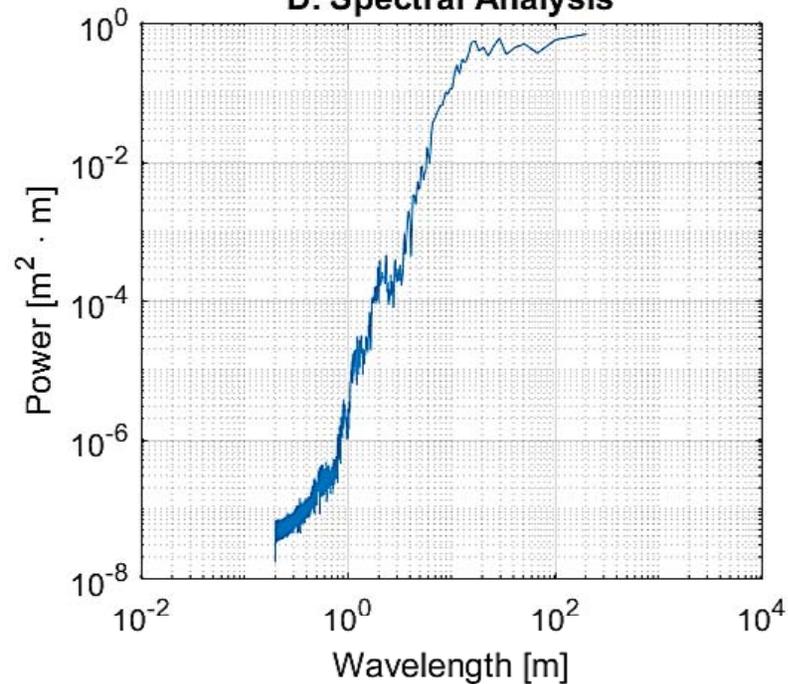
**B. Roughness**



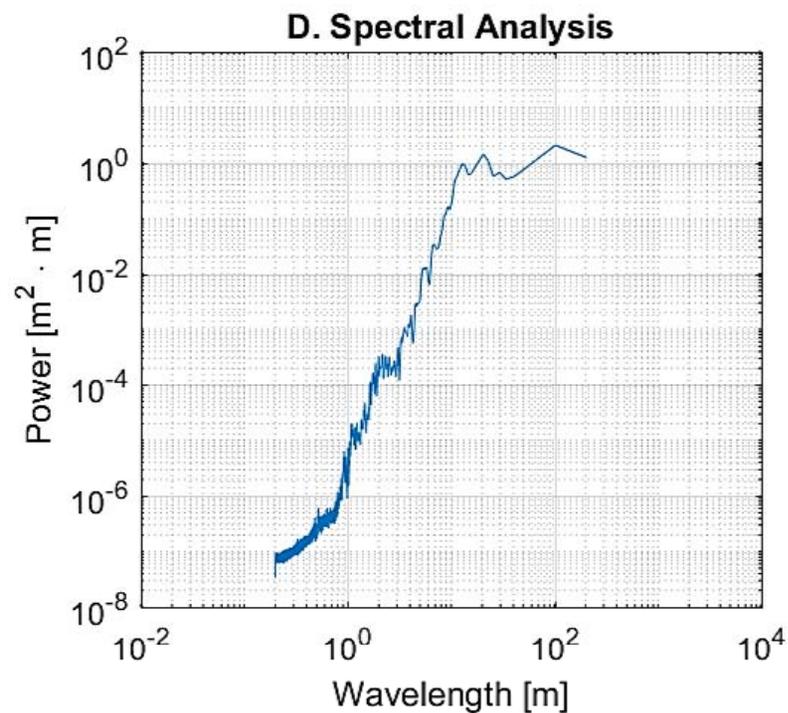
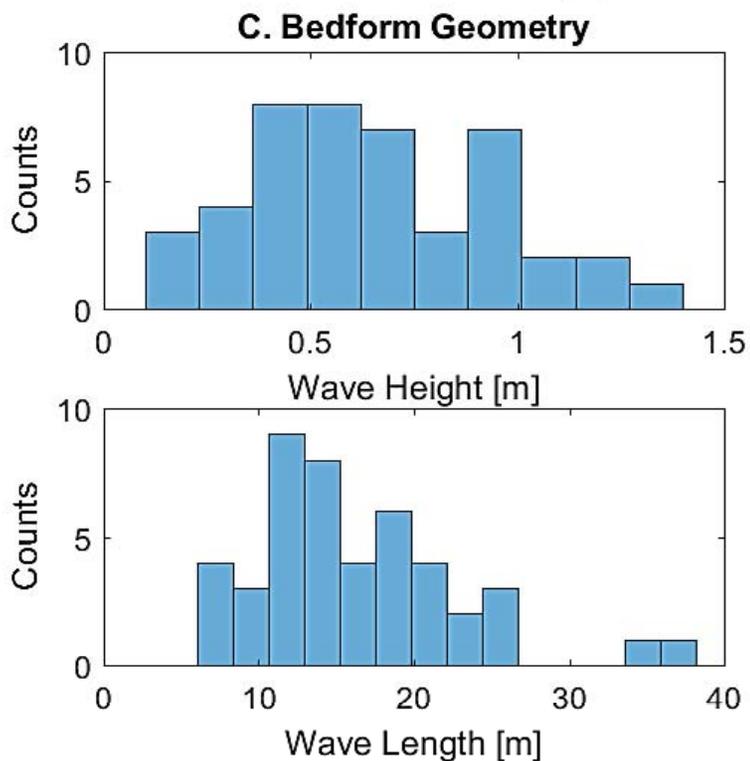
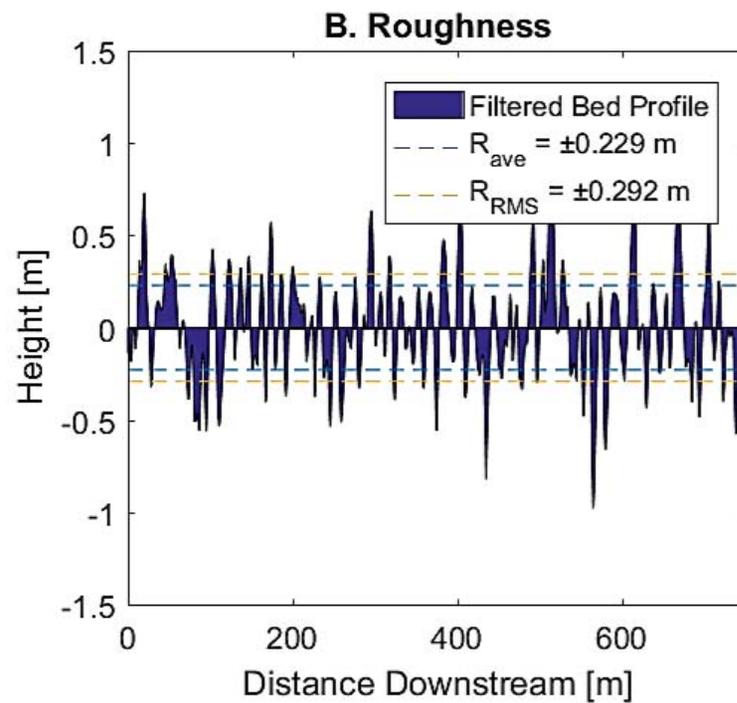
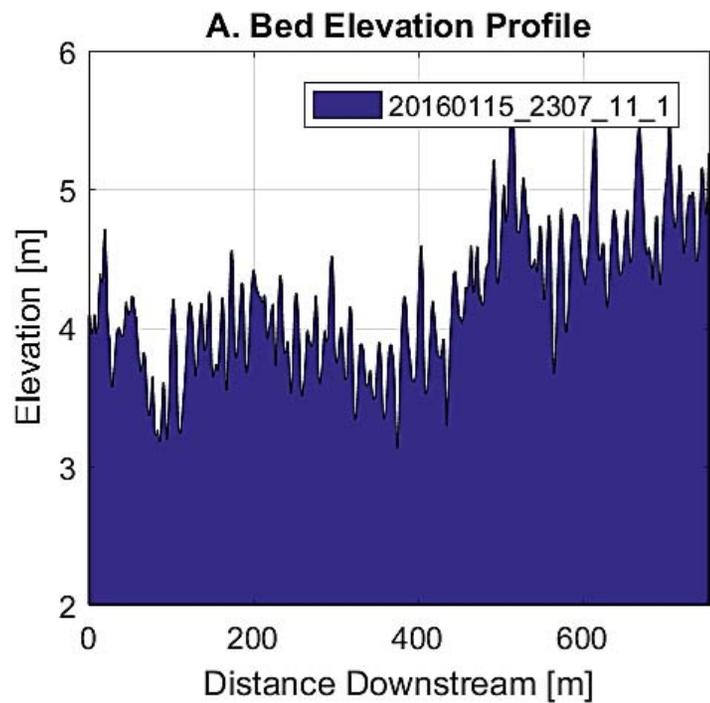
**C. Bedform Geometry**

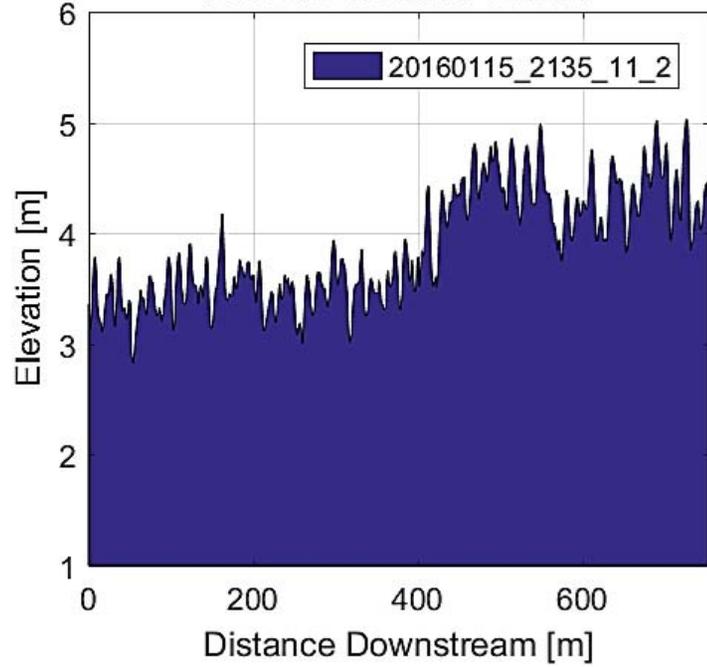
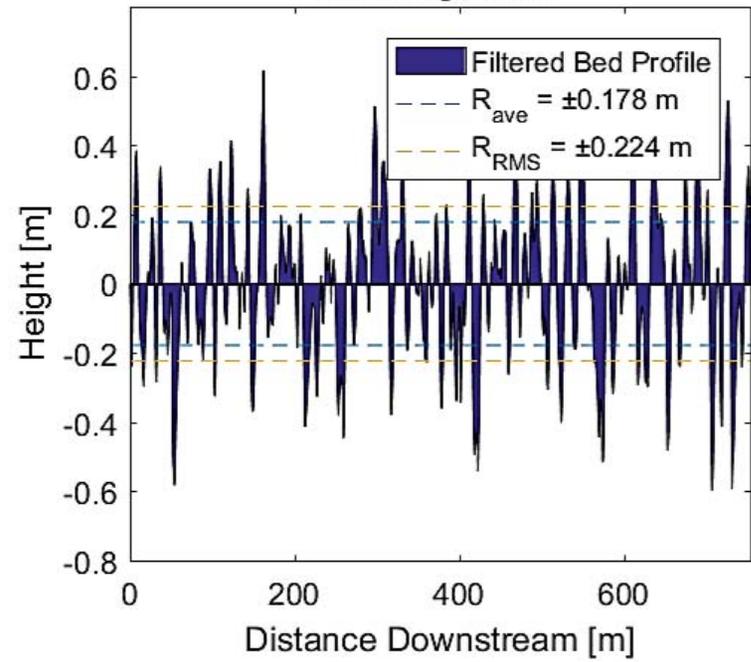
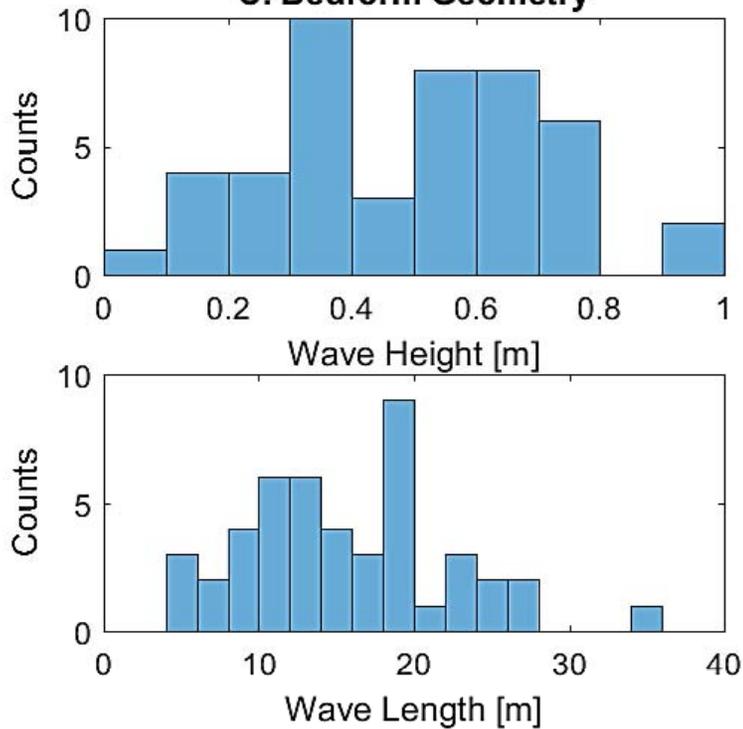
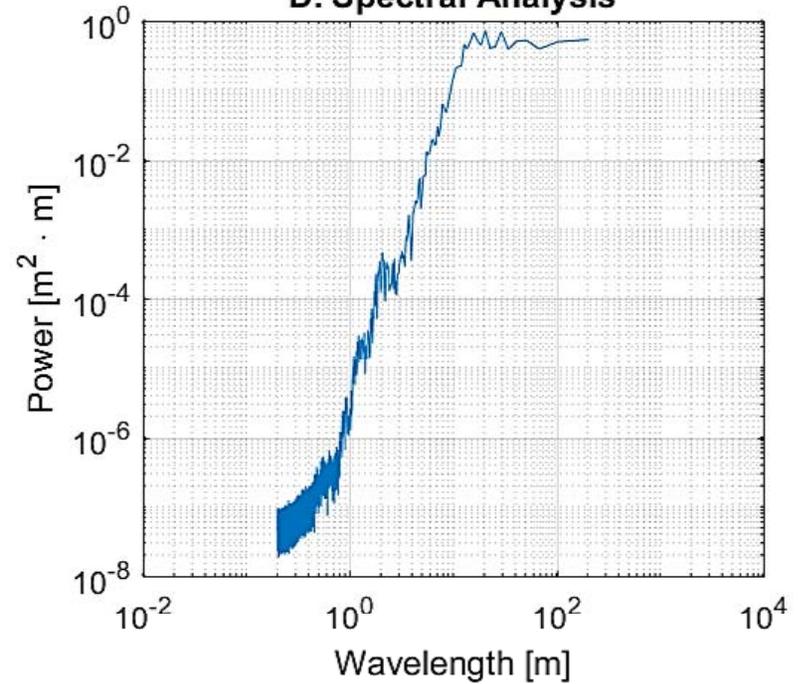


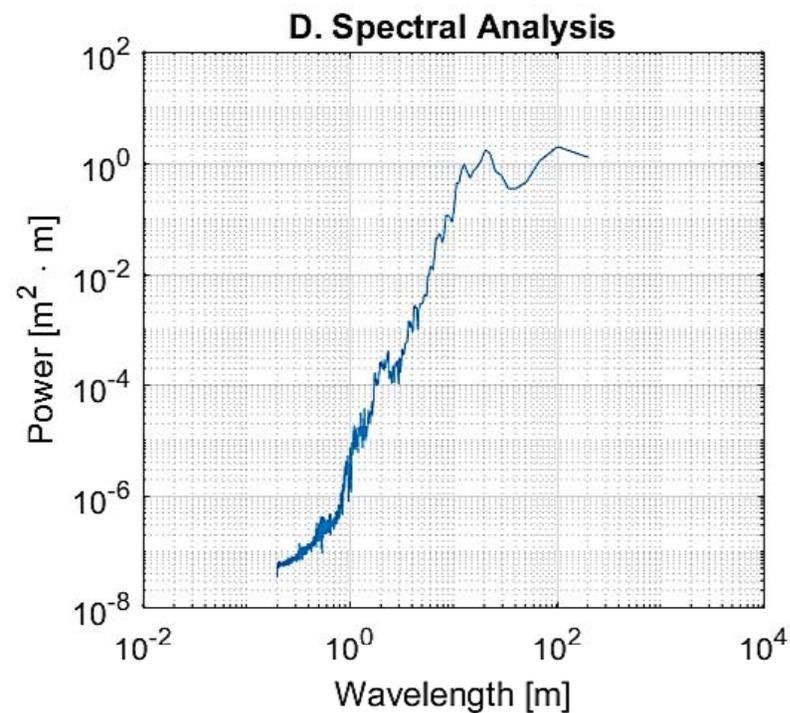
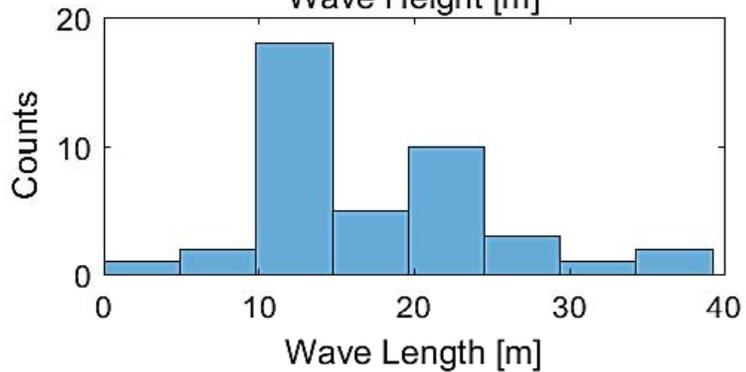
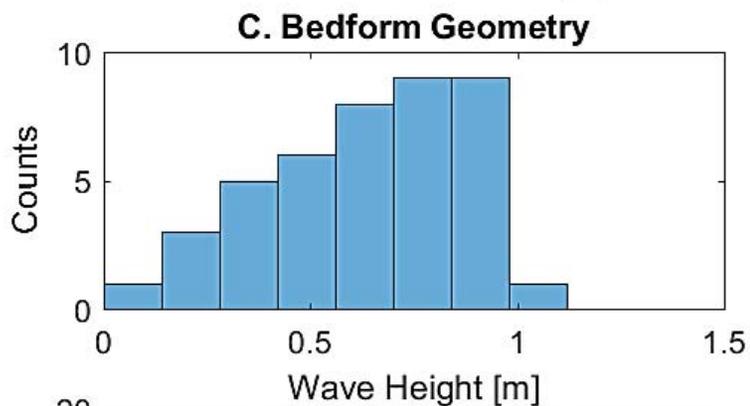
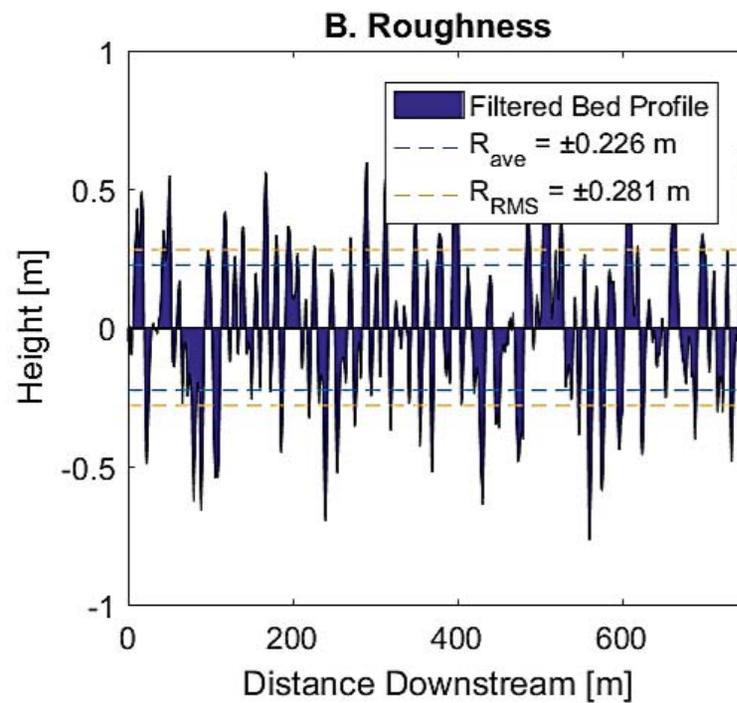
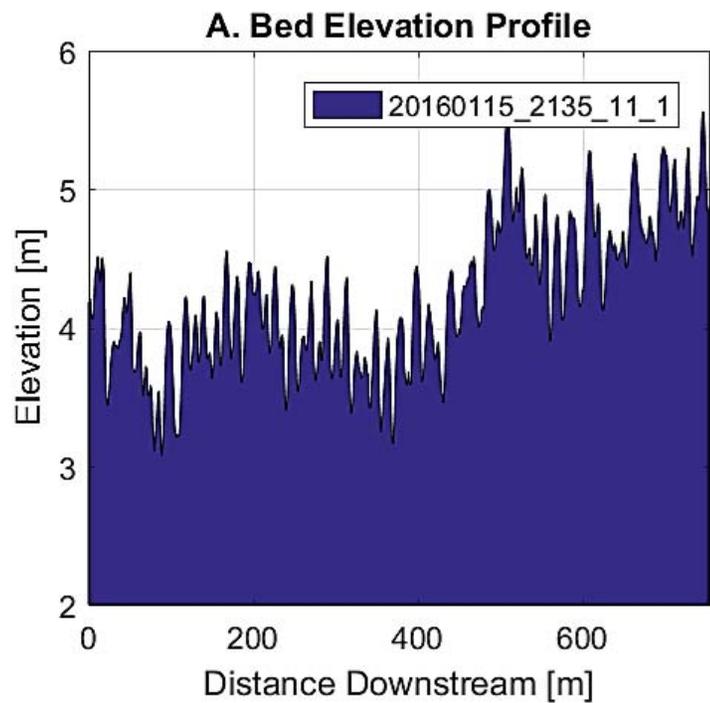
**D. Spectral Analysis**

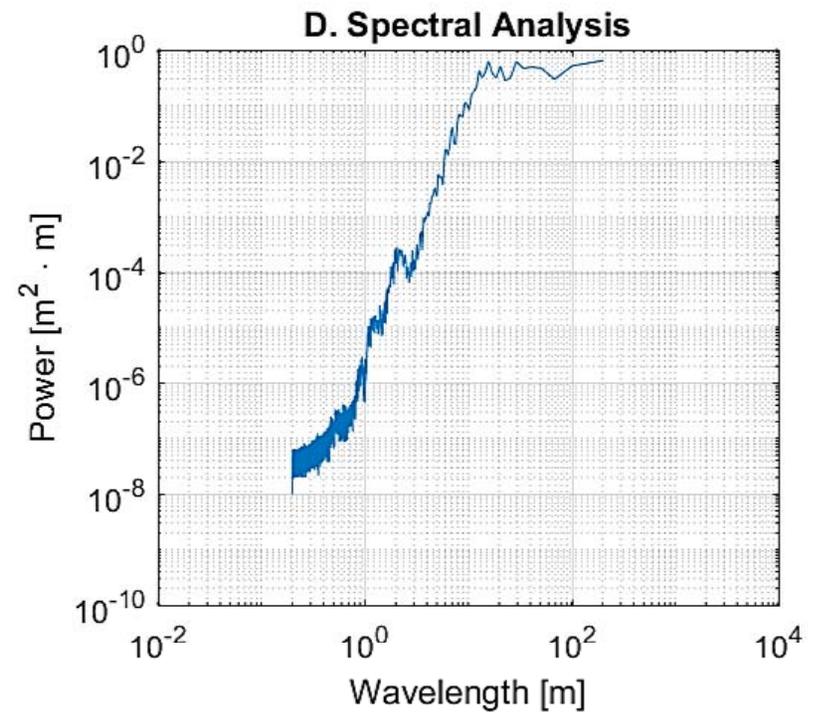
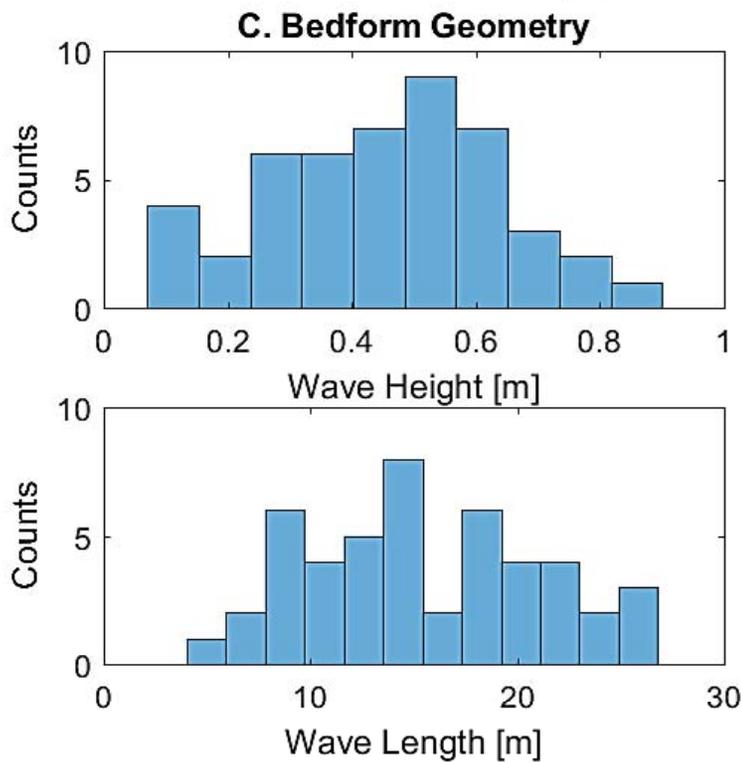
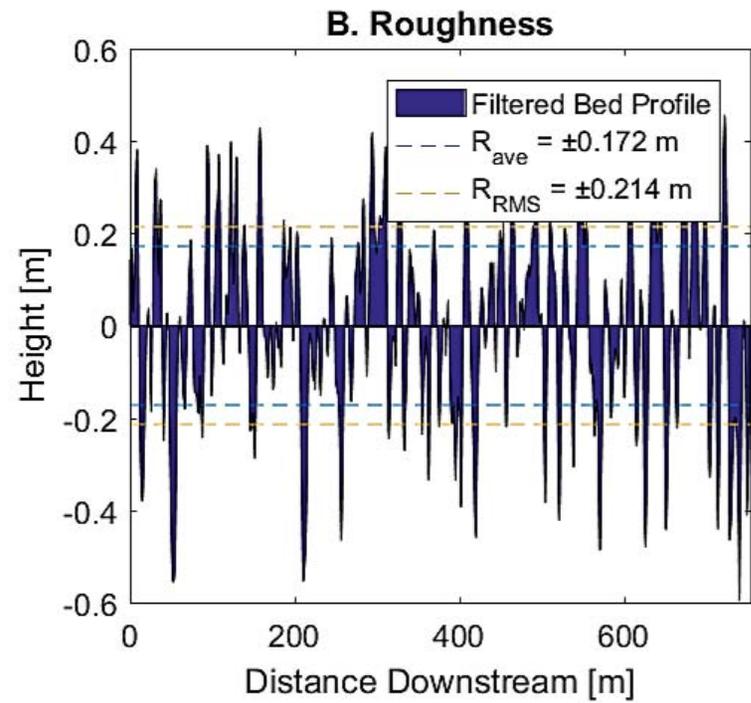
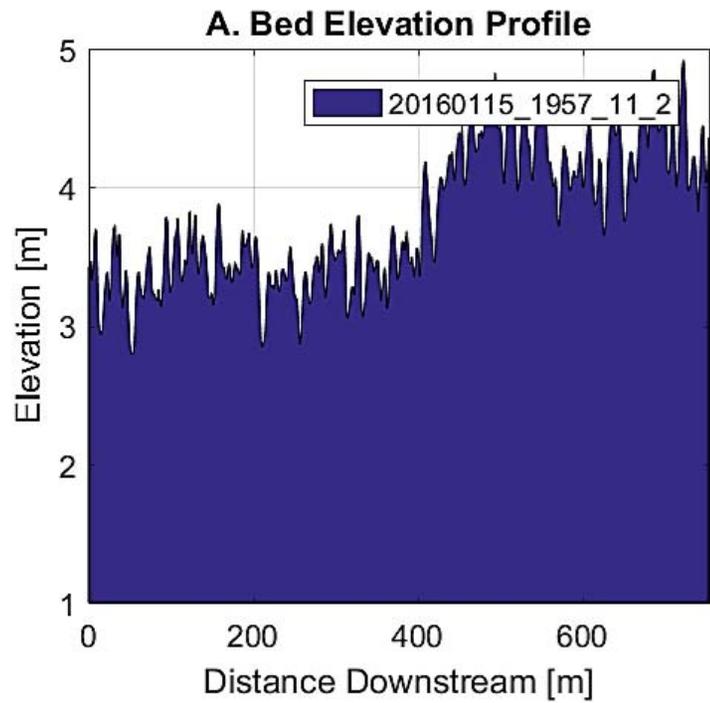


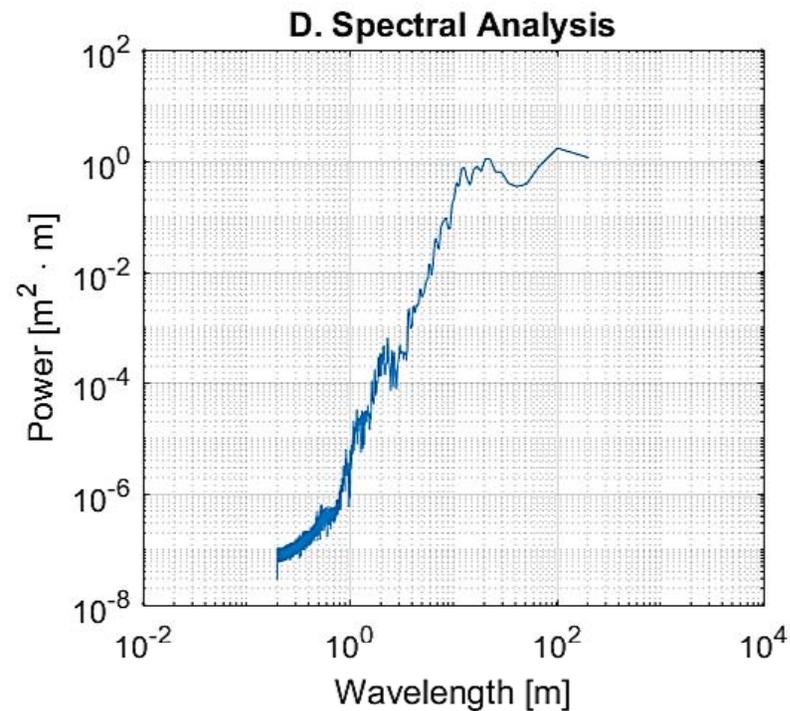
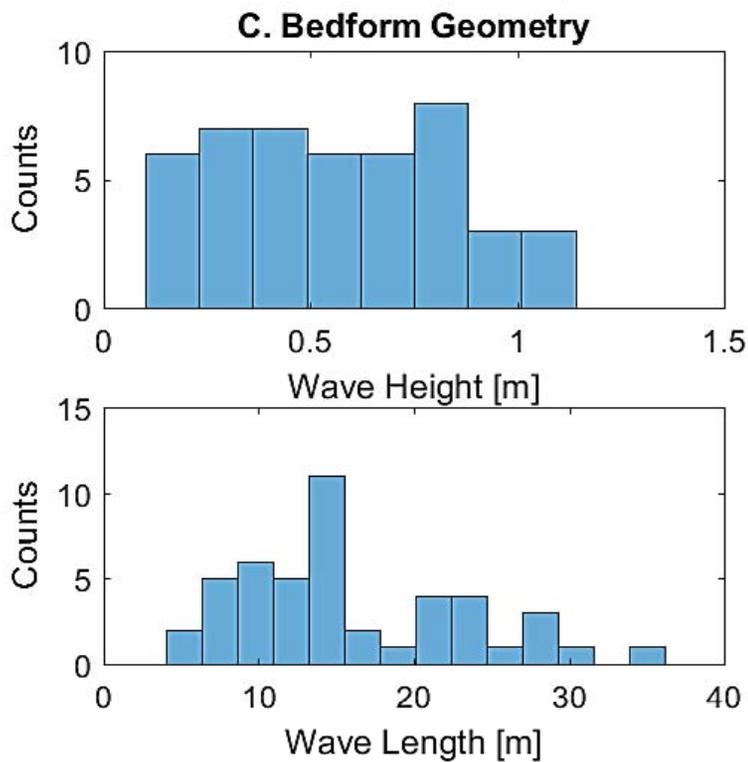
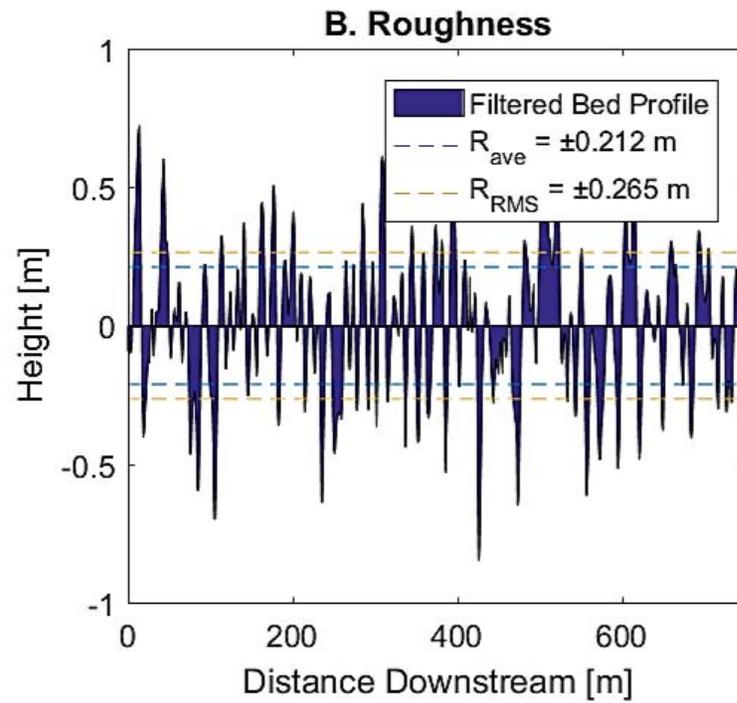
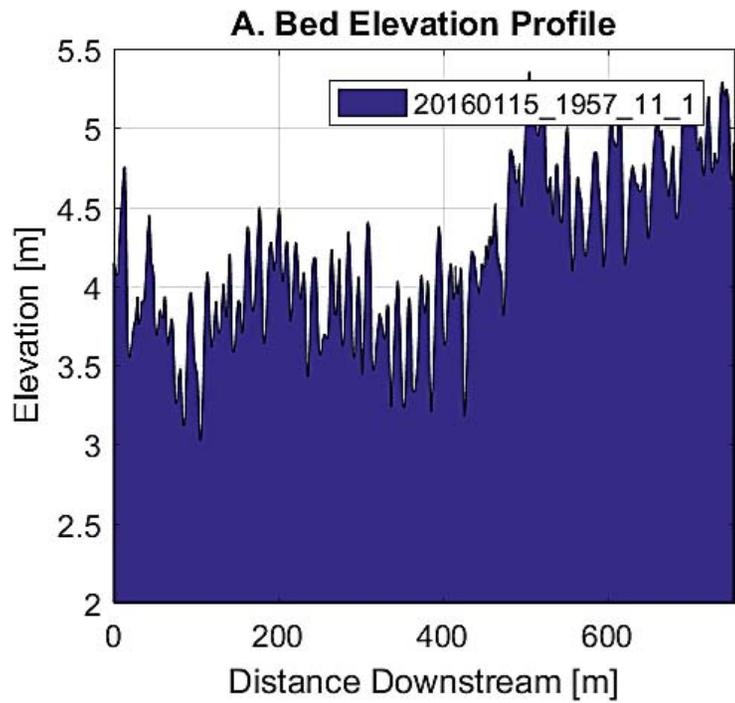


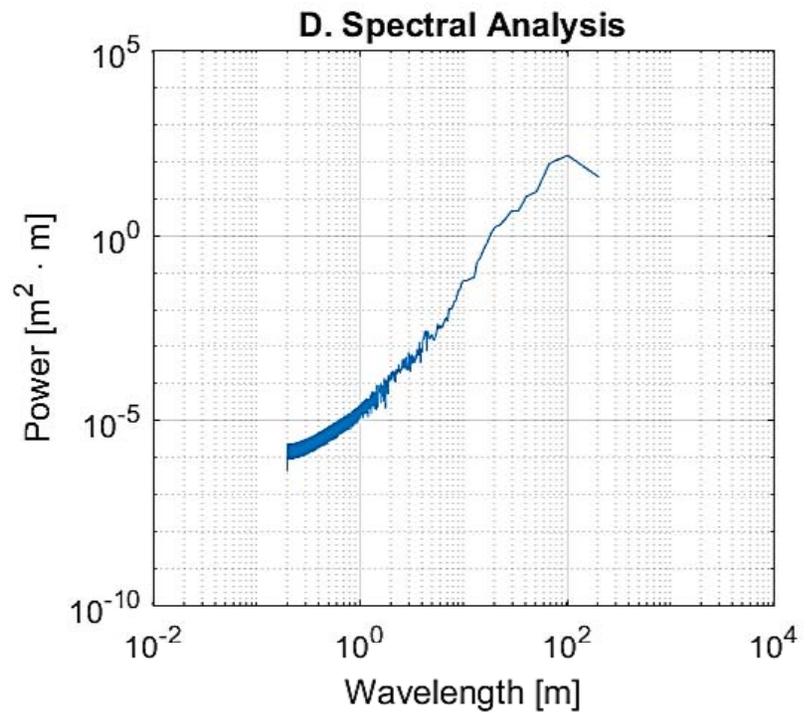
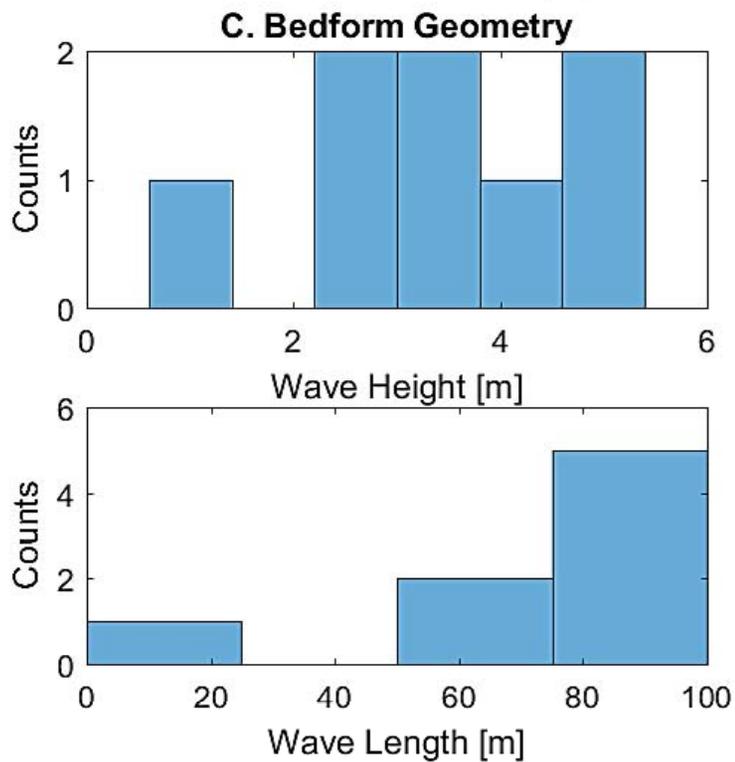
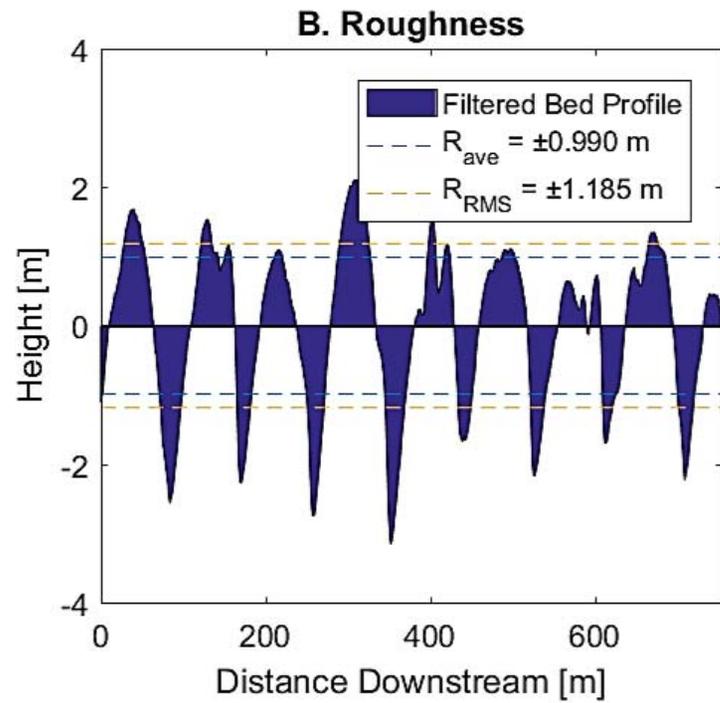
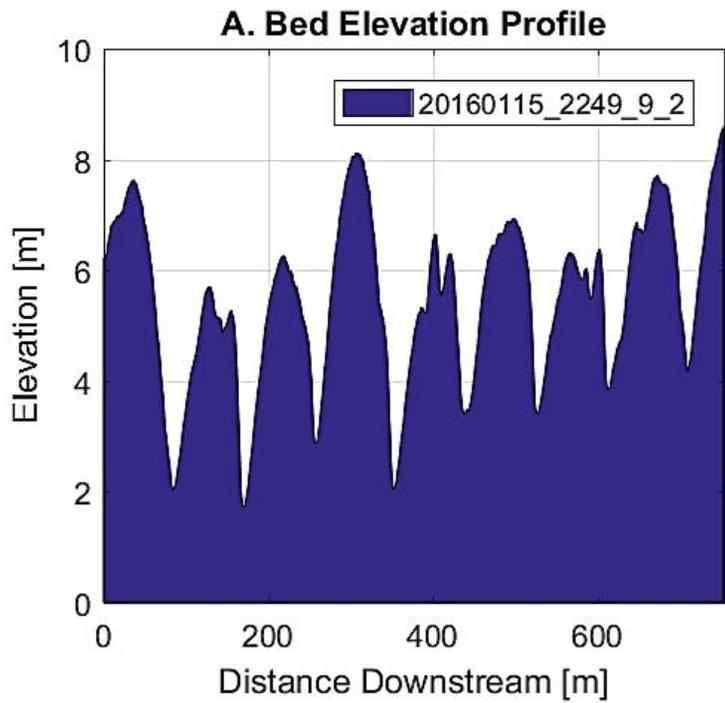


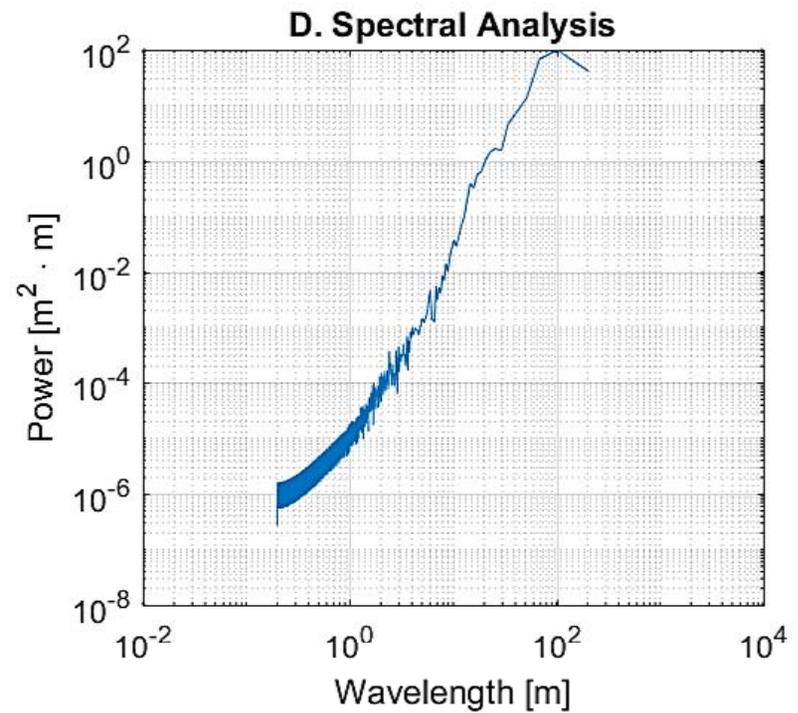
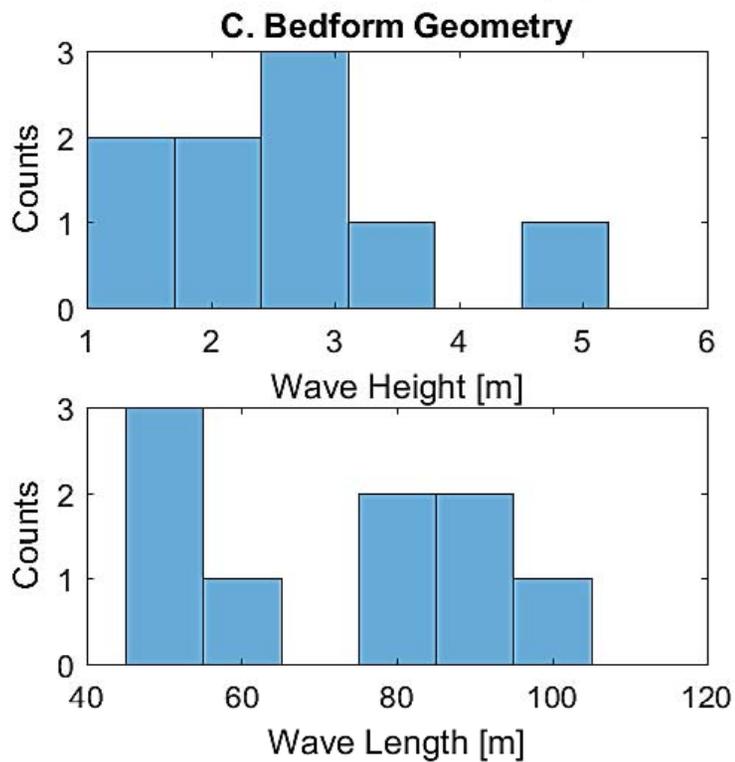
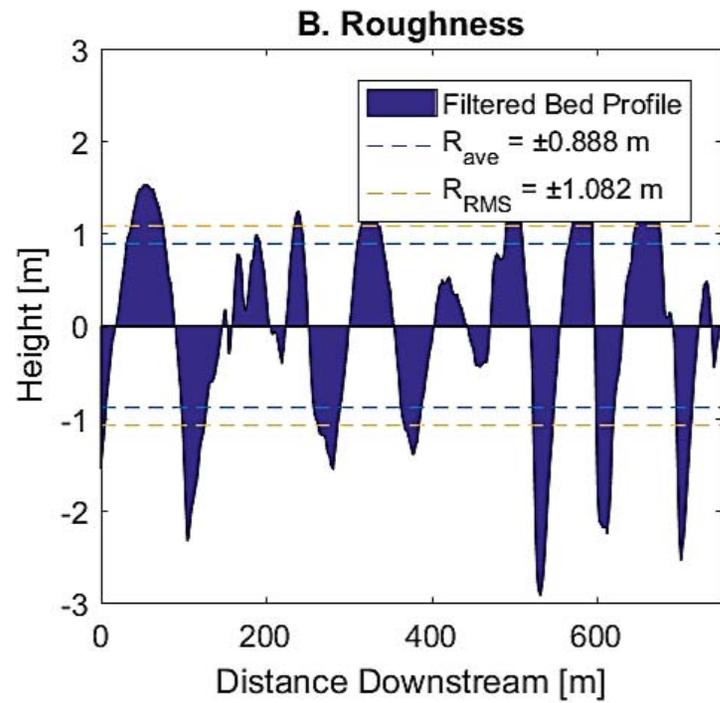
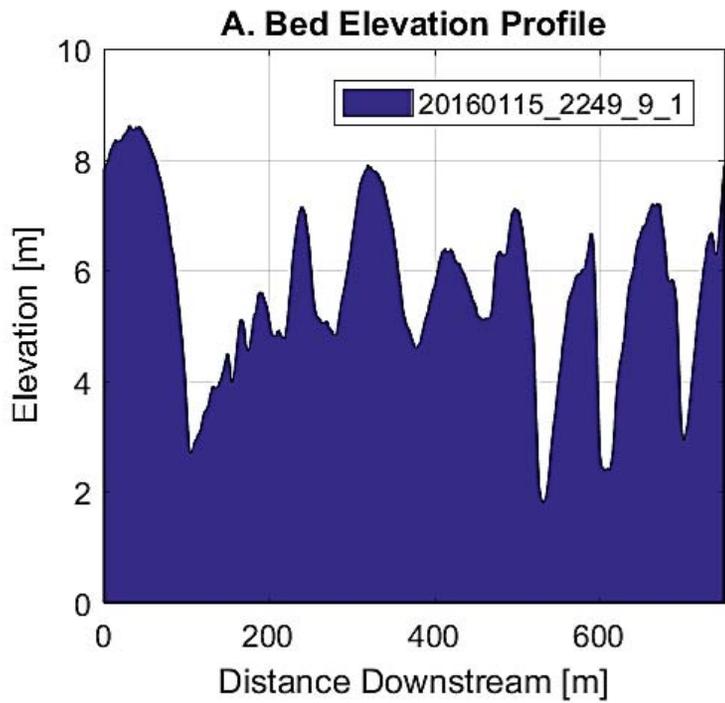
**A. Bed Elevation Profile****B. Roughness****C. Bedform Geometry****D. Spectral Analysis**

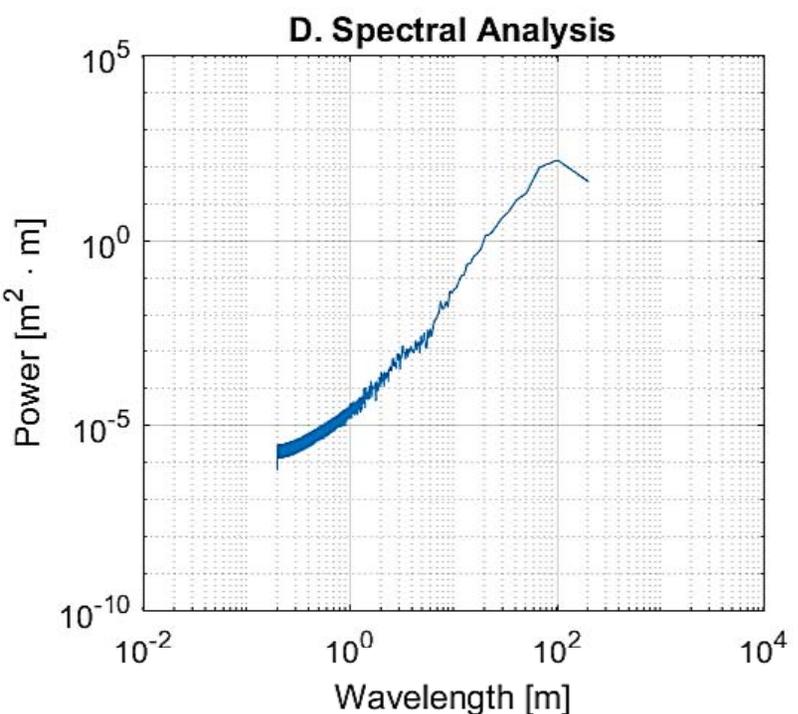
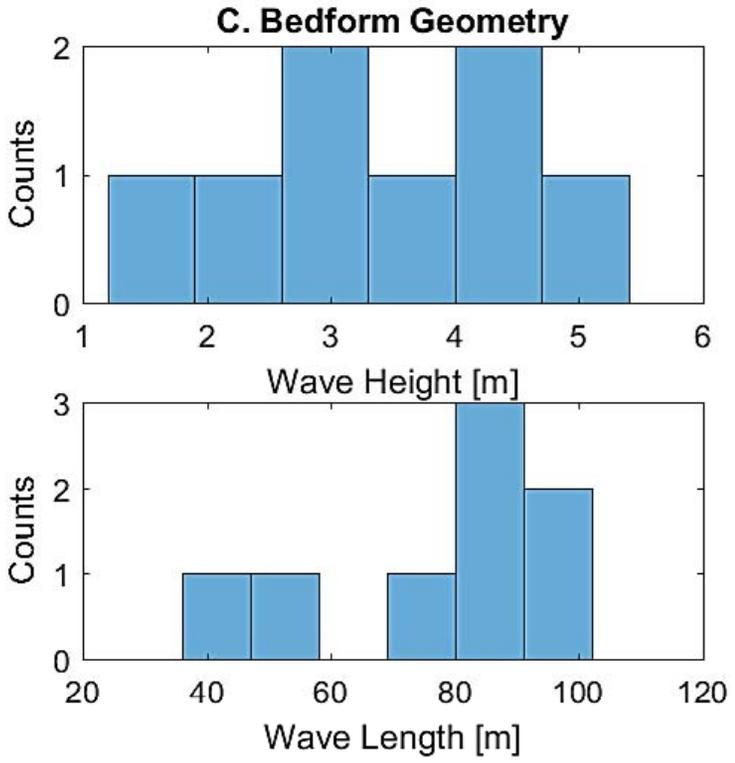
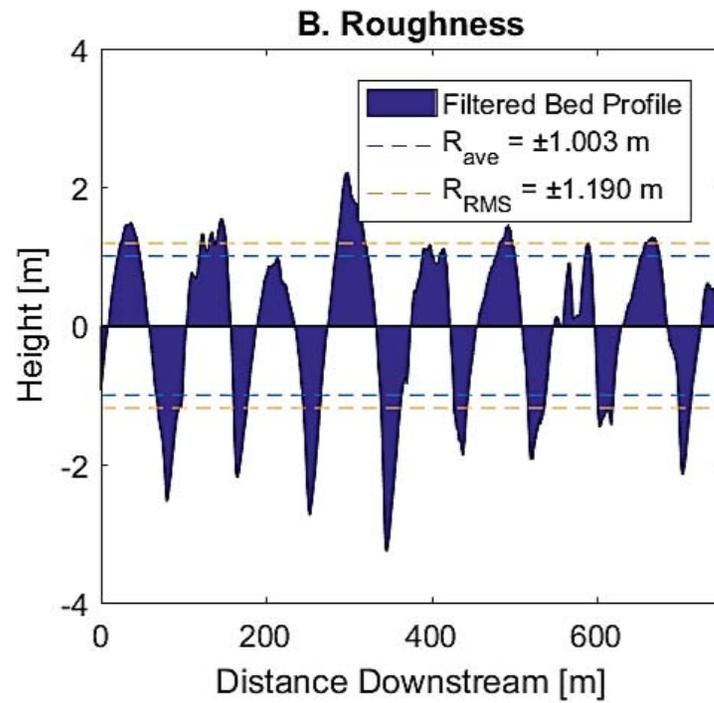
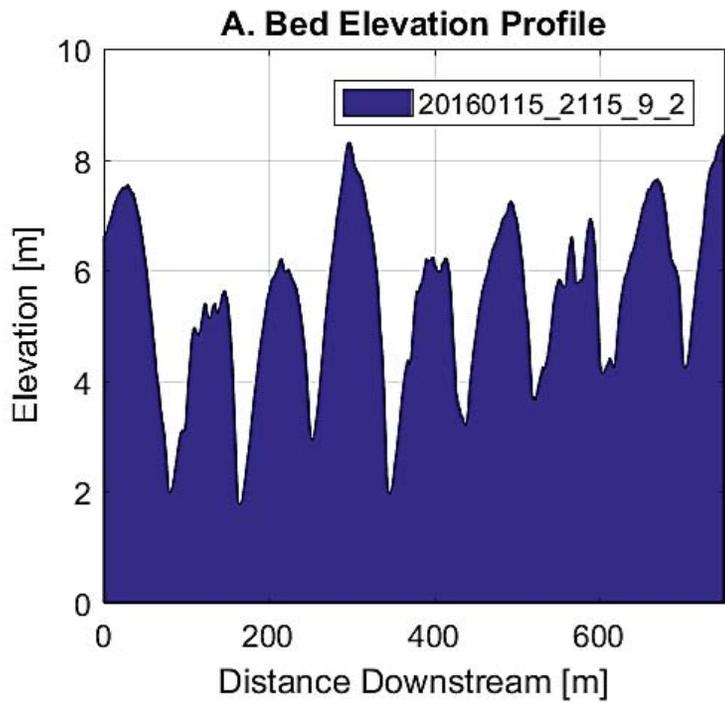




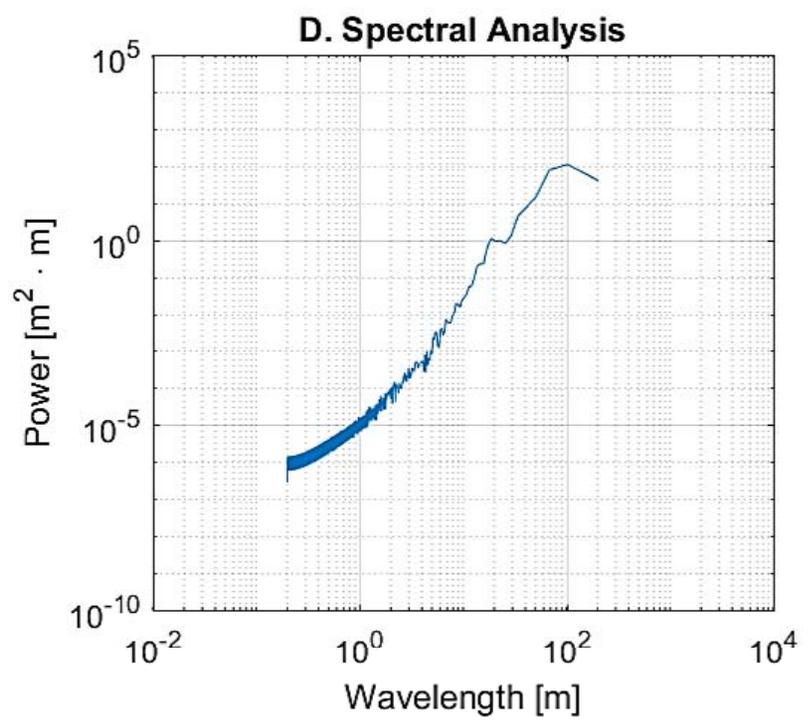
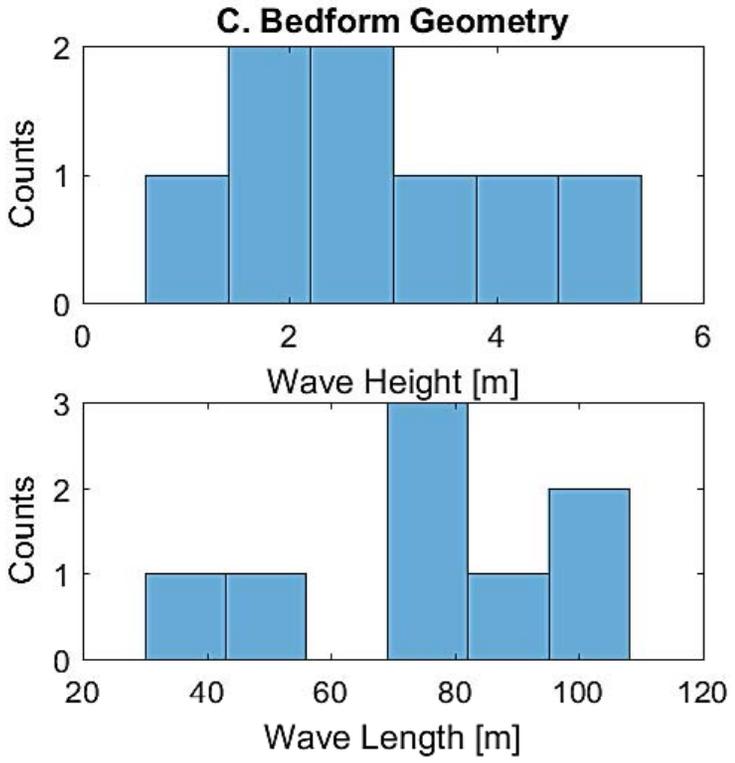
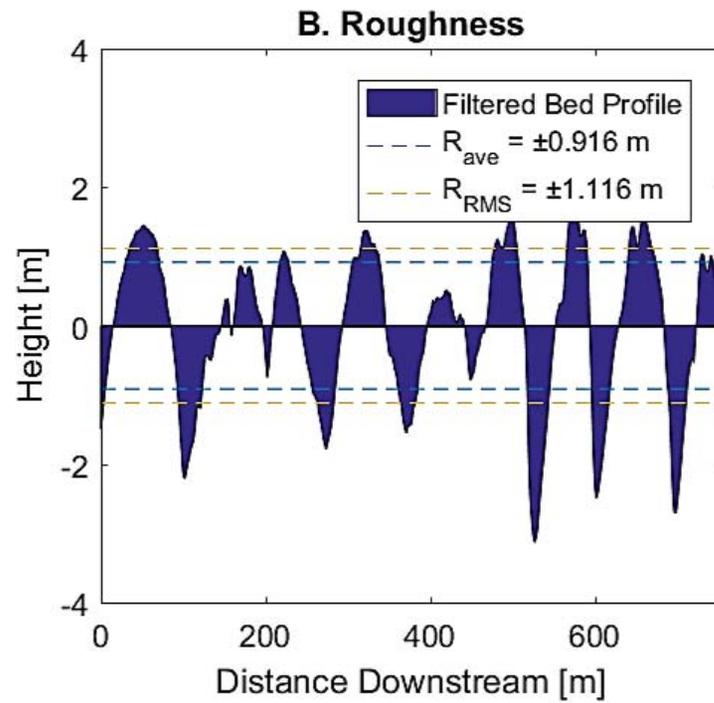
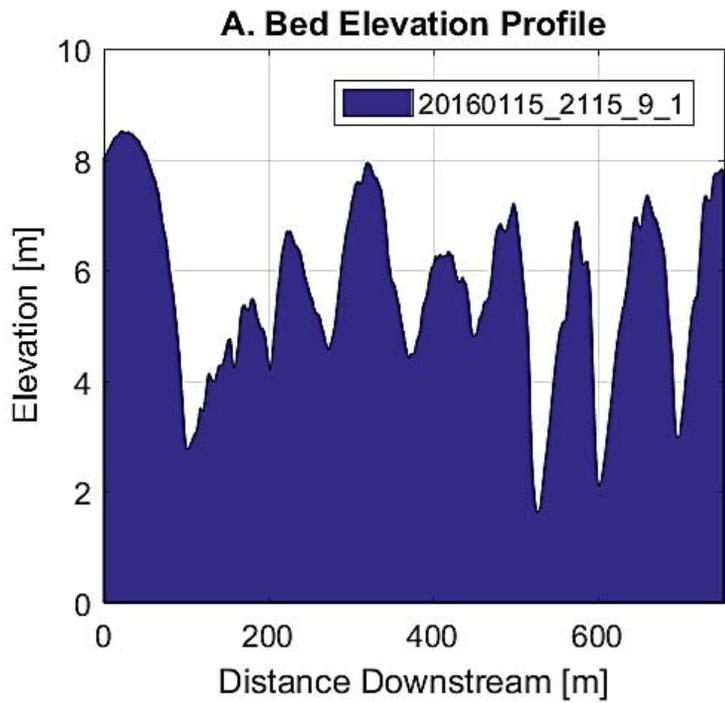


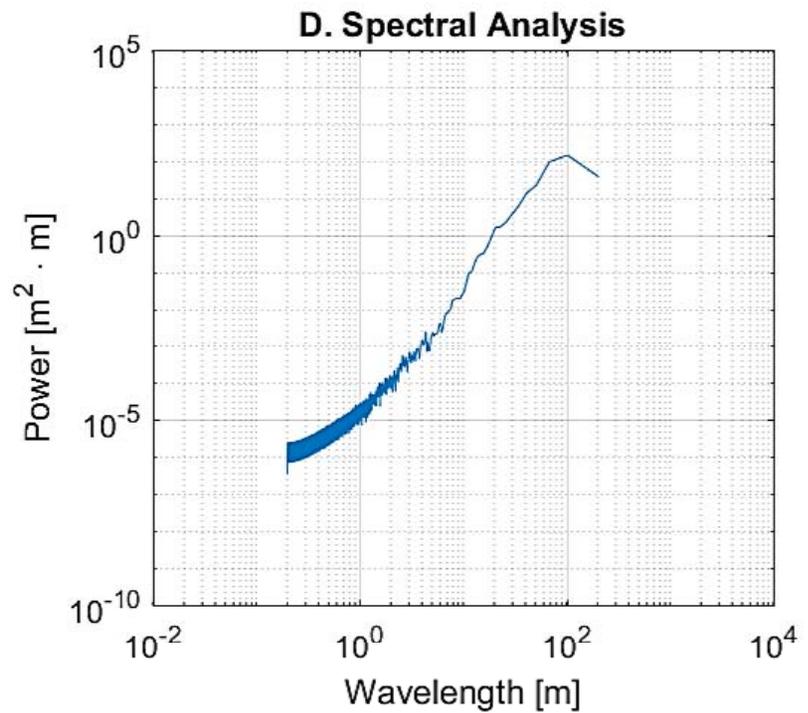
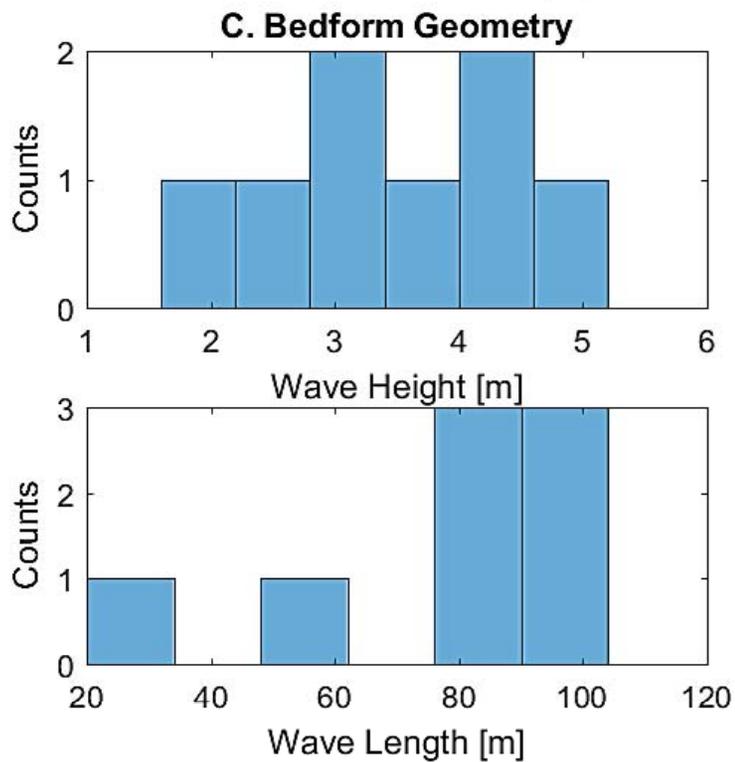
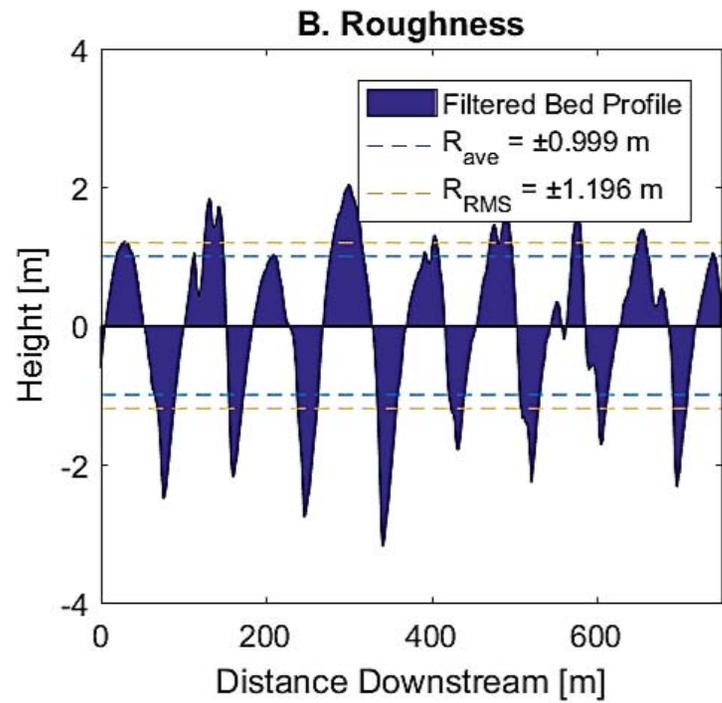
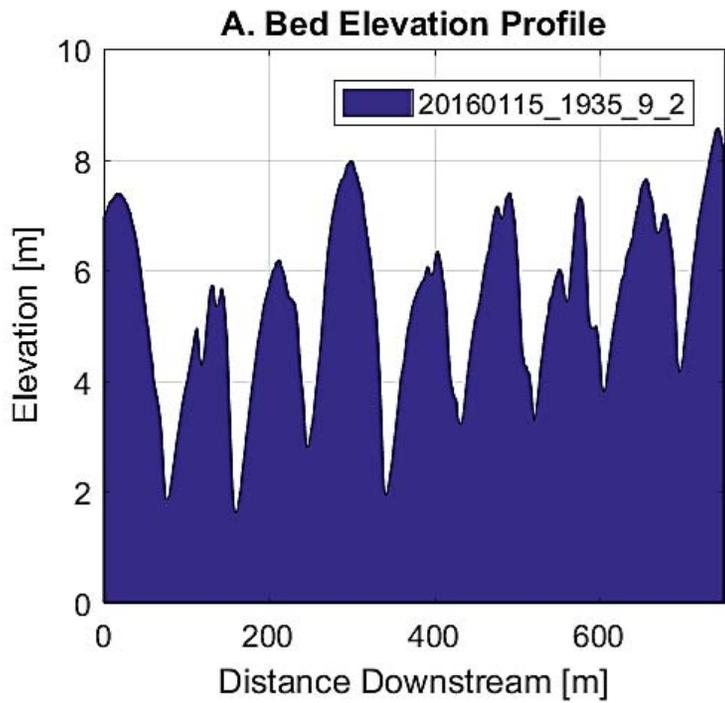


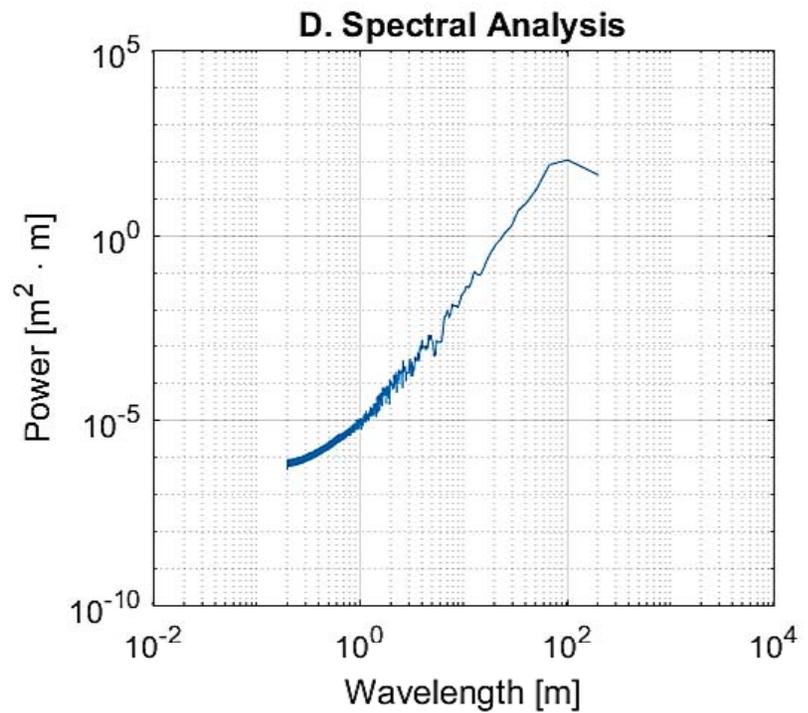
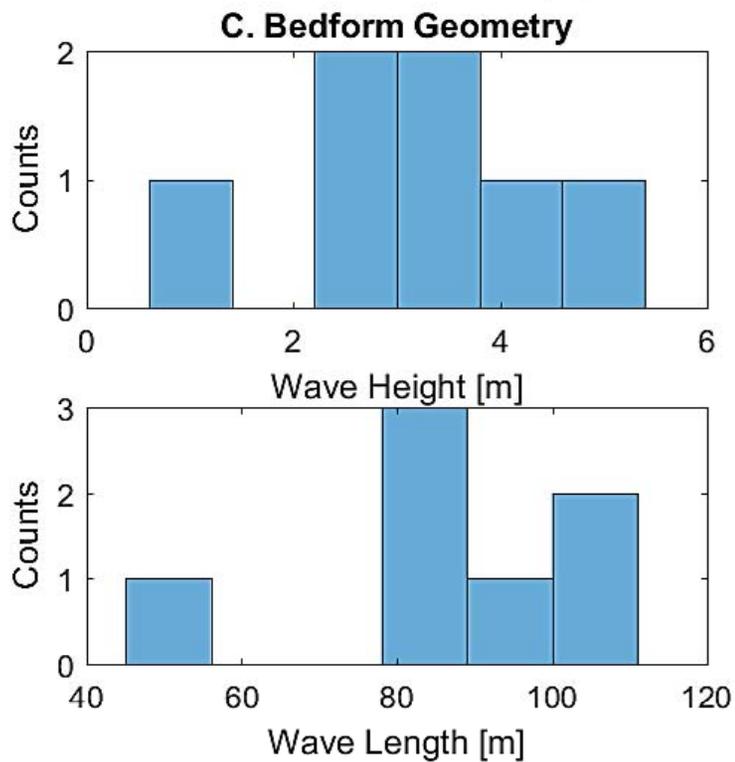
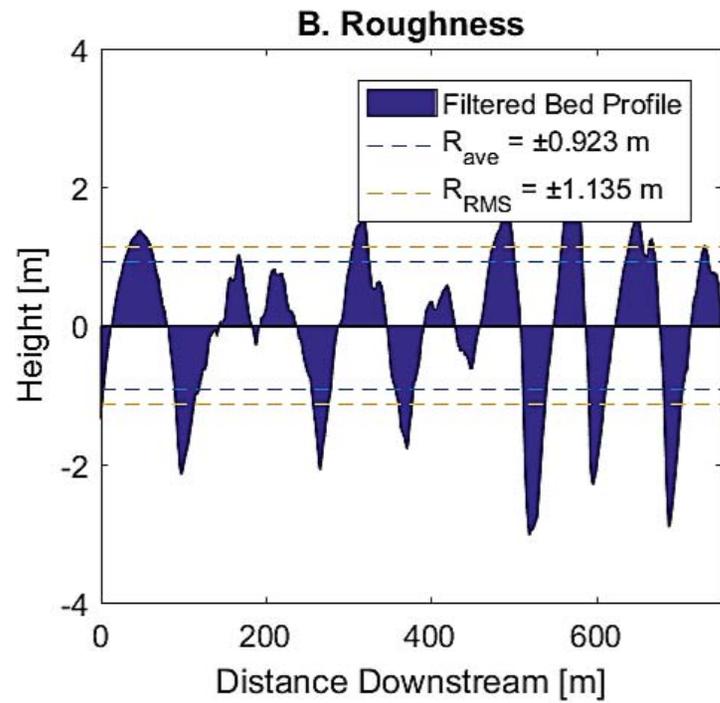
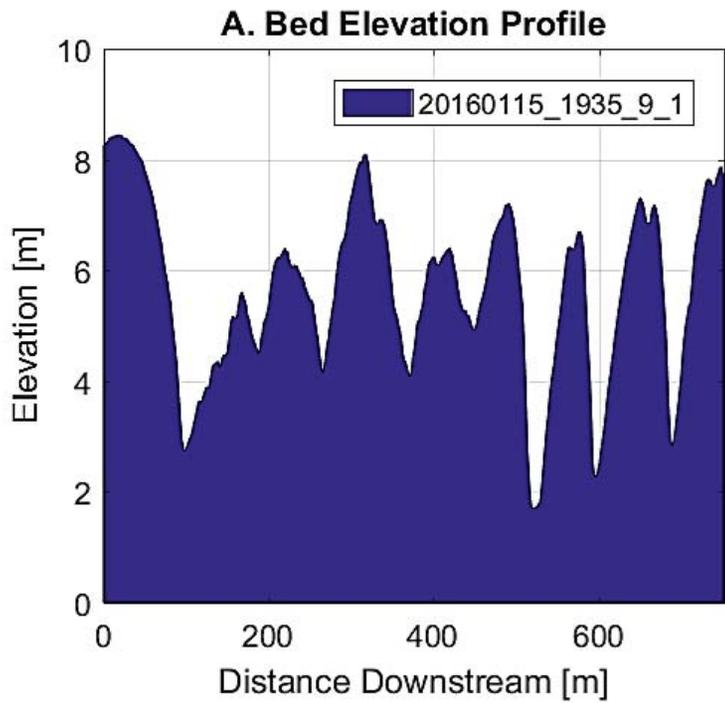


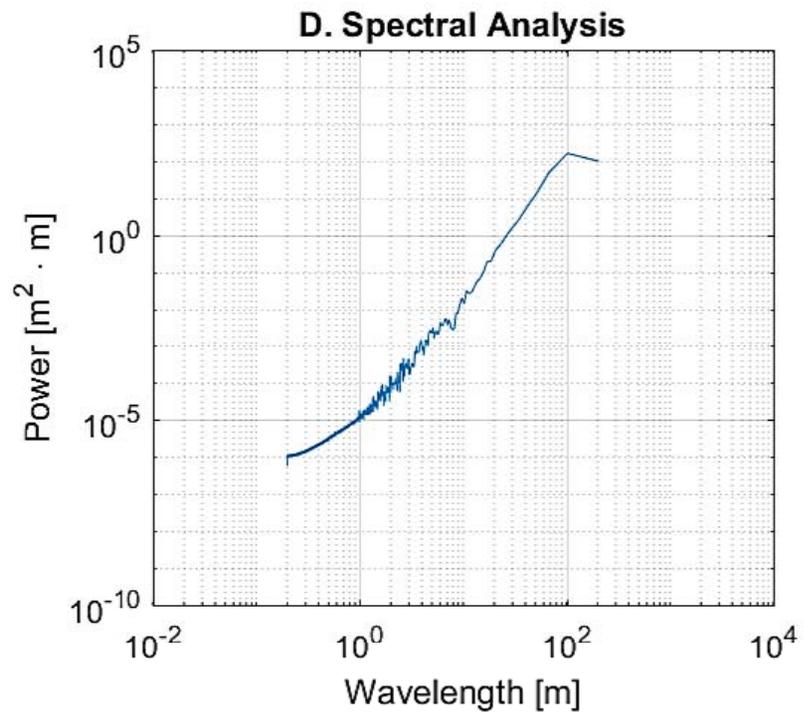
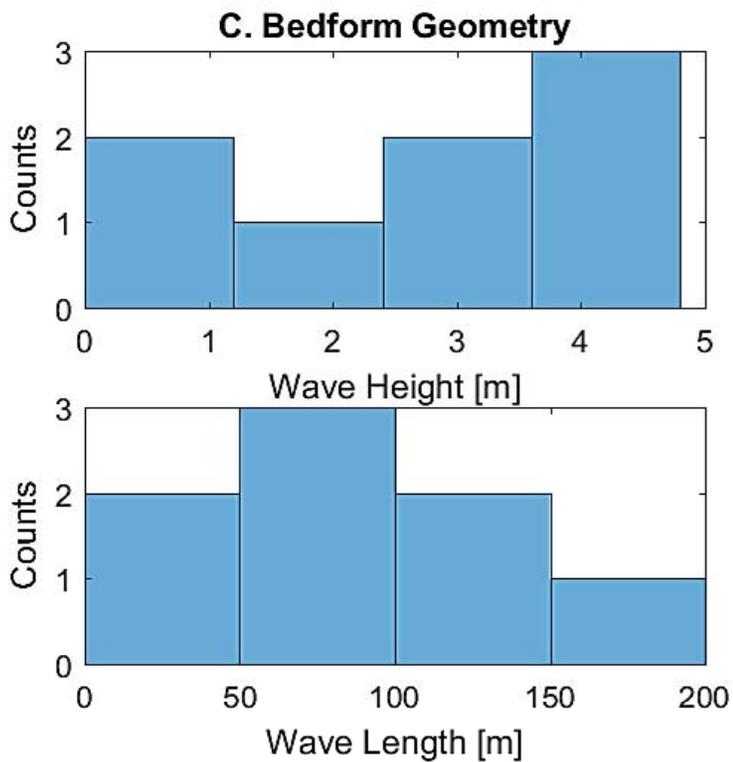
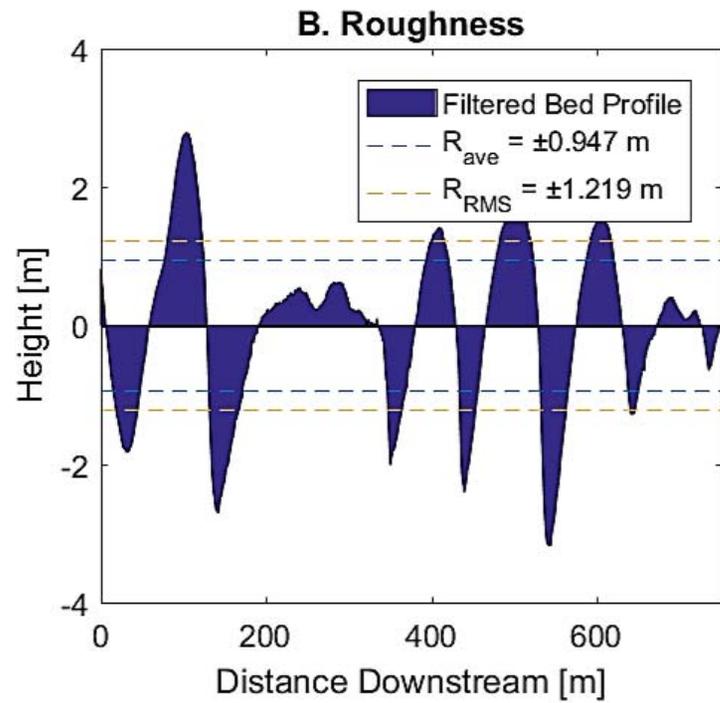
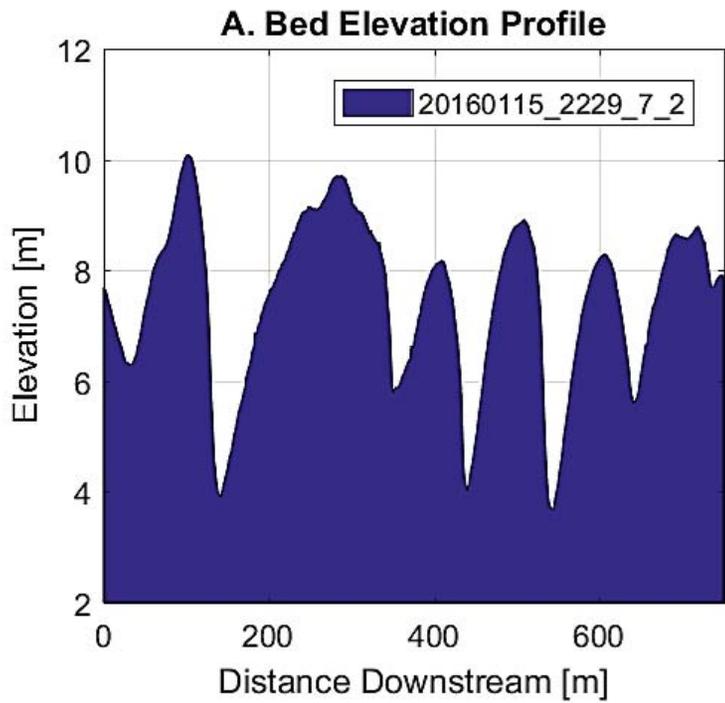


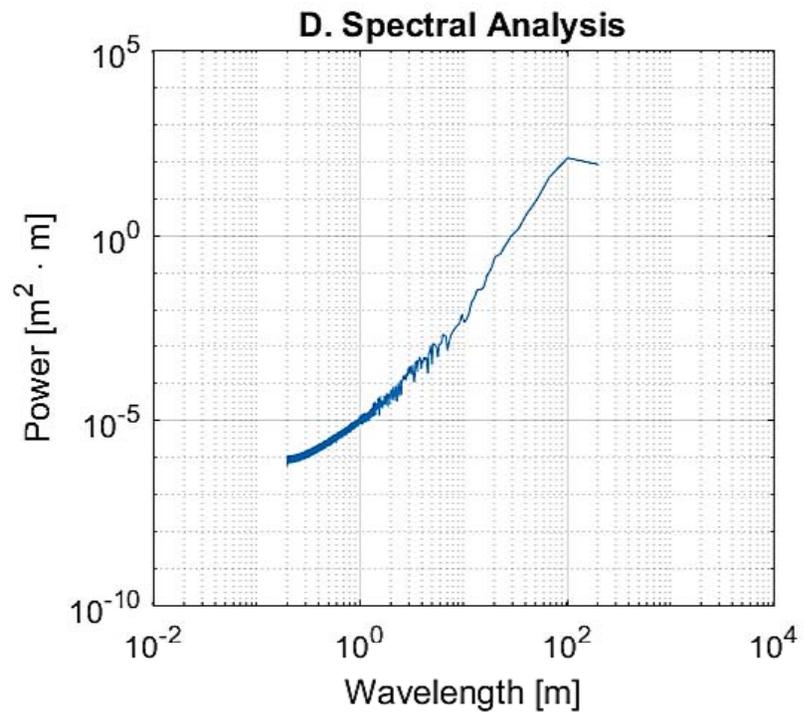
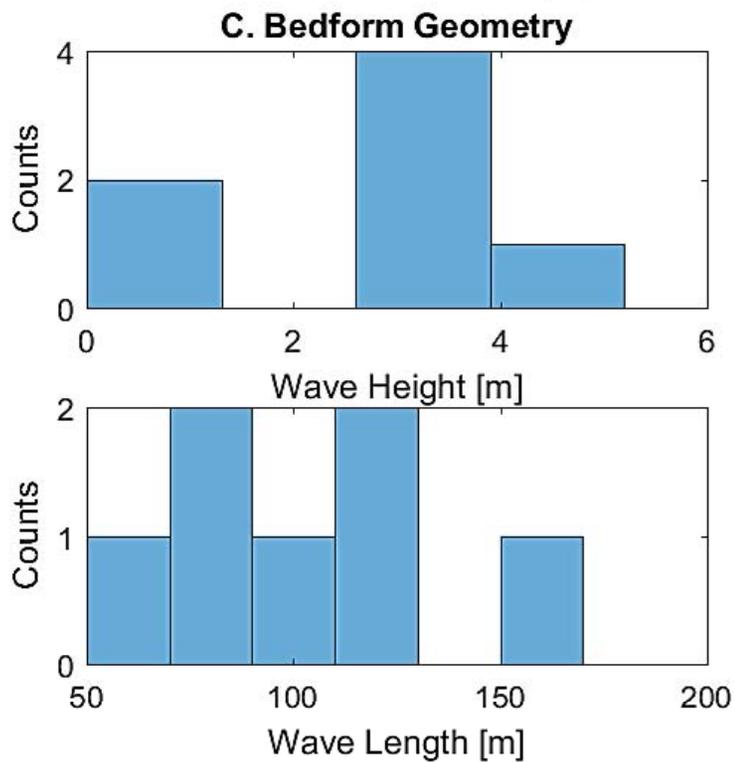
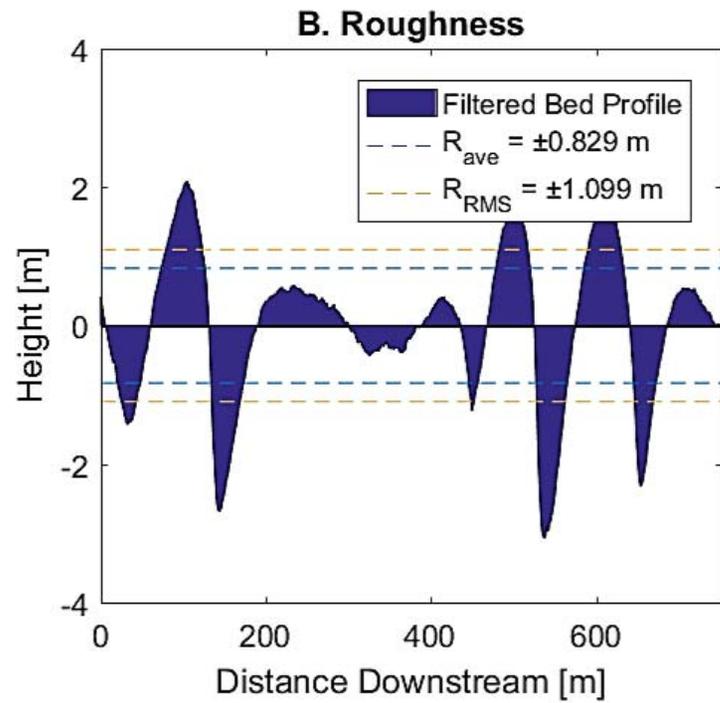
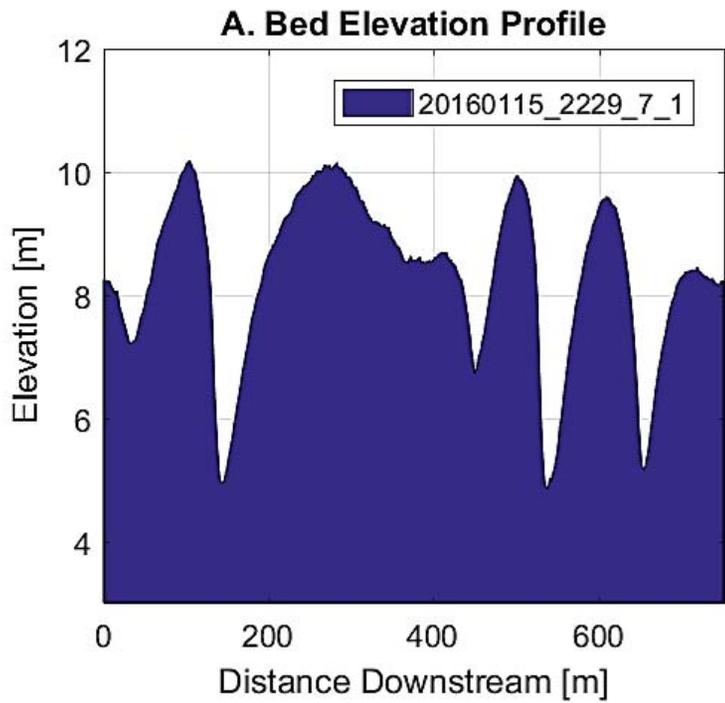


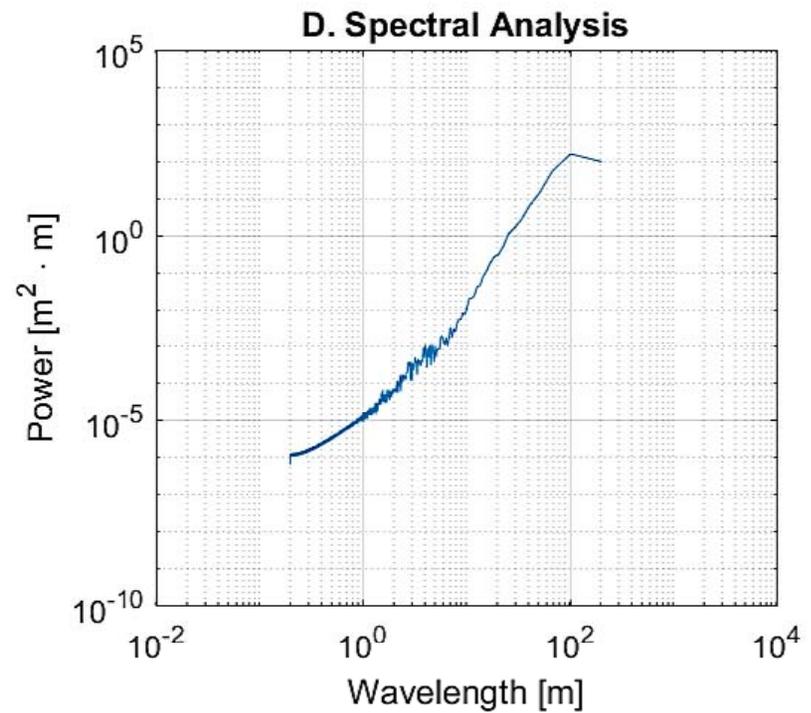
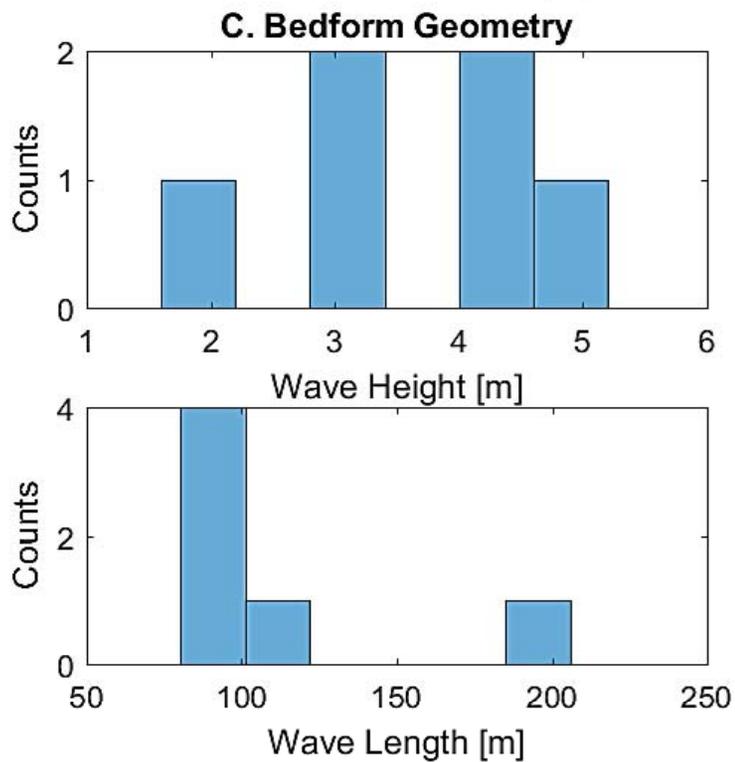
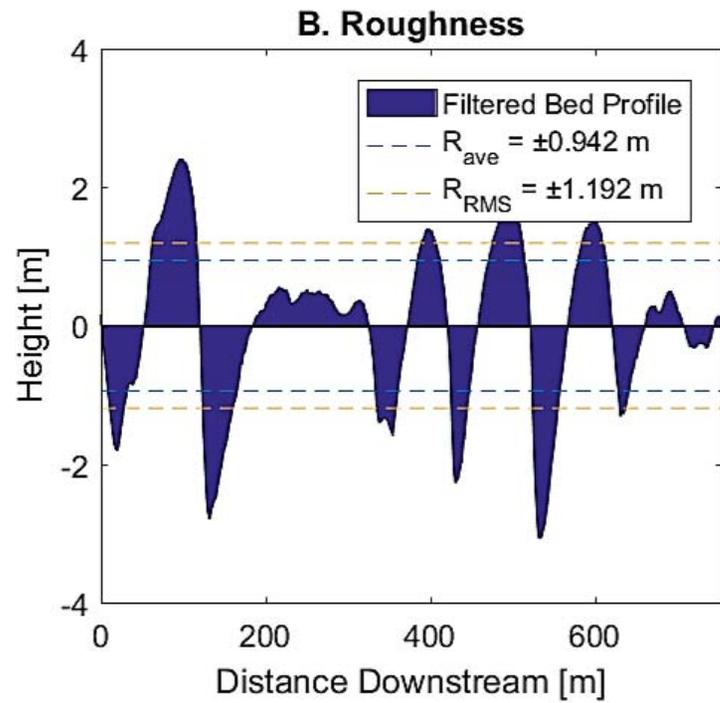
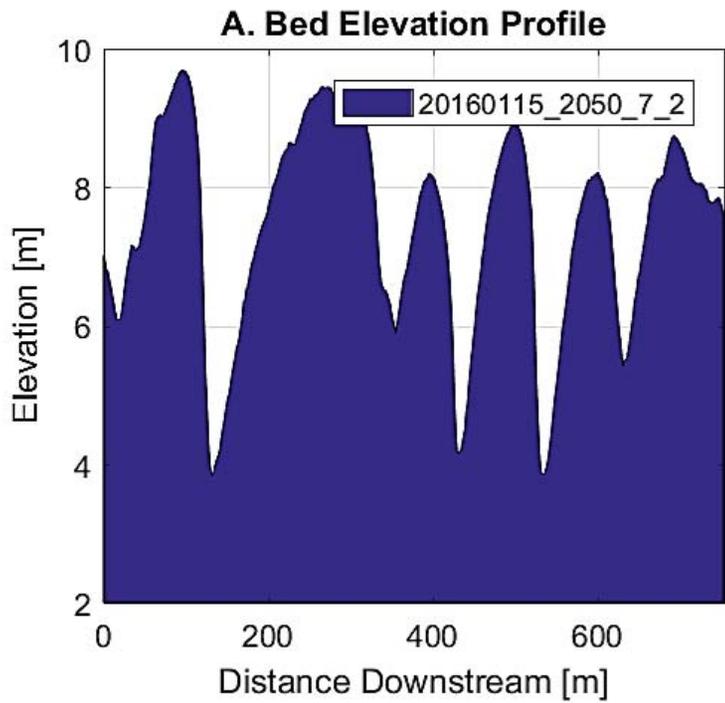


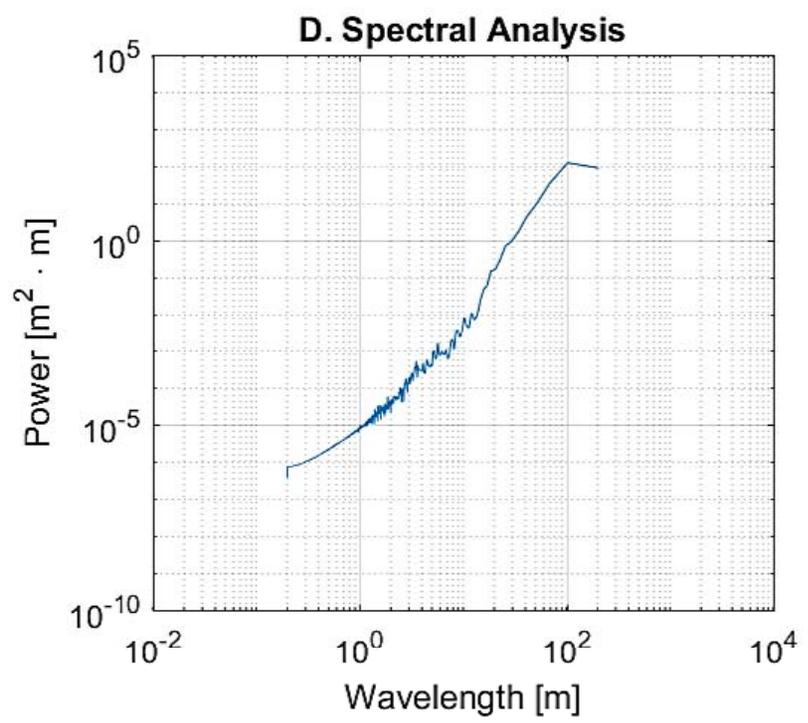
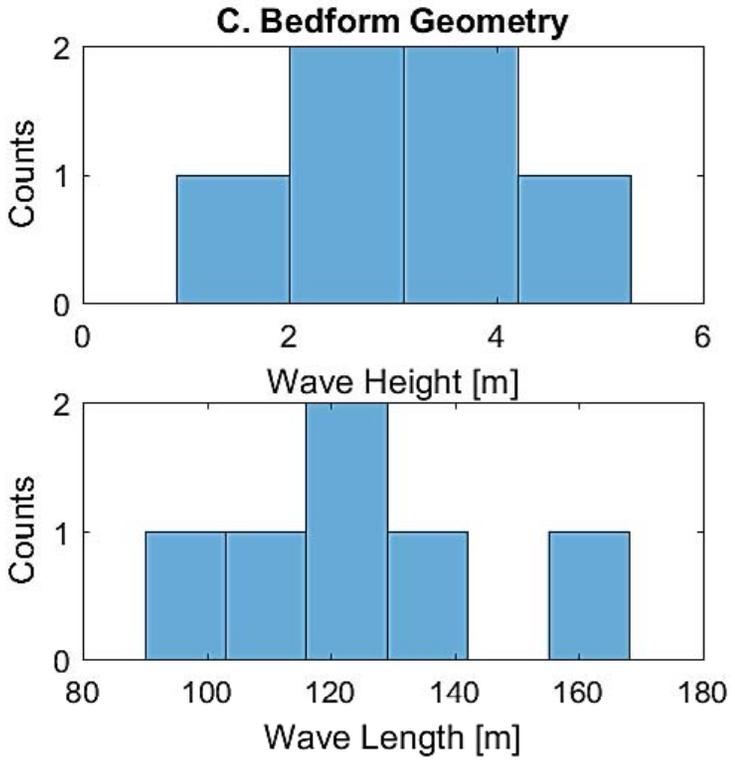
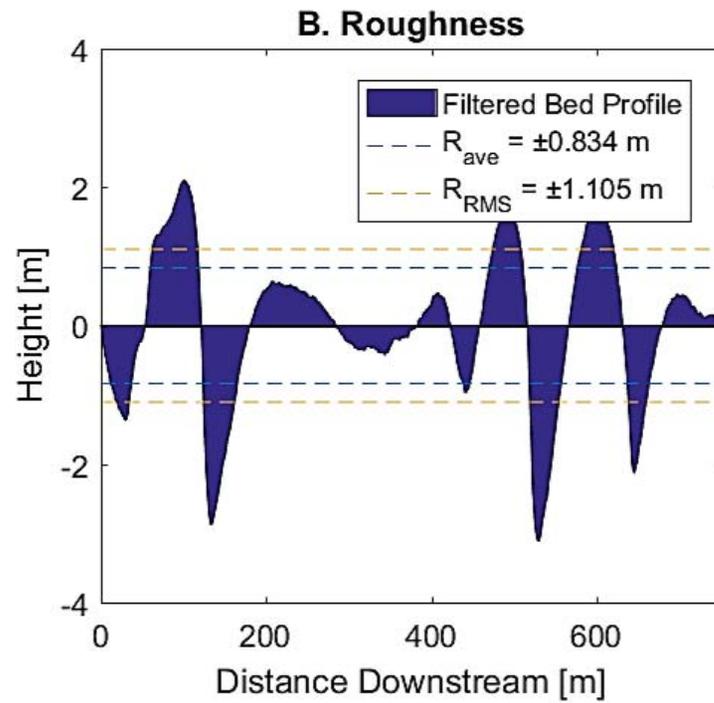
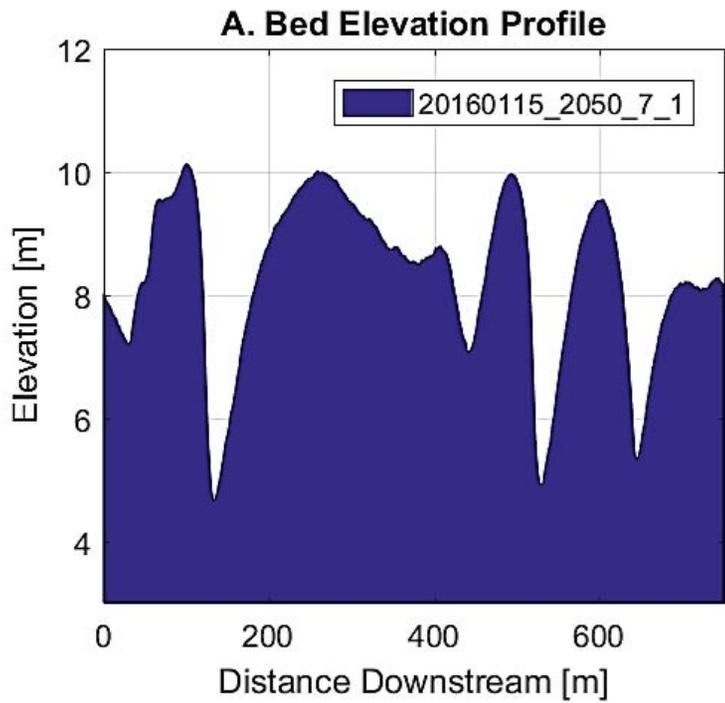


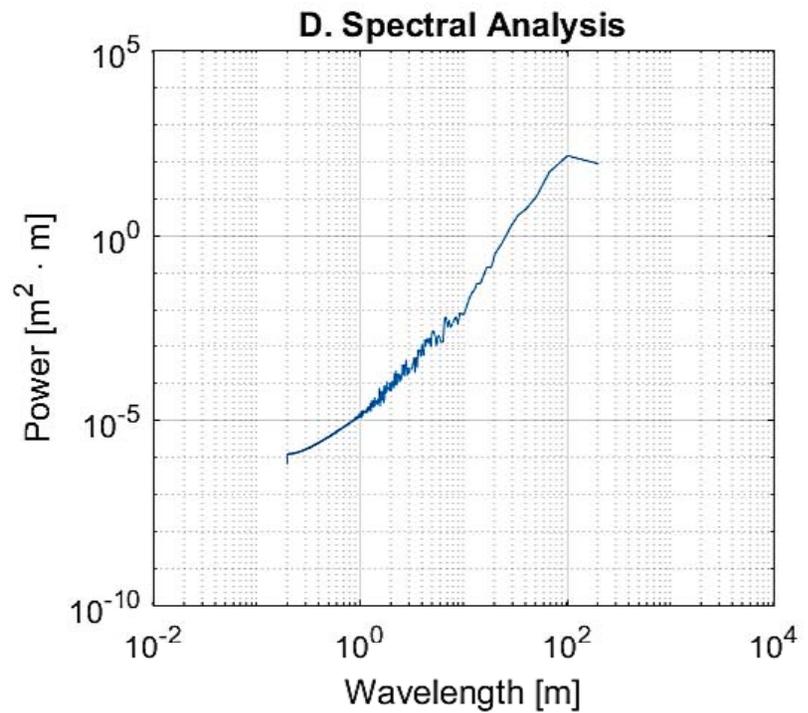
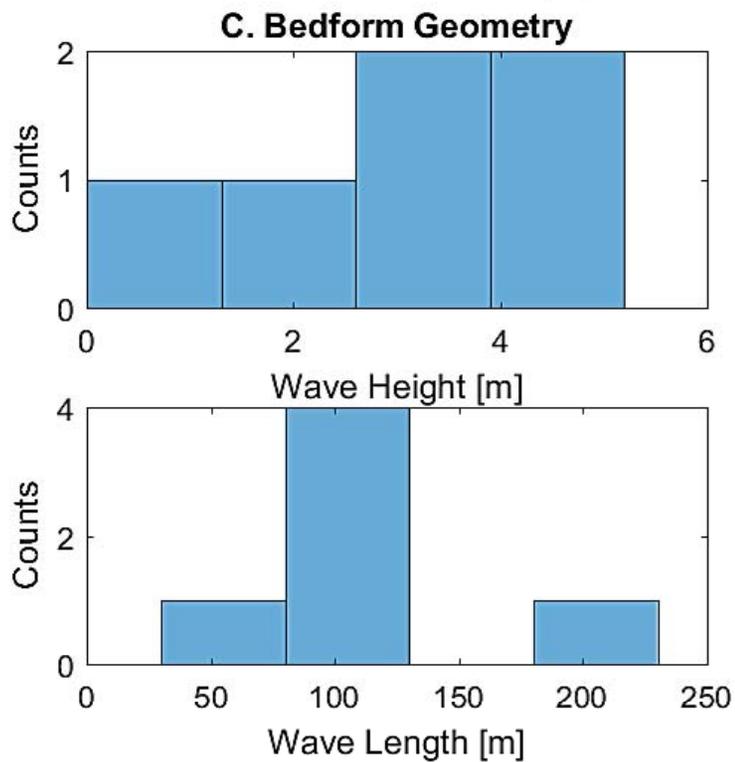
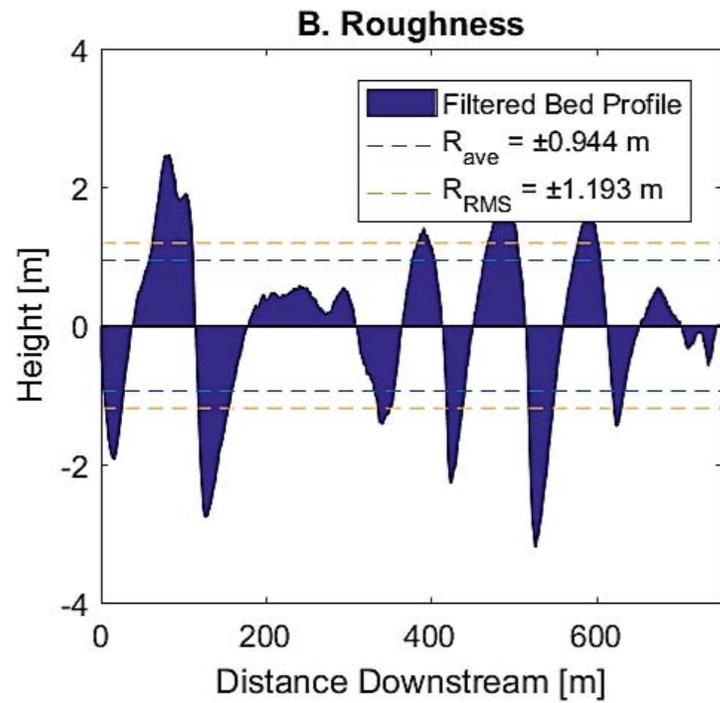
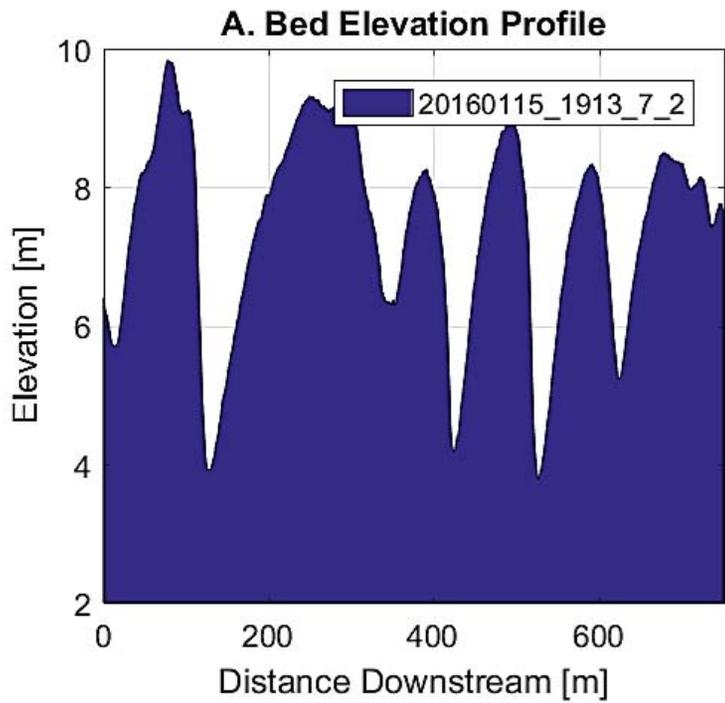




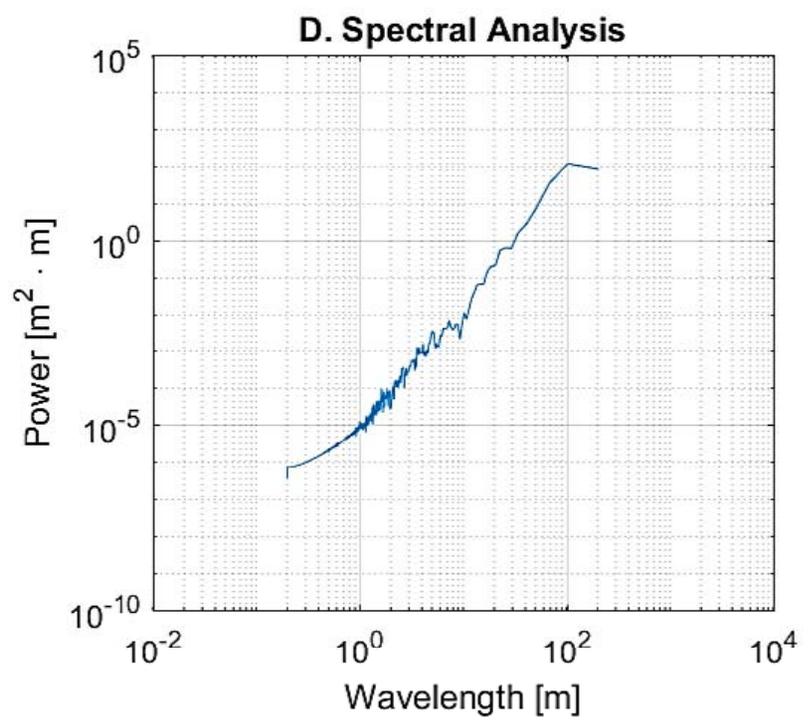
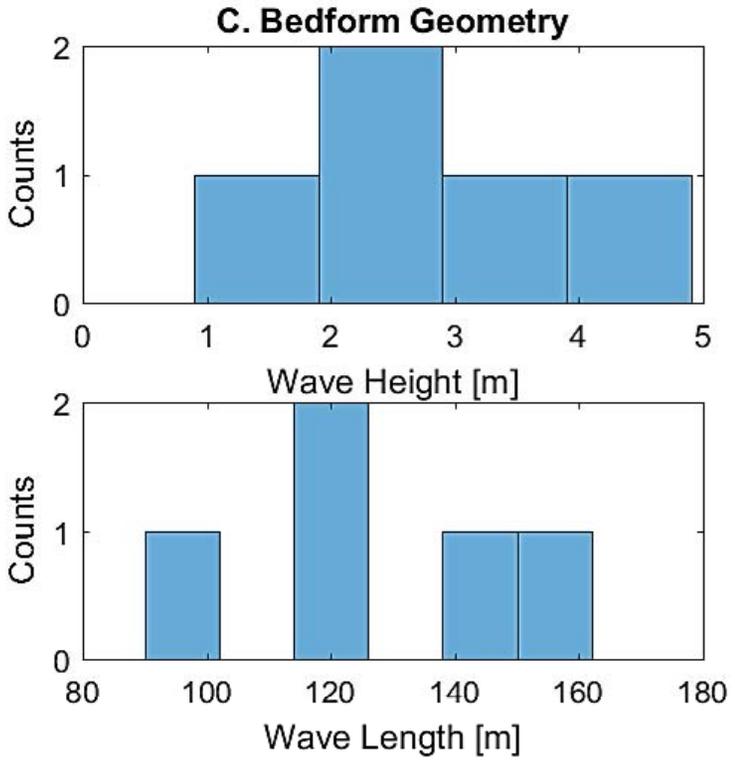
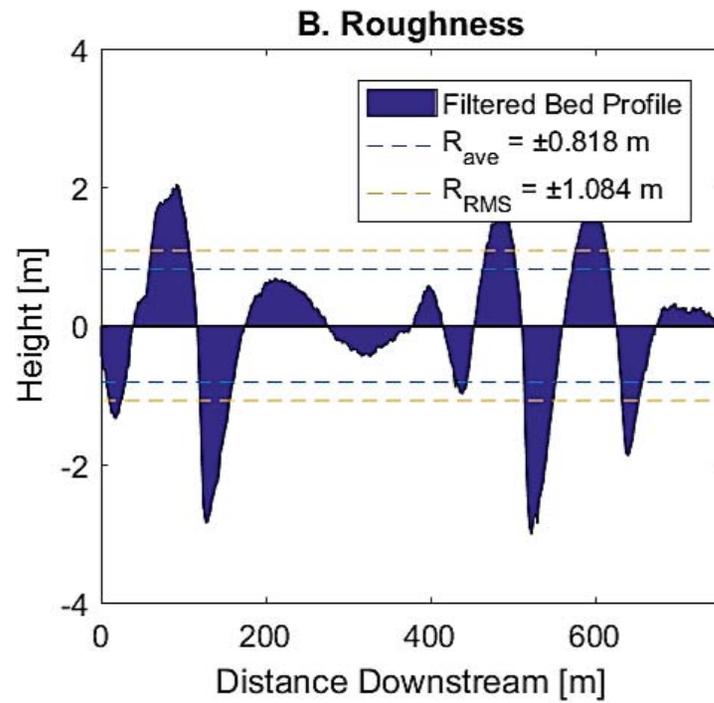
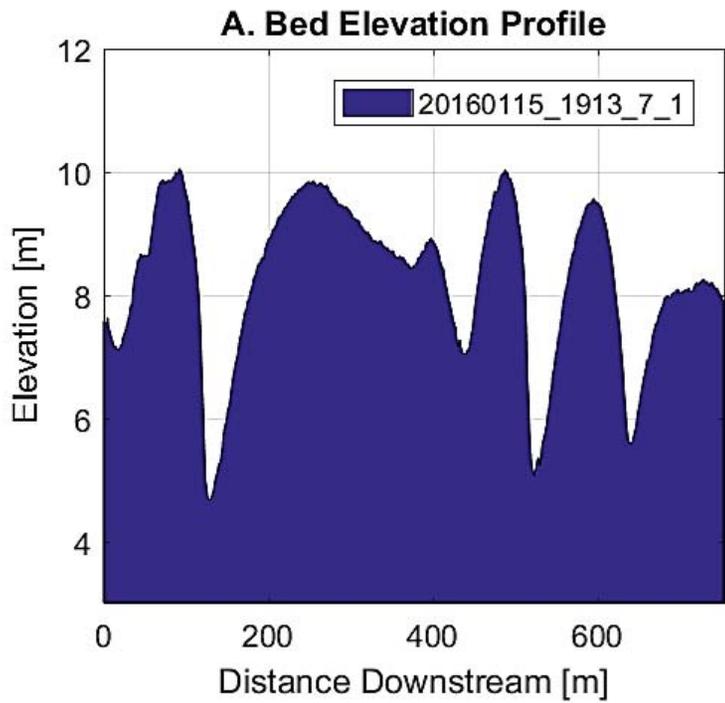


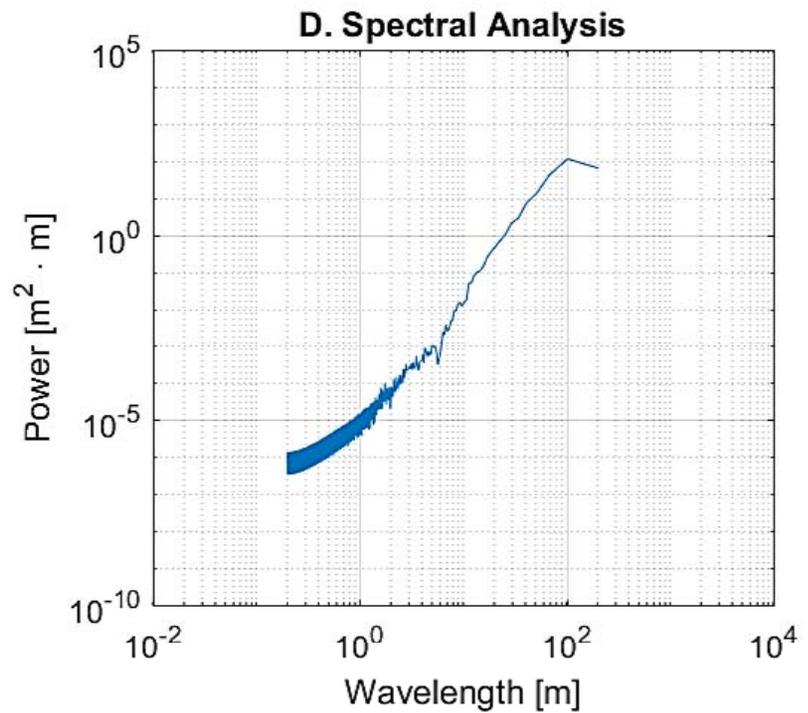
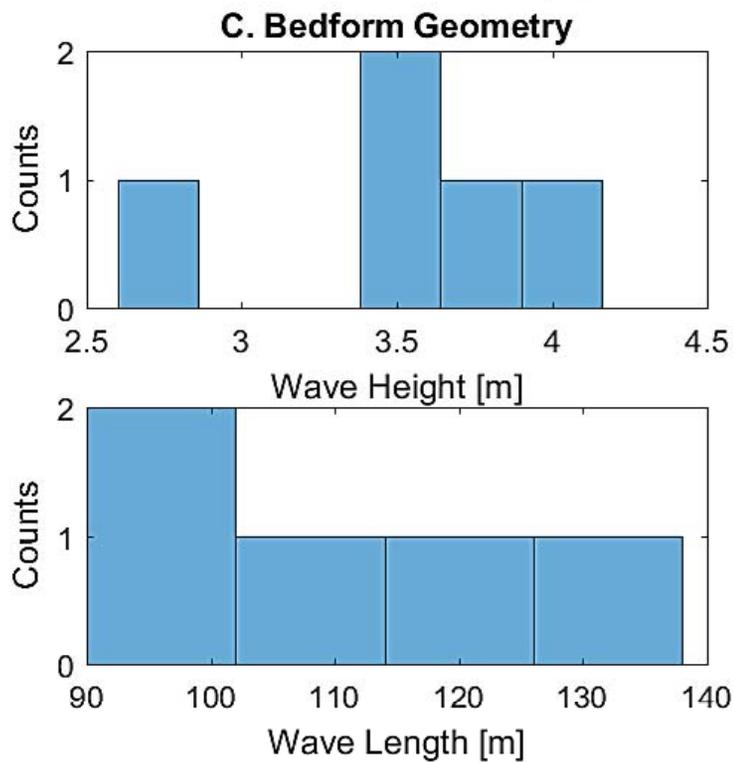
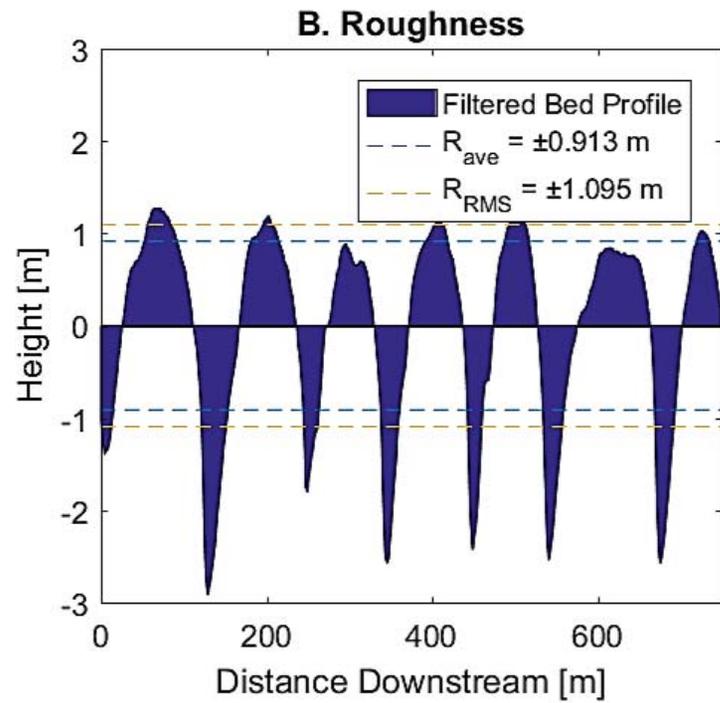
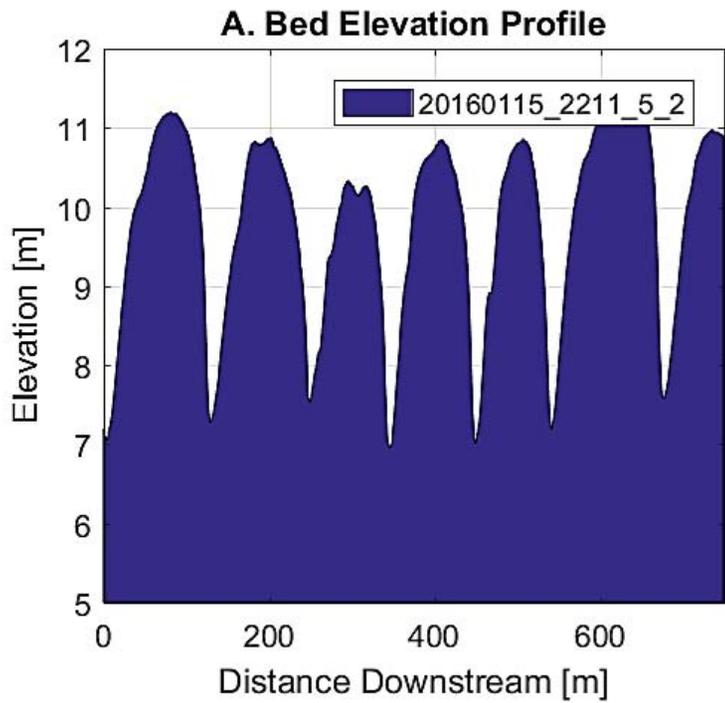


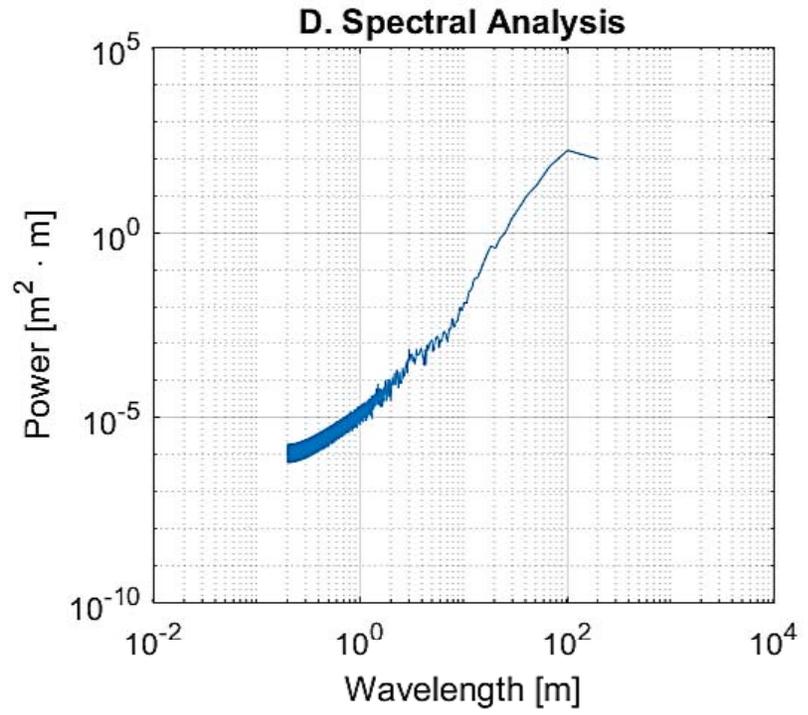
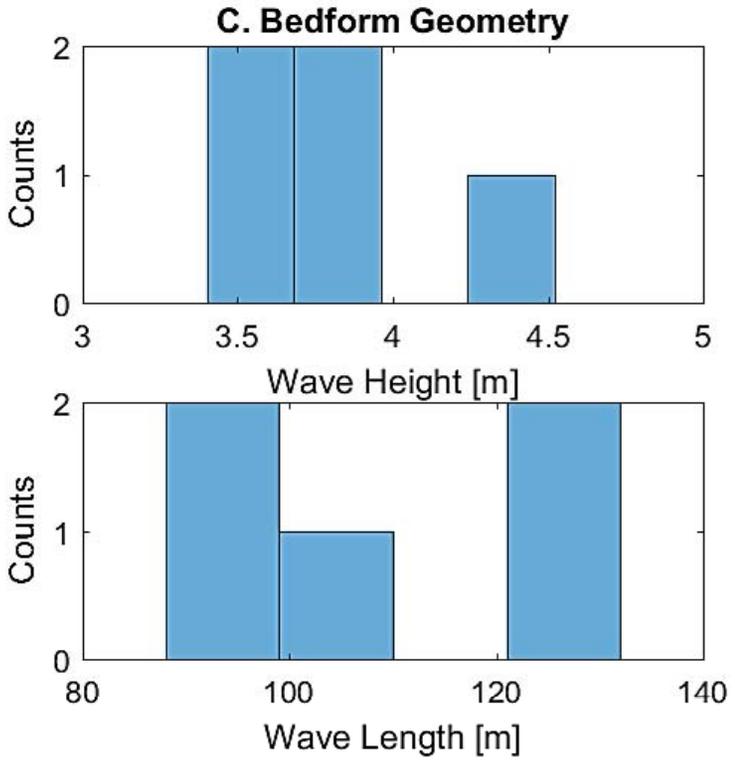
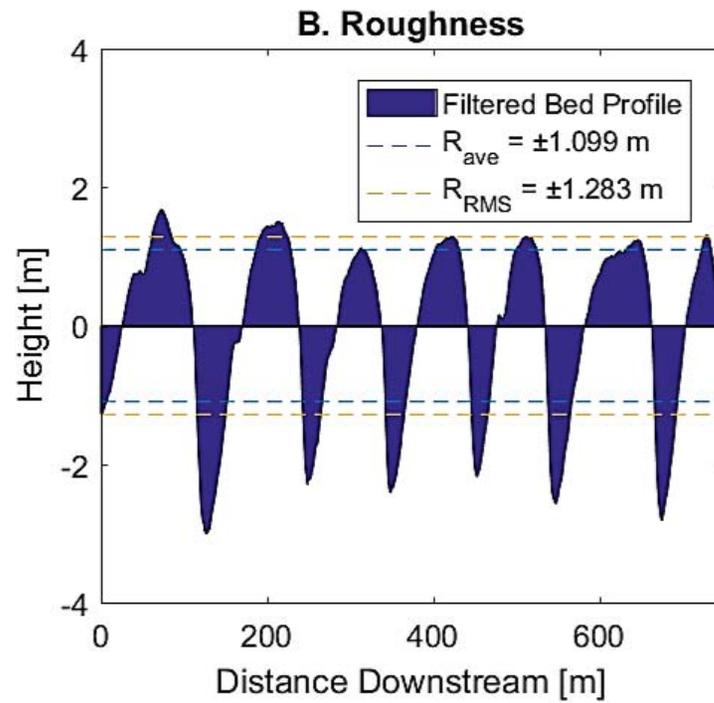
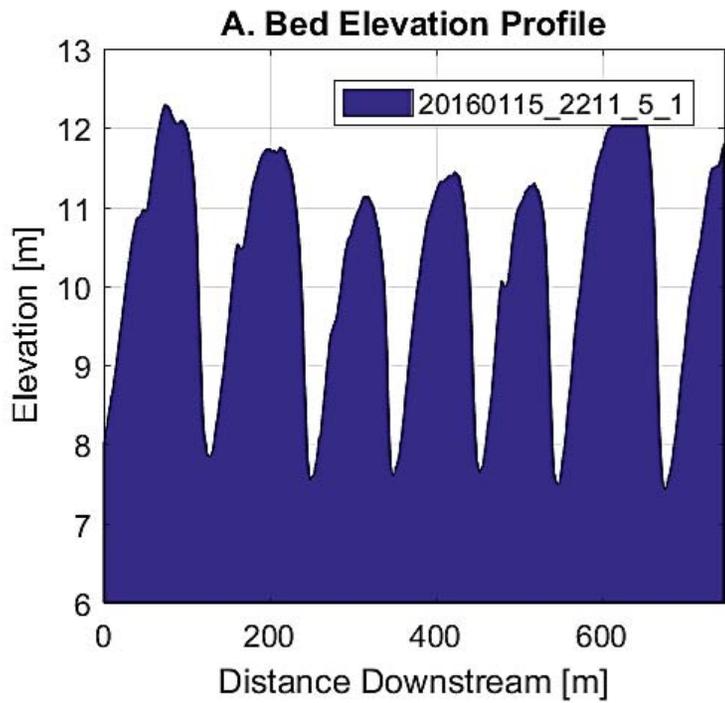


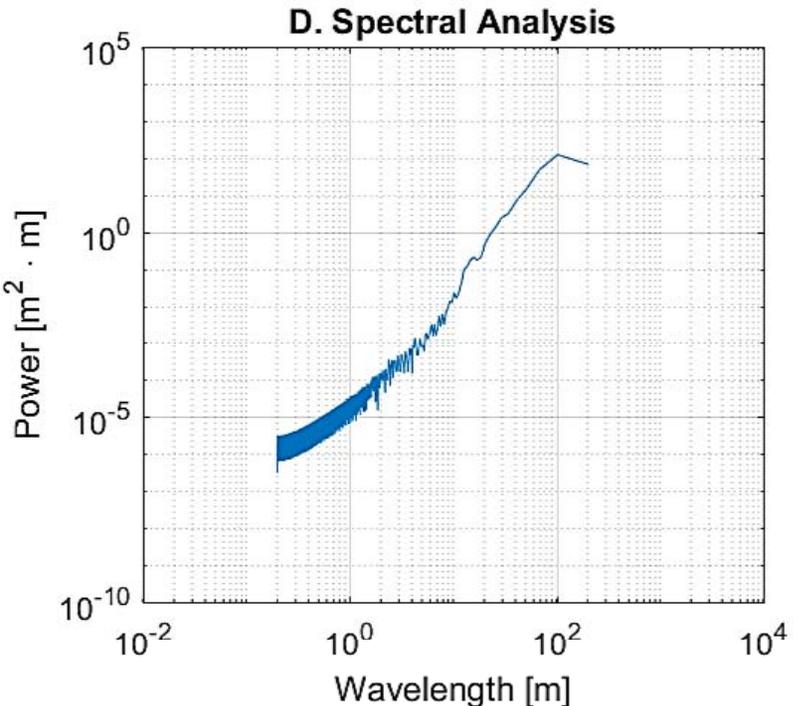
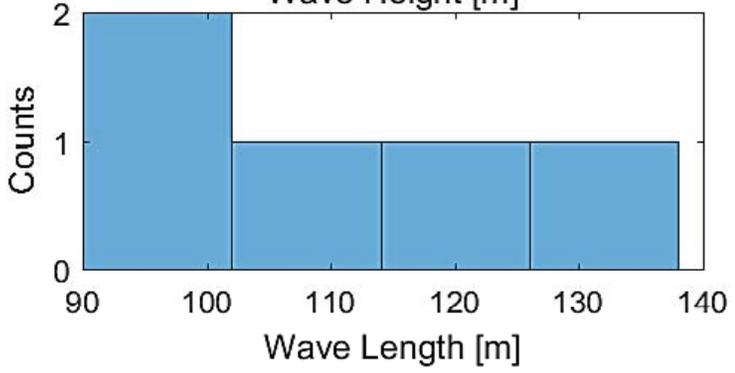
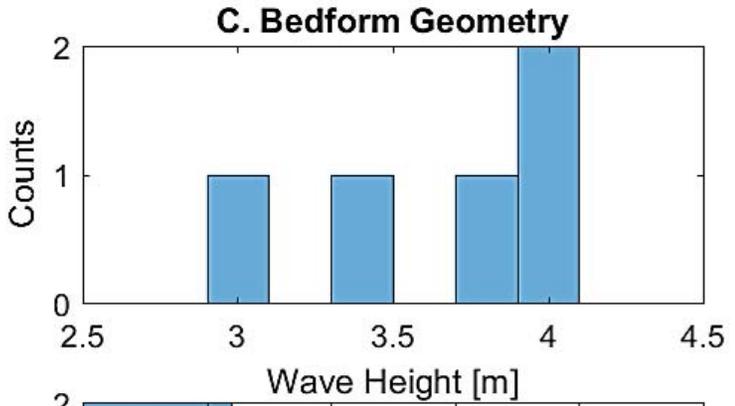
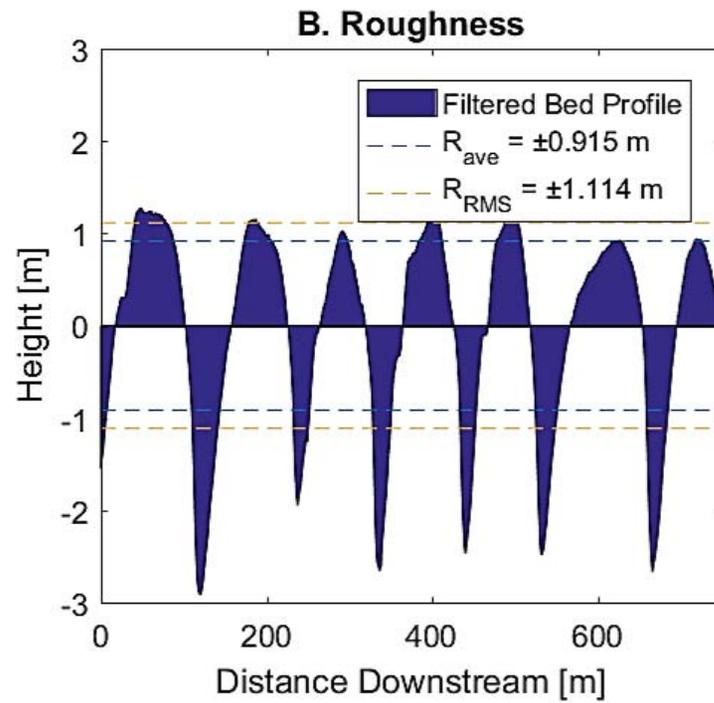
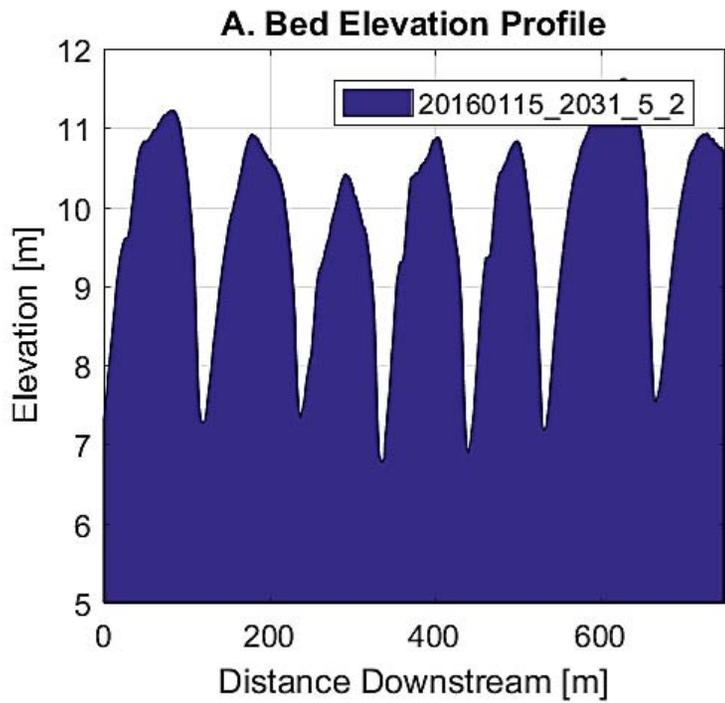


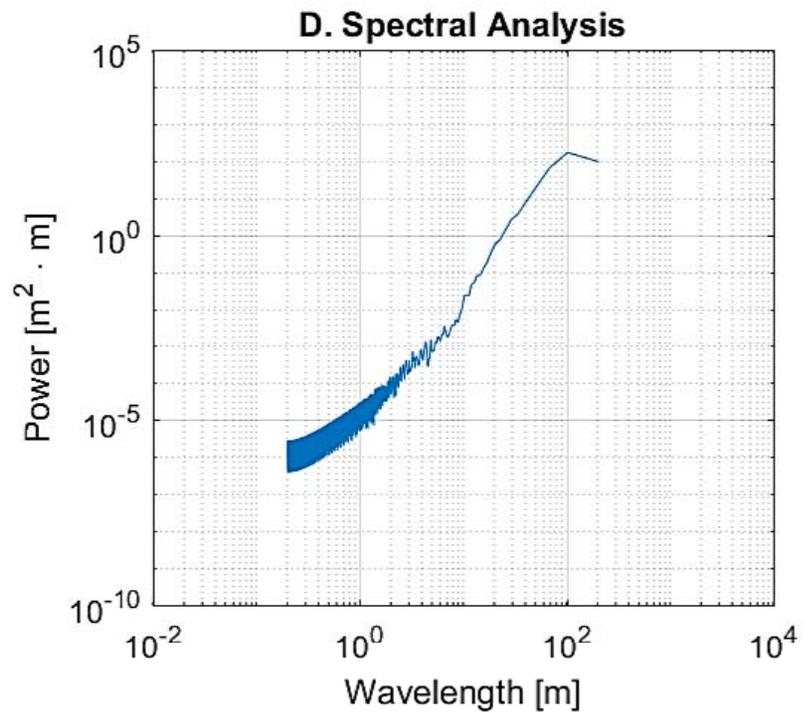
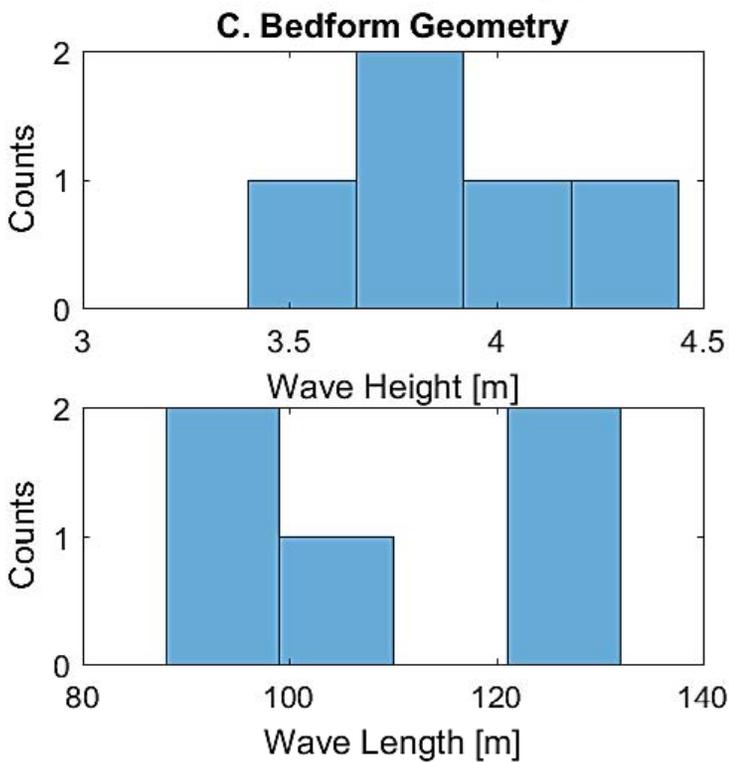
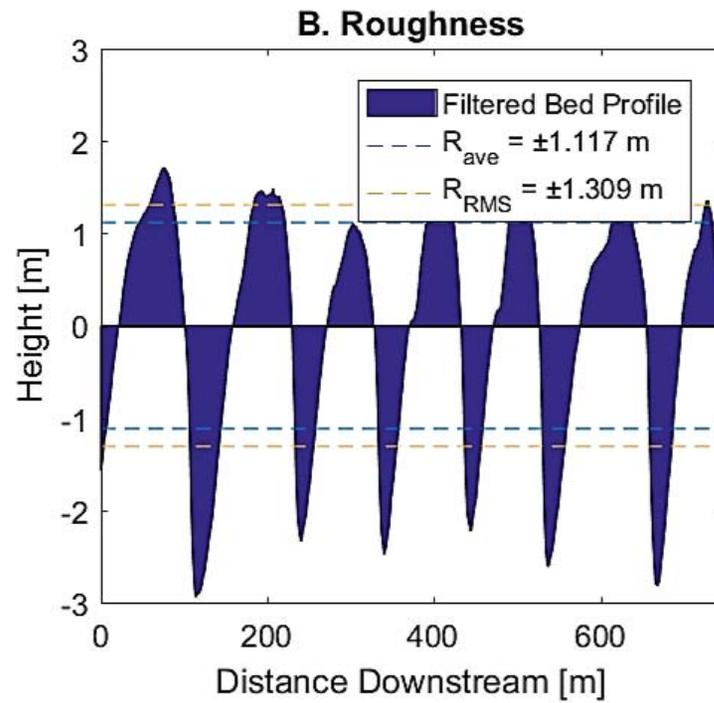
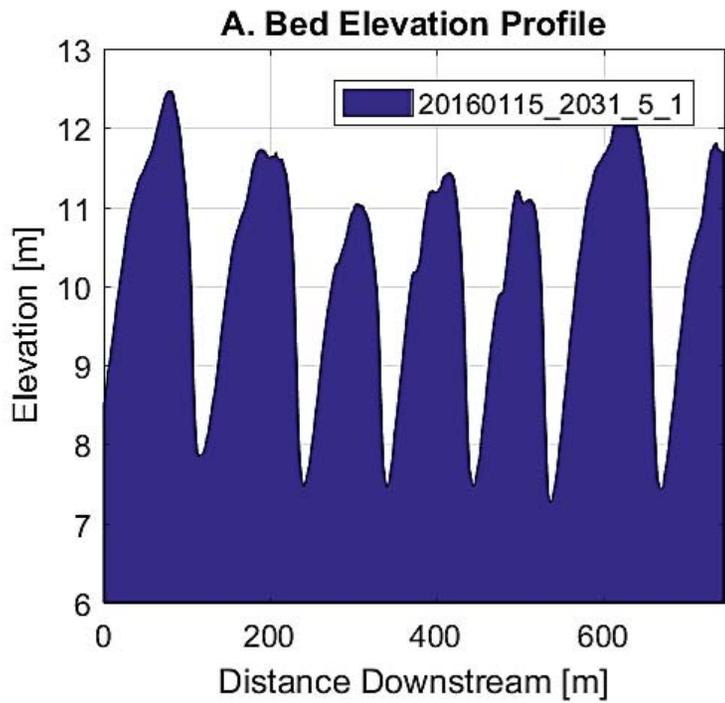


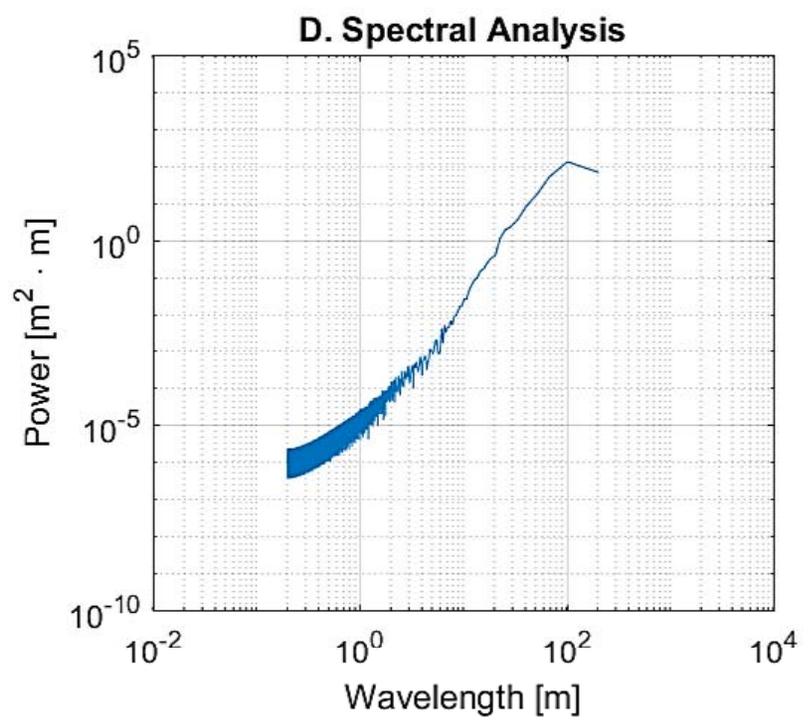
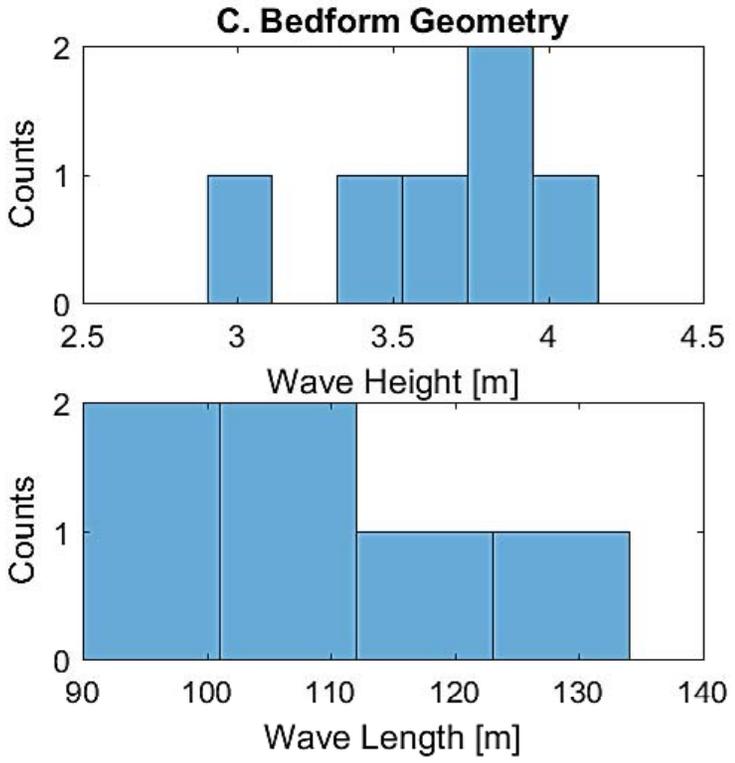
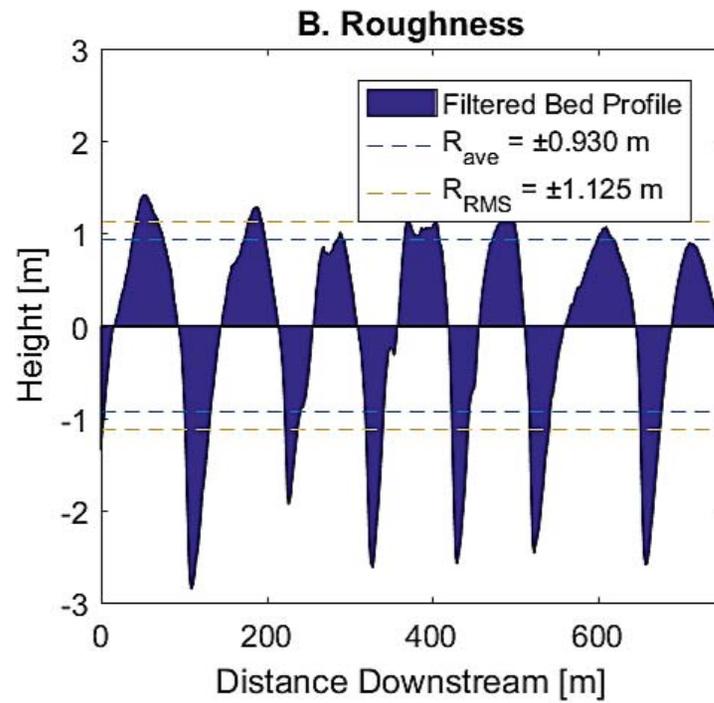
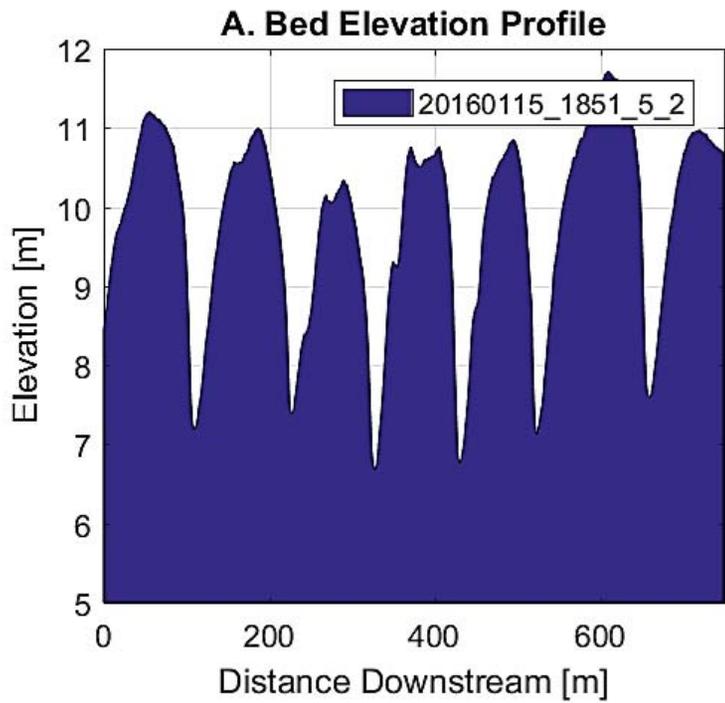


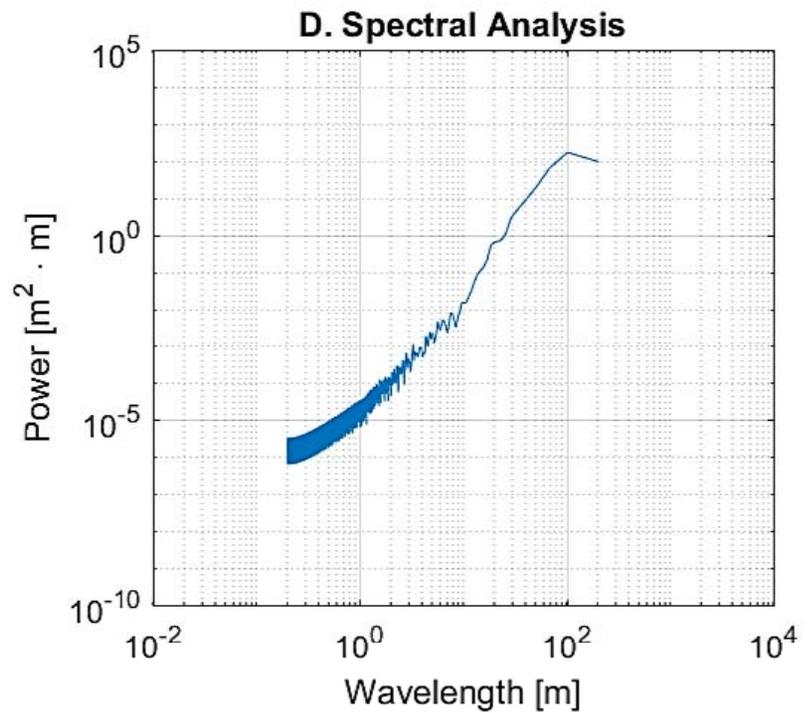
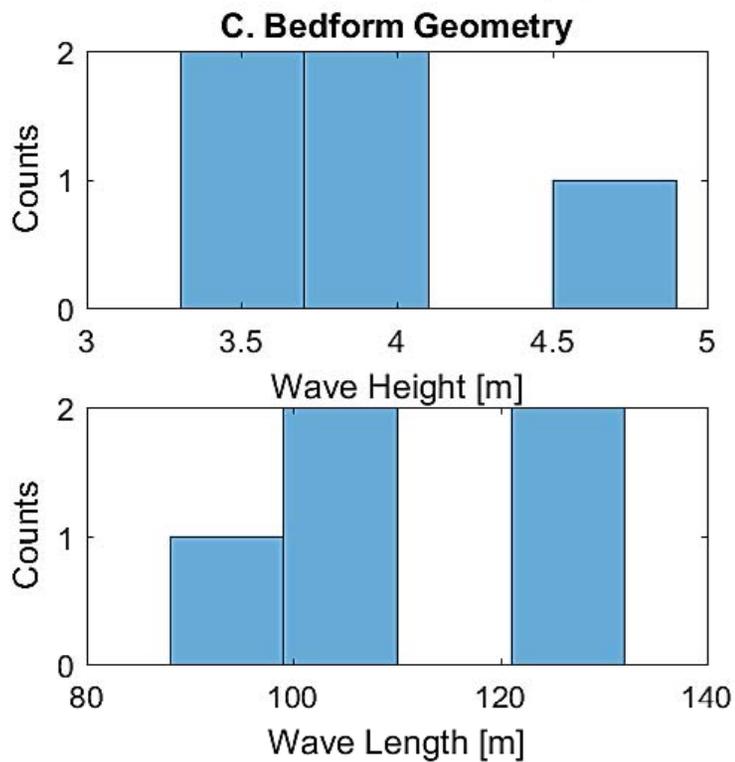
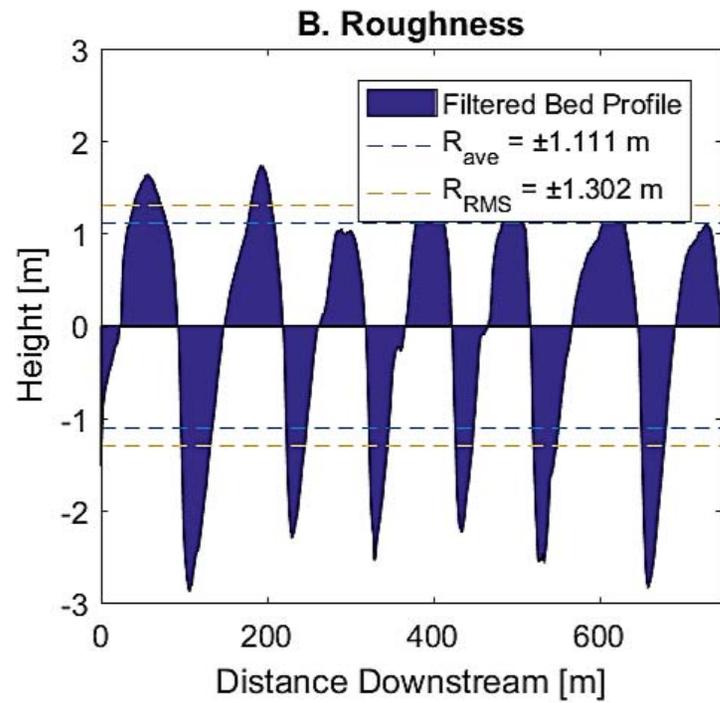
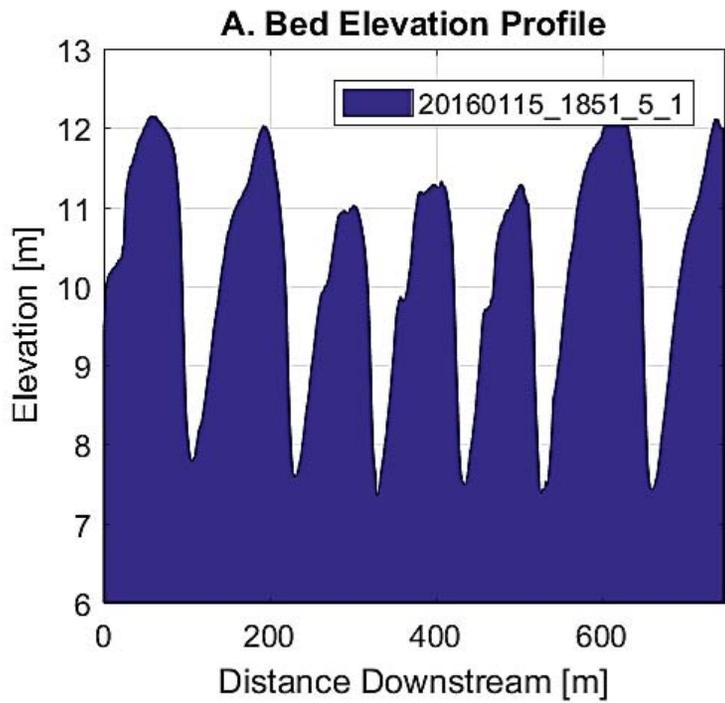


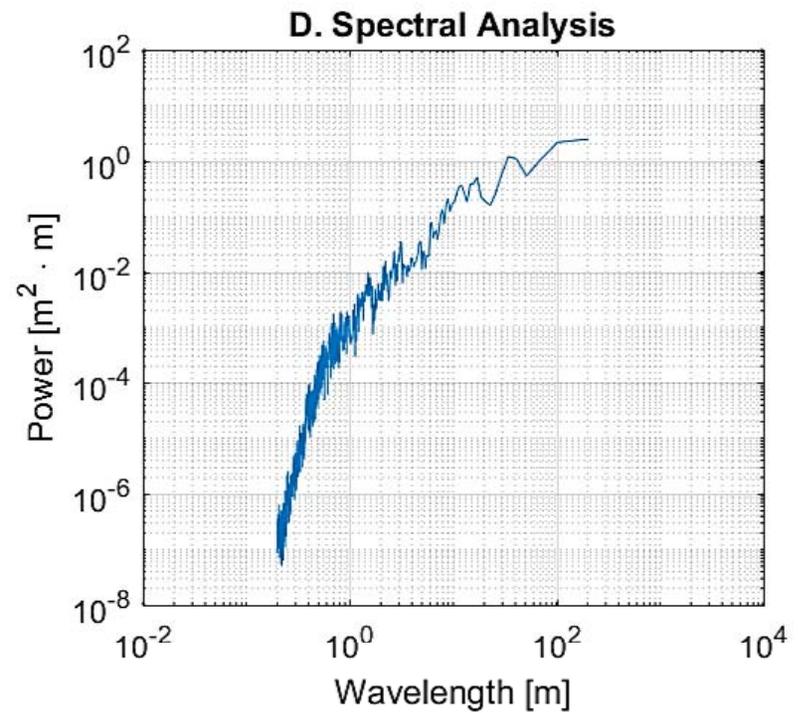
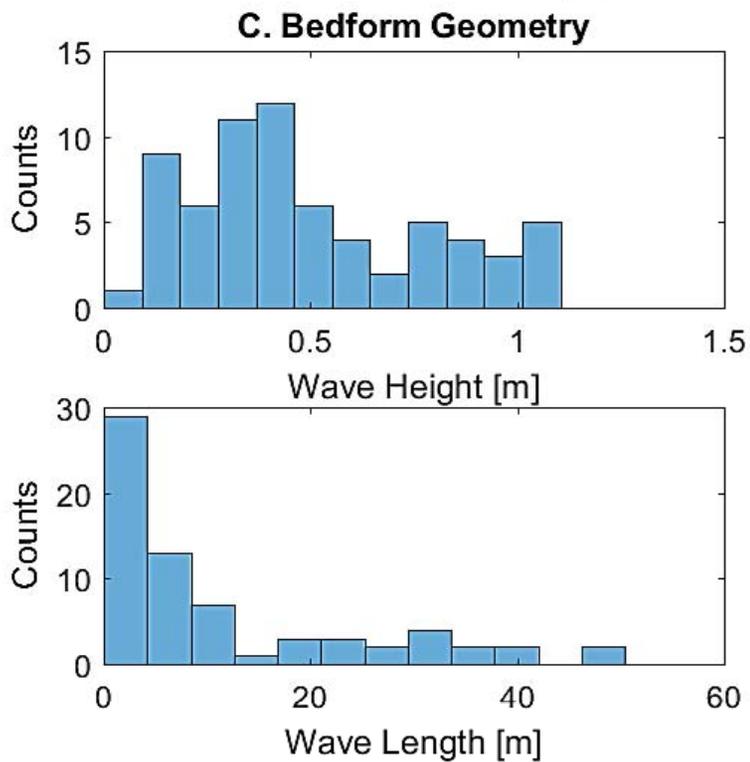
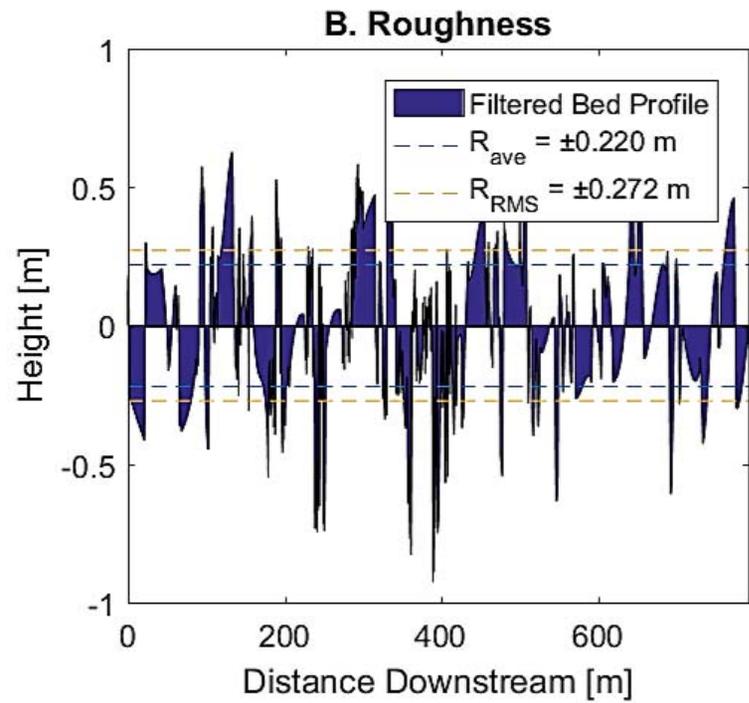
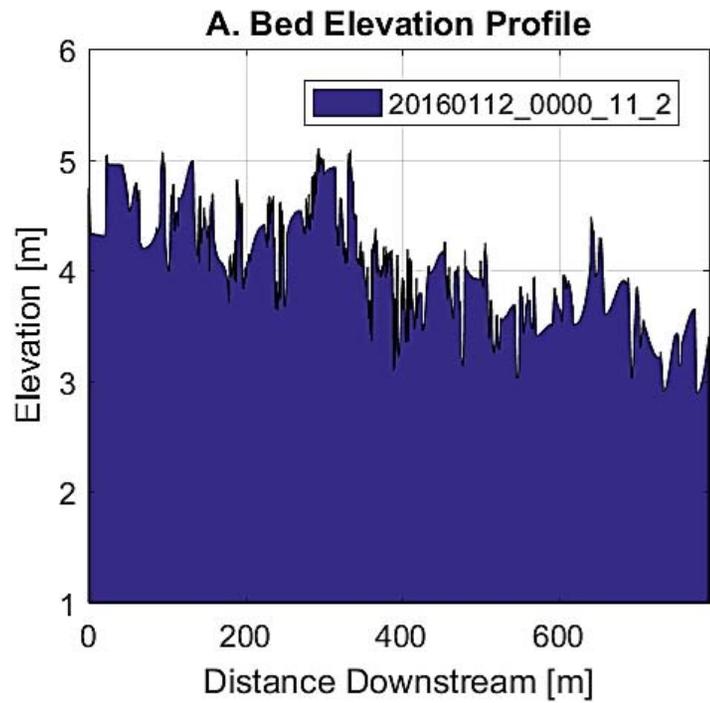




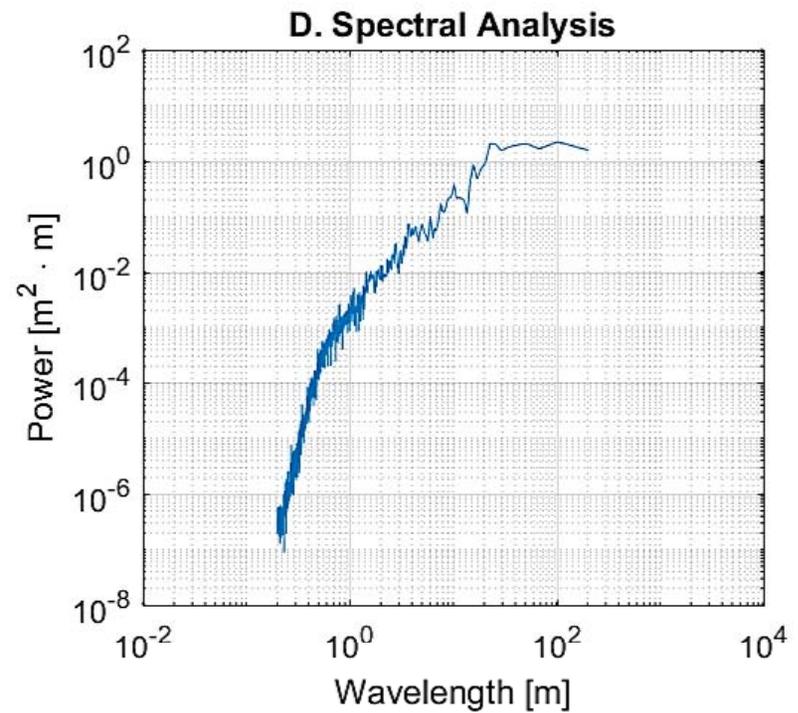
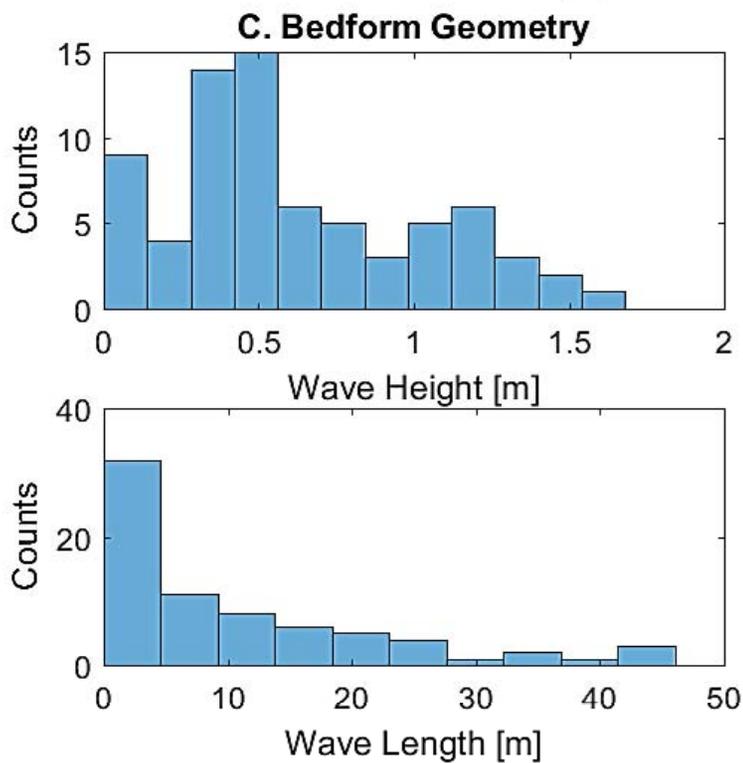
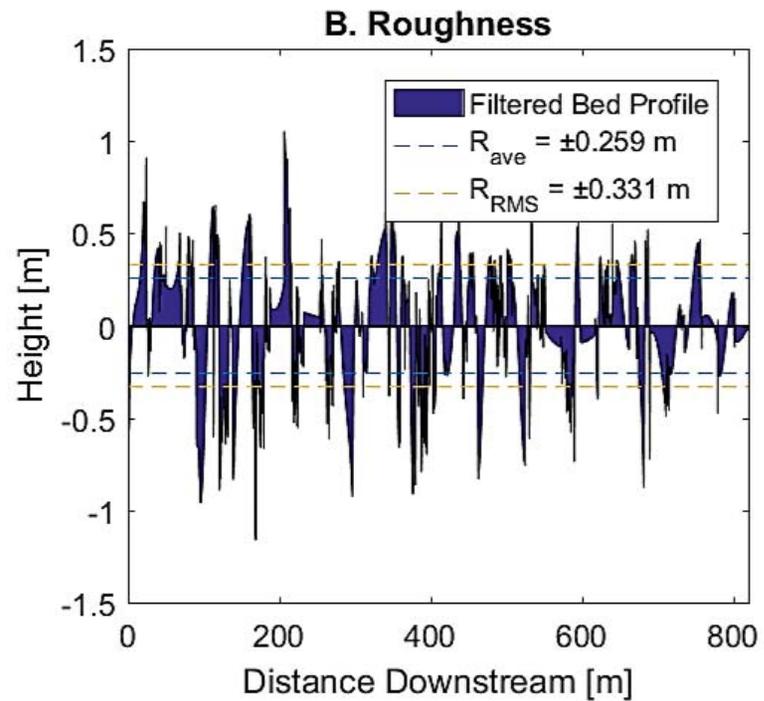
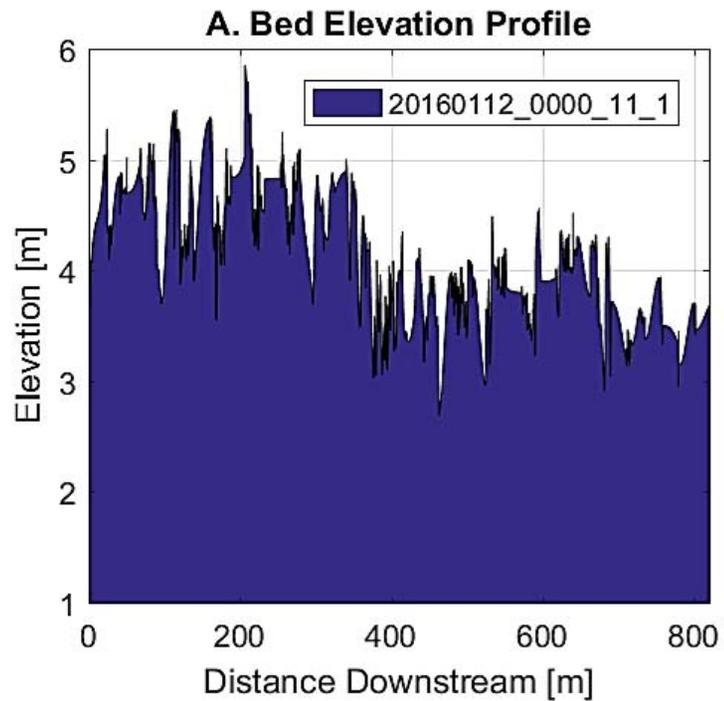


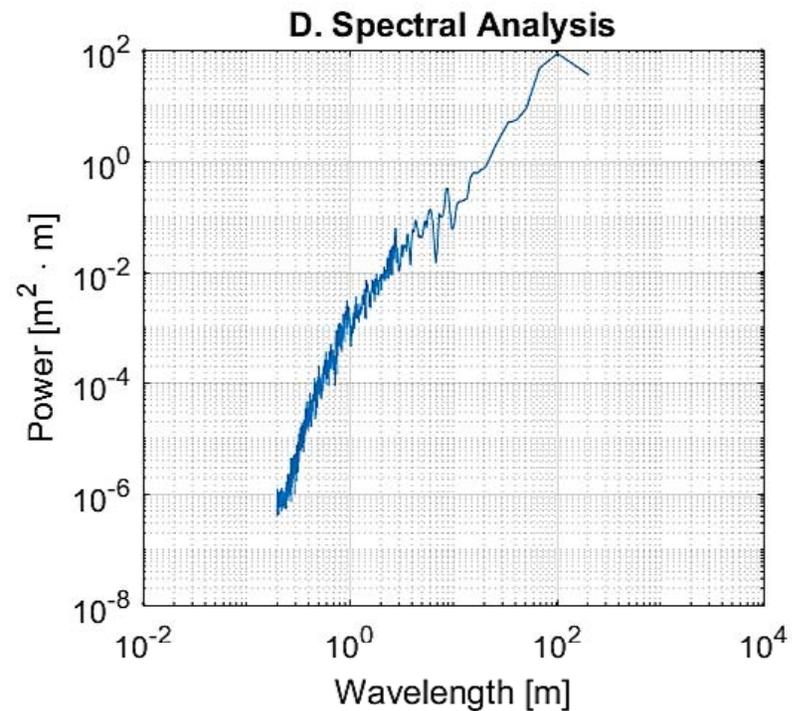
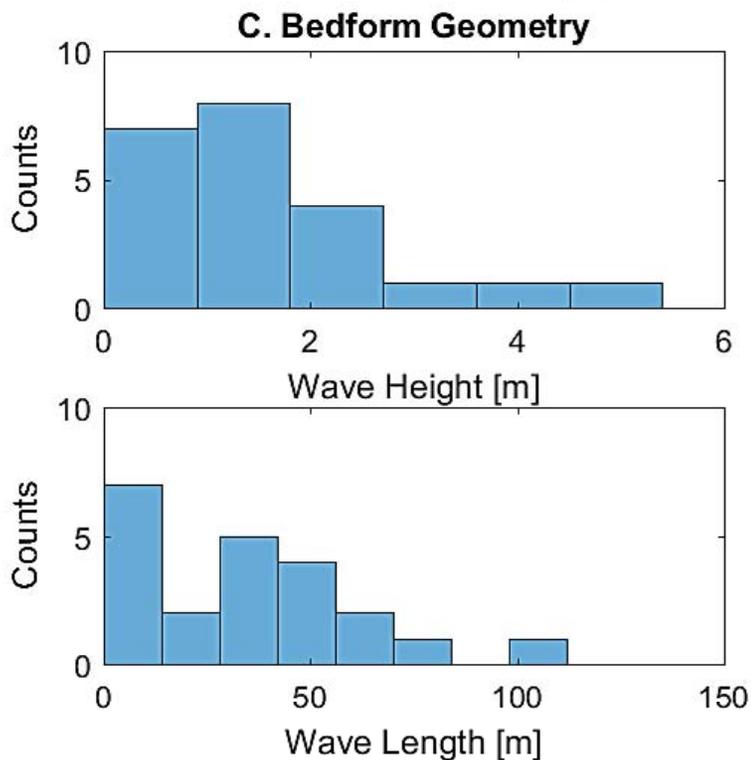
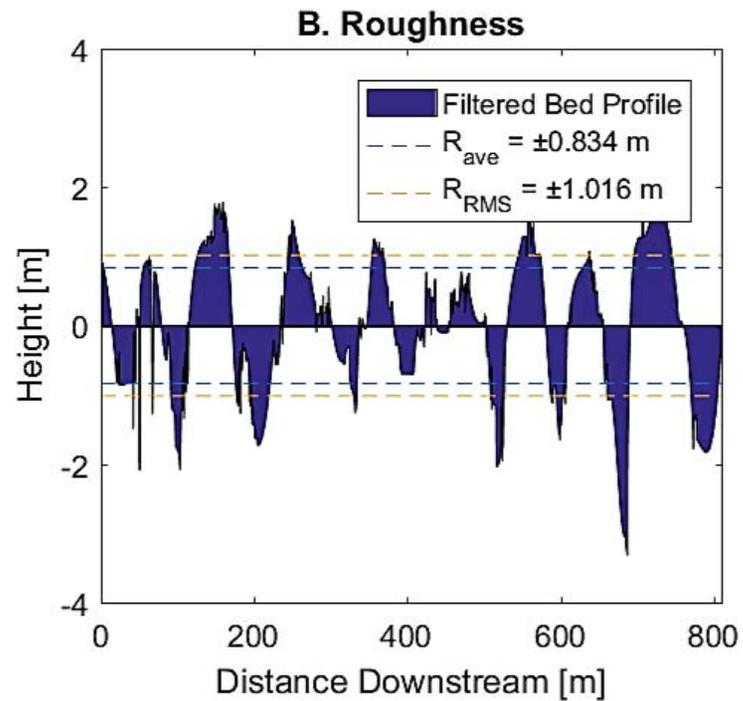
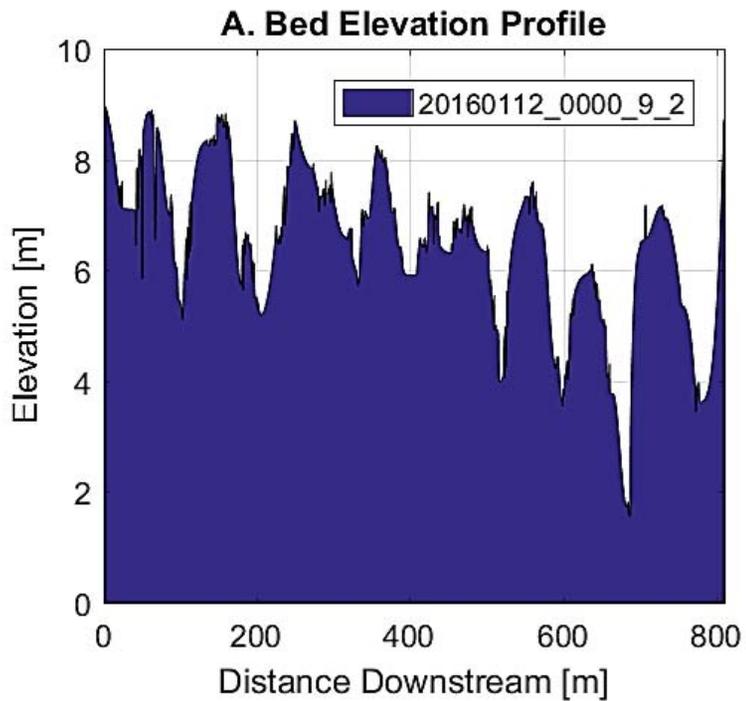


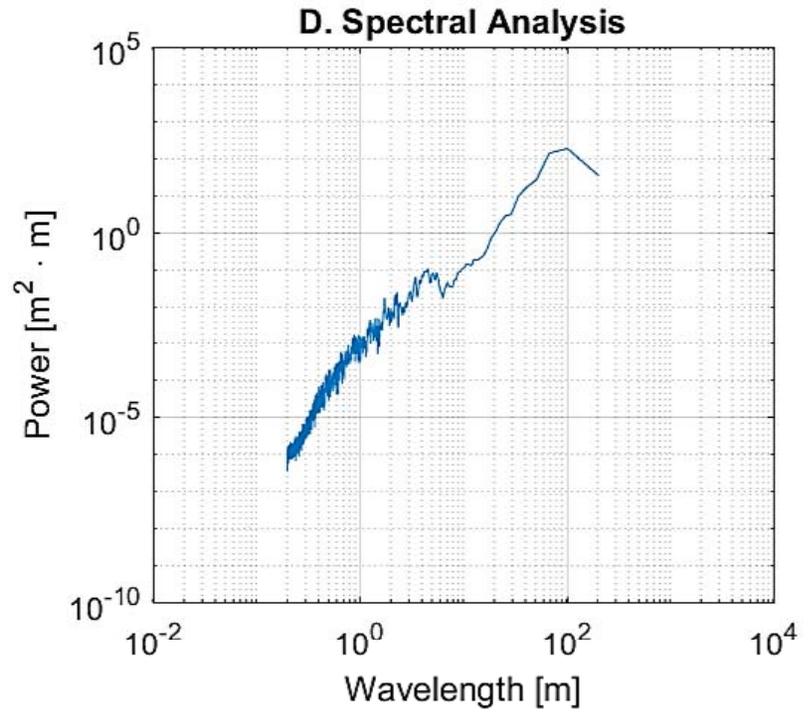
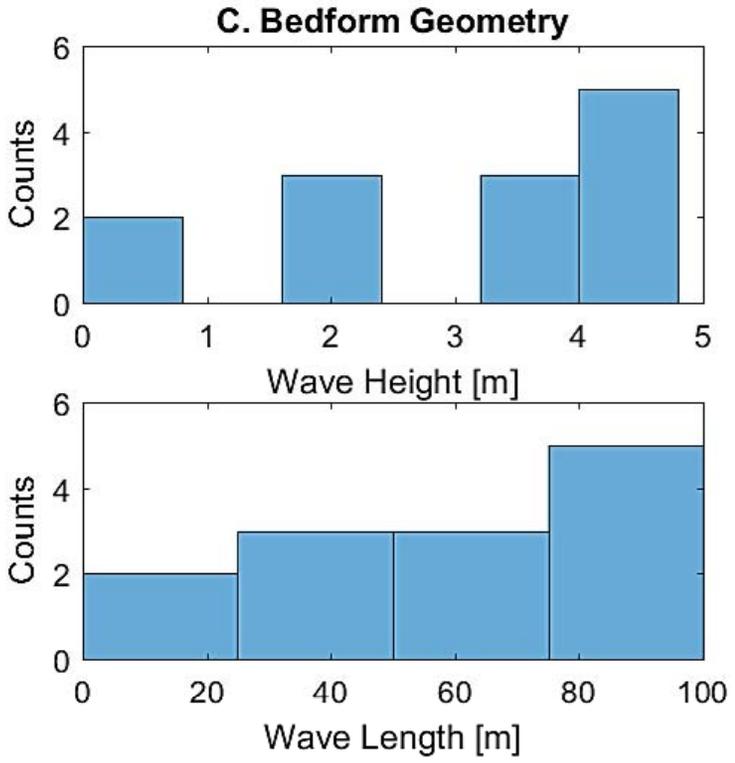
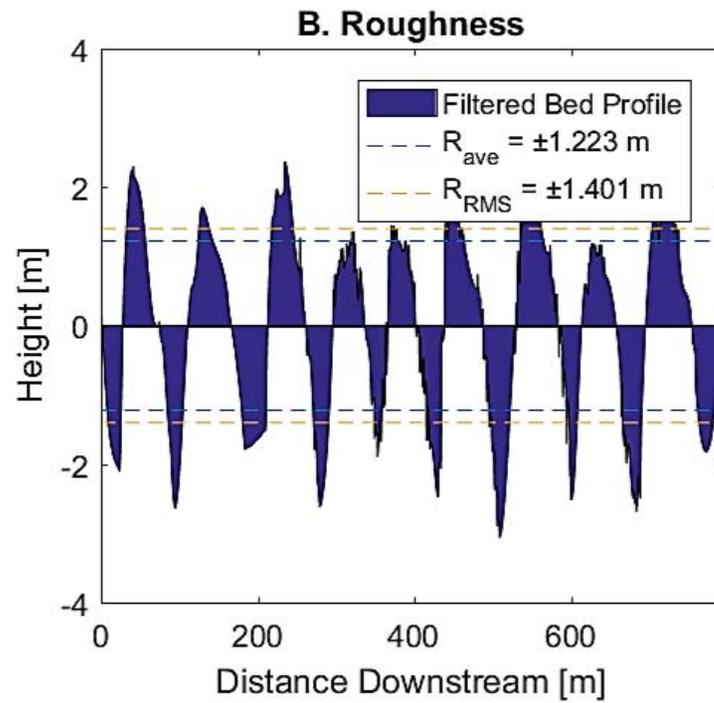
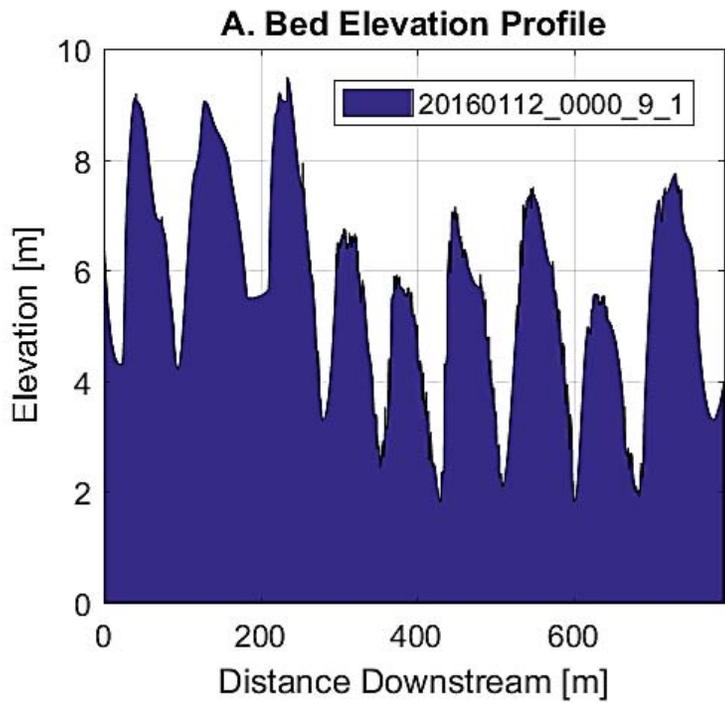


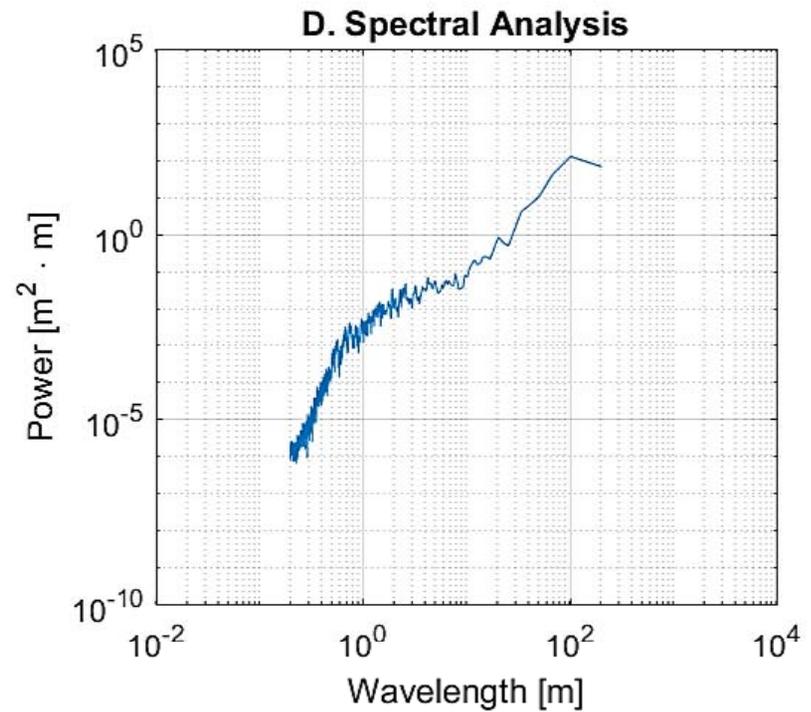
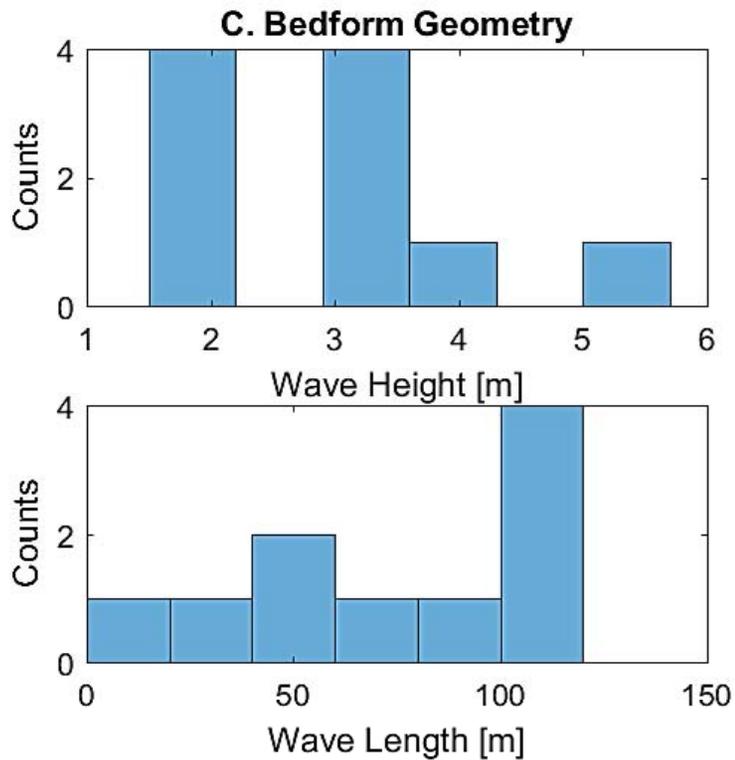
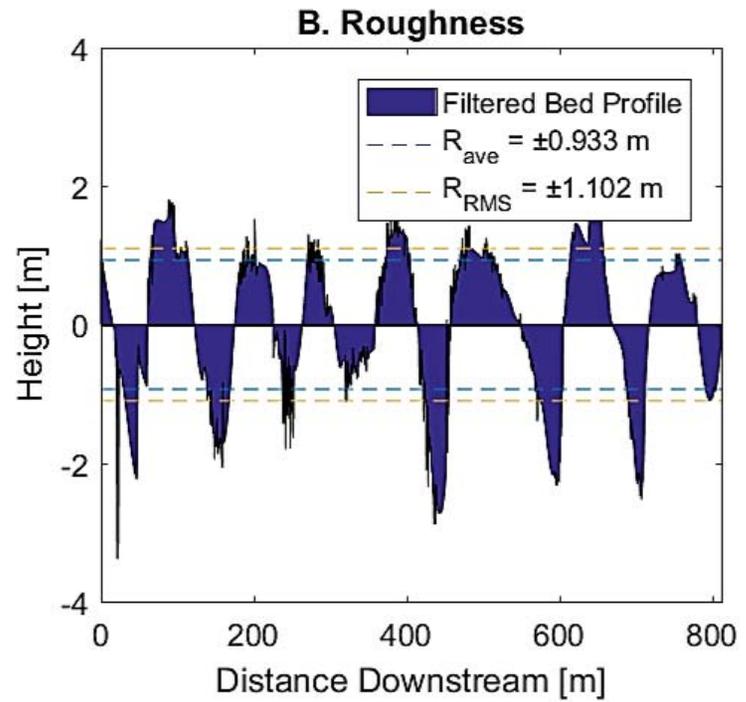
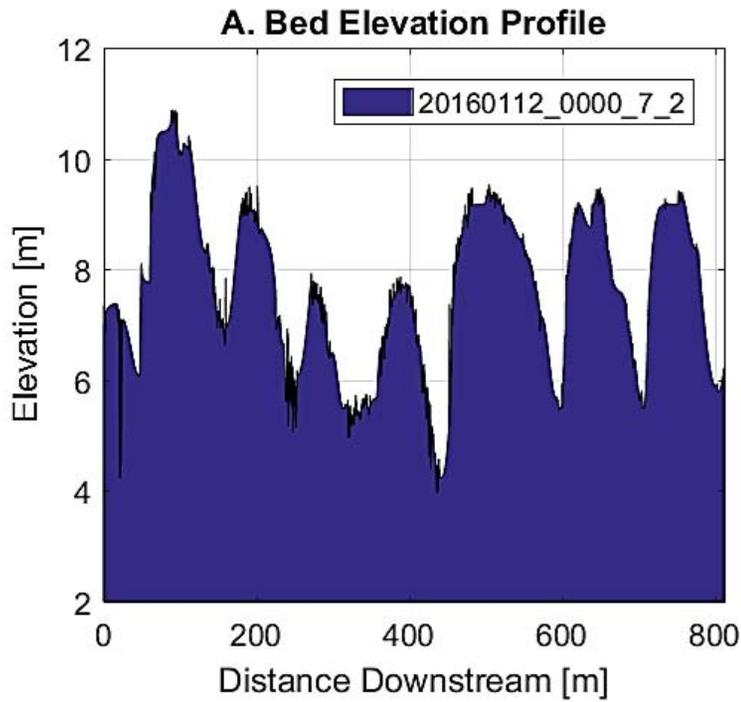


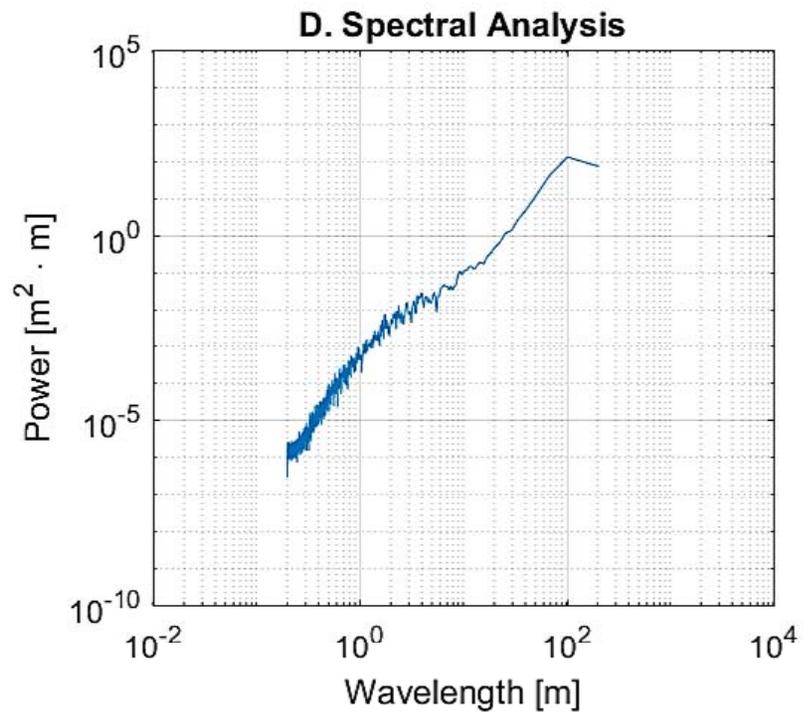
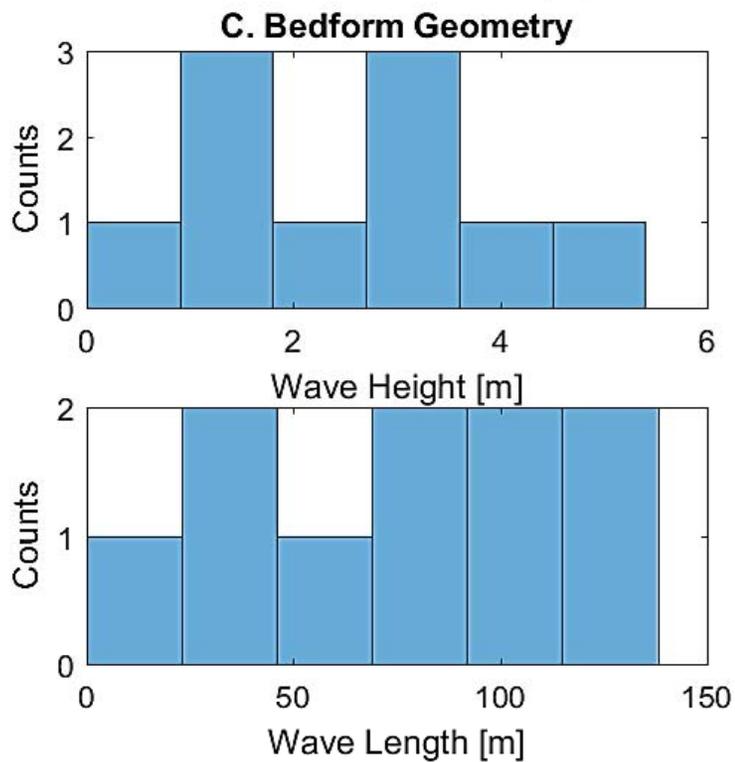
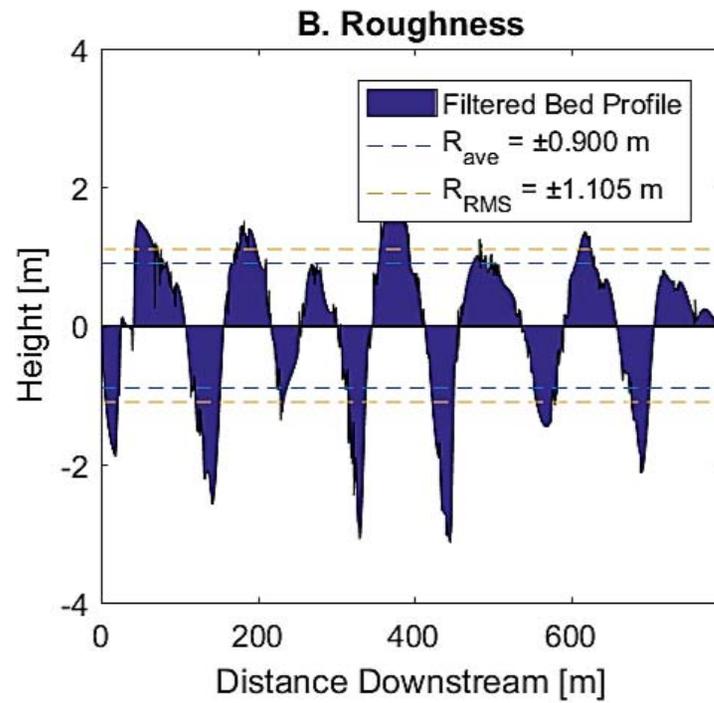
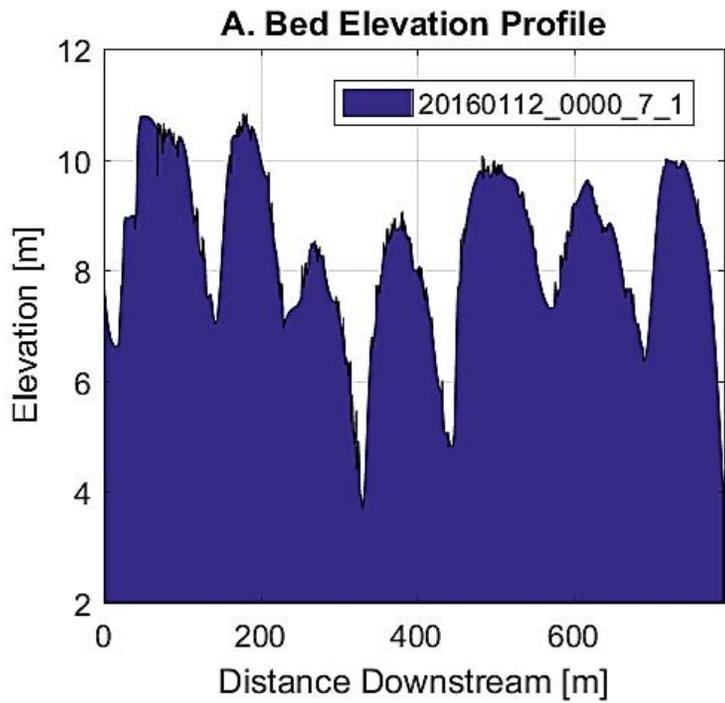


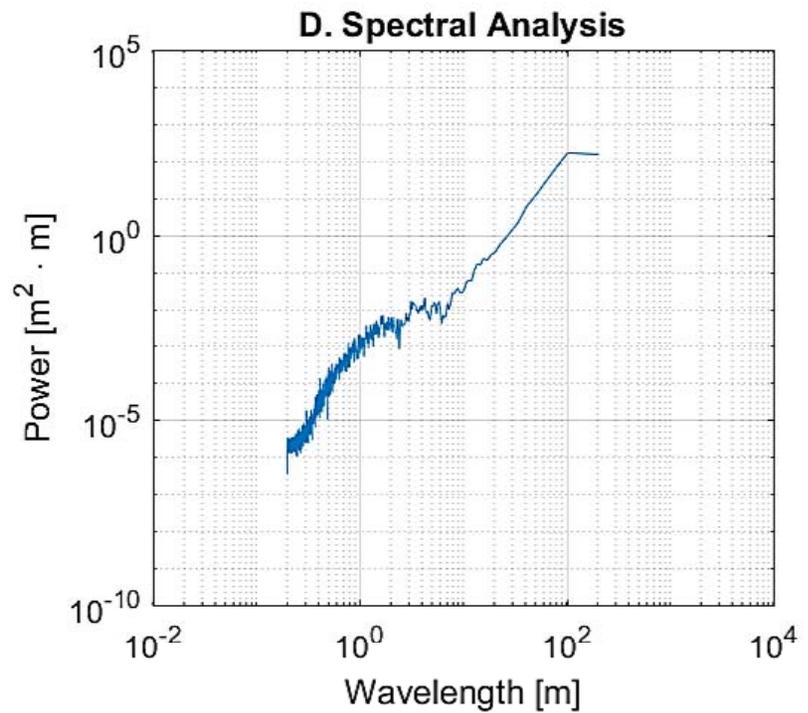
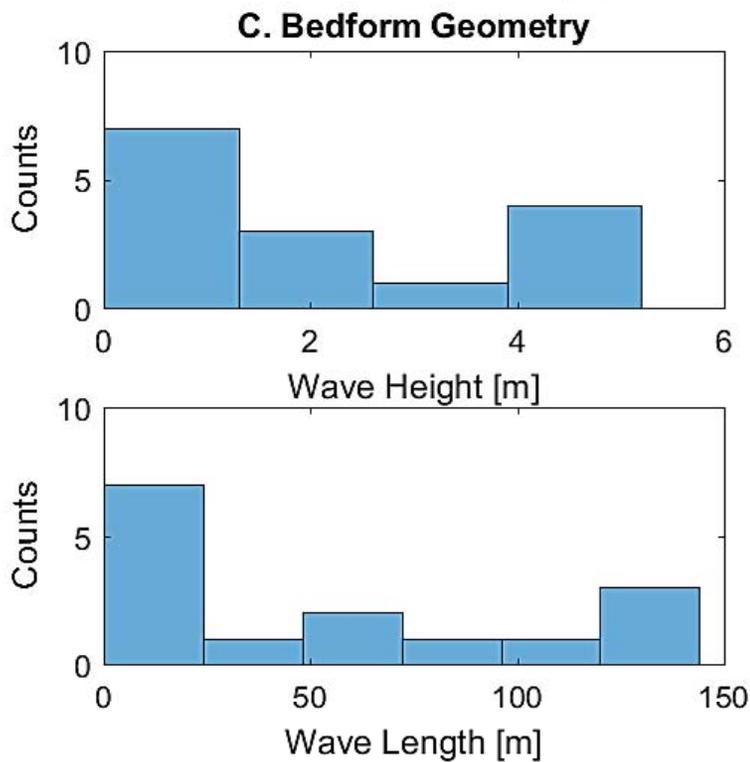
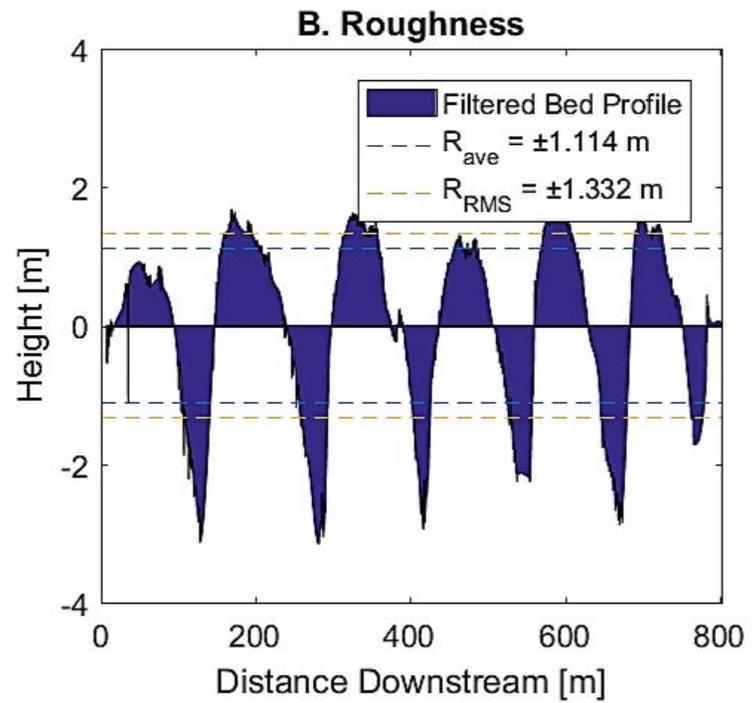
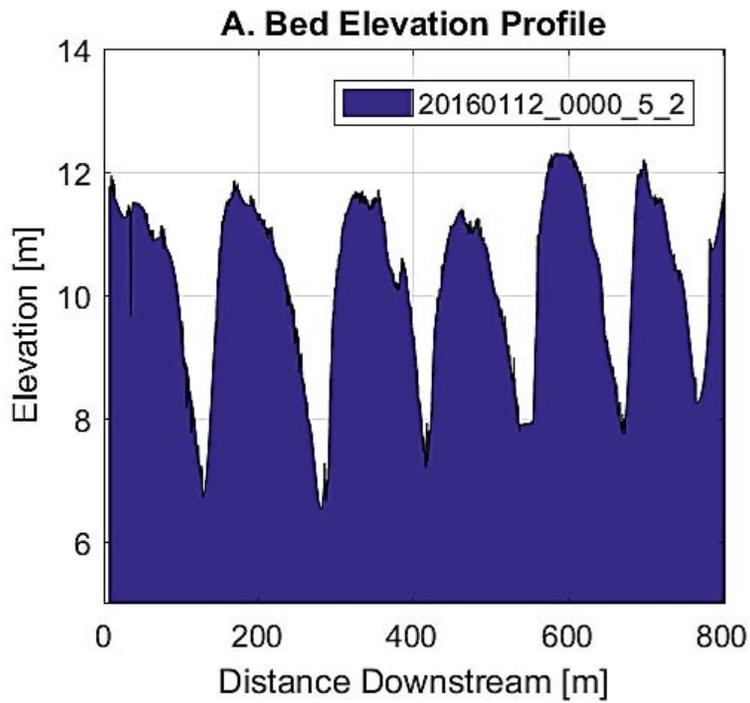


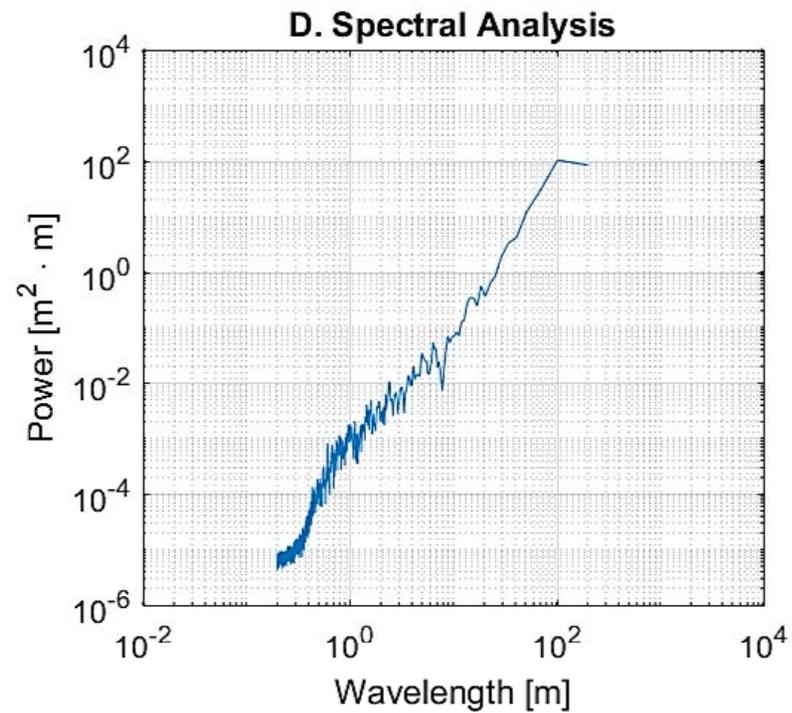
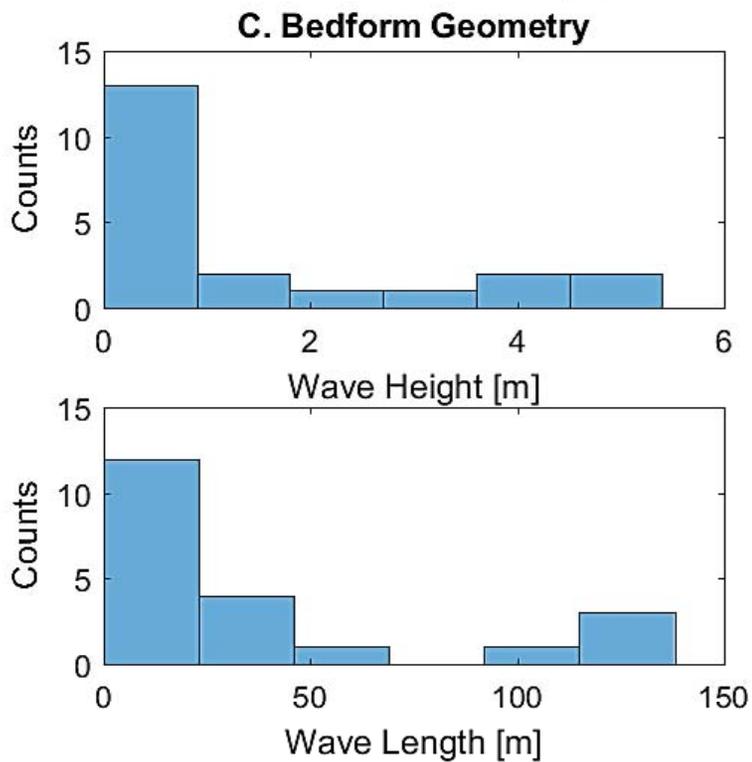
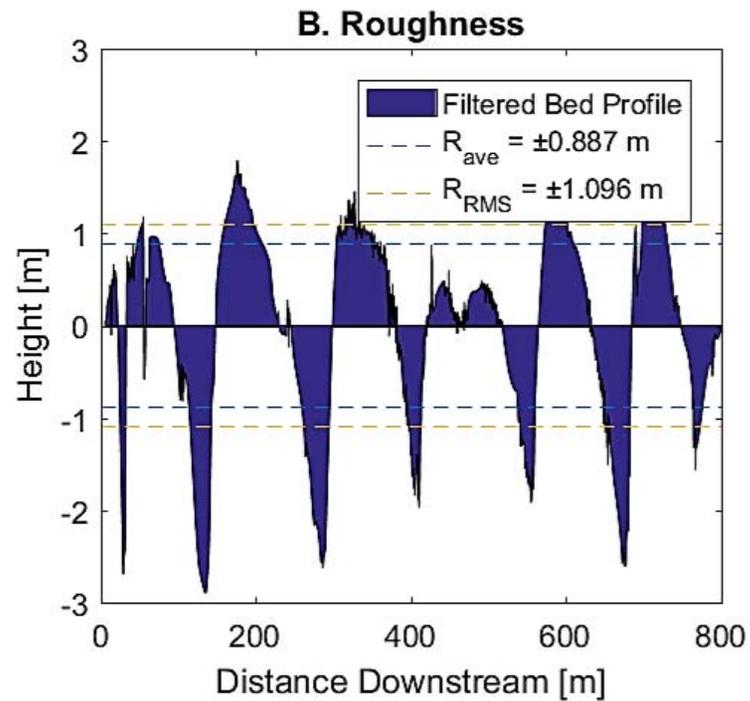
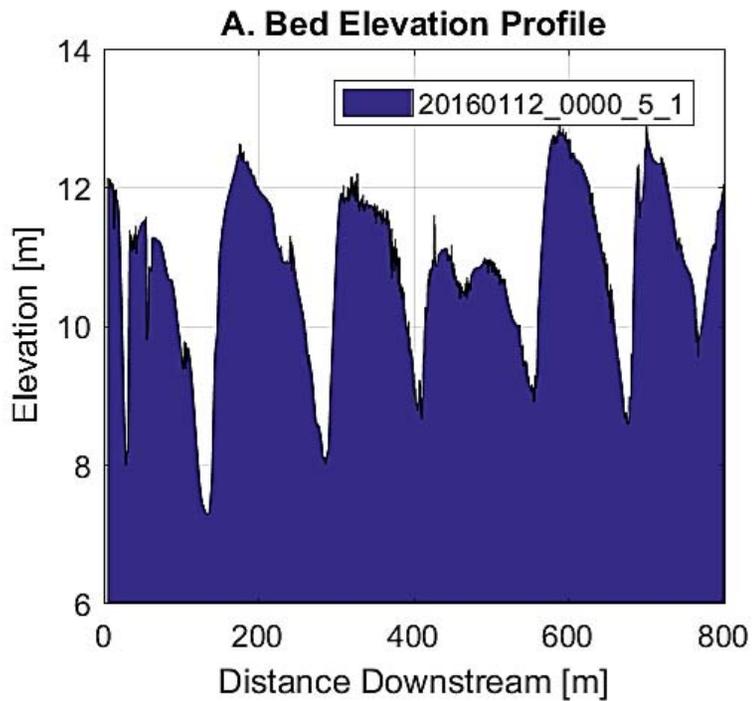


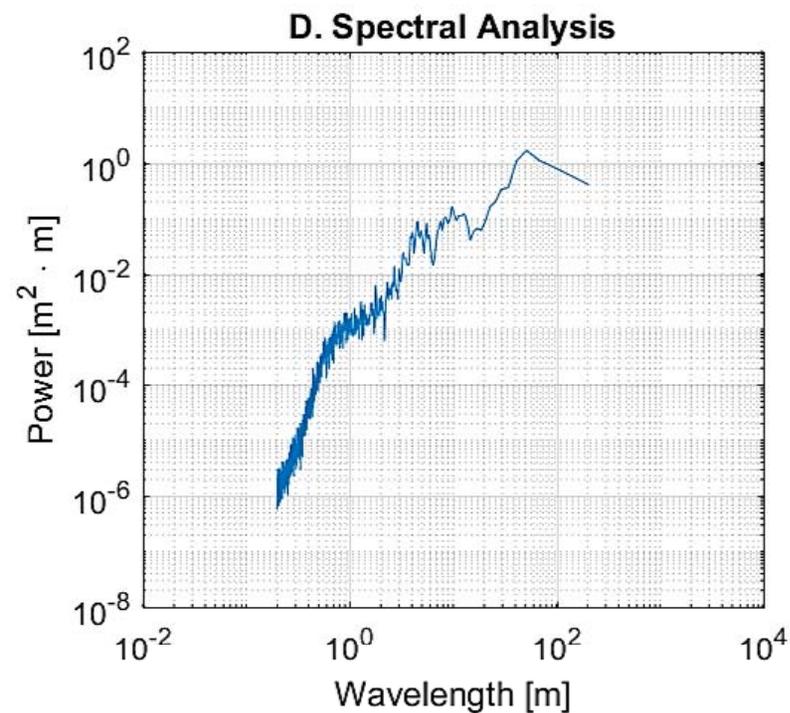
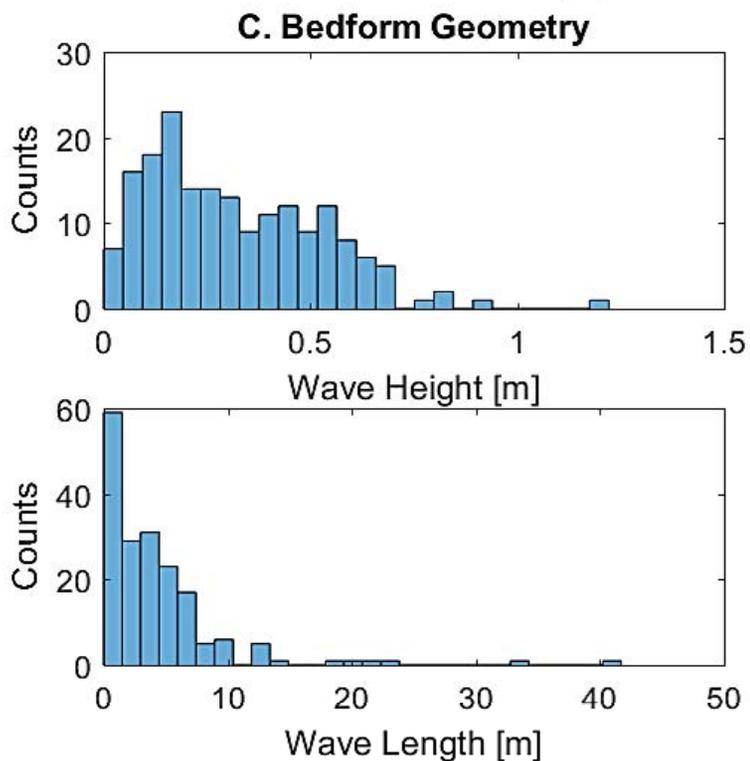
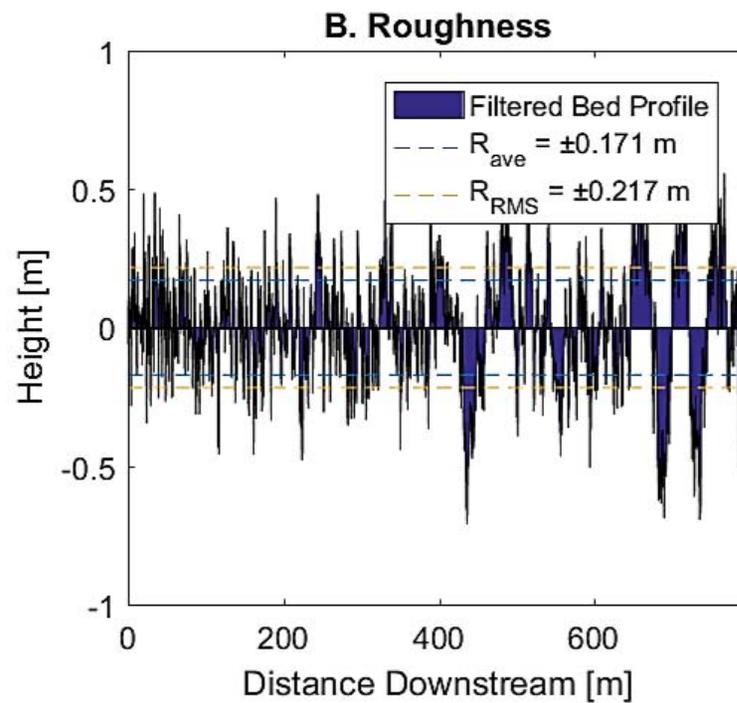
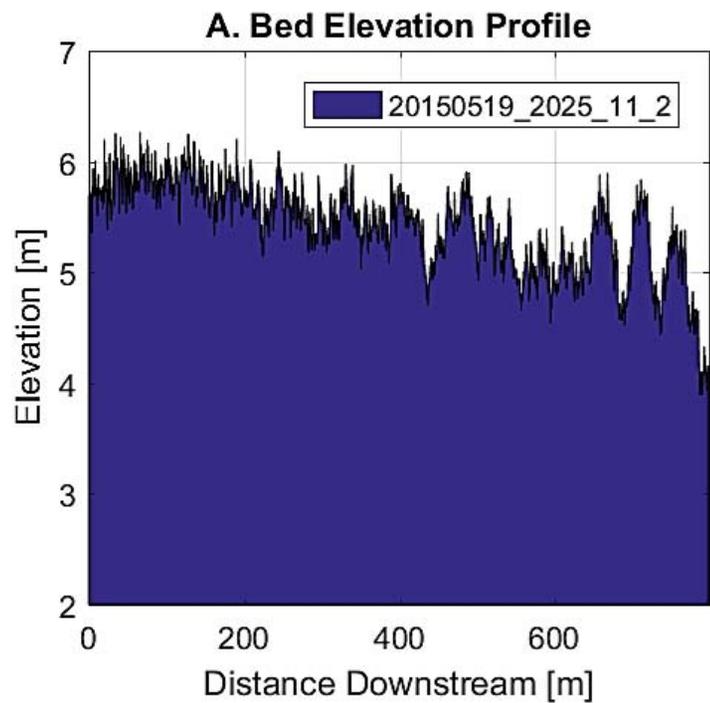




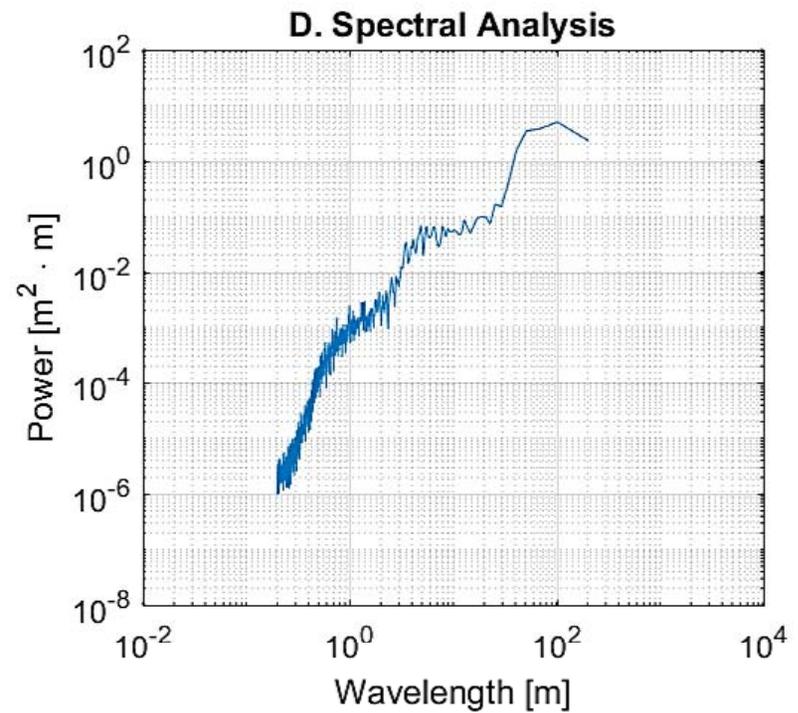
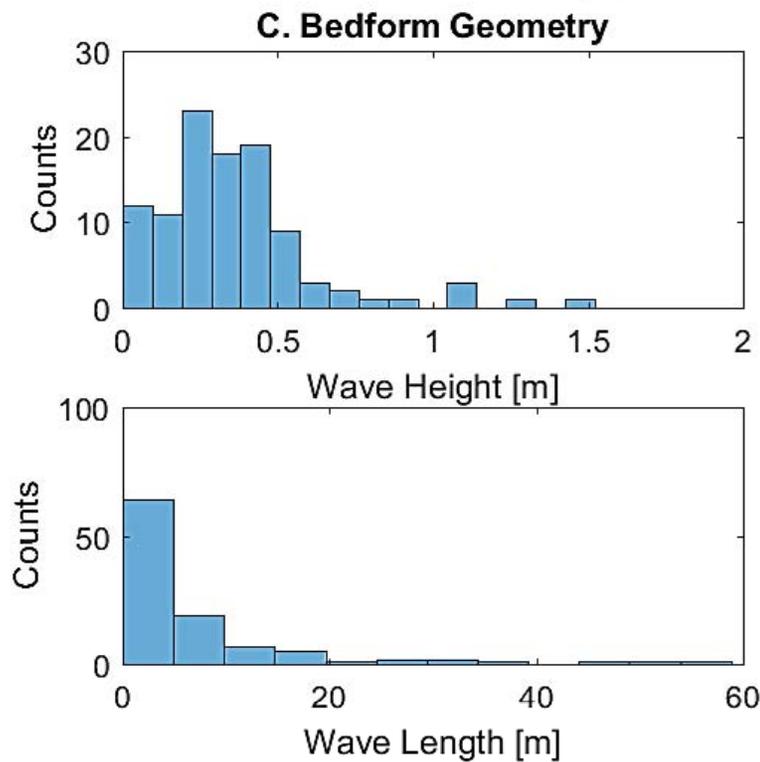
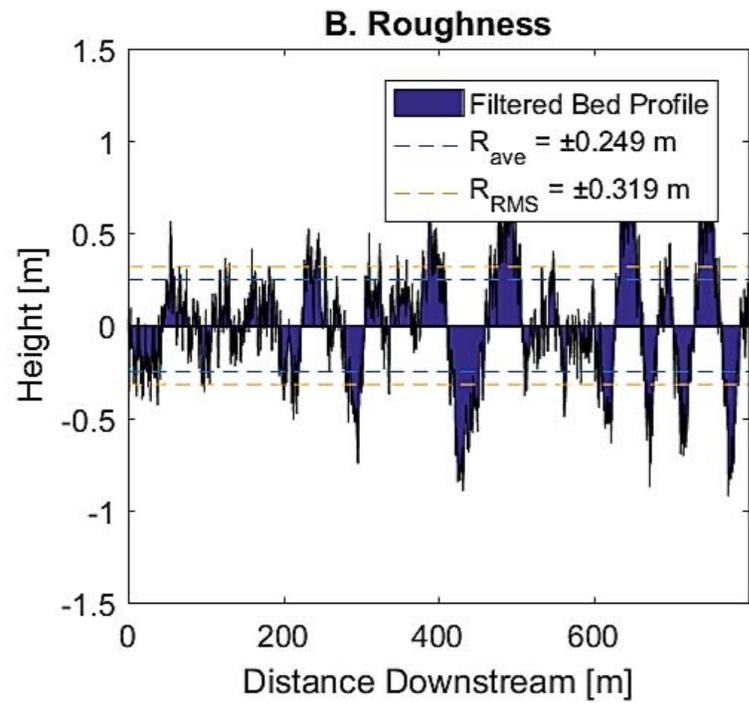
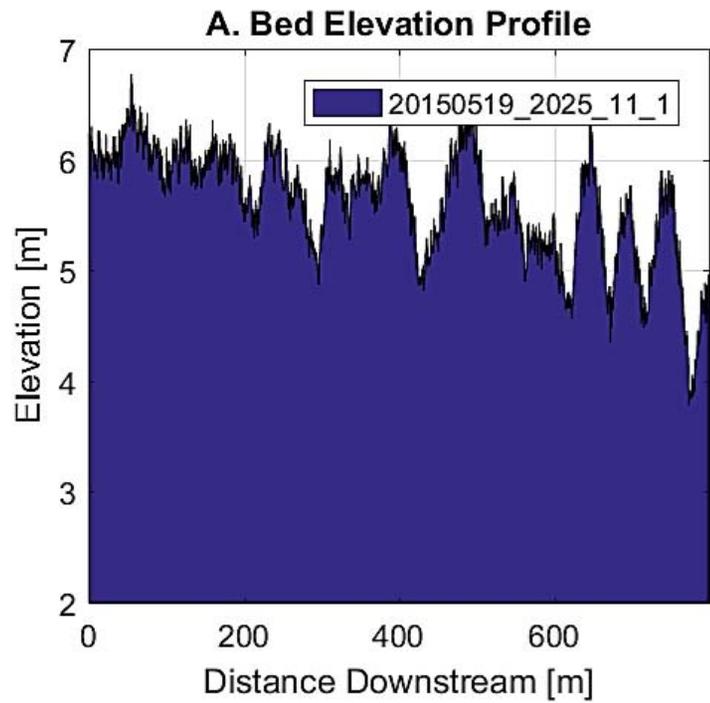


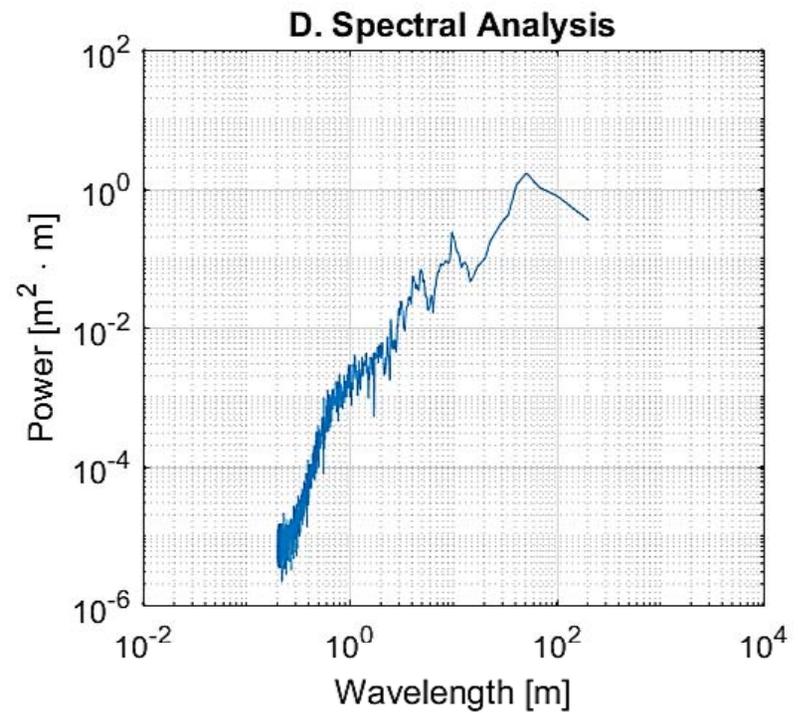
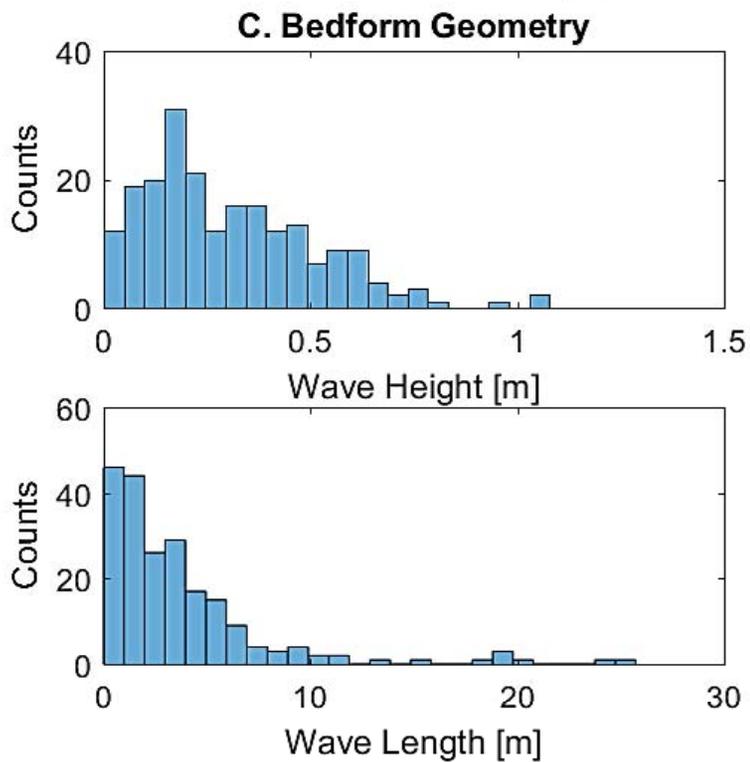
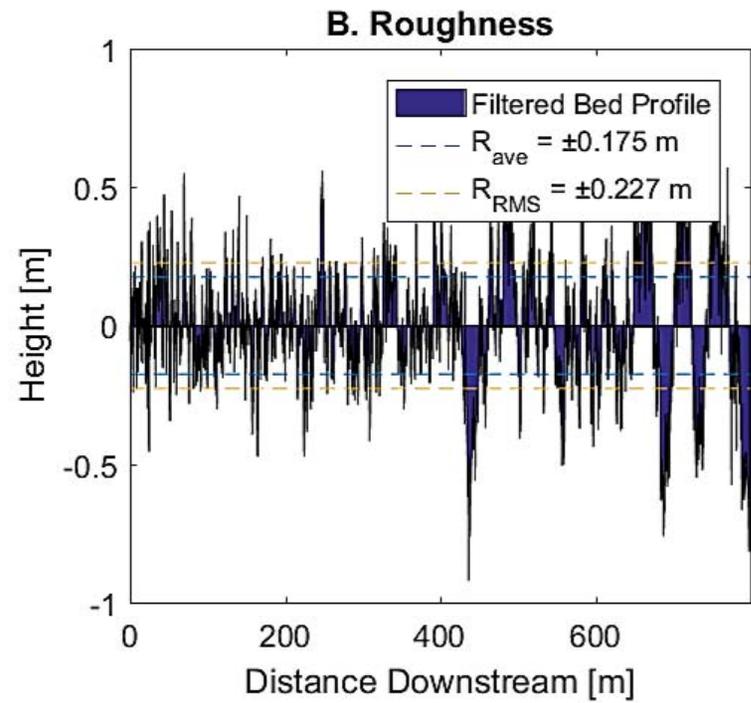
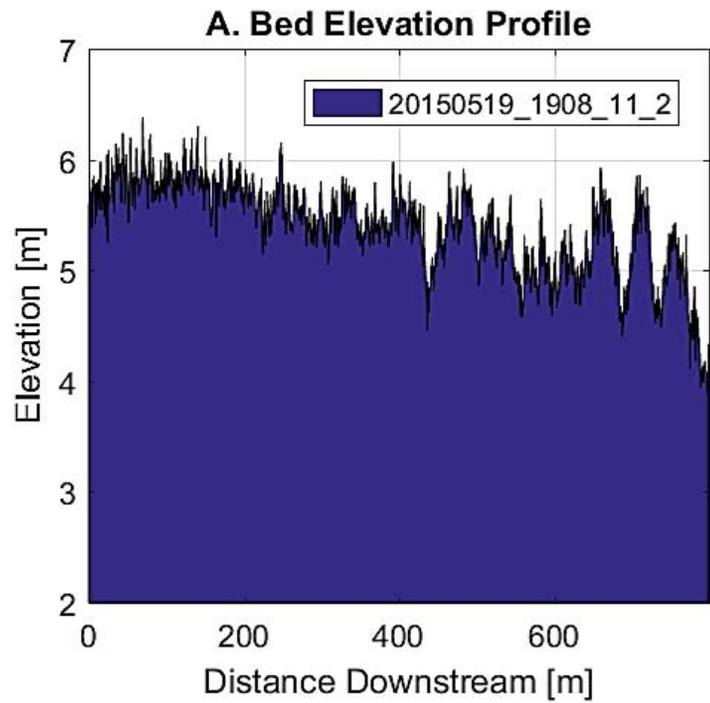


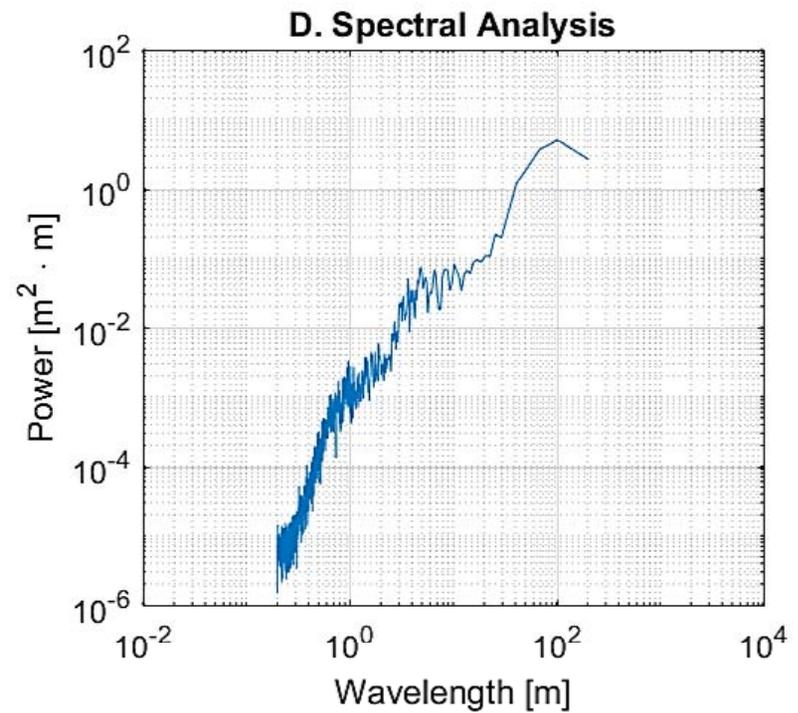
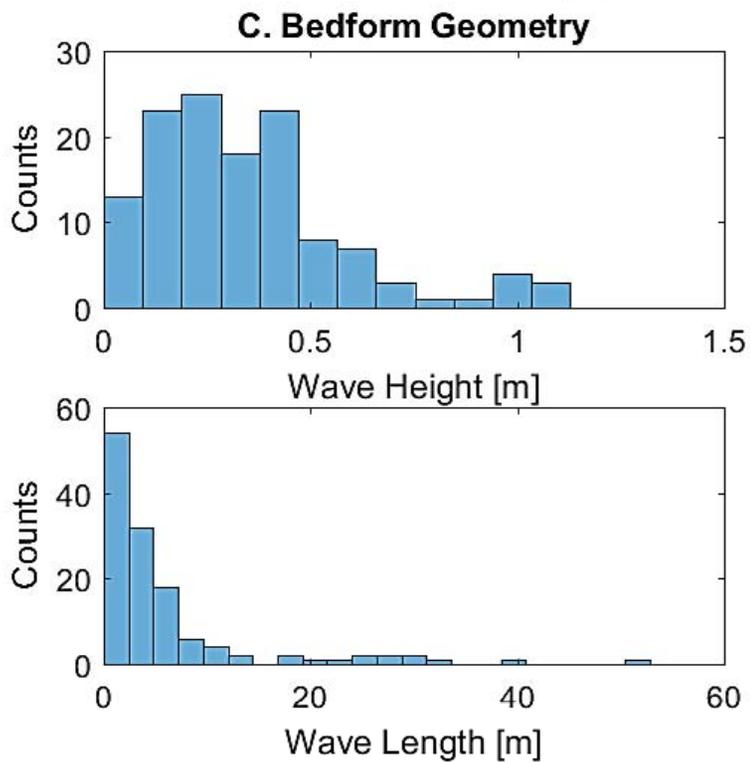
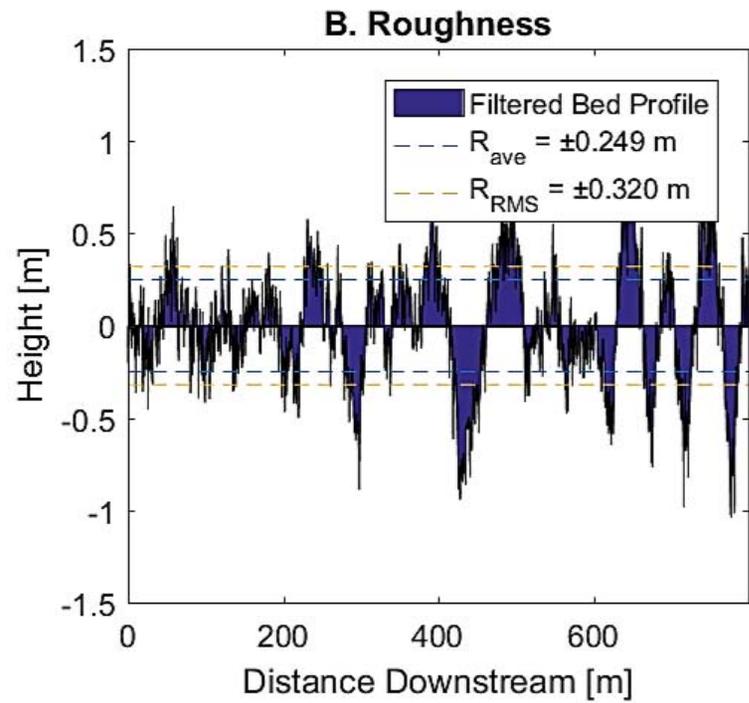
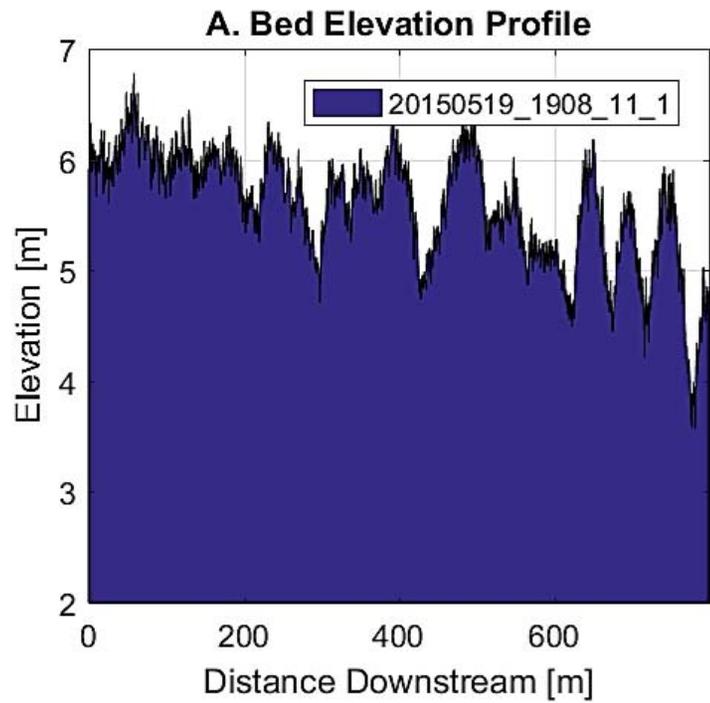


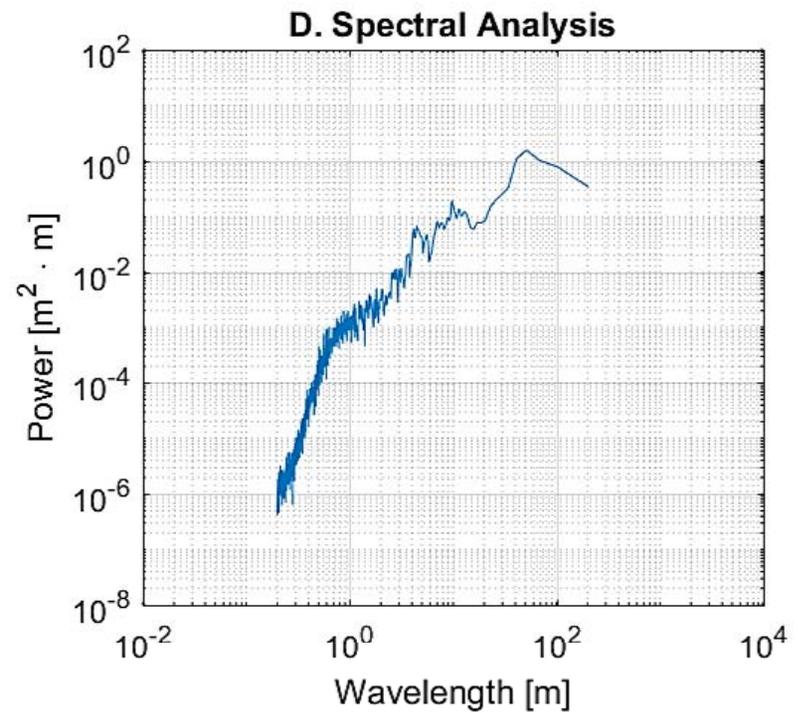
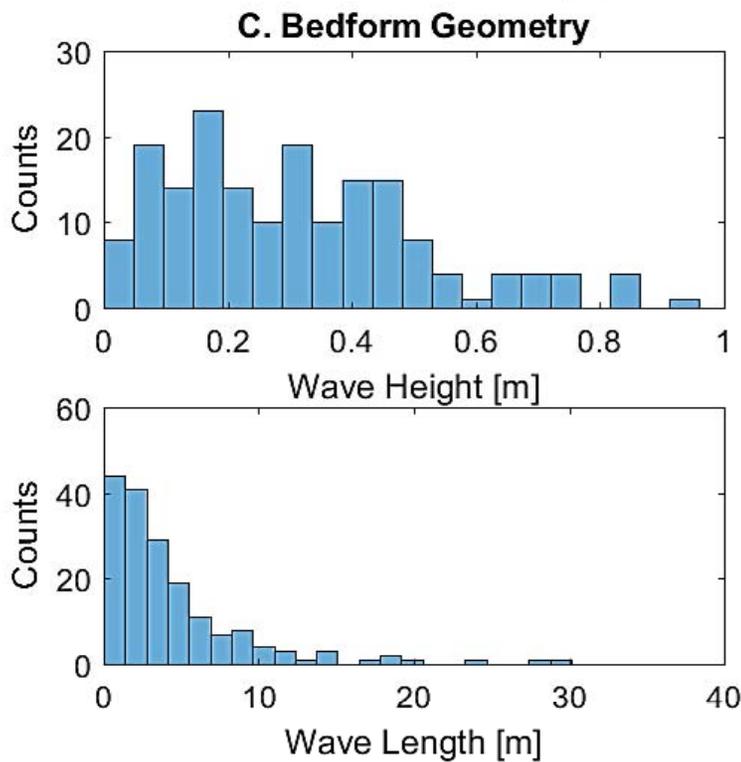
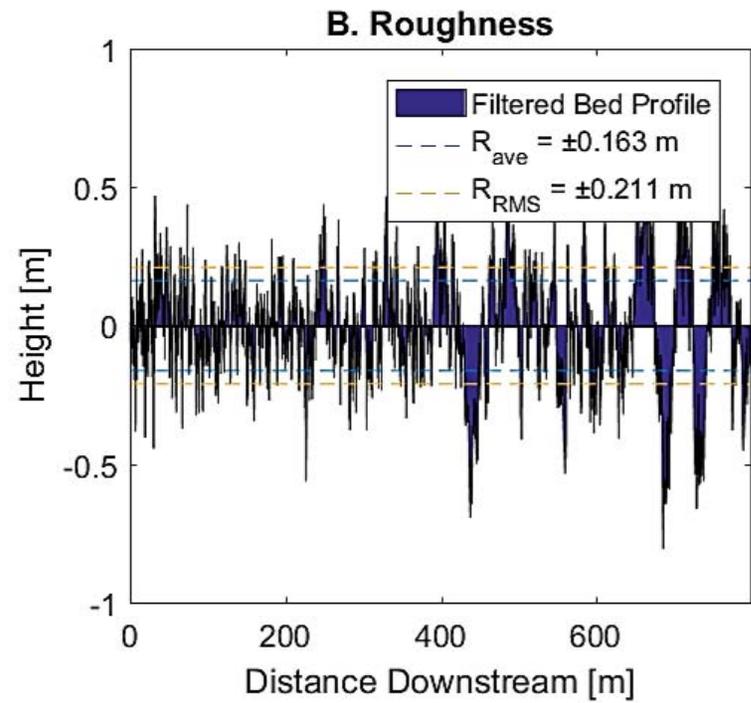
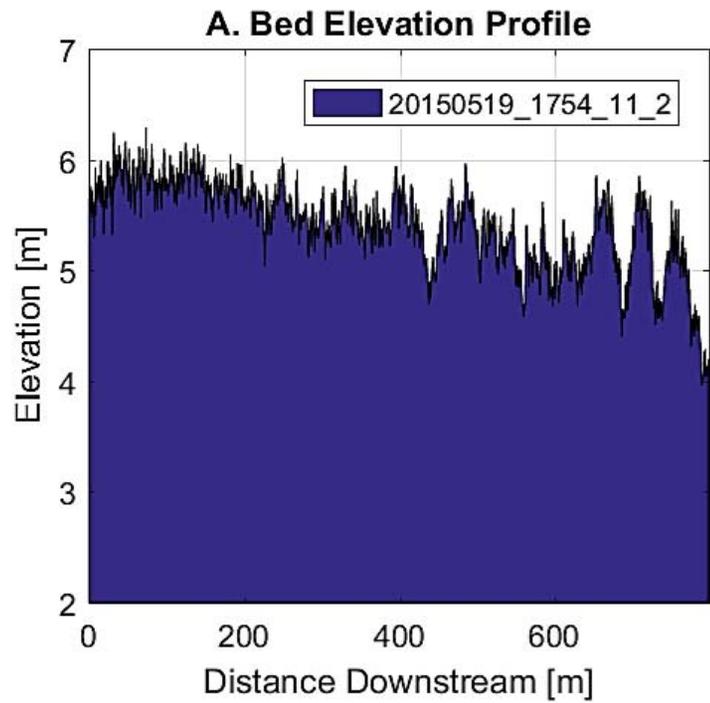


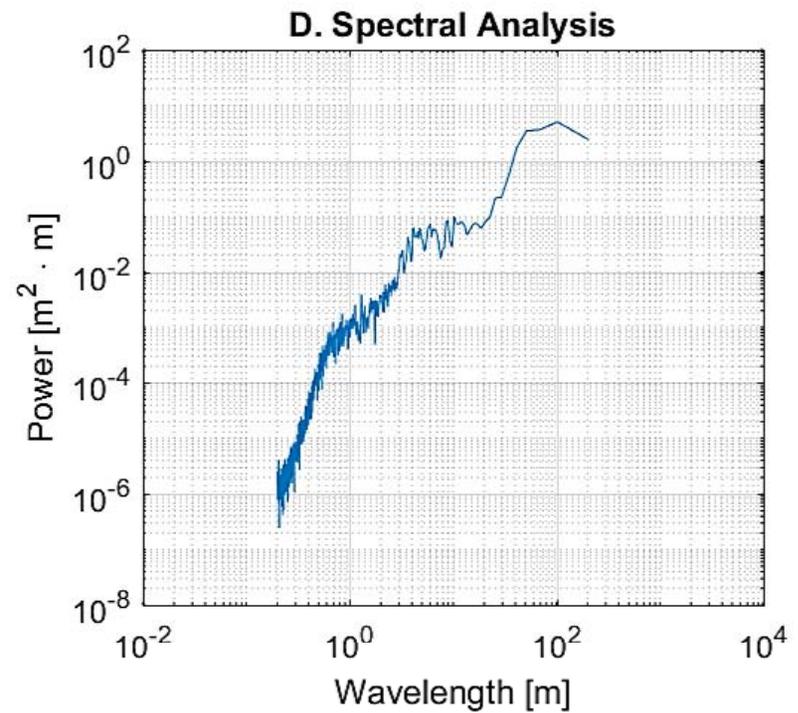
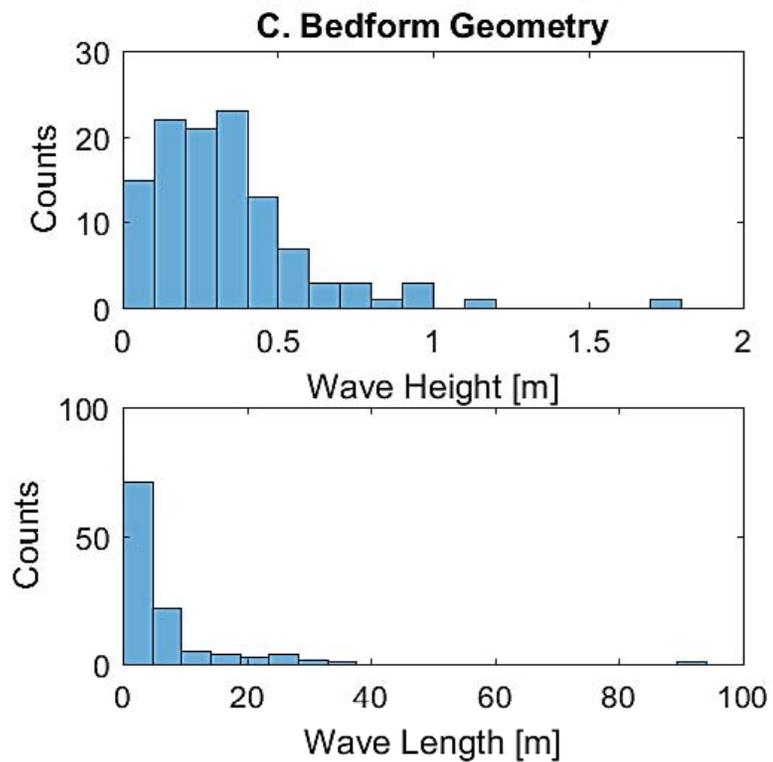
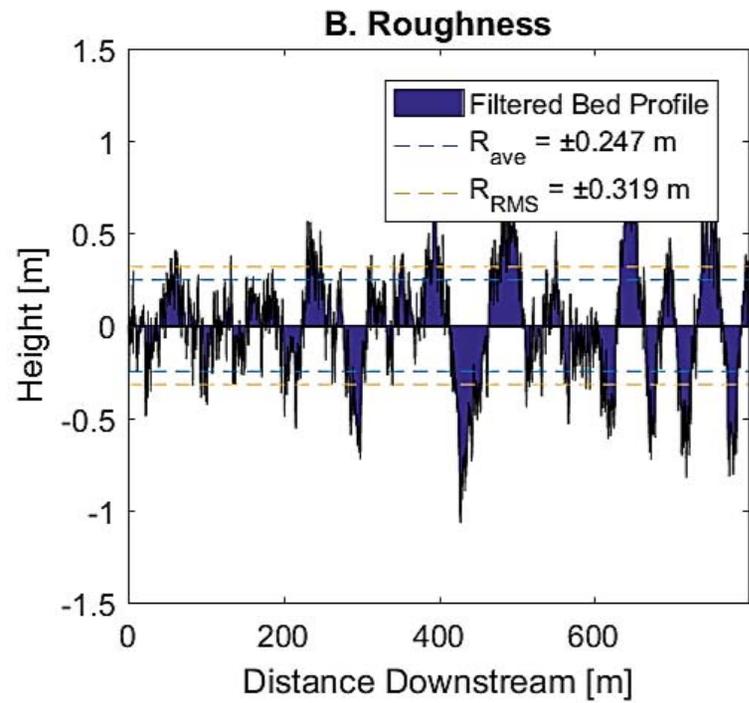
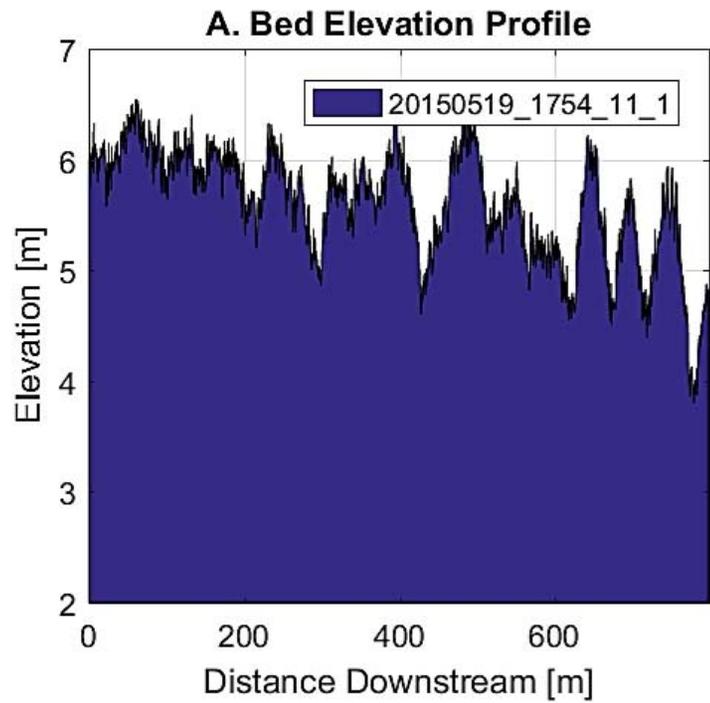


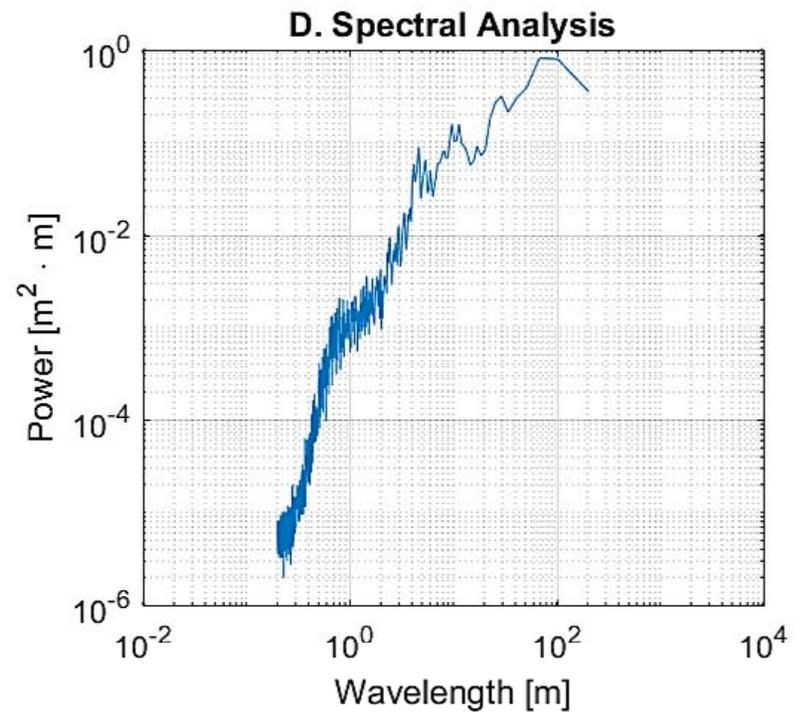
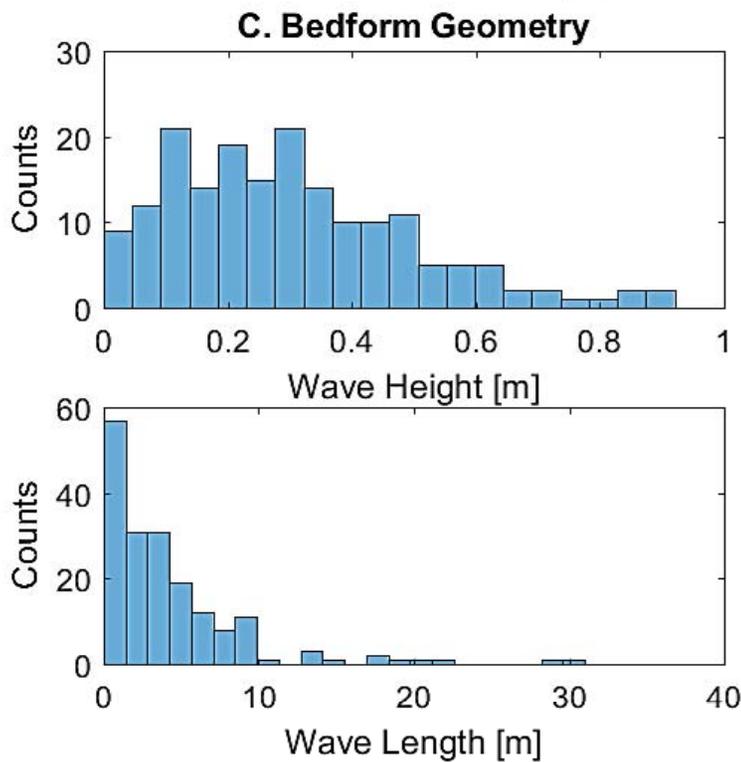
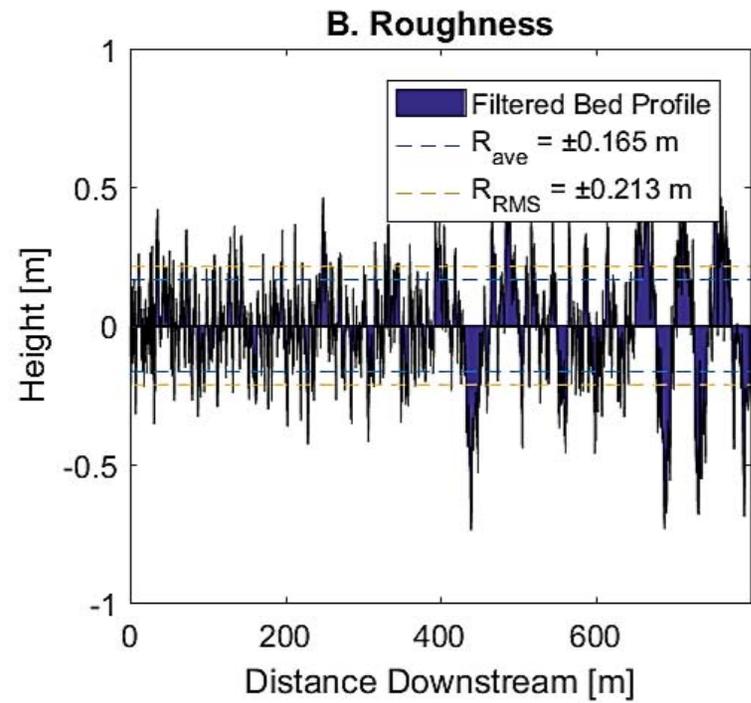
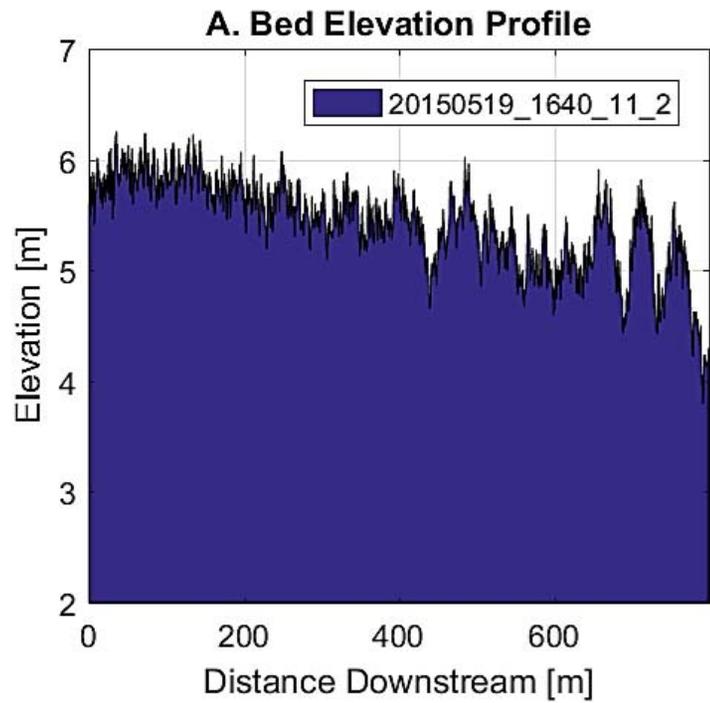


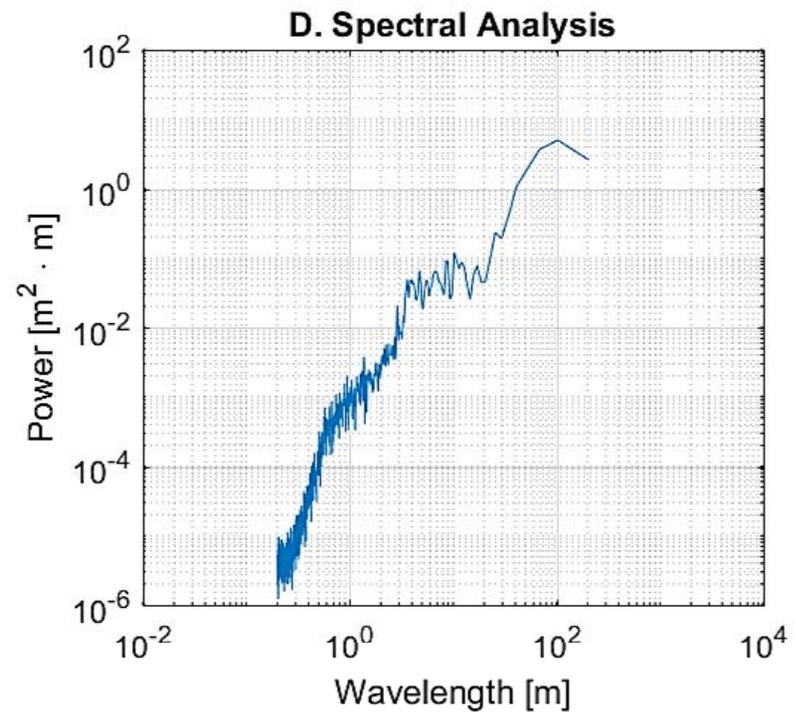
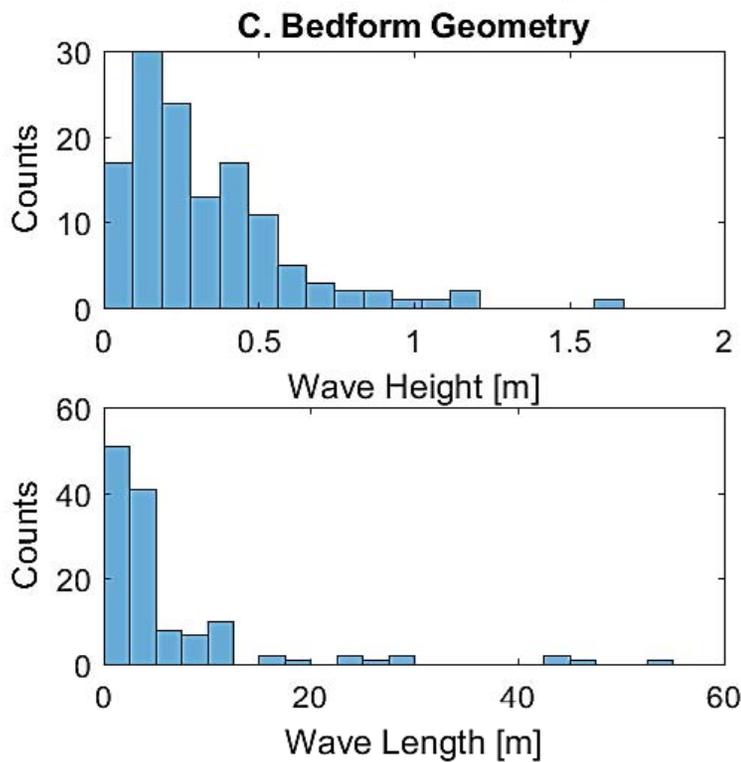
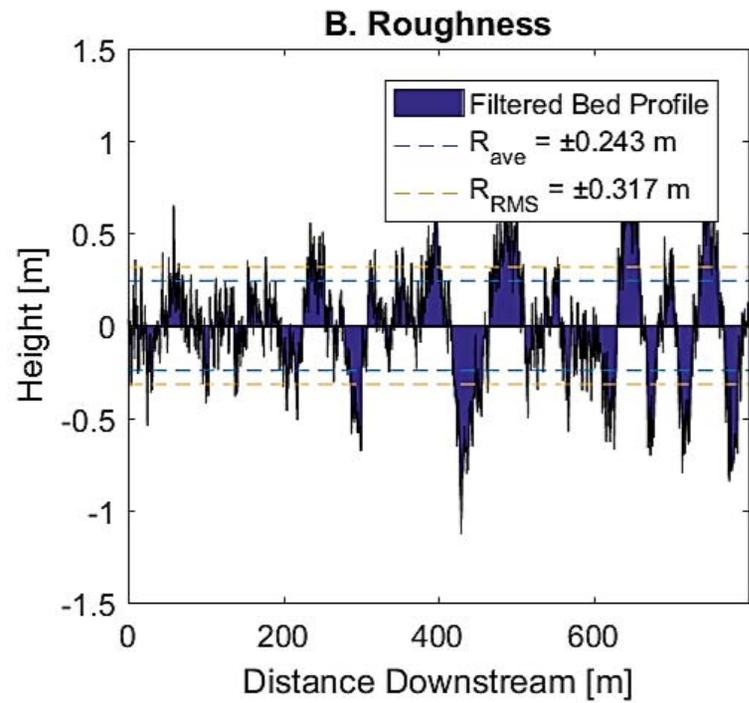
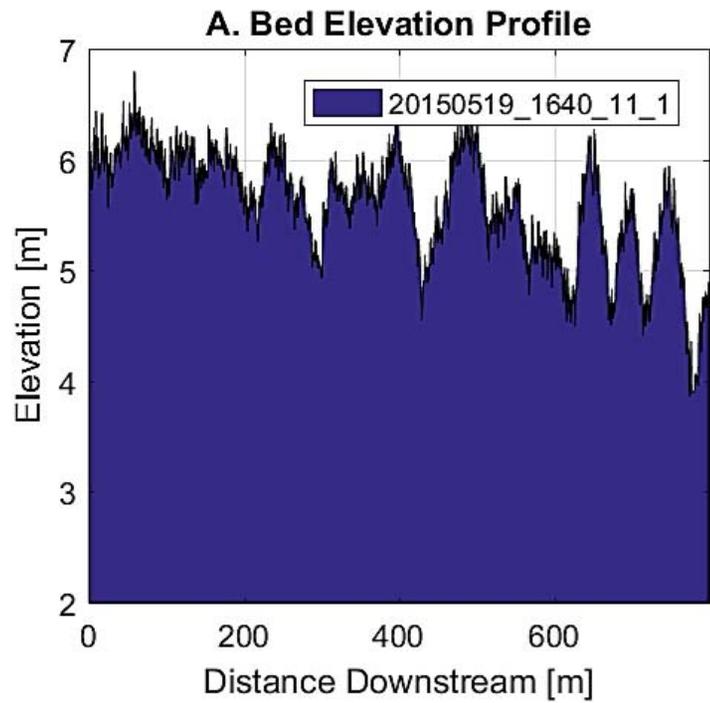


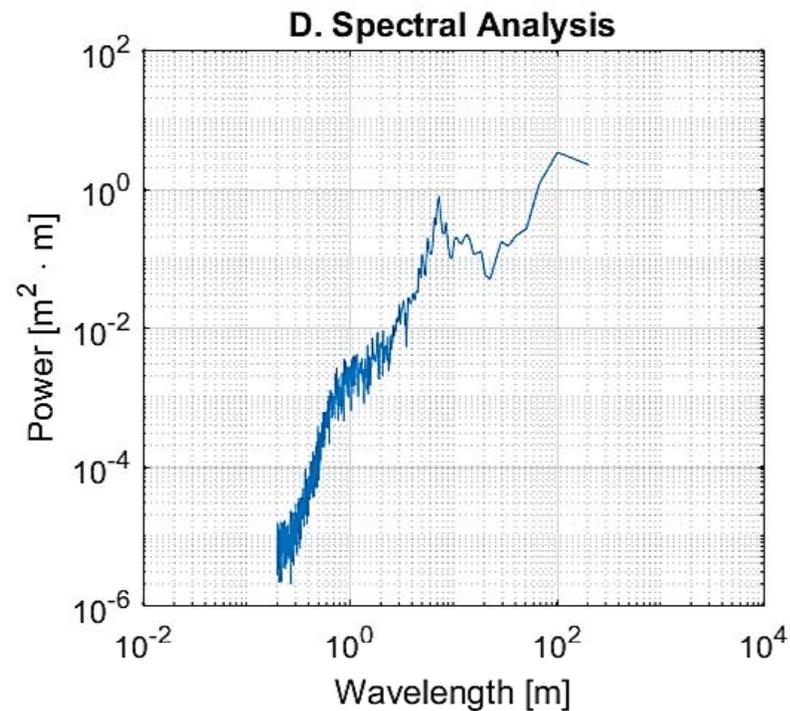
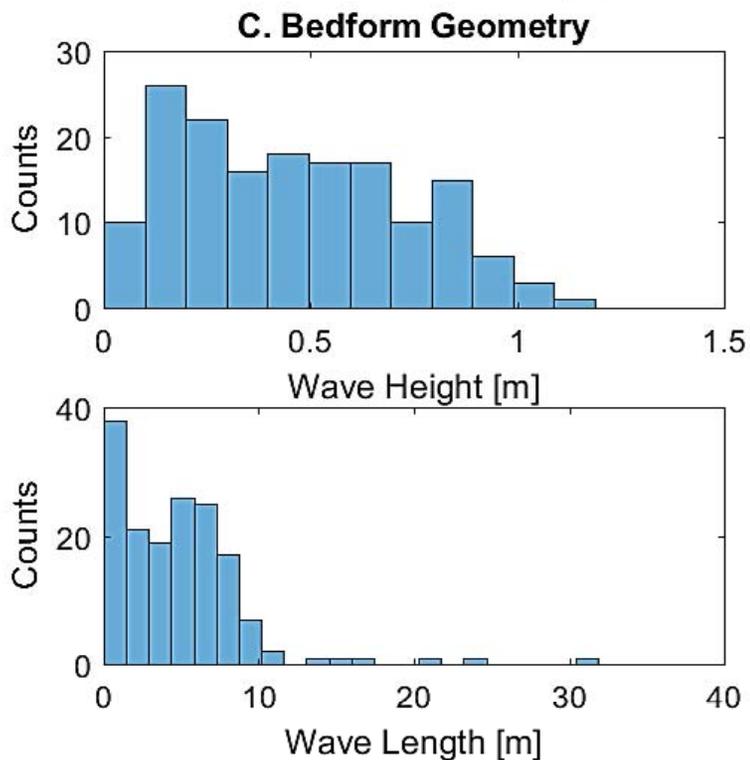
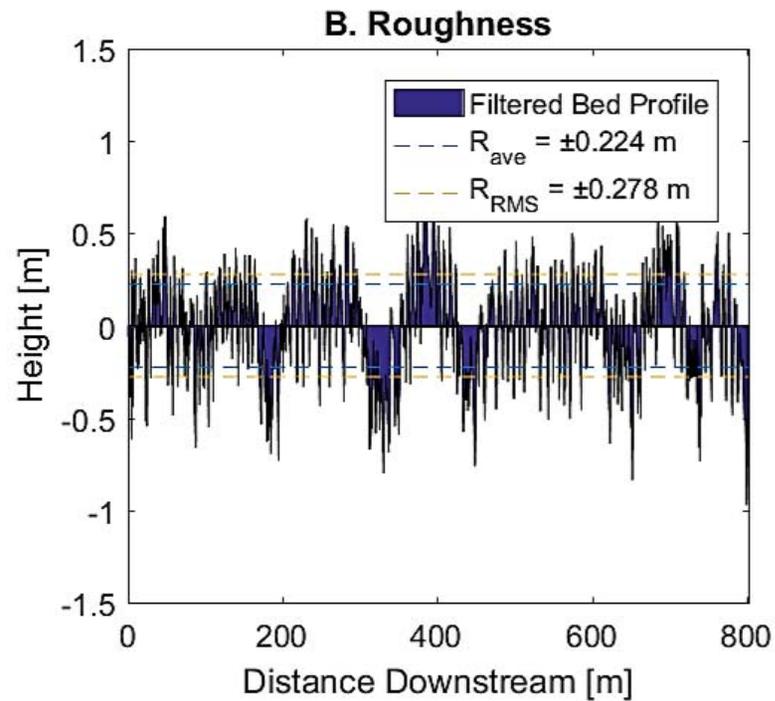
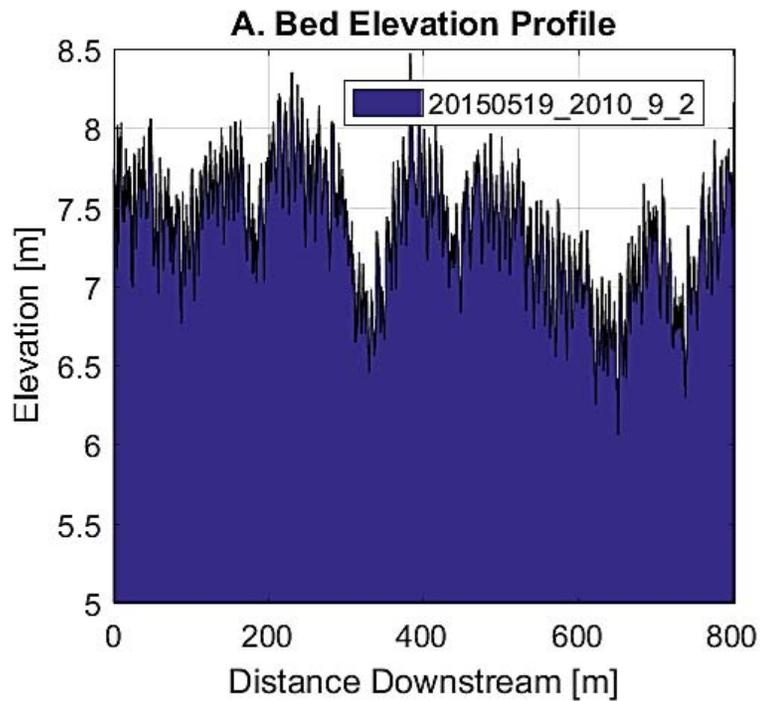




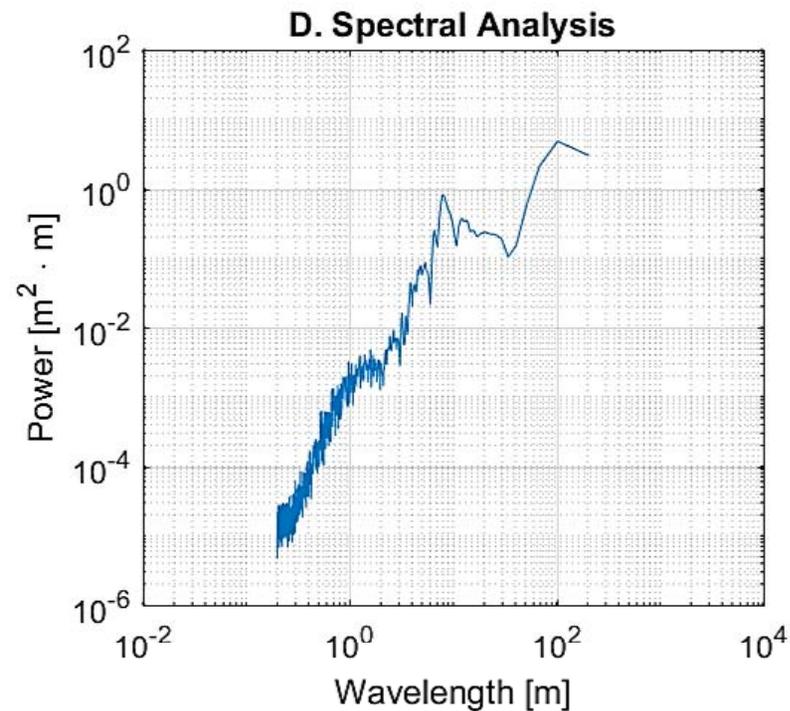
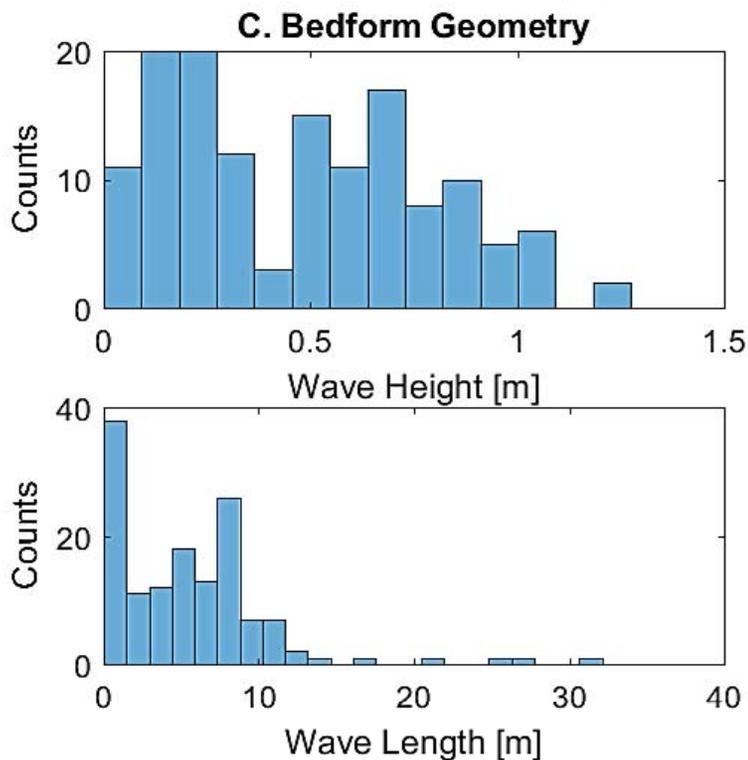
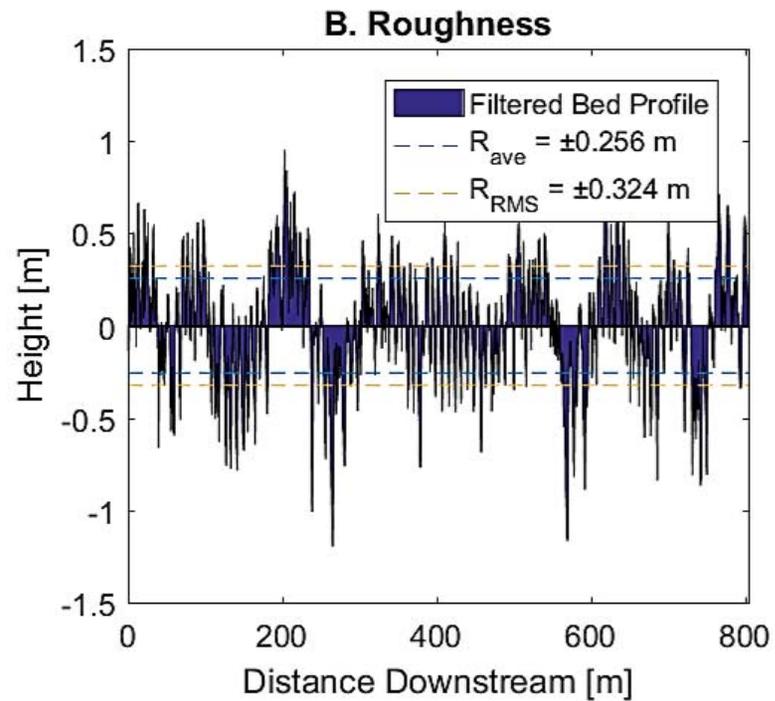
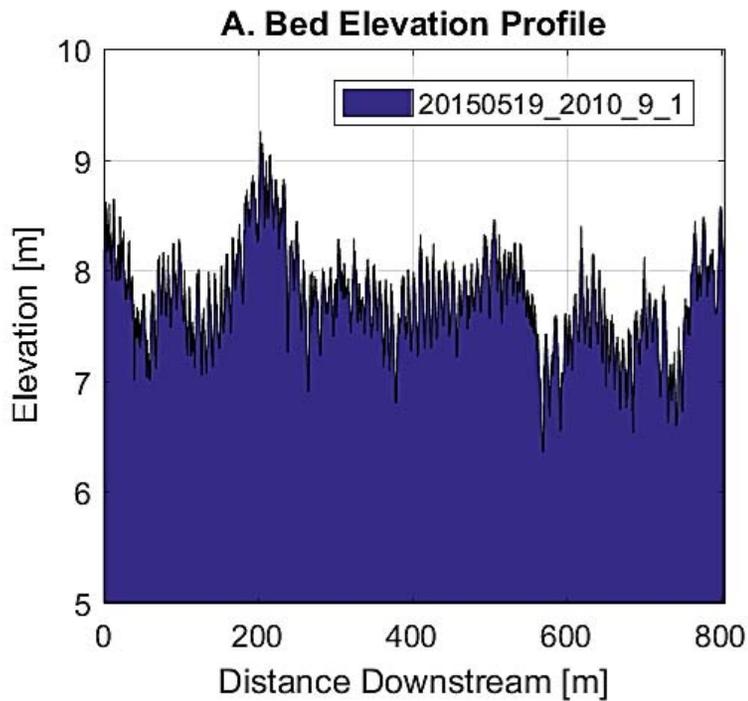


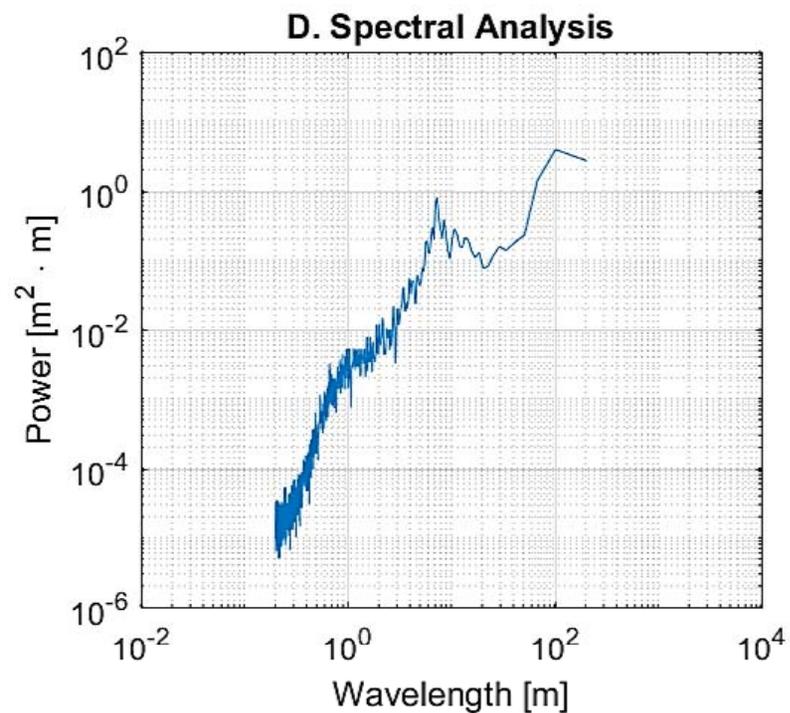
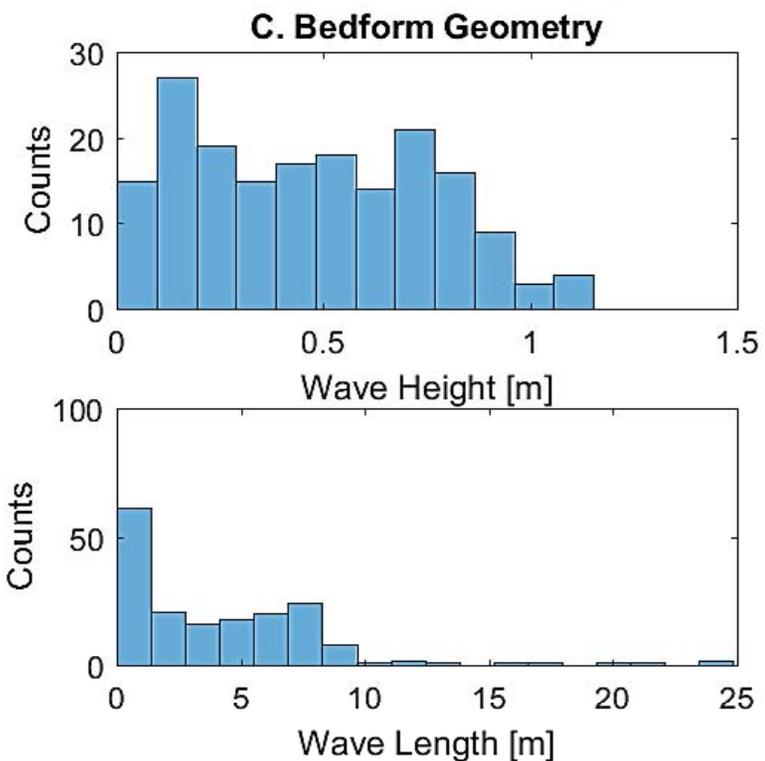
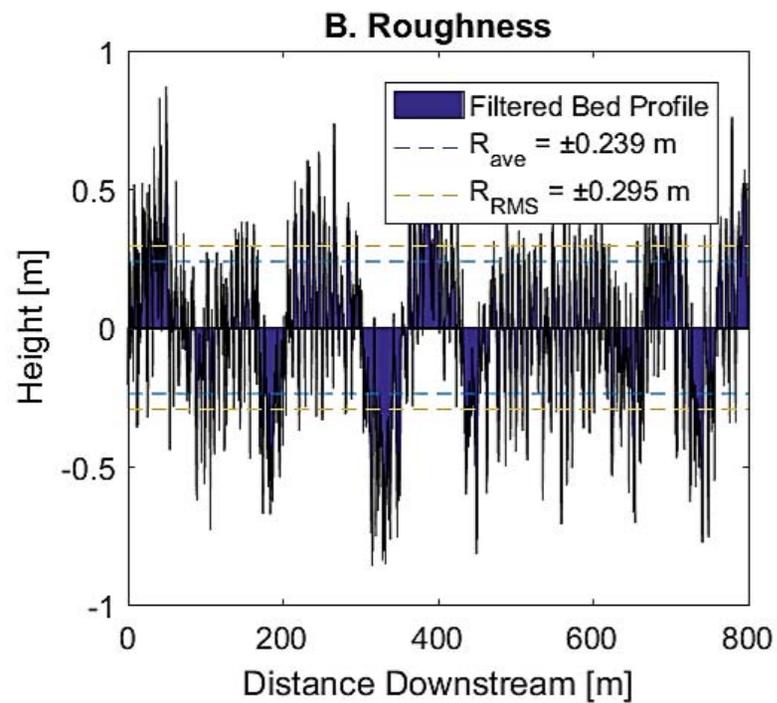
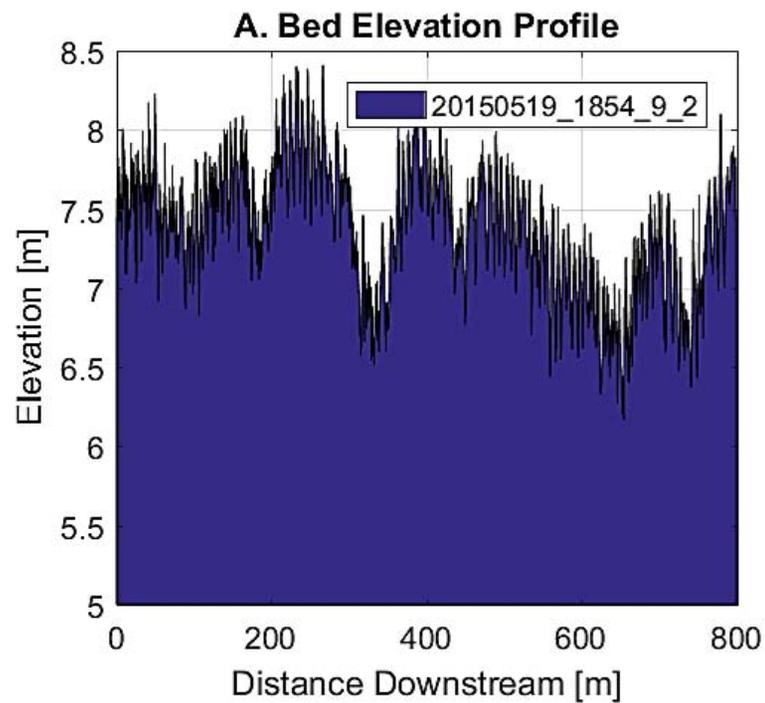


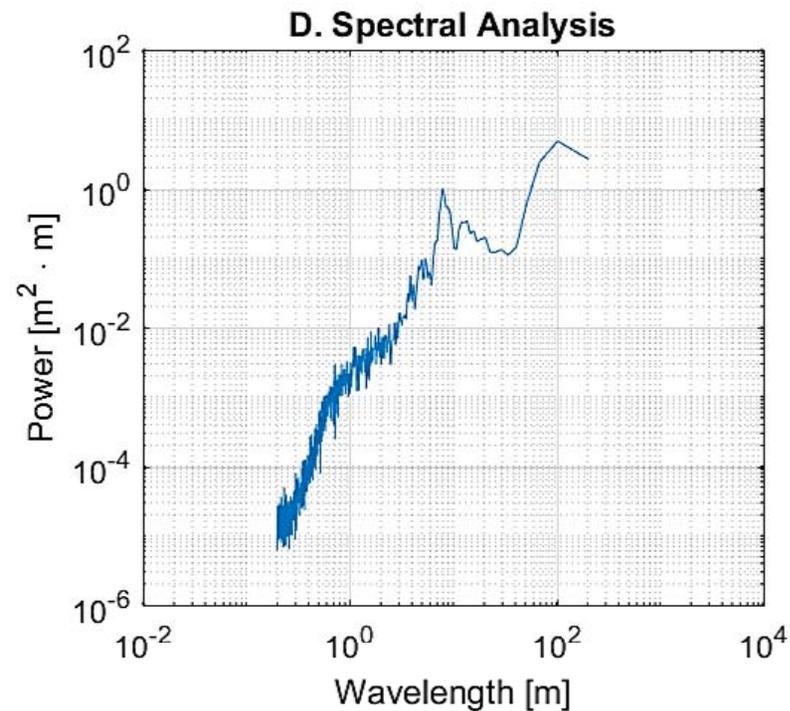
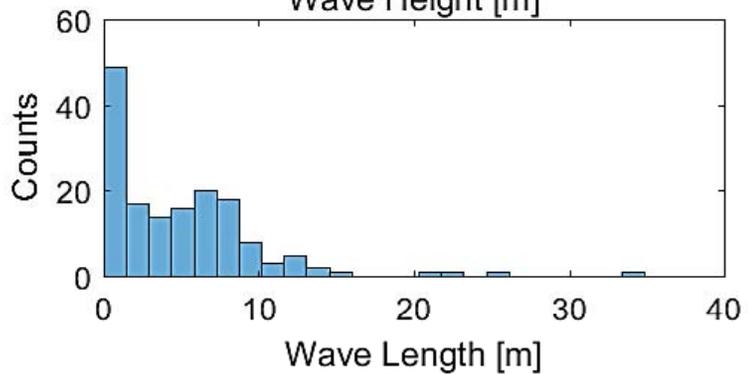
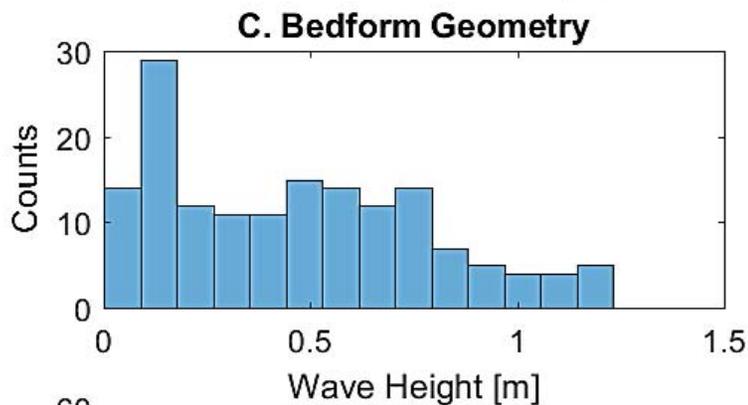
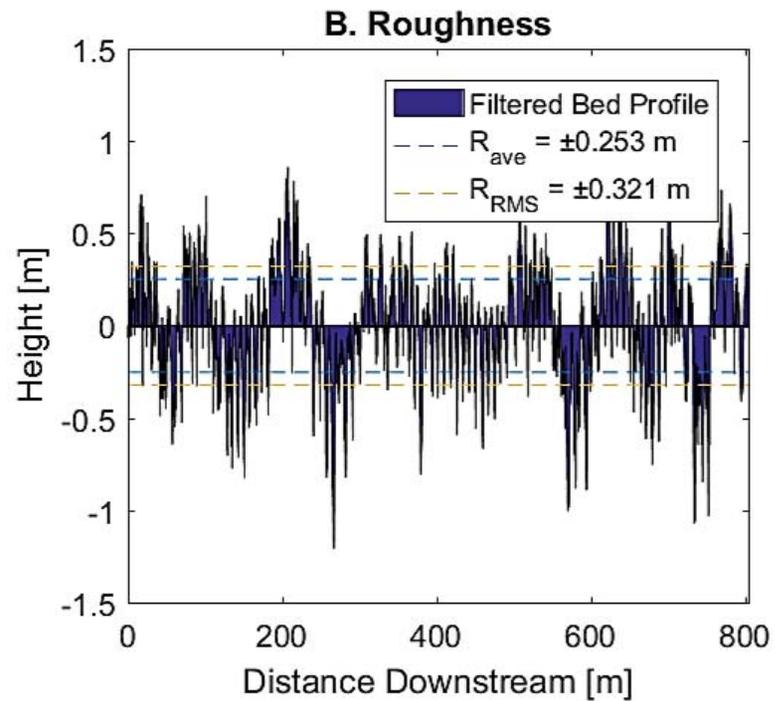
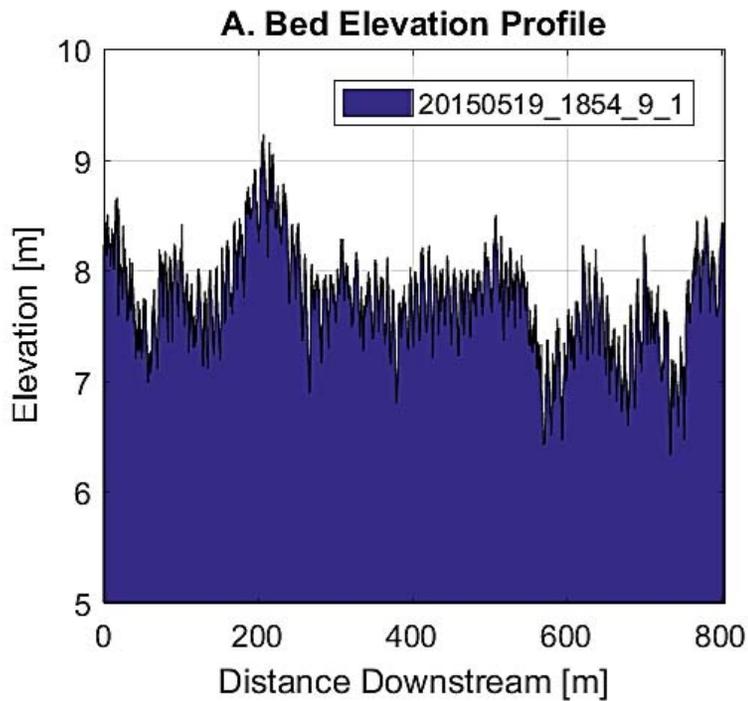


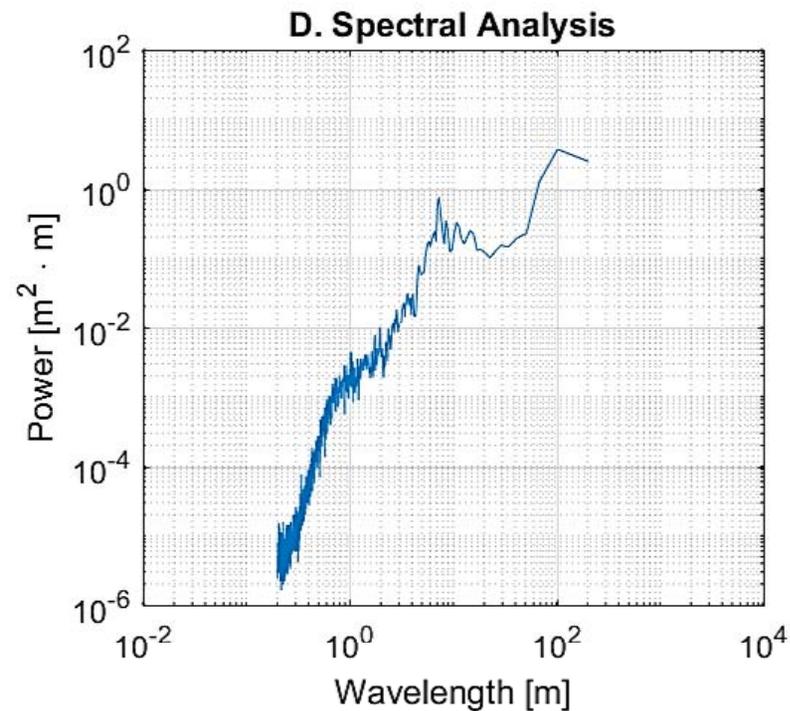
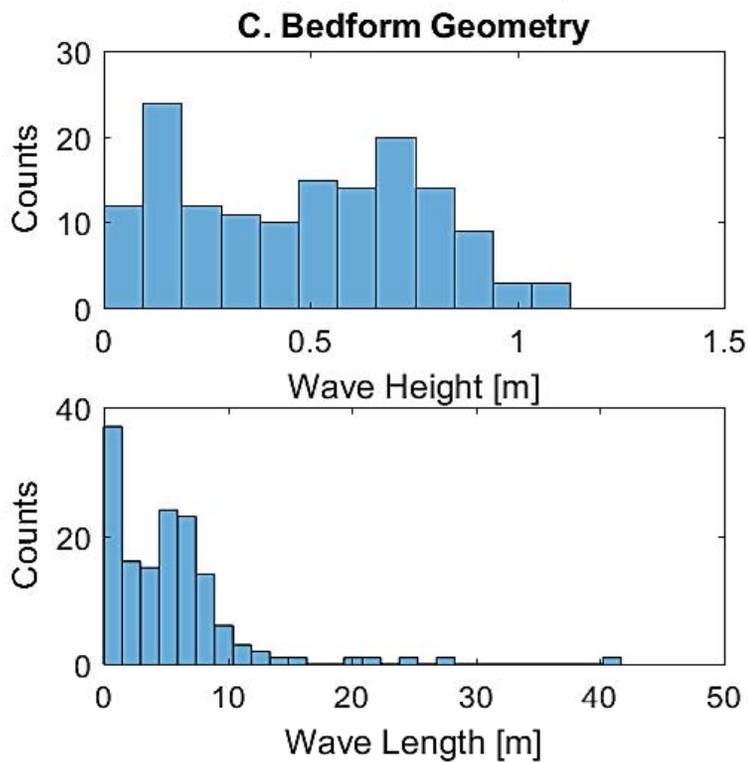
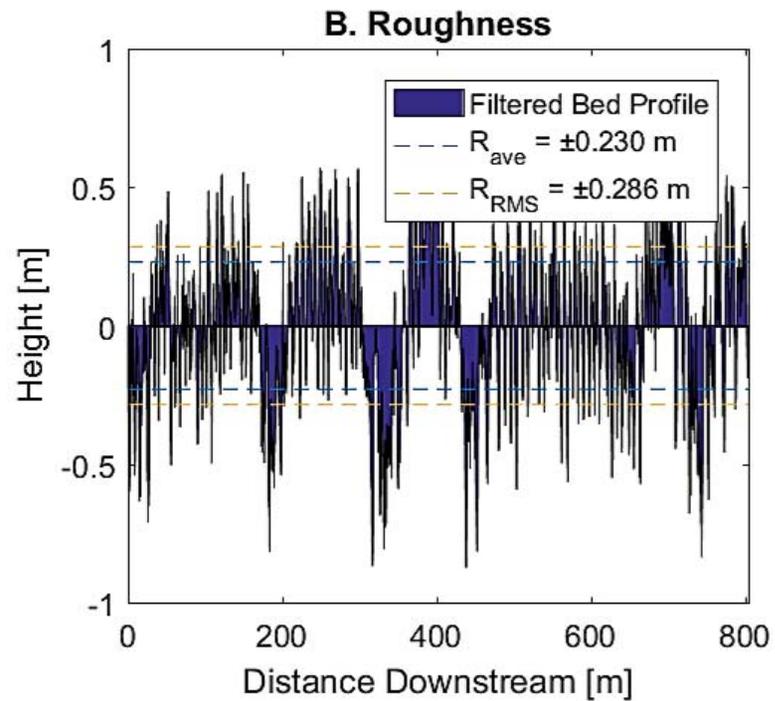
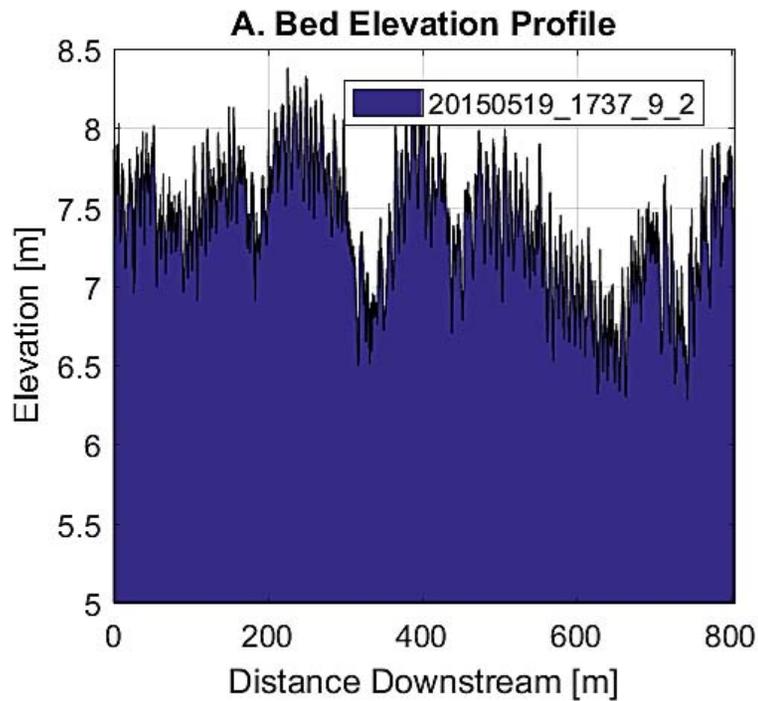


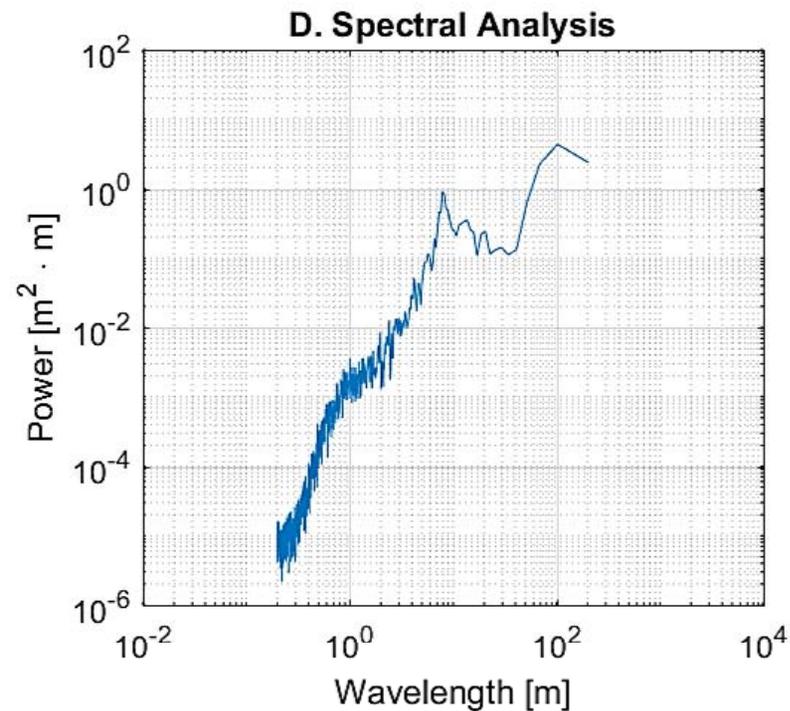
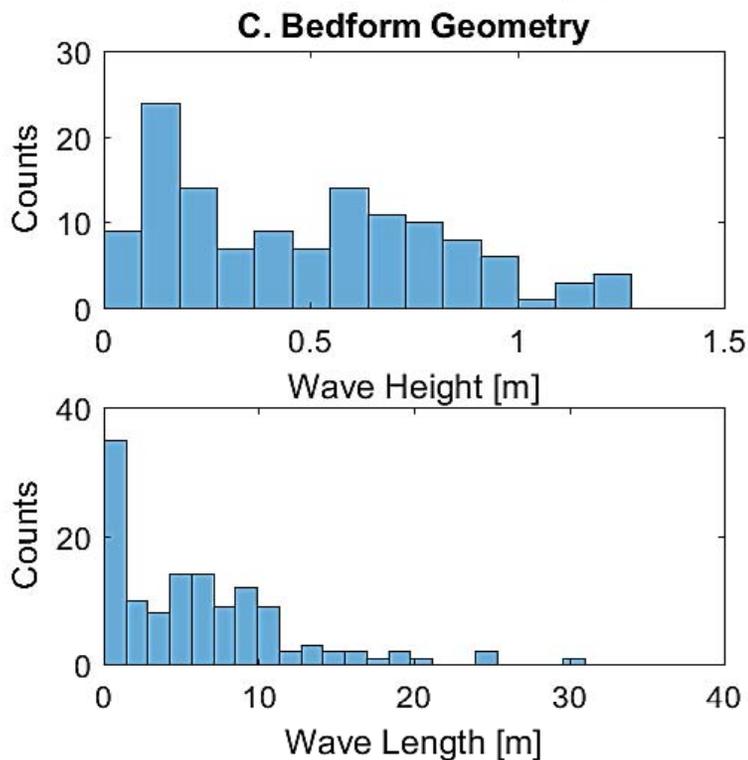
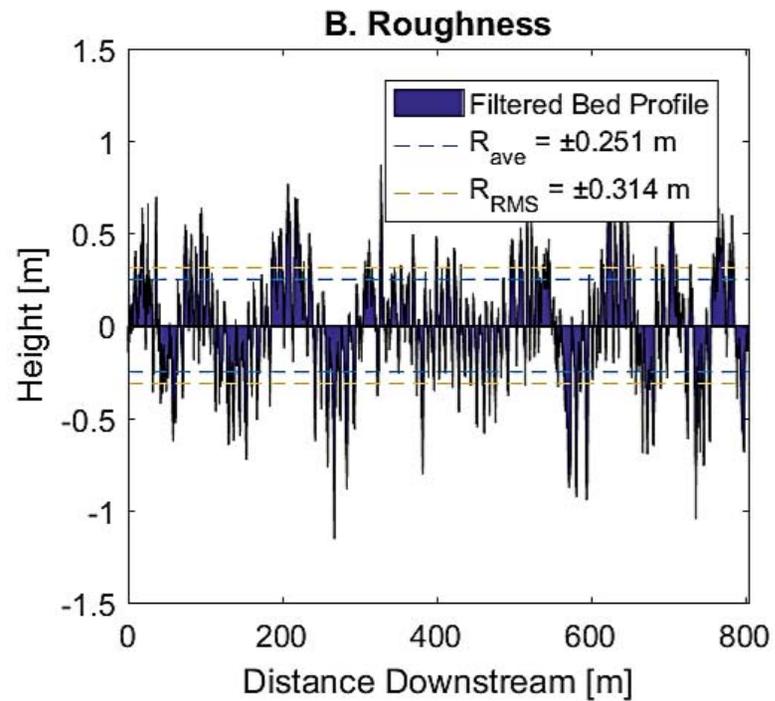
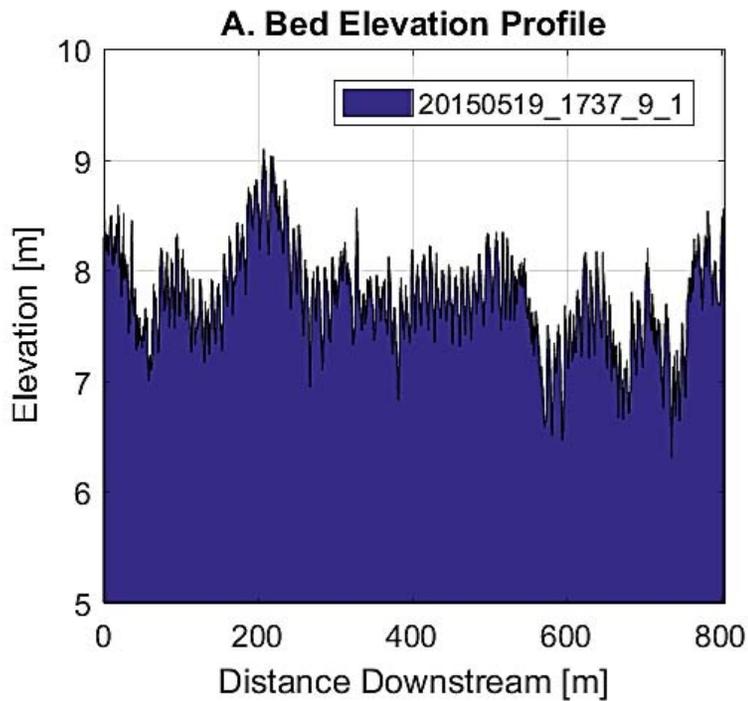


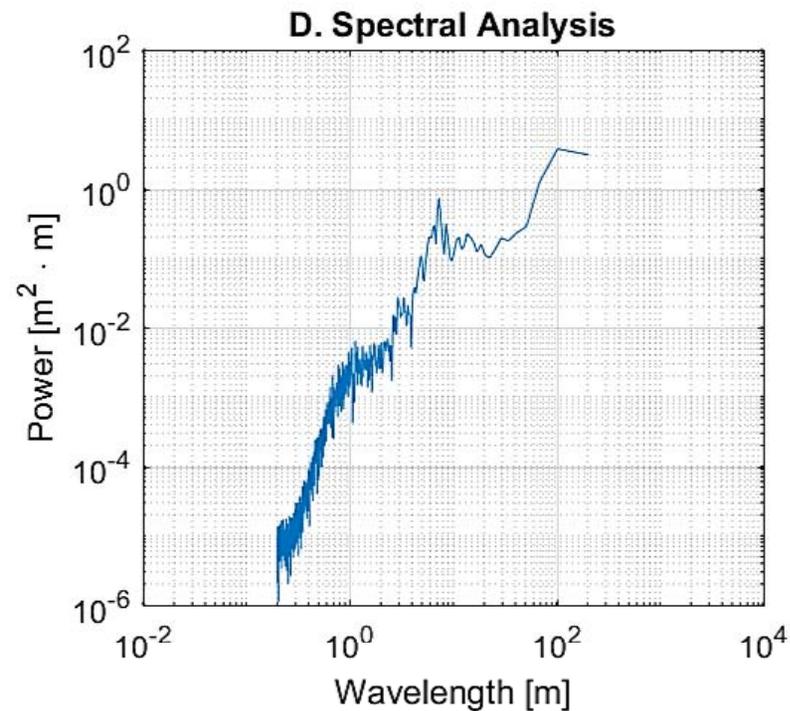
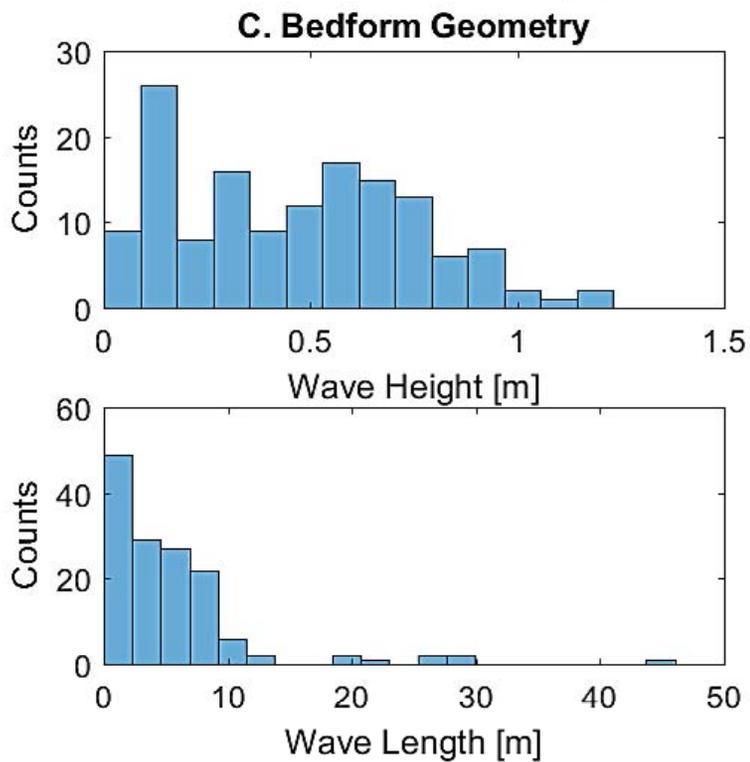
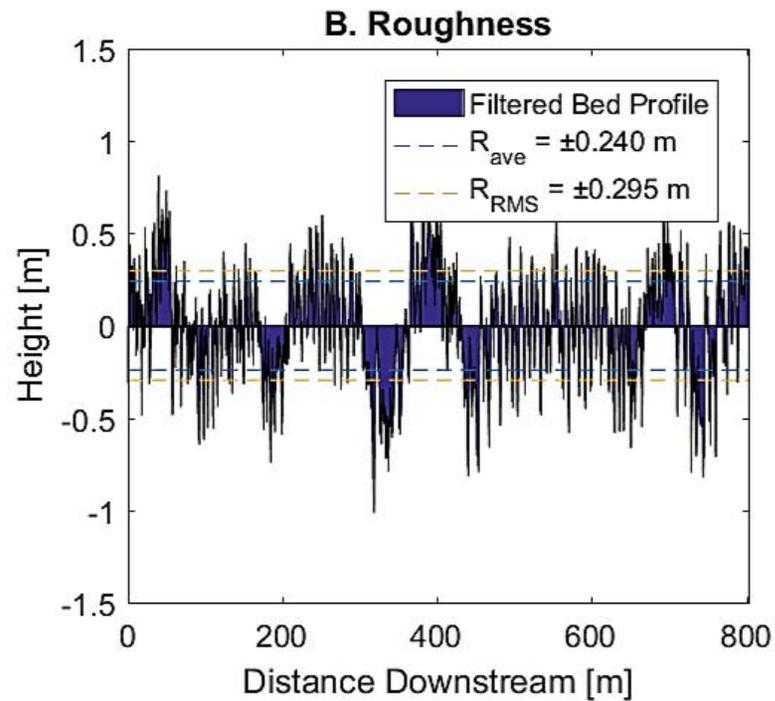
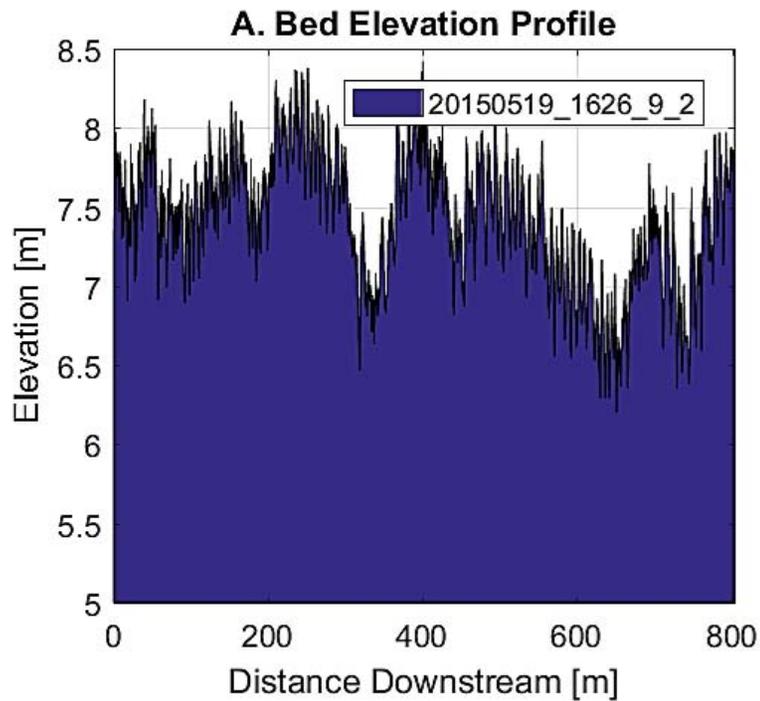


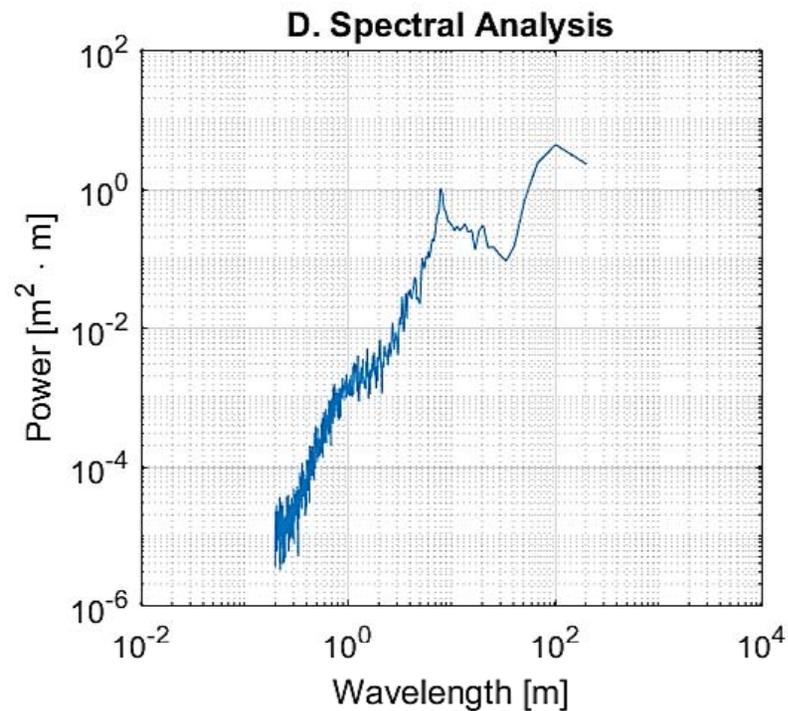
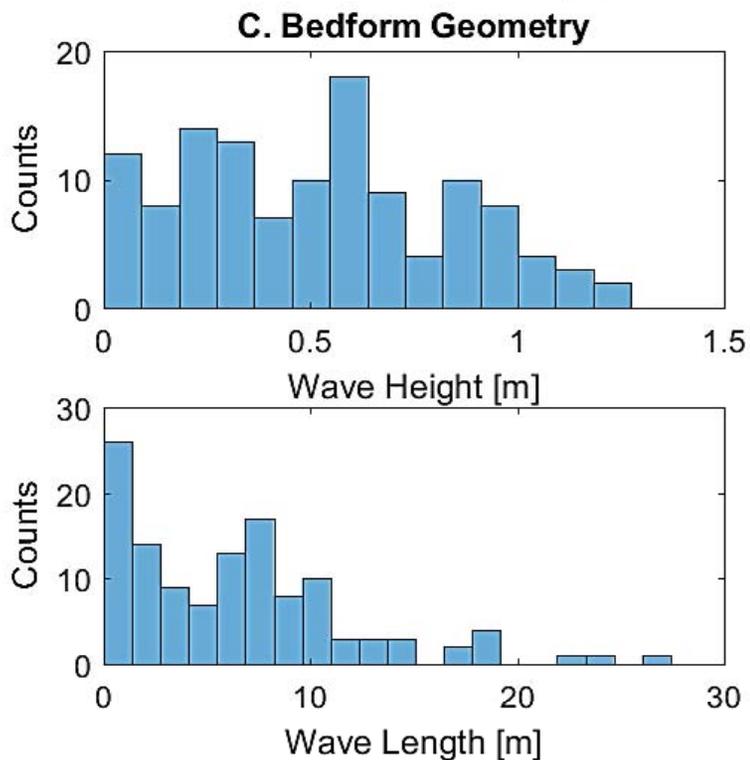
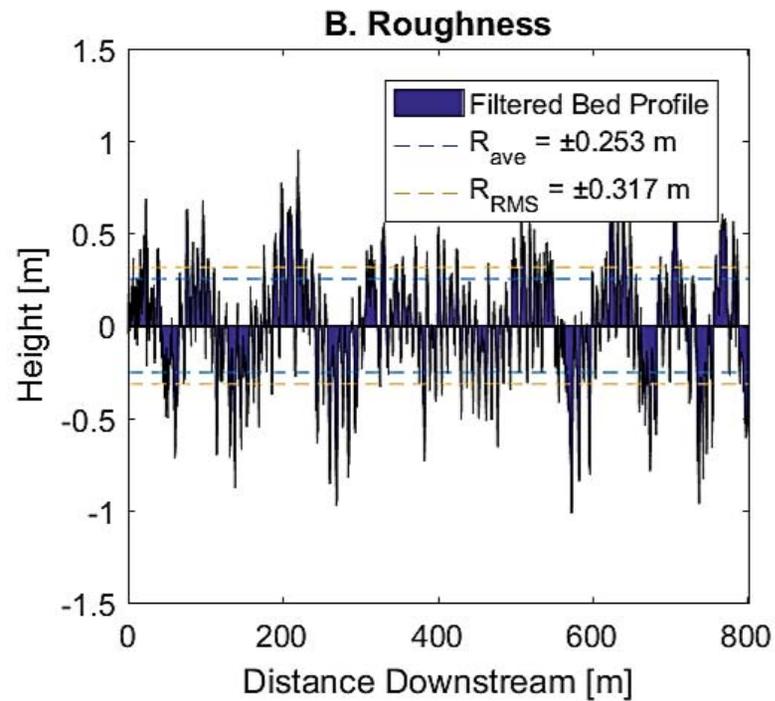
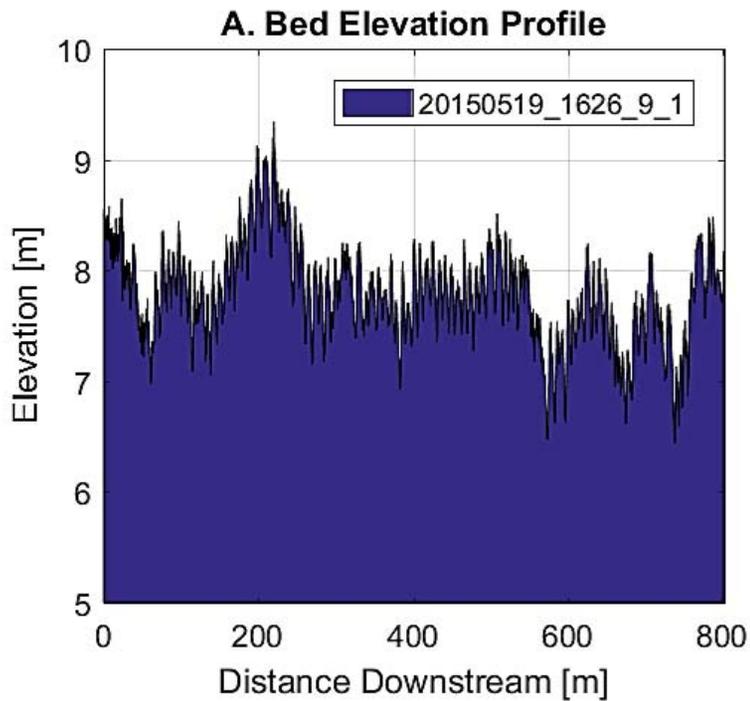


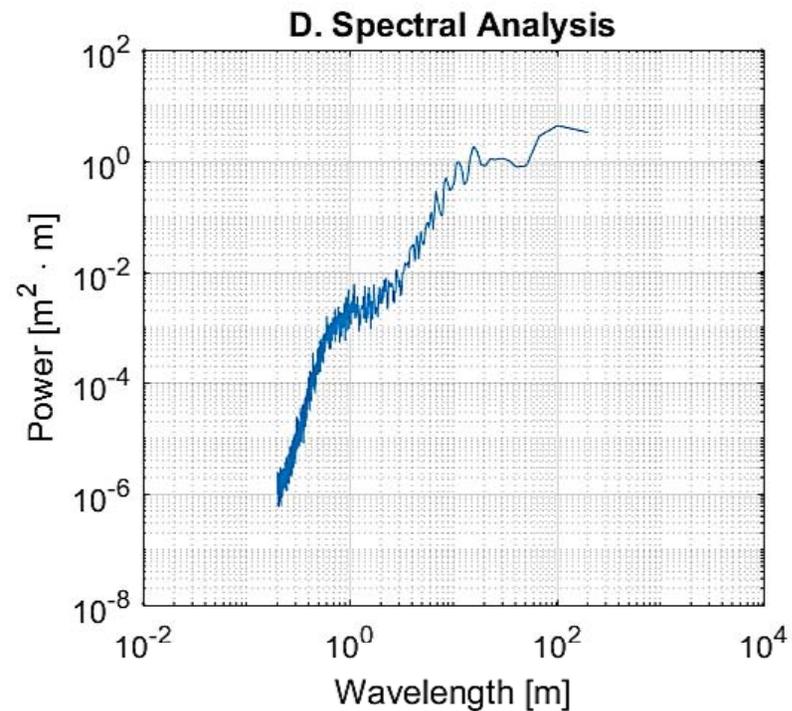
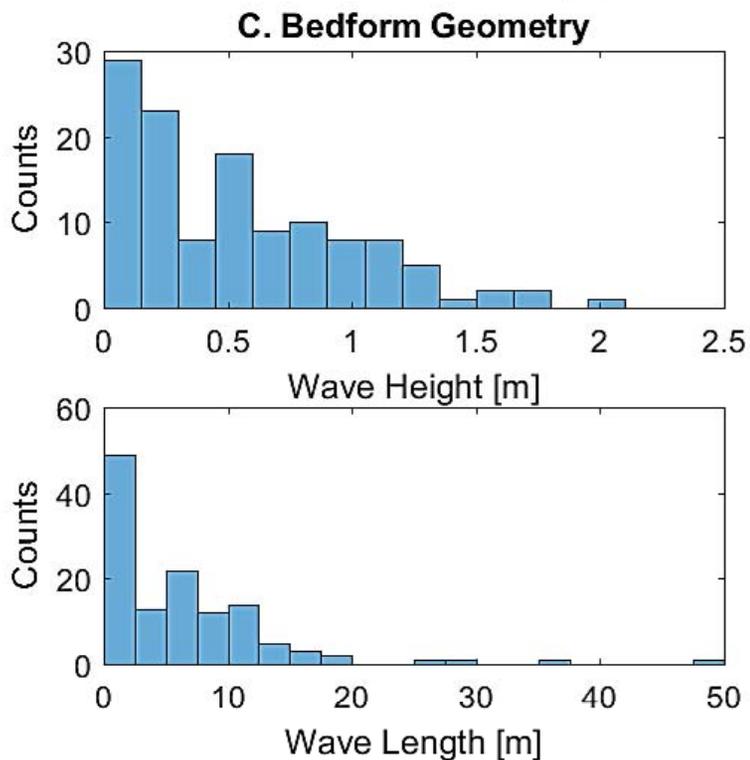
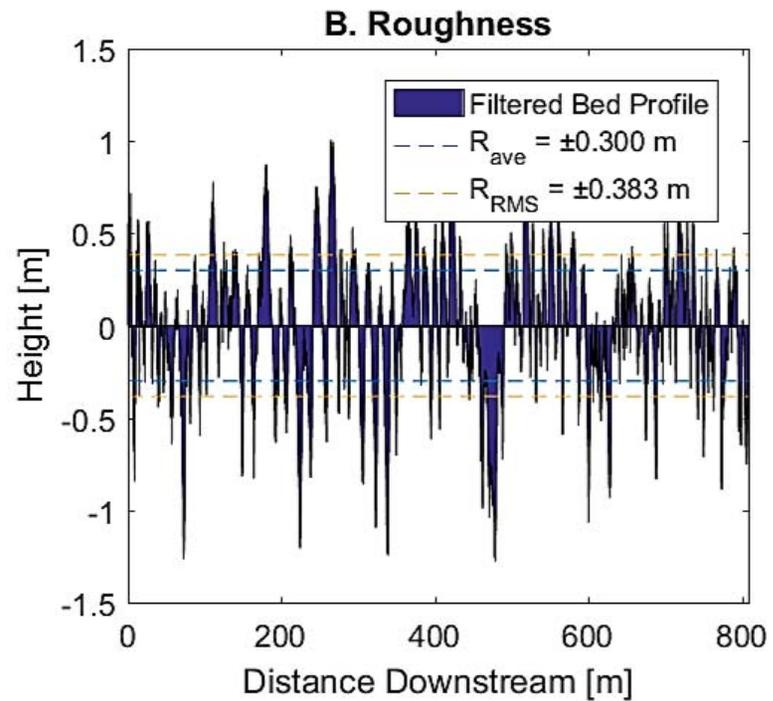
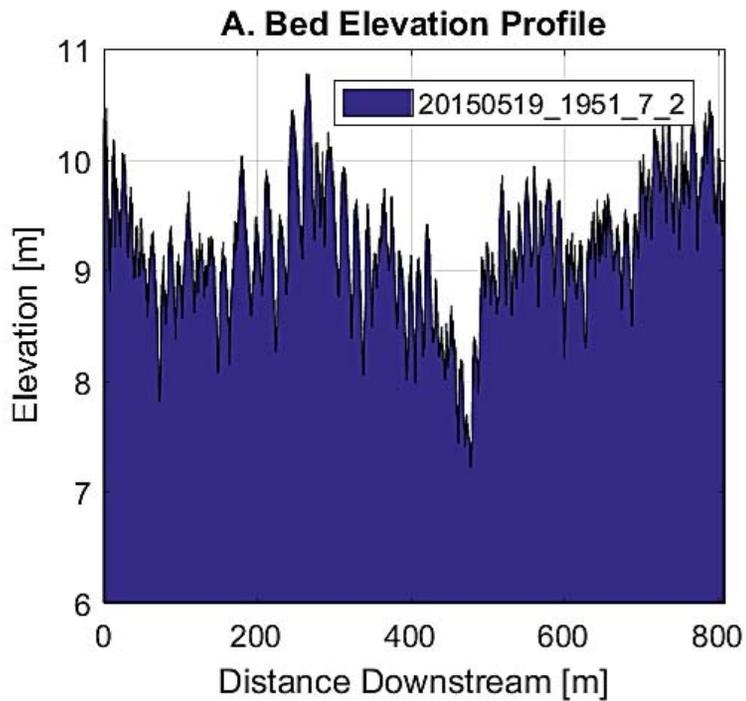




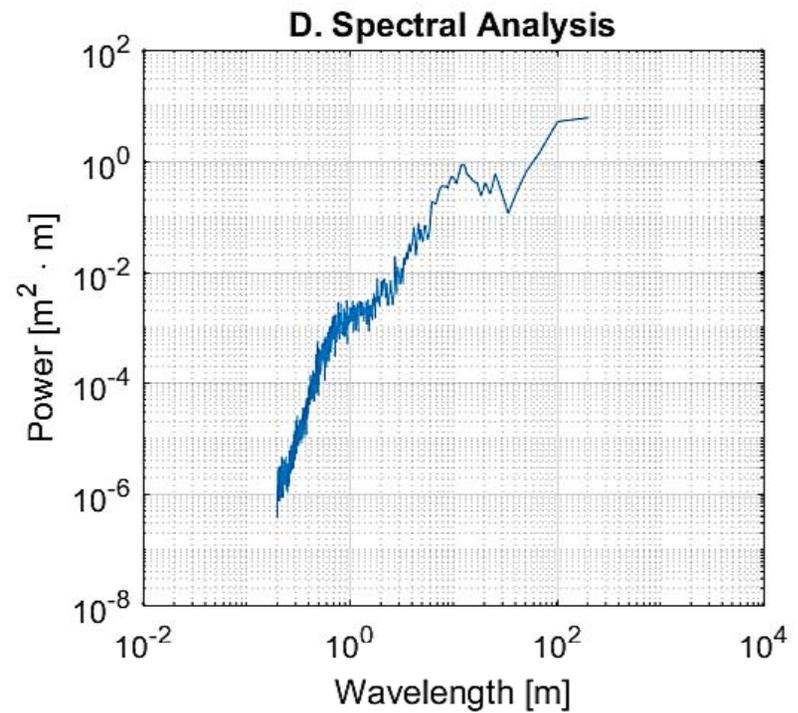
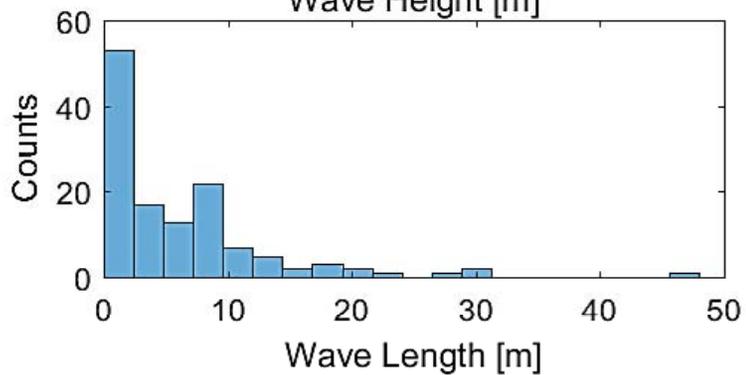
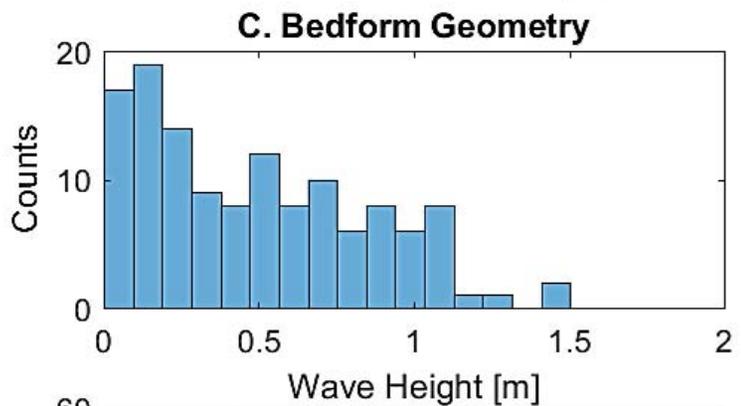
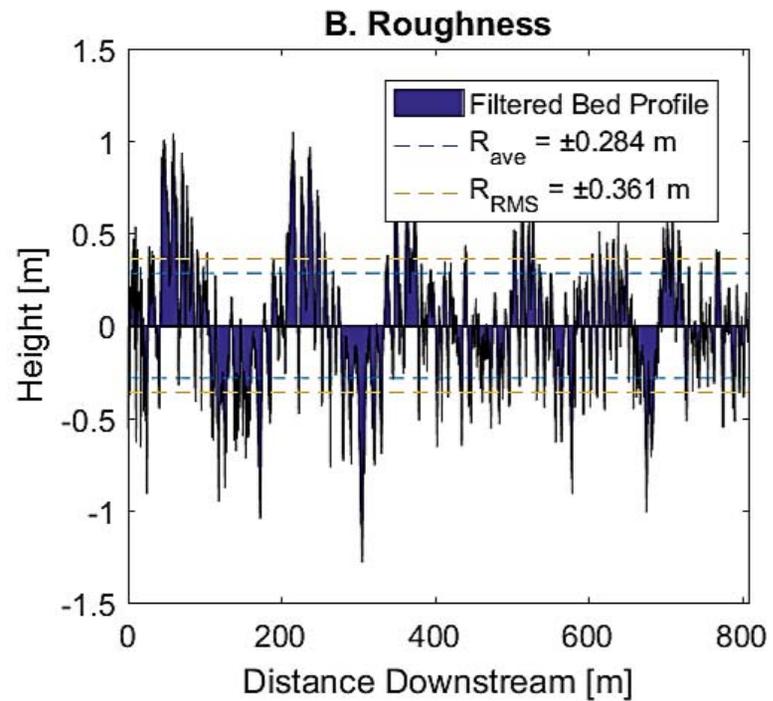
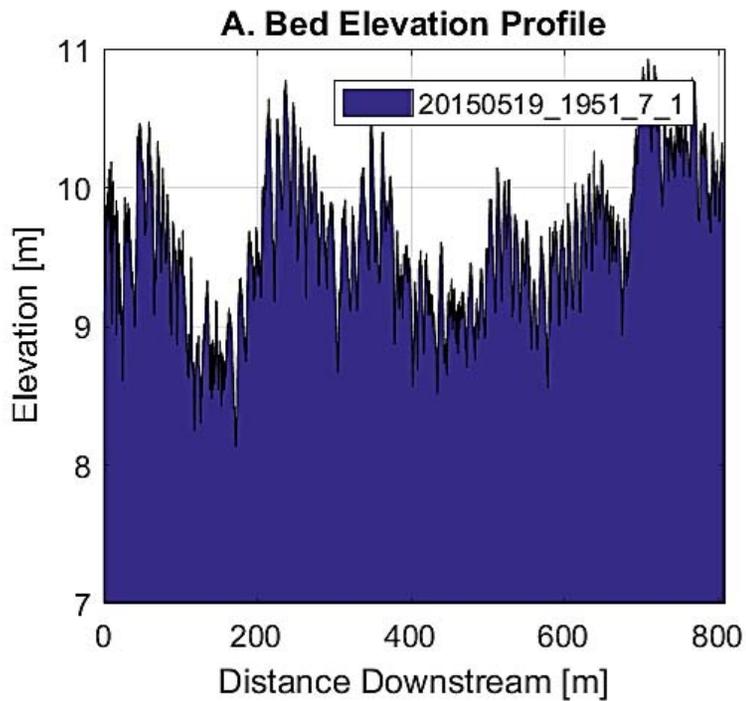


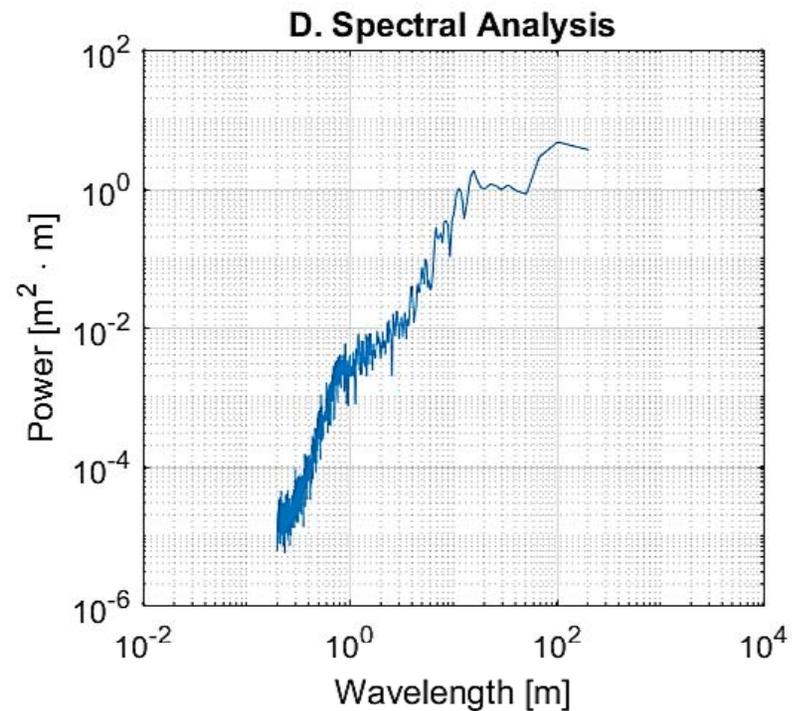
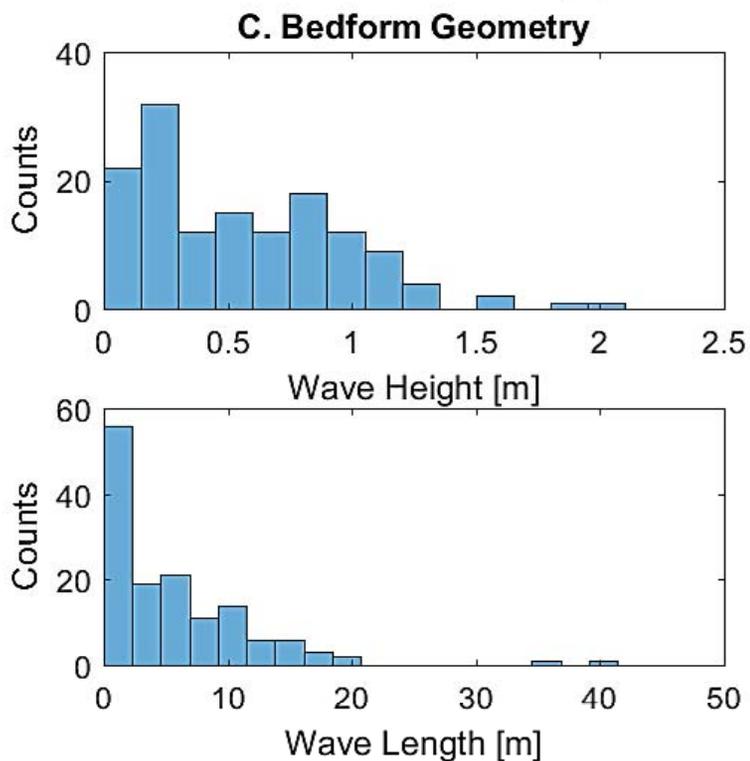
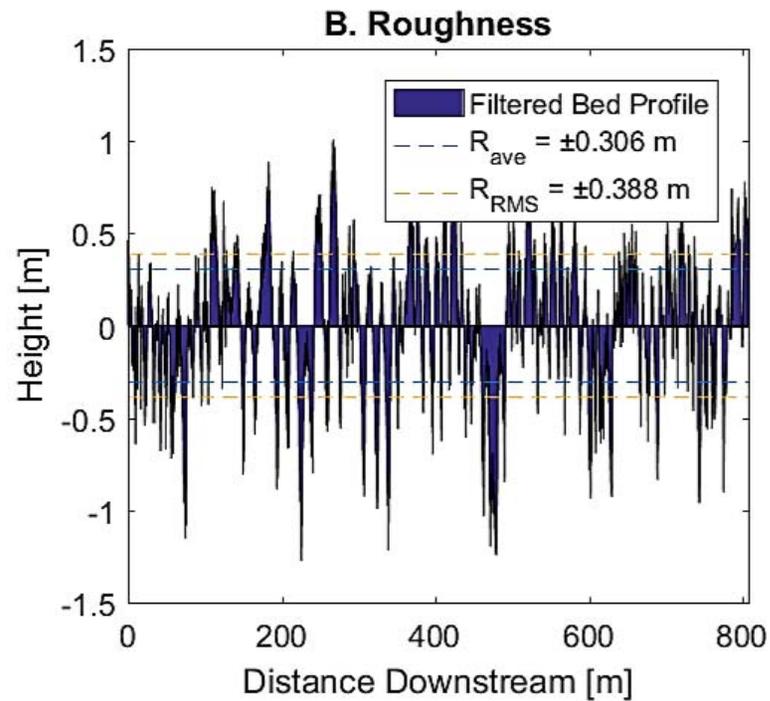
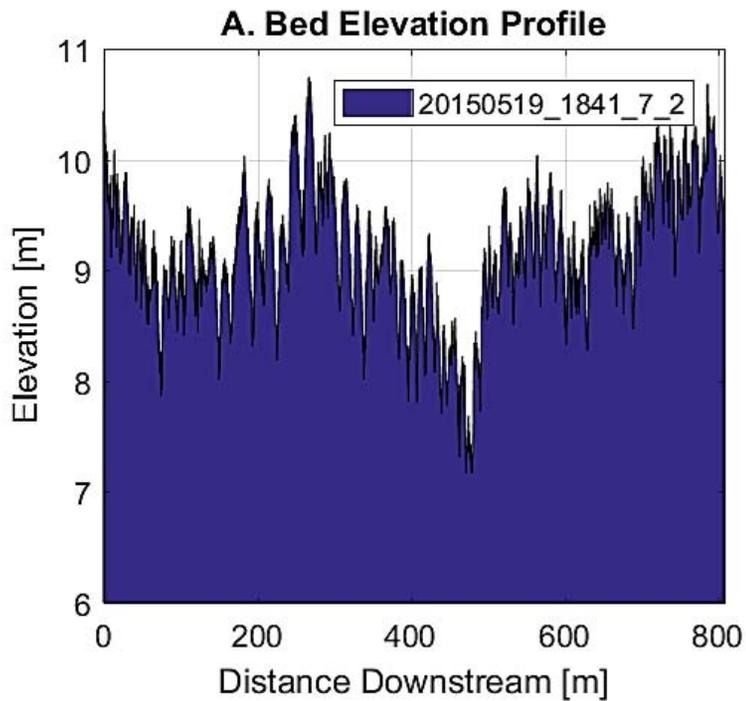


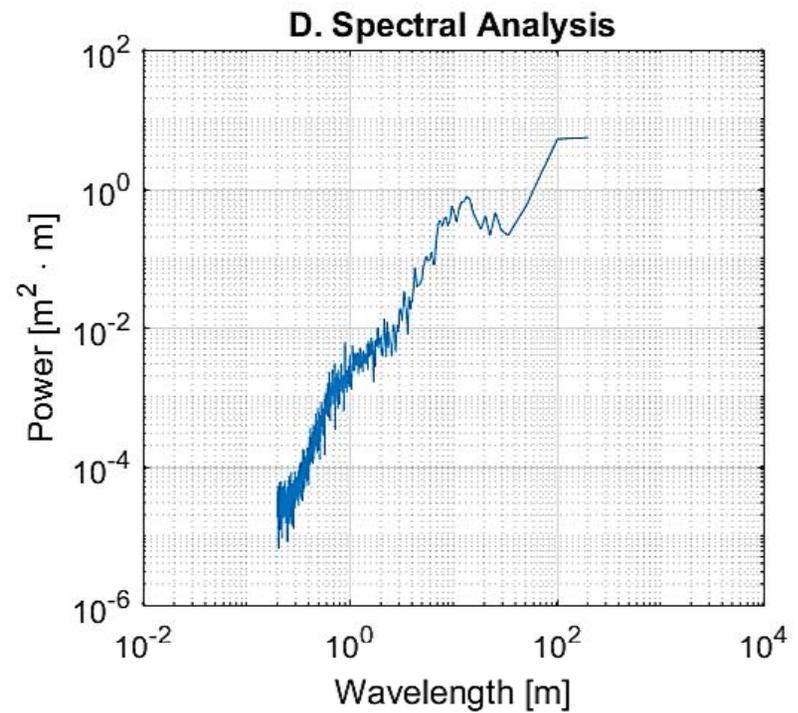
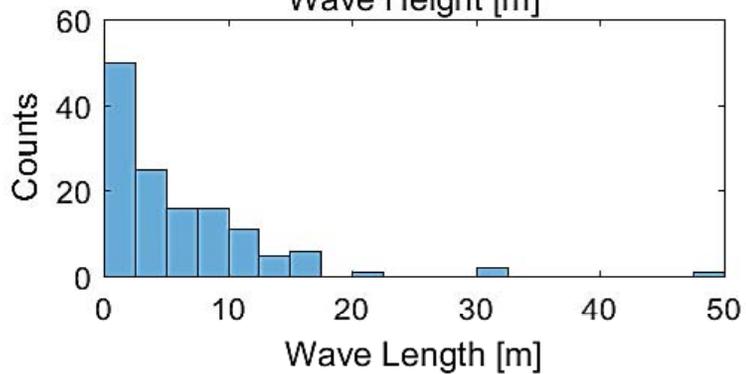
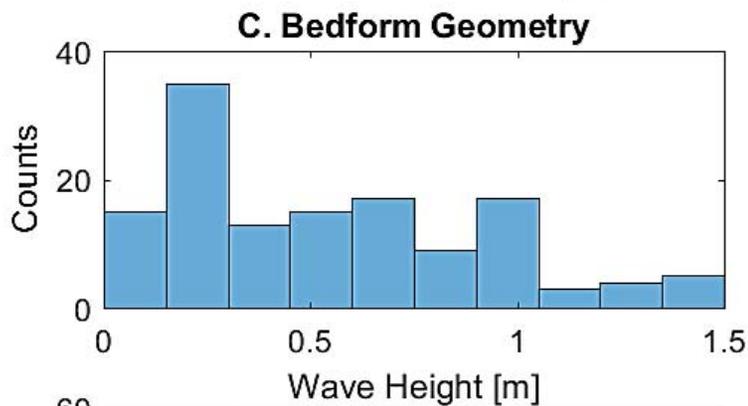
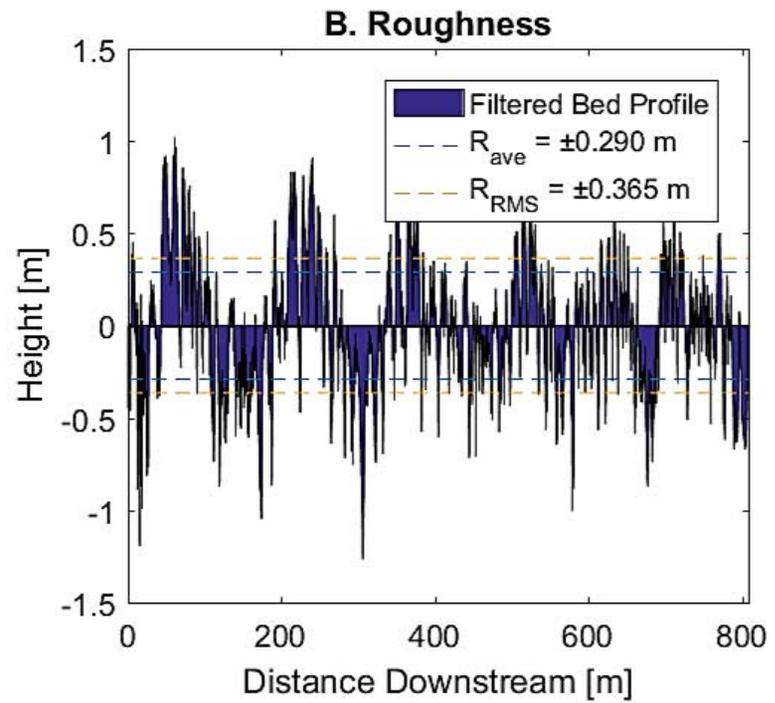
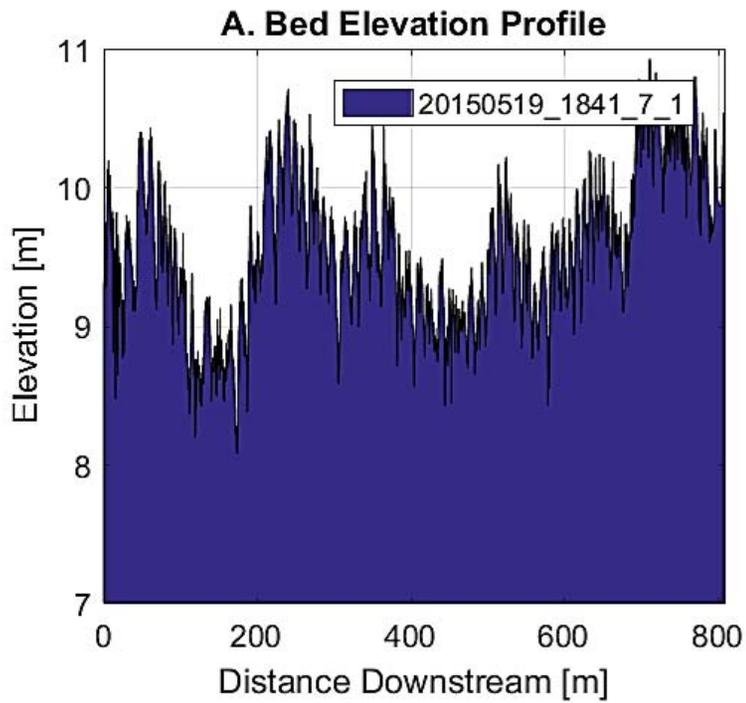


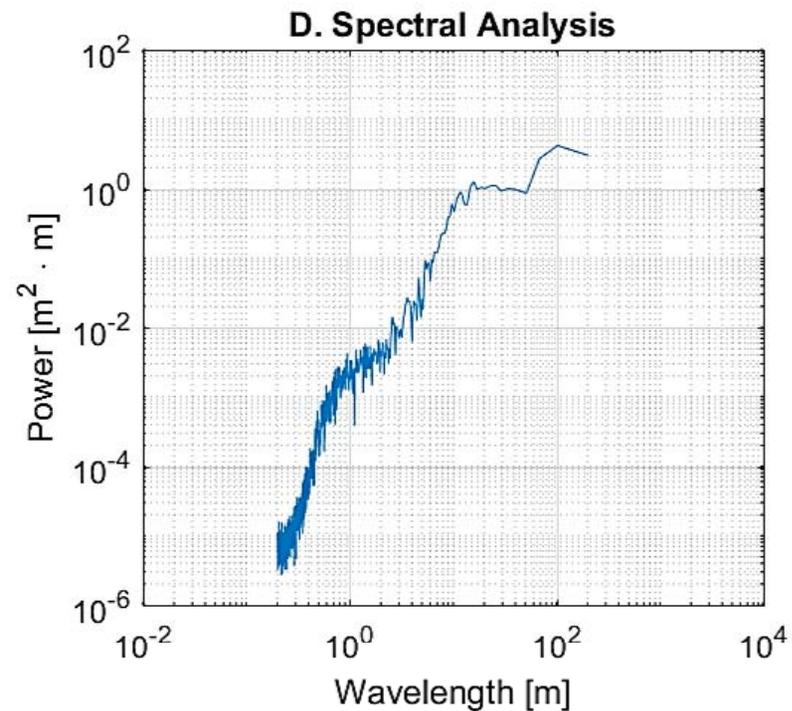
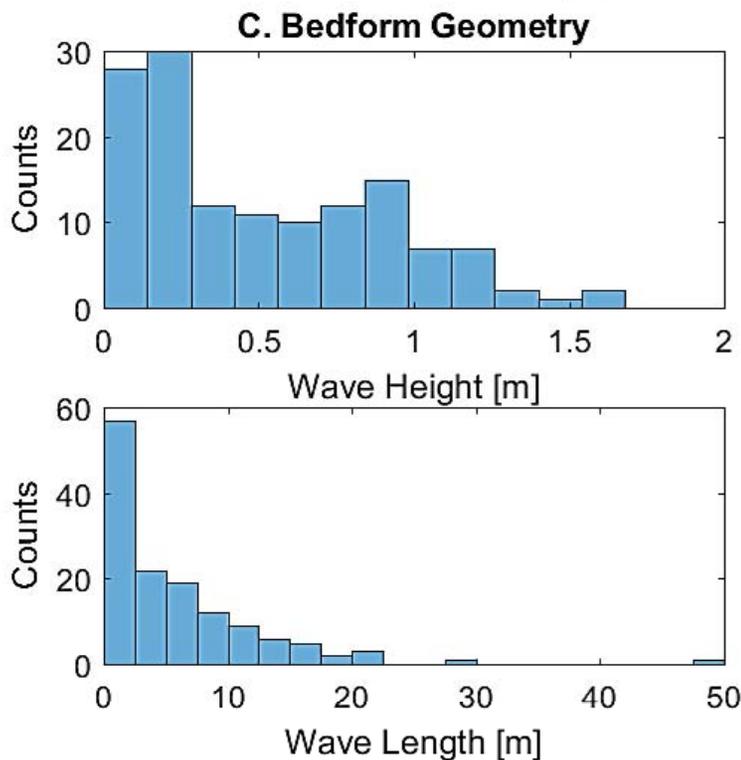
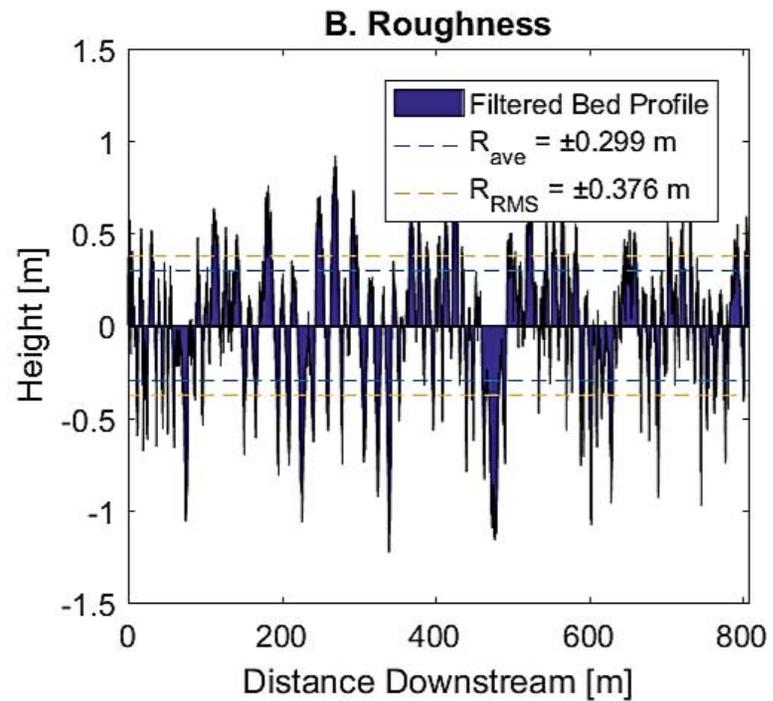
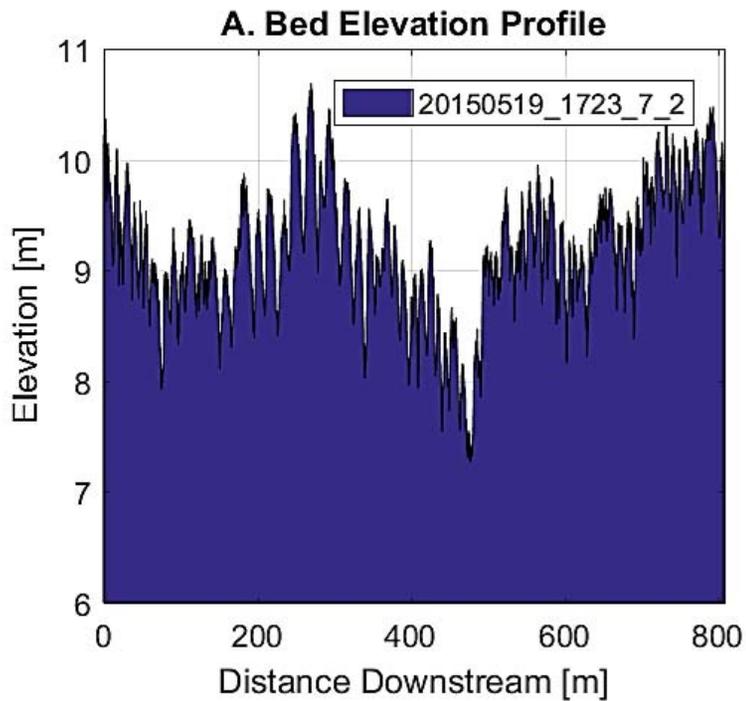


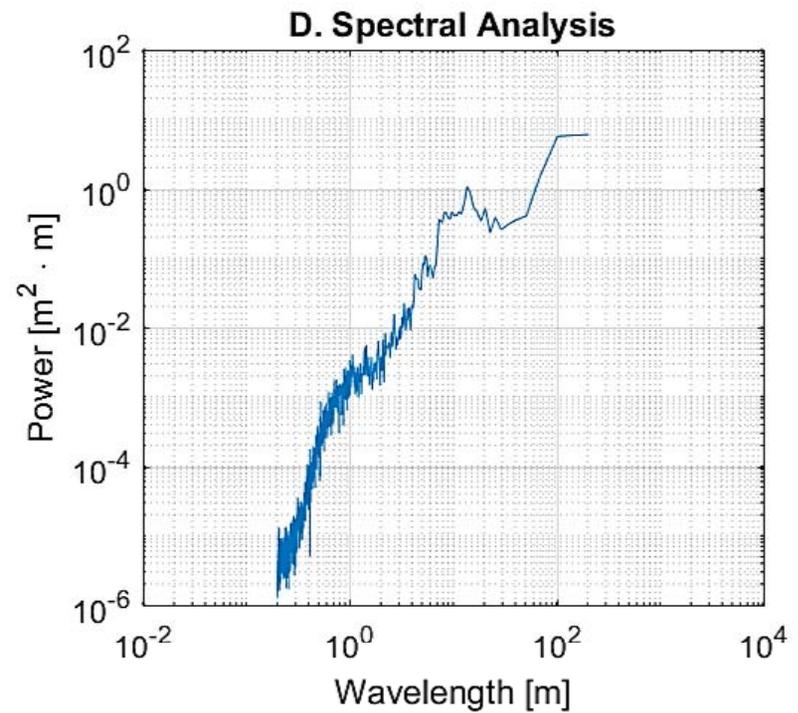
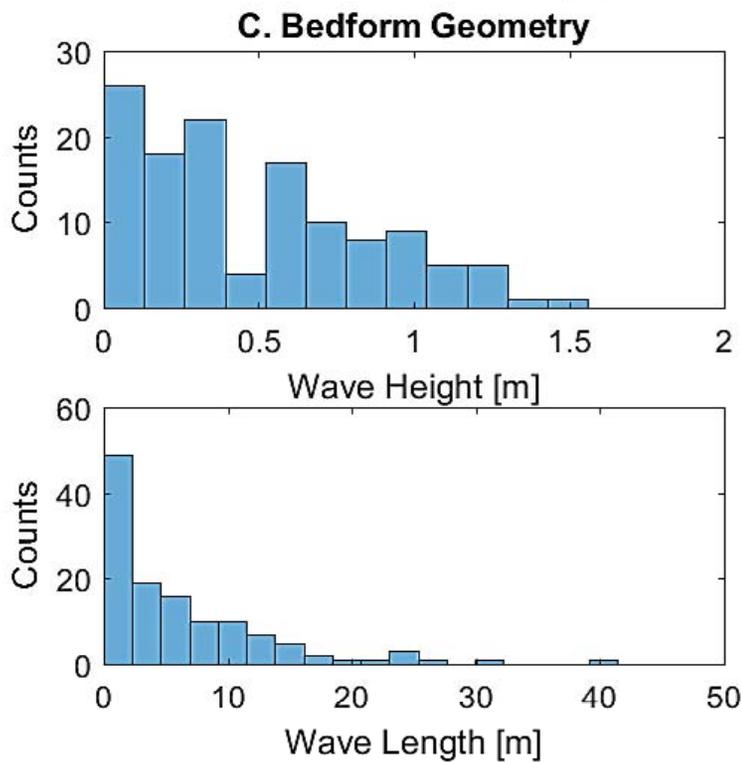
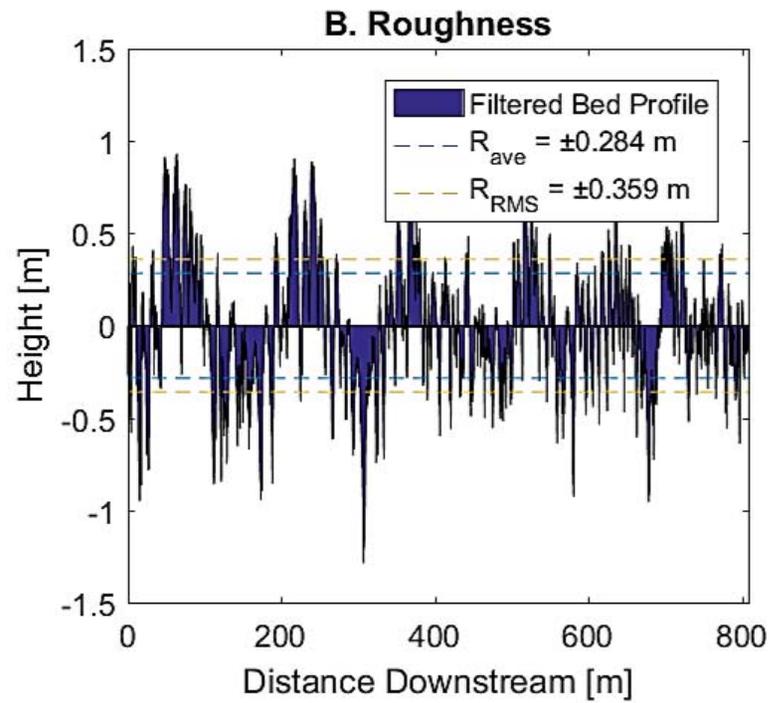
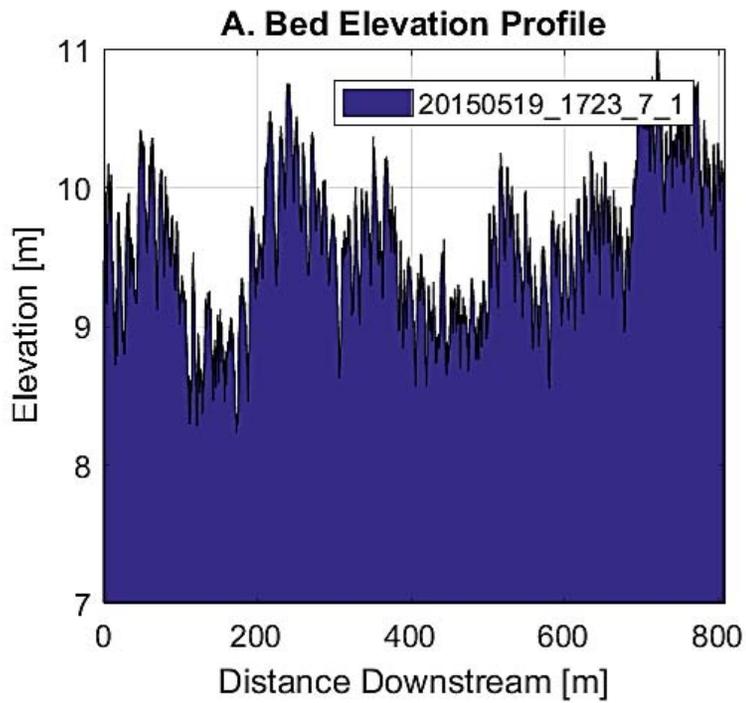


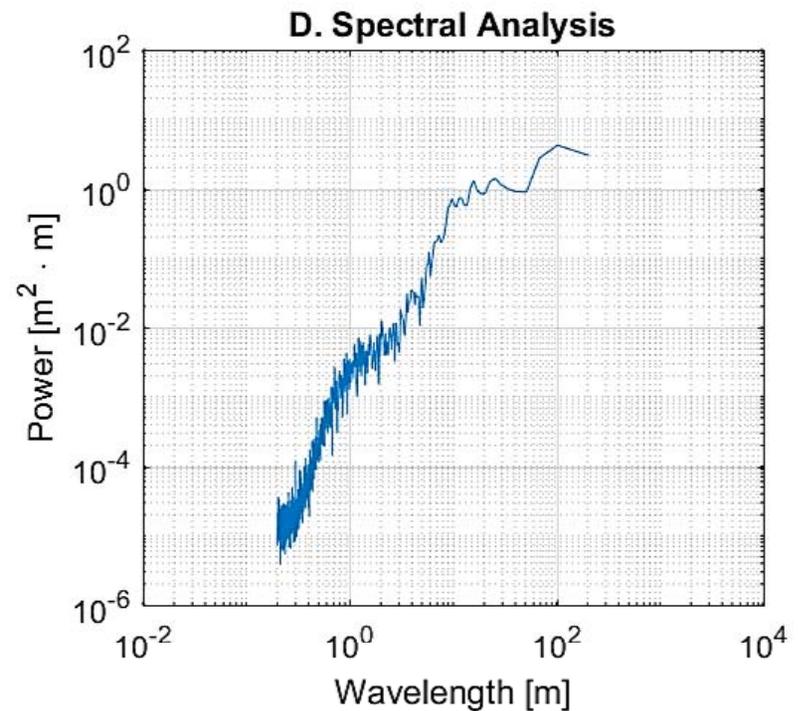
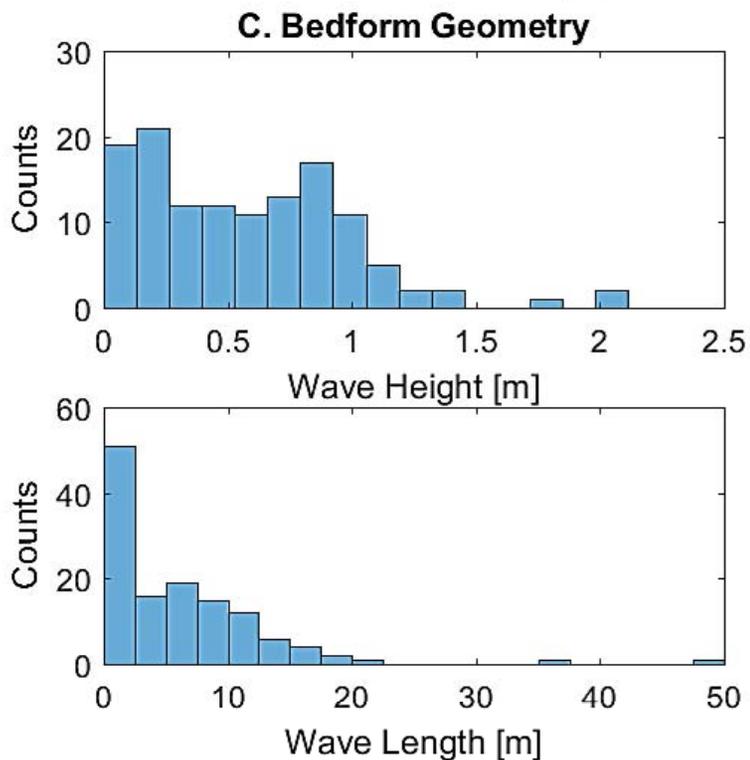
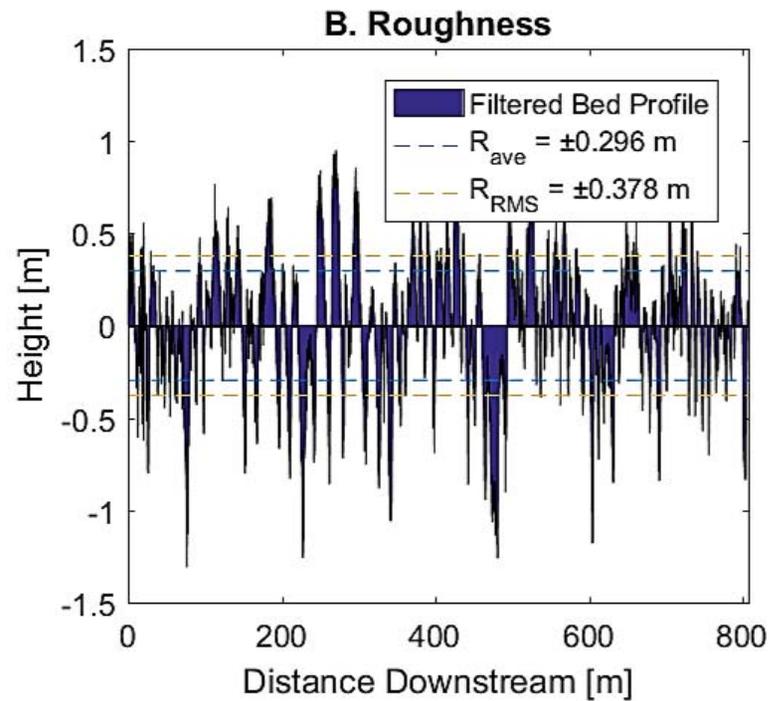
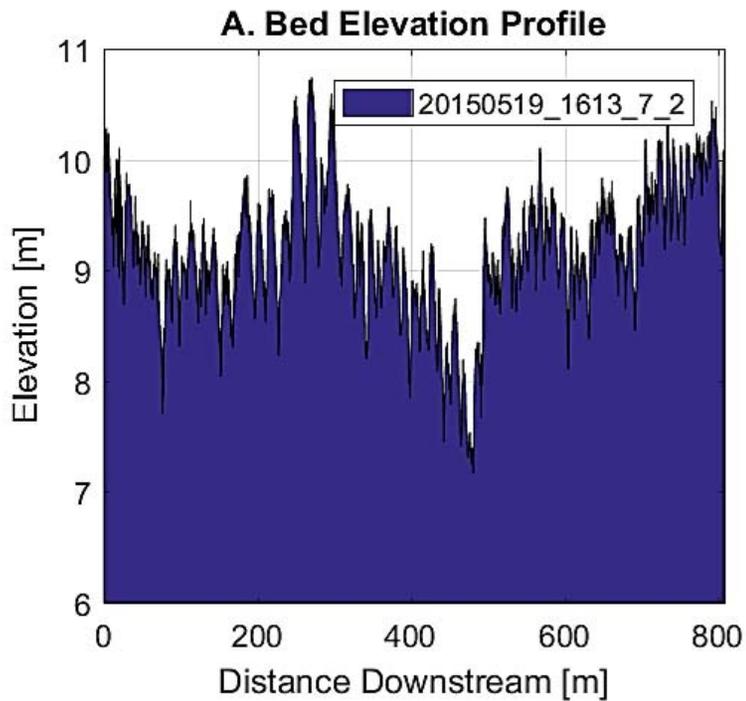


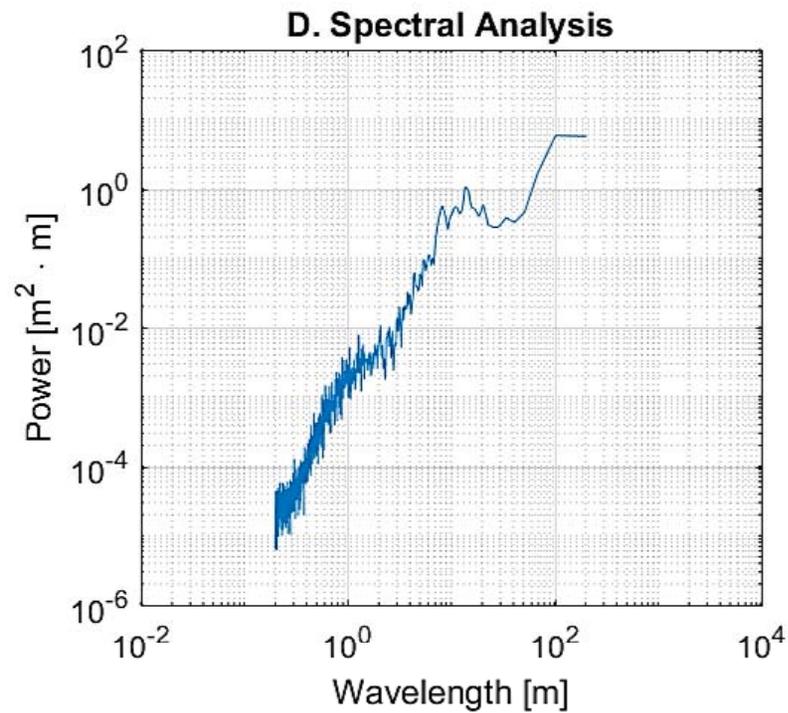
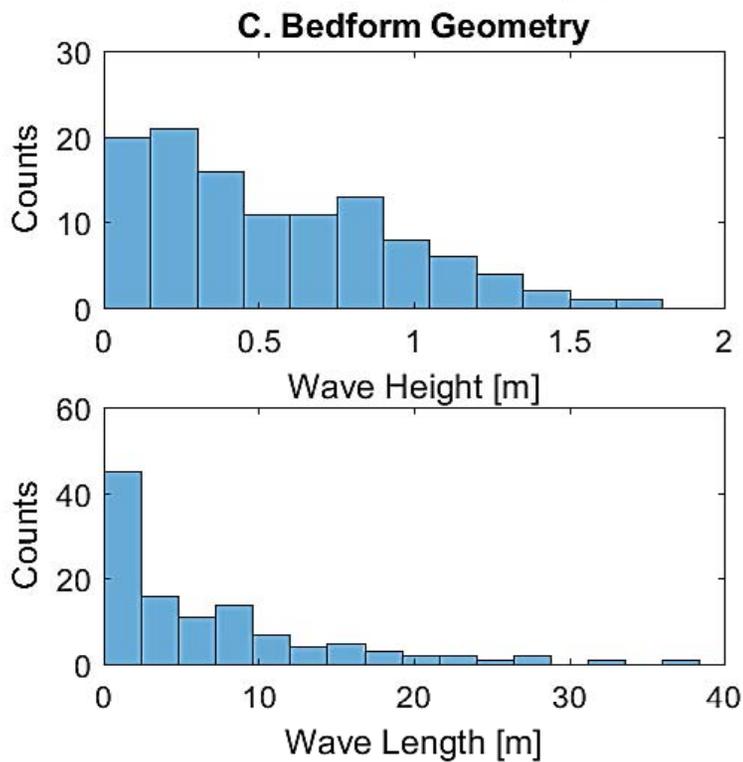
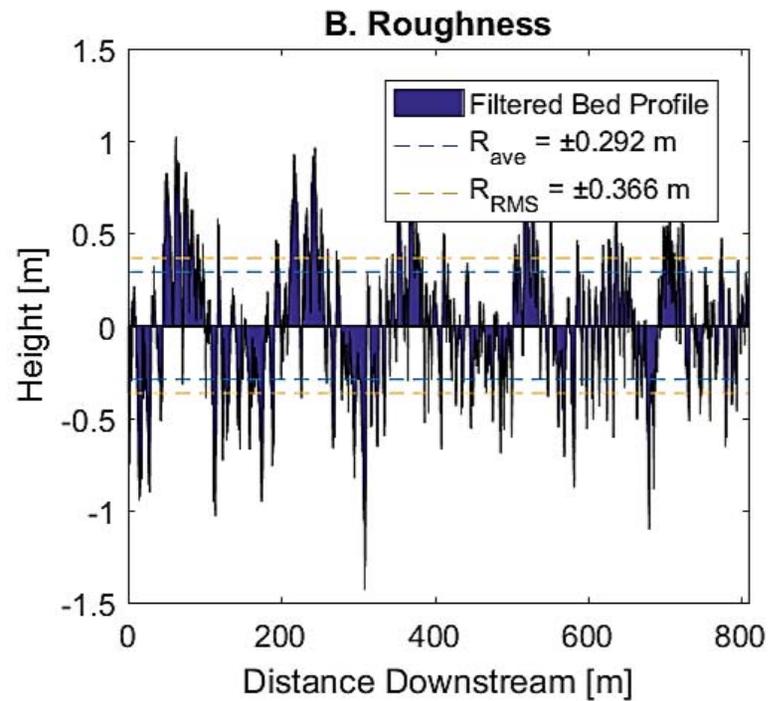
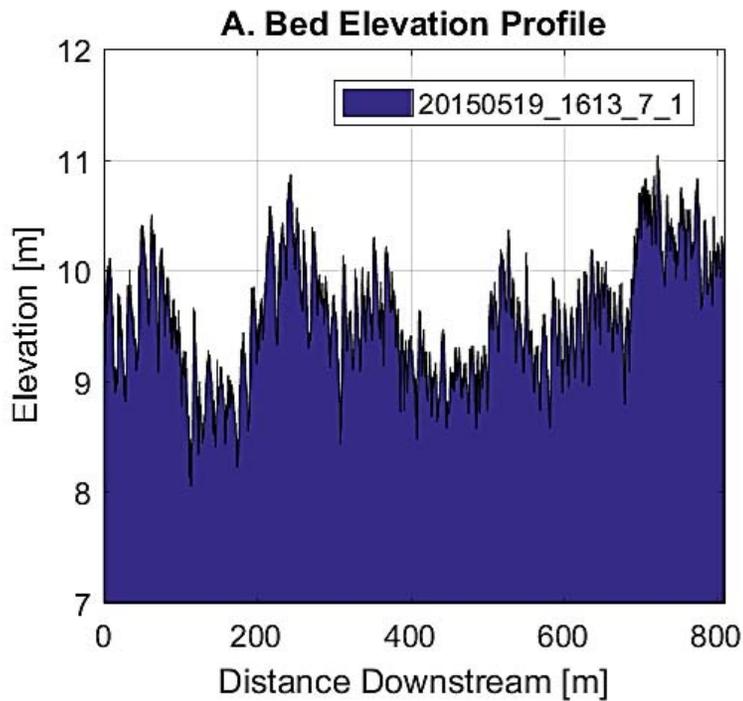


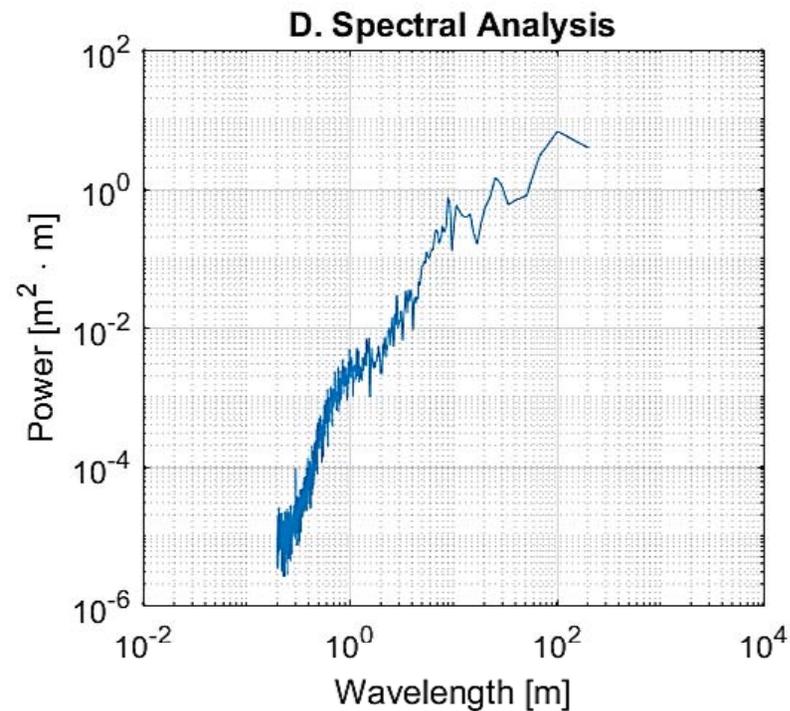
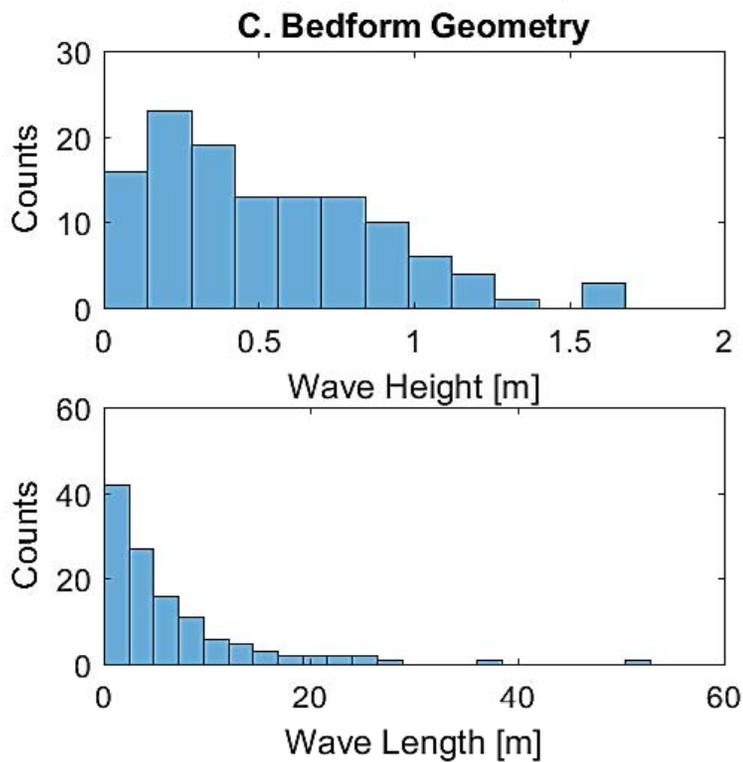
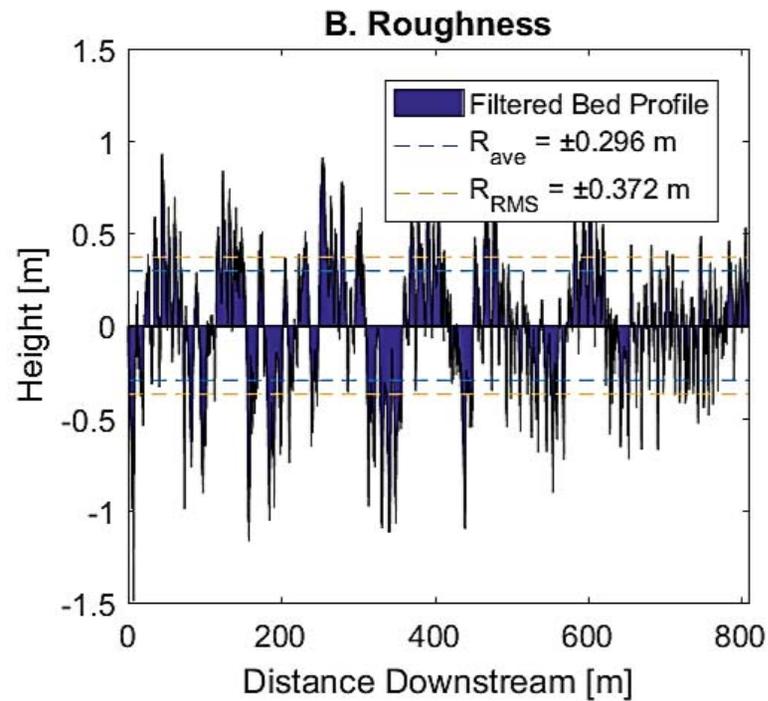
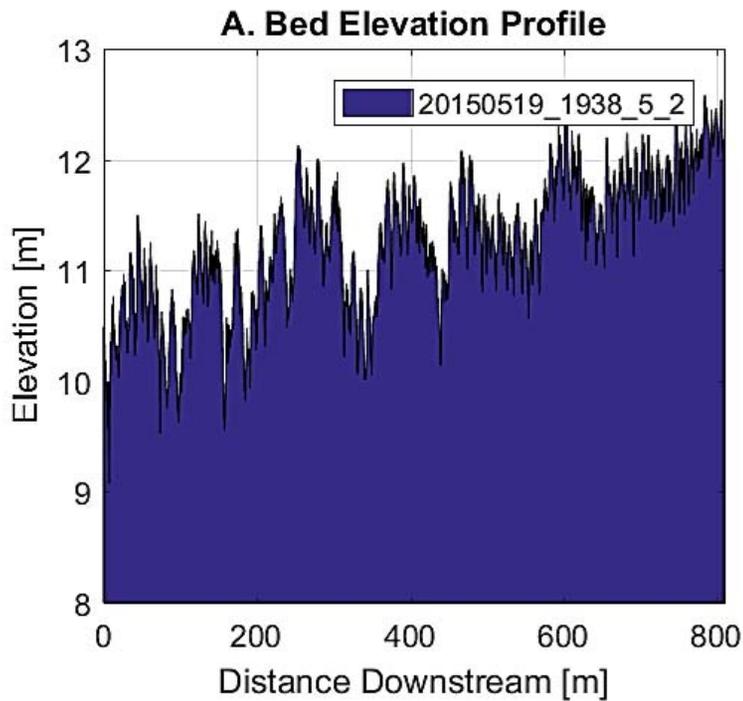




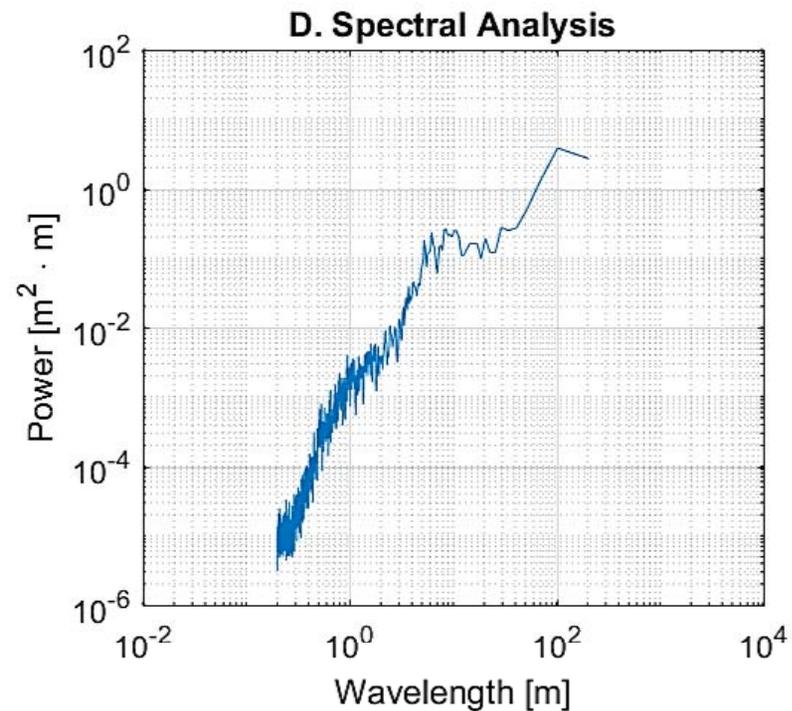
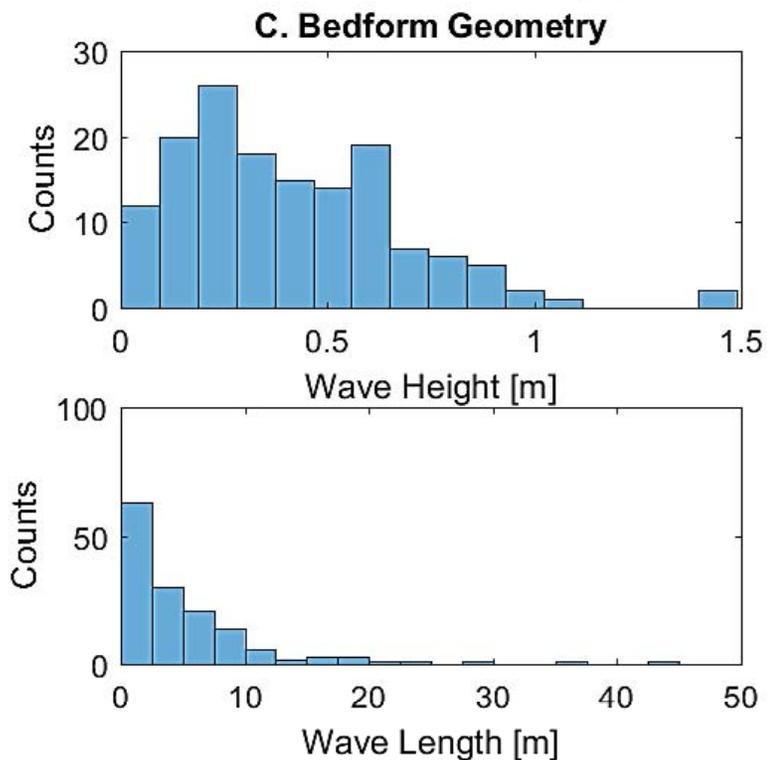
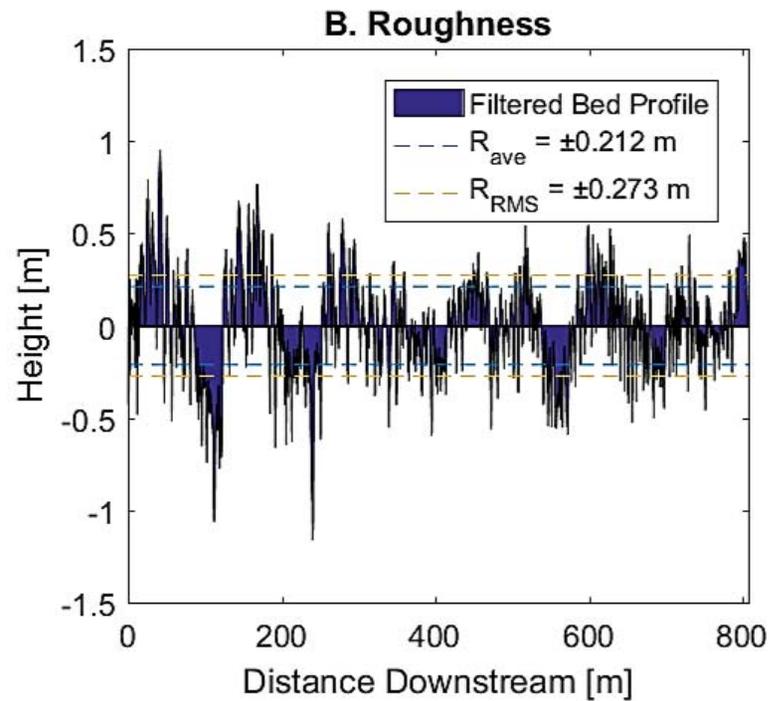
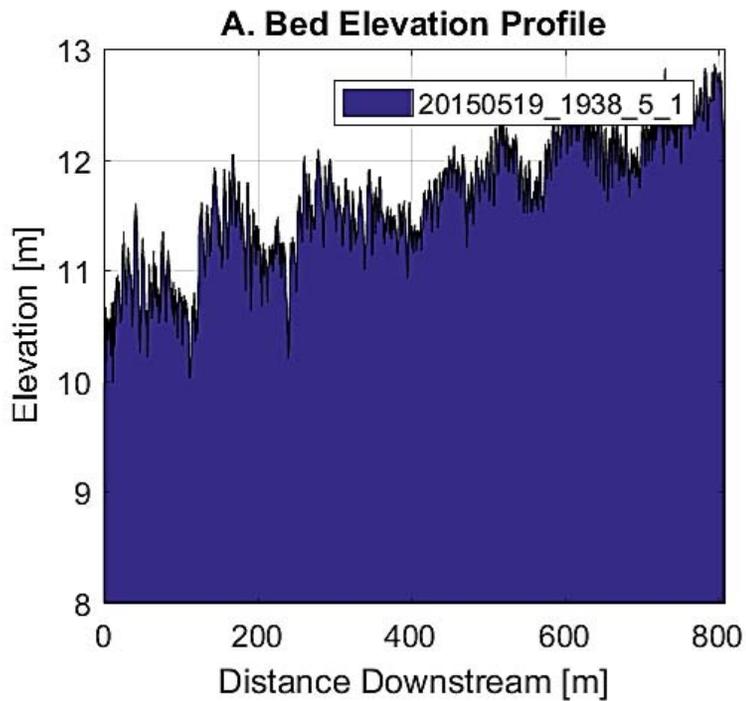


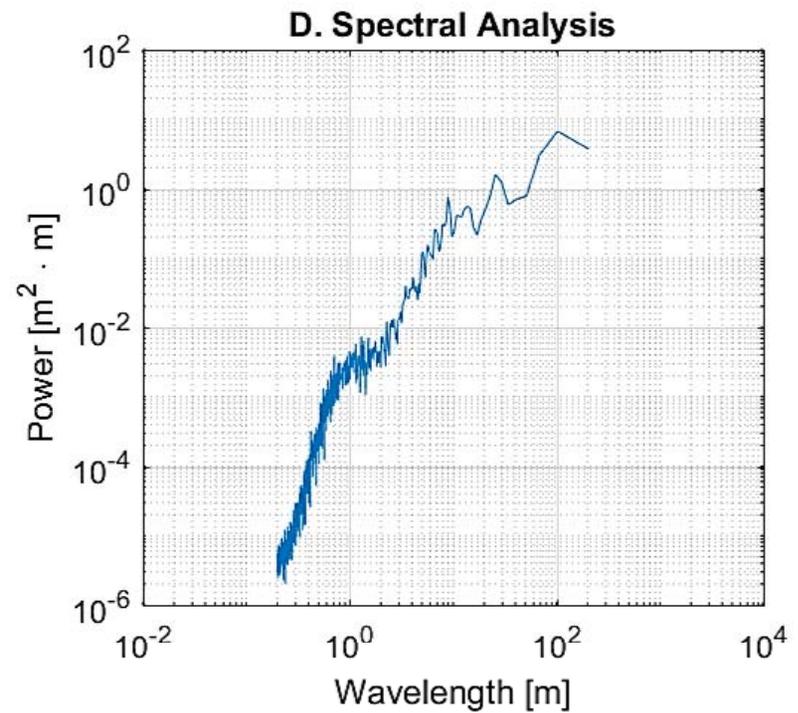
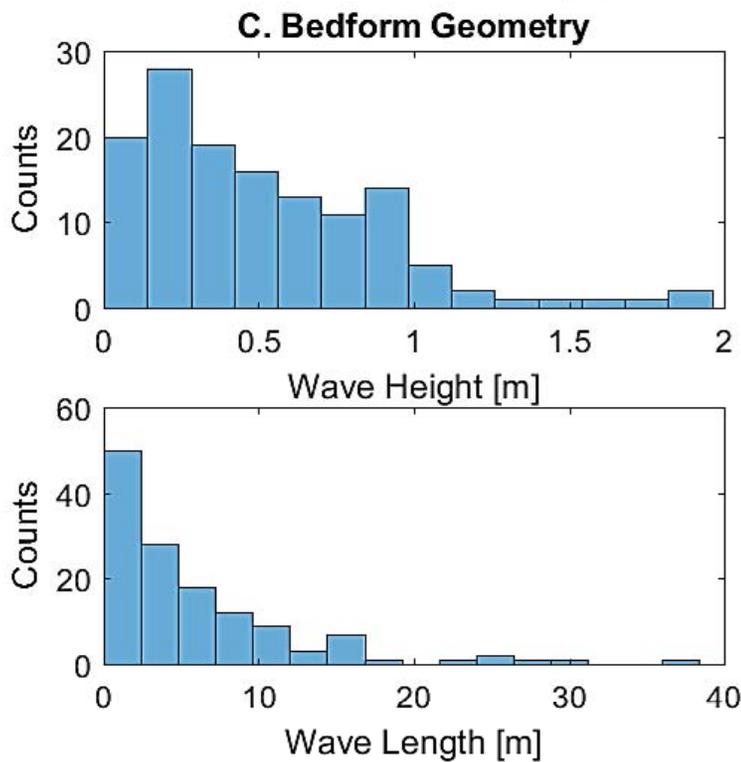
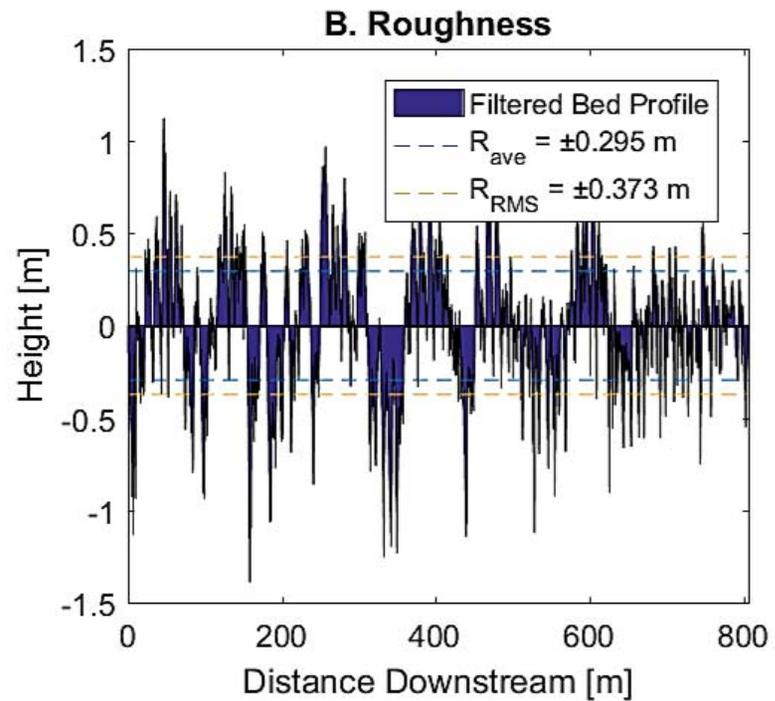
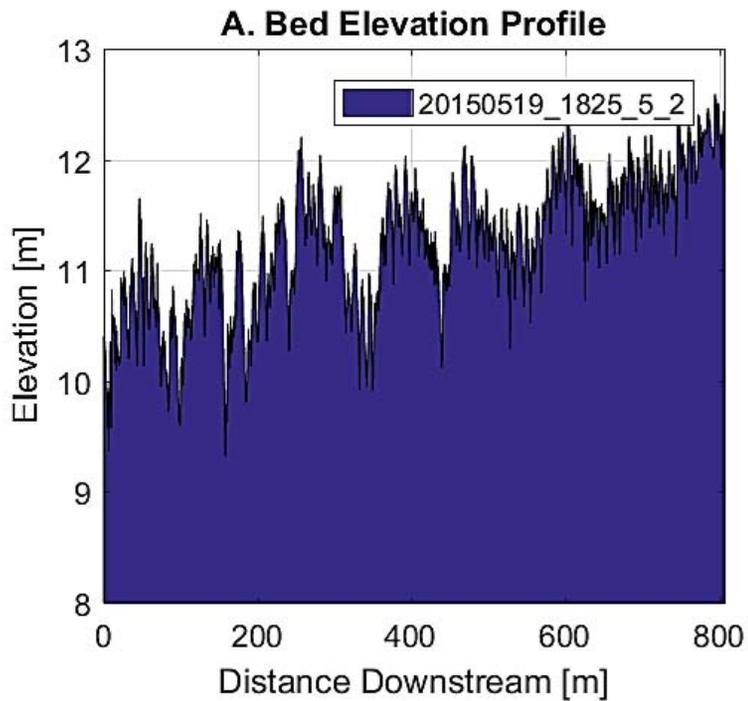


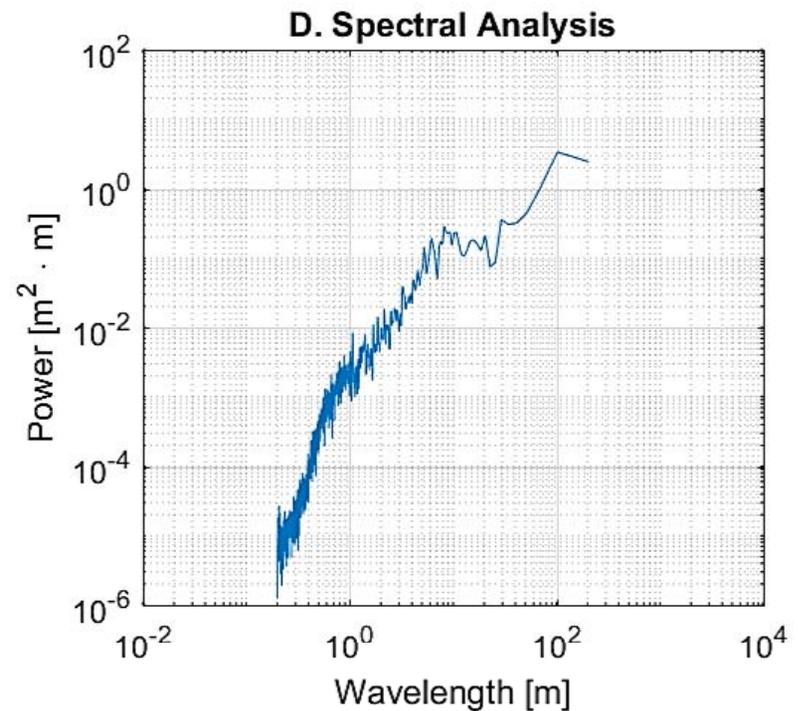
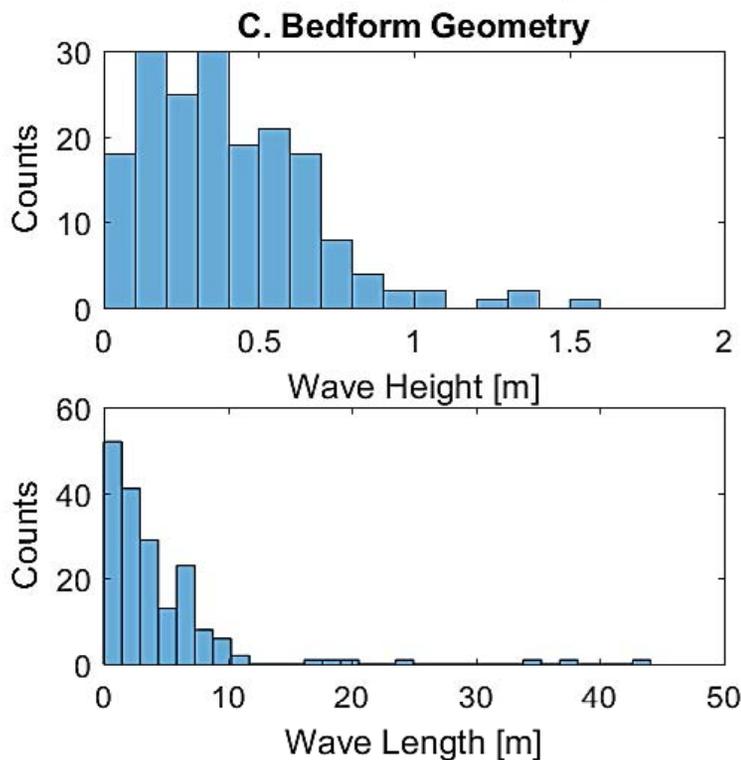
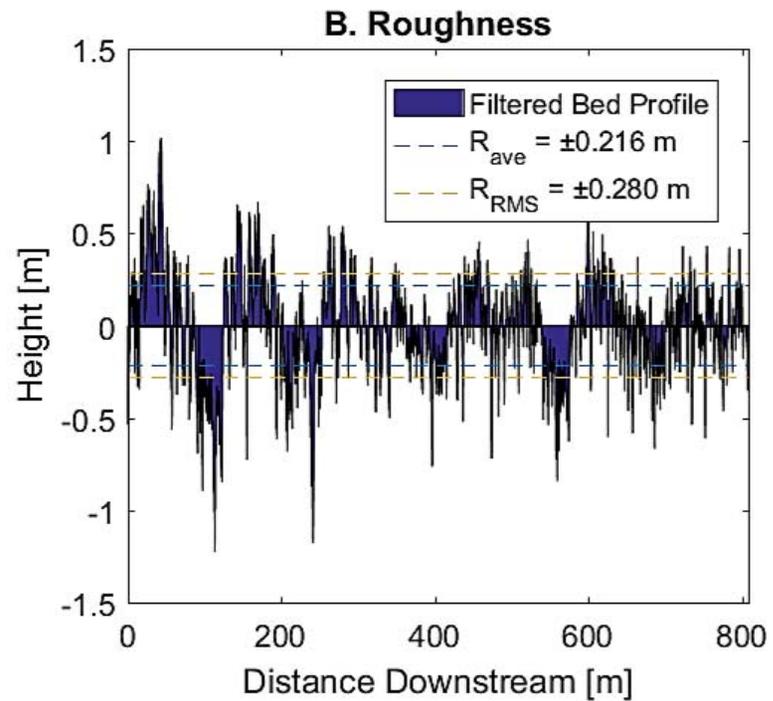
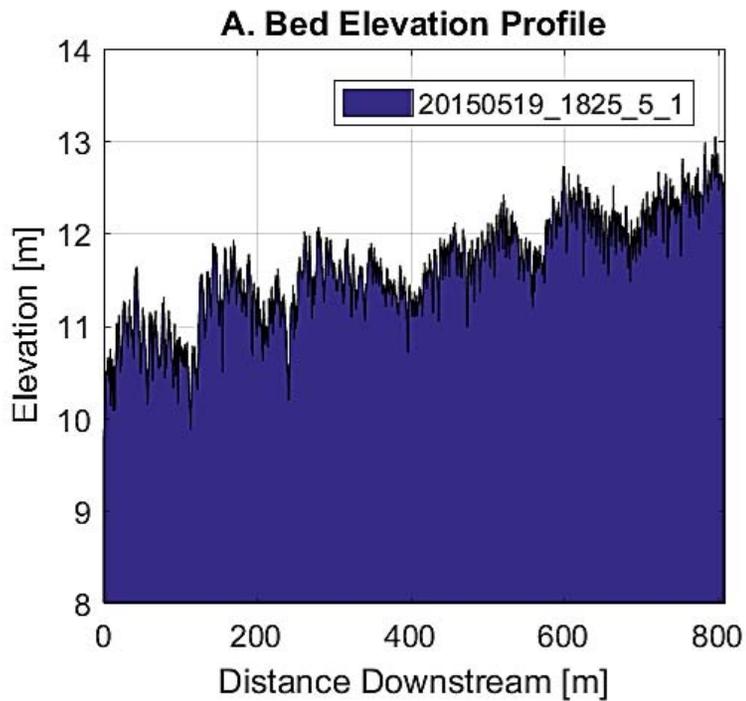


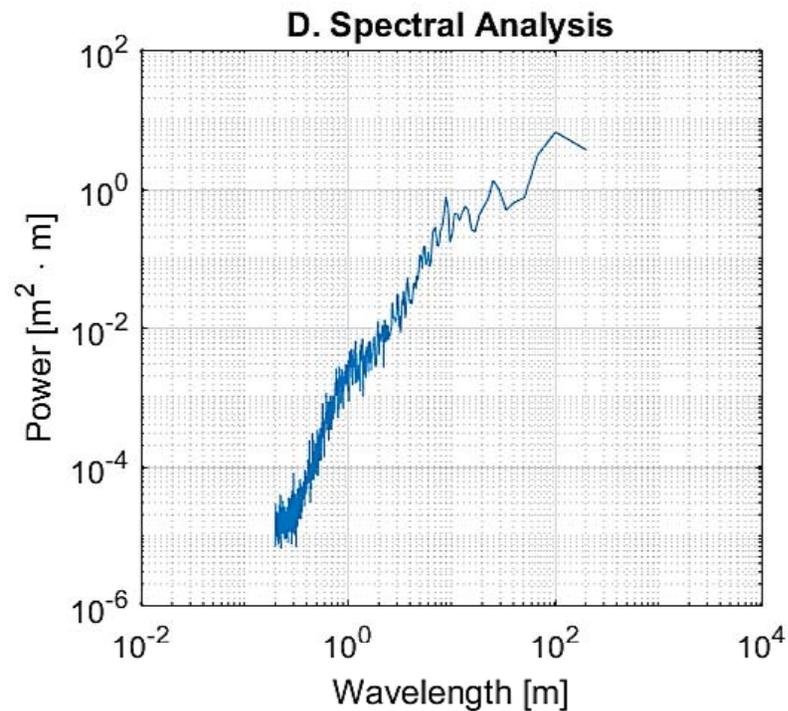
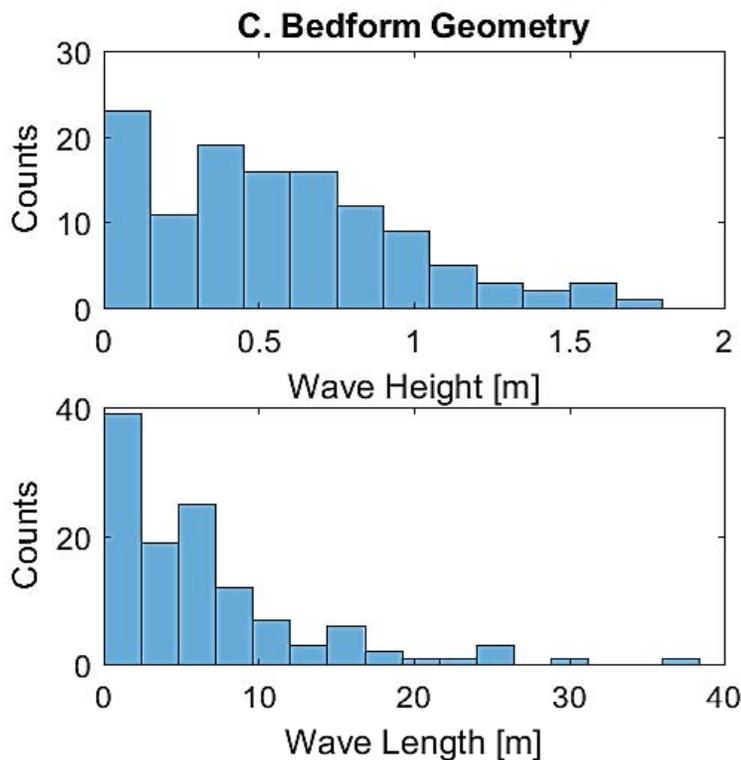
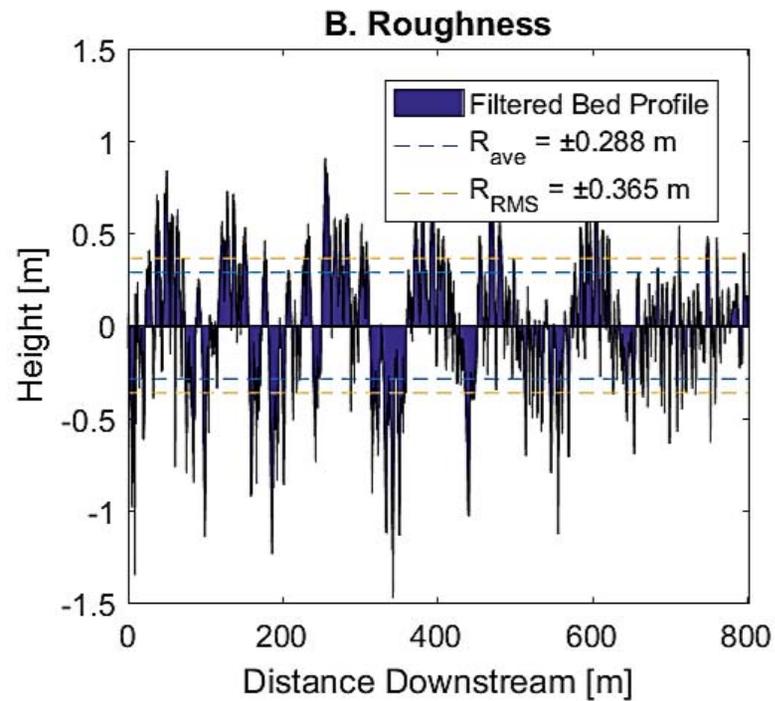
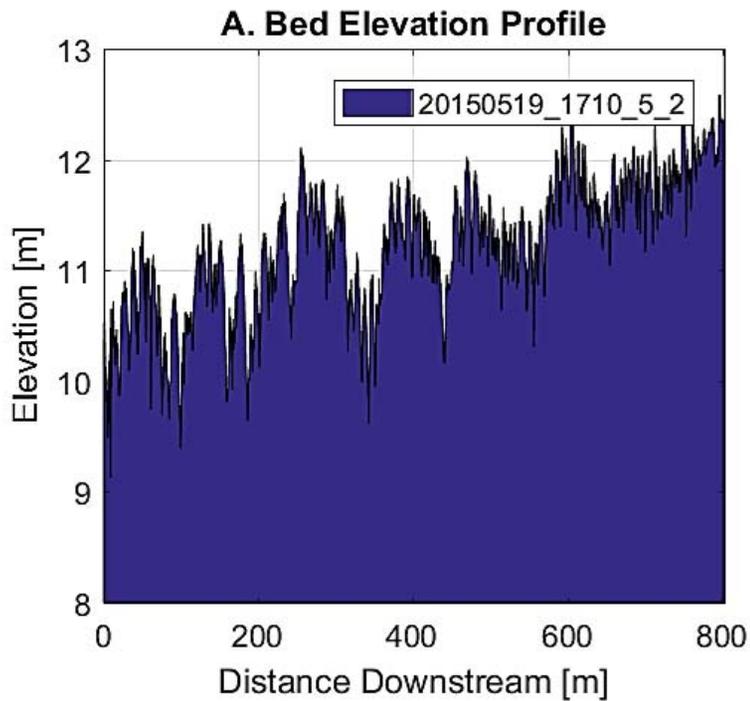


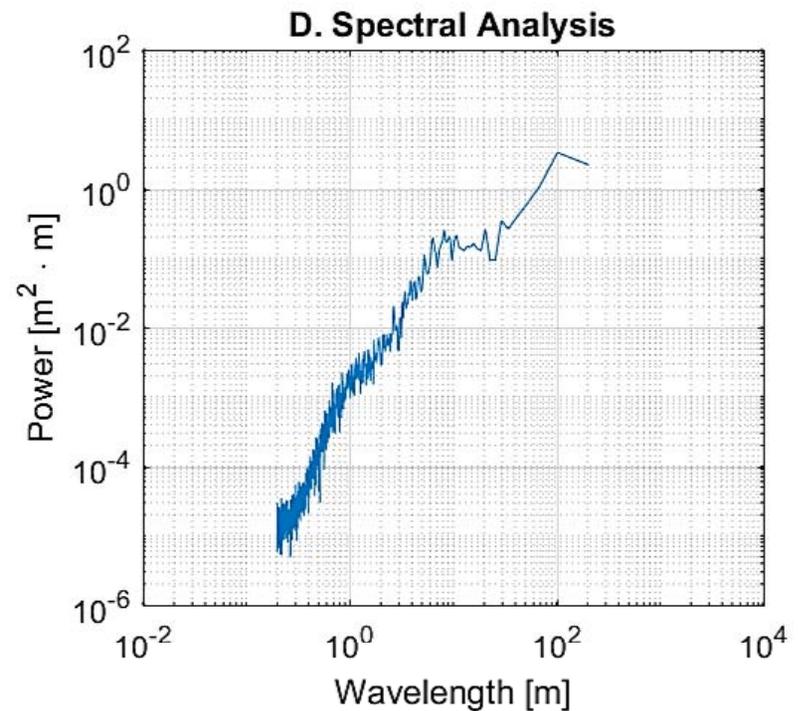
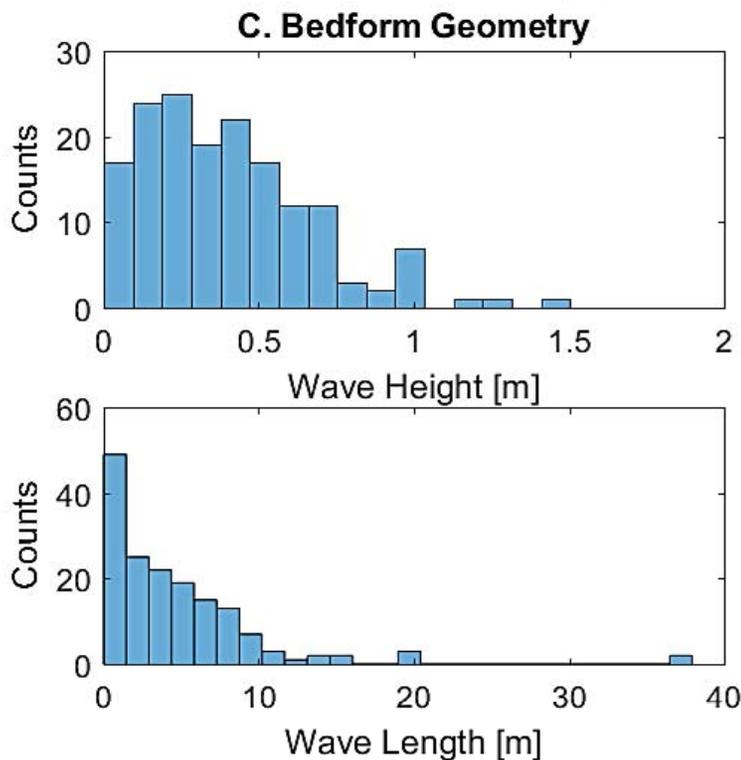
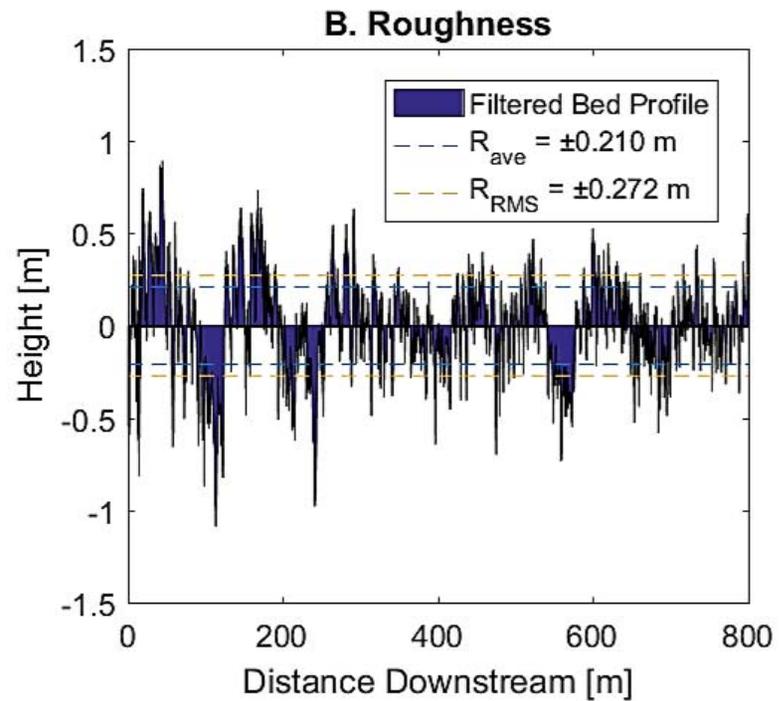
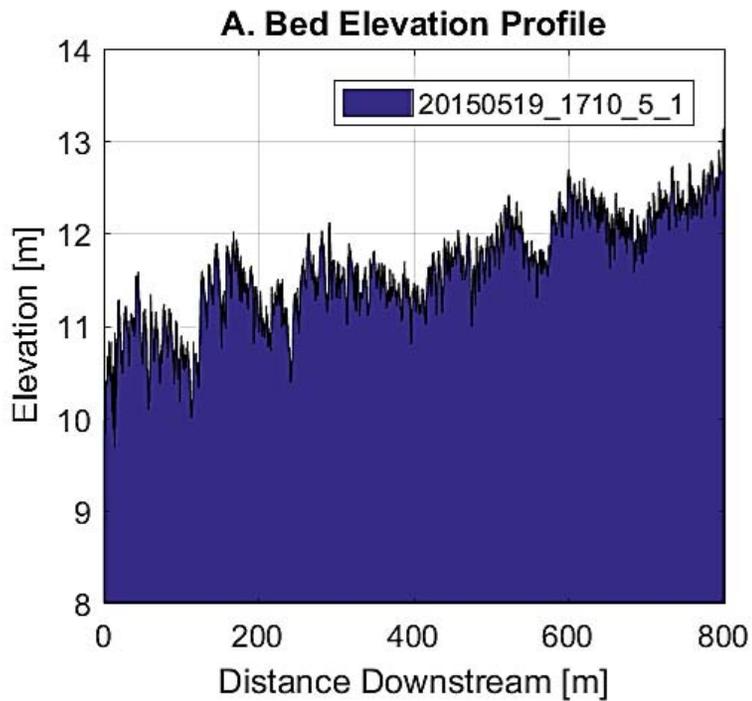


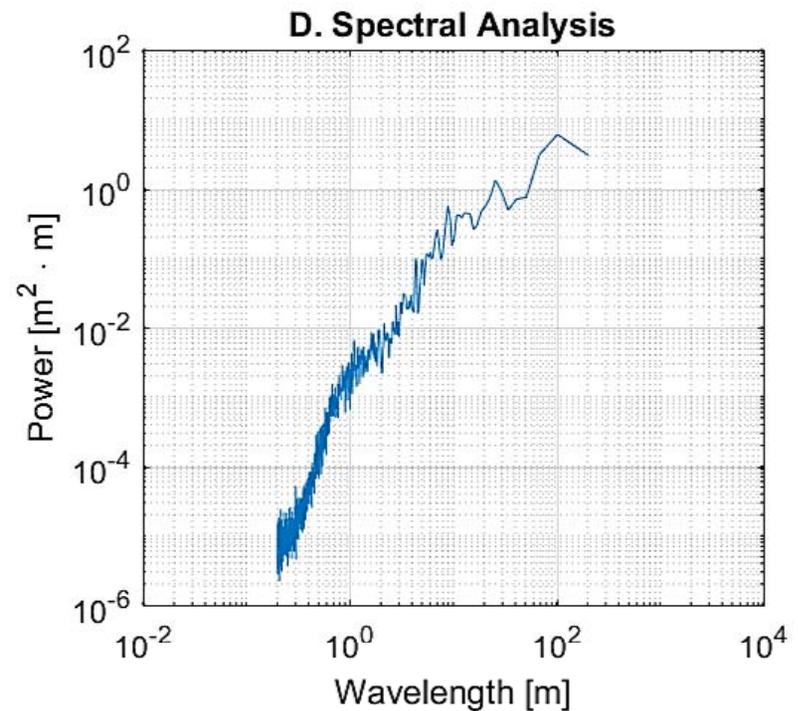
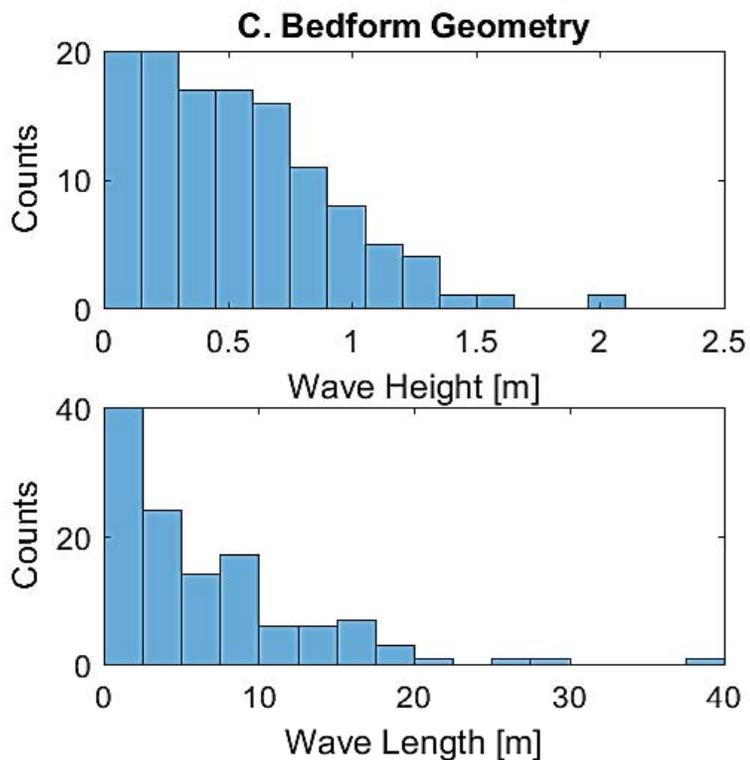
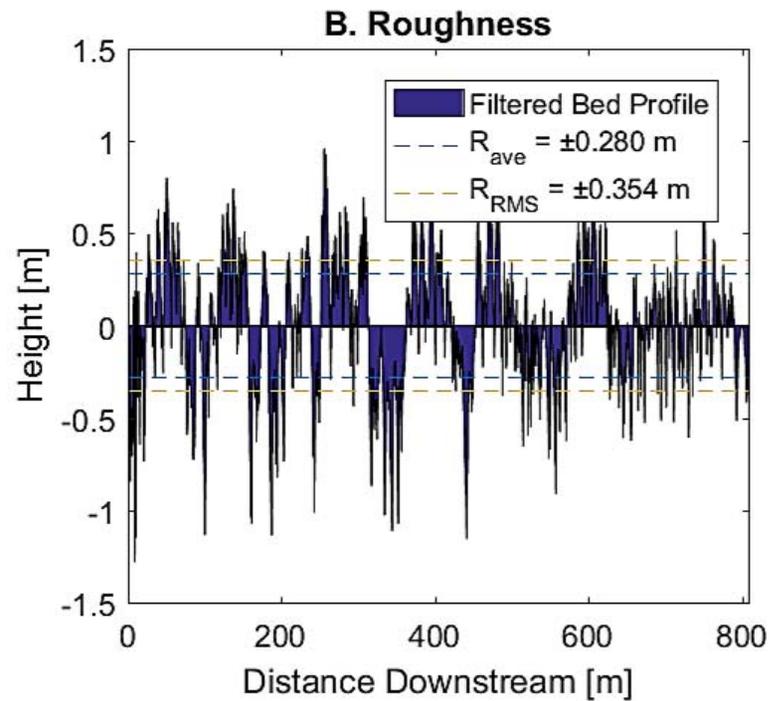
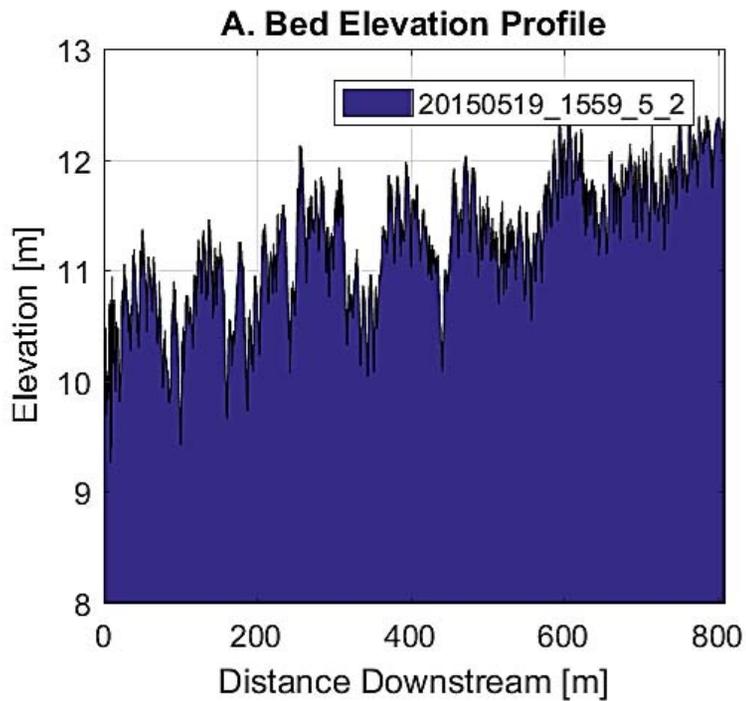


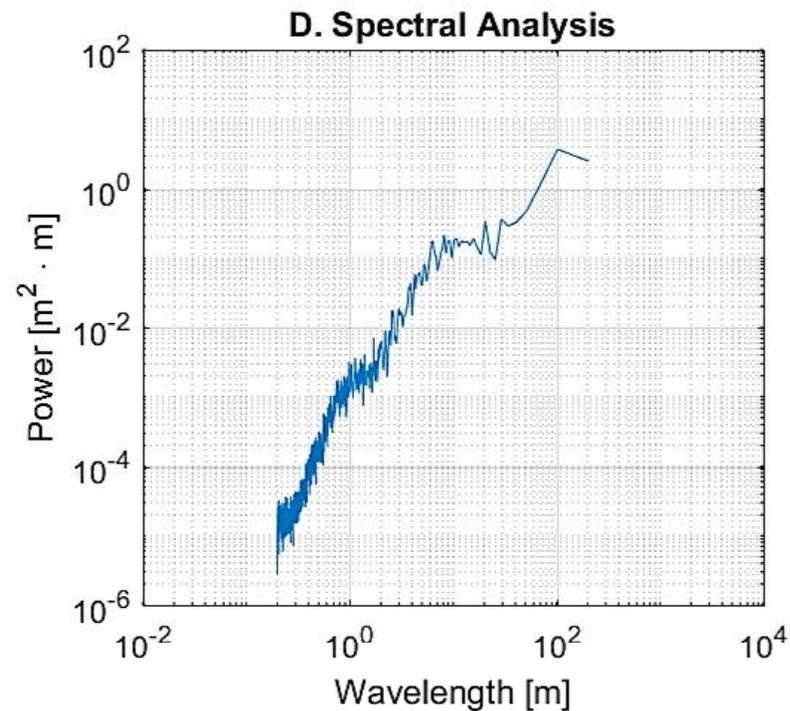
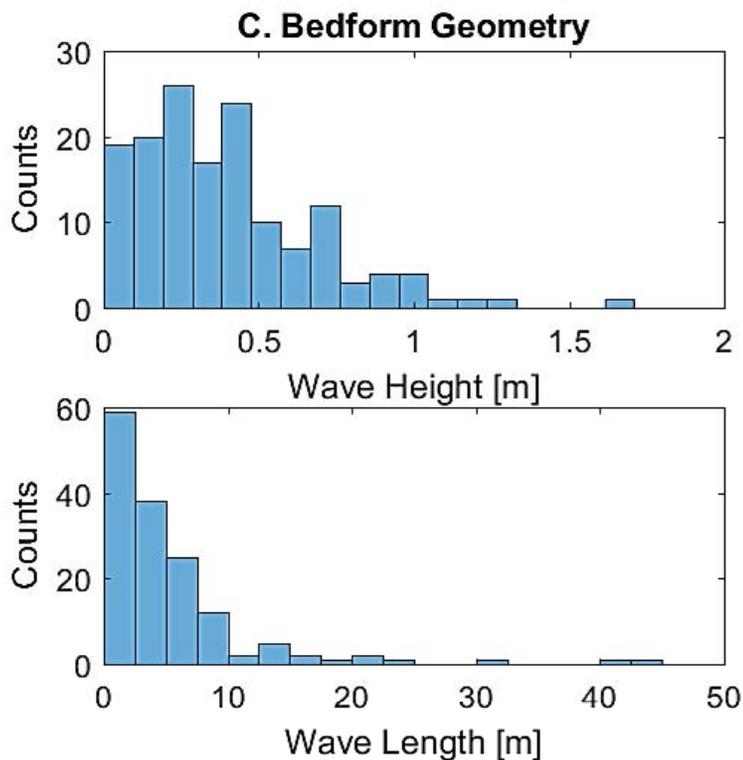
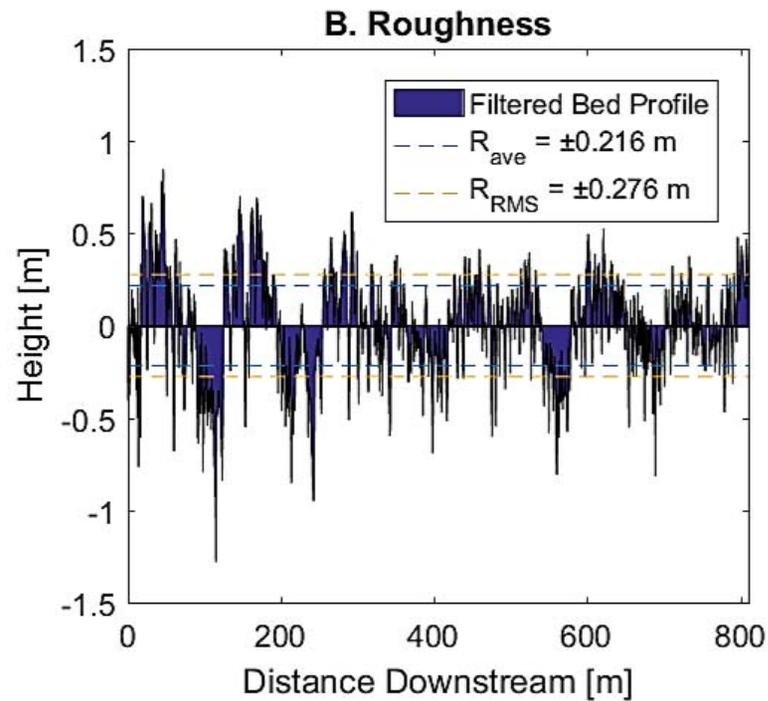
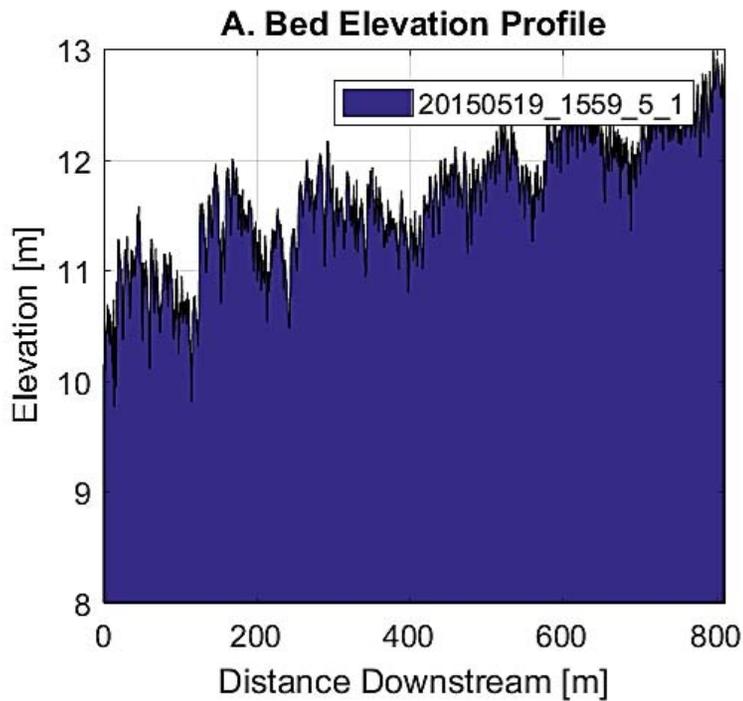


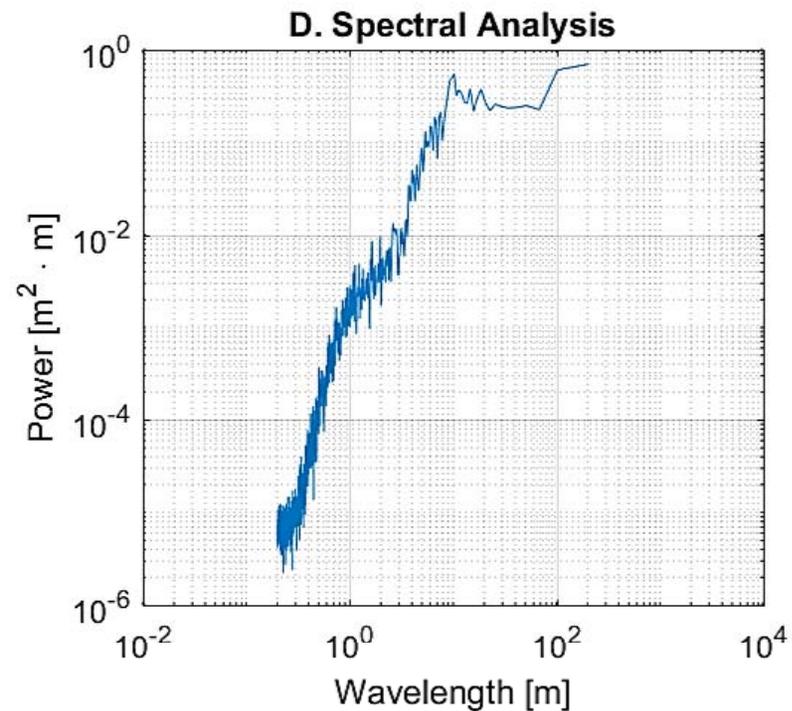
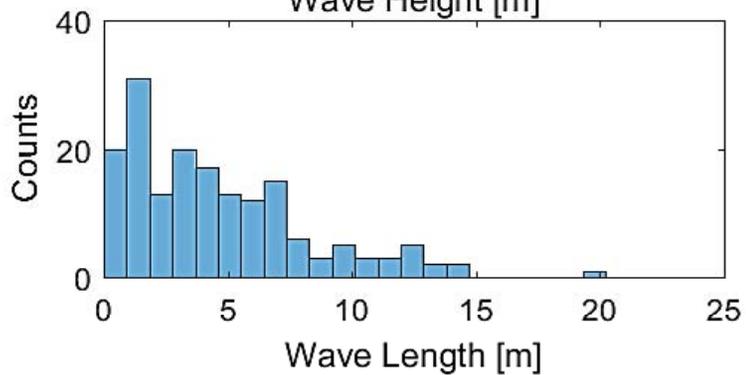
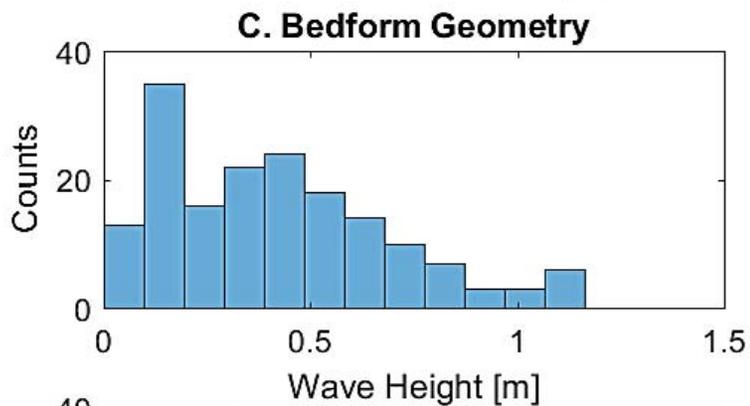
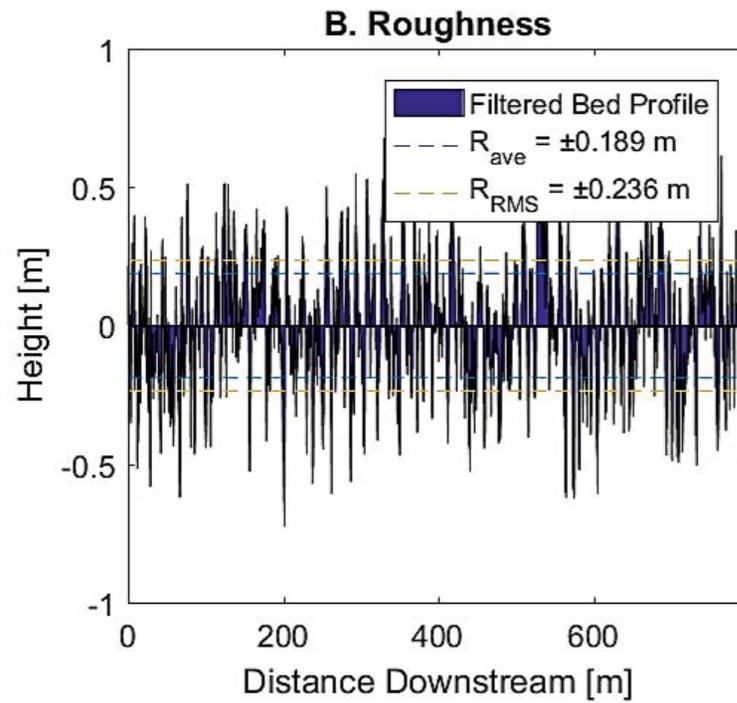
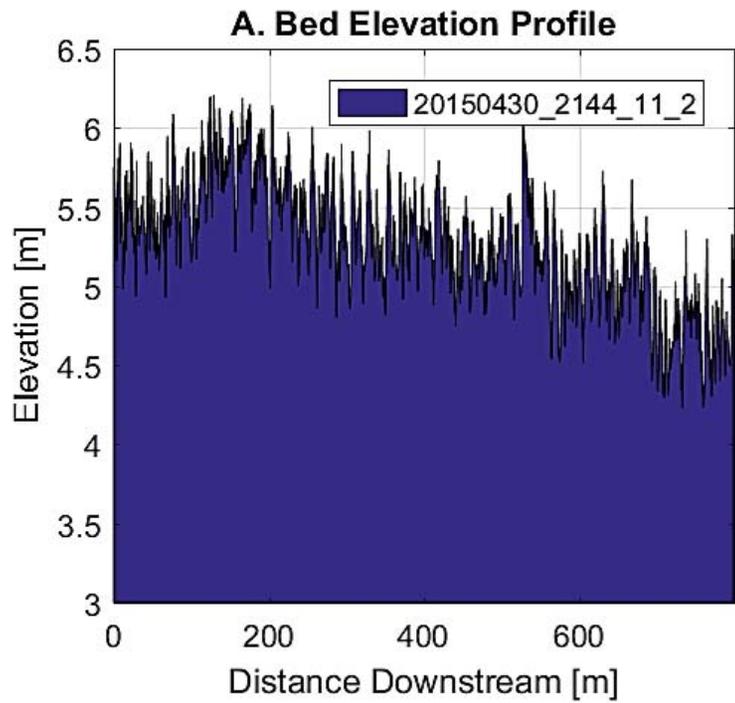




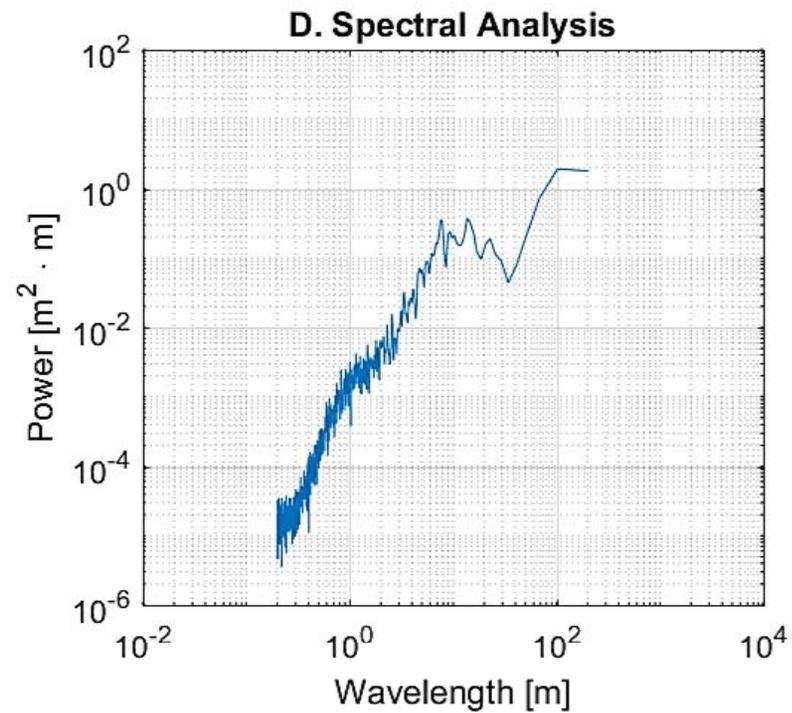
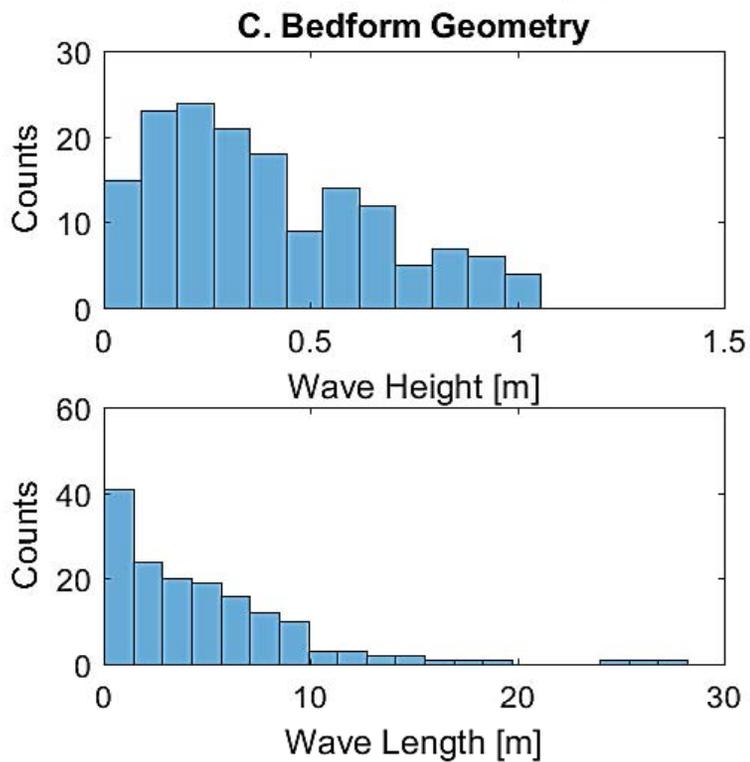
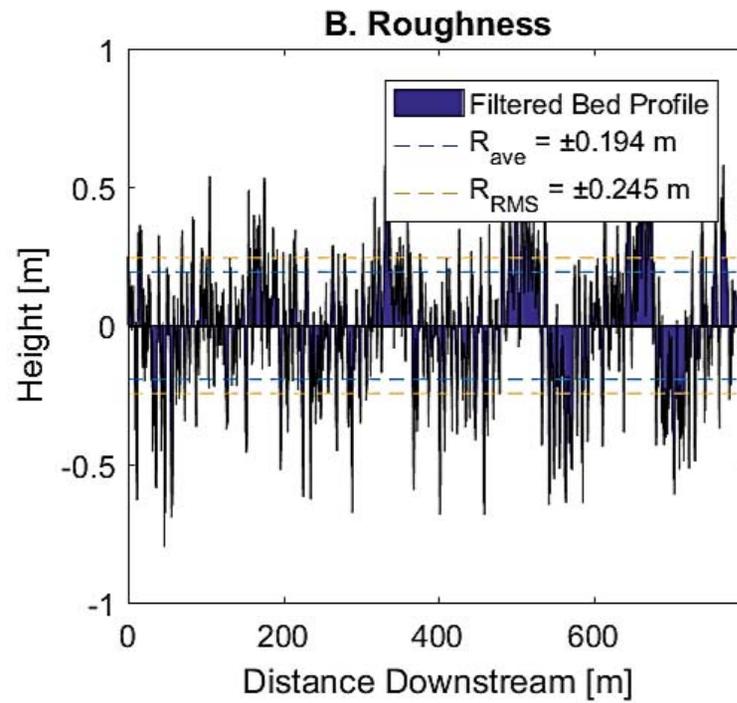
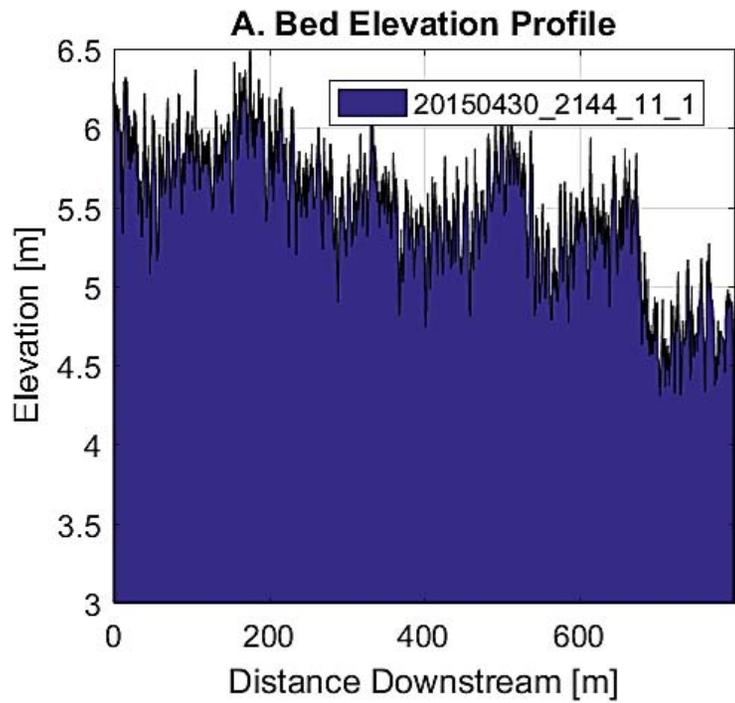


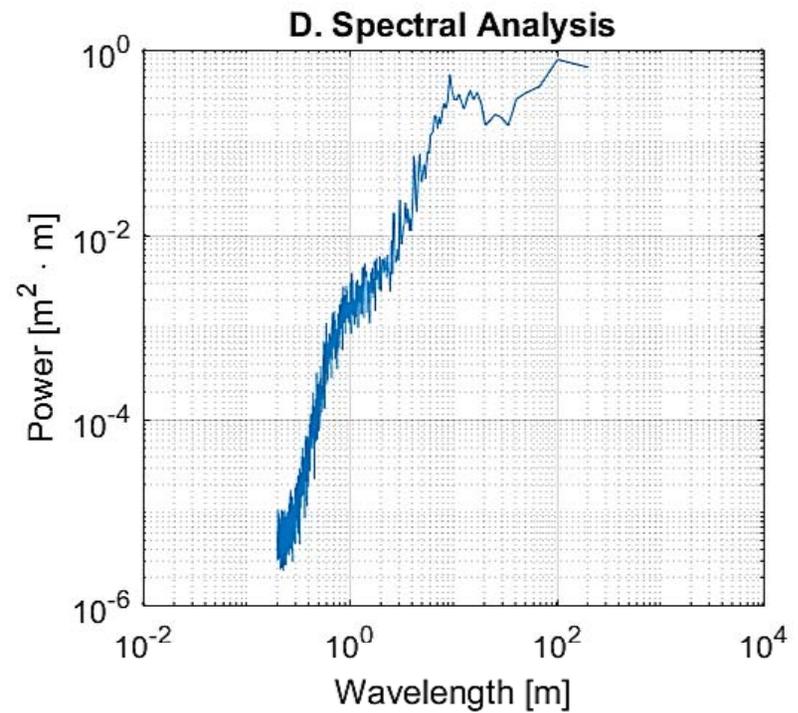
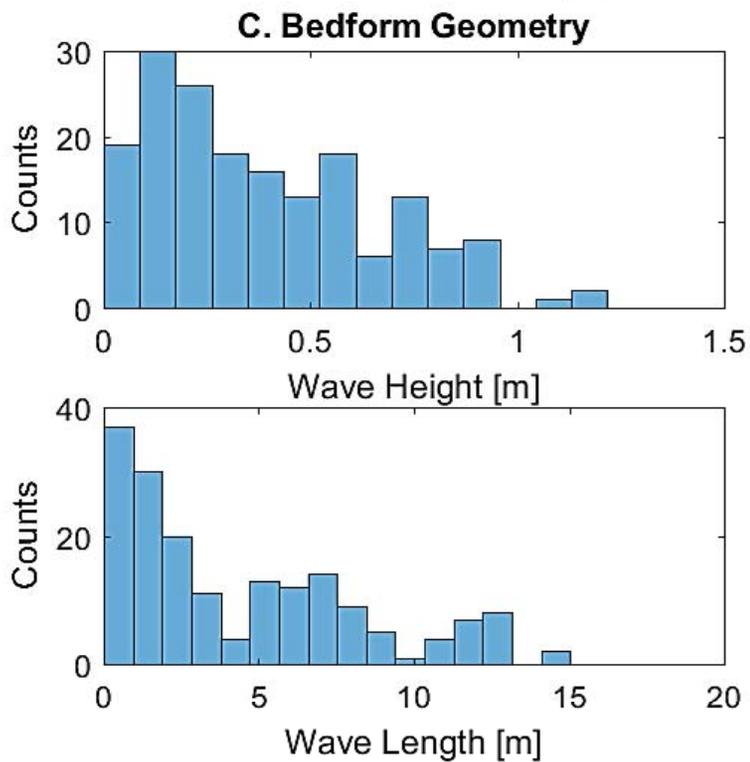
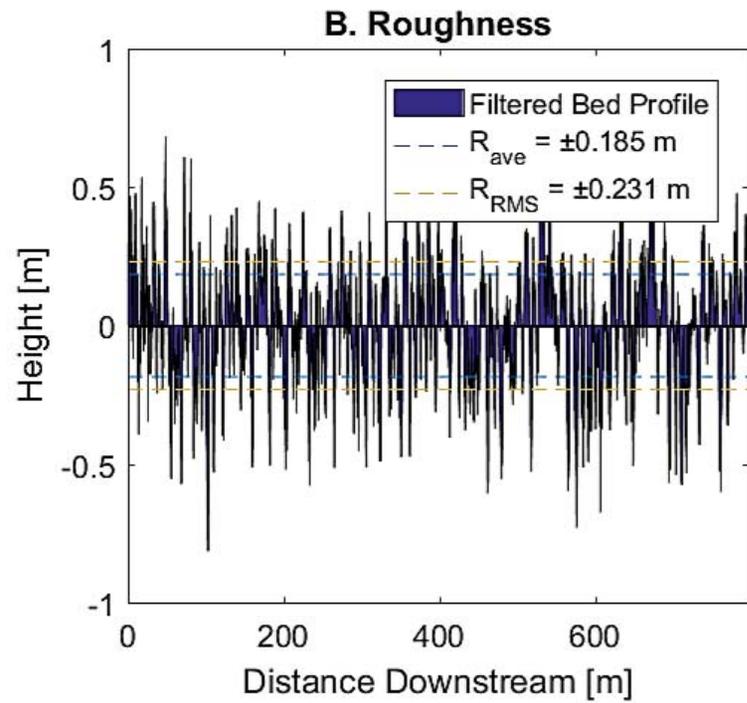
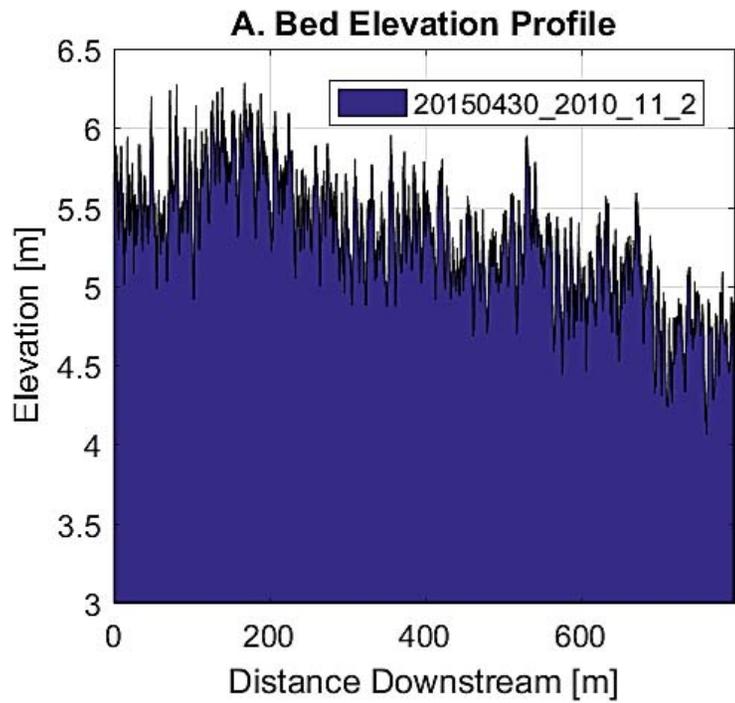


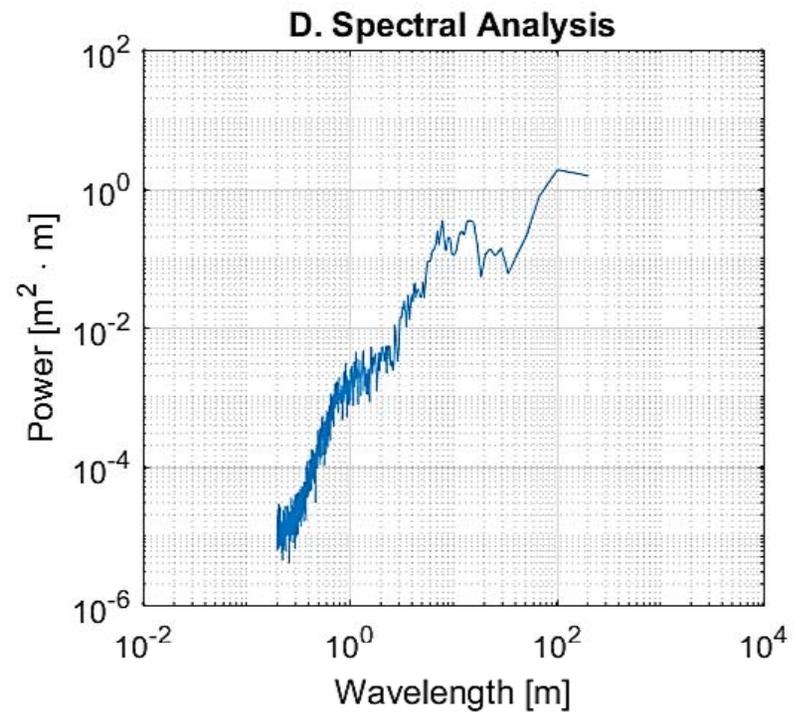
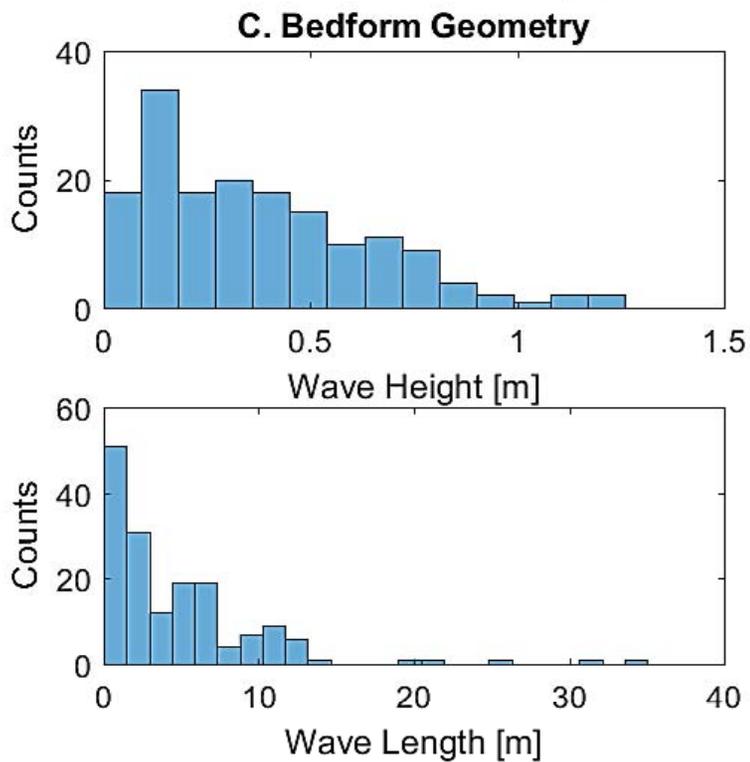
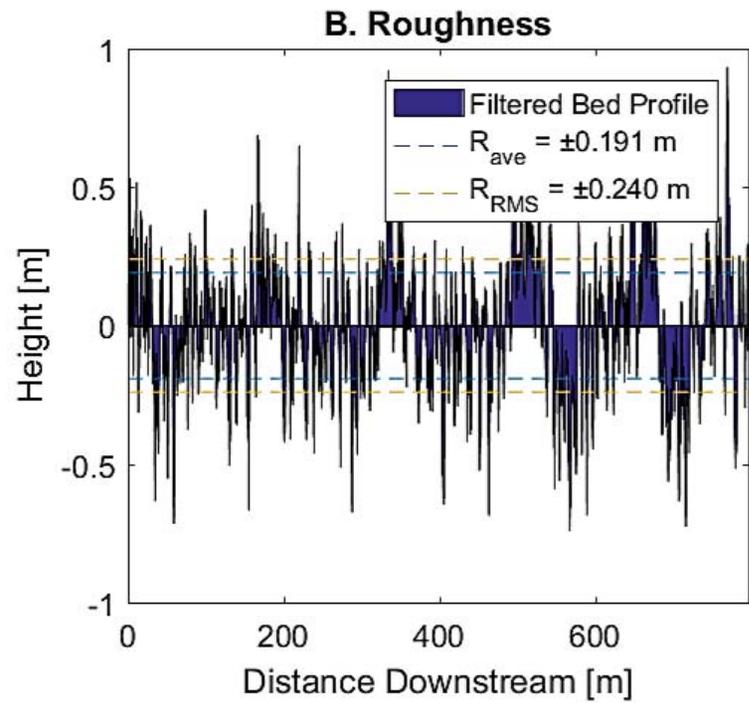
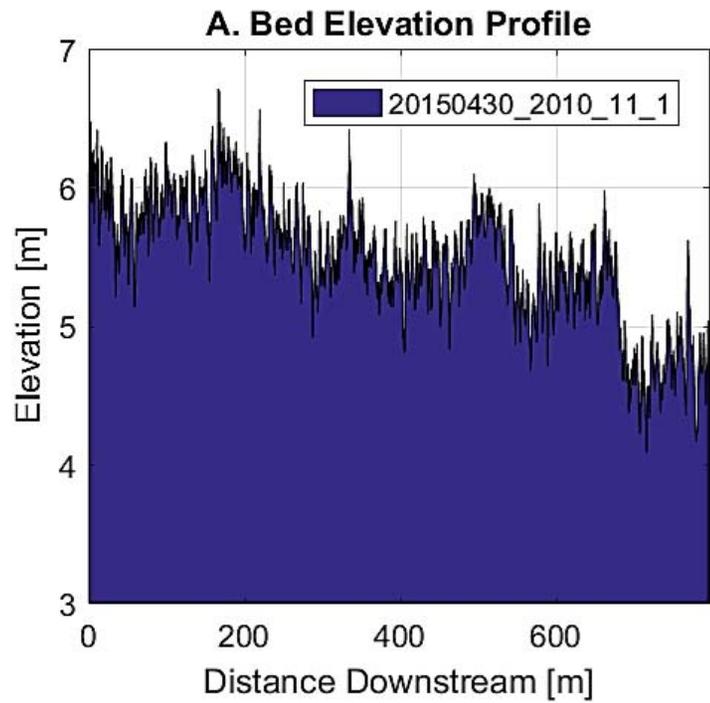


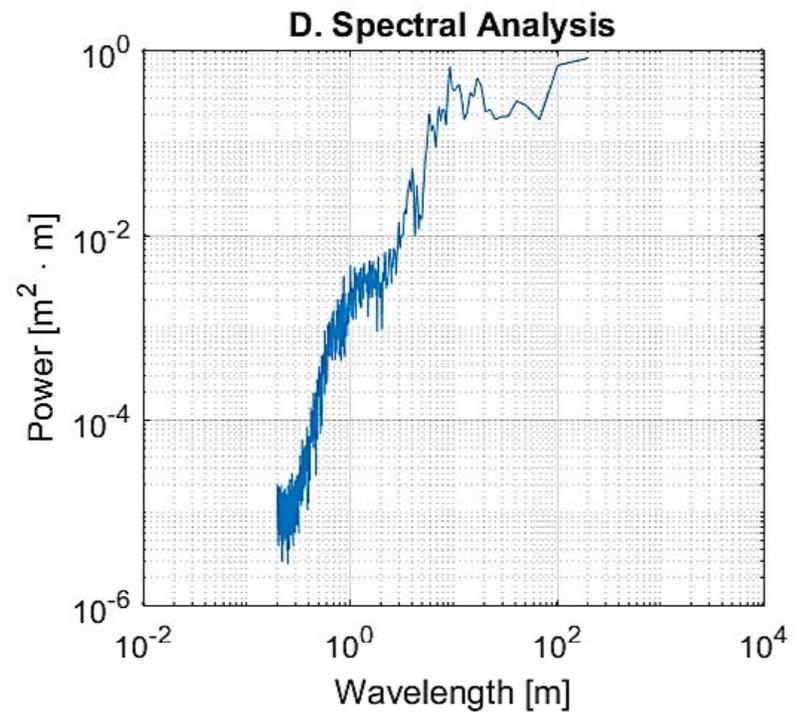
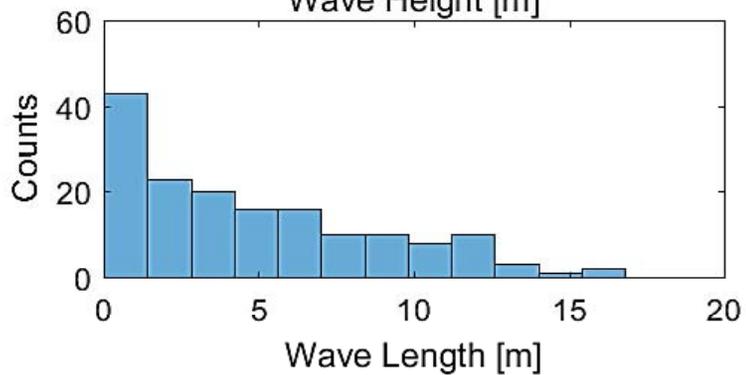
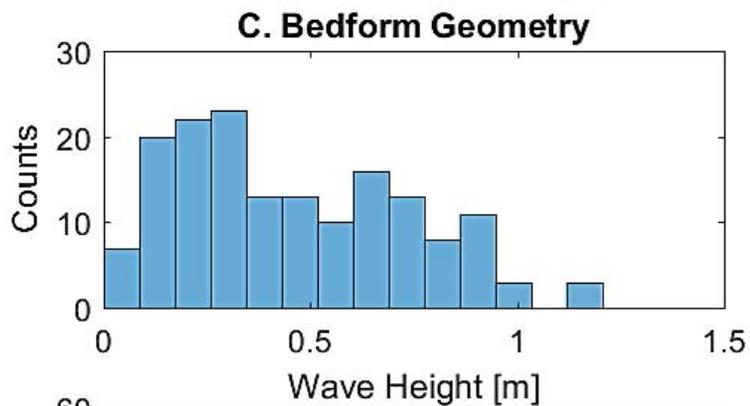
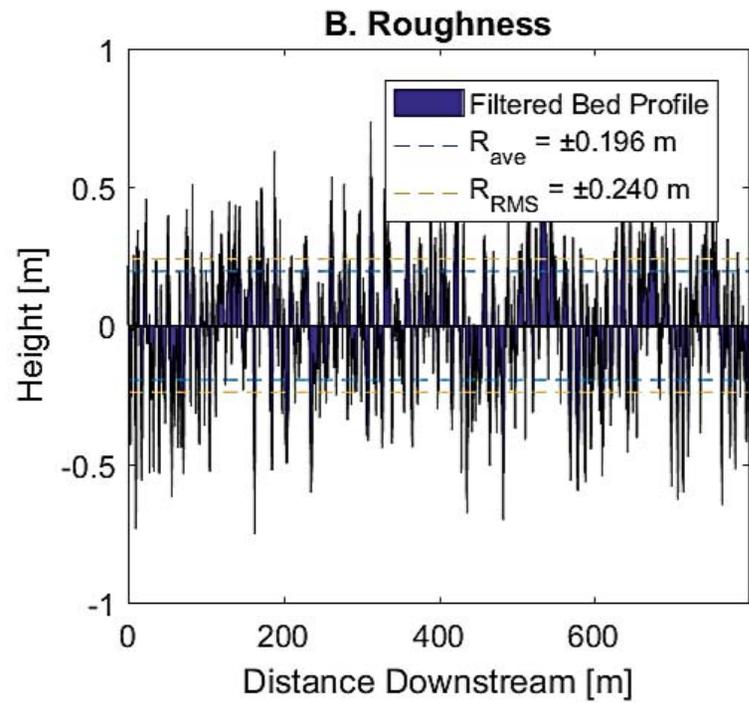
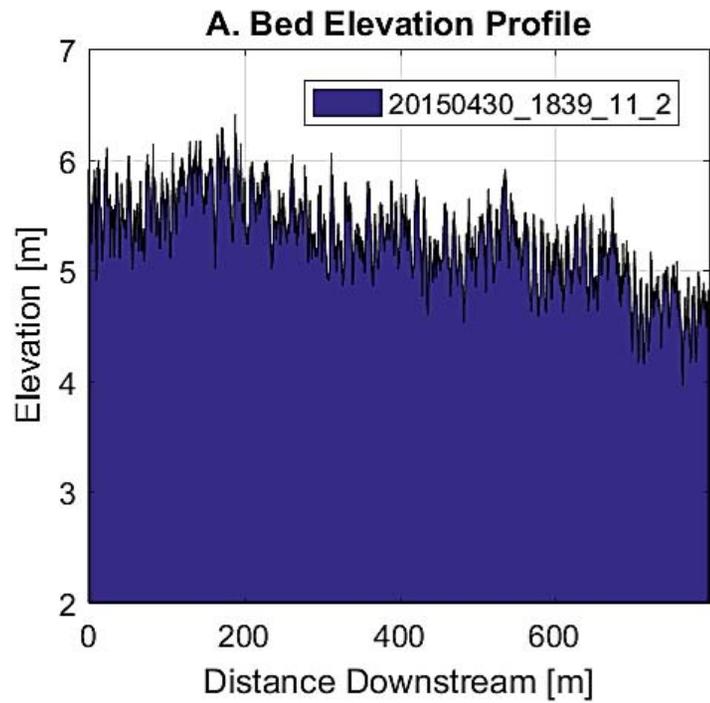


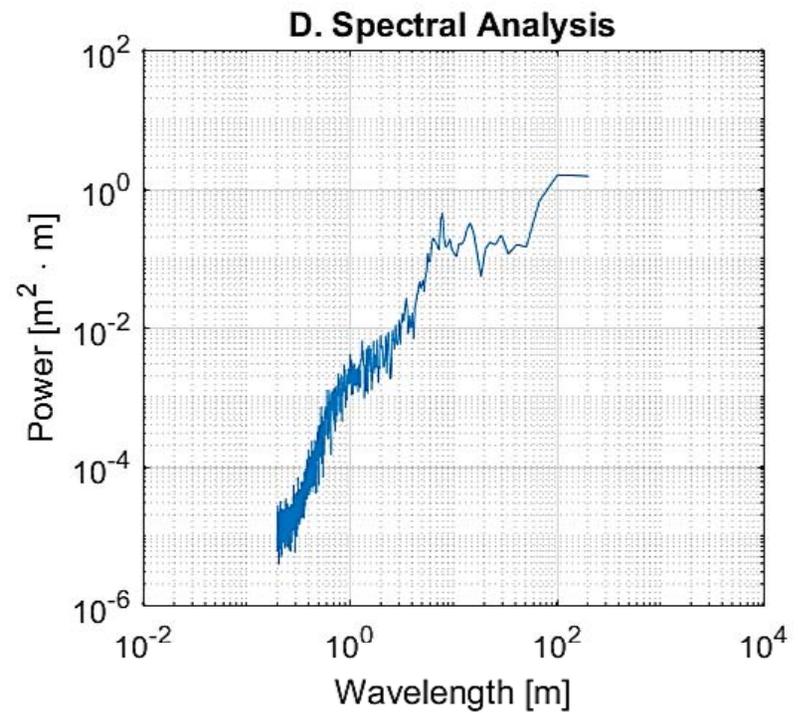
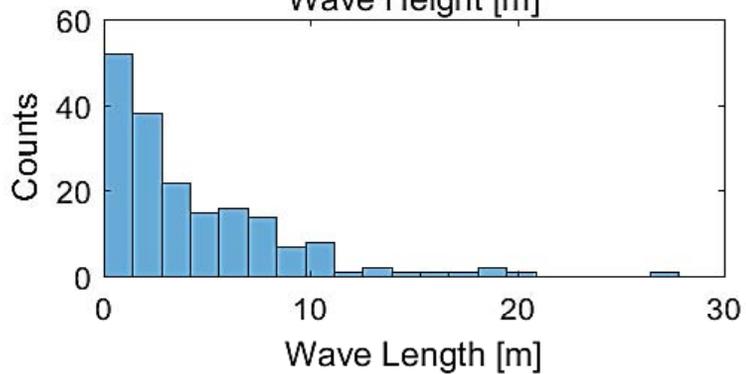
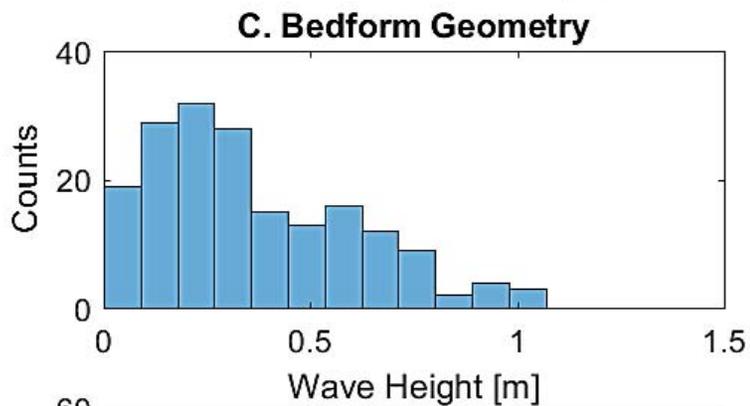
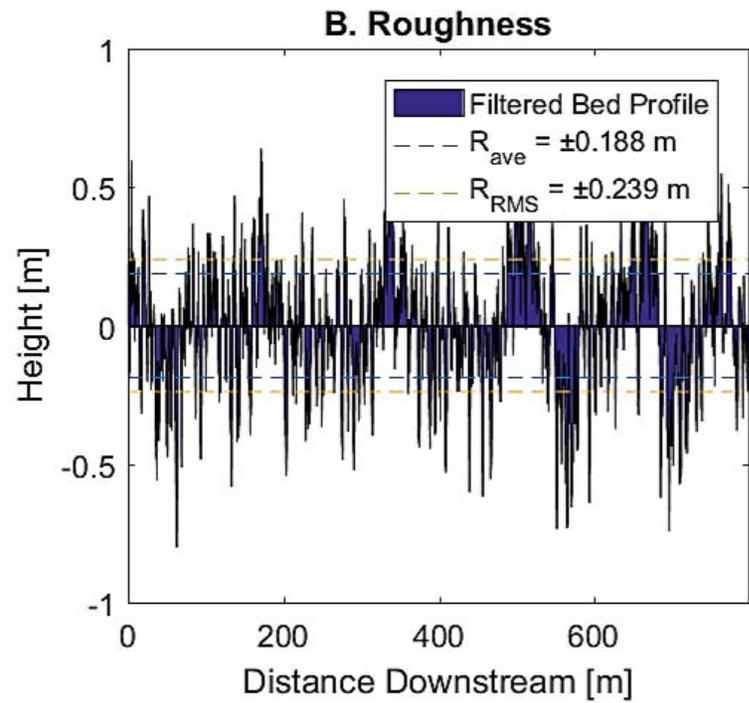
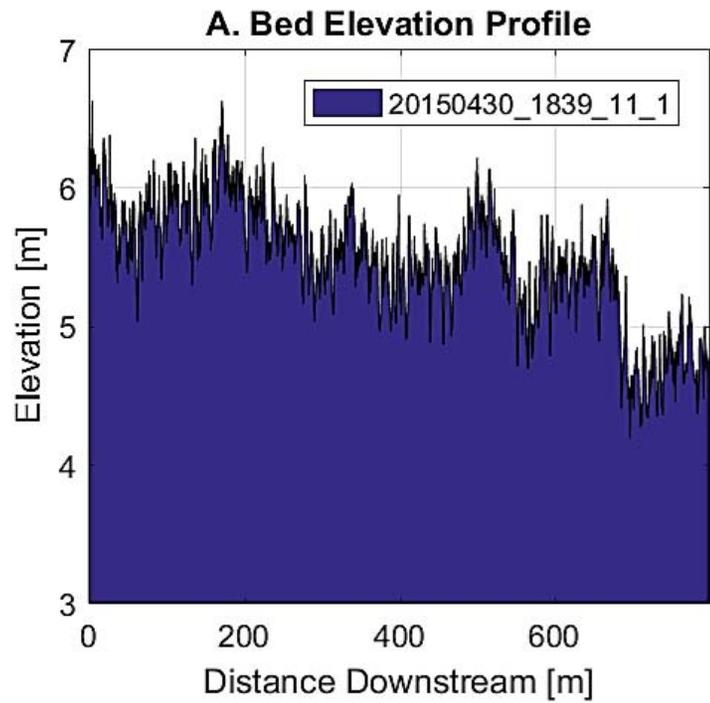


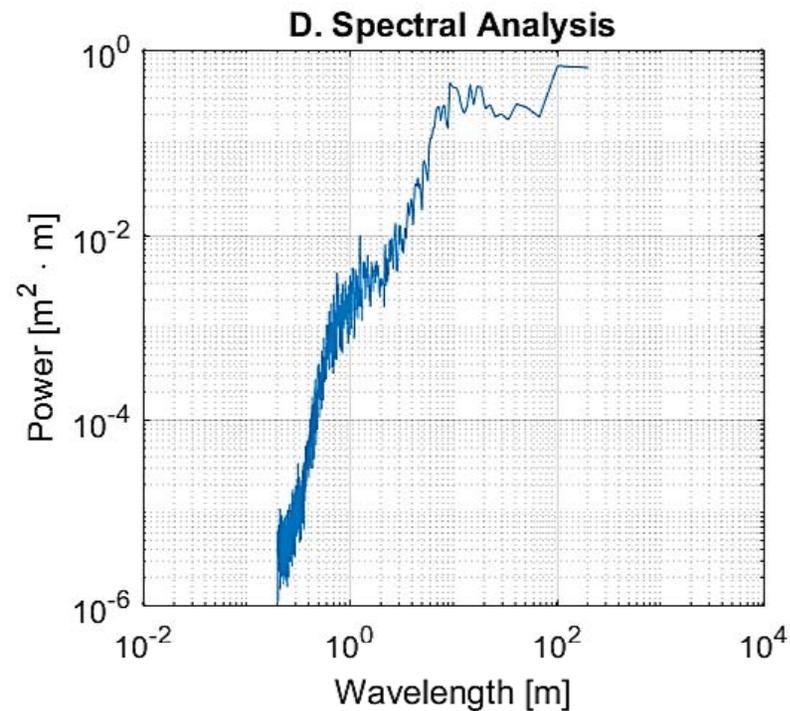
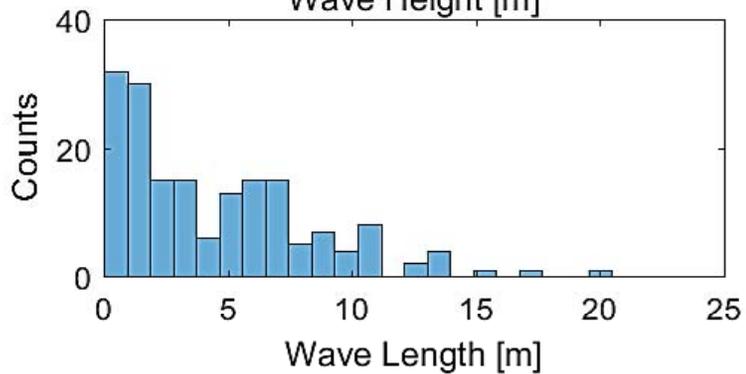
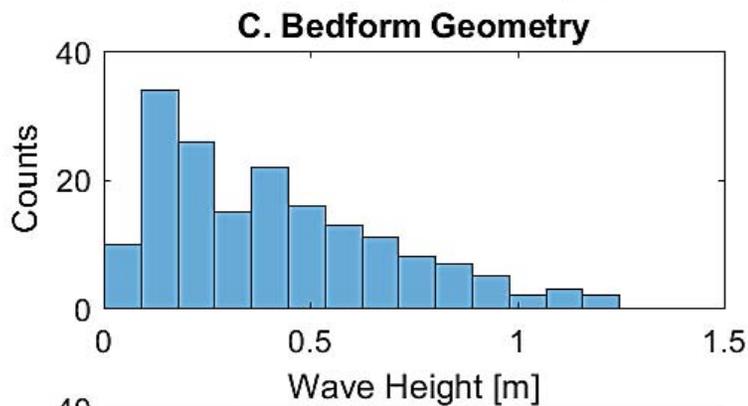
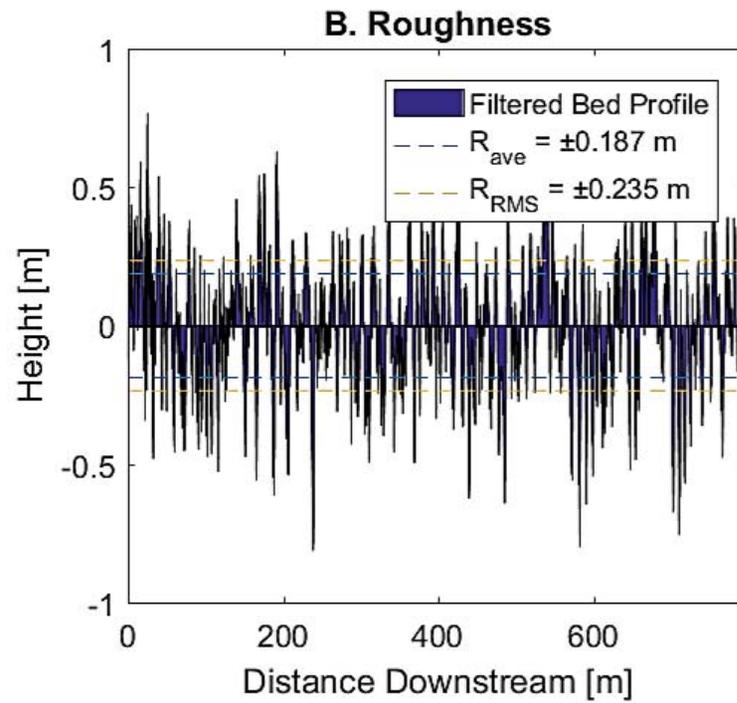
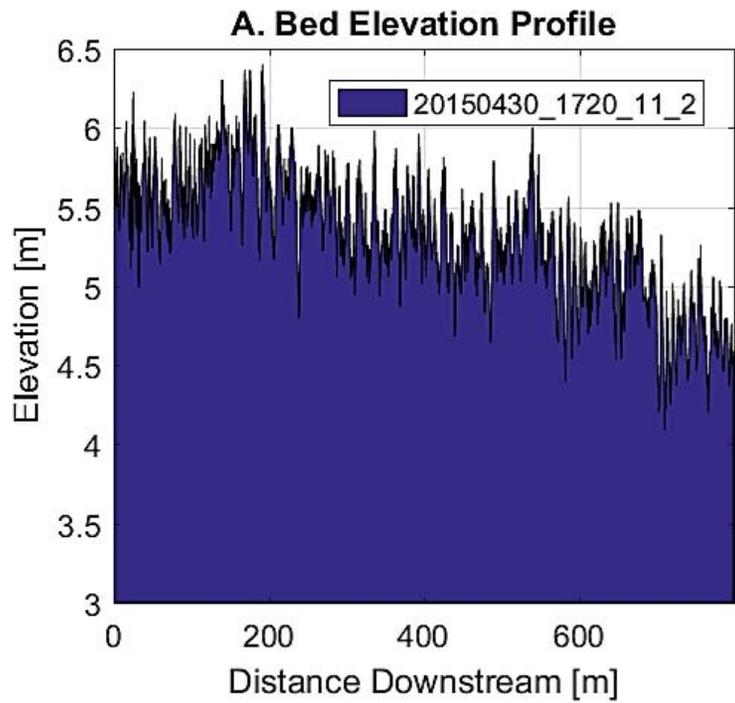


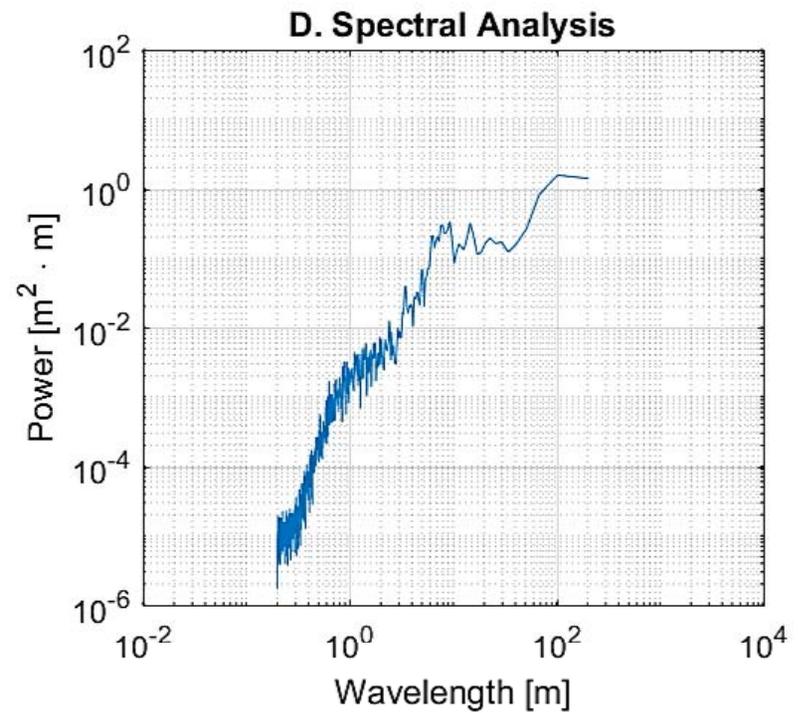
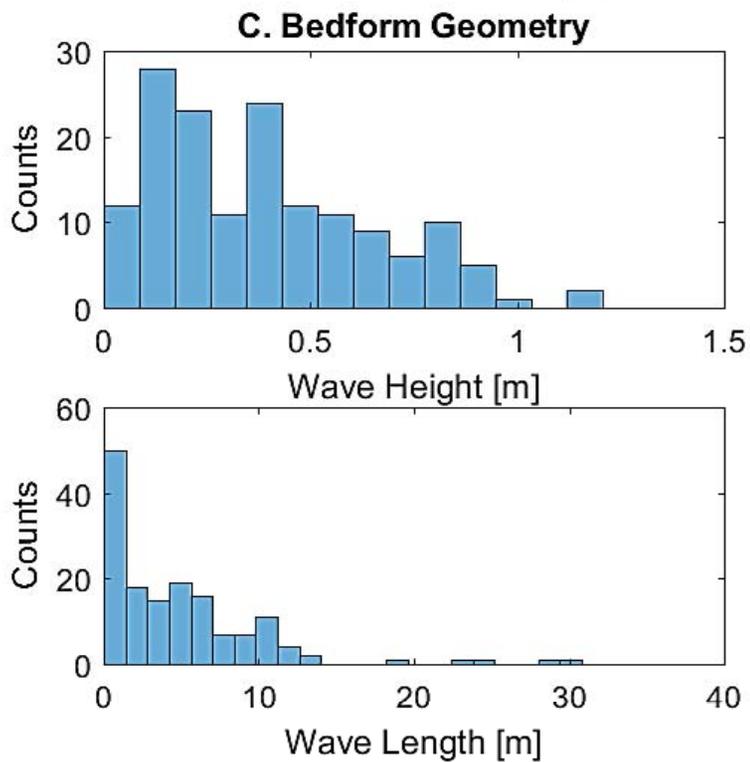
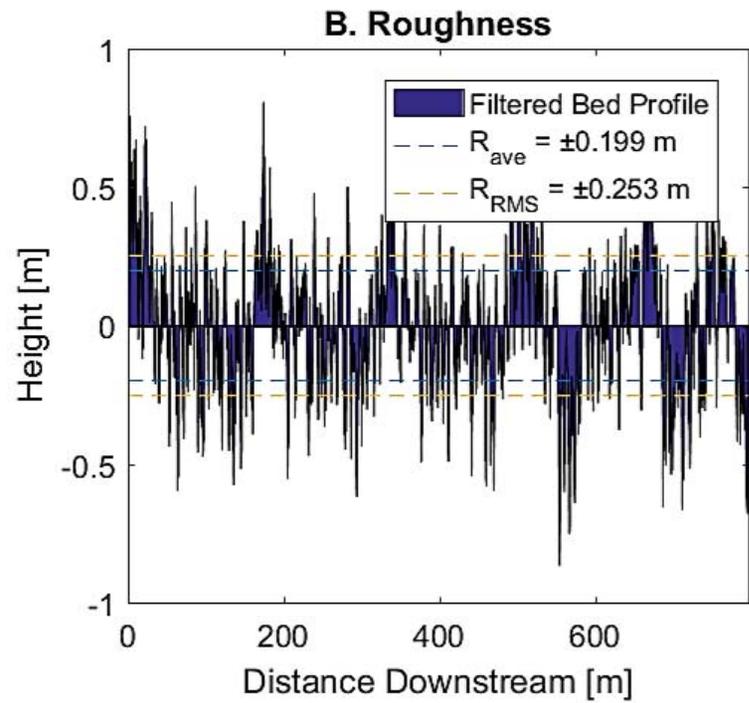
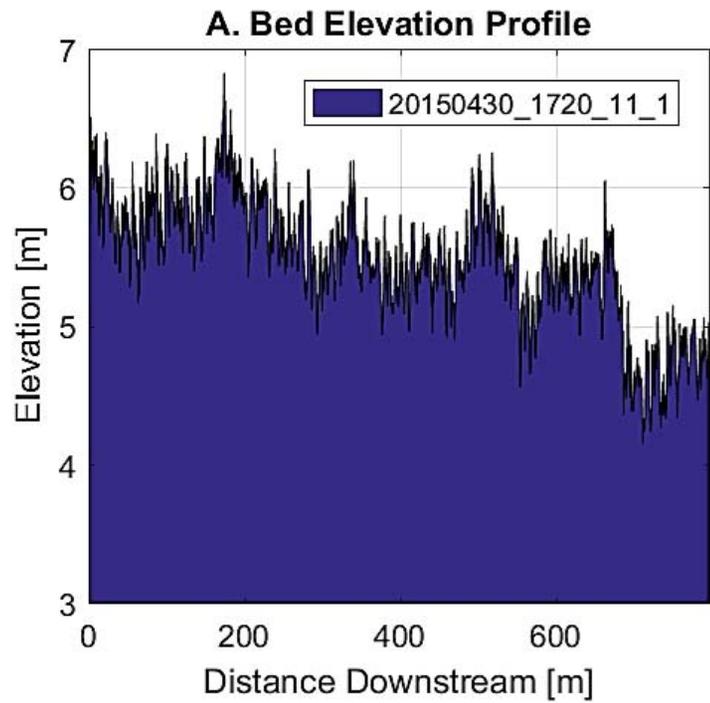


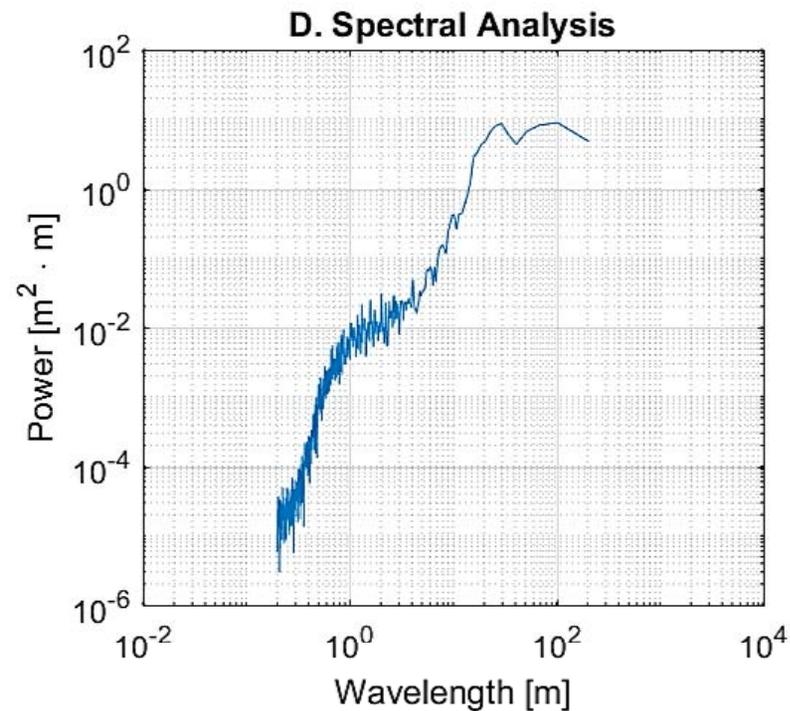
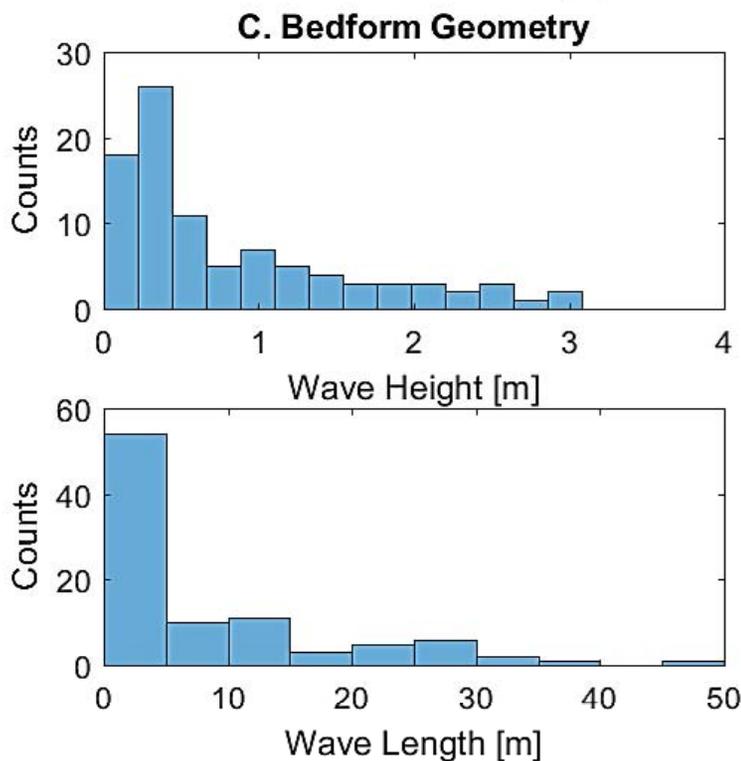
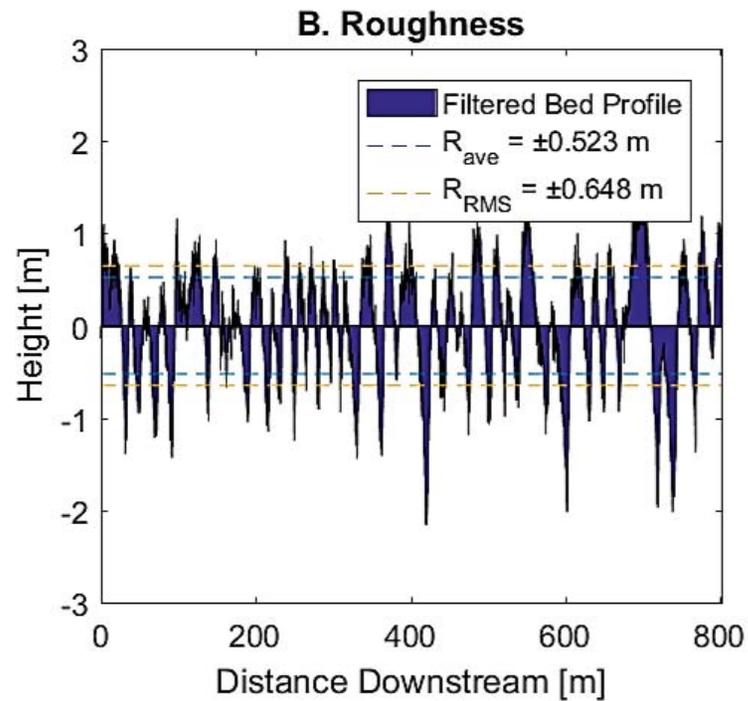
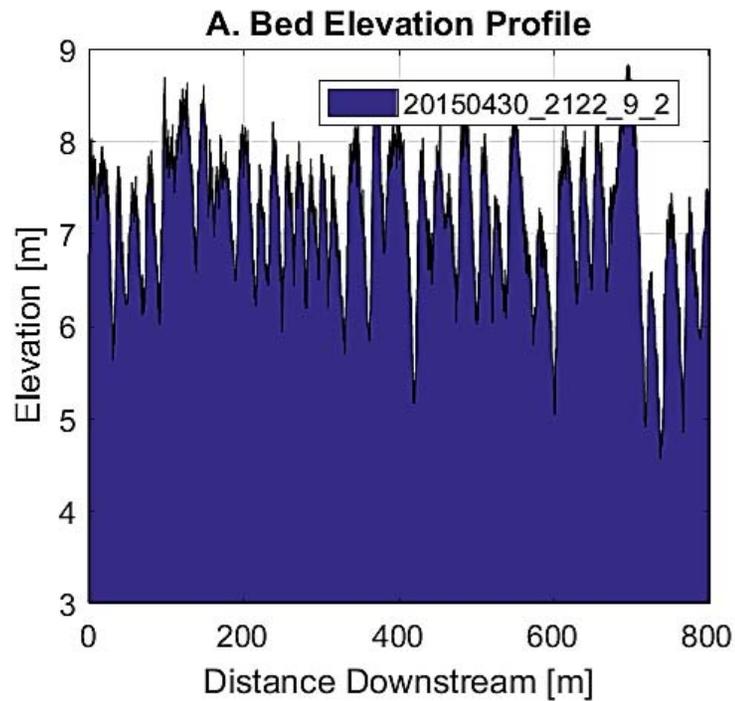




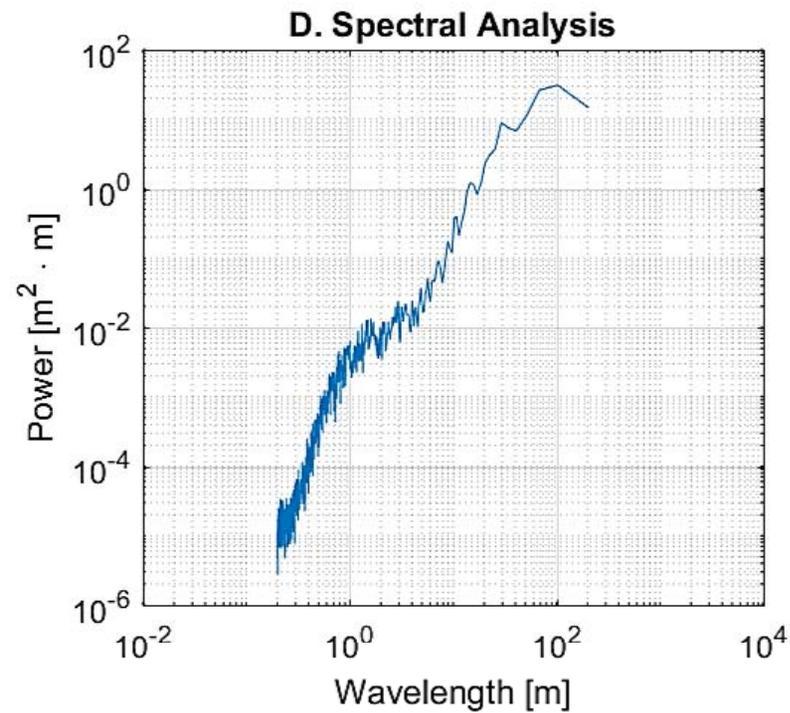
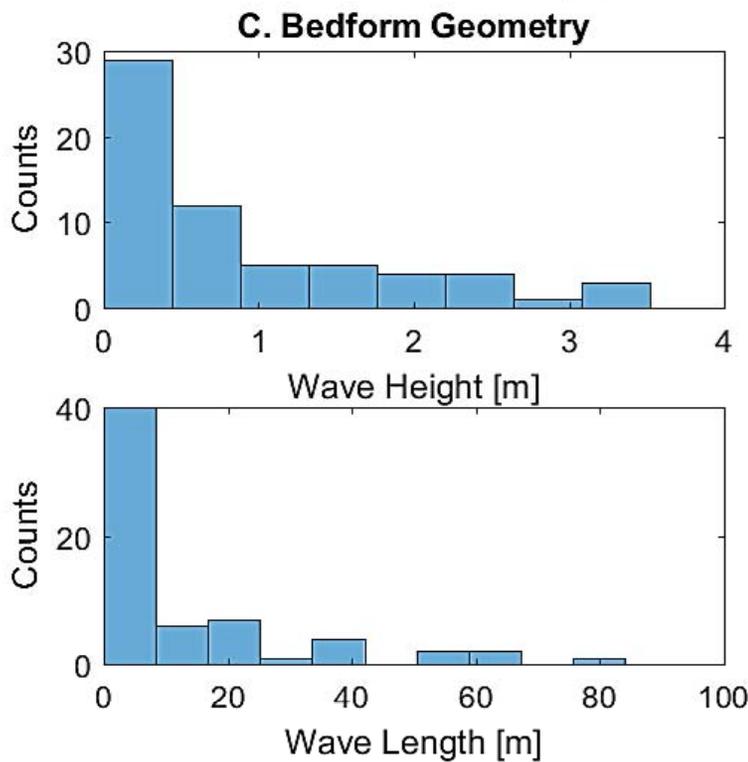
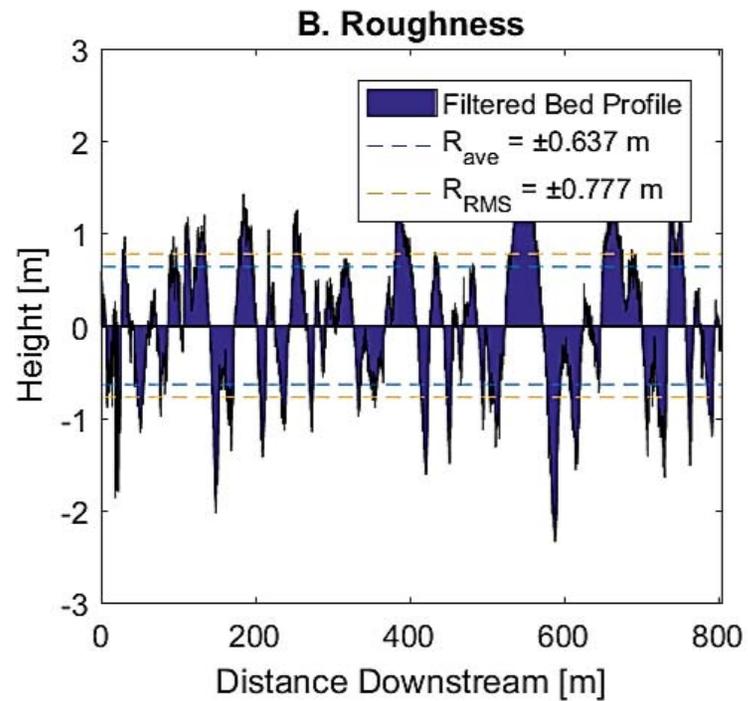
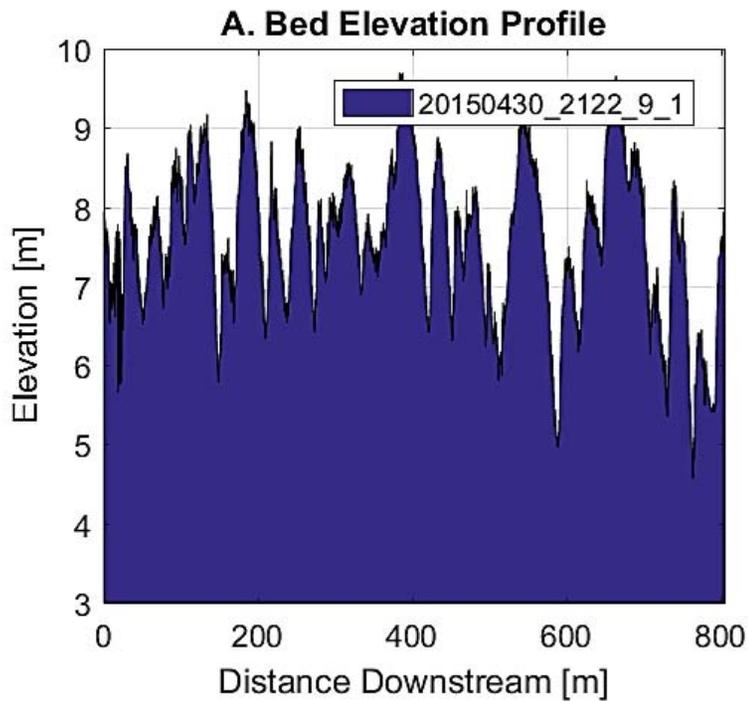


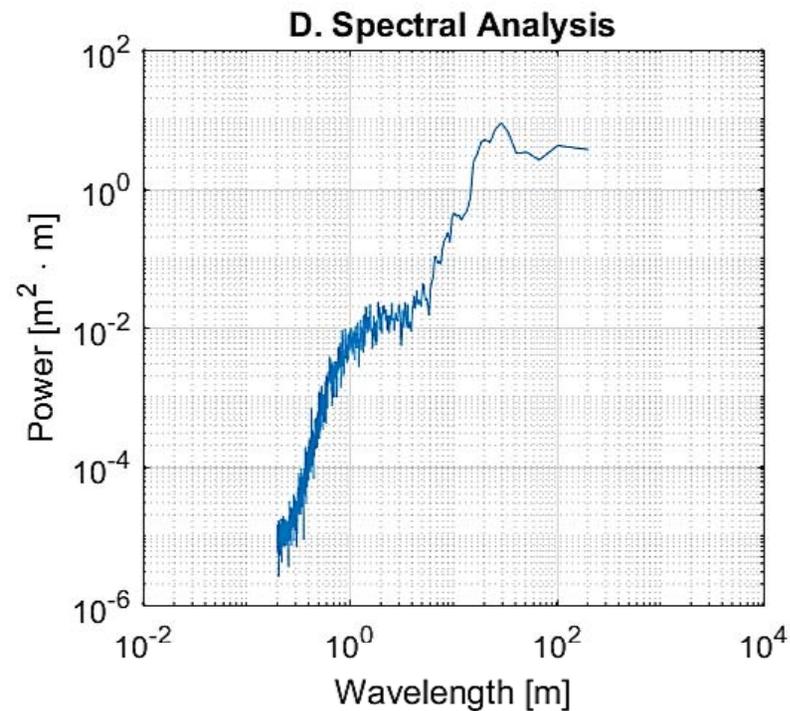
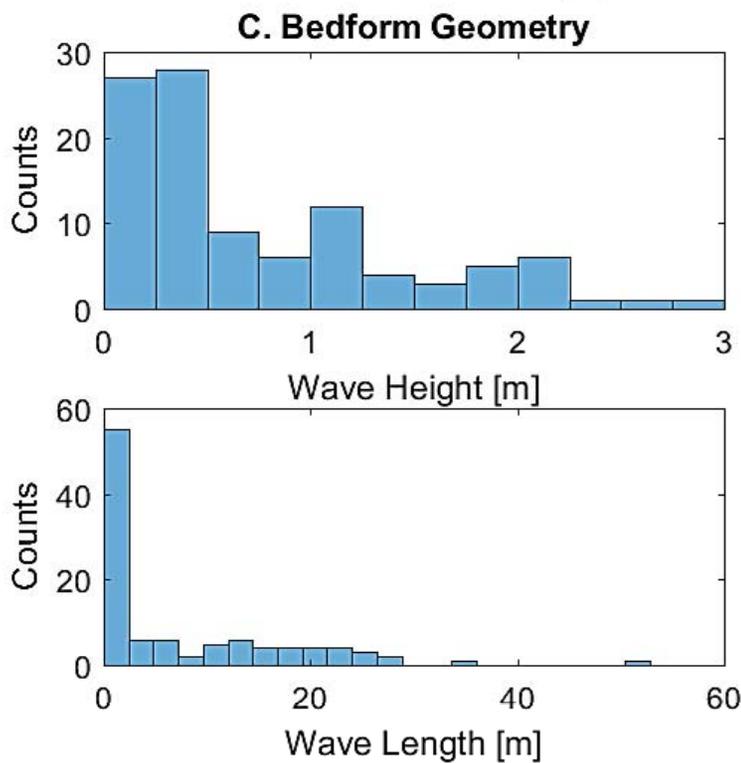
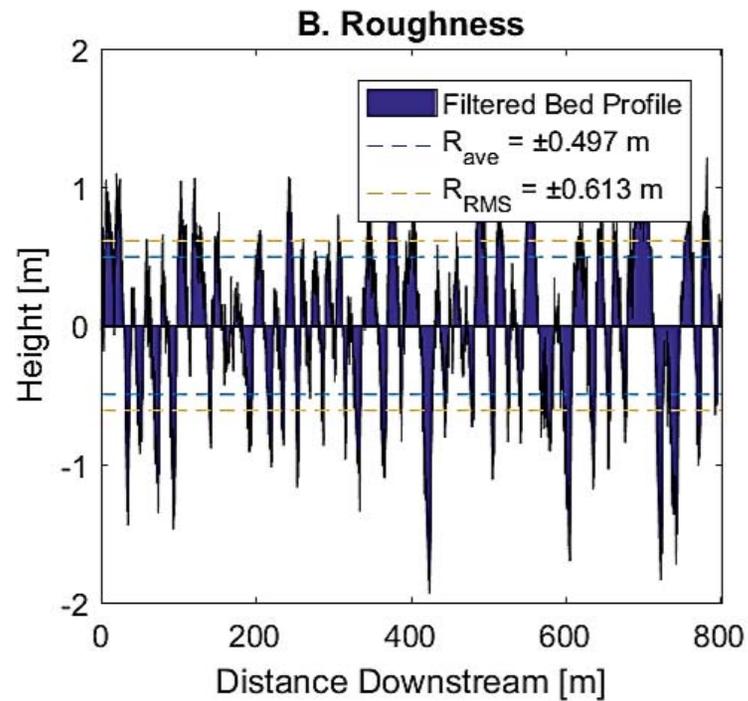
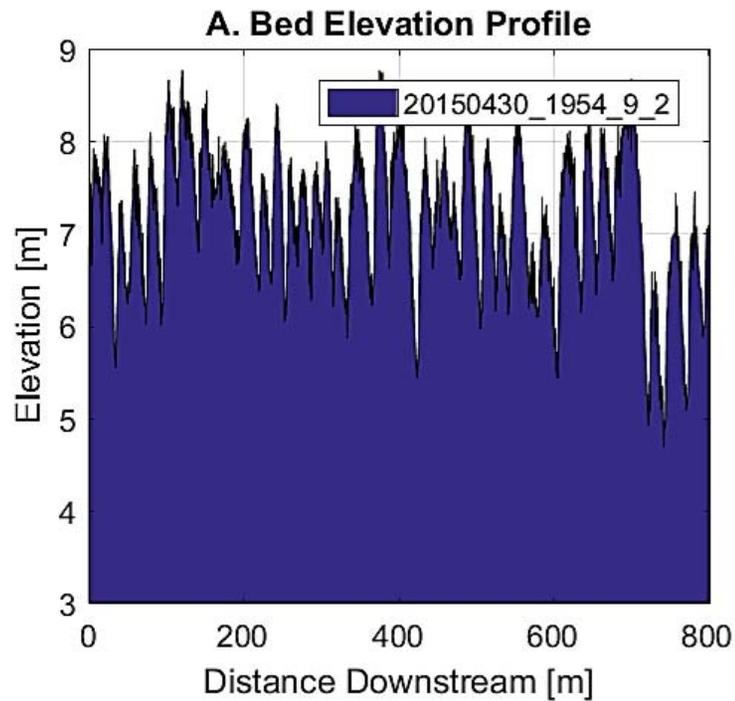


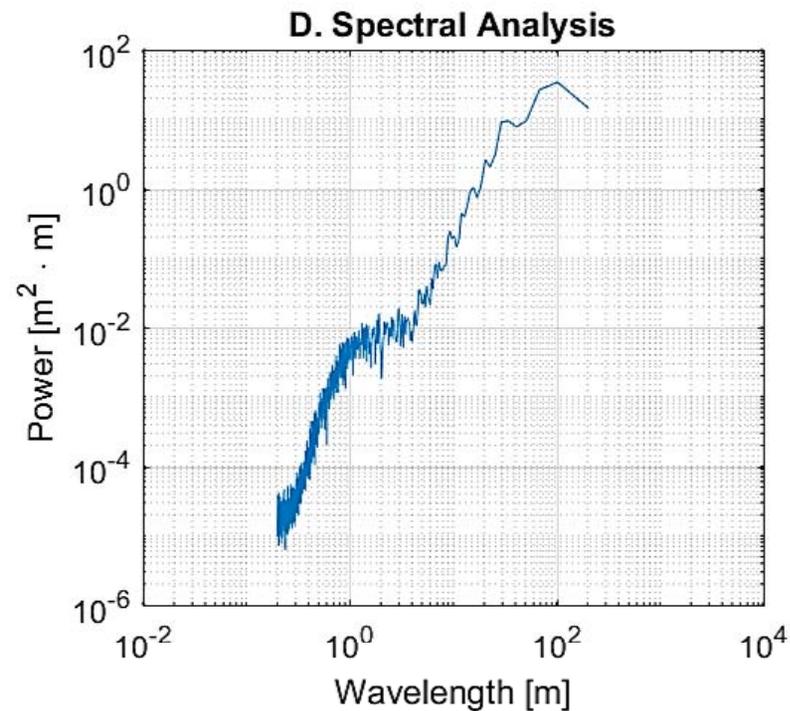
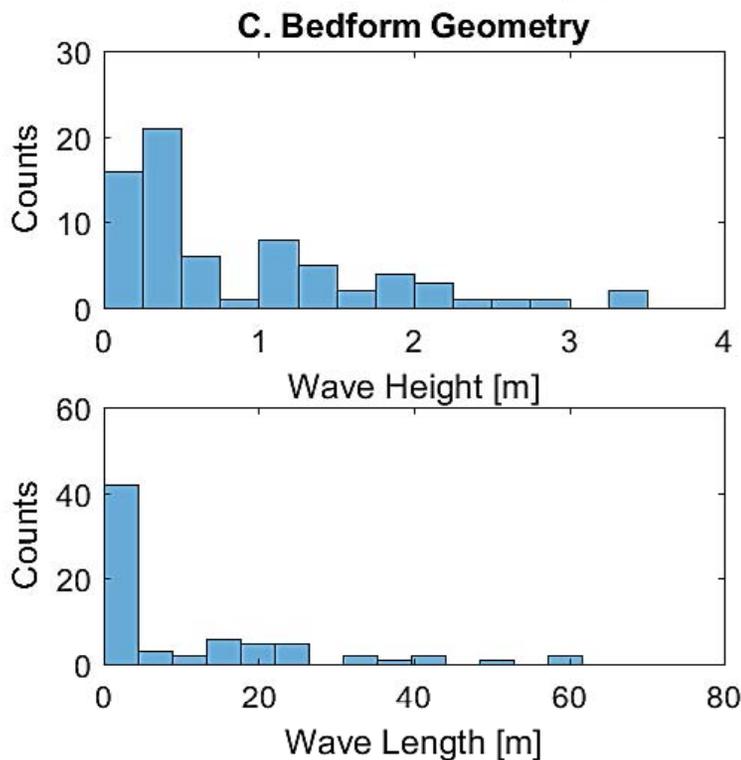
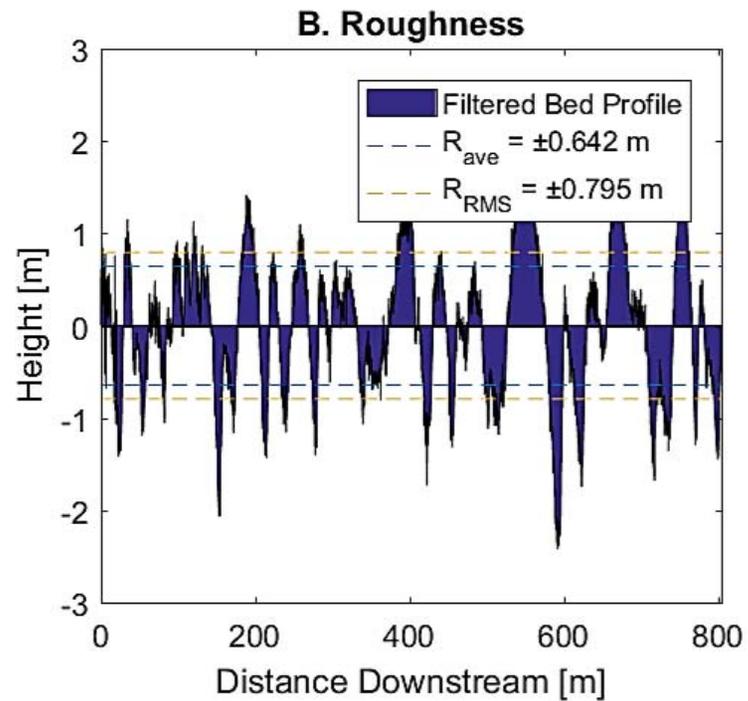
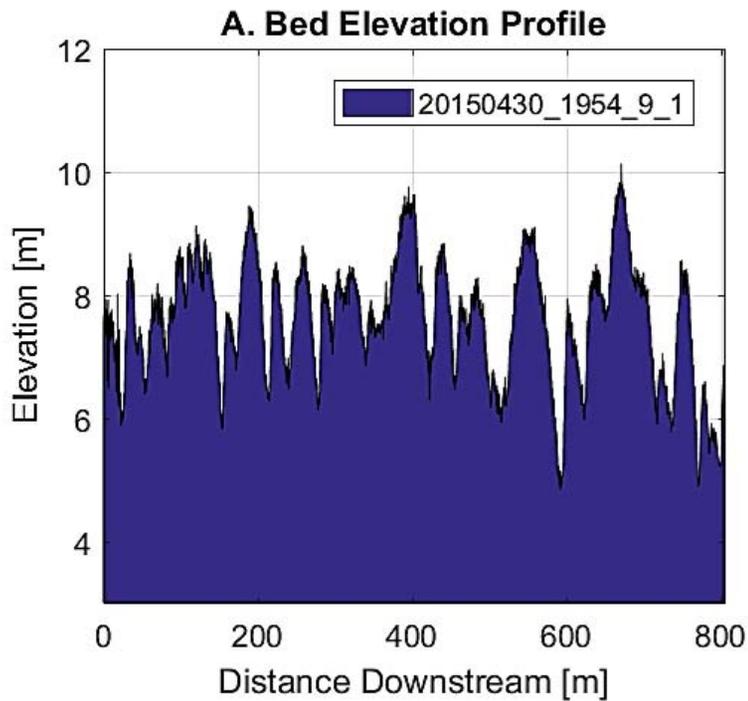


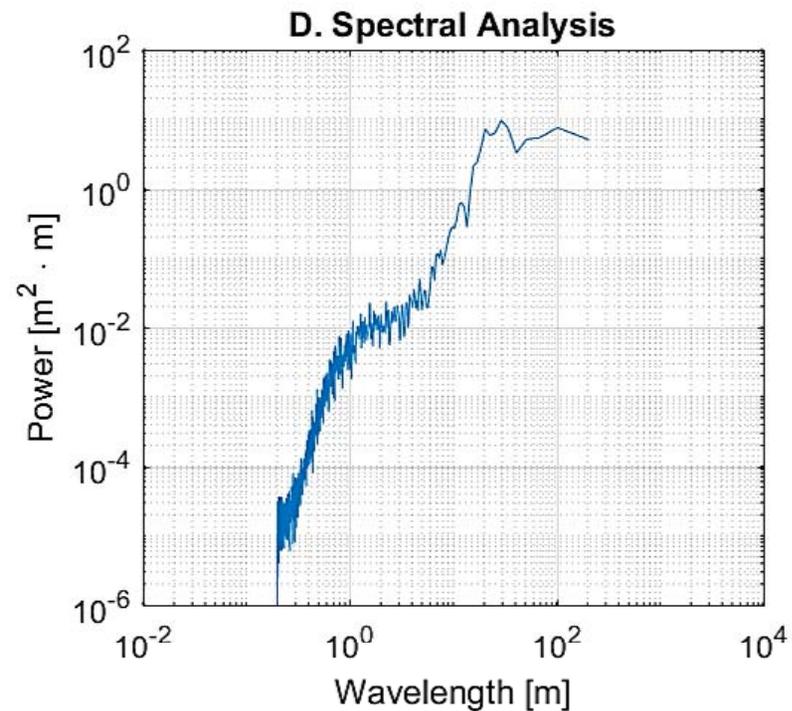
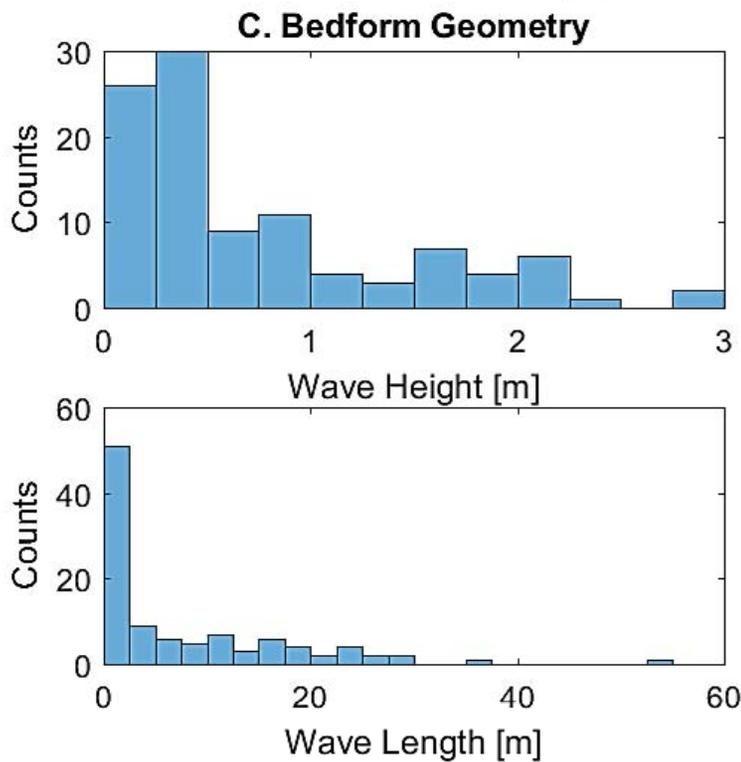
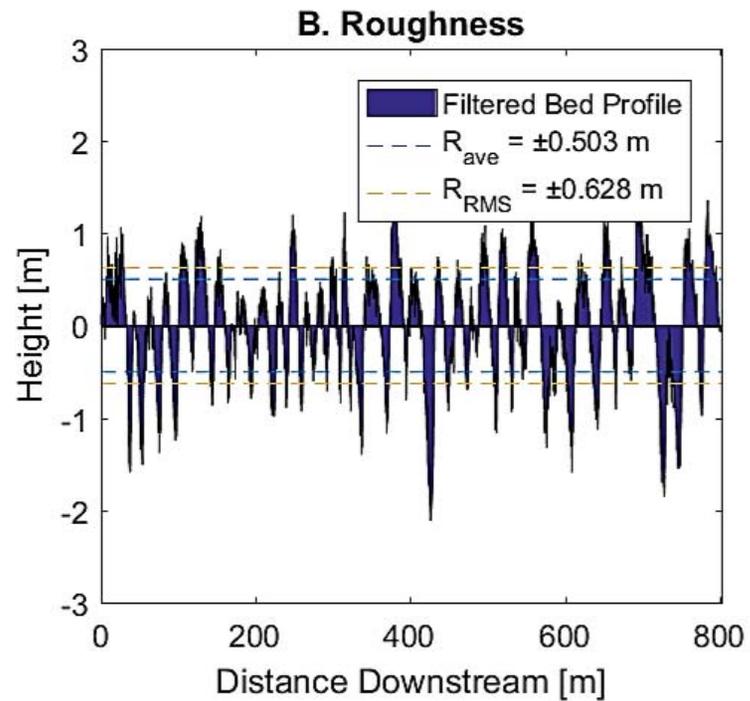
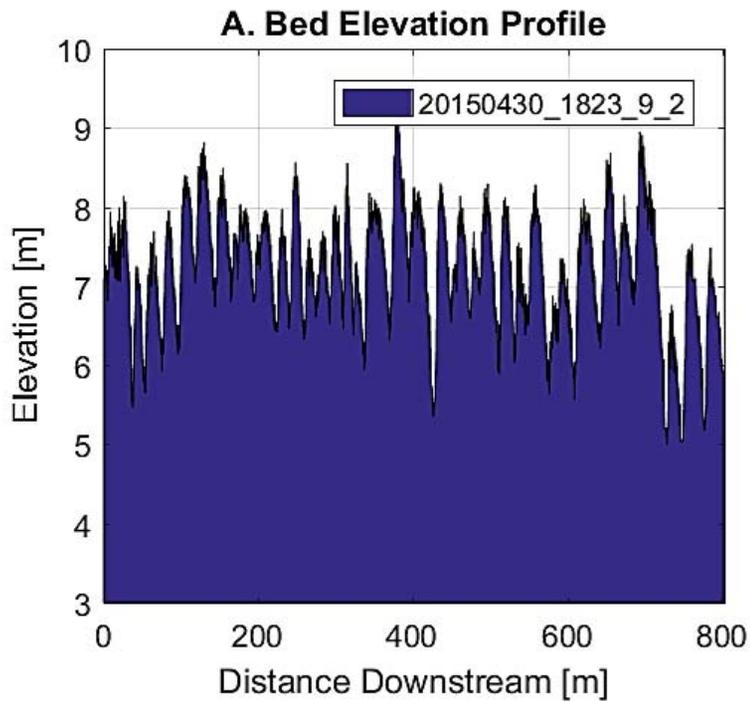


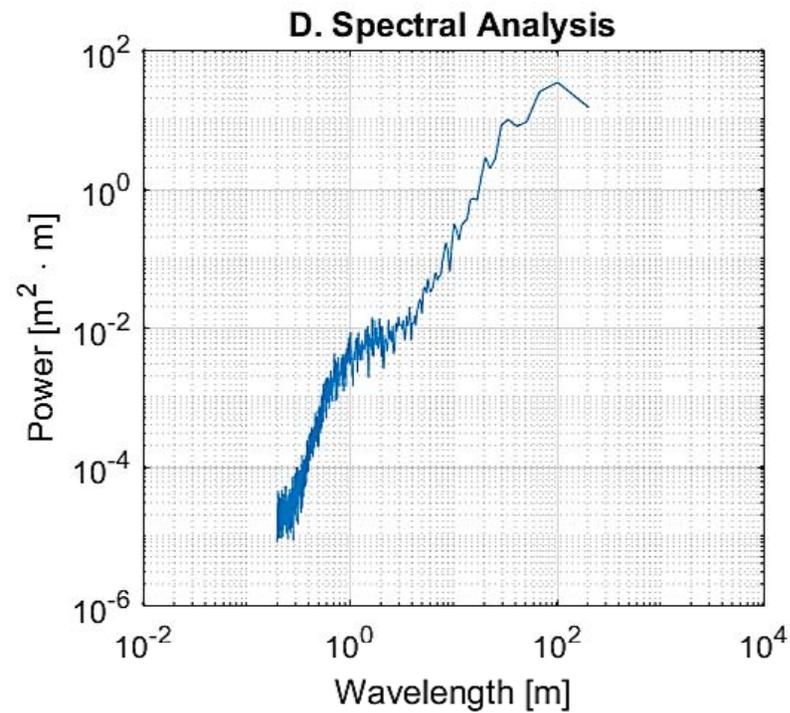
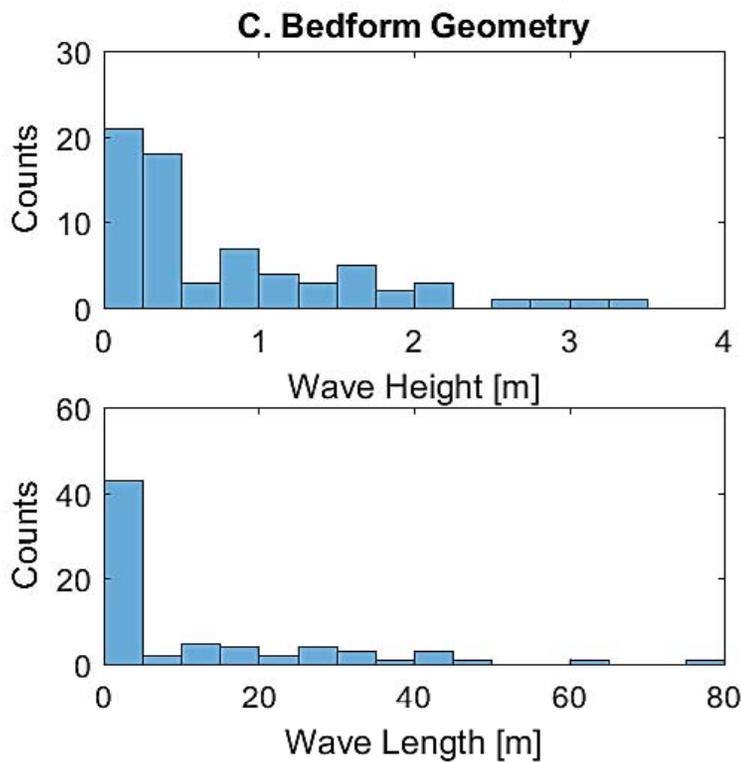
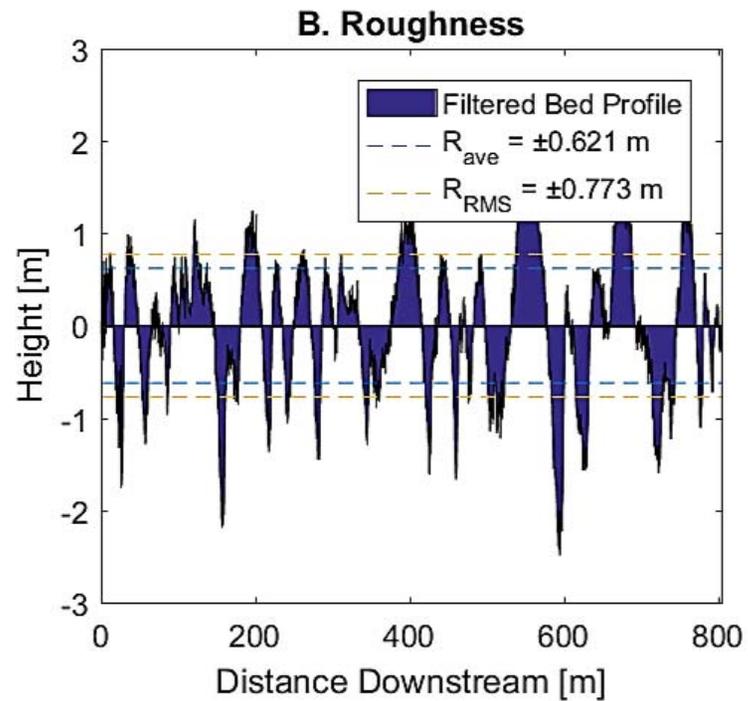
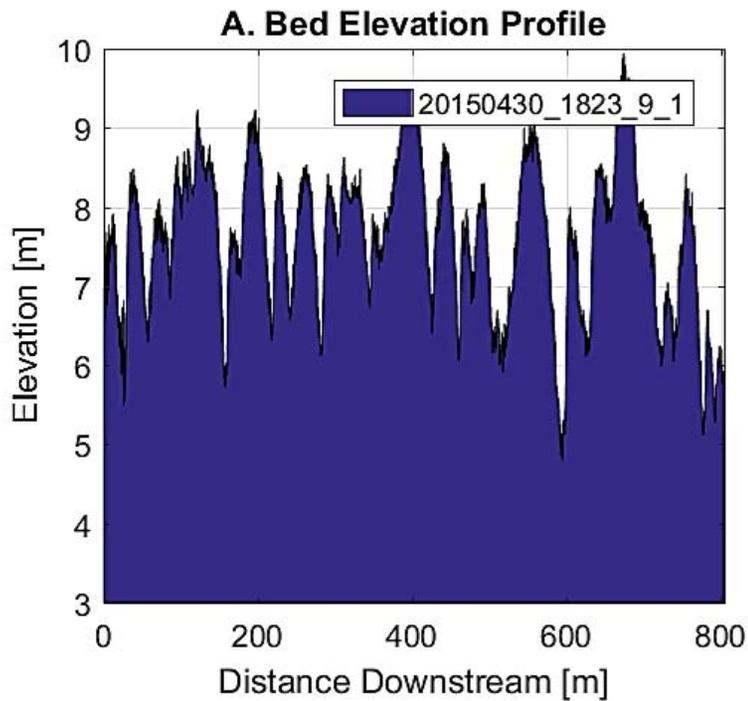


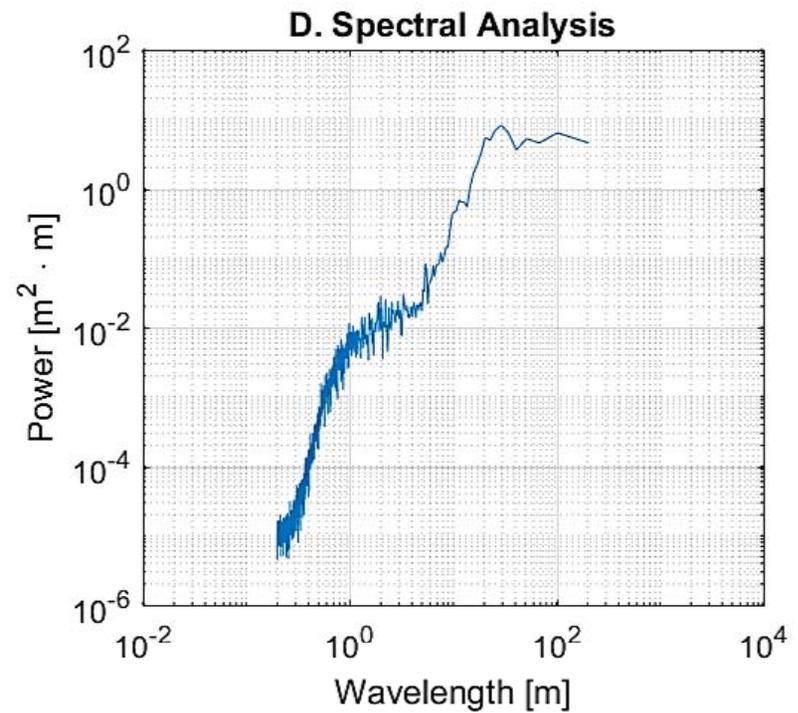
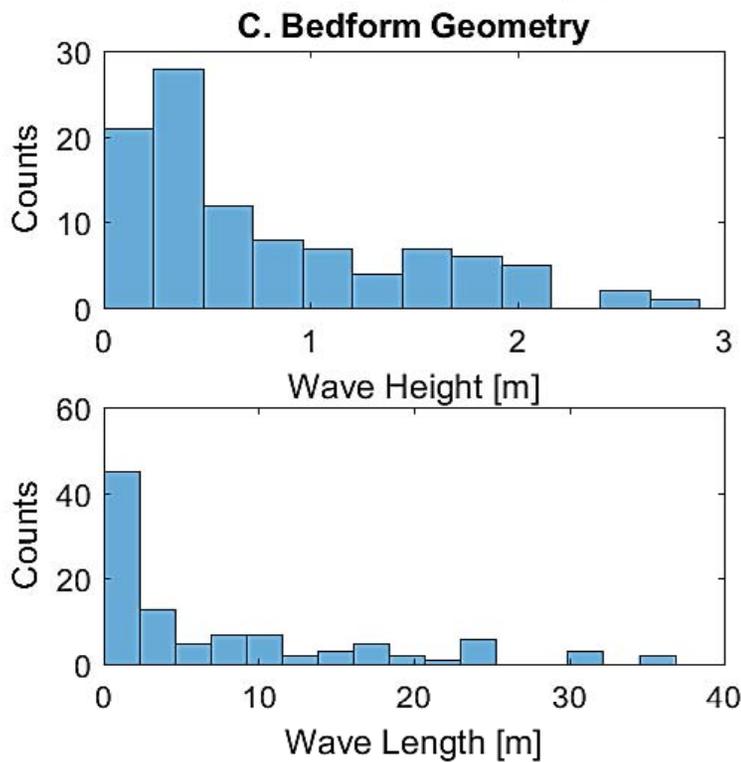
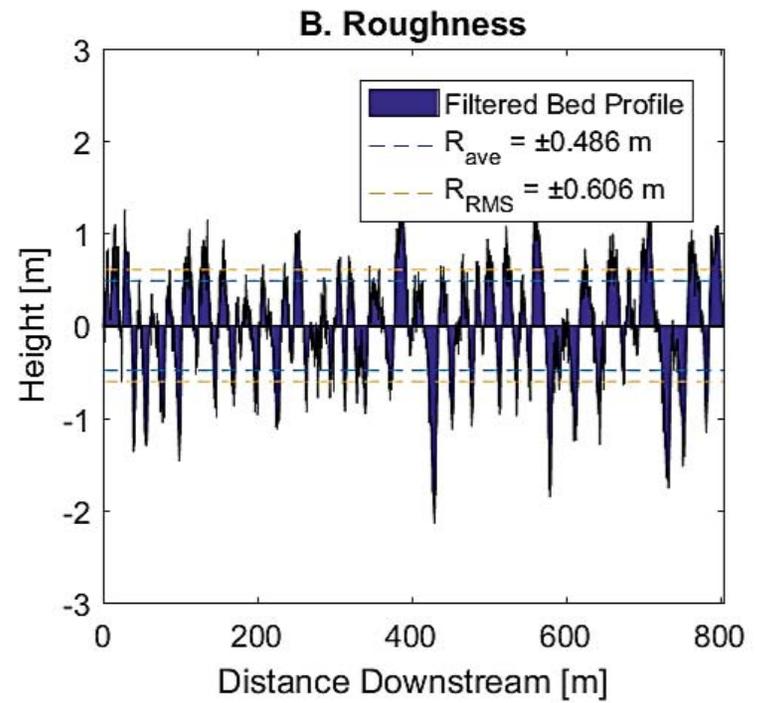
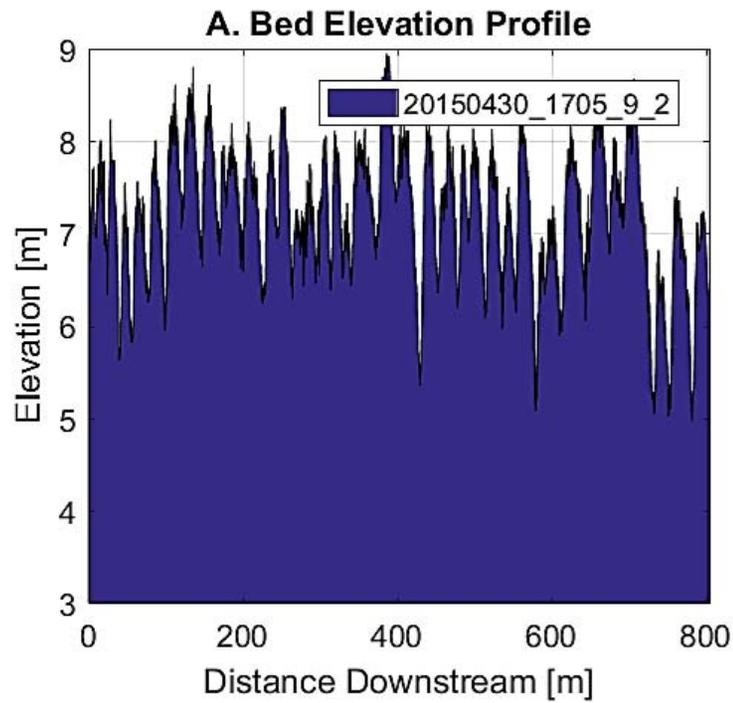


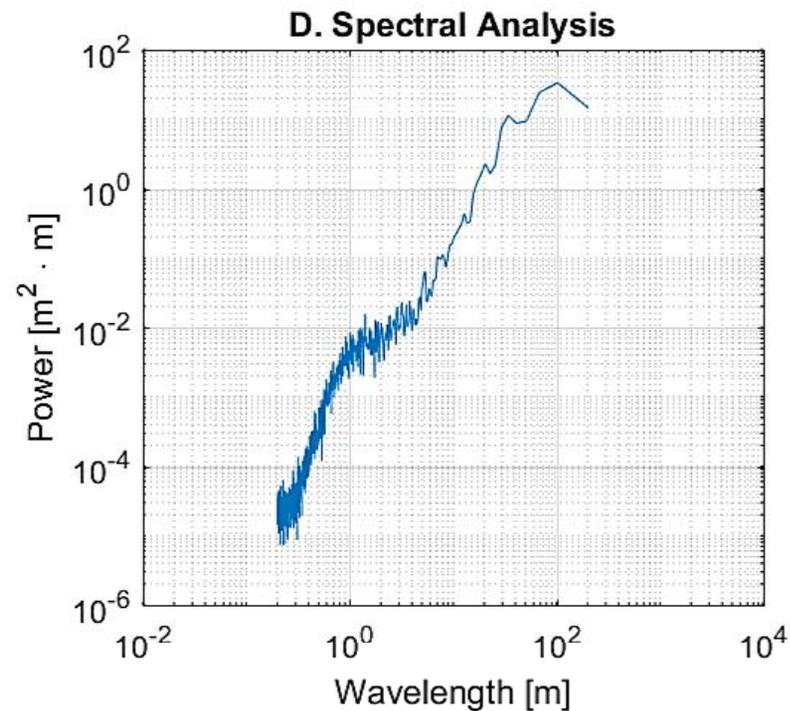
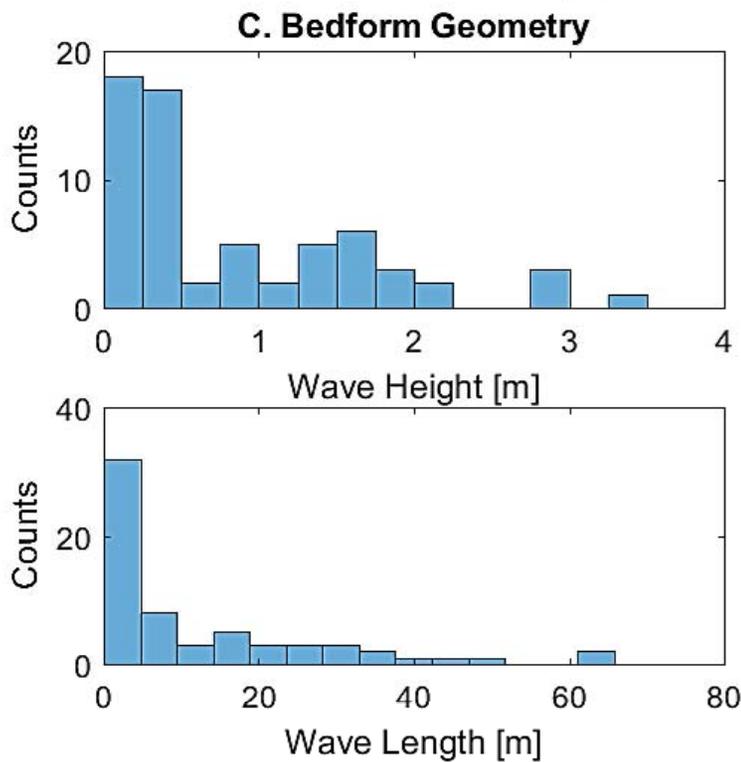
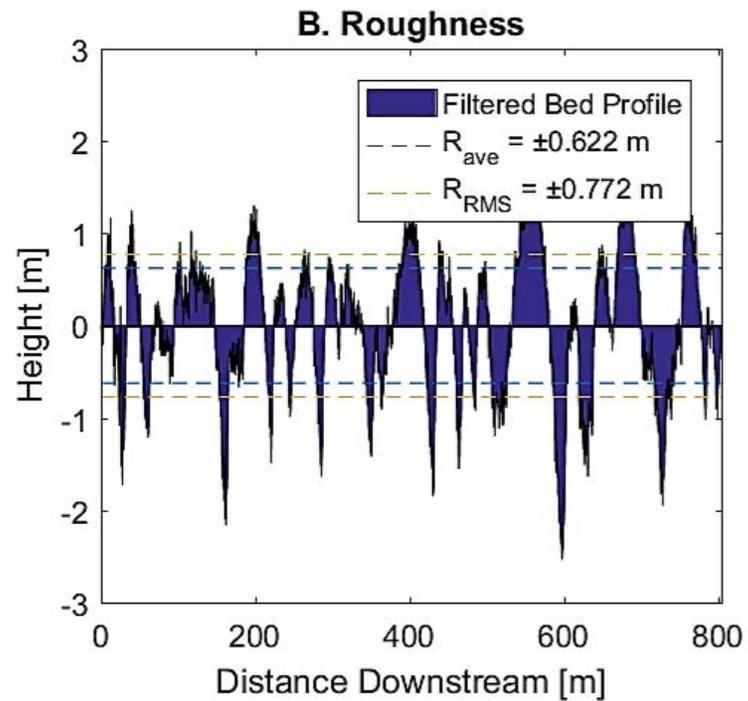
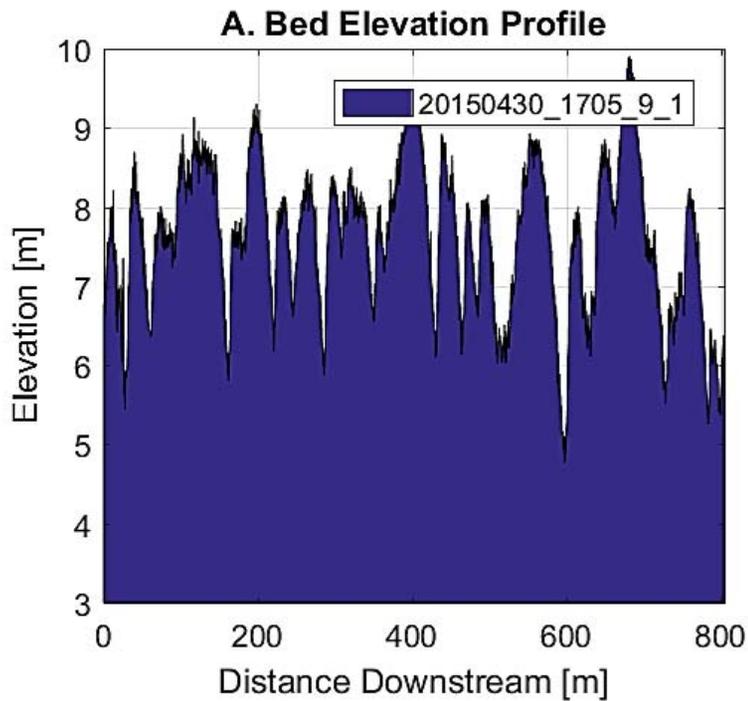


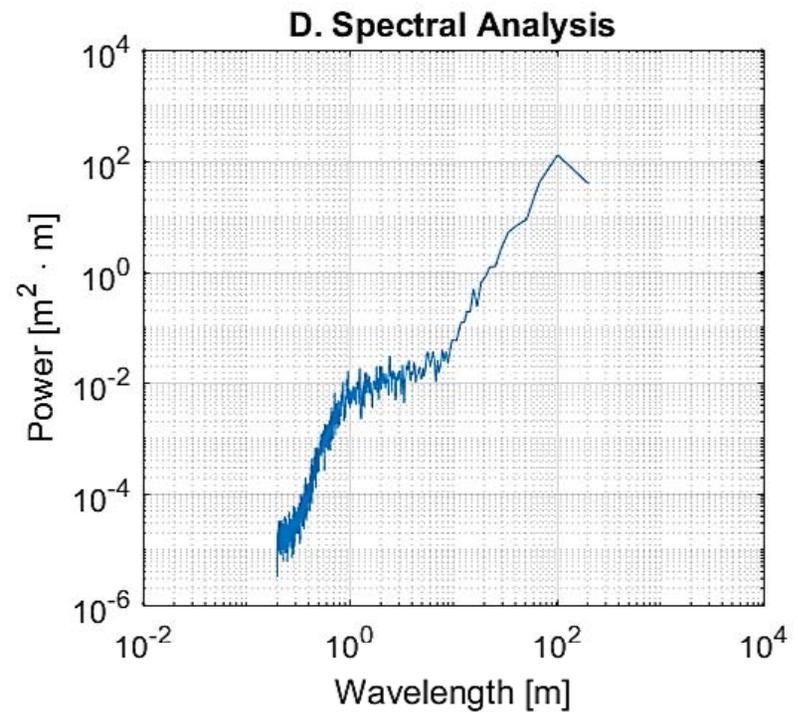
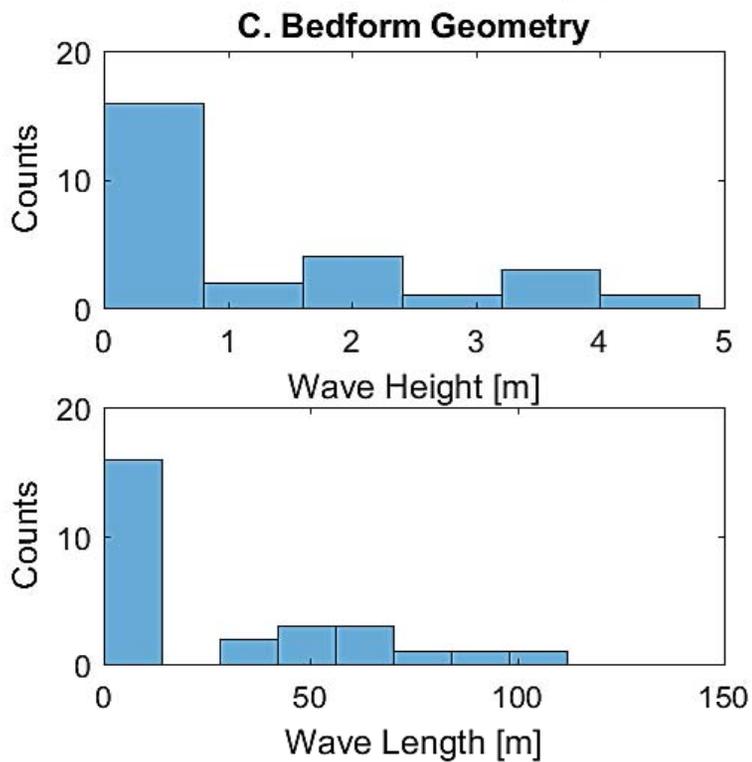
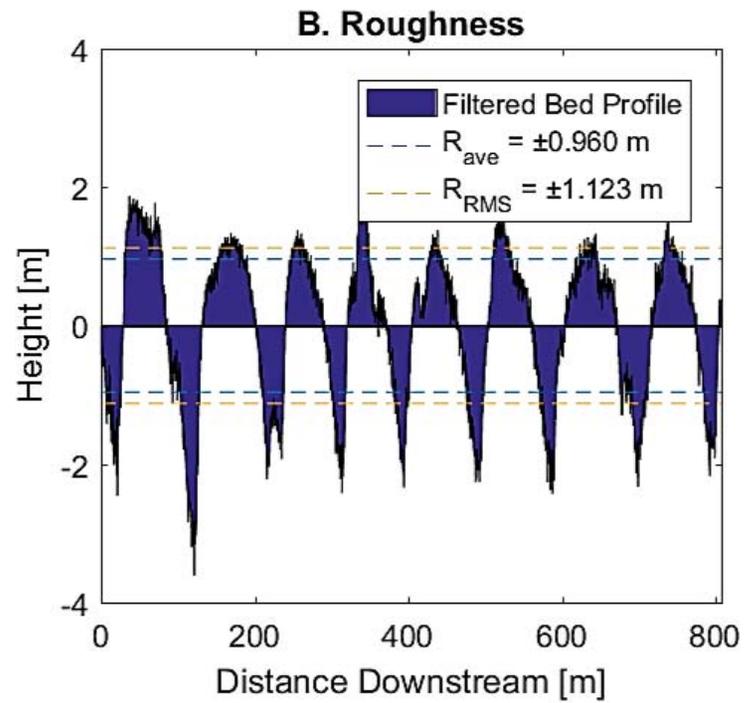
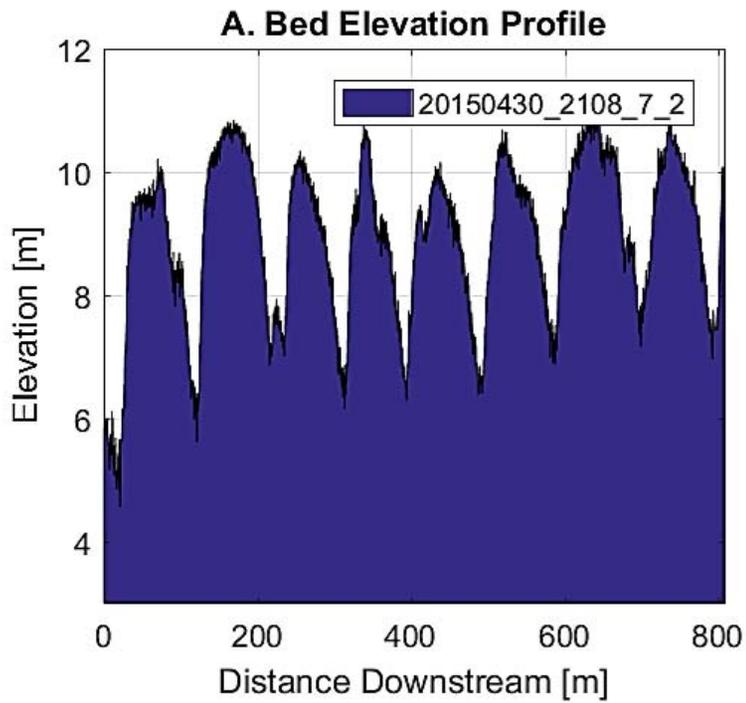




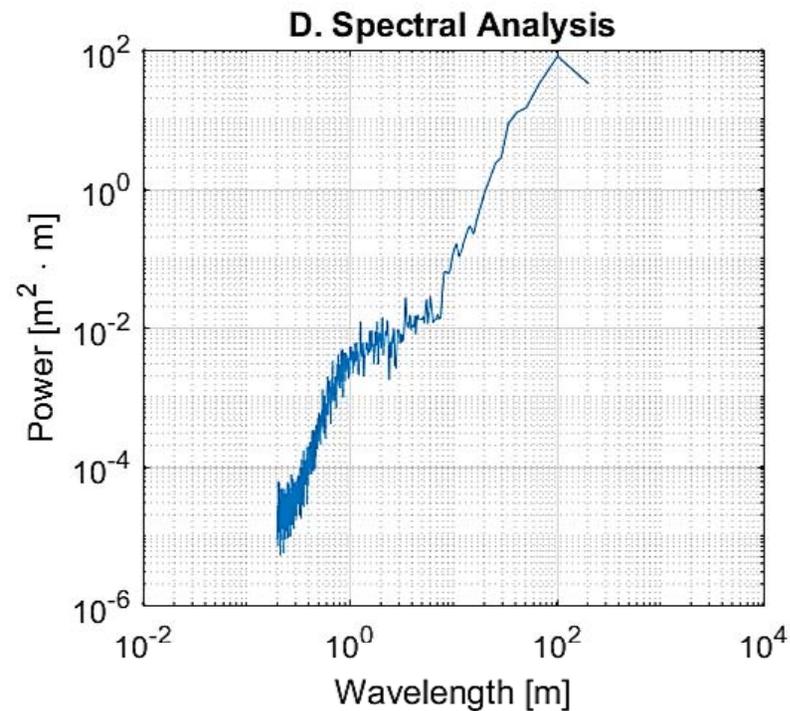
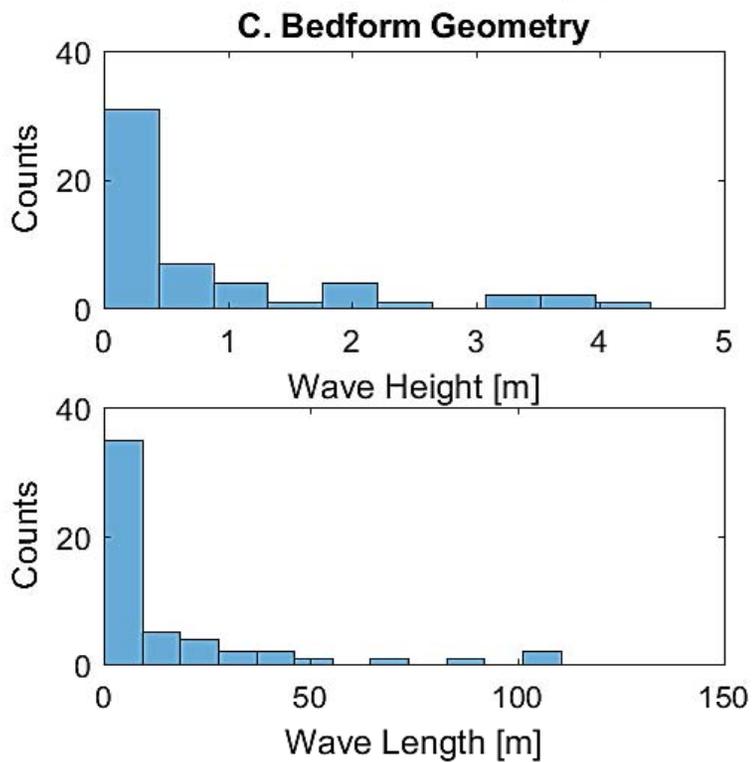
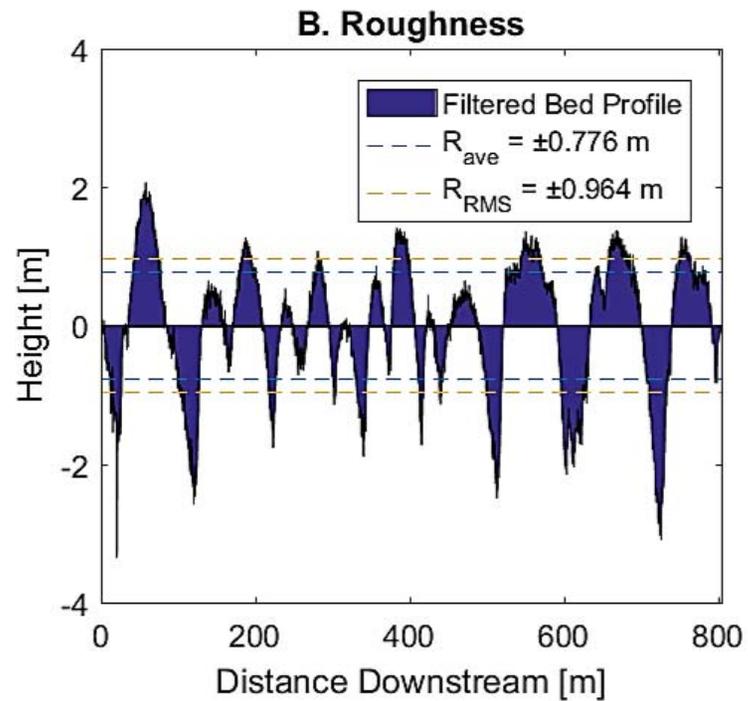
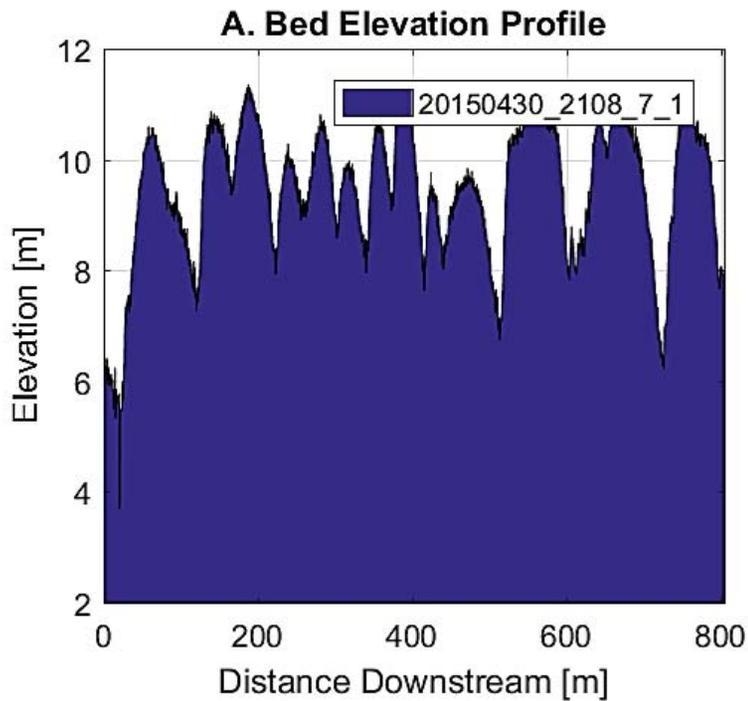


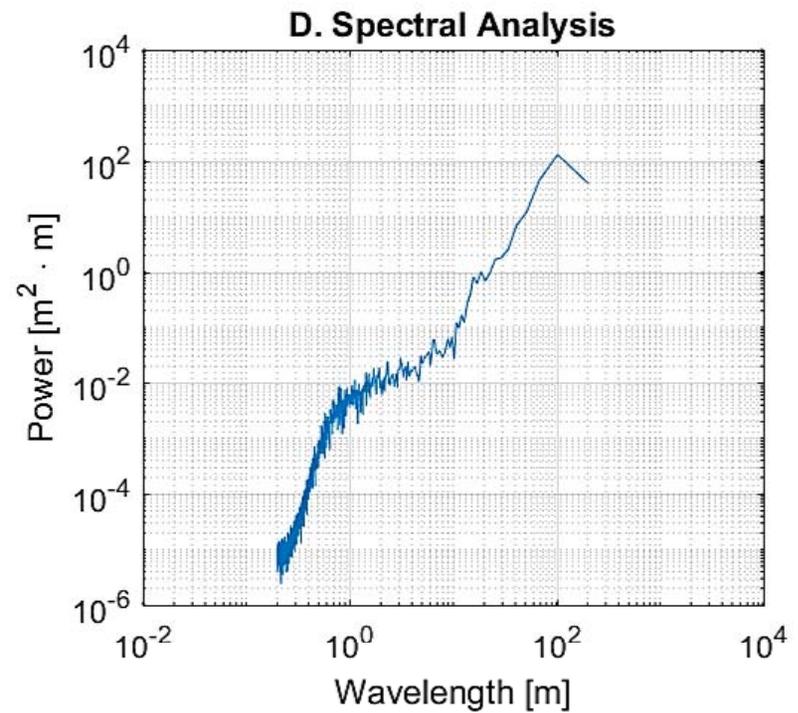
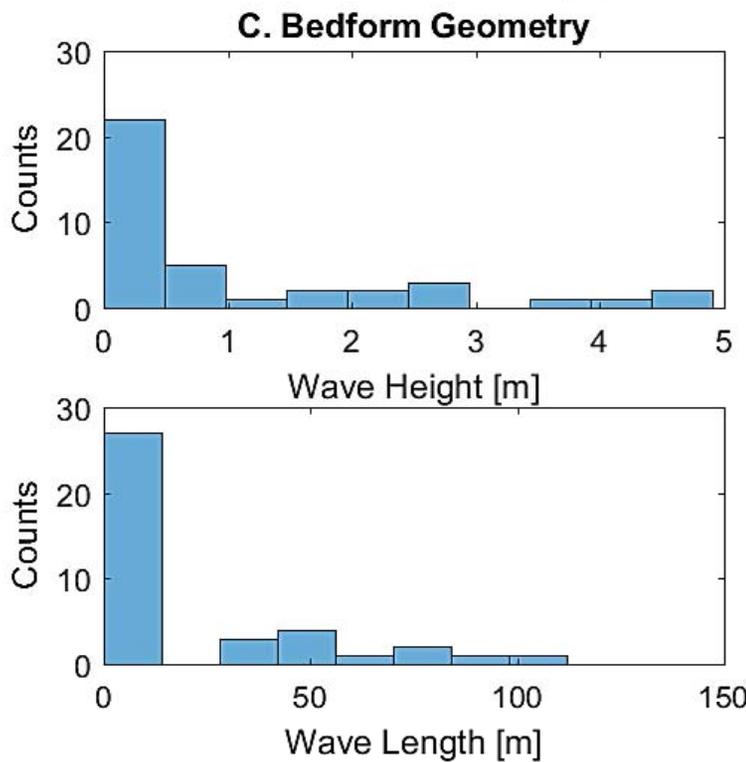
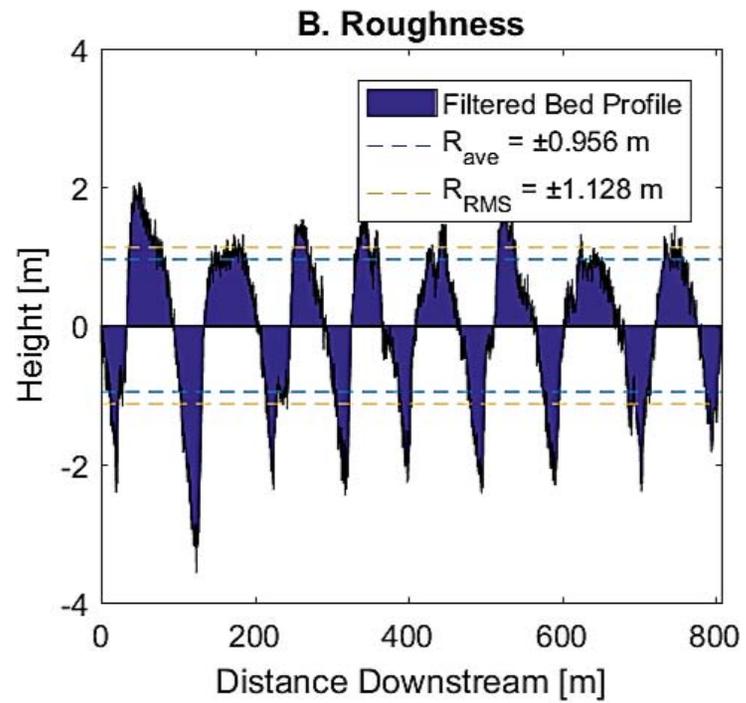
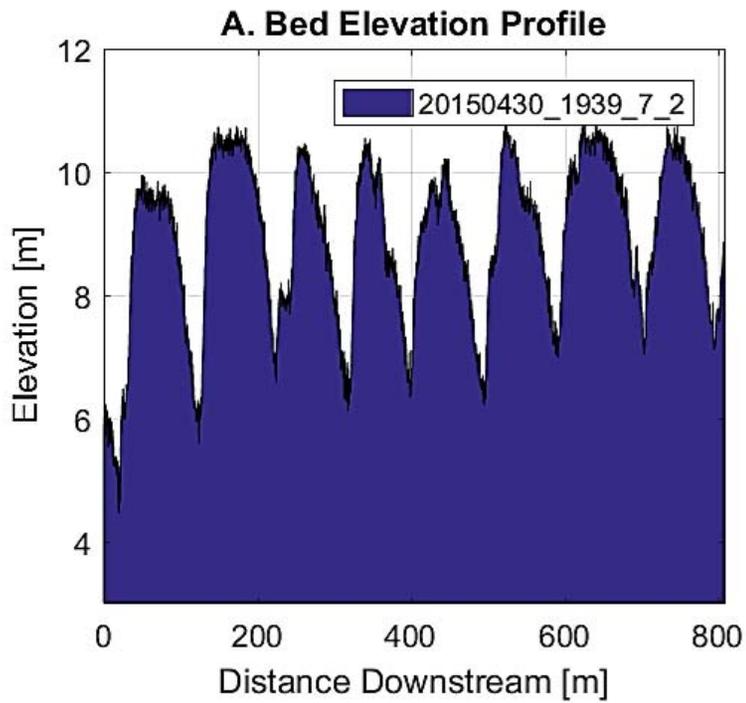


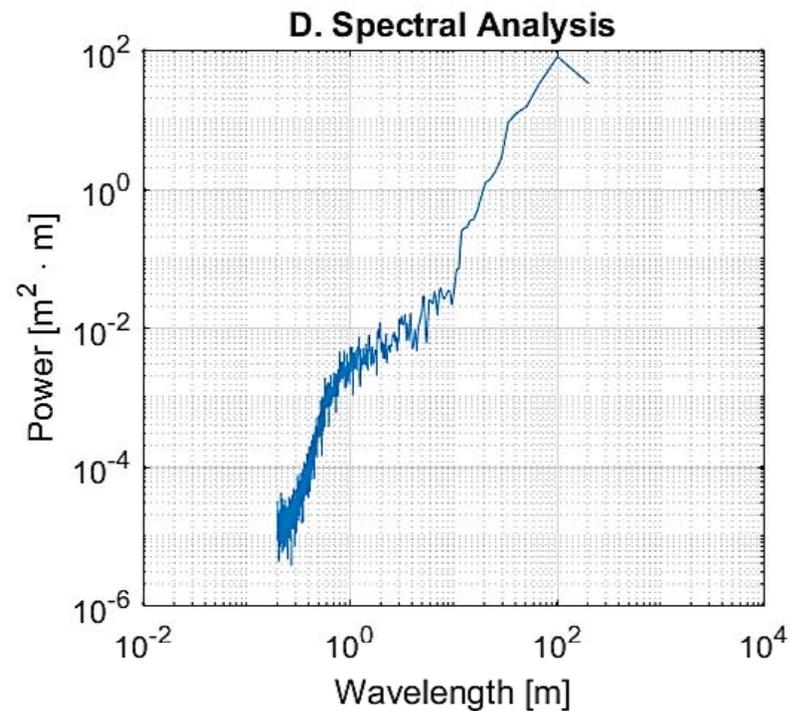
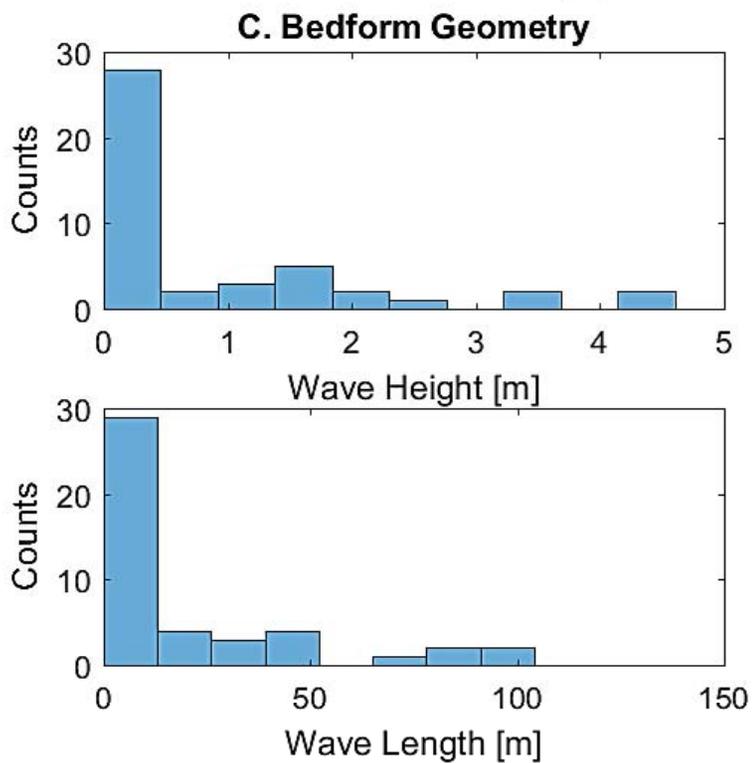
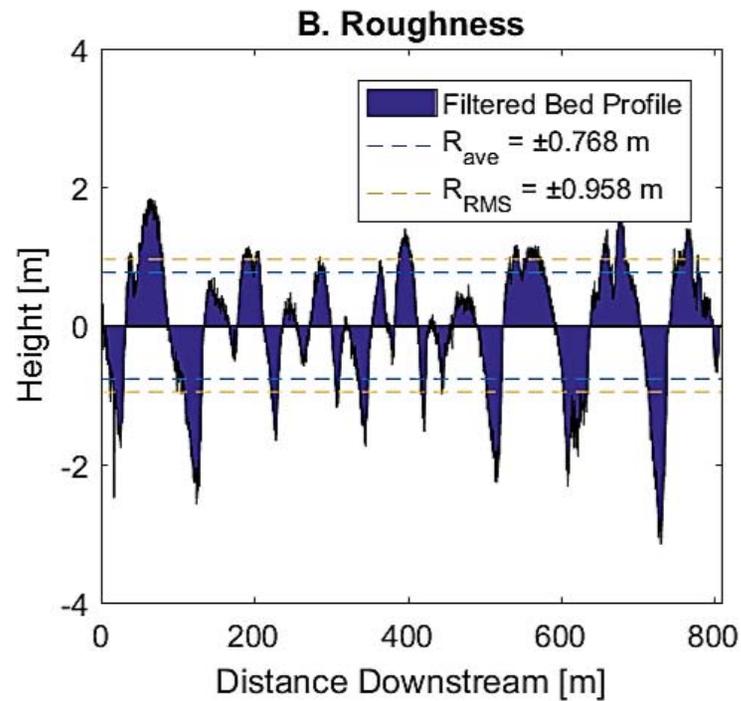
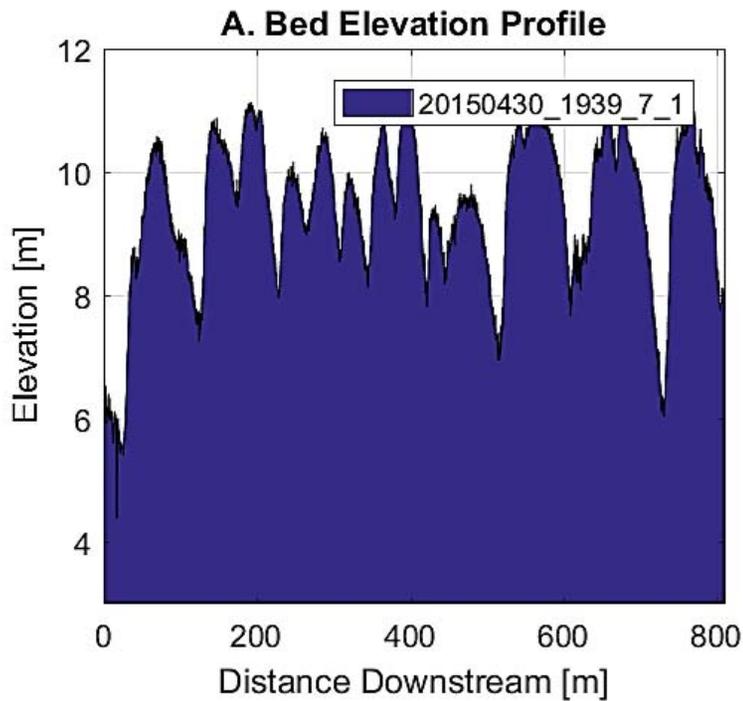


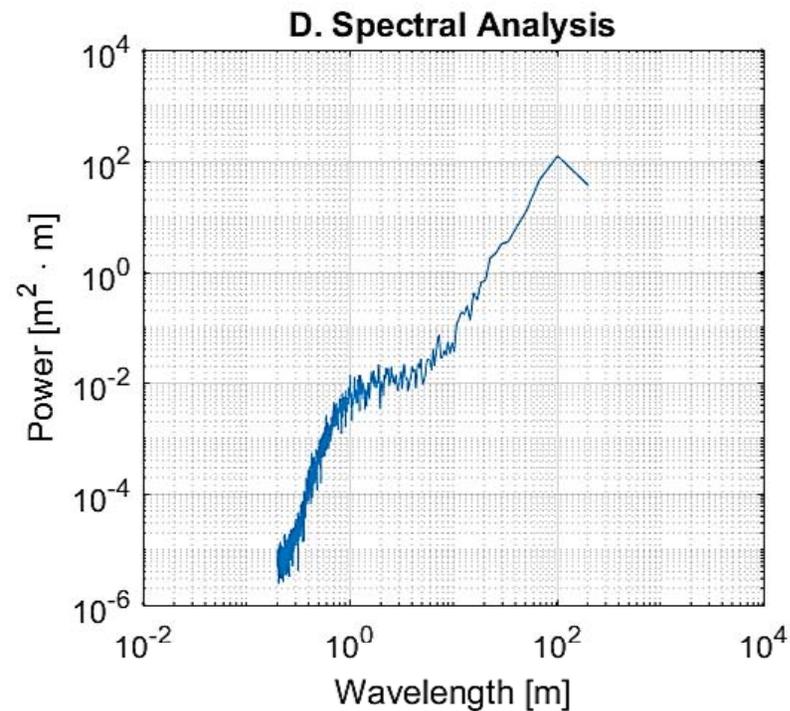
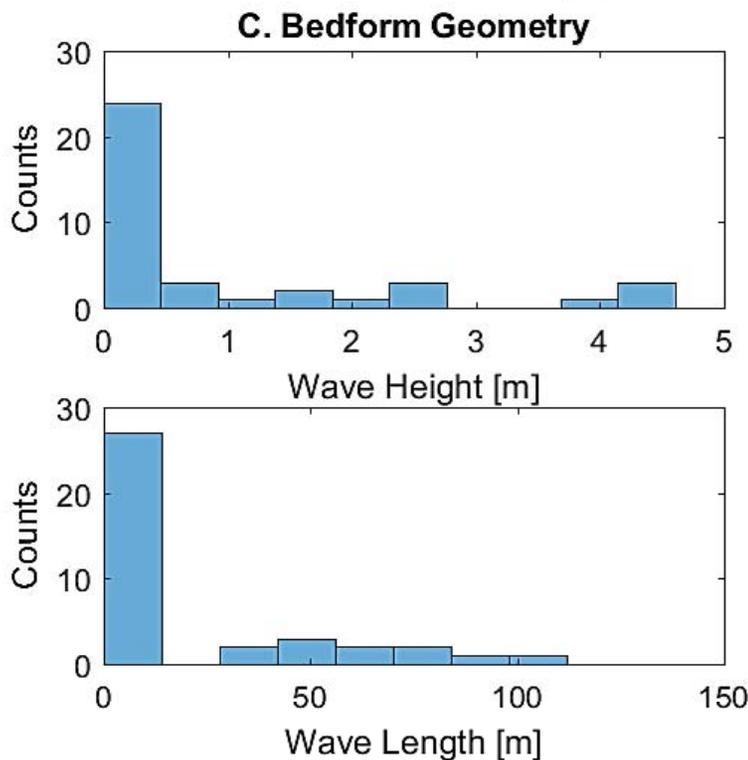
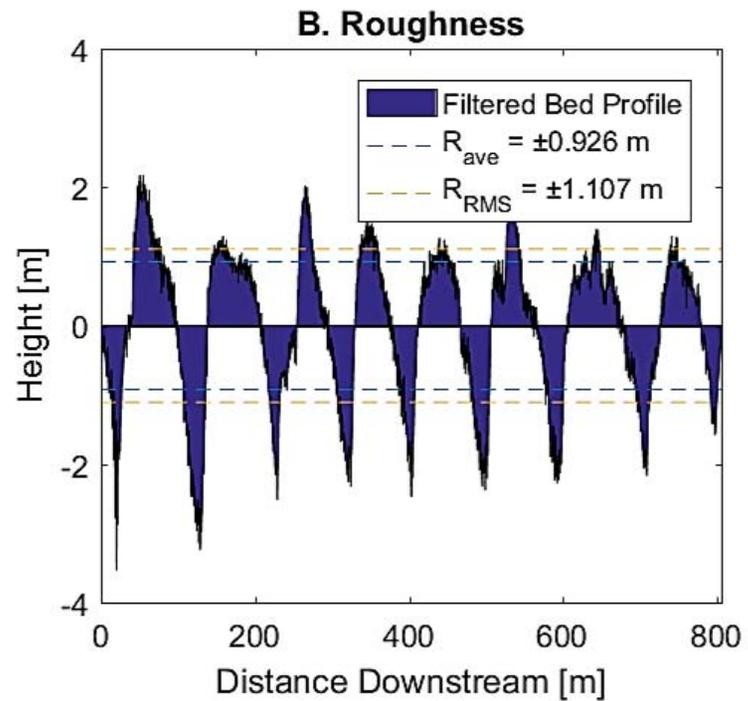
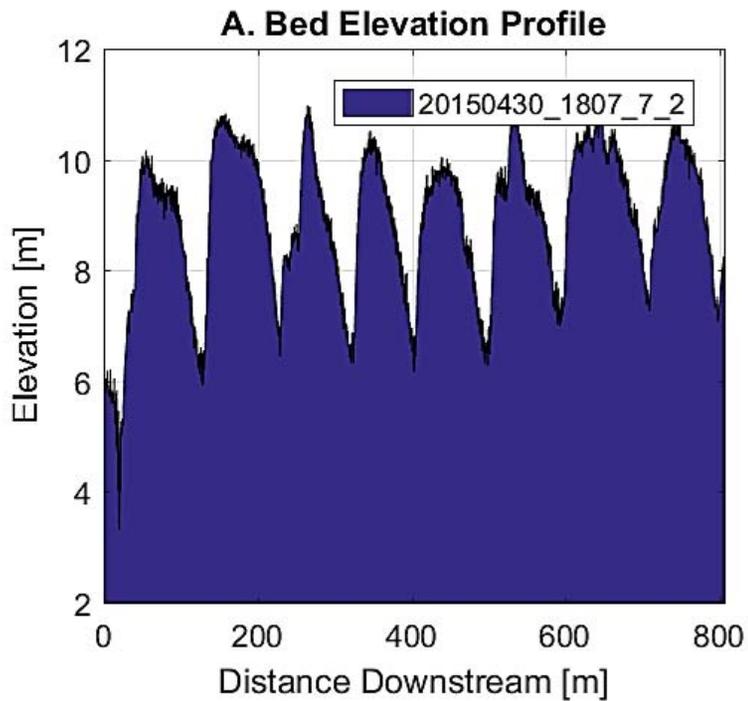


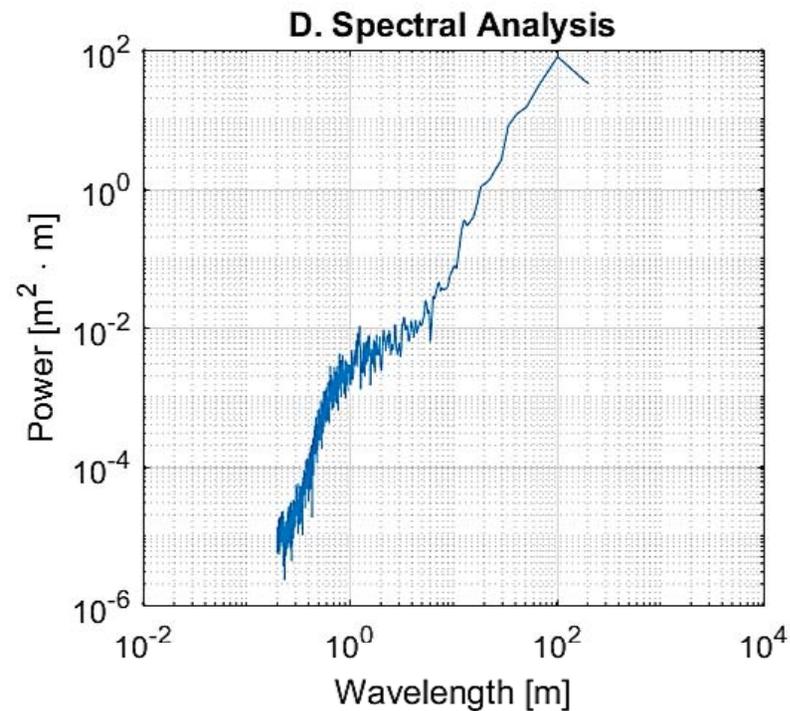
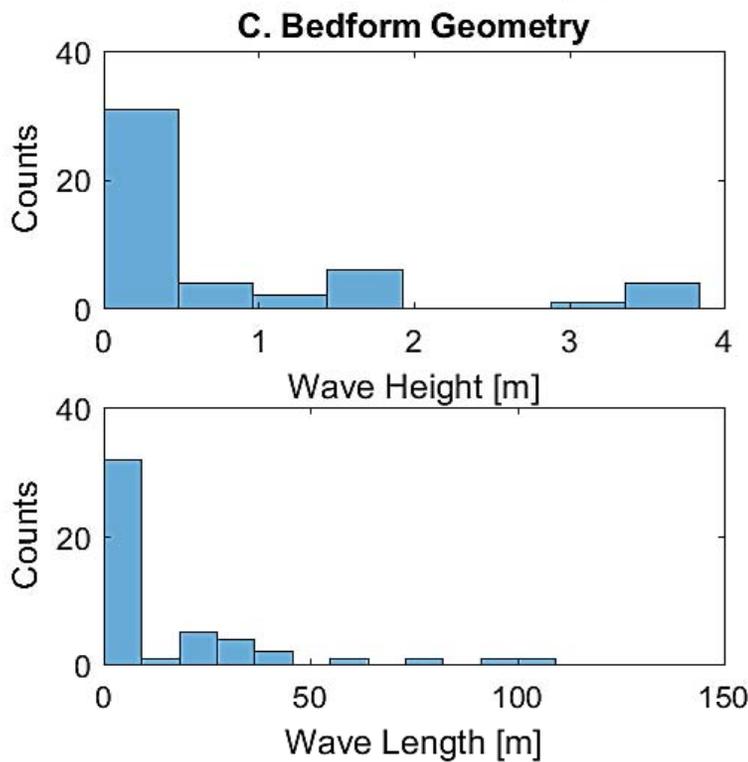
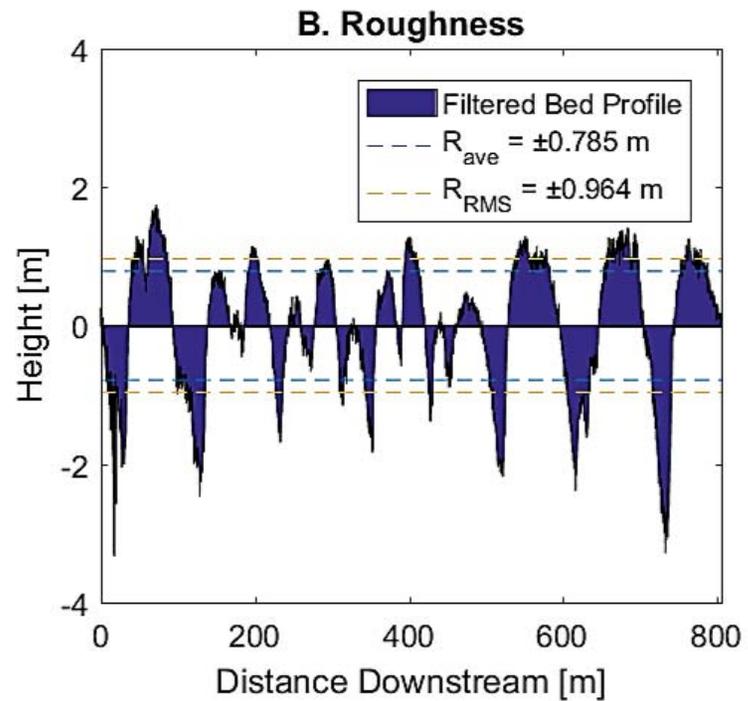
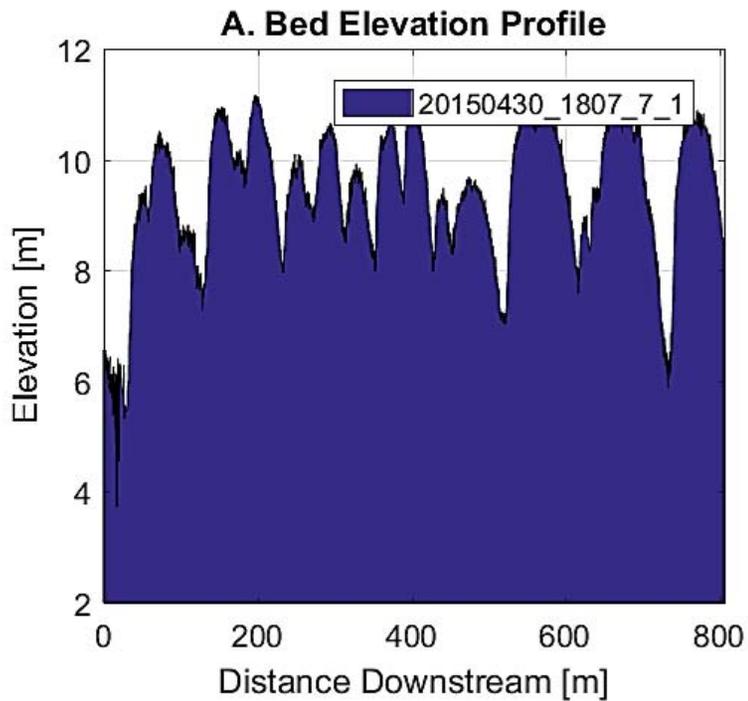


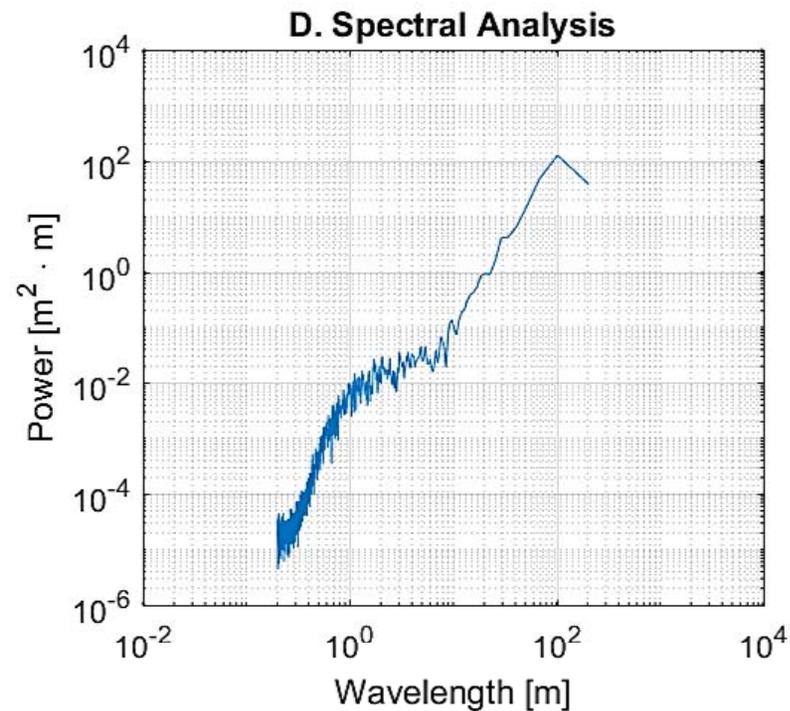
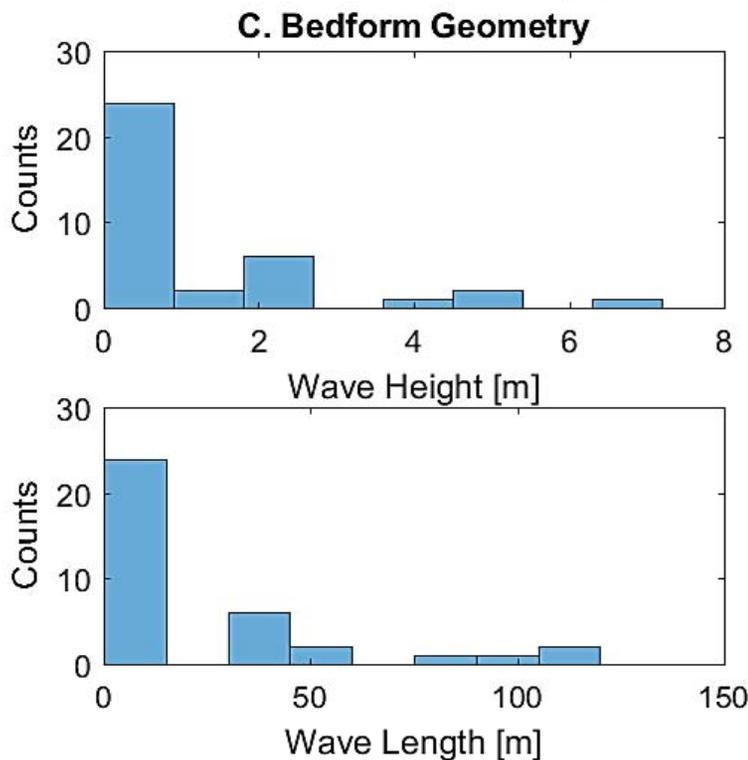
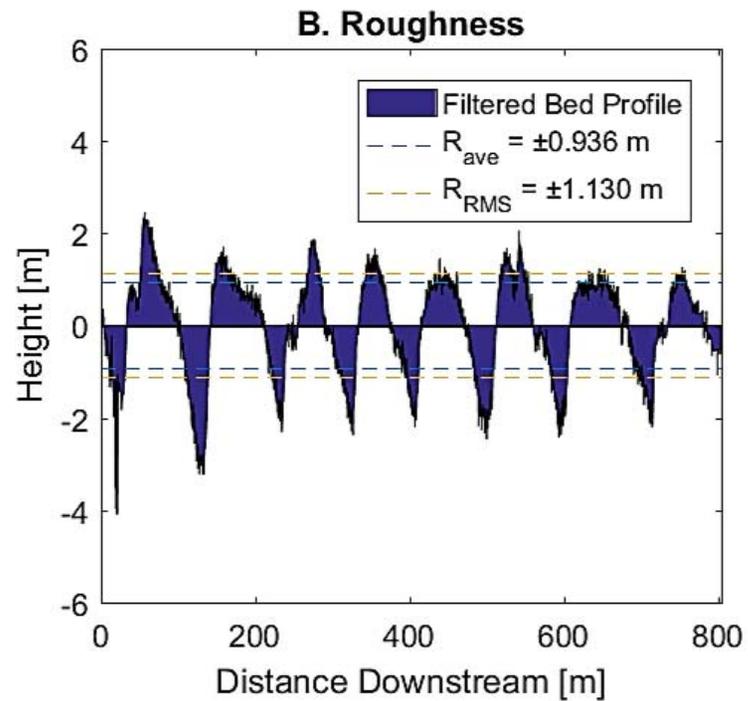
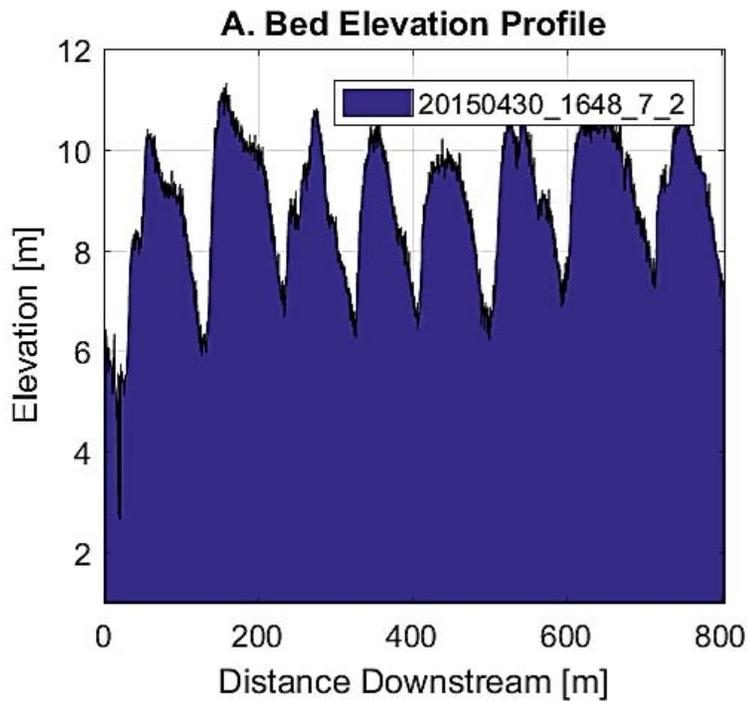


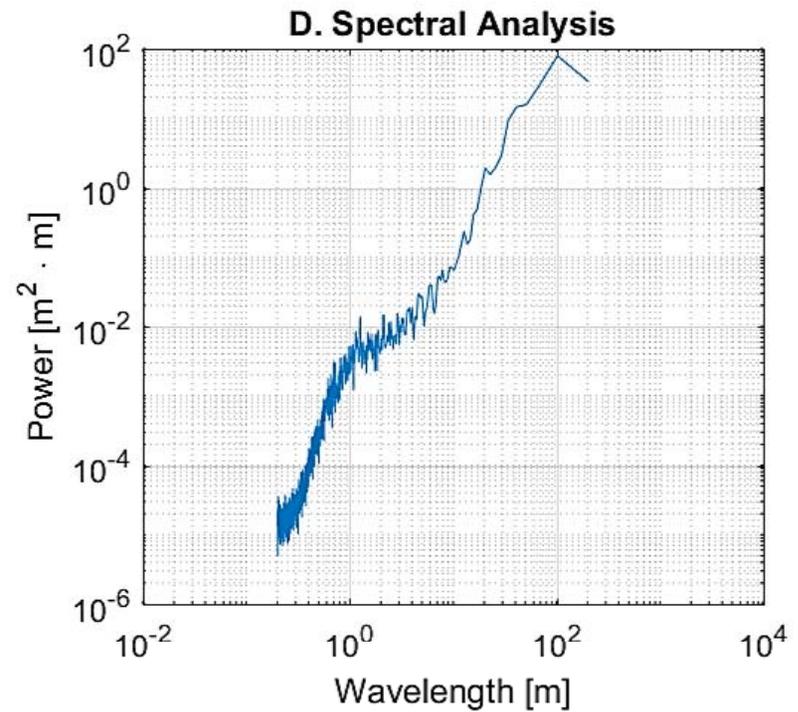
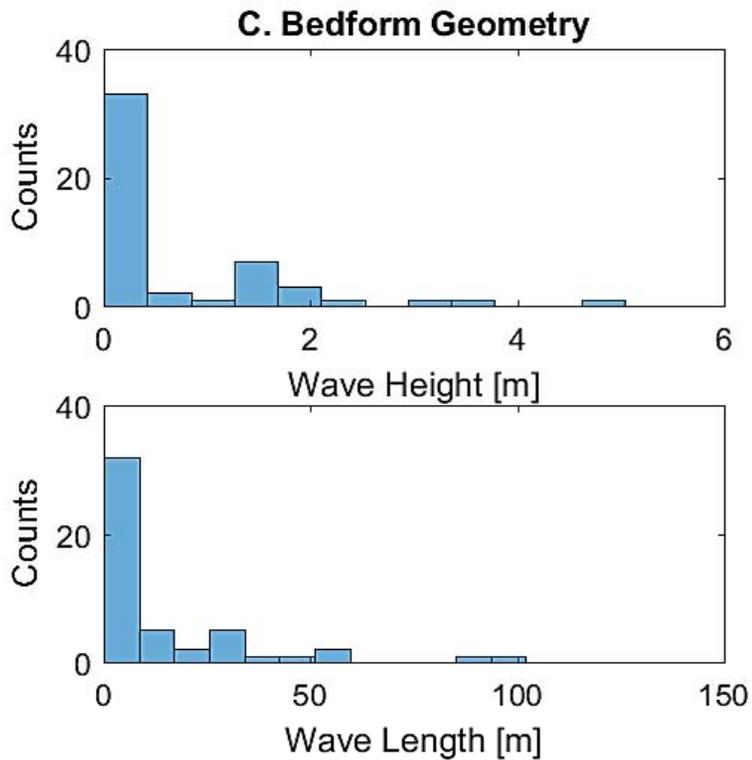
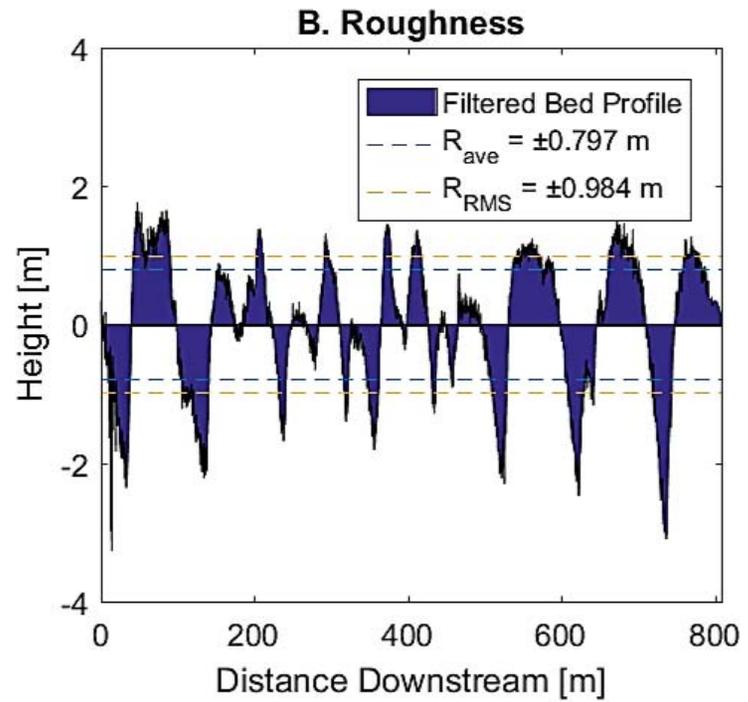
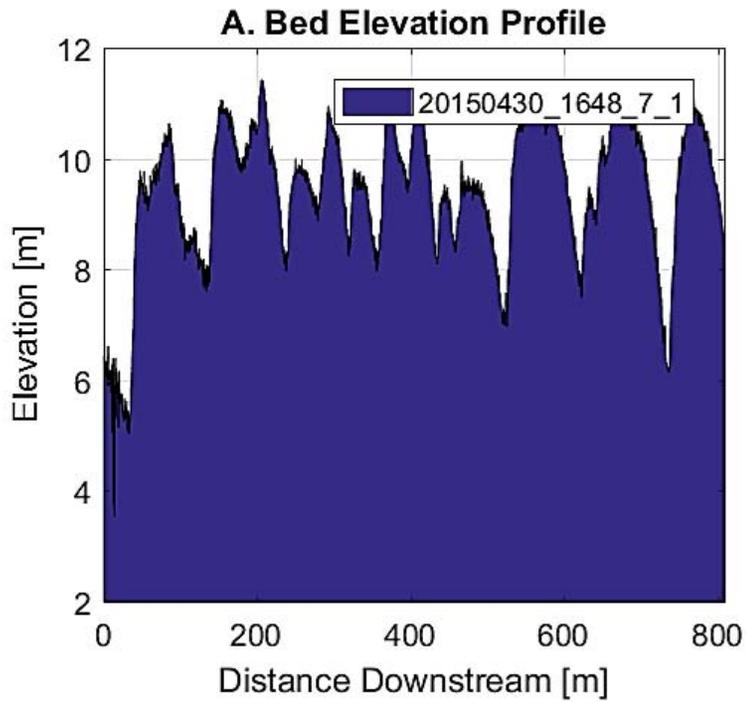


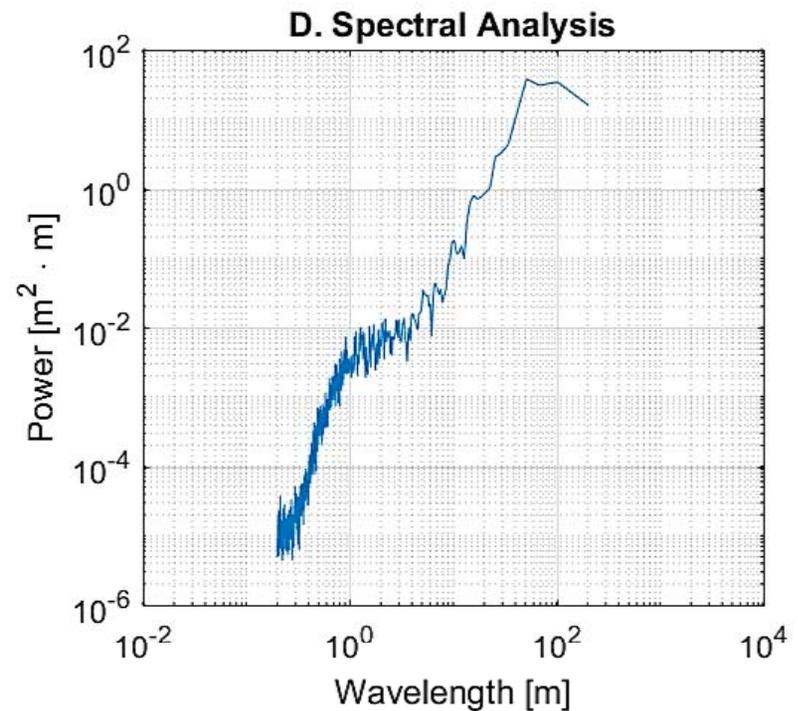
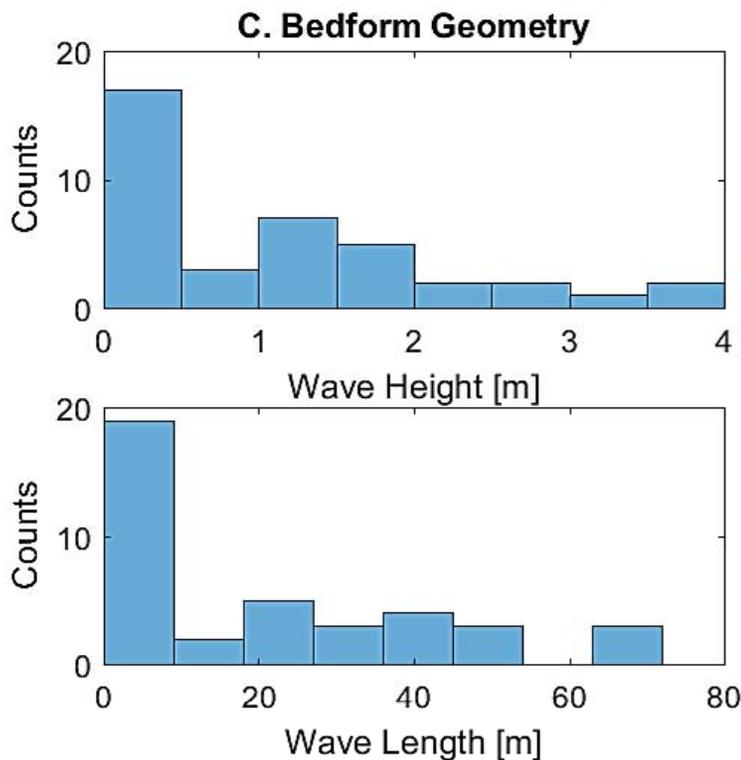
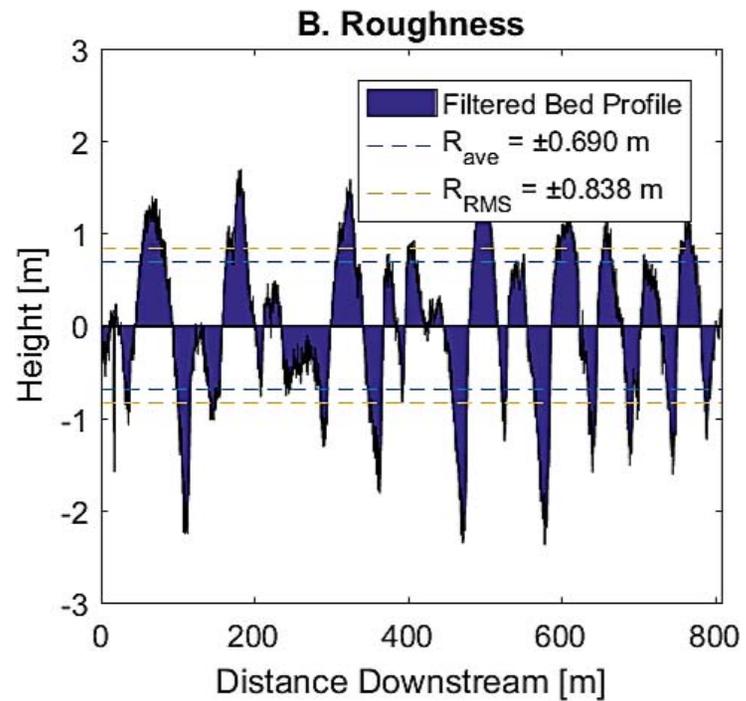
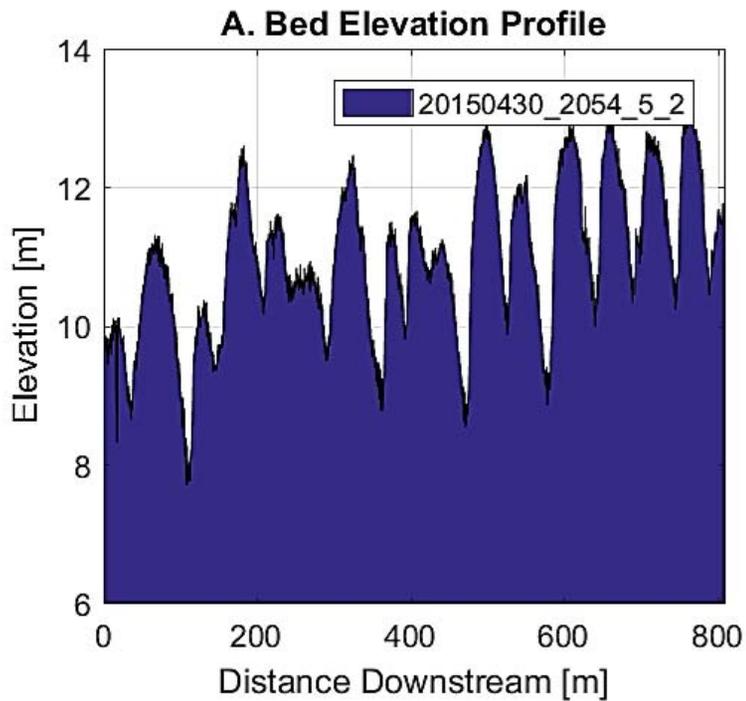




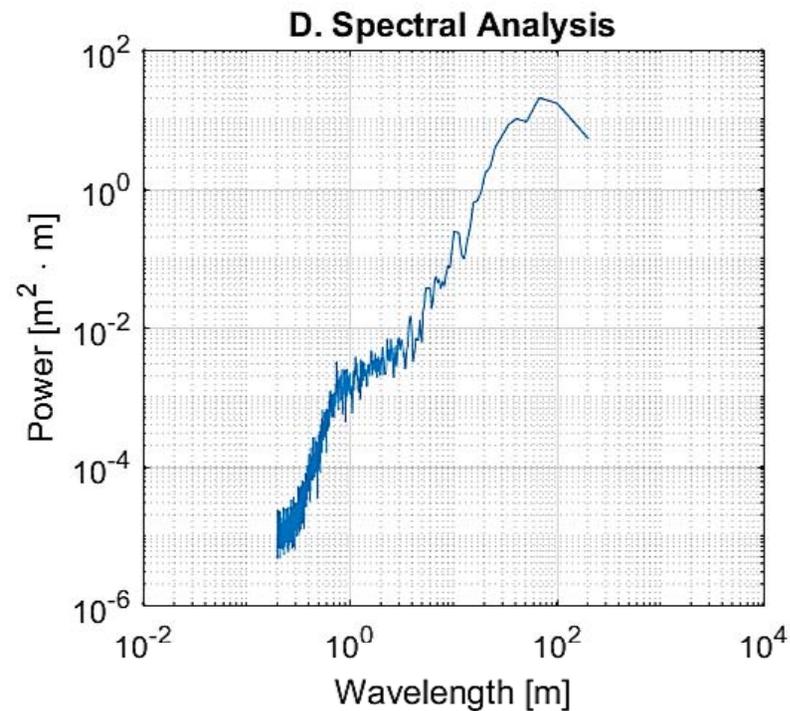
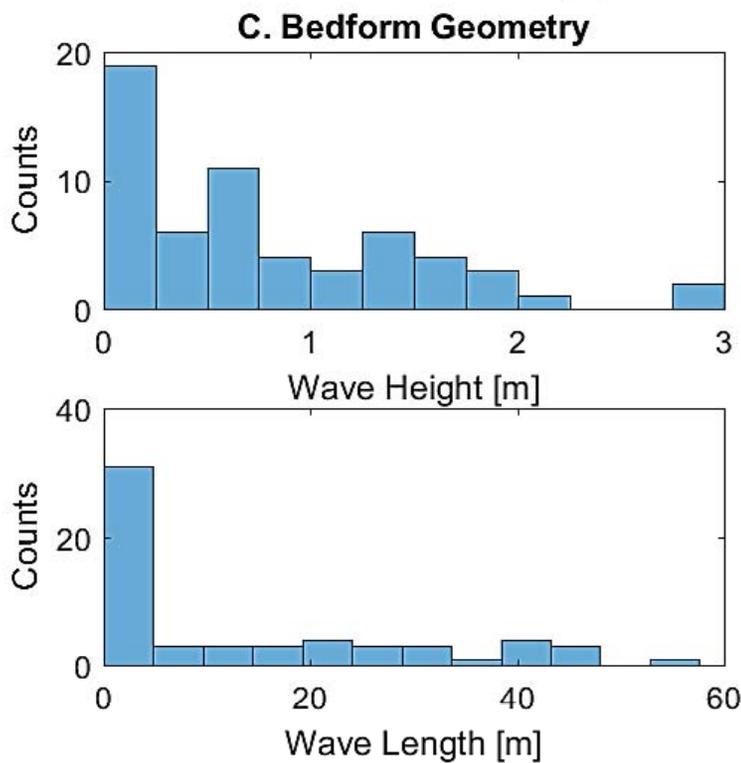
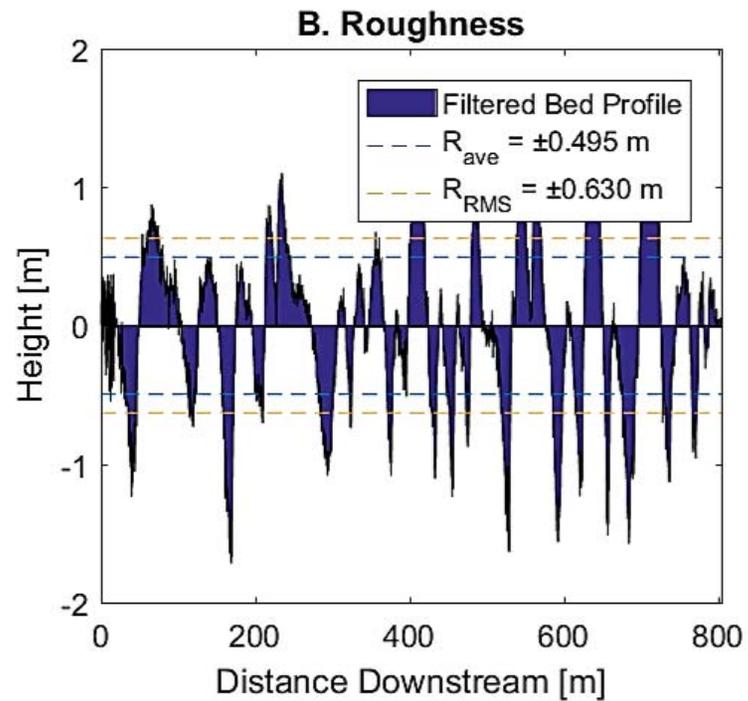
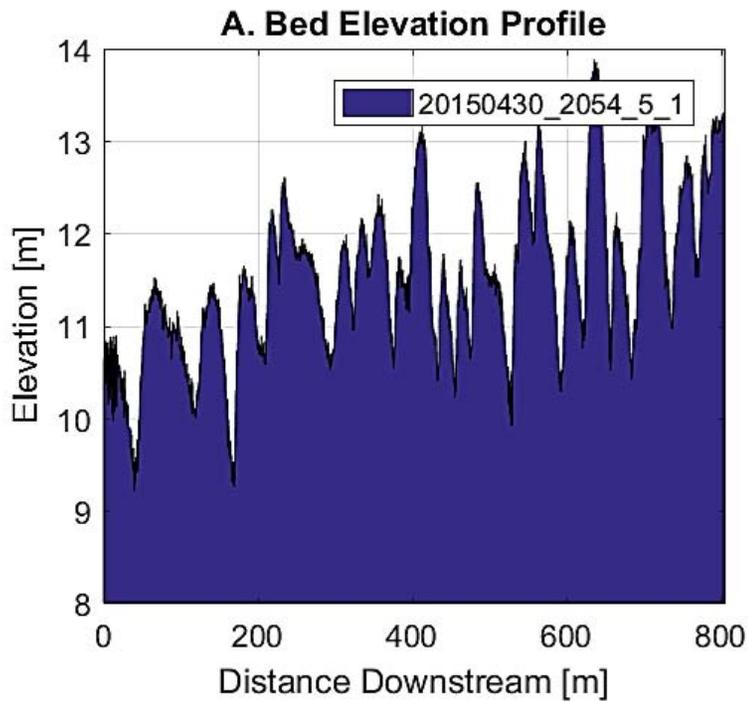


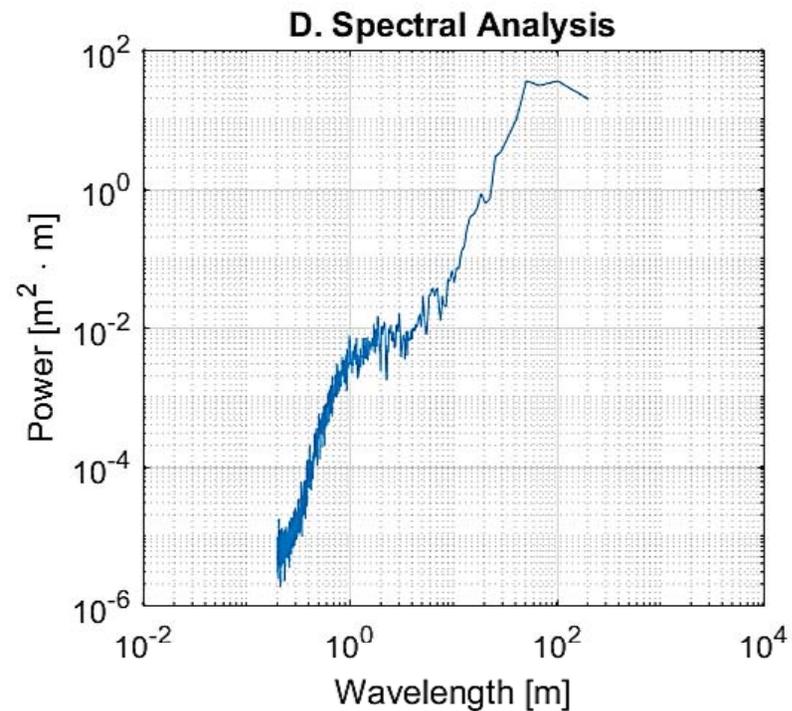
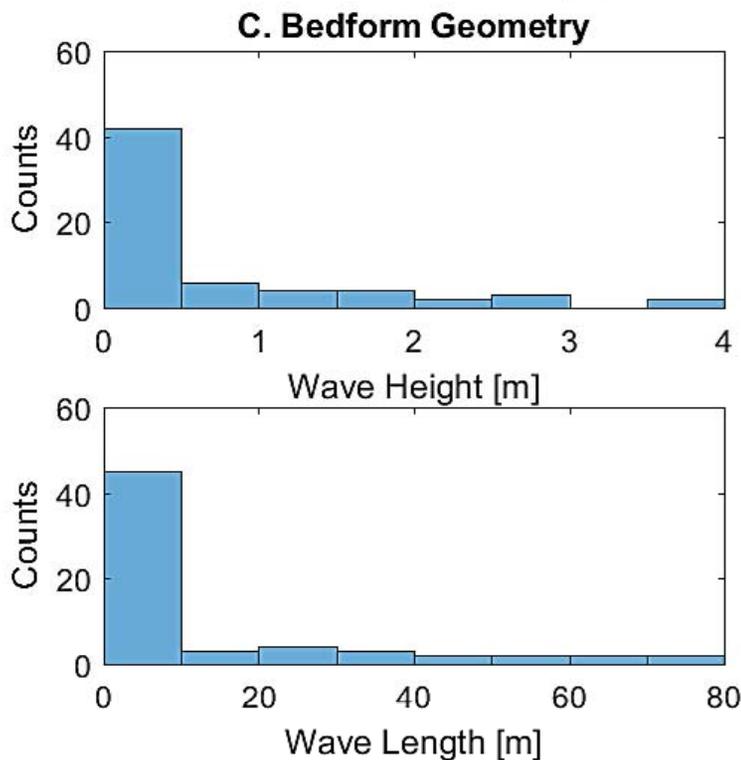
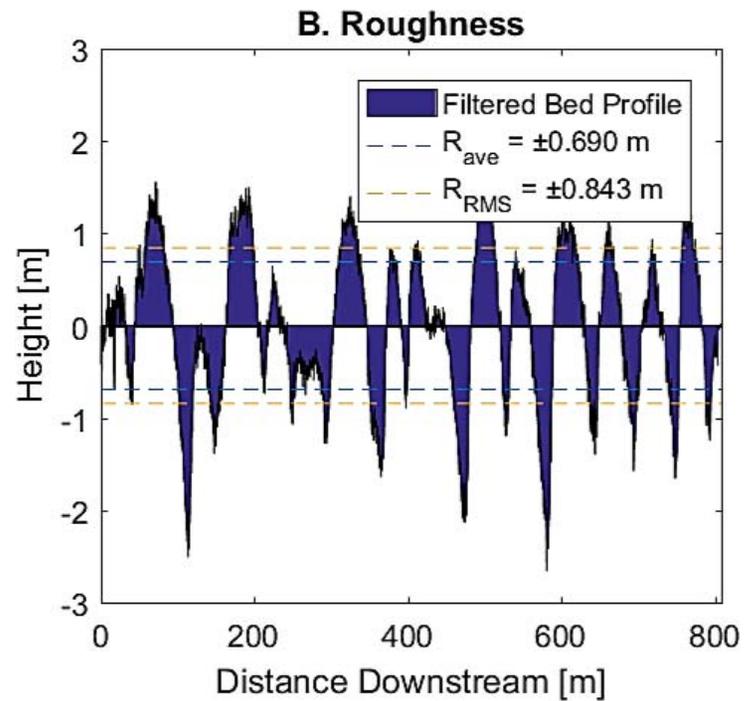
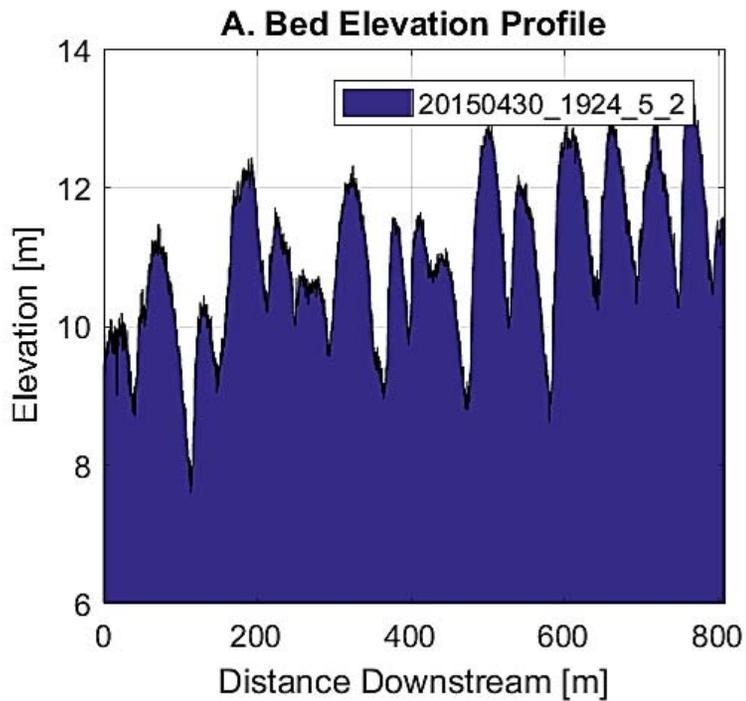


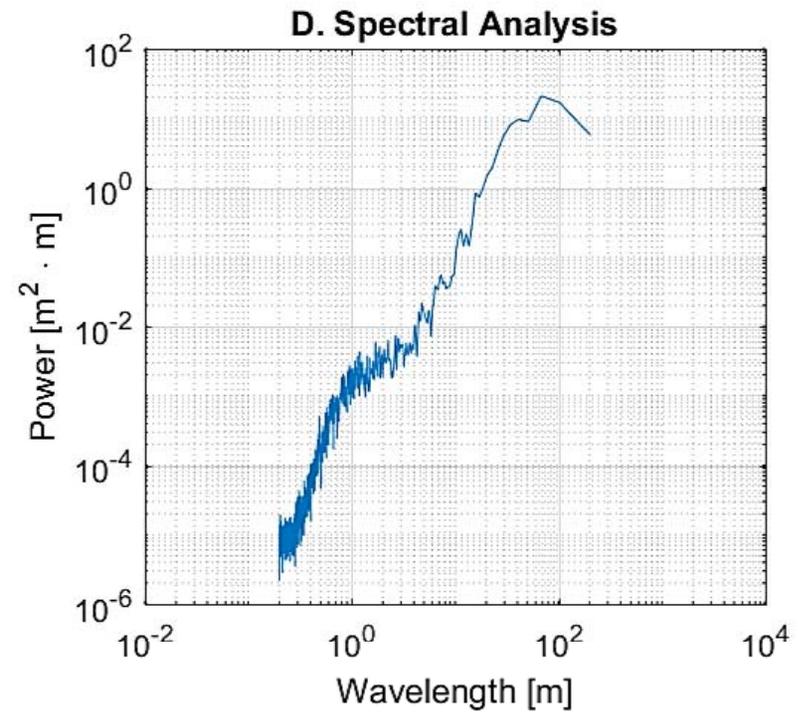
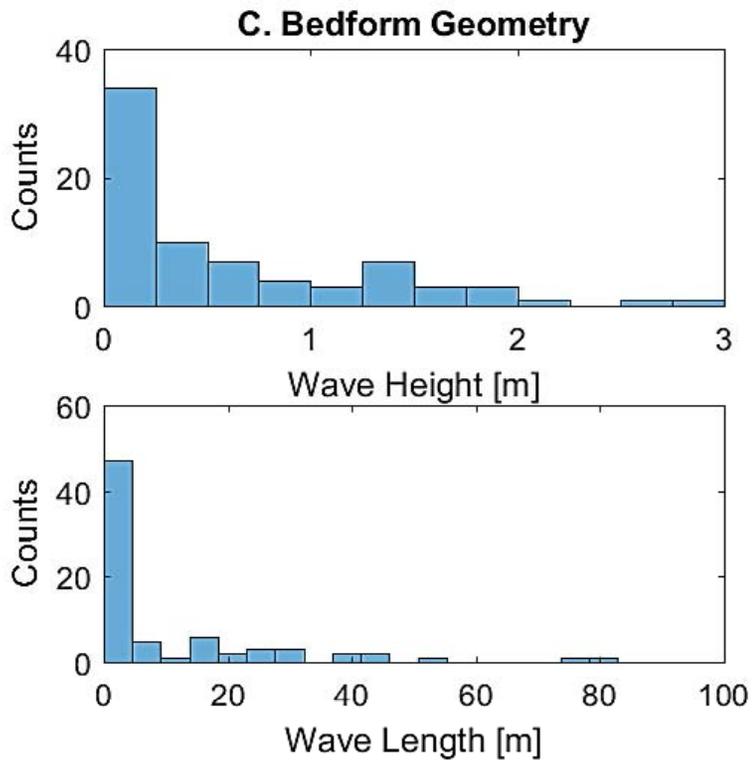
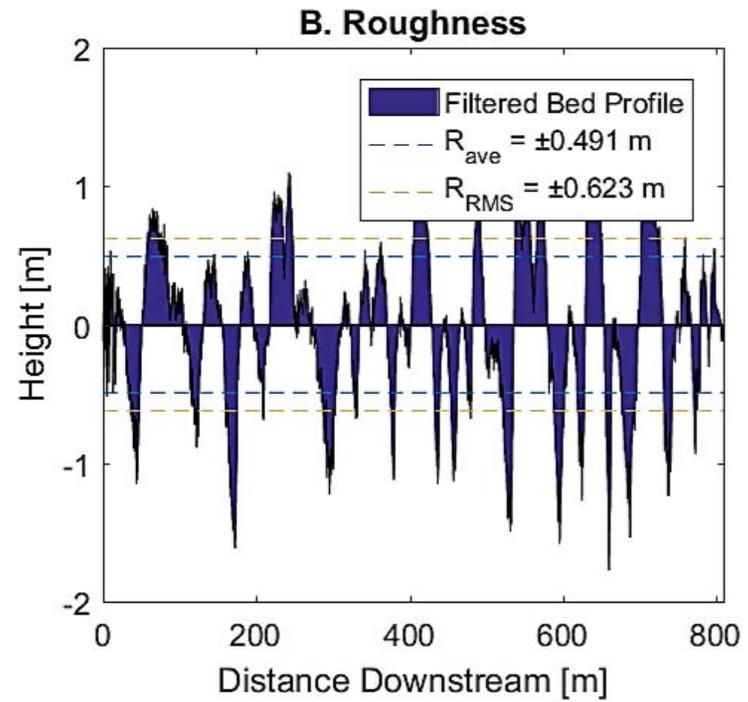
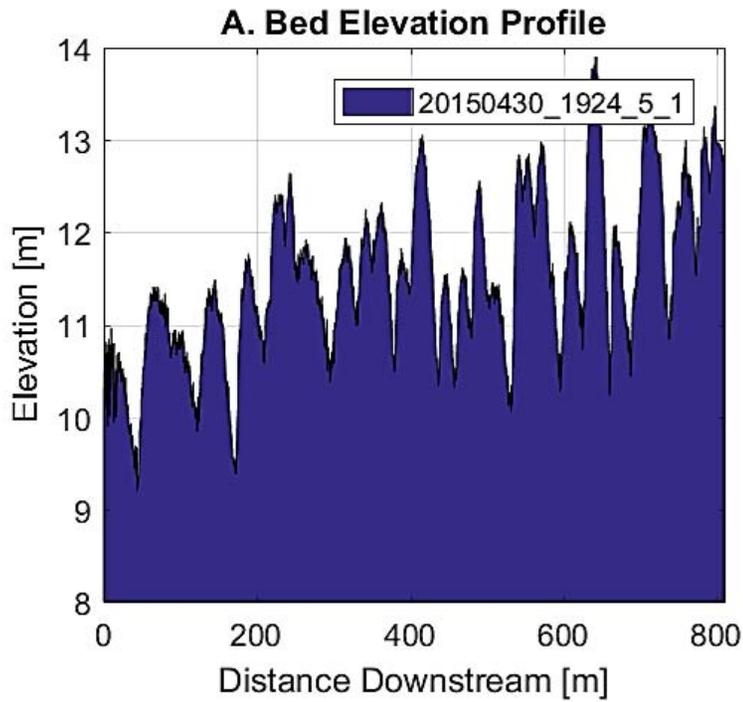


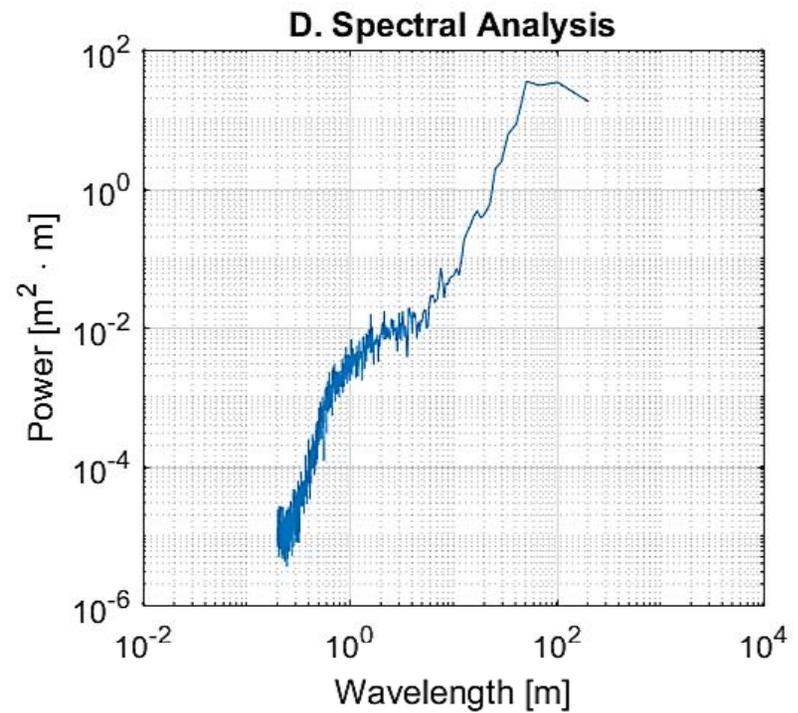
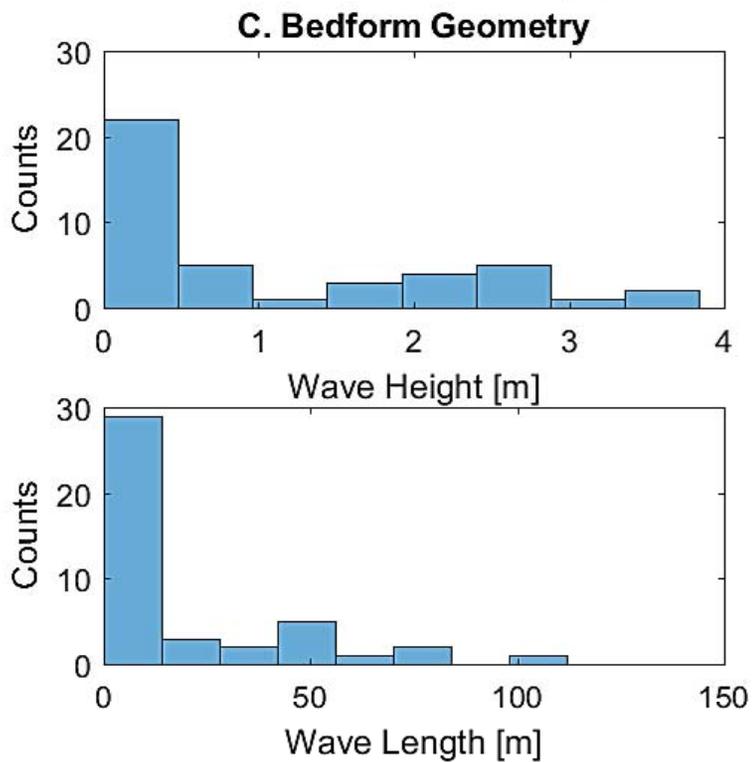
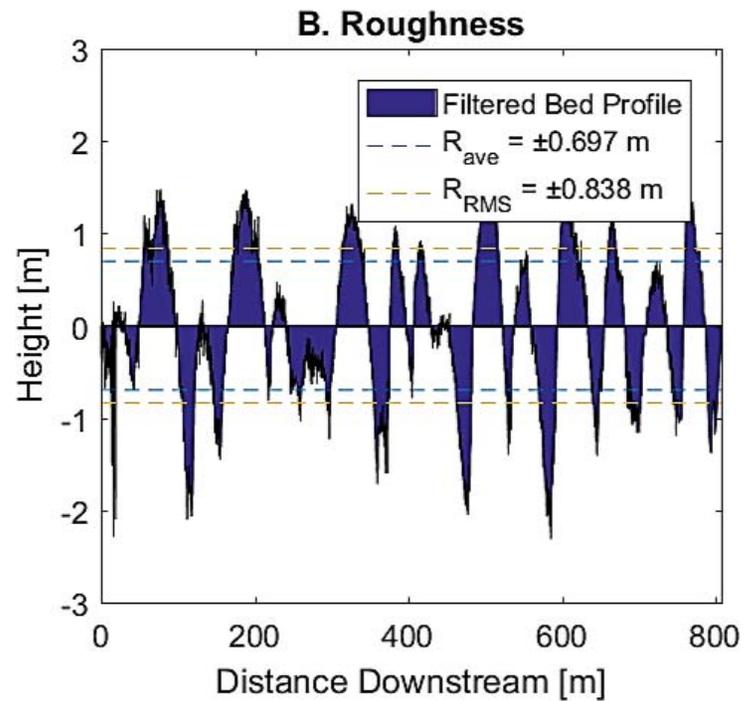
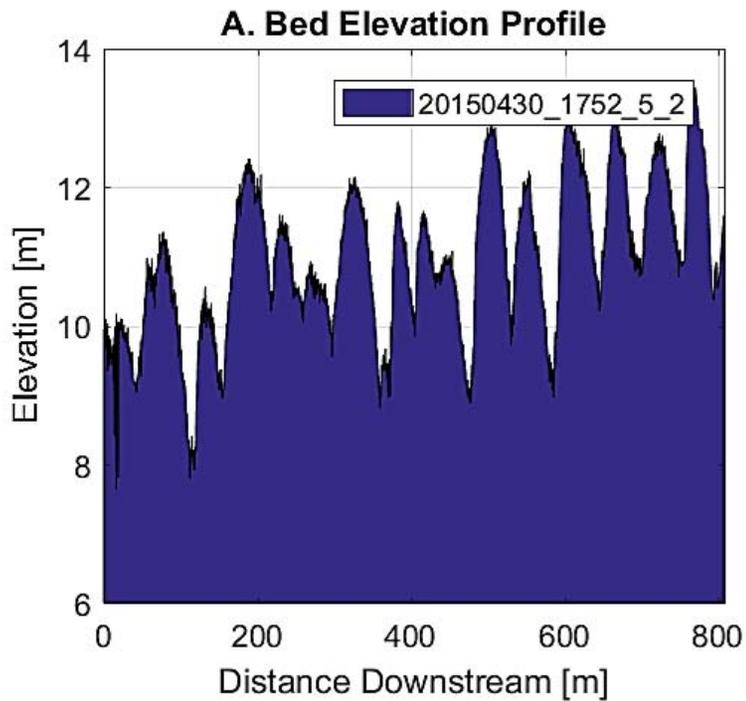


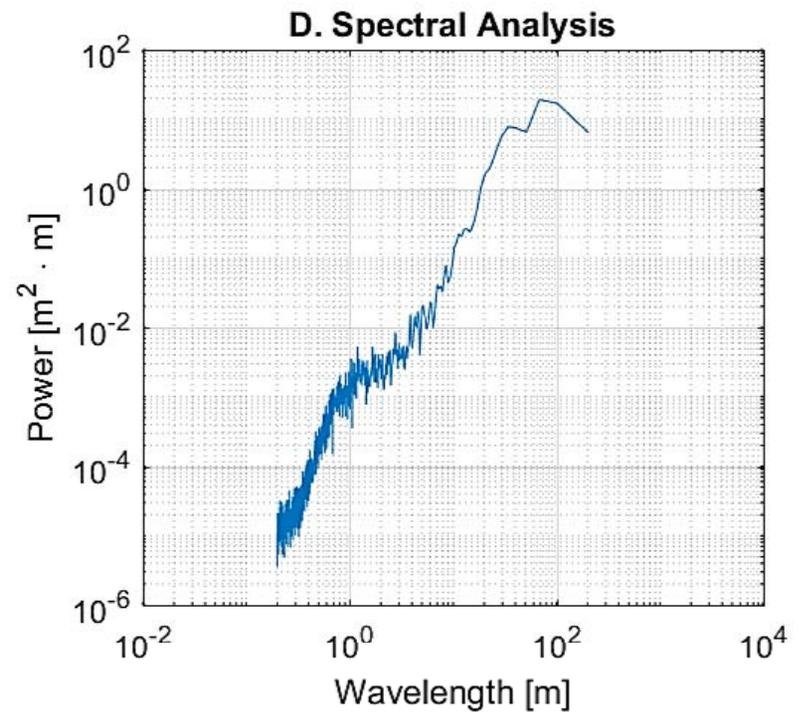
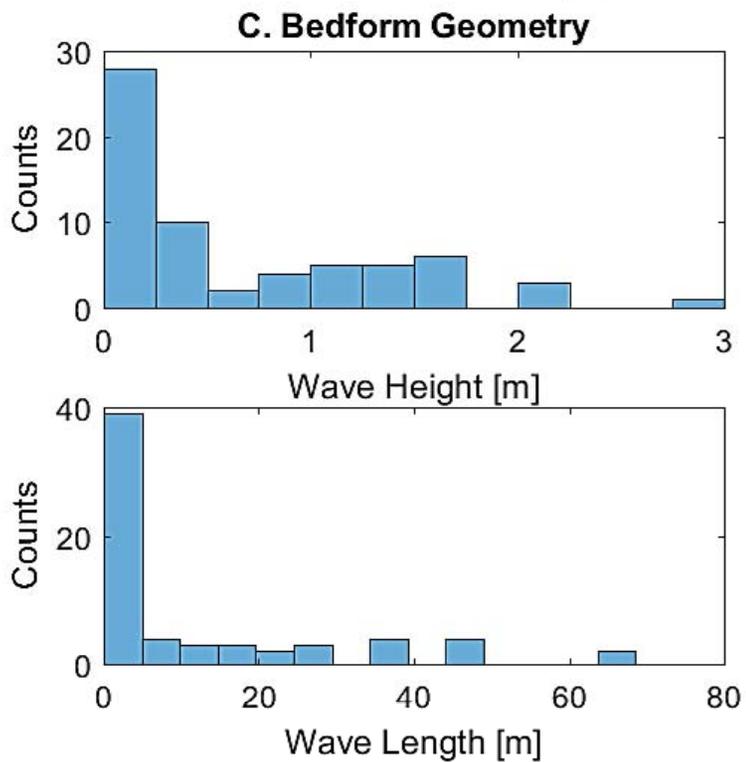
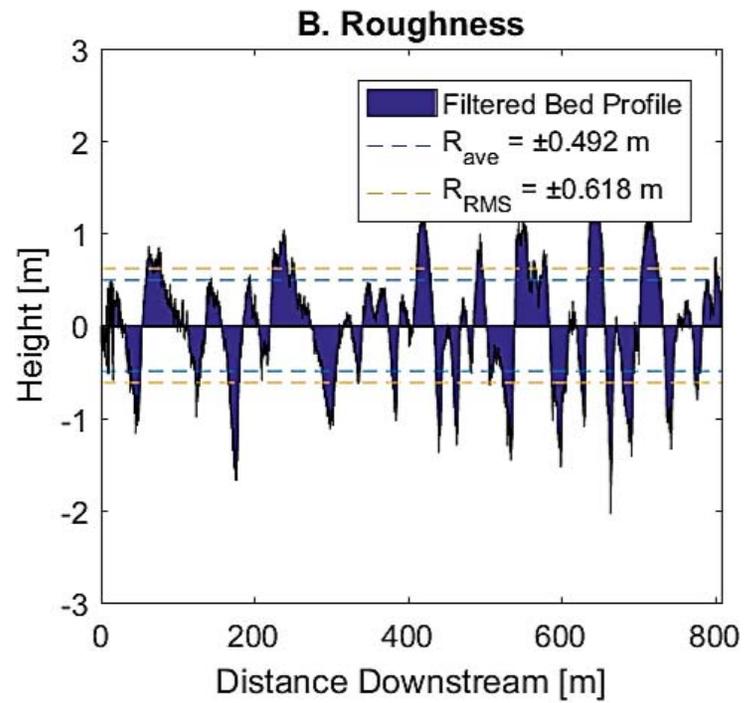
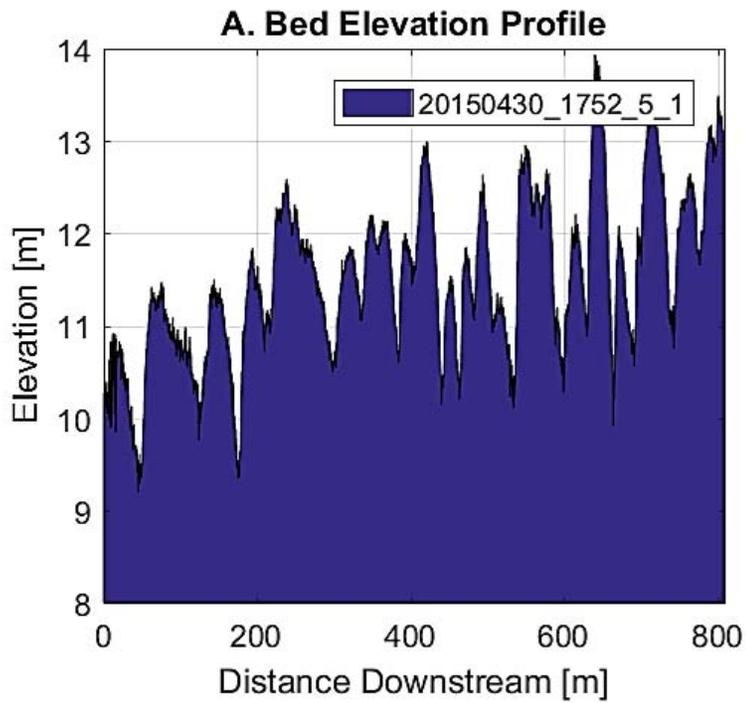


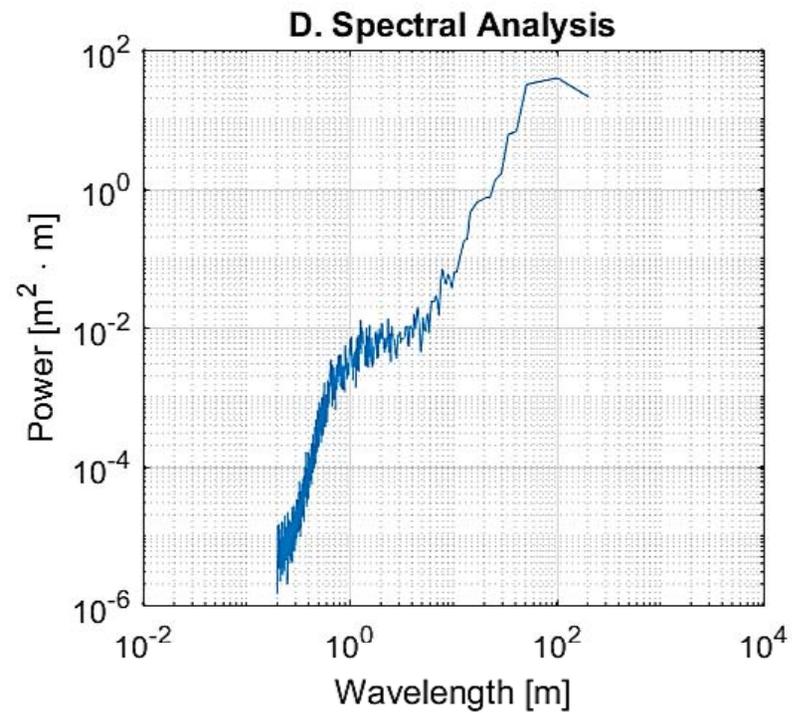
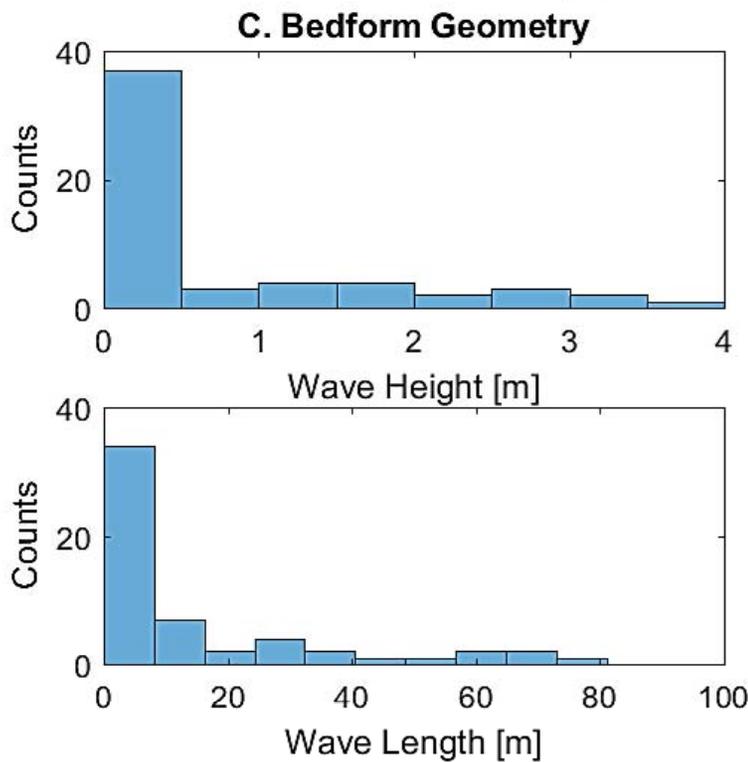
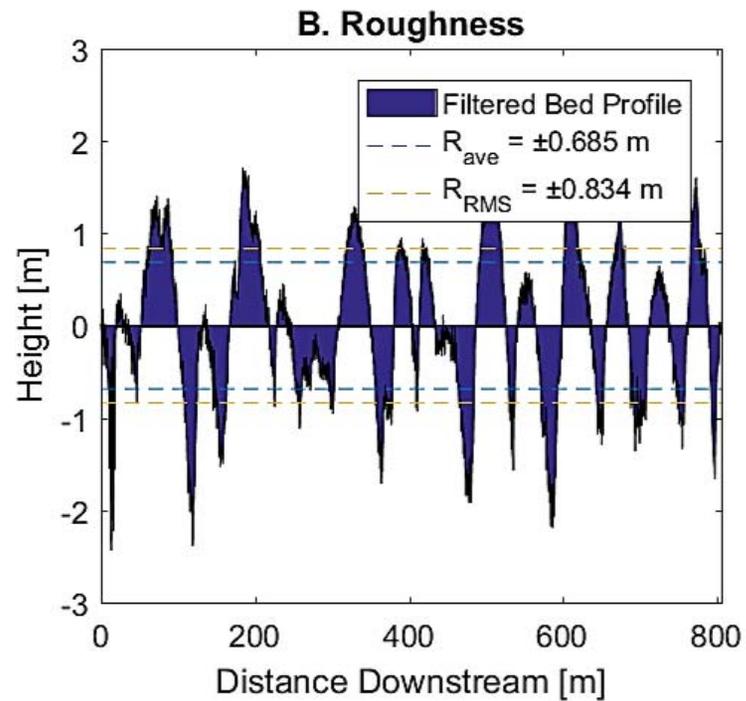
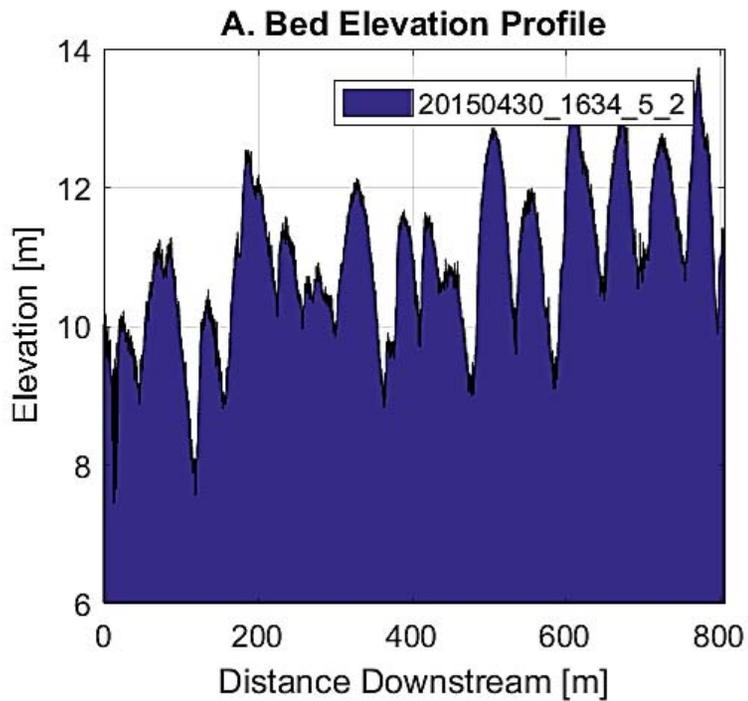


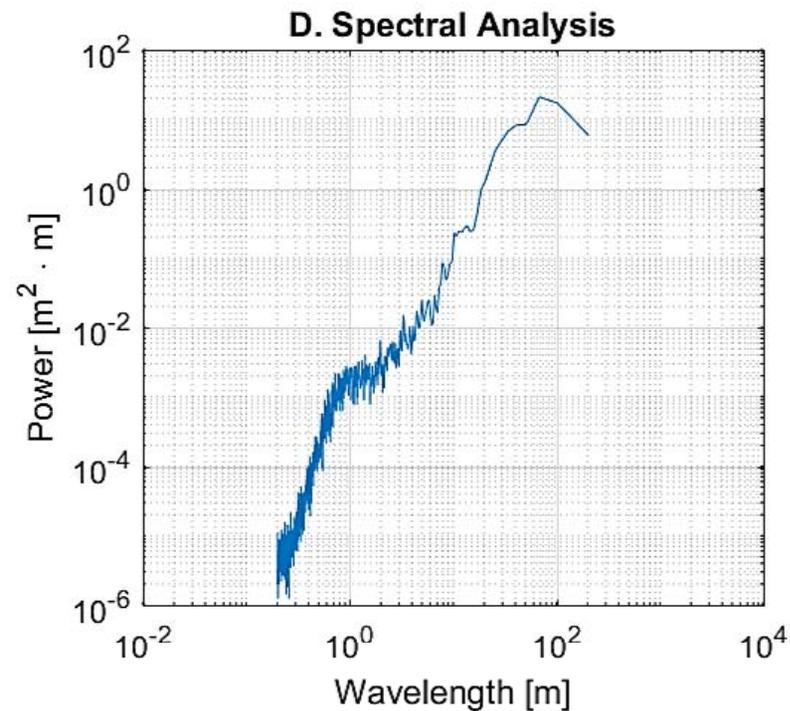
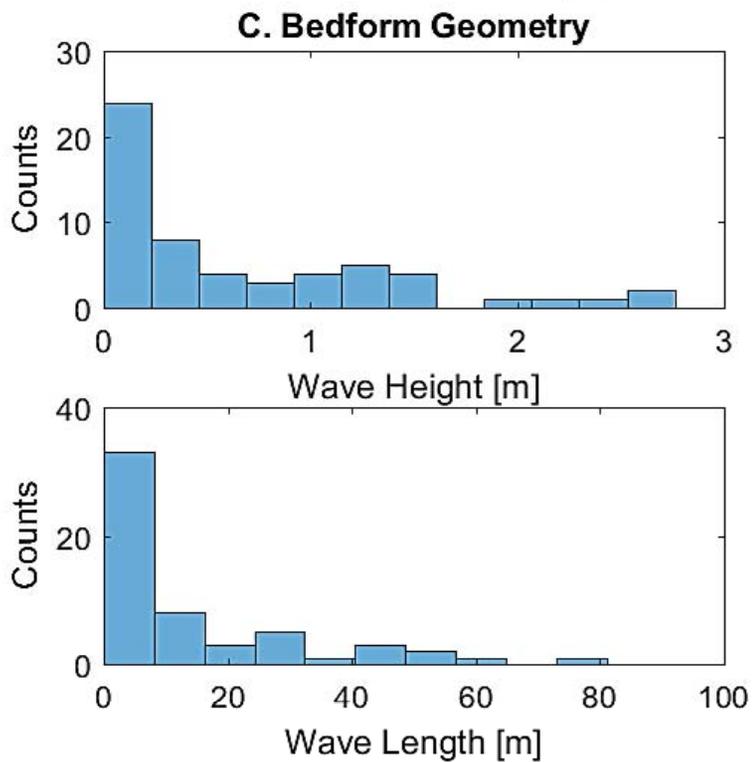
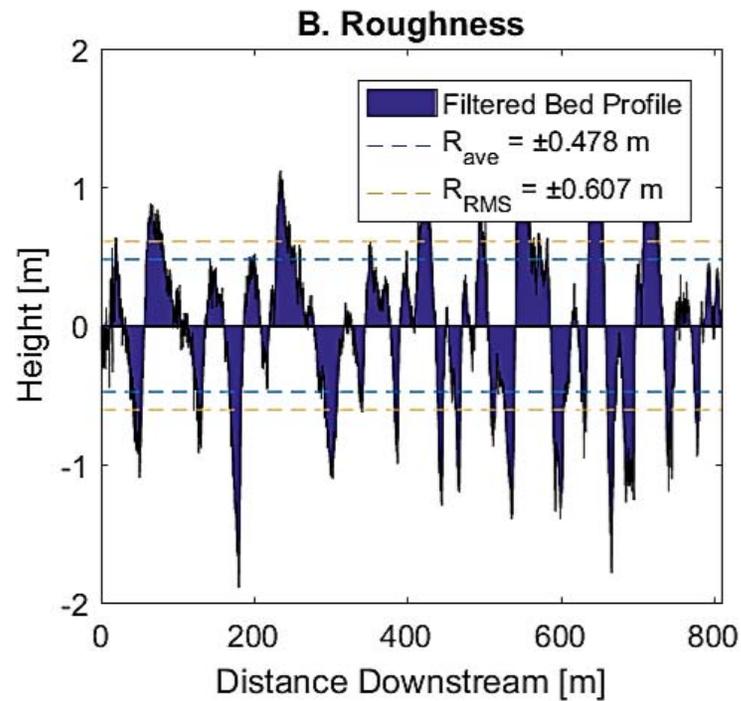
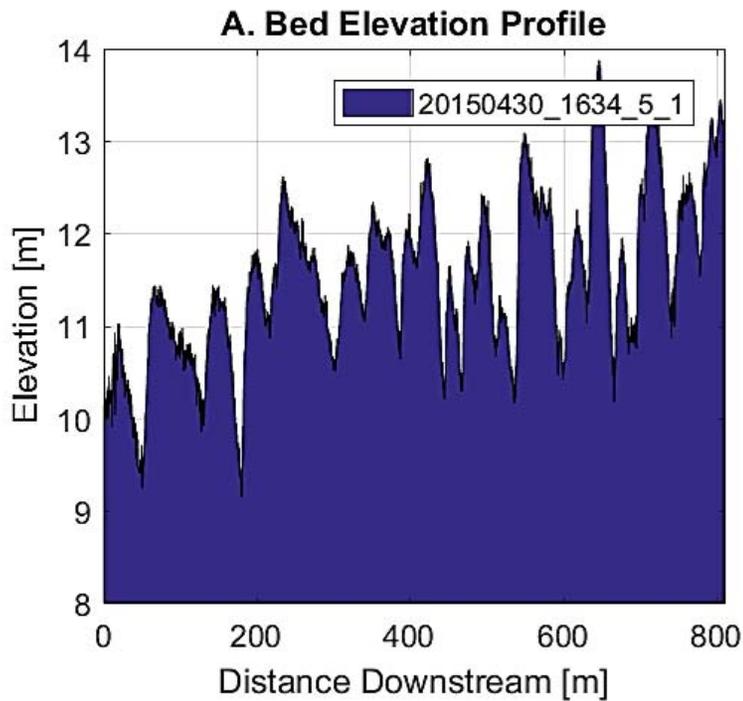


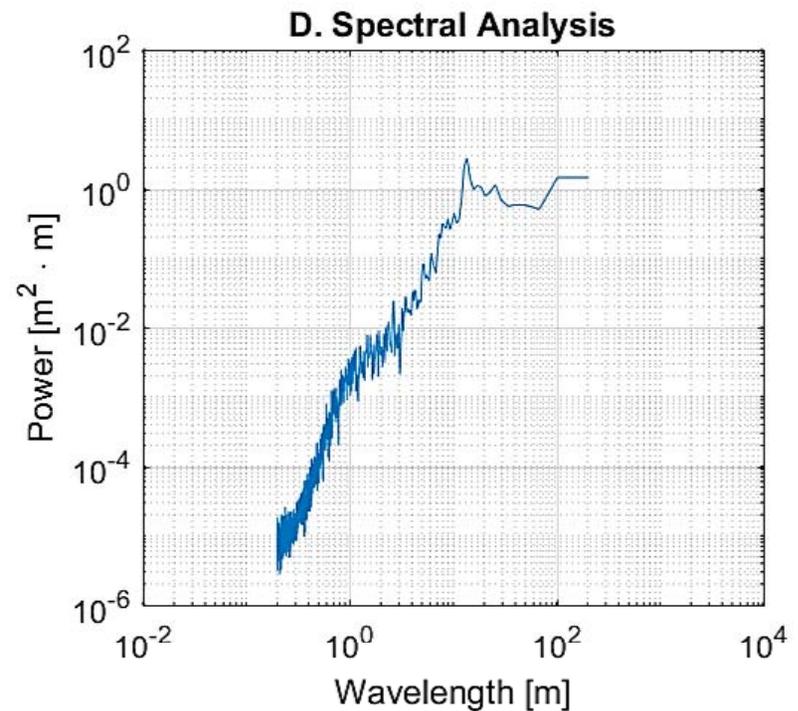
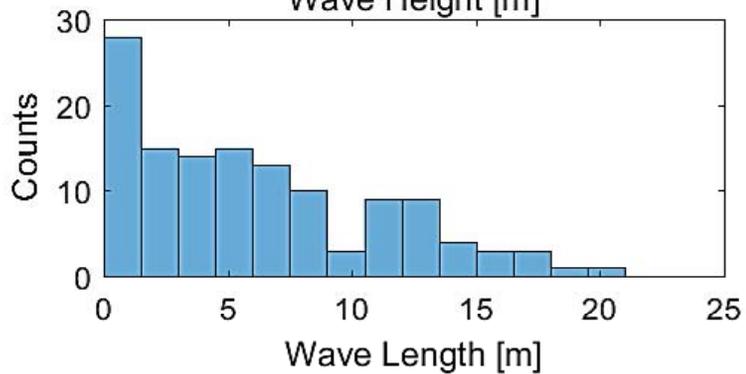
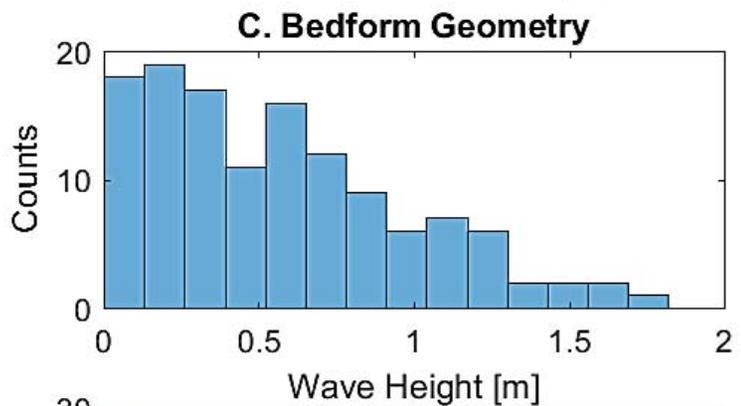
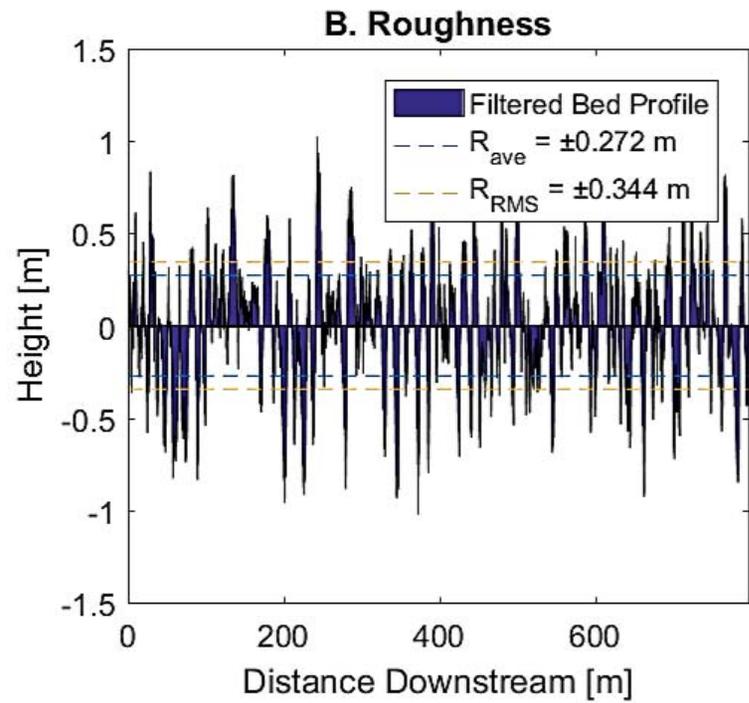
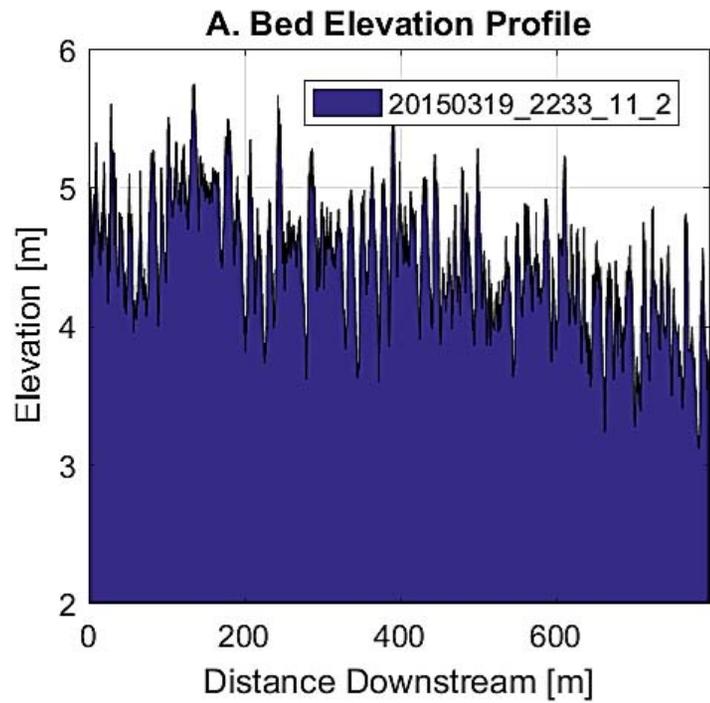




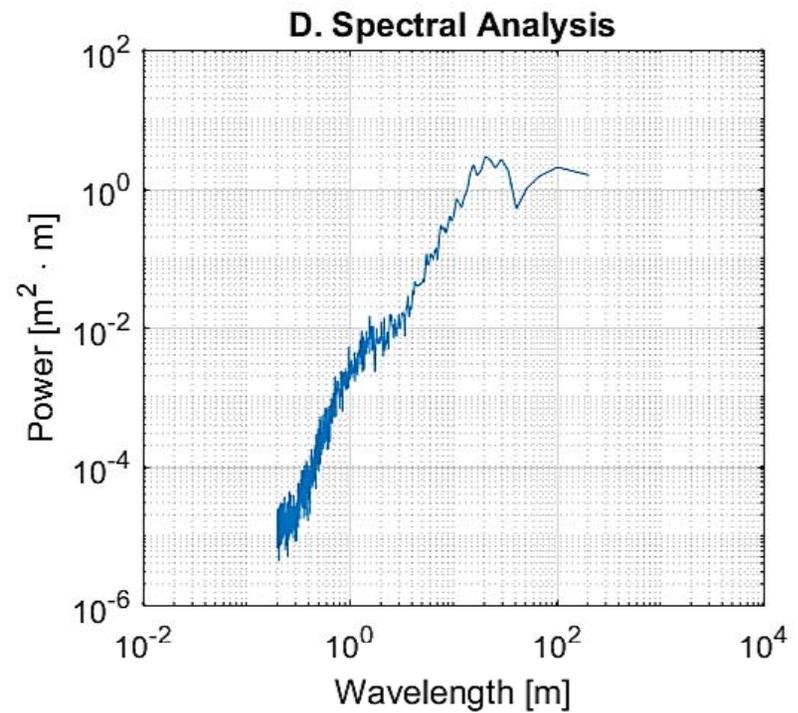
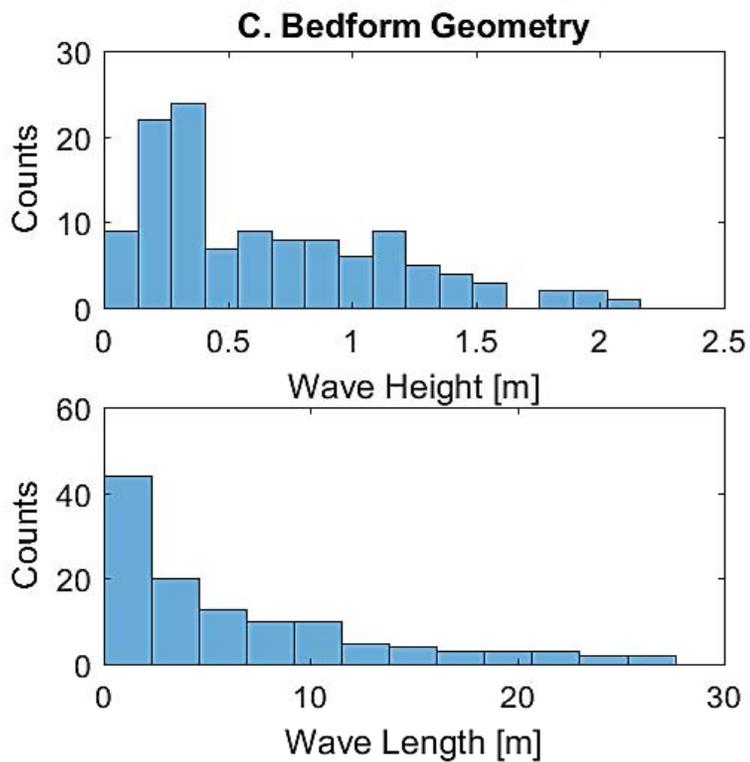
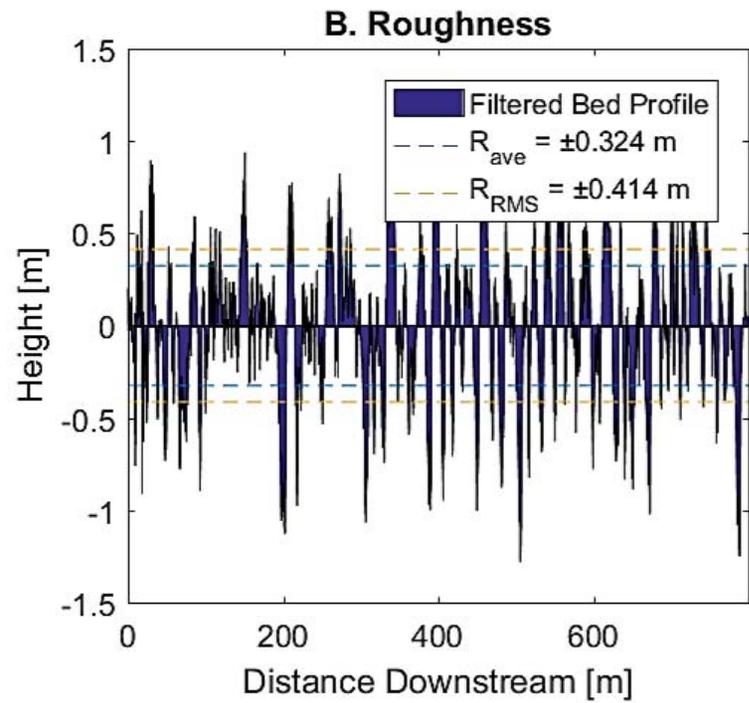
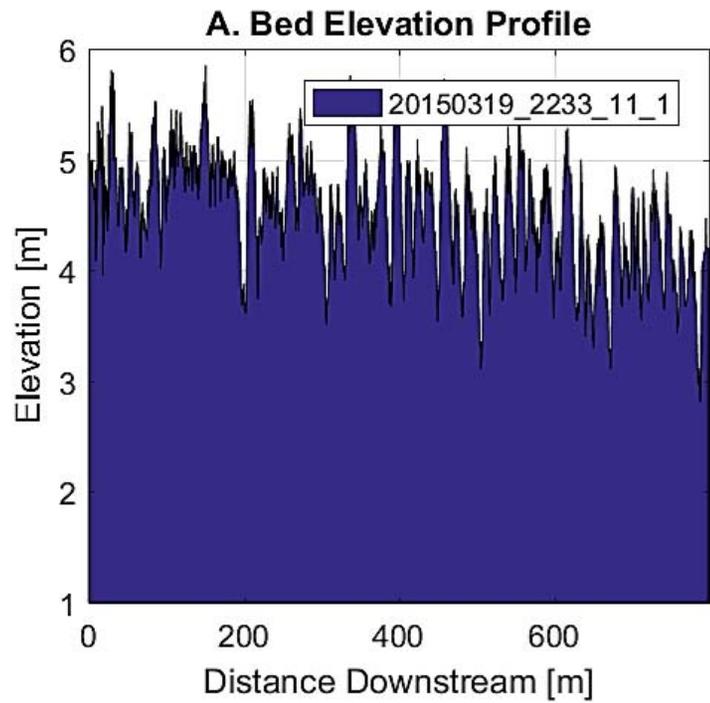


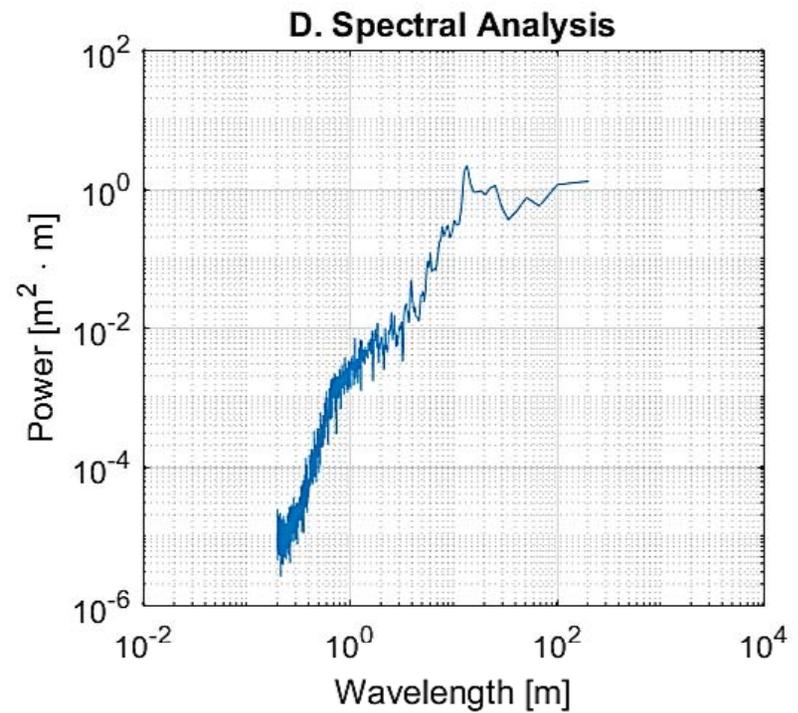
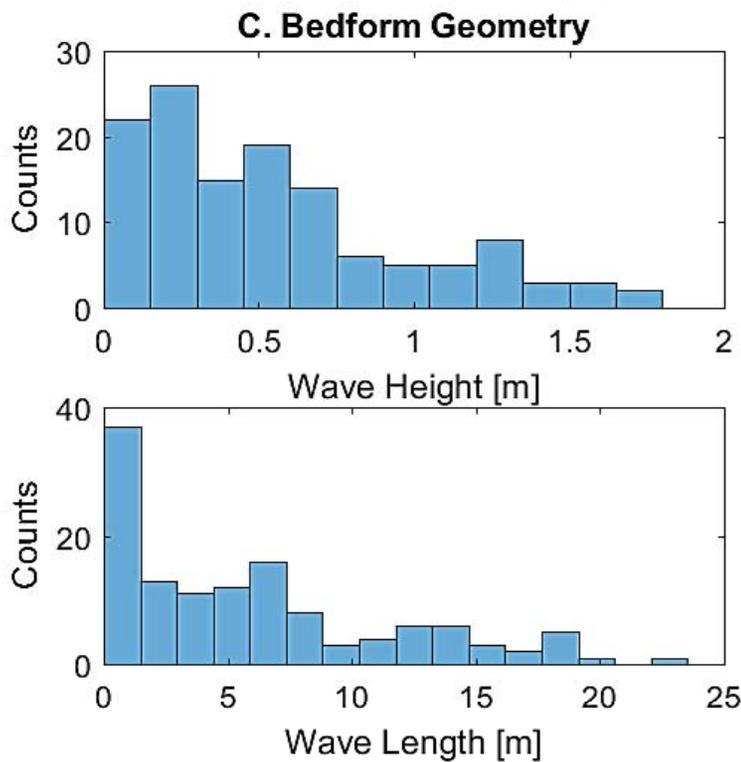
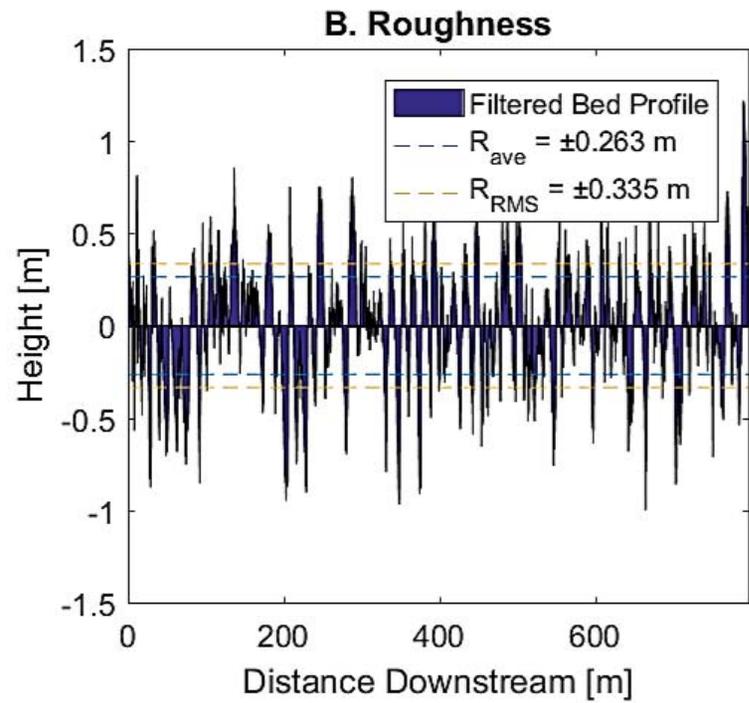
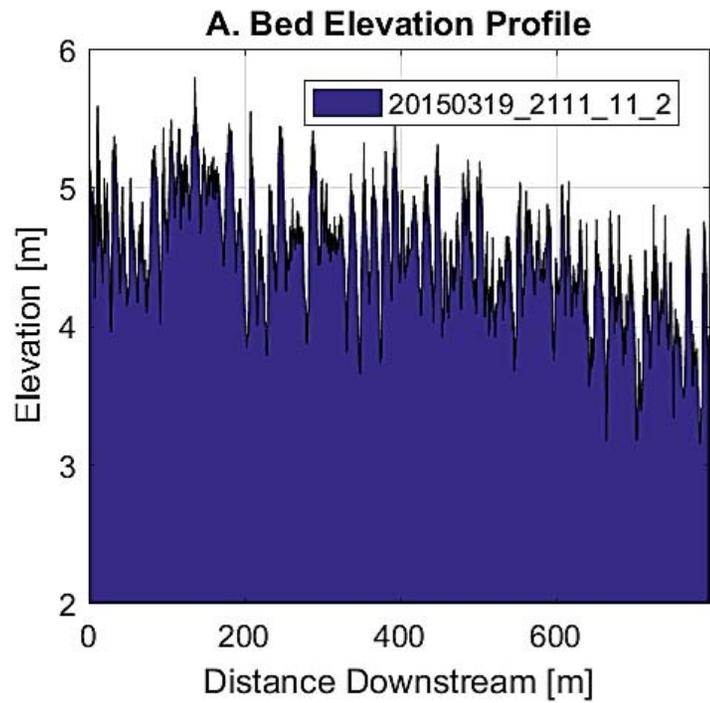


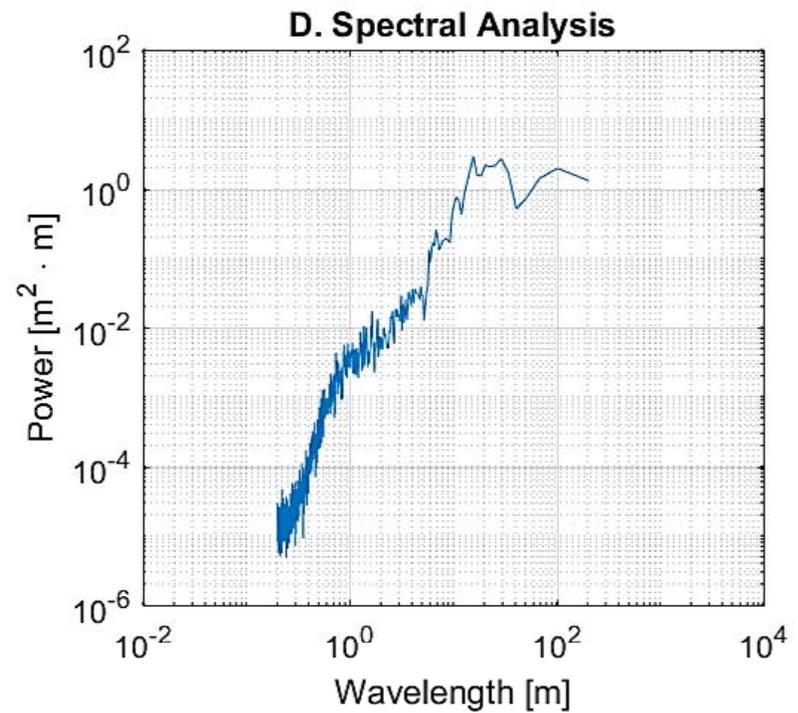
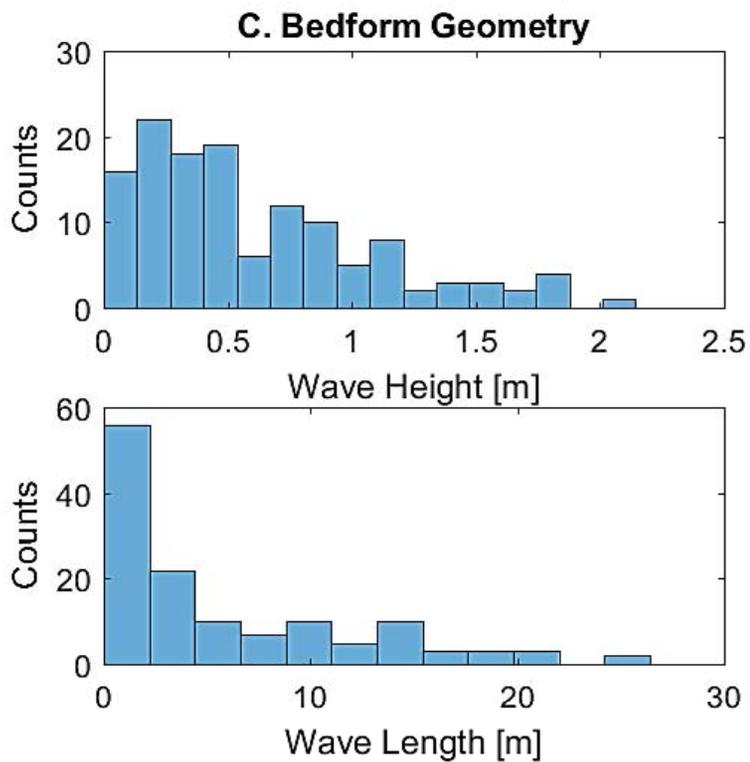
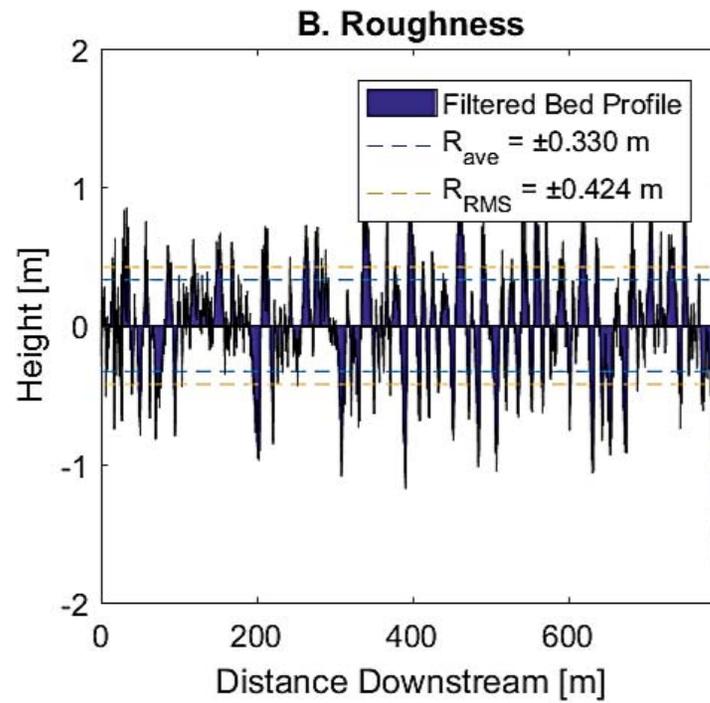
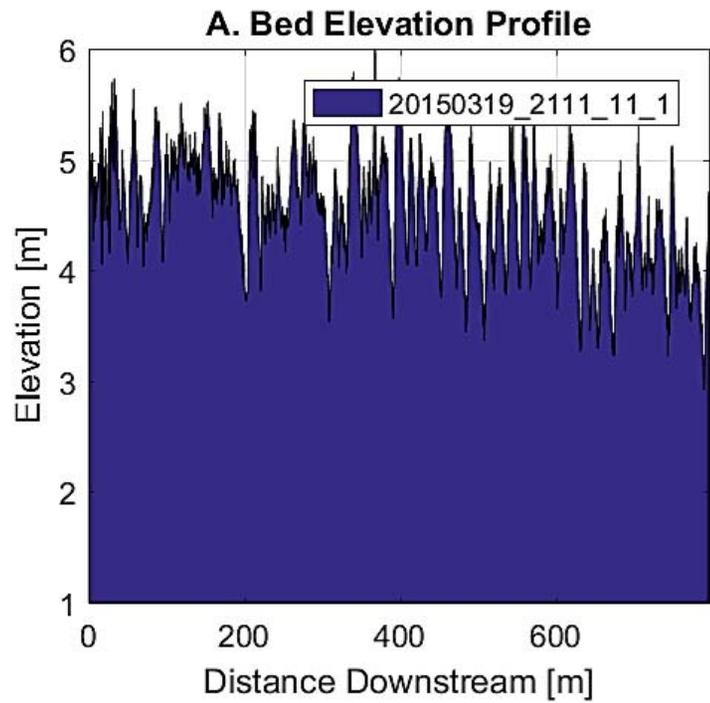


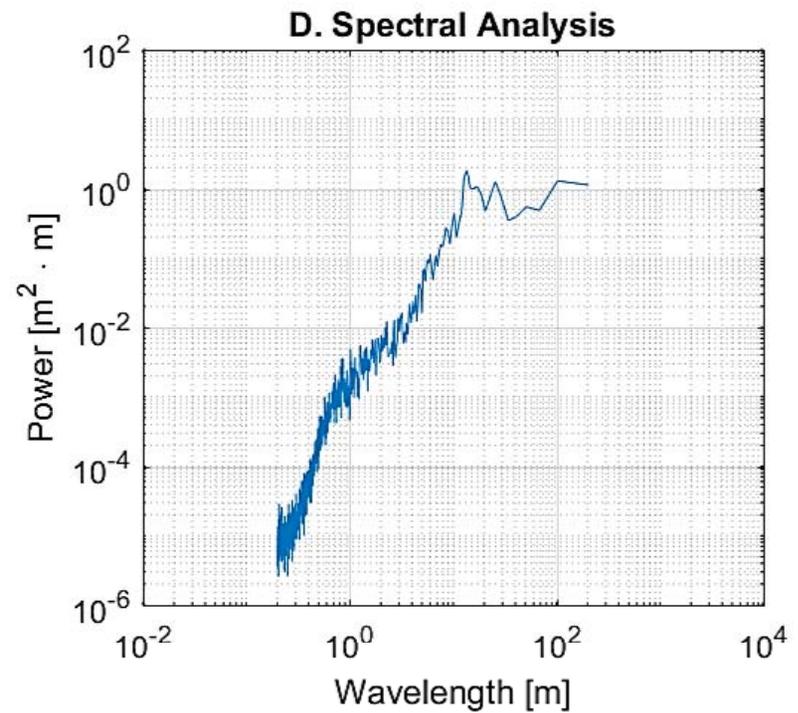
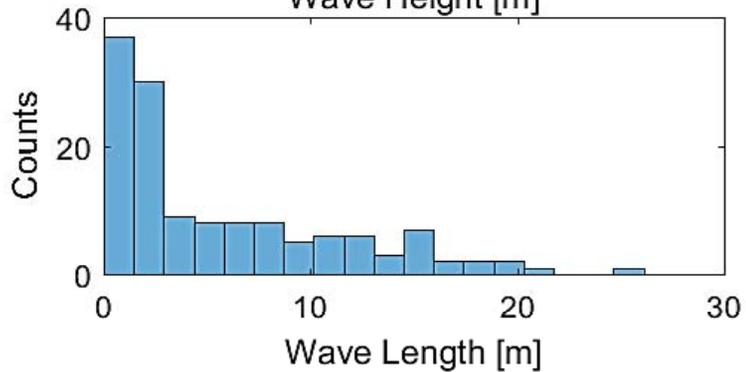
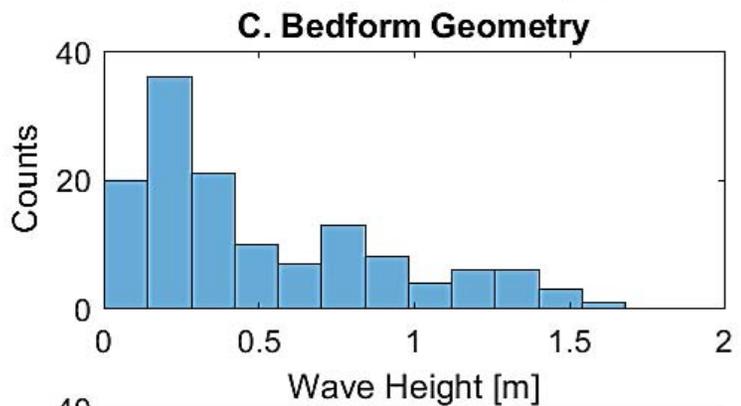
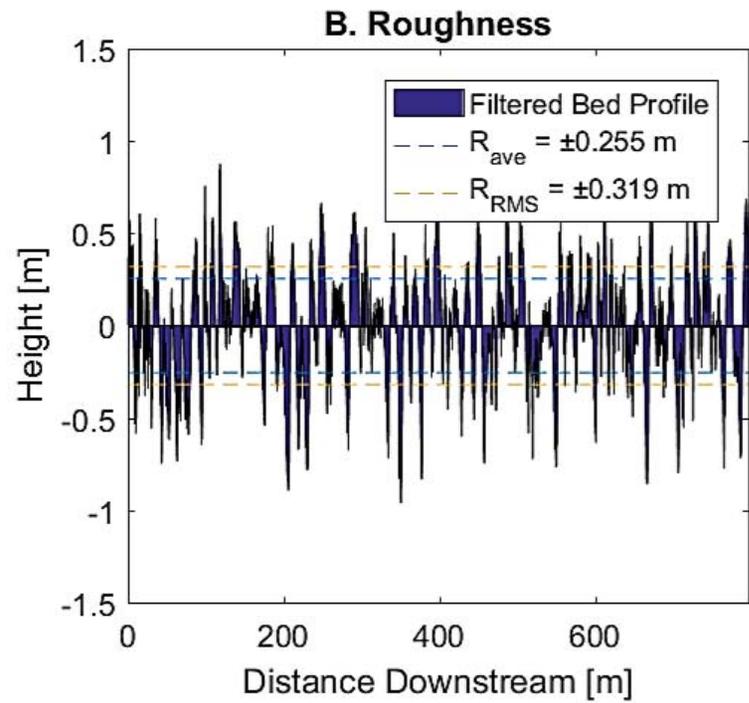
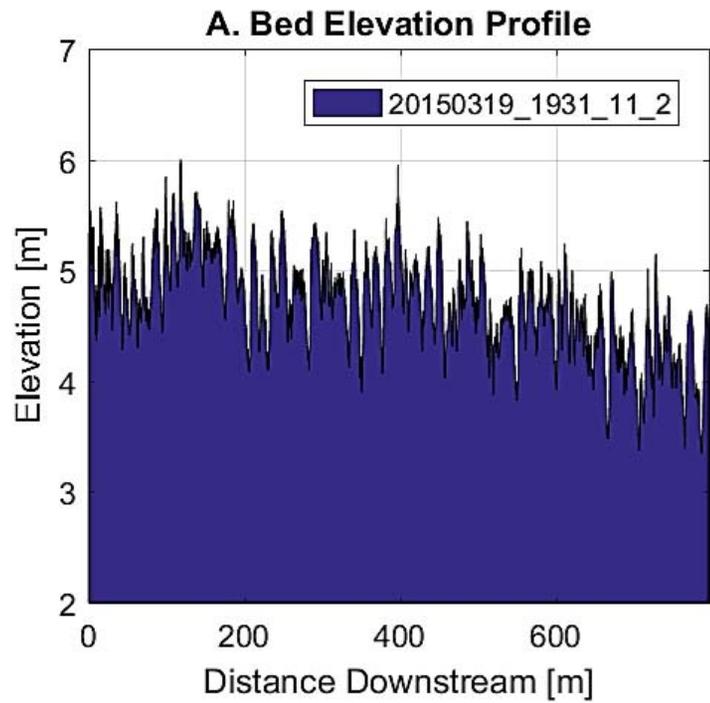


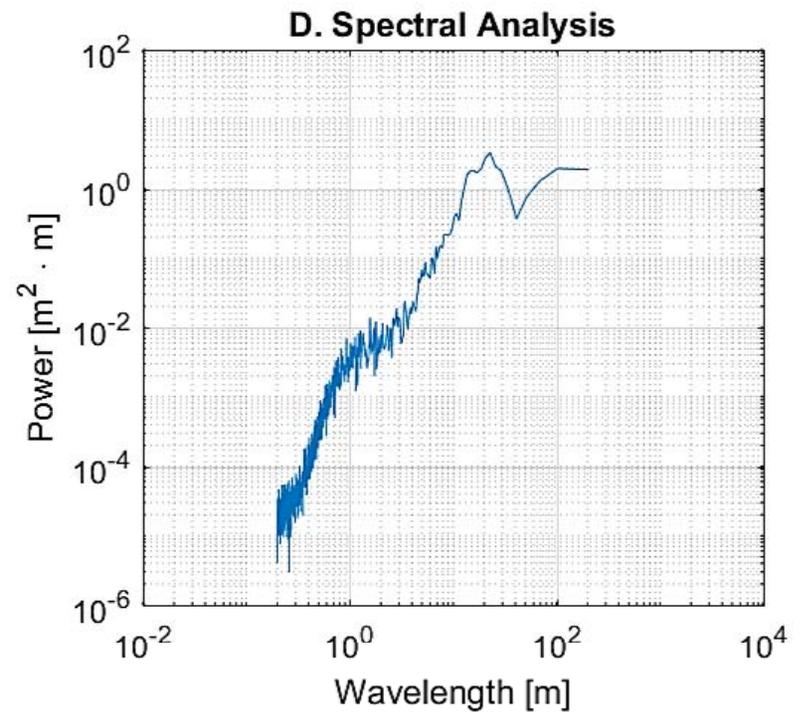
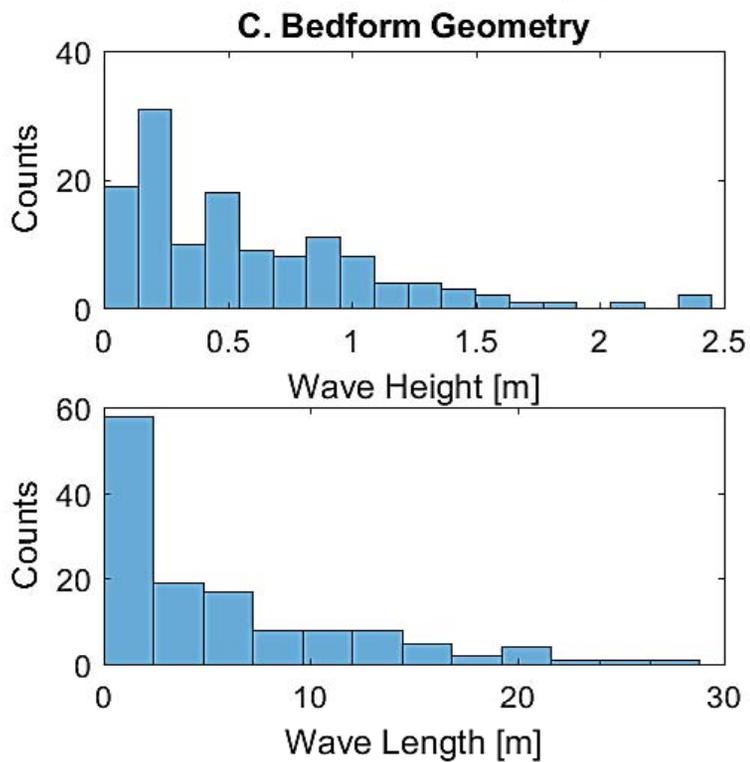
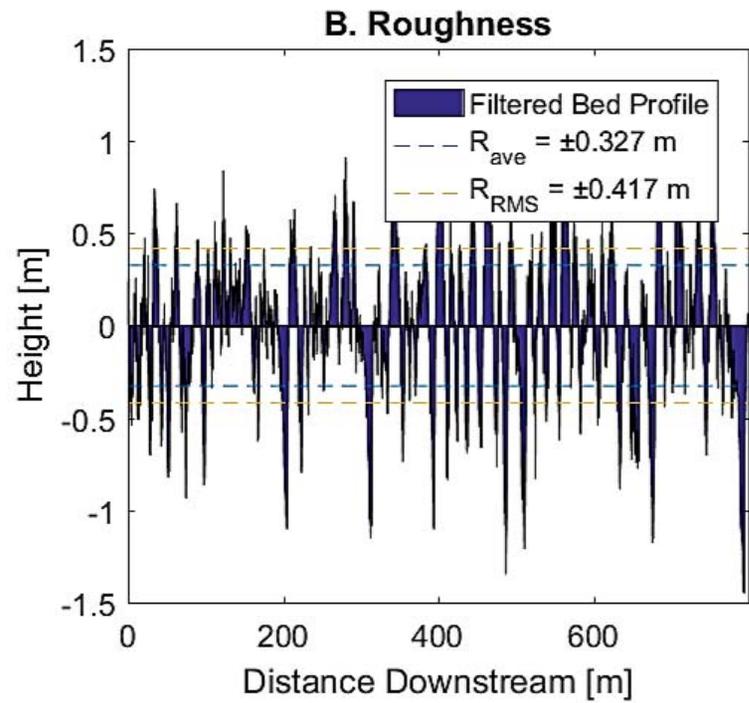
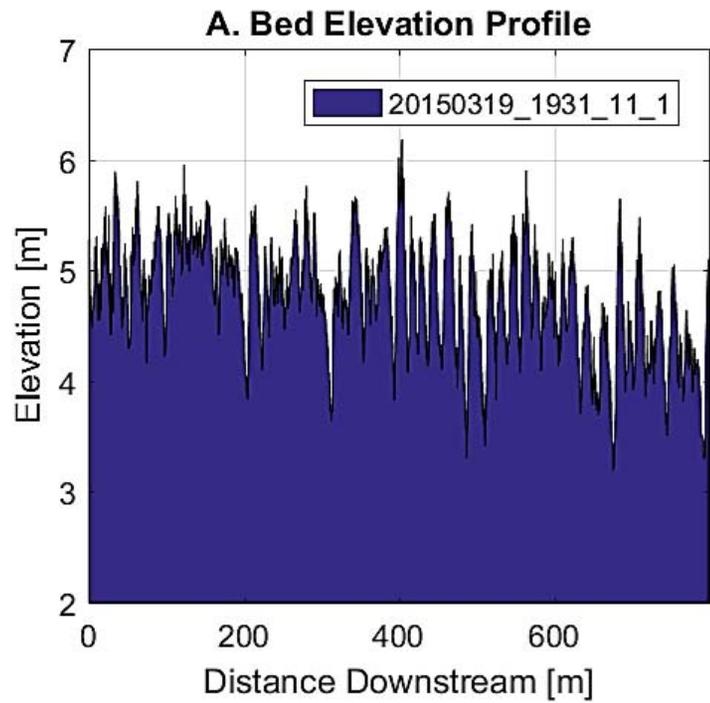


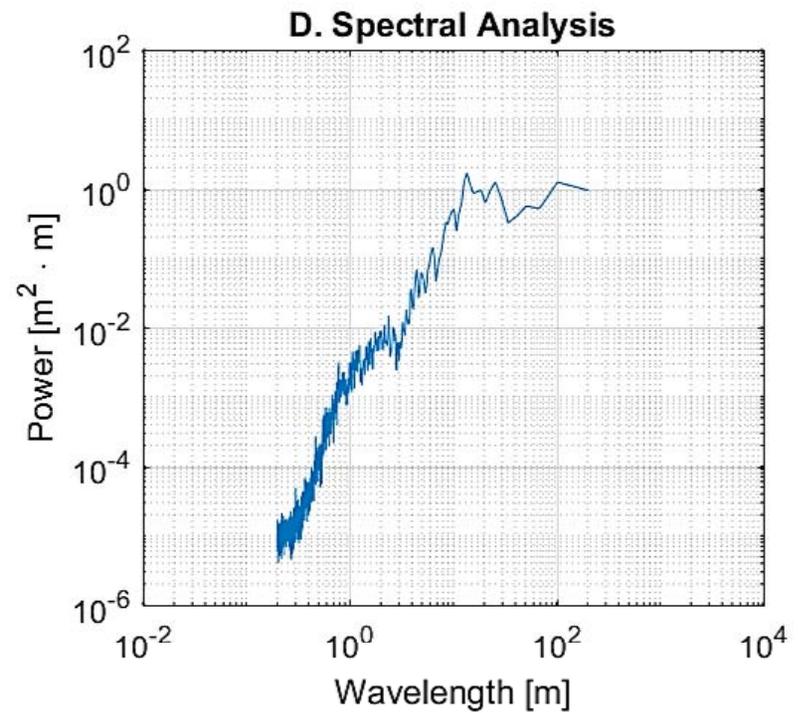
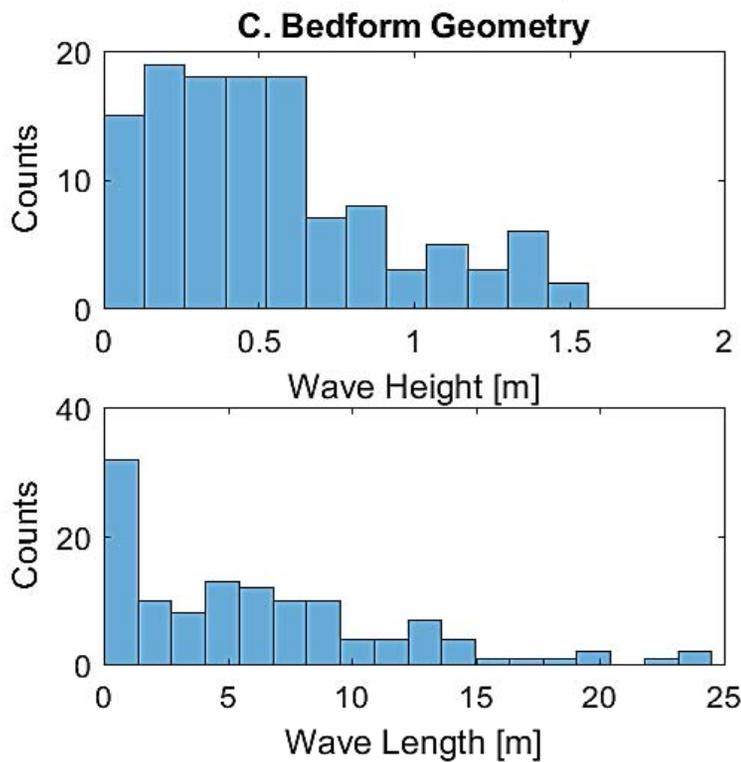
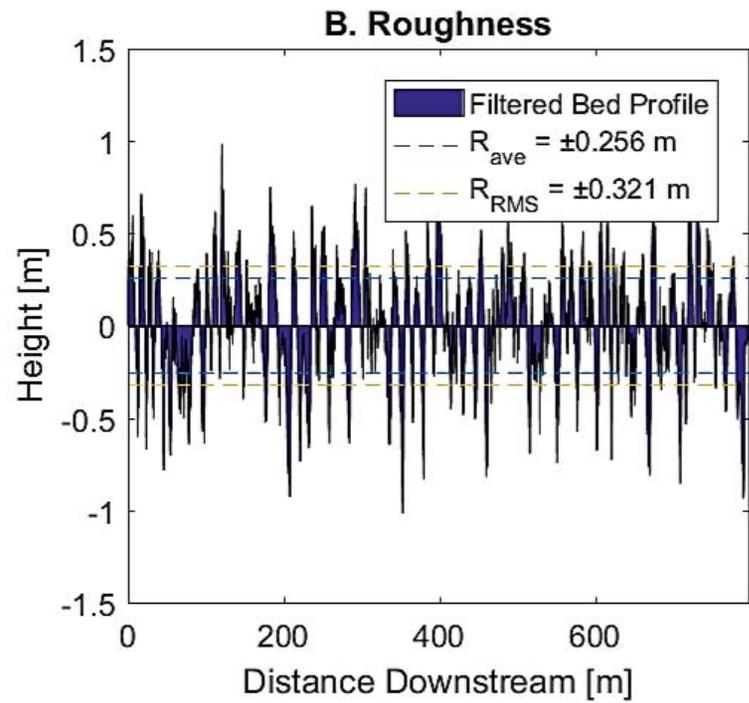
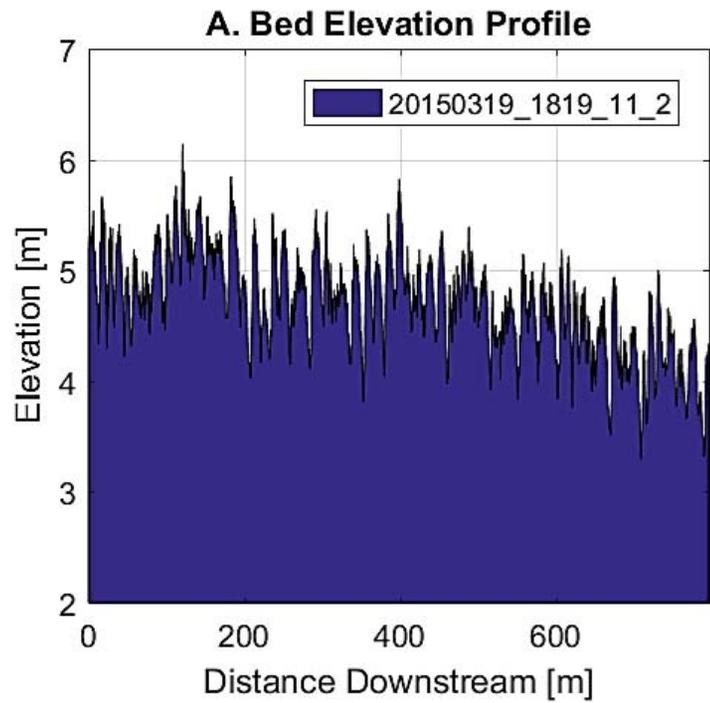


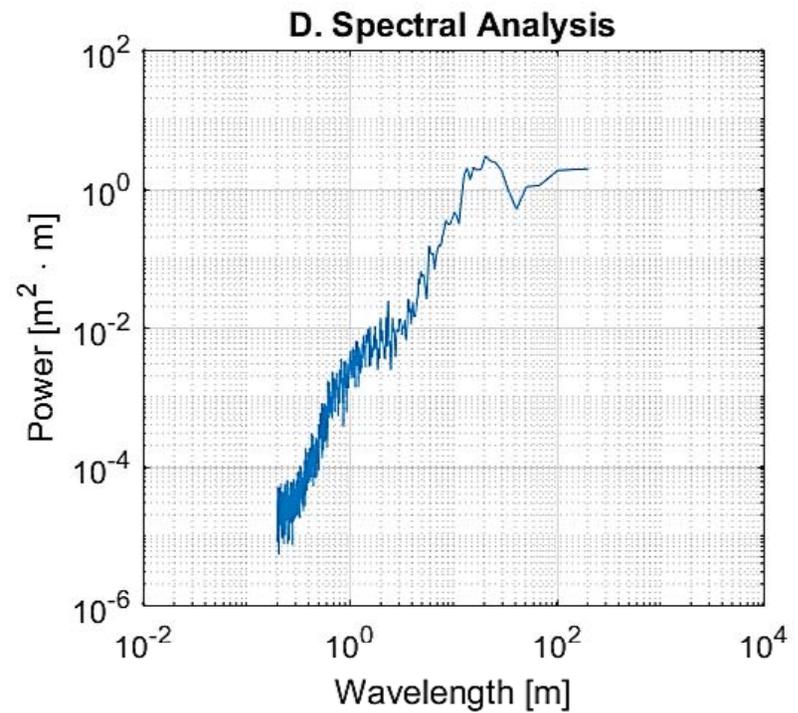
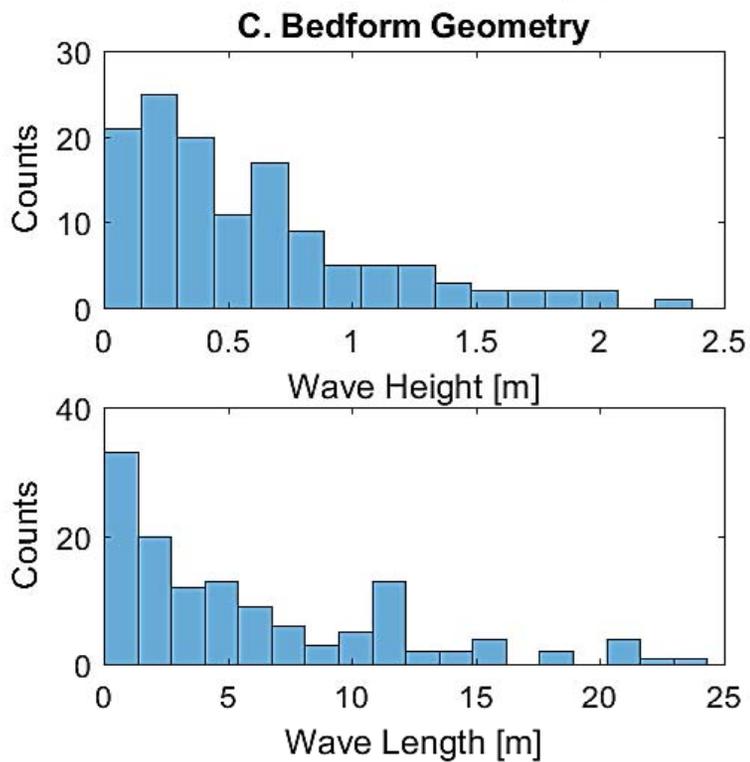
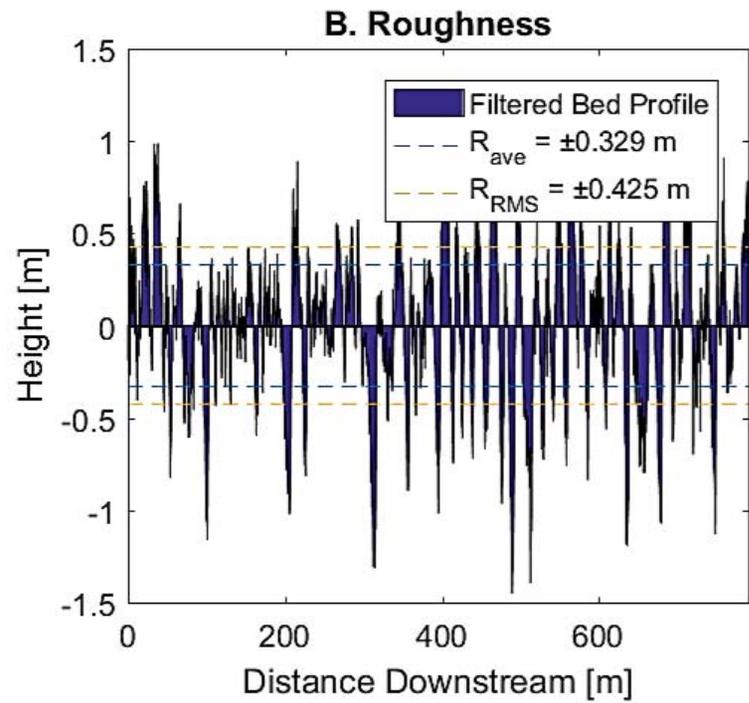
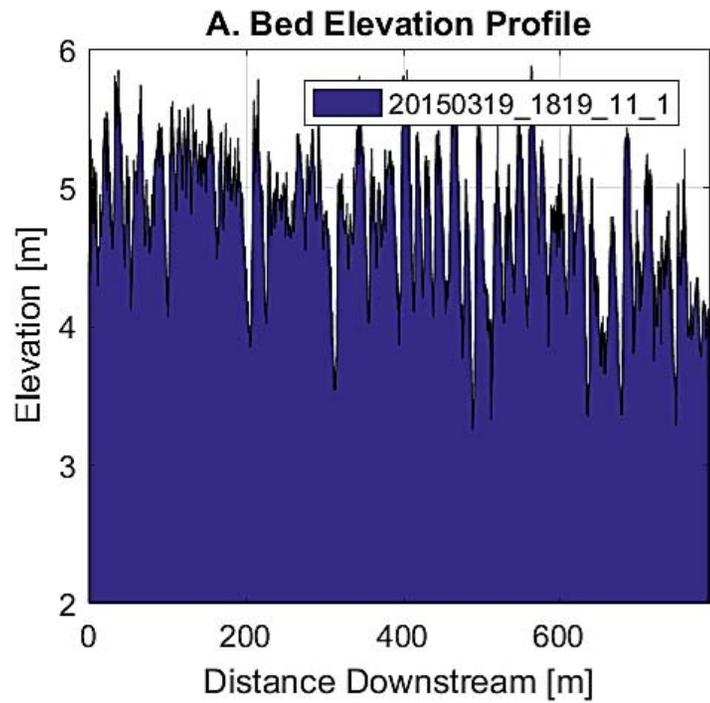


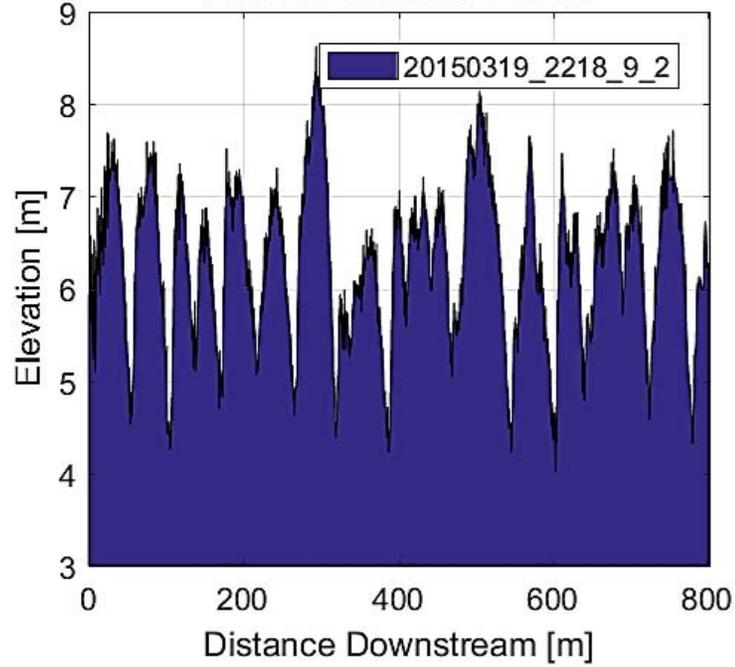
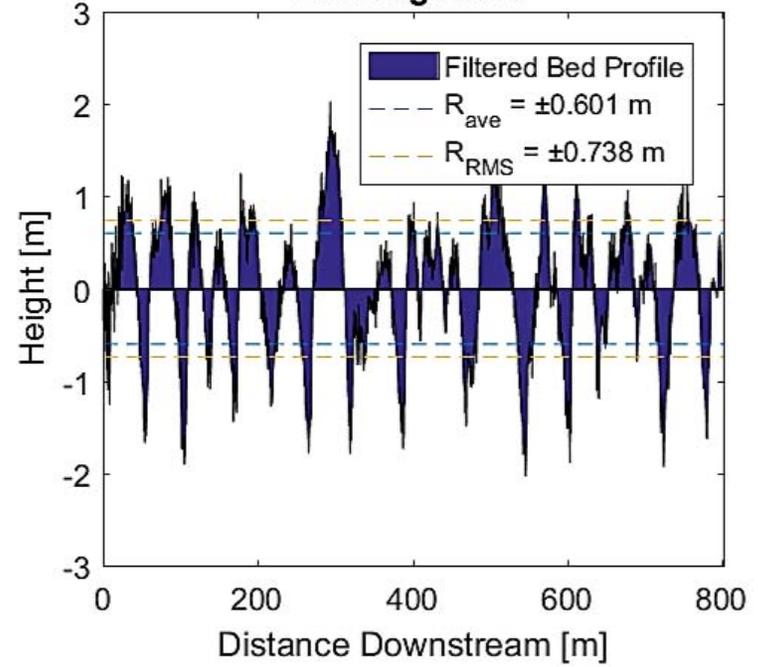
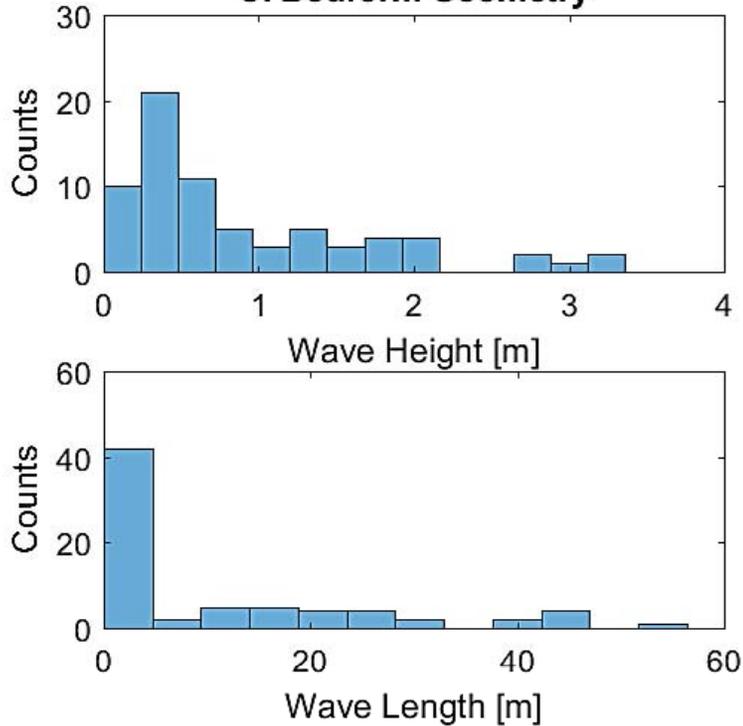
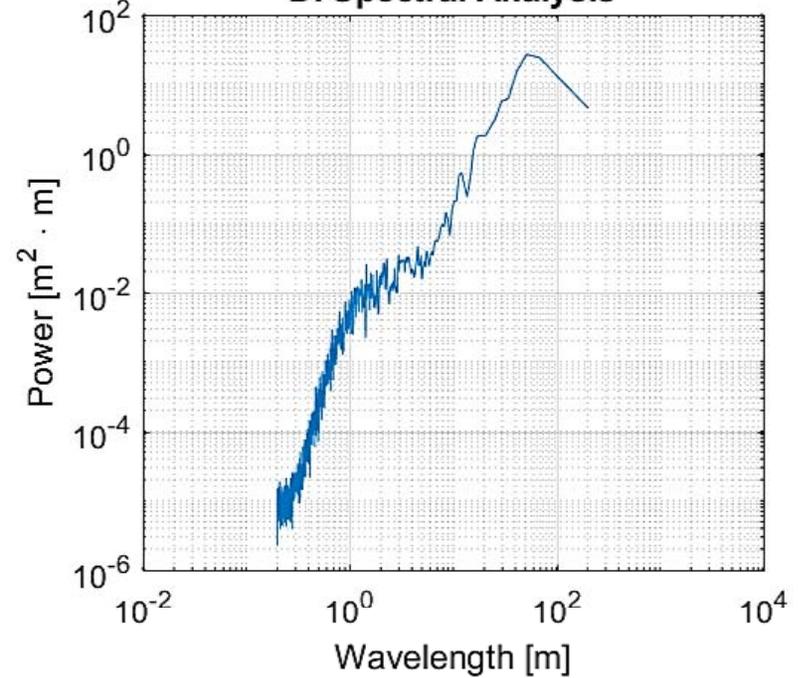




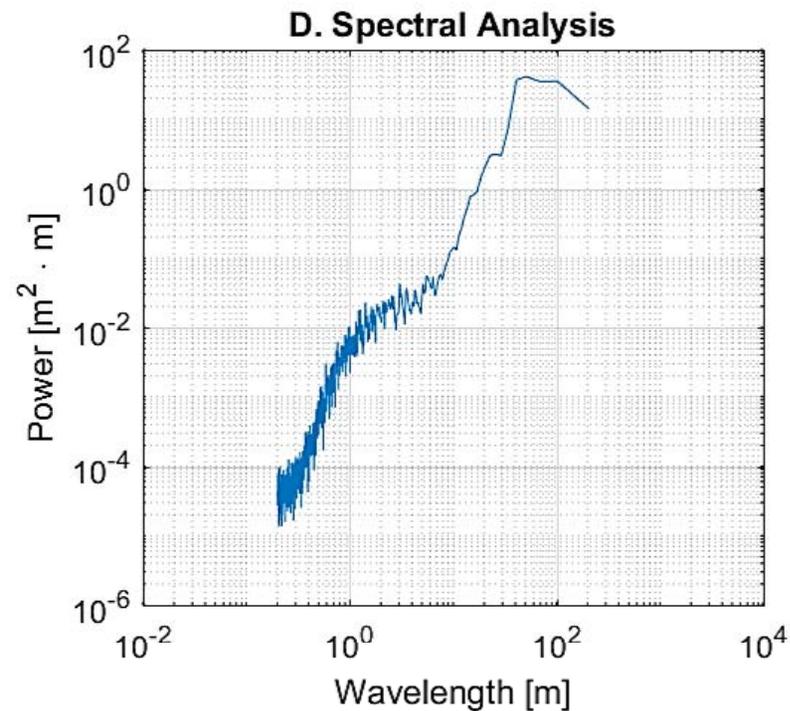
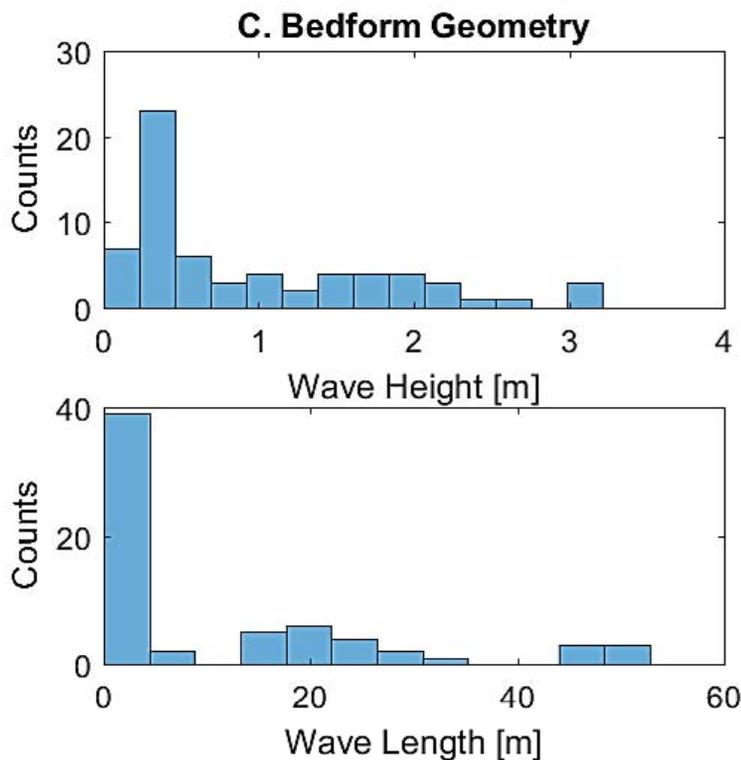
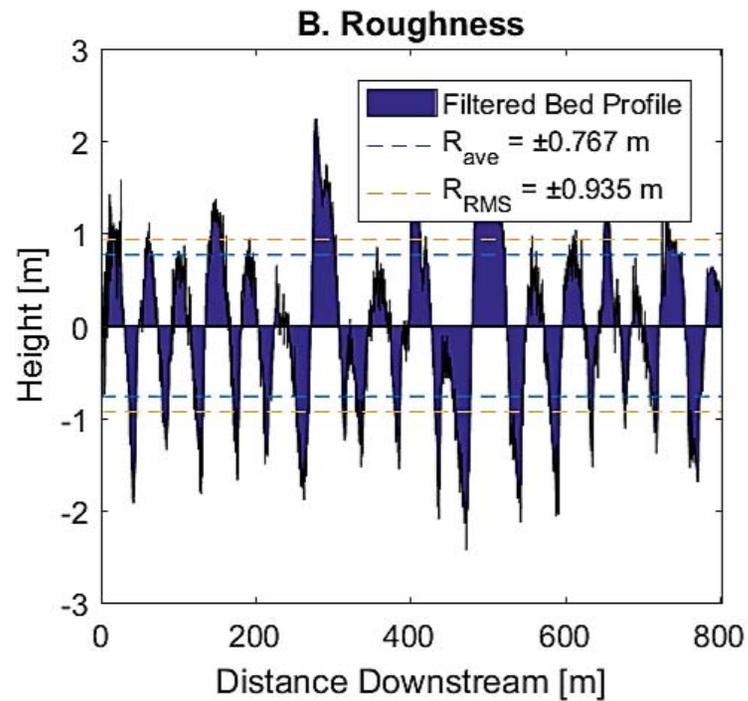
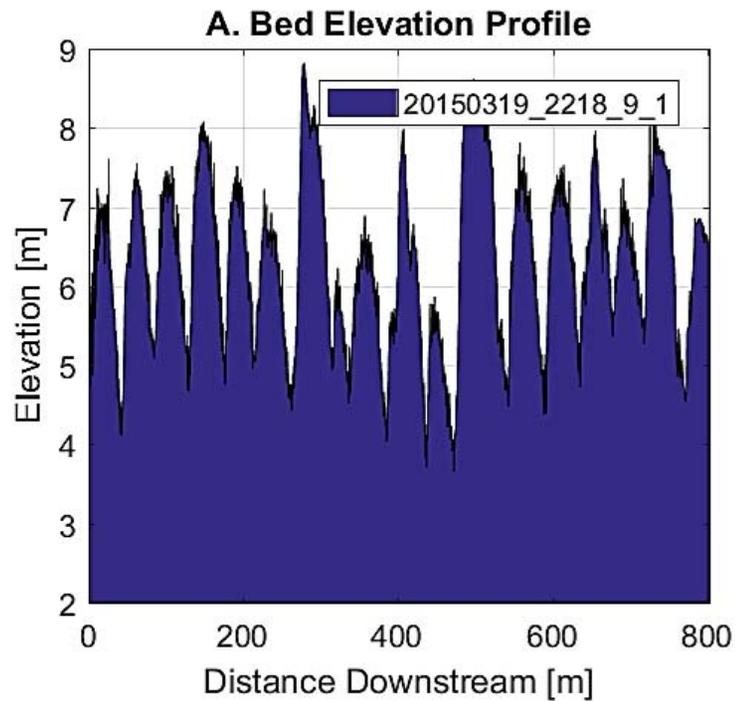


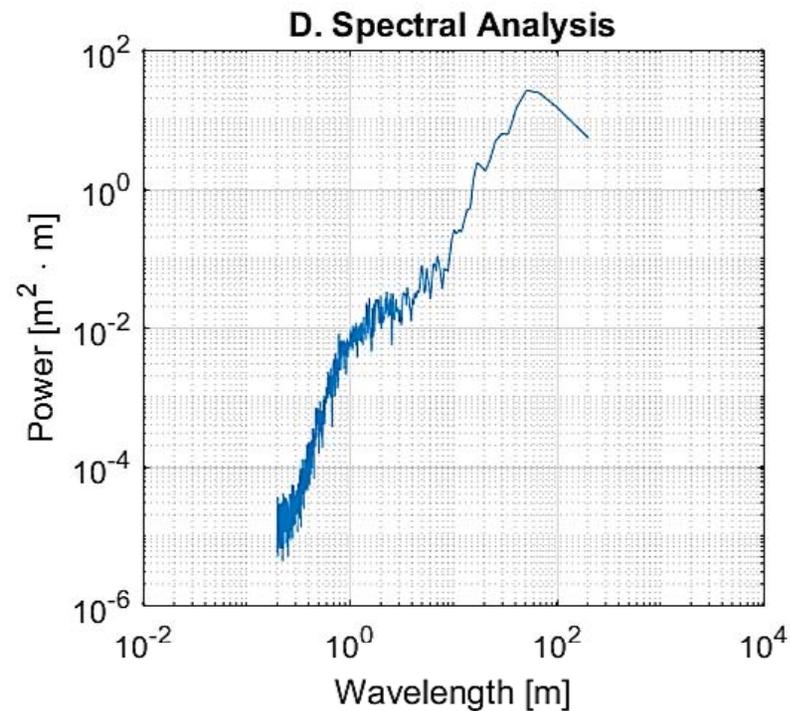
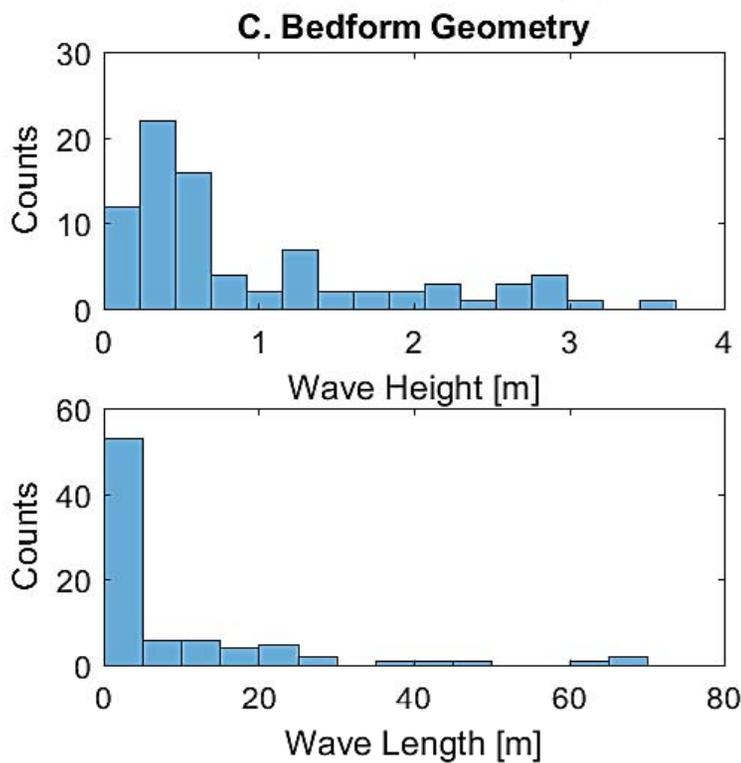
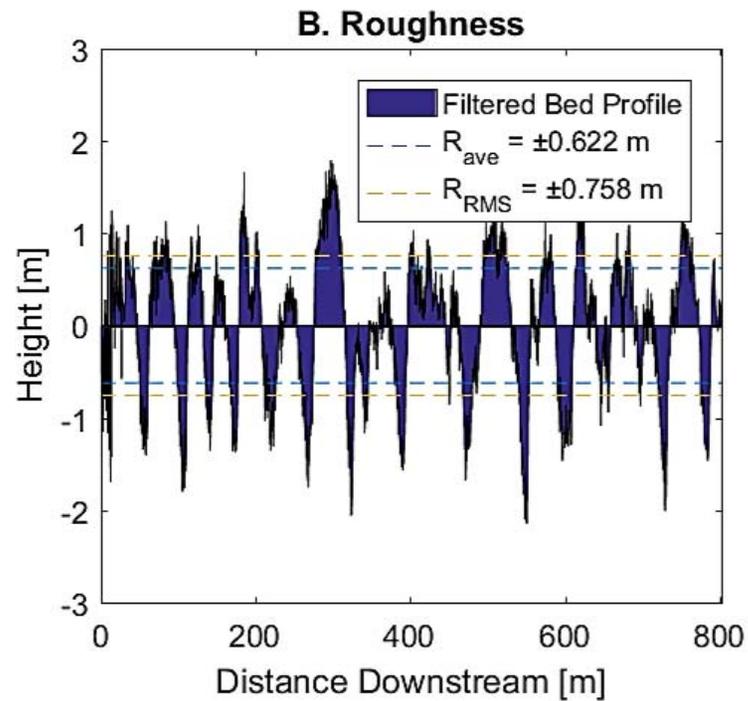
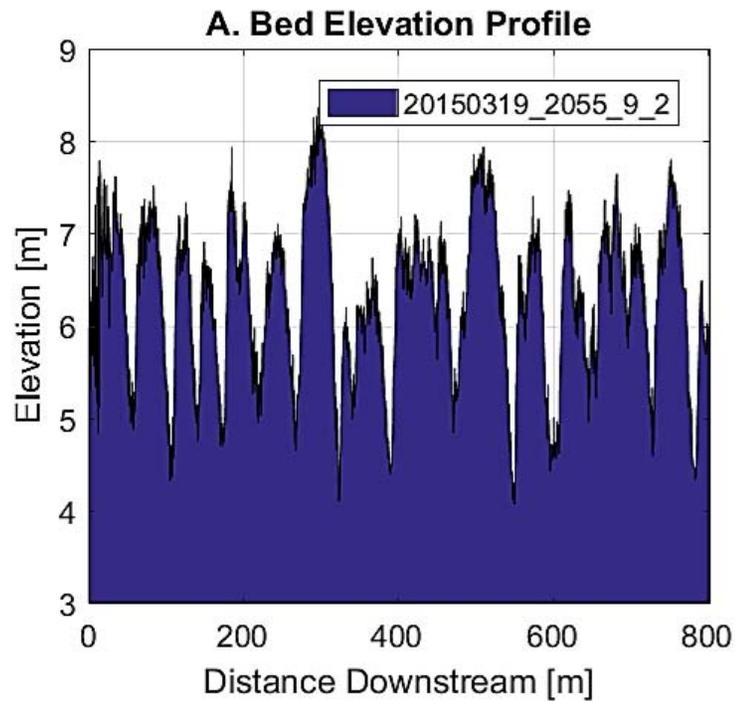


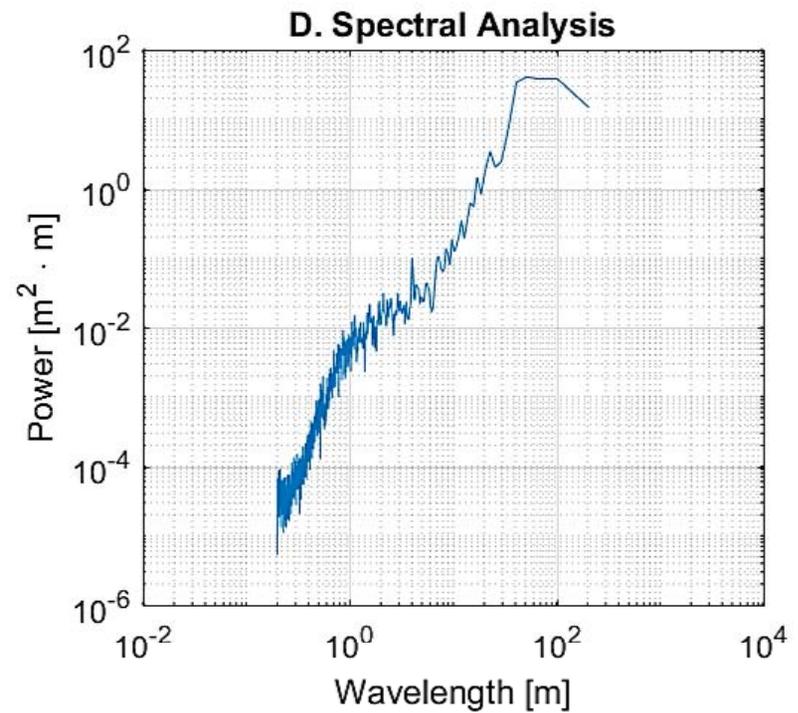
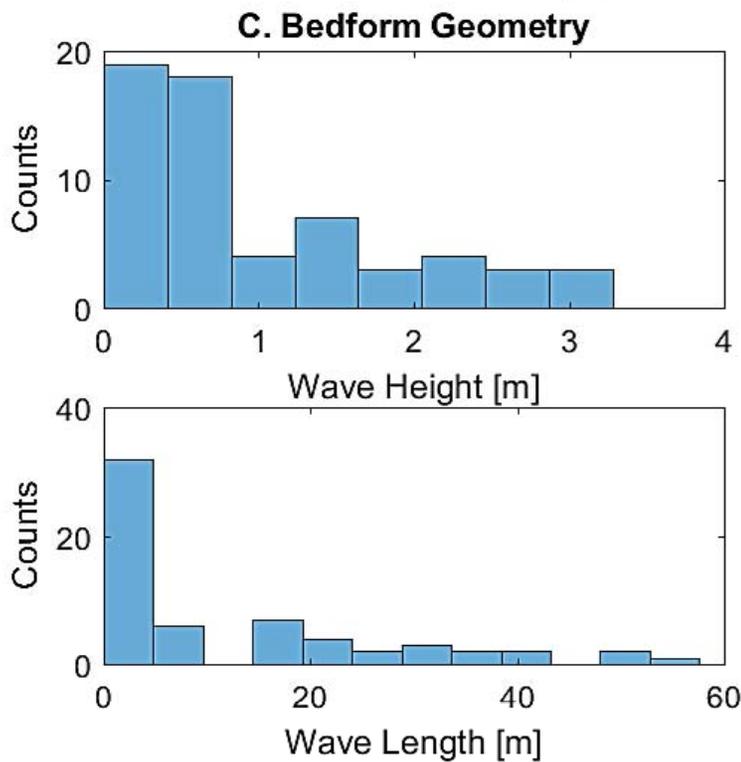
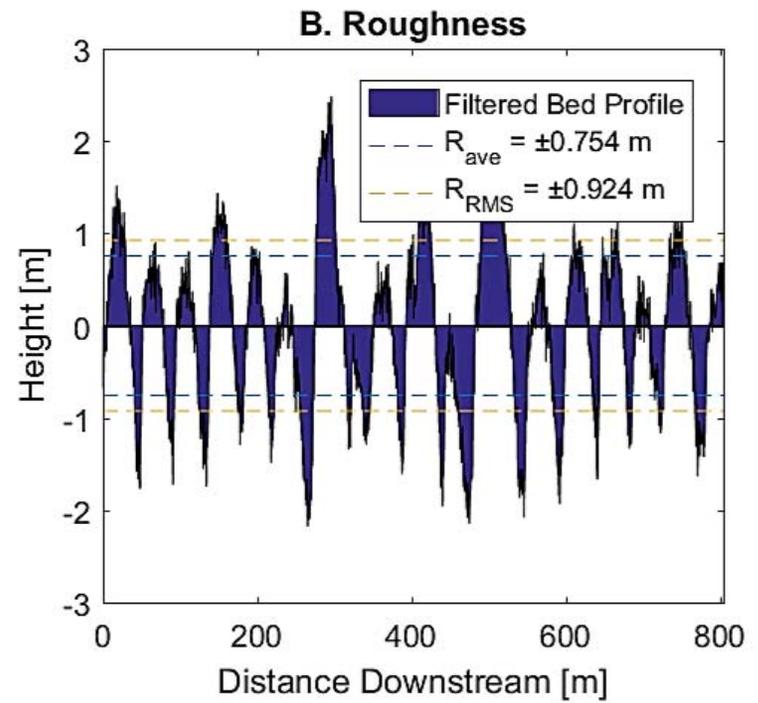
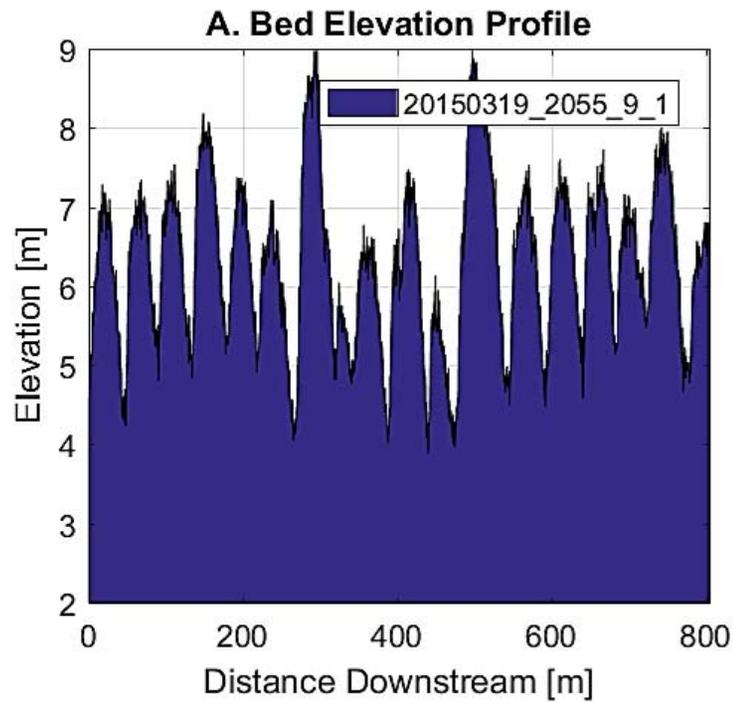


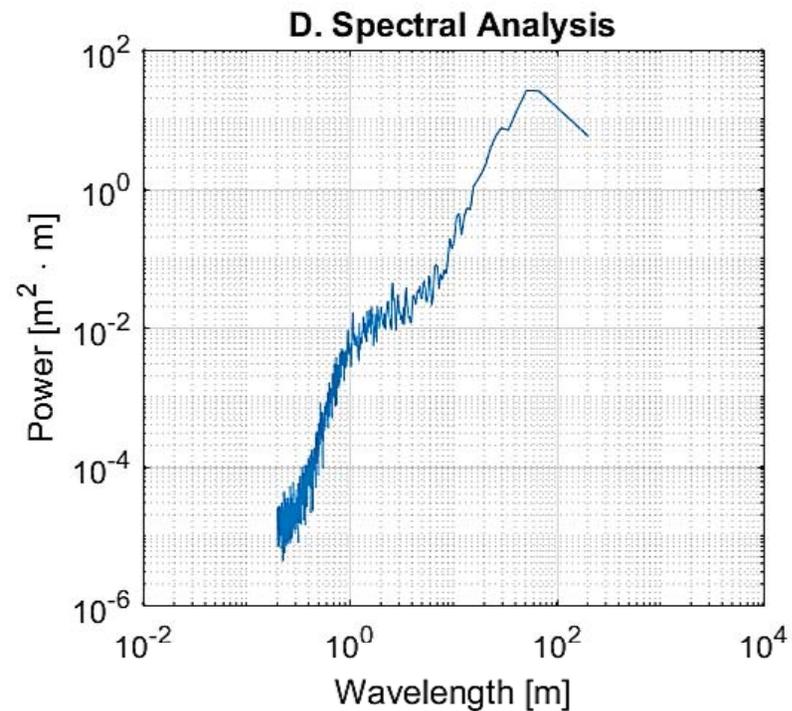
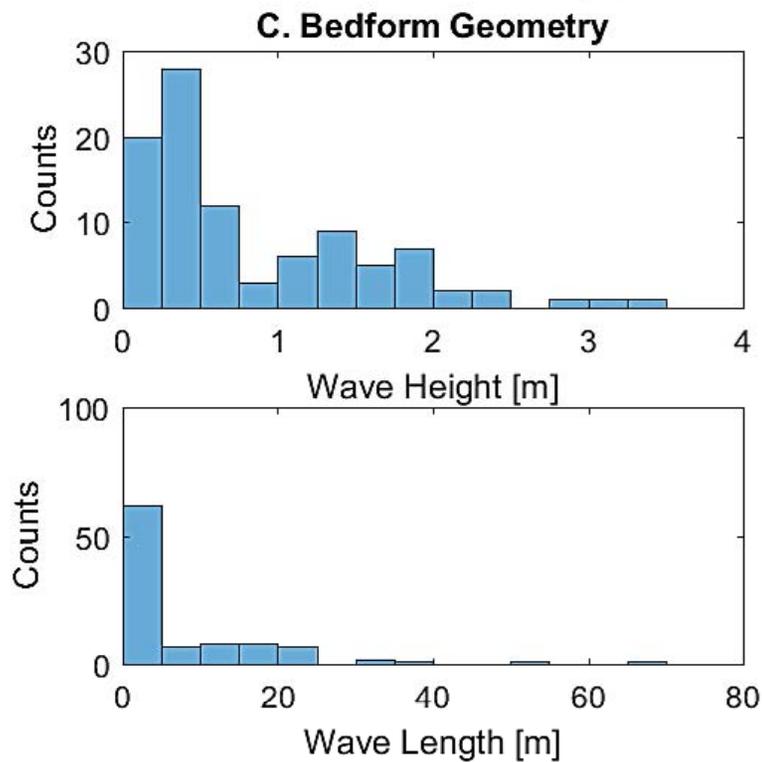
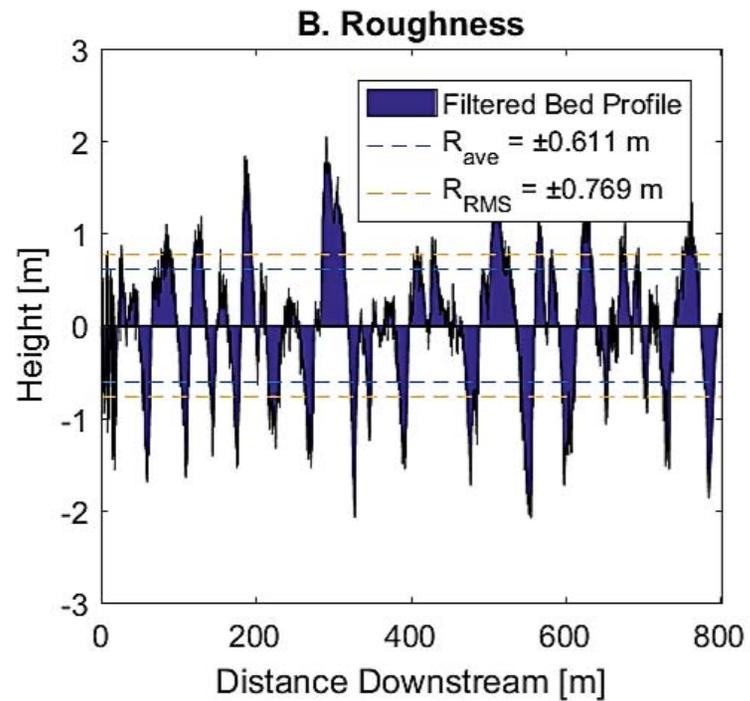
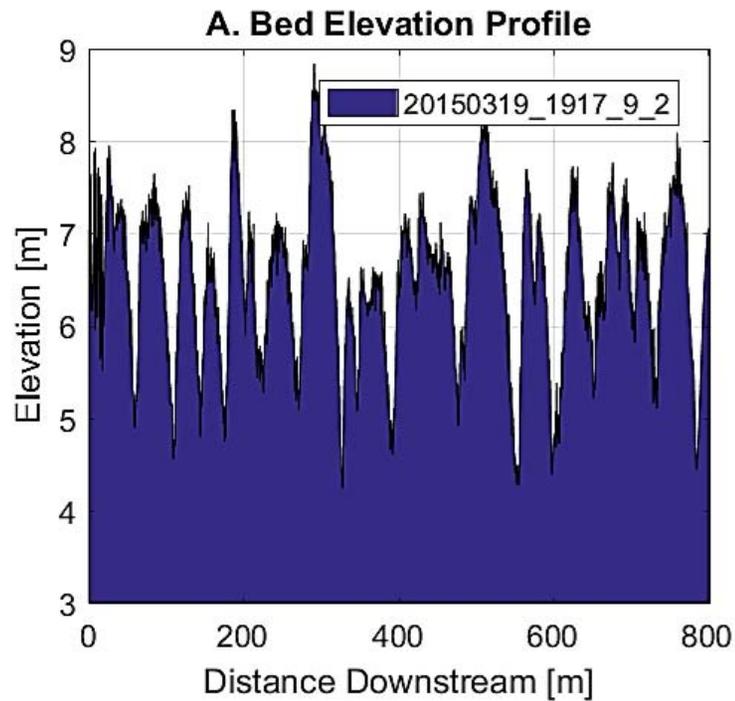
**A. Bed Elevation Profile****B. Roughness****C. Bedform Geometry****D. Spectral Analysis**

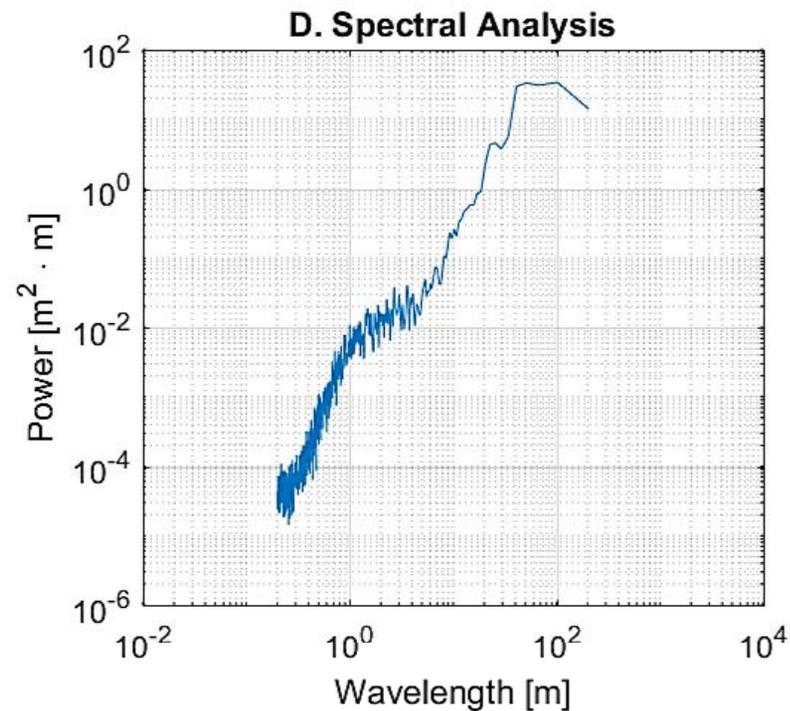
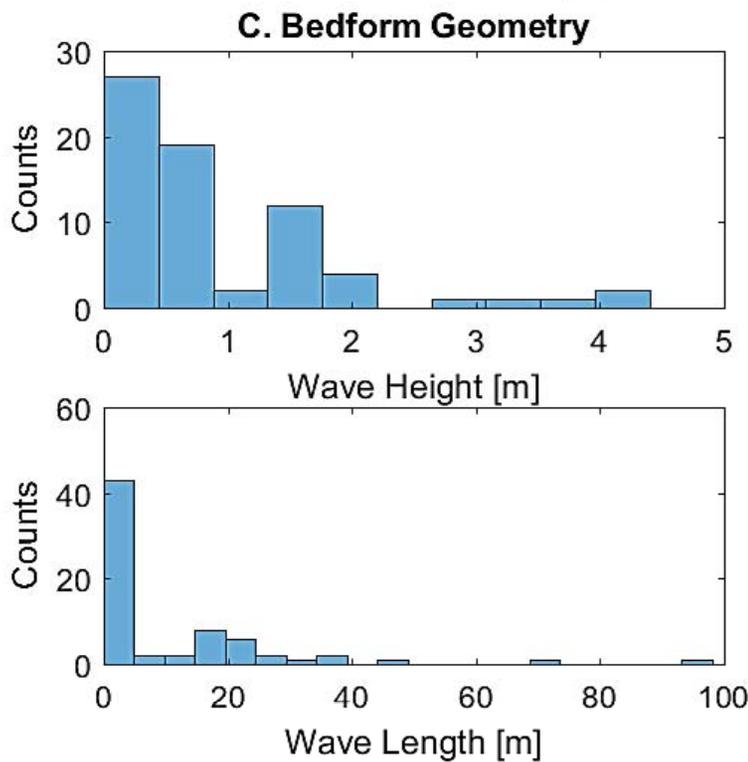
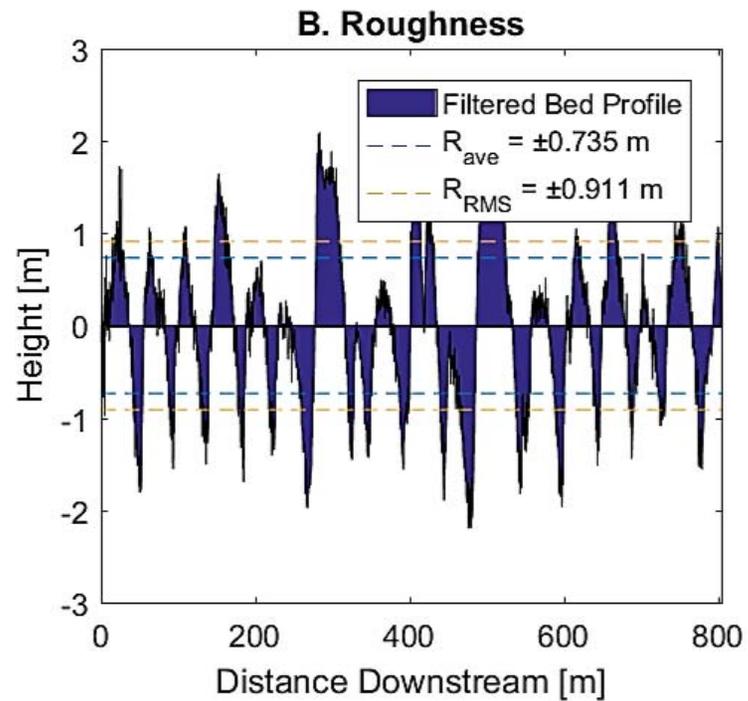
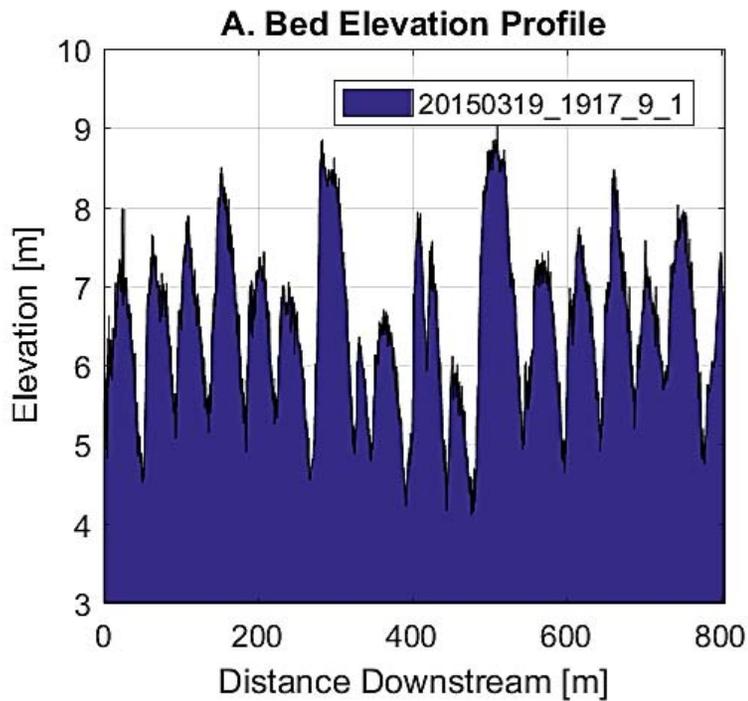


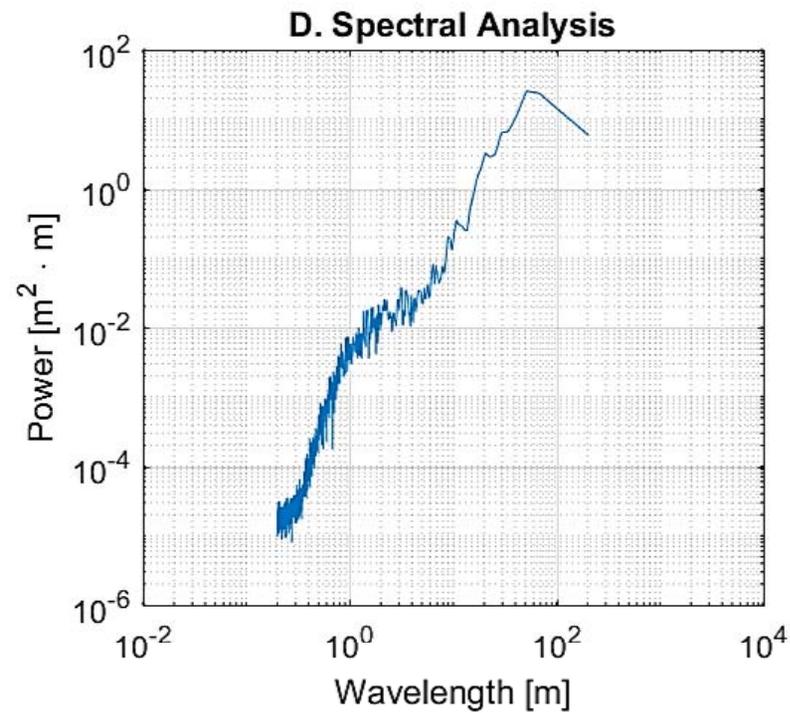
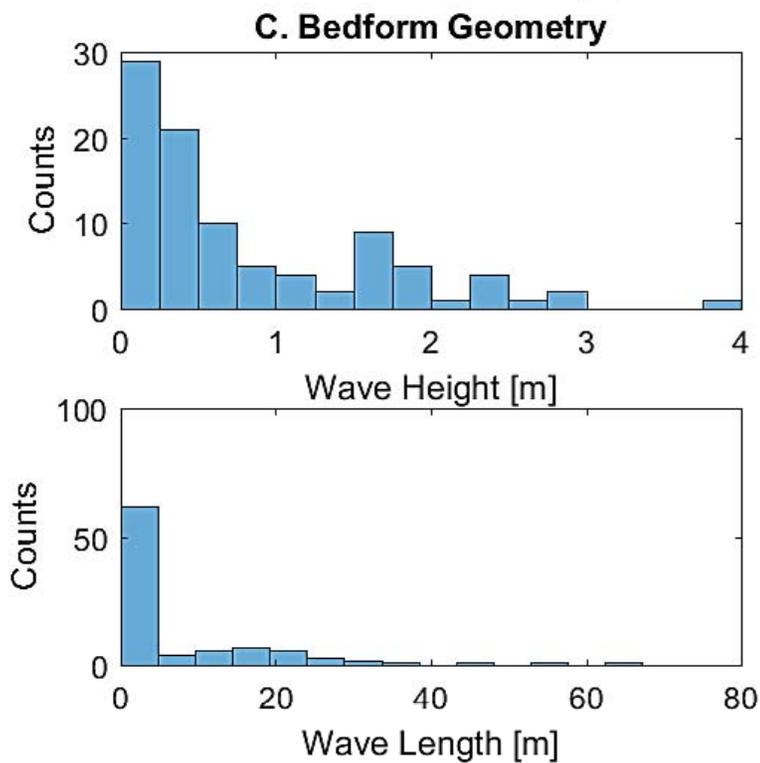
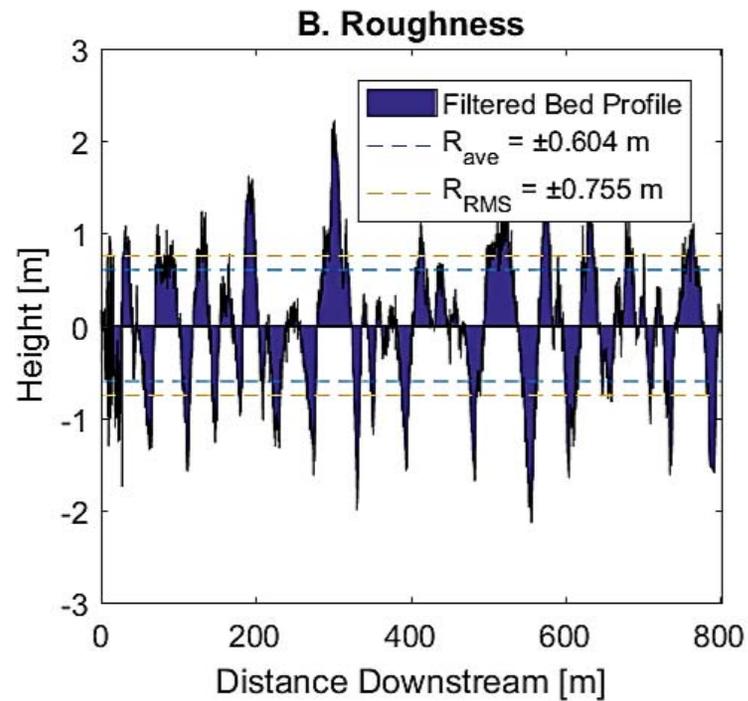
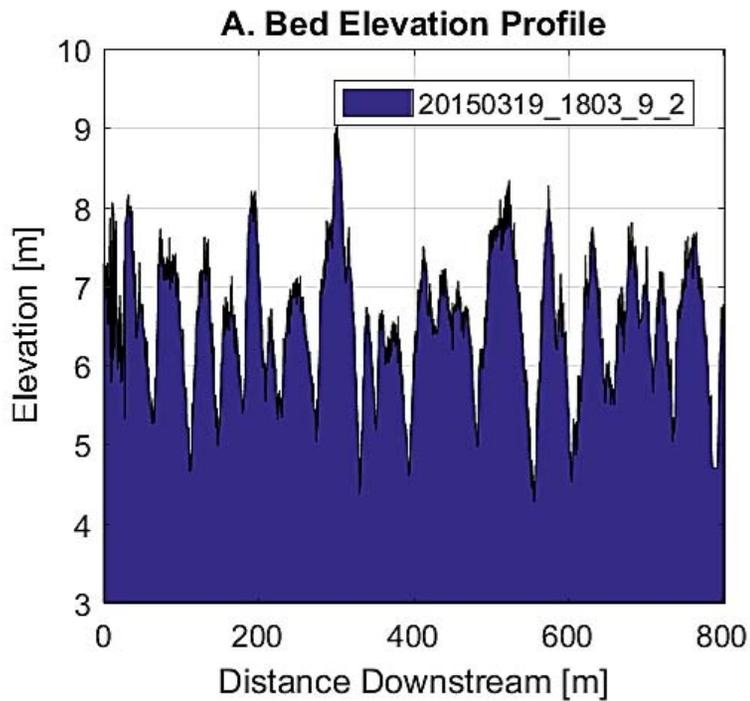


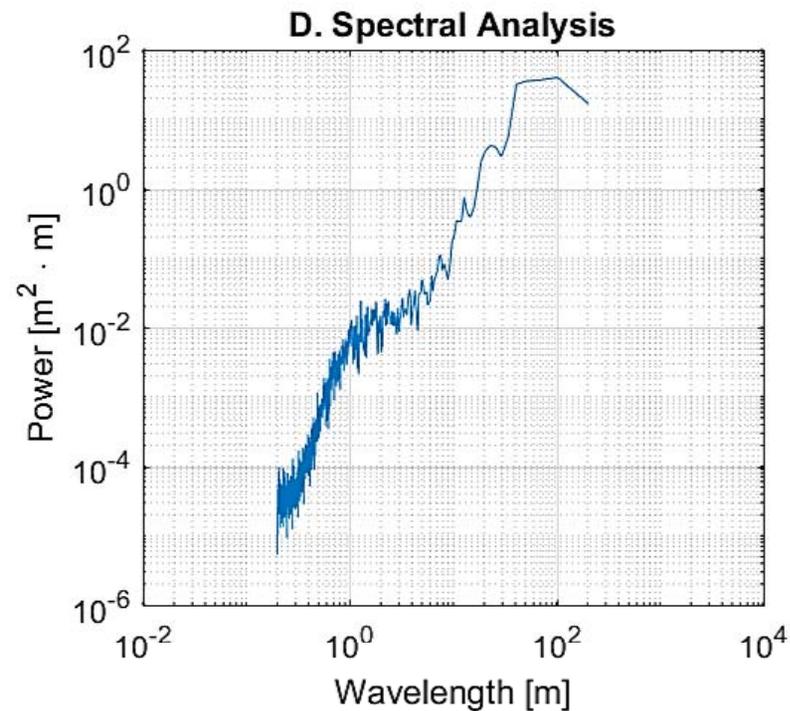
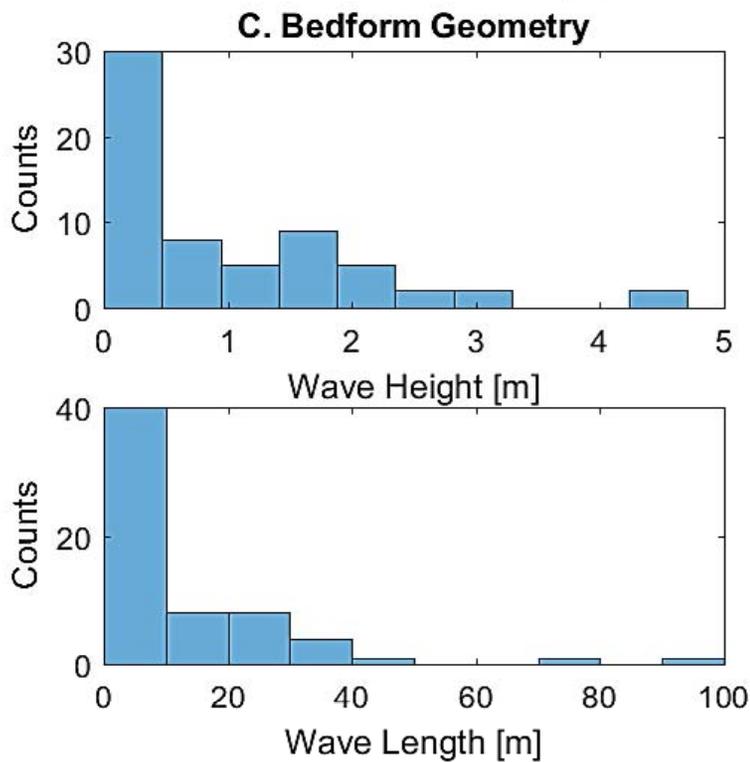
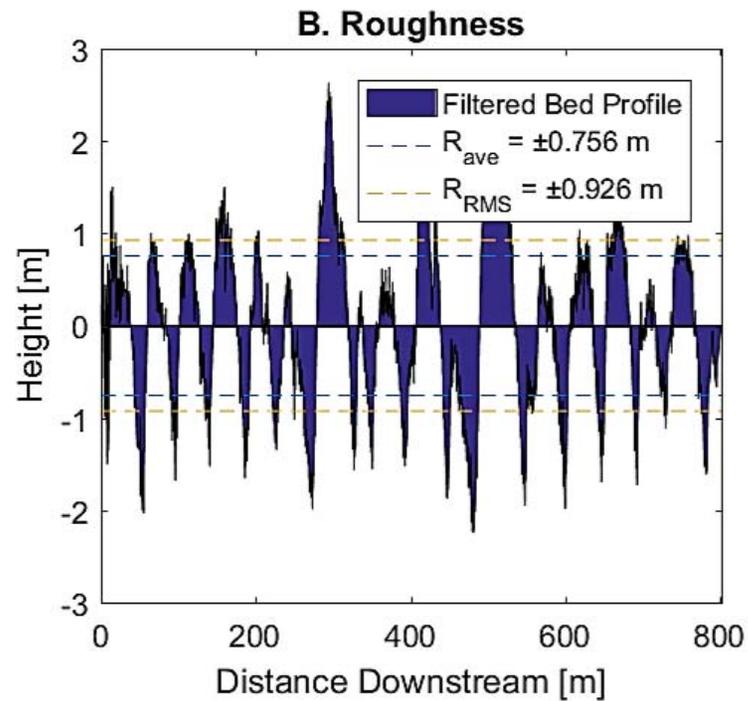
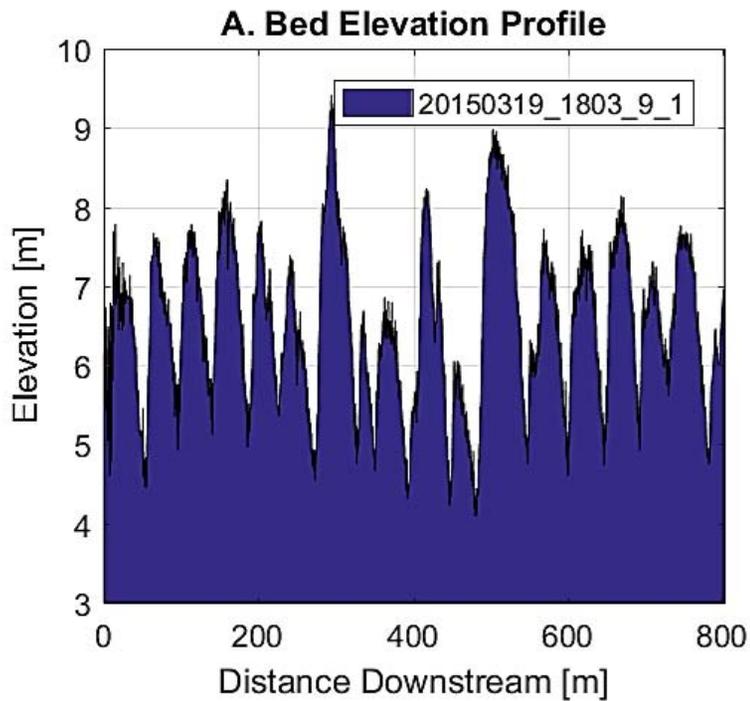


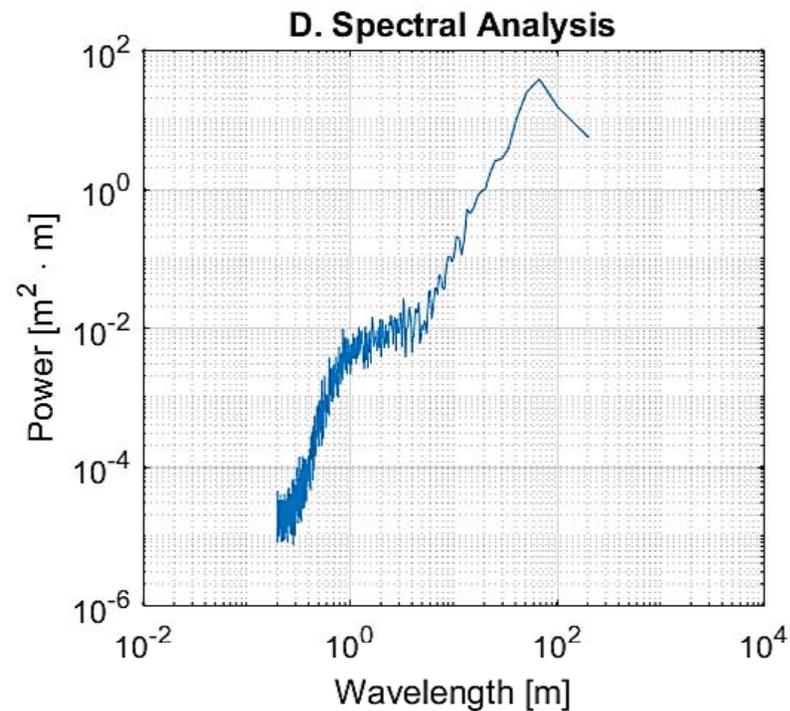
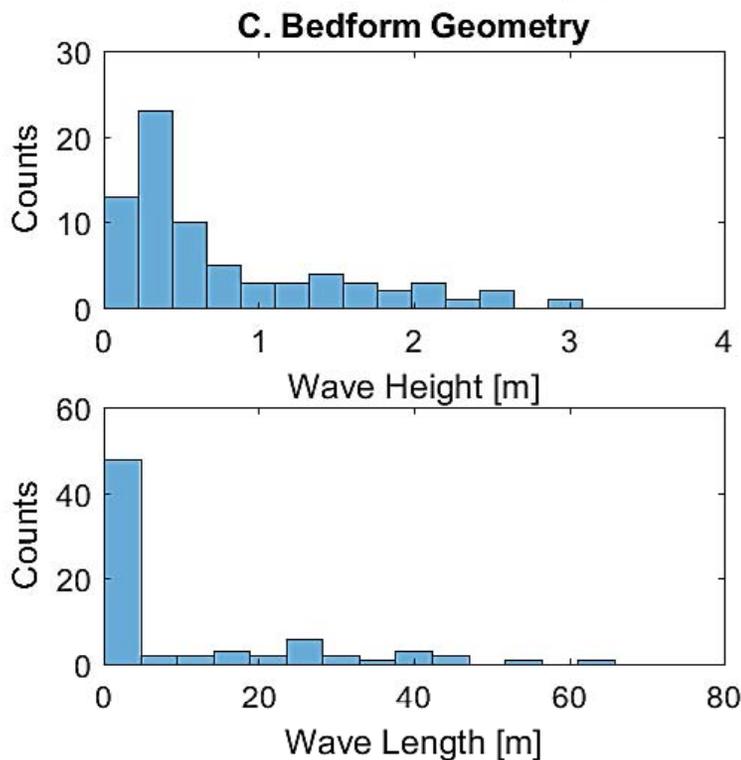
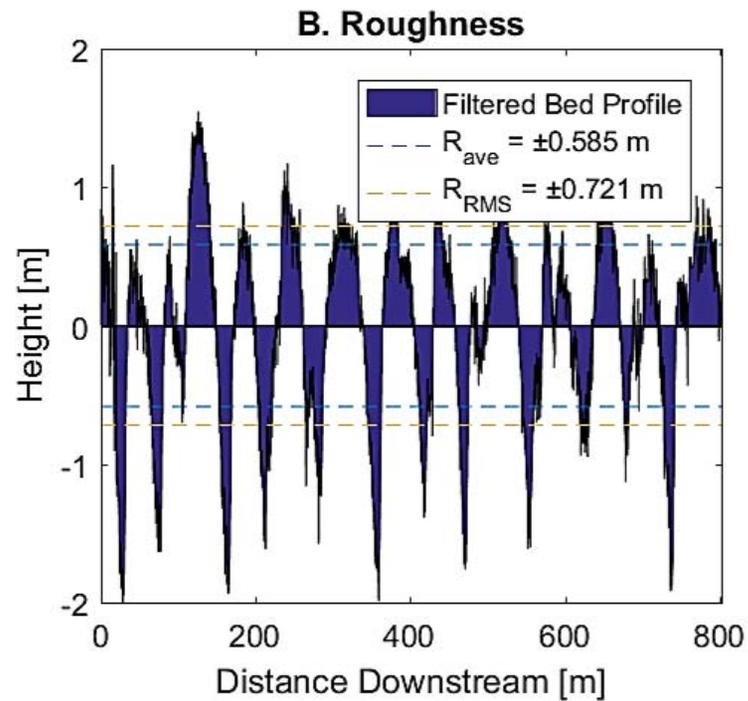
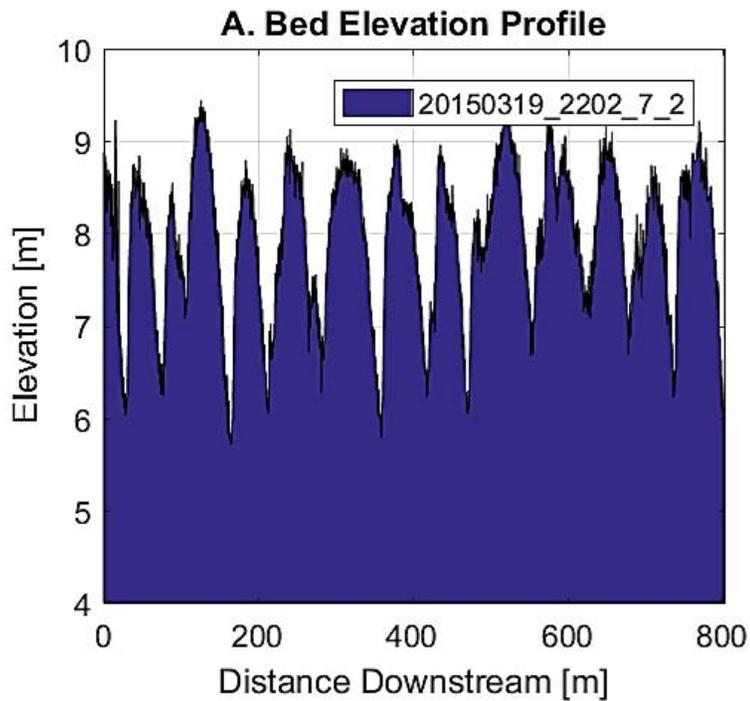




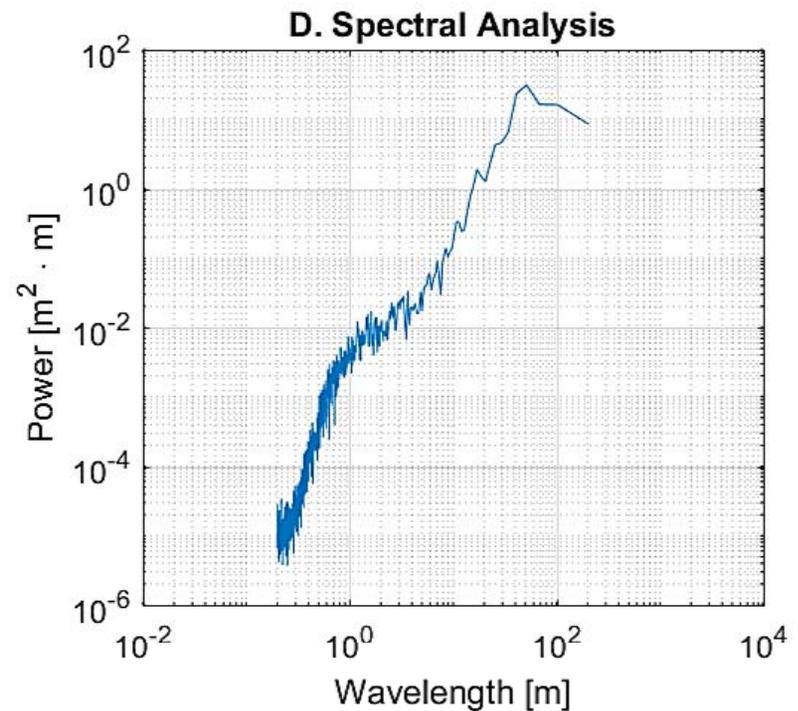
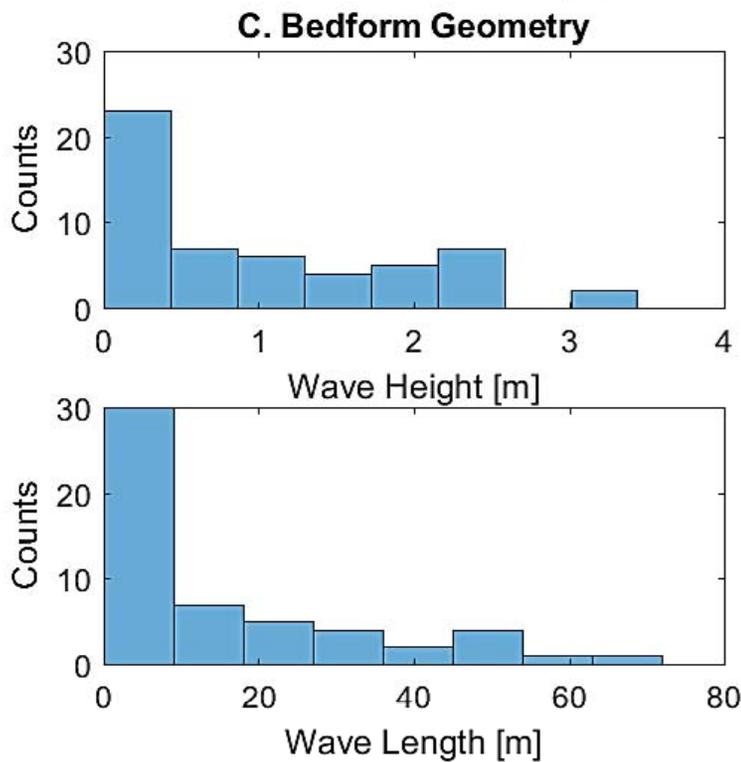
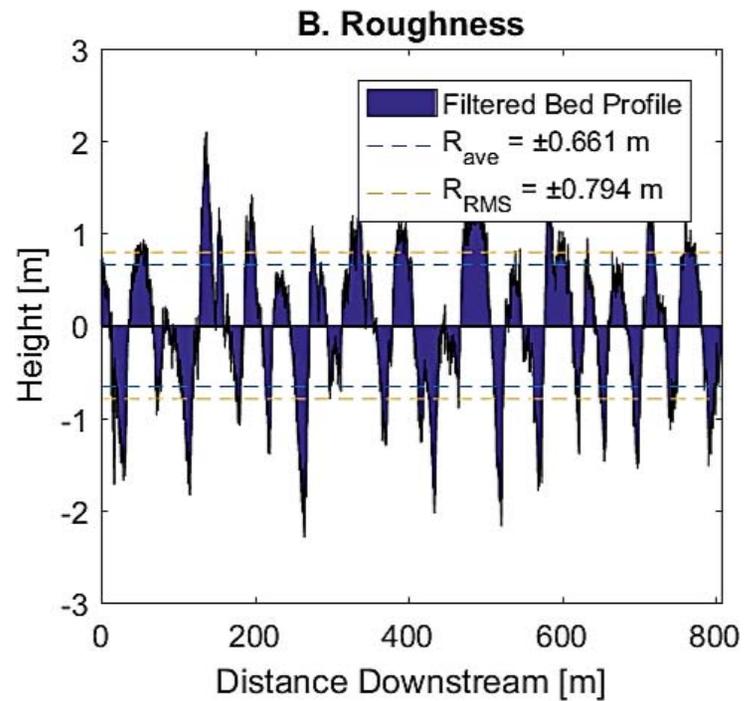
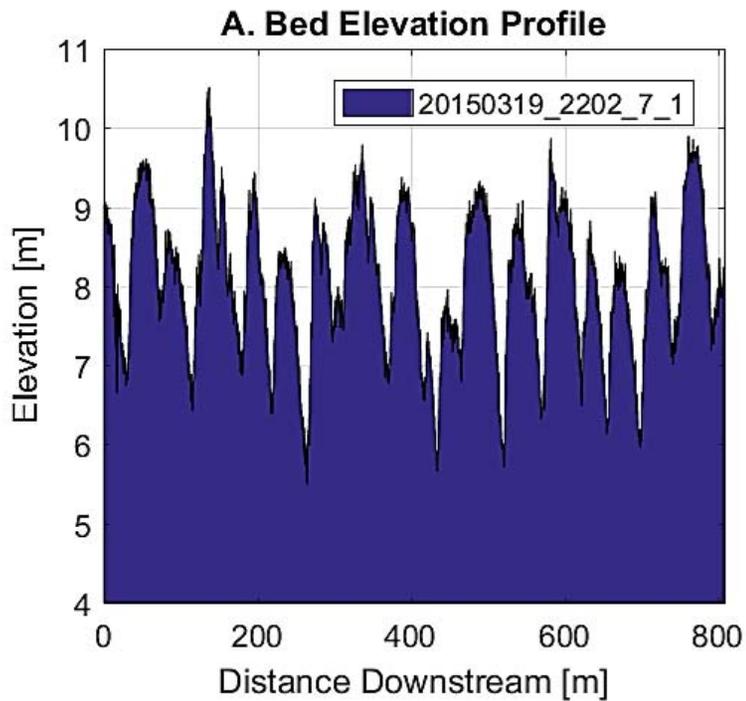


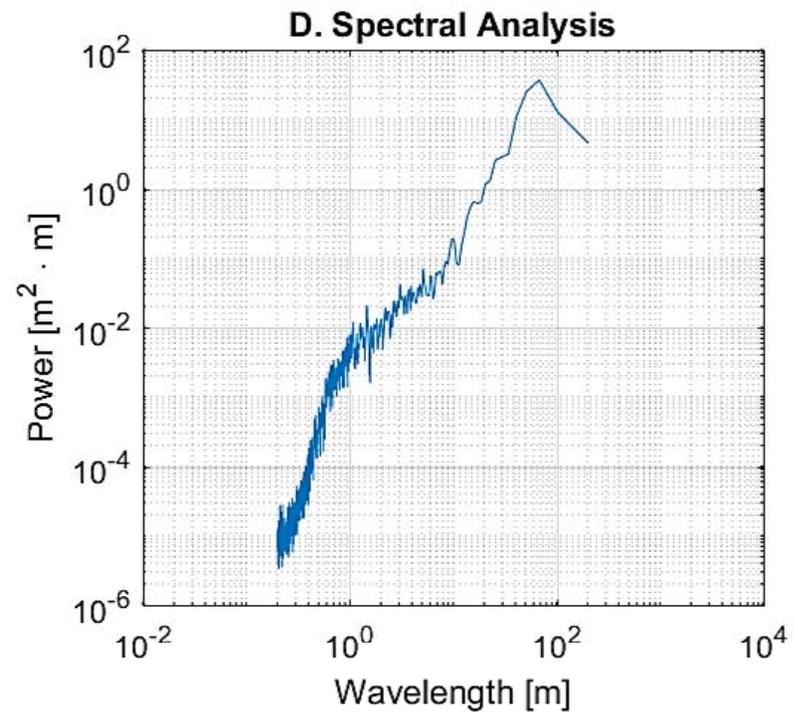
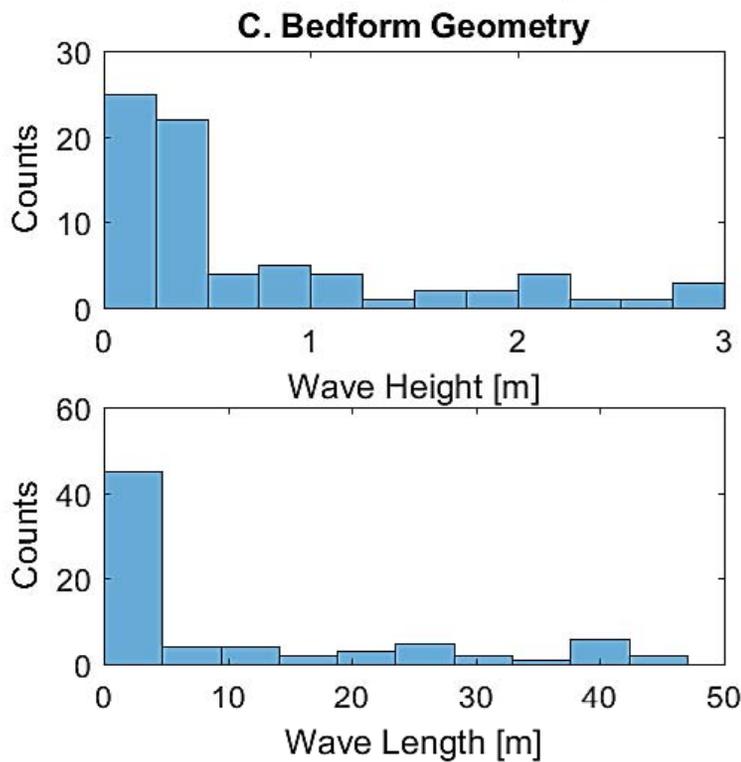
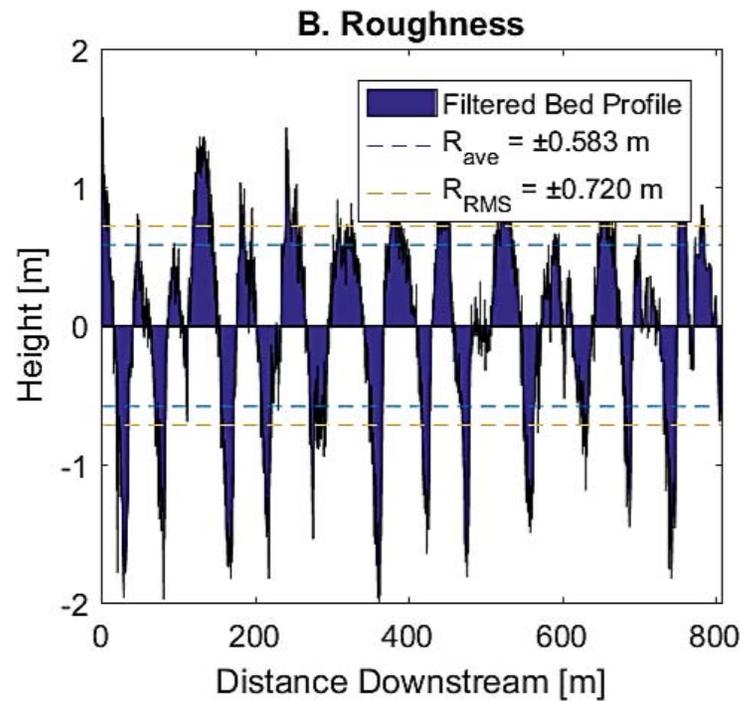
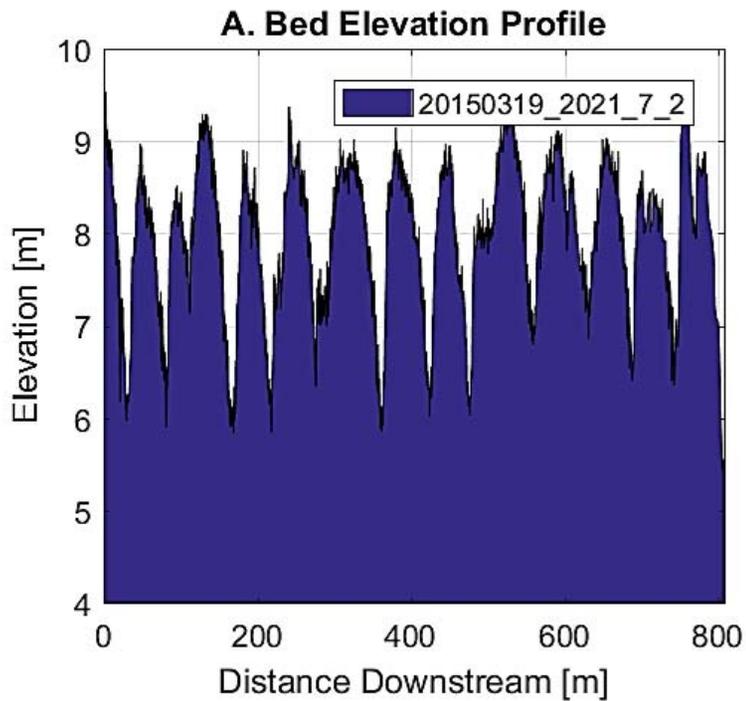


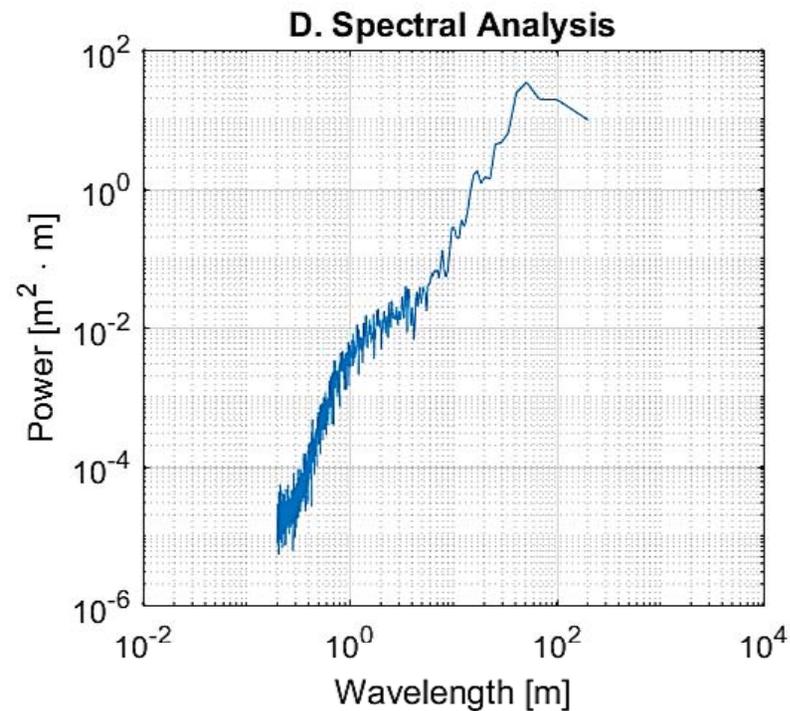
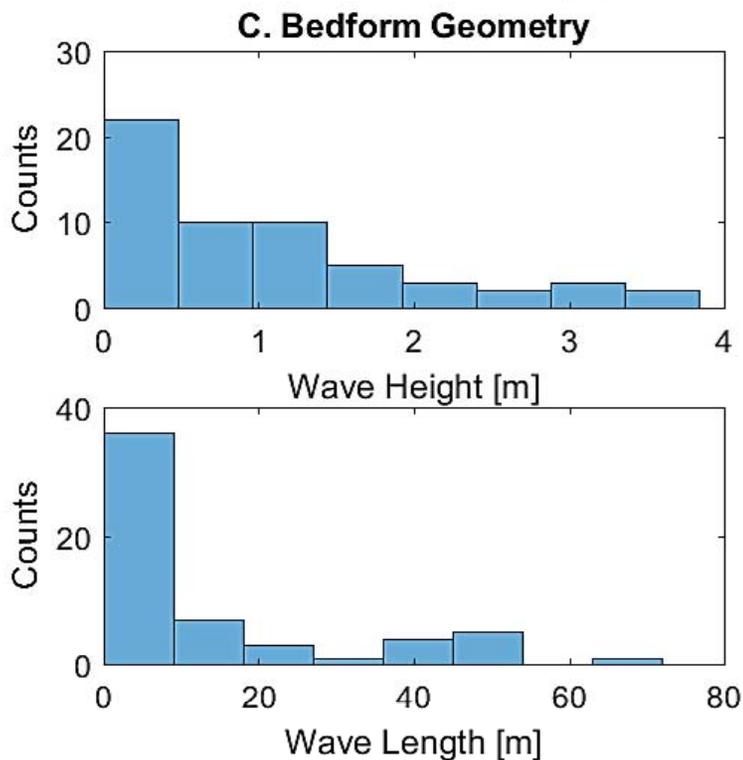
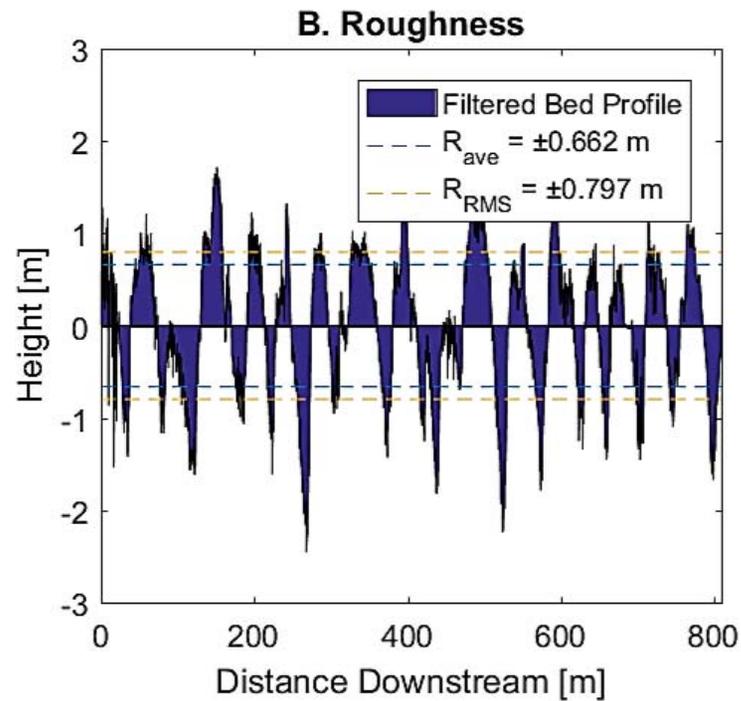
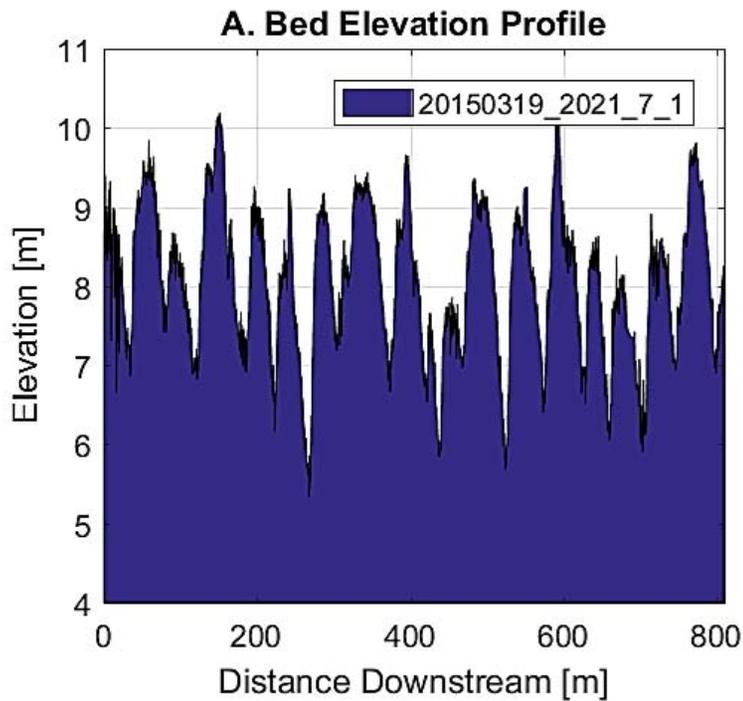


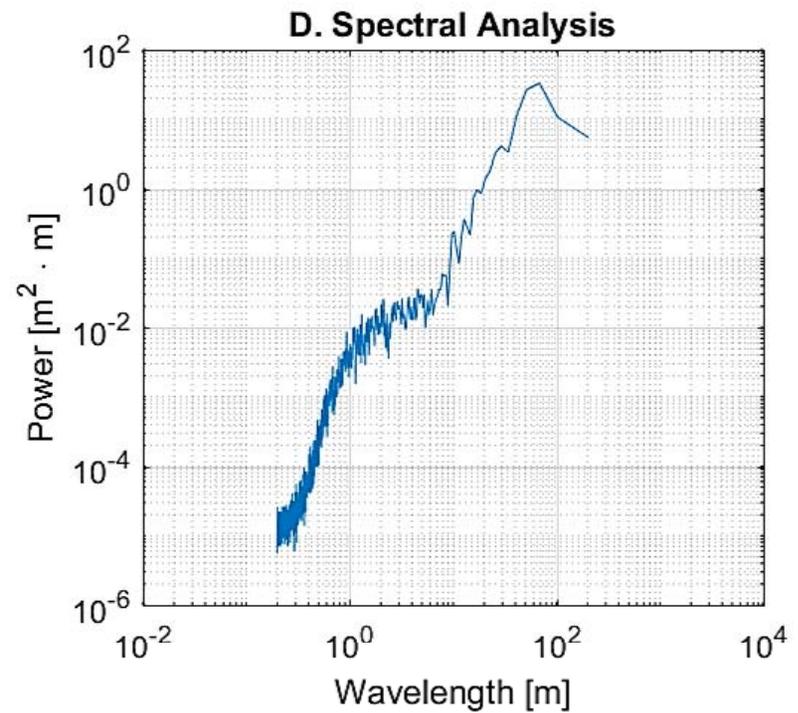
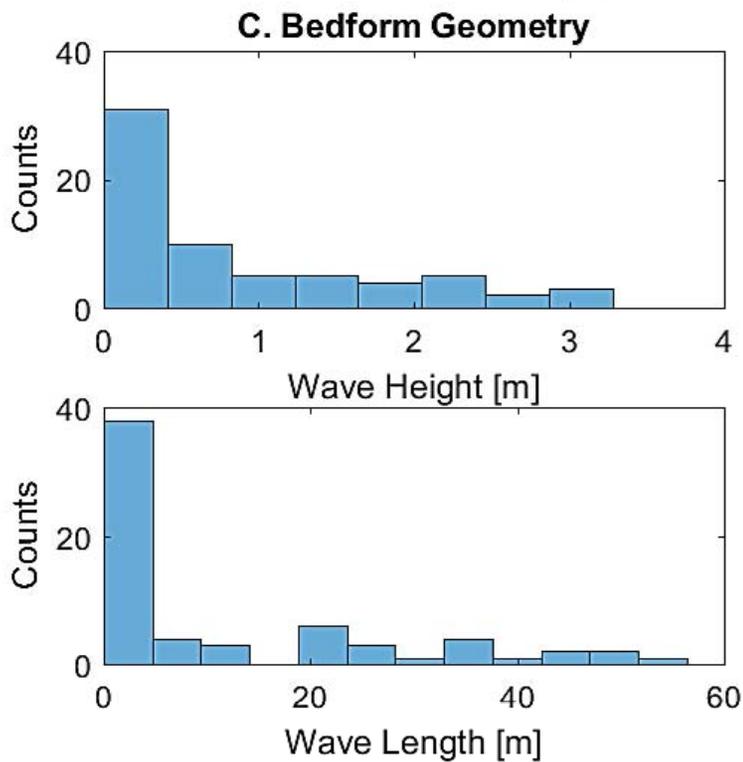
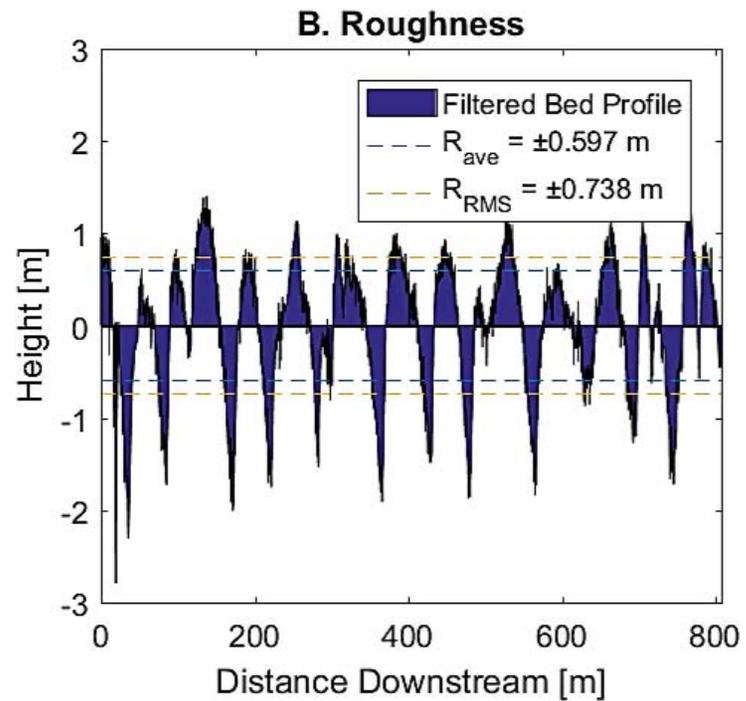
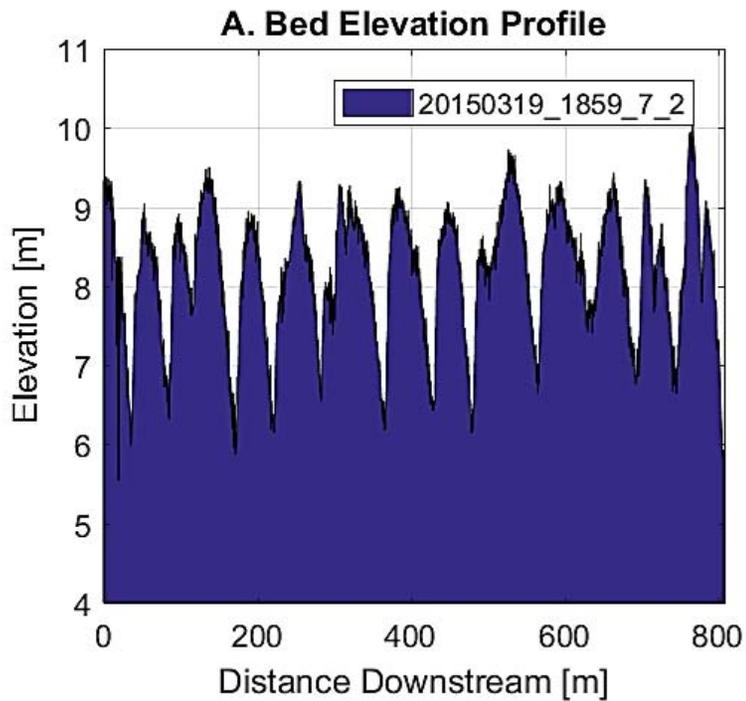


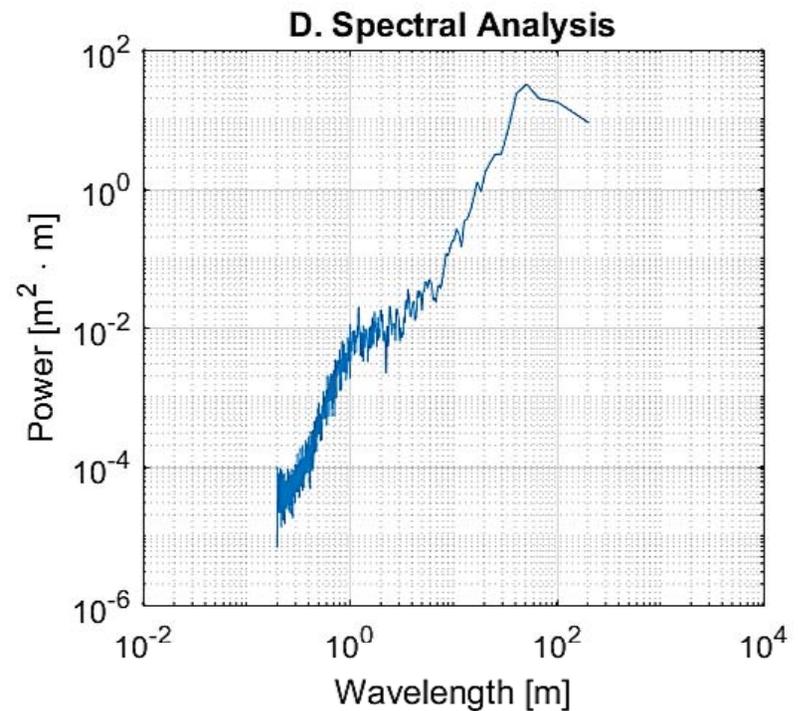
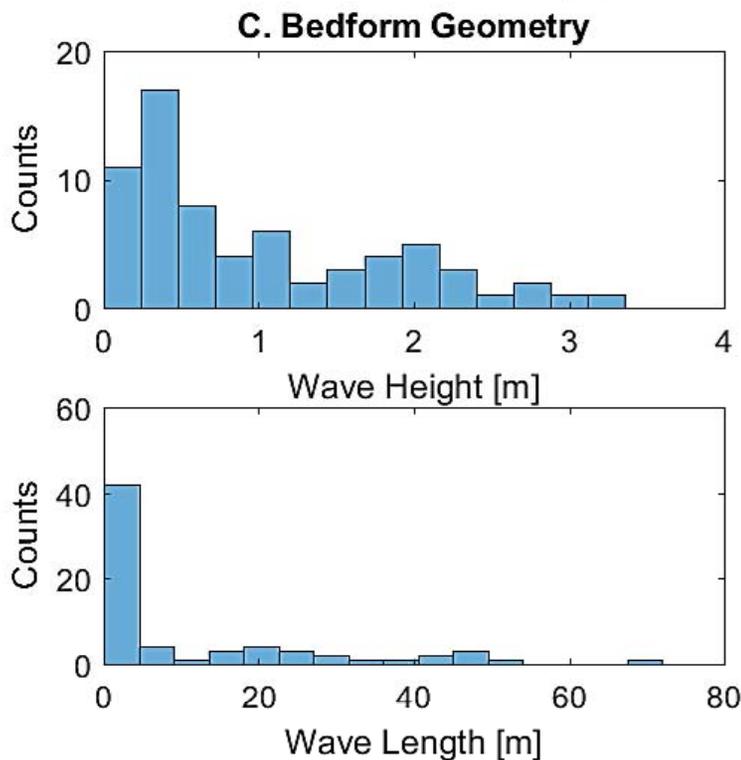
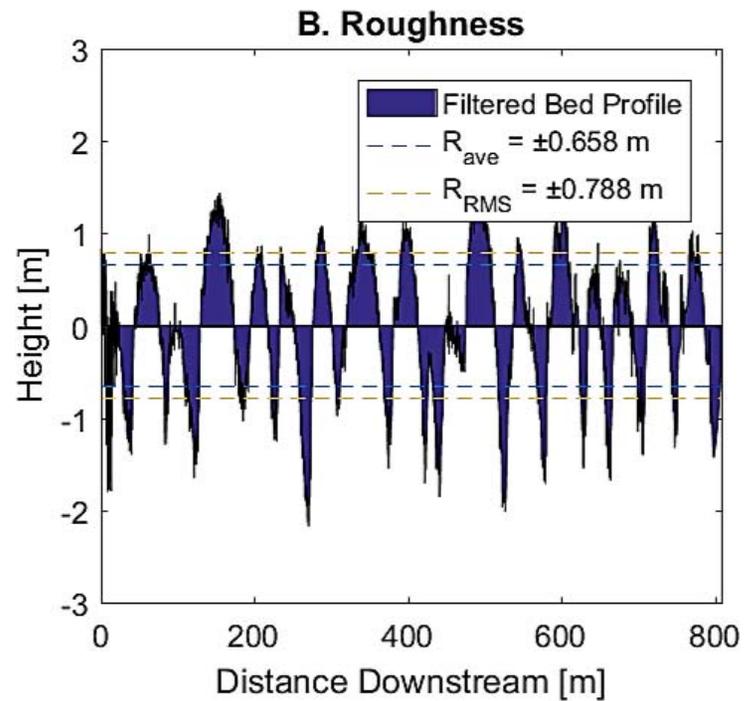
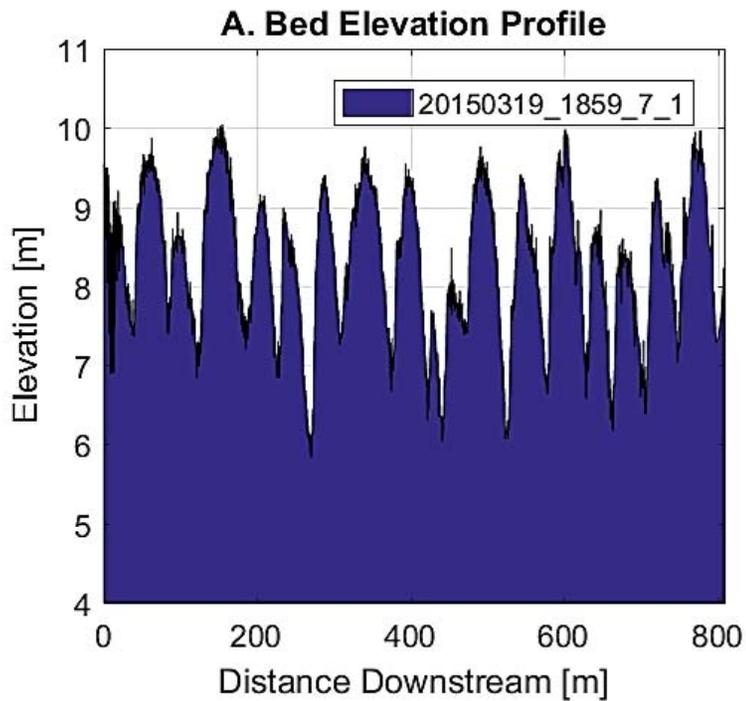


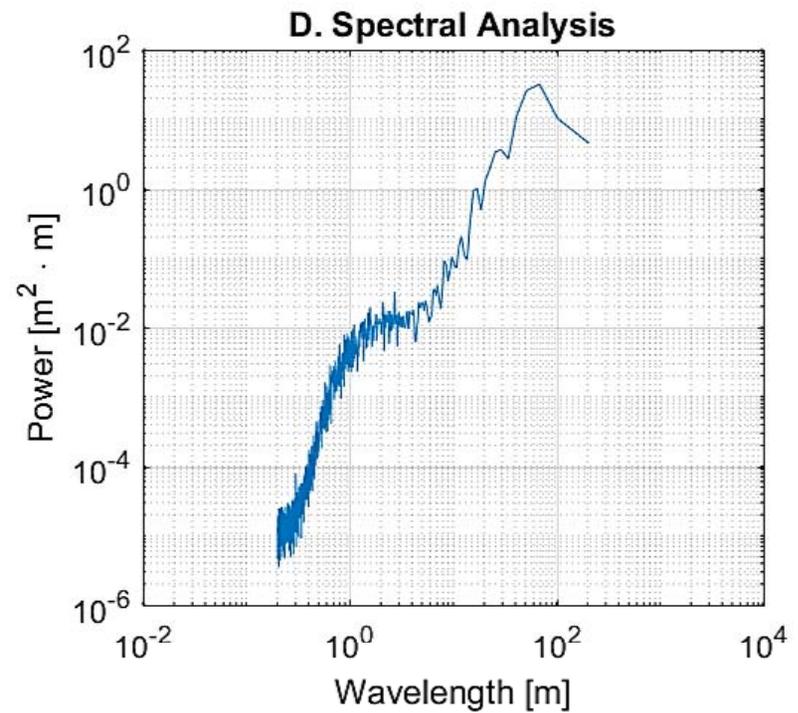
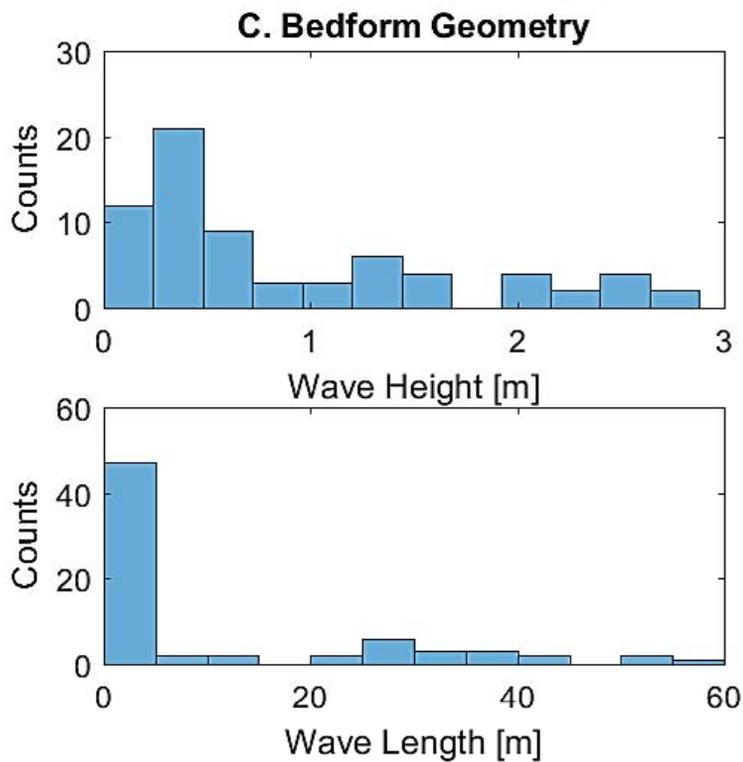
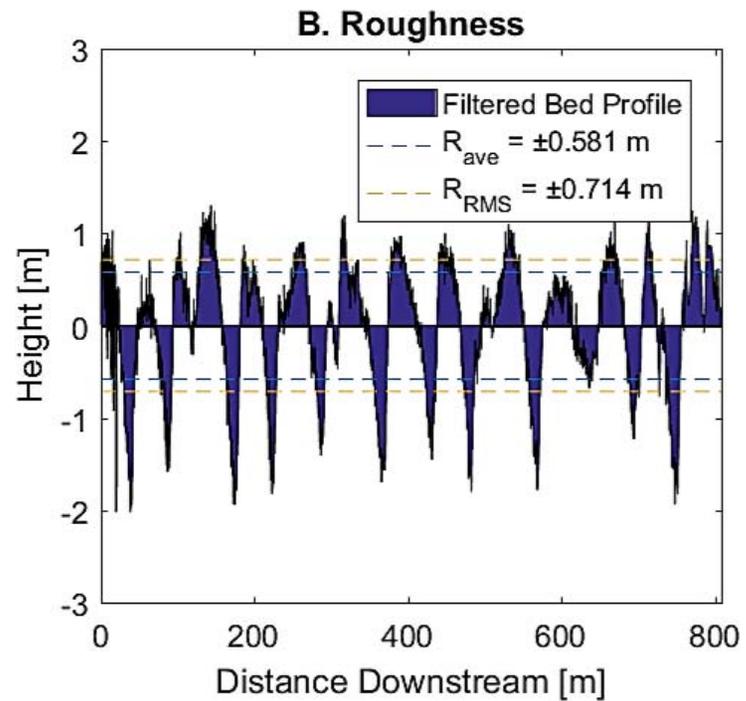
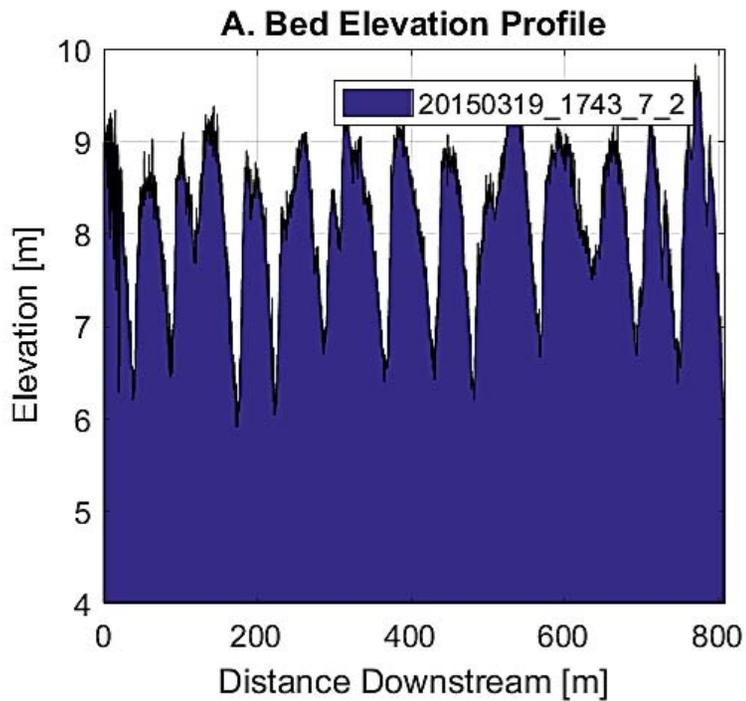


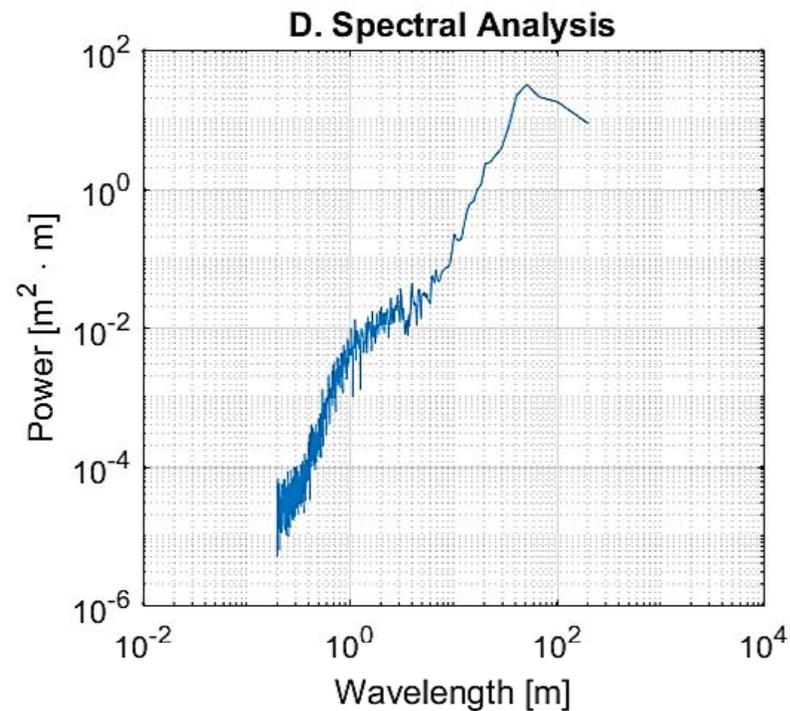
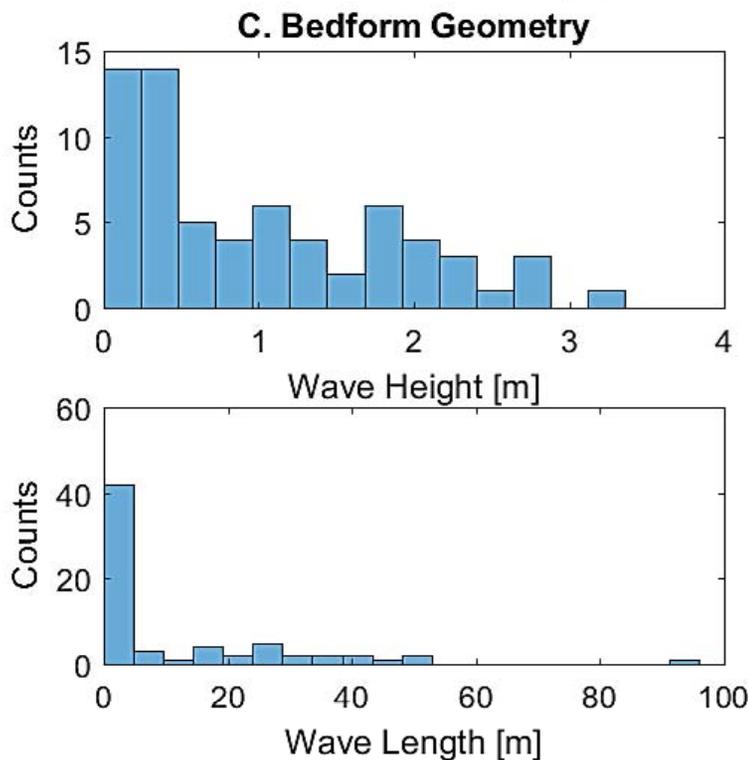
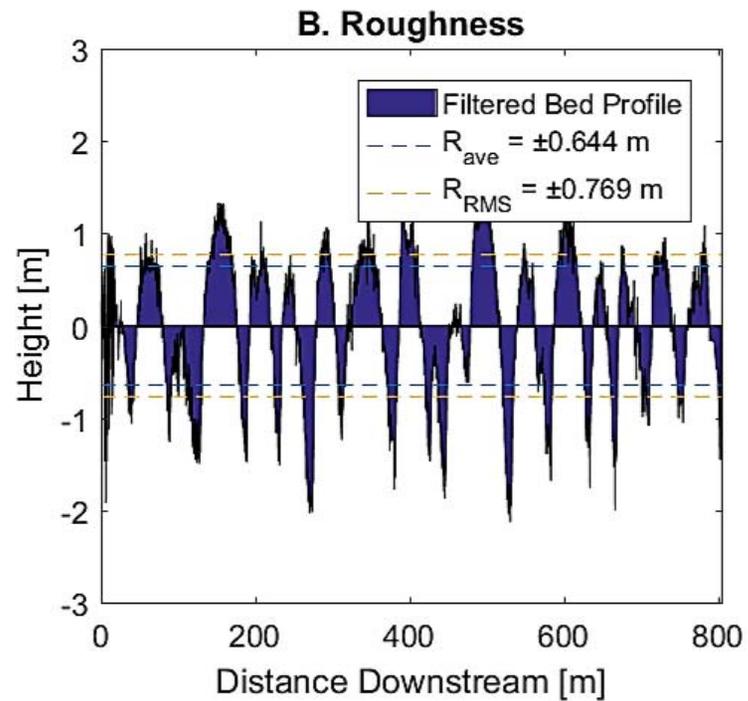
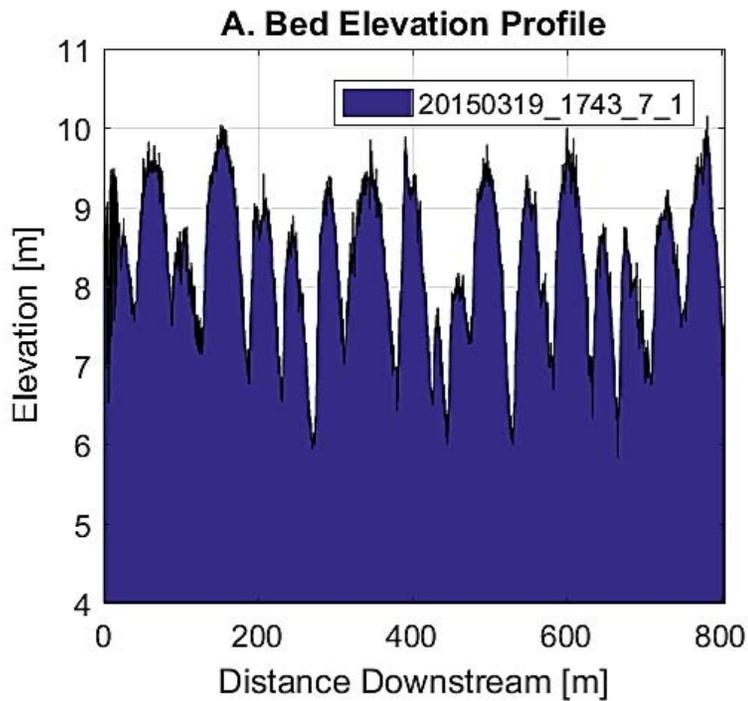


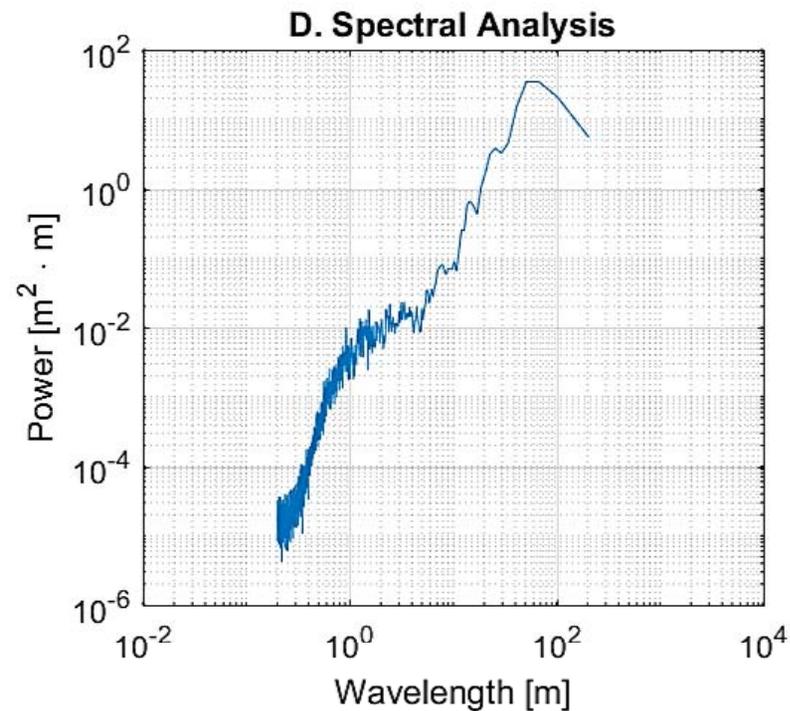
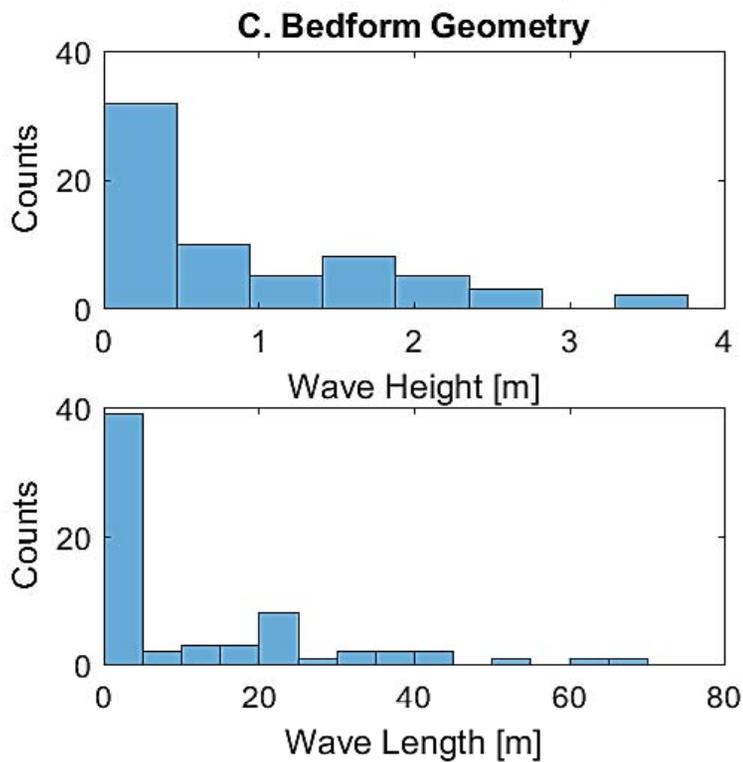
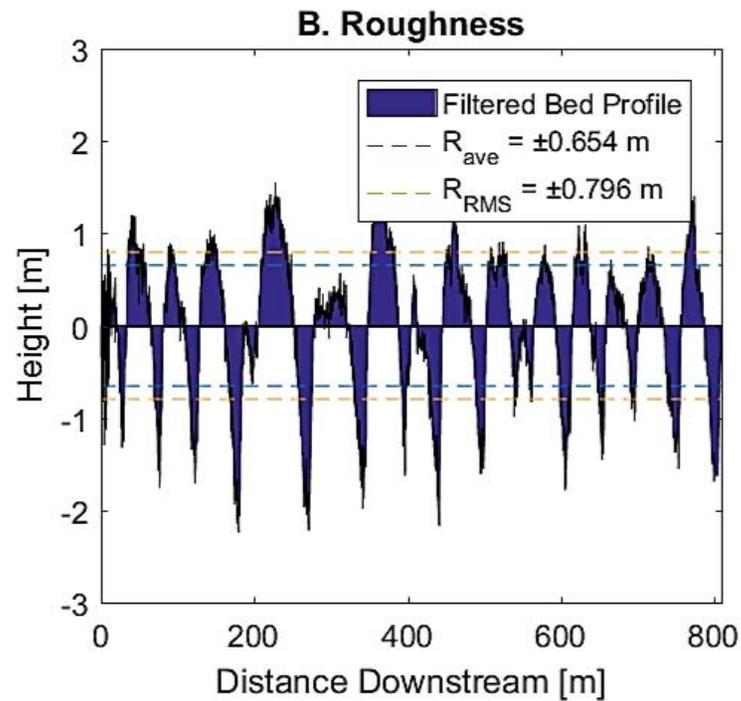
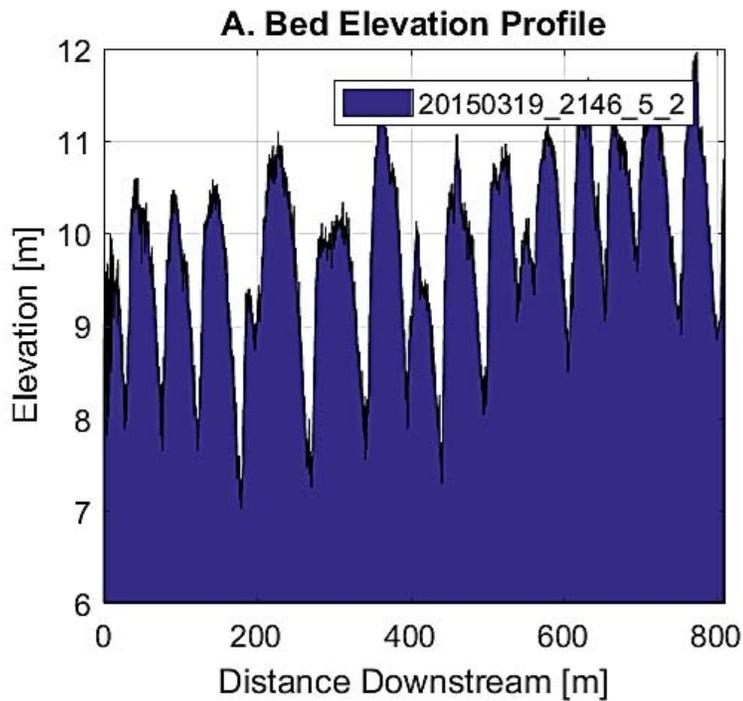




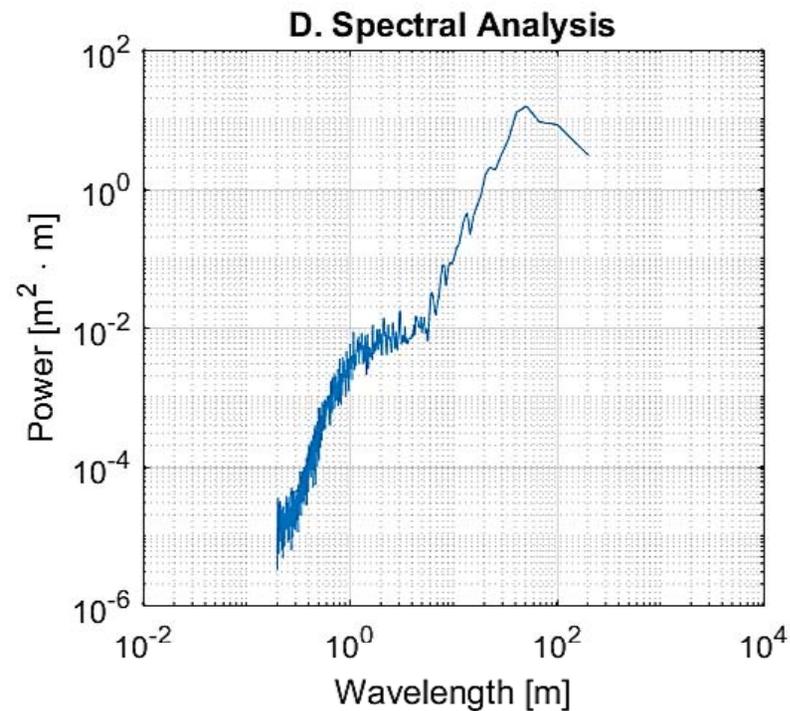
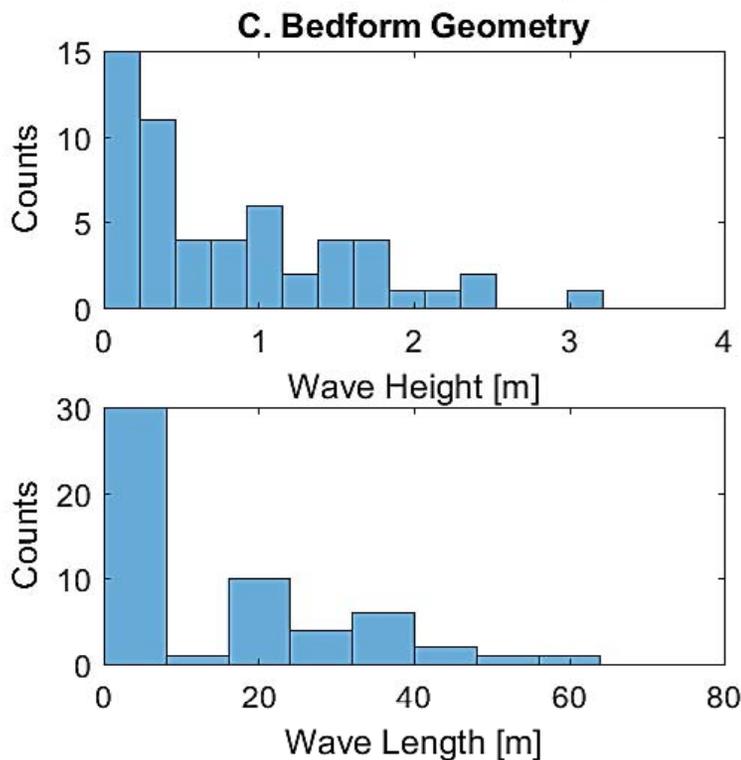
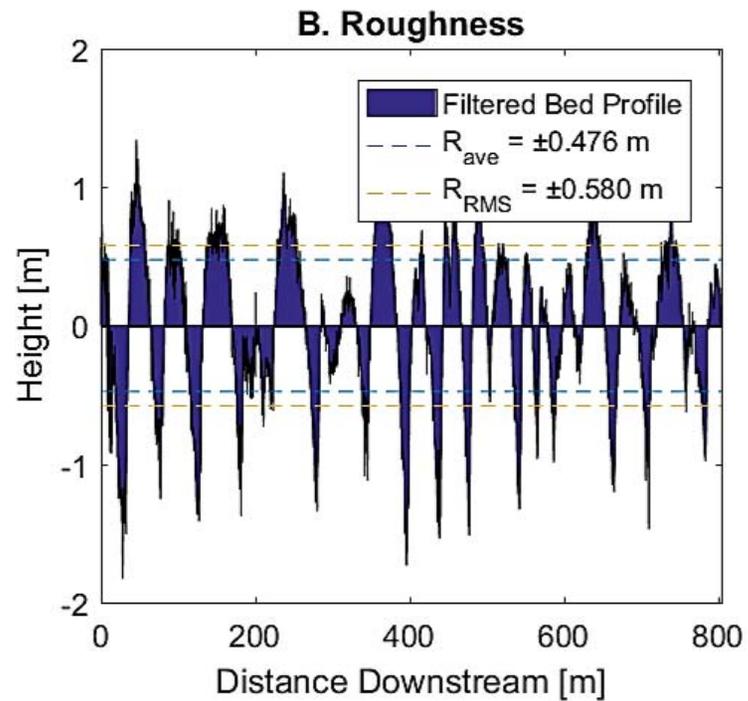
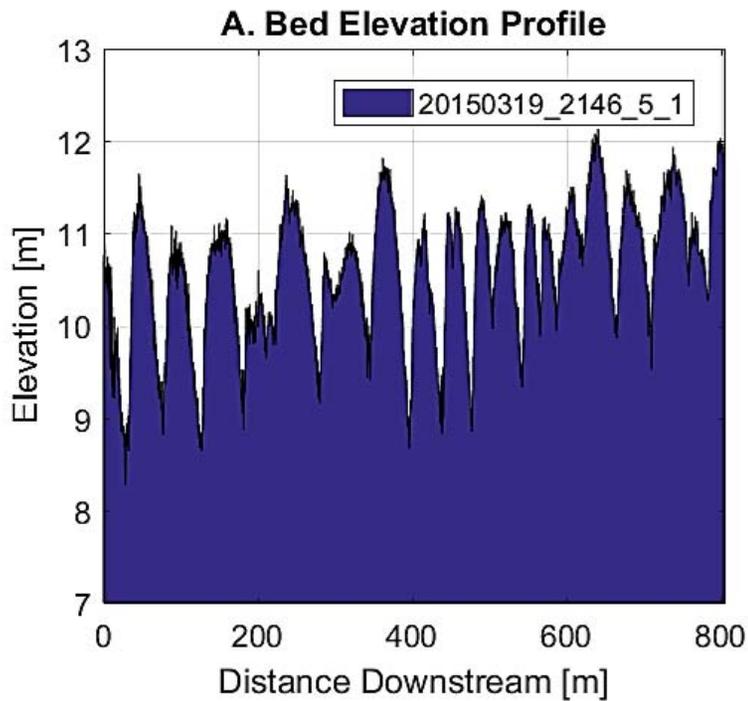


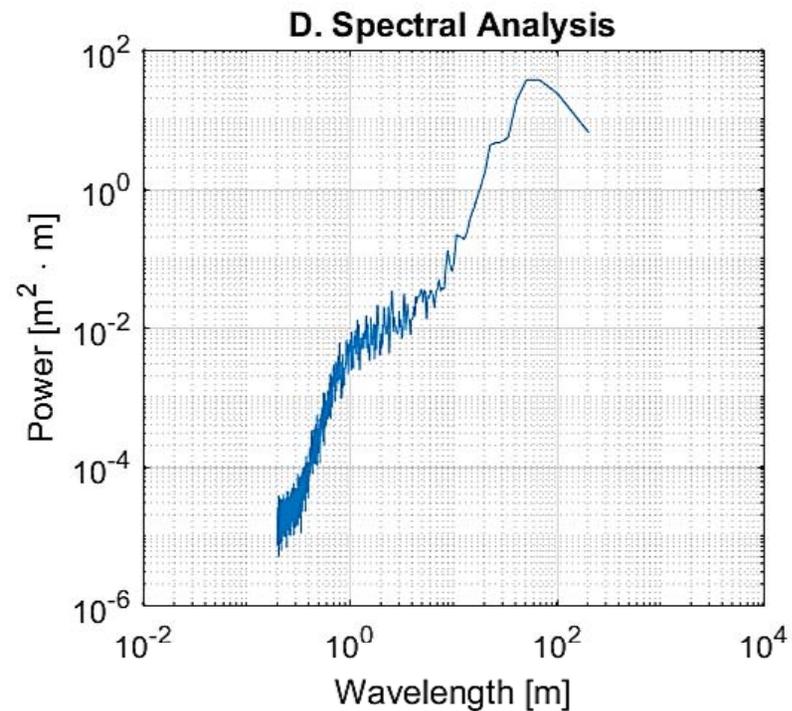
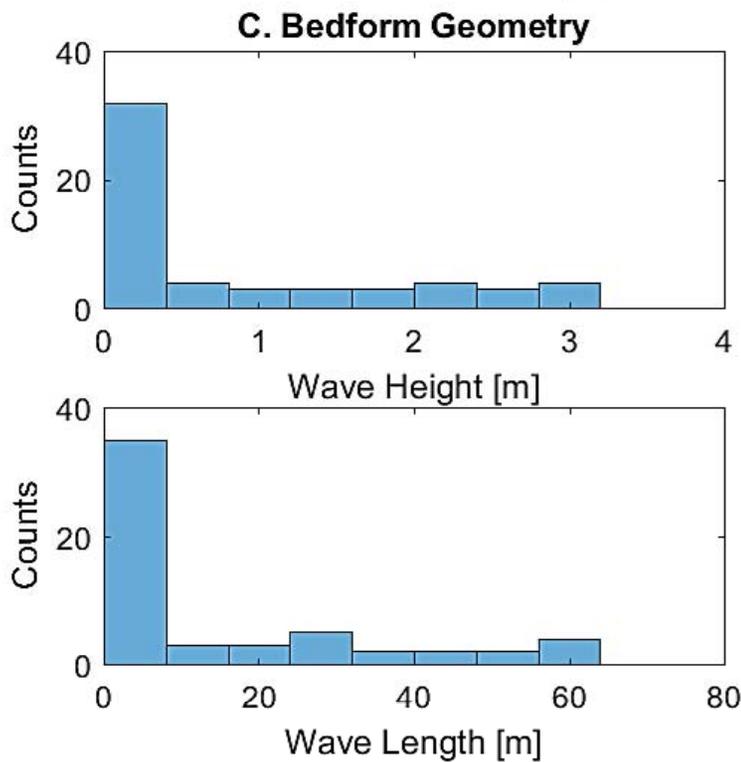
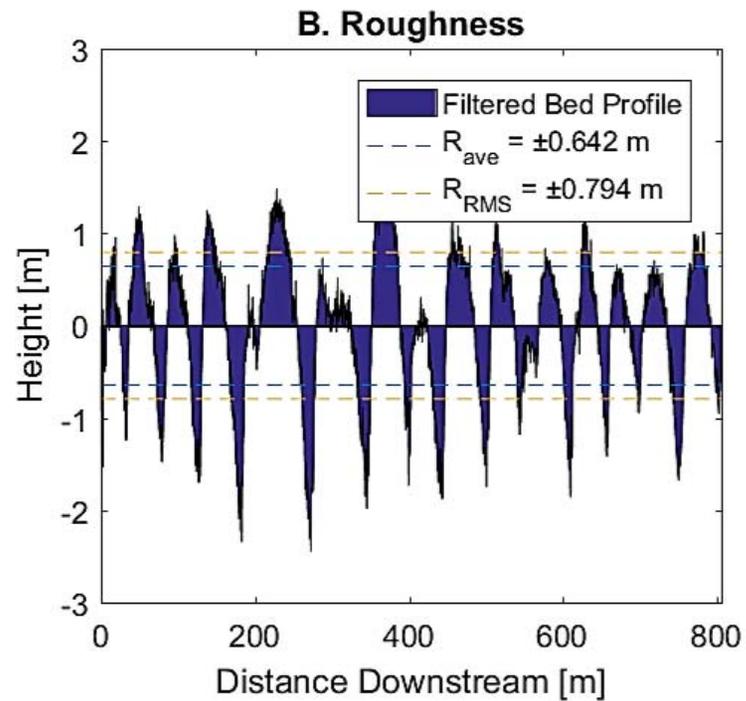
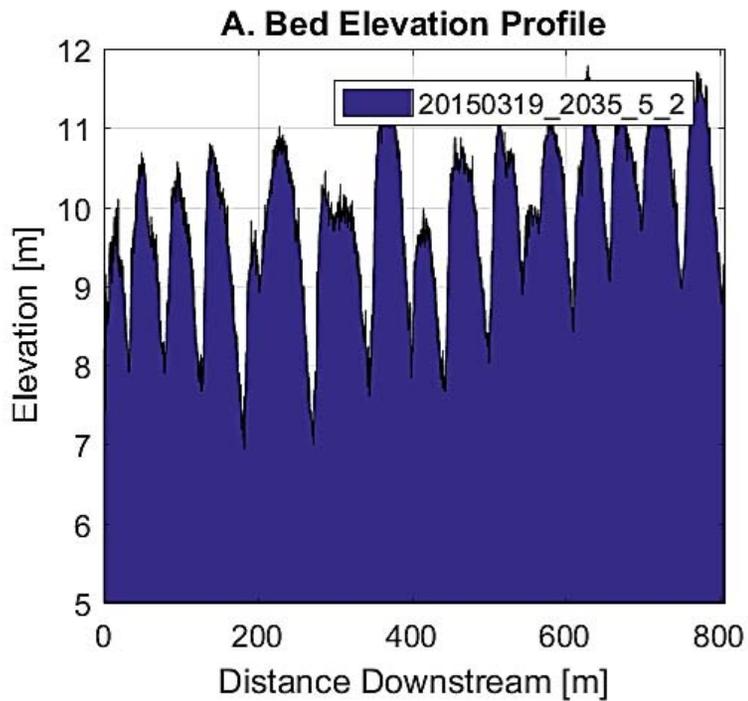


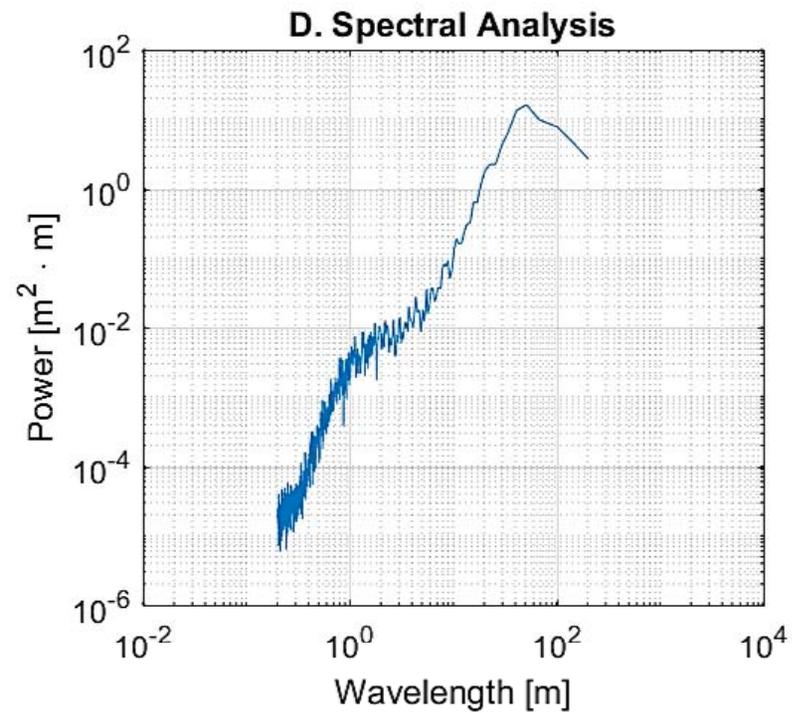
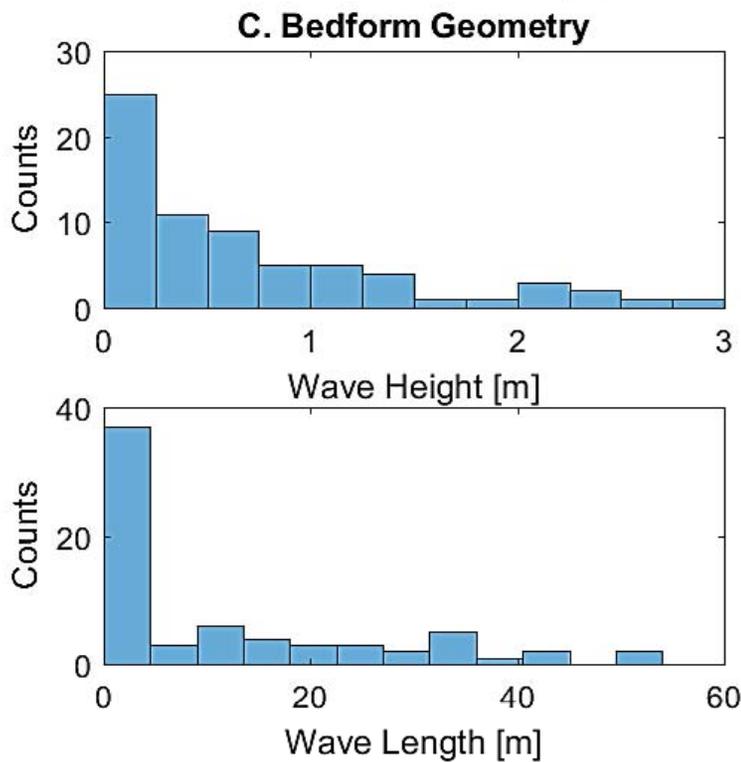
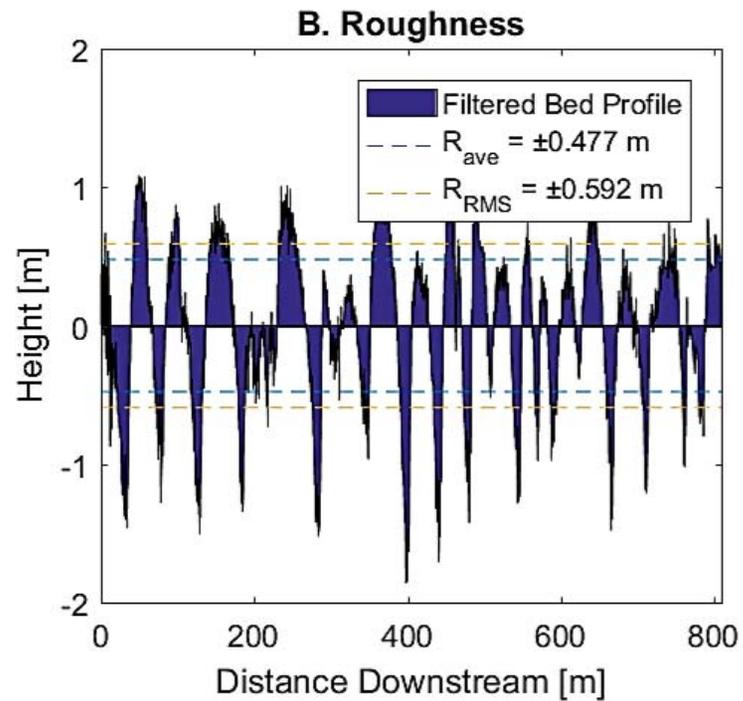
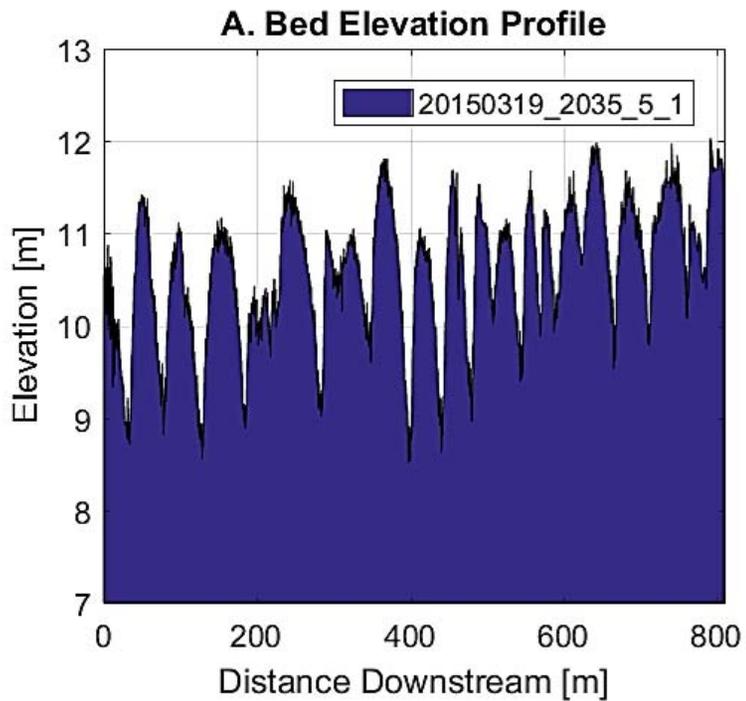


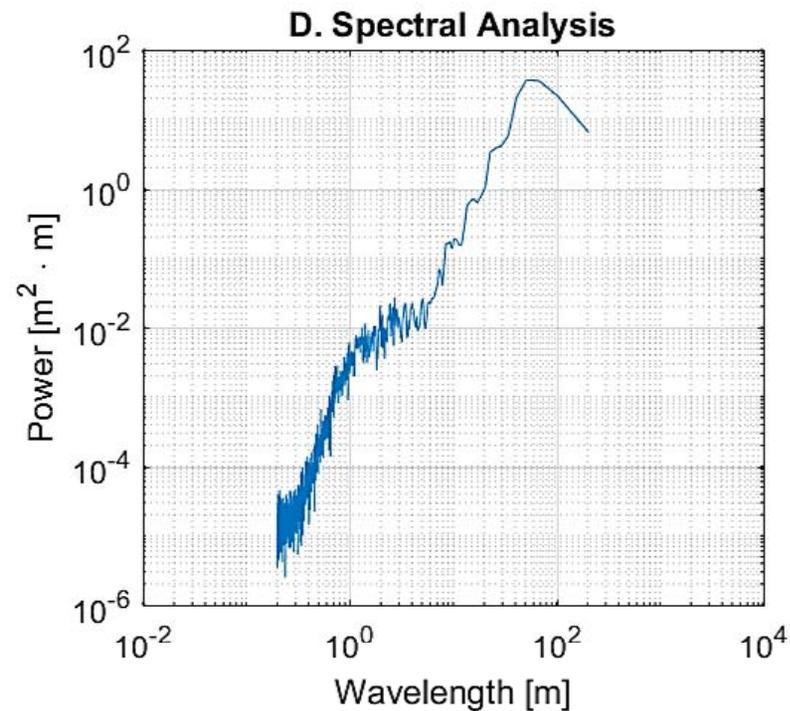
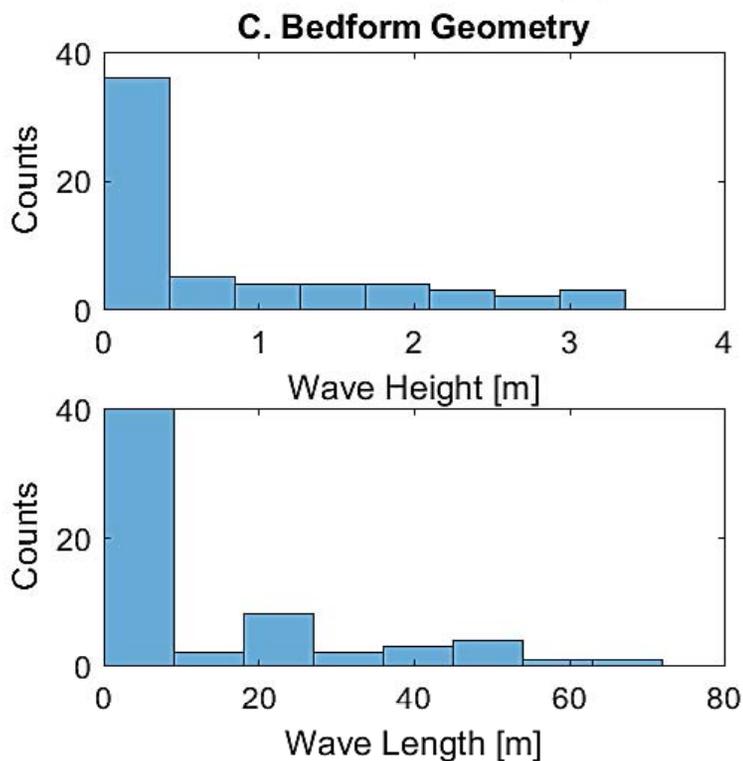
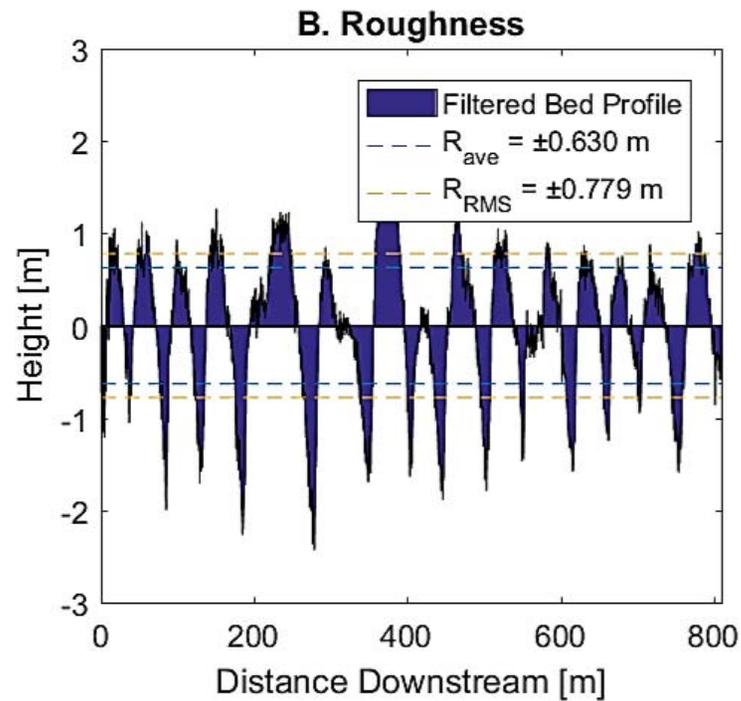
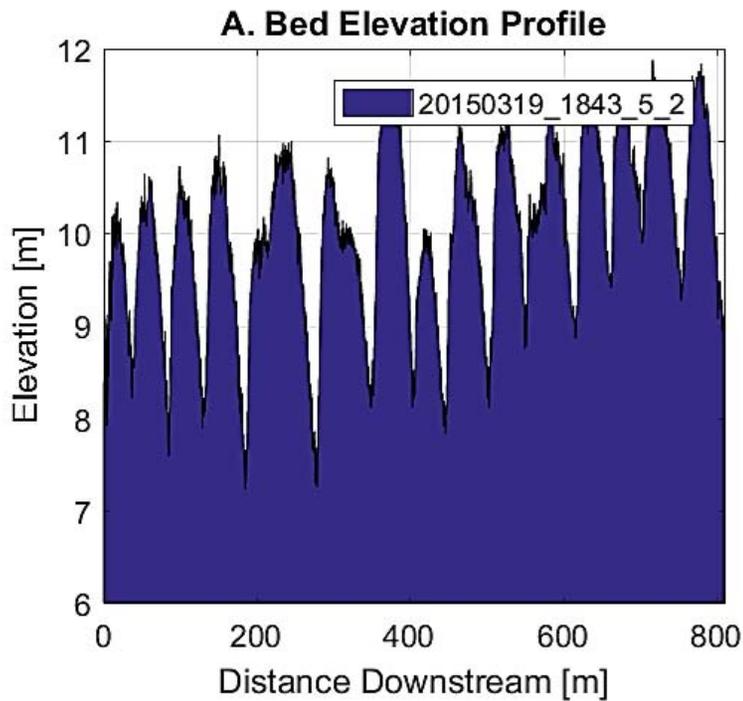


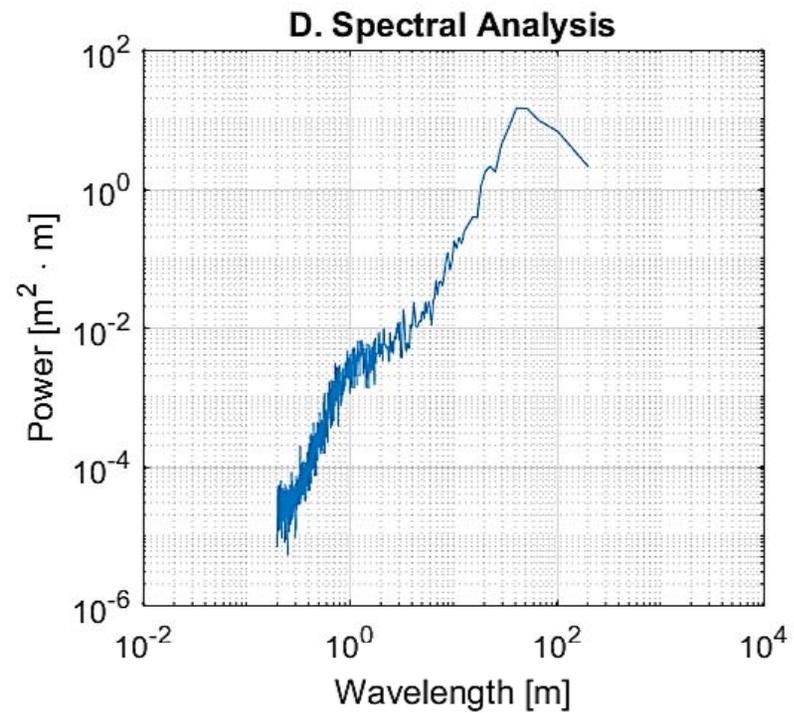
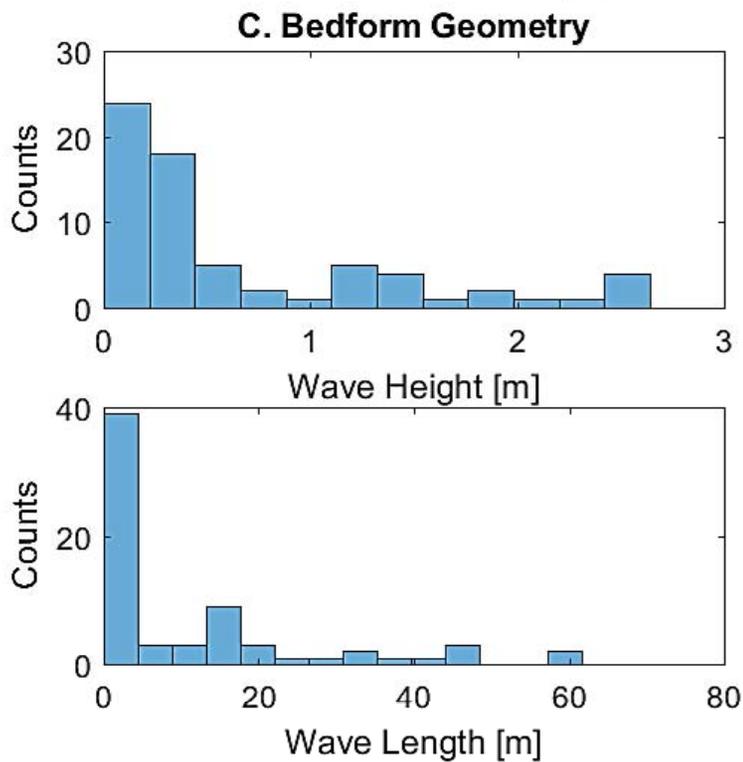
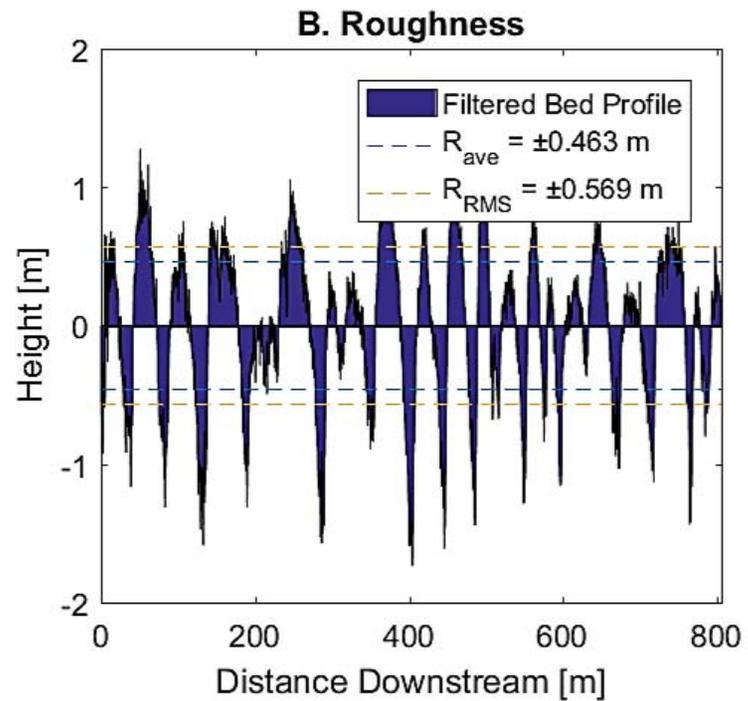
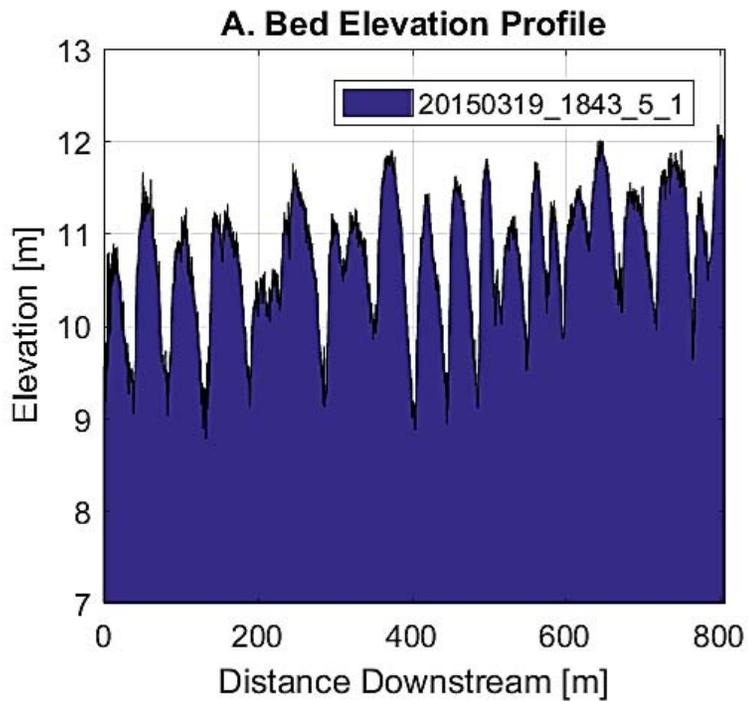


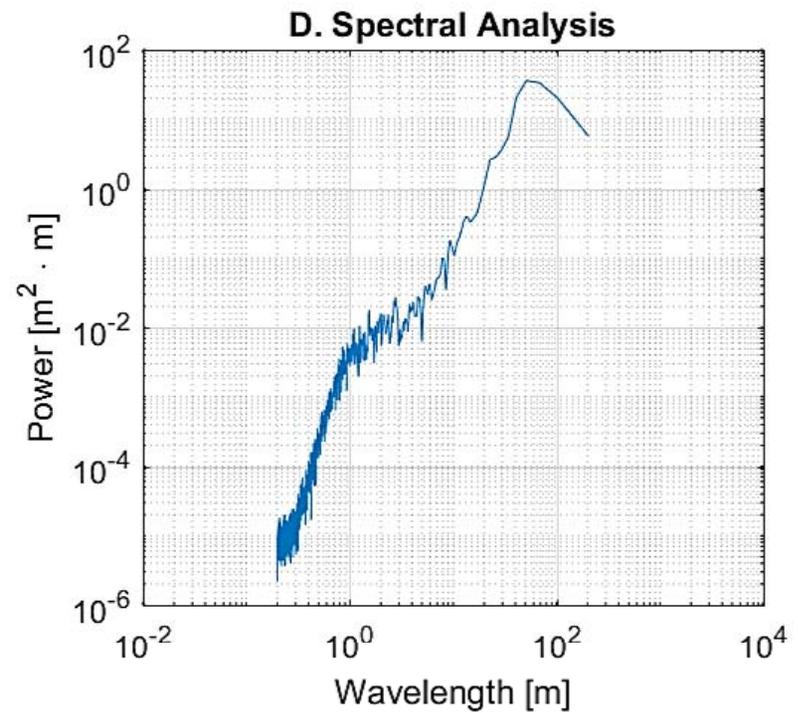
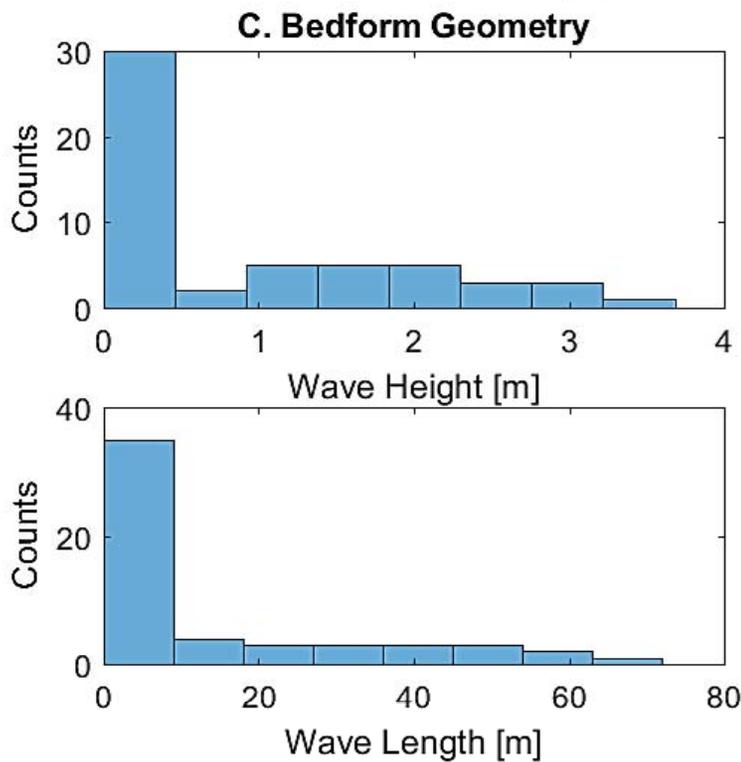
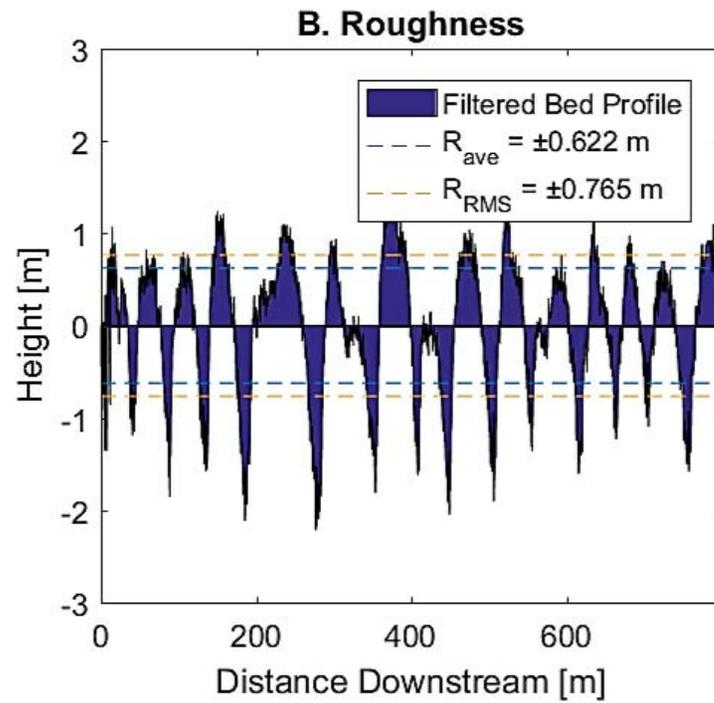
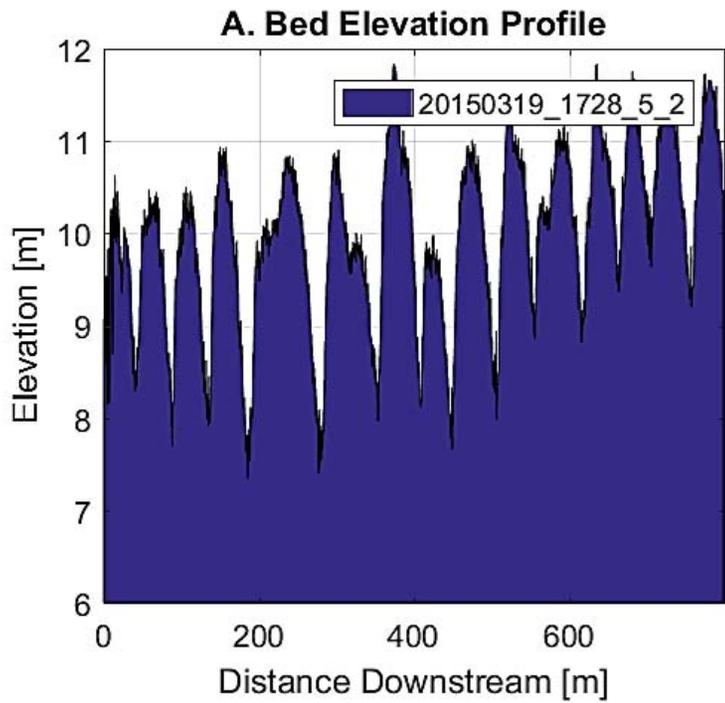


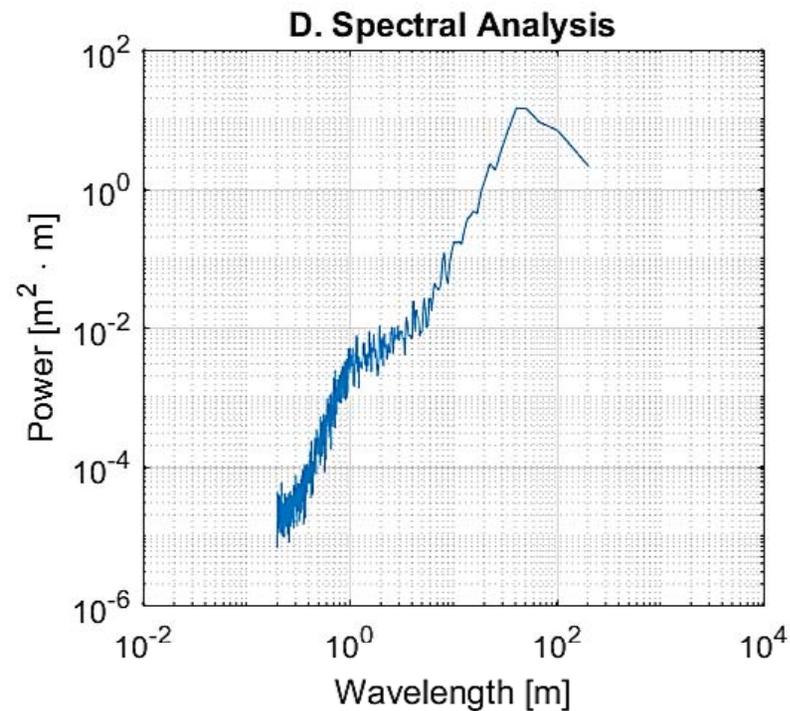
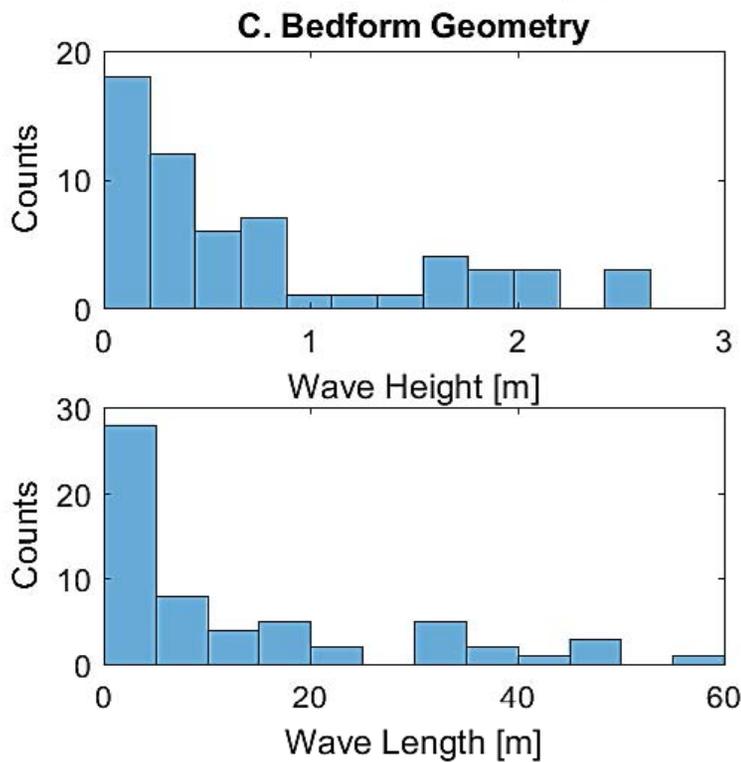
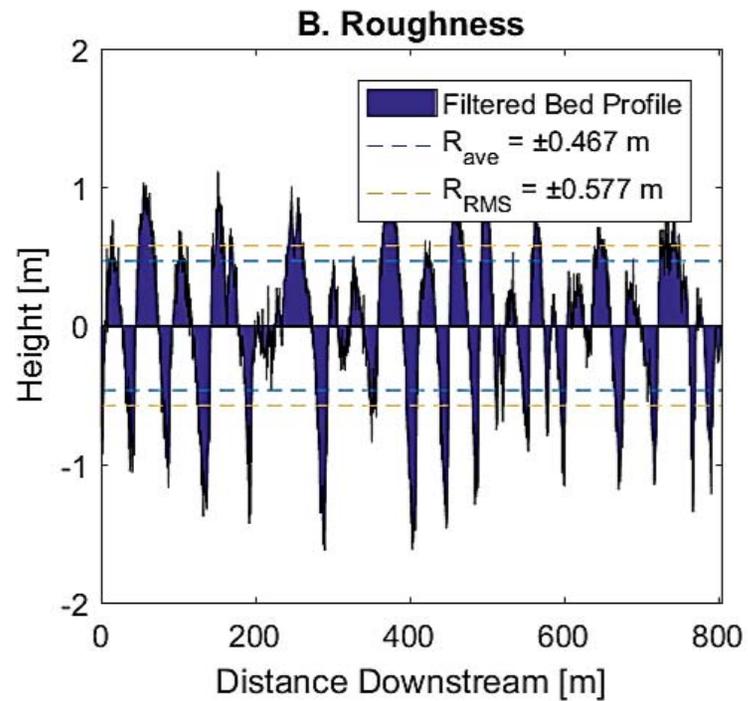
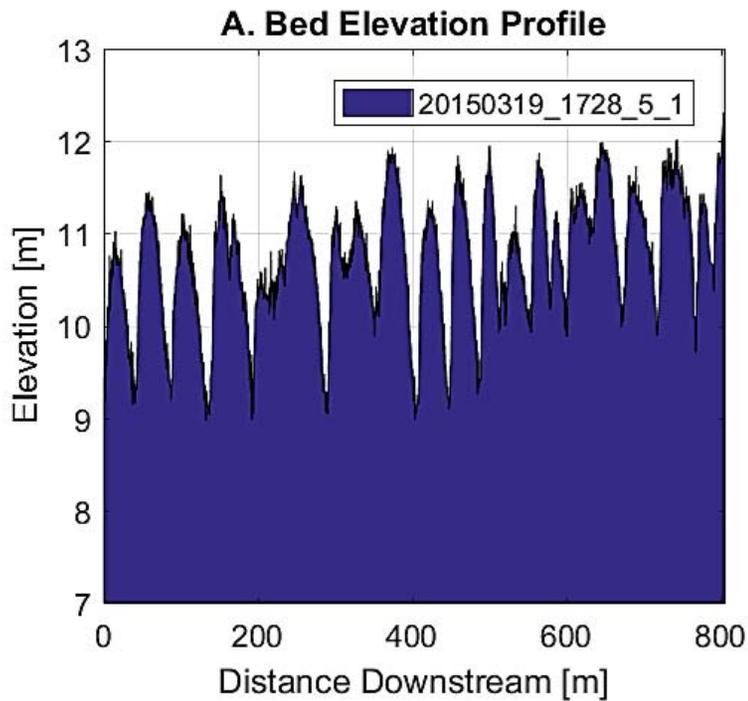


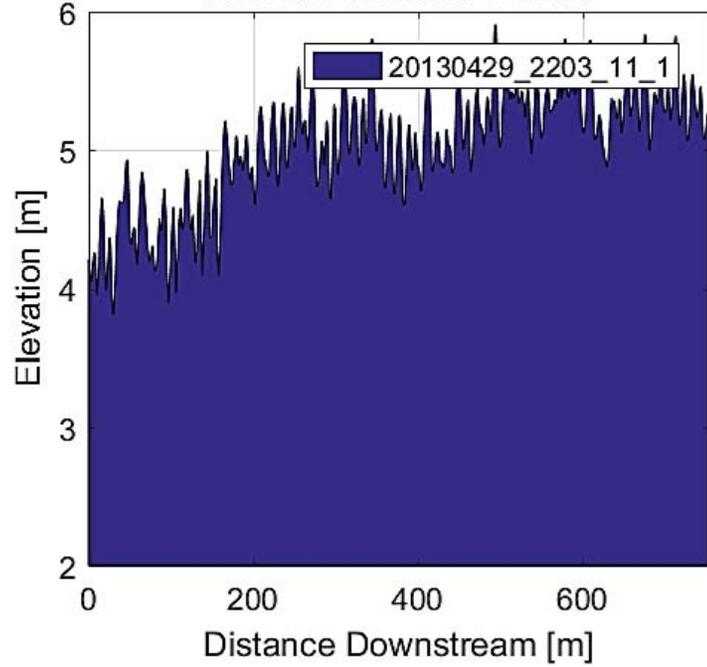
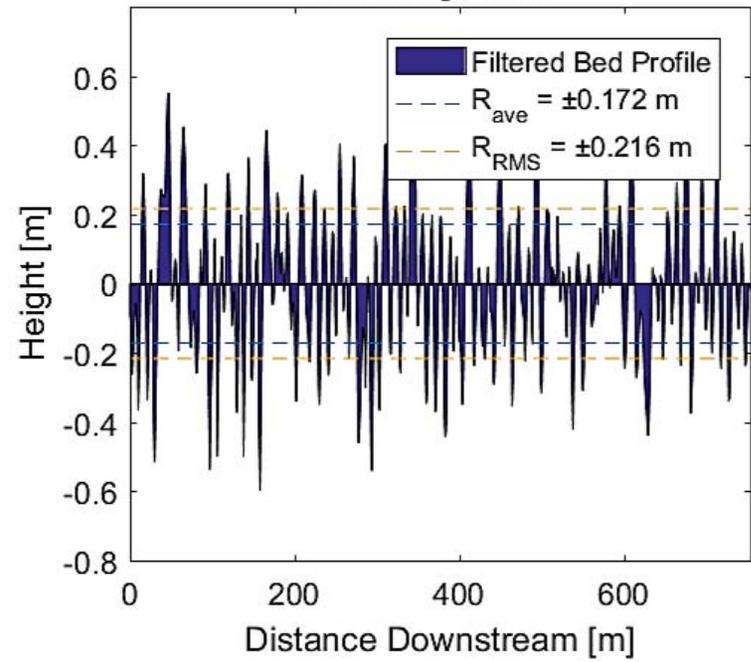
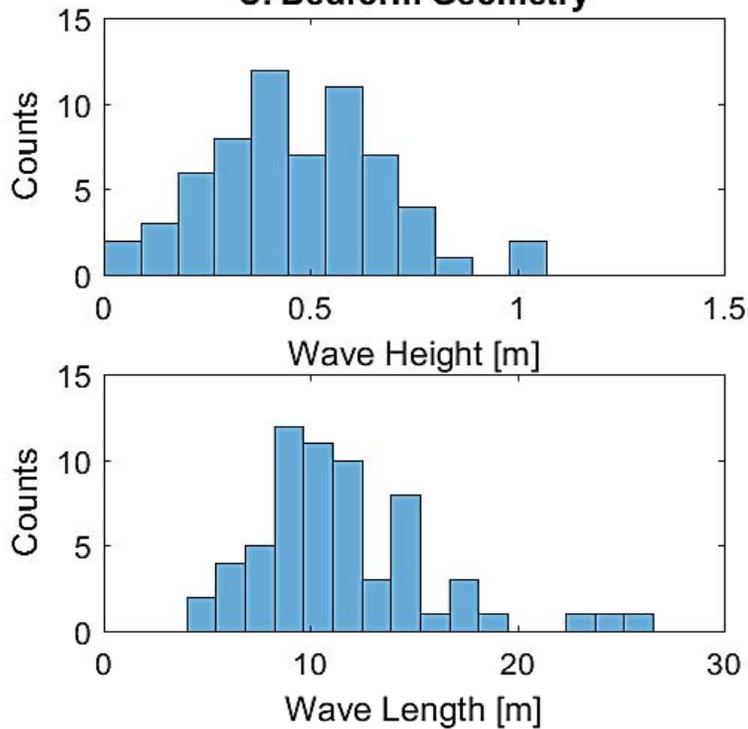
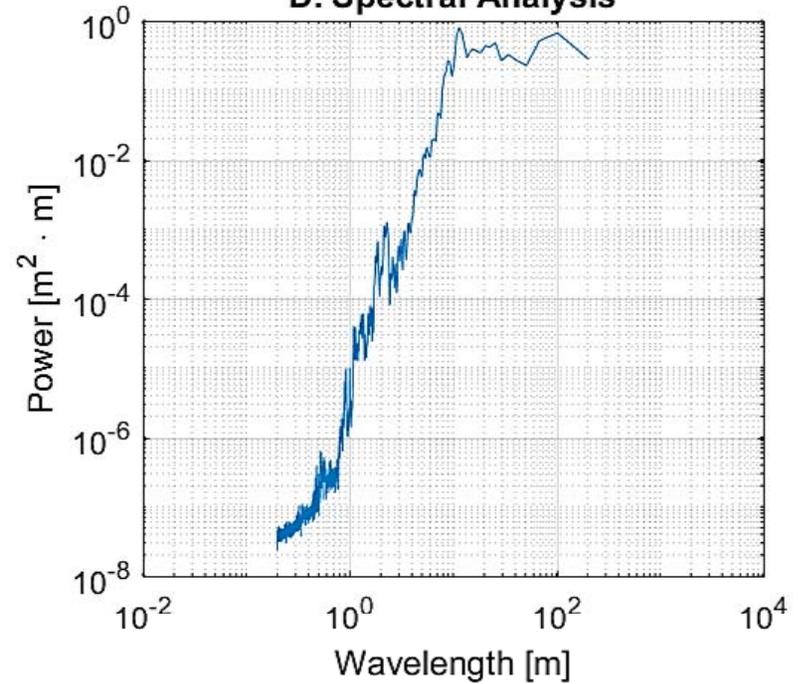




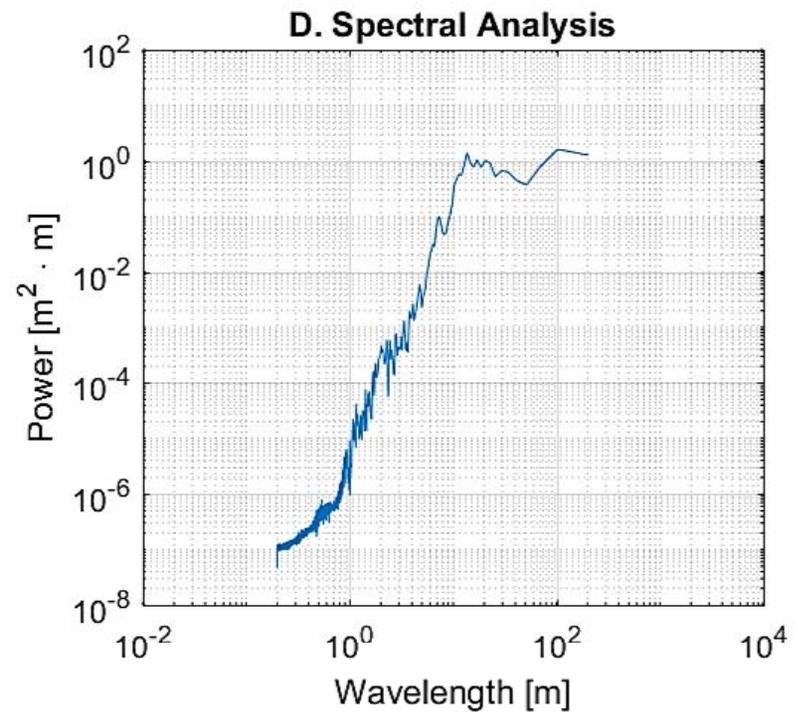
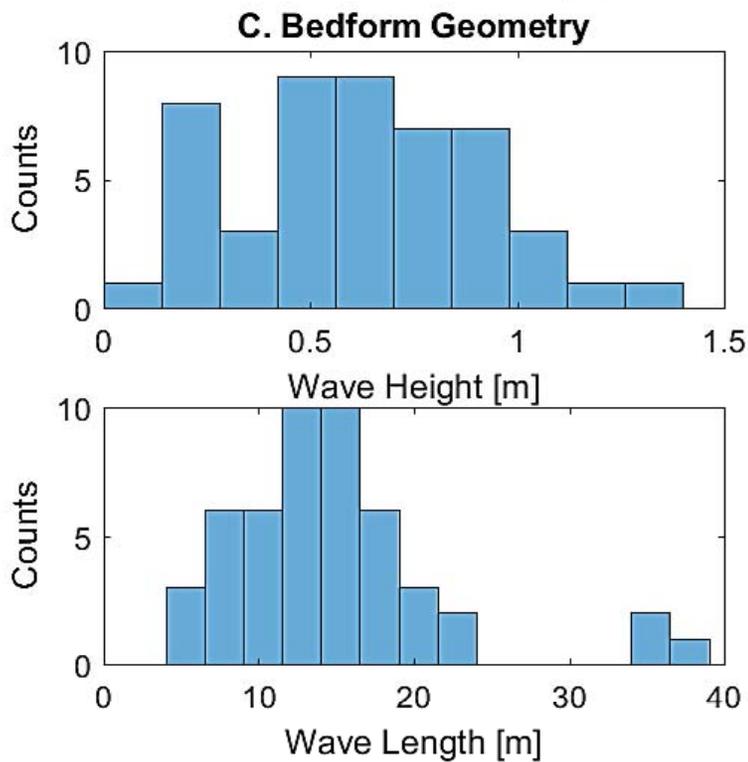
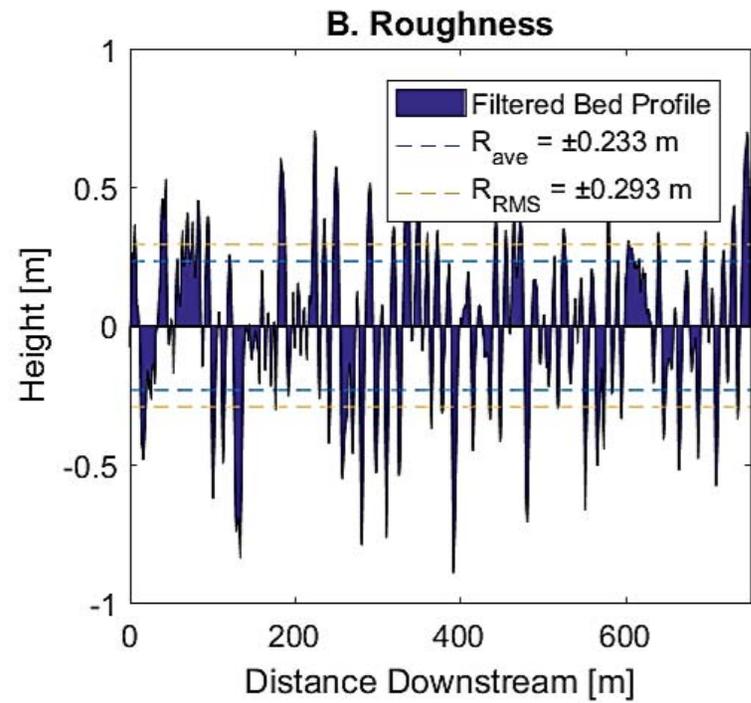
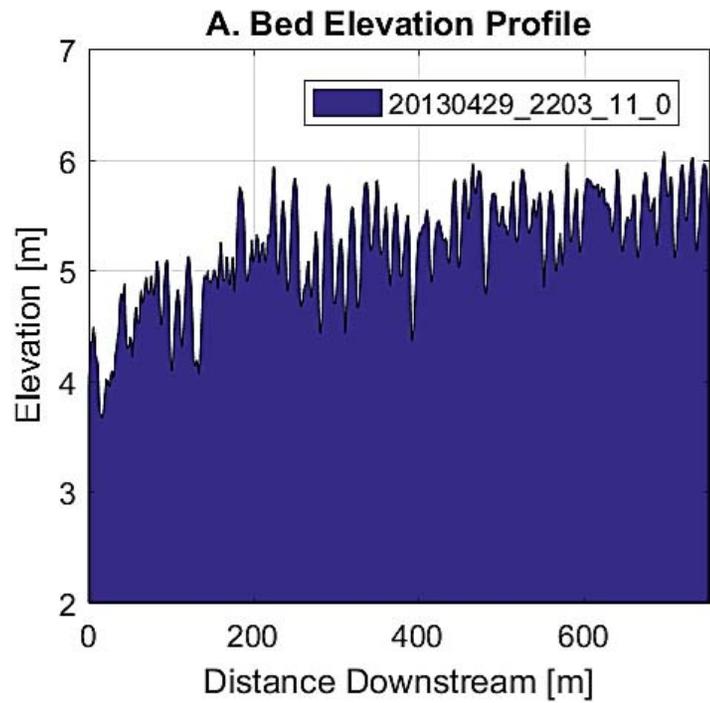


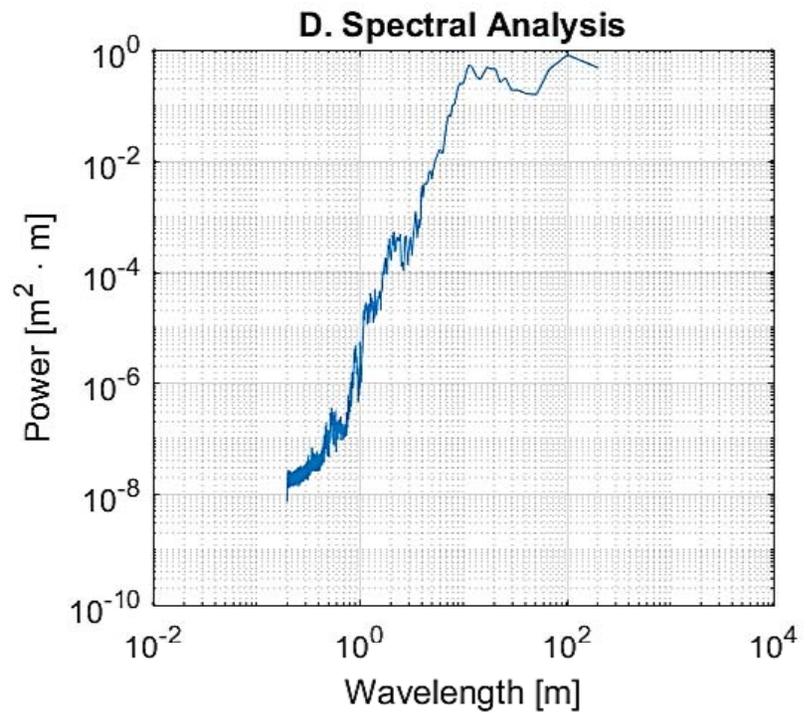
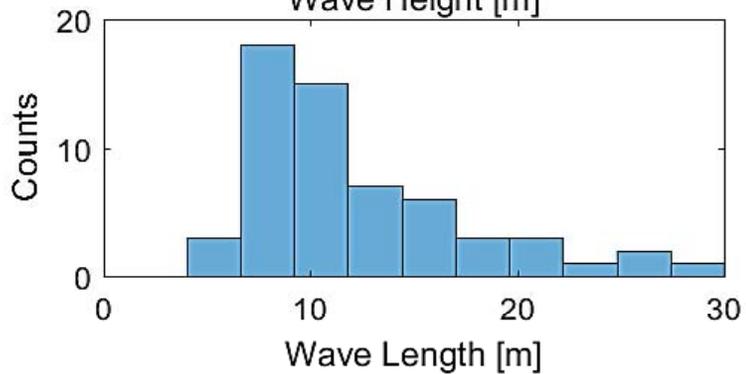
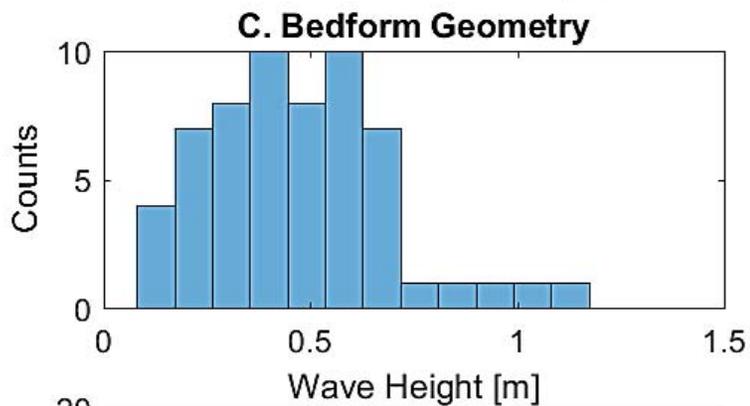
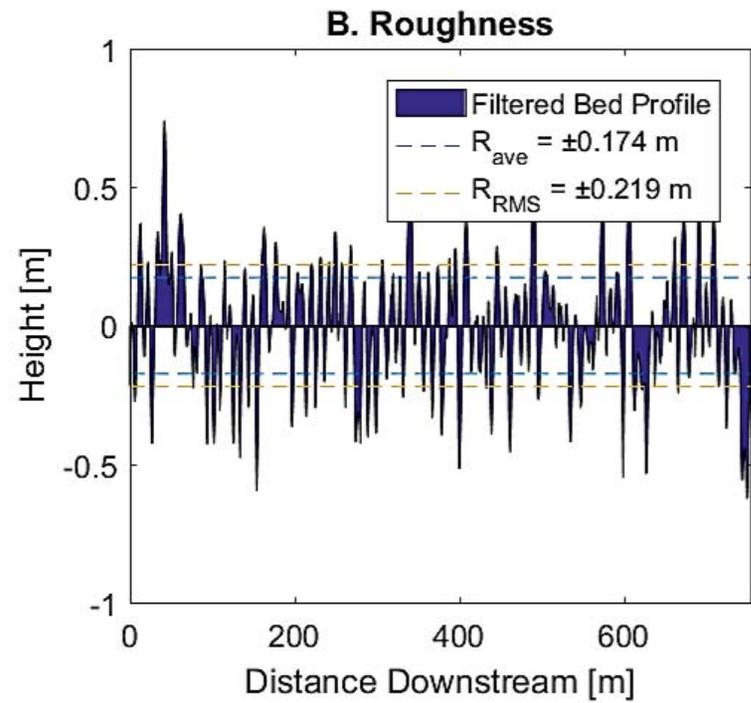
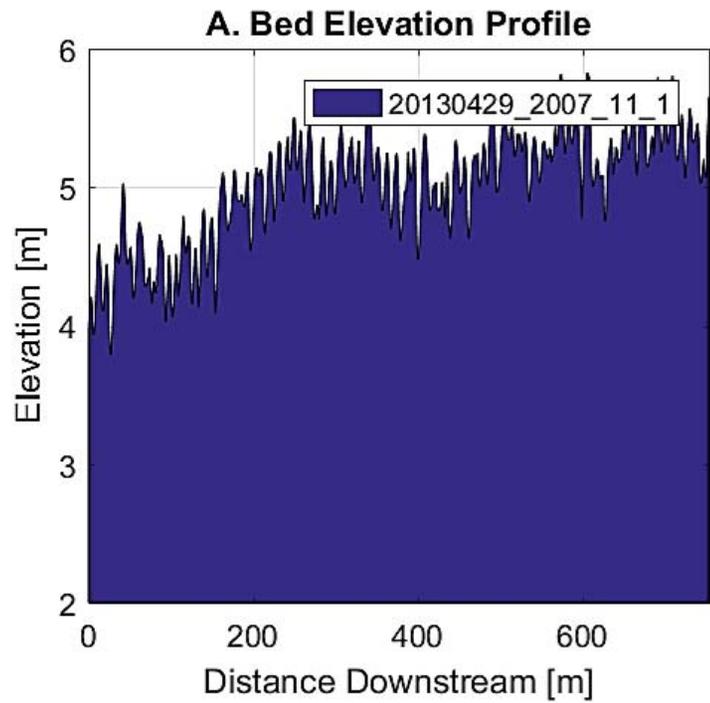


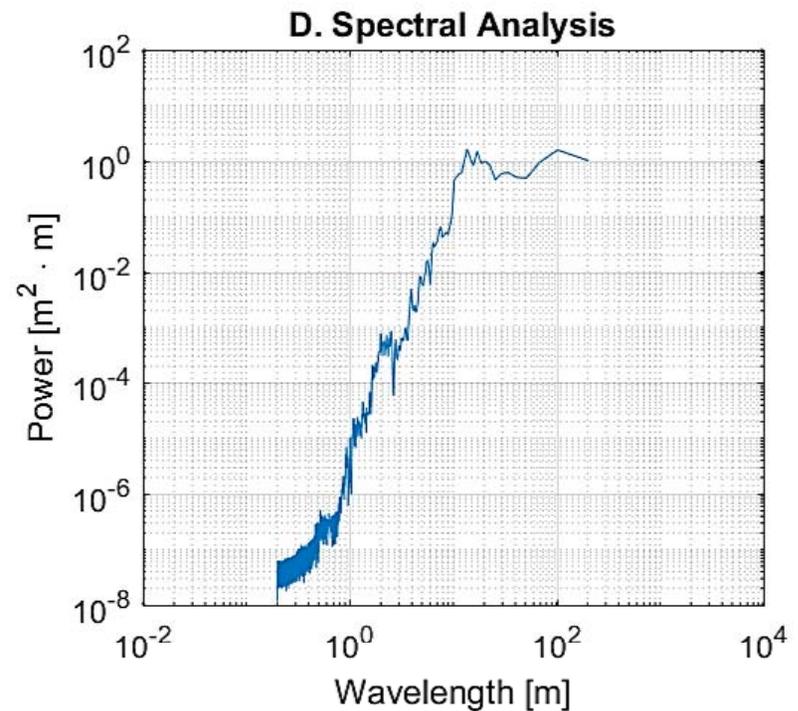
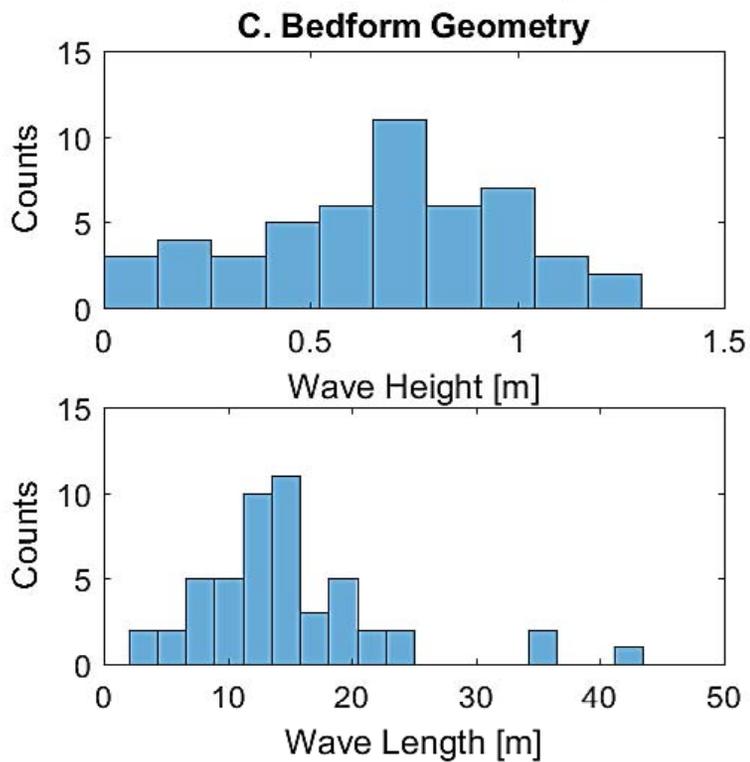
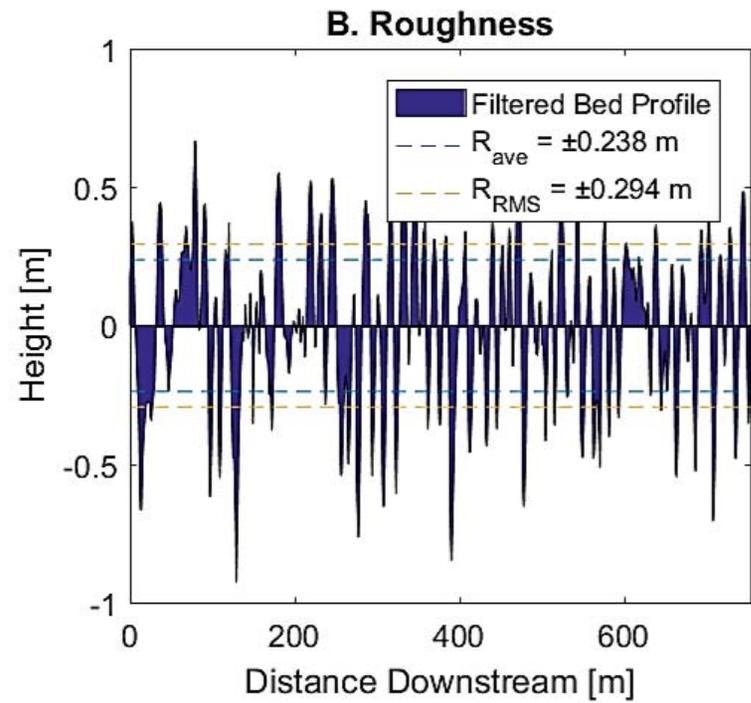
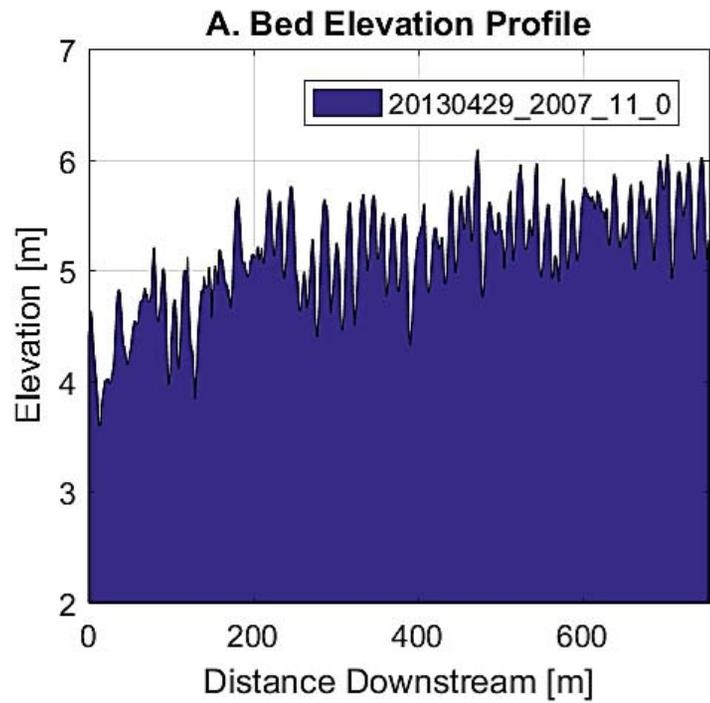


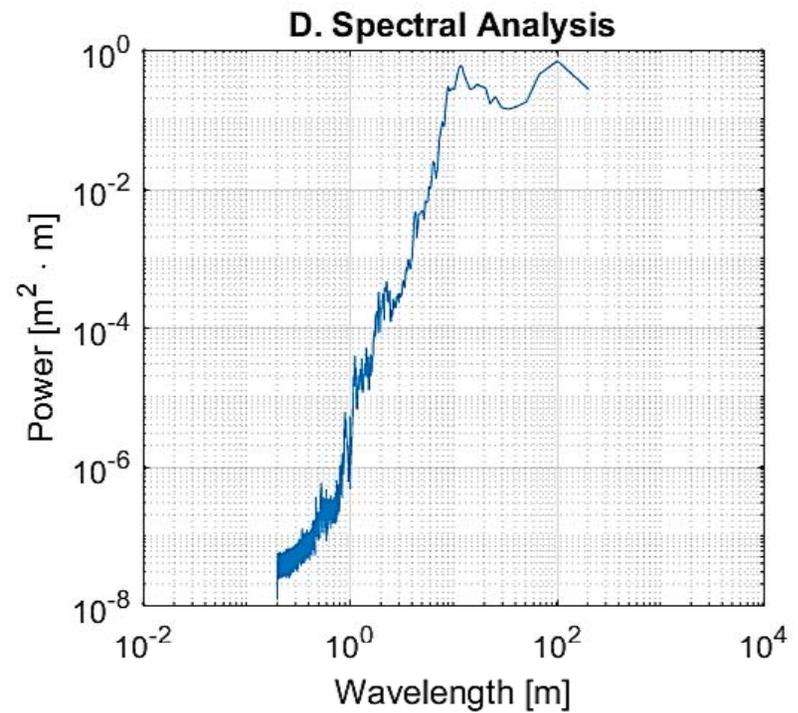
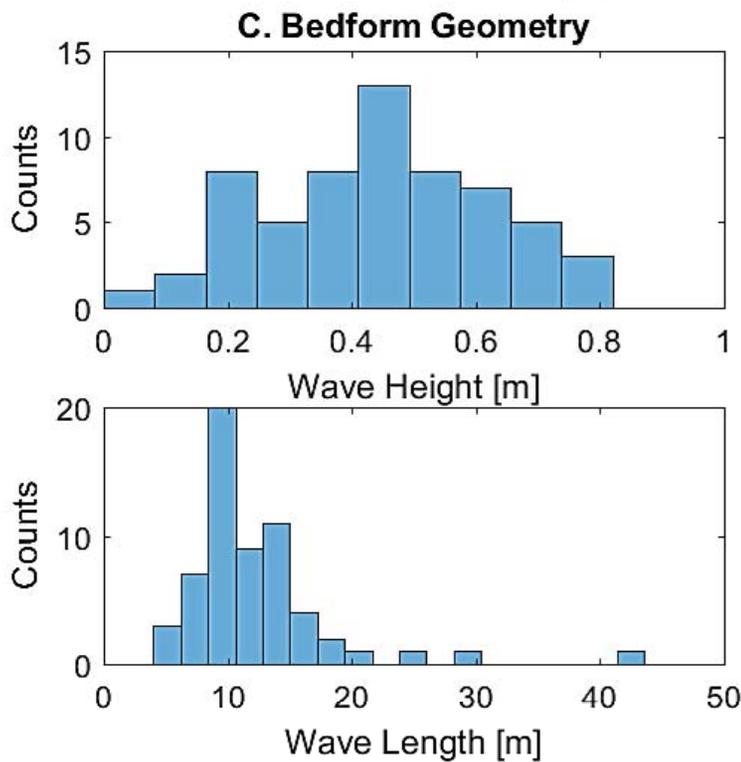
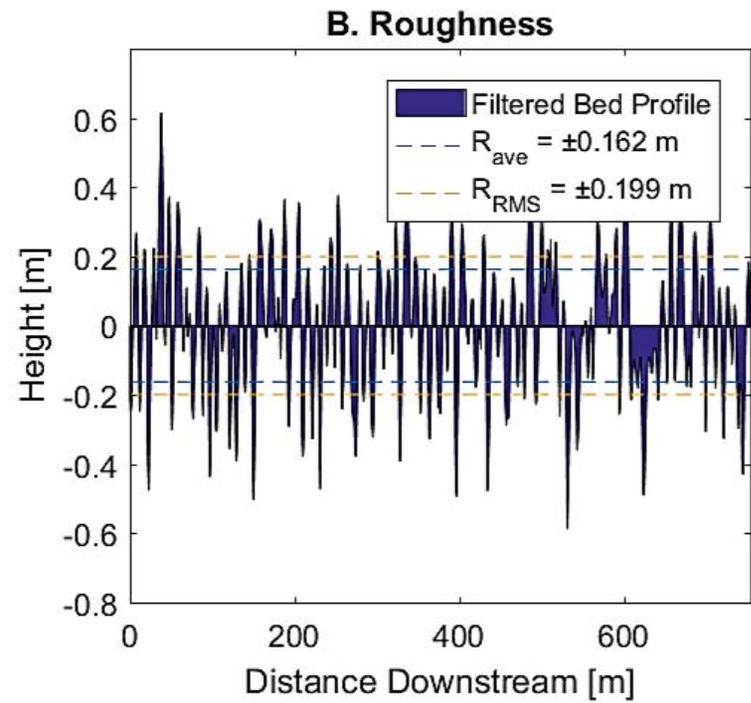
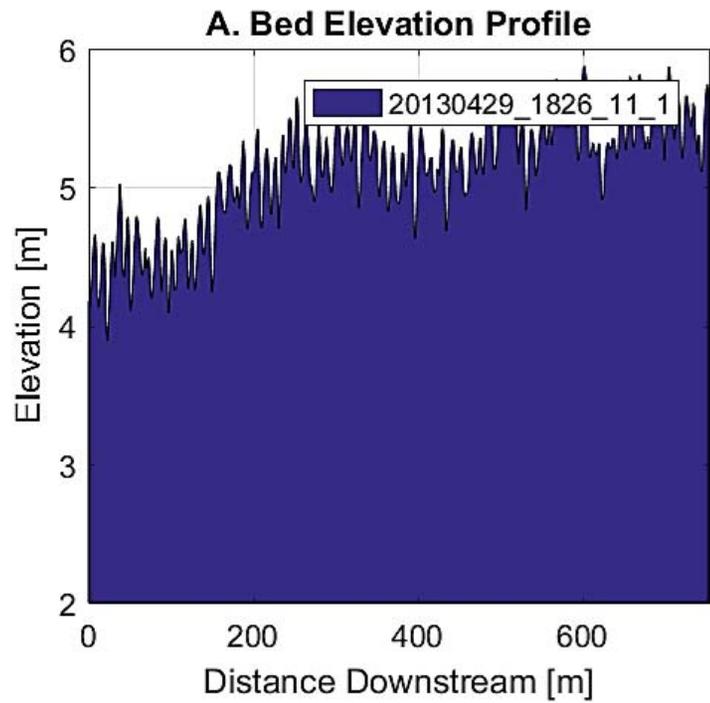
**A. Bed Elevation Profile****B. Roughness****C. Bedform Geometry****D. Spectral Analysis**

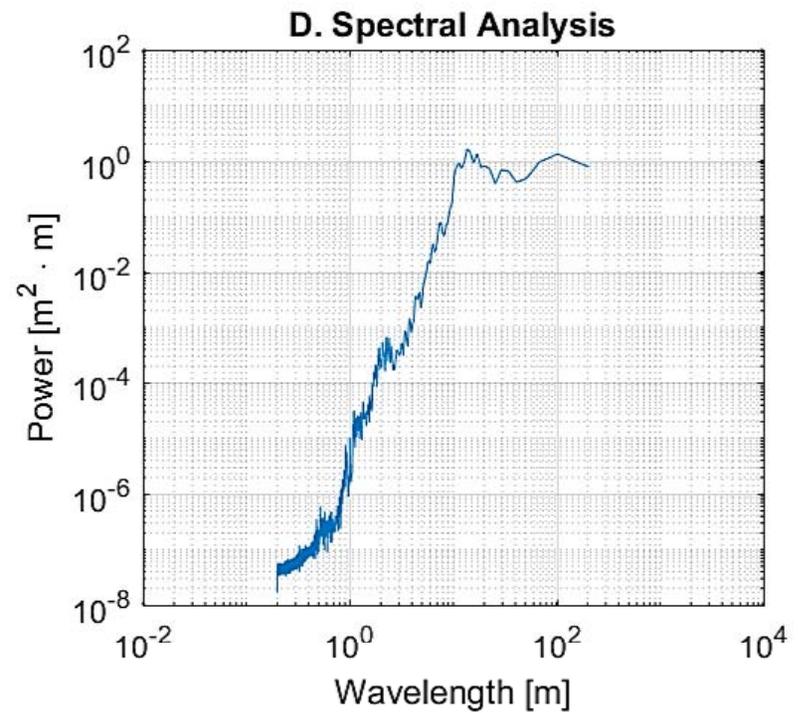
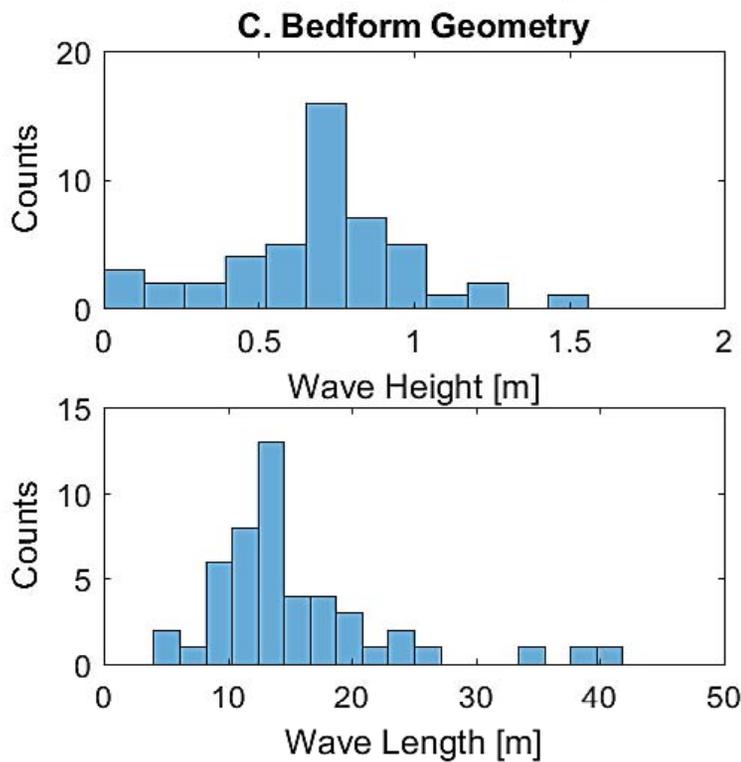
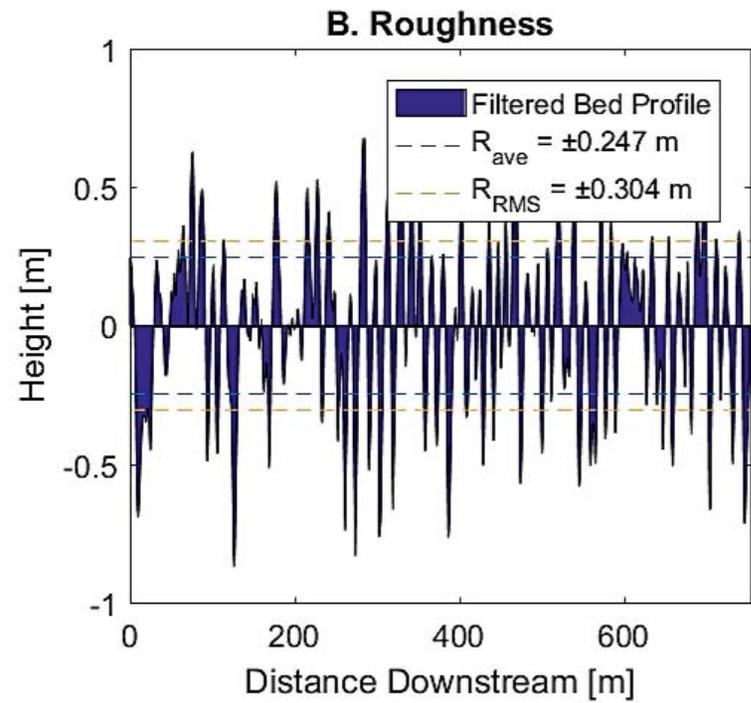
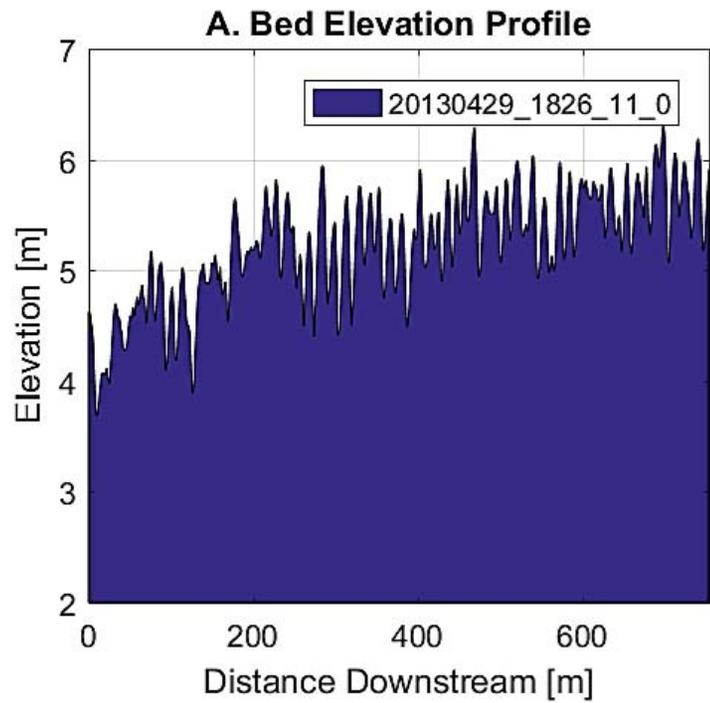


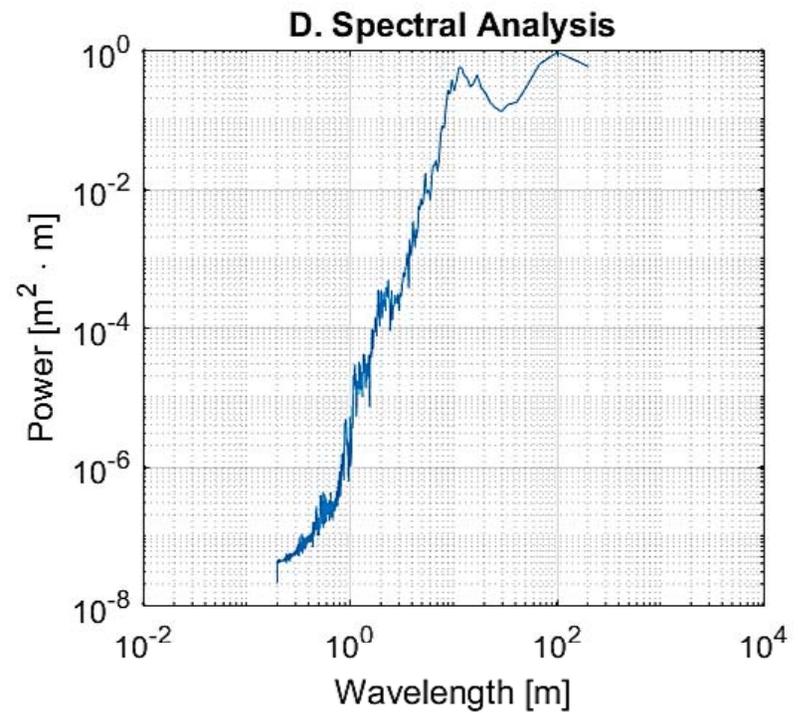
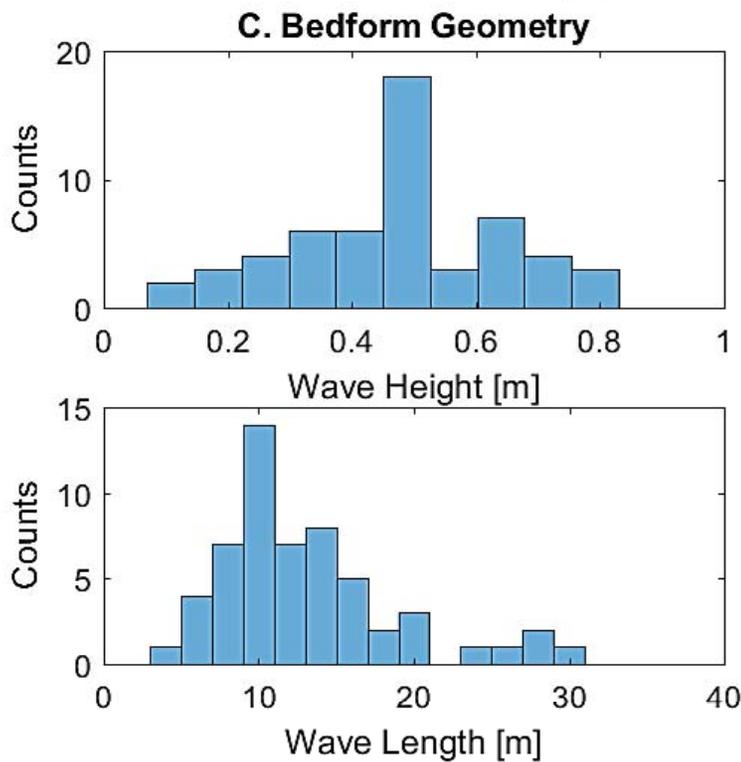
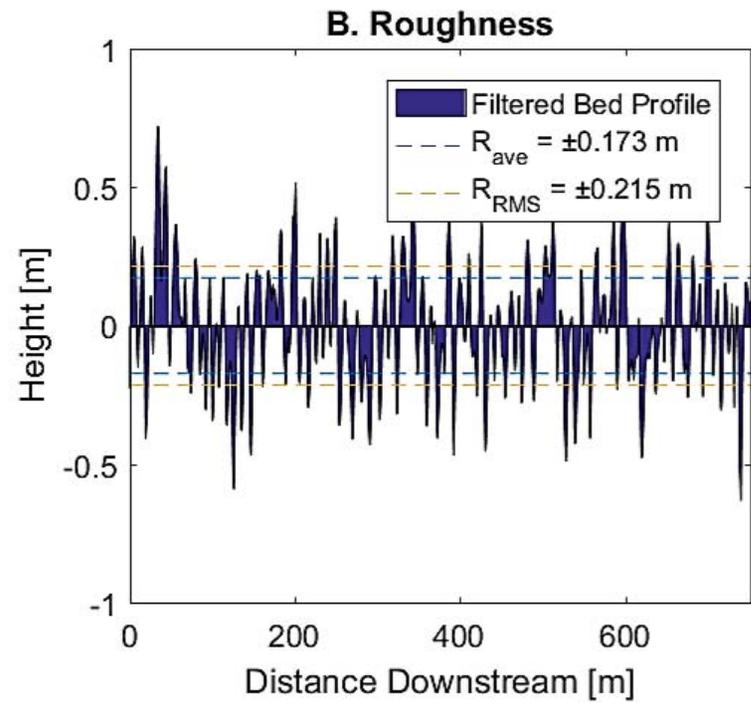
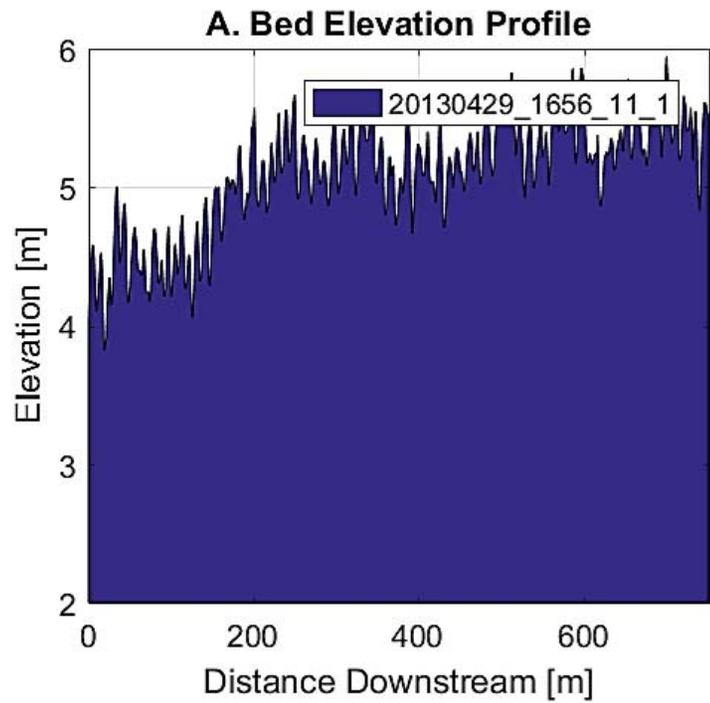




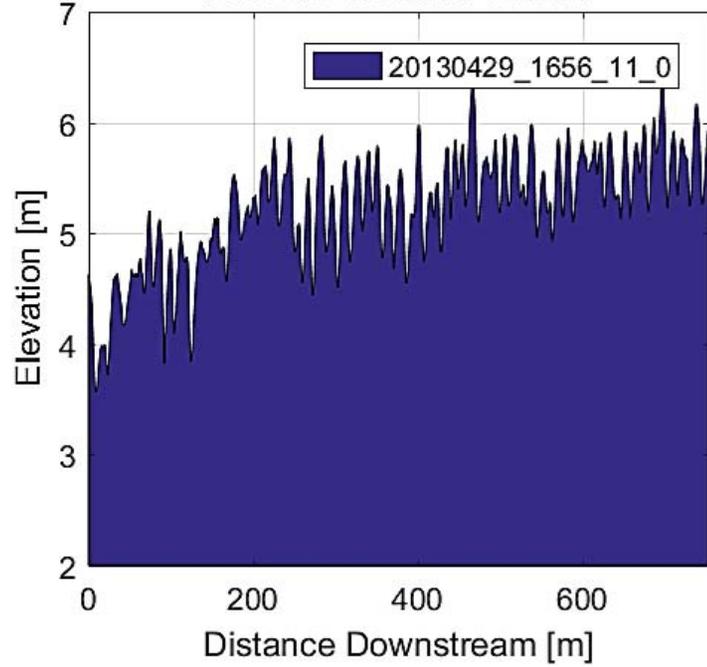




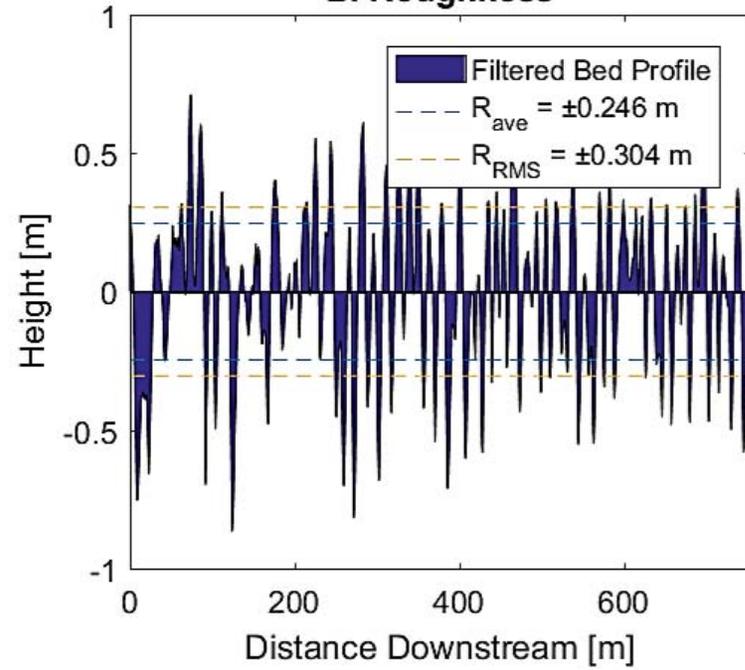




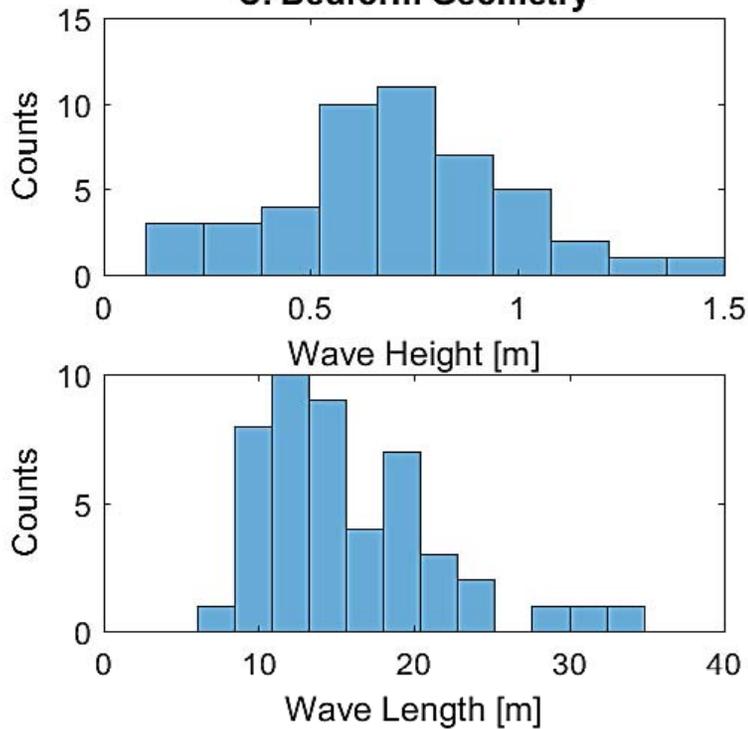
### A. Bed Elevation Profile



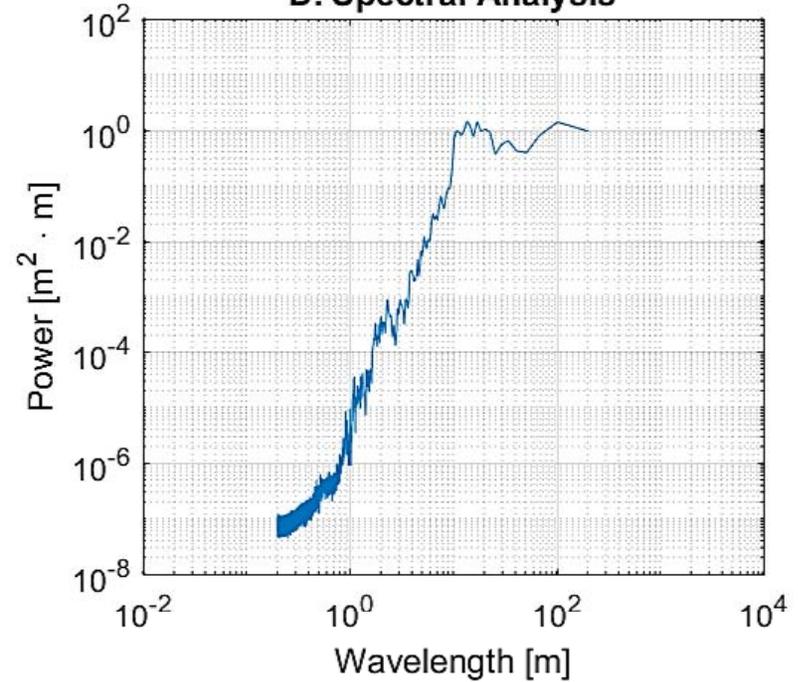
### B. Roughness

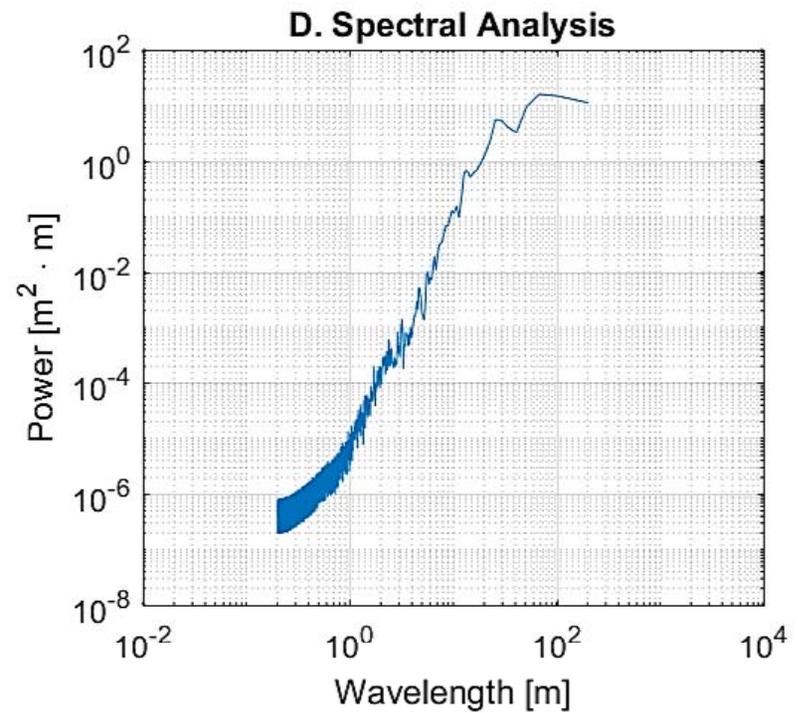
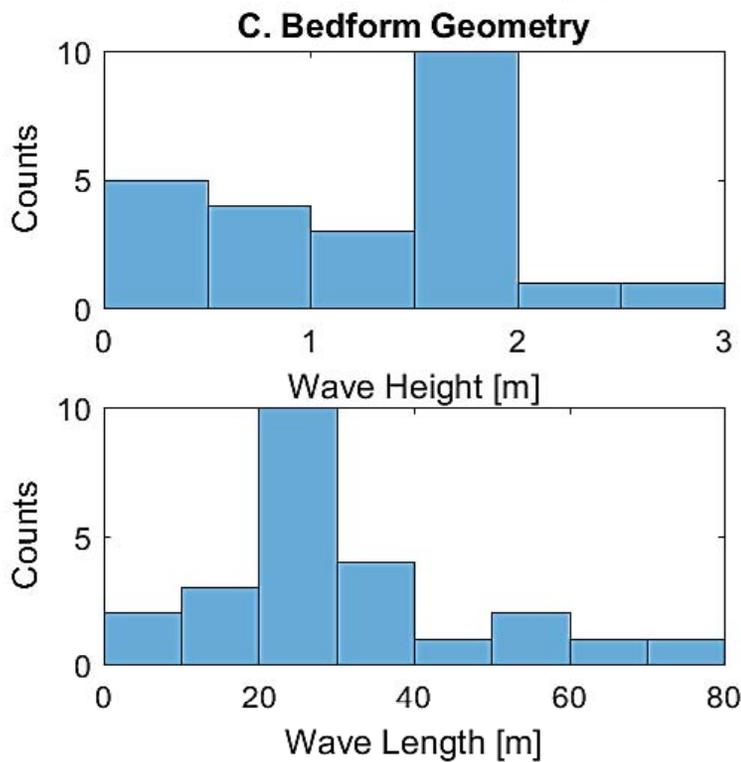
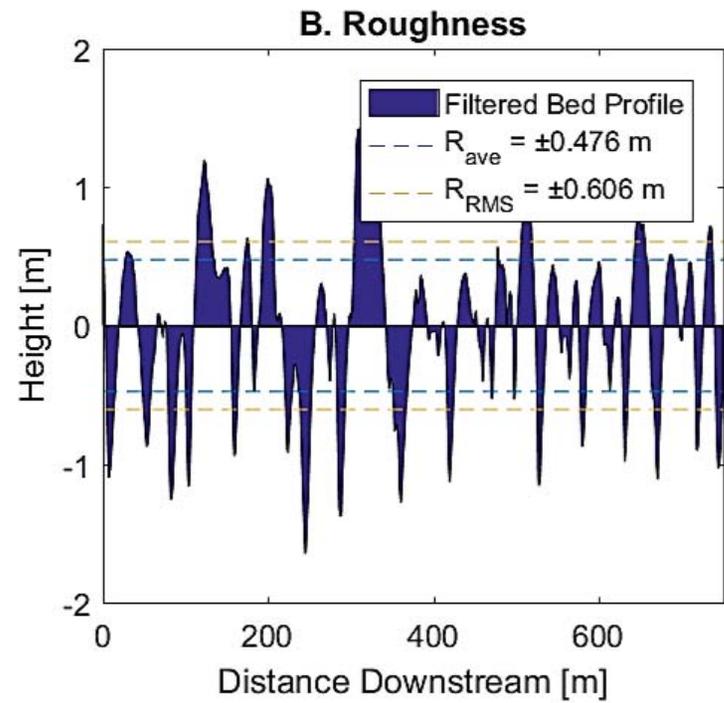
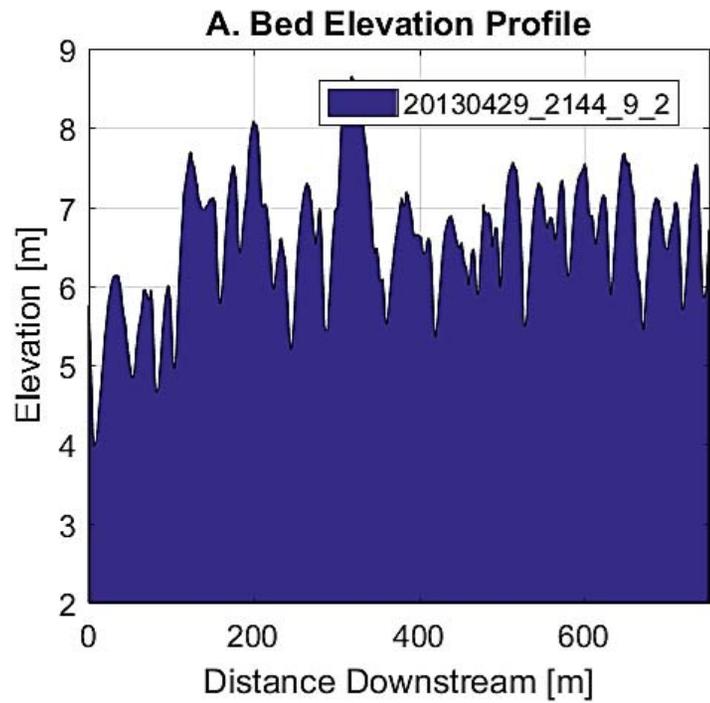


### C. Bedform Geometry

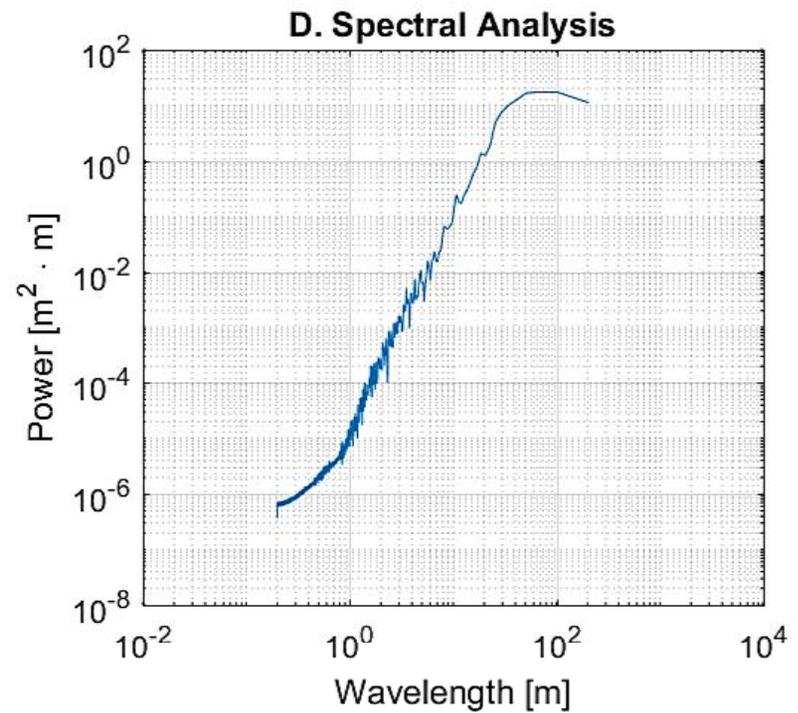
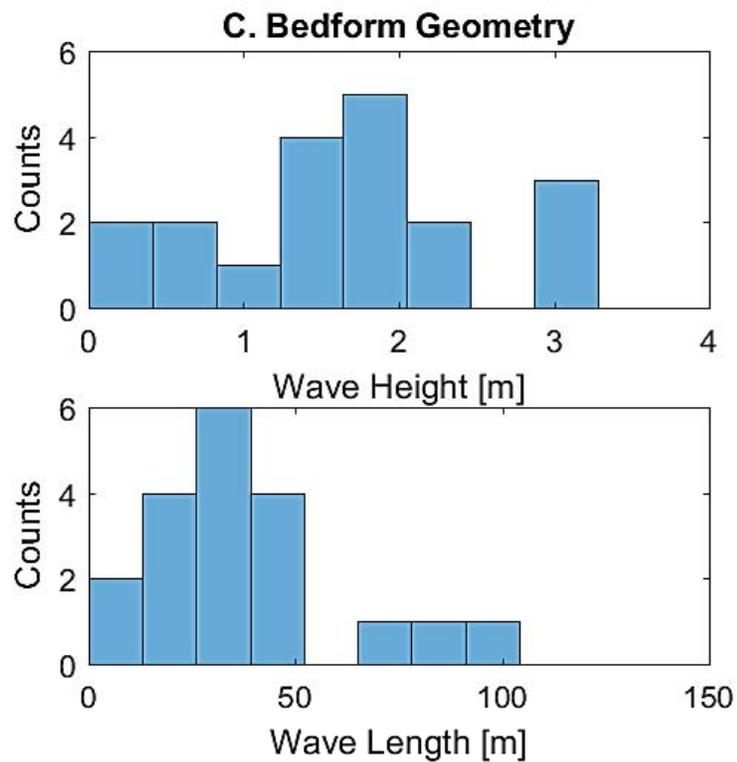
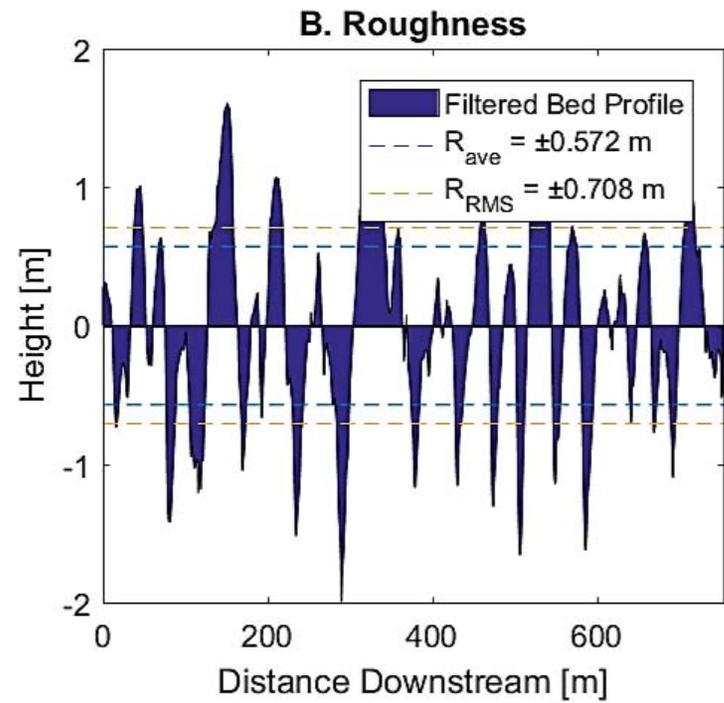
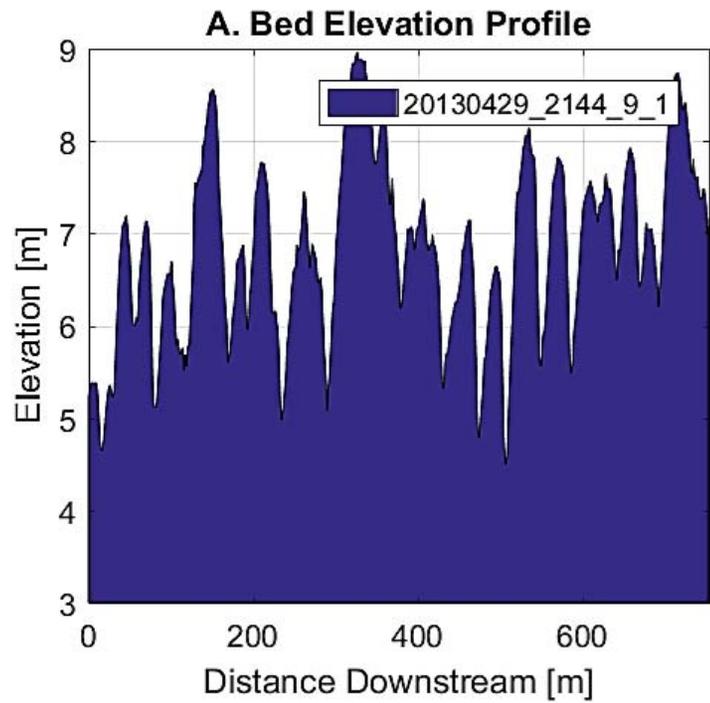


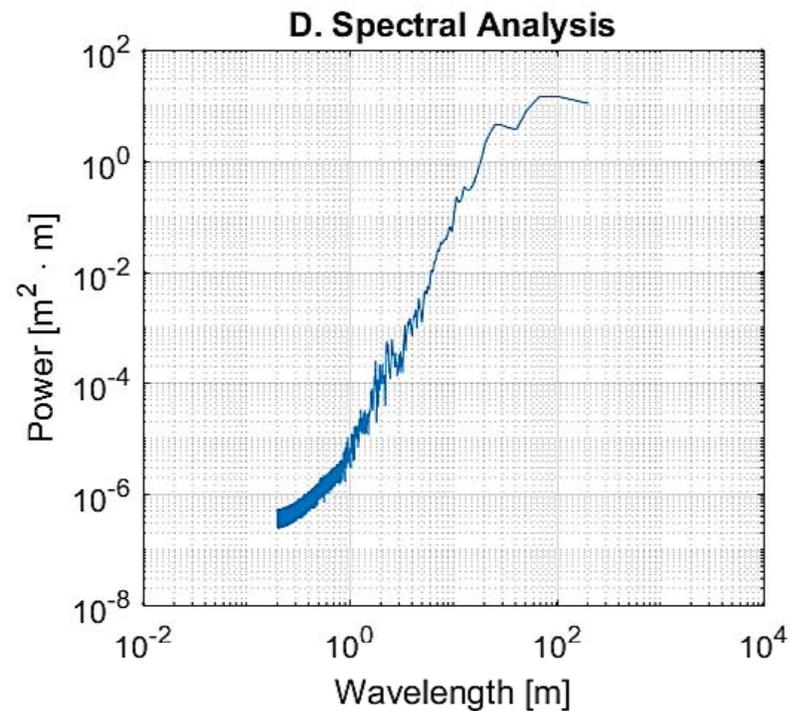
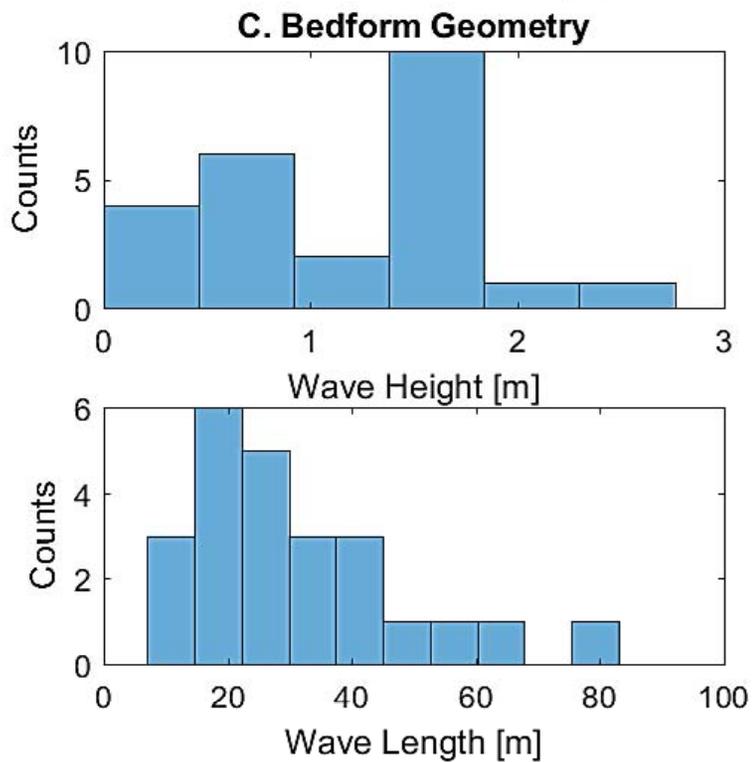
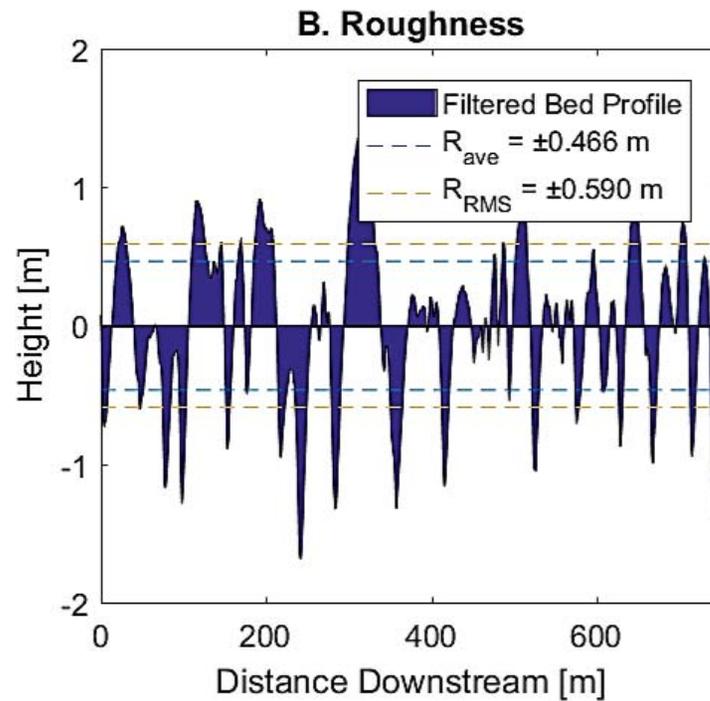
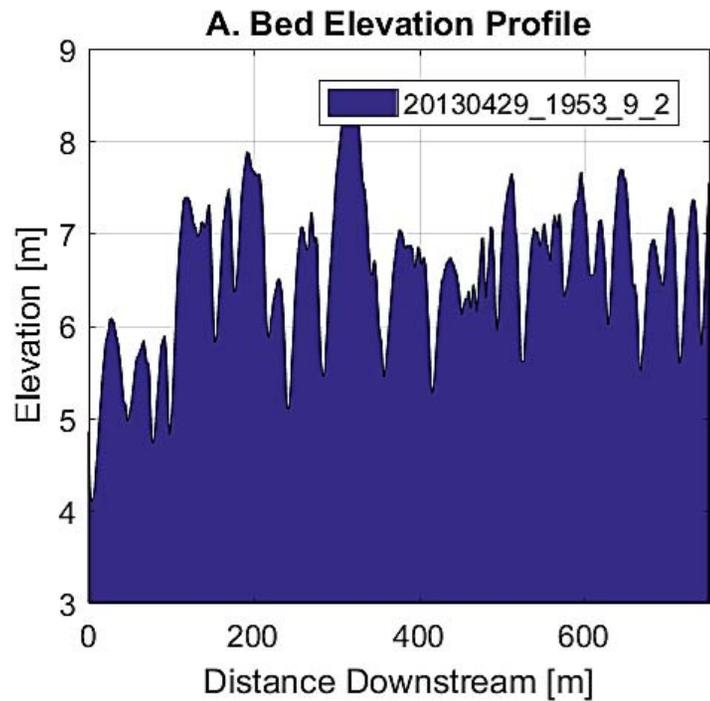
### D. Spectral Analysis

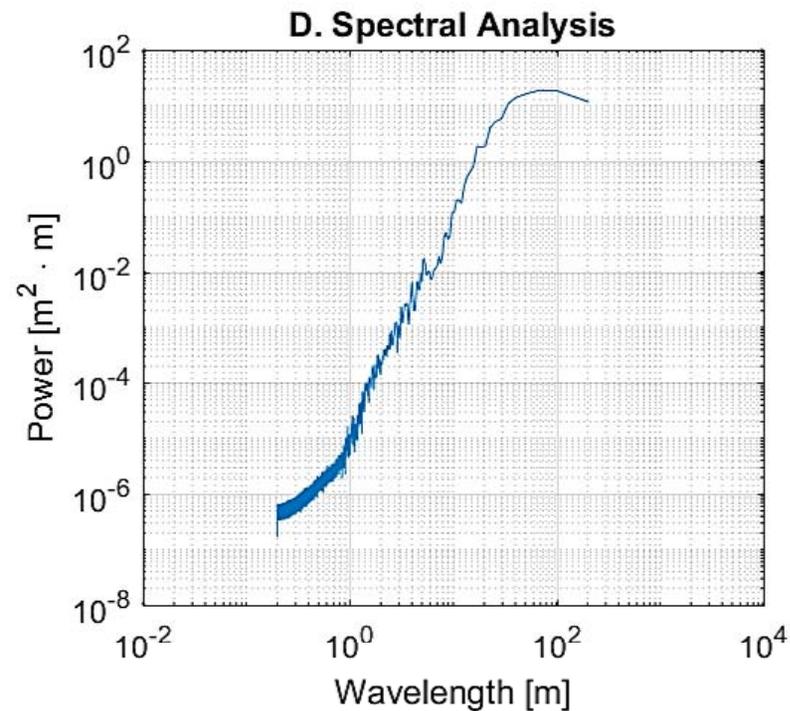
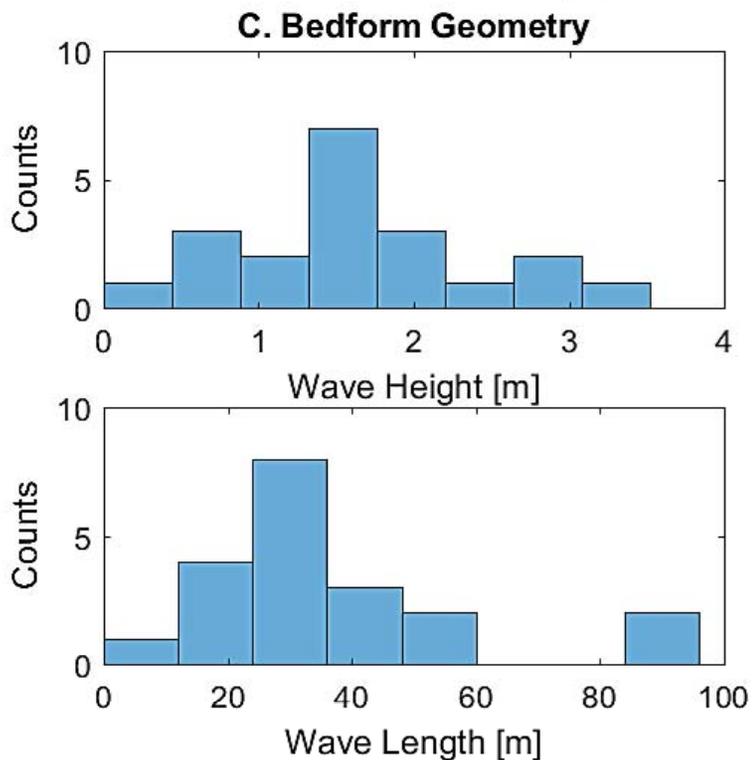
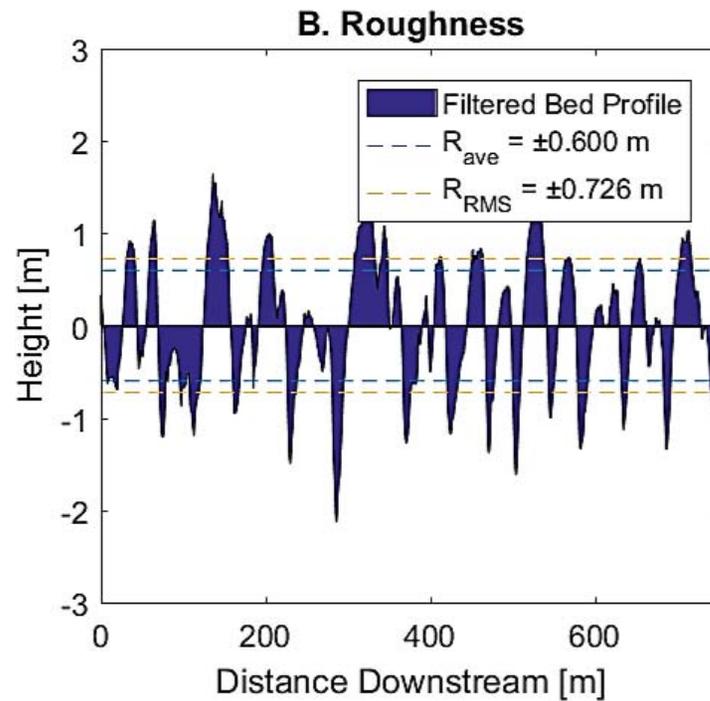
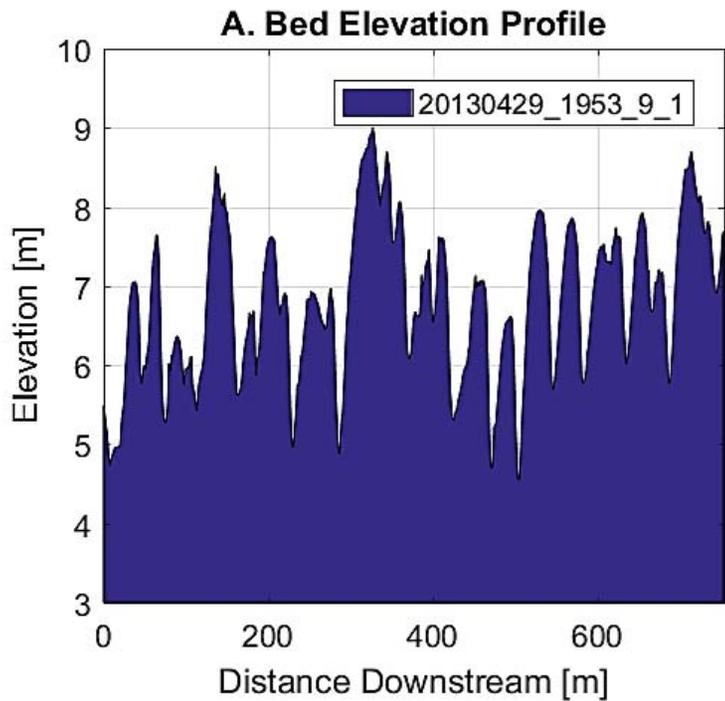


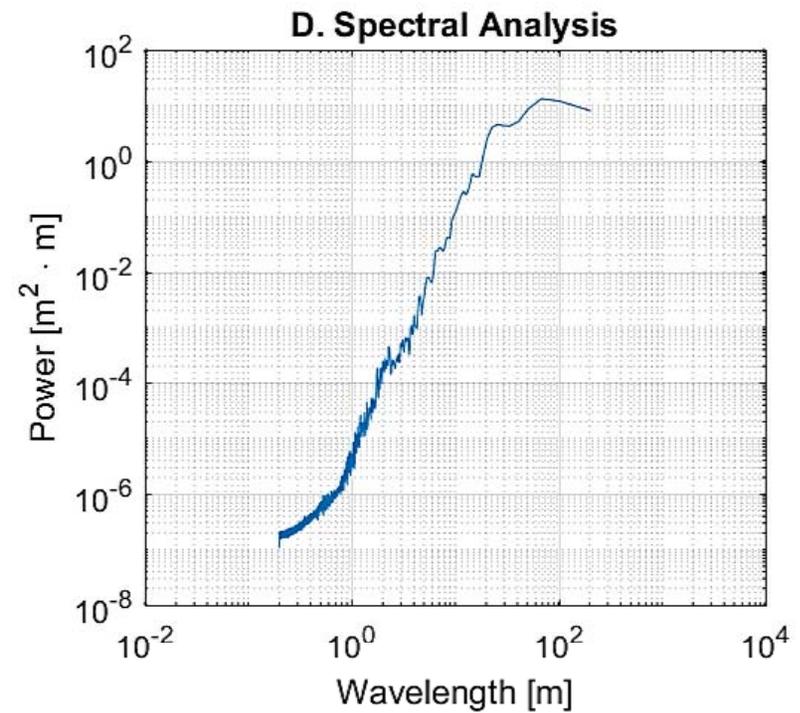
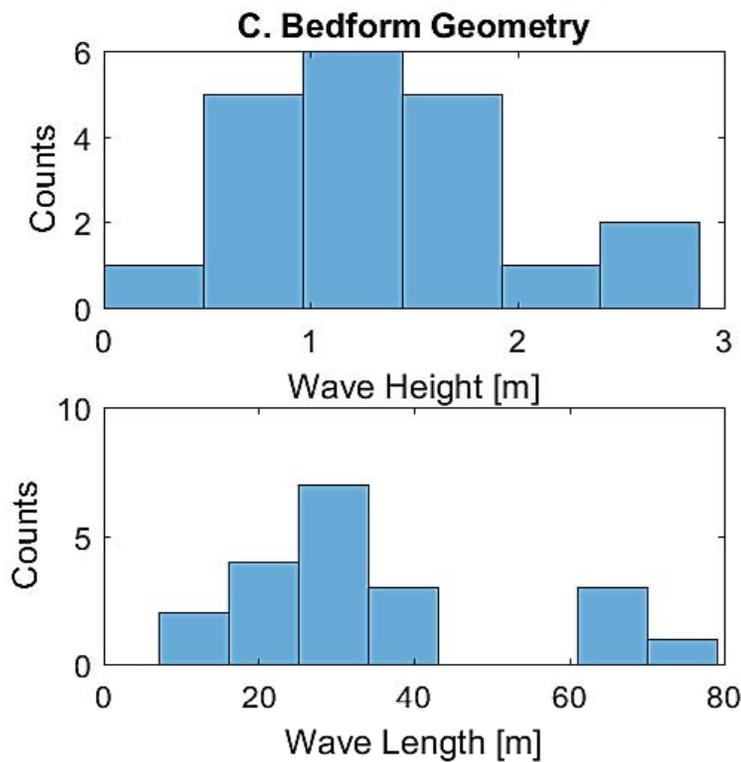
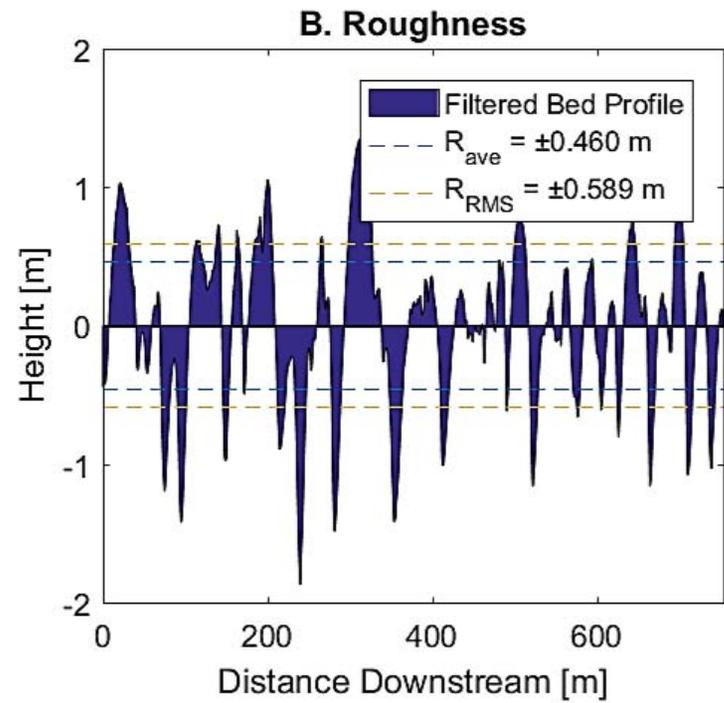
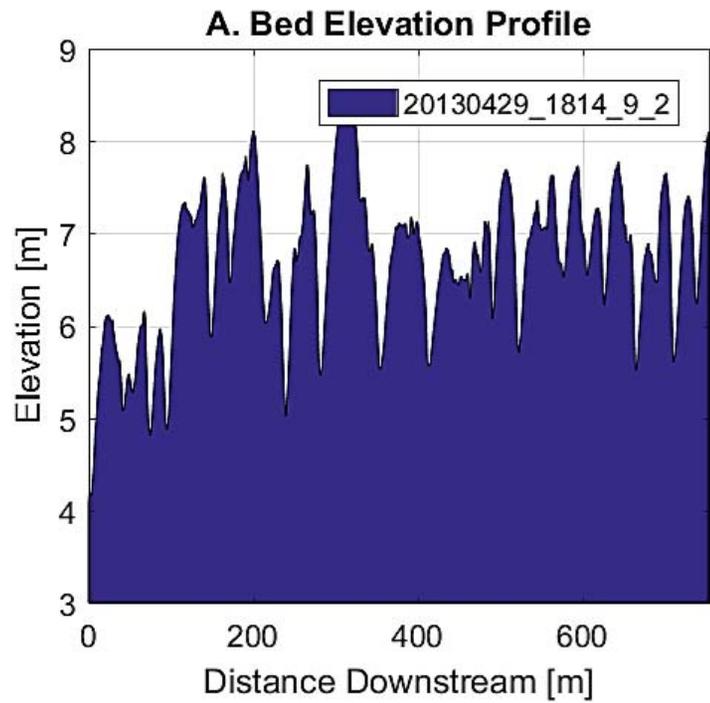


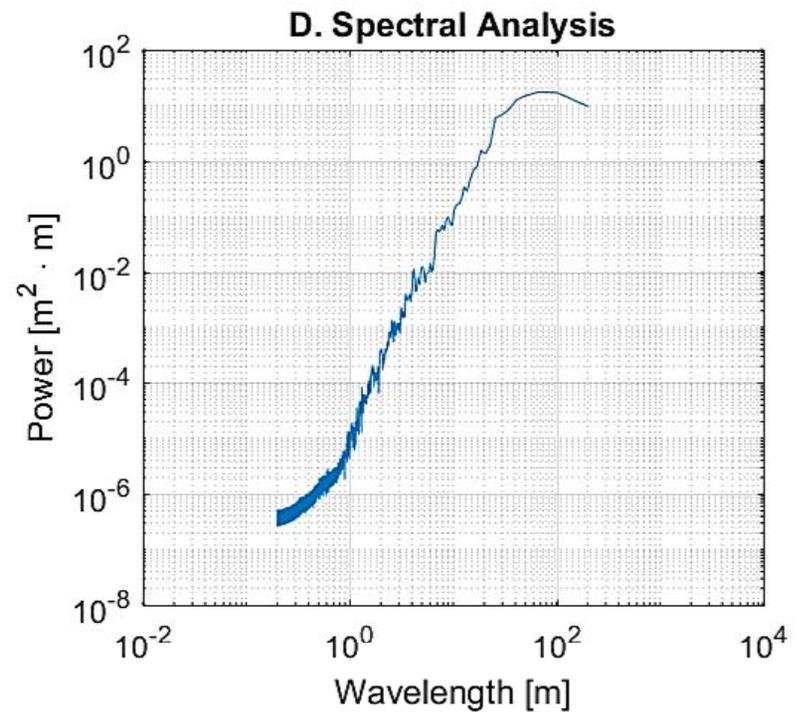
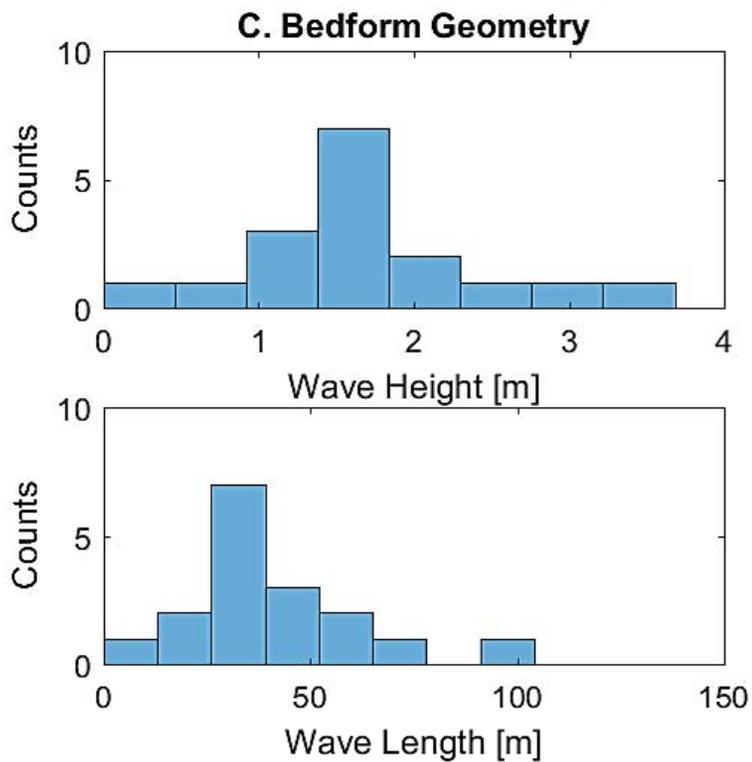
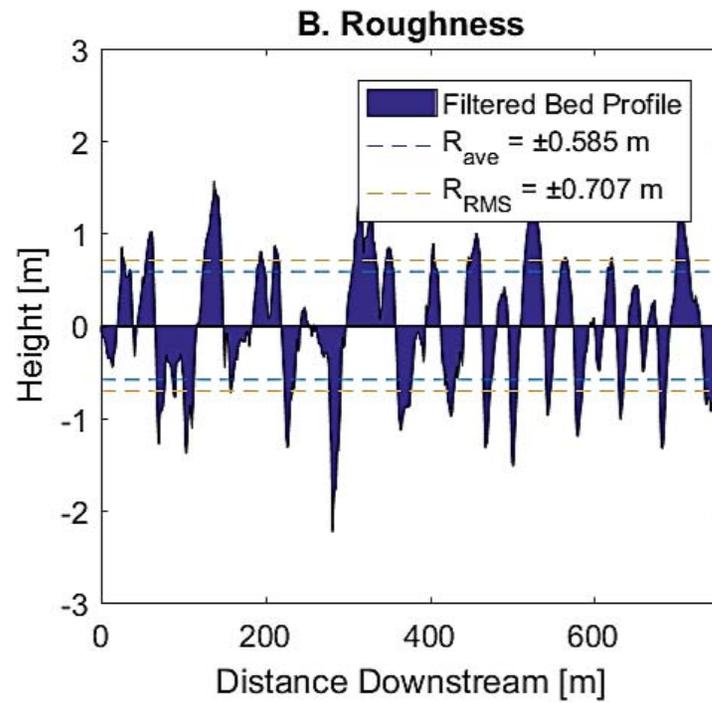
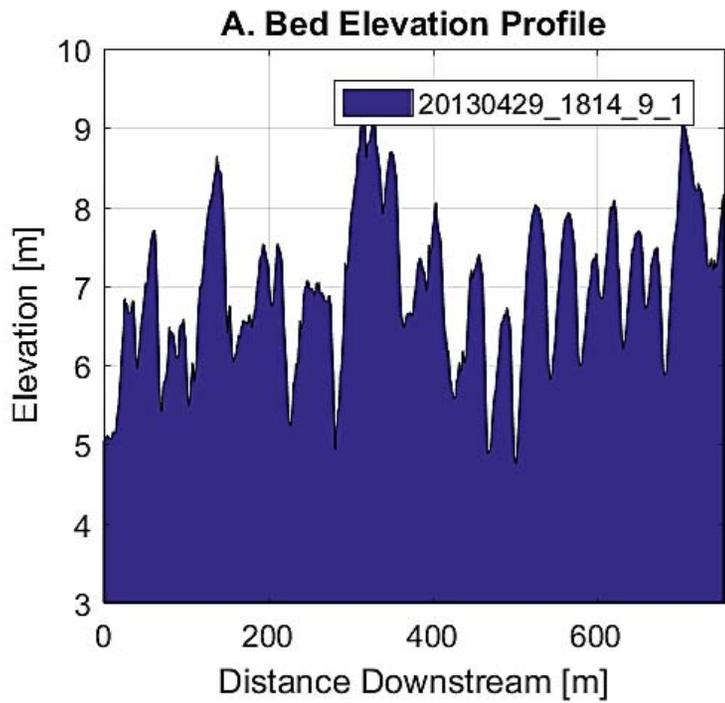


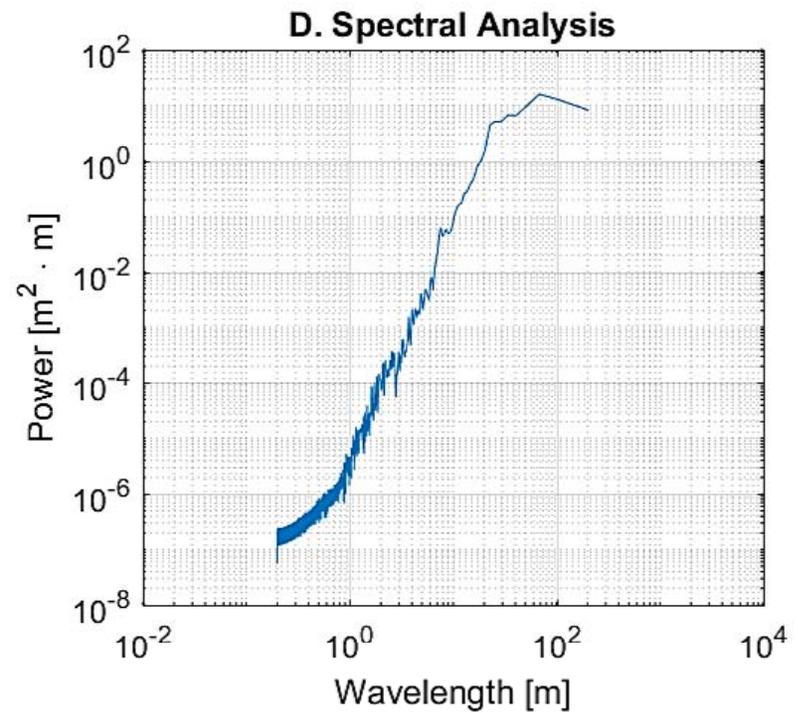
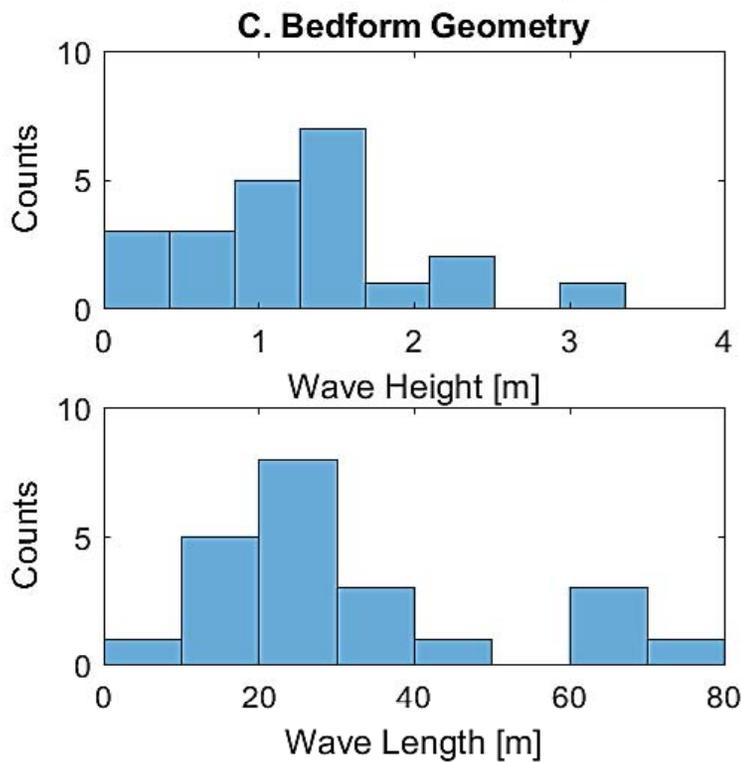
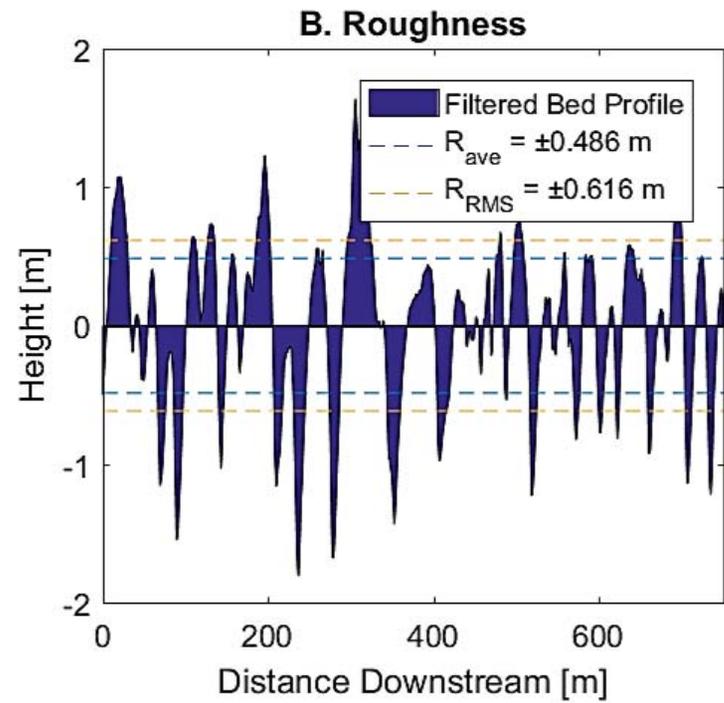
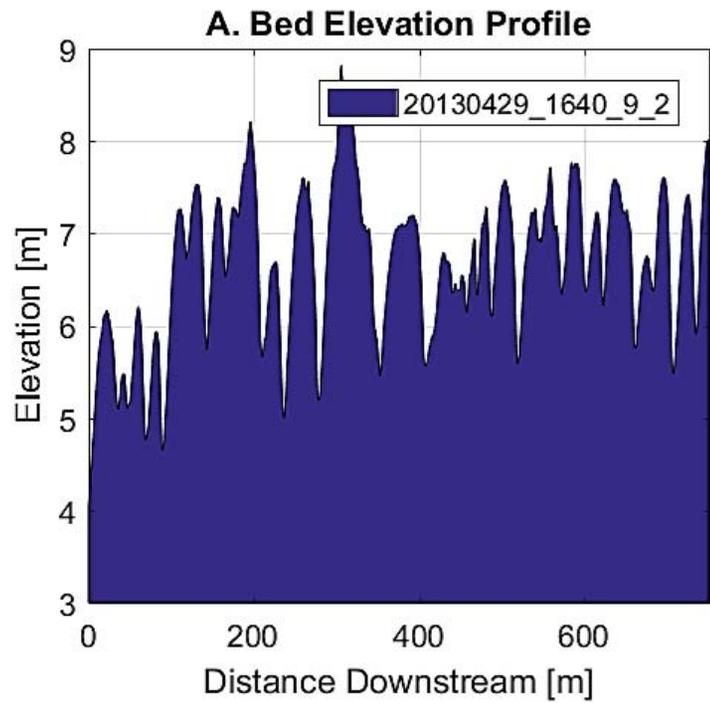


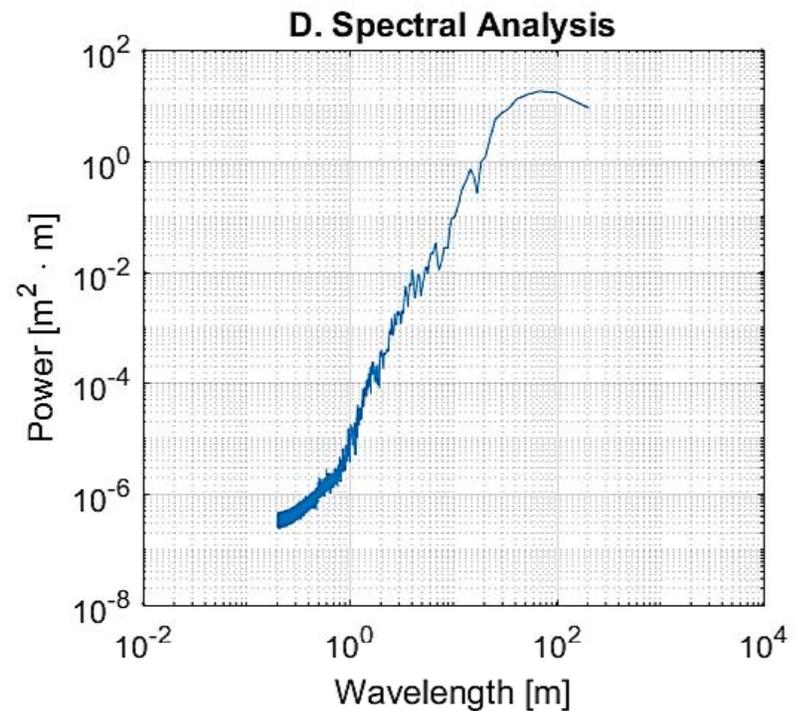
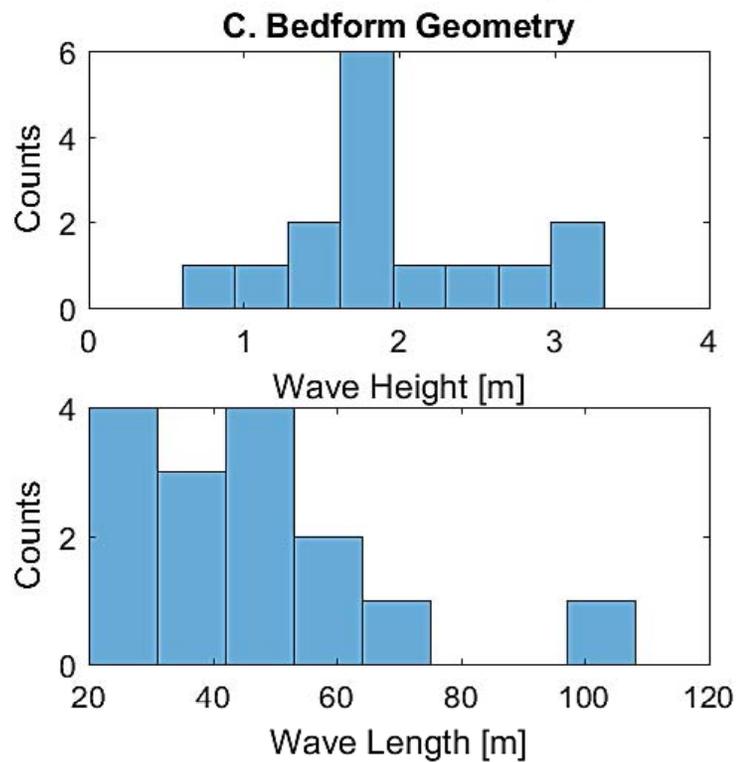
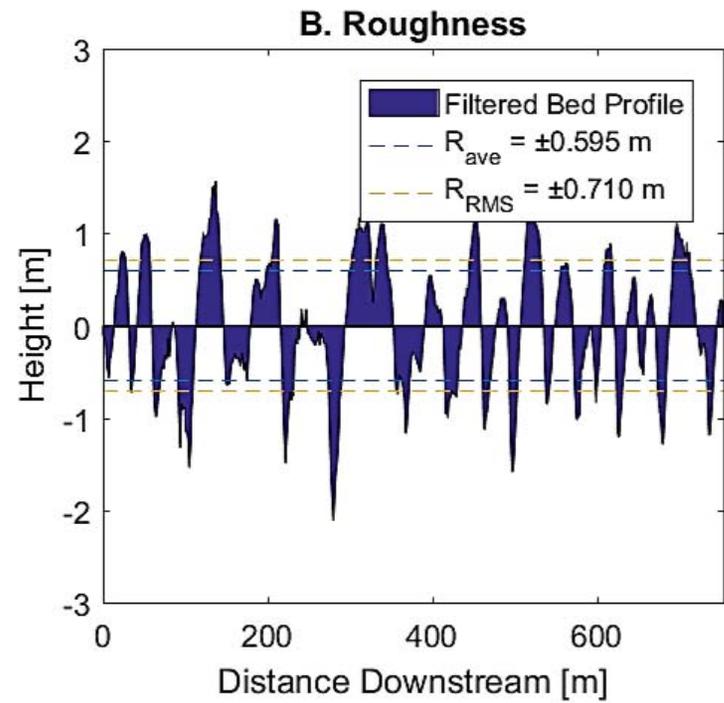
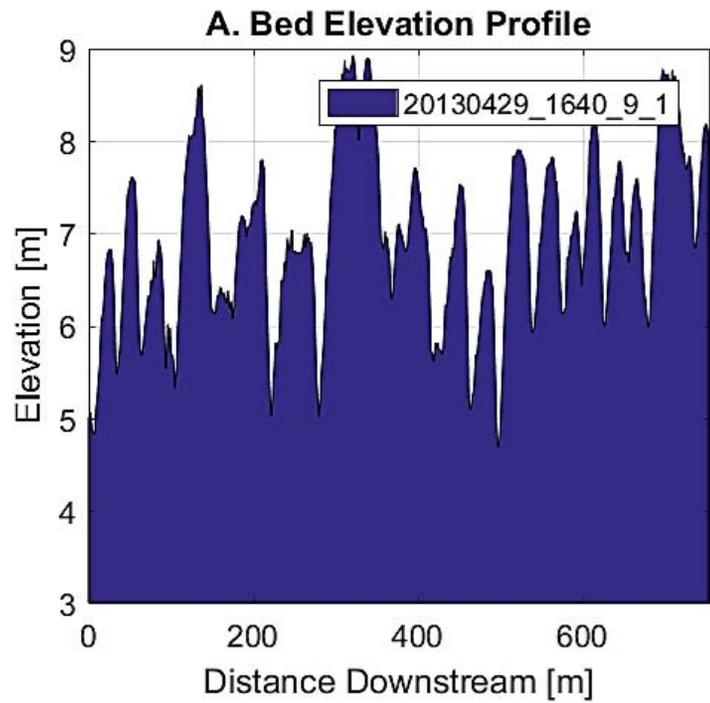


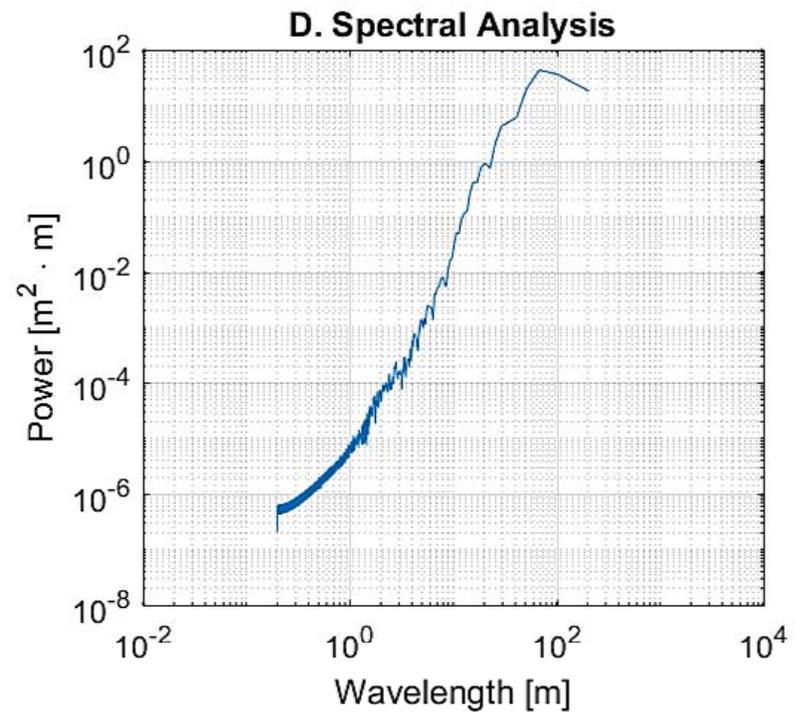
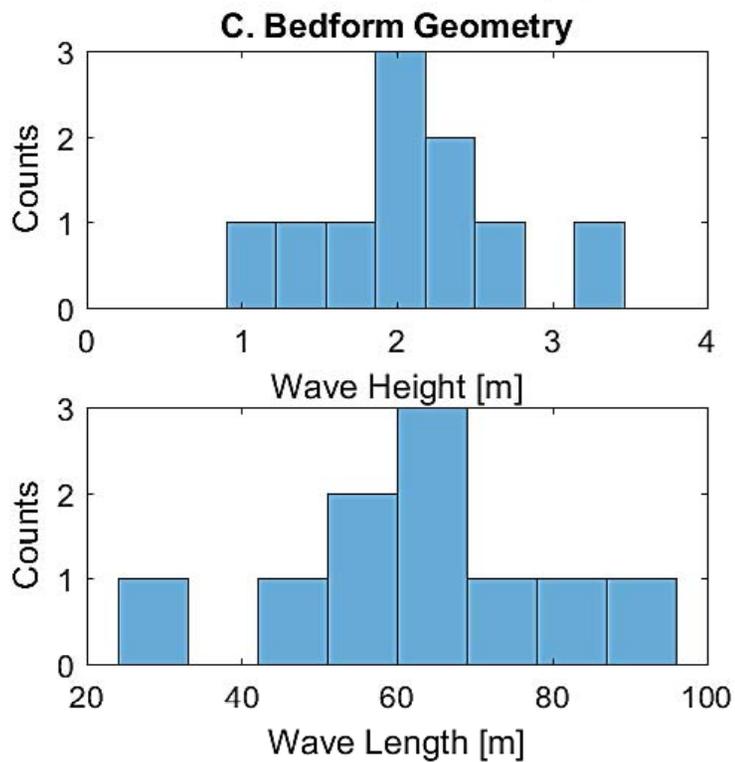
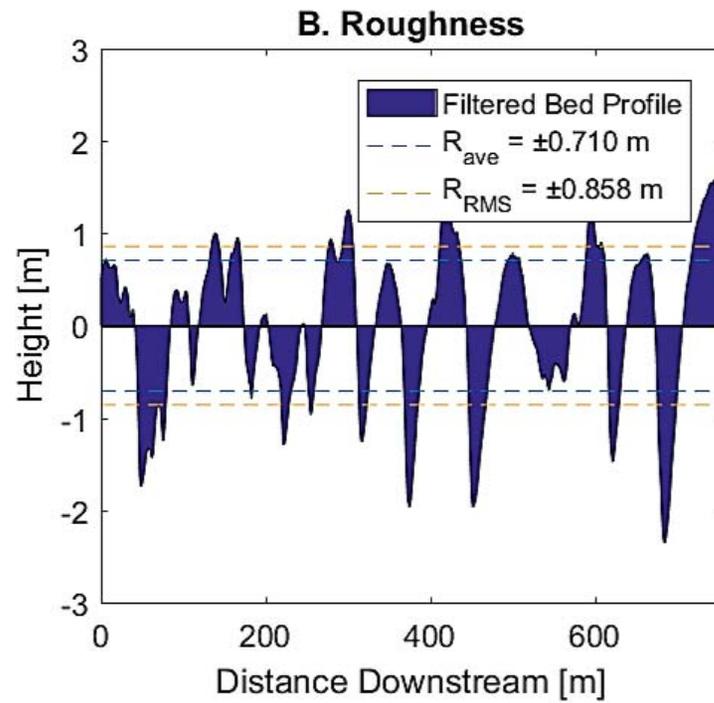
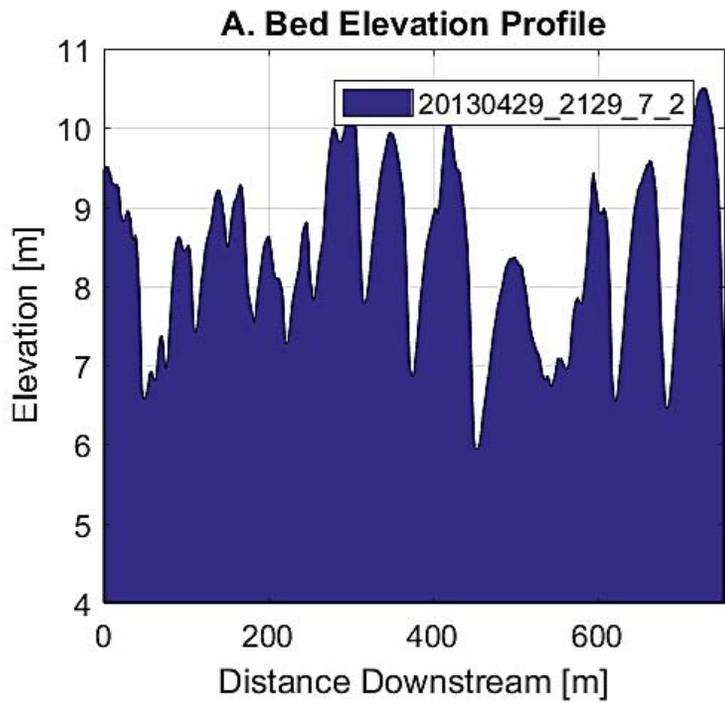




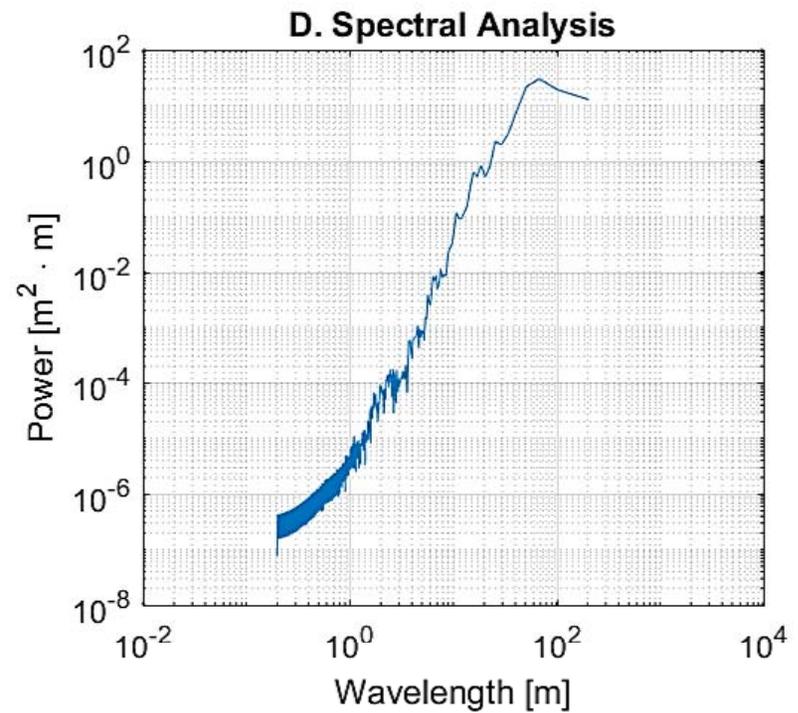
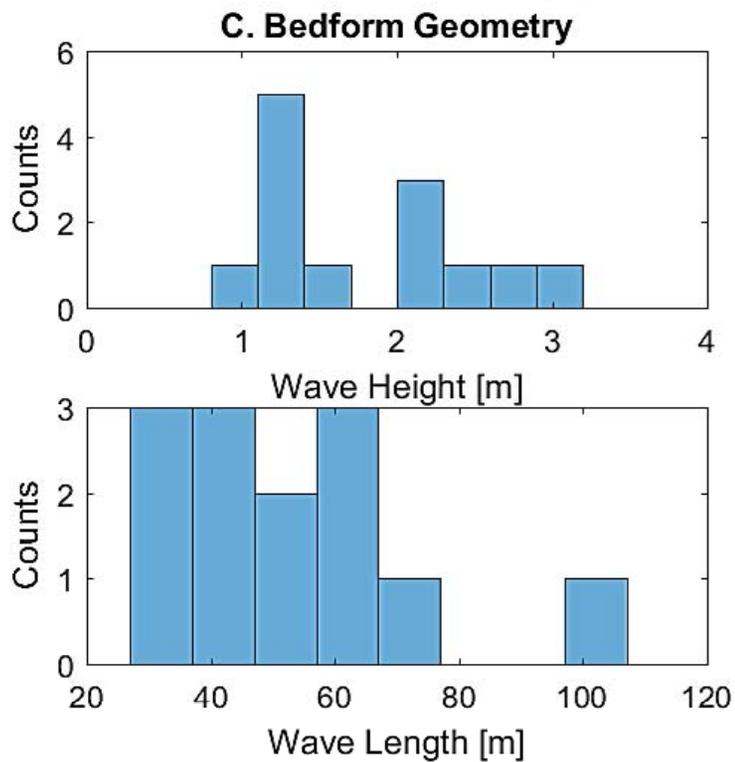
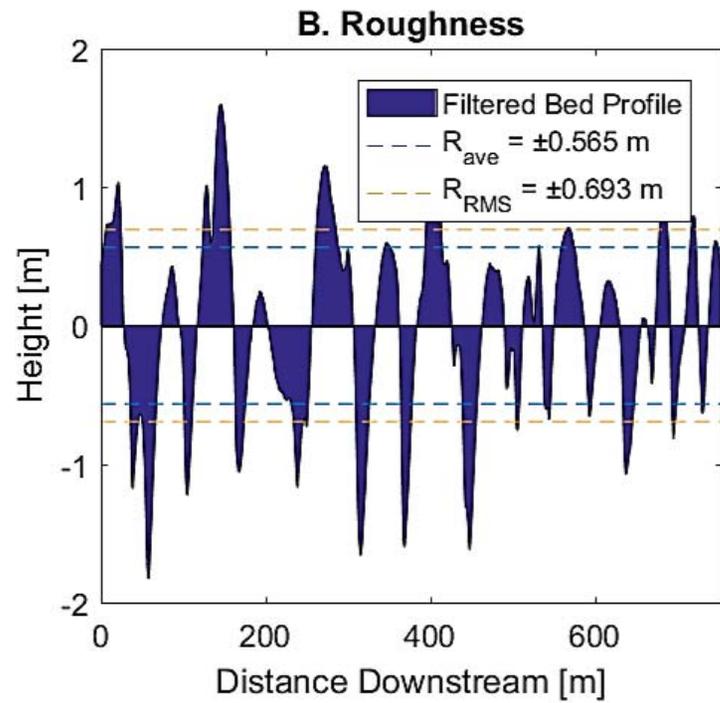
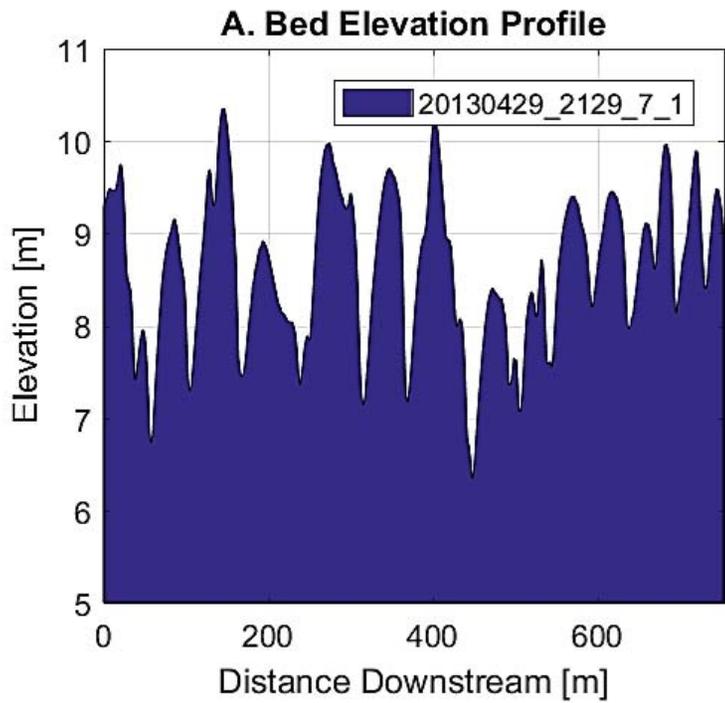


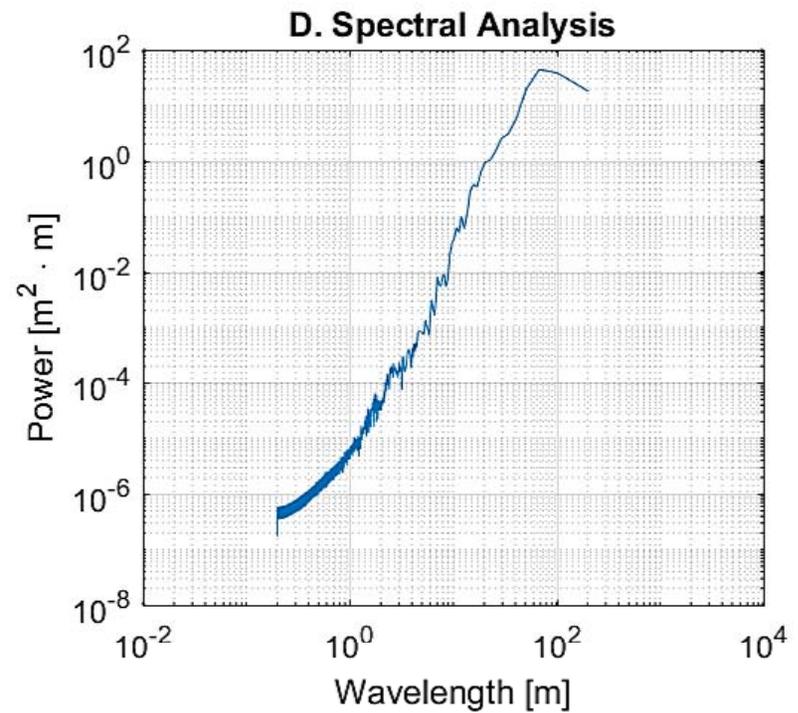
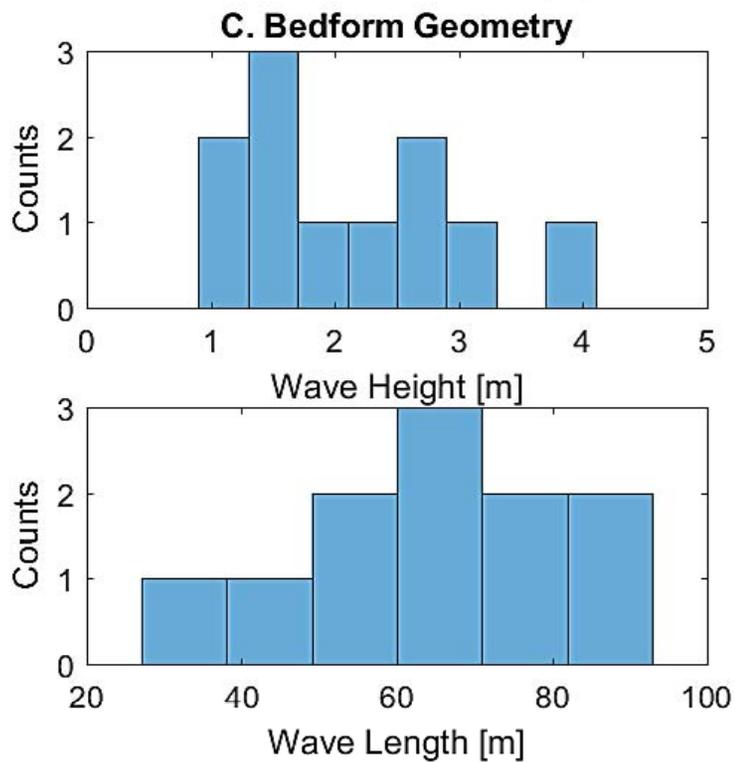
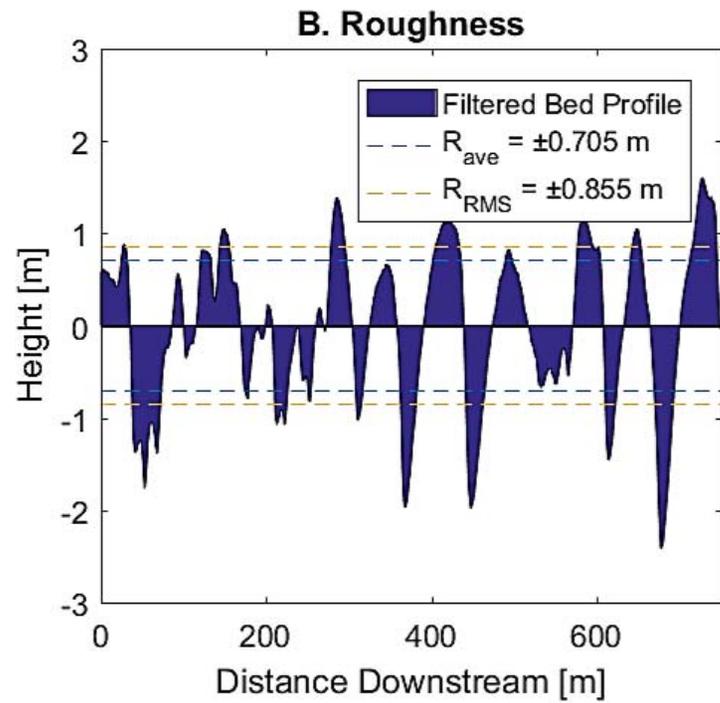
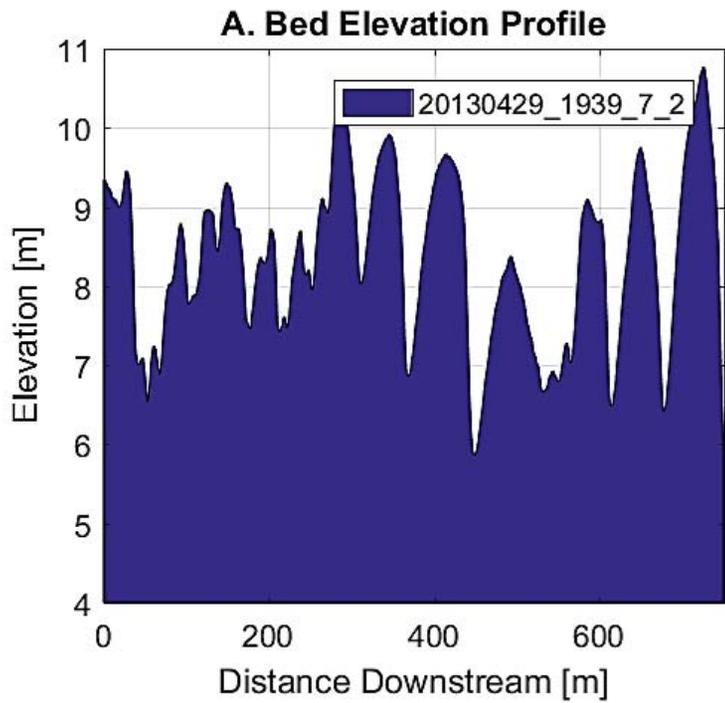


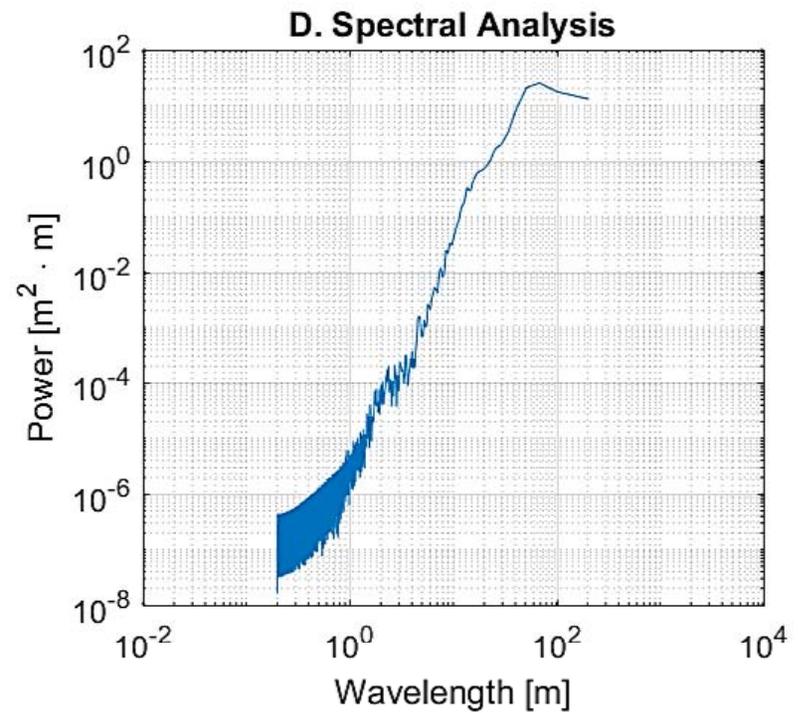
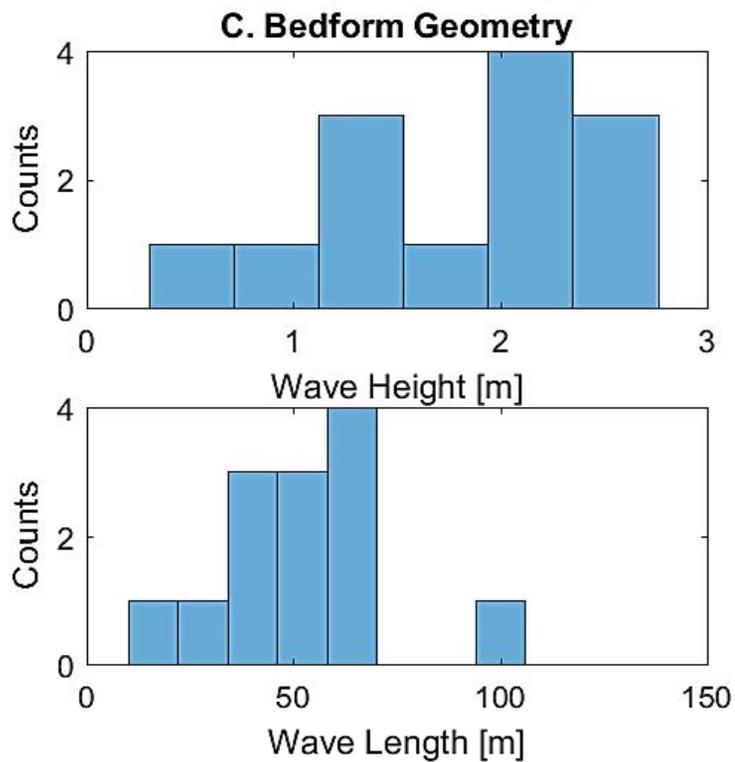
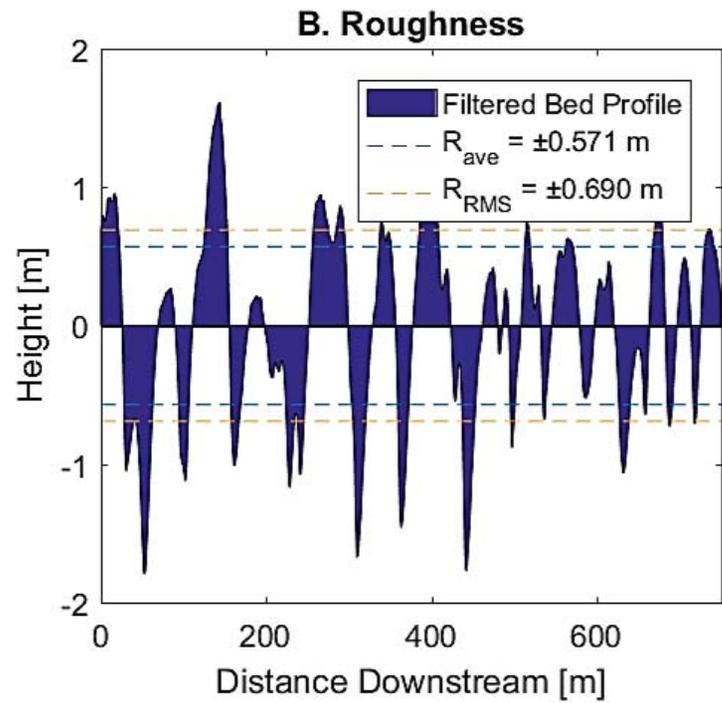
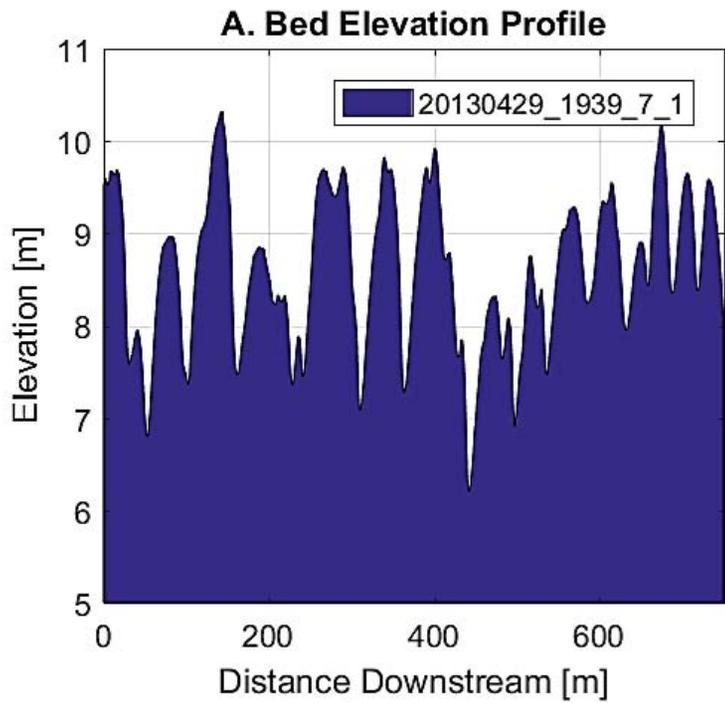


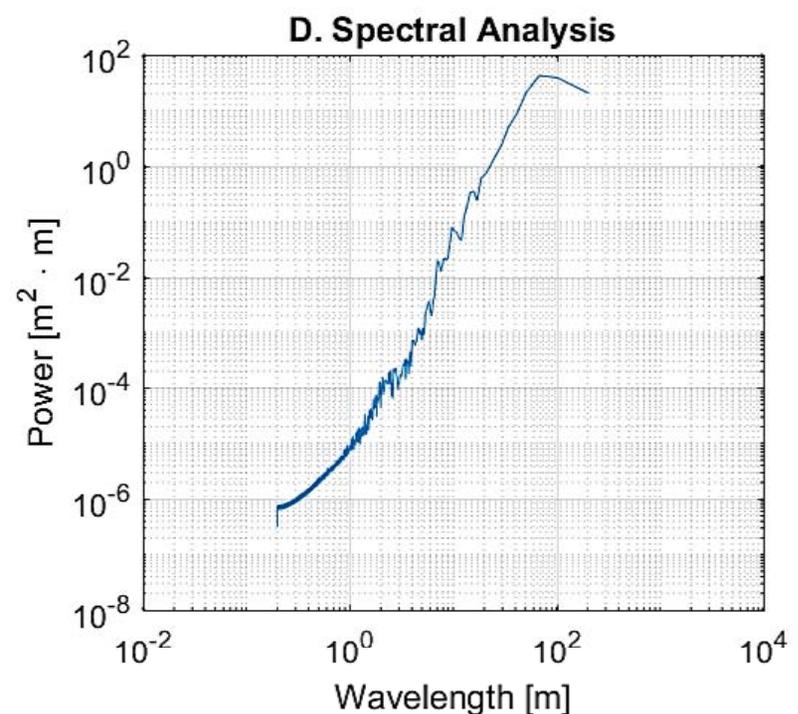
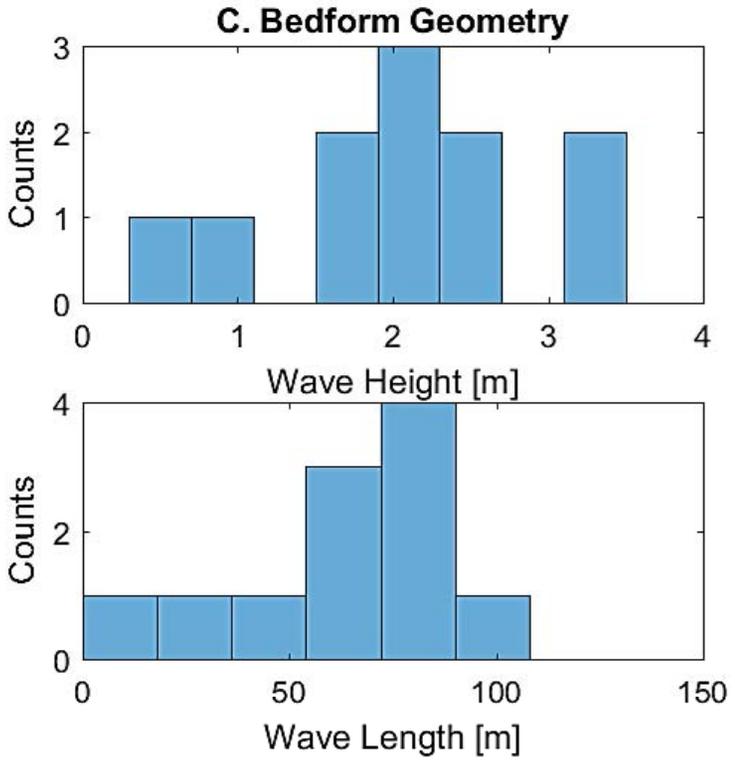
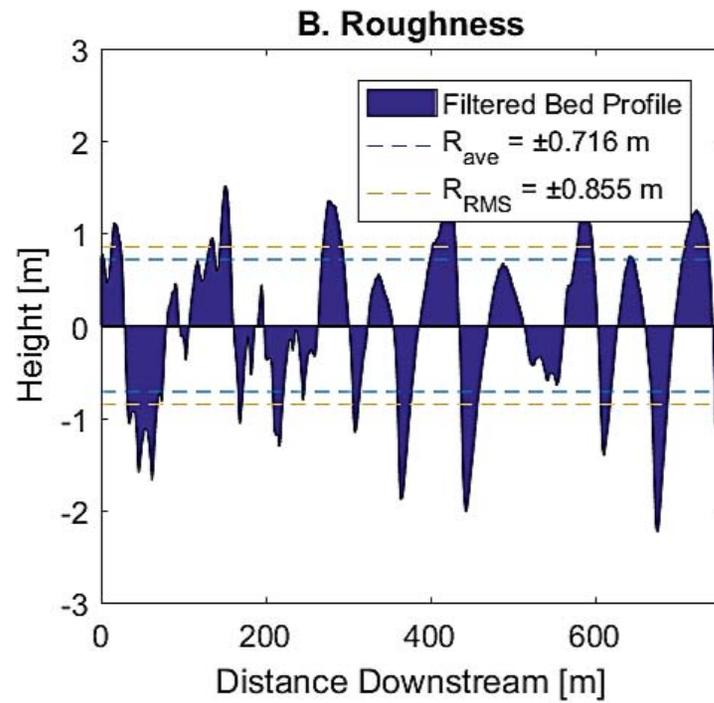
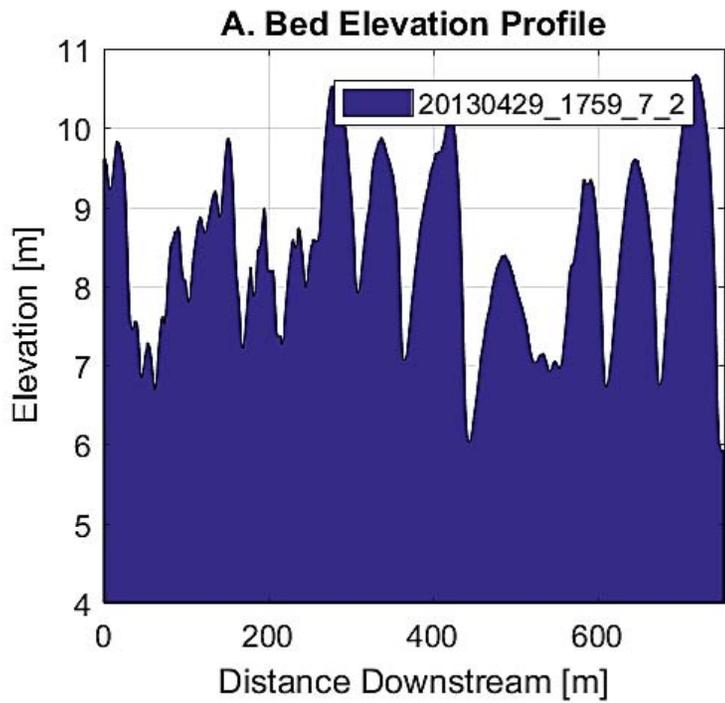


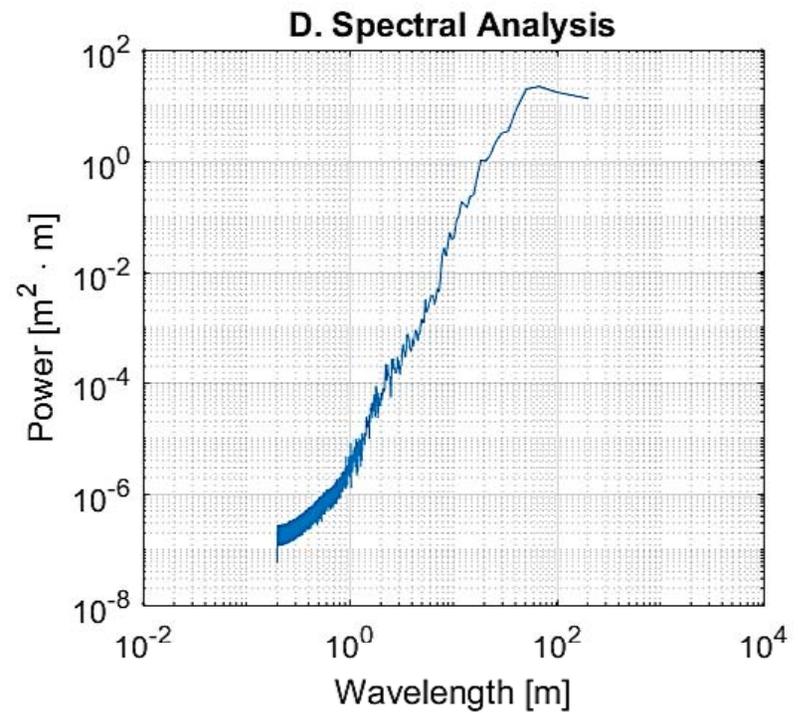
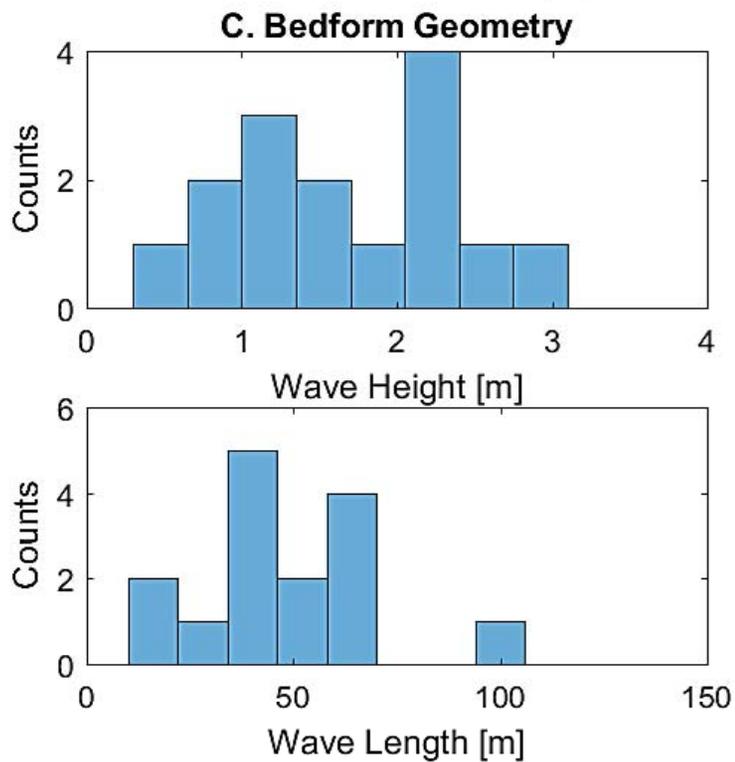
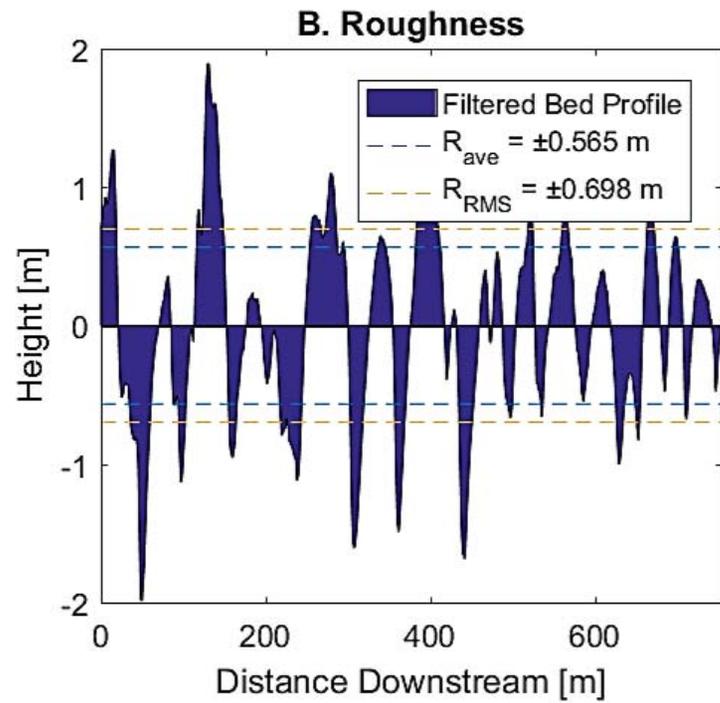
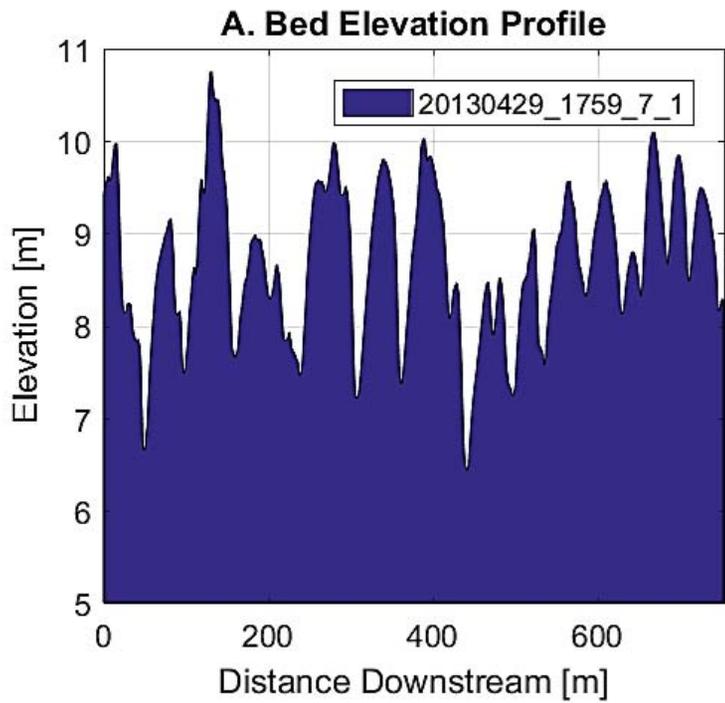


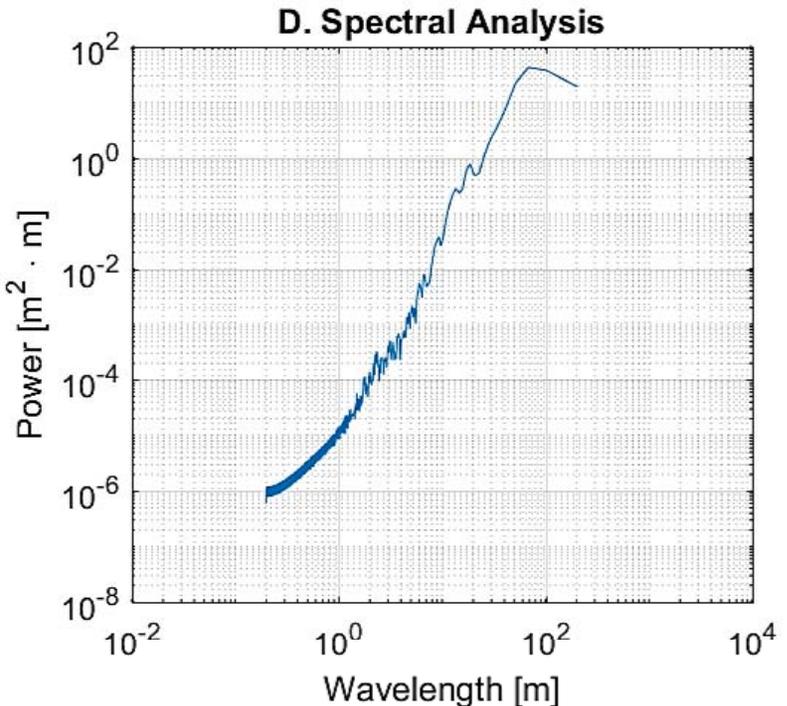
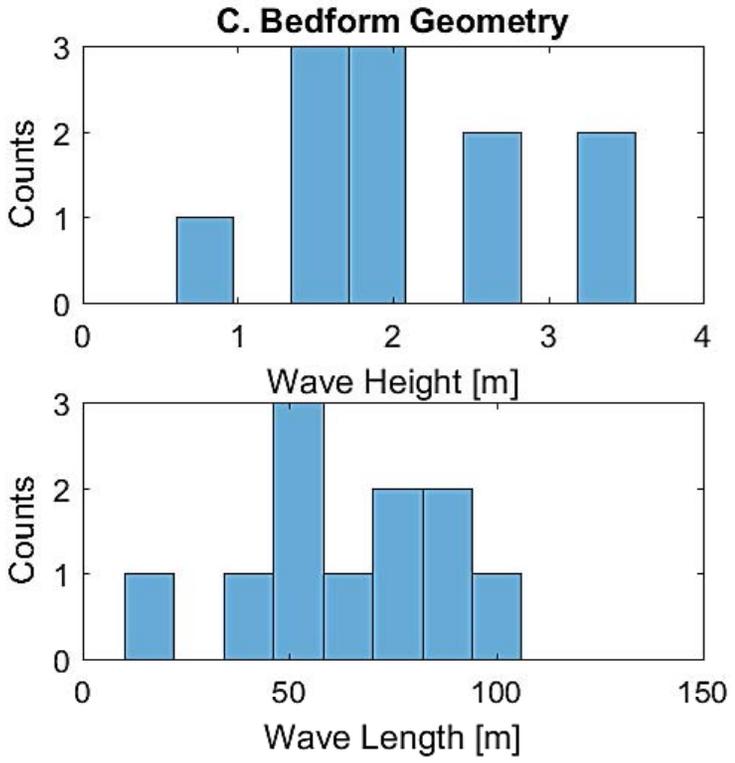
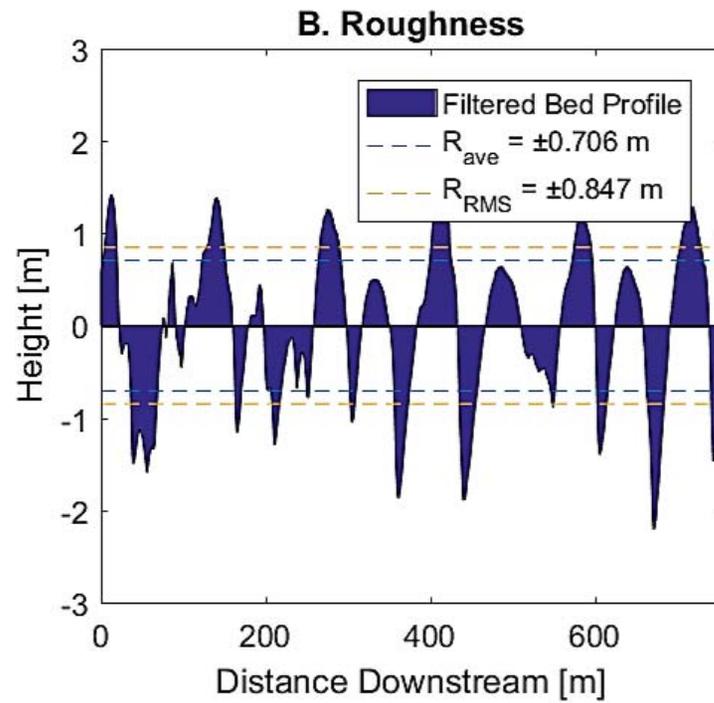
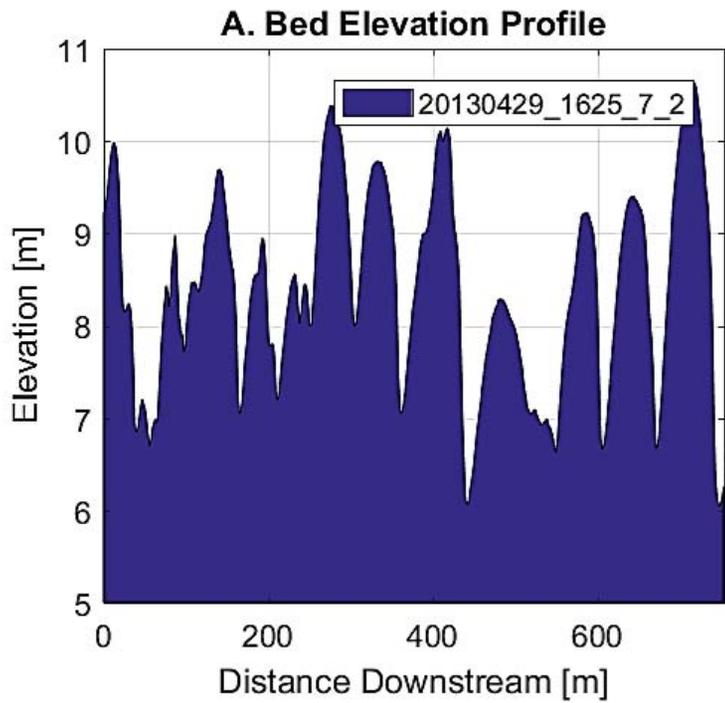


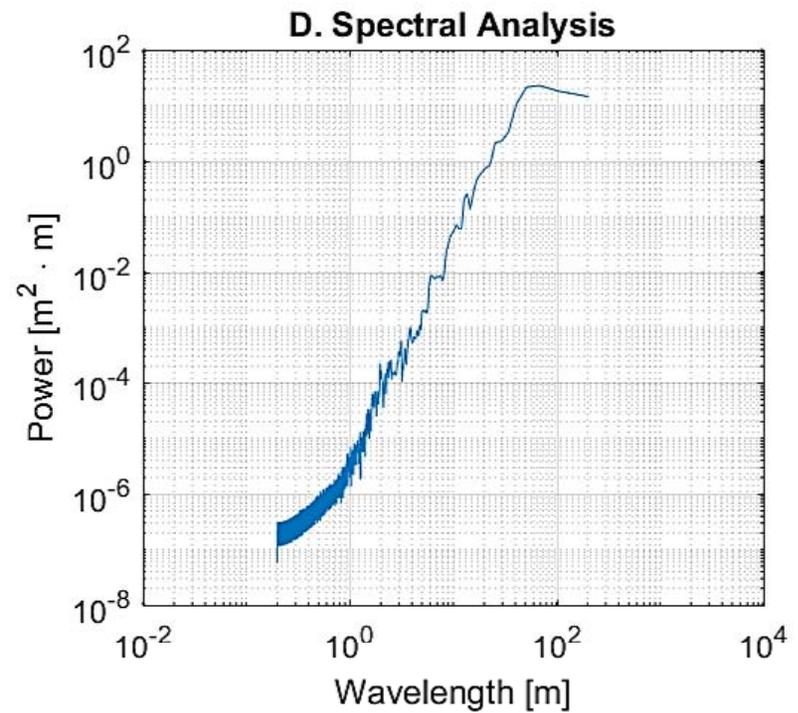
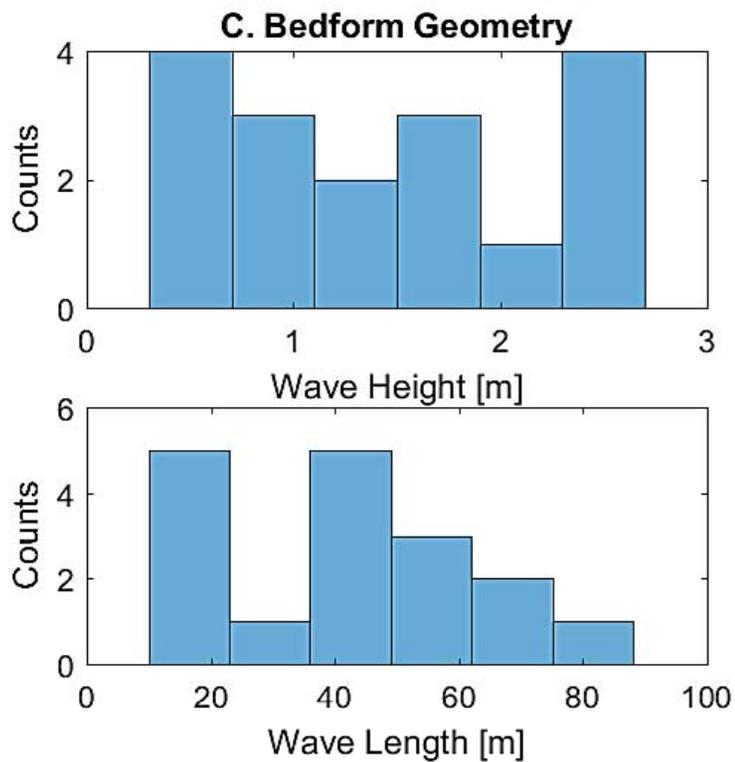
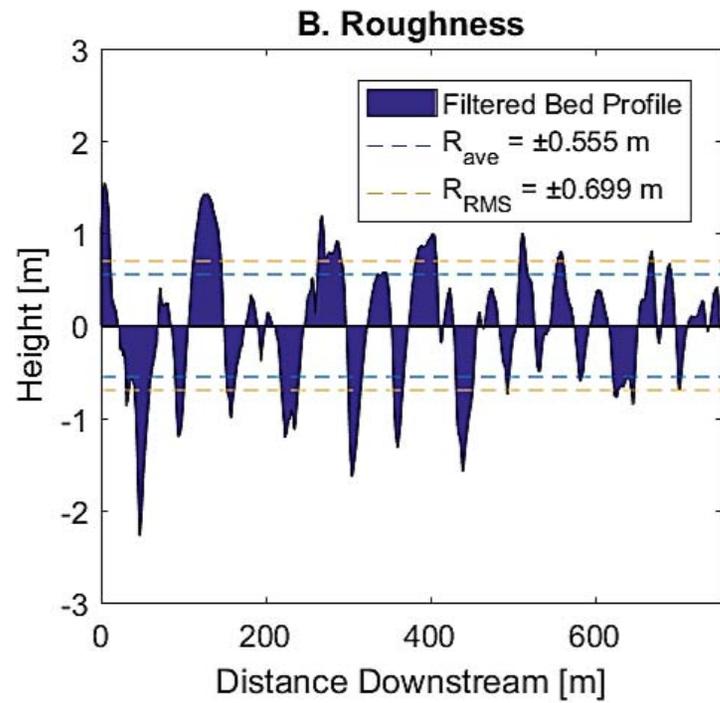
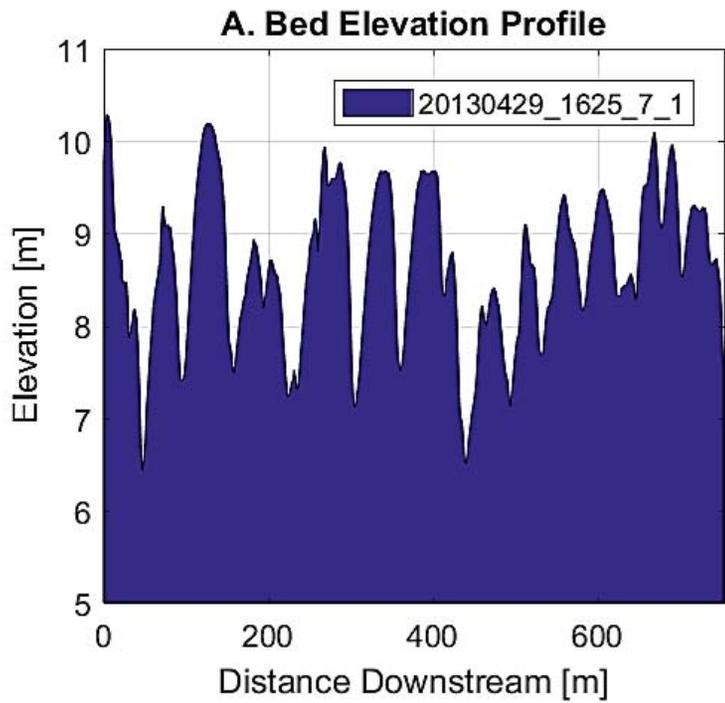


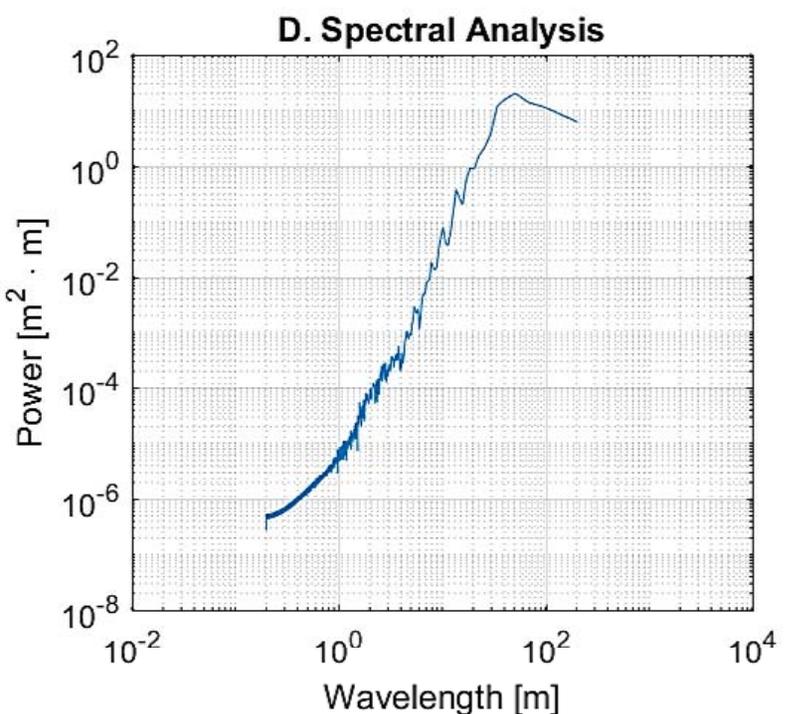
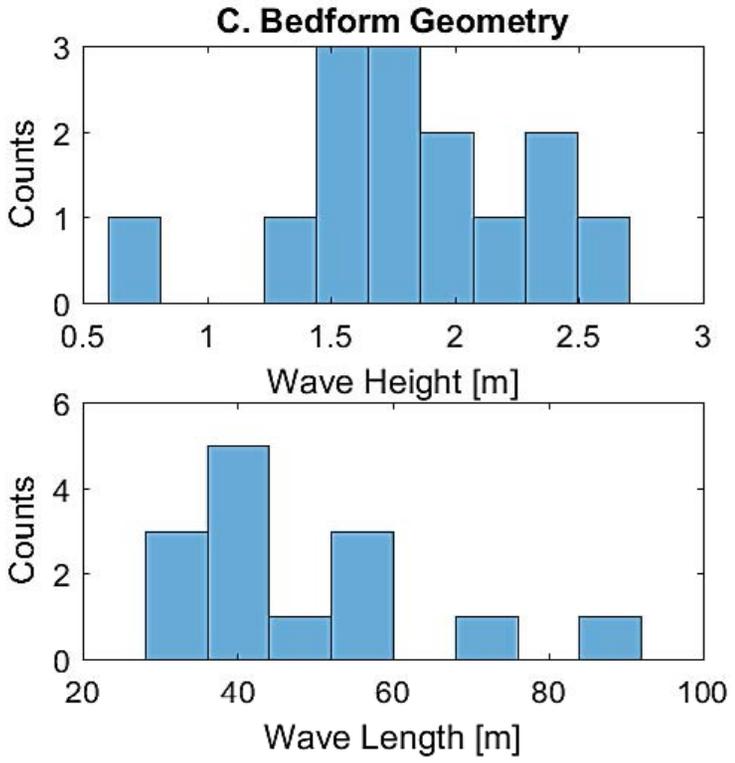
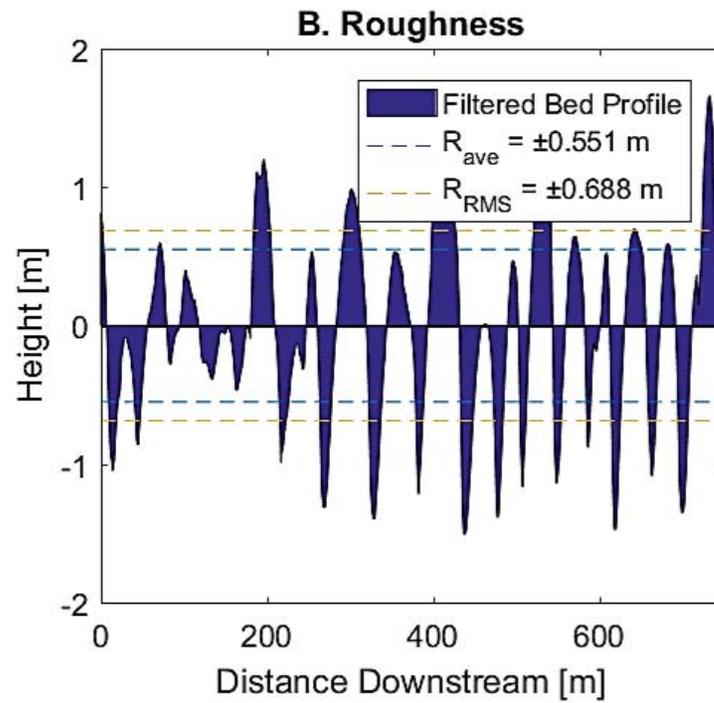
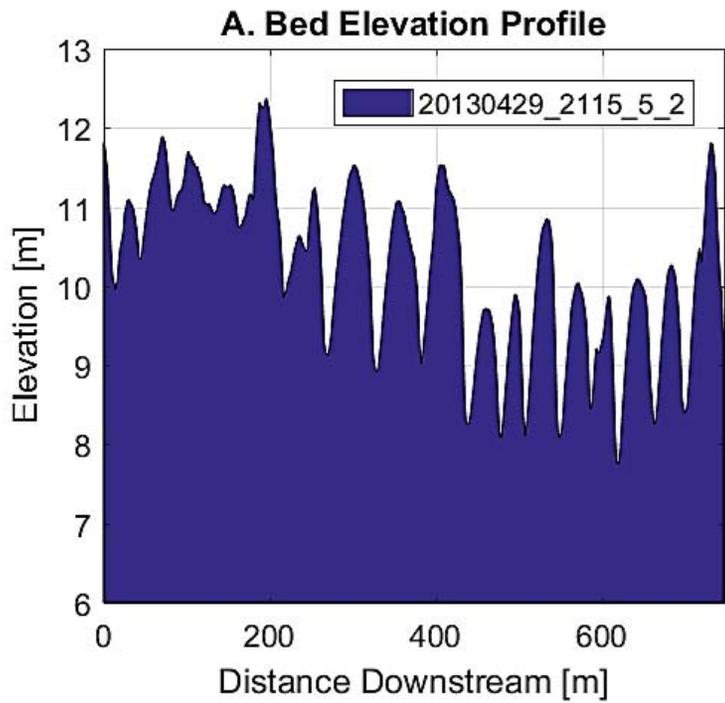




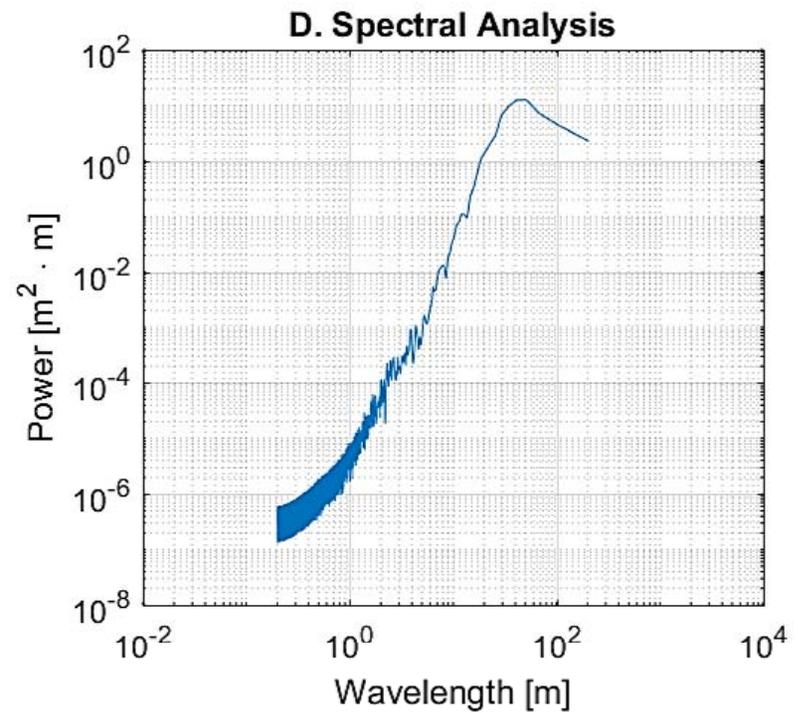
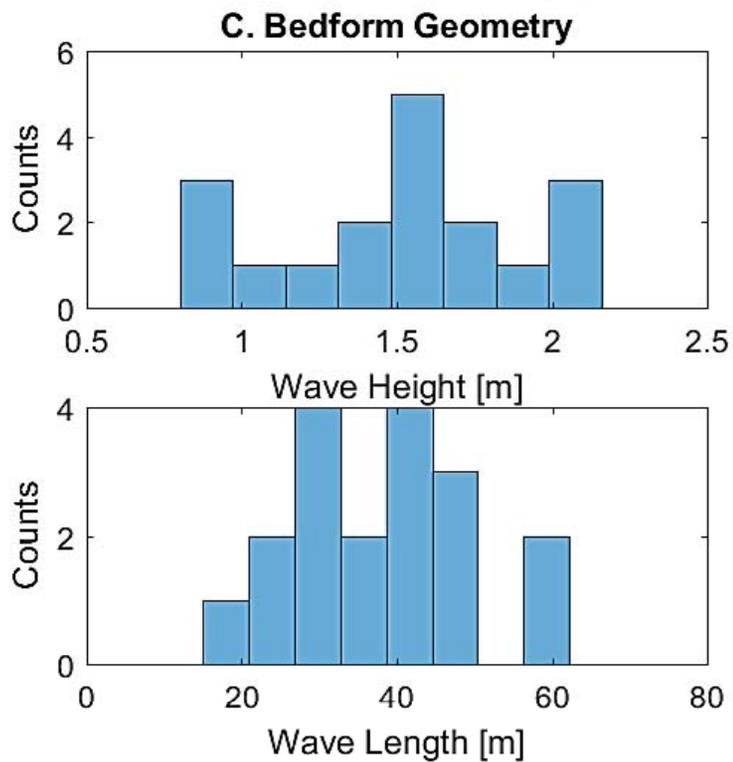
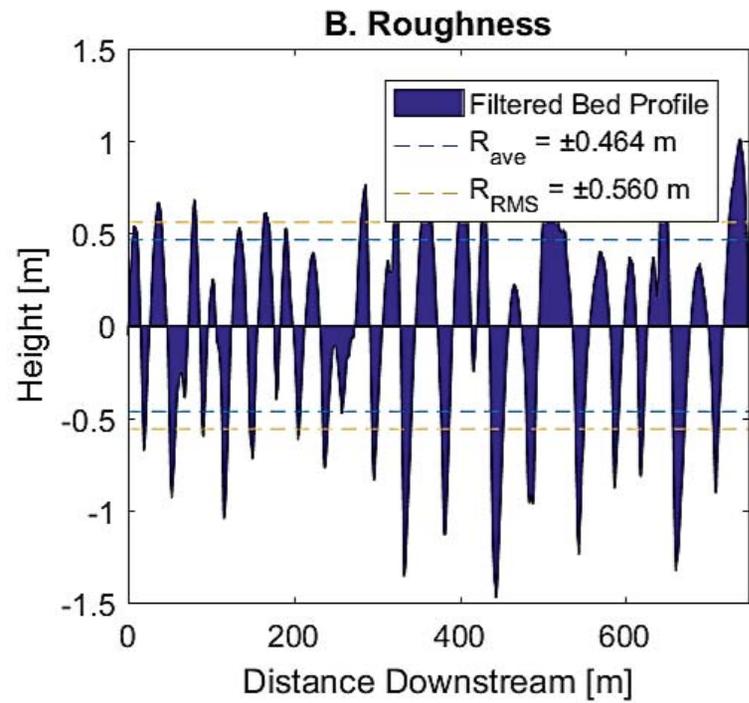
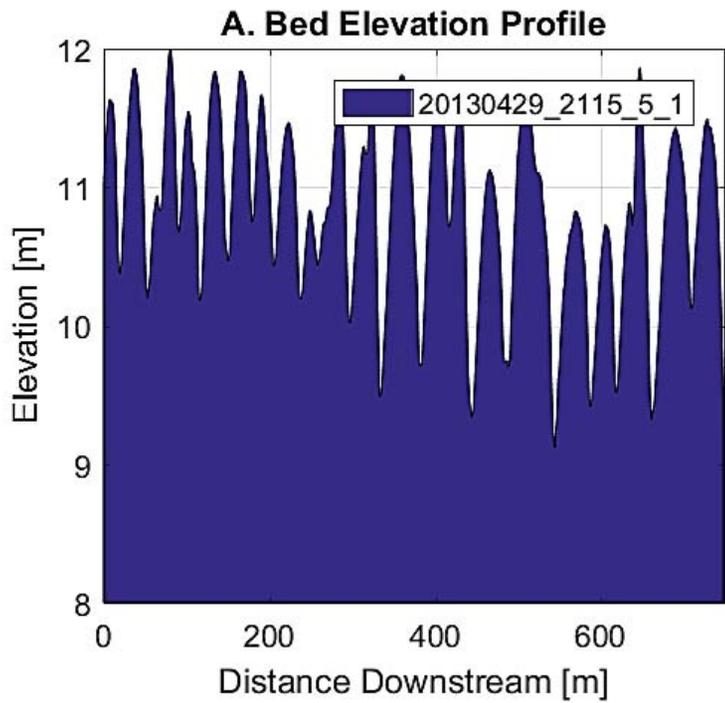


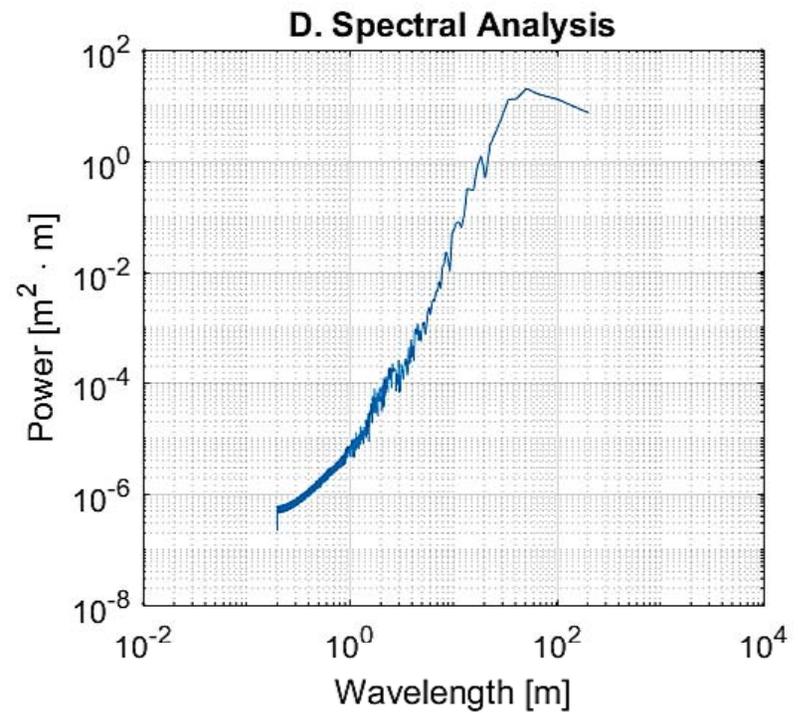
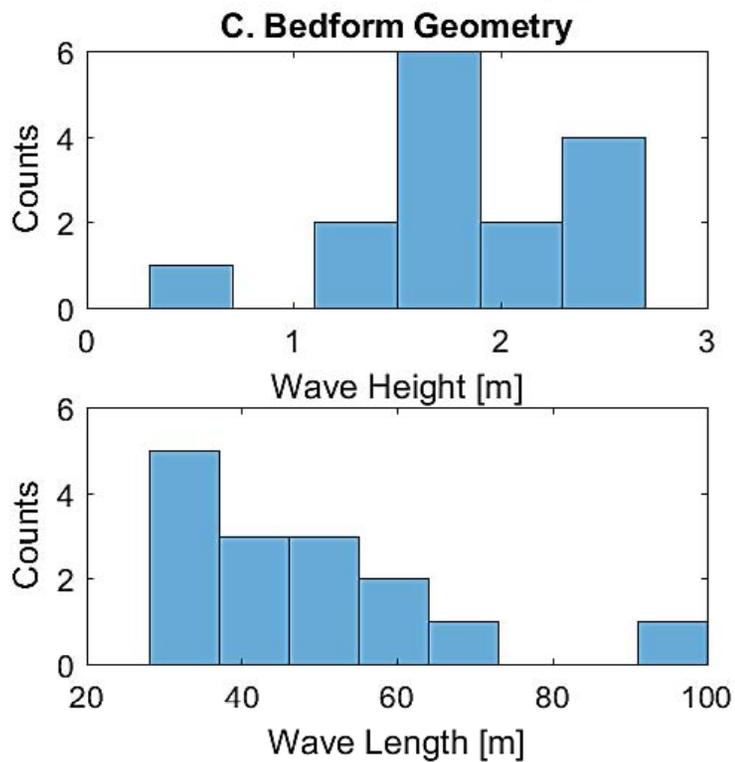
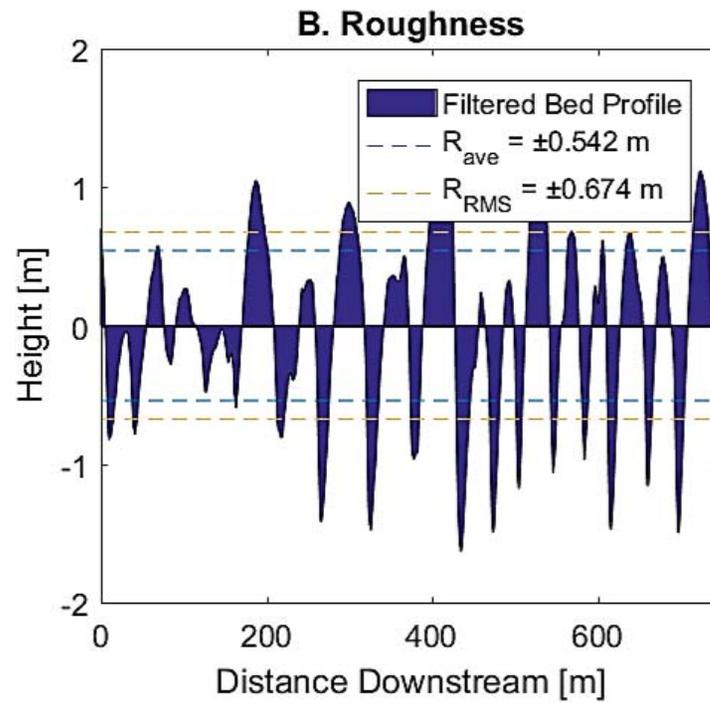
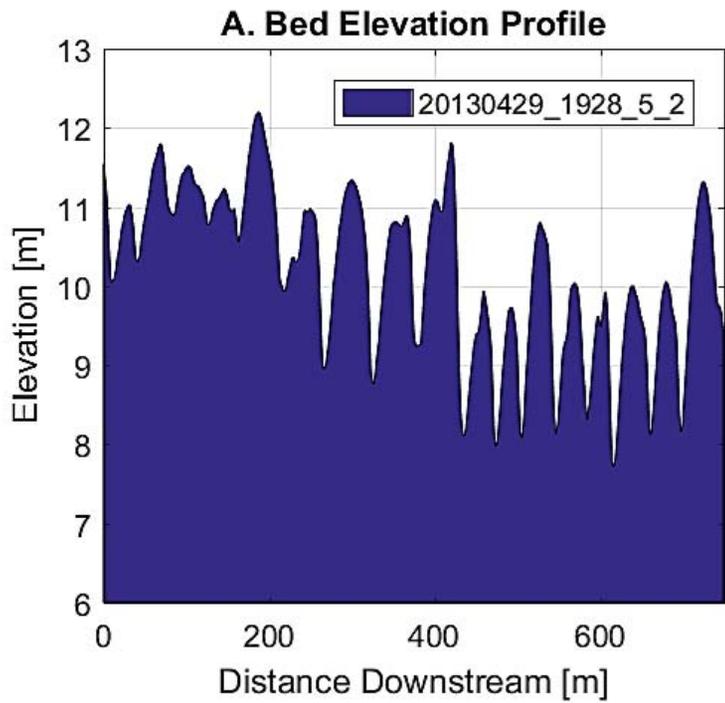


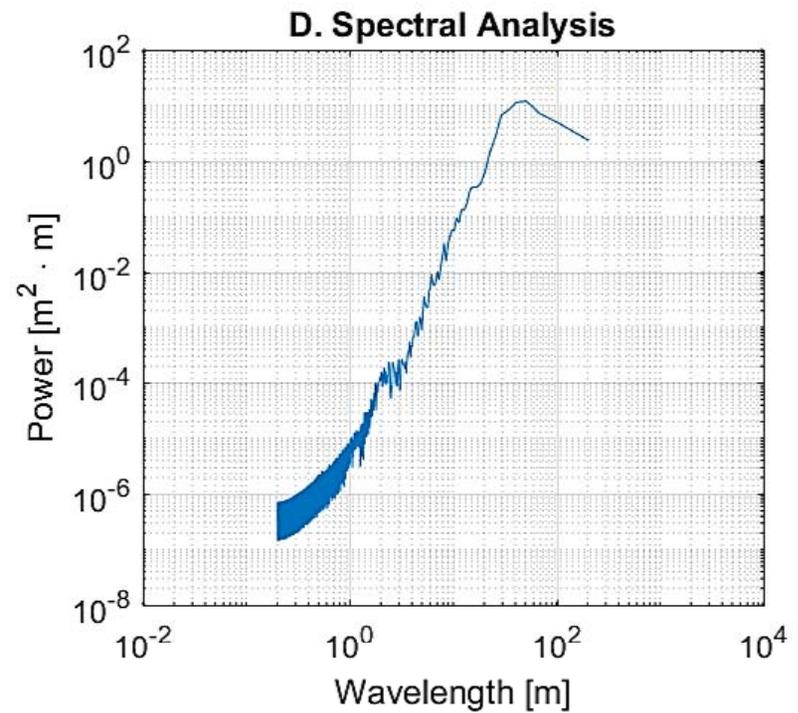
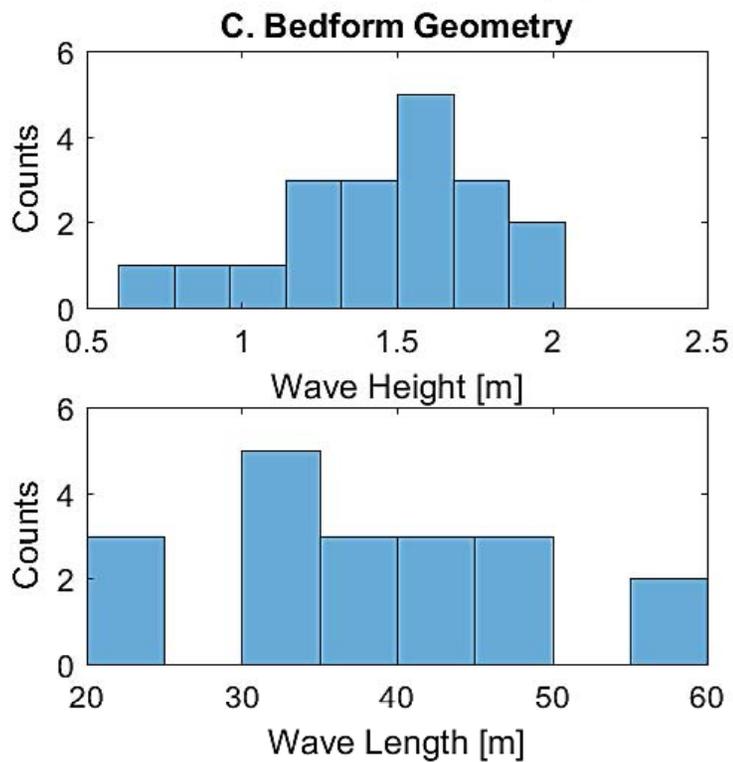
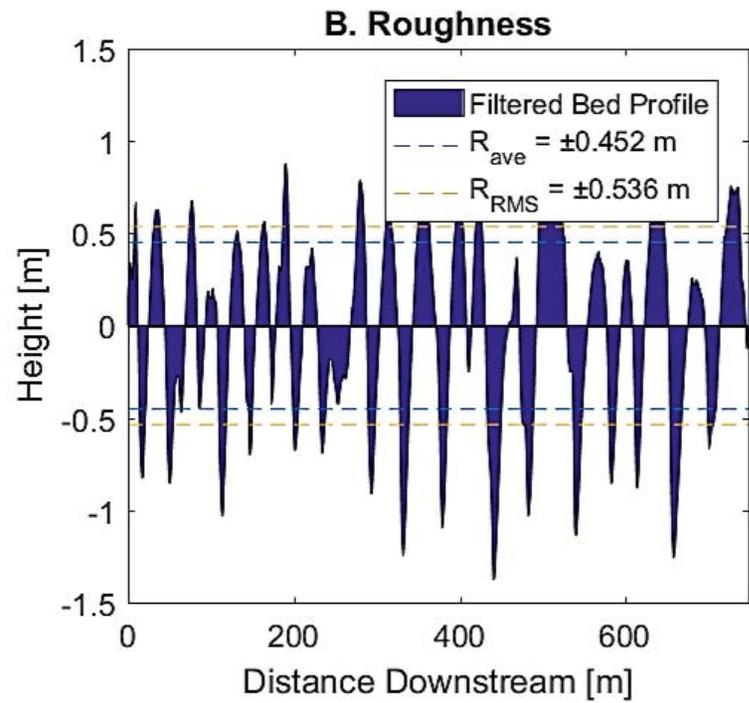
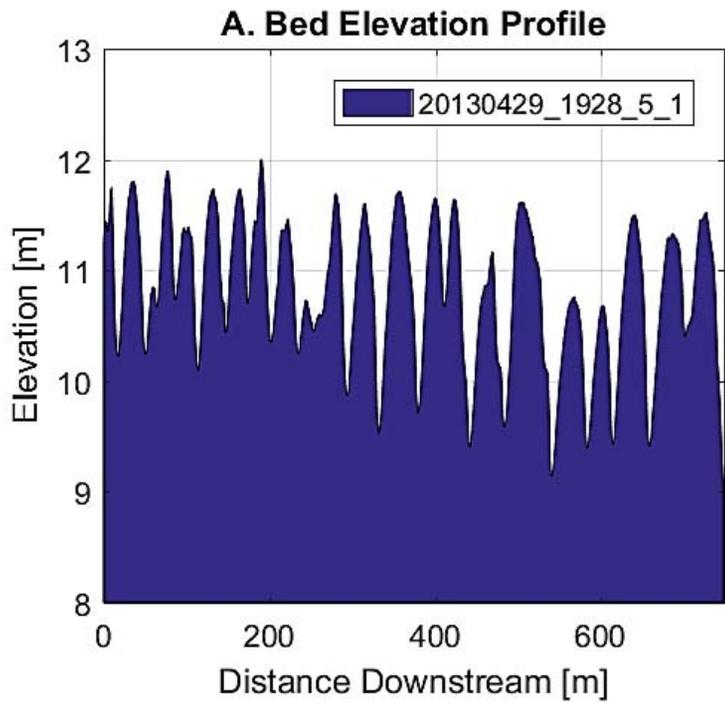


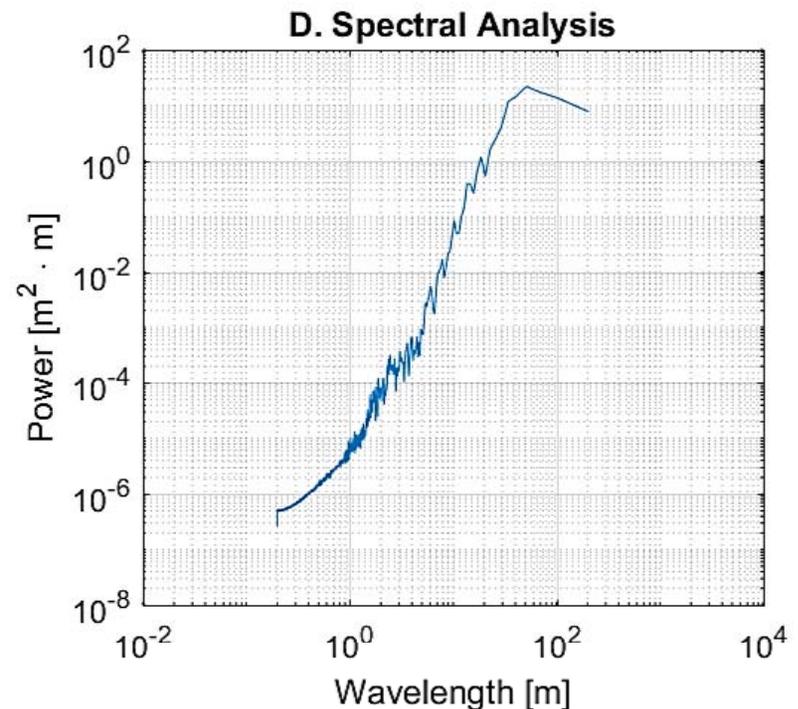
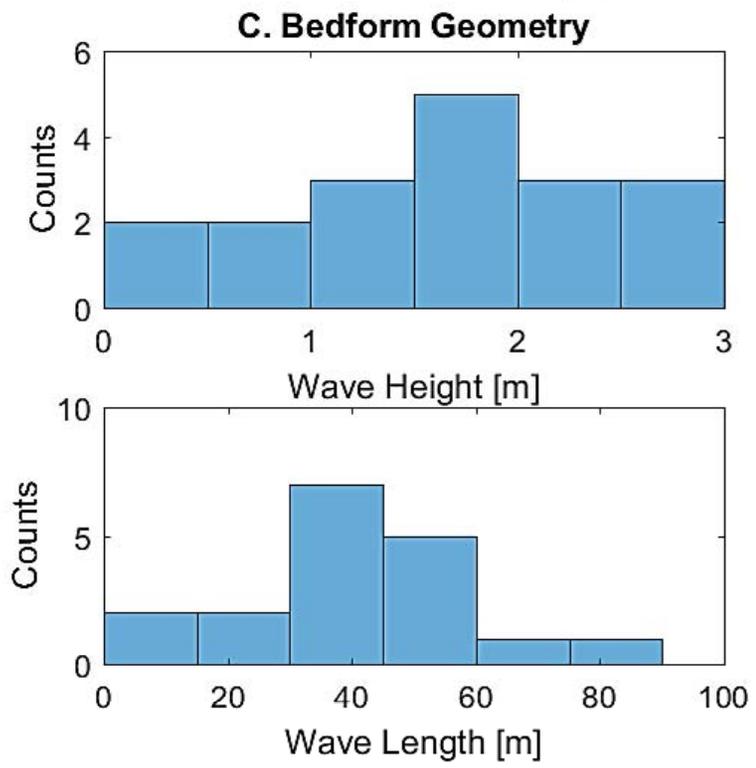
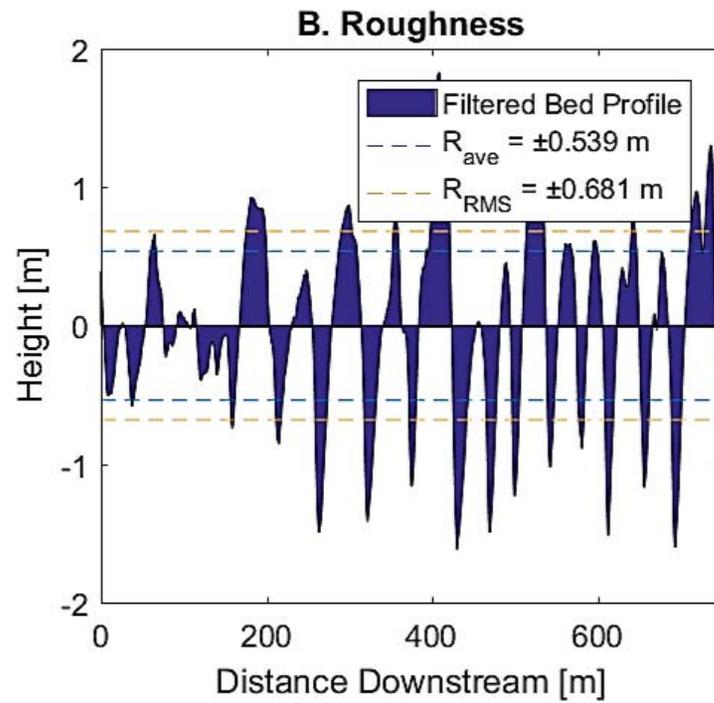
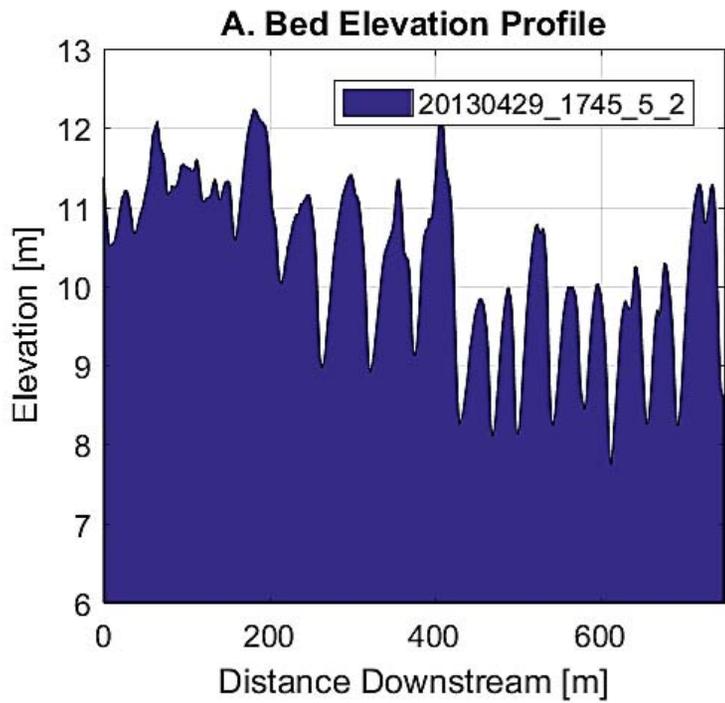


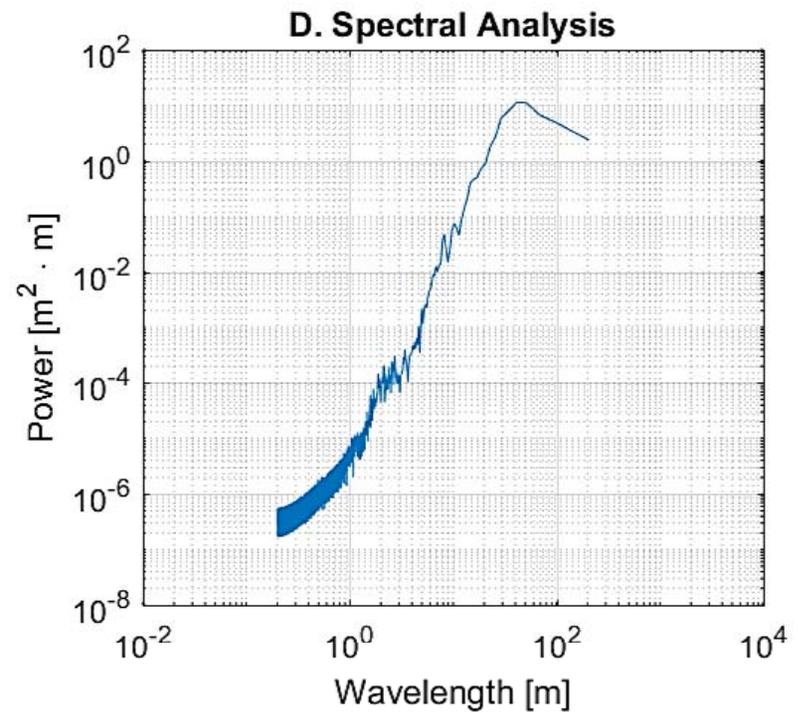
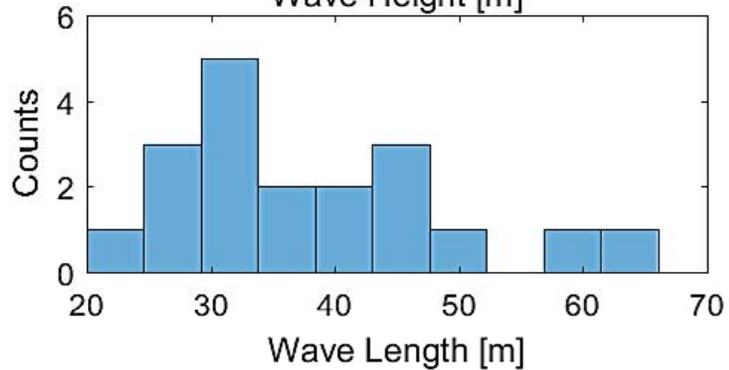
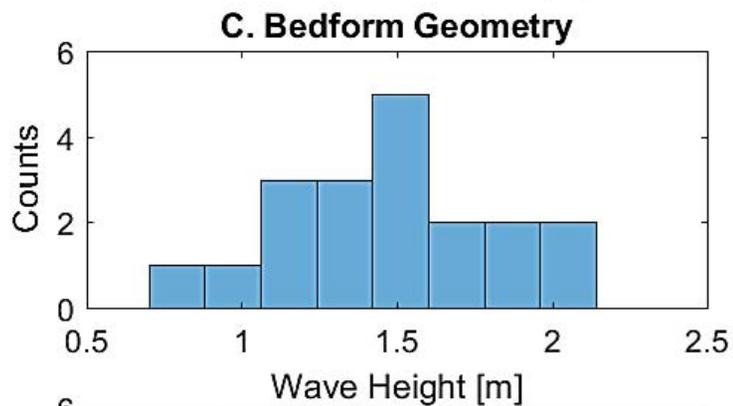
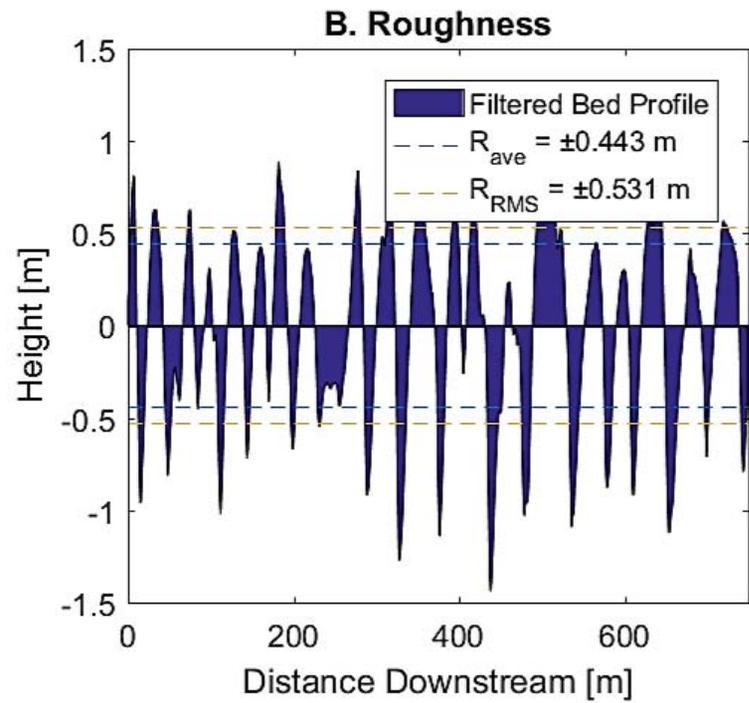
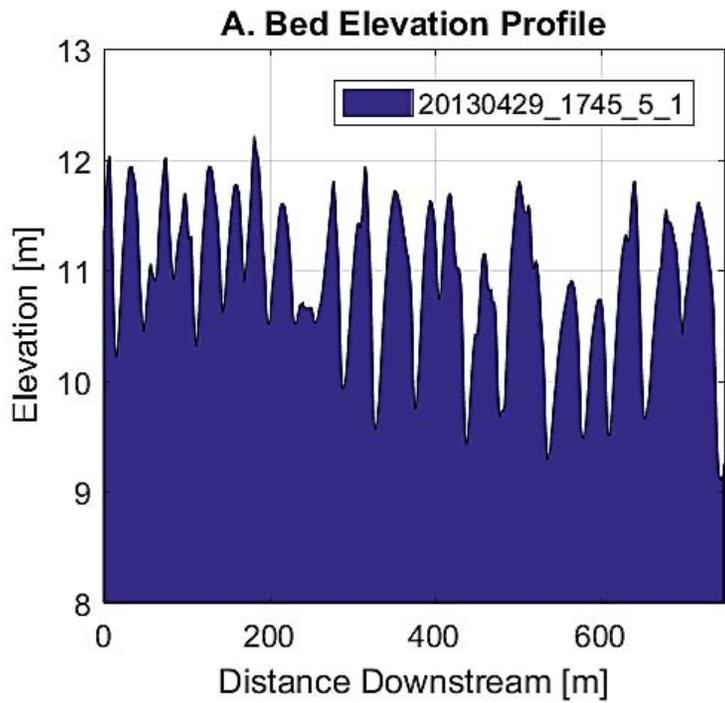


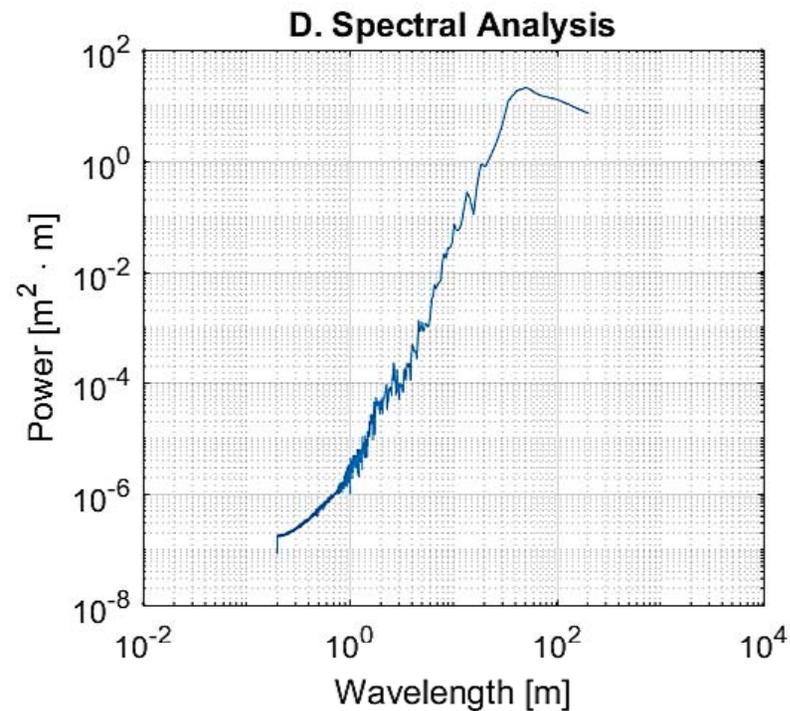
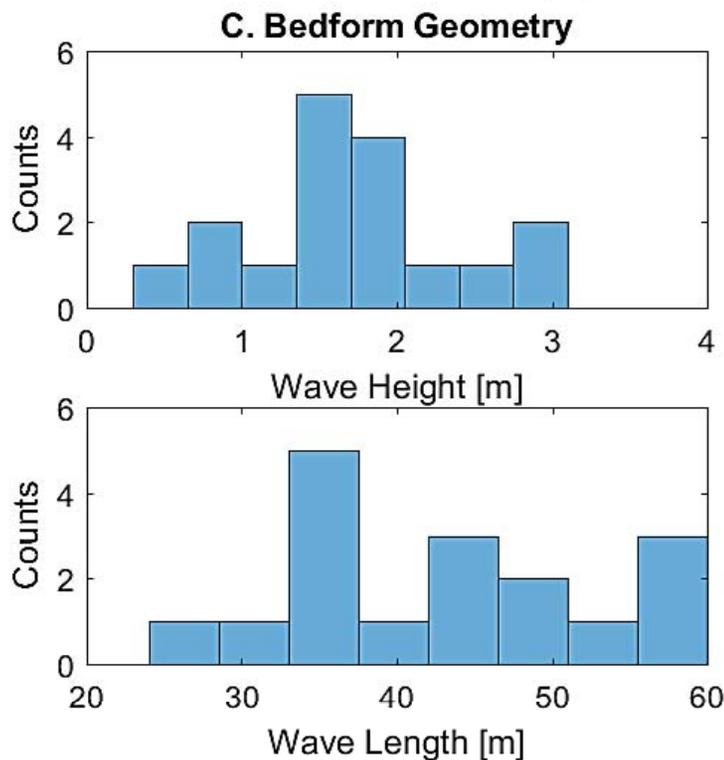
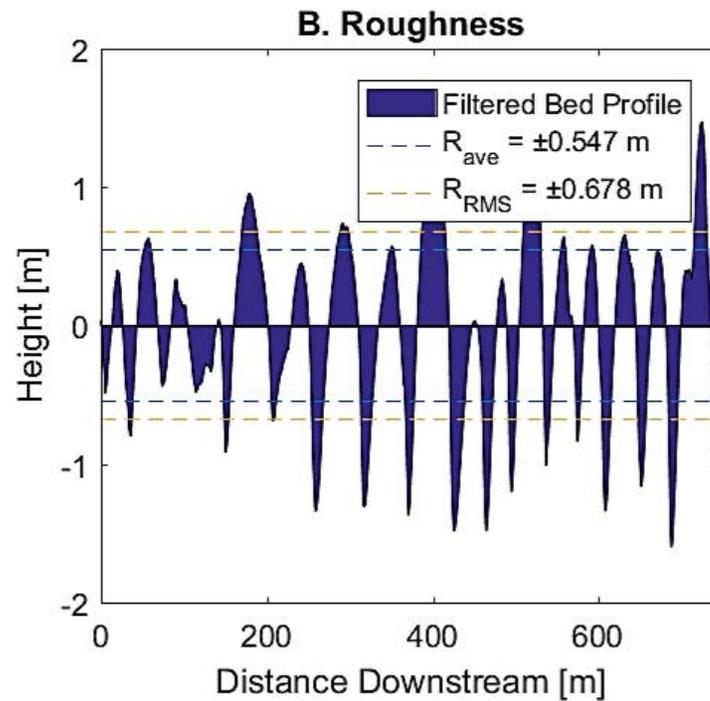
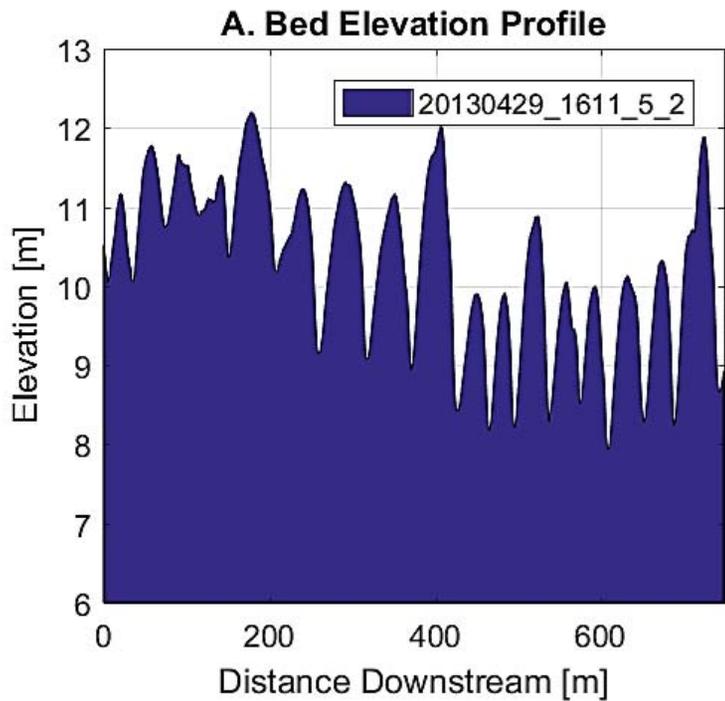


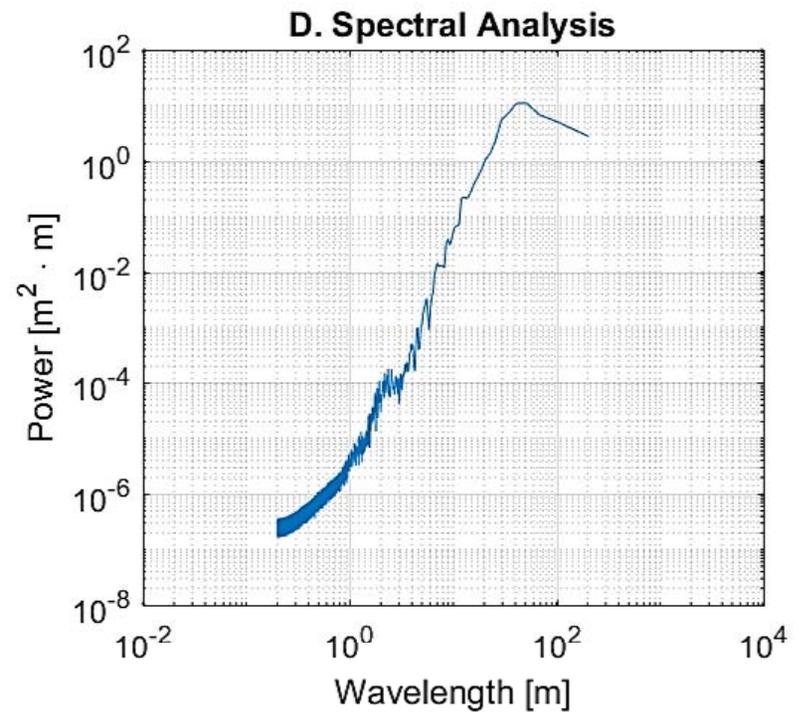
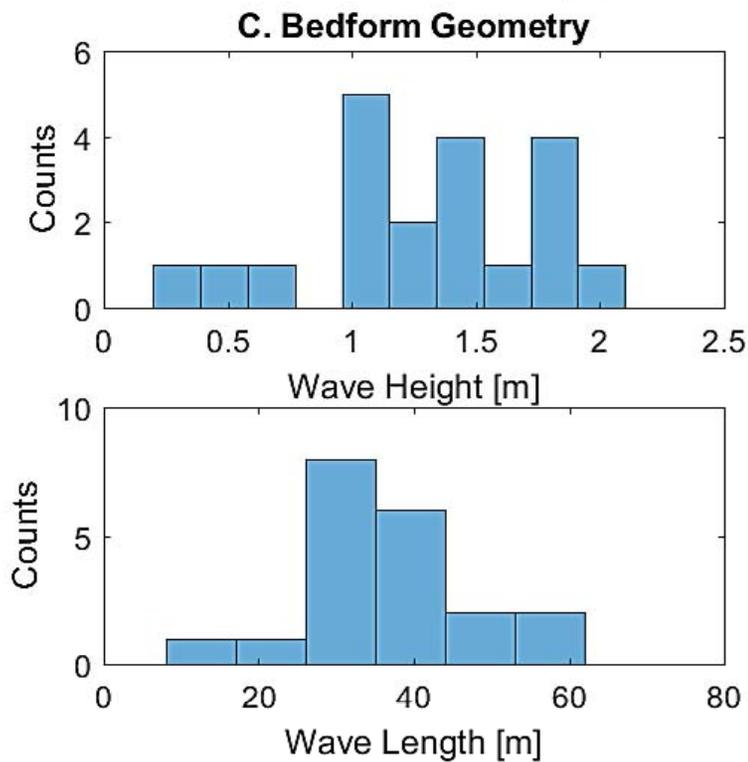
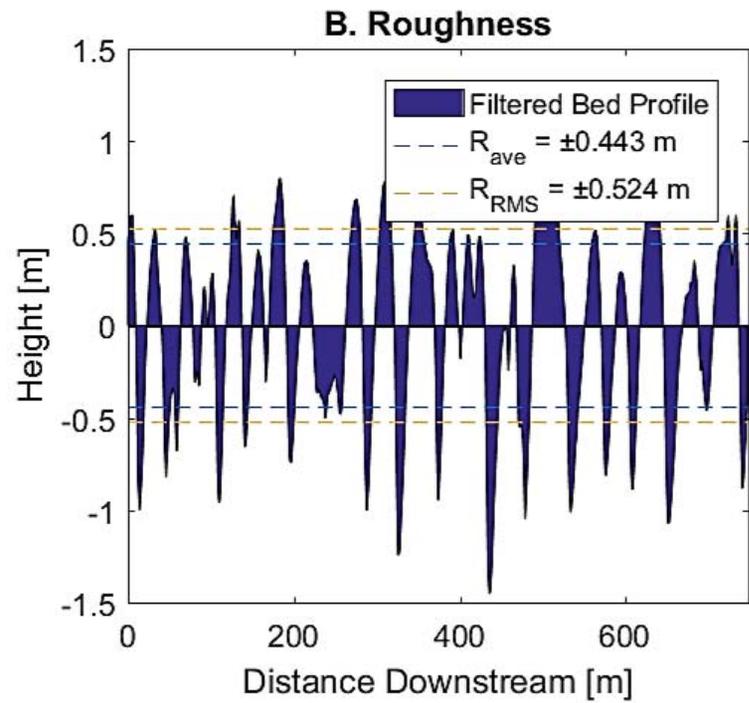
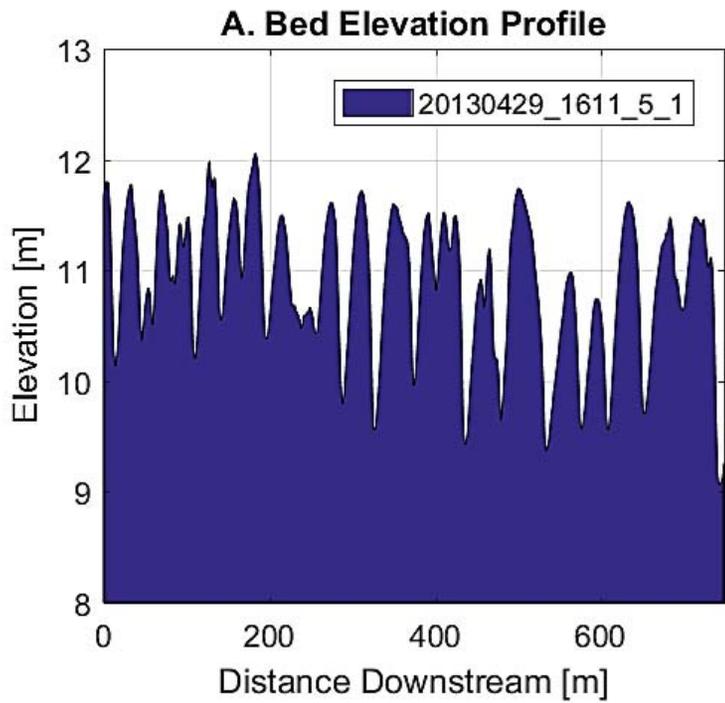


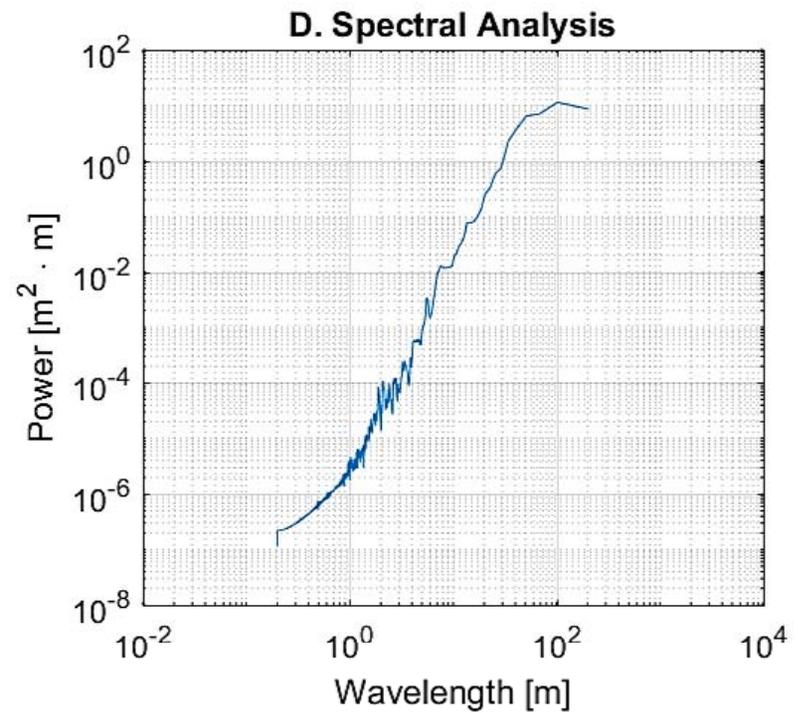
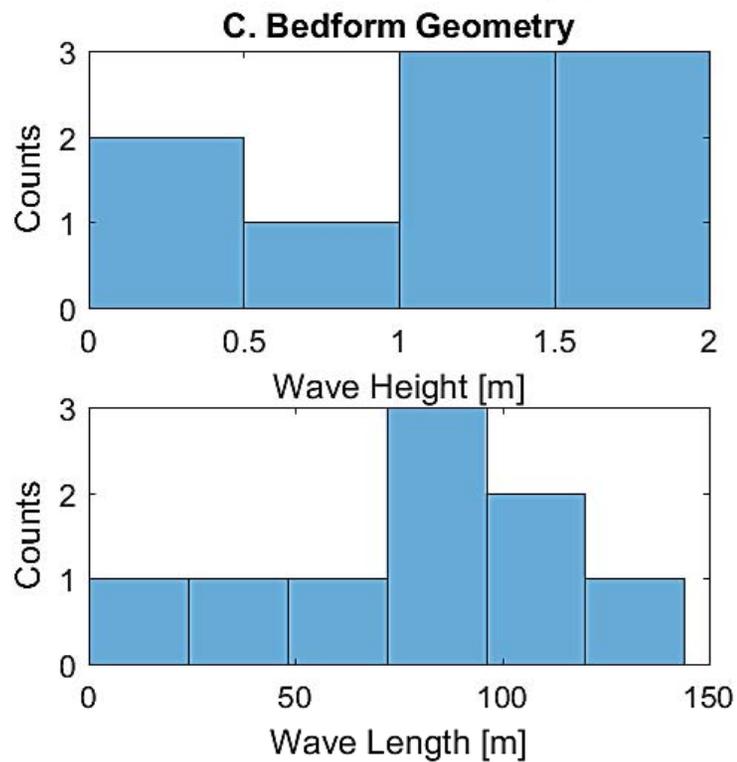
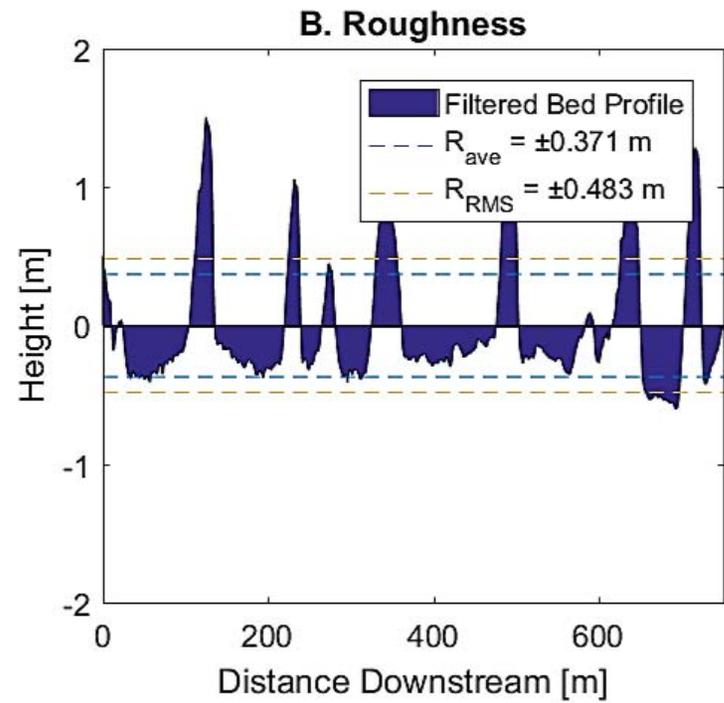
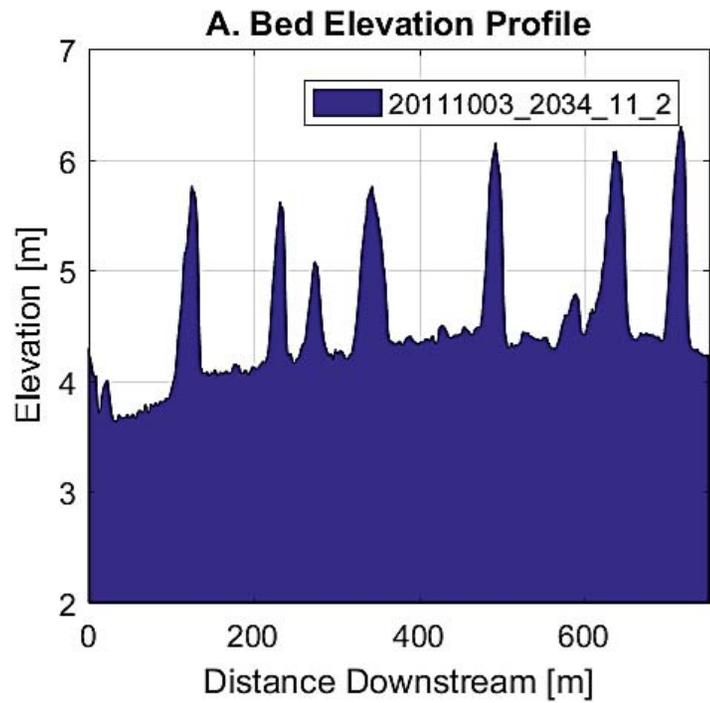




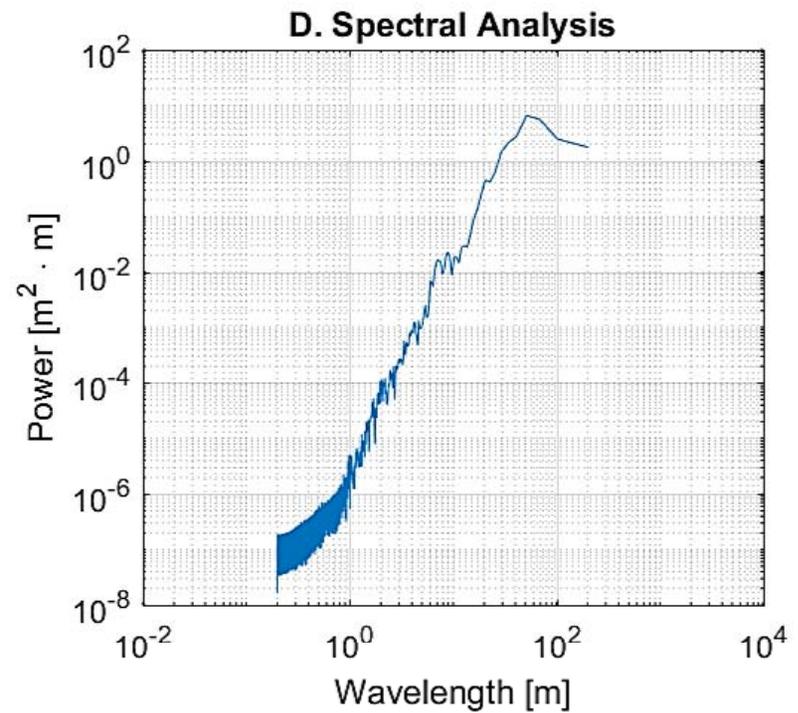
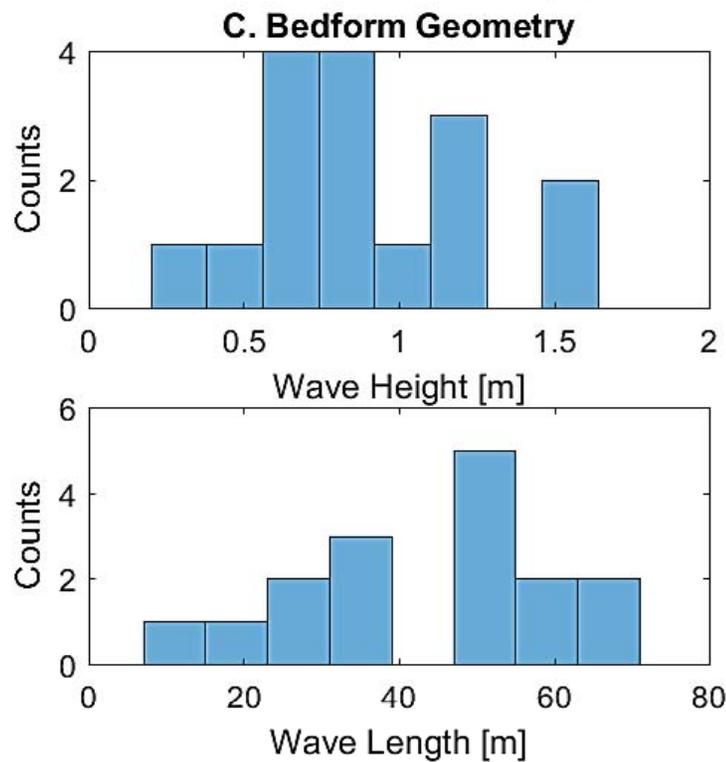
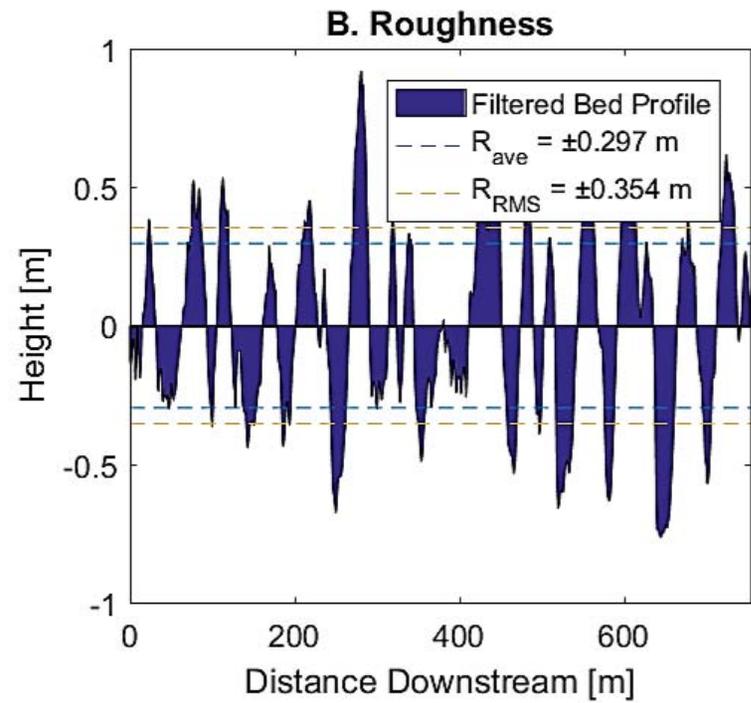
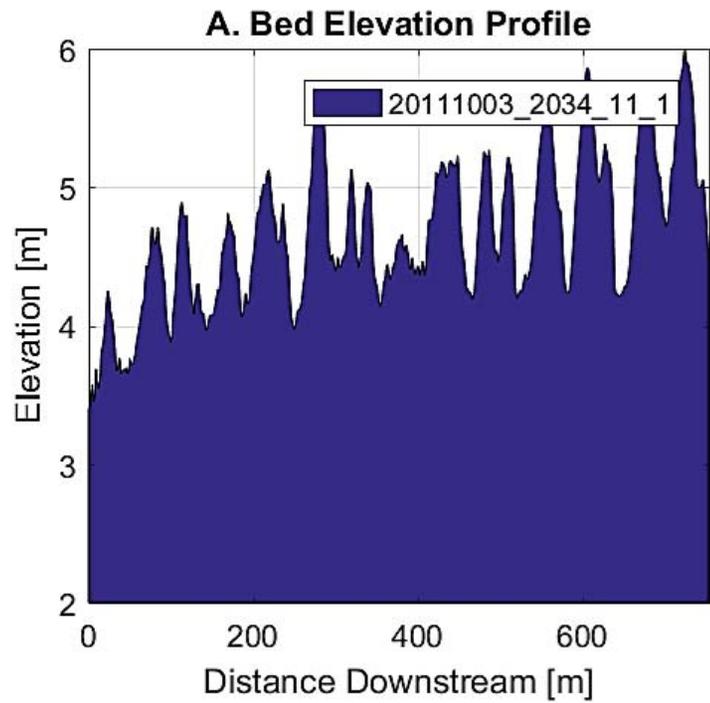


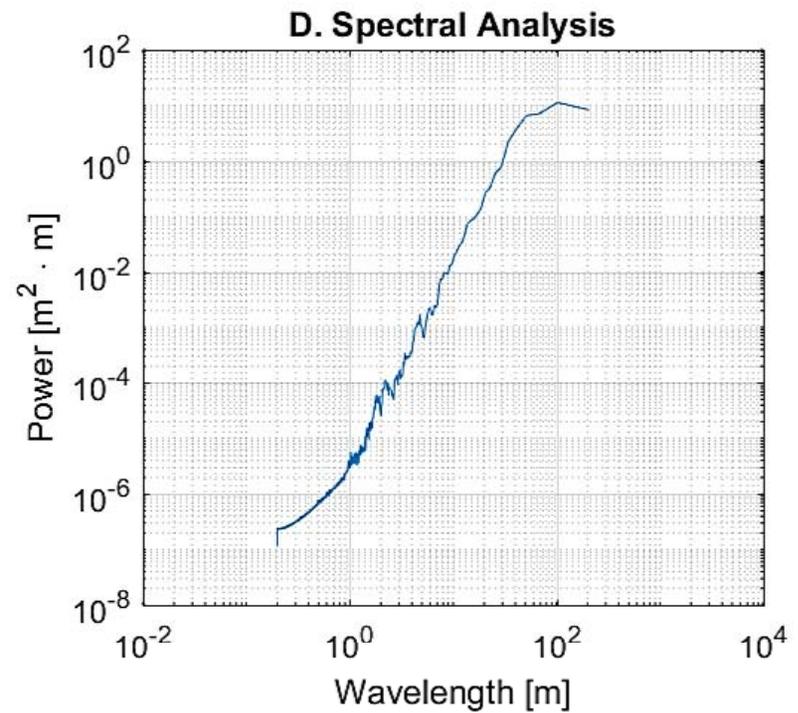
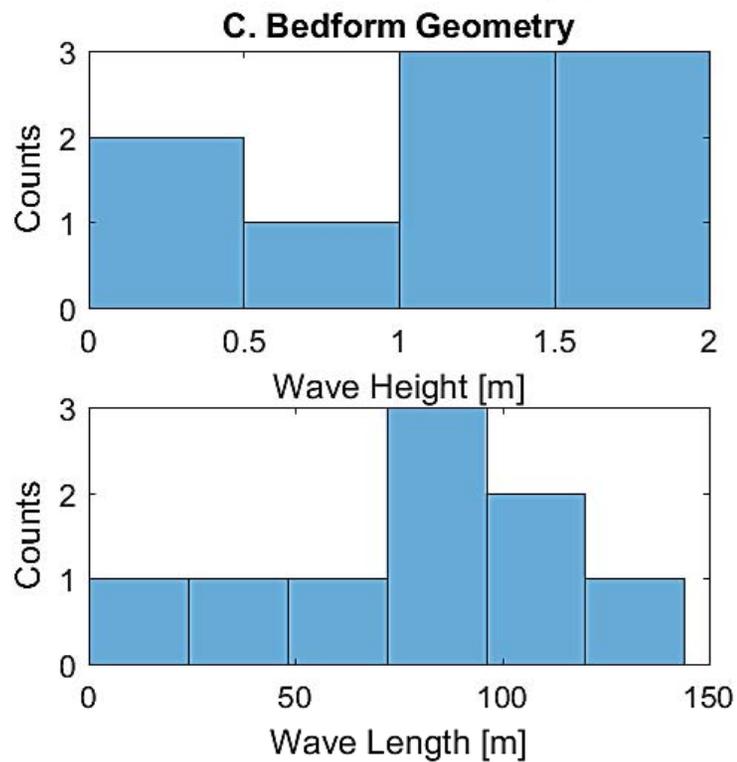
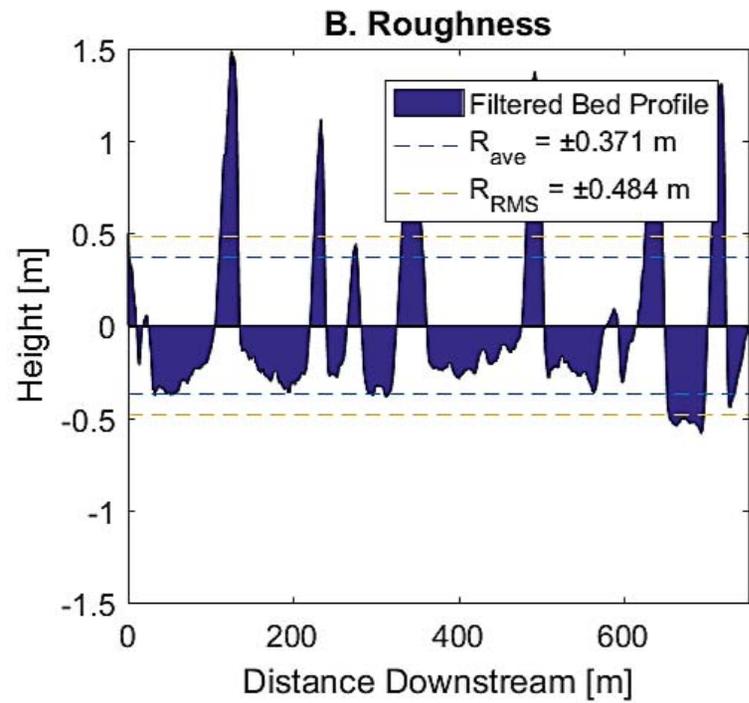
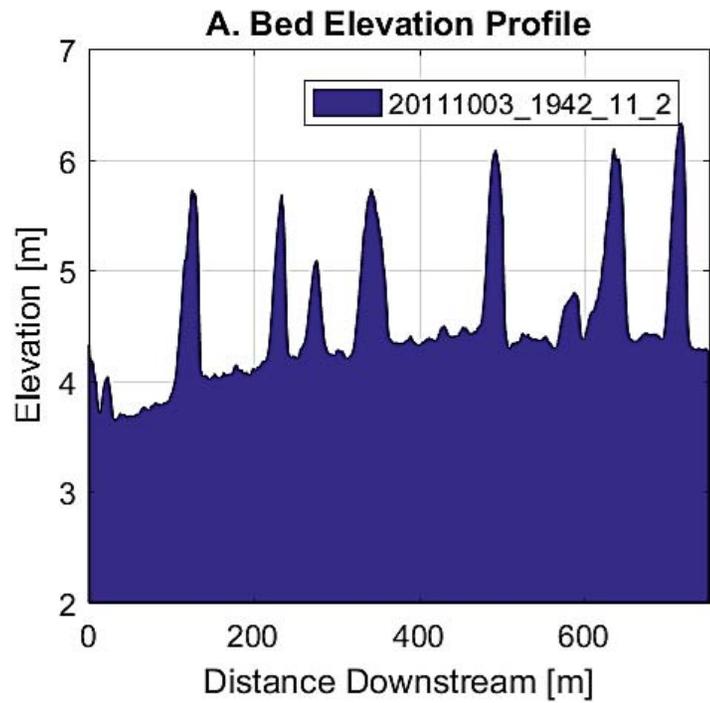


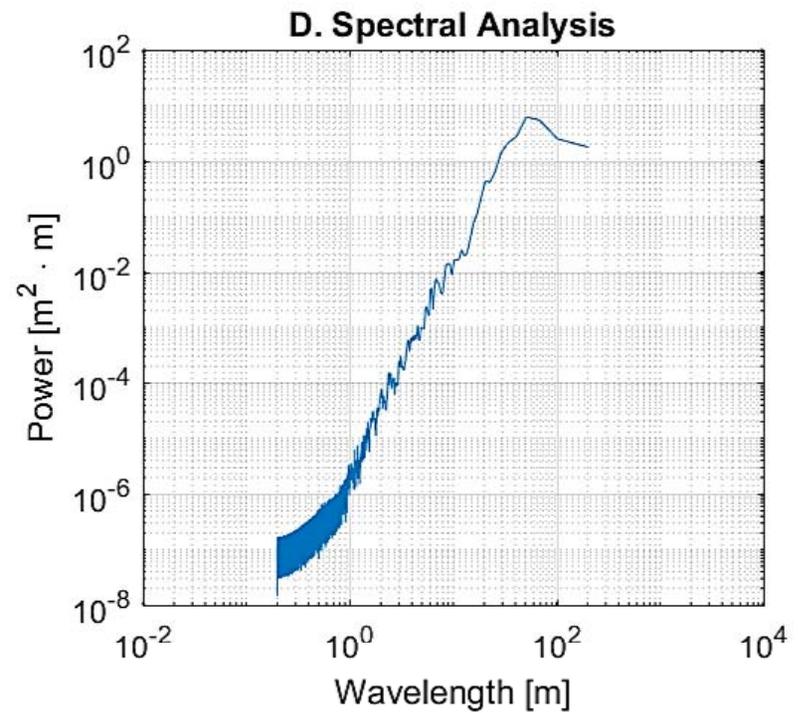
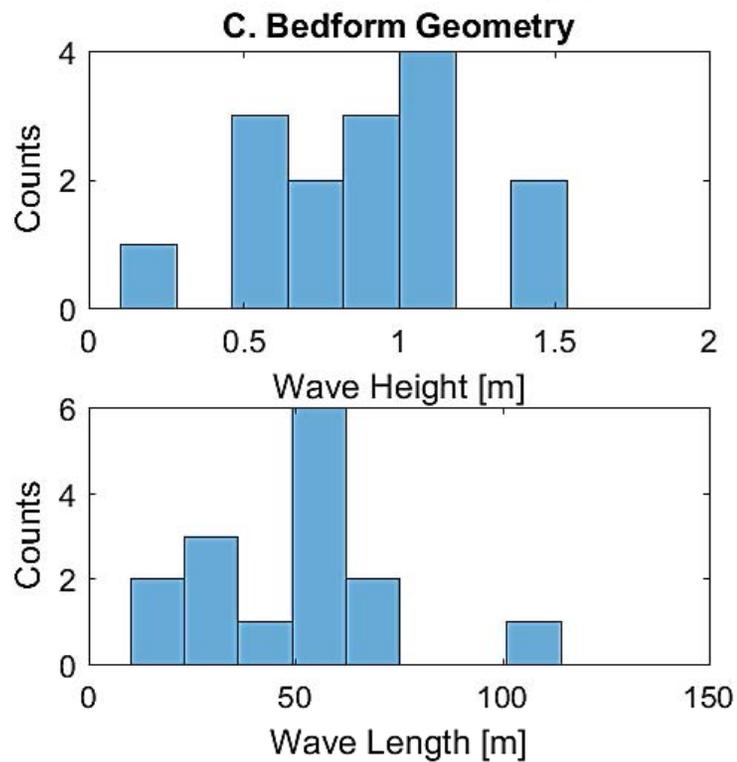
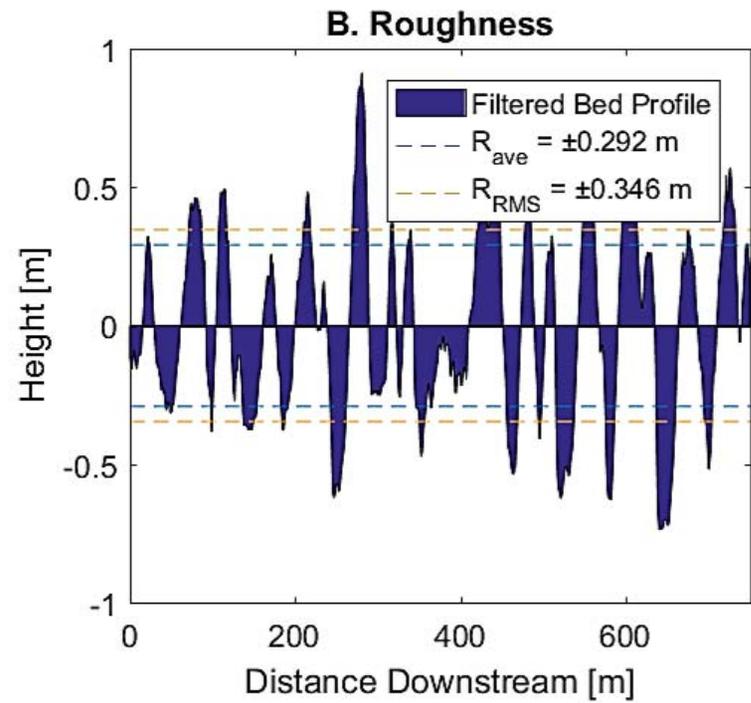
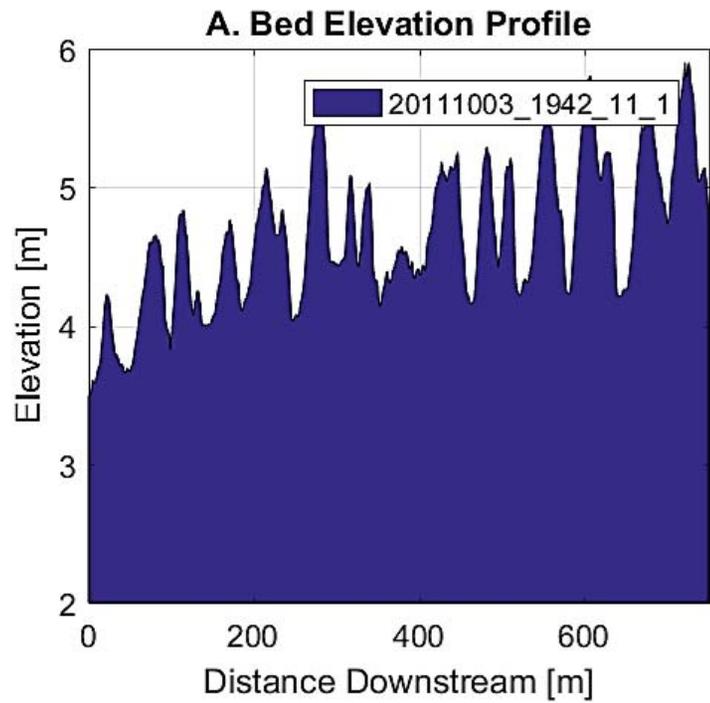


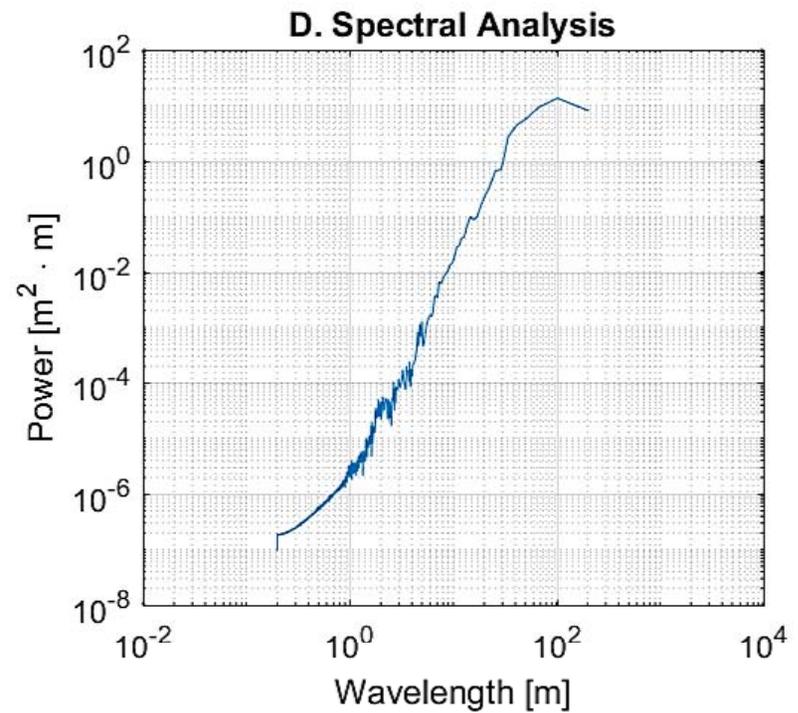
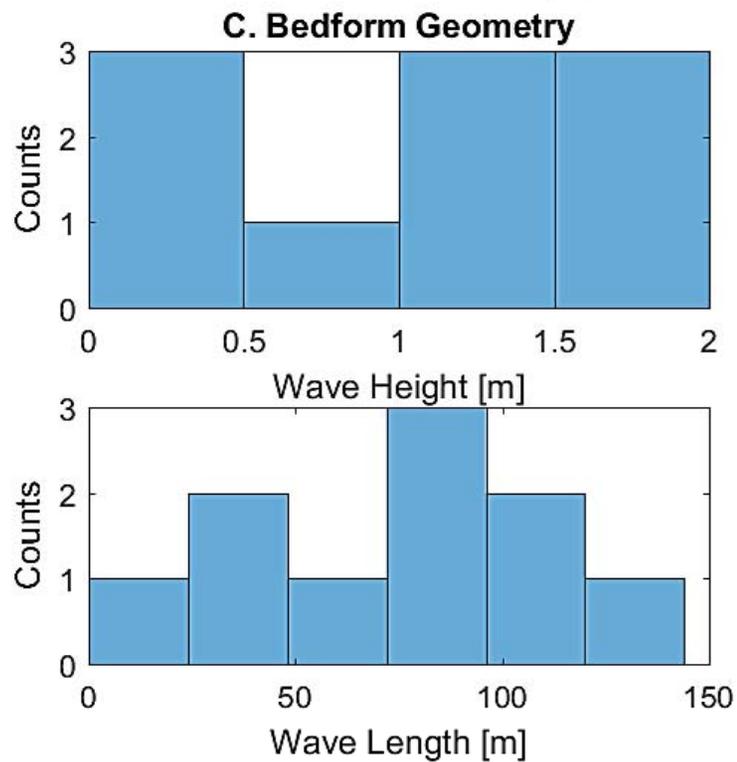
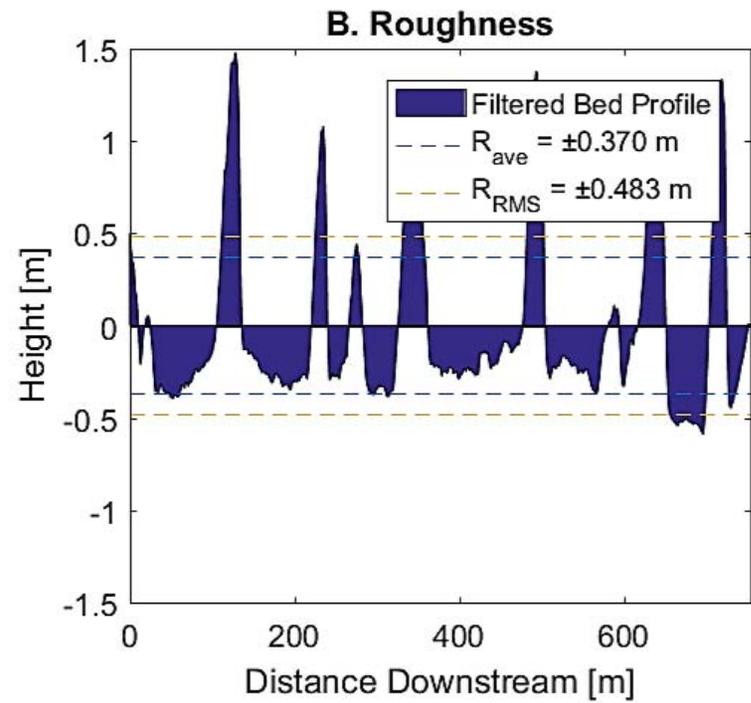
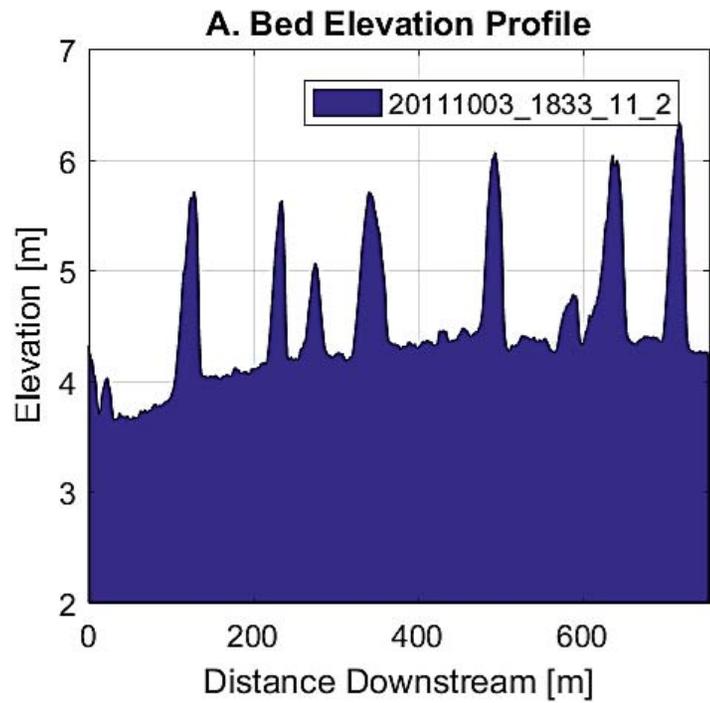


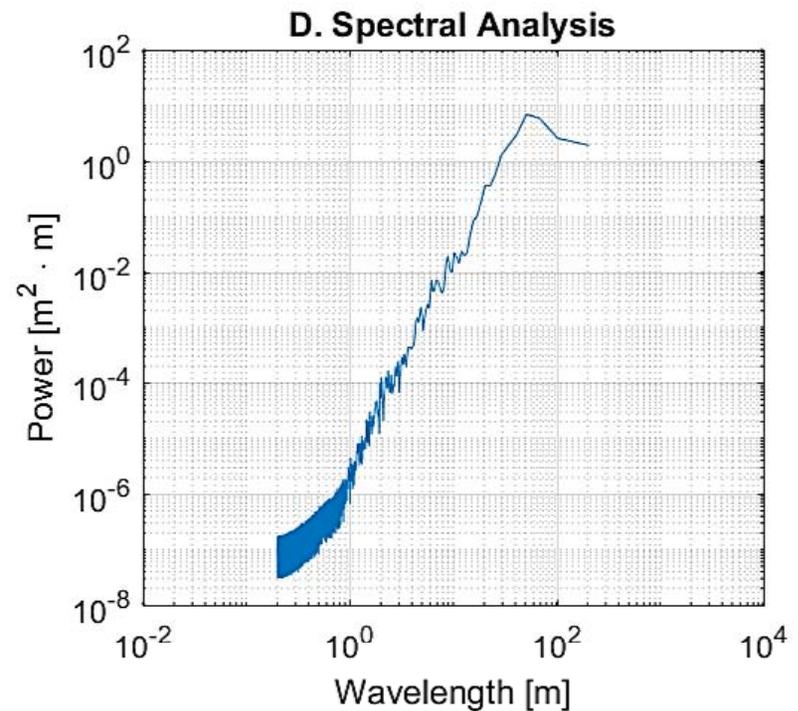
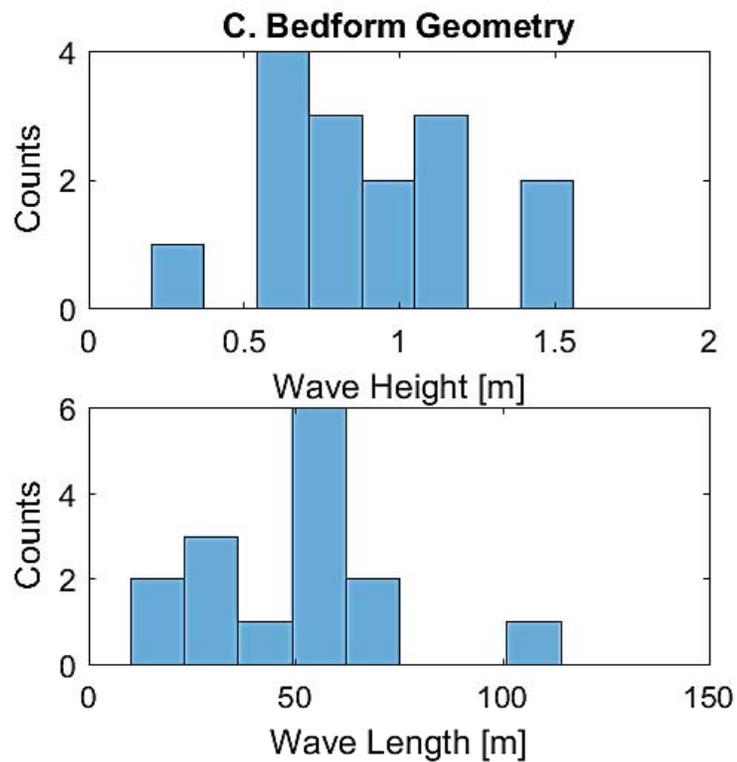
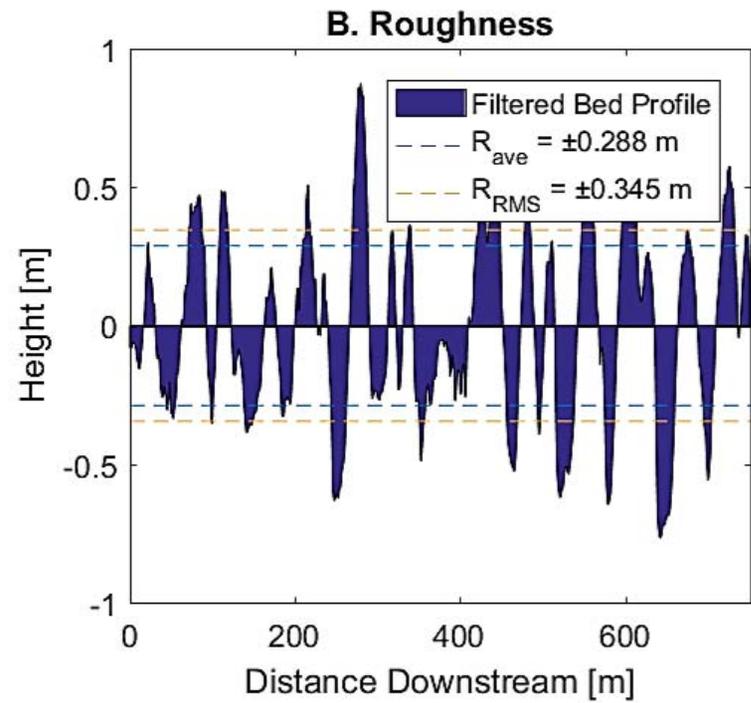
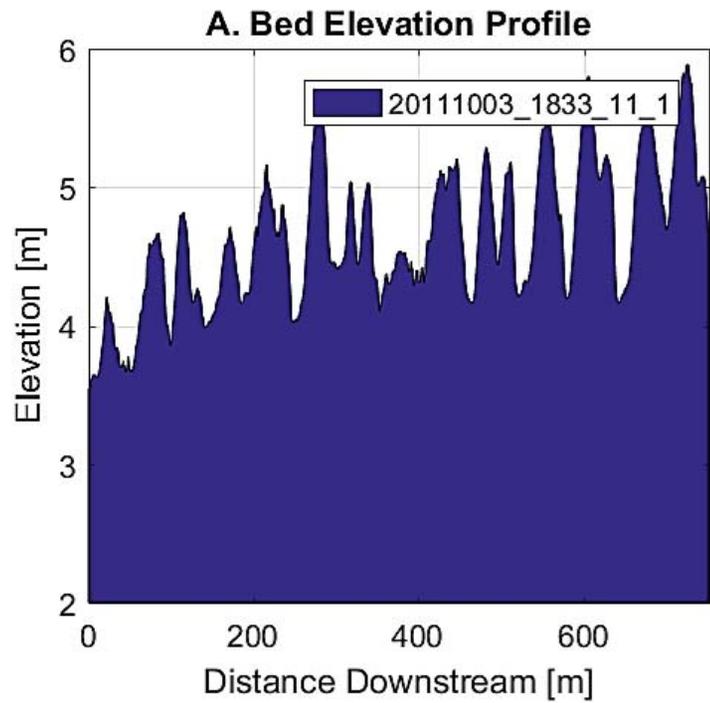


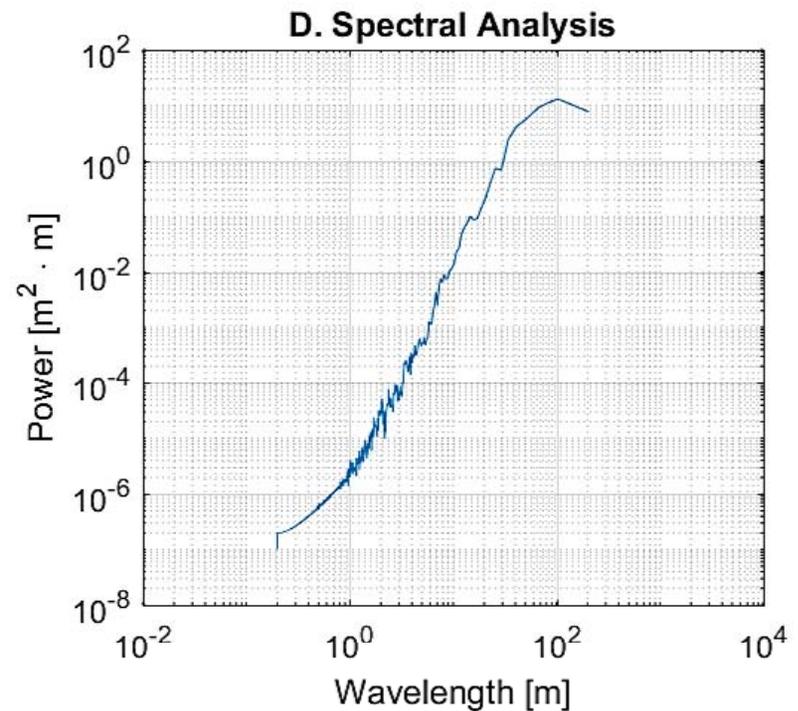
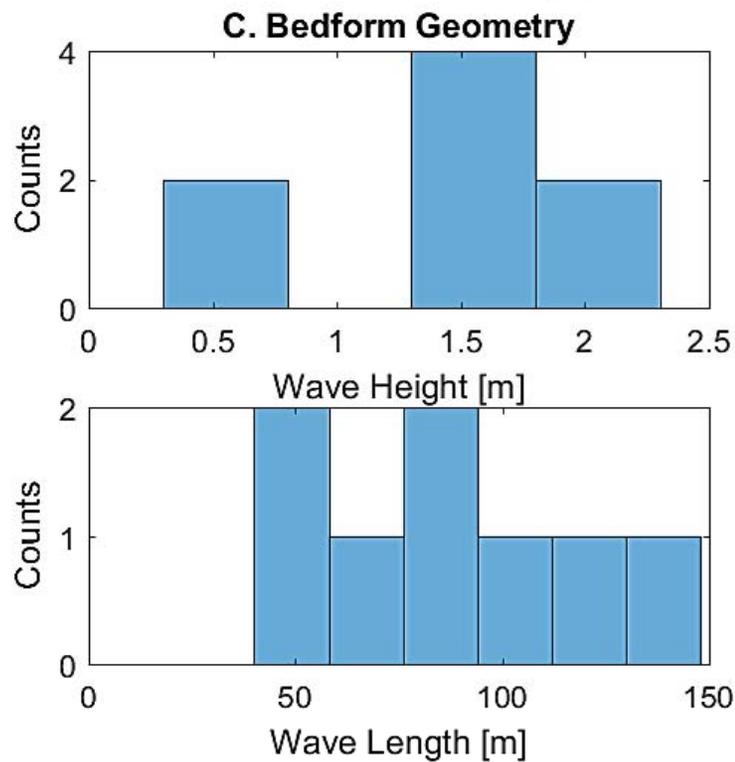
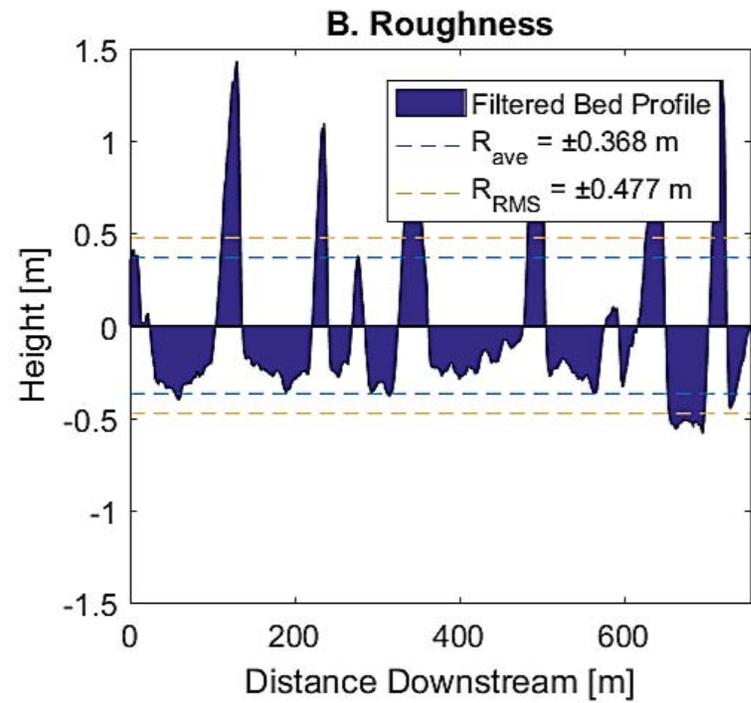
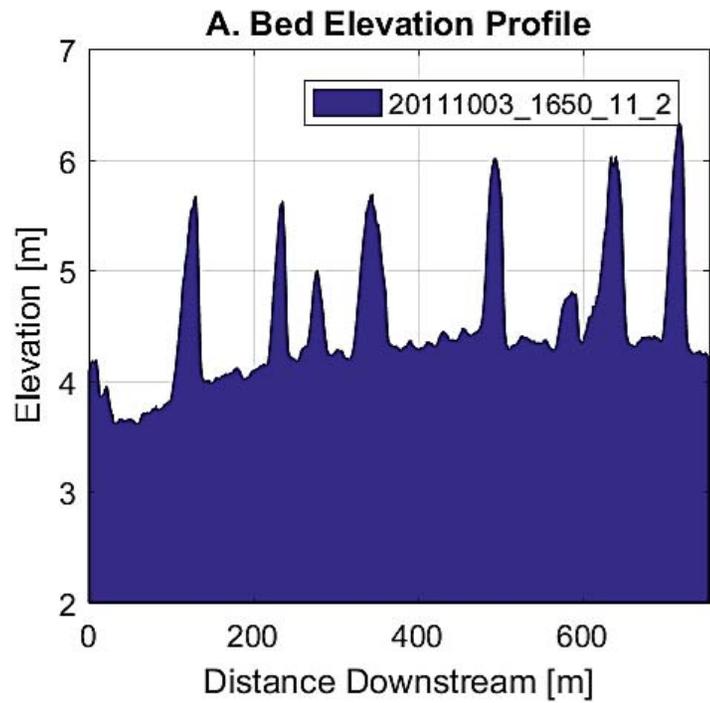


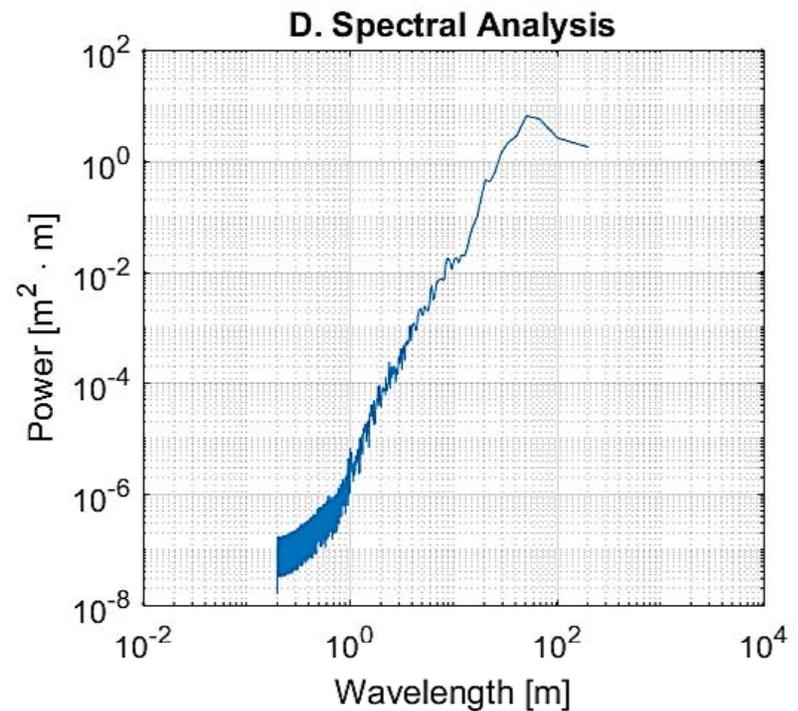
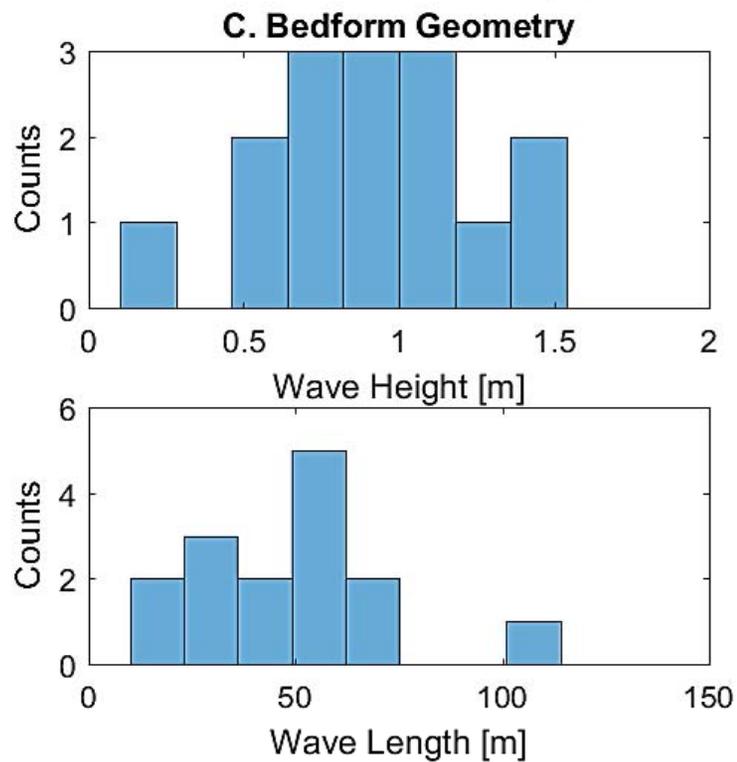
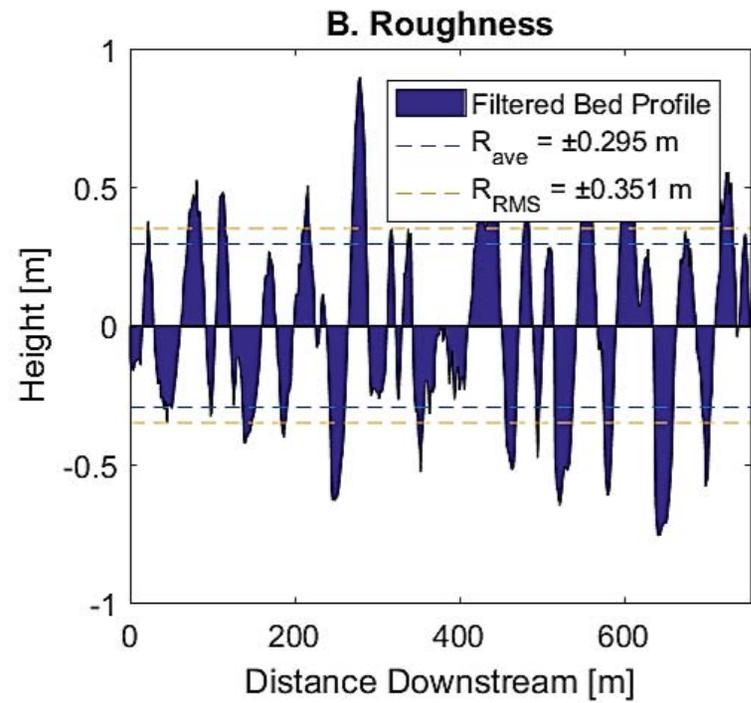
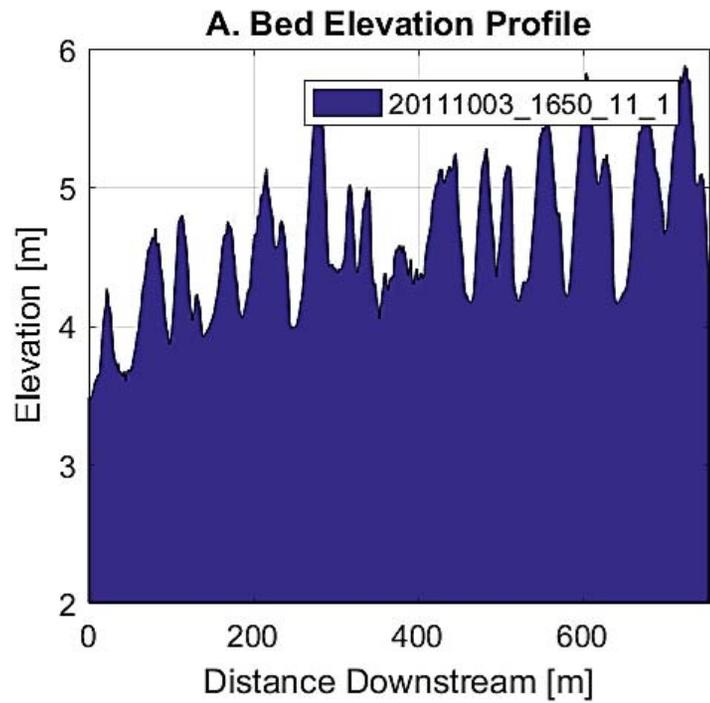


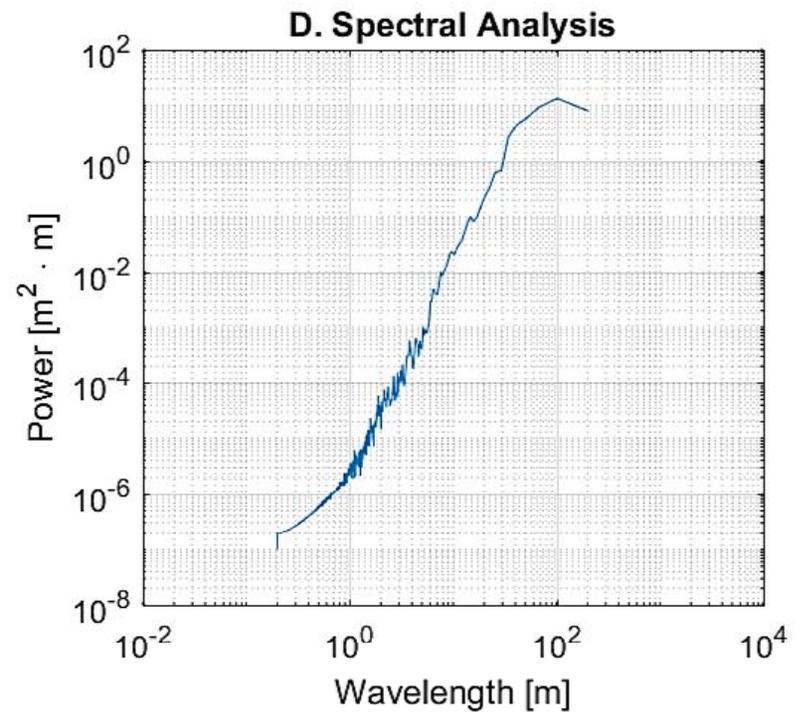
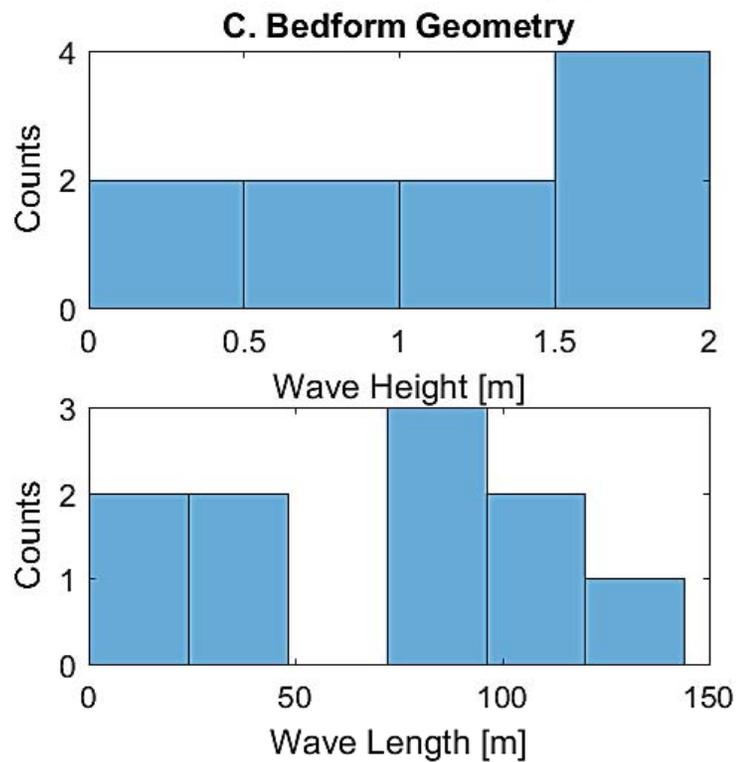
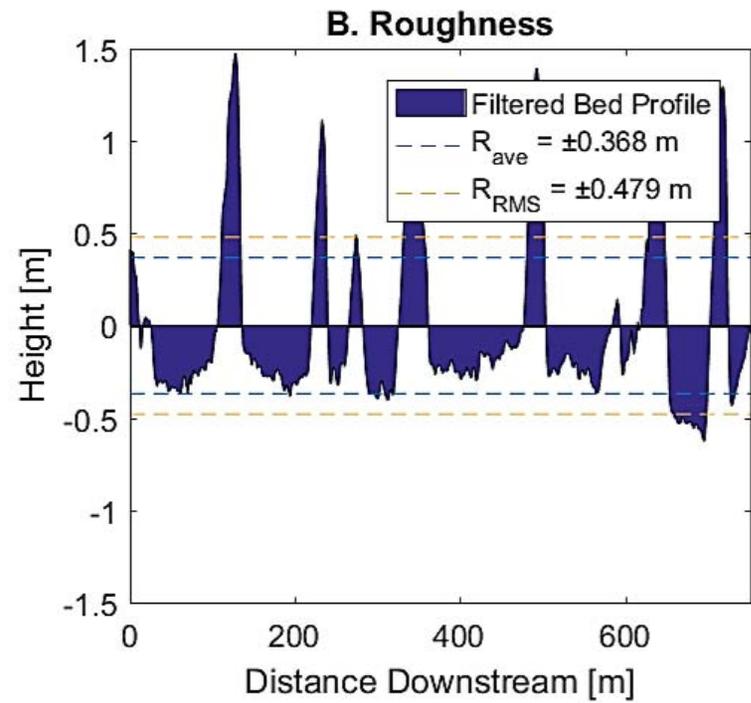
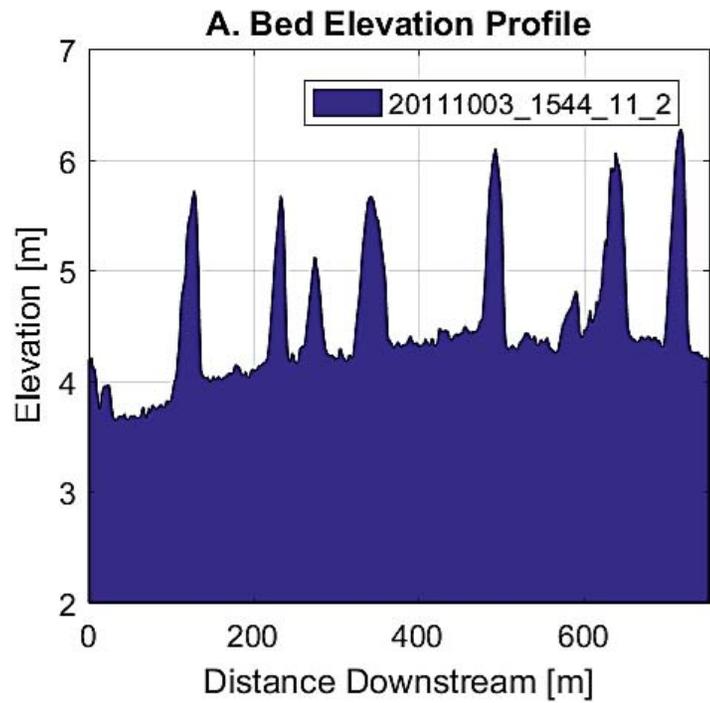




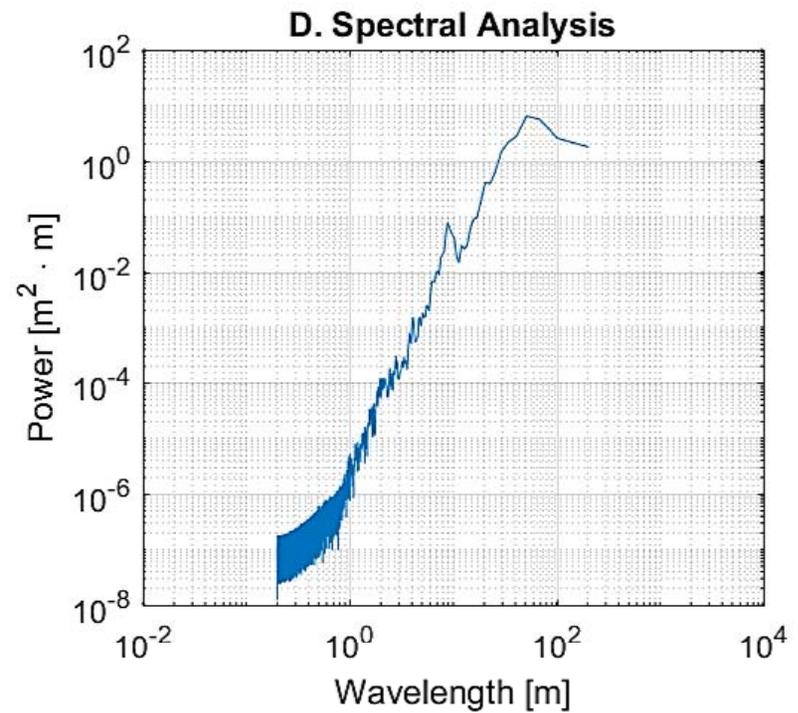
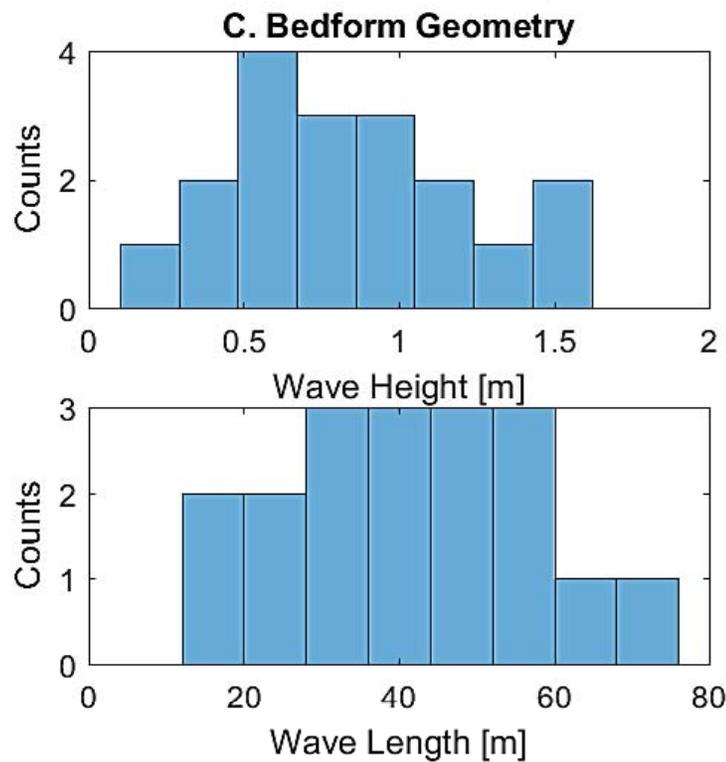
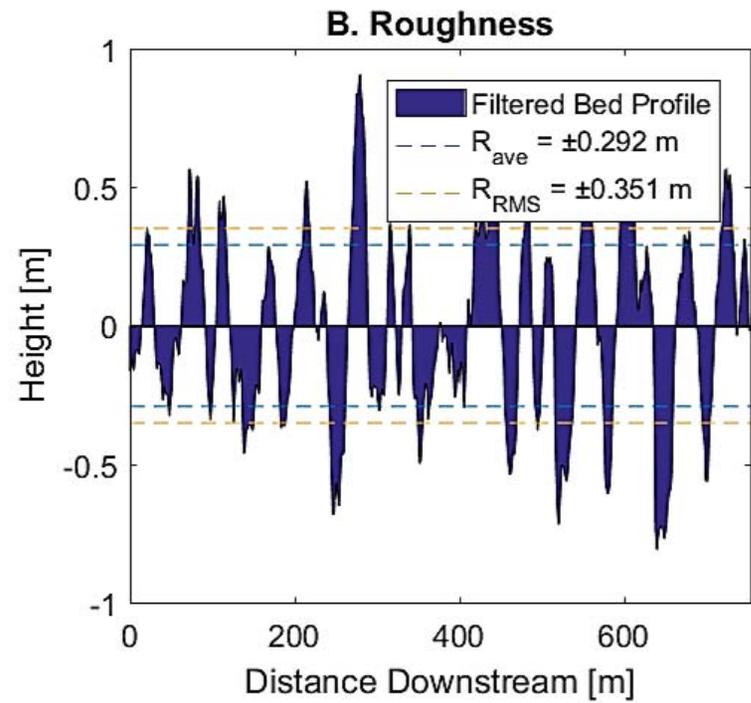
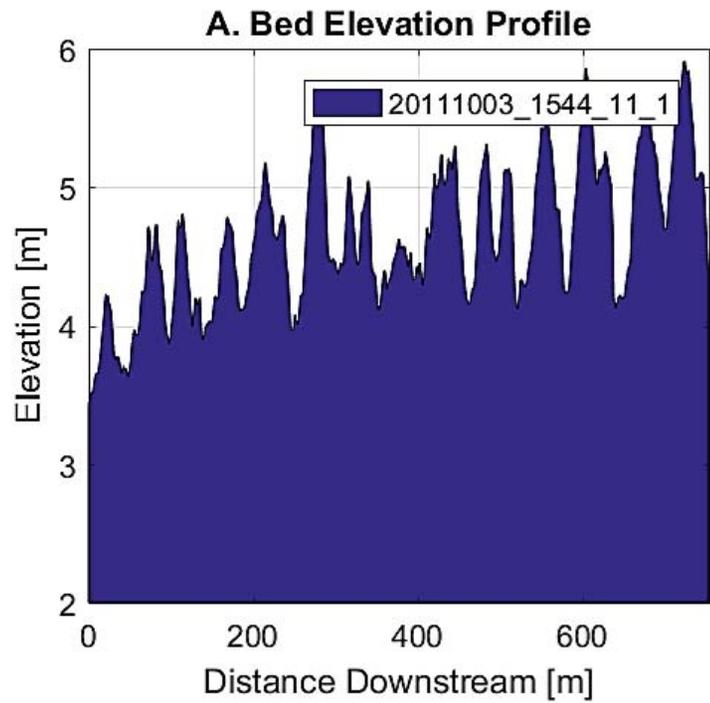


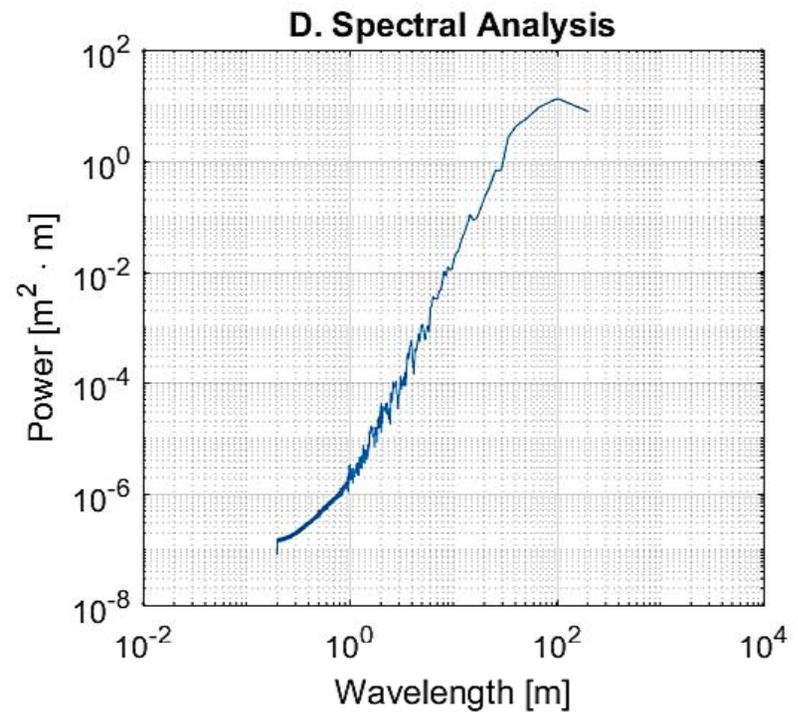
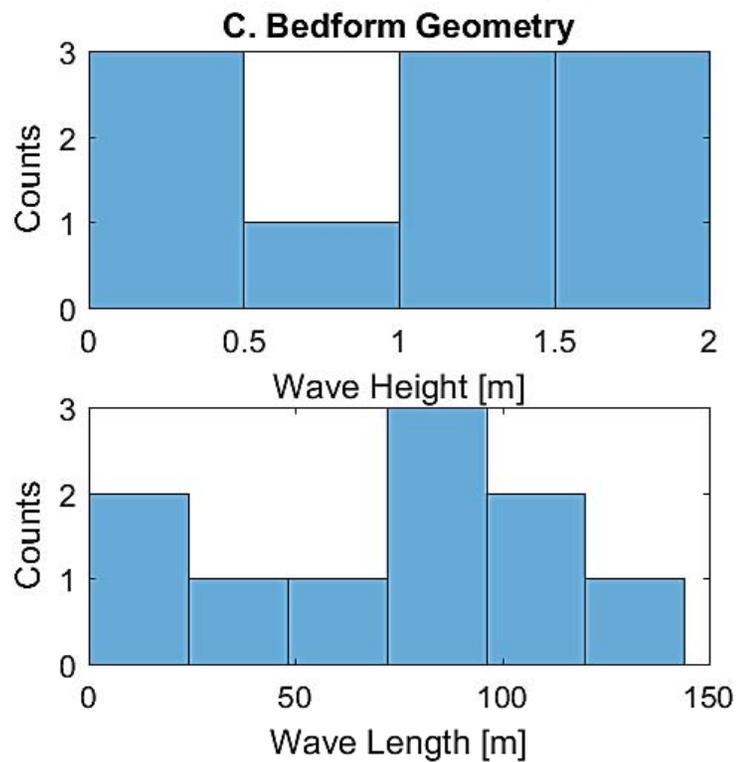
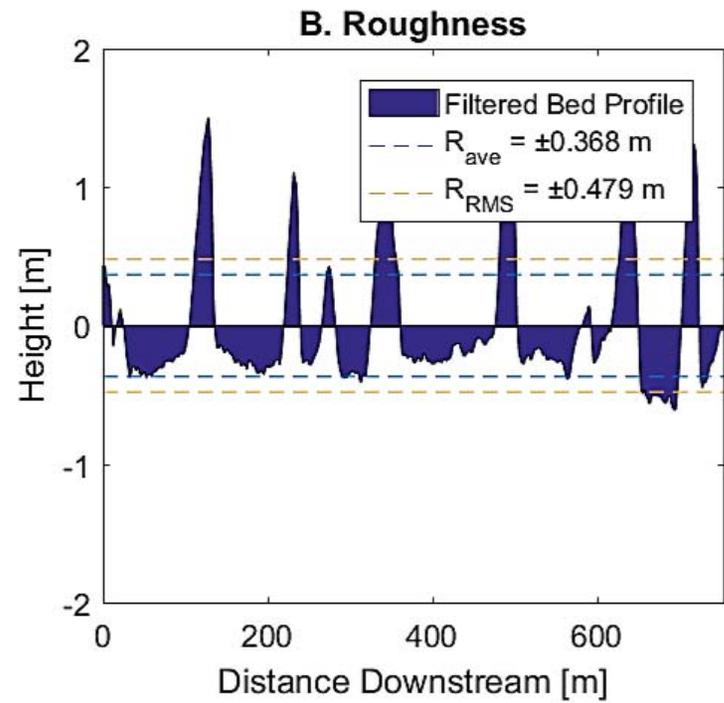
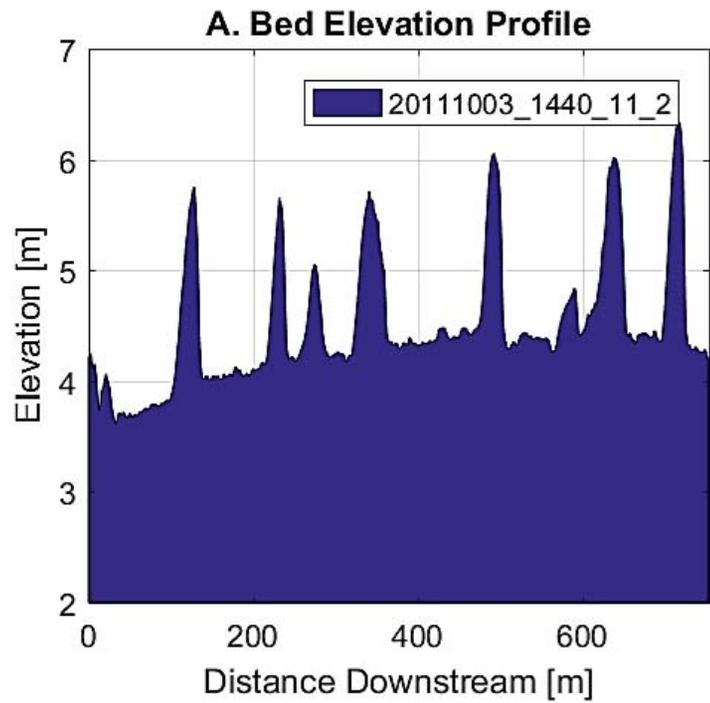


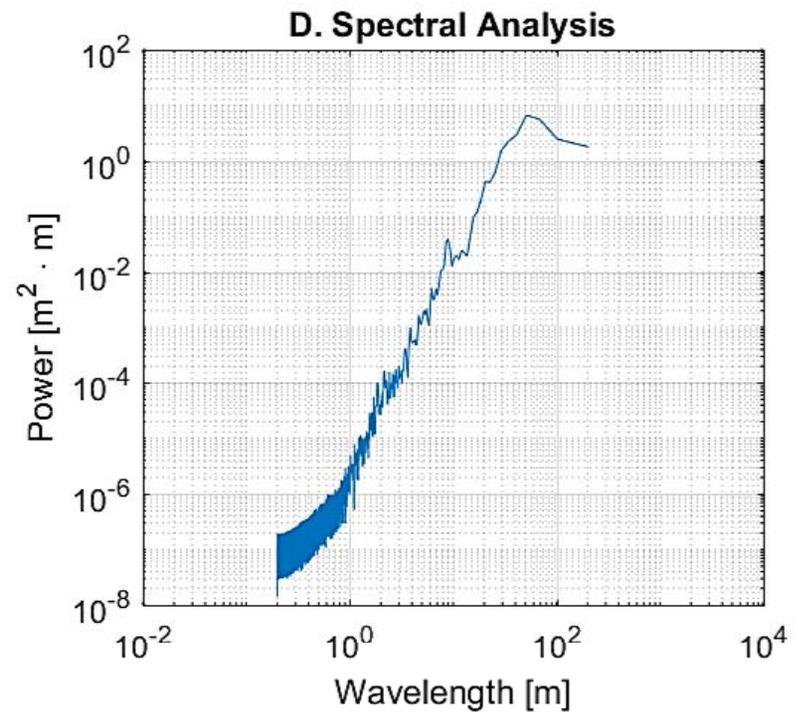
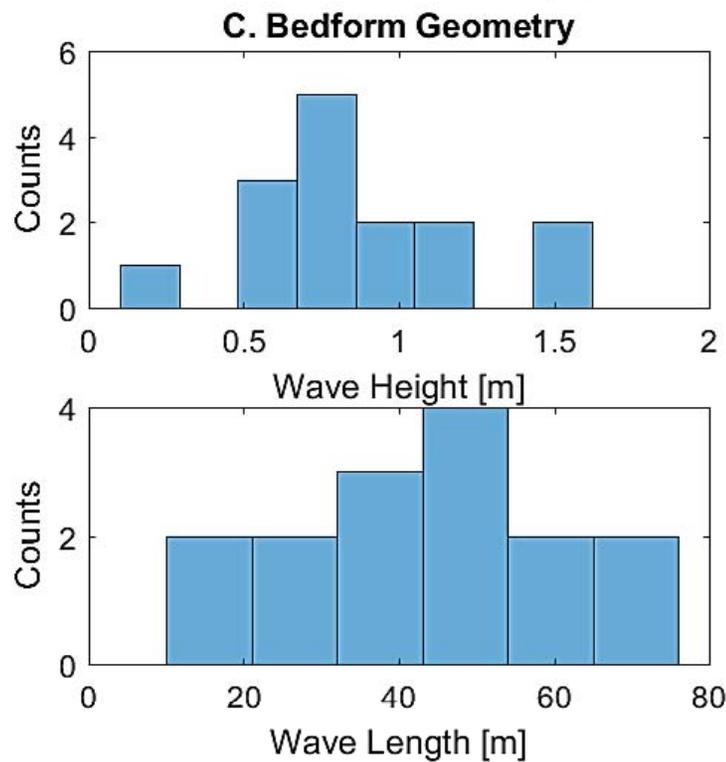
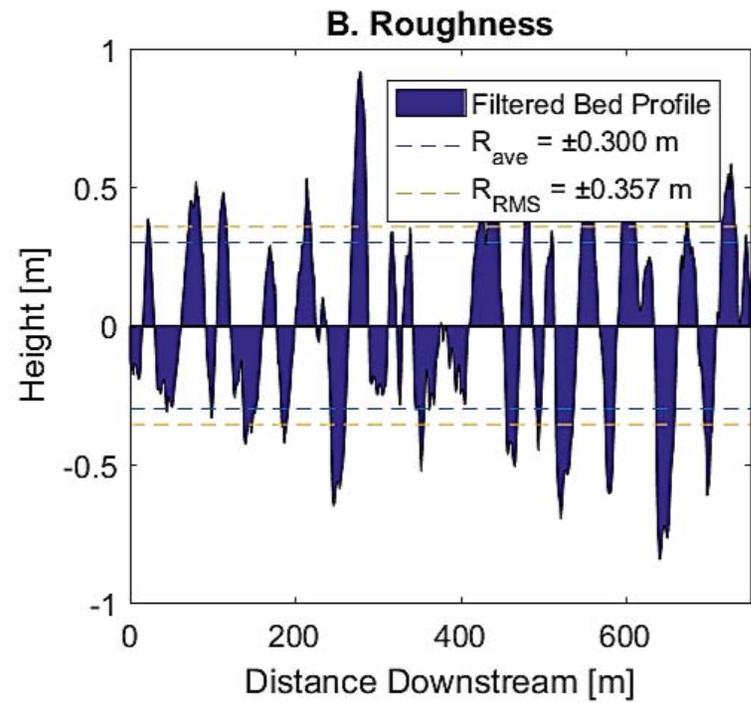
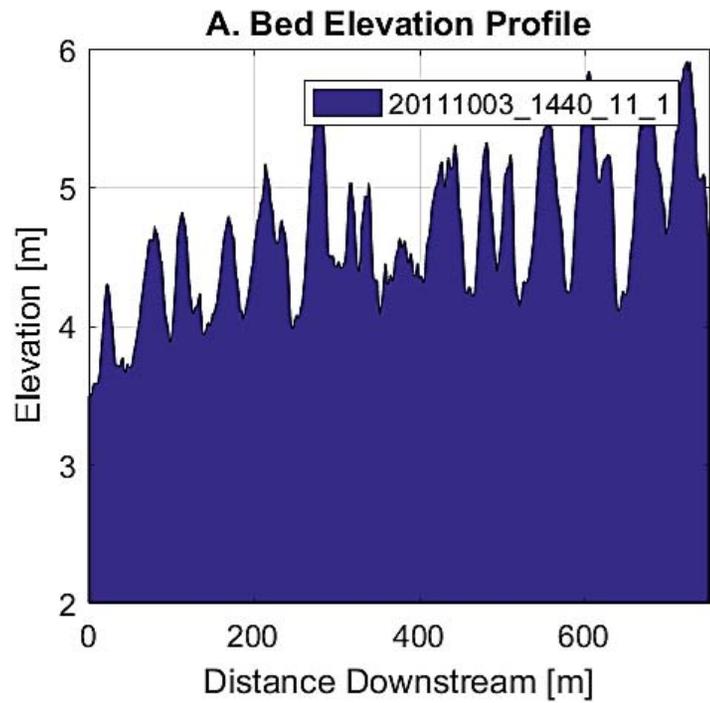


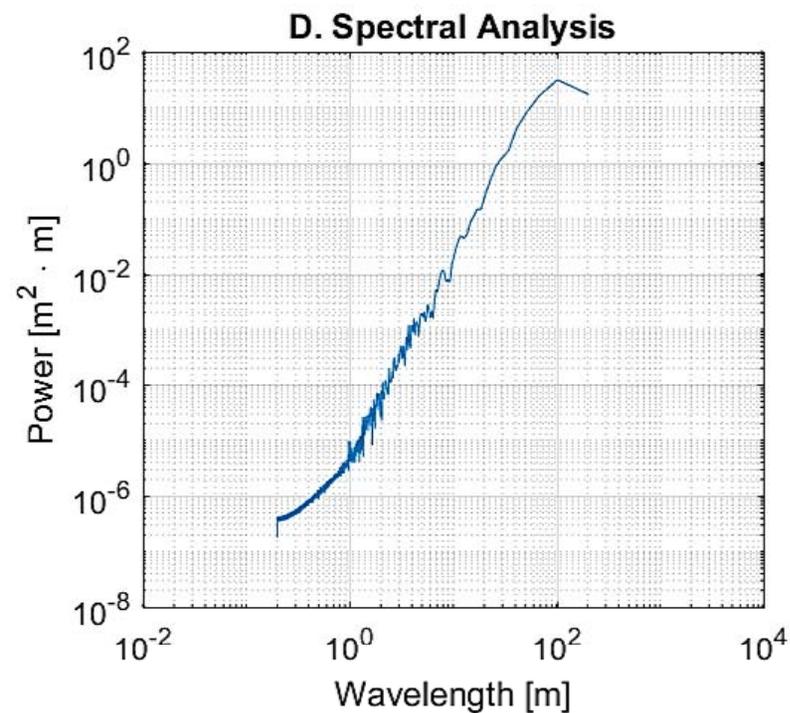
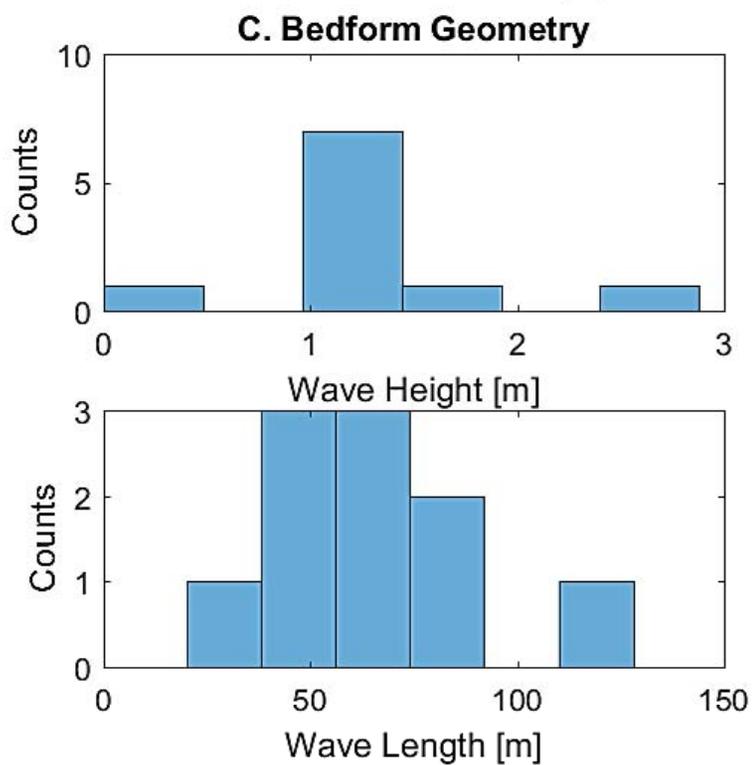
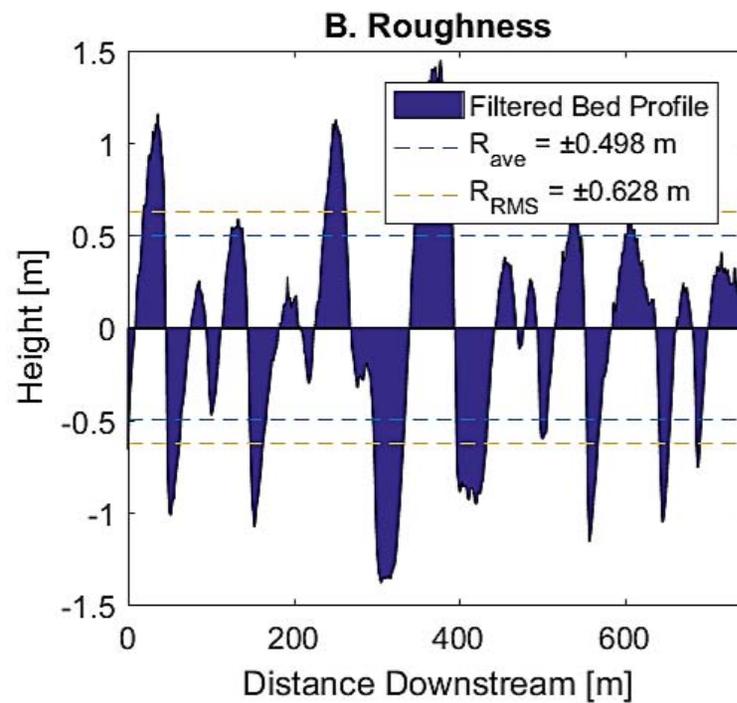
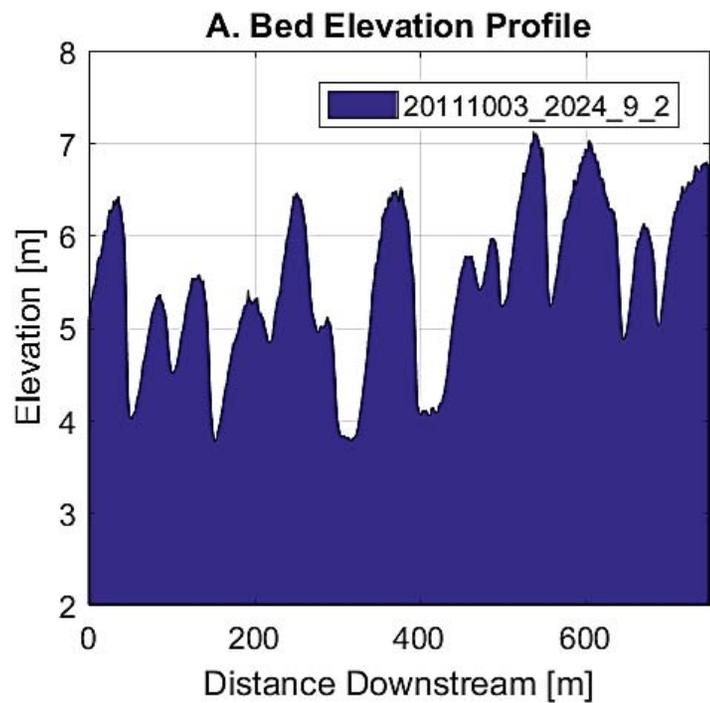


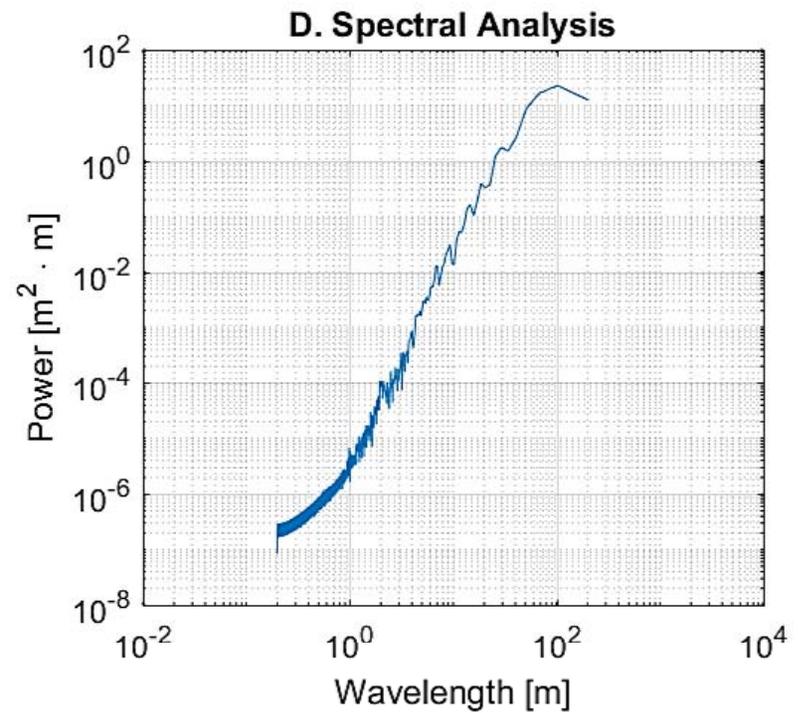
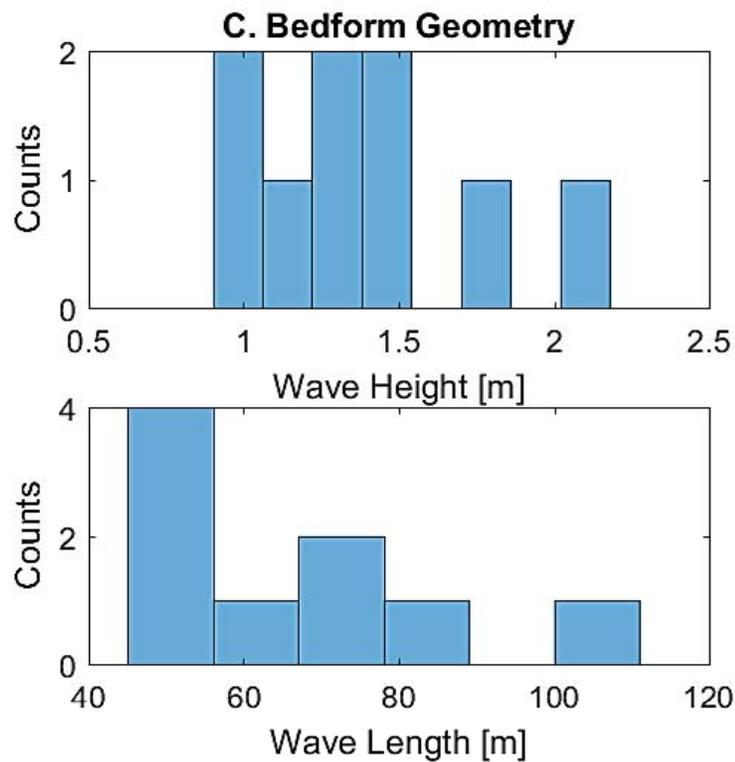
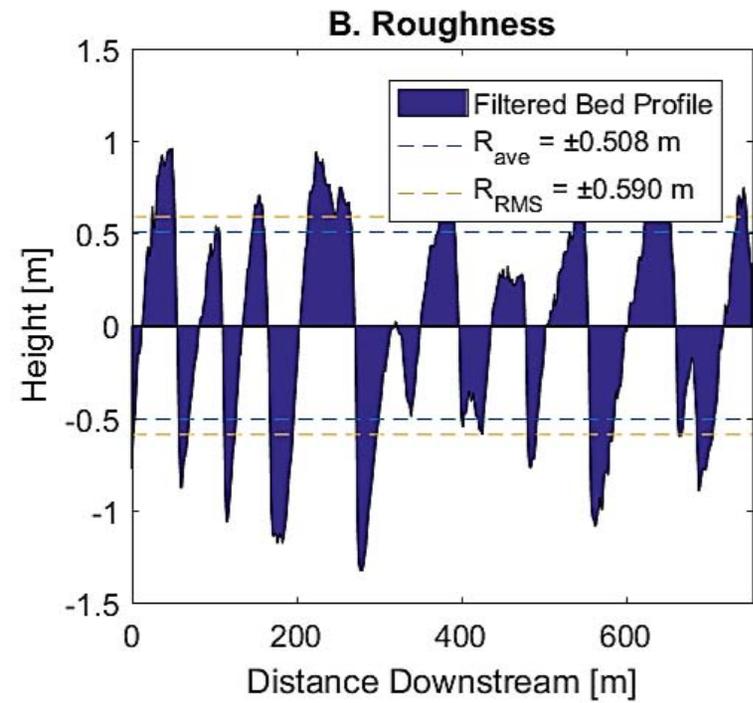
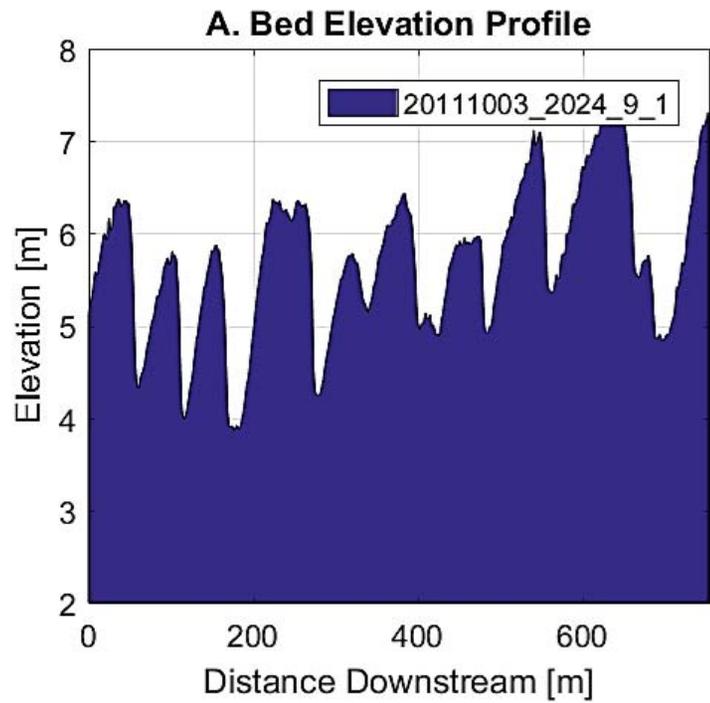


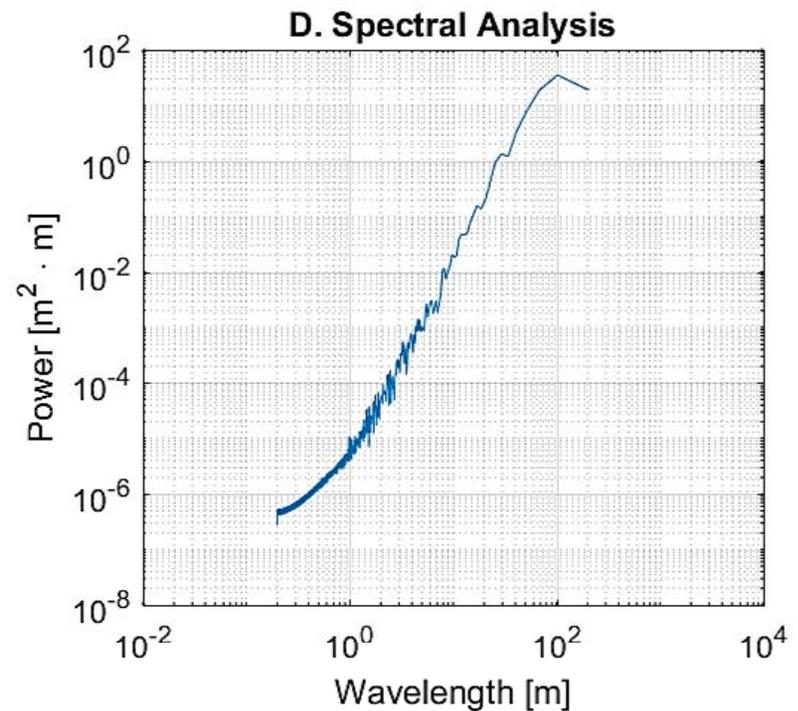
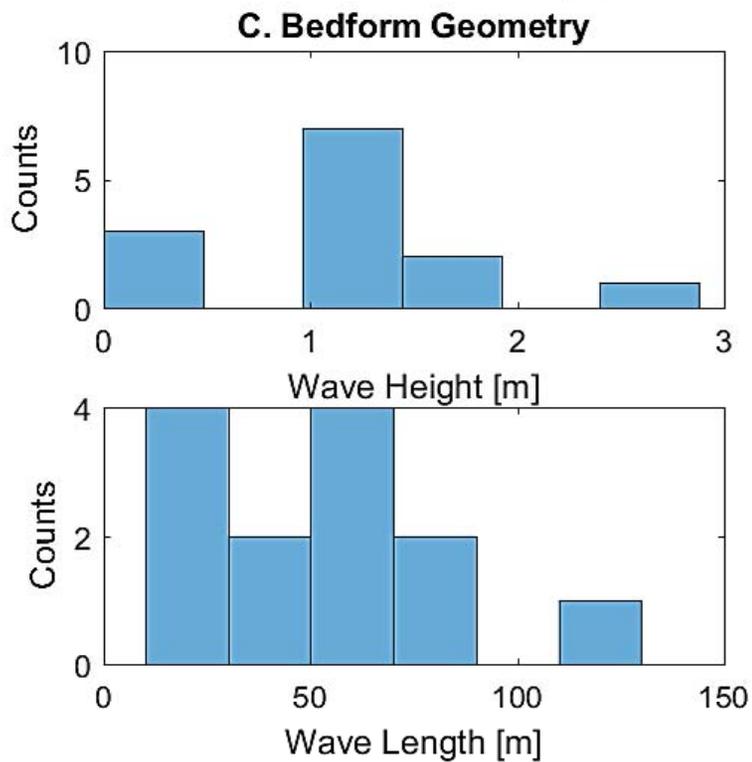
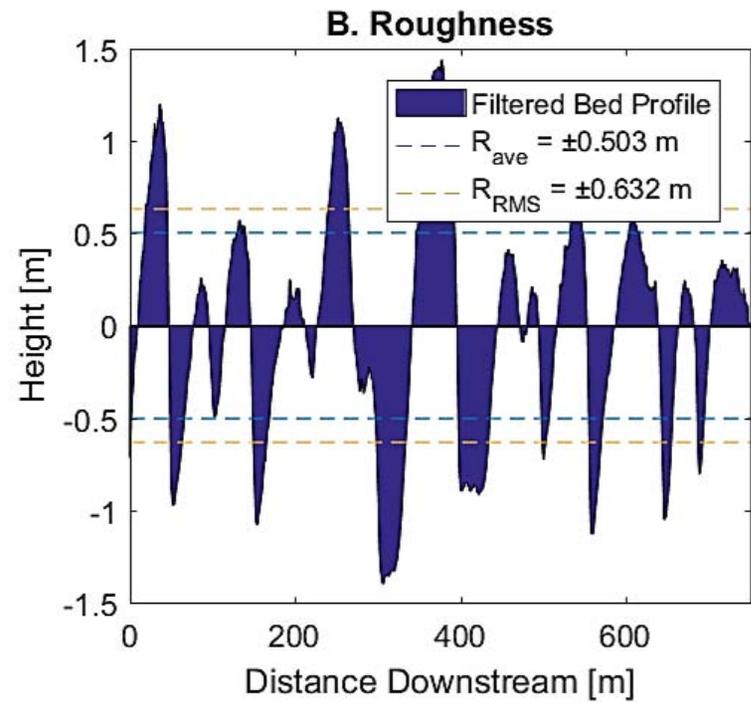
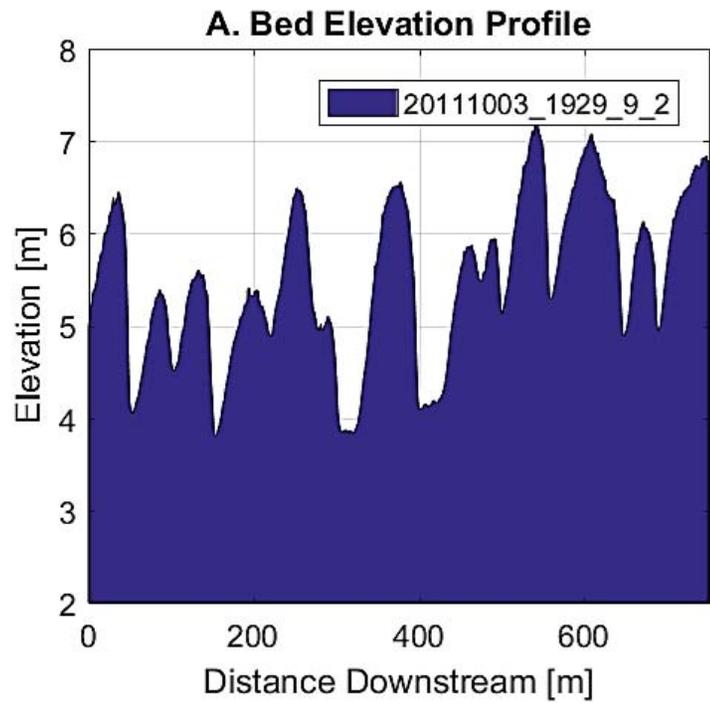


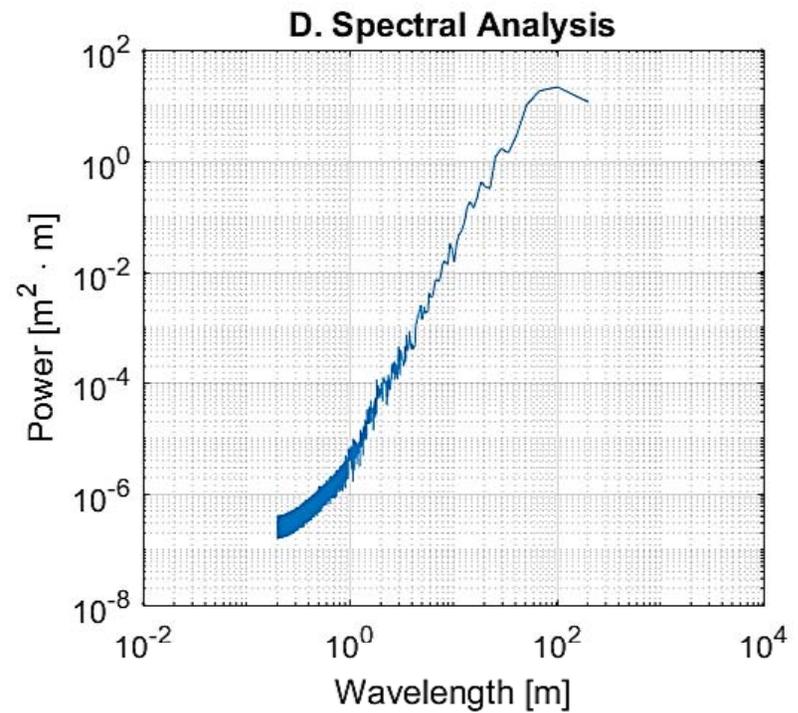
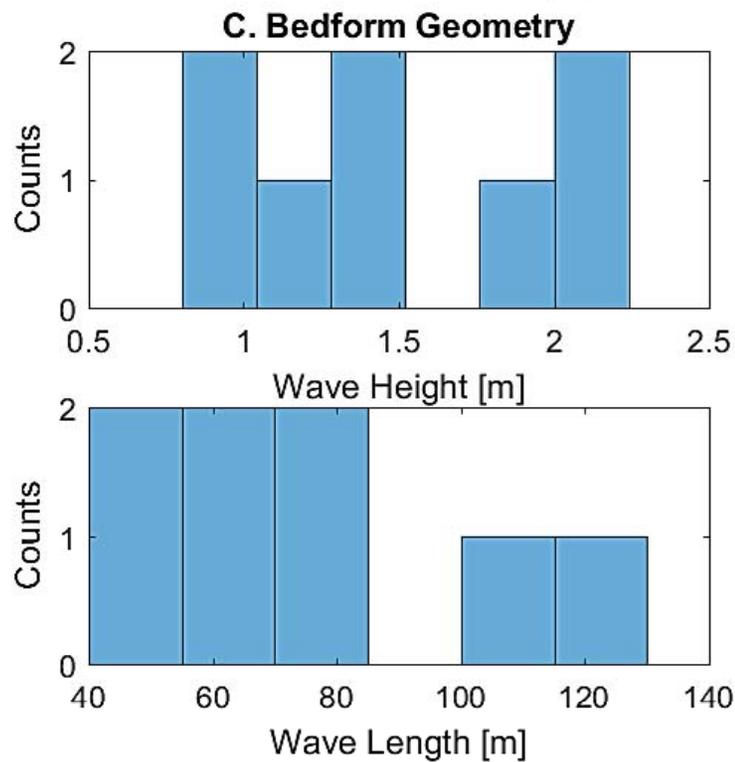
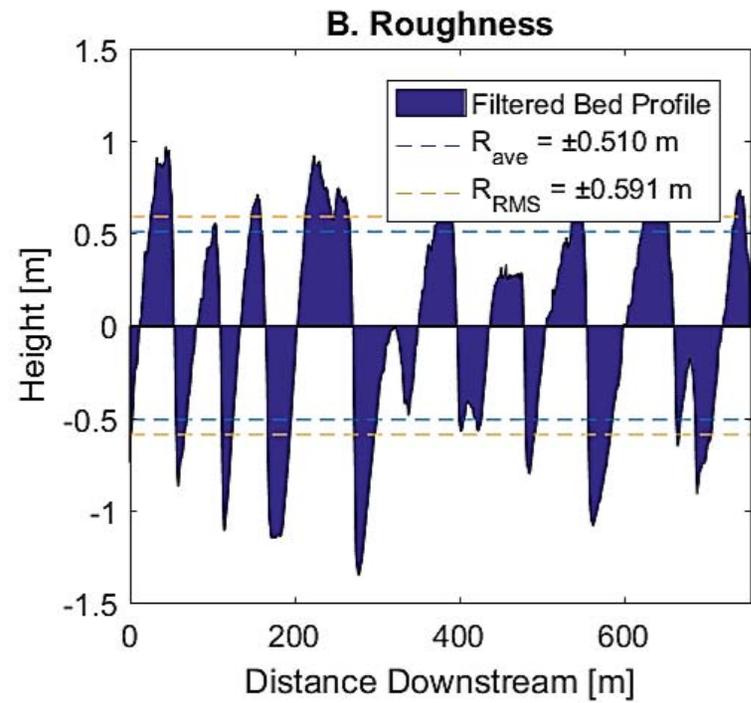
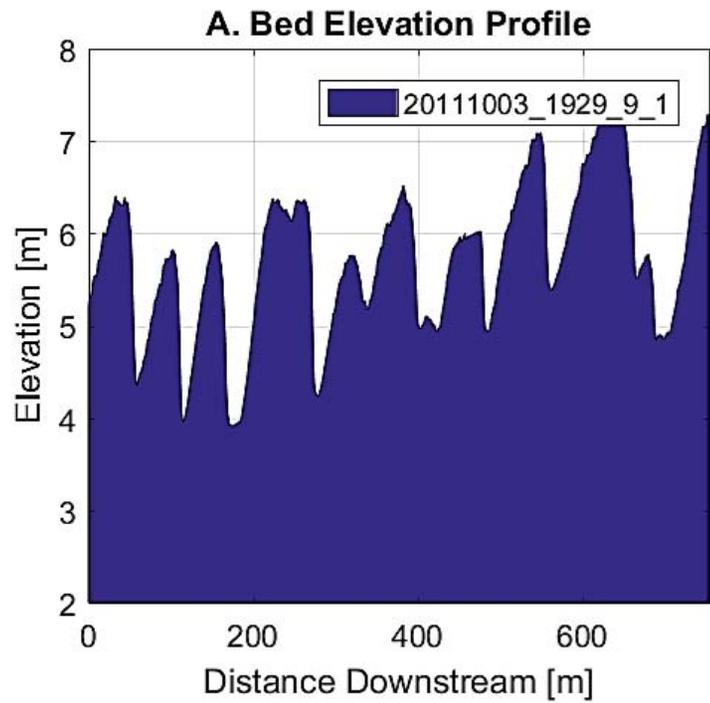


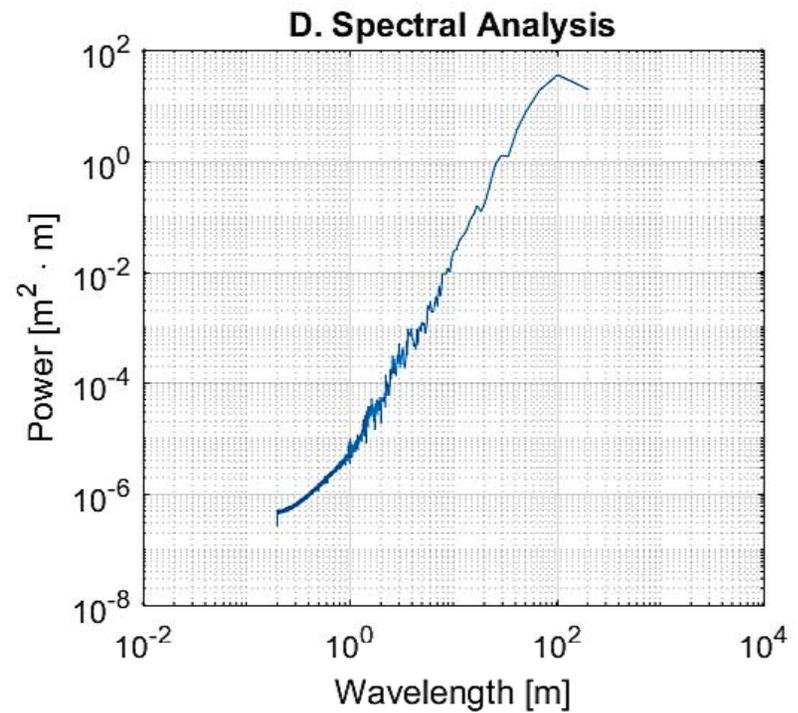
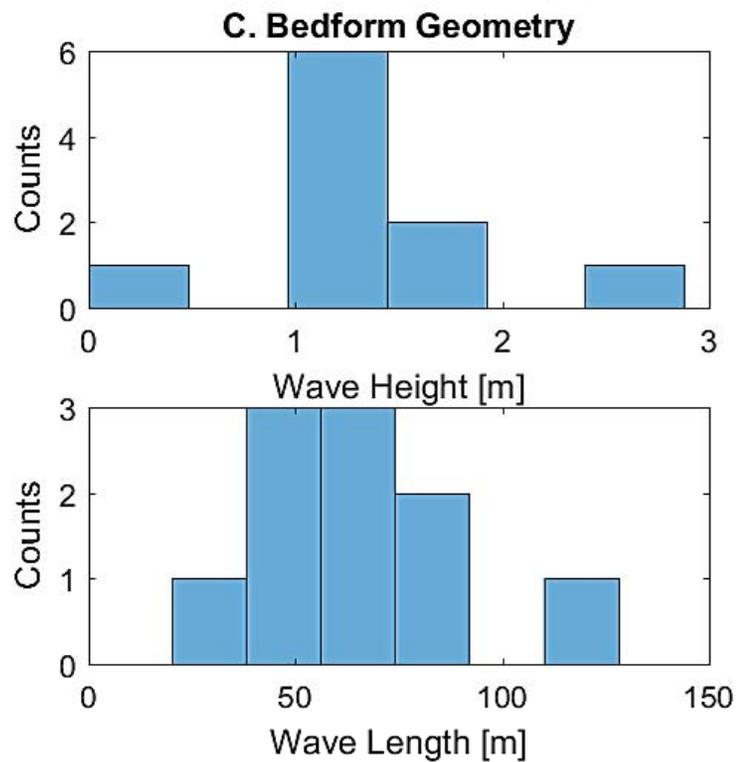
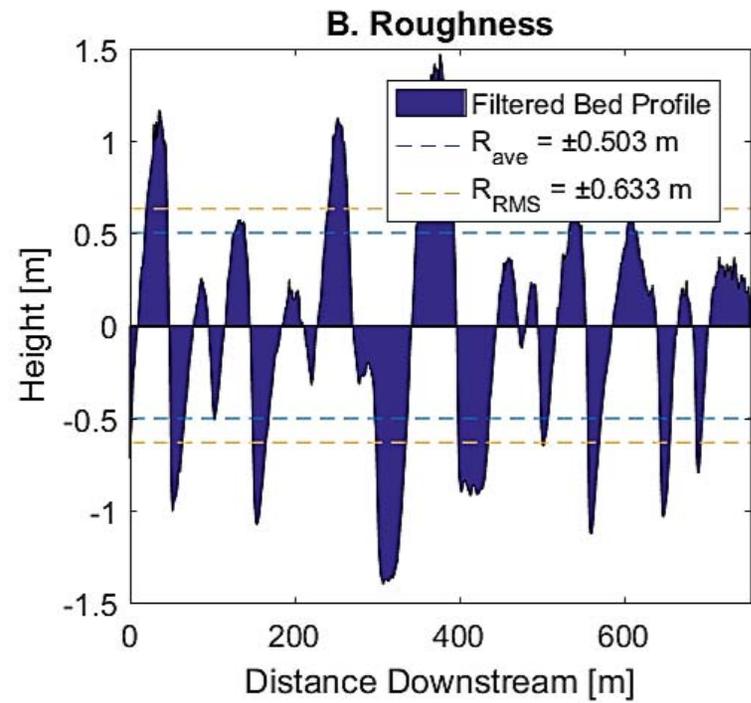
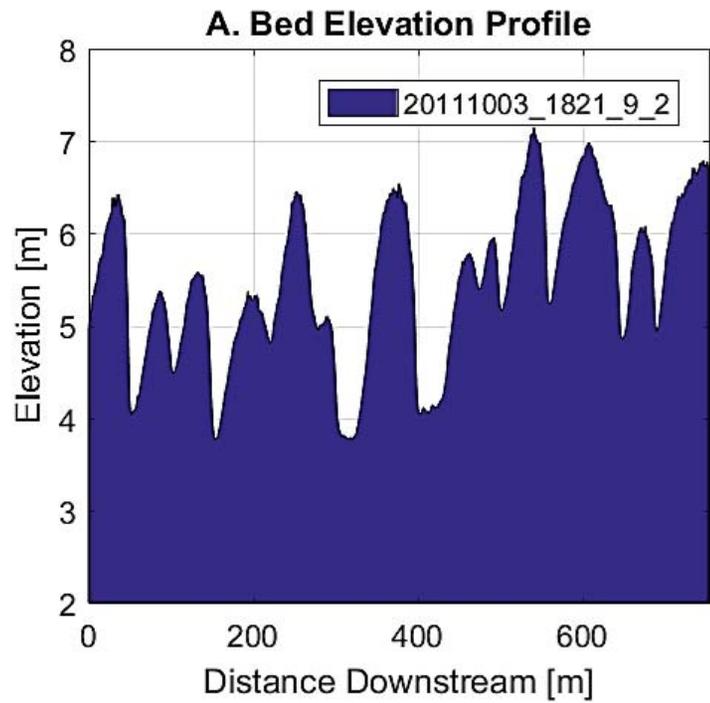




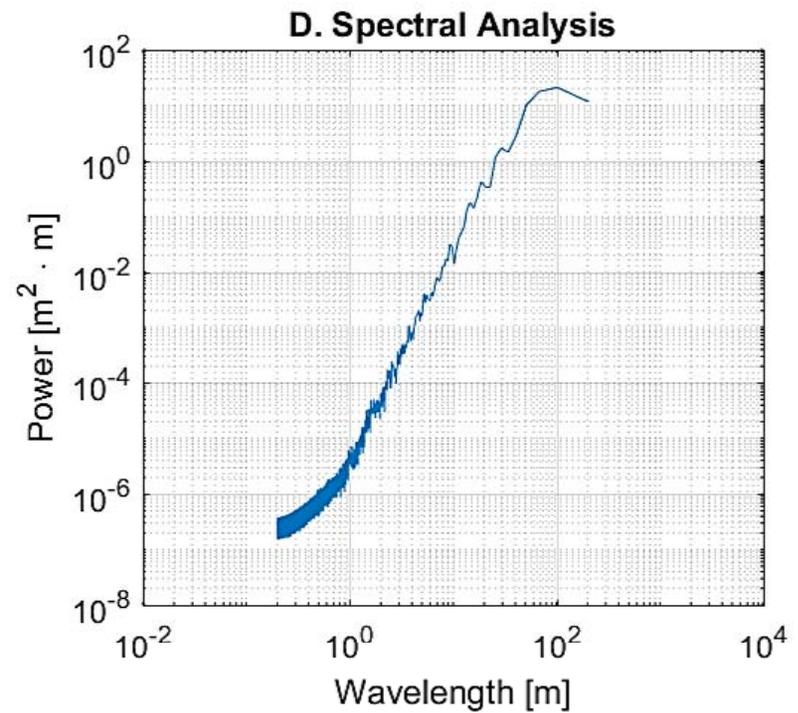
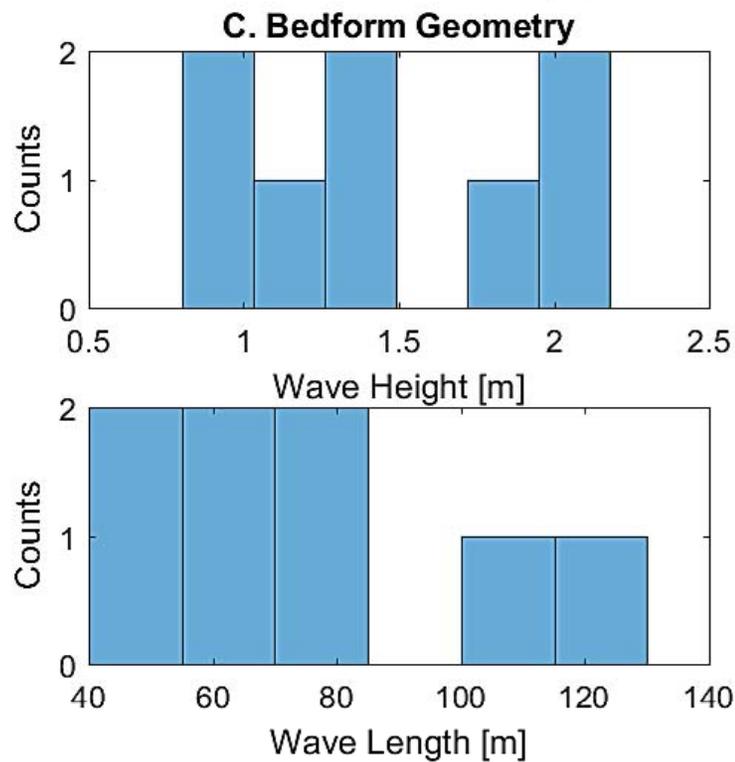
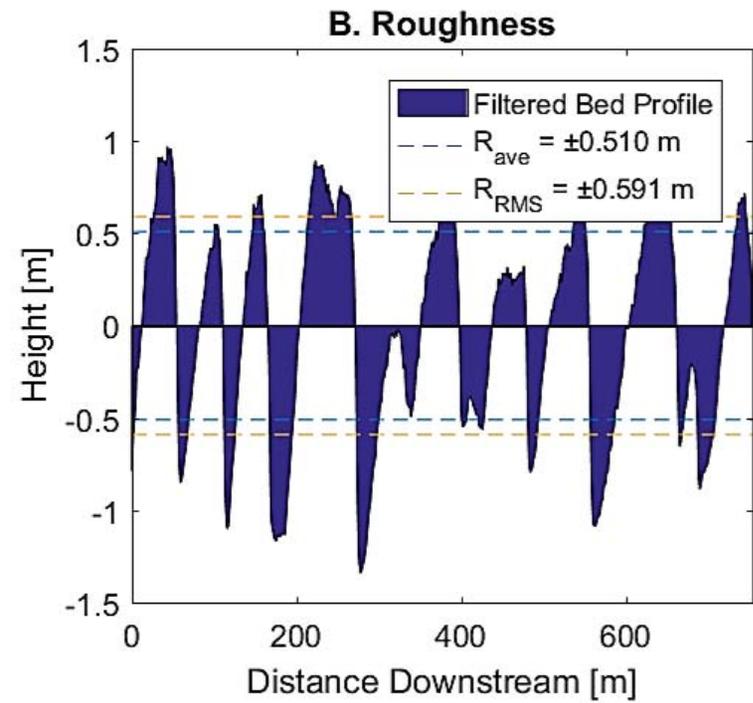
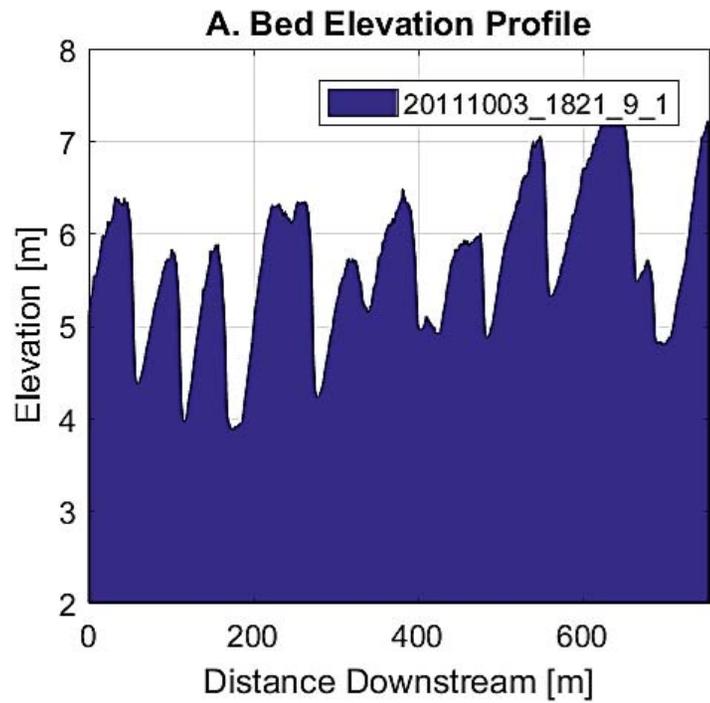


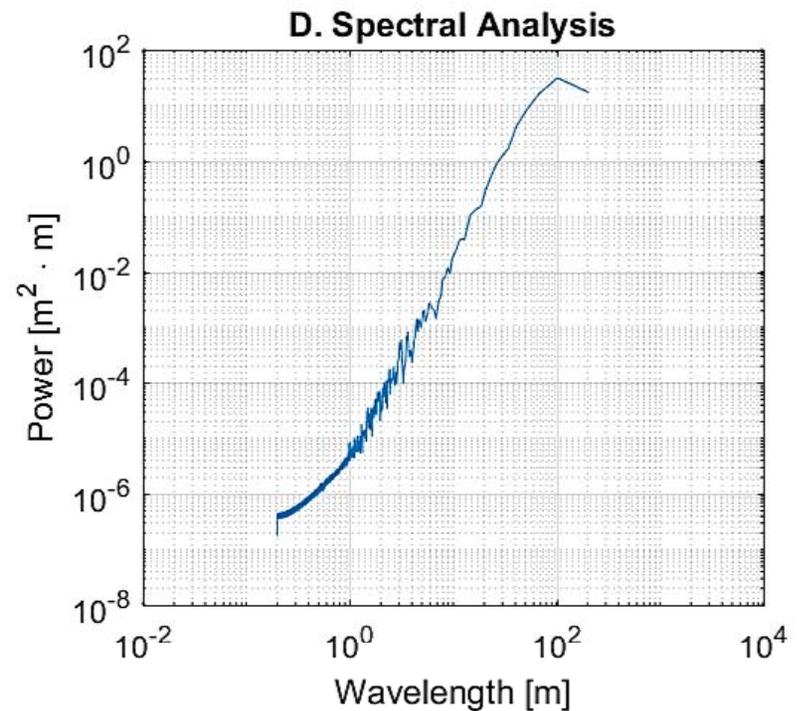
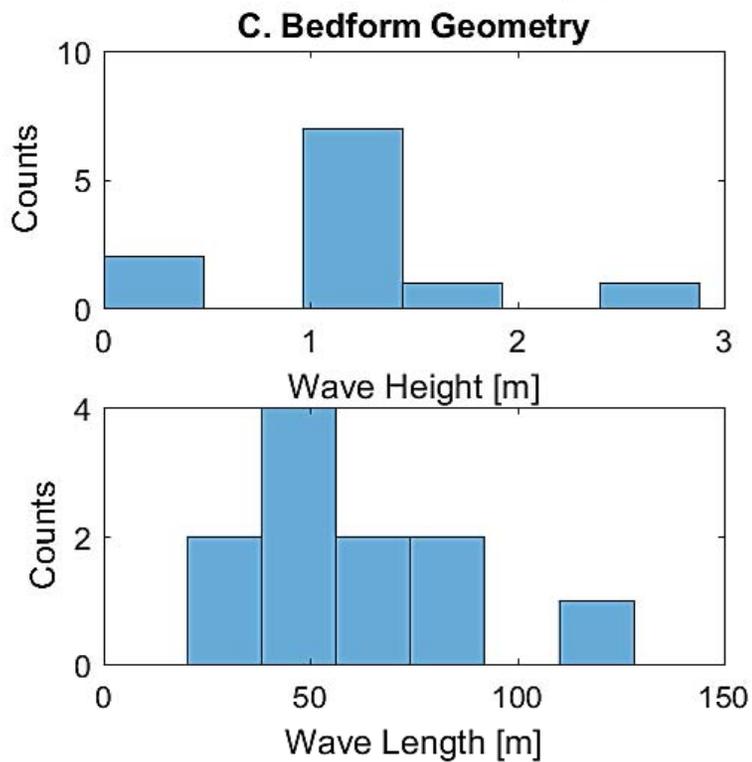
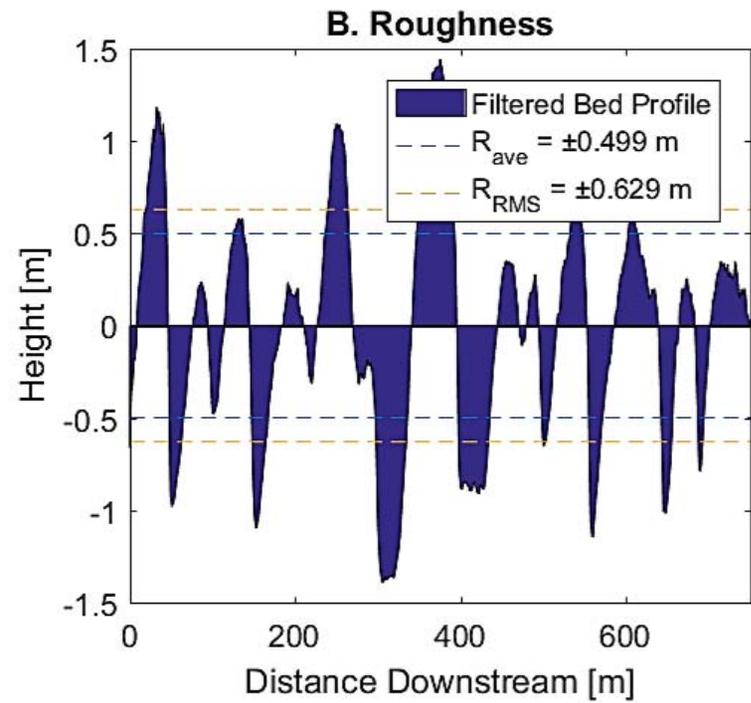
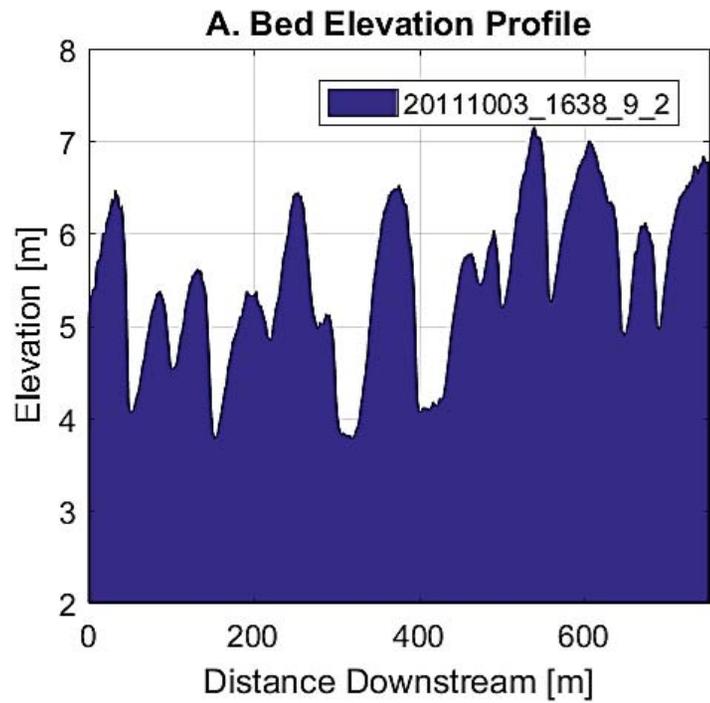


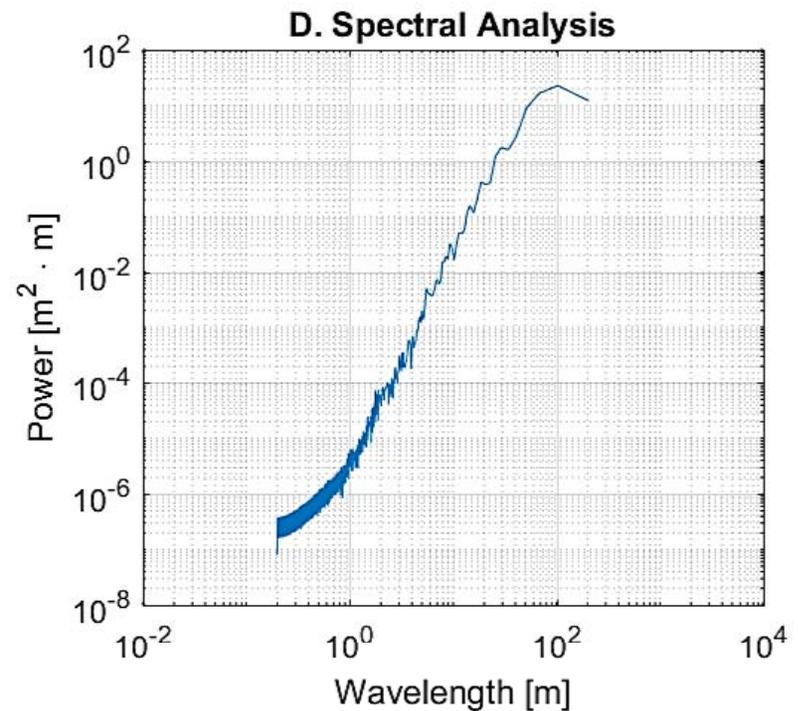
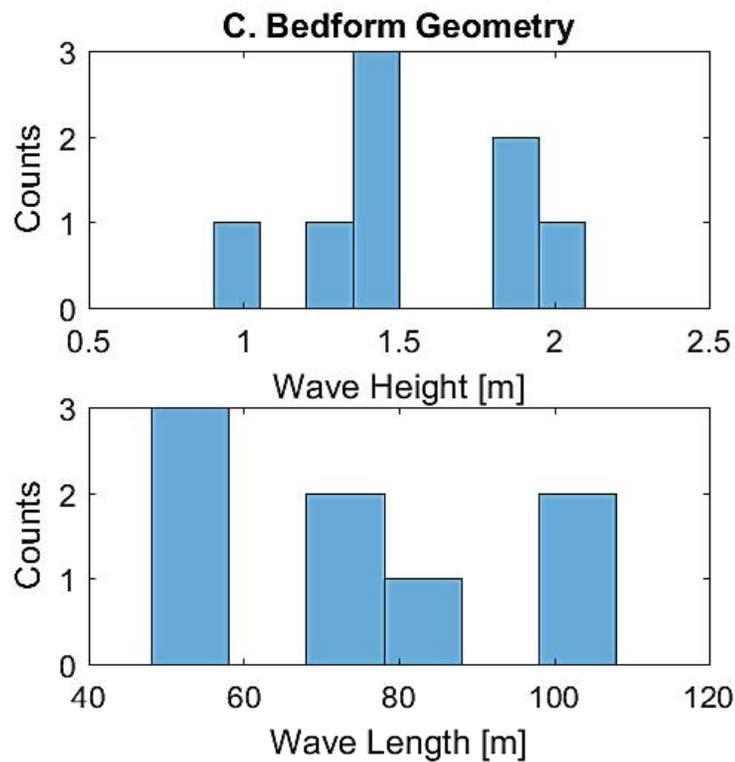
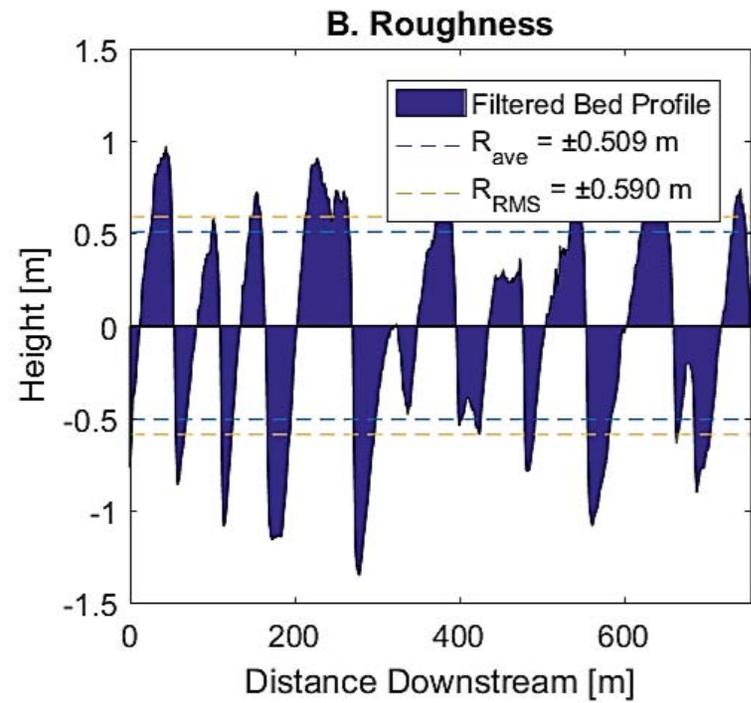
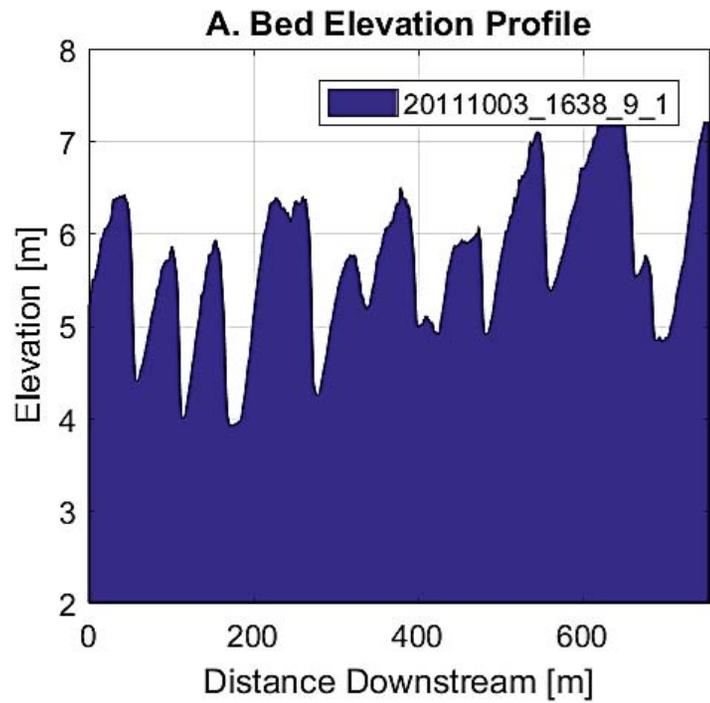


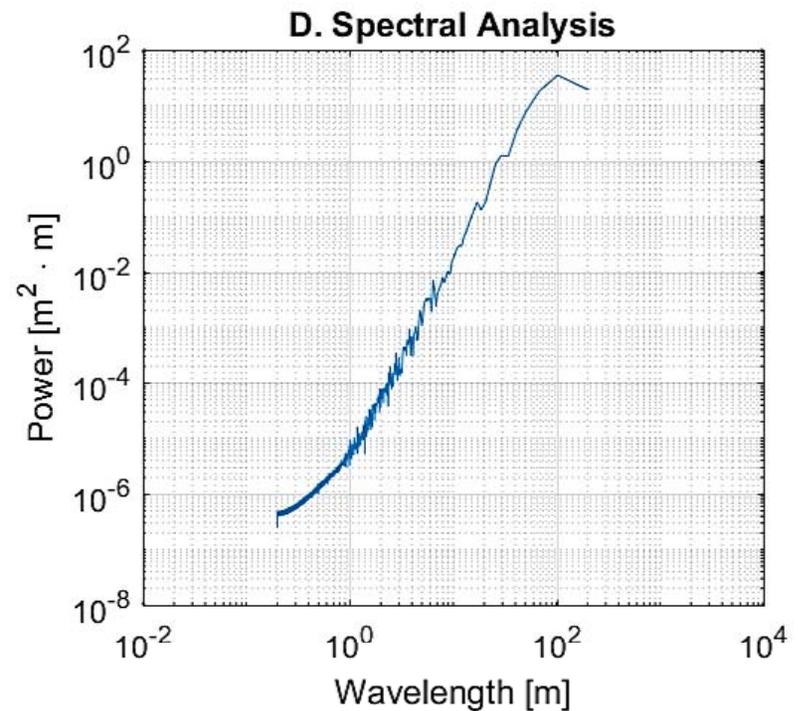
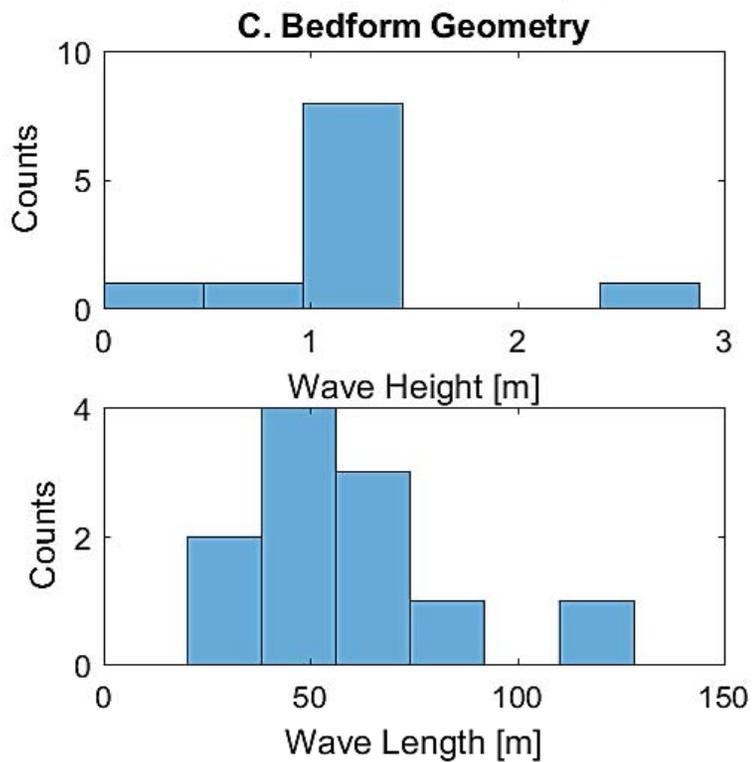
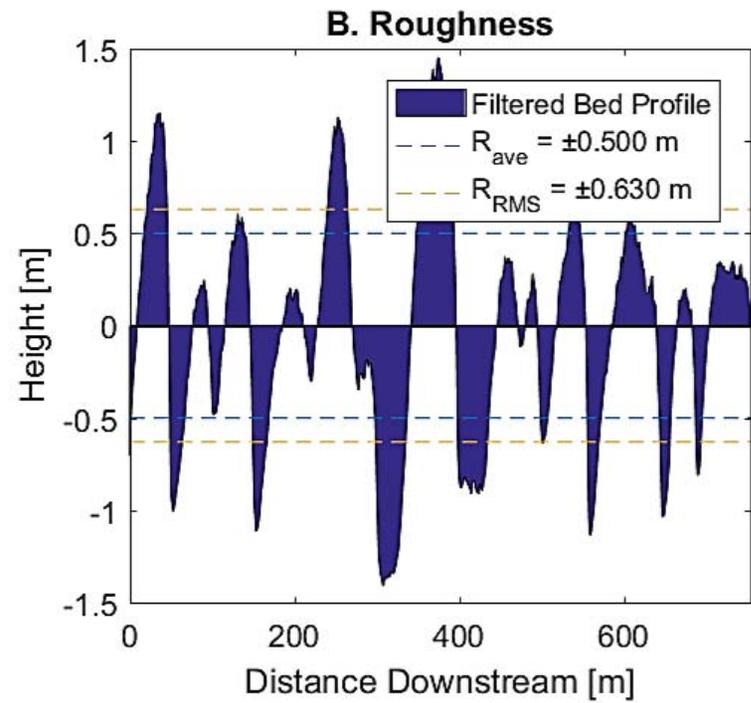
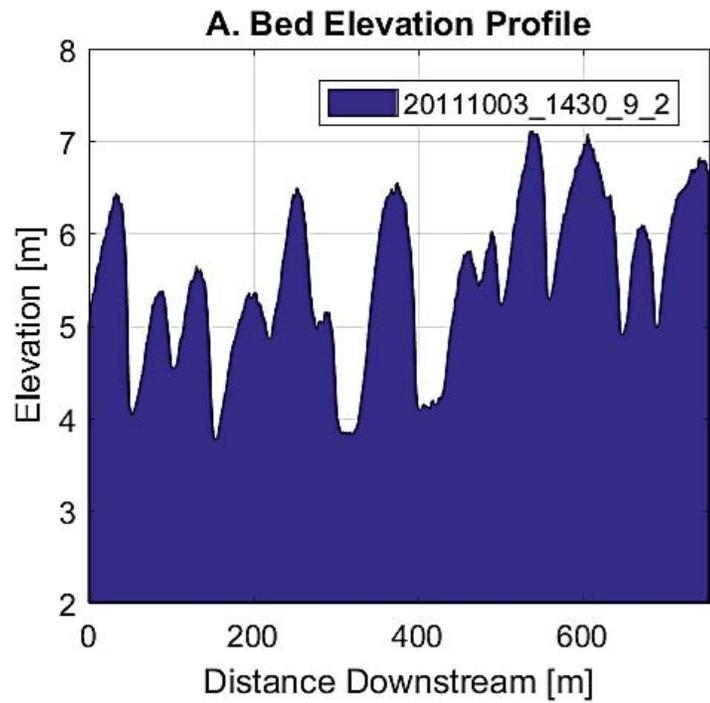


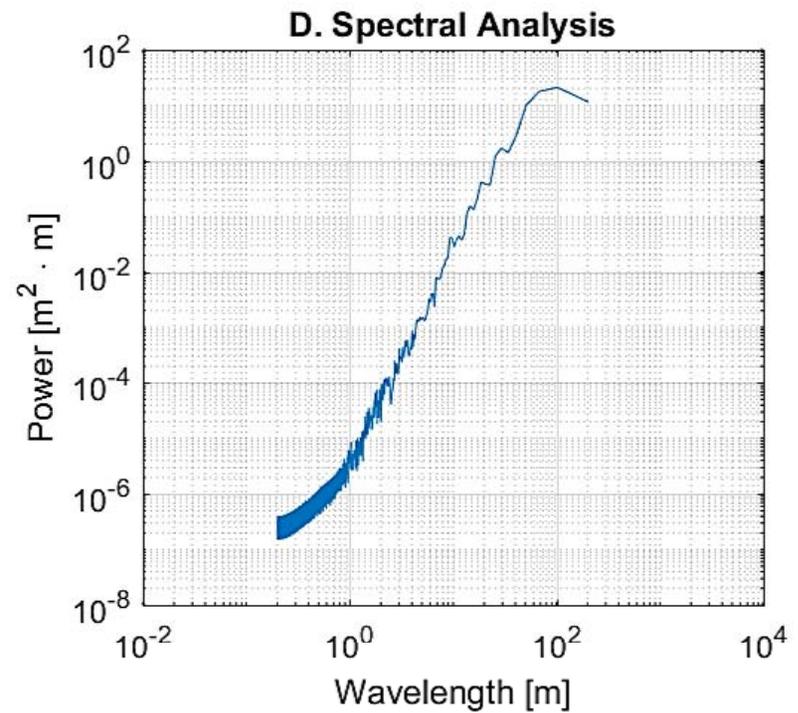
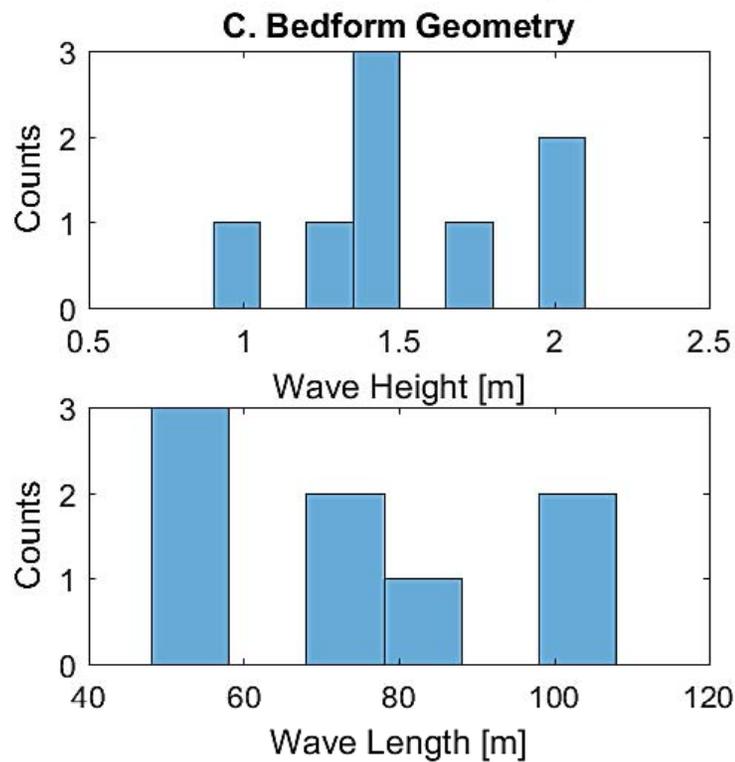
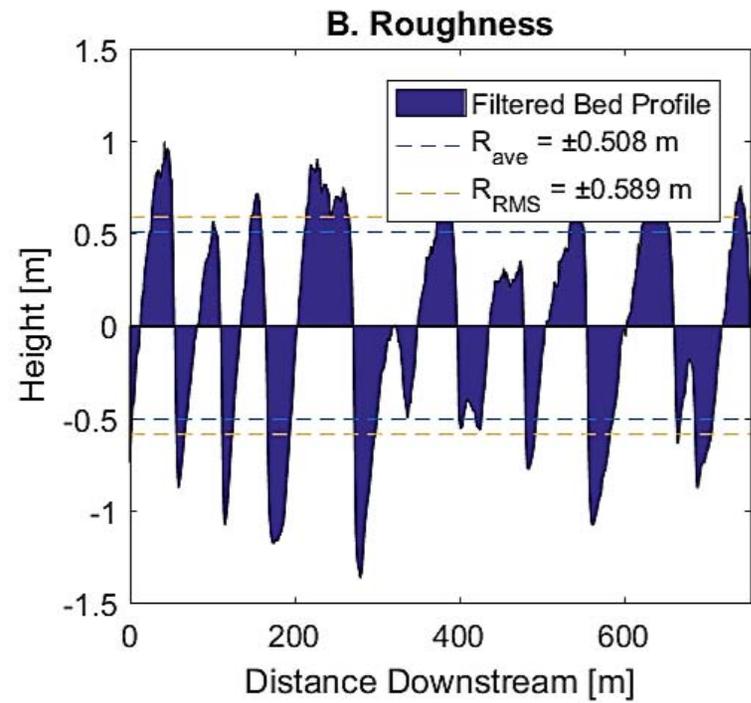
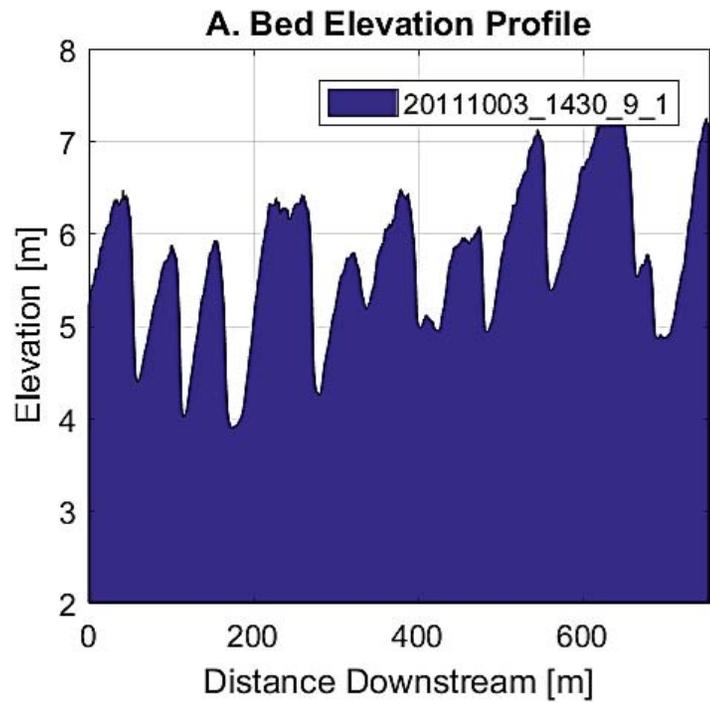


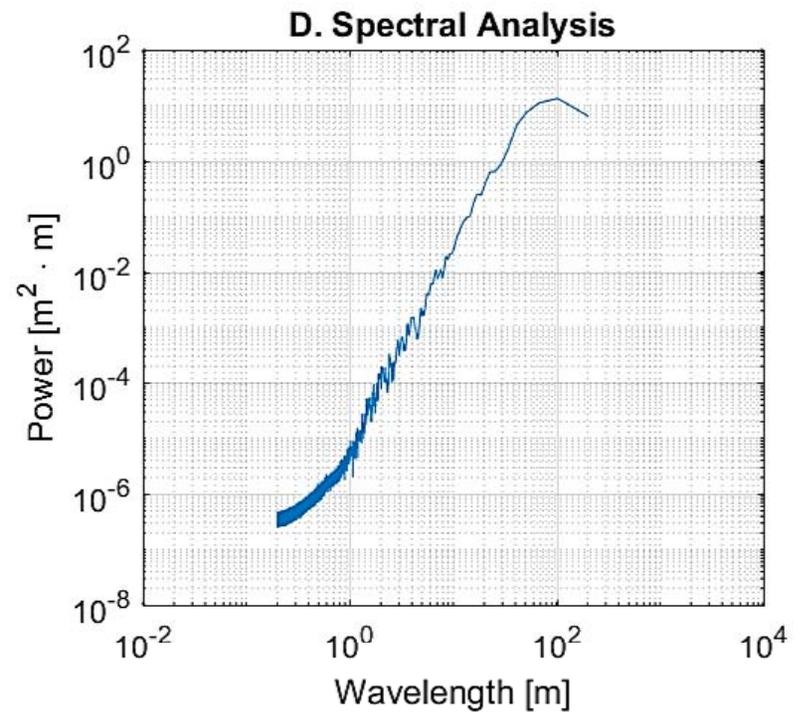
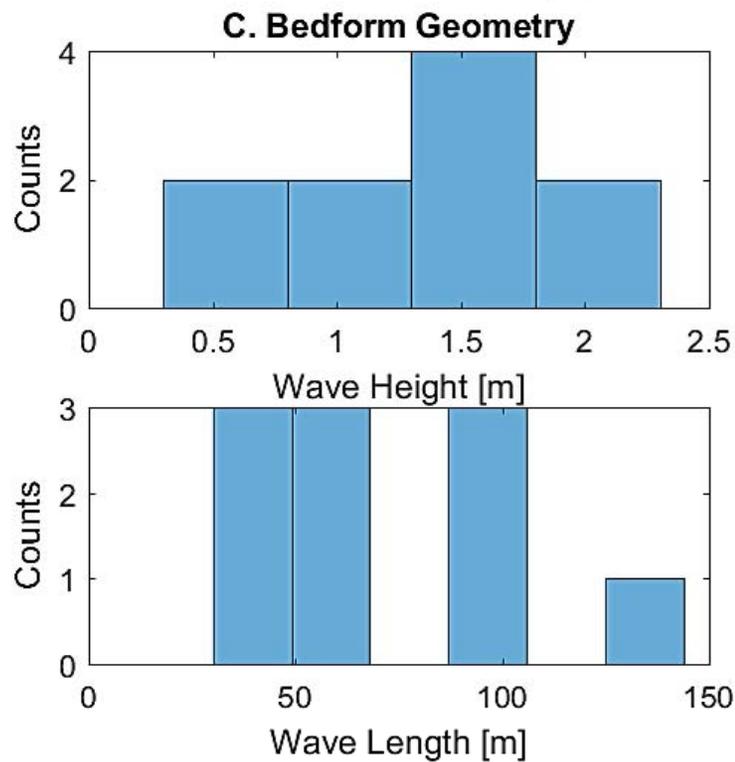
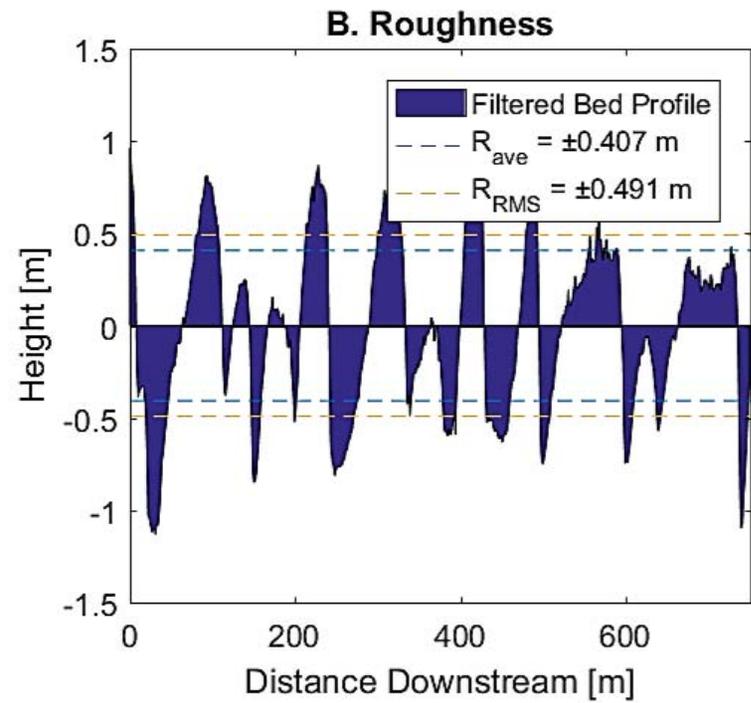
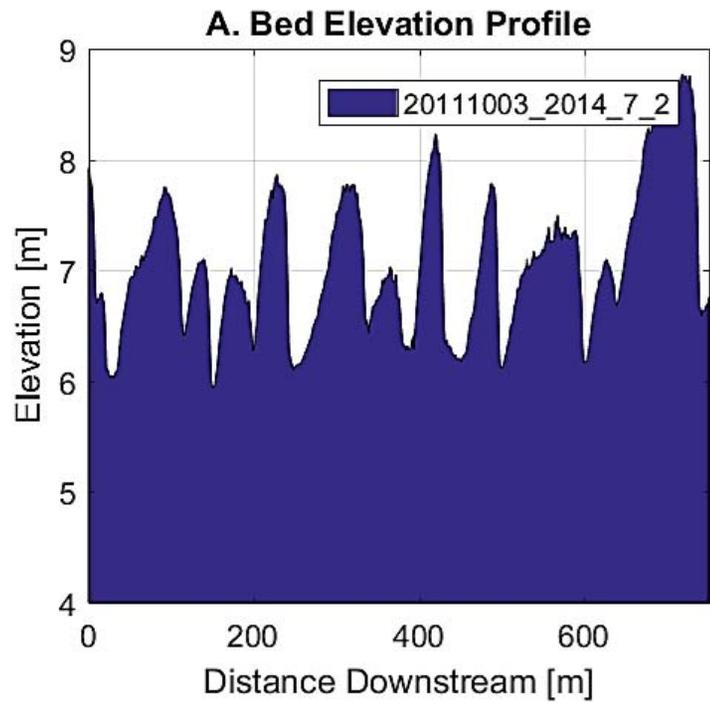


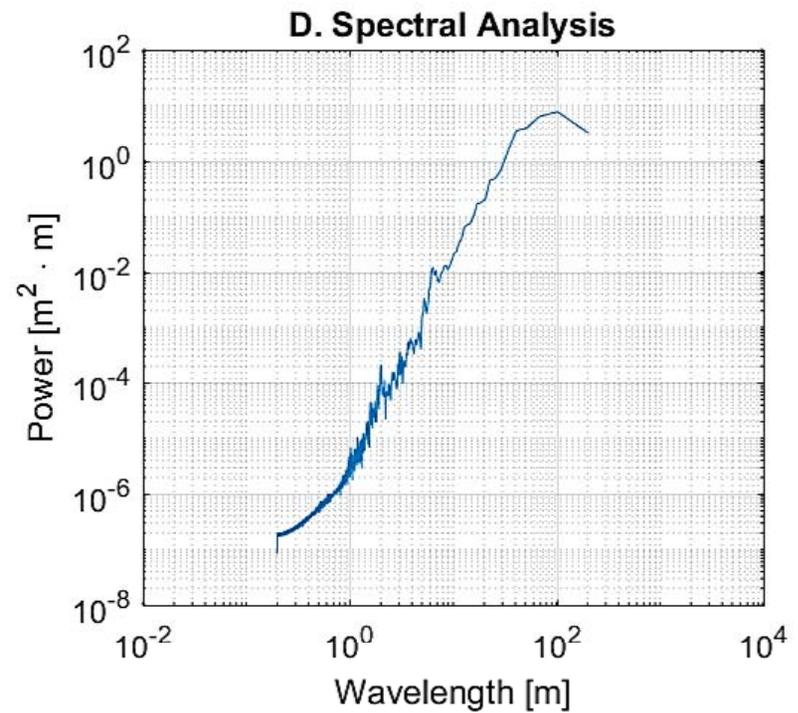
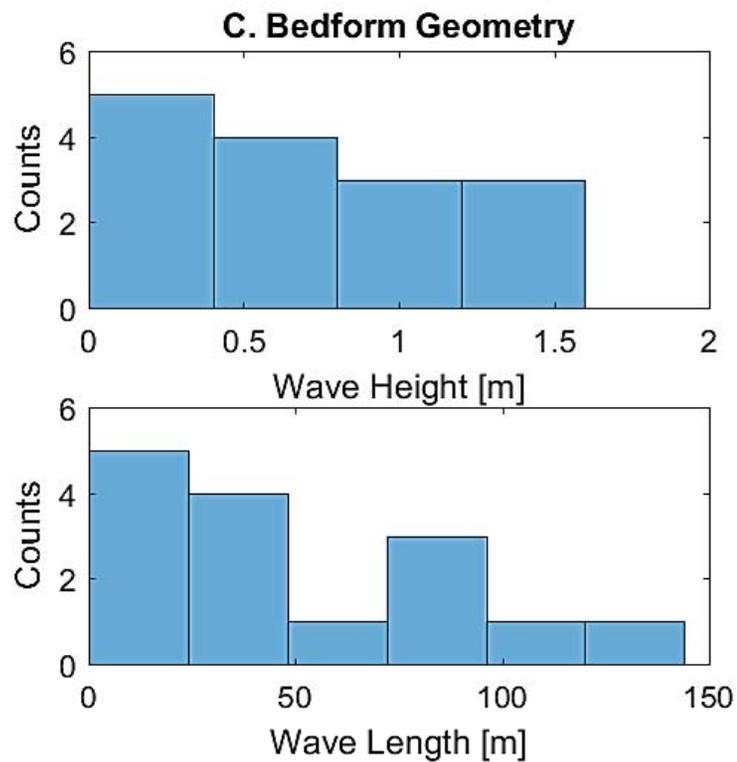
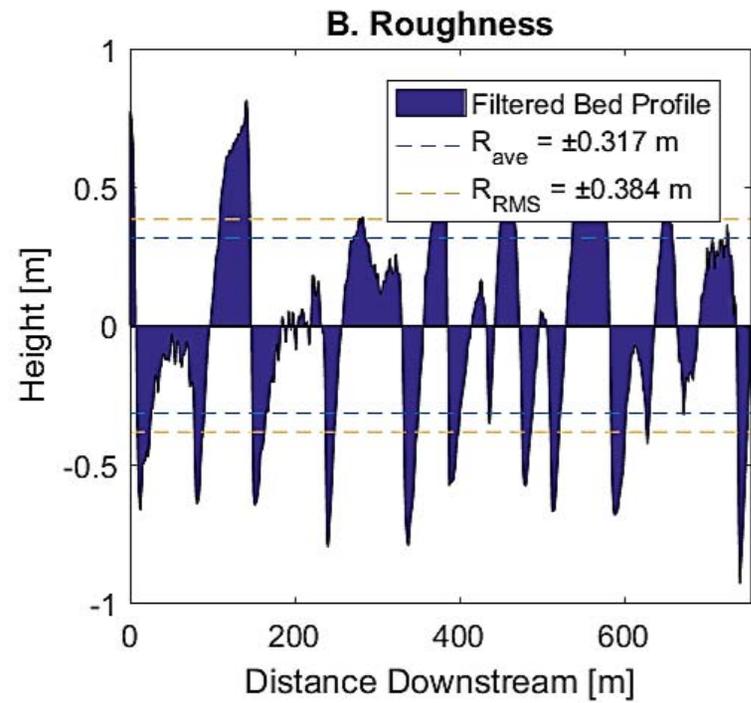
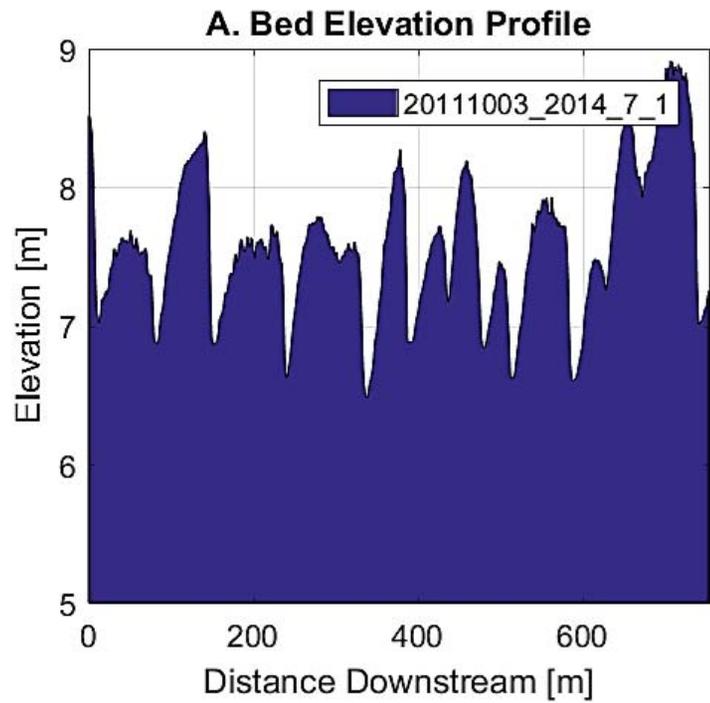


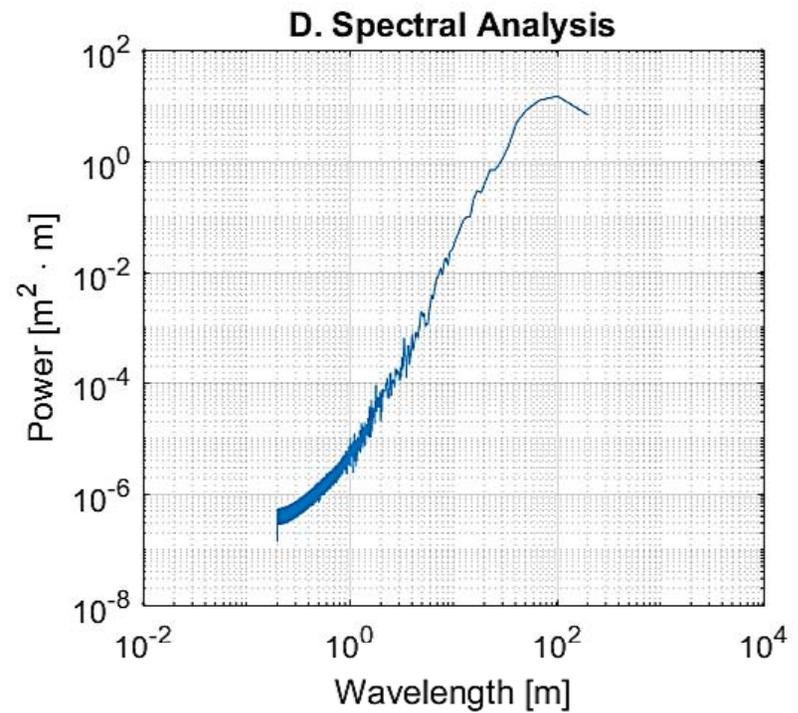
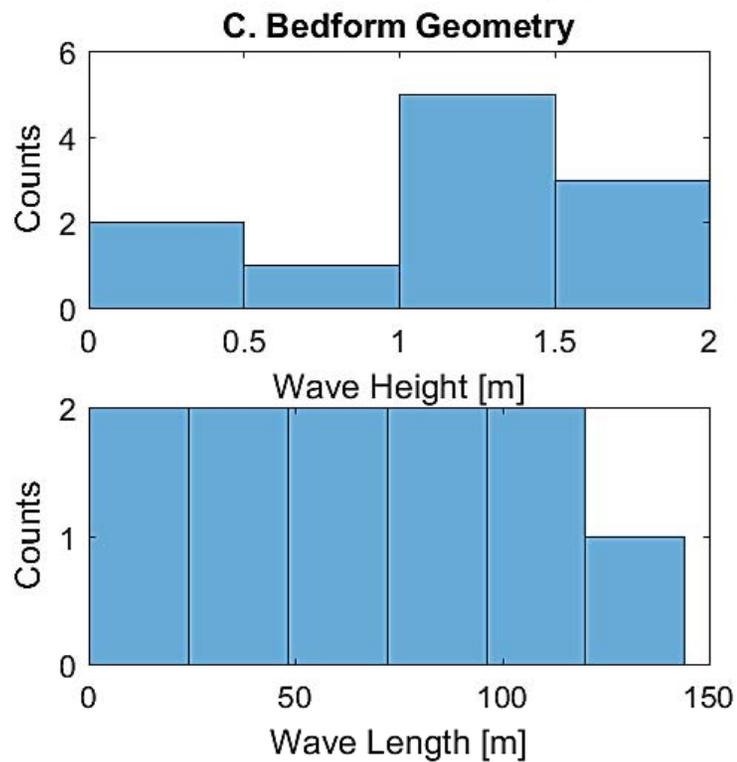
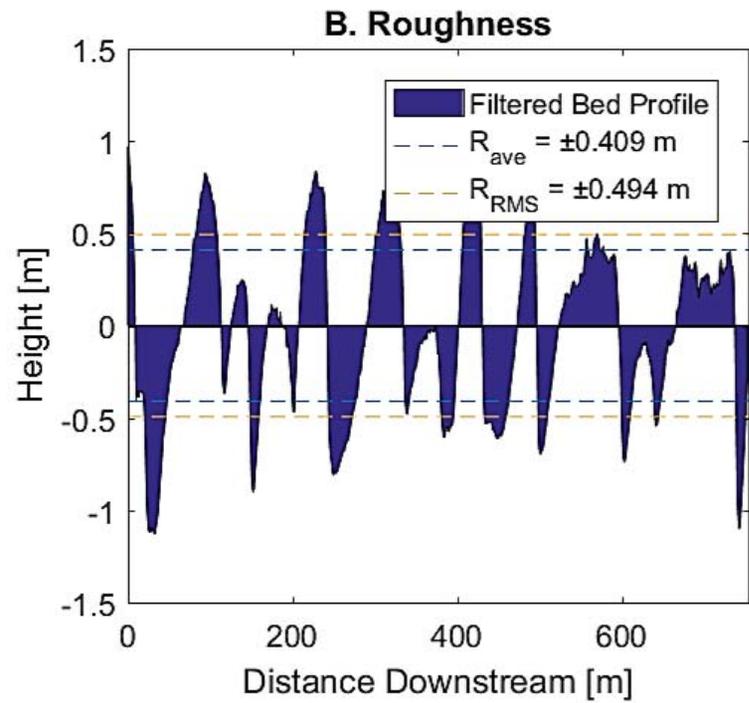
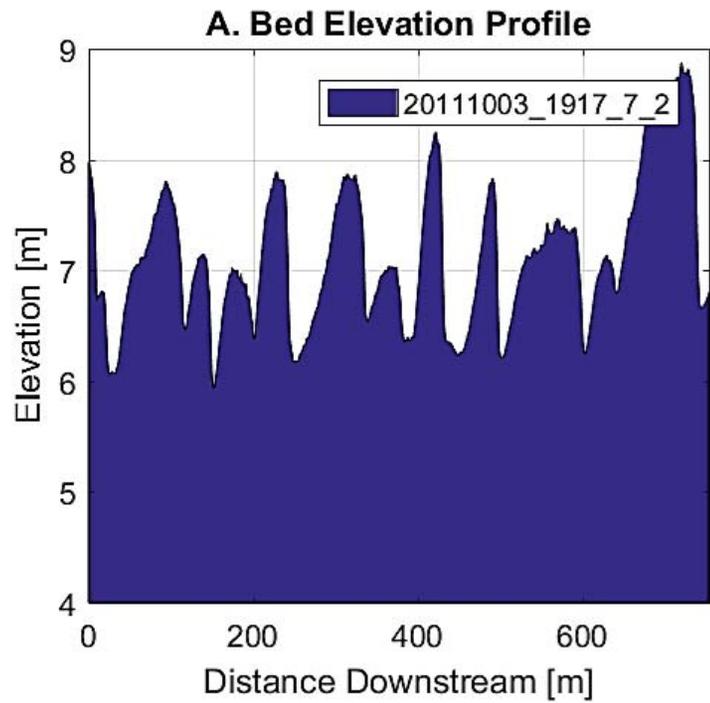




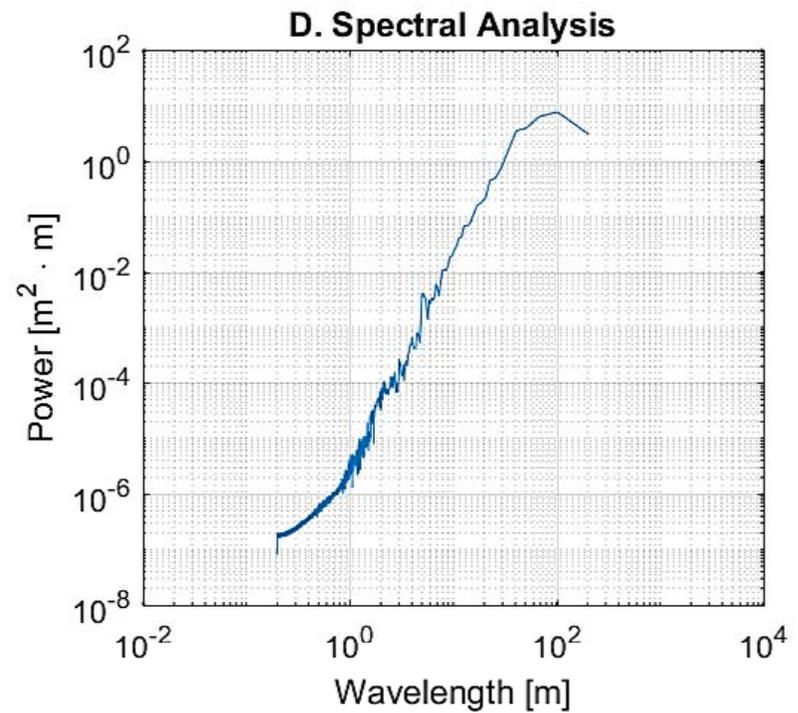
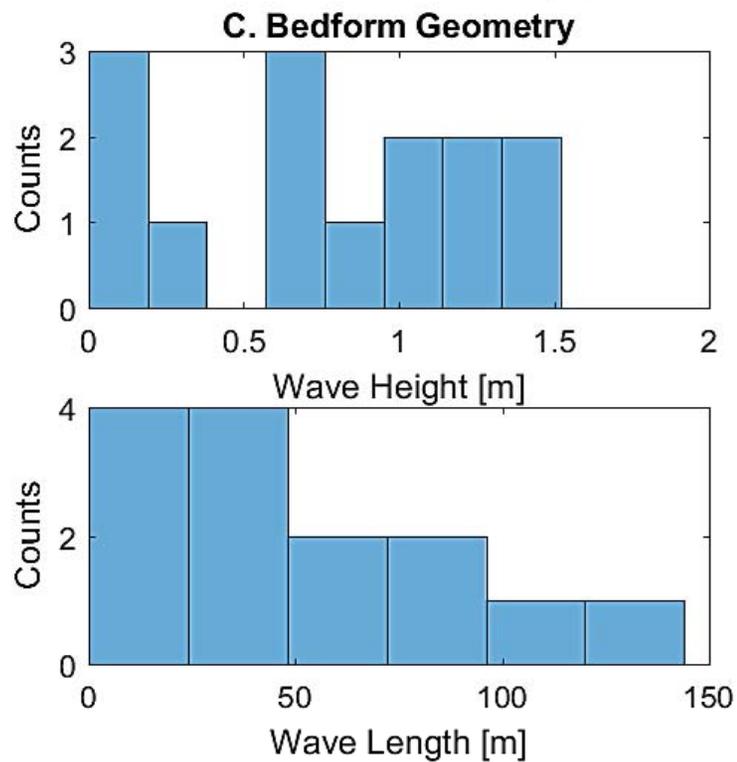
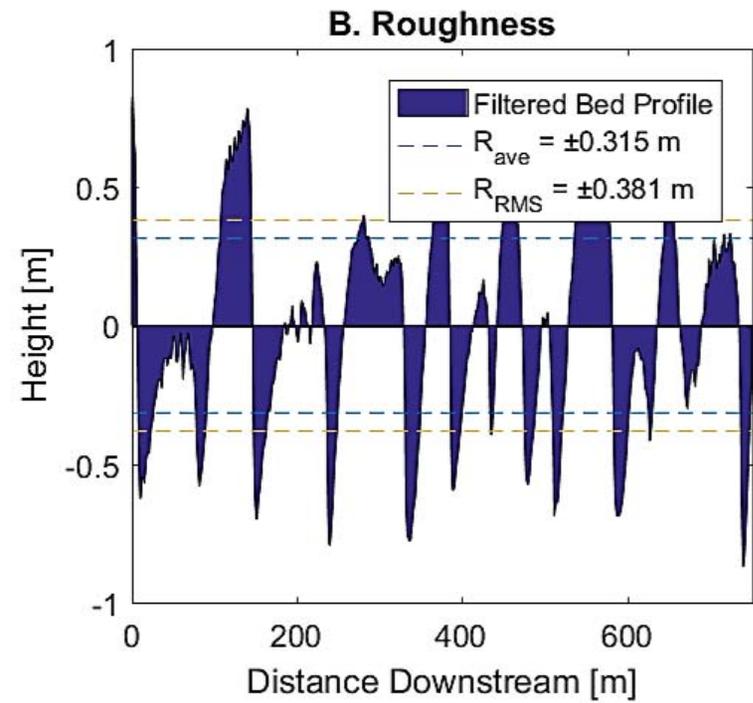
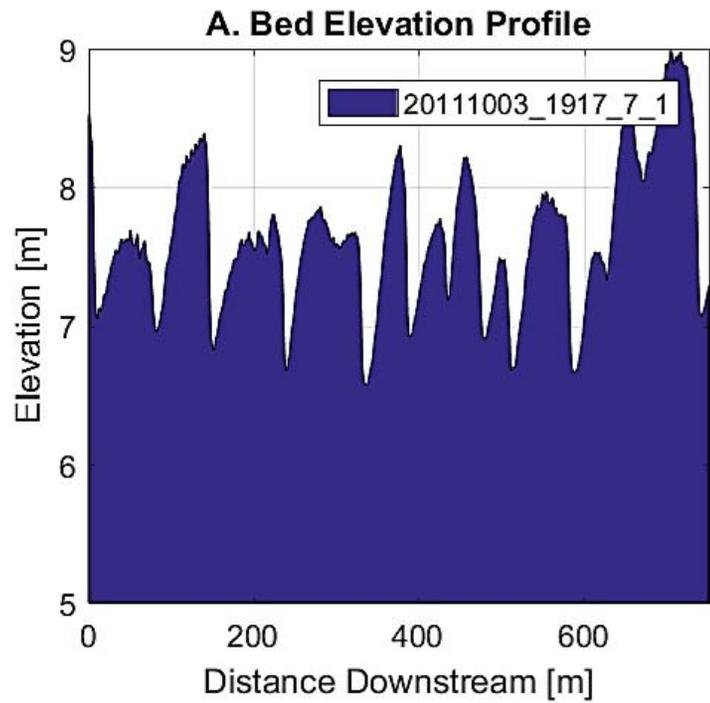


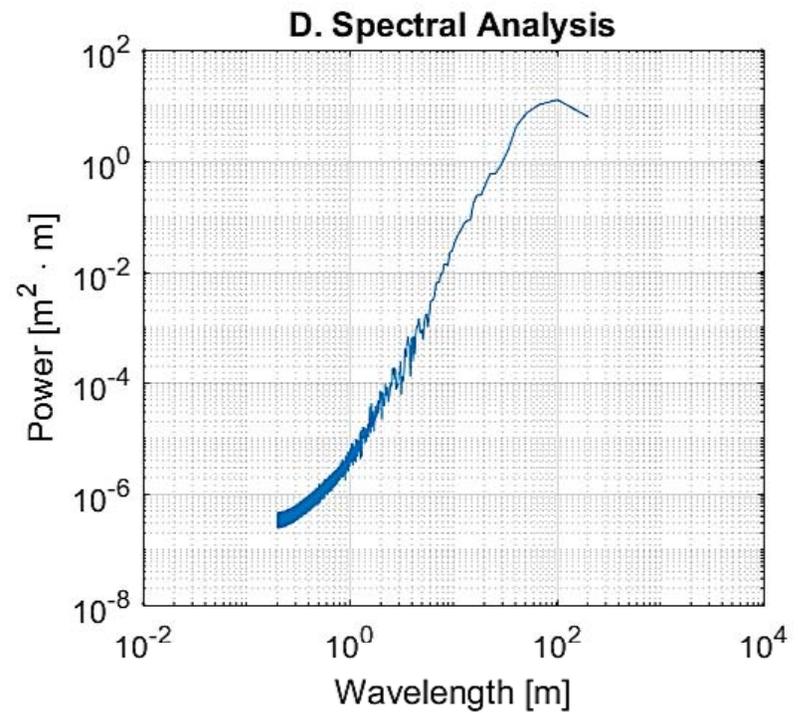
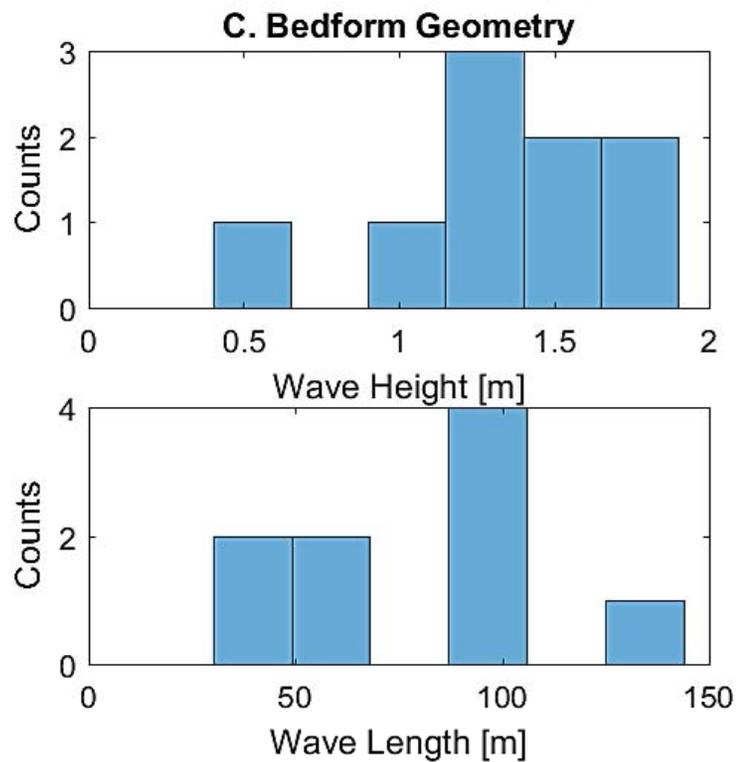
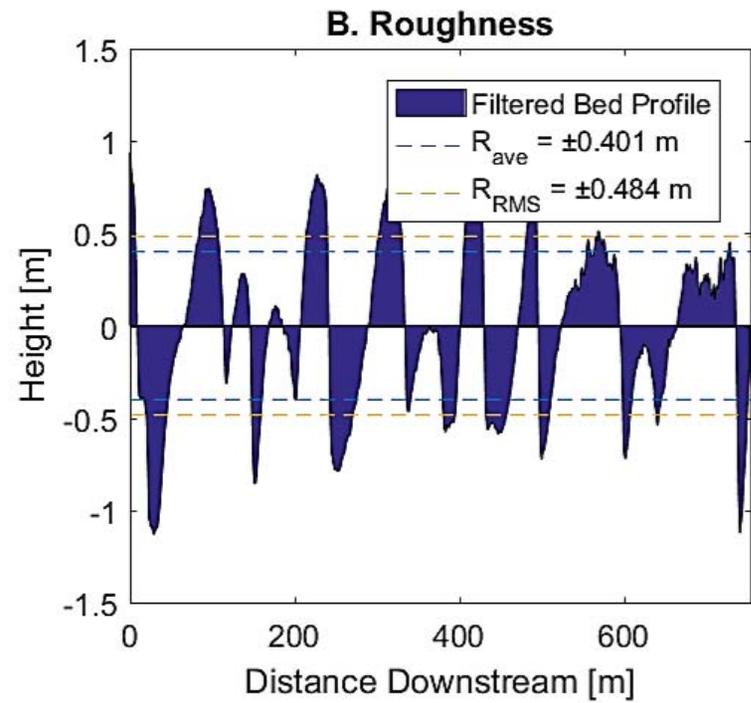
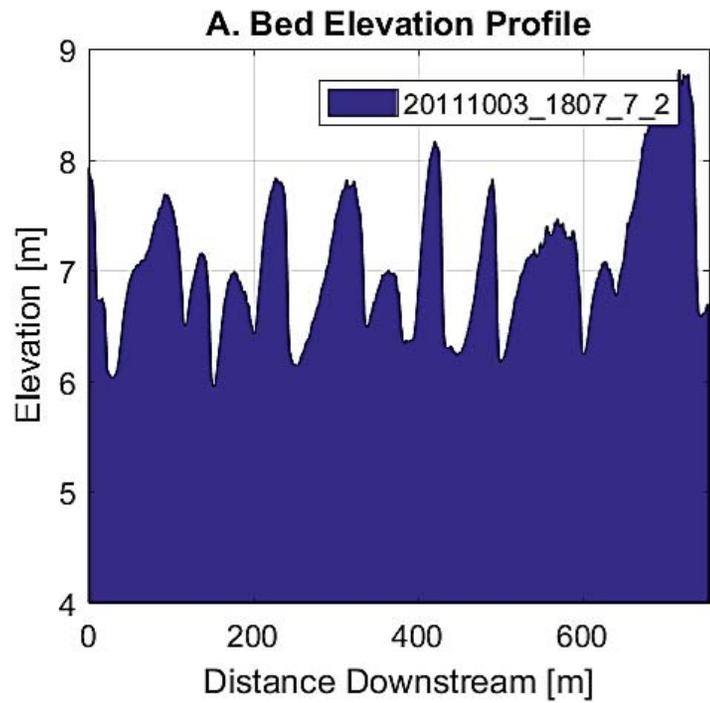


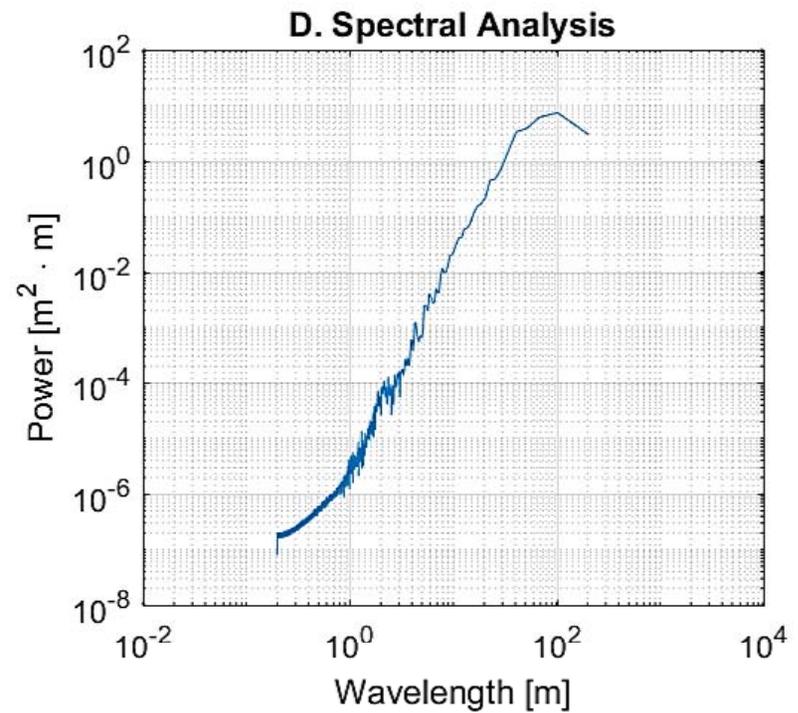
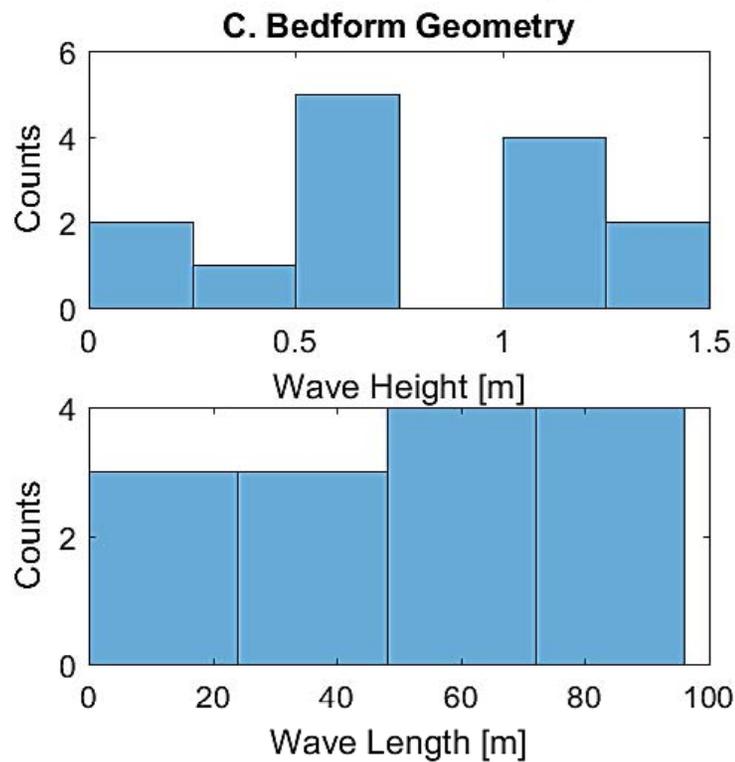
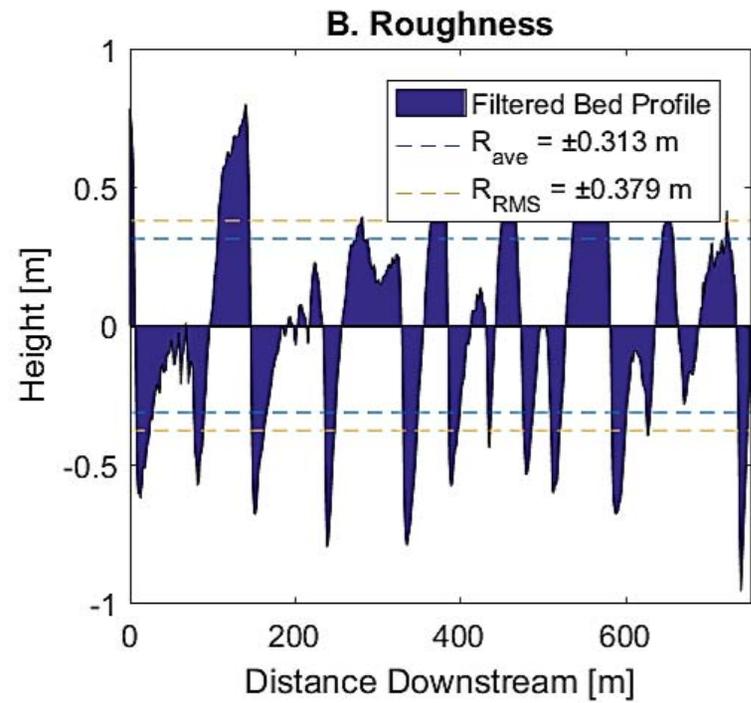
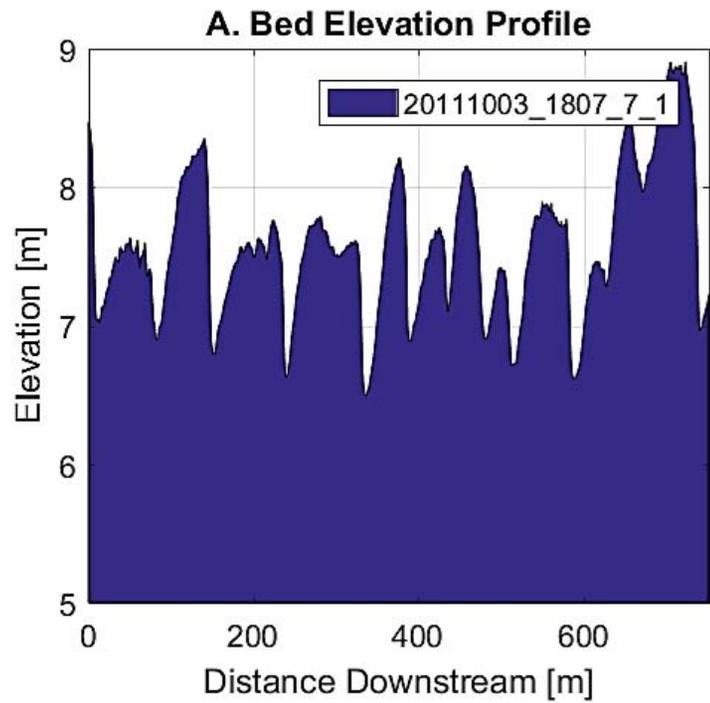


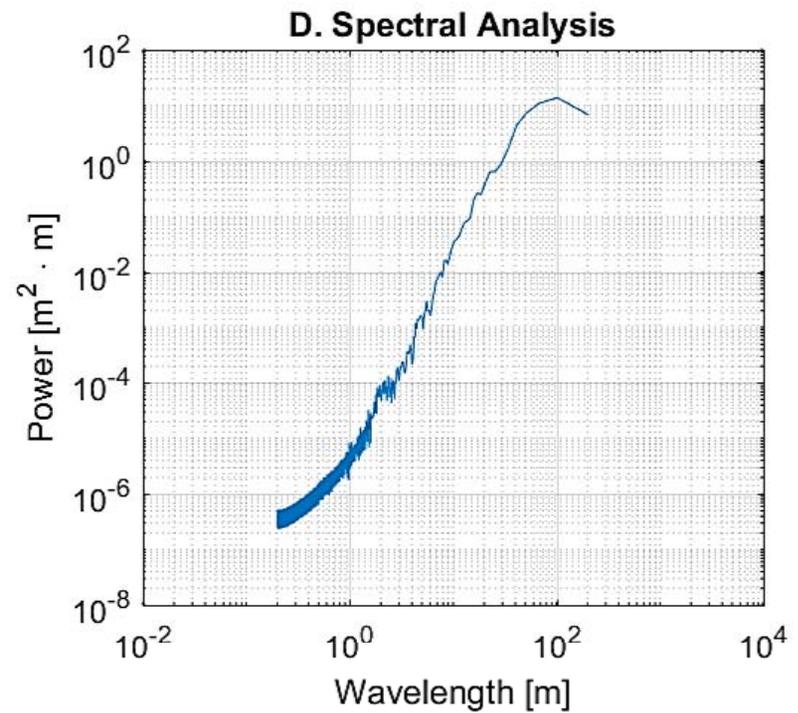
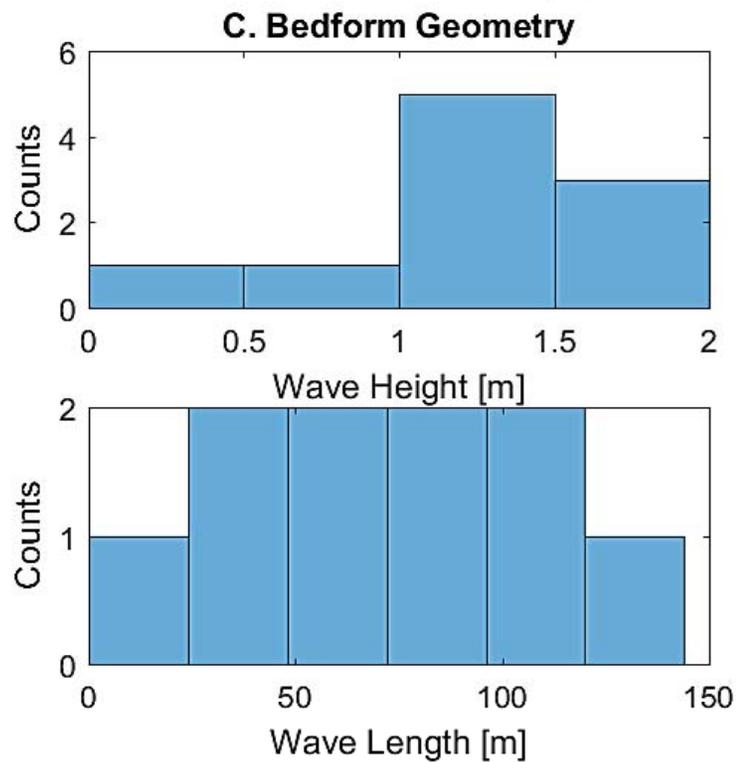
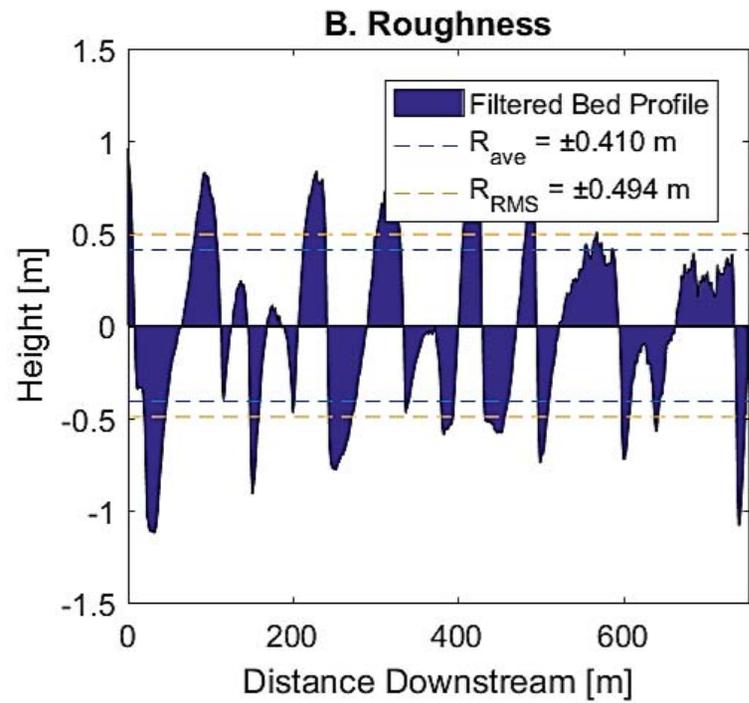
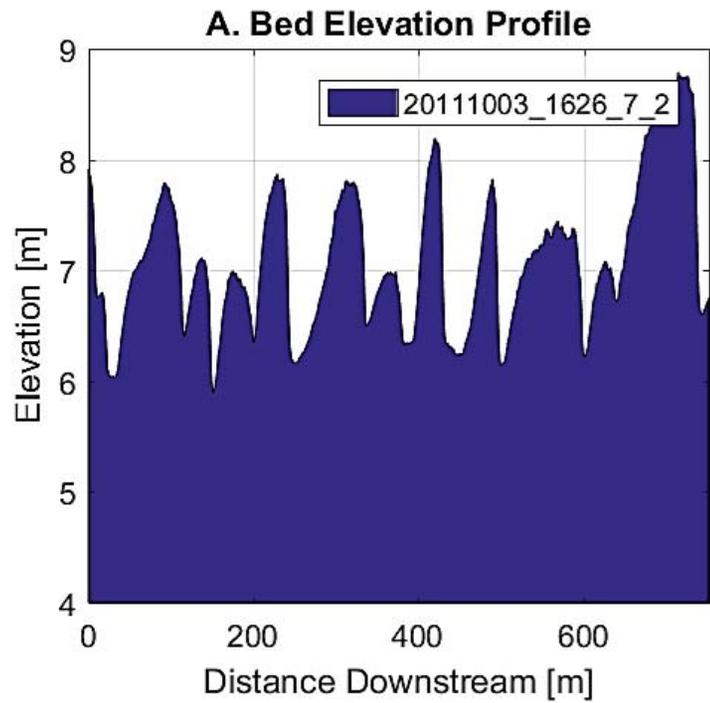


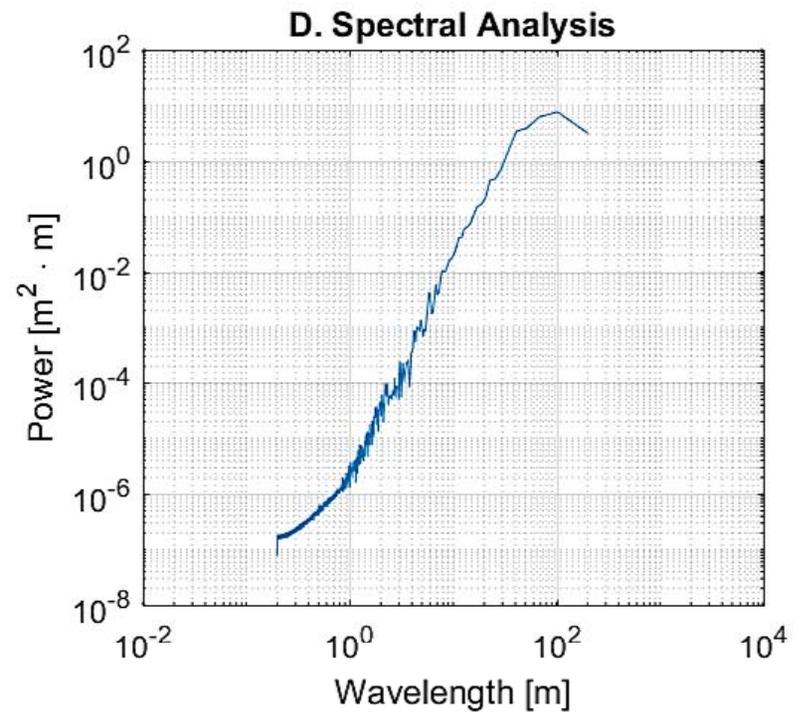
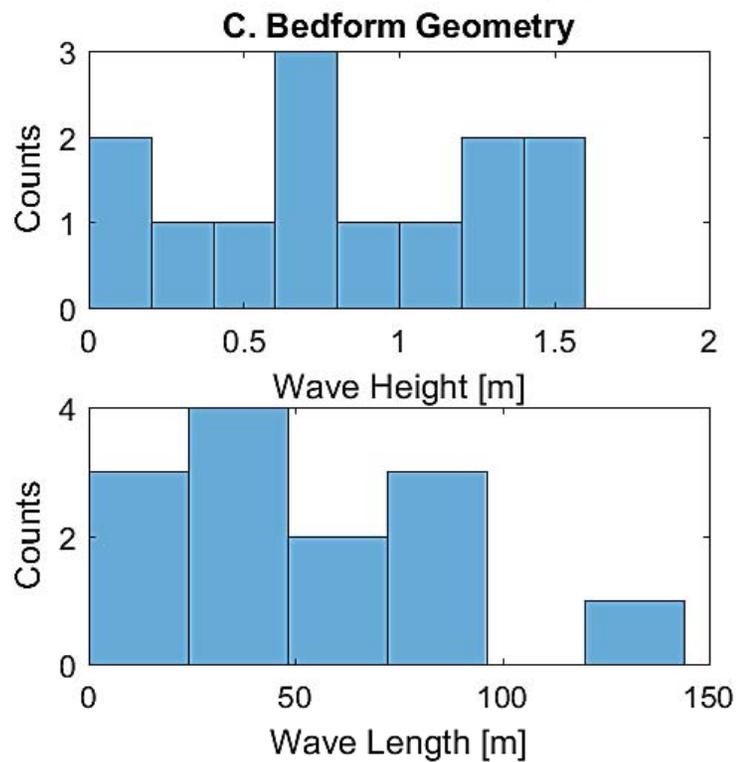
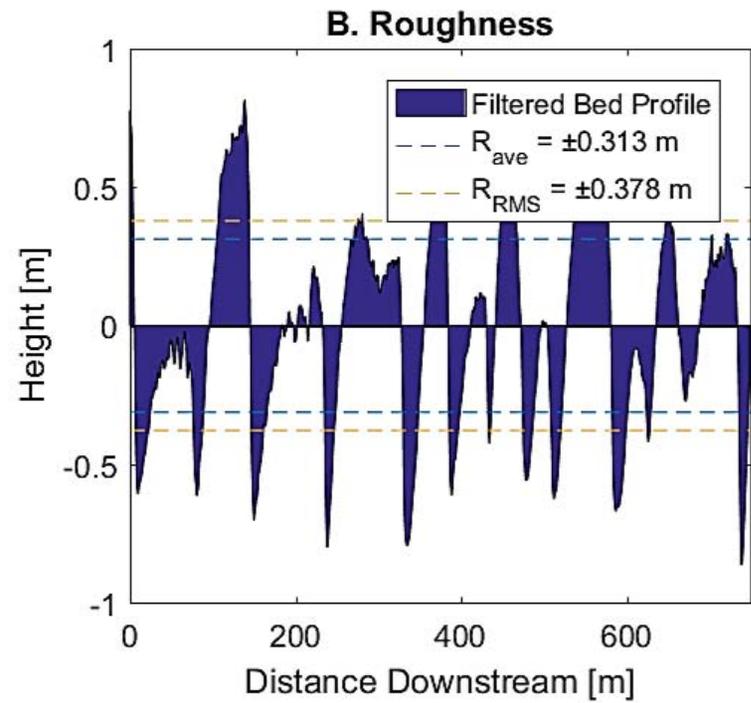
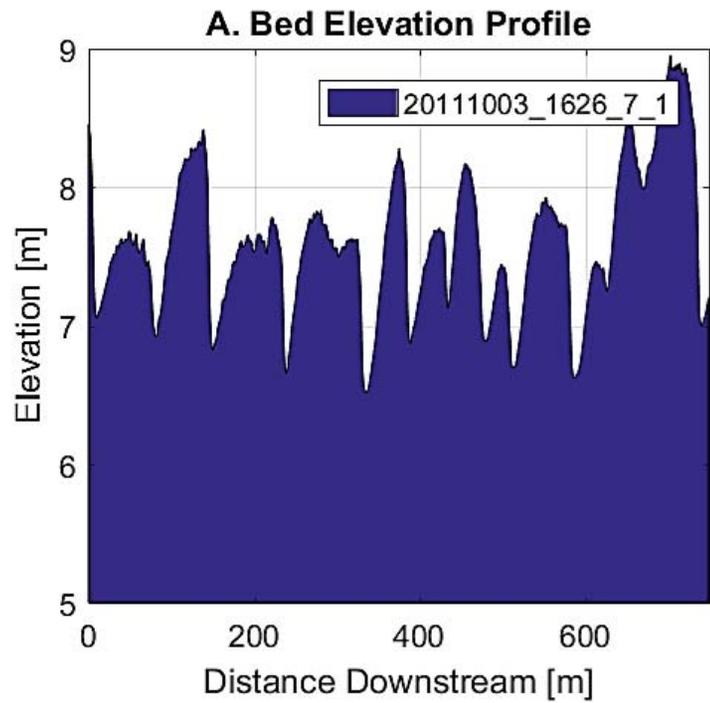


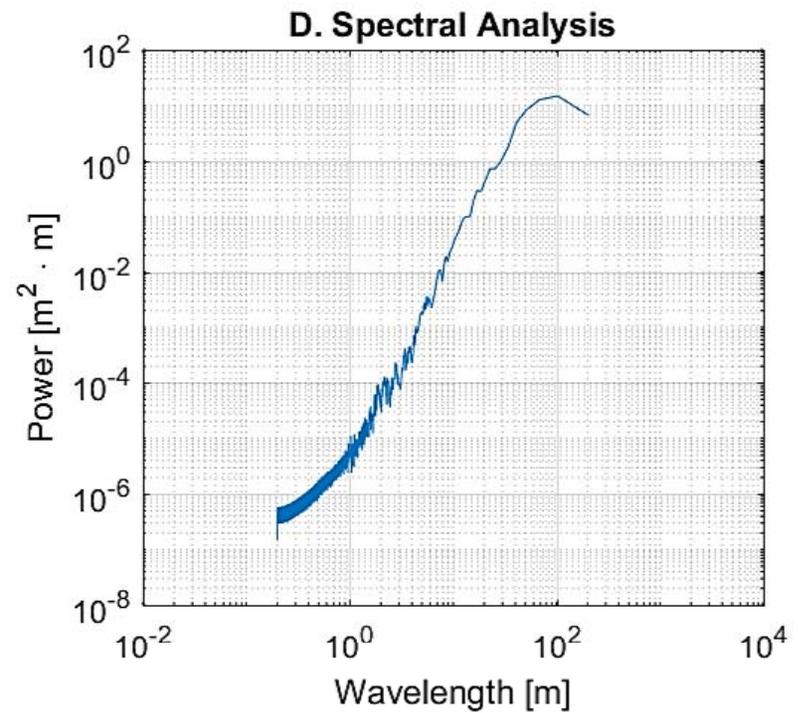
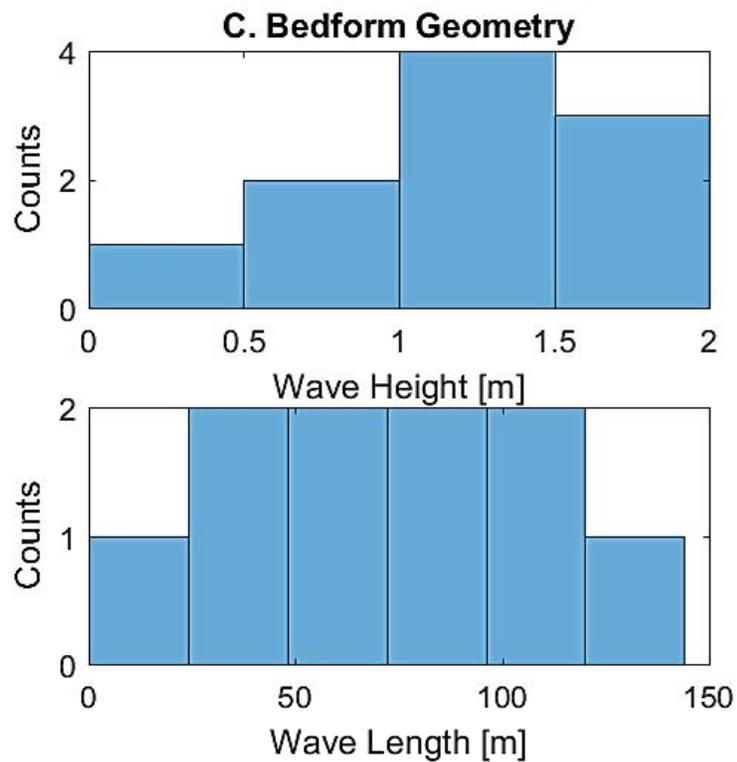
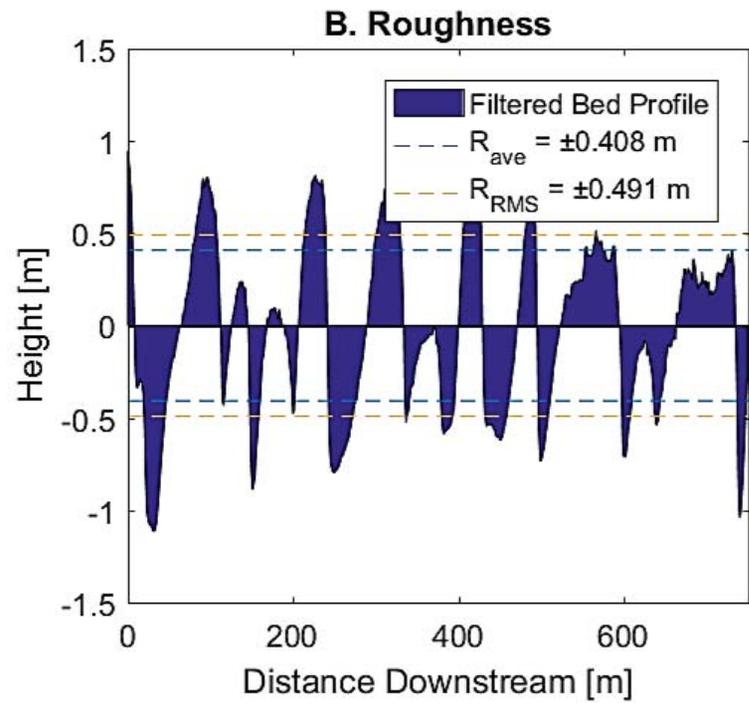
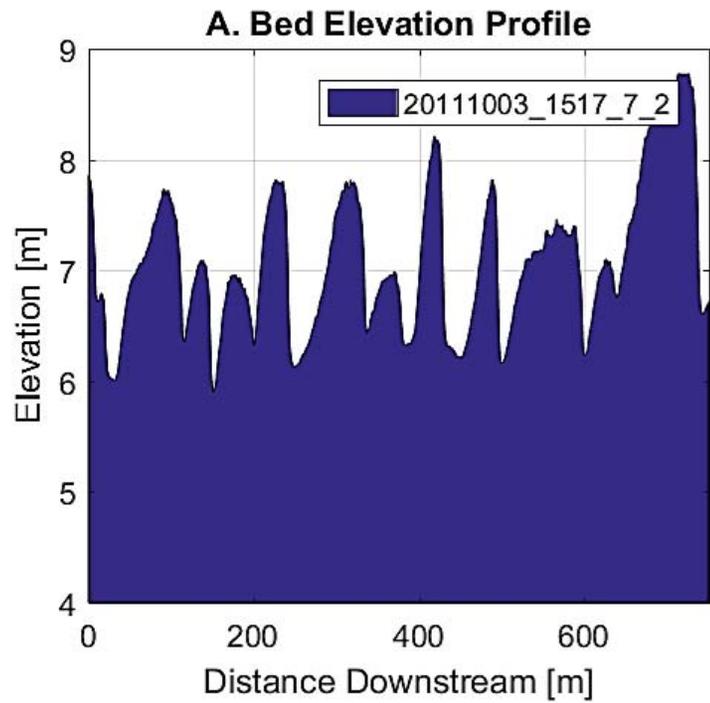


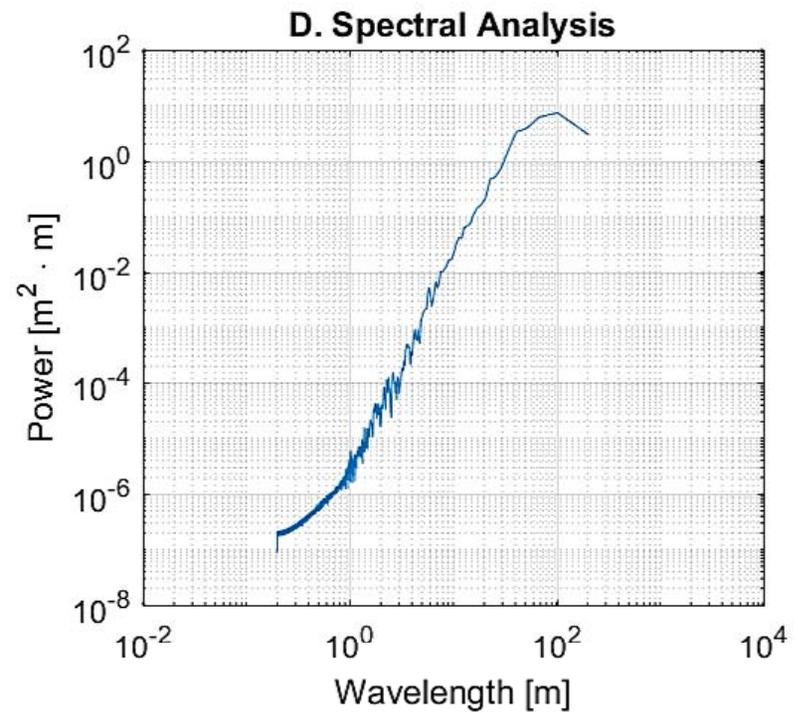
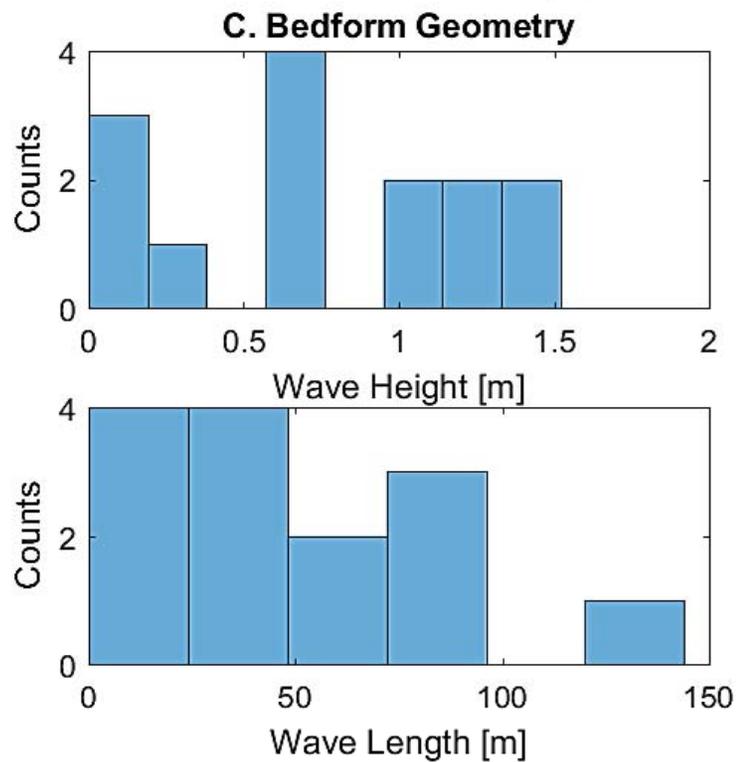
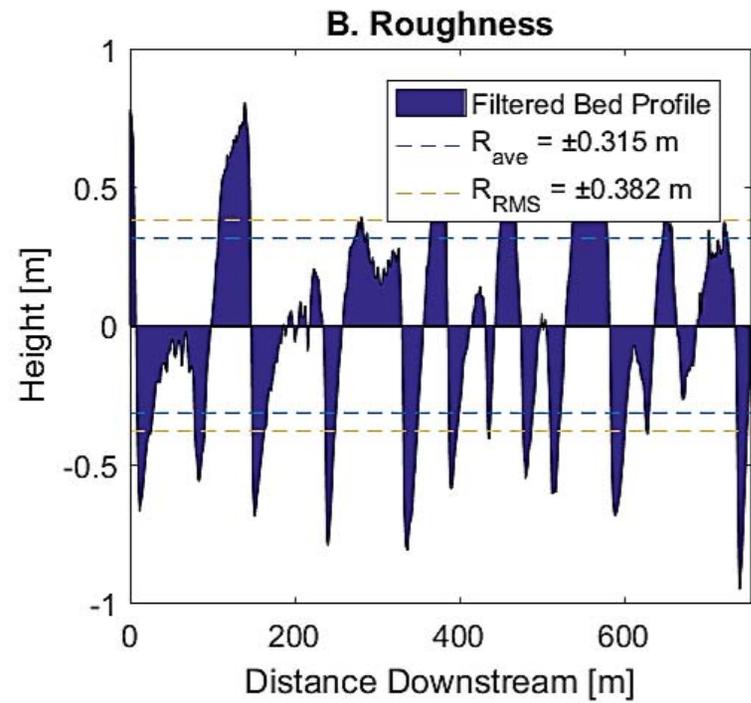
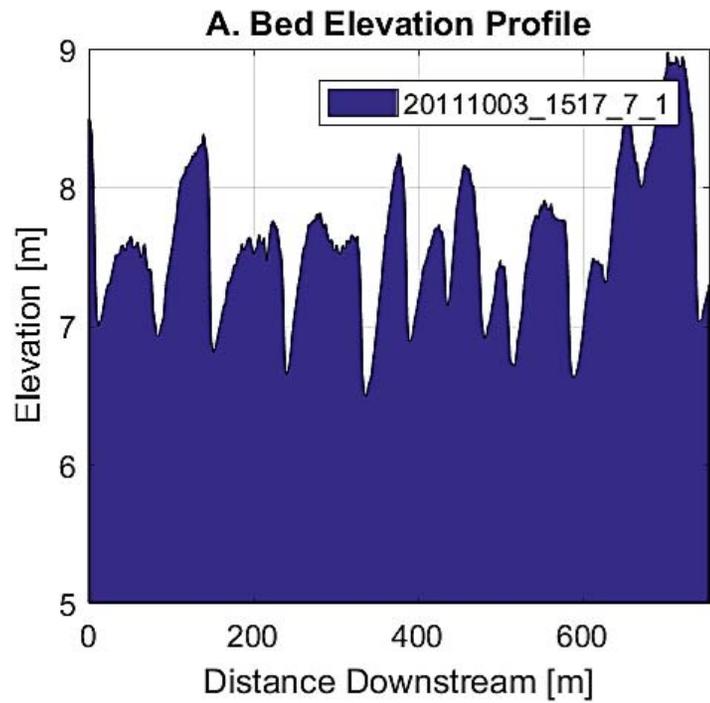


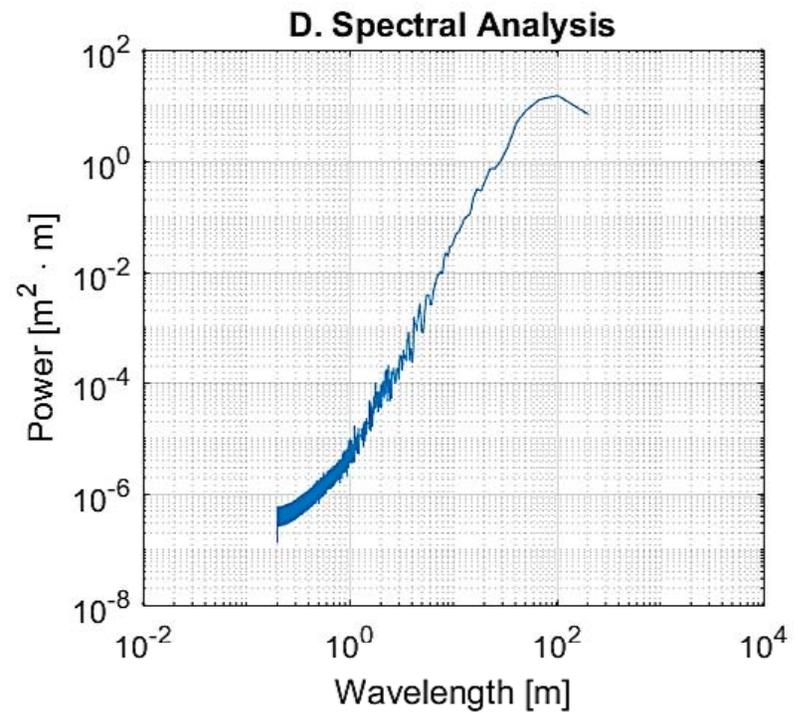
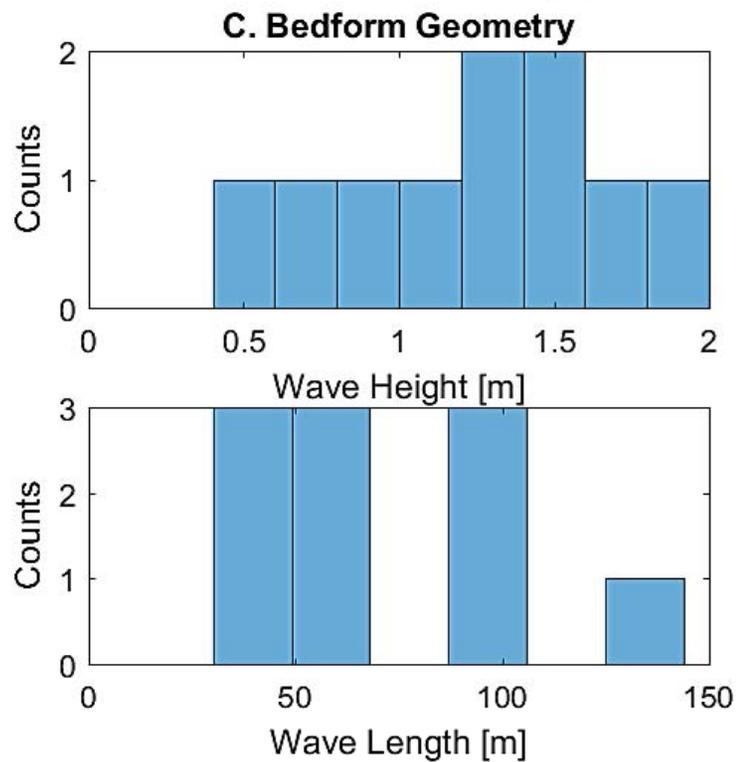
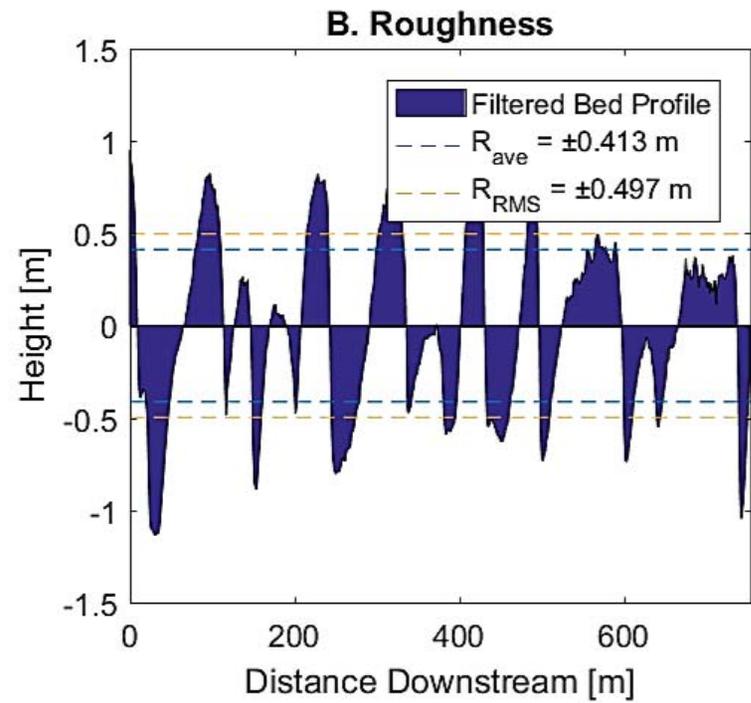
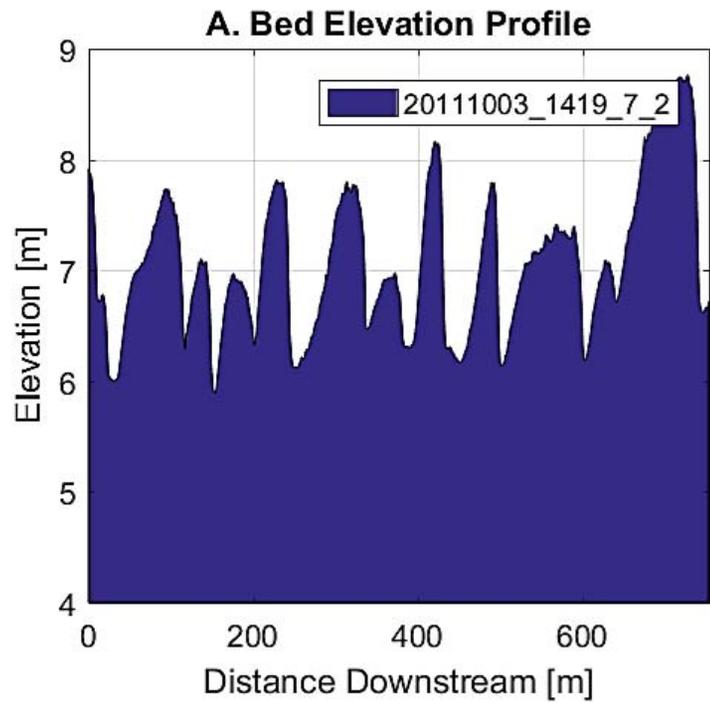




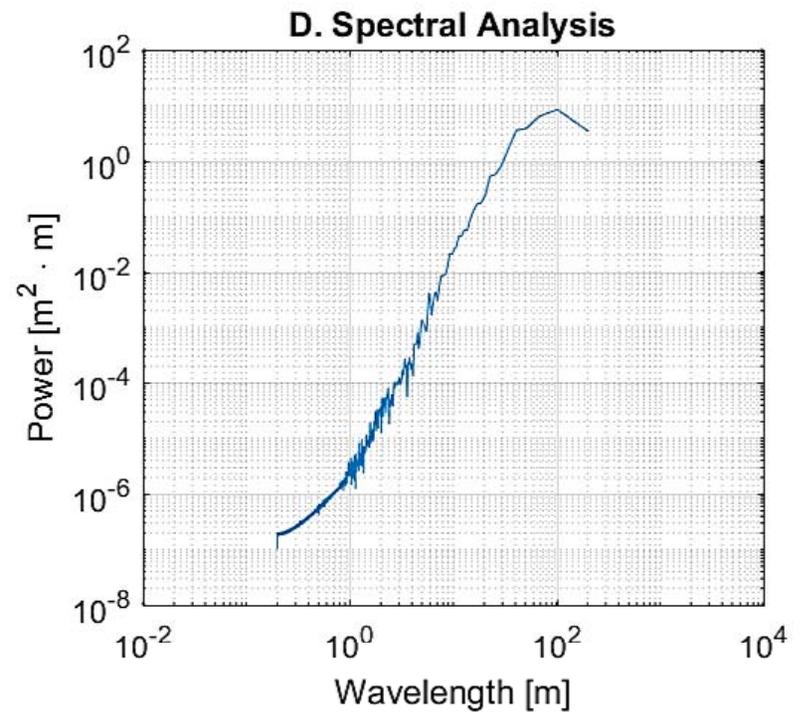
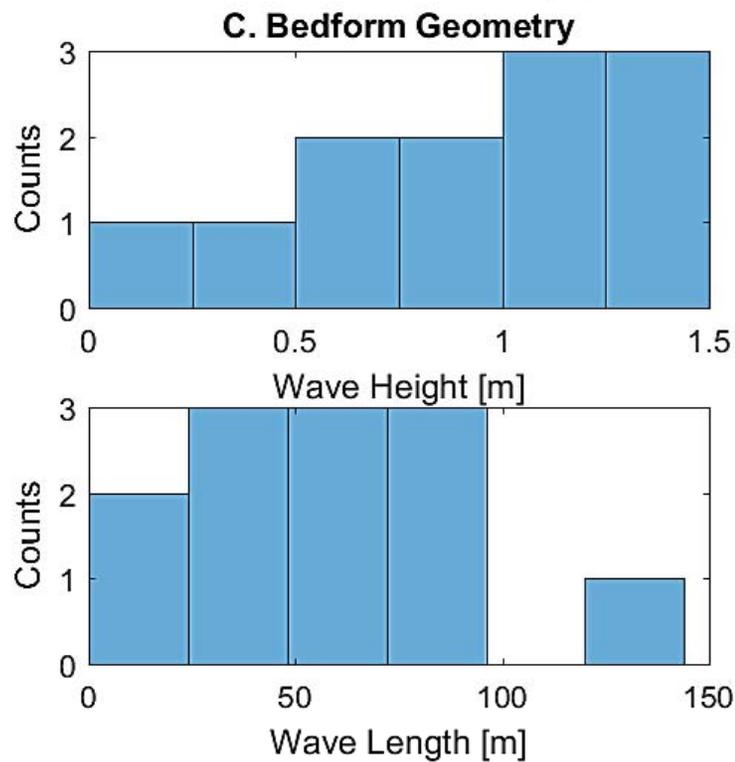
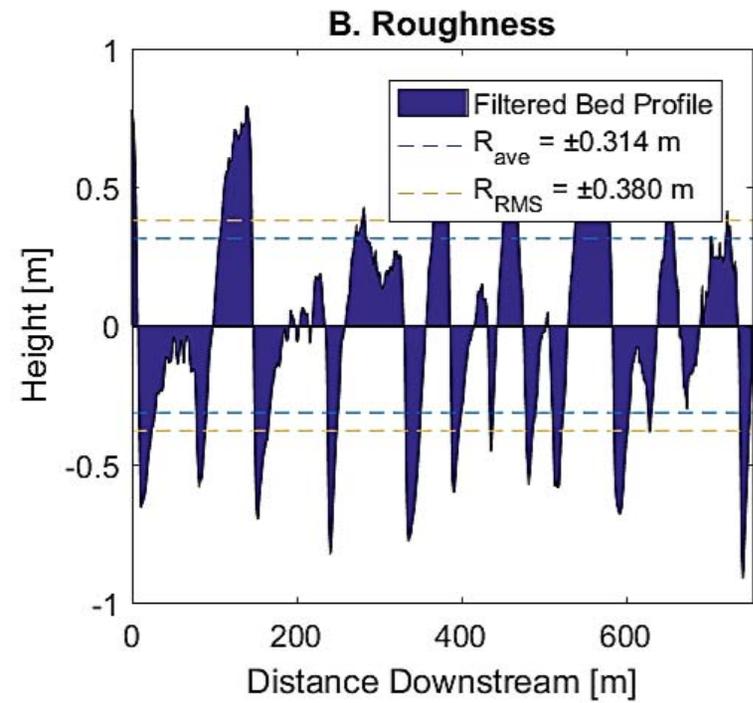
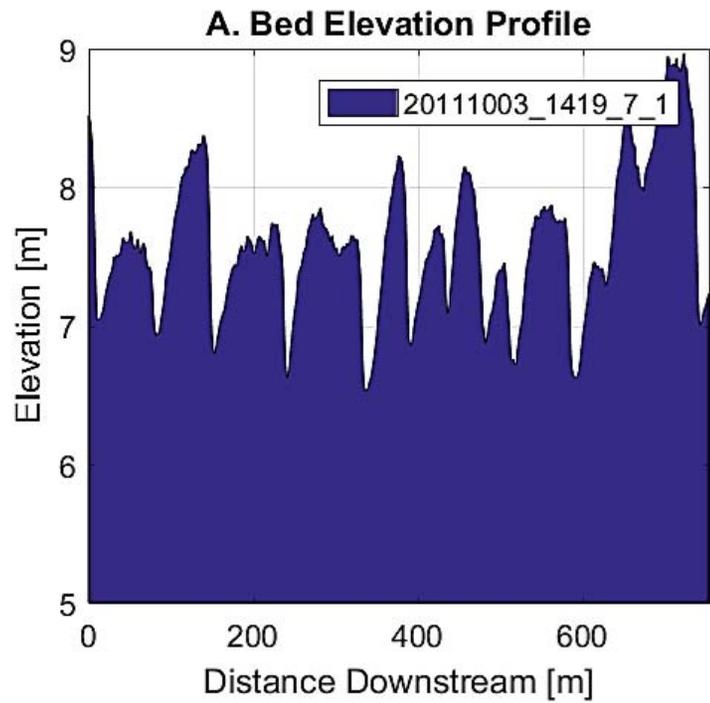


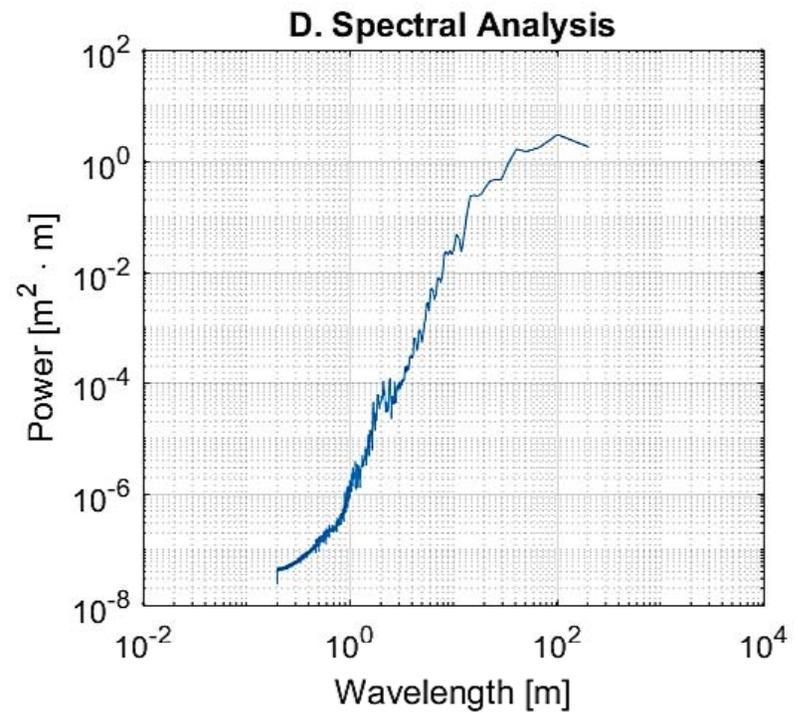
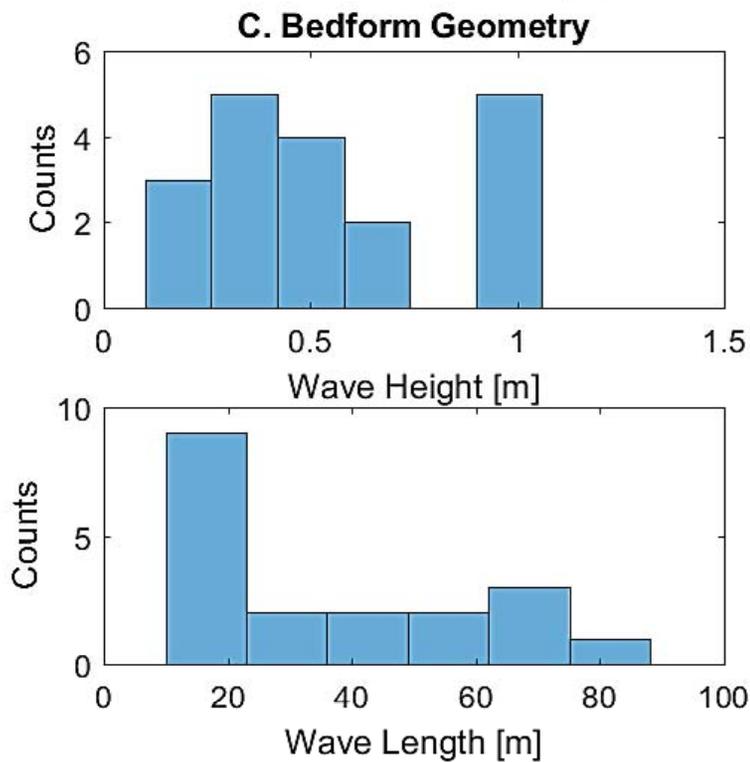
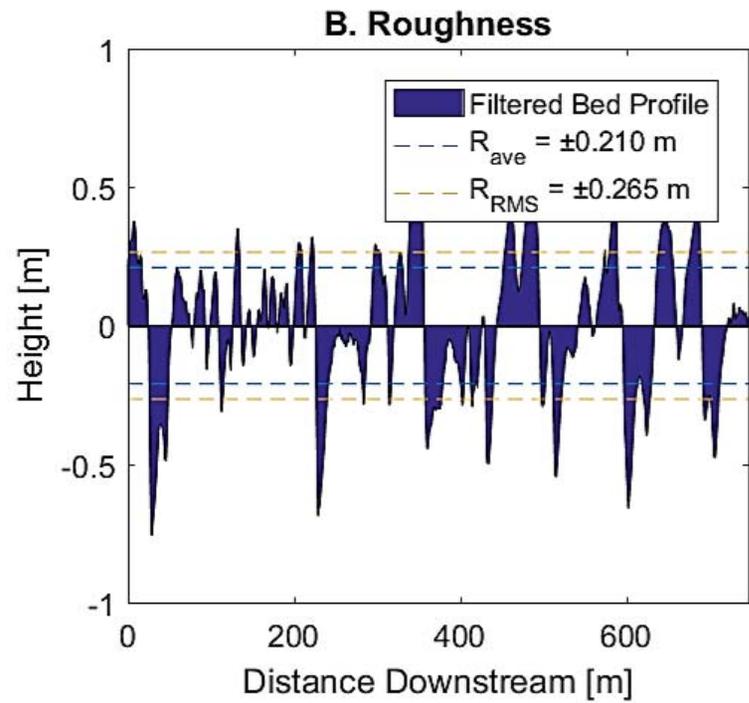
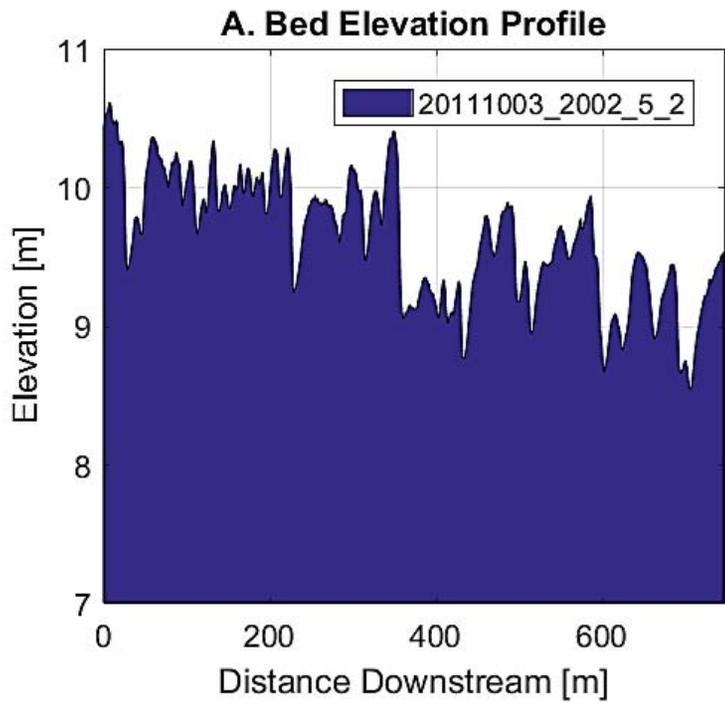


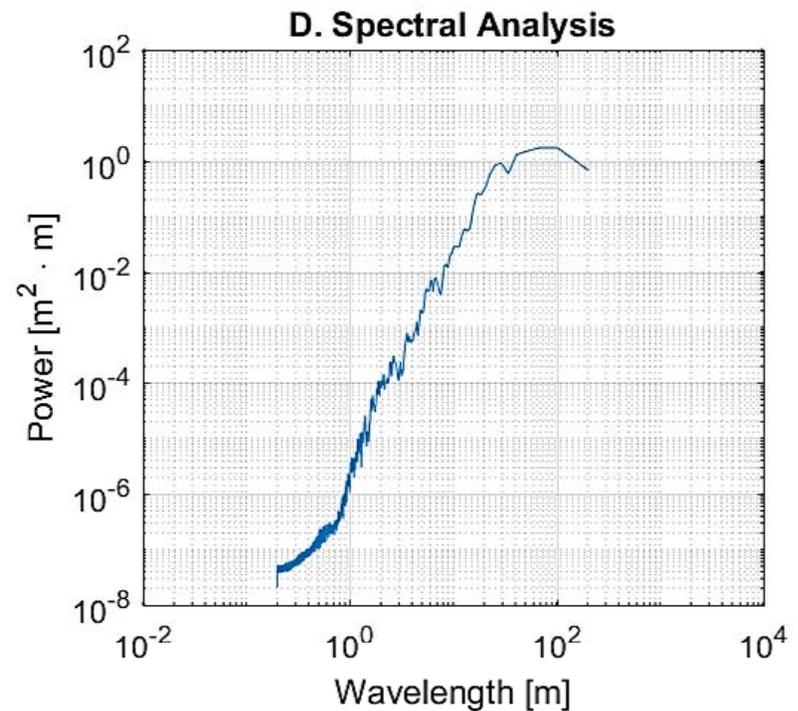
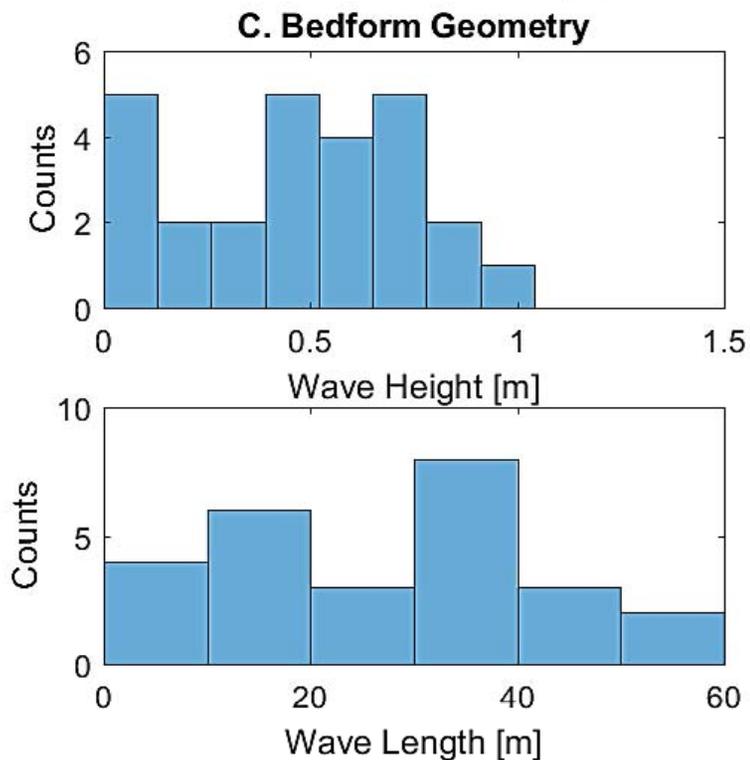
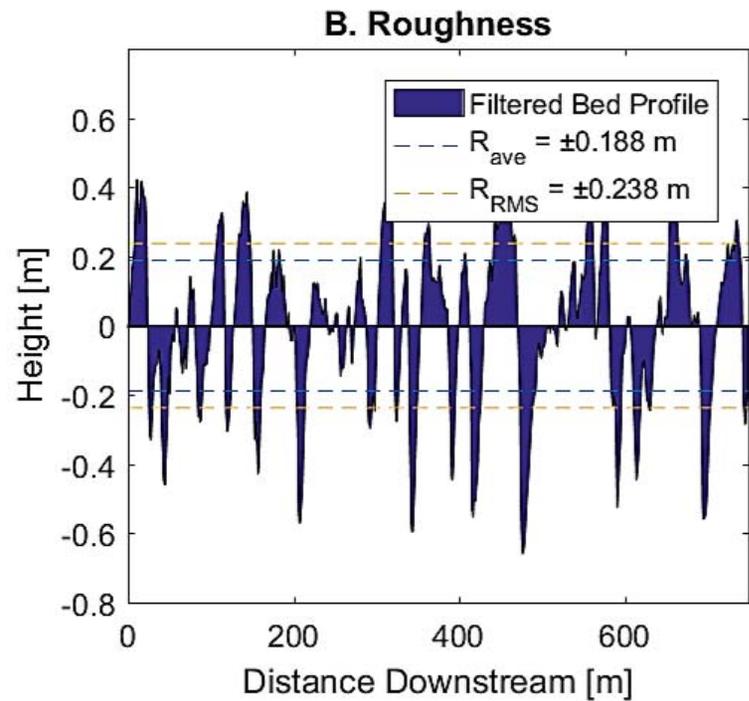
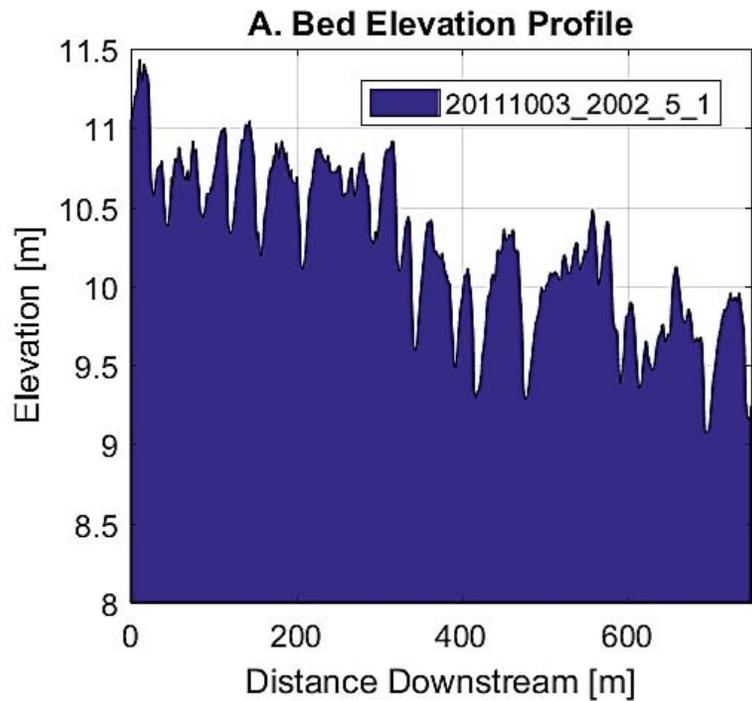


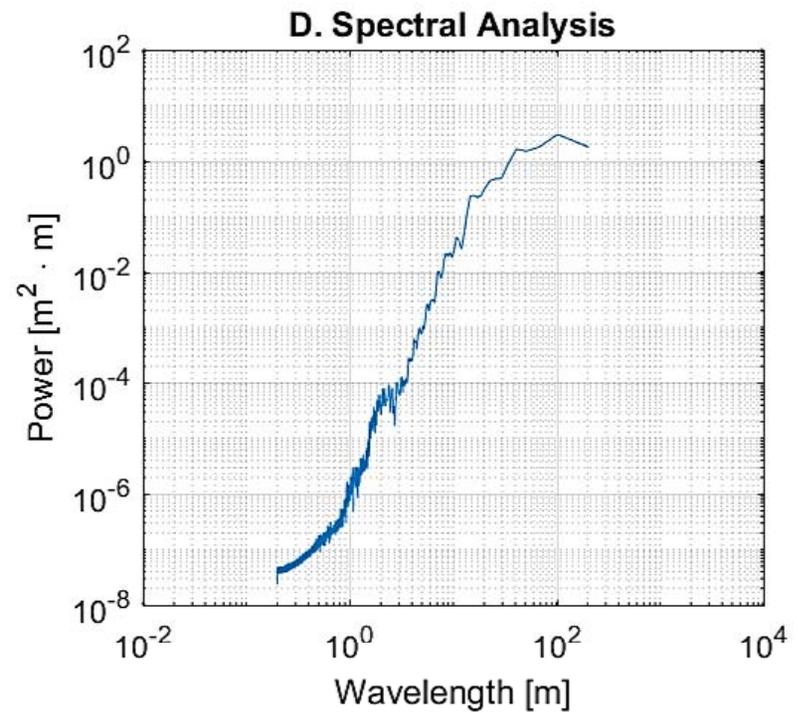
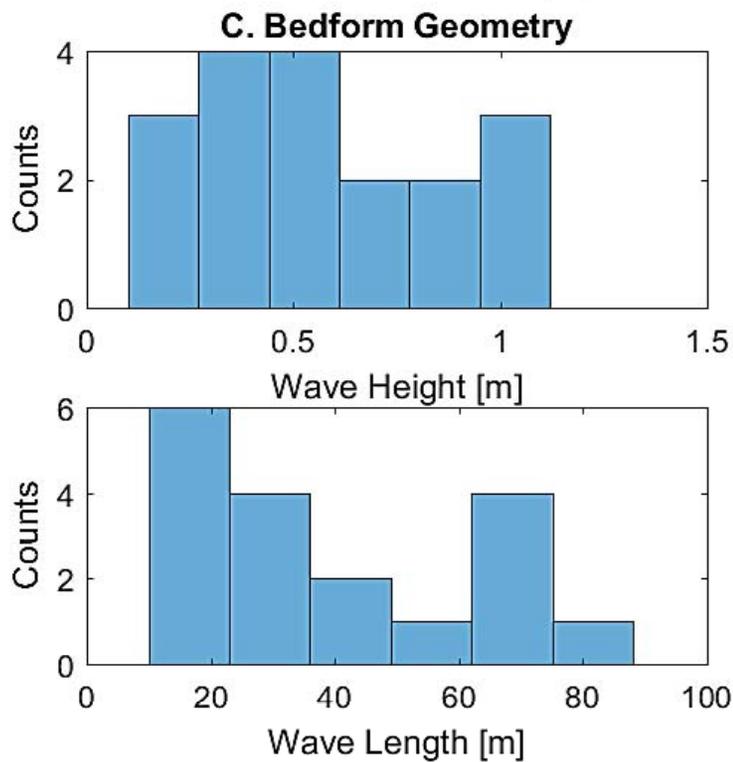
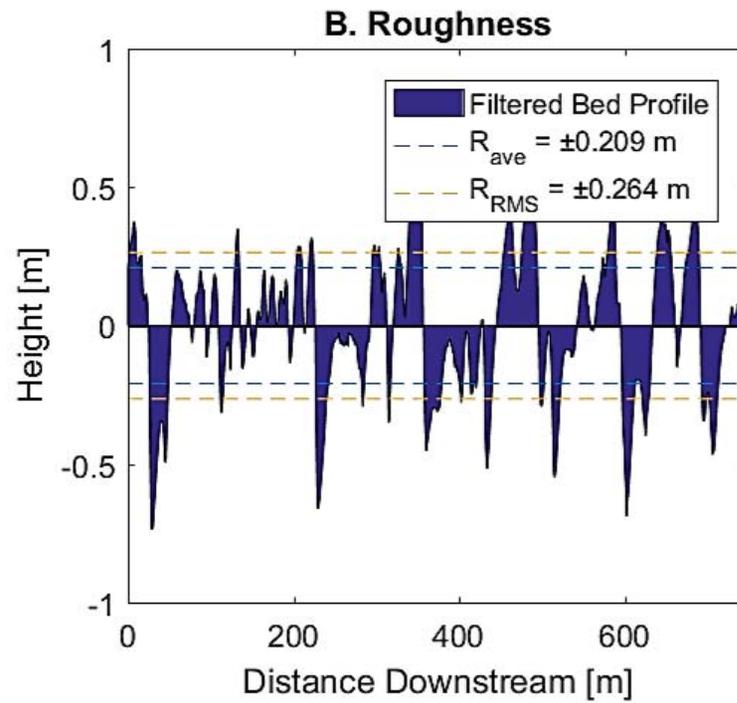
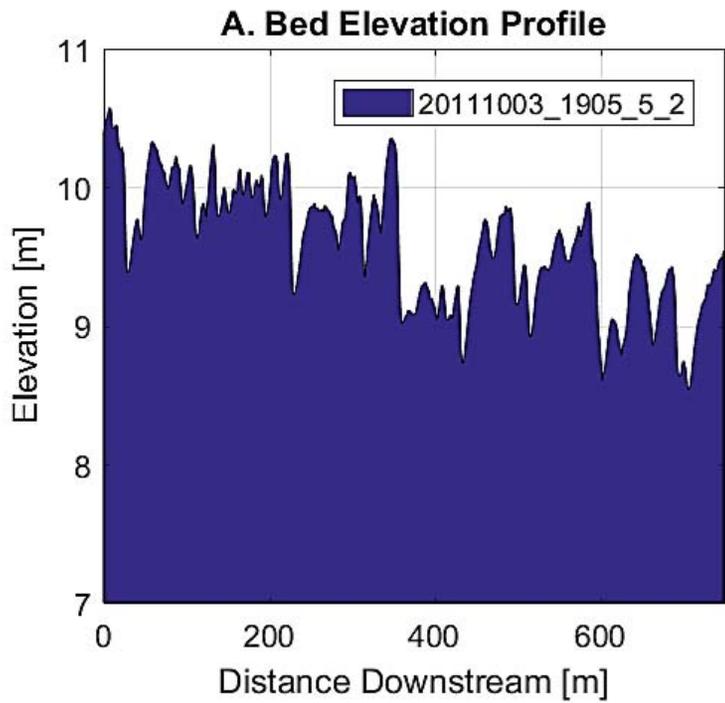


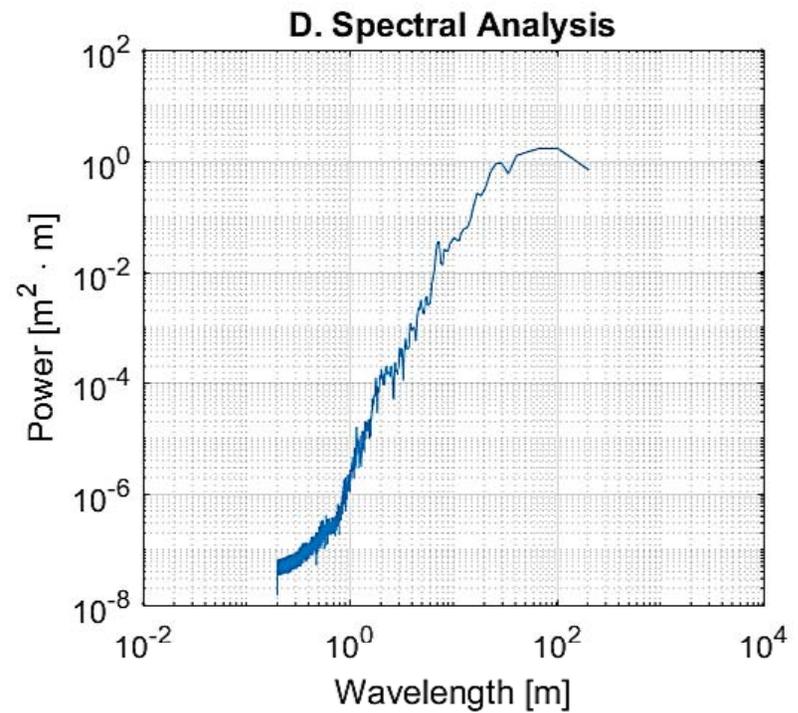
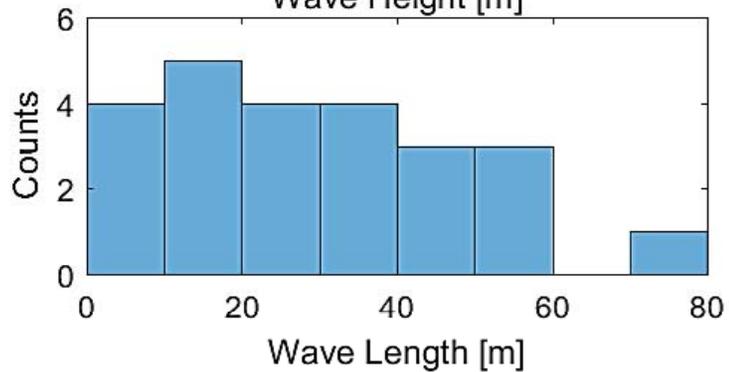
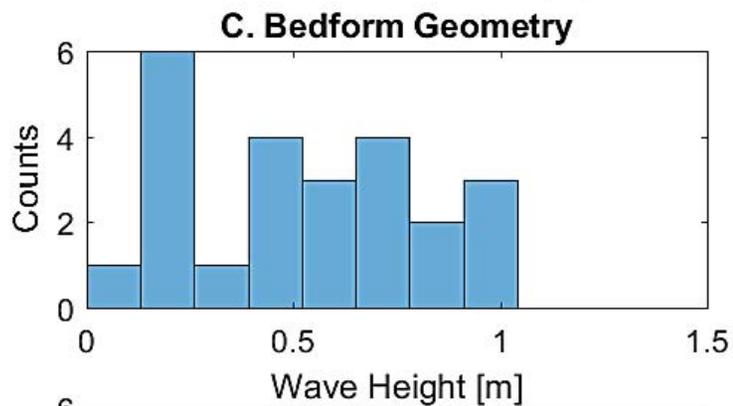
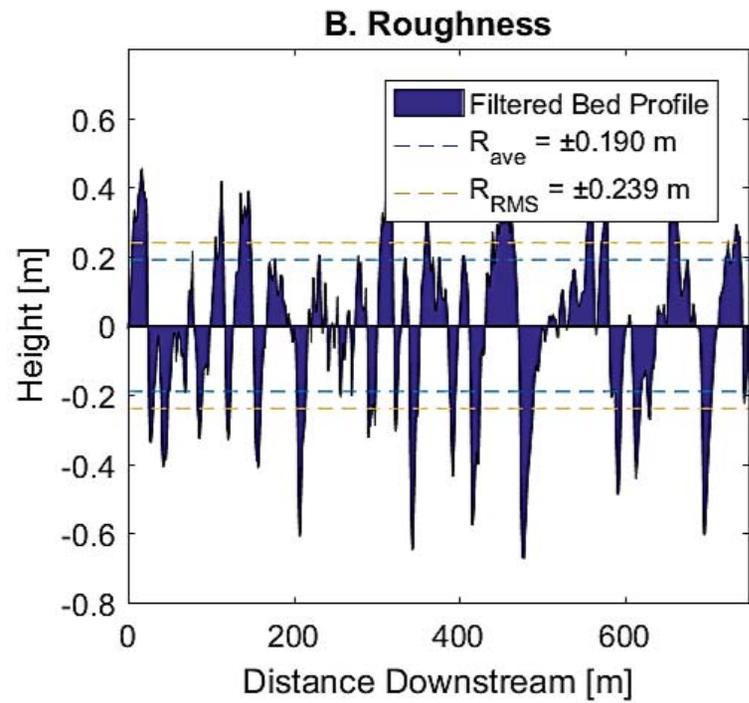
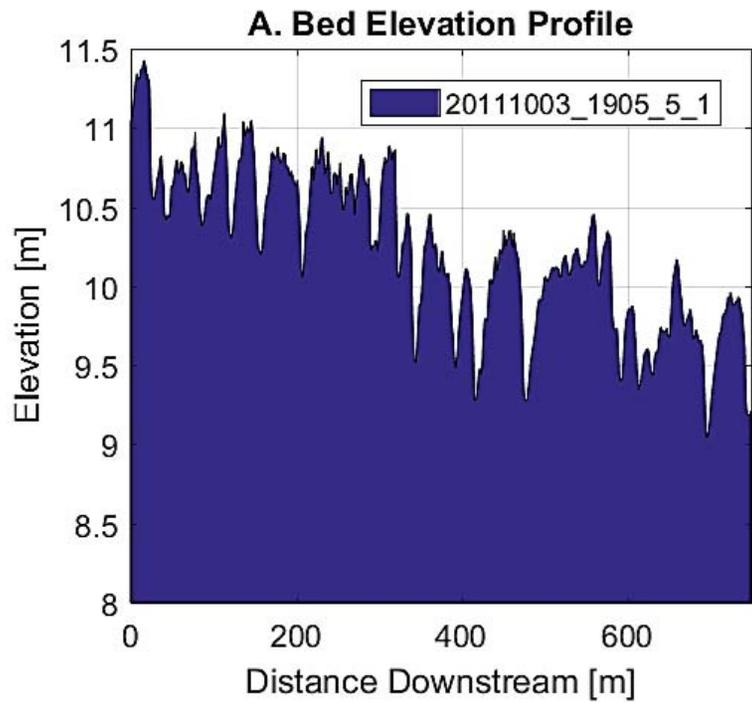


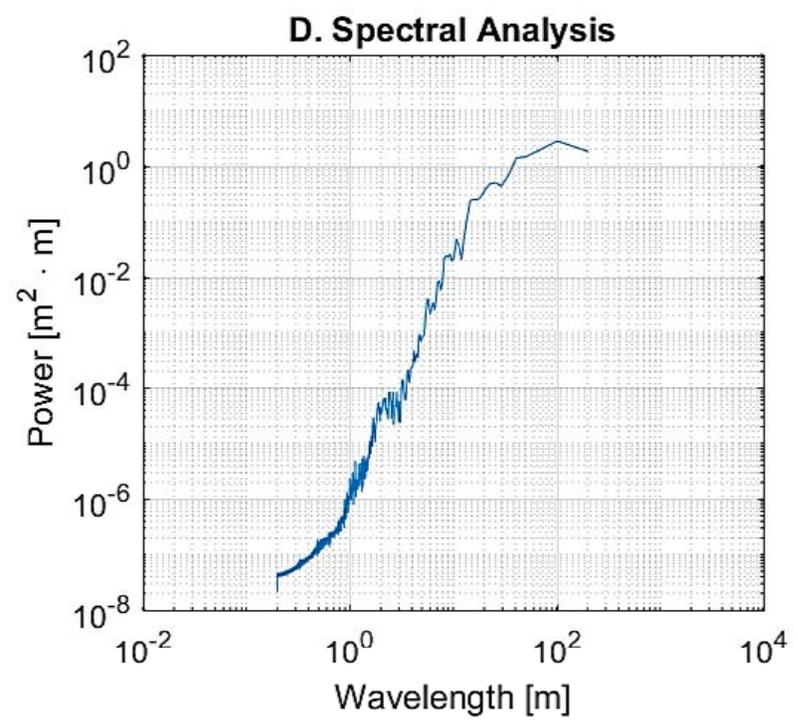
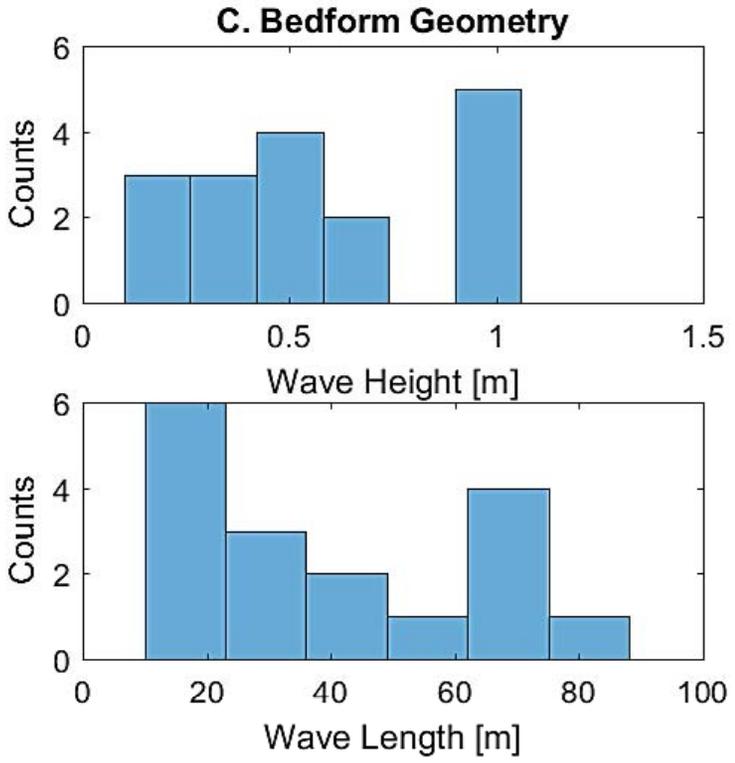
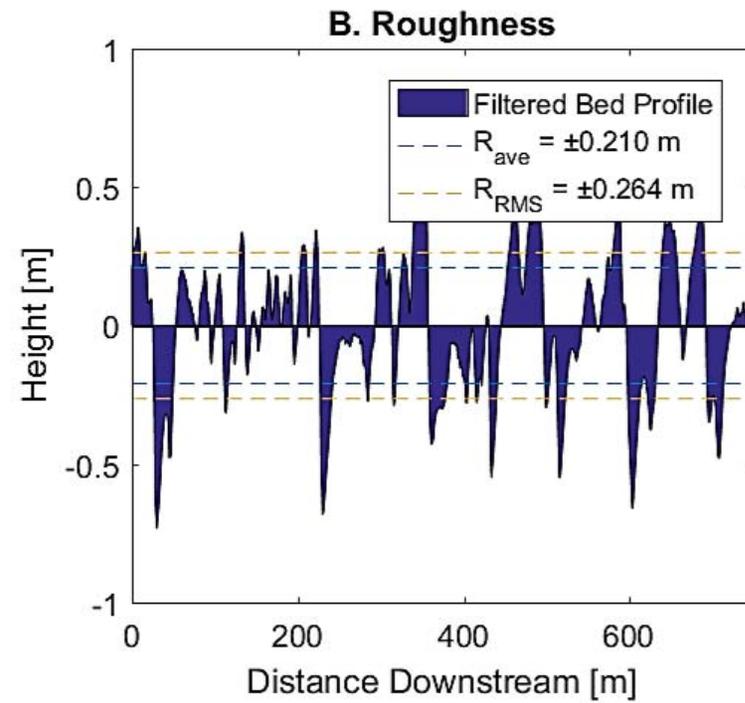
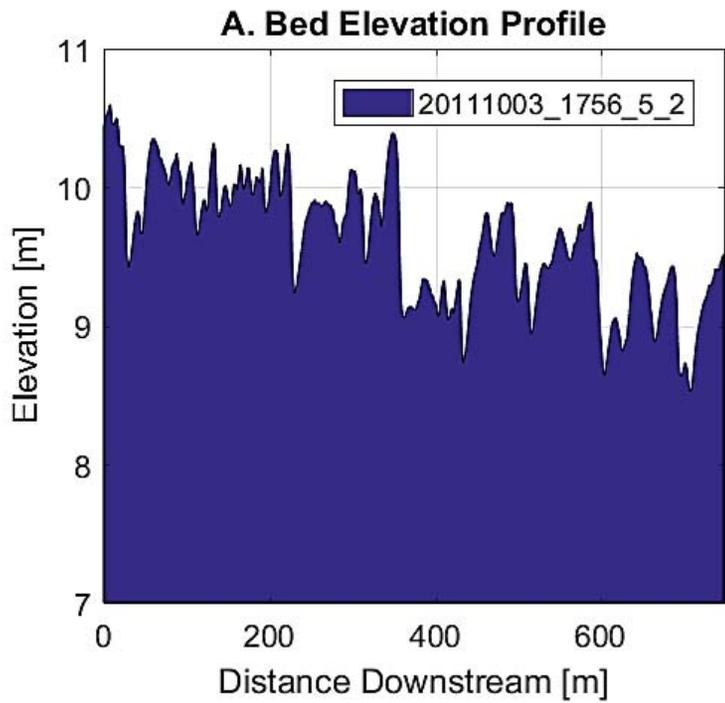


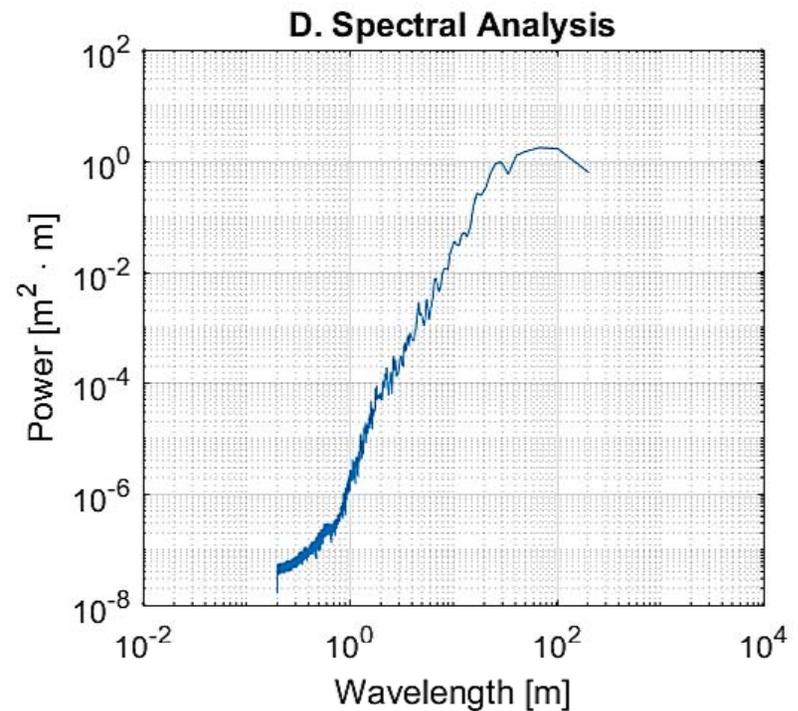
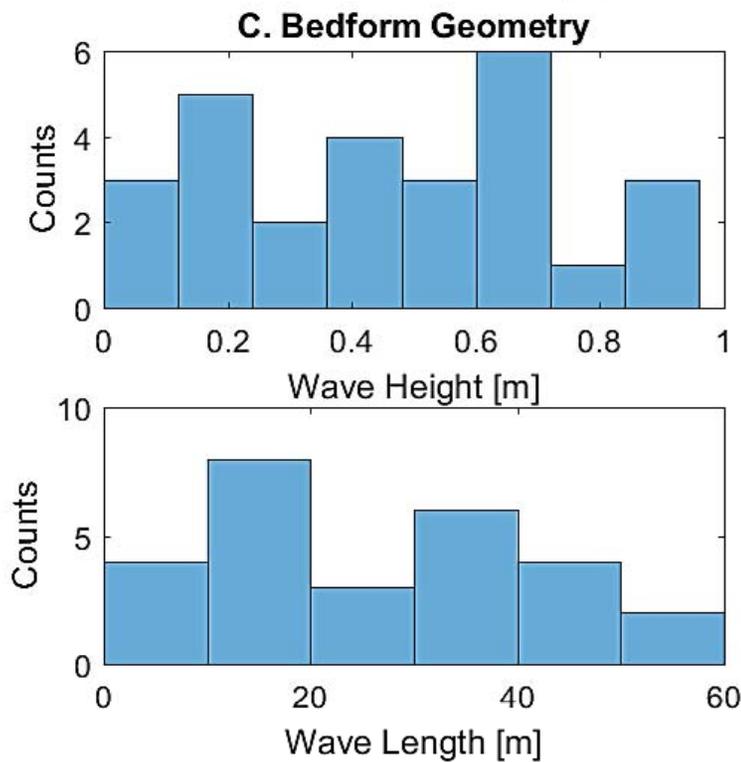
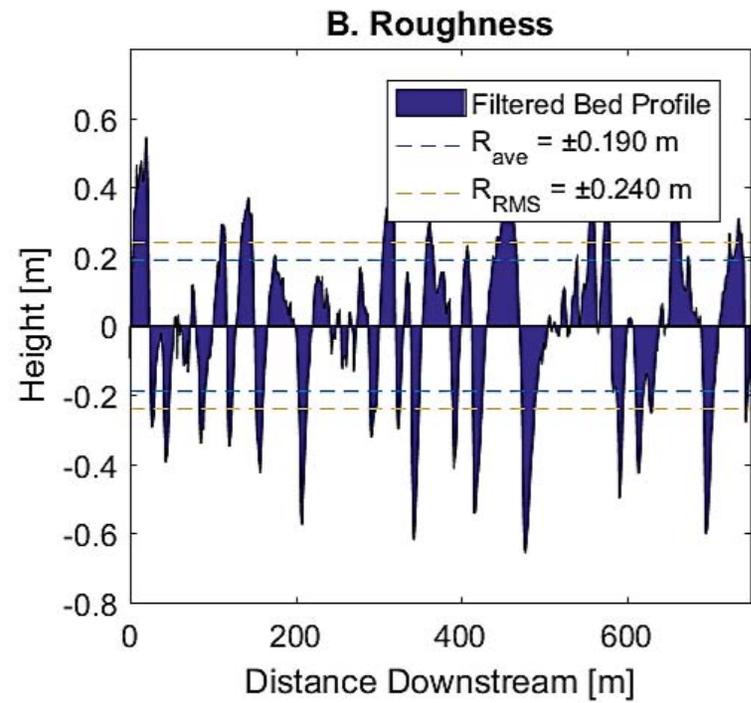
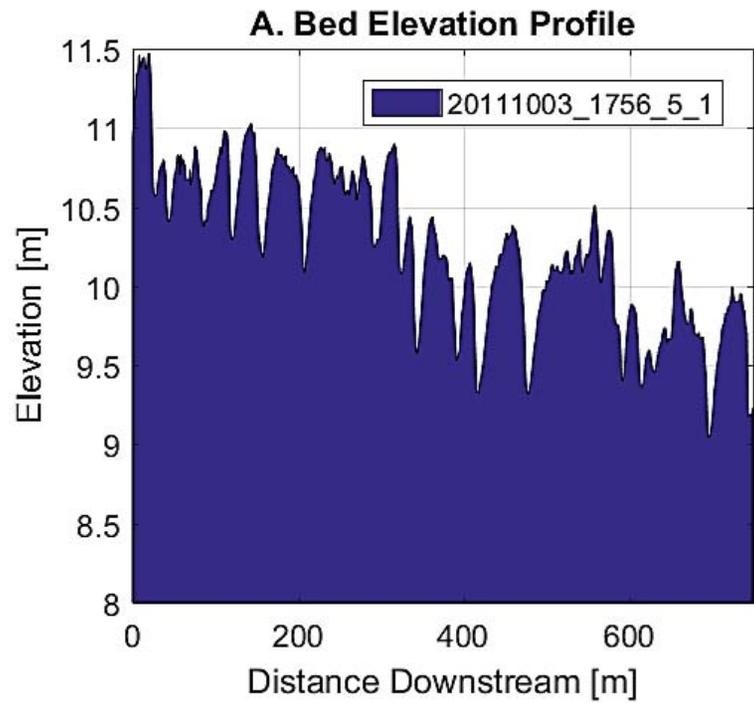


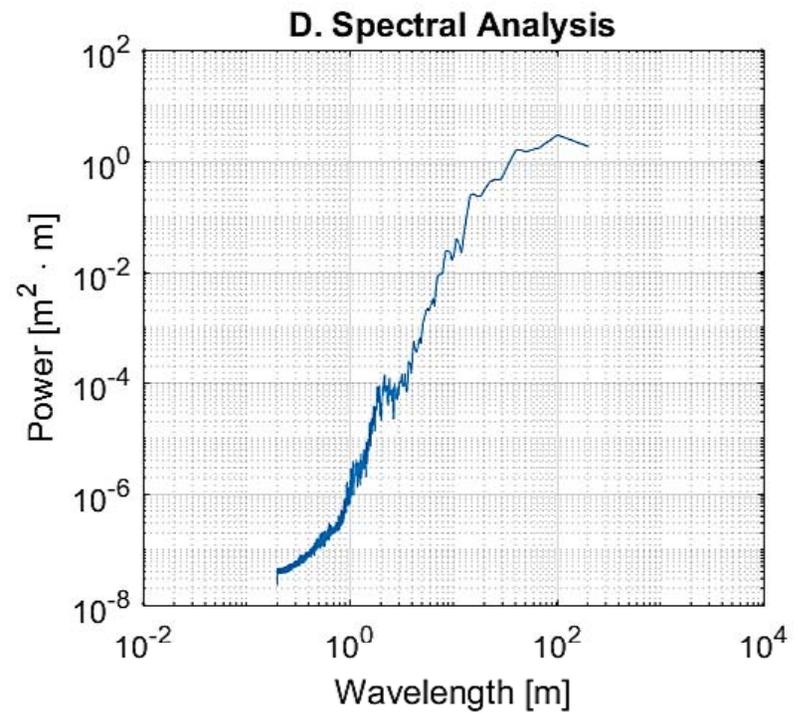
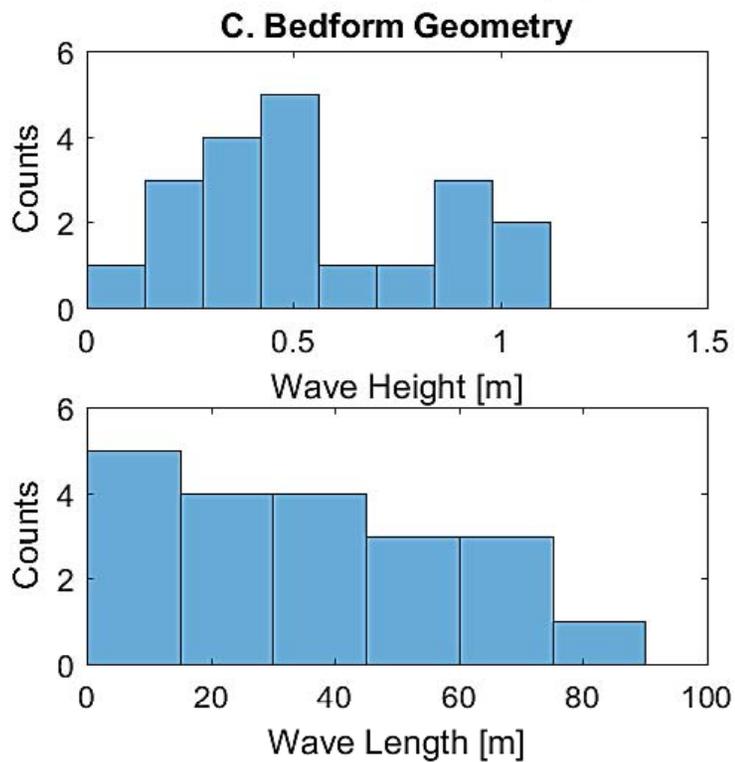
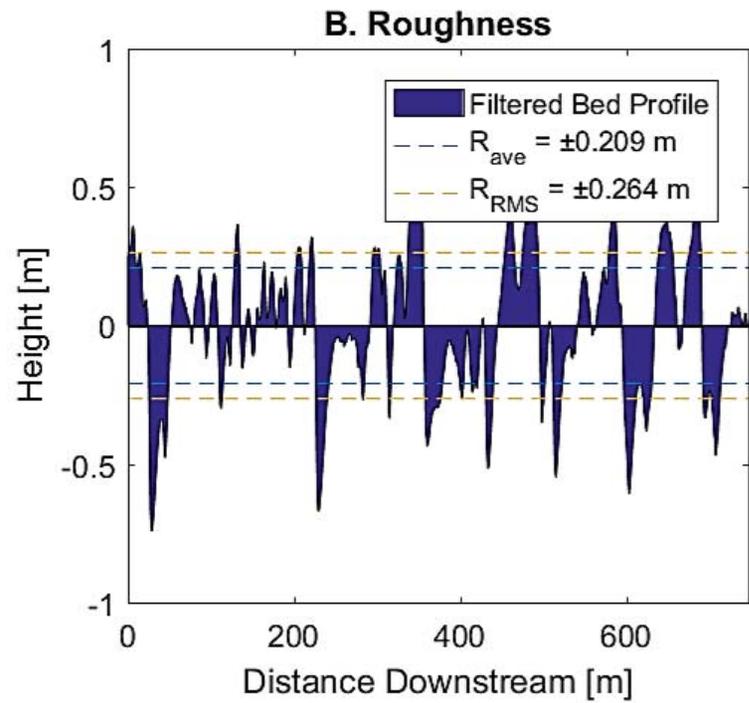
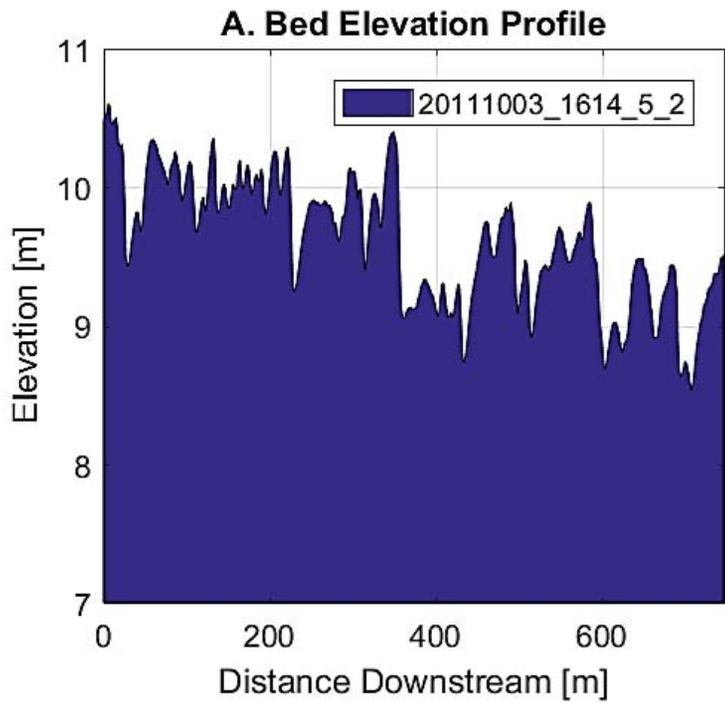




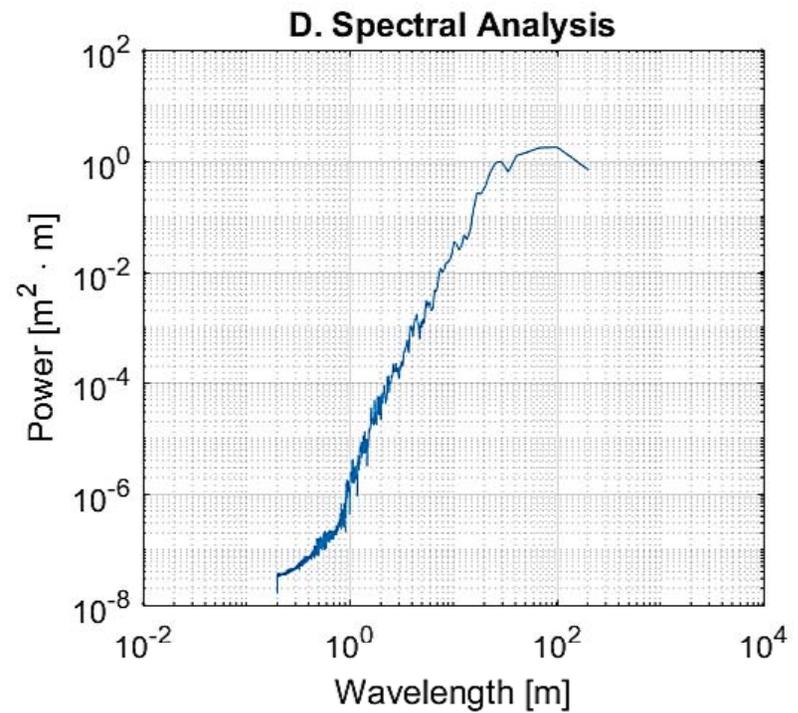
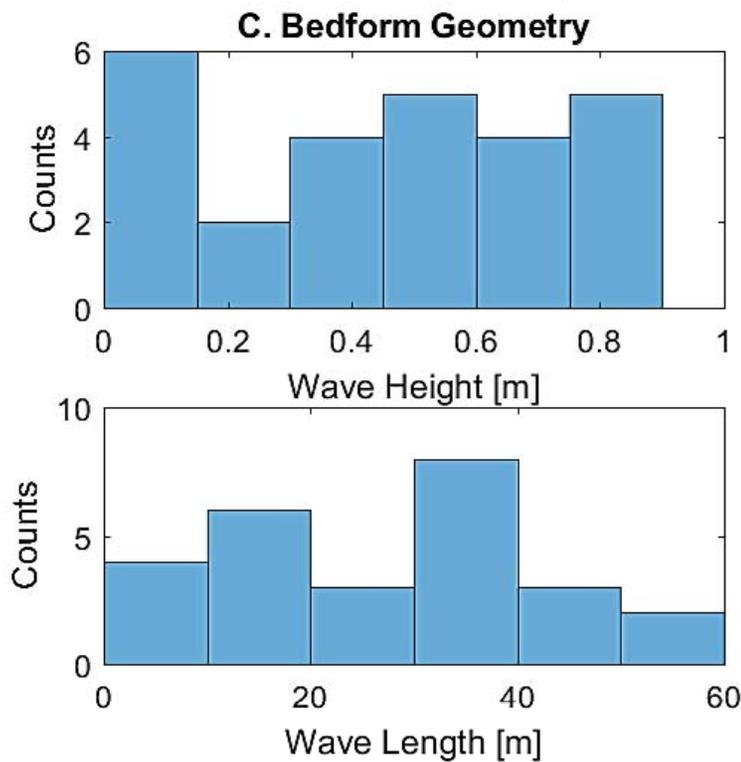
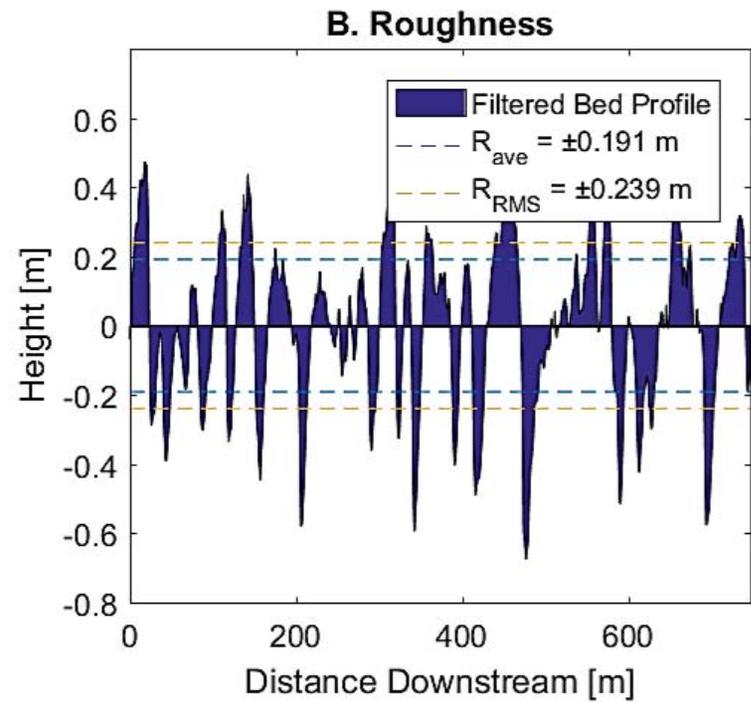
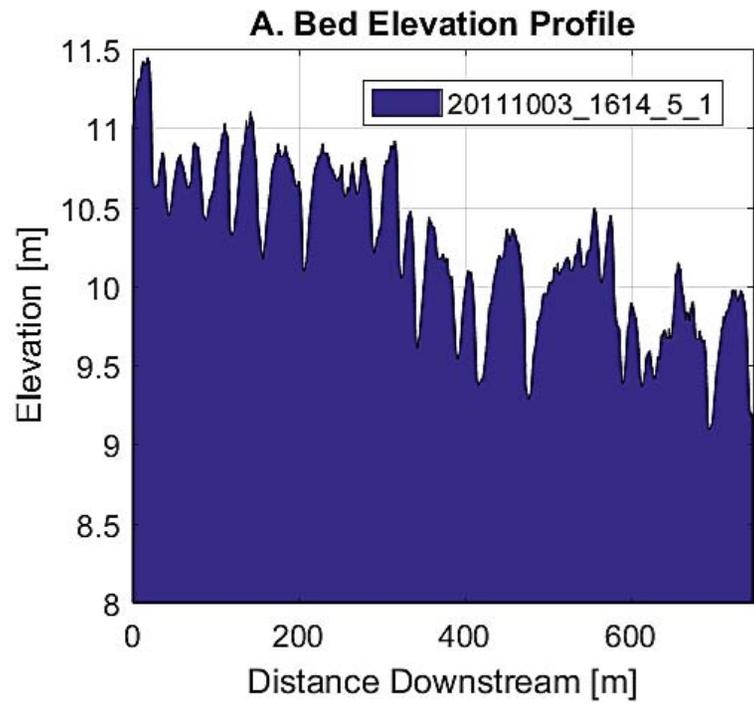


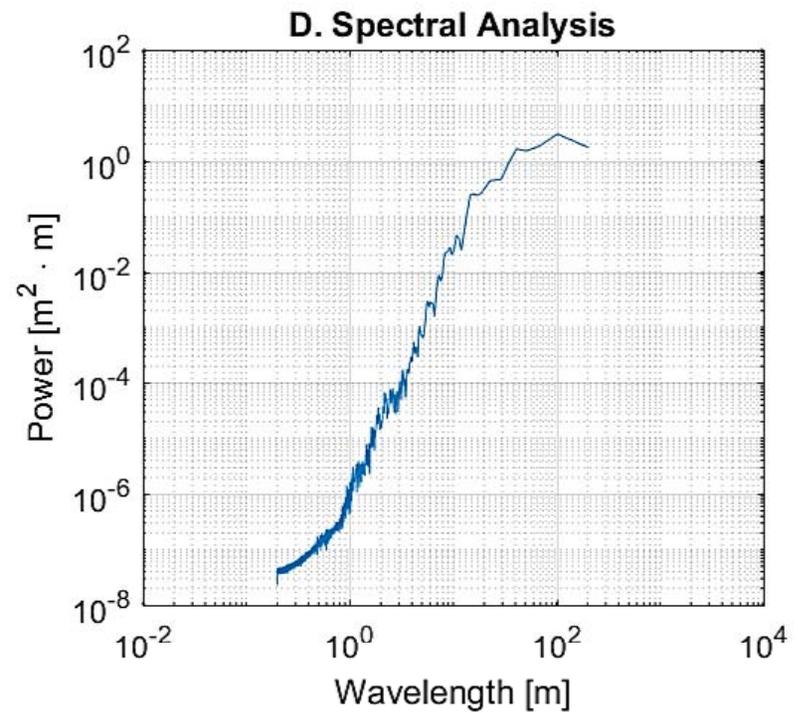
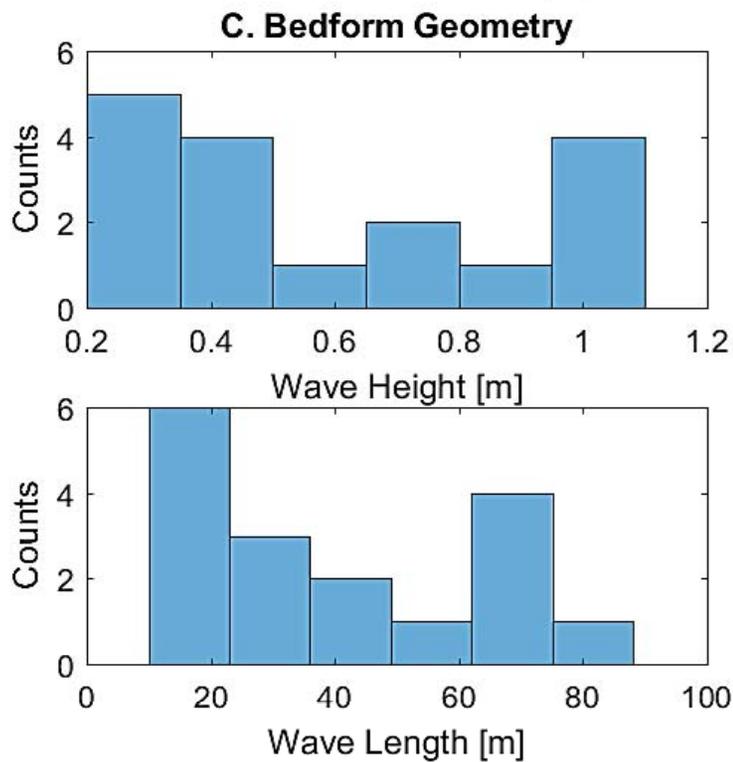
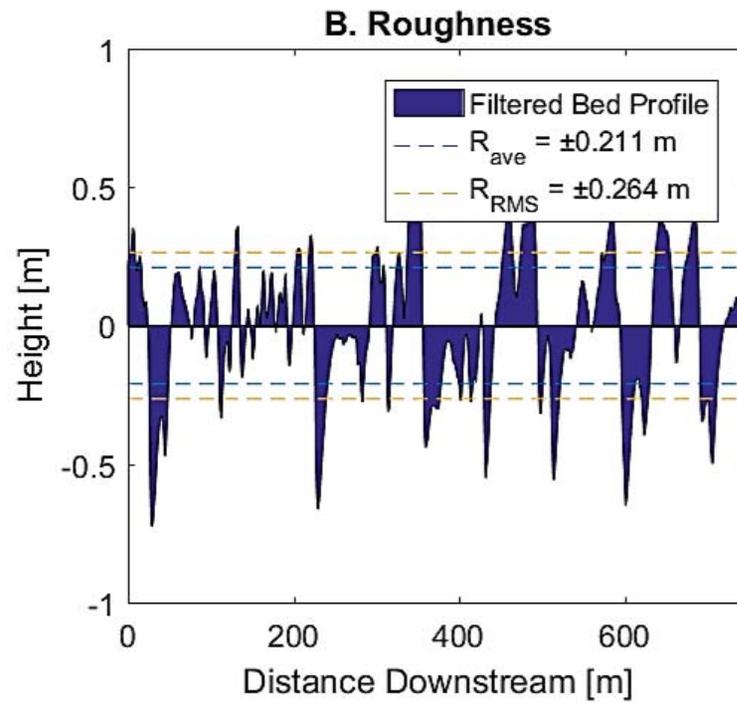
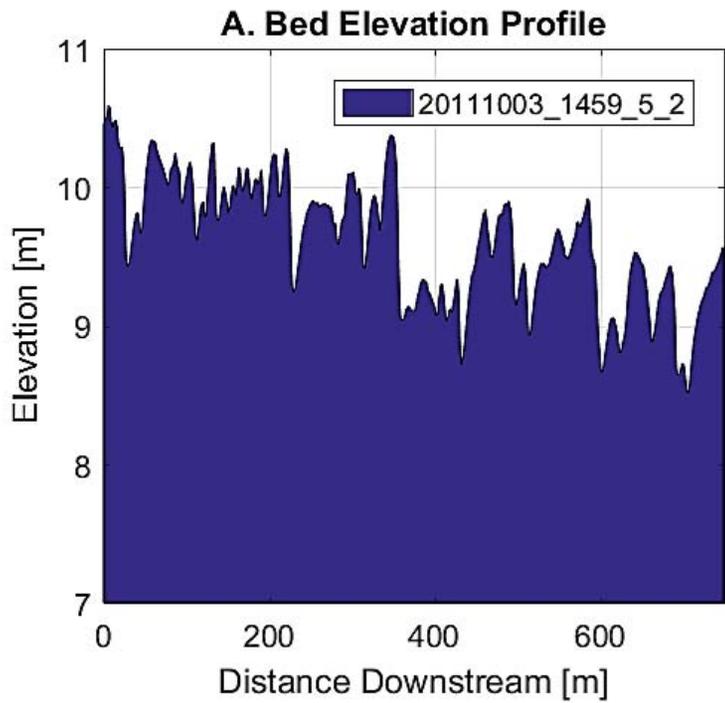


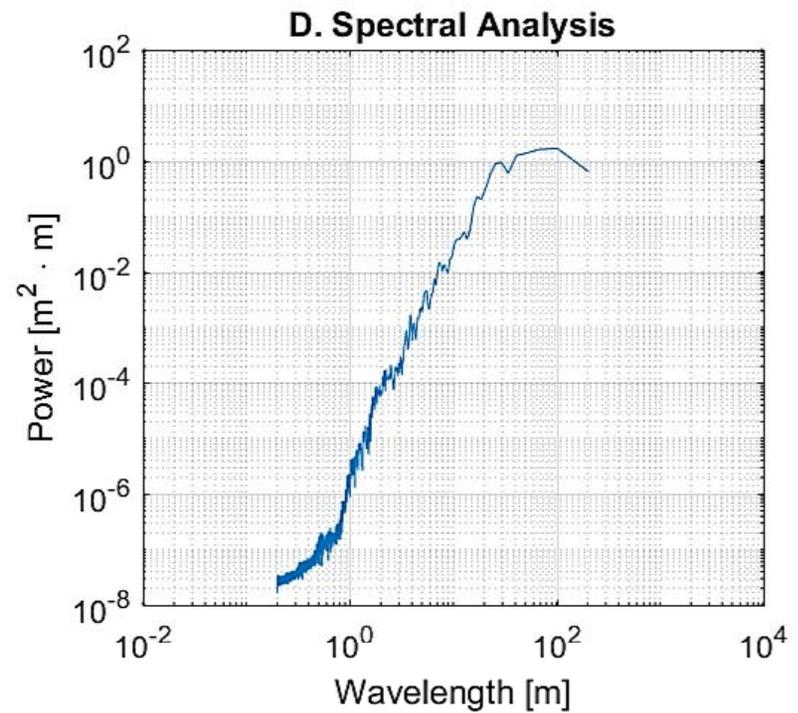
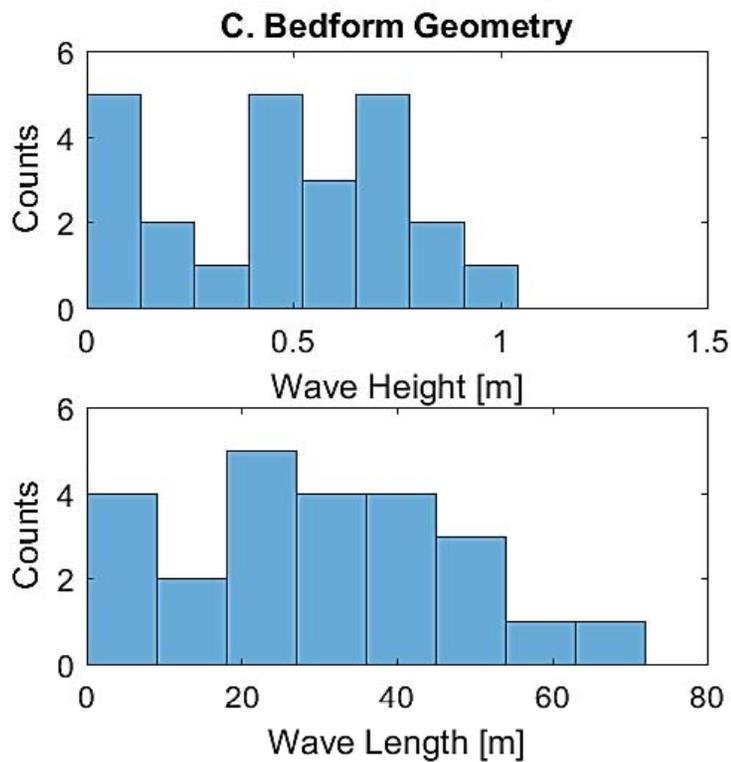
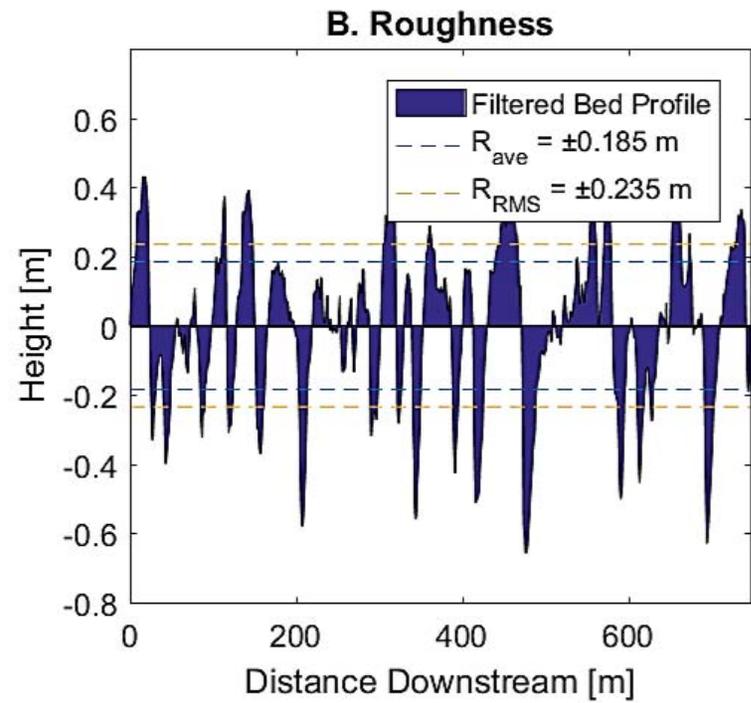
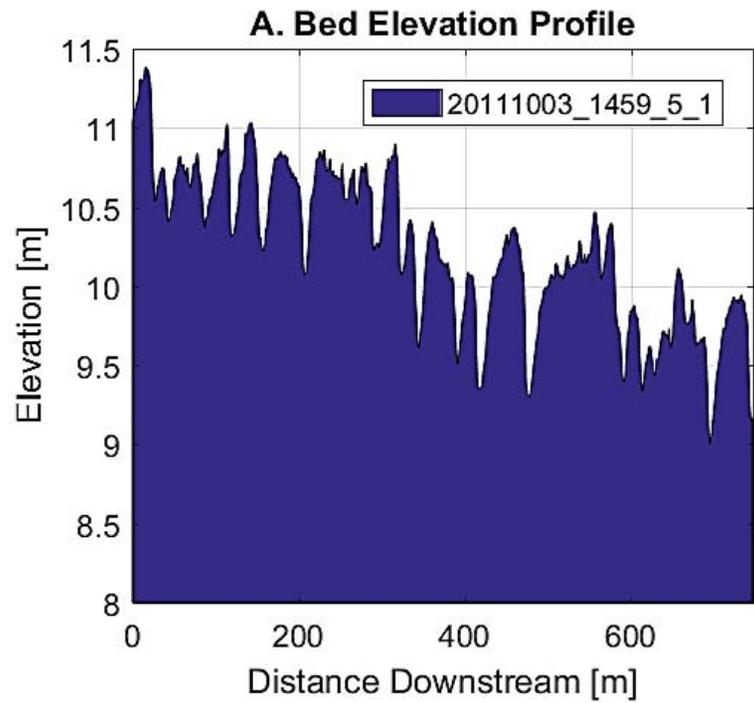


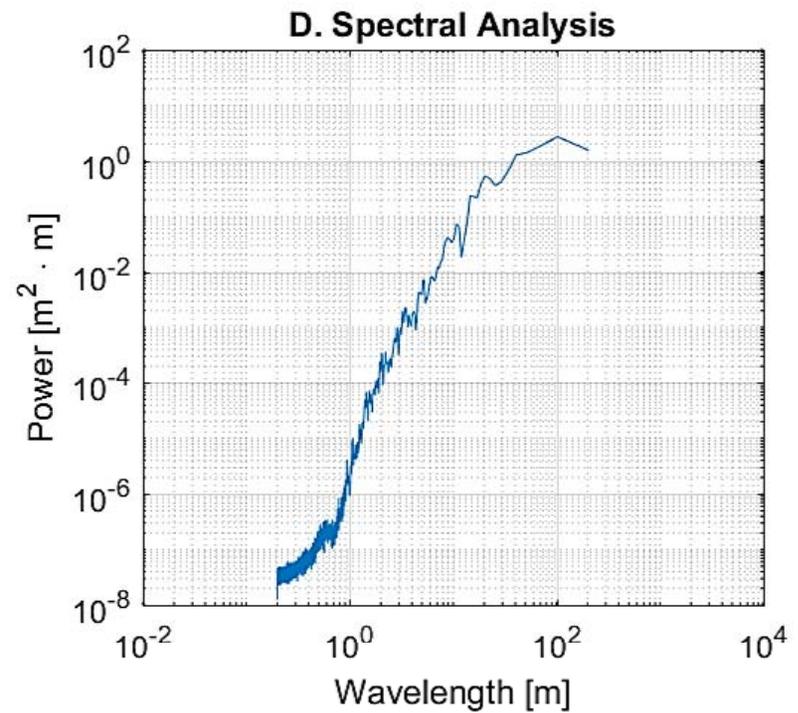
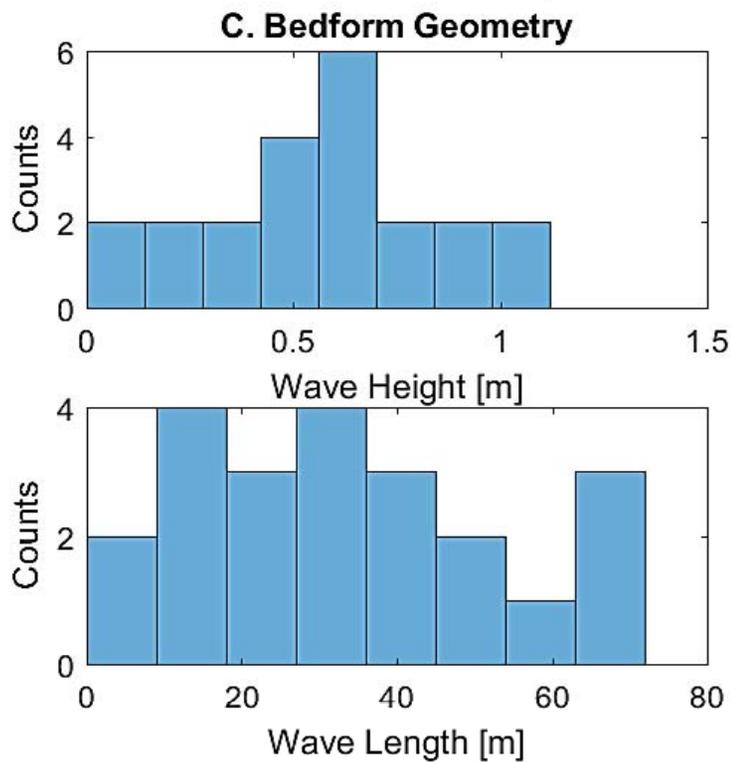
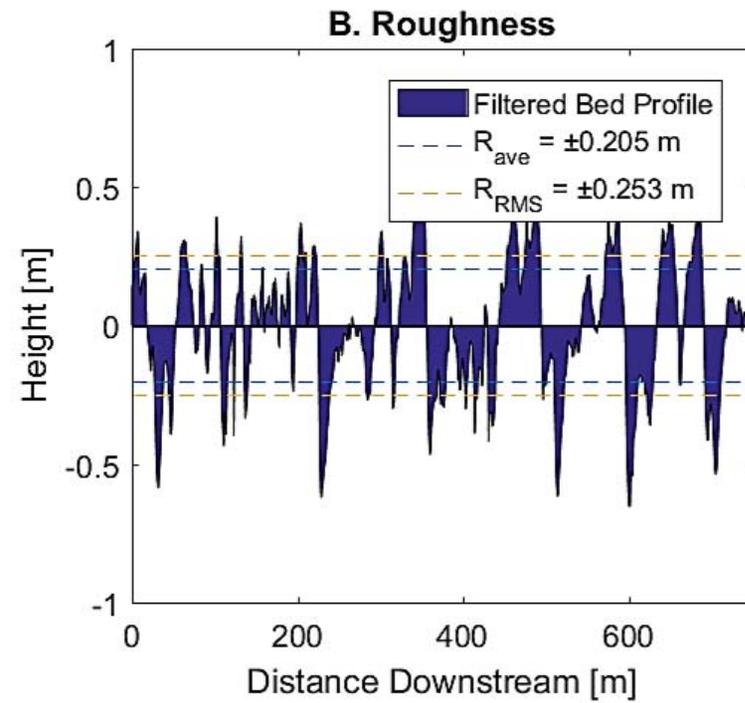
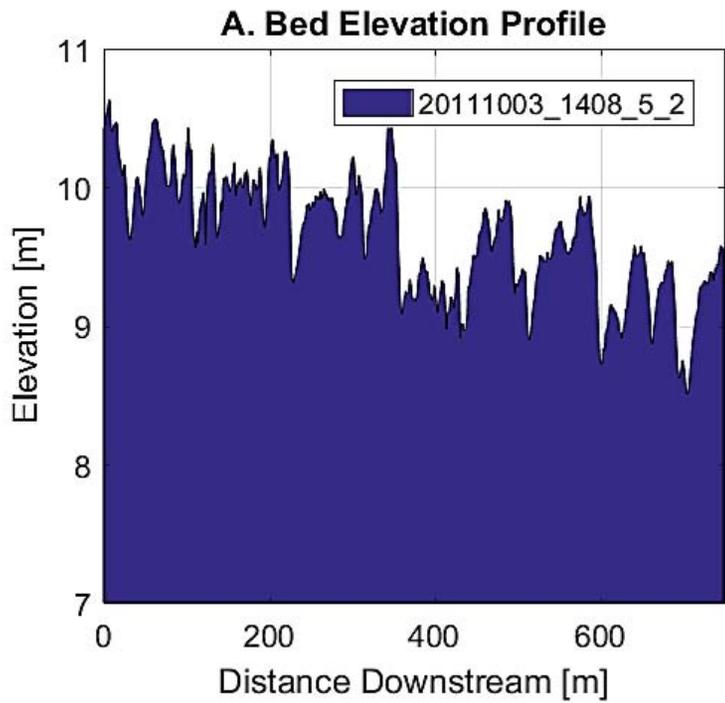


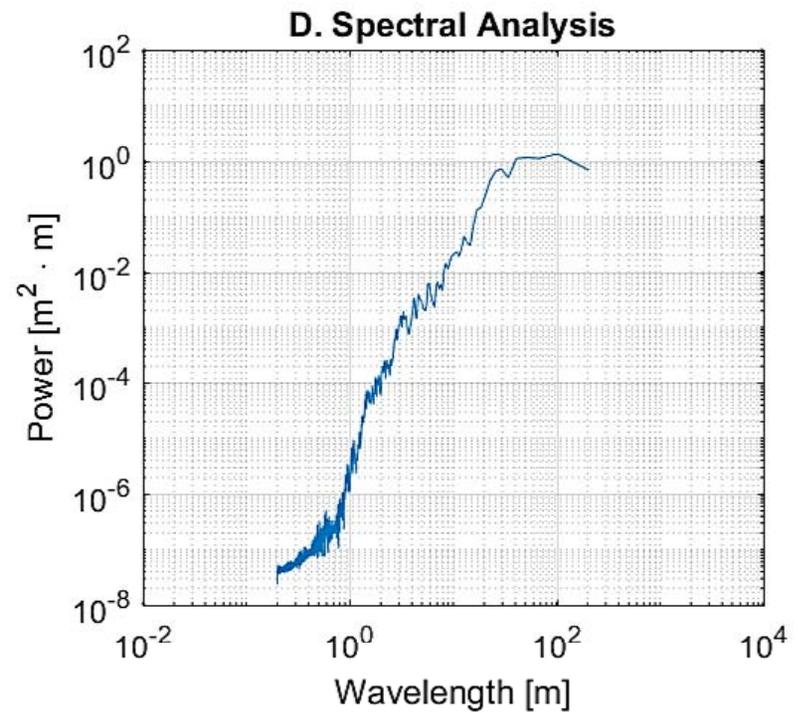
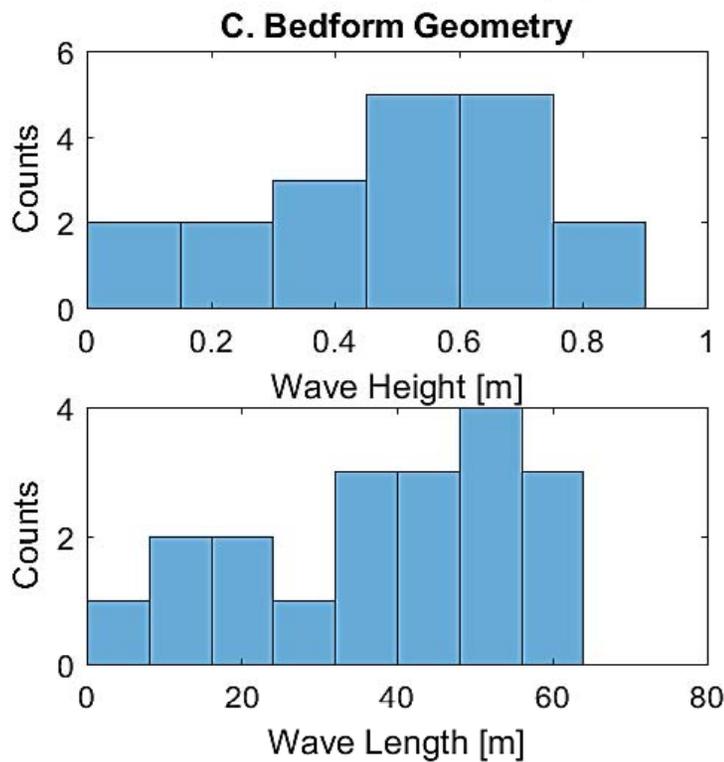
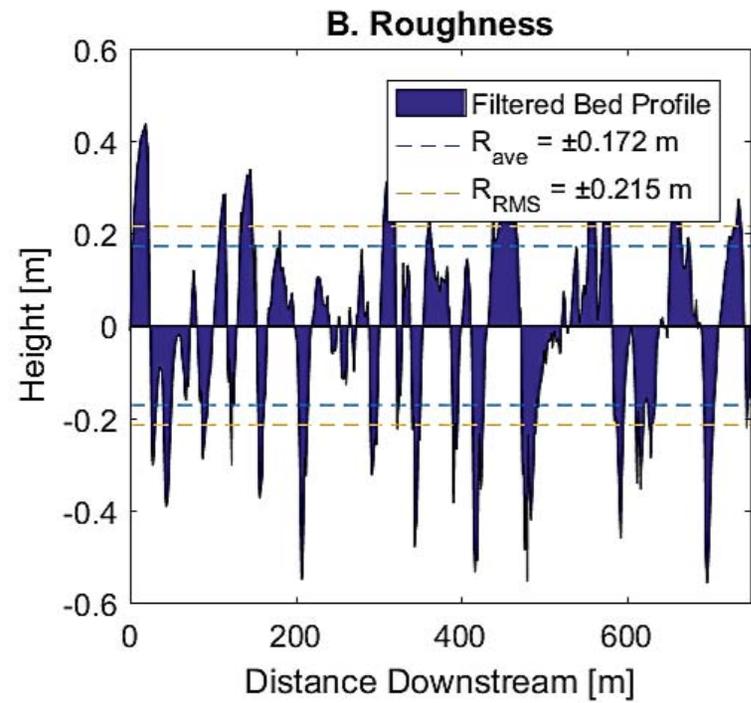
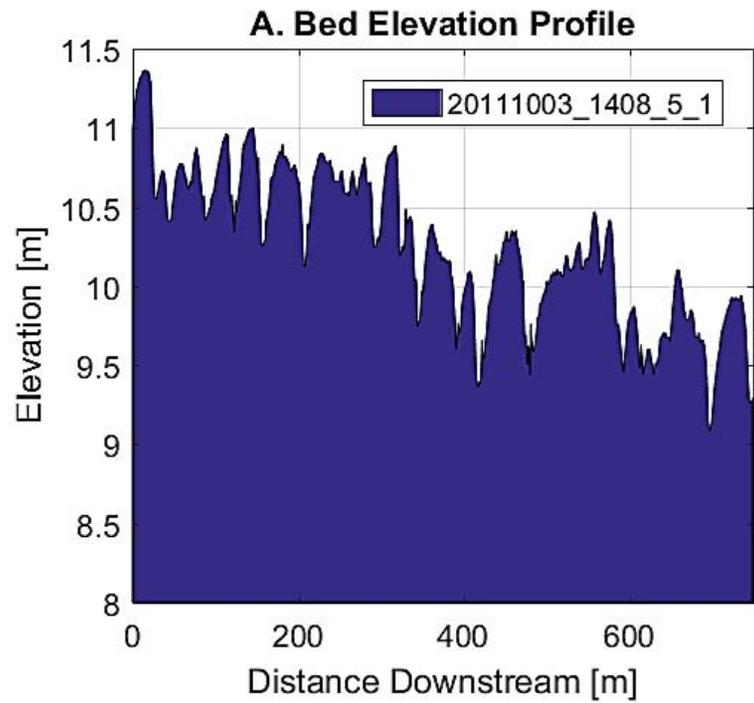


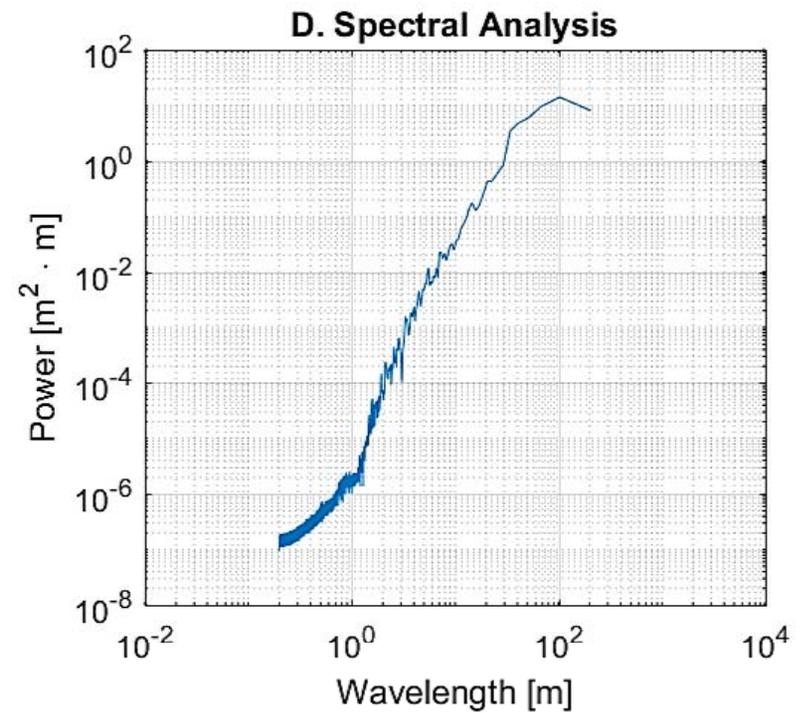
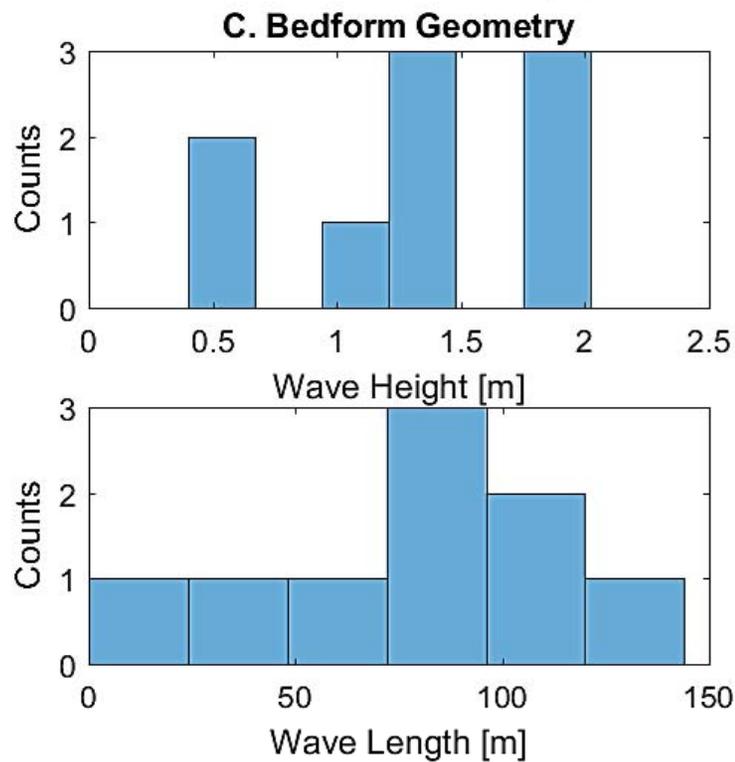
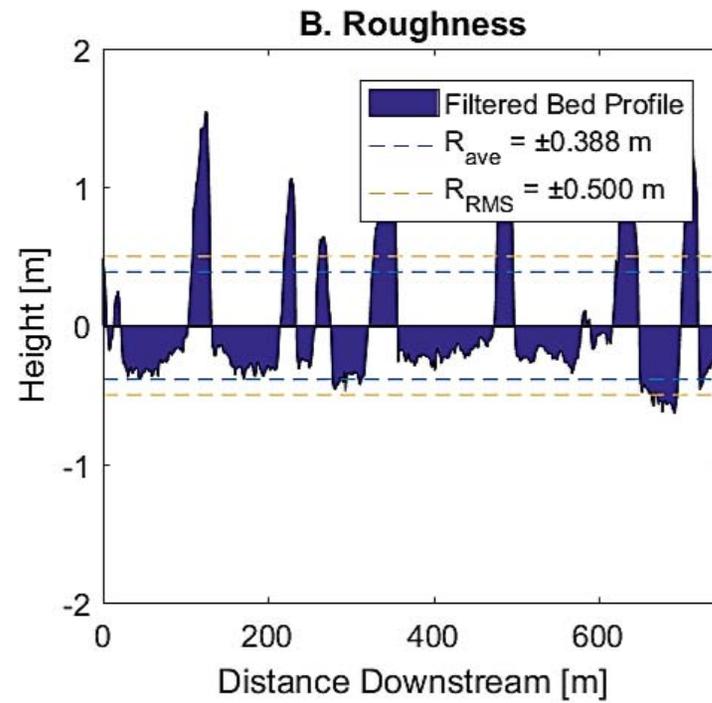
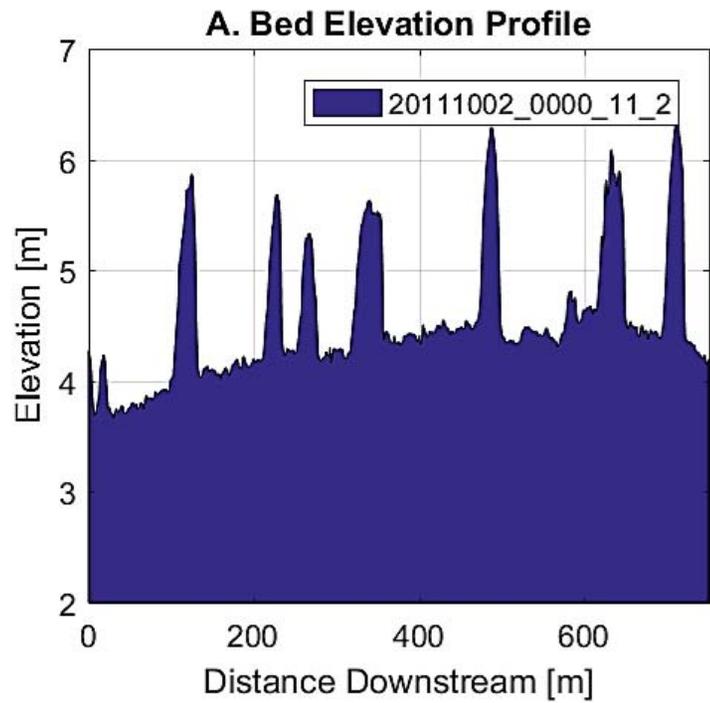


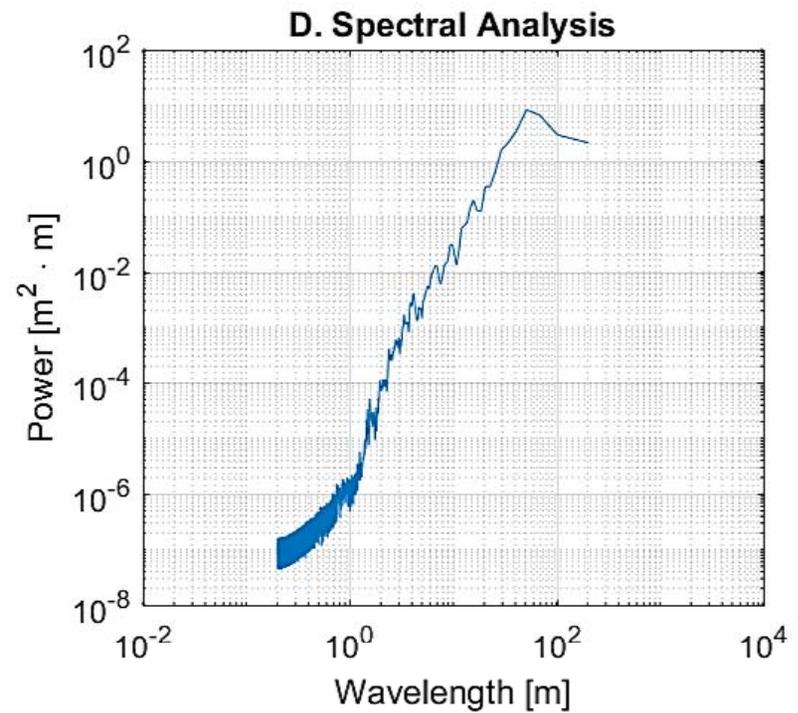
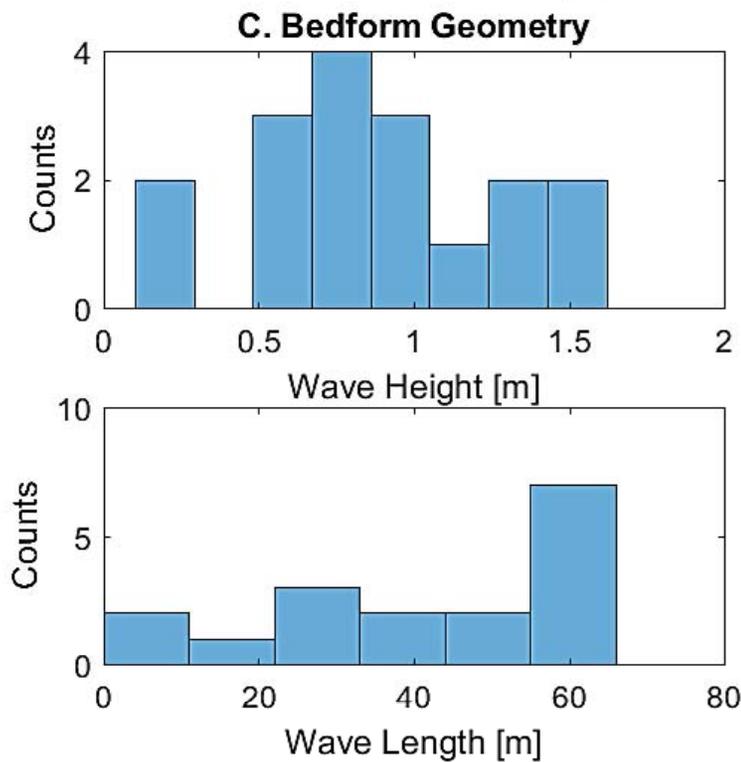
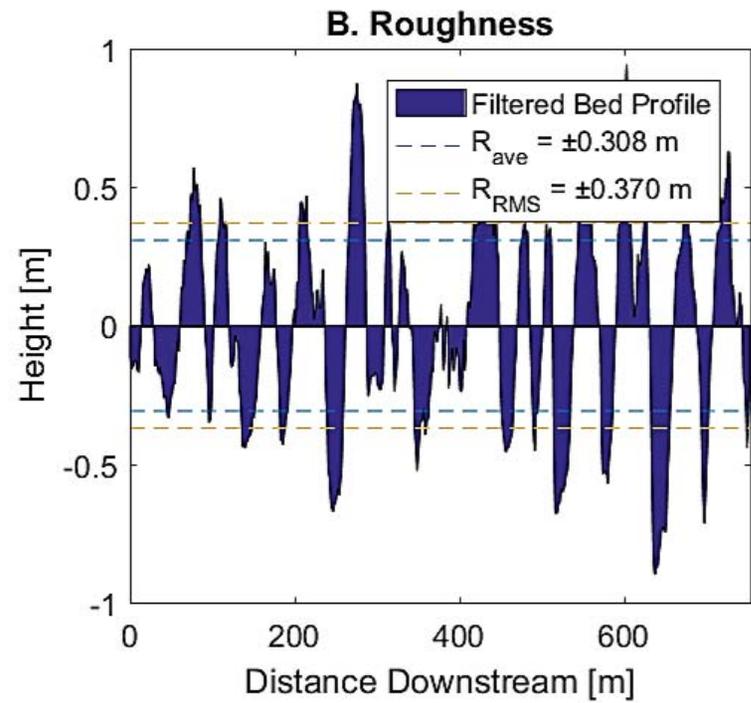
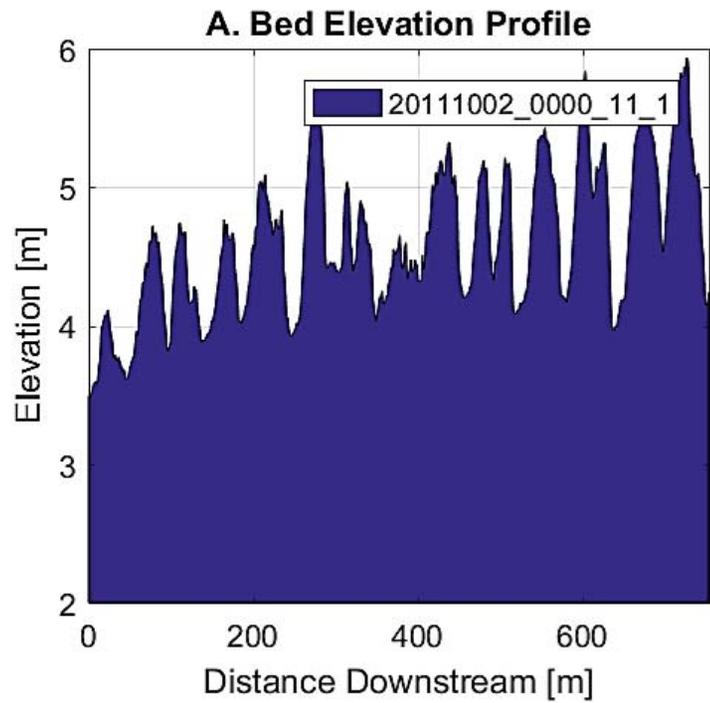


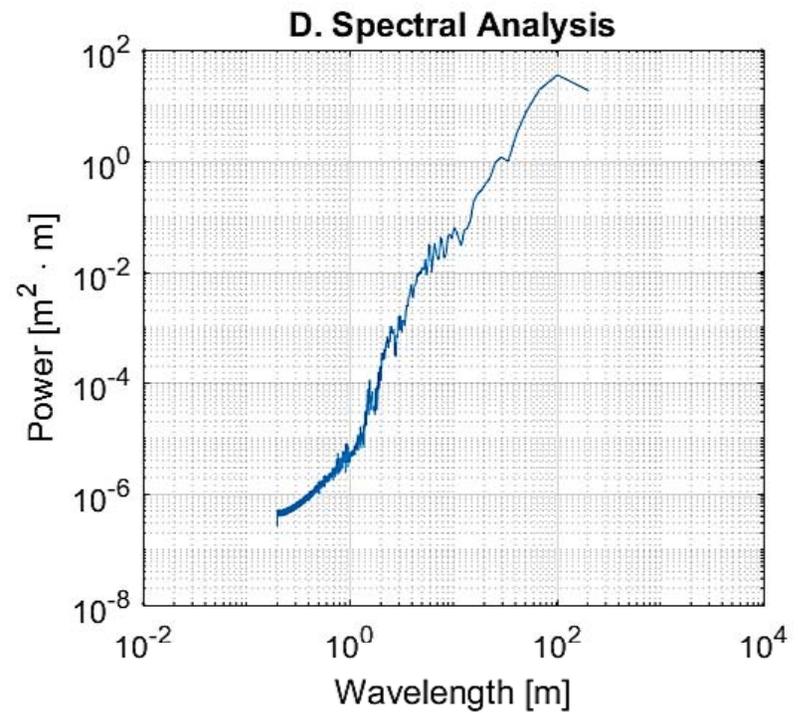
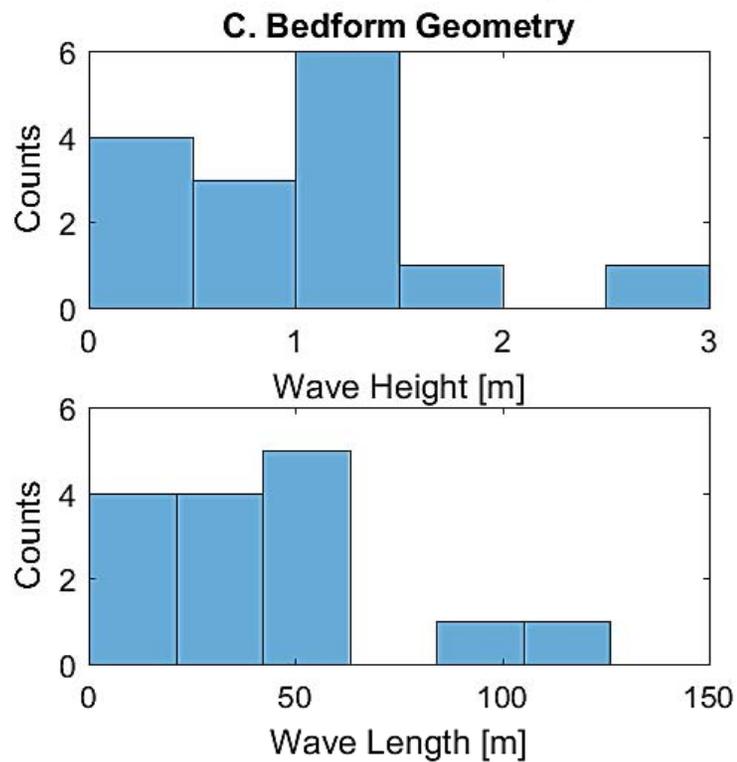
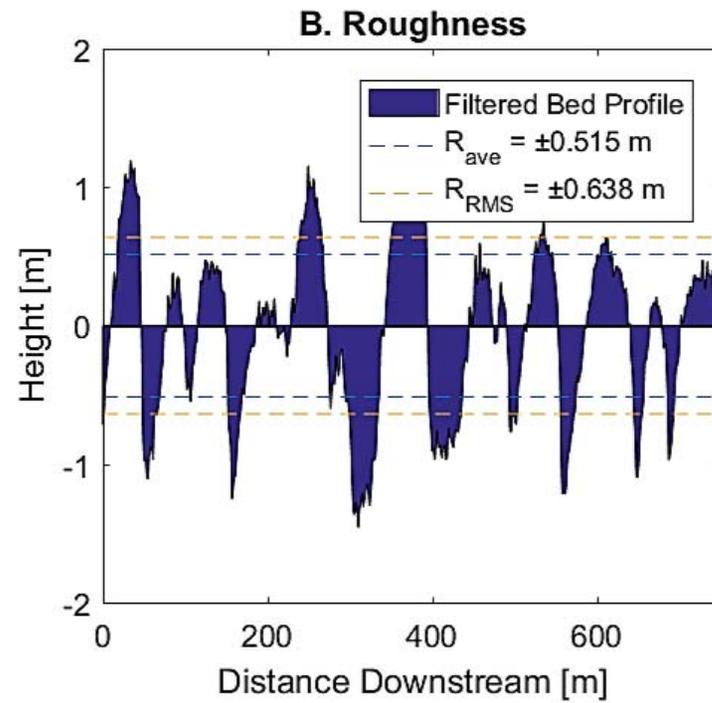
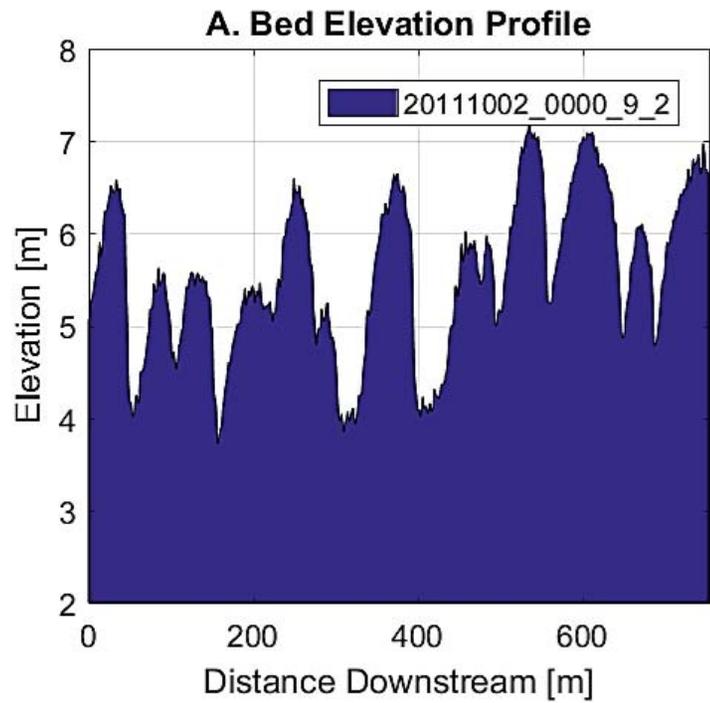




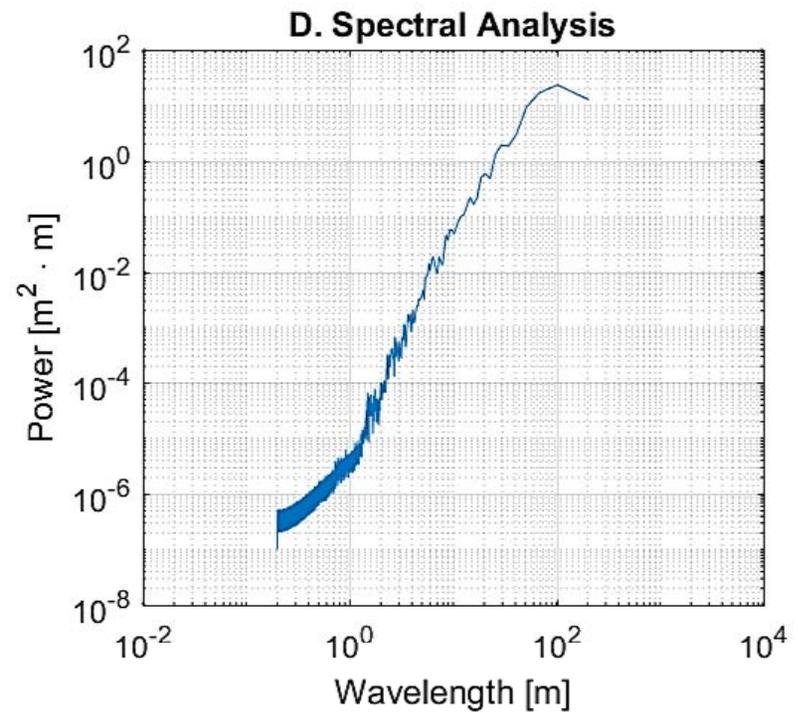
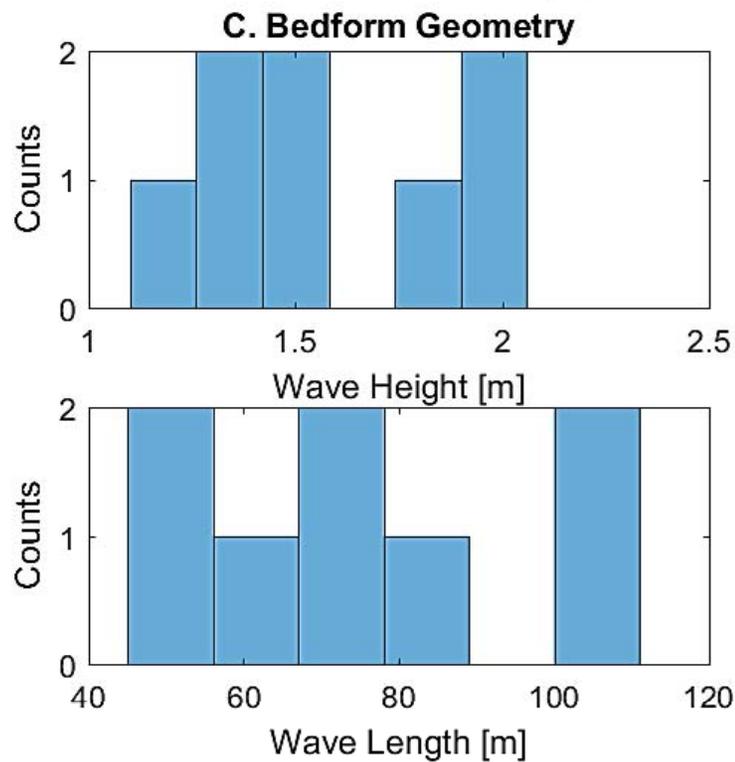
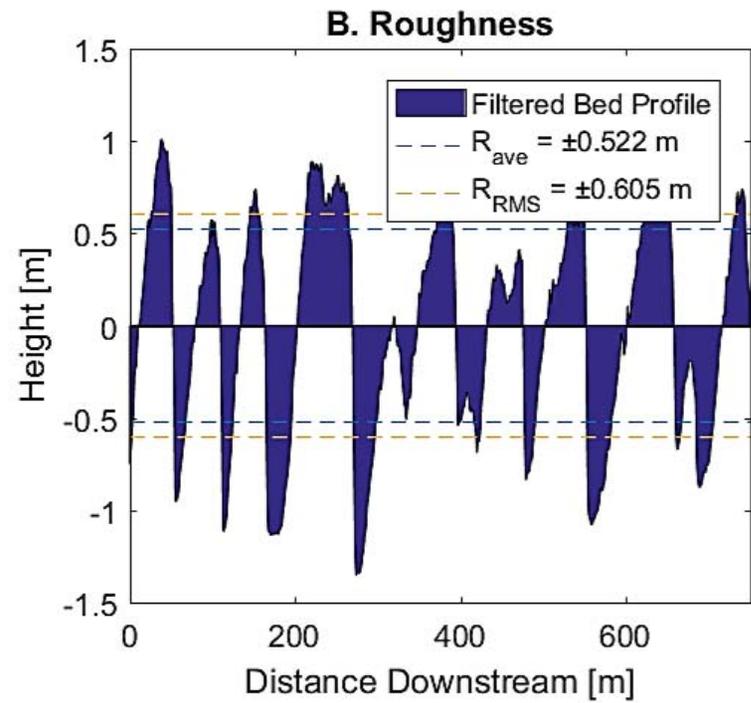
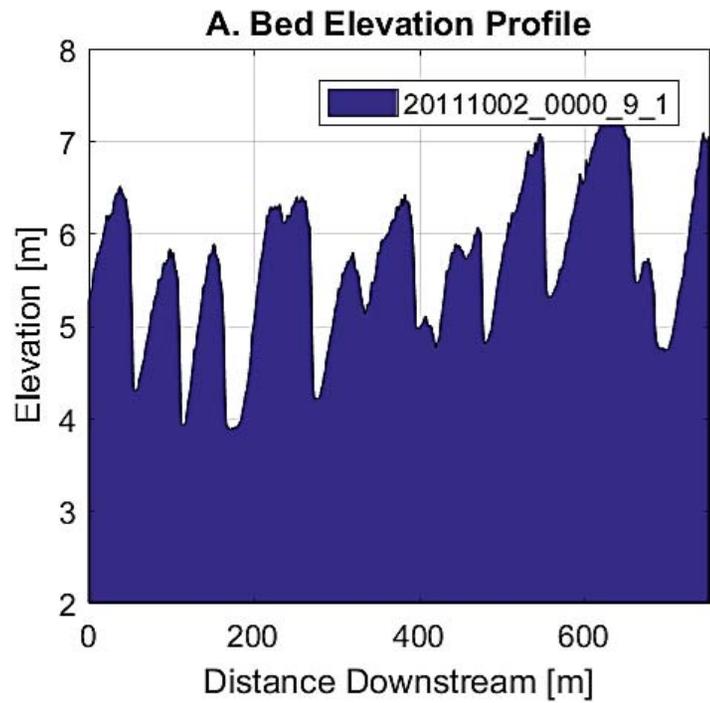


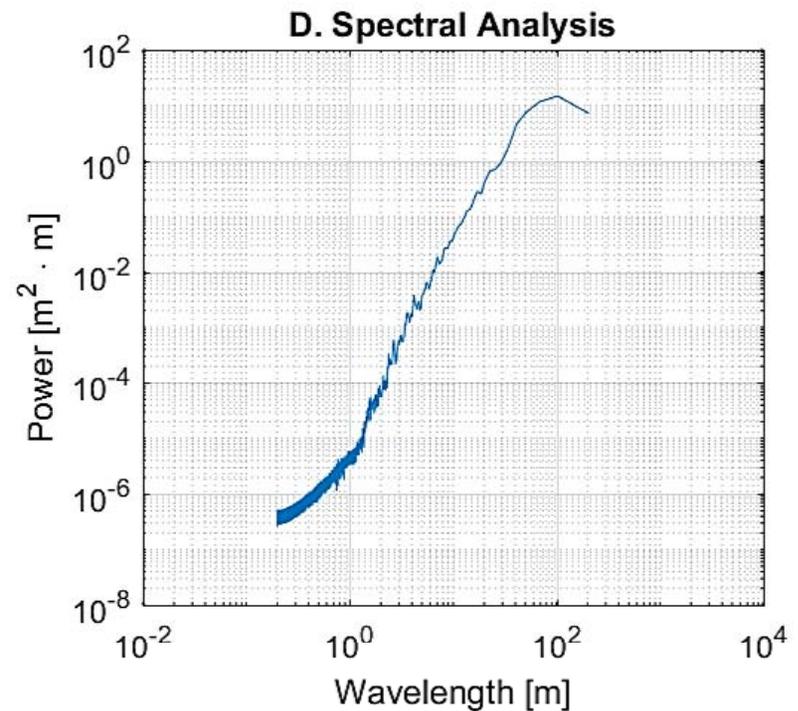
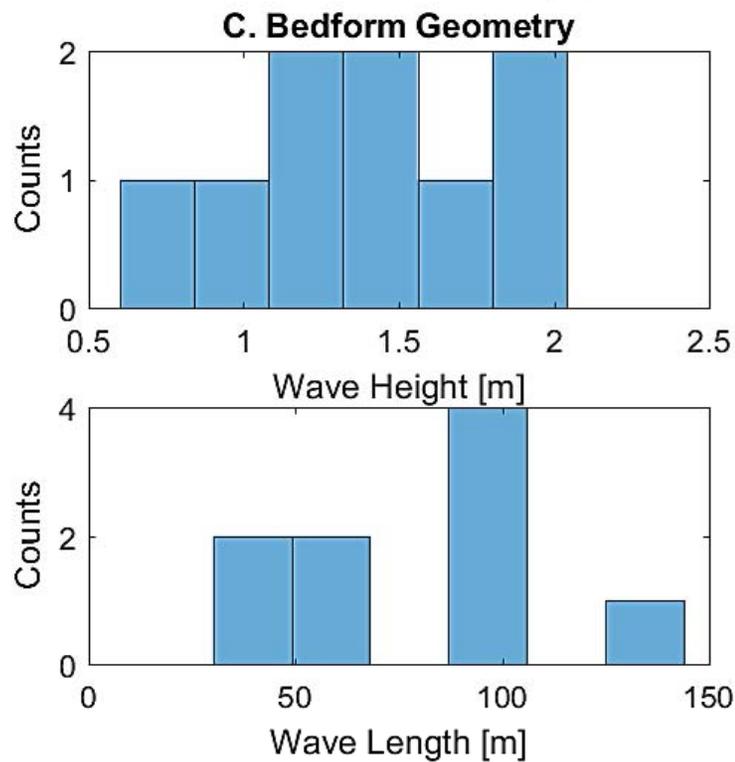
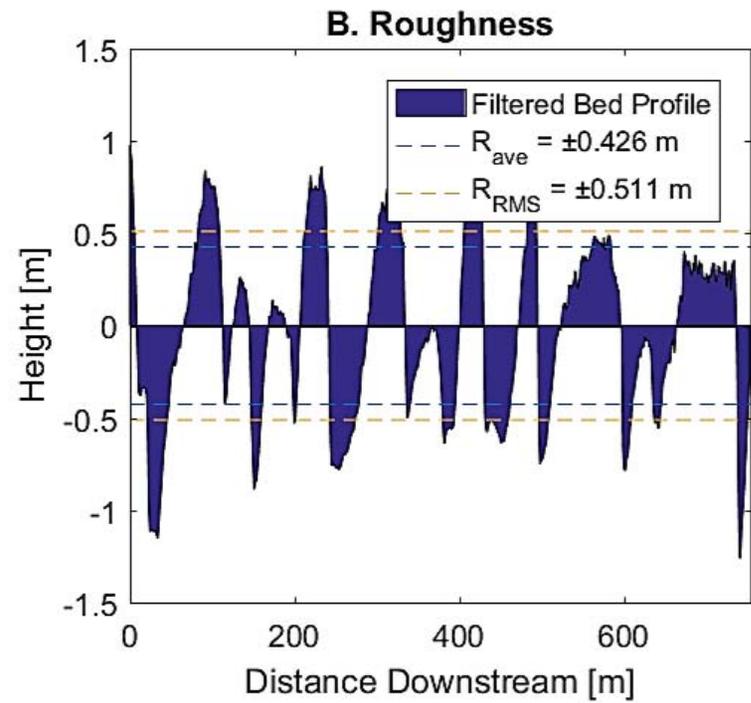
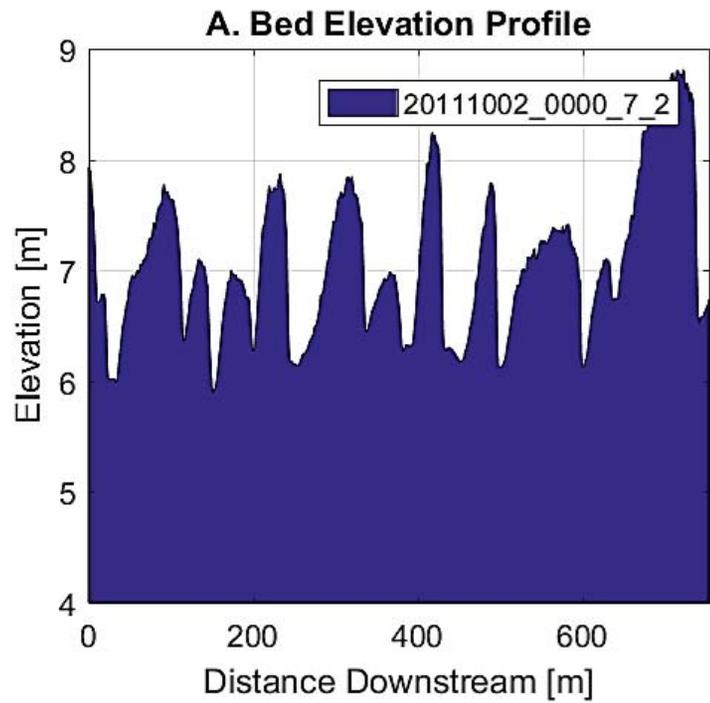


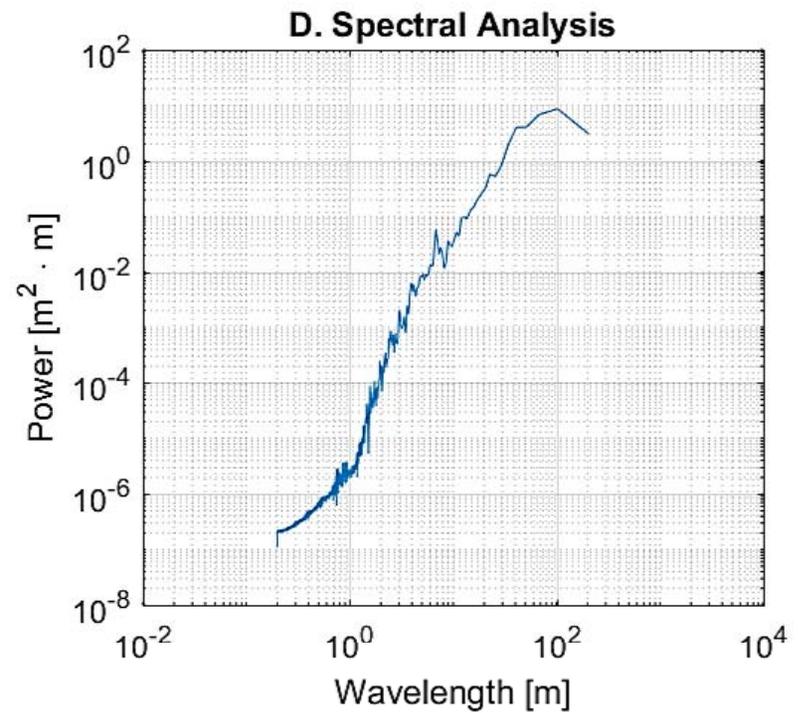
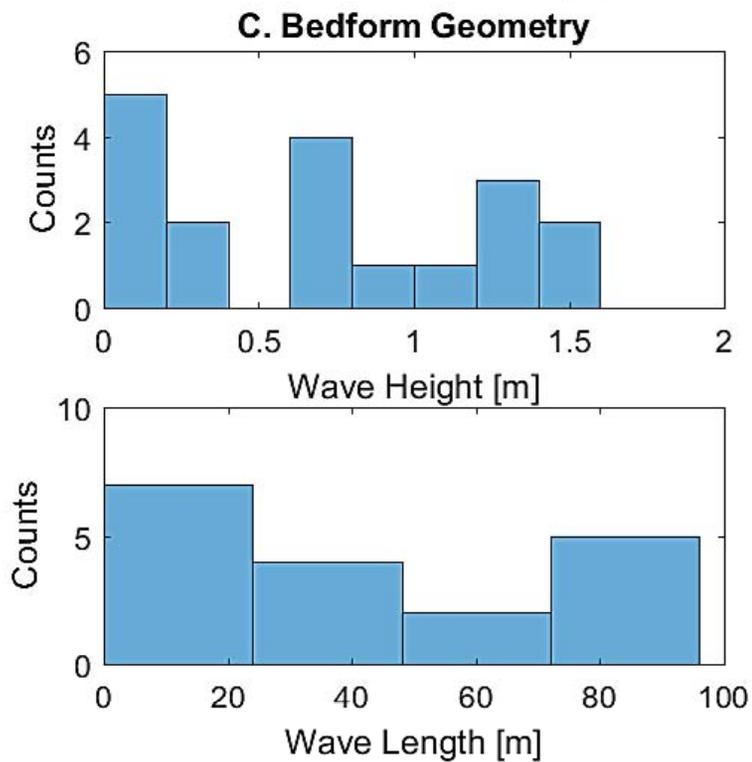
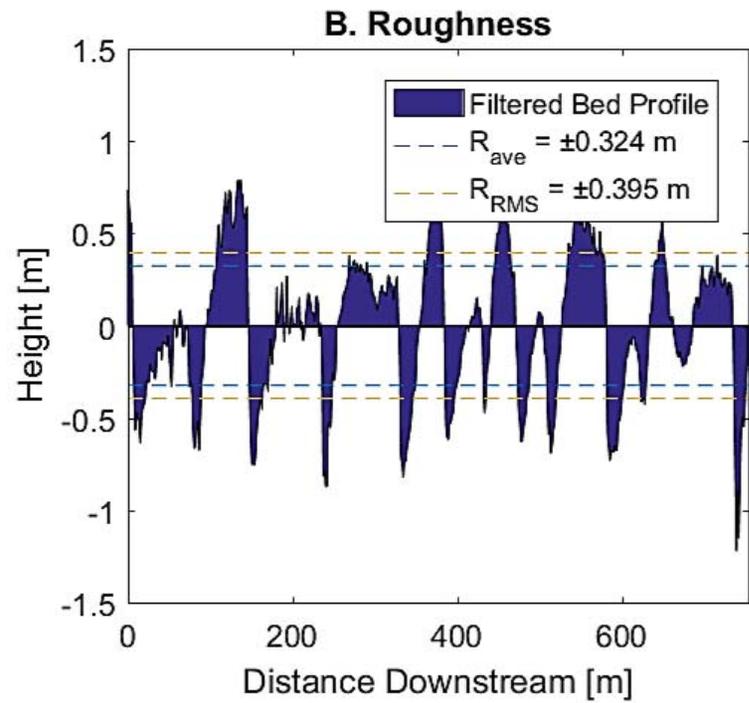
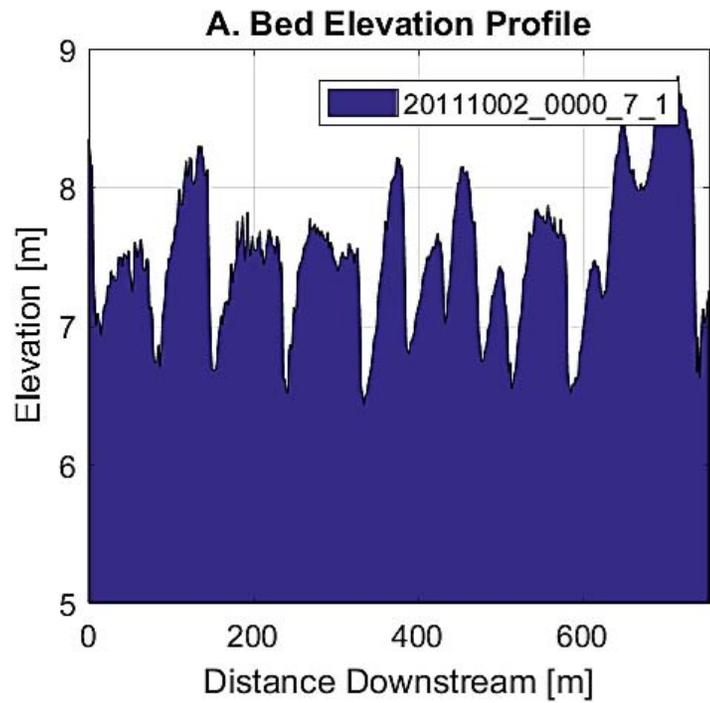


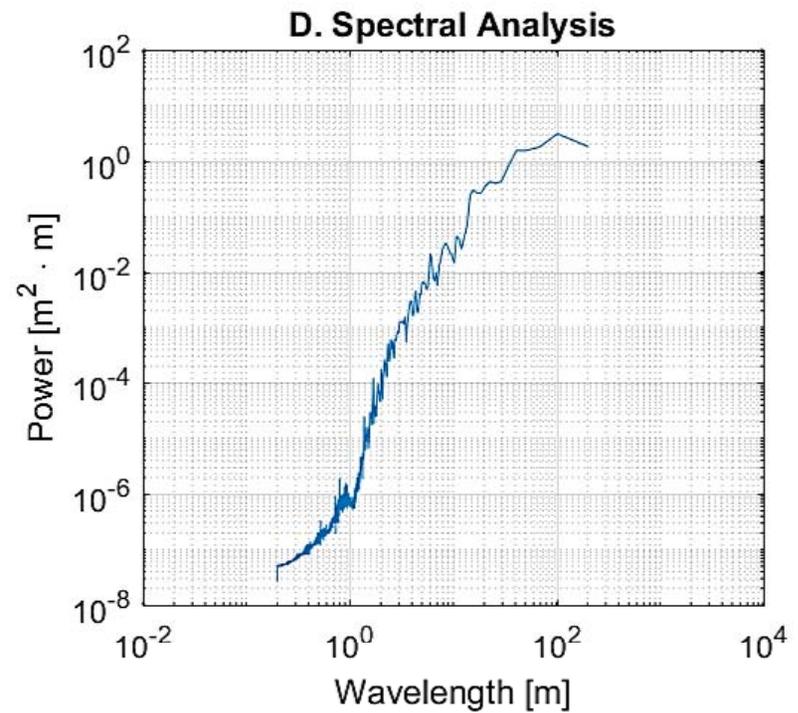
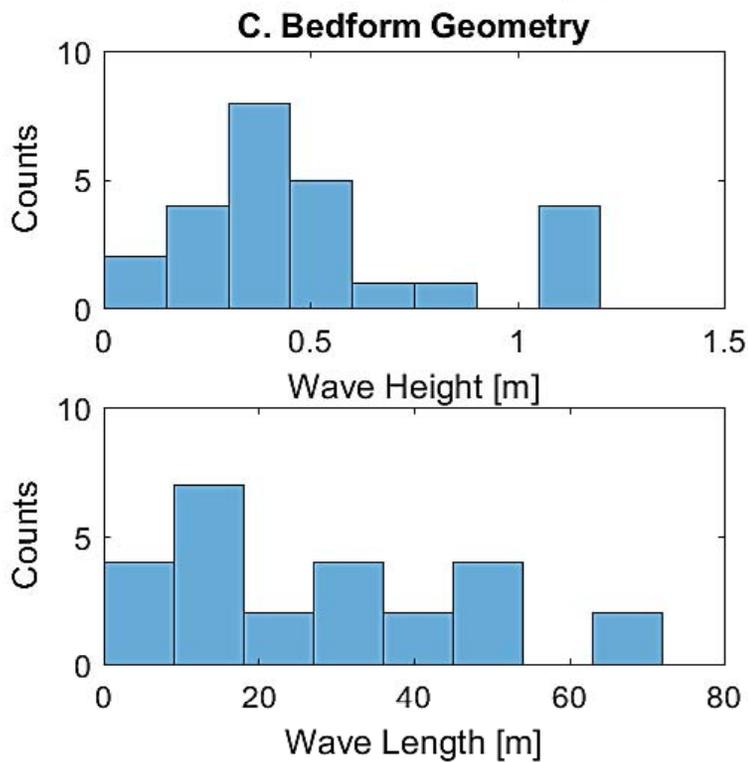
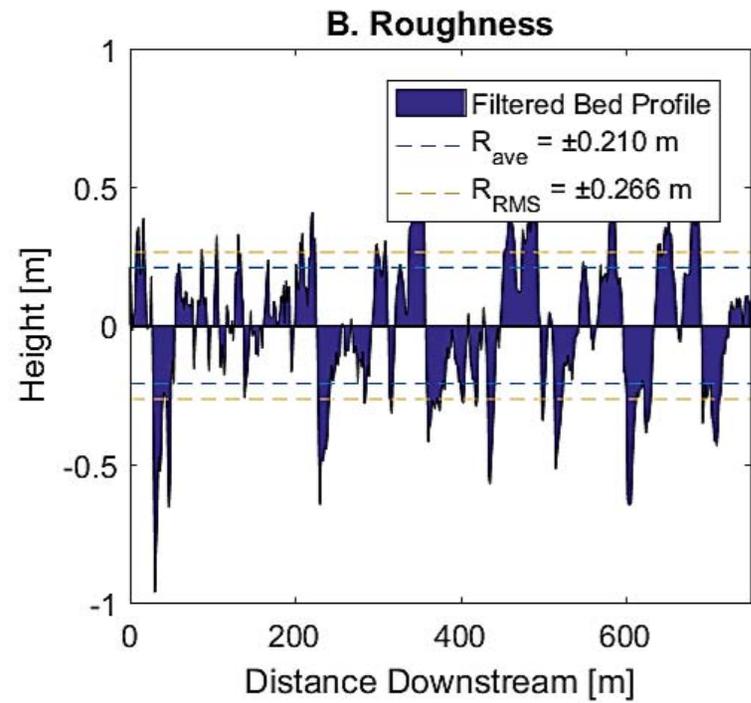
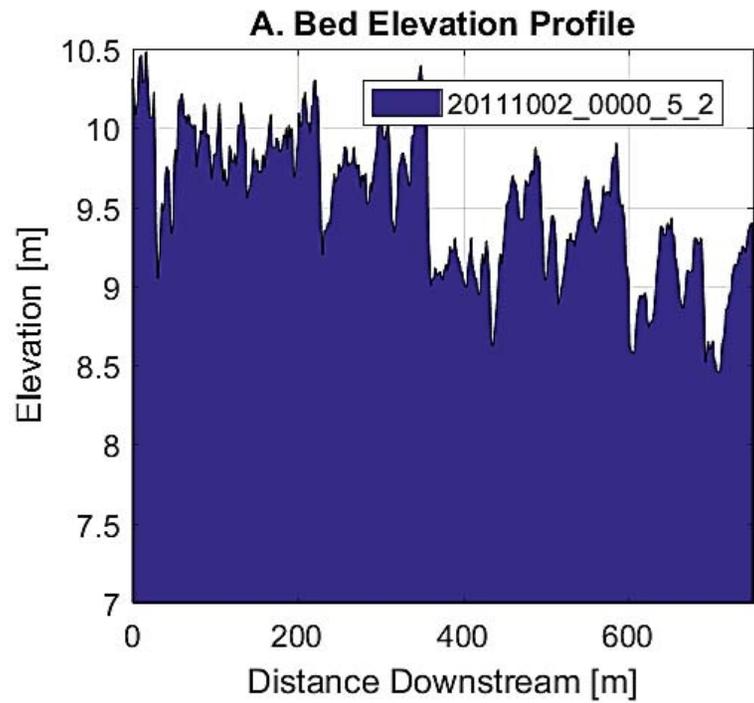


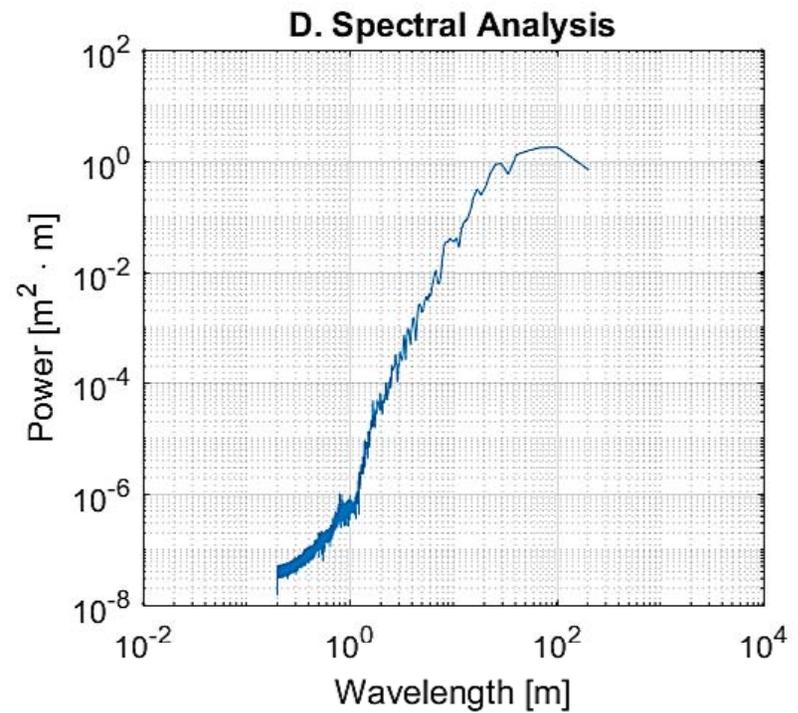
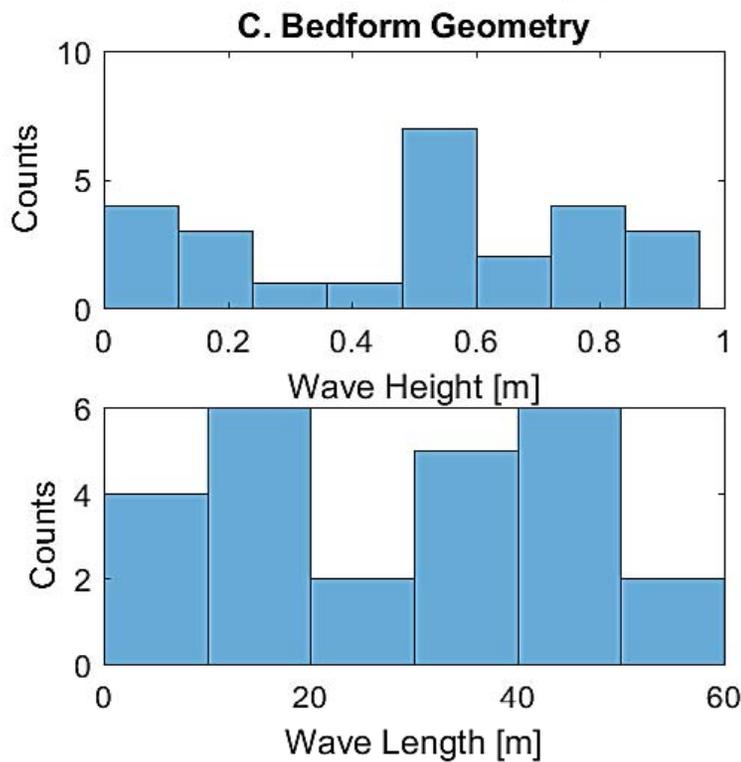
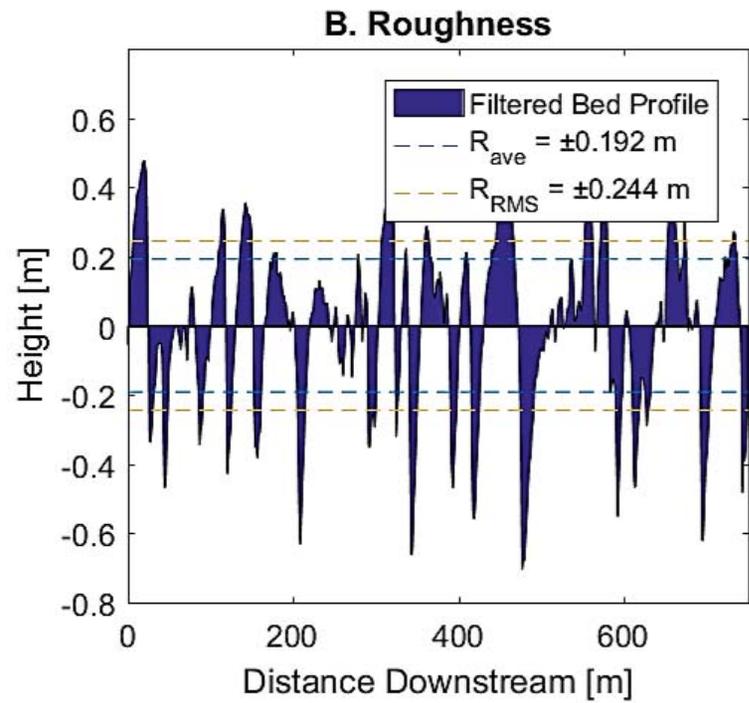
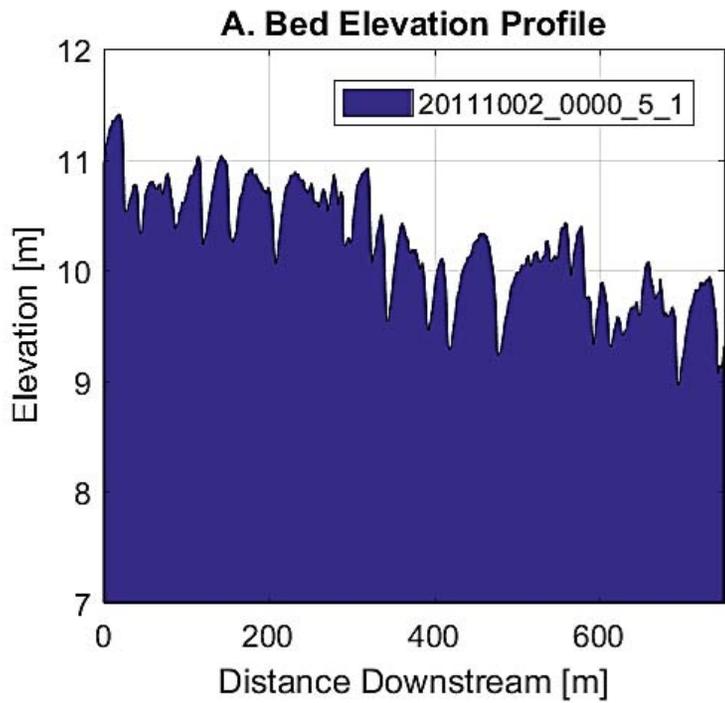


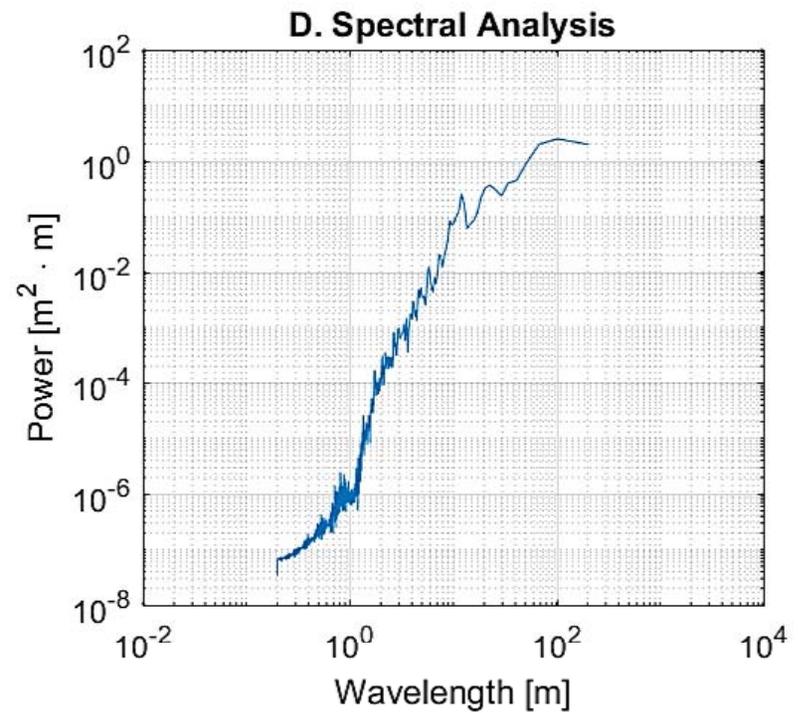
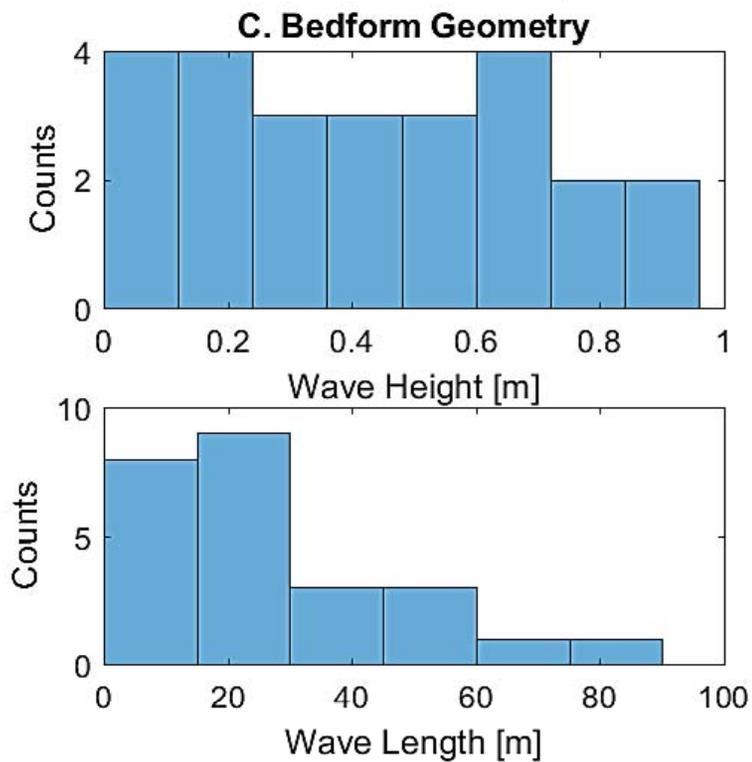
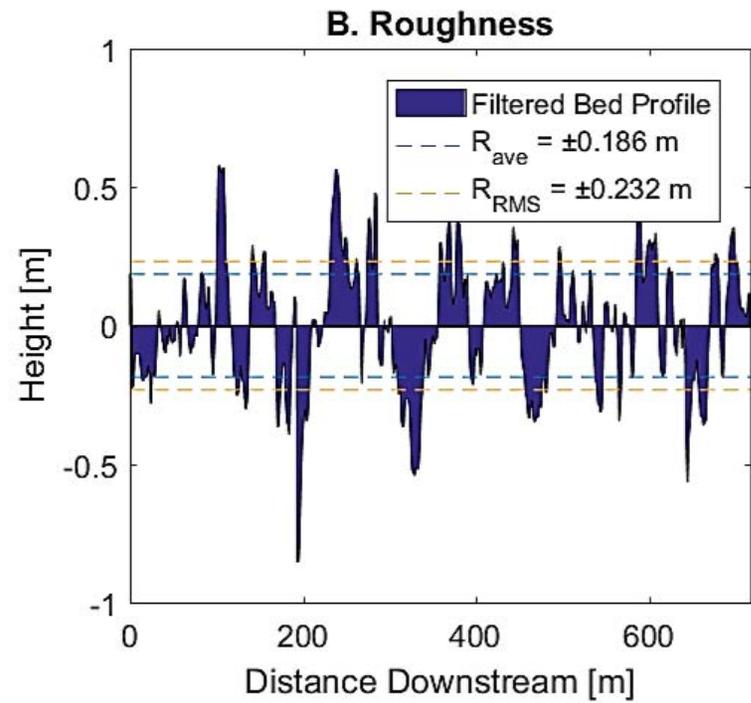
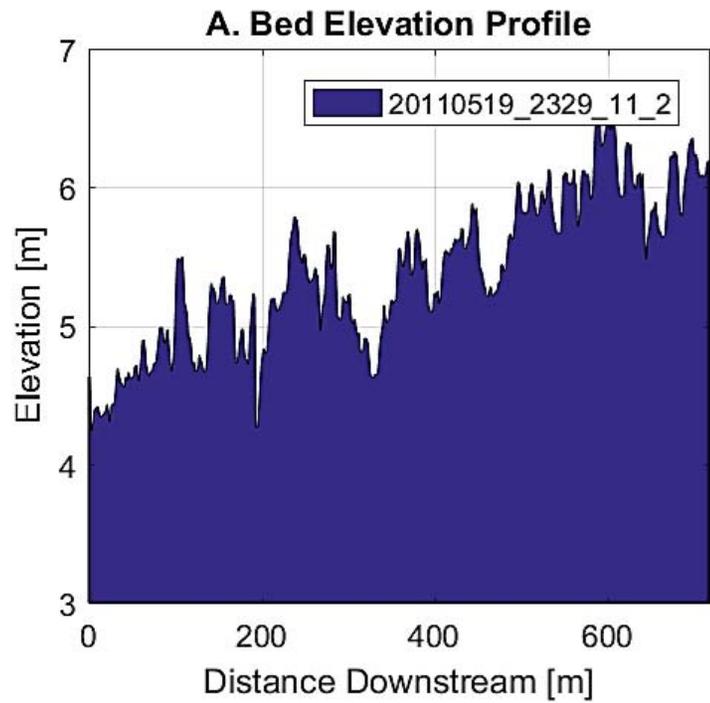


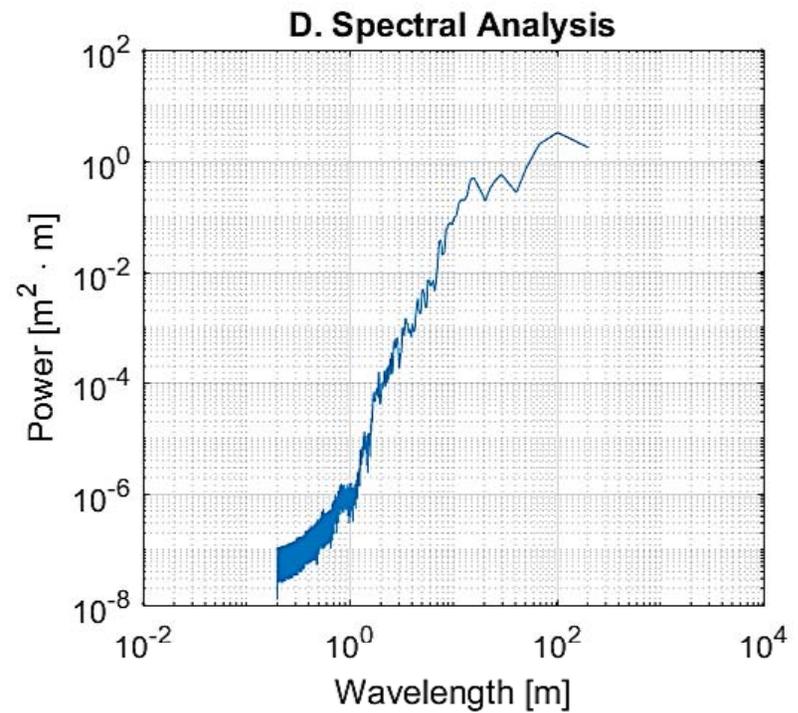
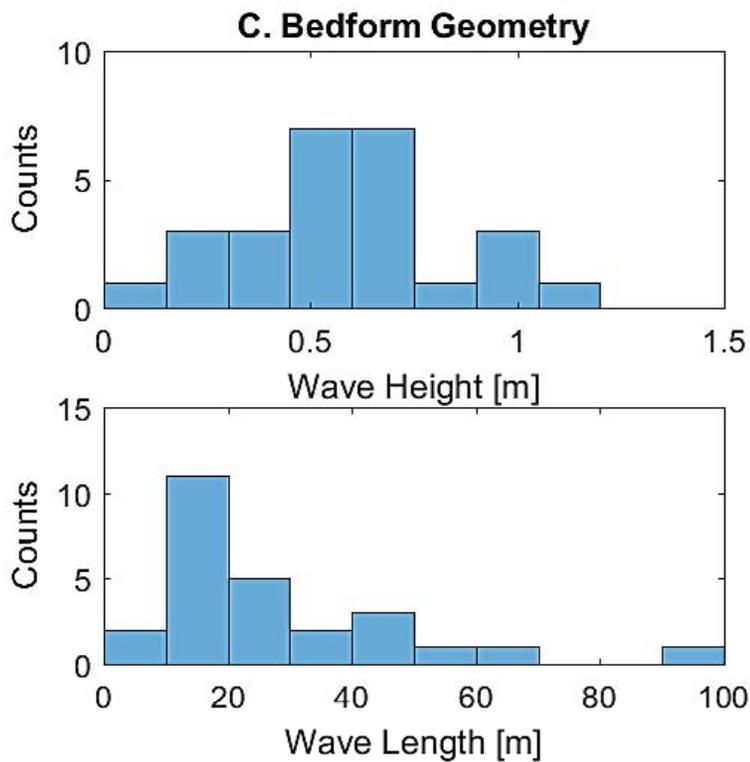
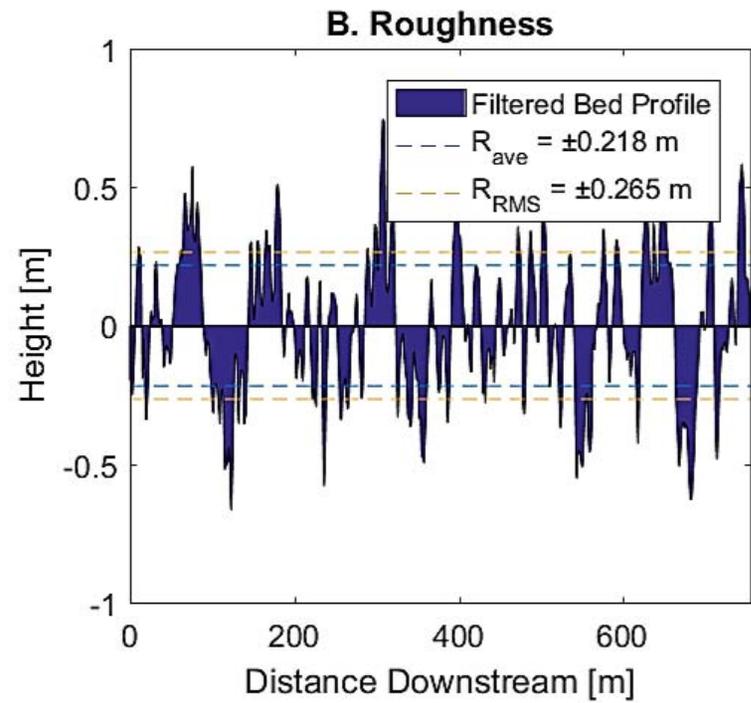
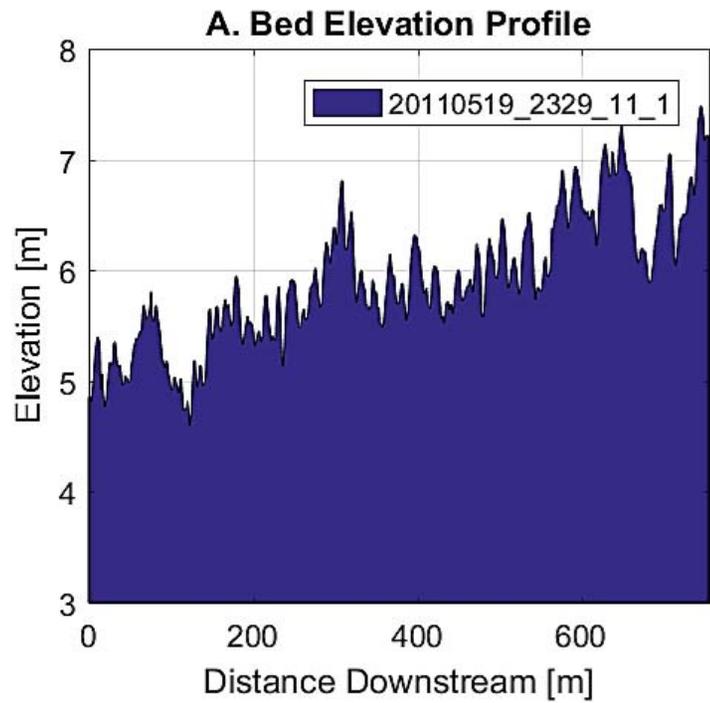


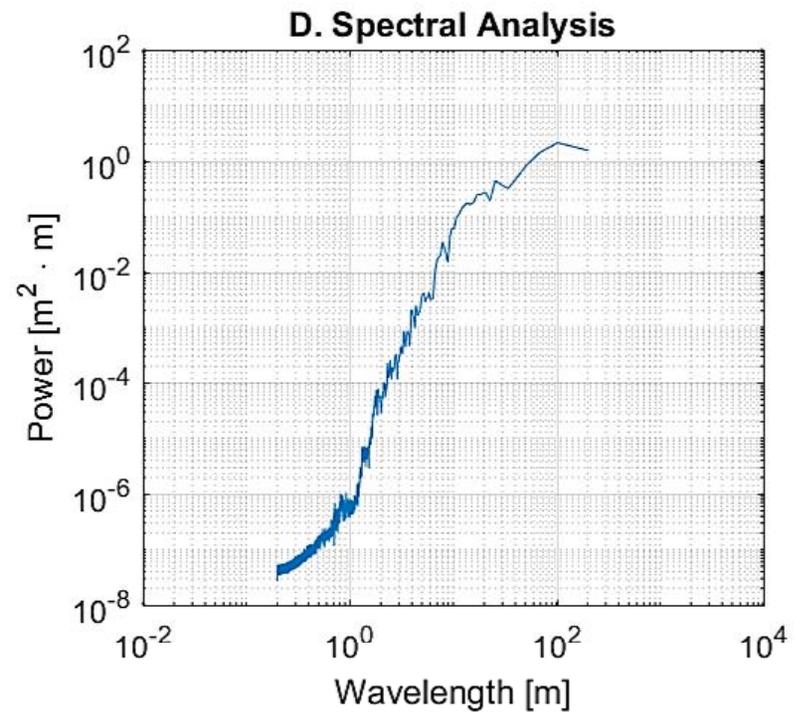
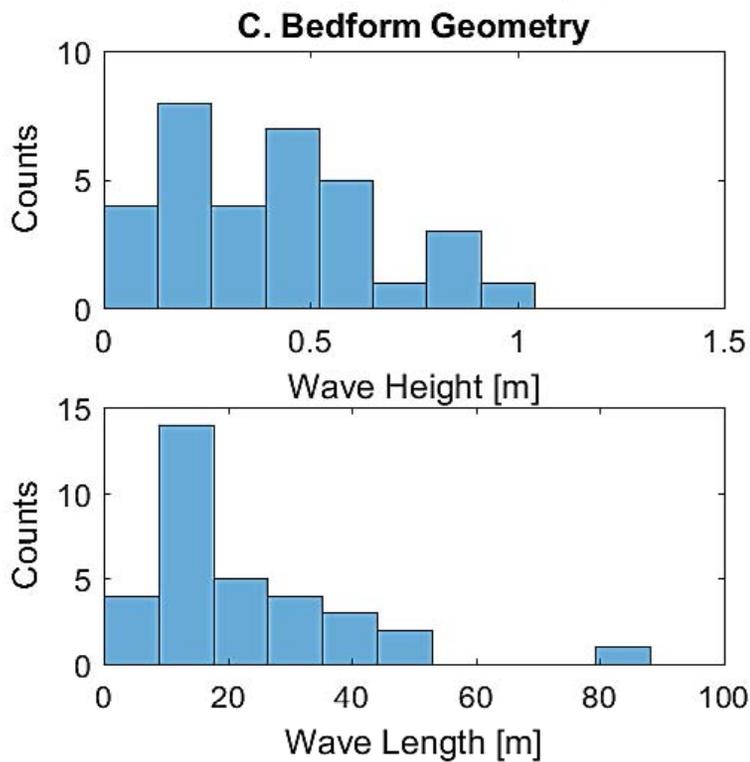
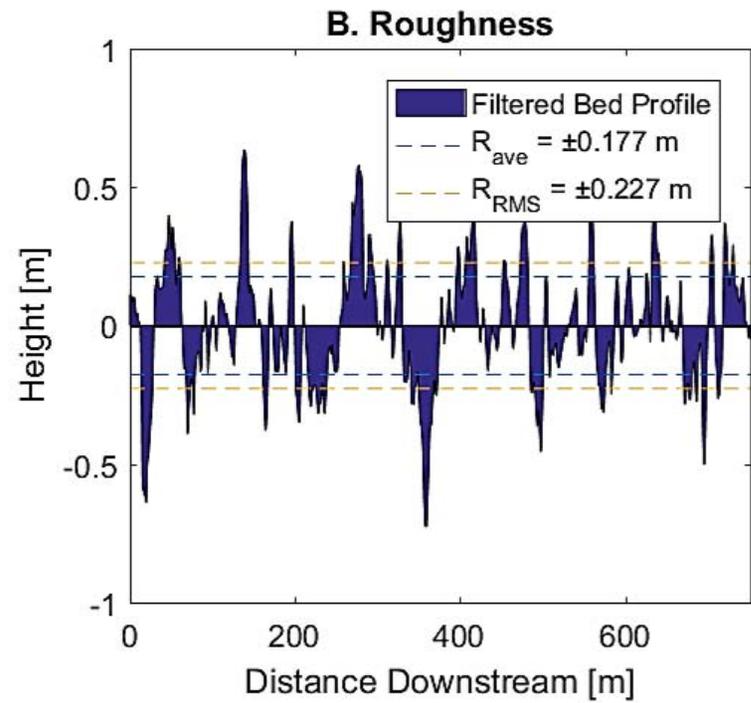
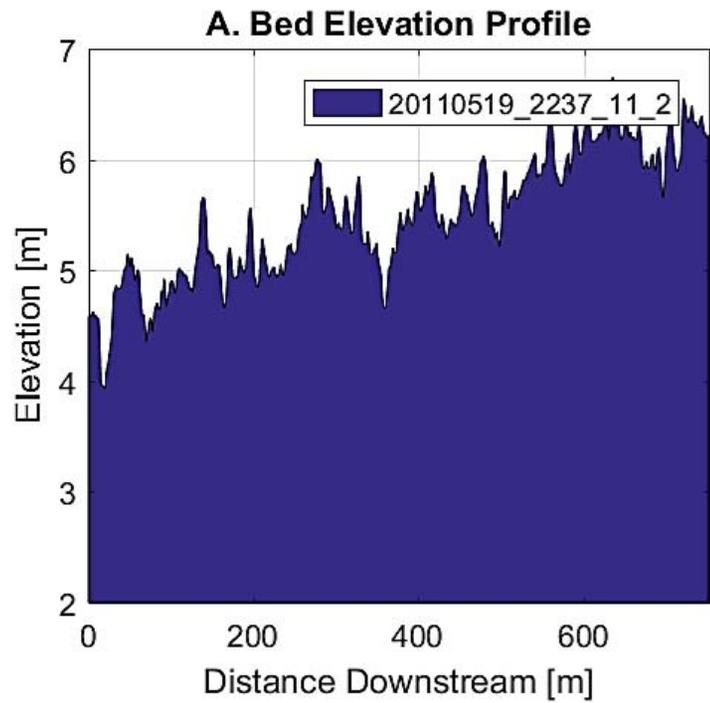




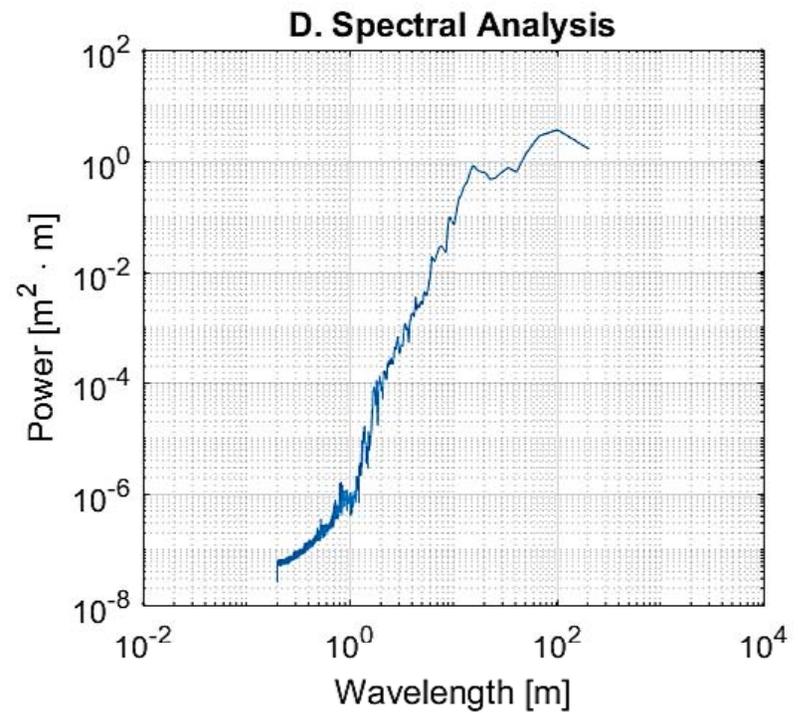
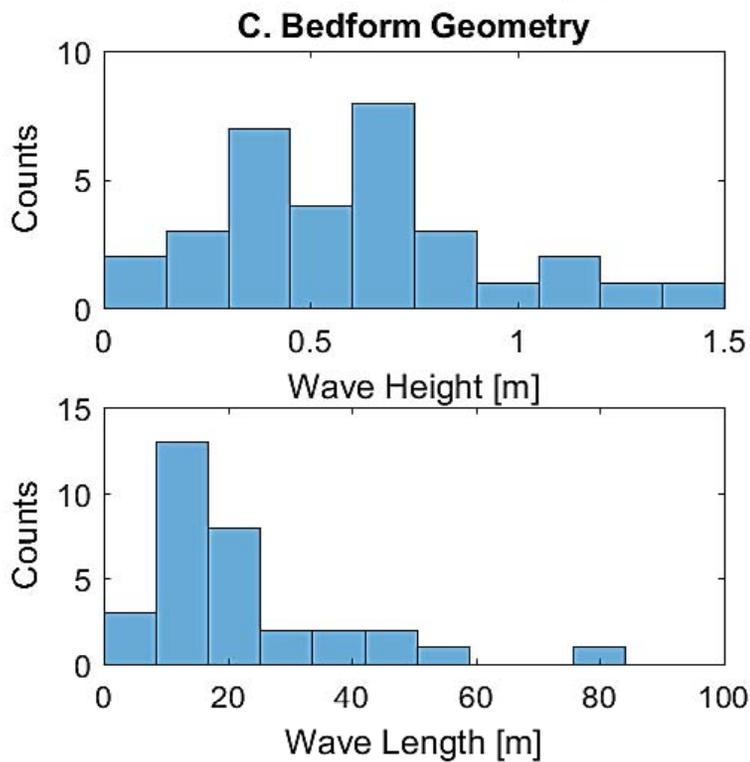
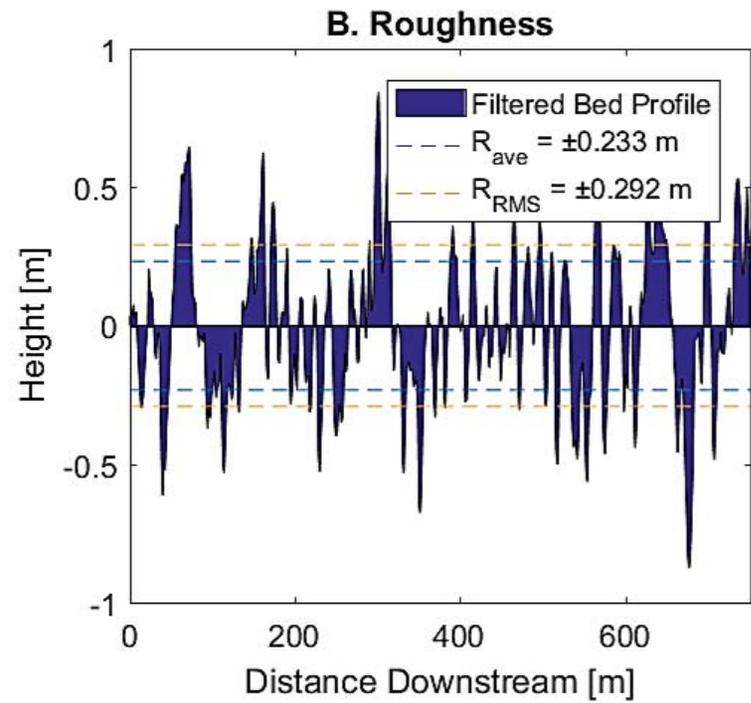
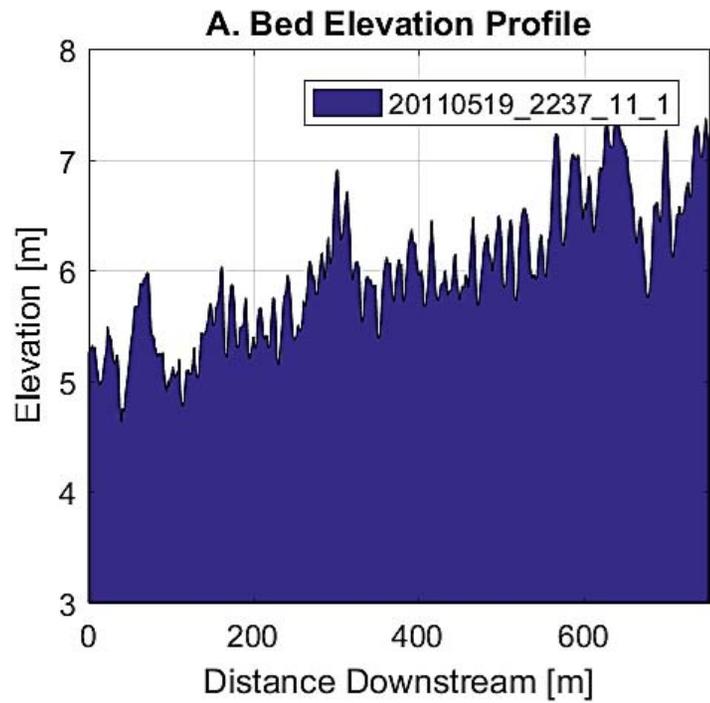


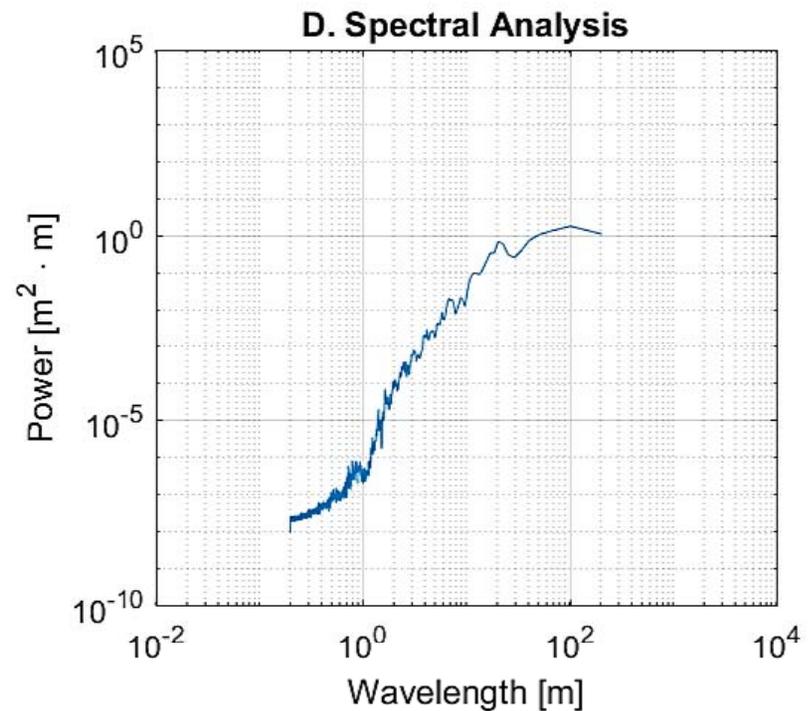
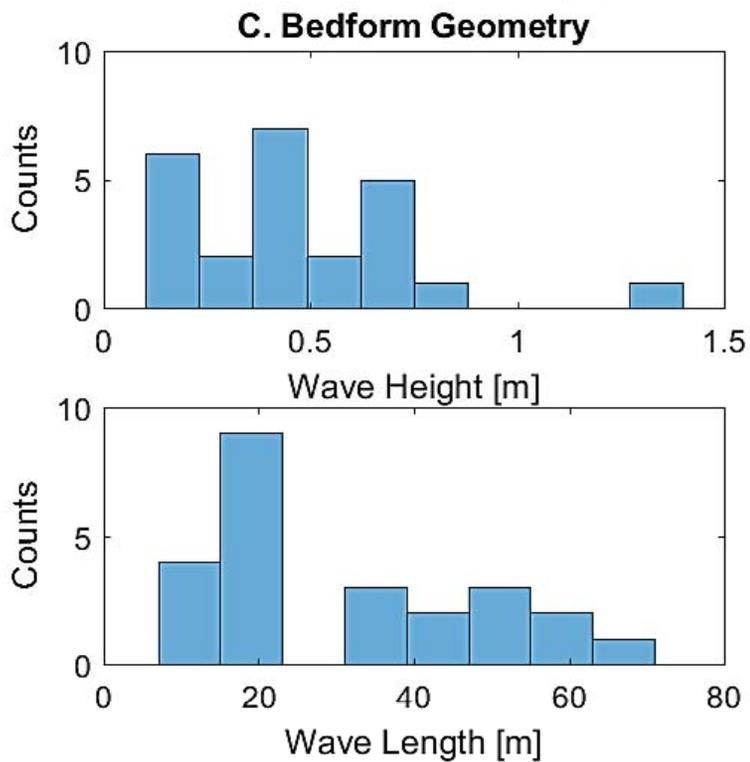
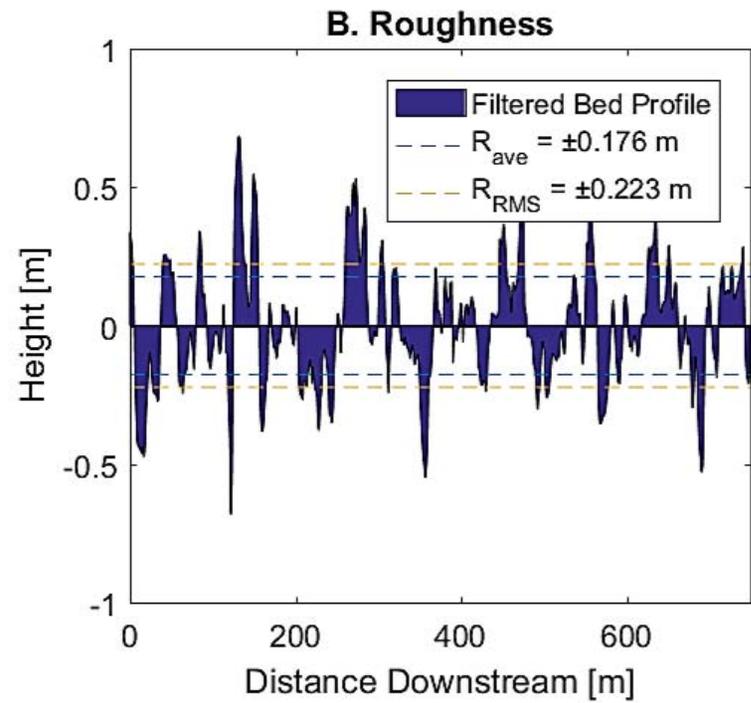
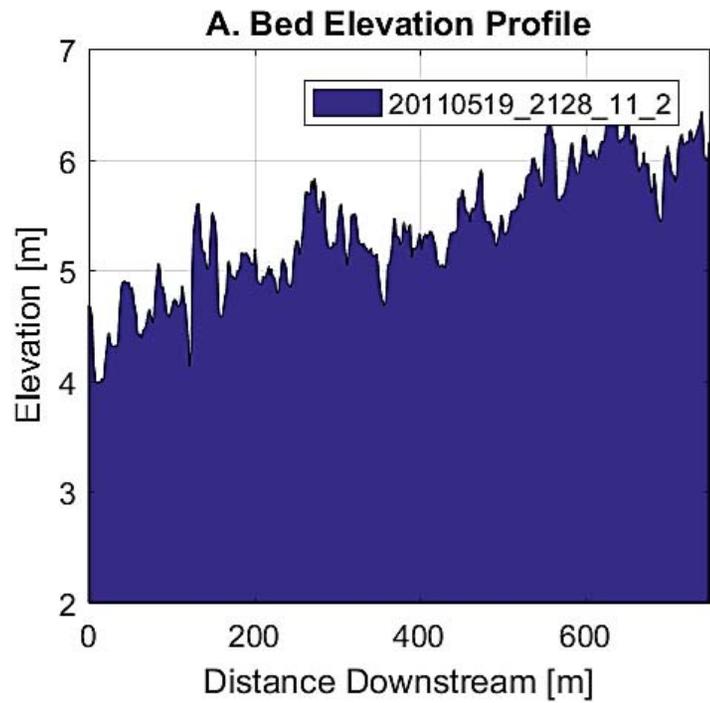


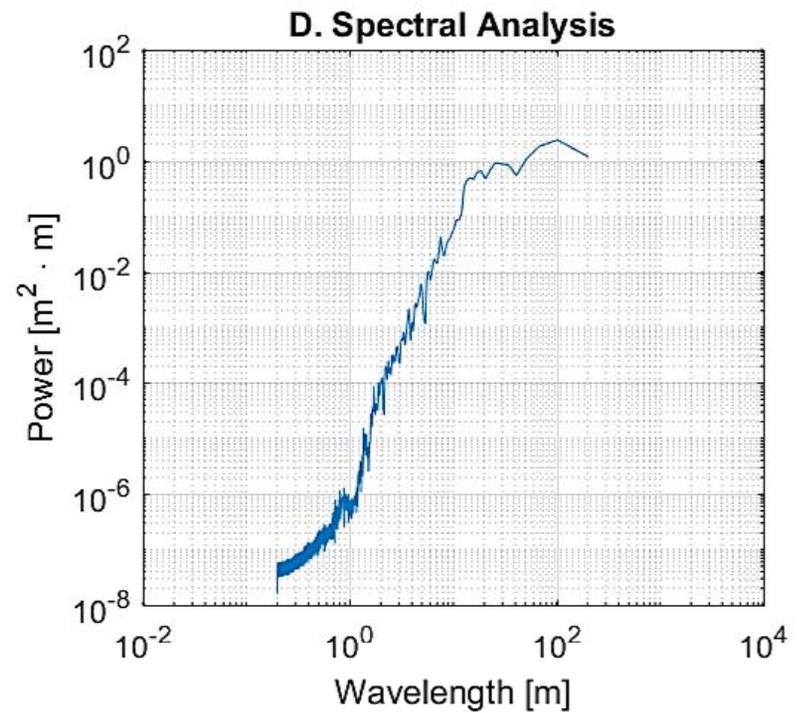
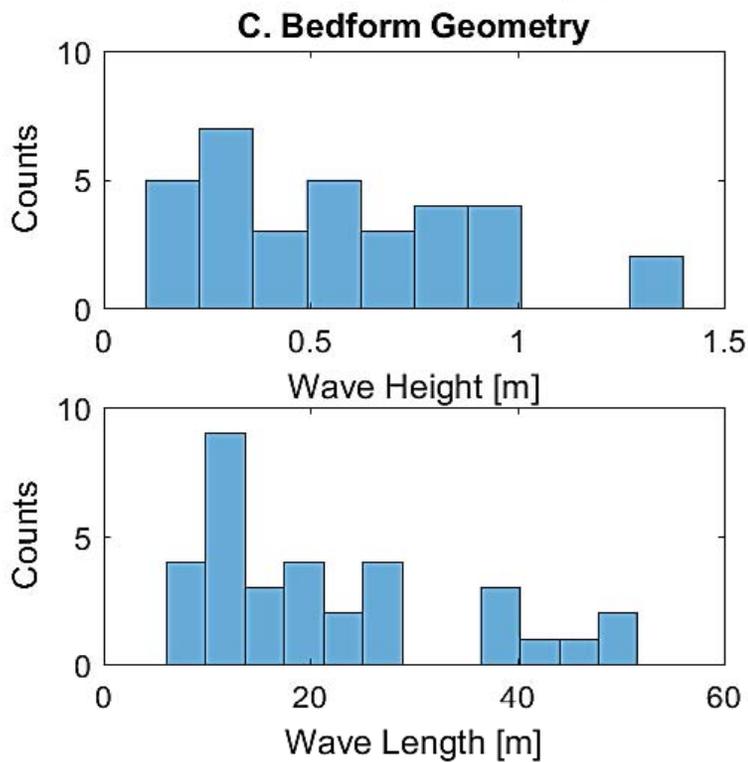
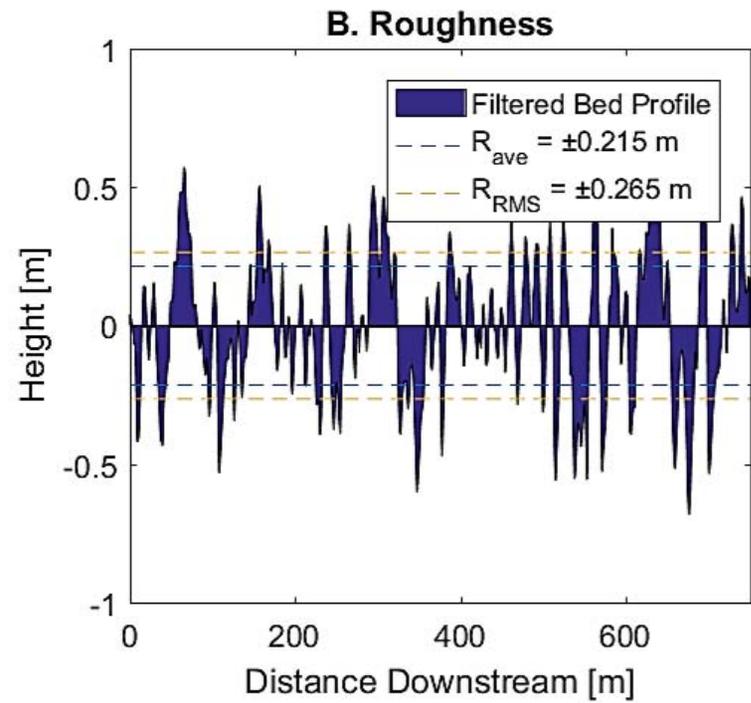
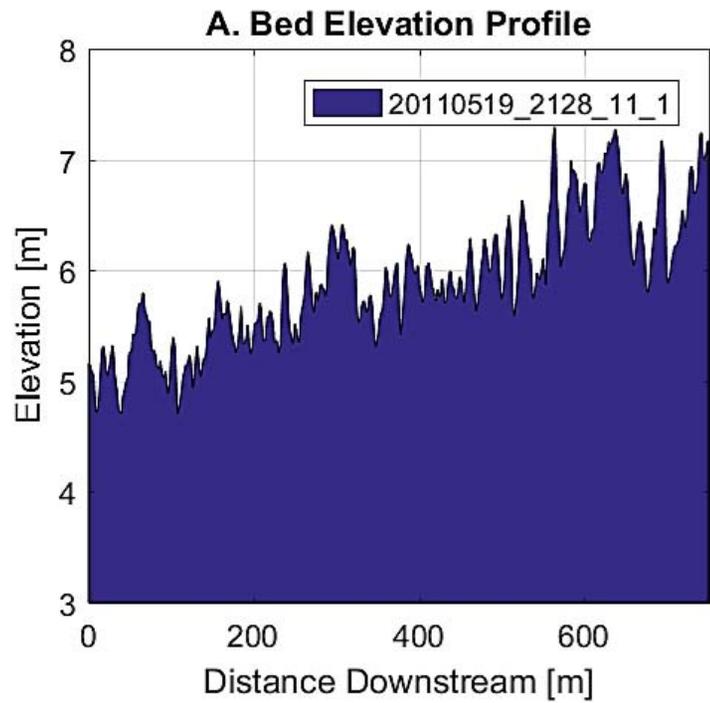


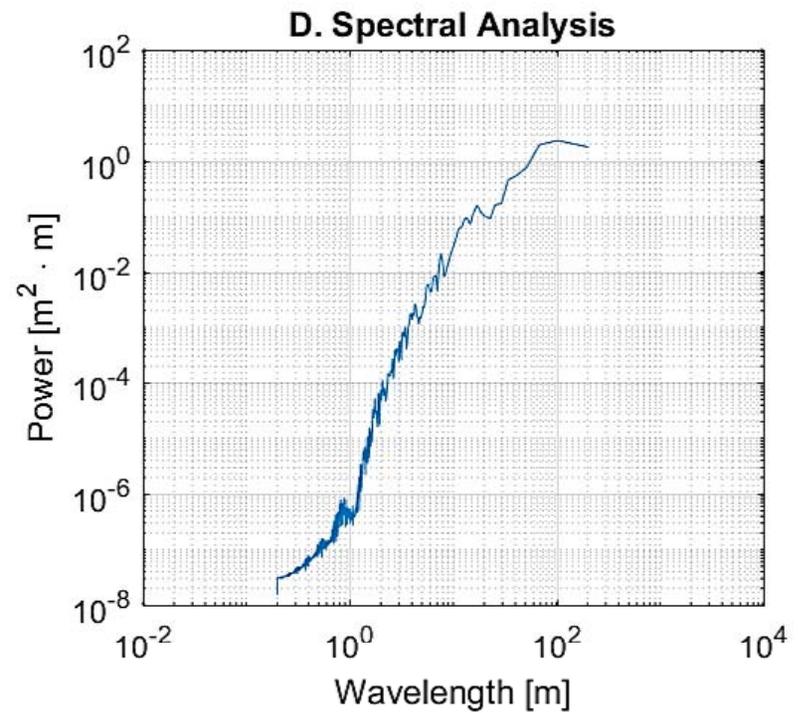
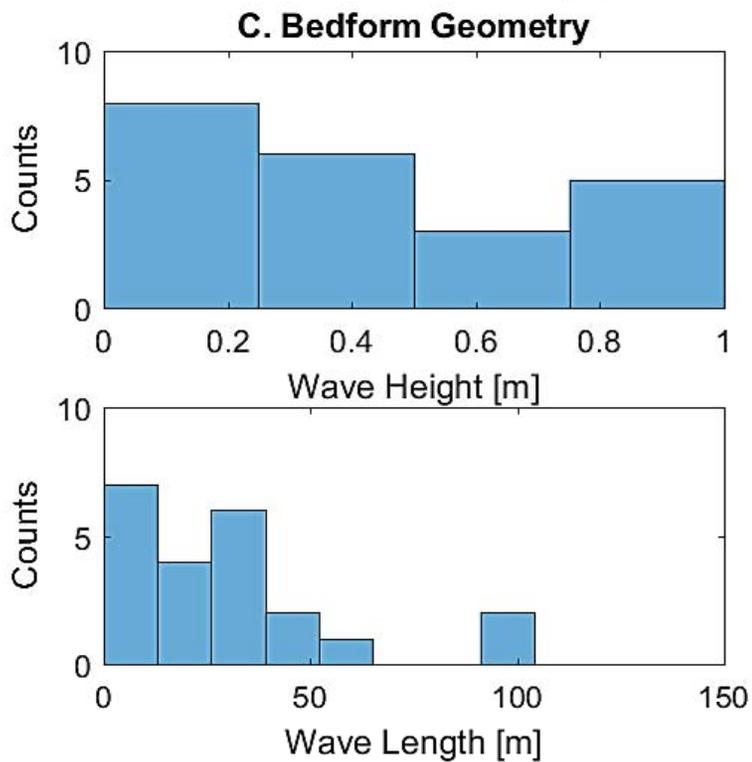
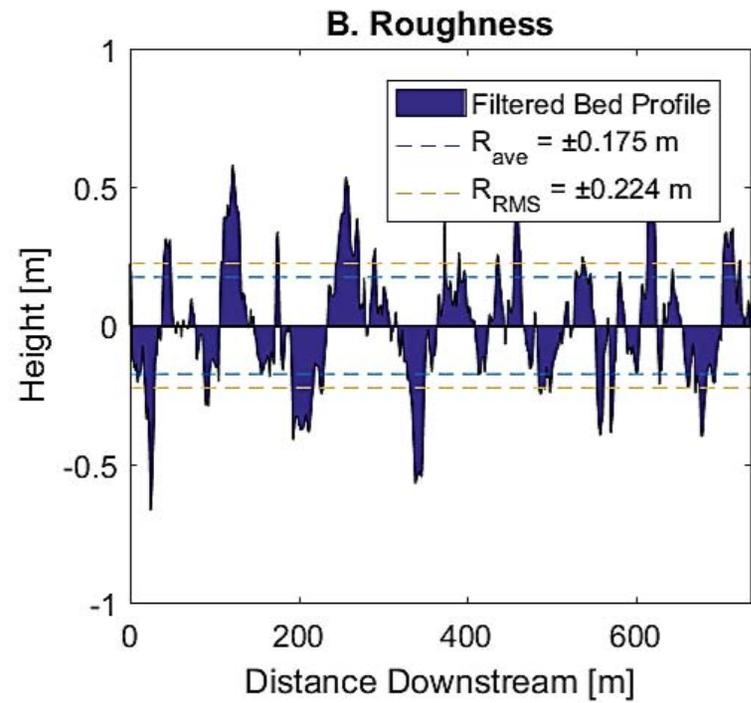
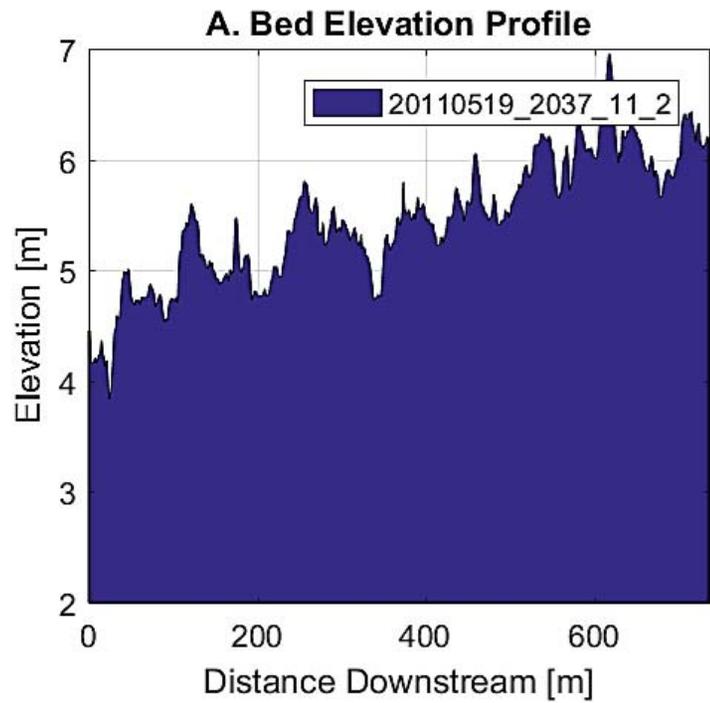


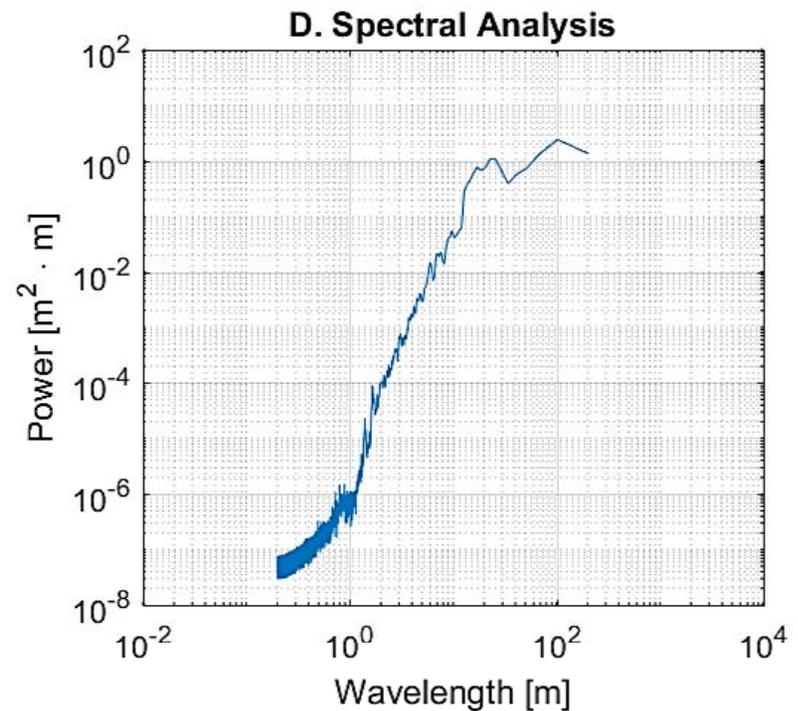
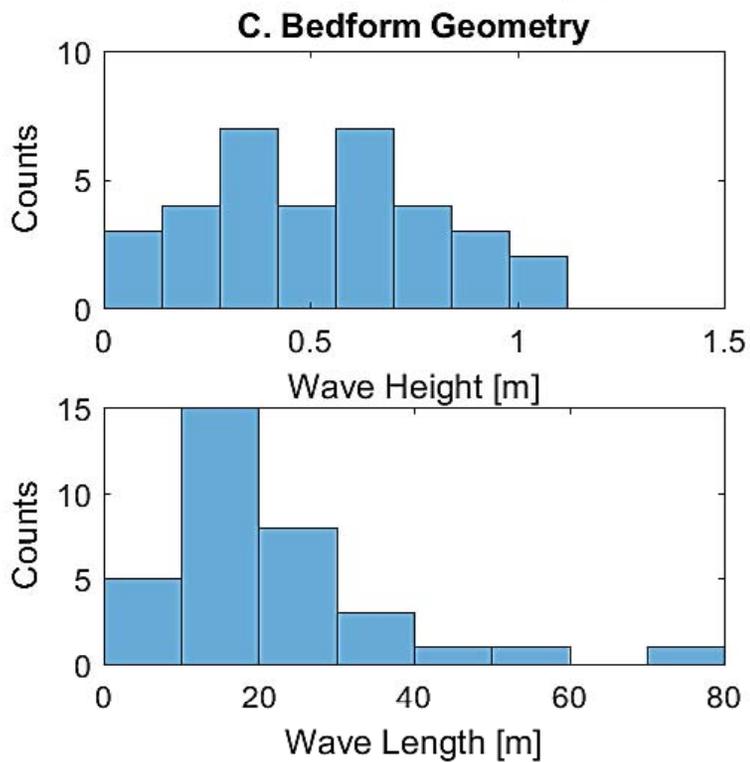
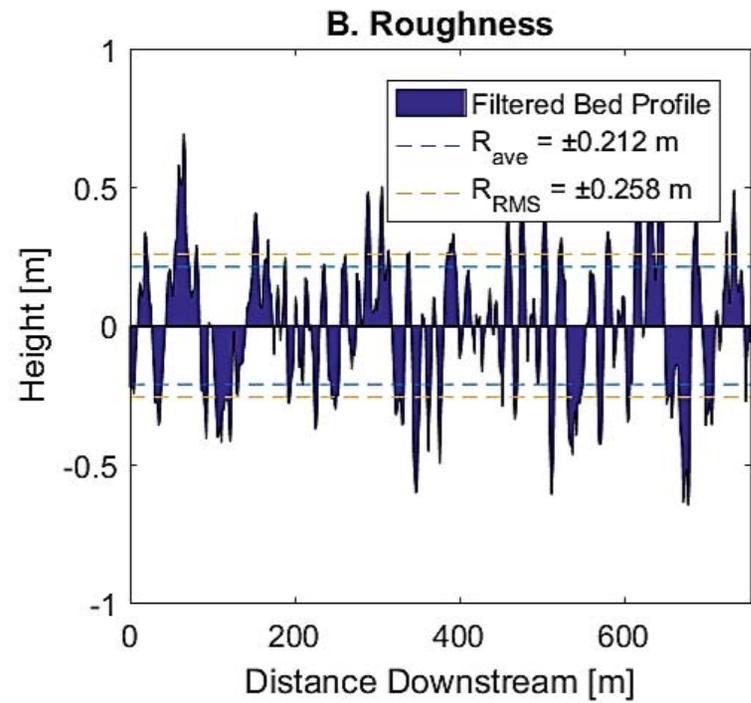
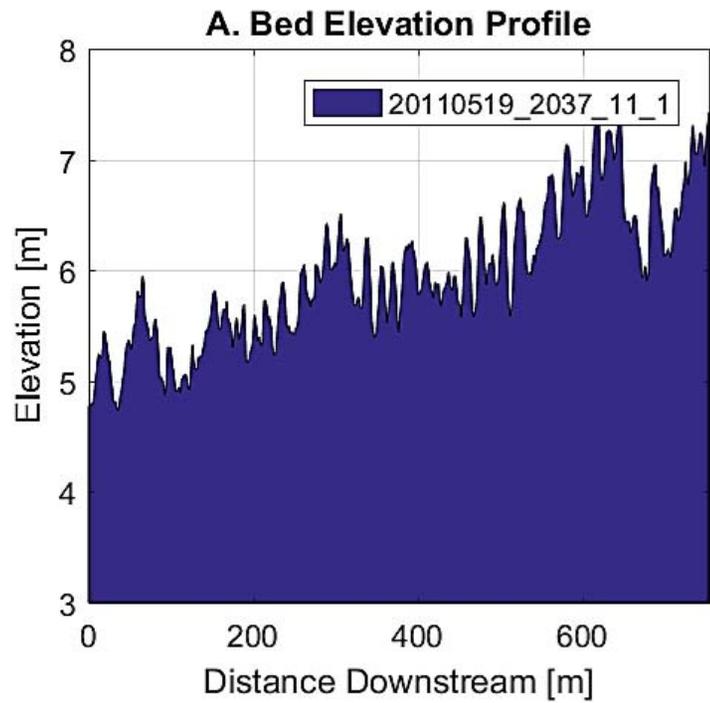


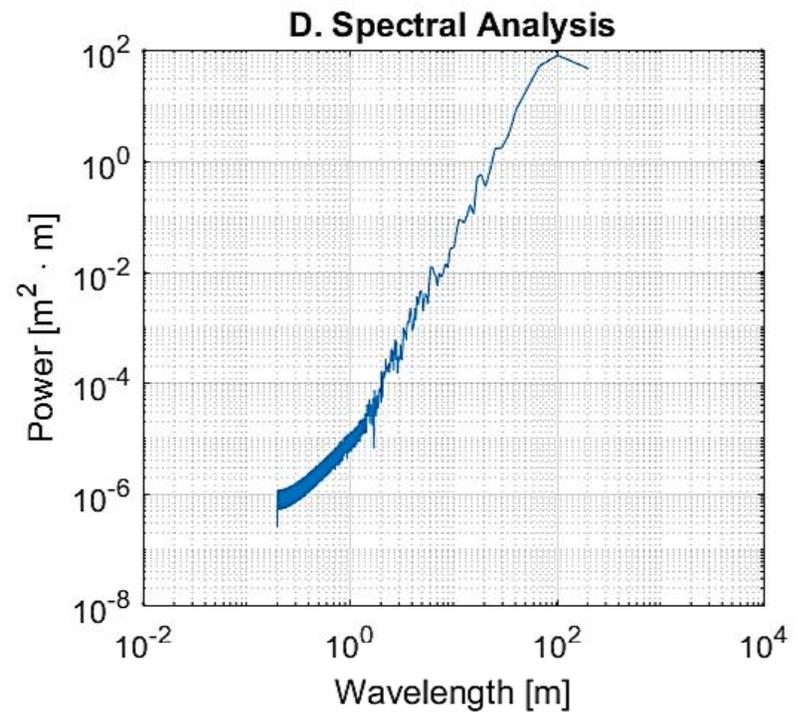
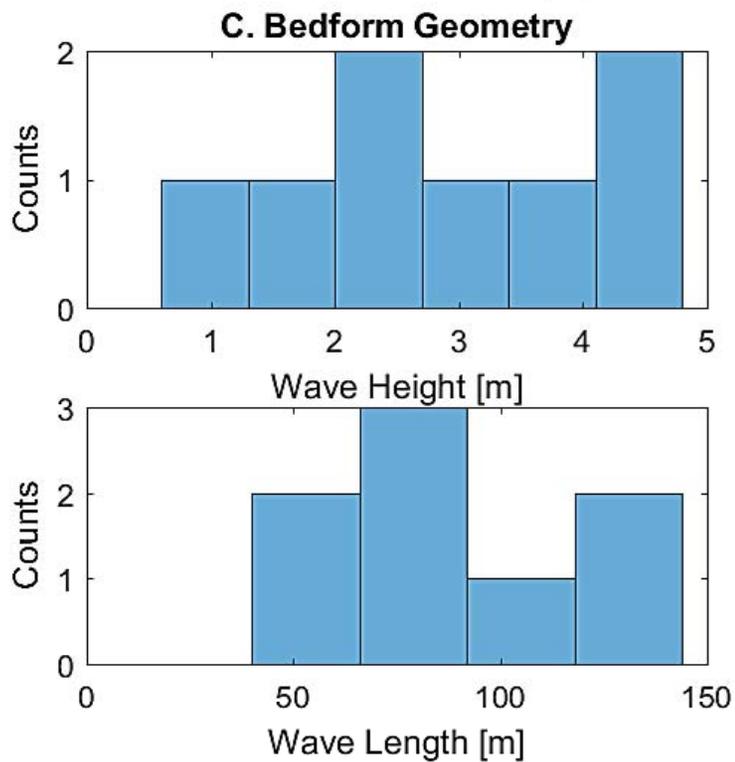
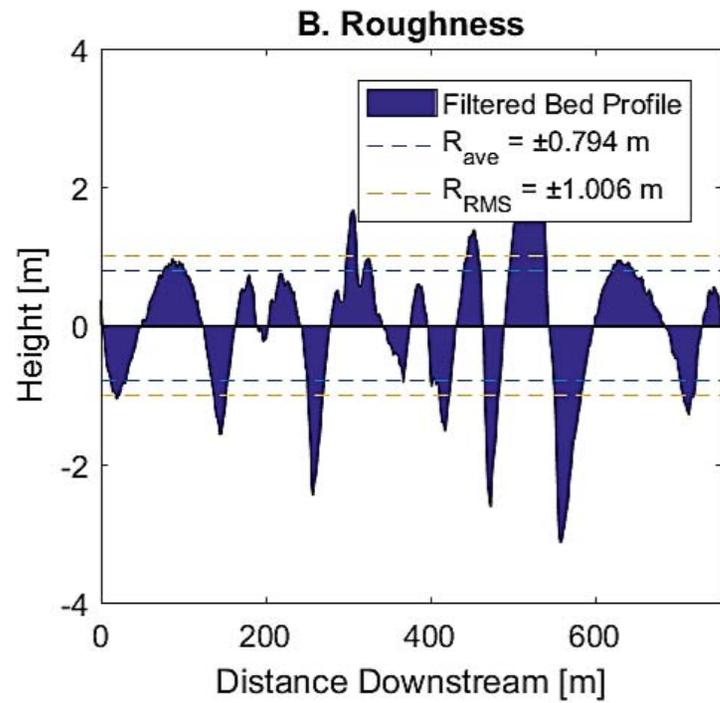
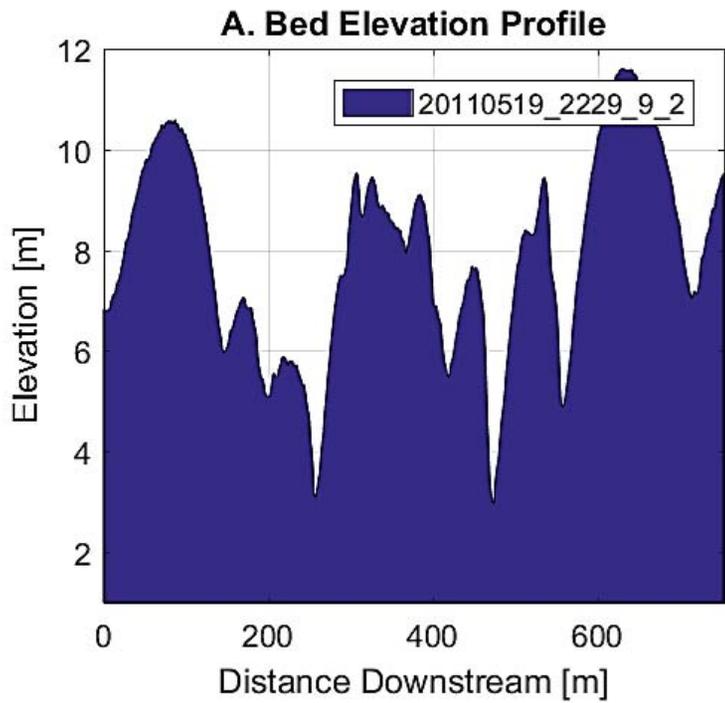


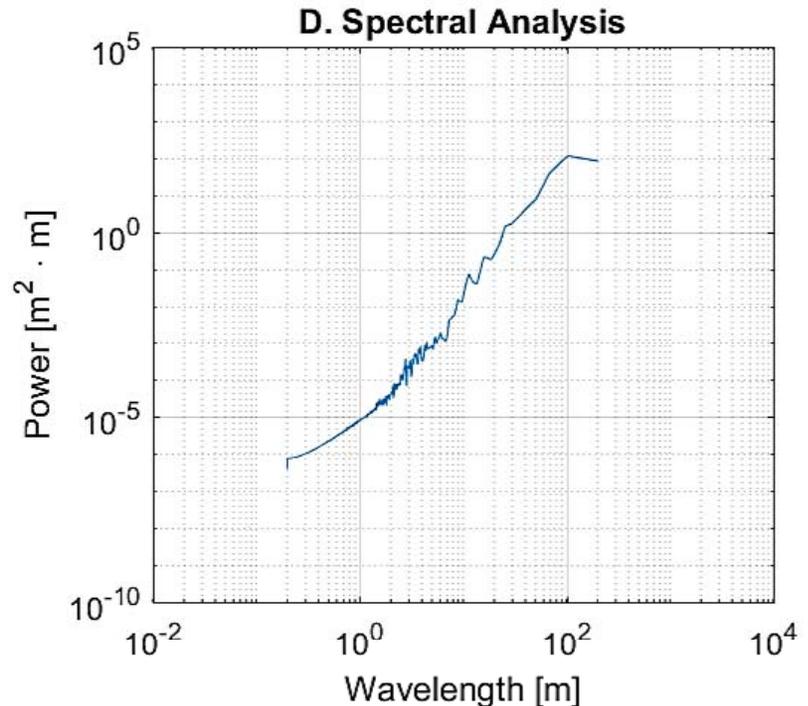
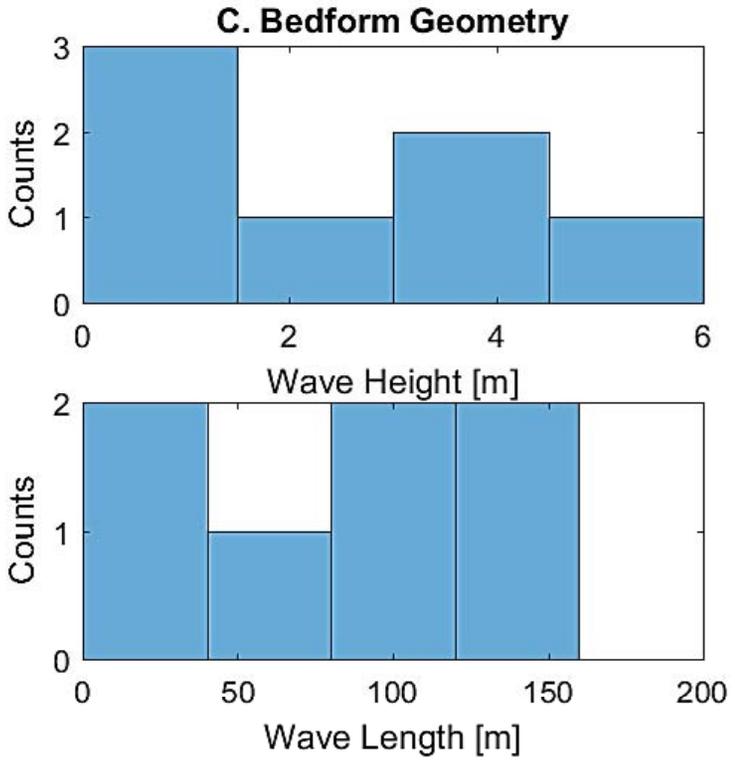
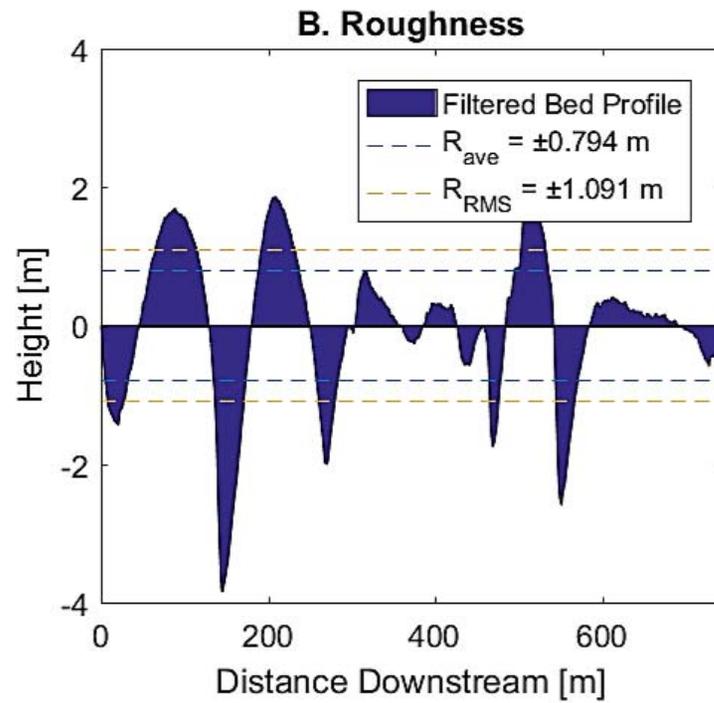
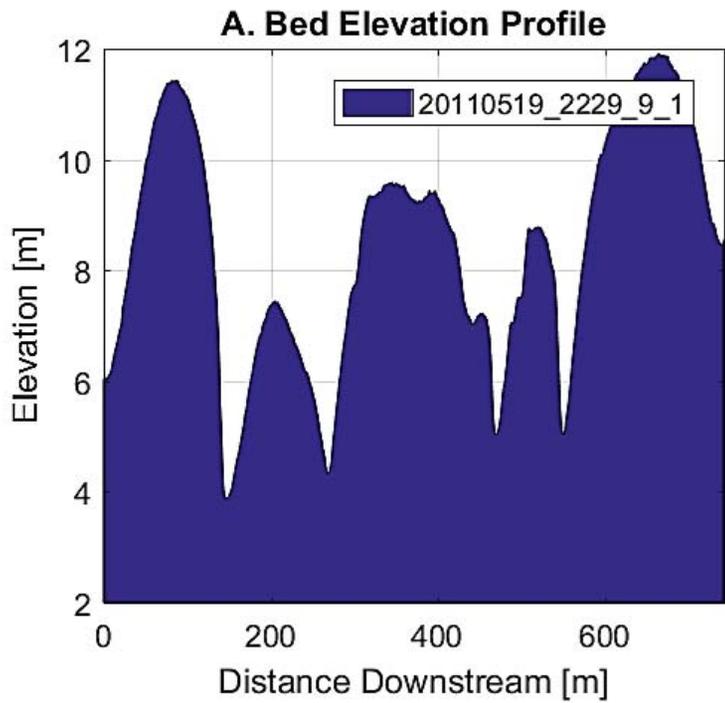


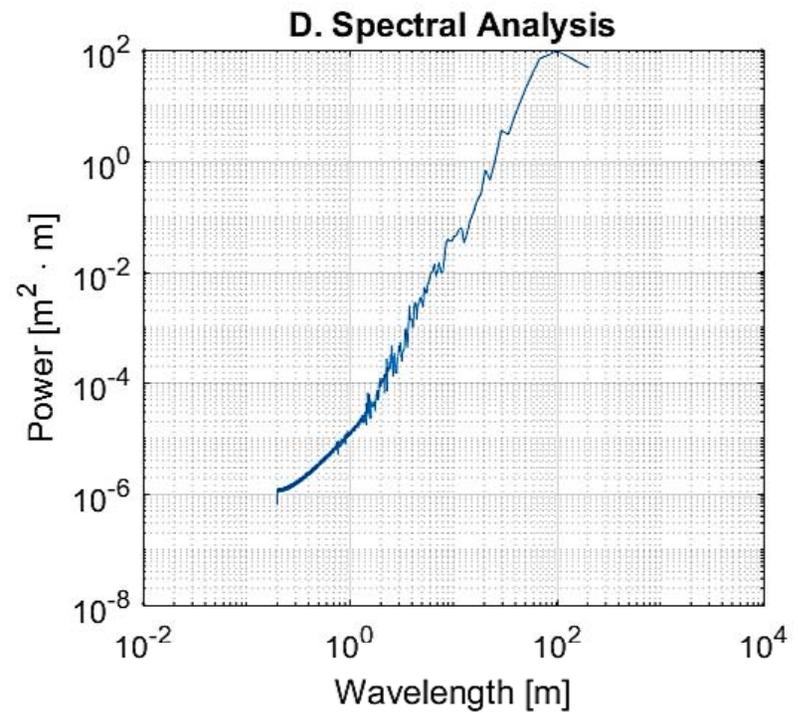
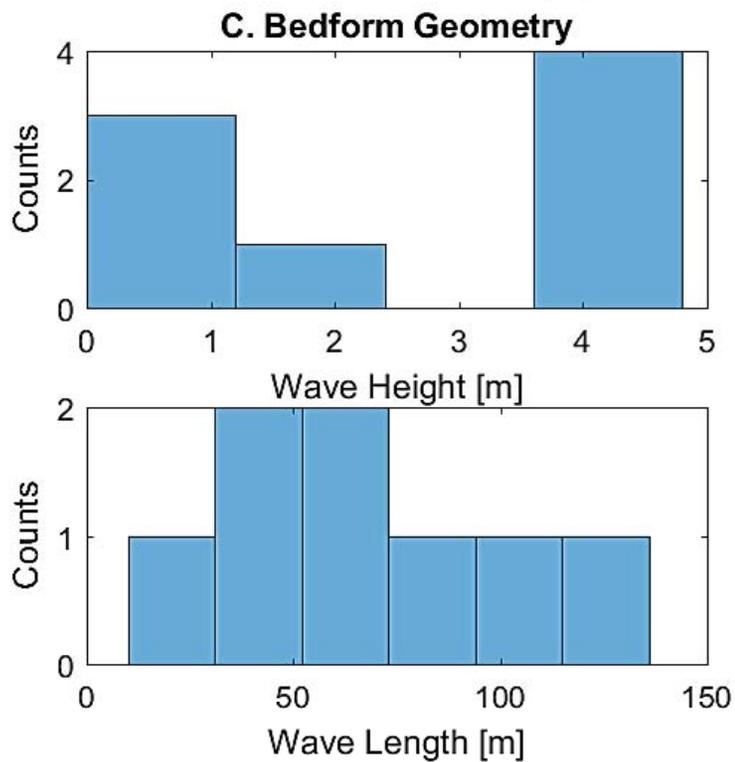
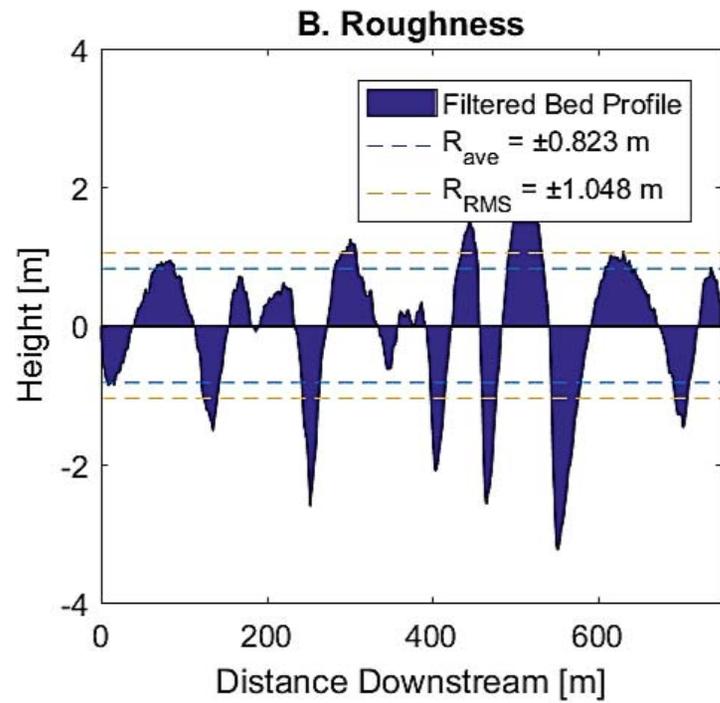
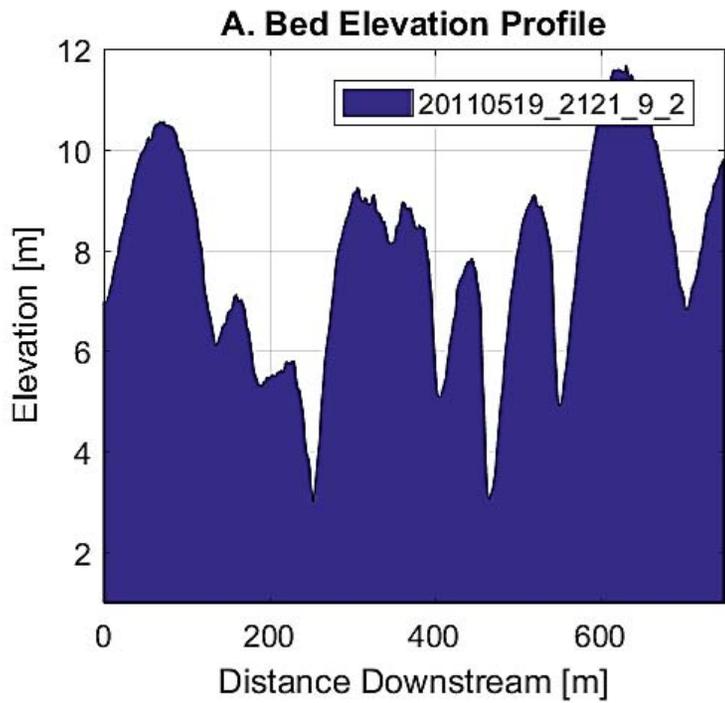




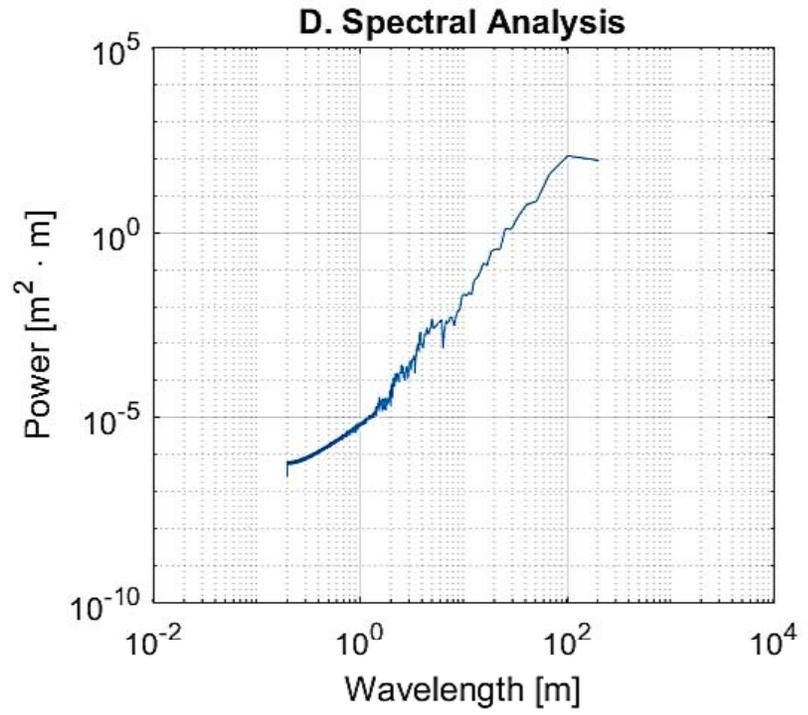
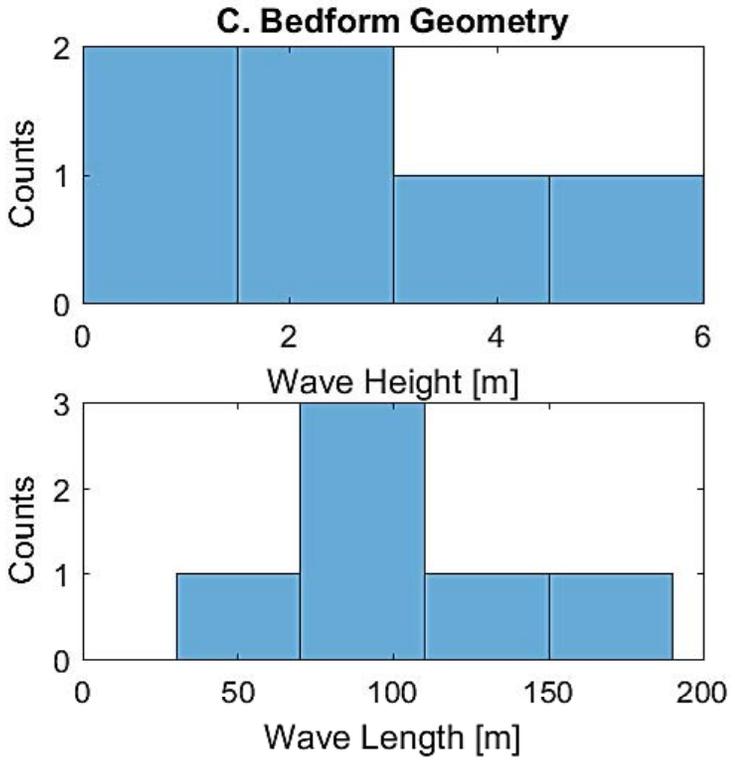
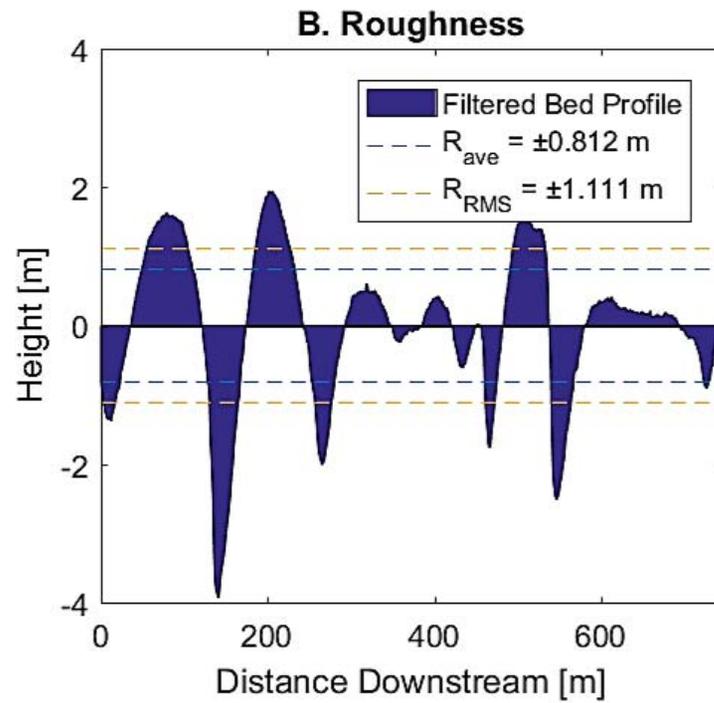
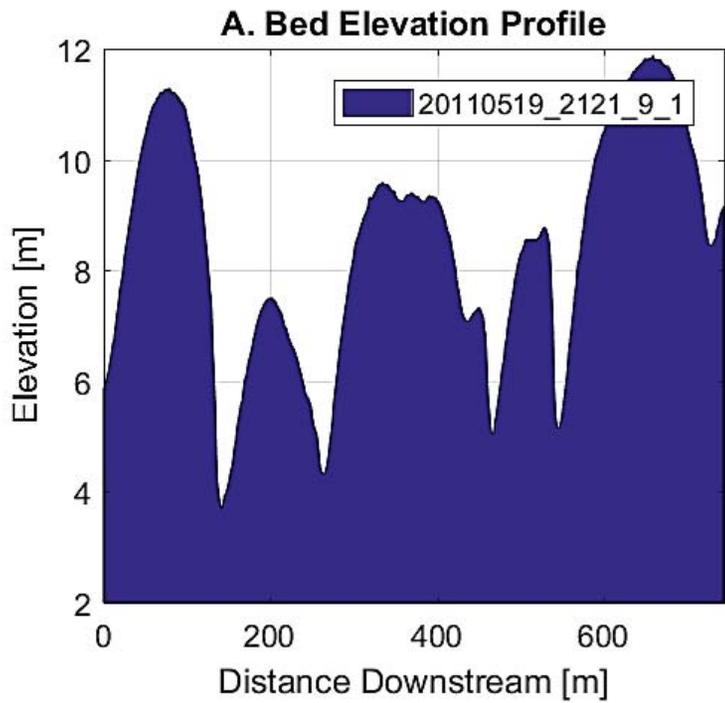


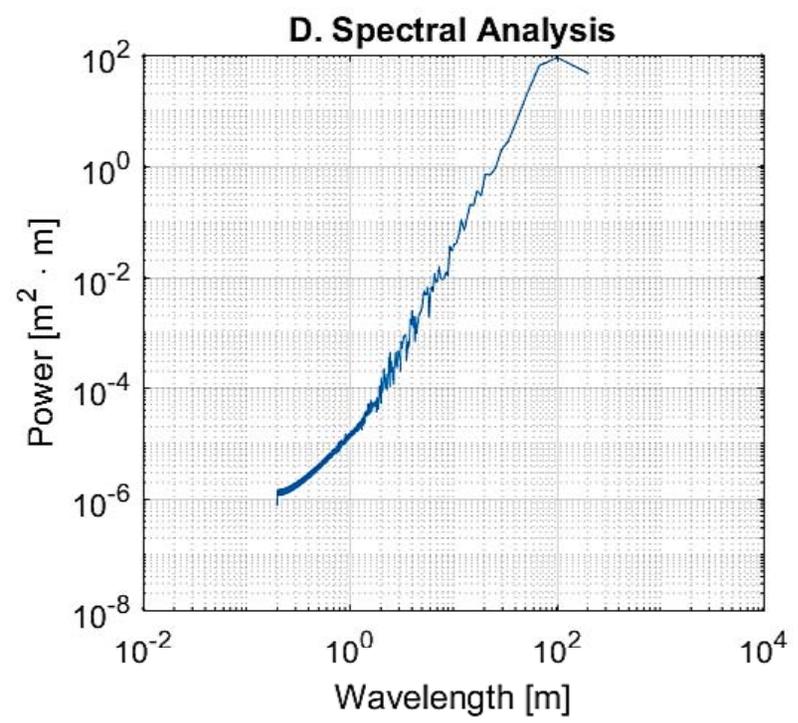
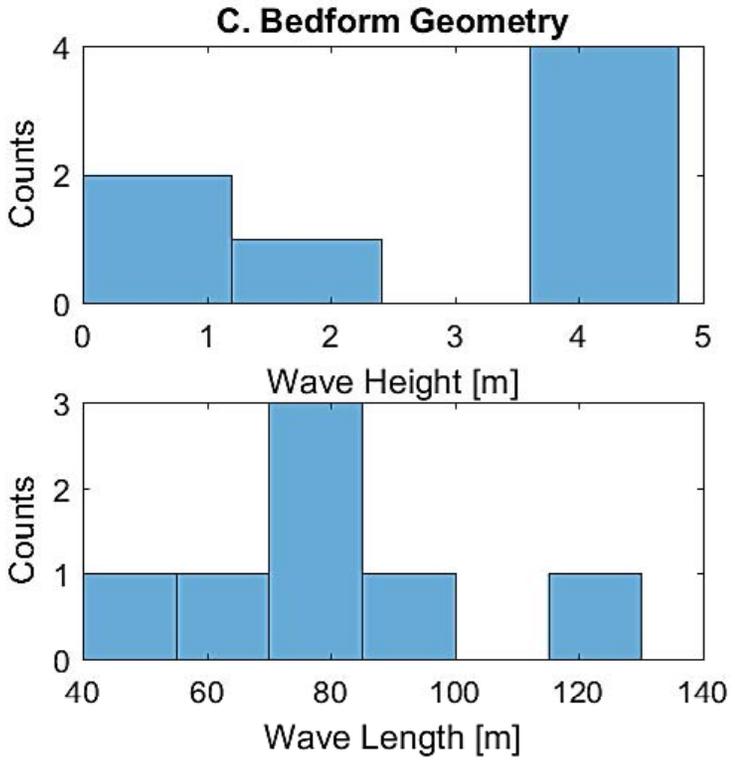
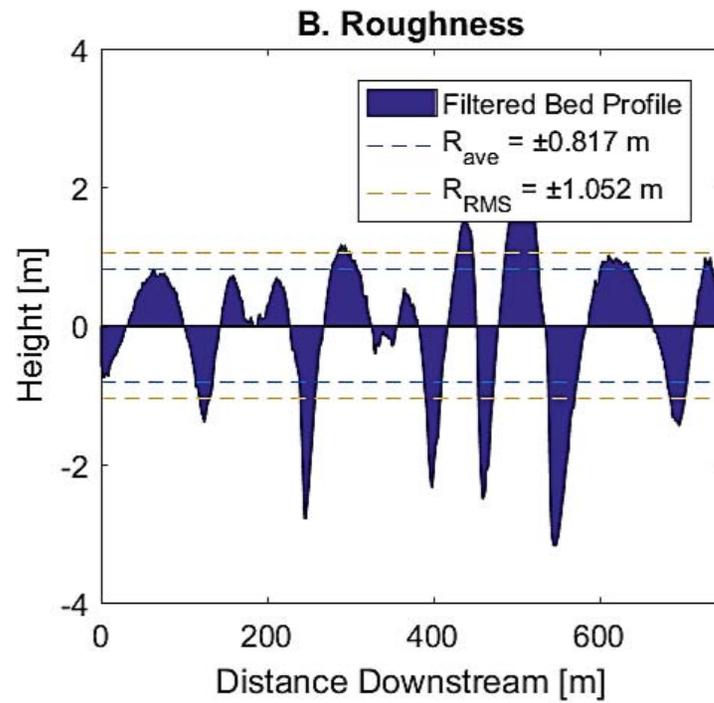
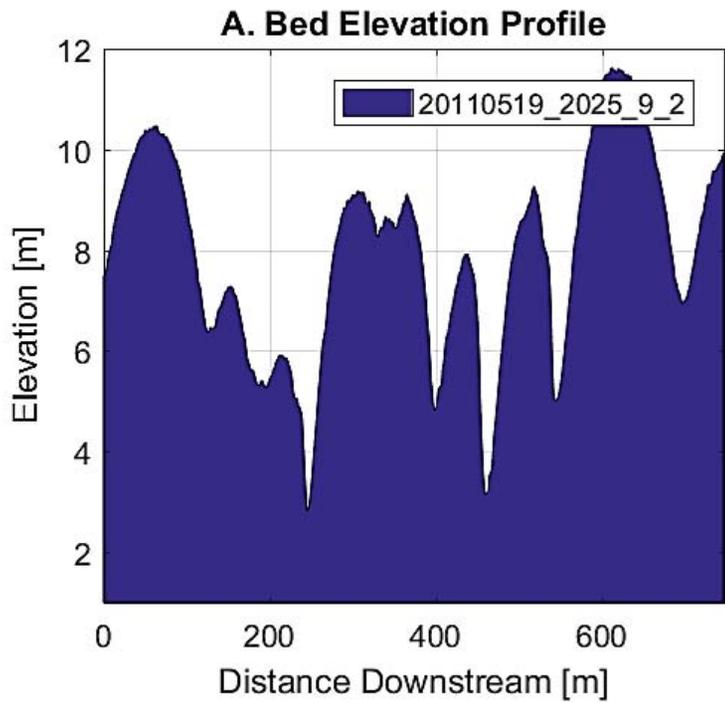


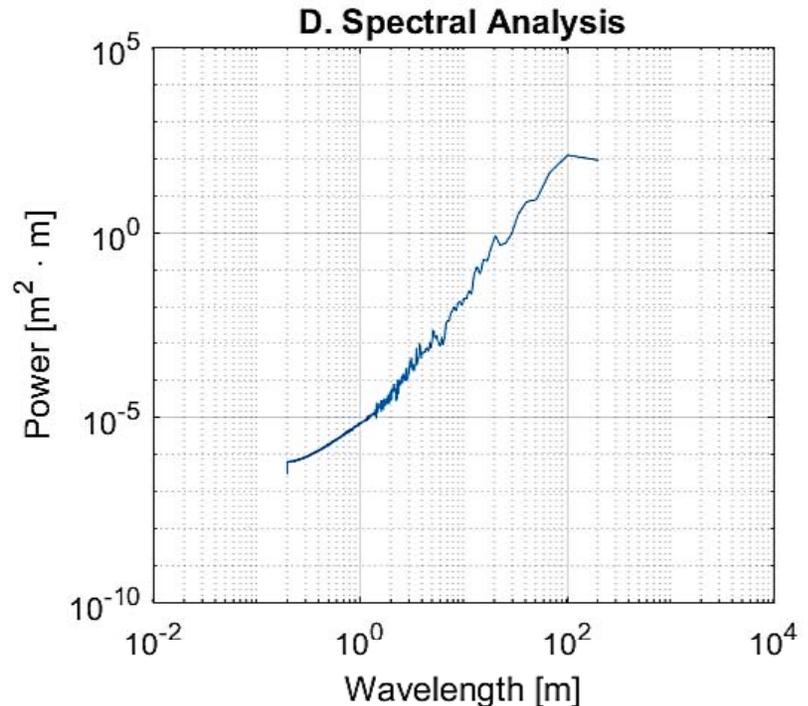
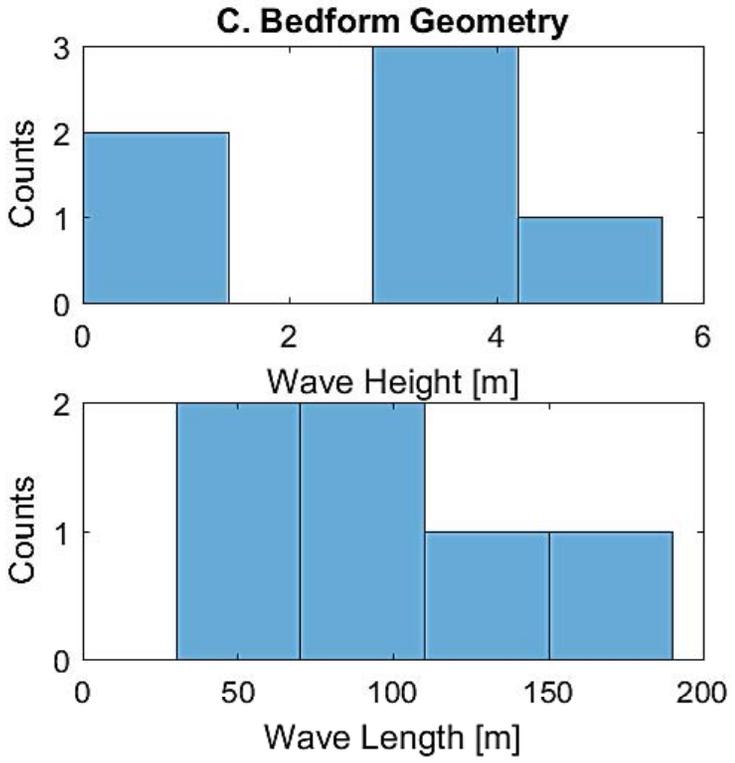
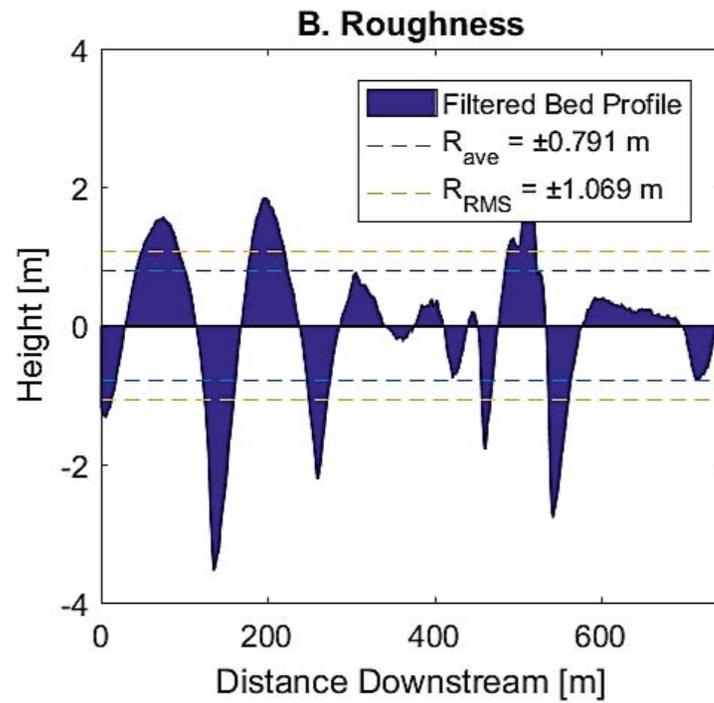
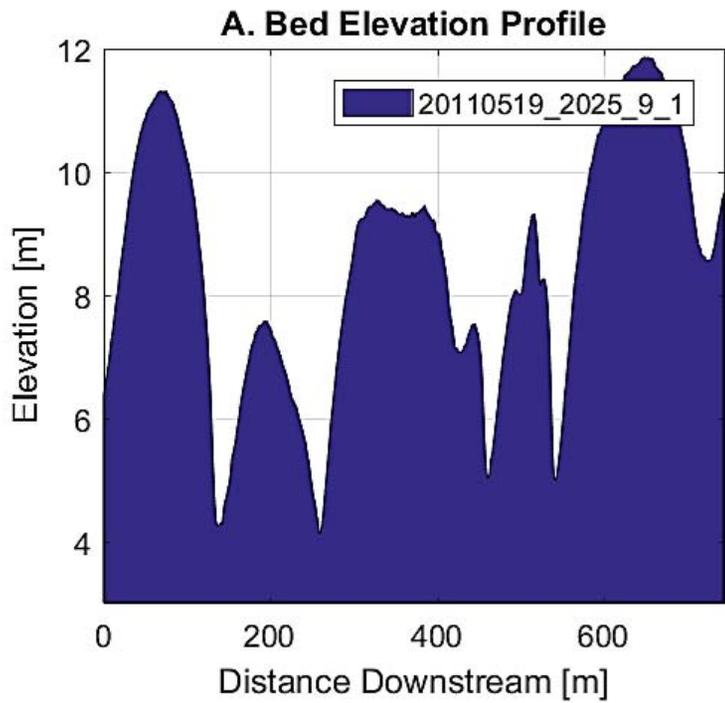


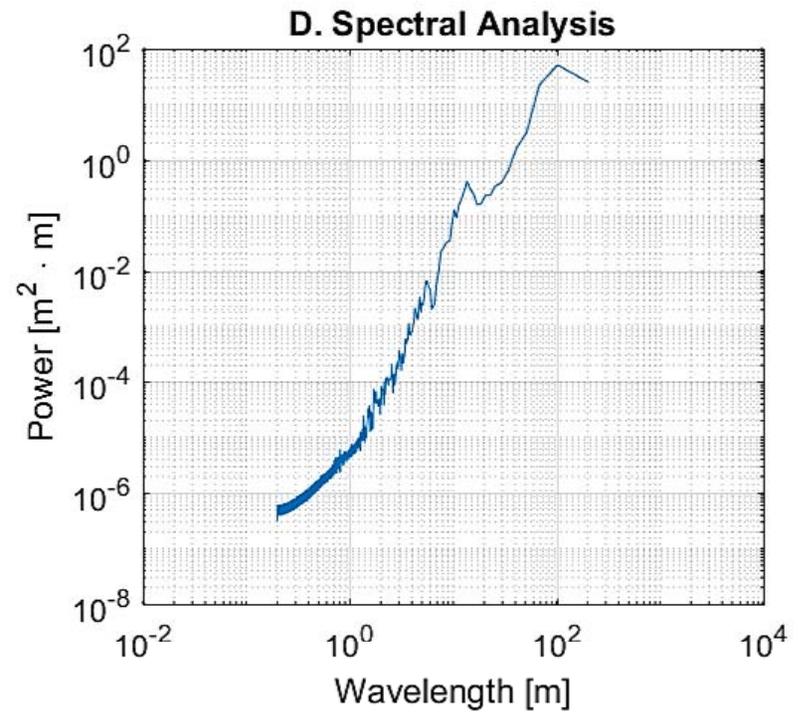
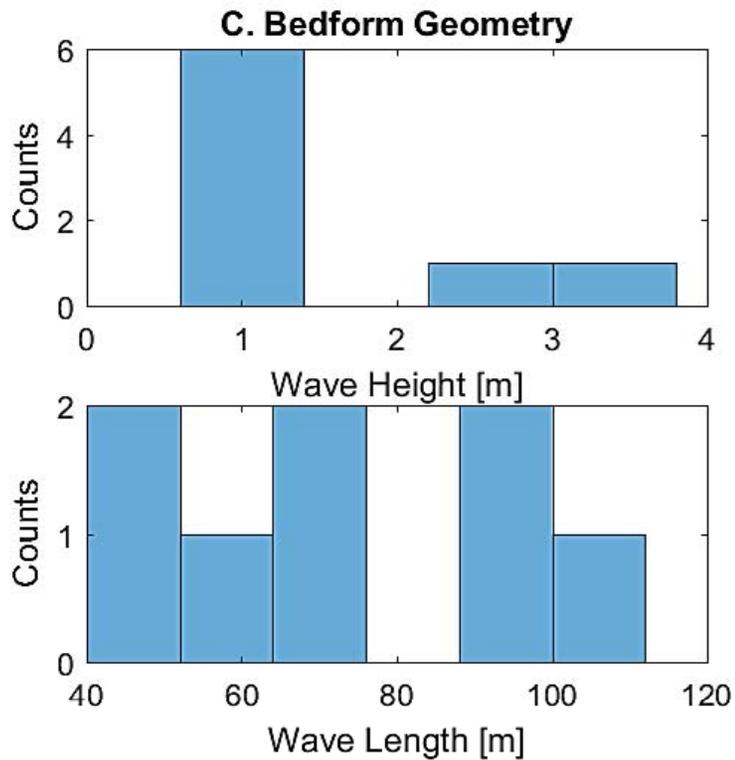
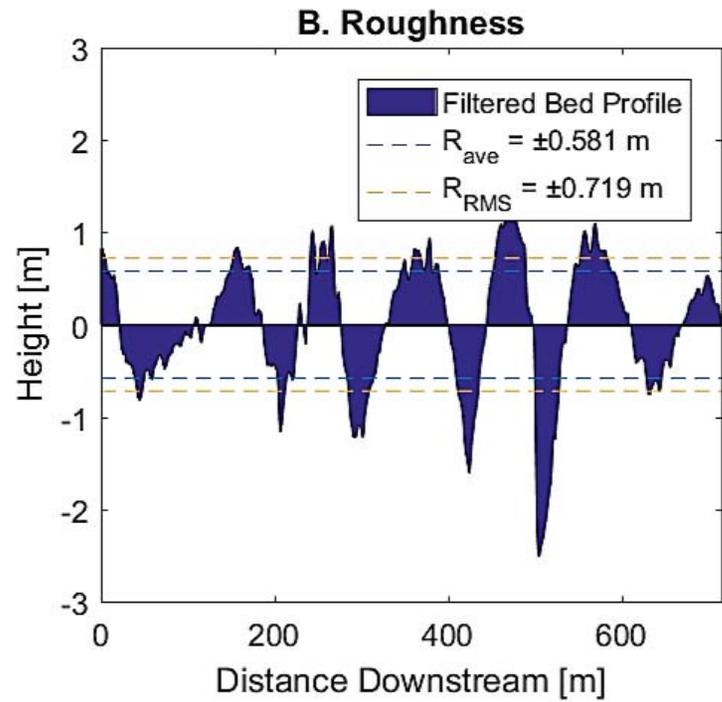
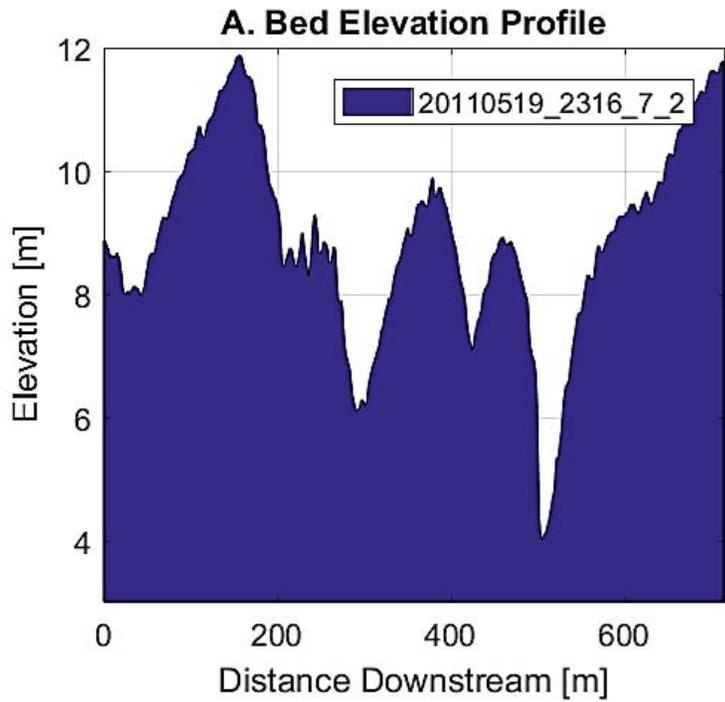


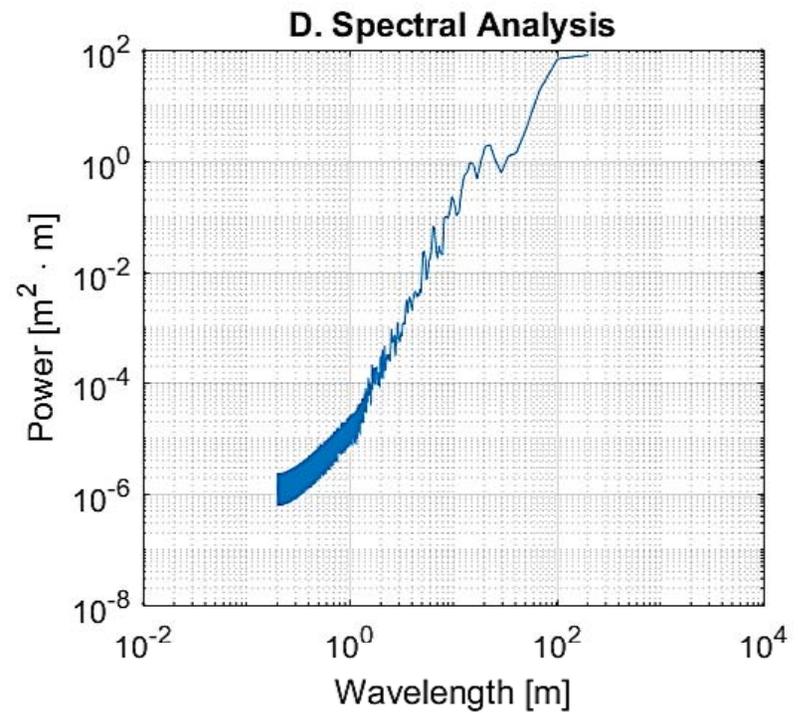
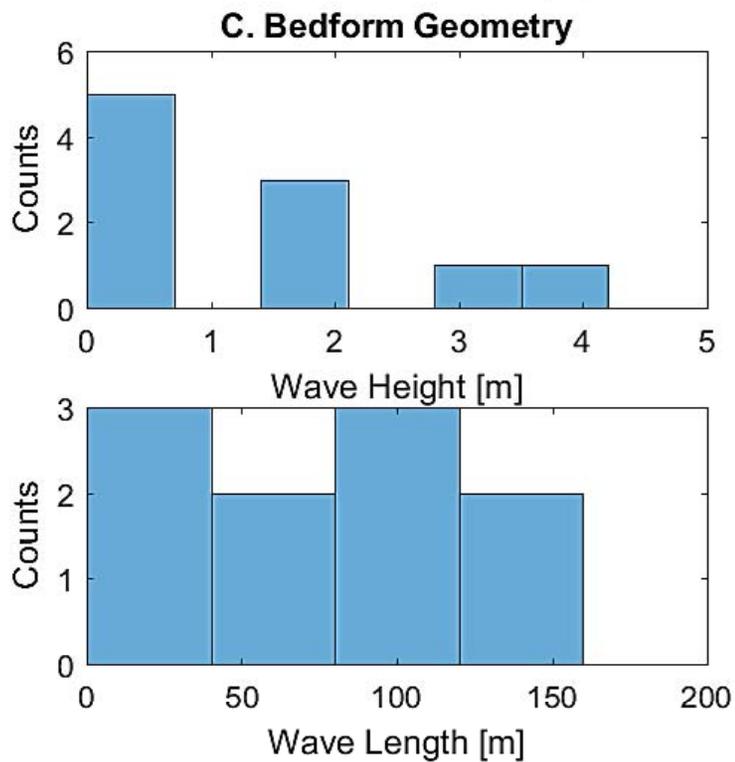
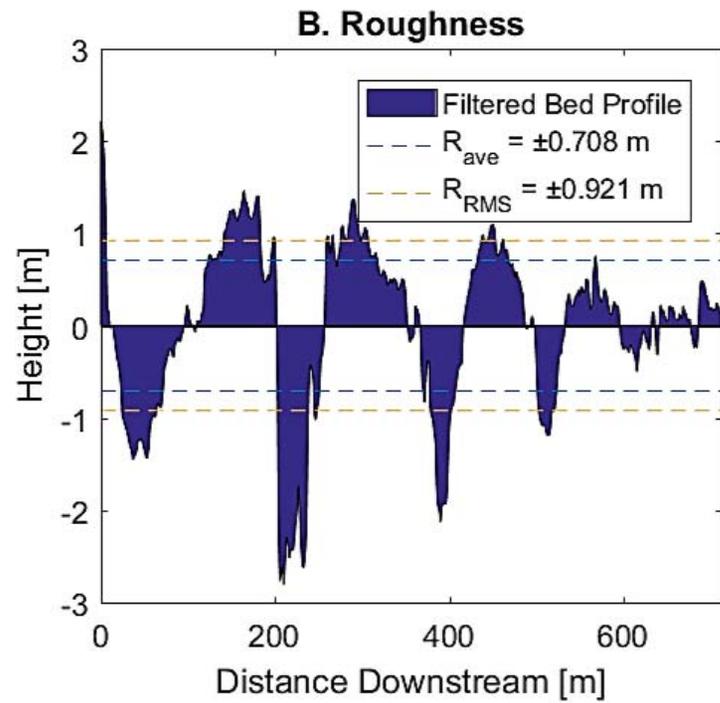
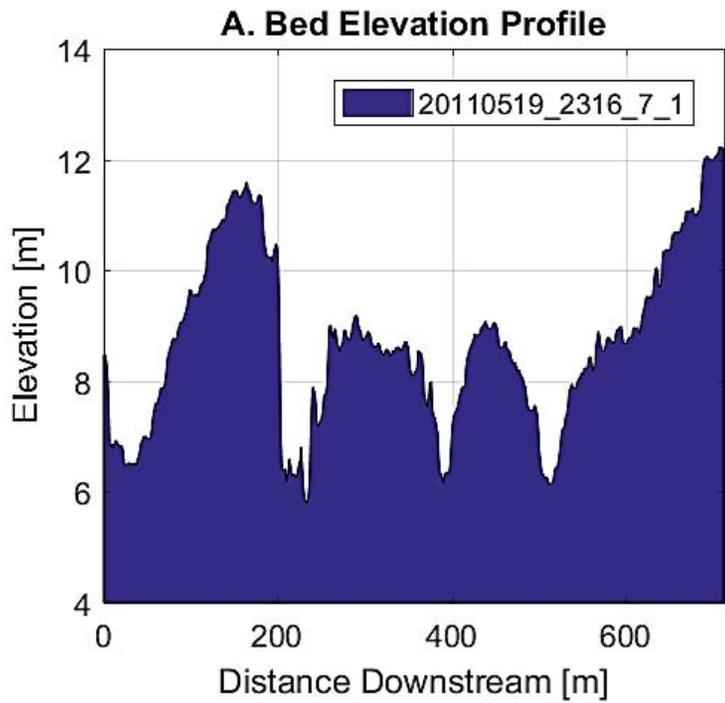


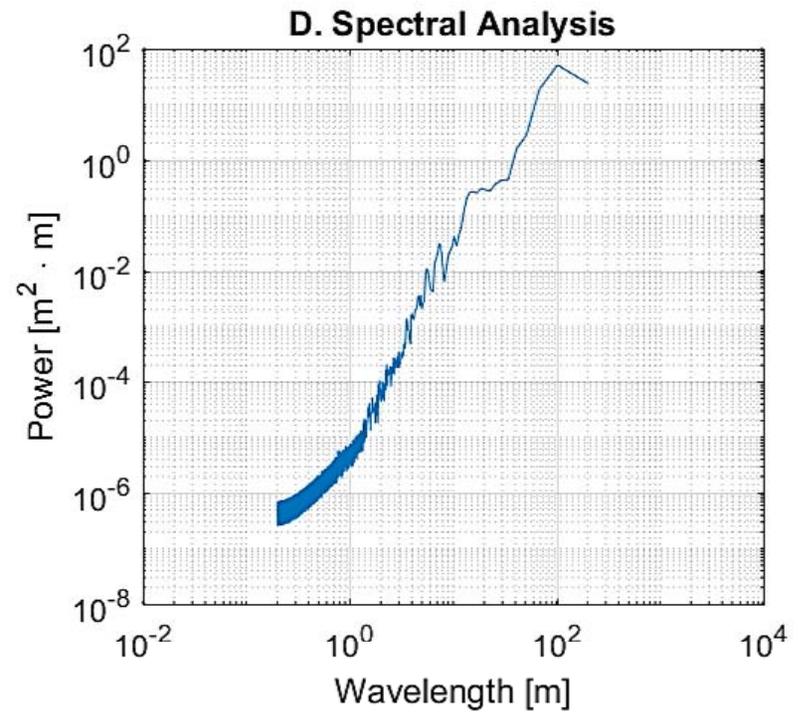
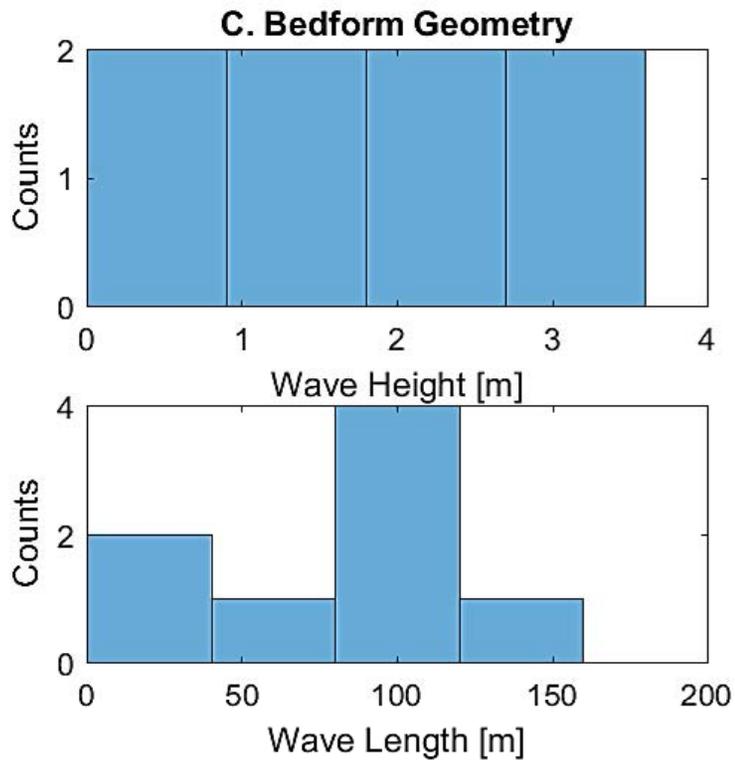
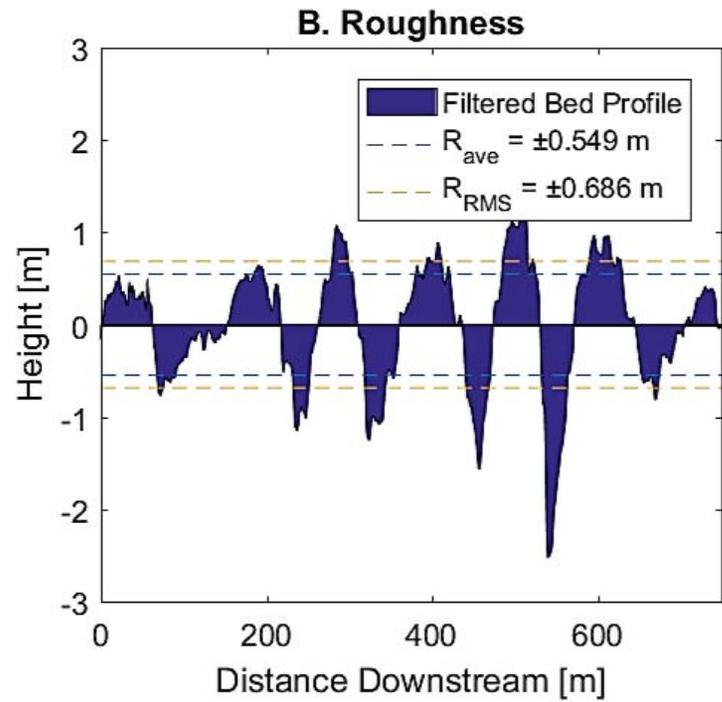
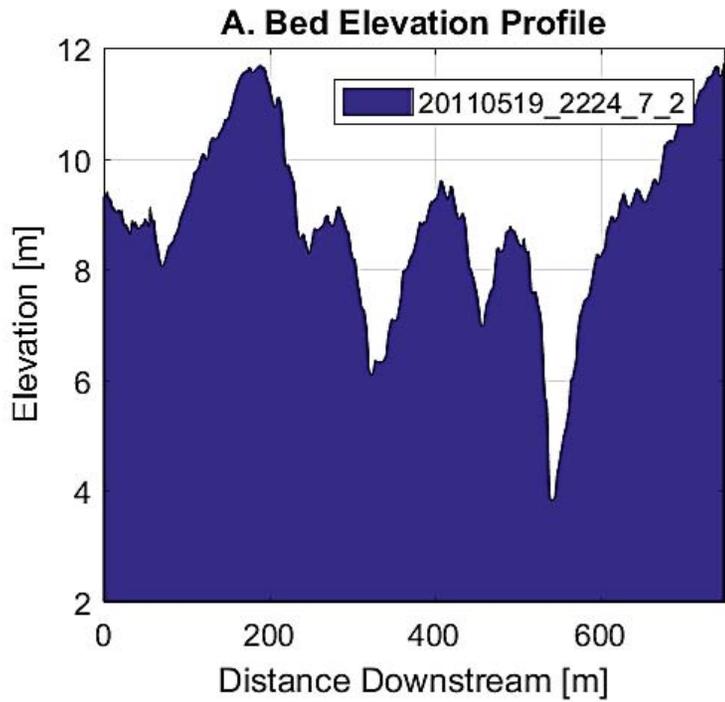


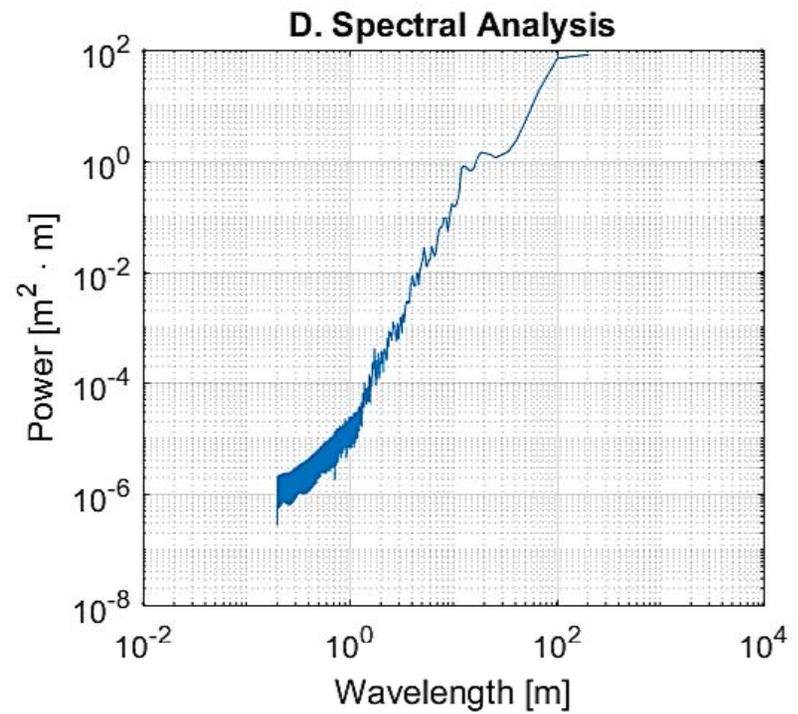
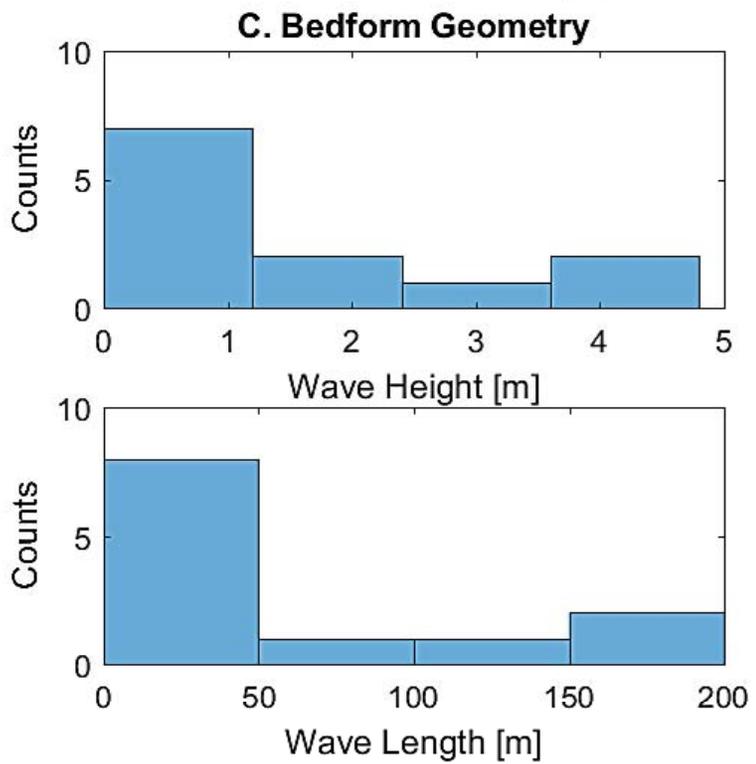
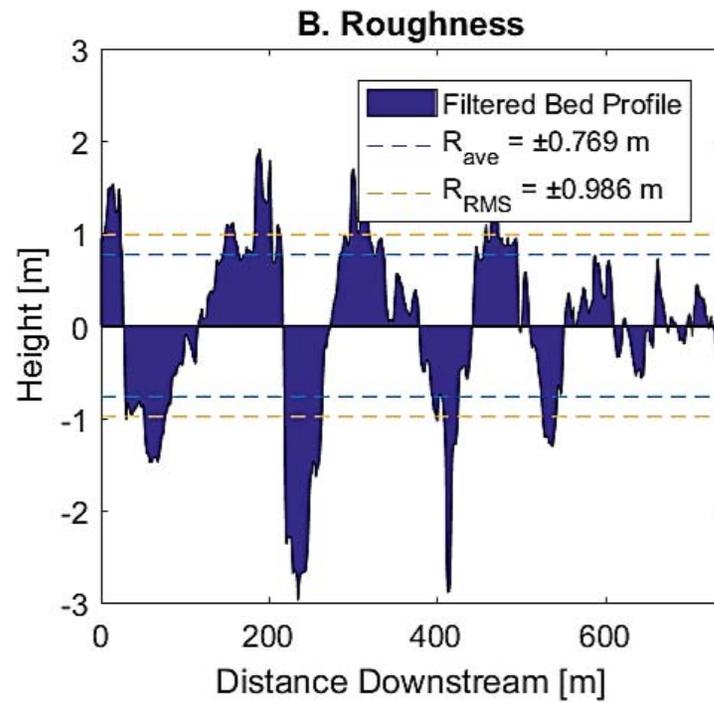
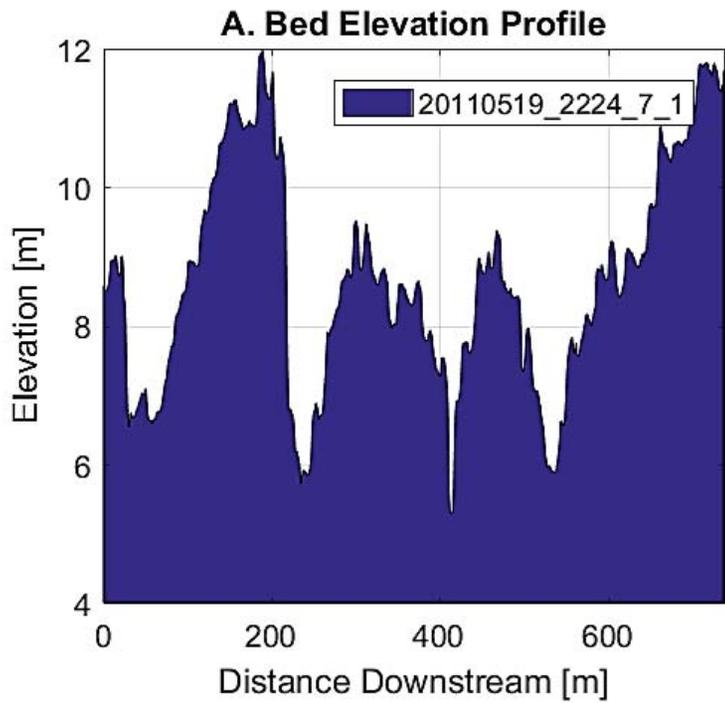


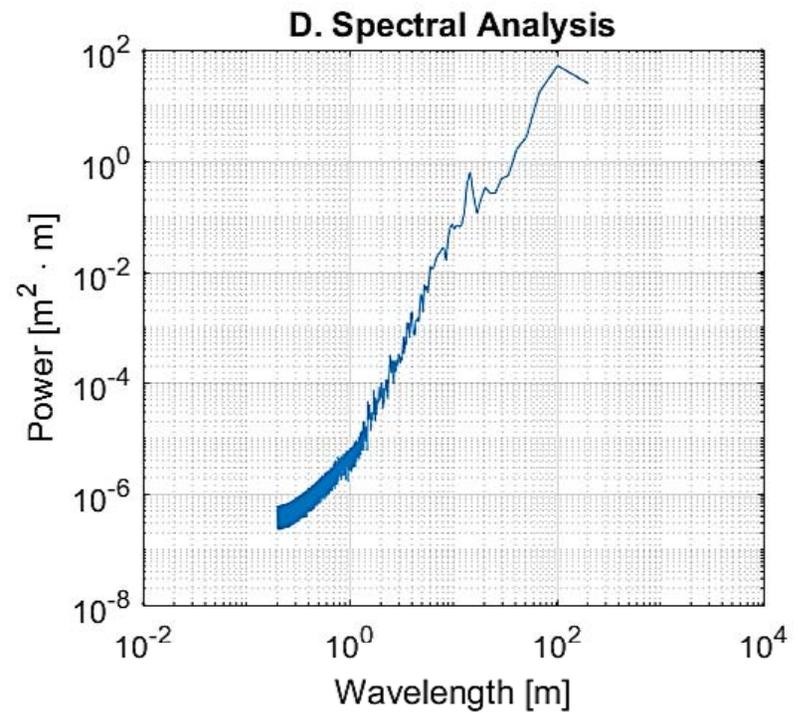
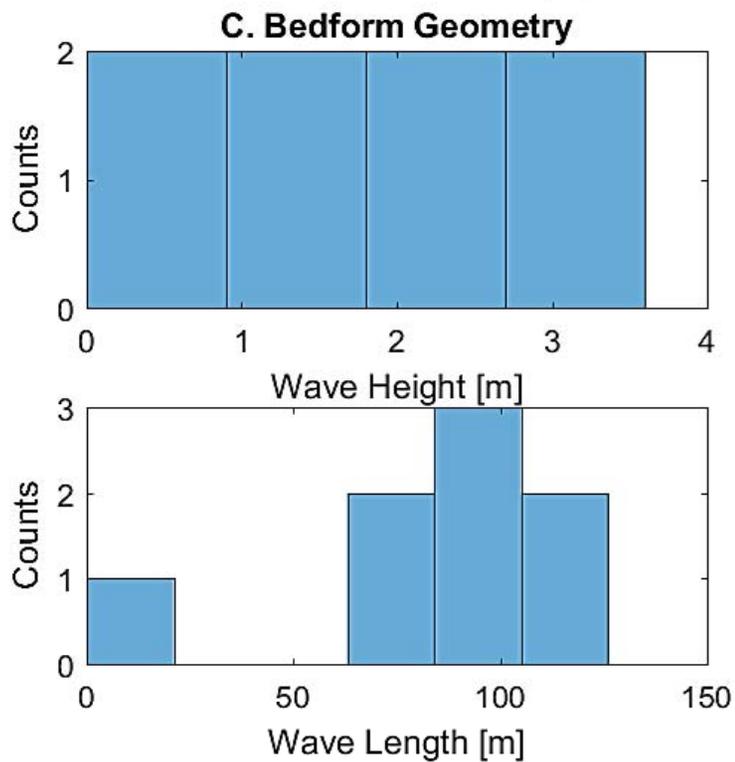
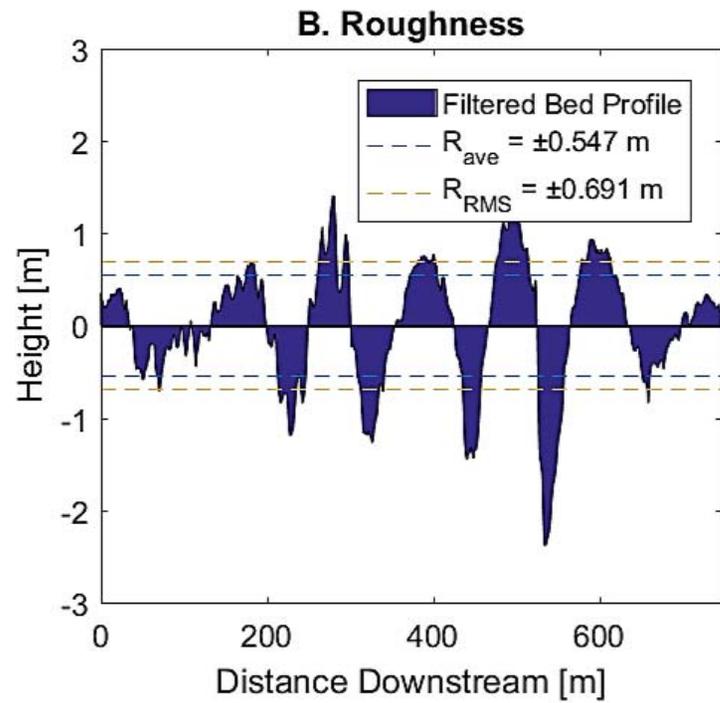
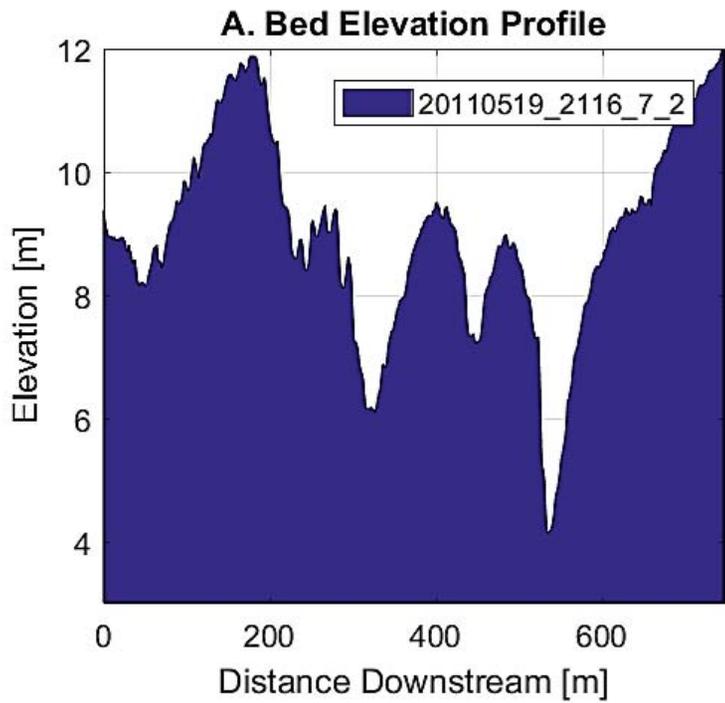




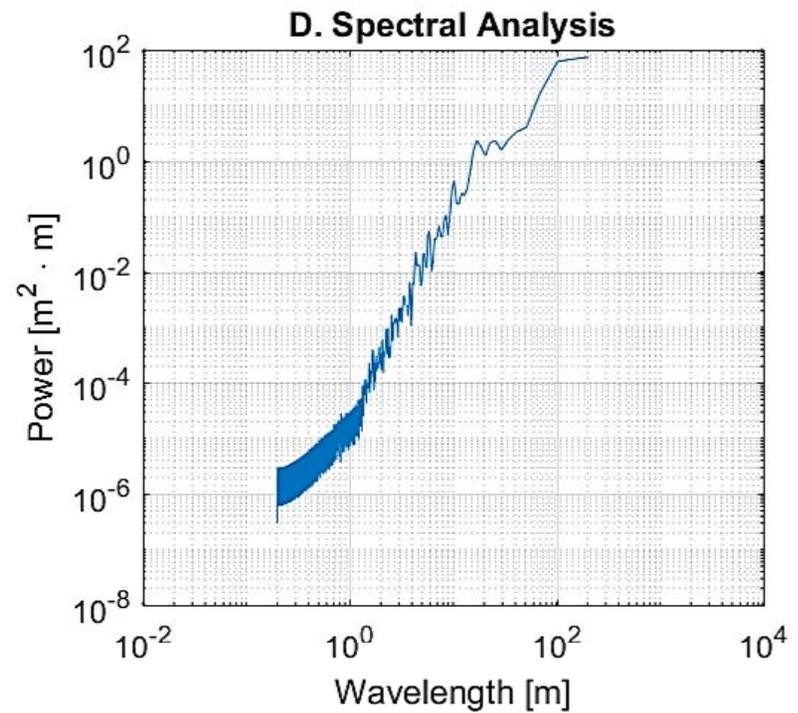
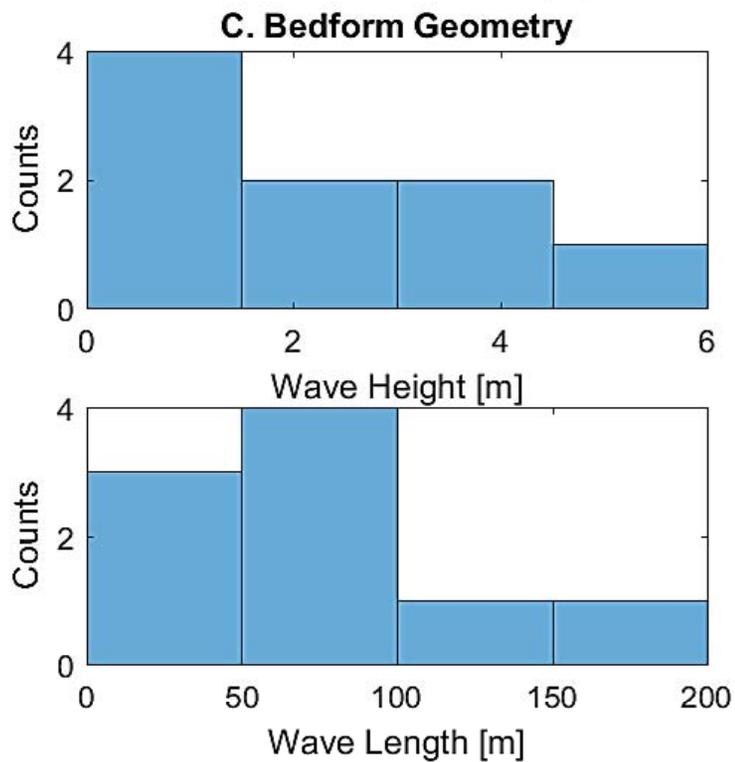
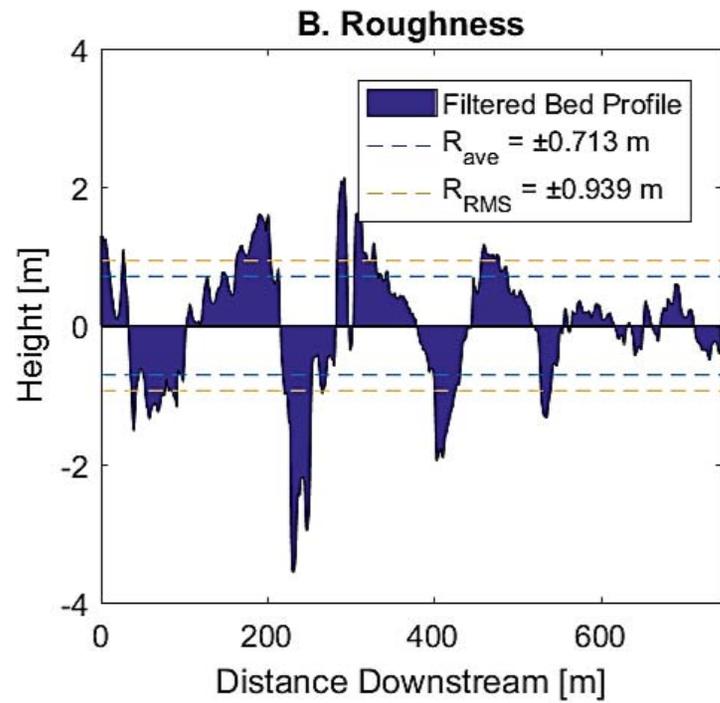
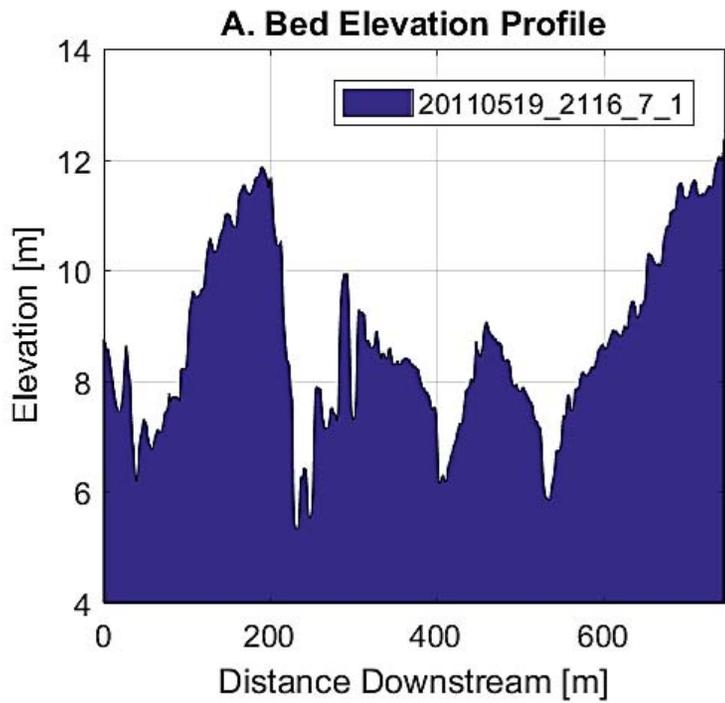


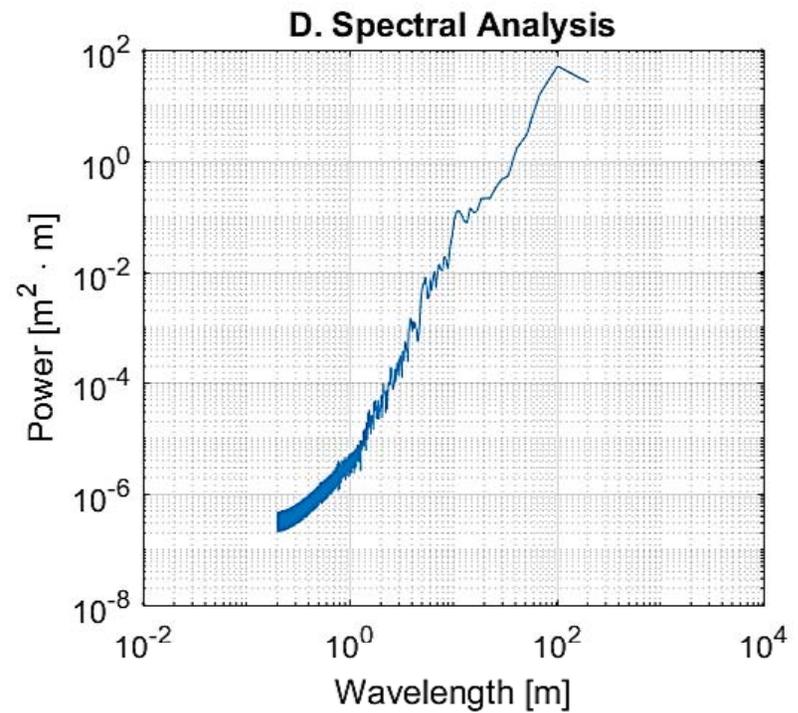
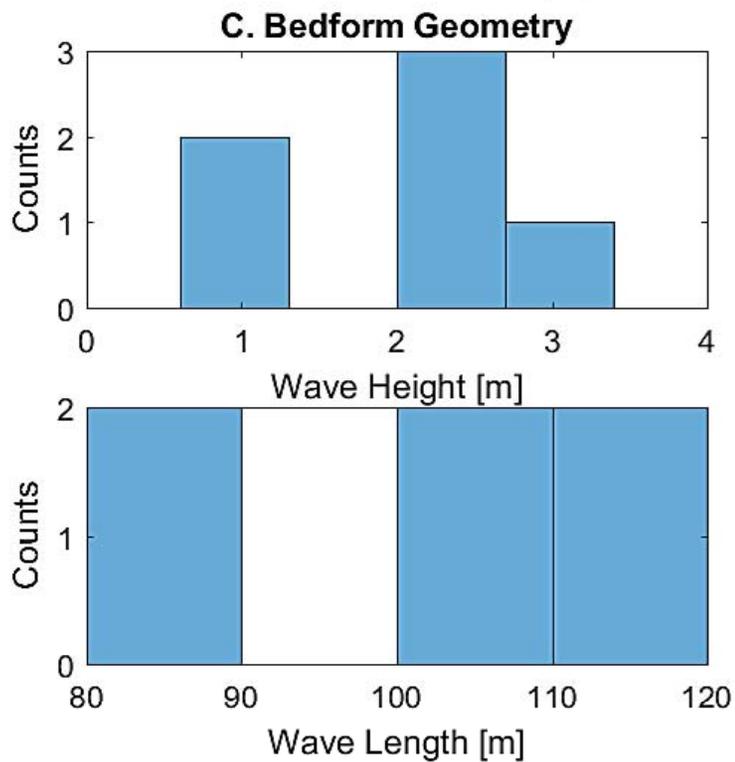
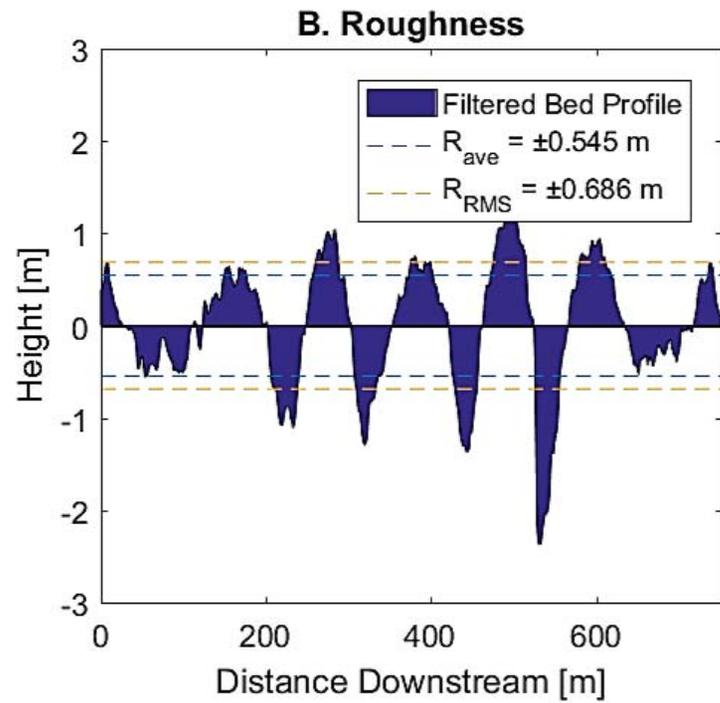
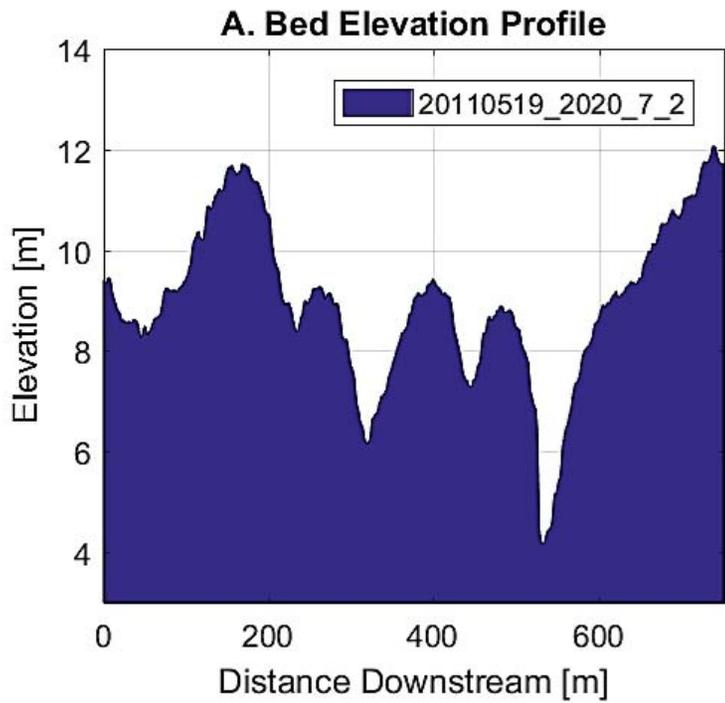


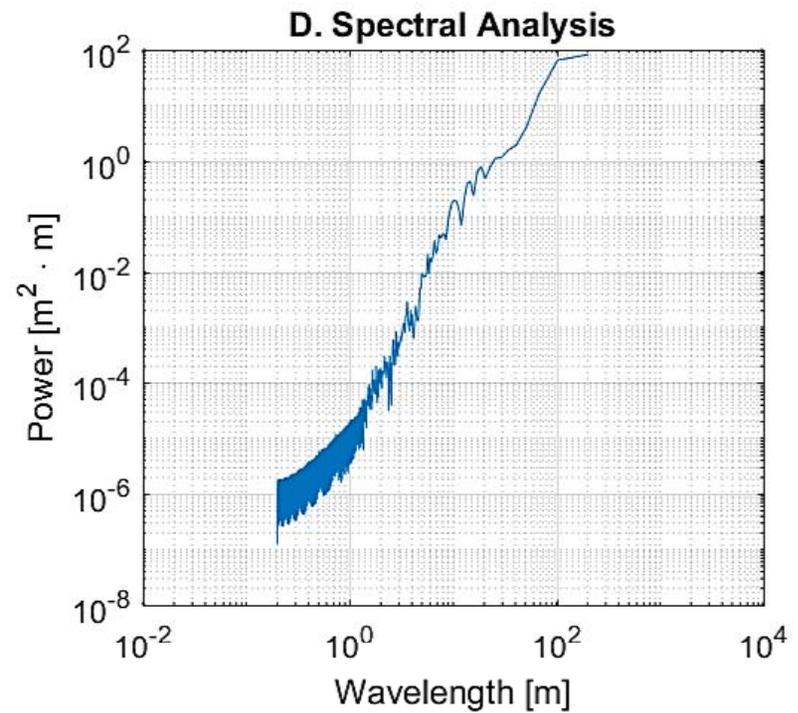
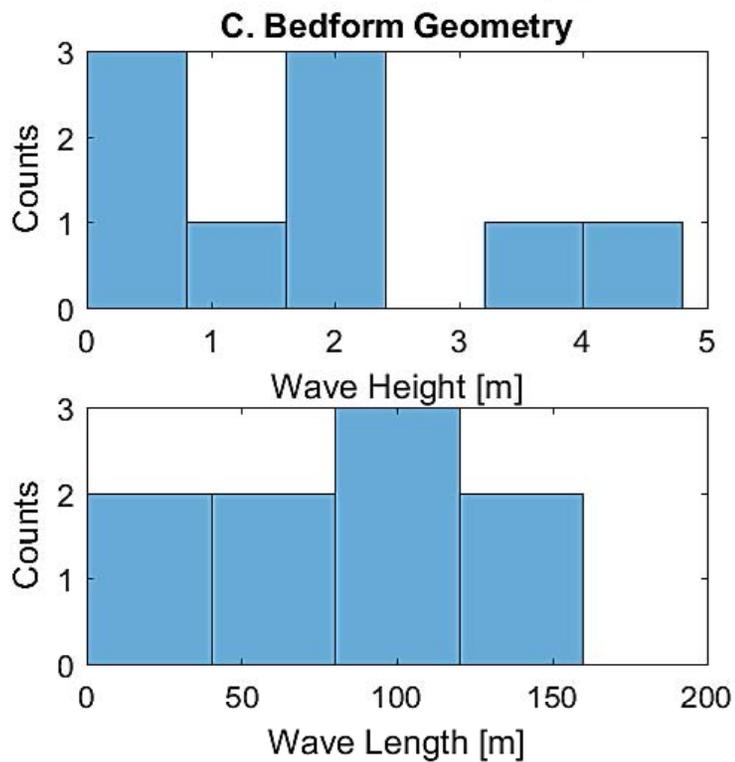
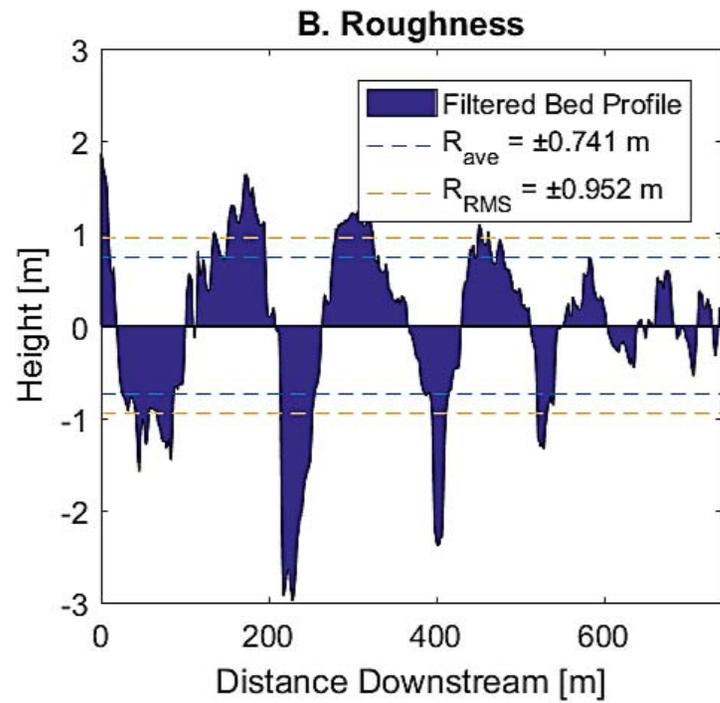
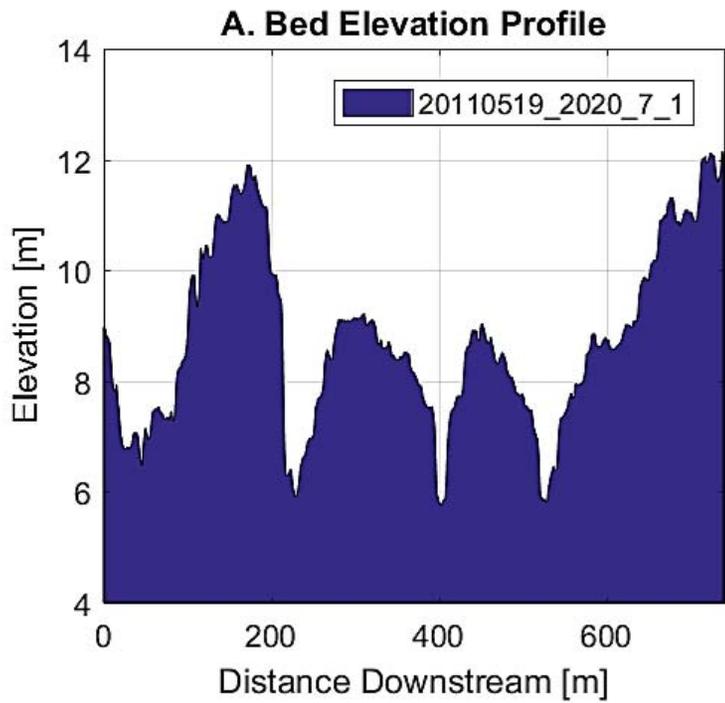


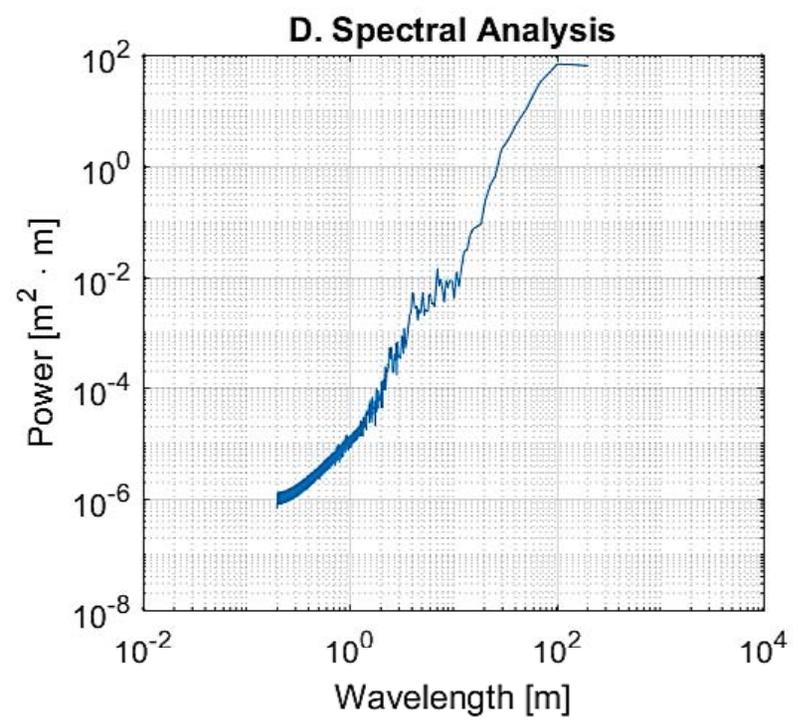
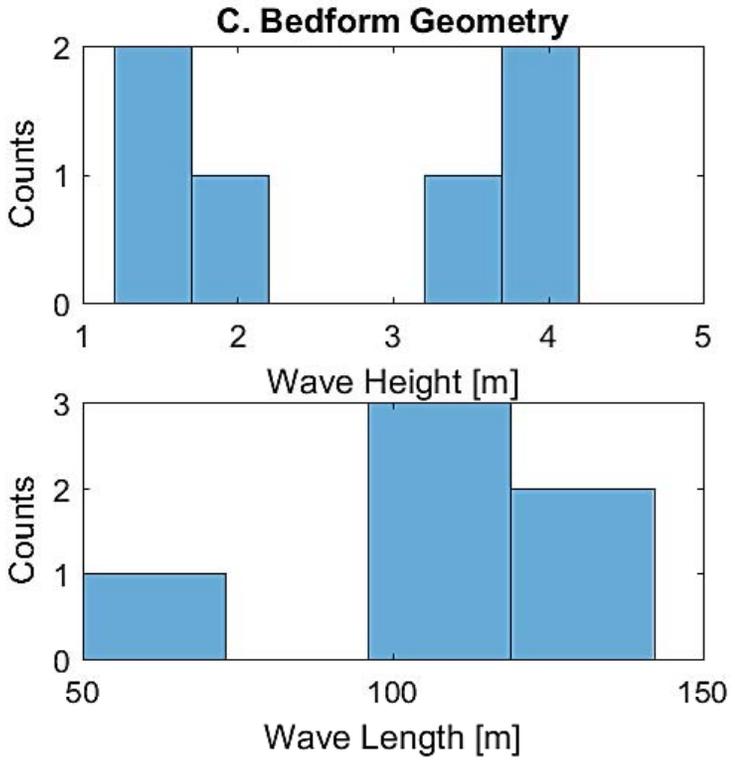
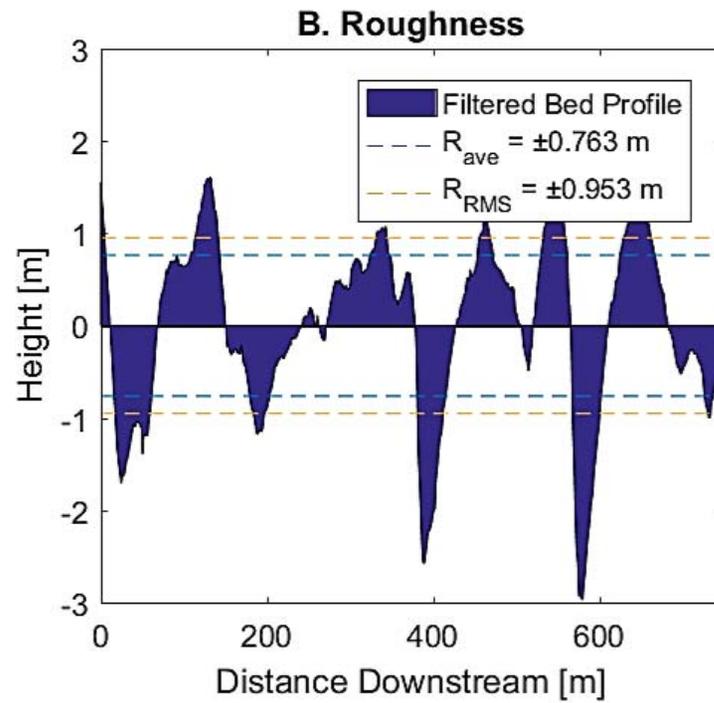
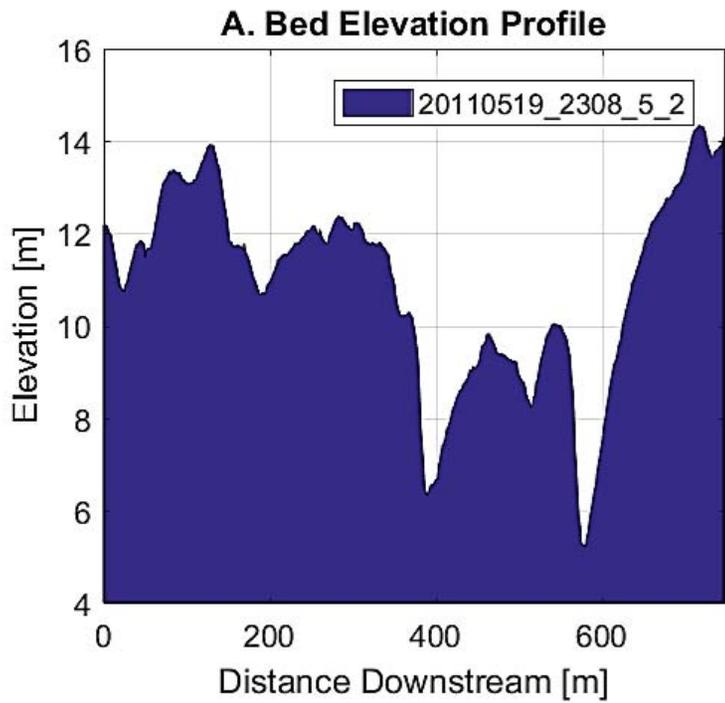


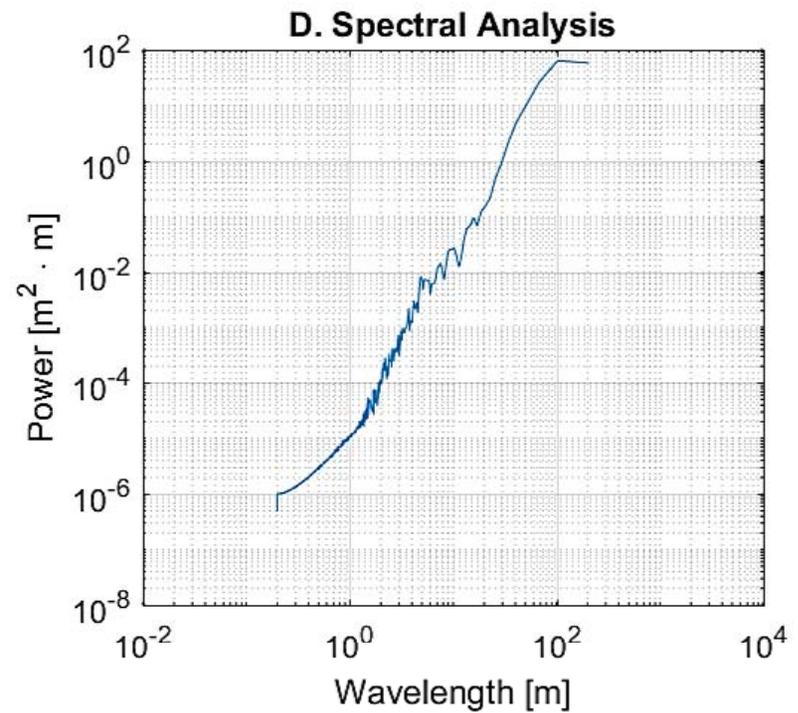
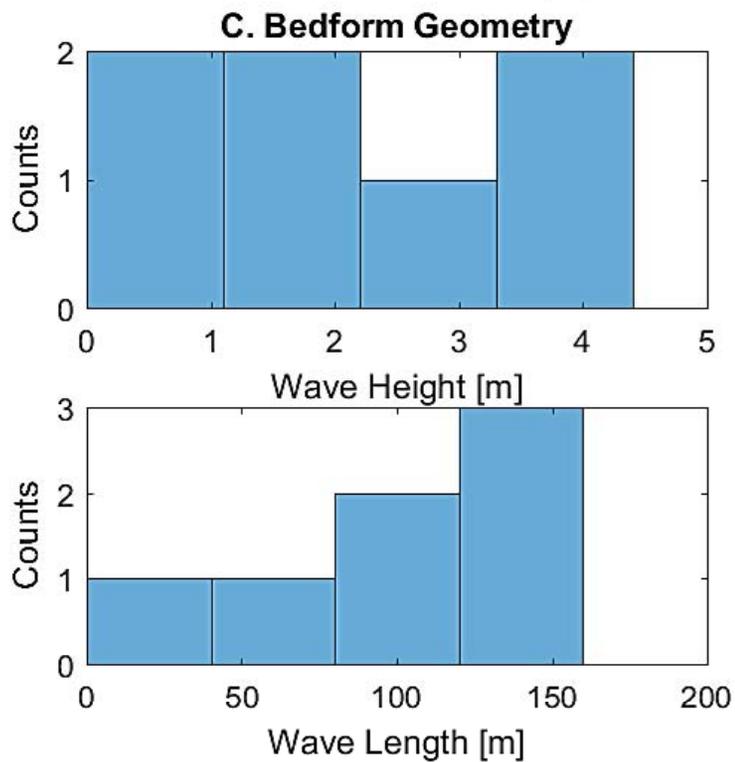
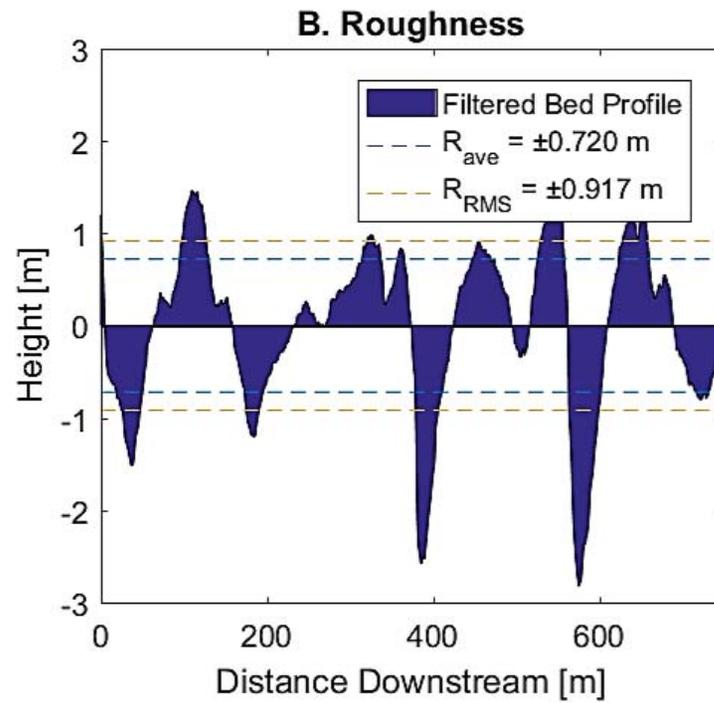
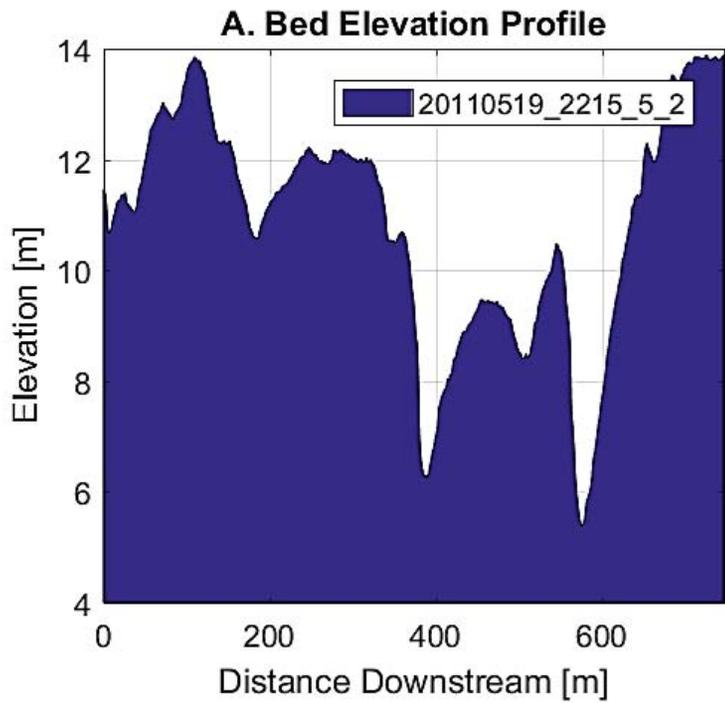


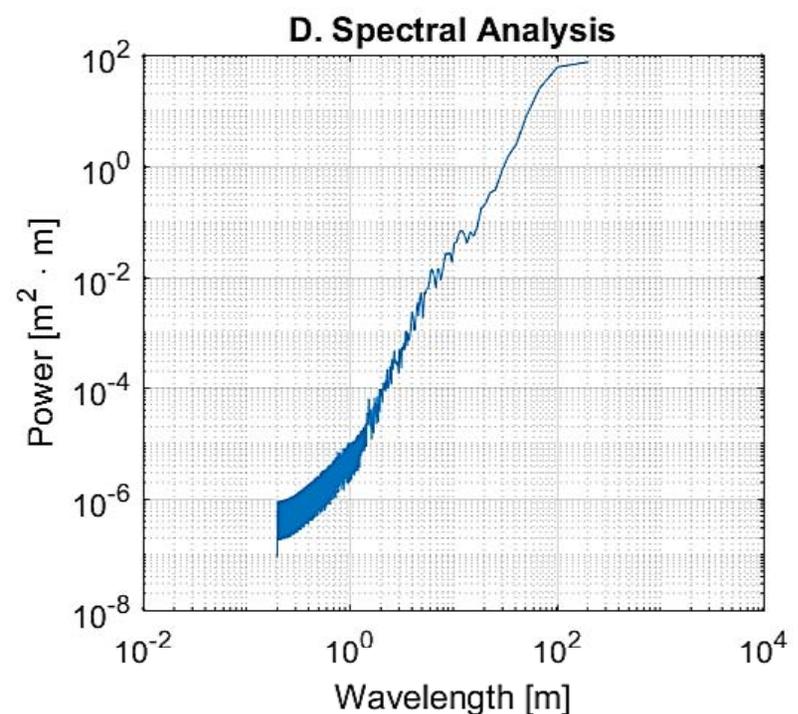
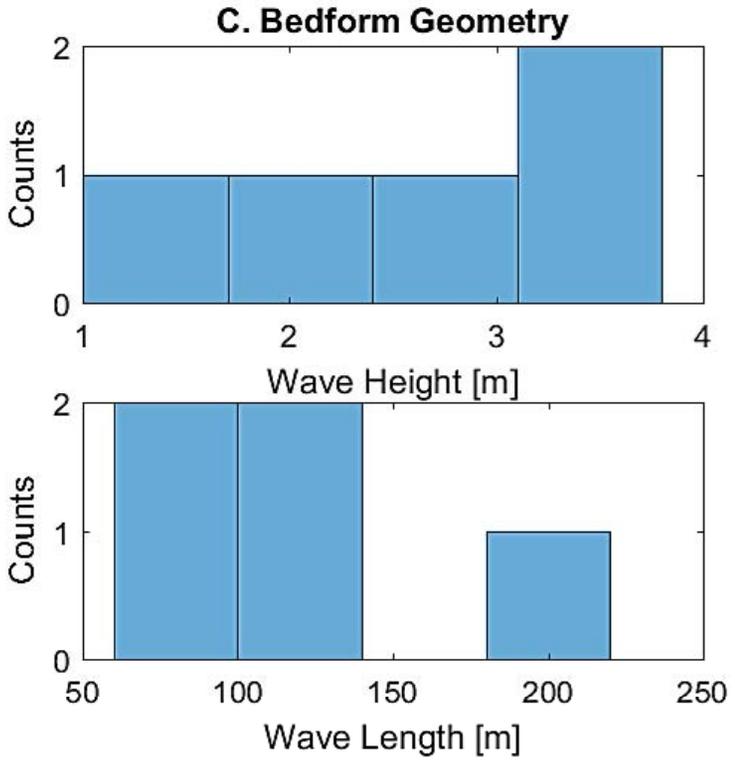
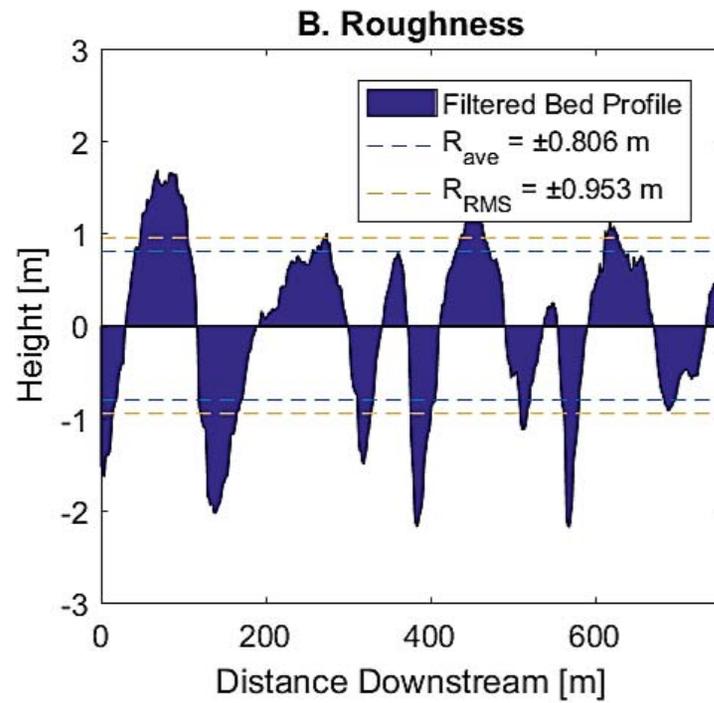
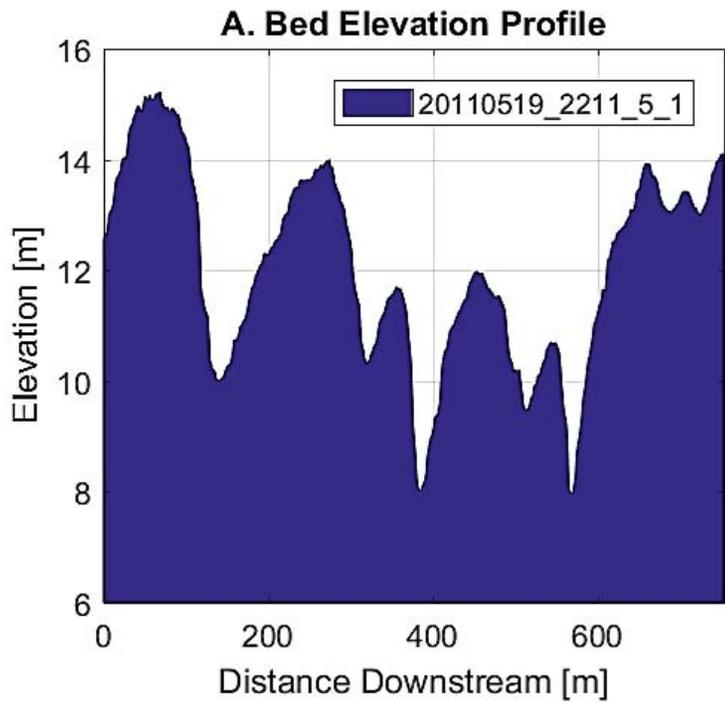


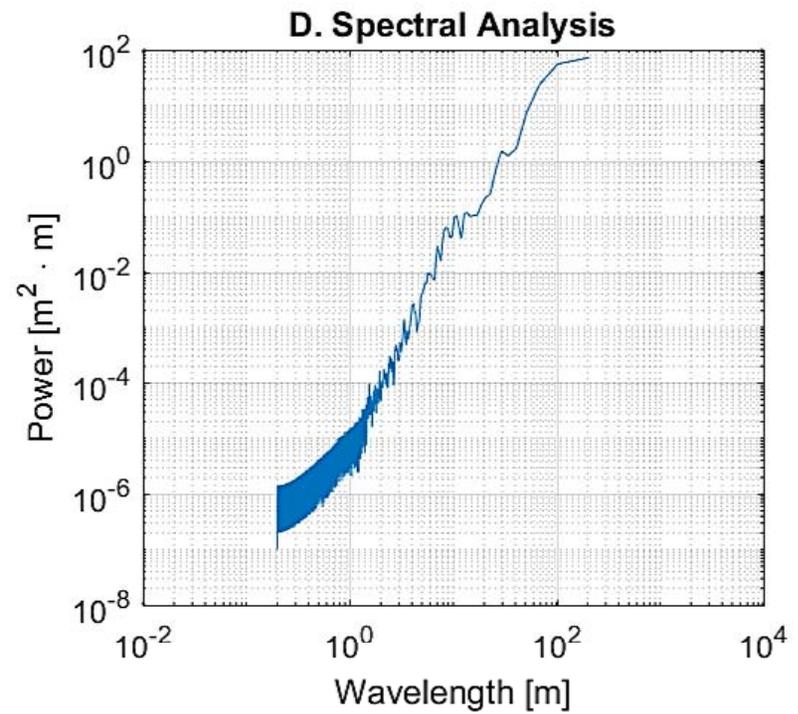
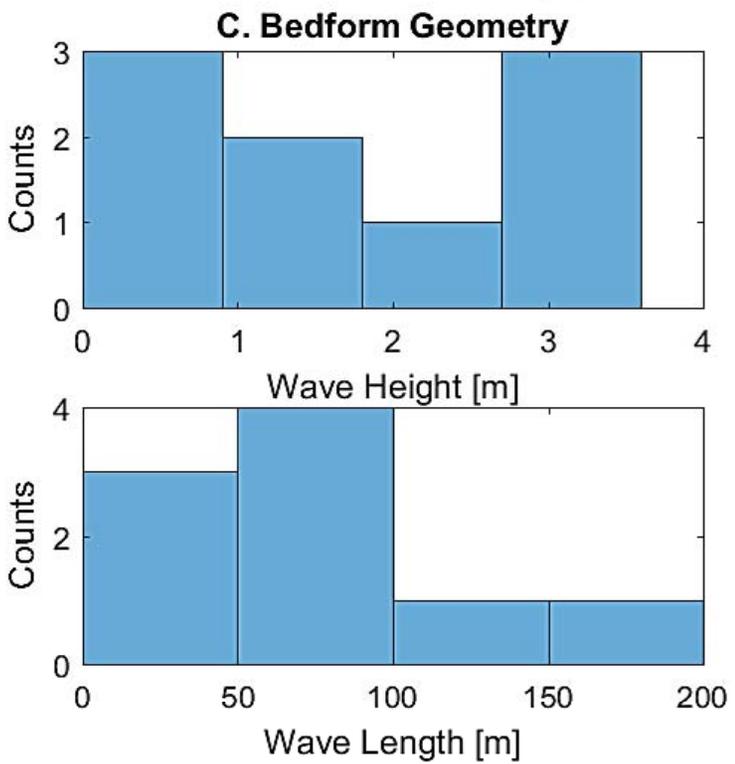
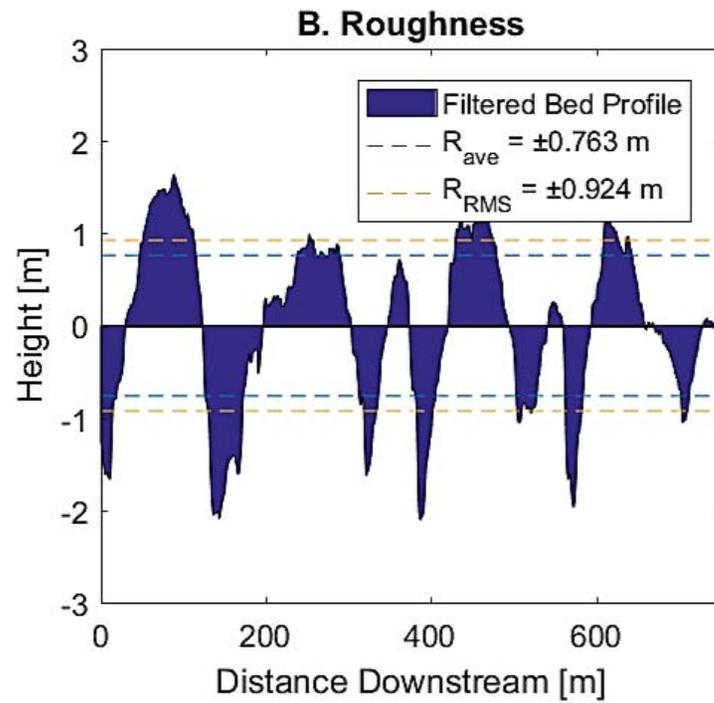
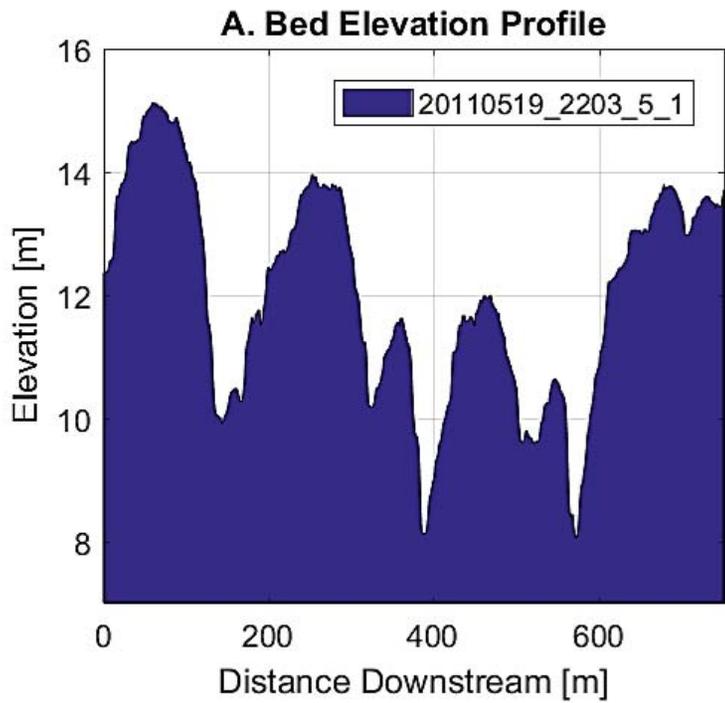


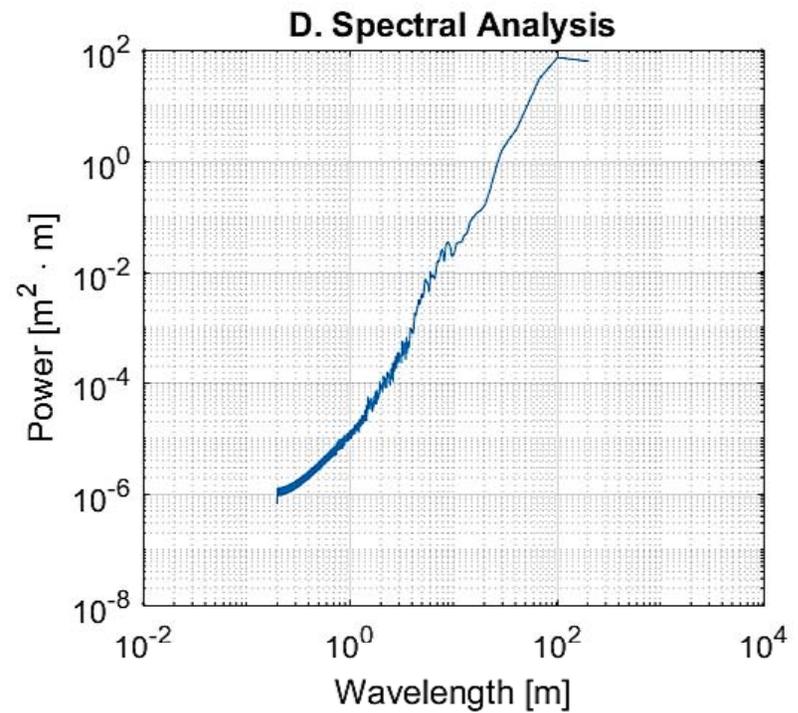
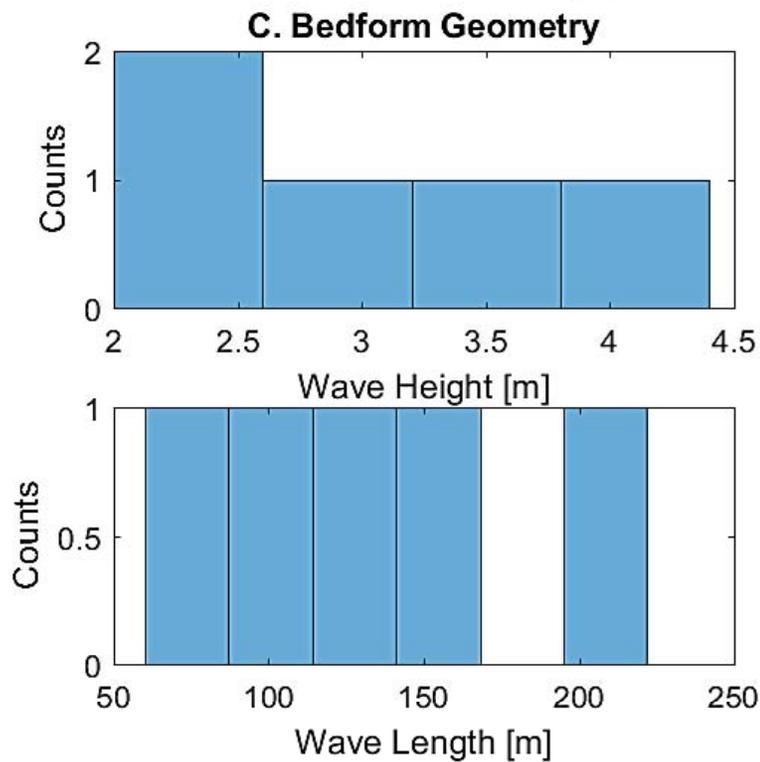
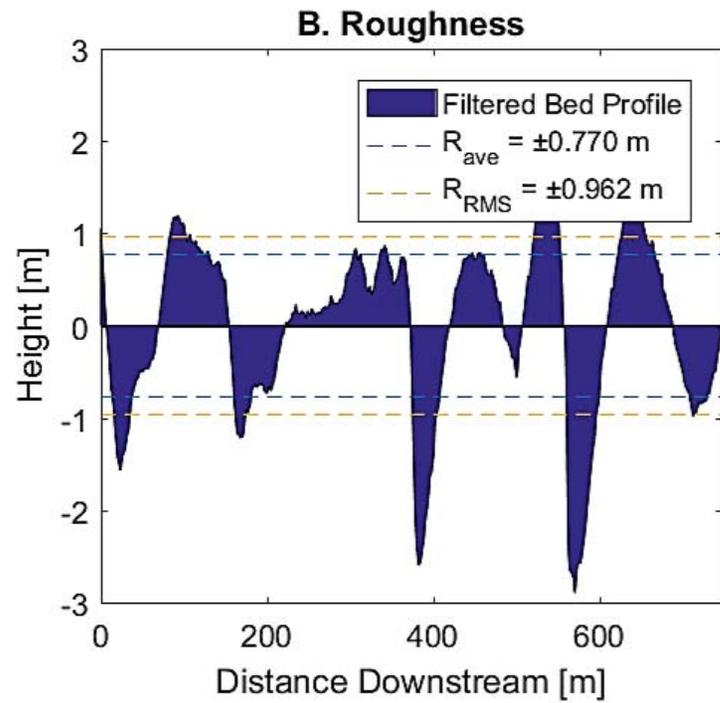
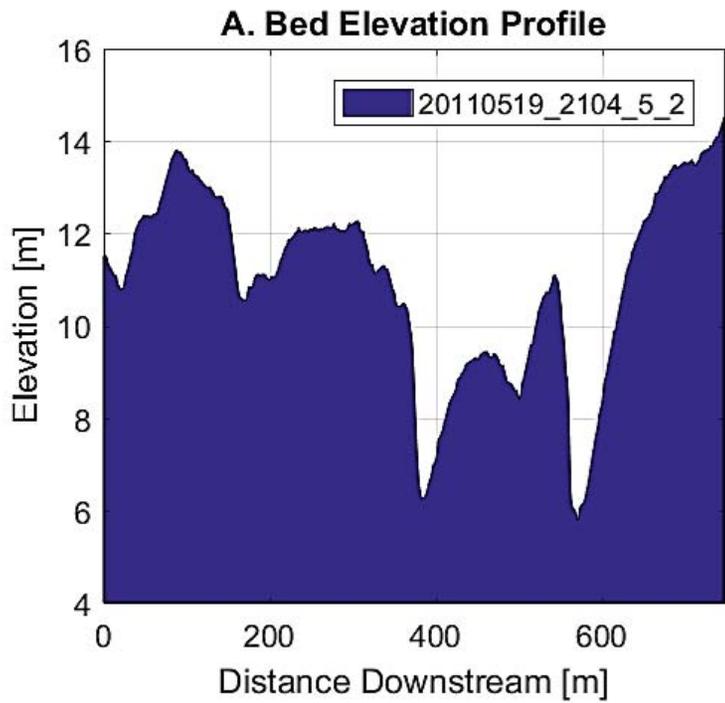




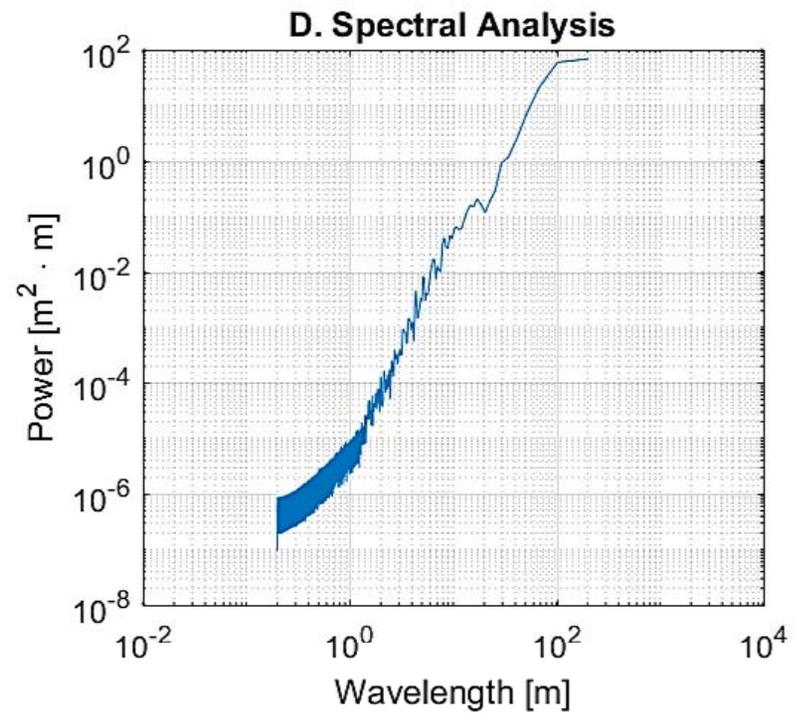
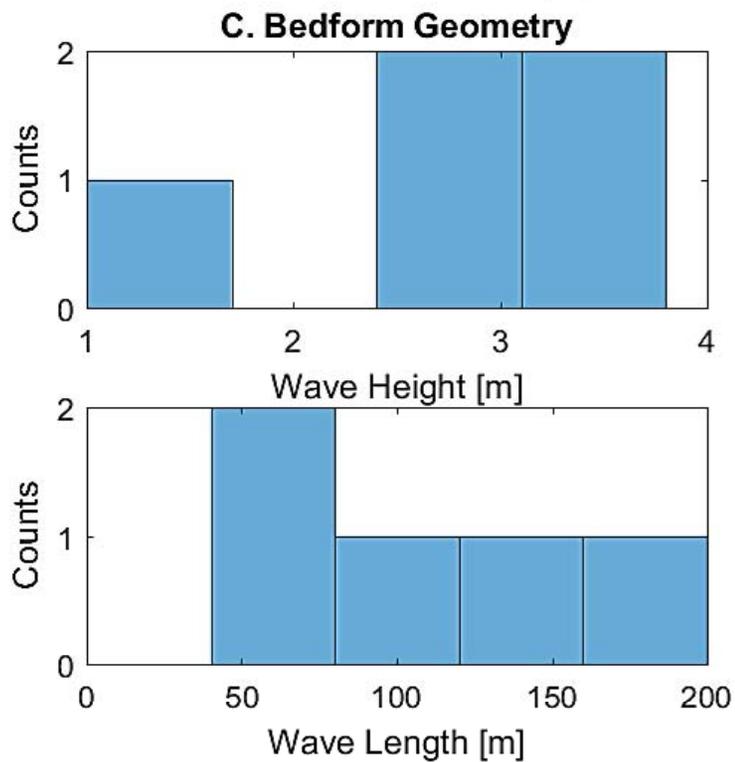
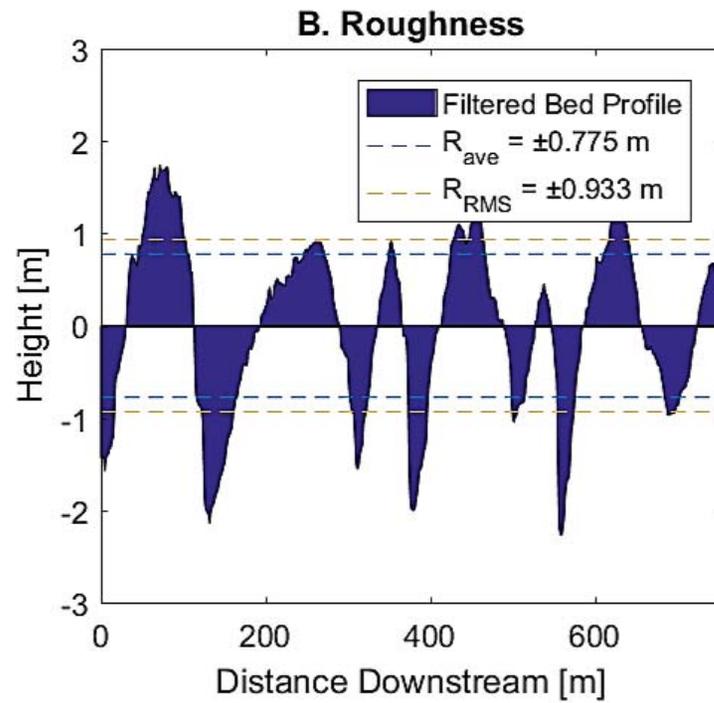
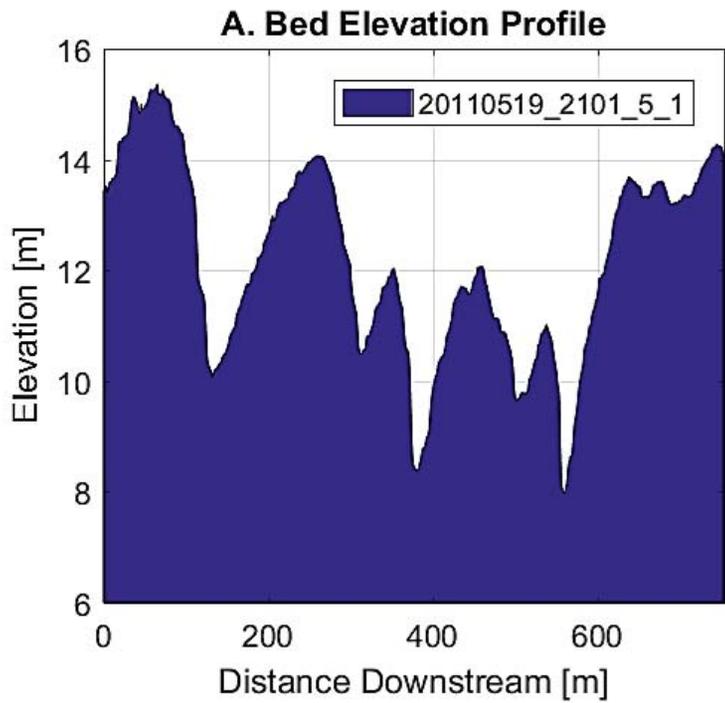


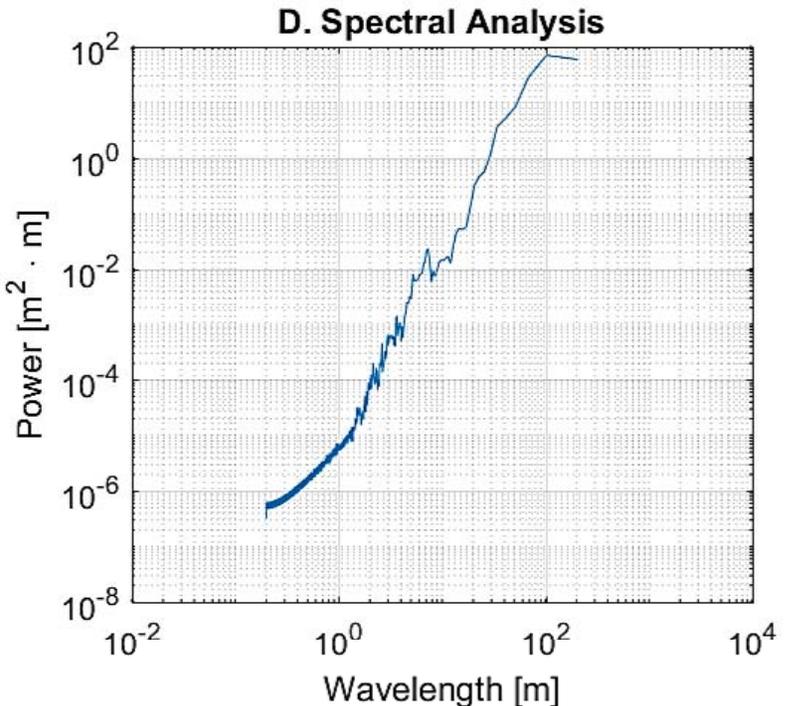
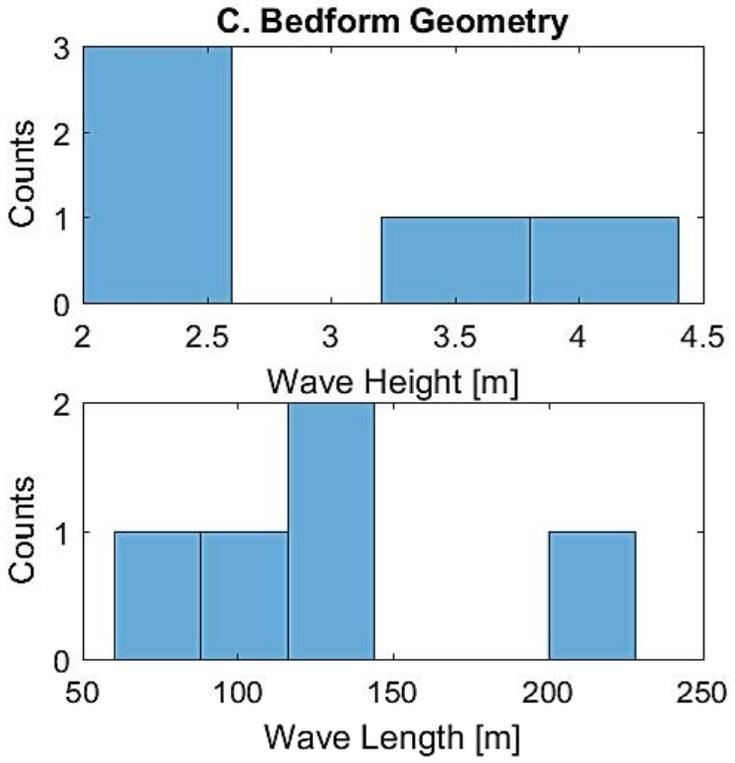
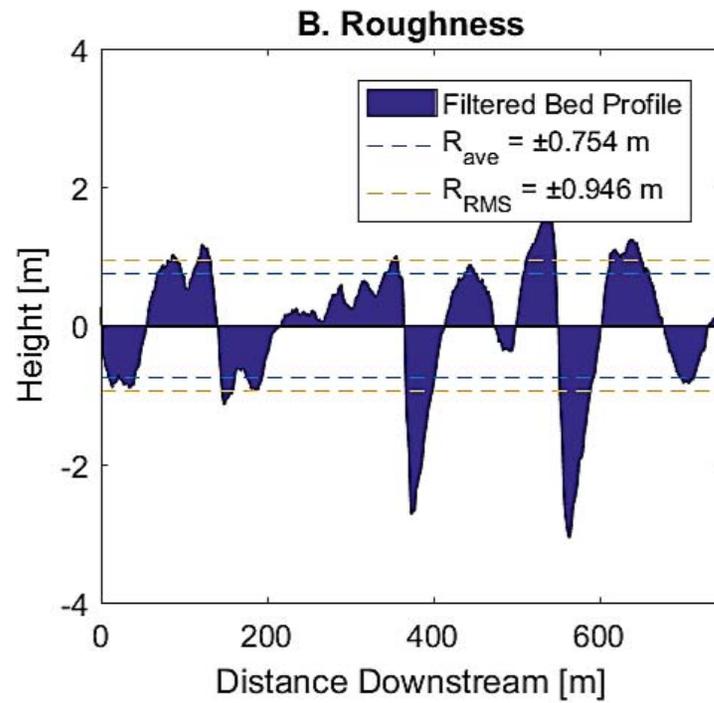
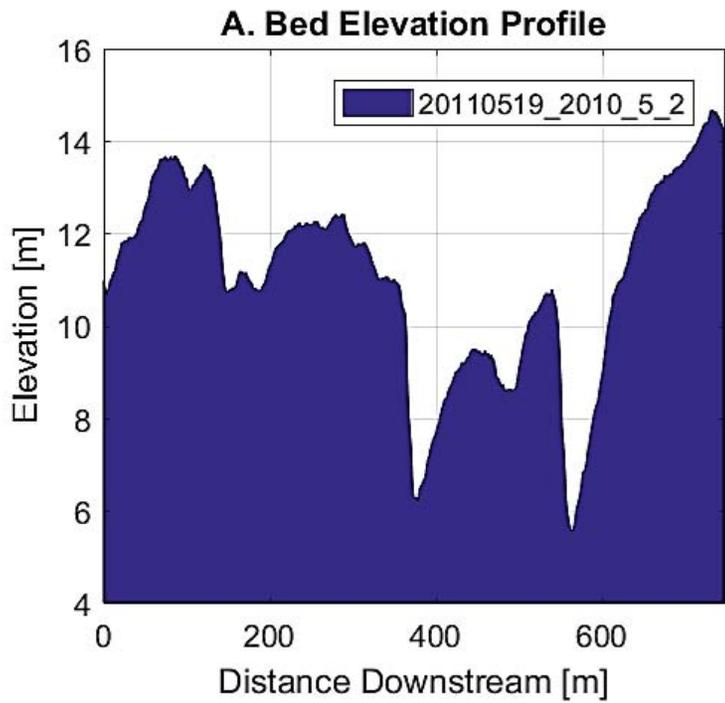


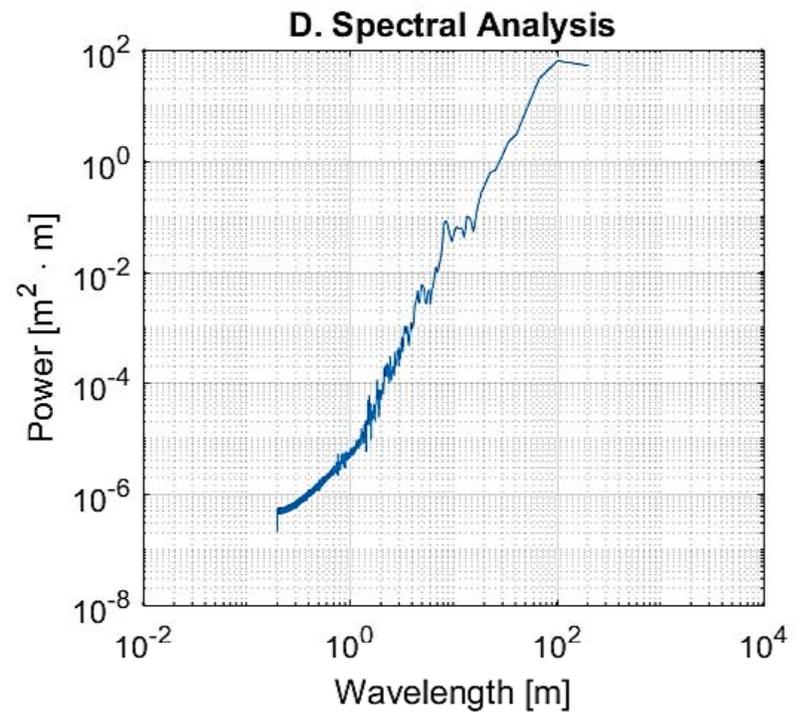
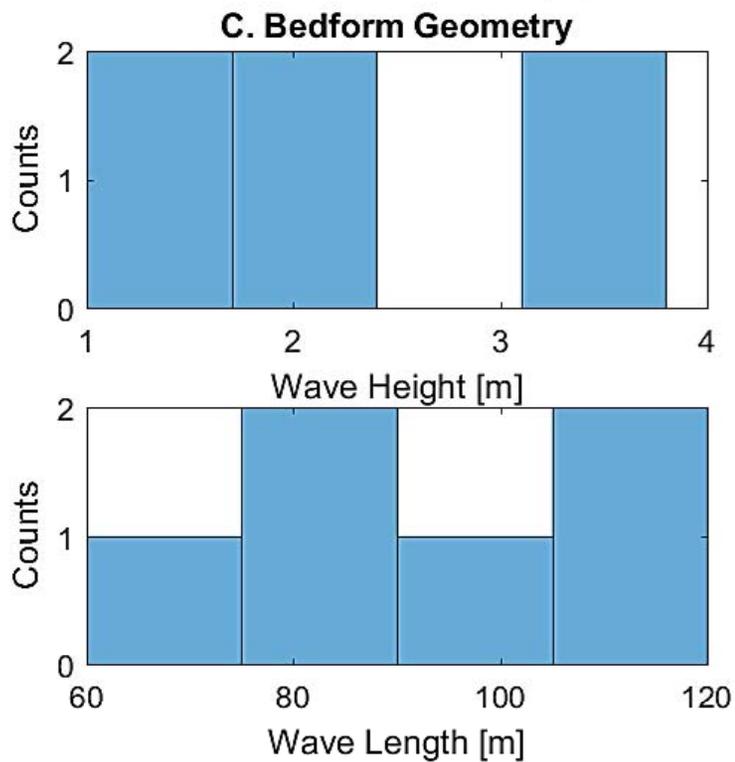
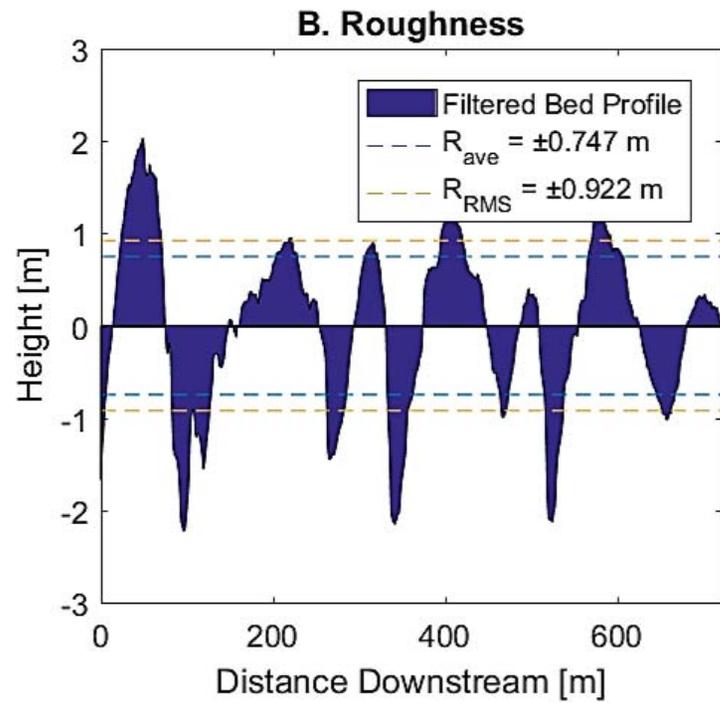
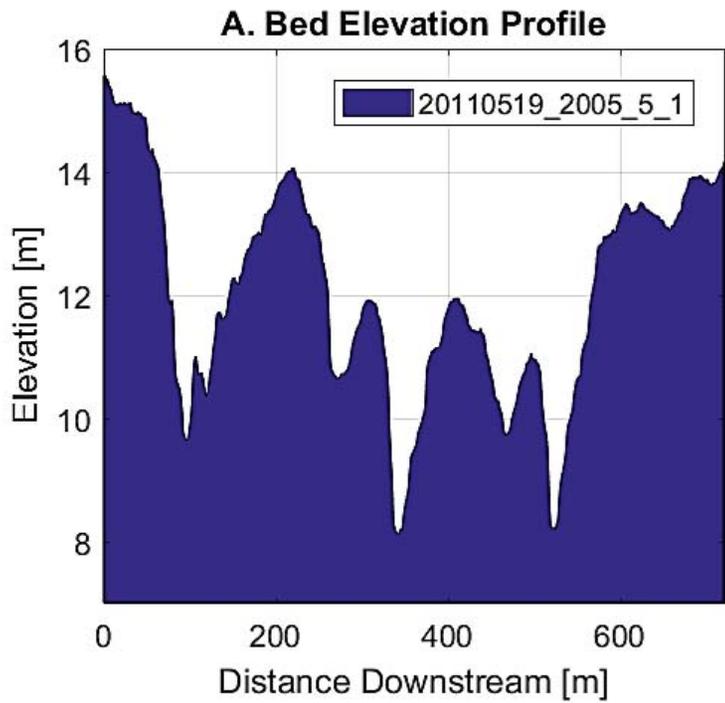


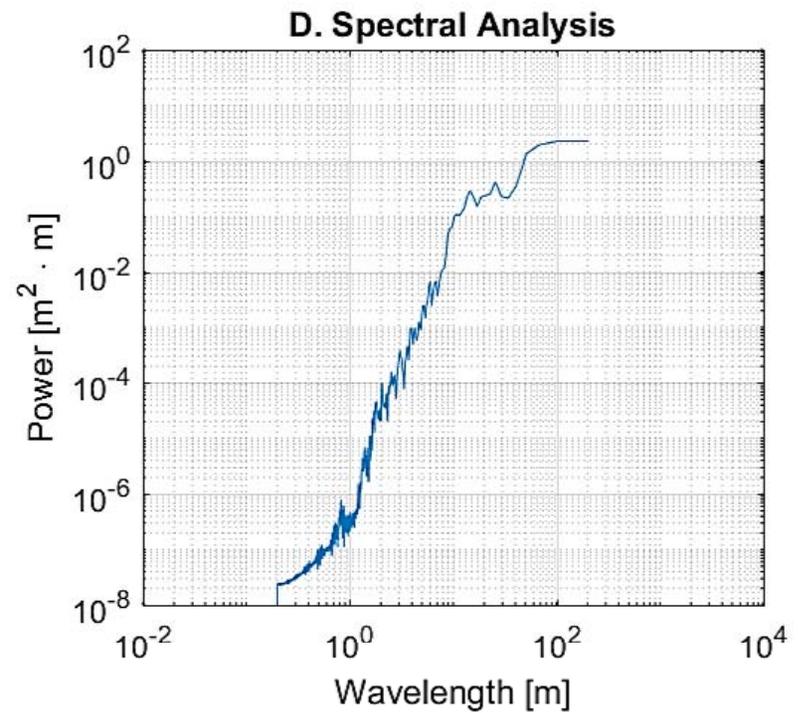
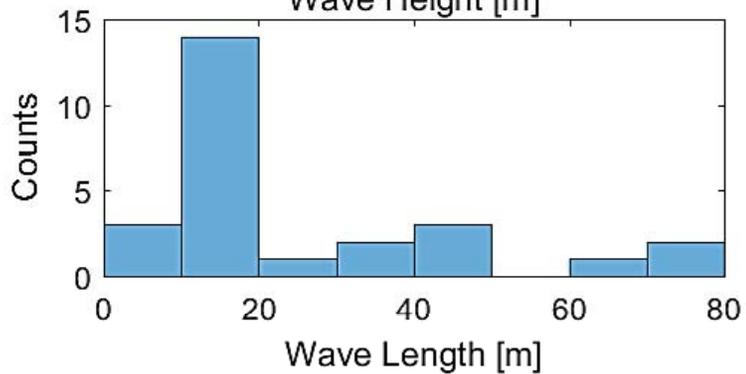
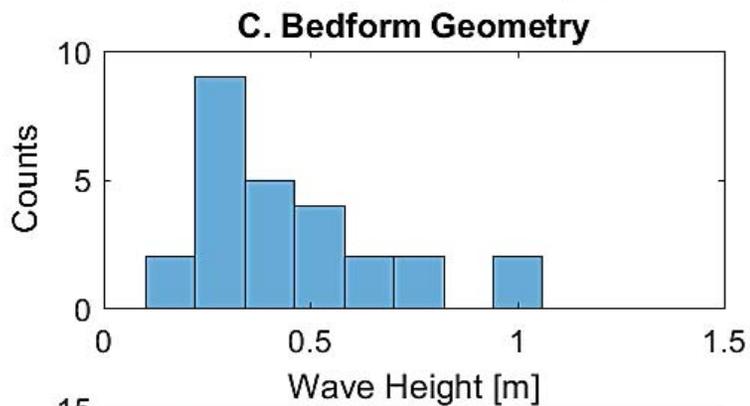
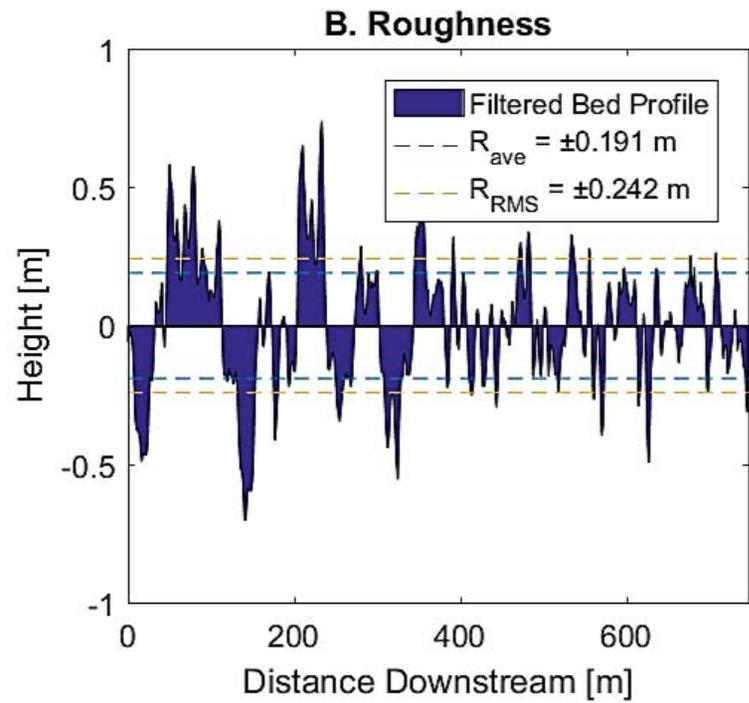
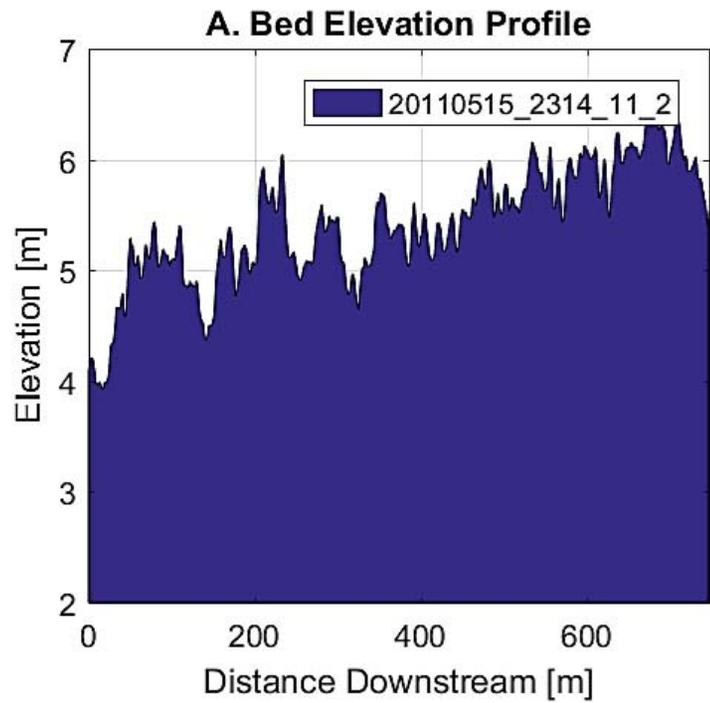


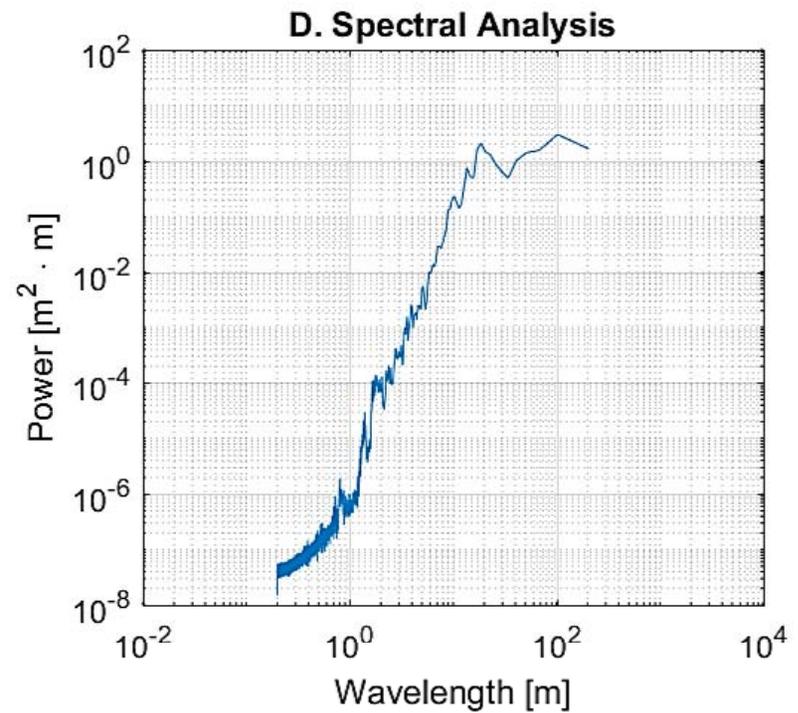
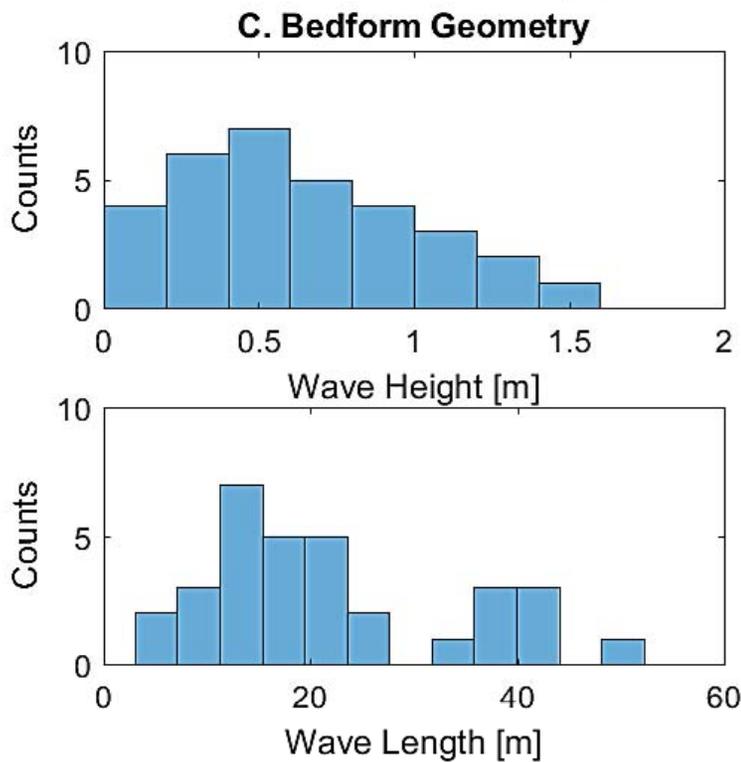
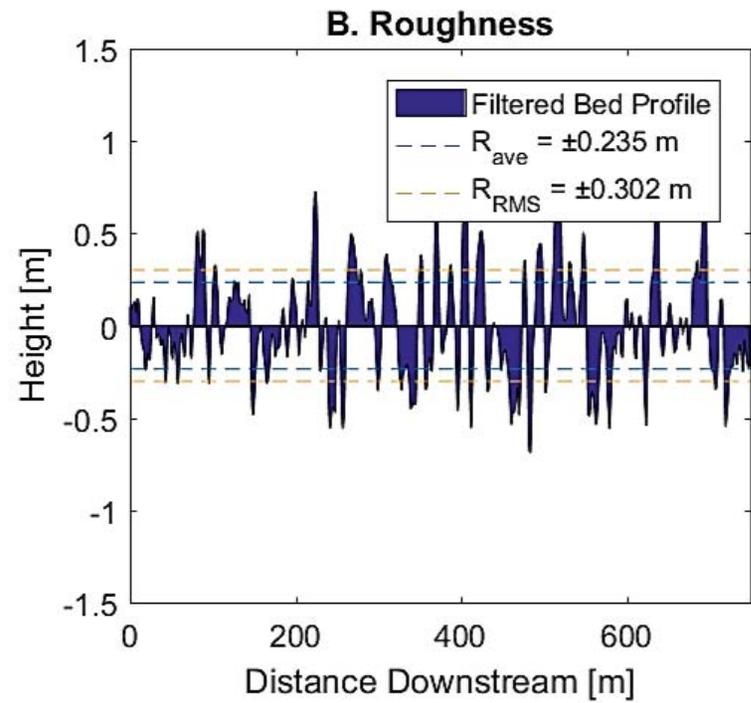
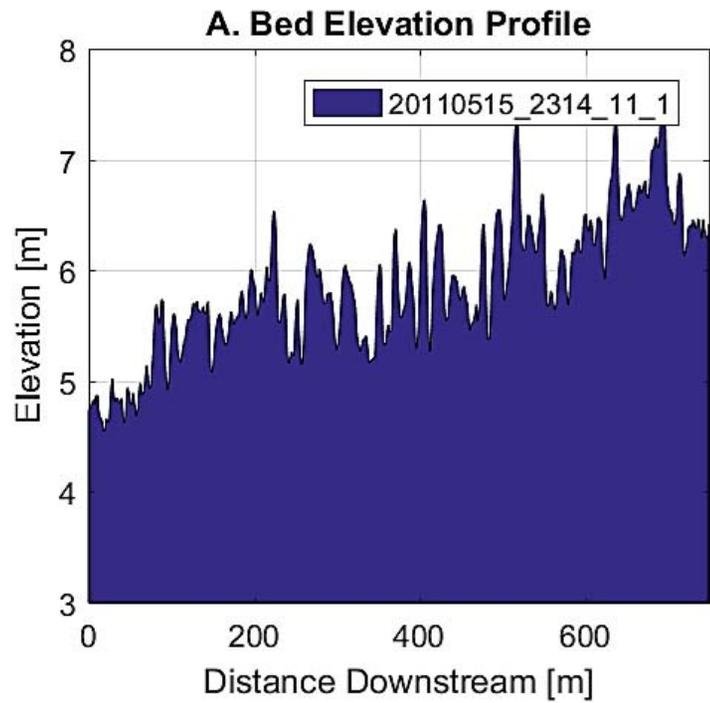


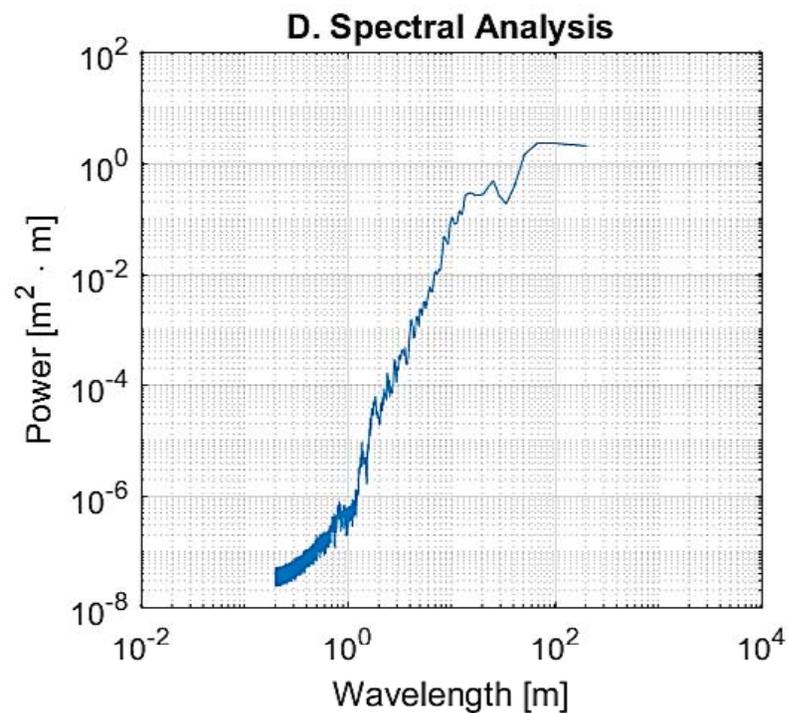
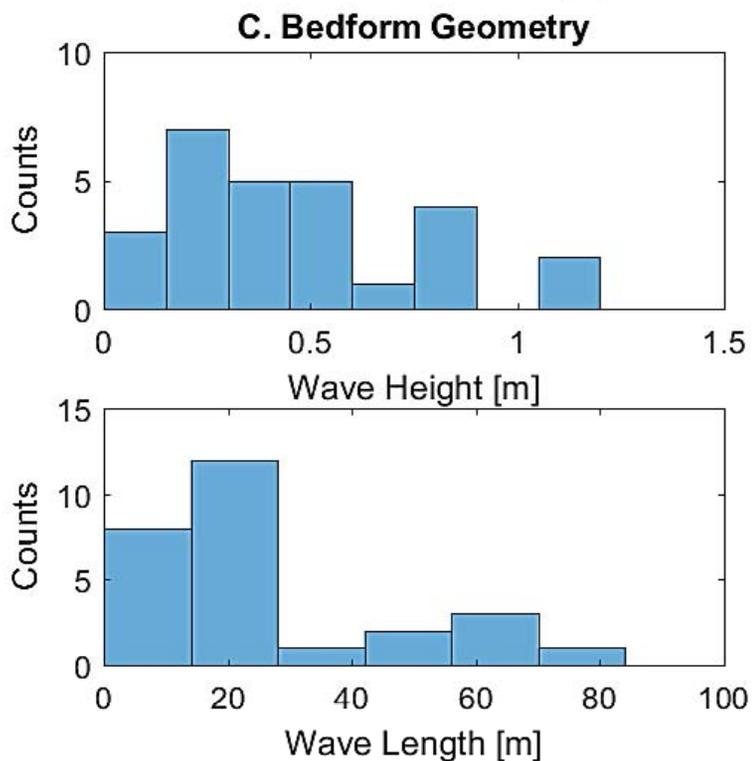
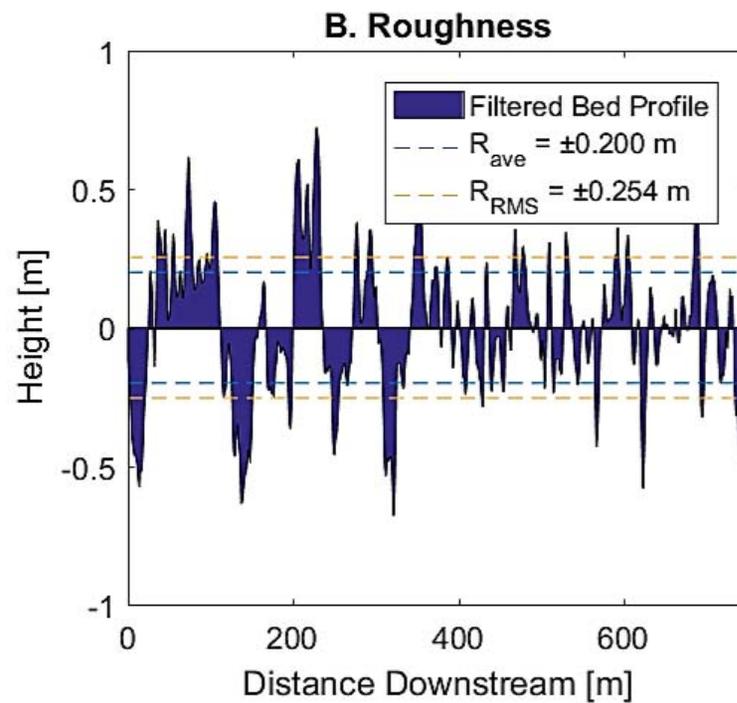
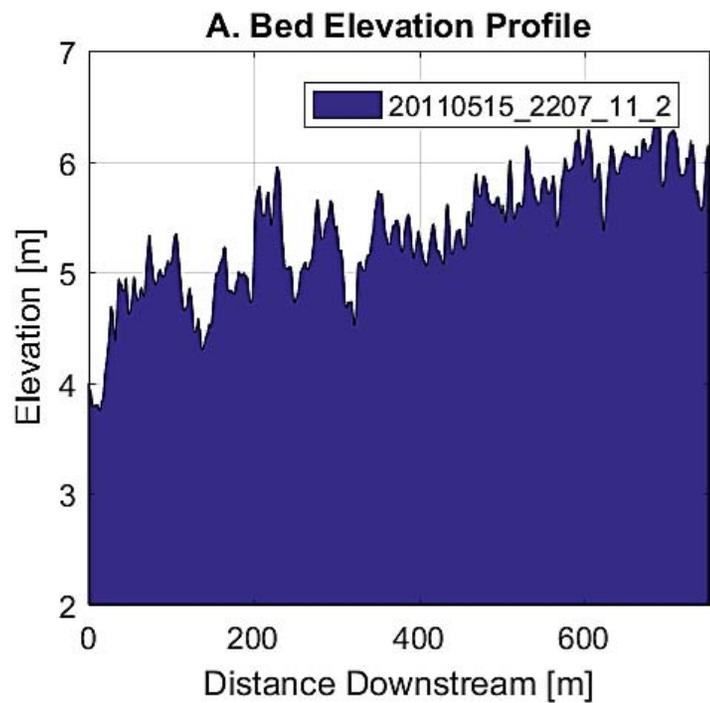


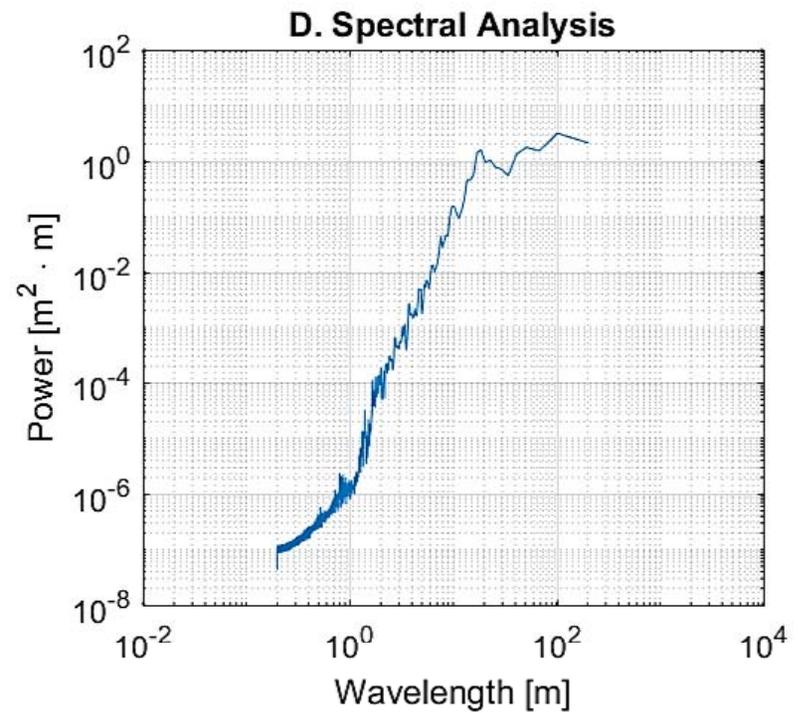
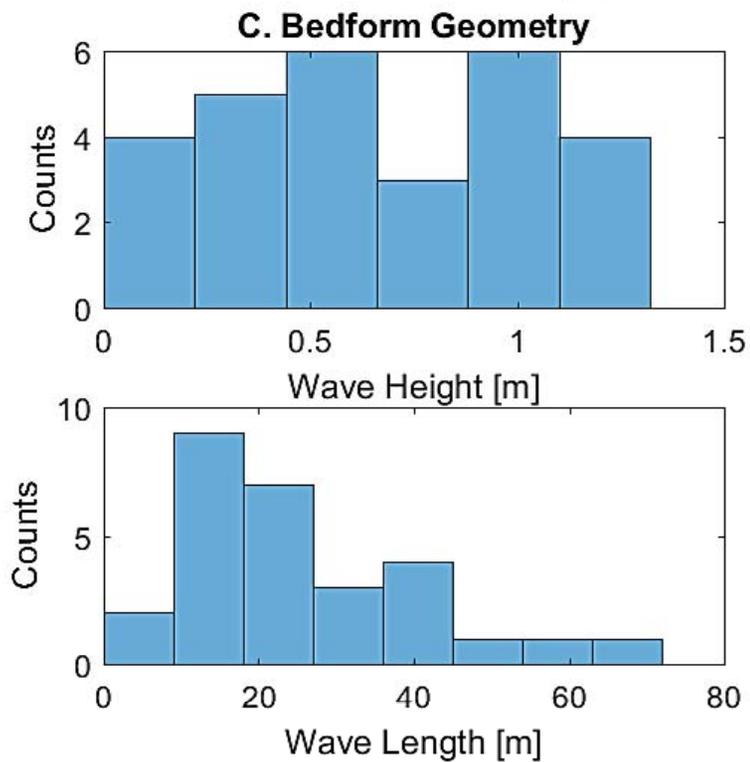
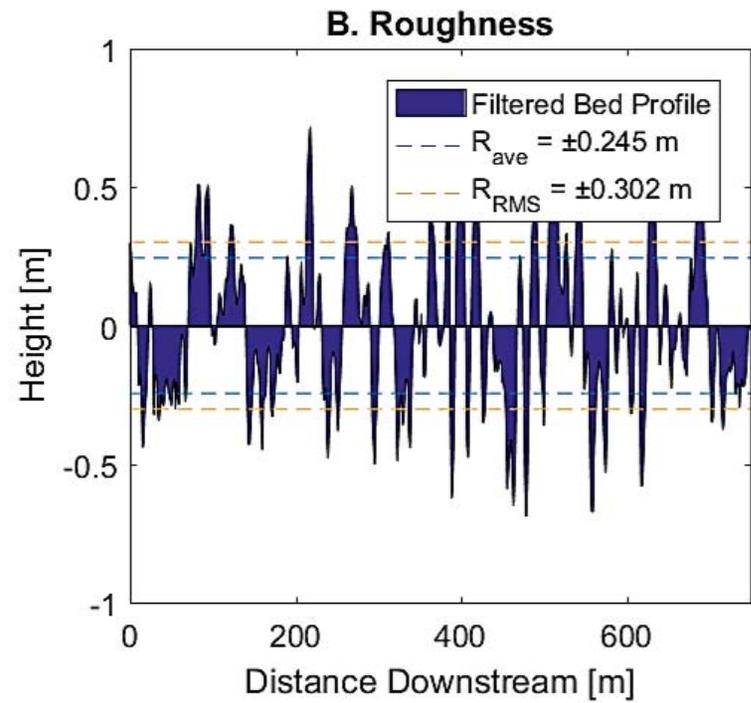
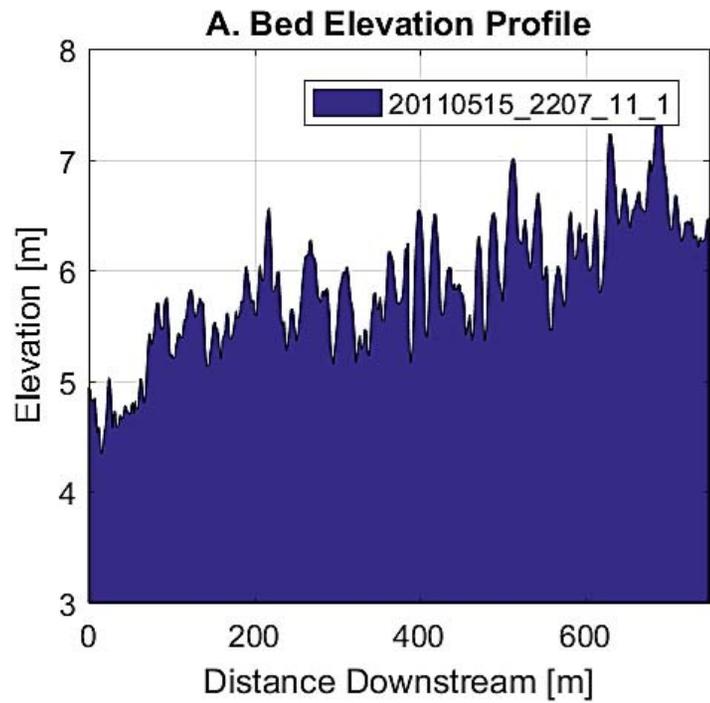


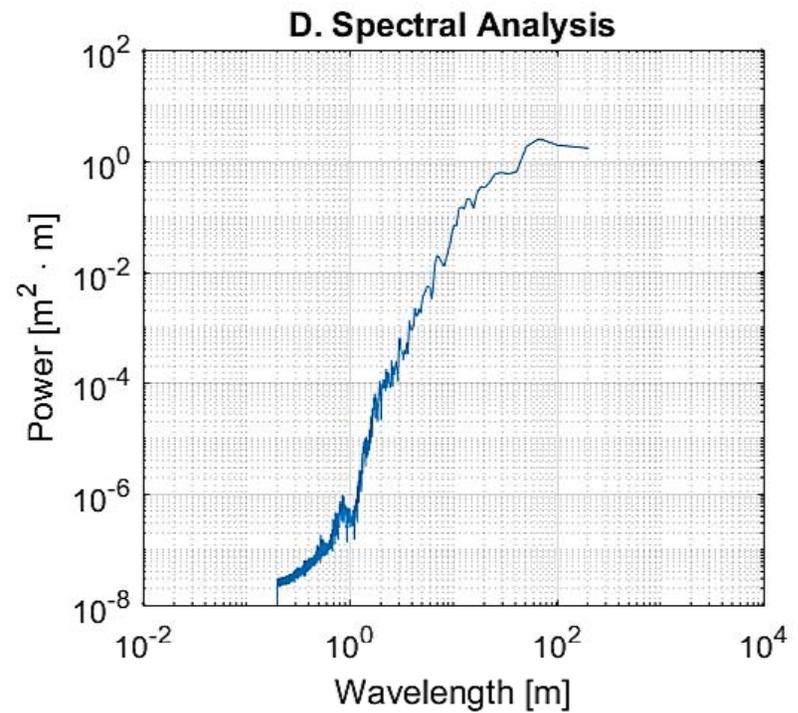
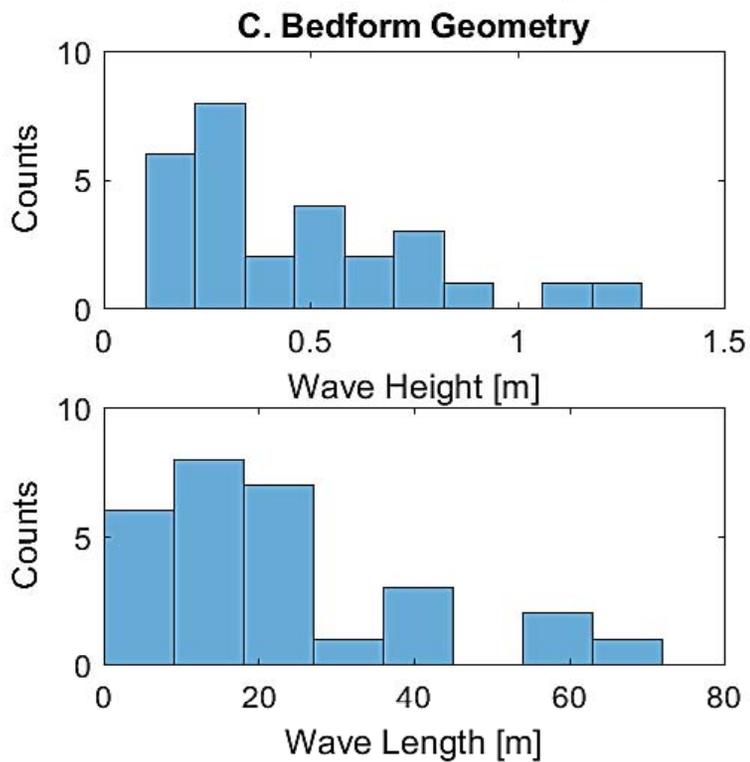
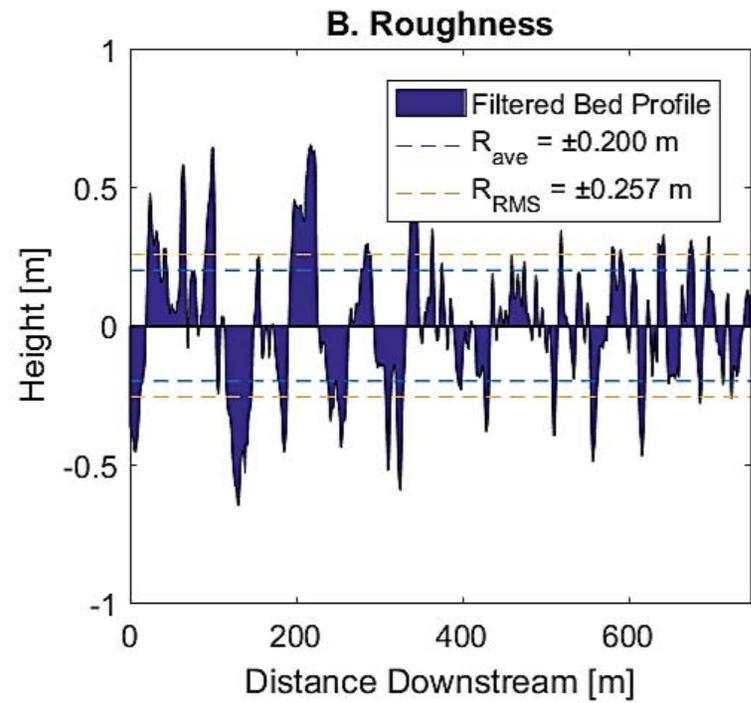
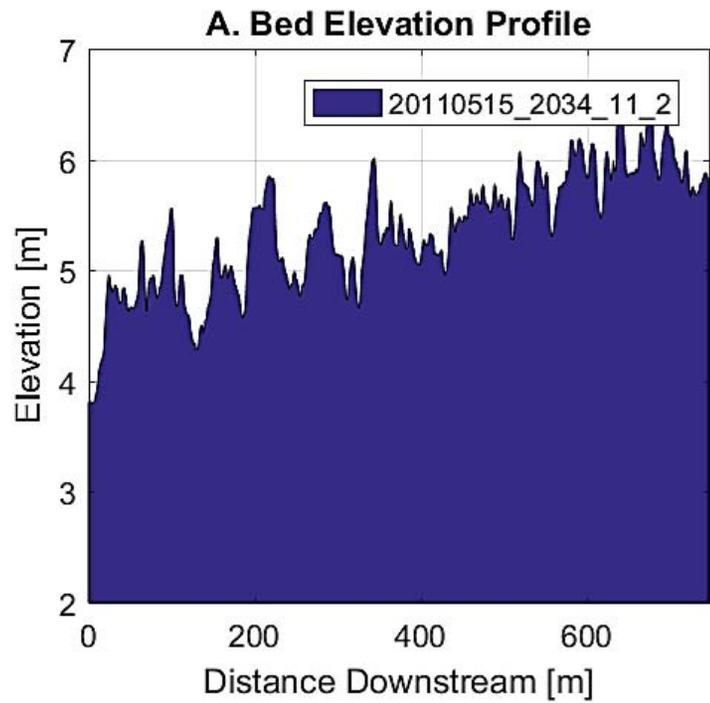




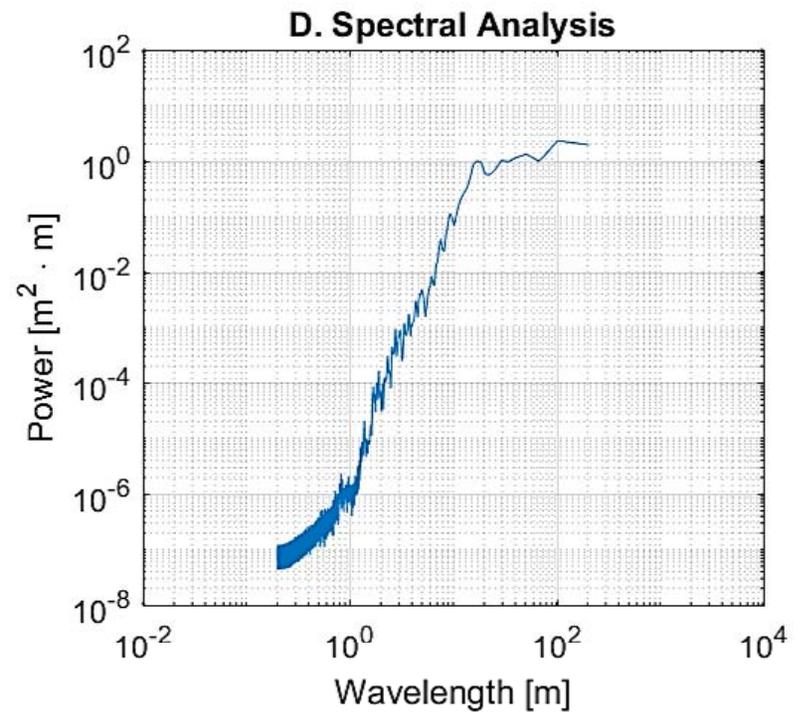
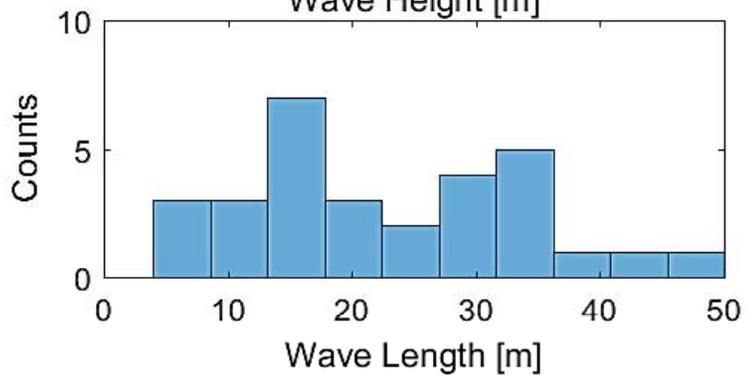
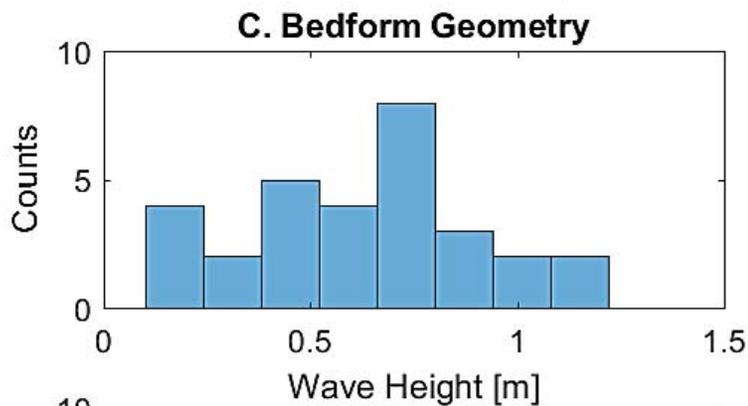
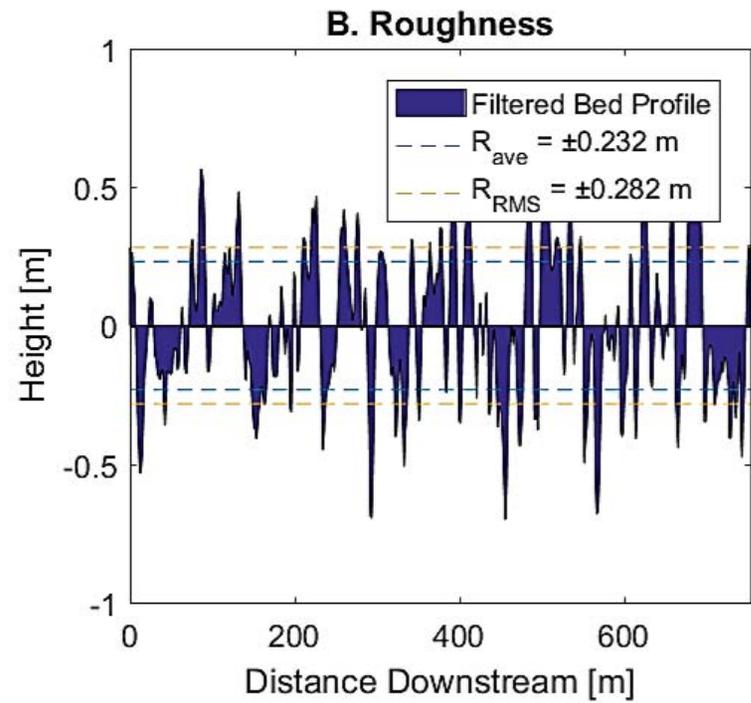
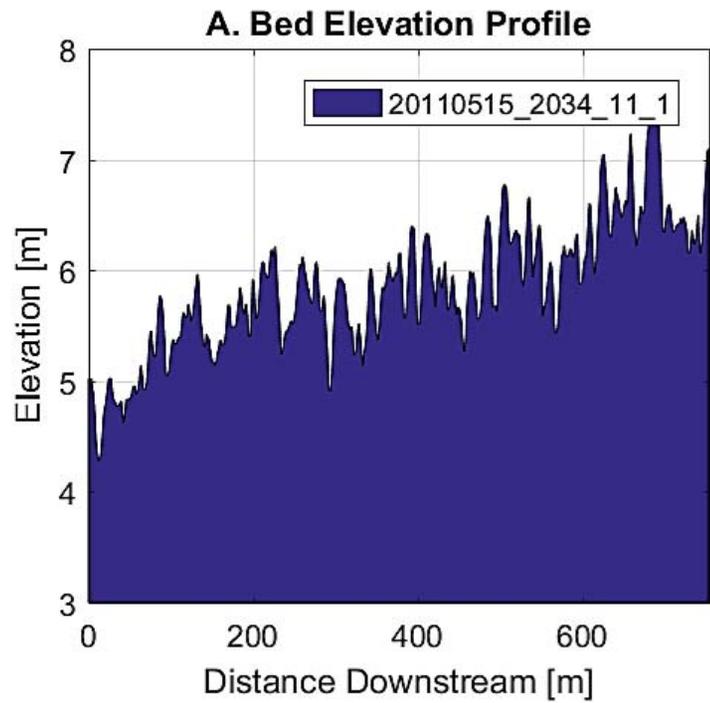


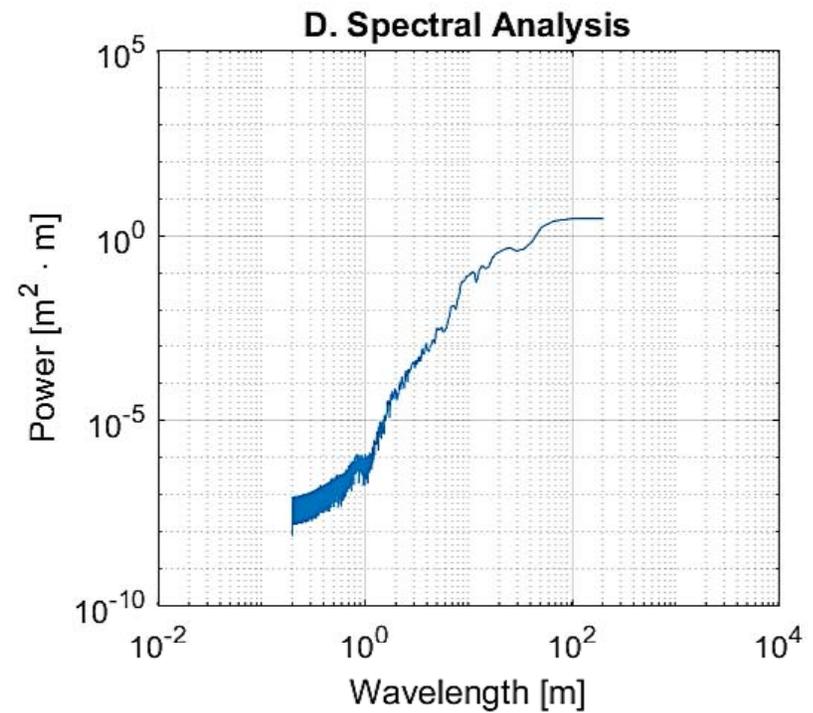
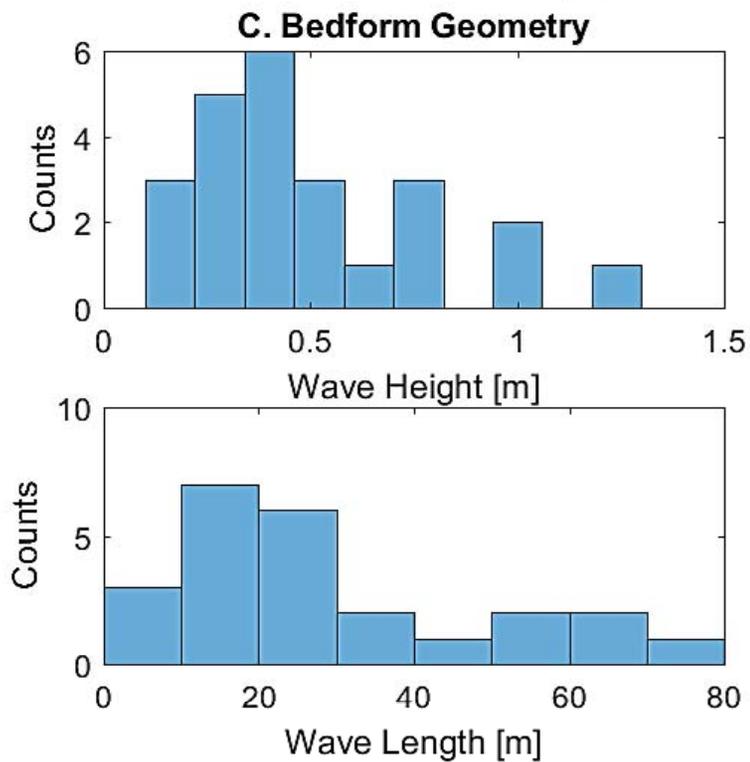
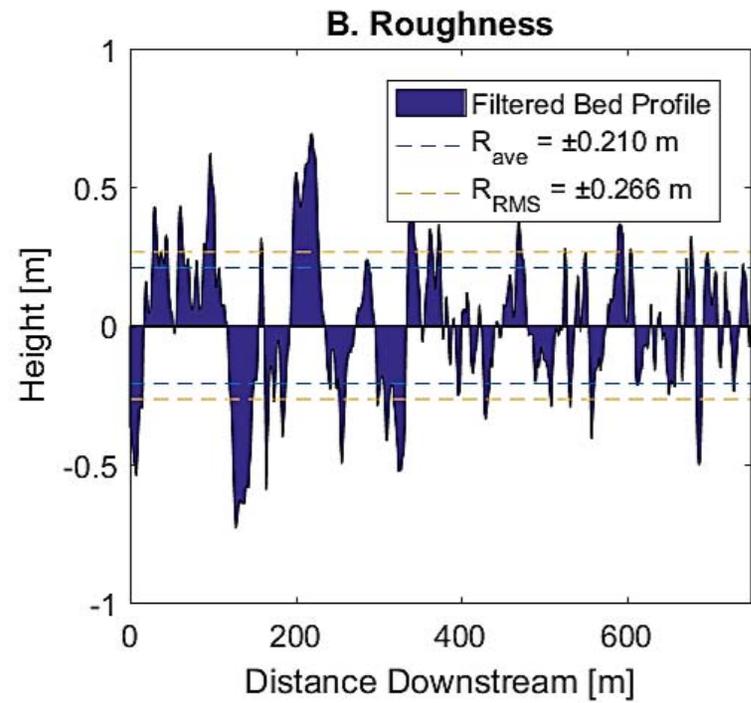
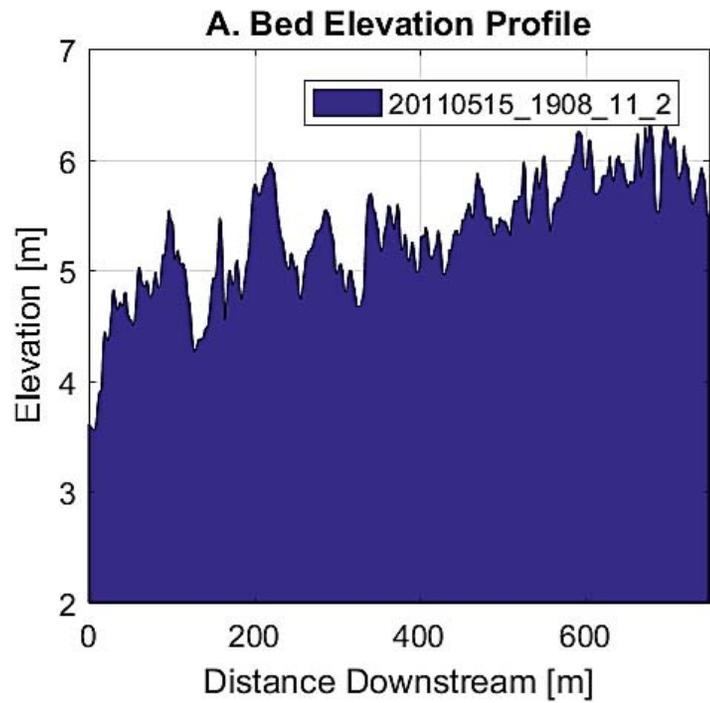


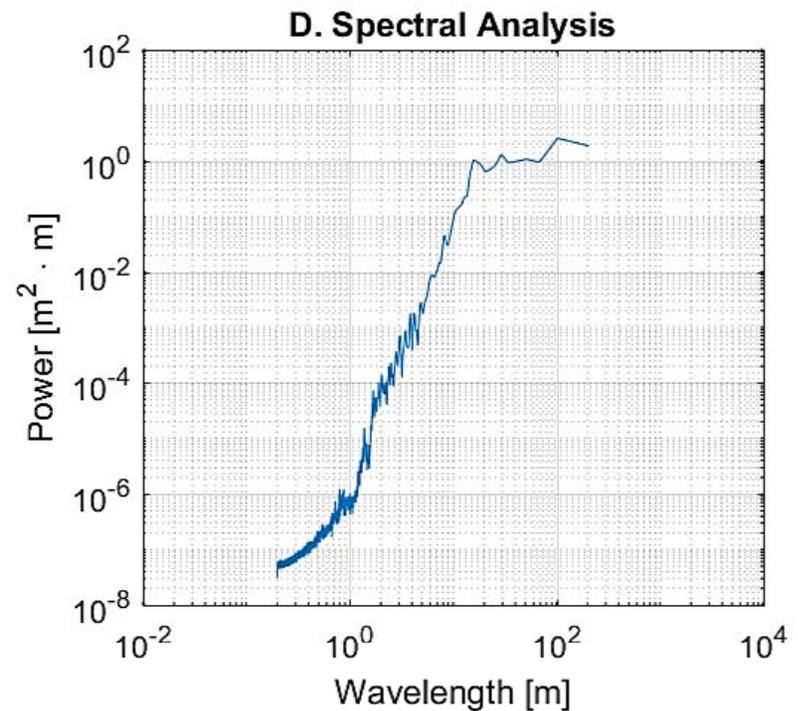
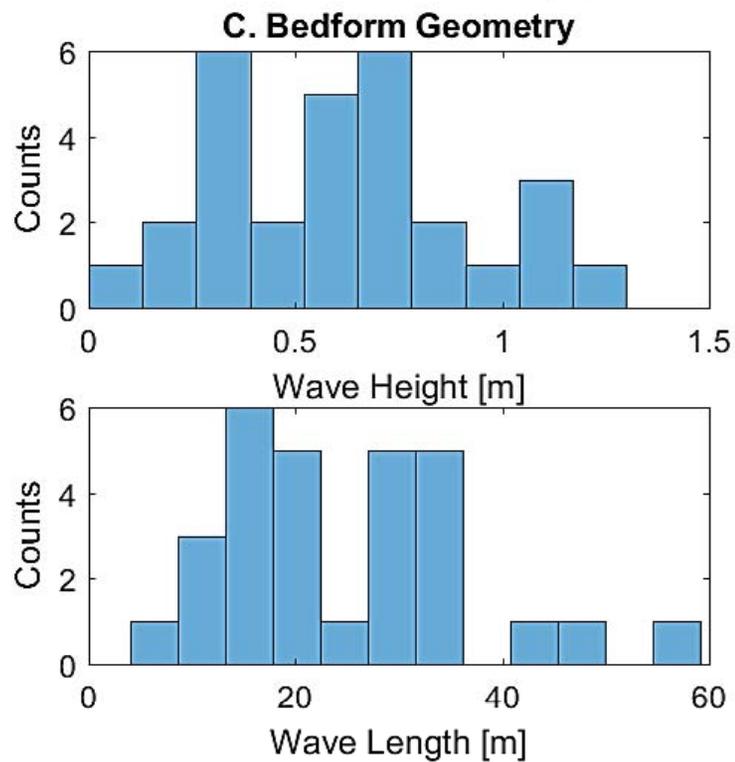
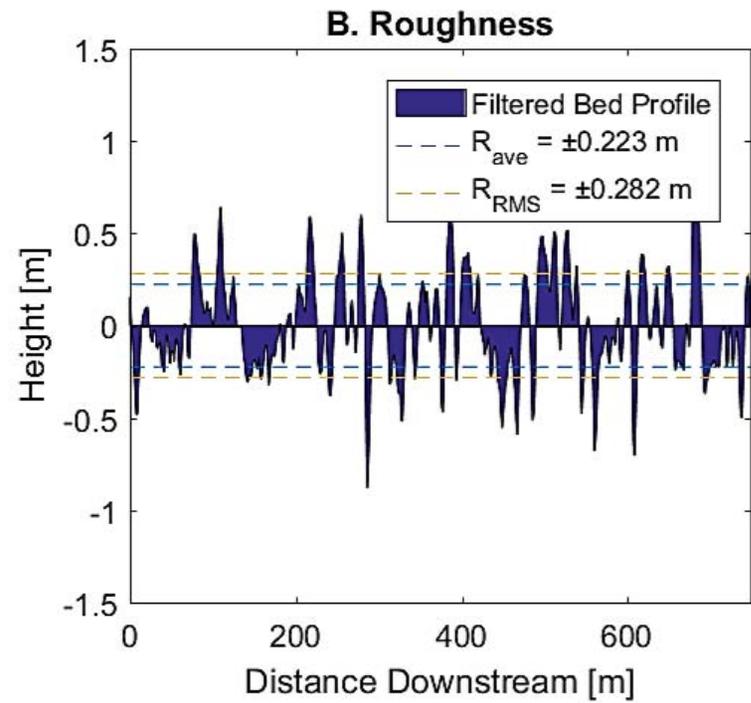
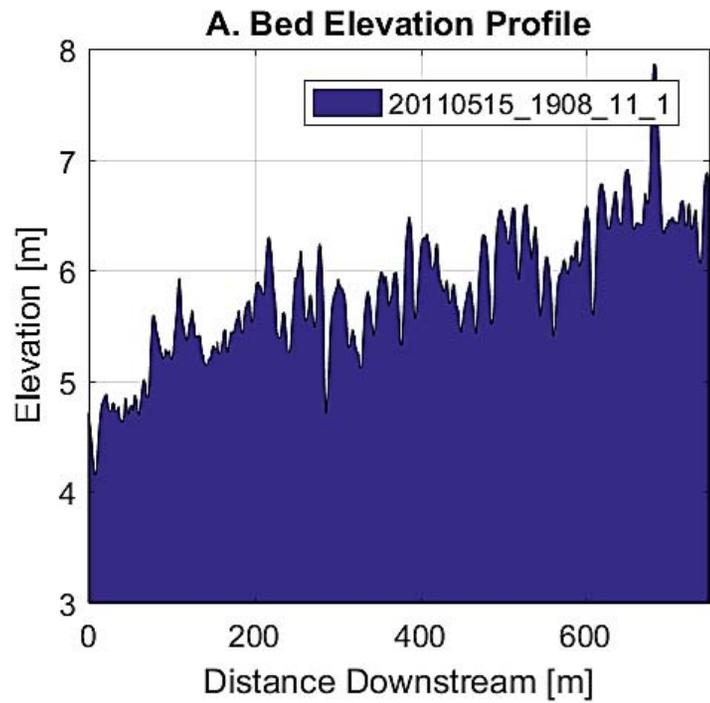


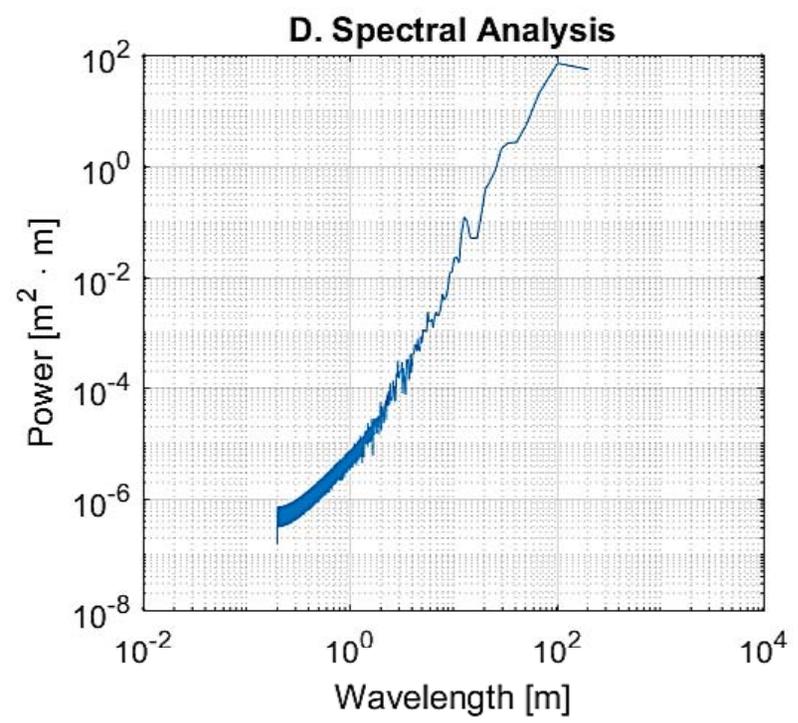
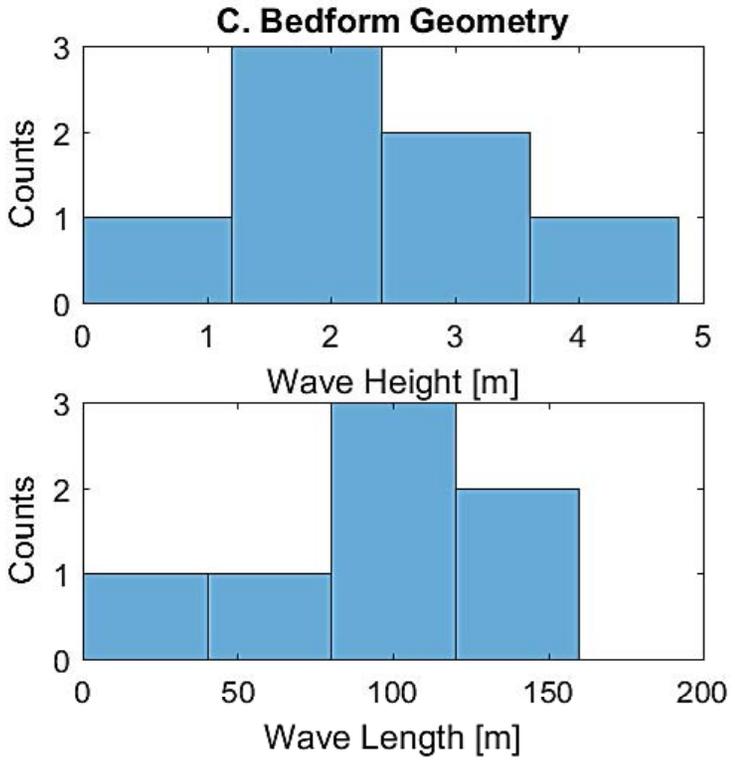
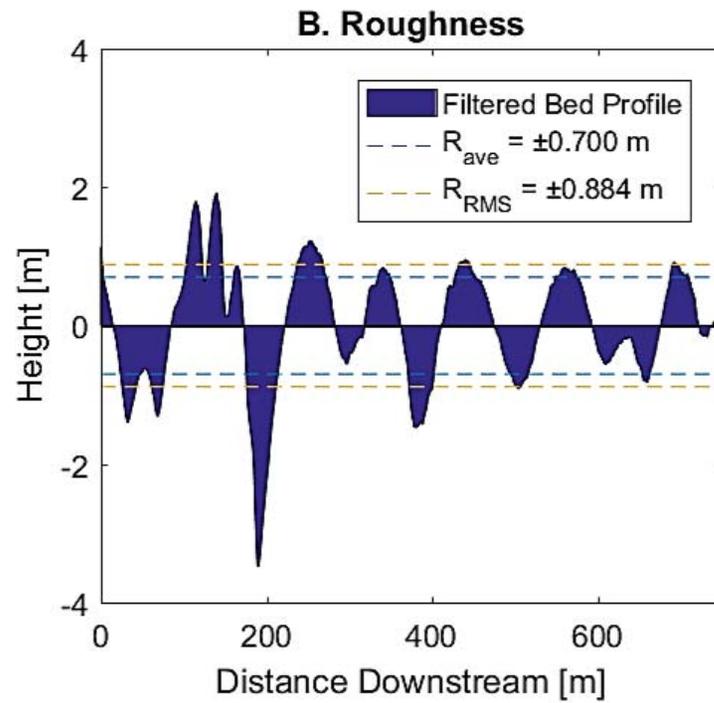
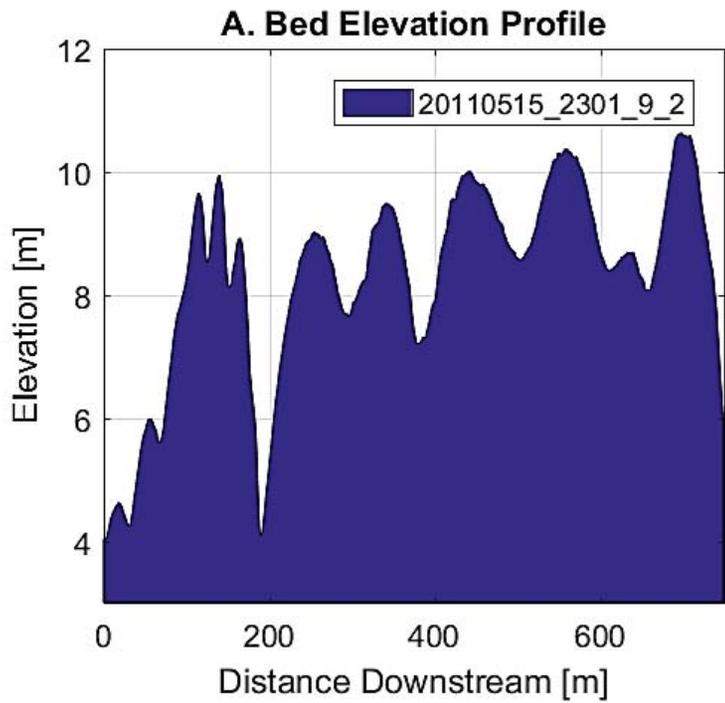


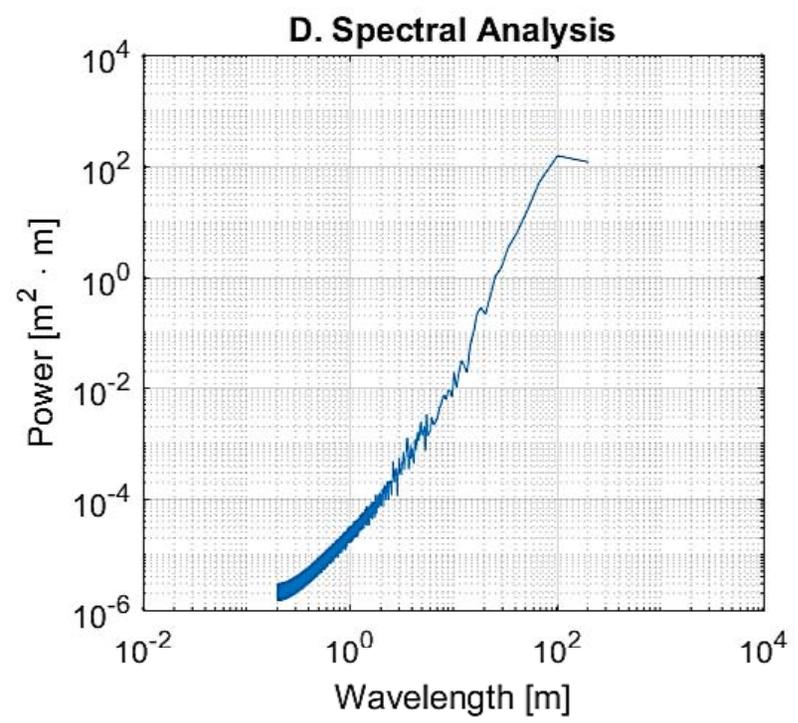
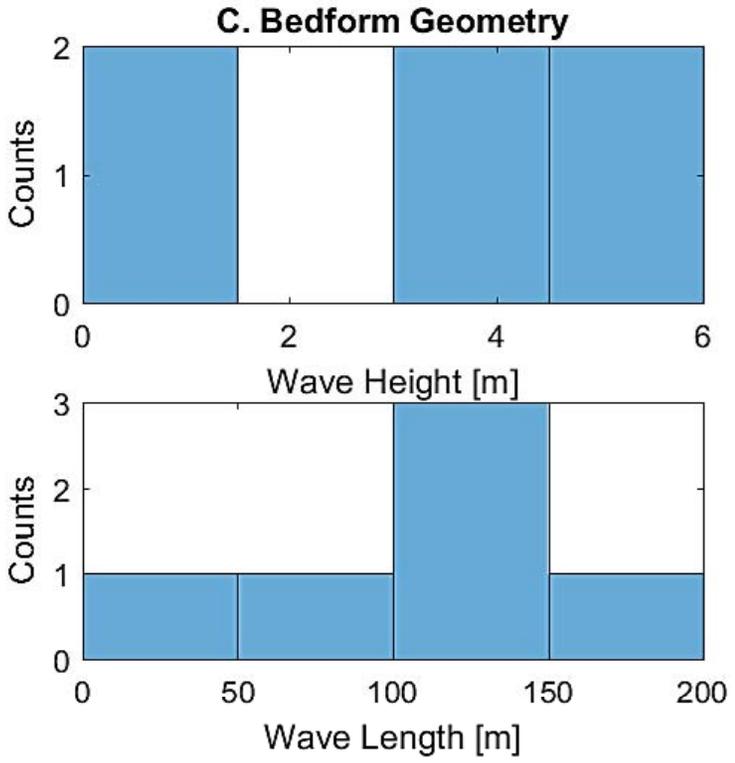
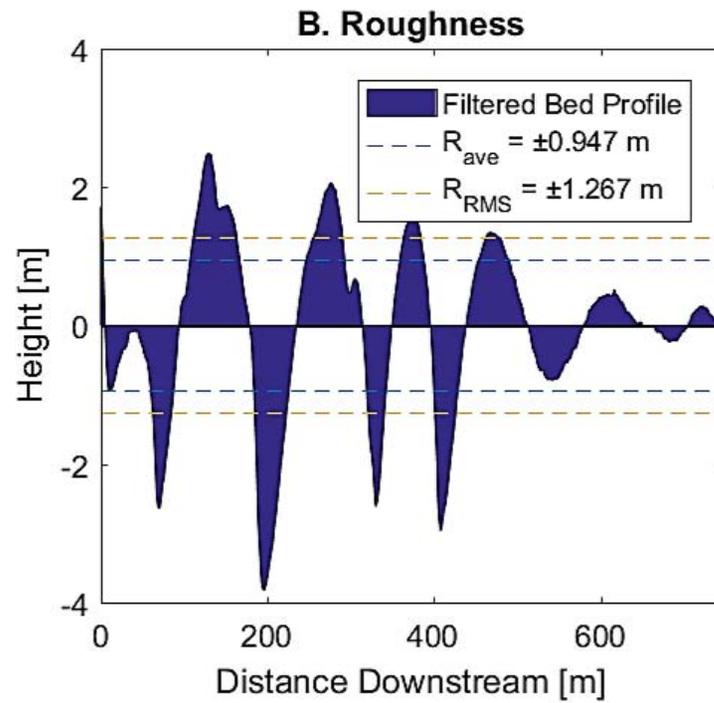
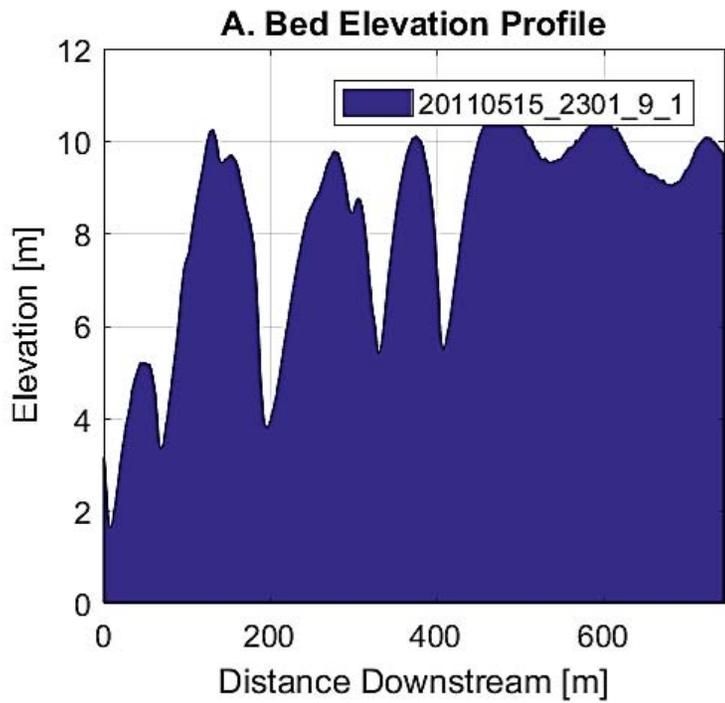


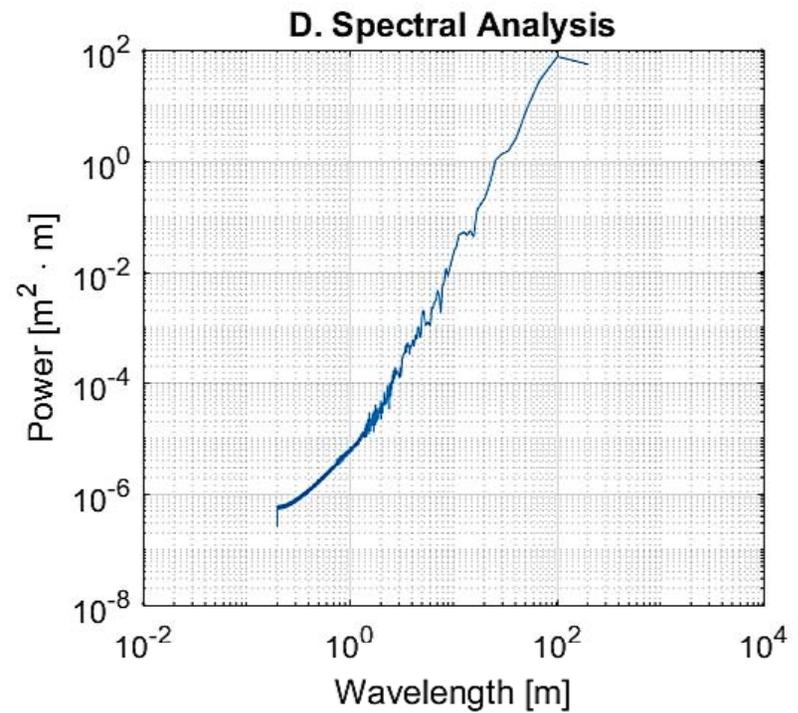
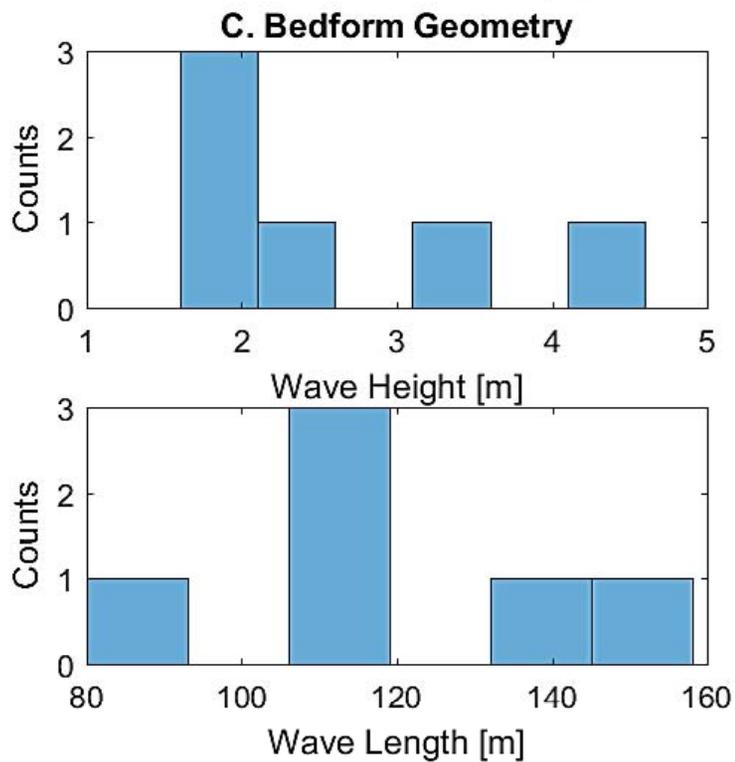
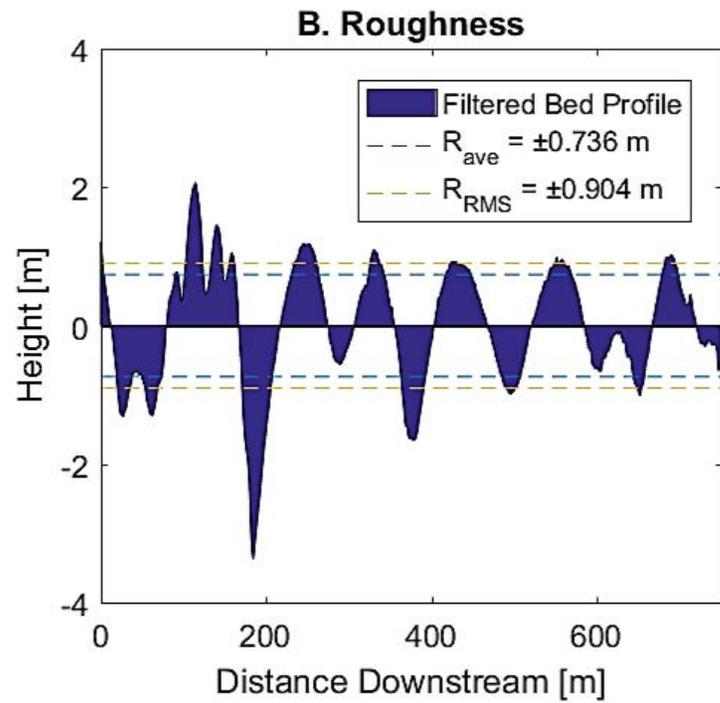
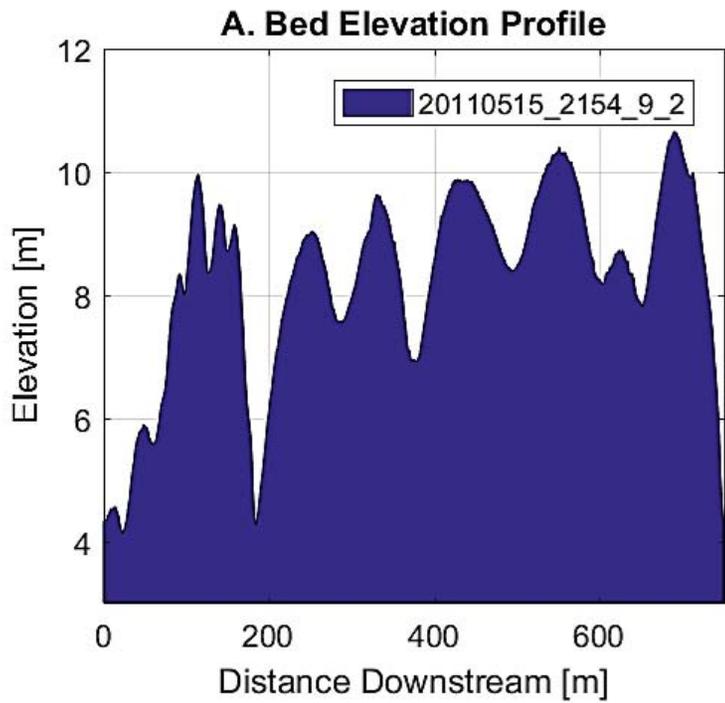


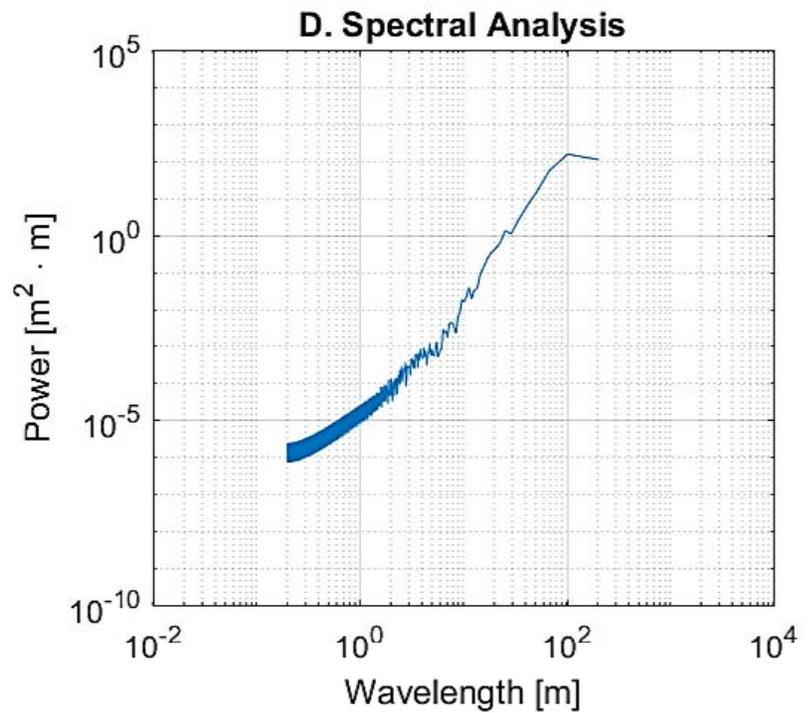
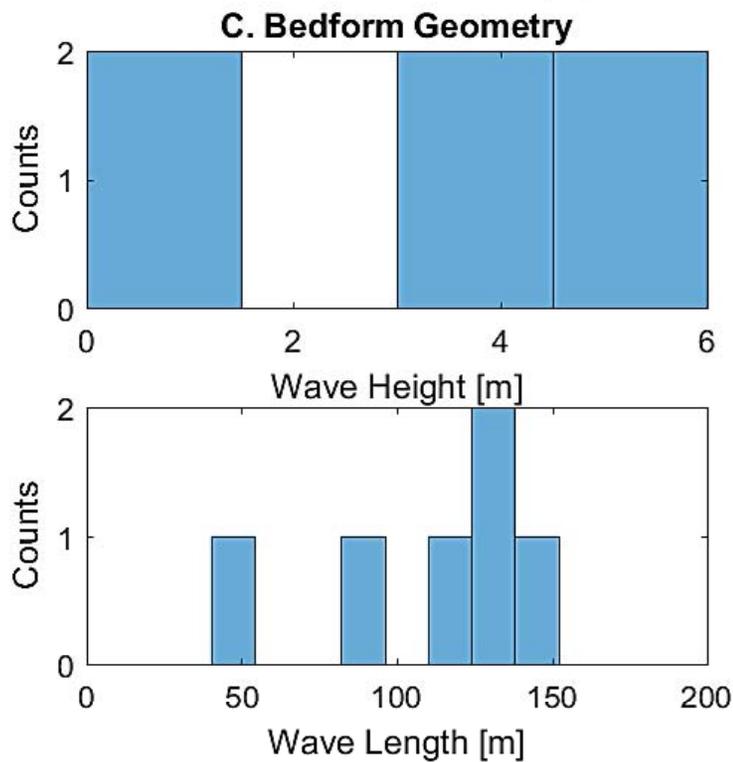
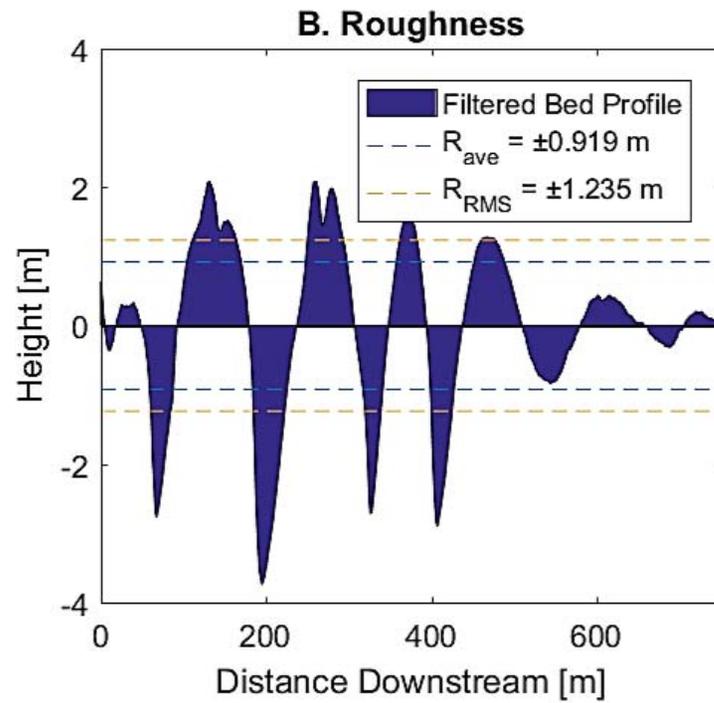
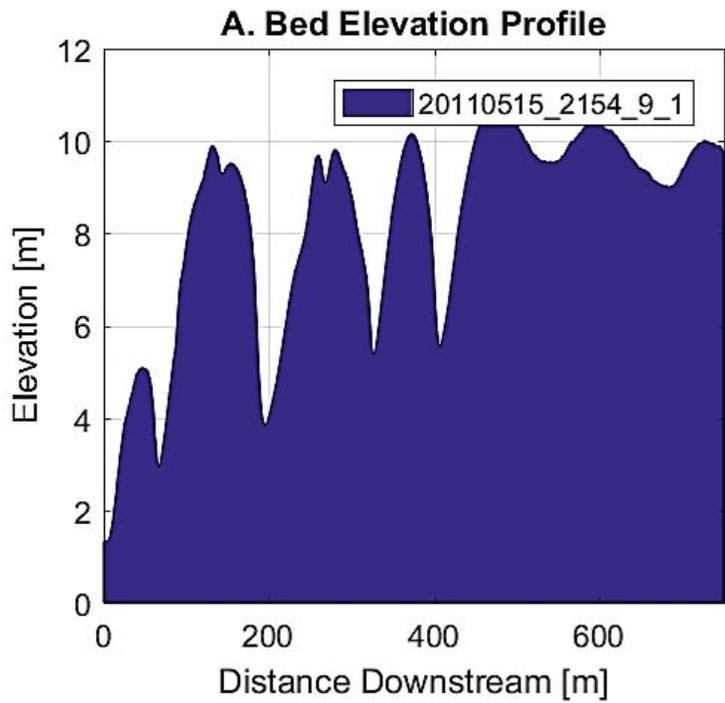


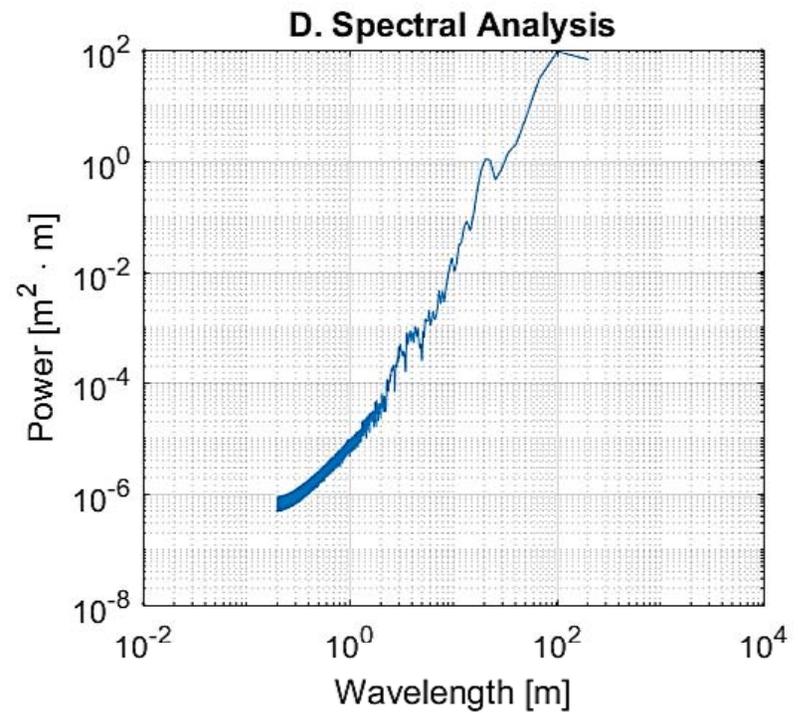
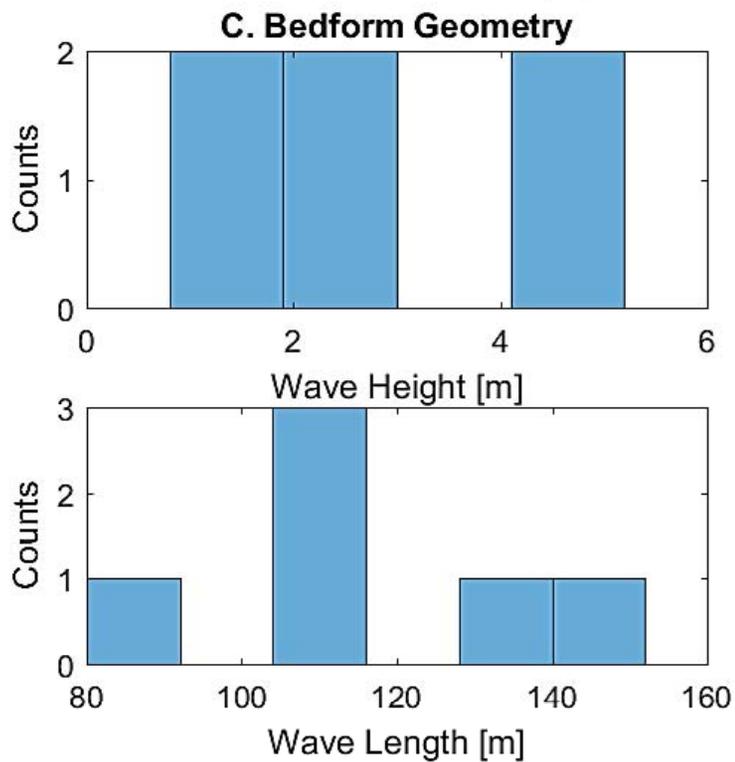
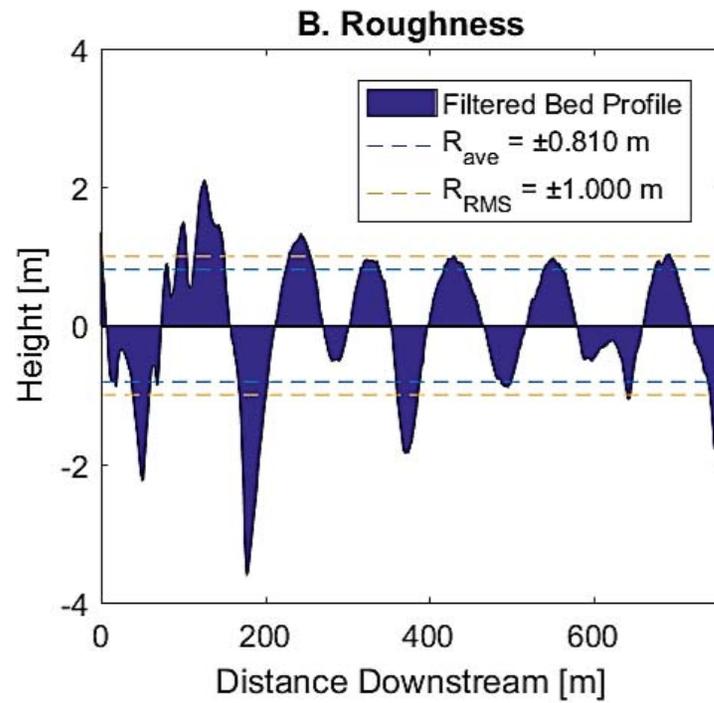
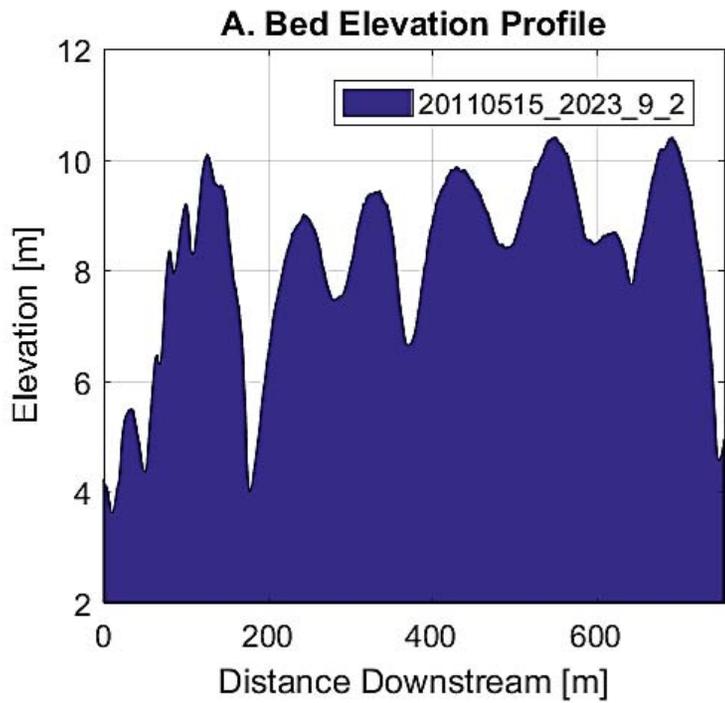




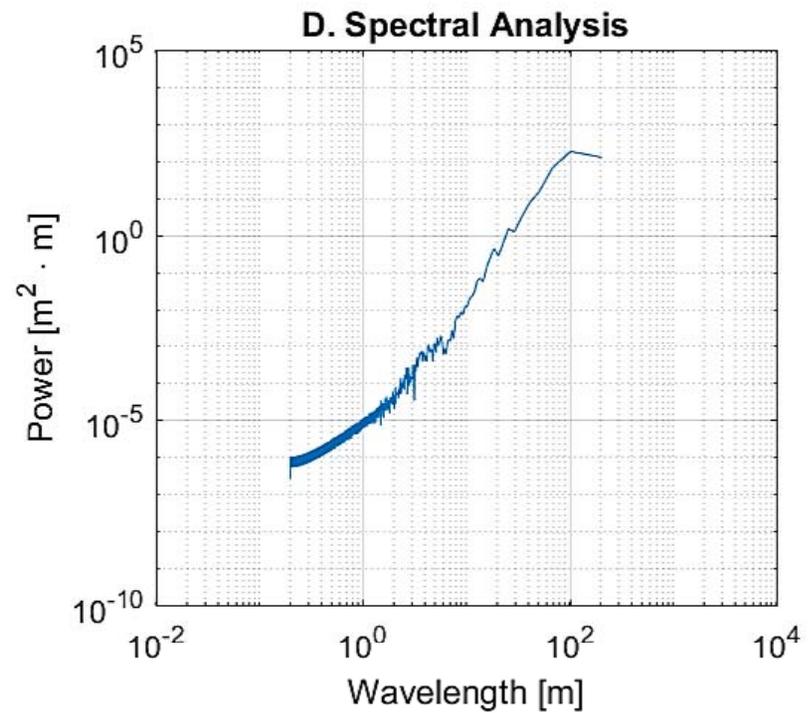
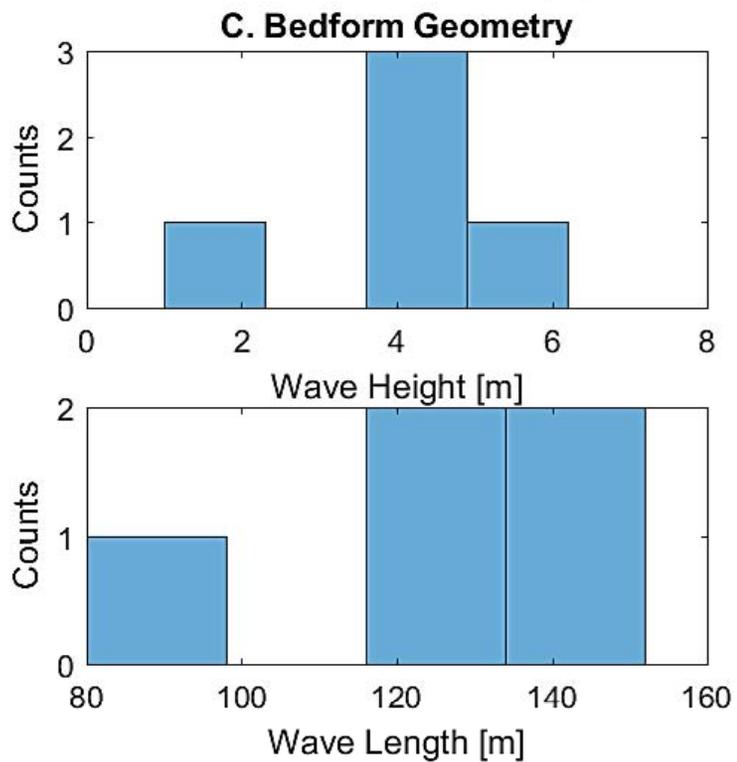
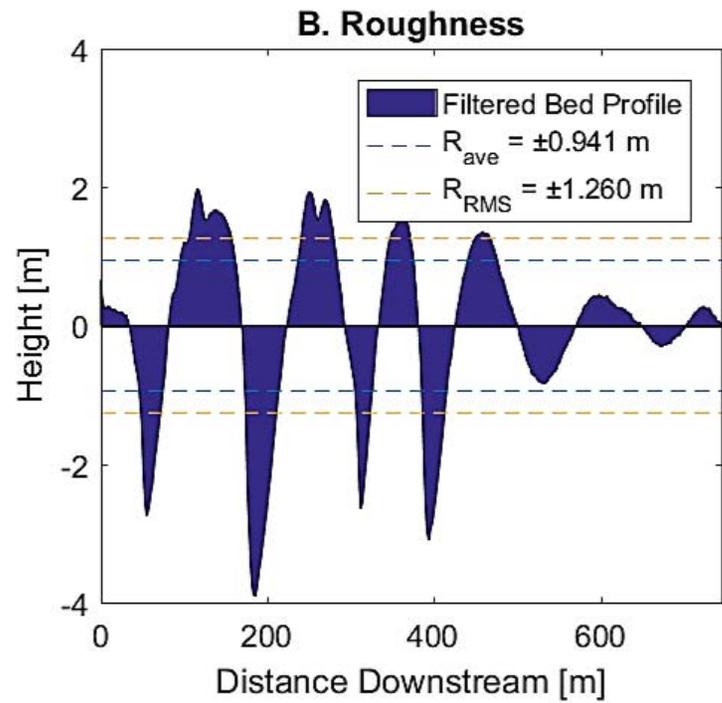
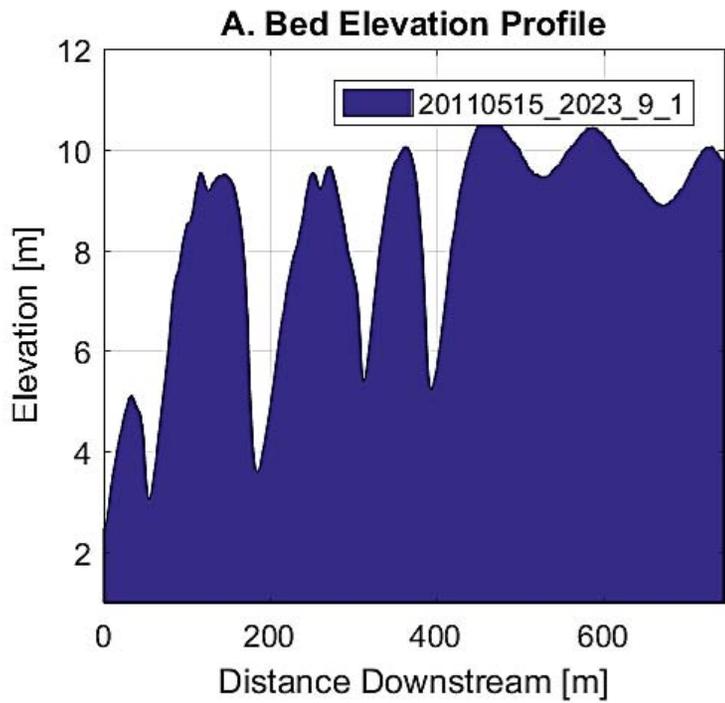


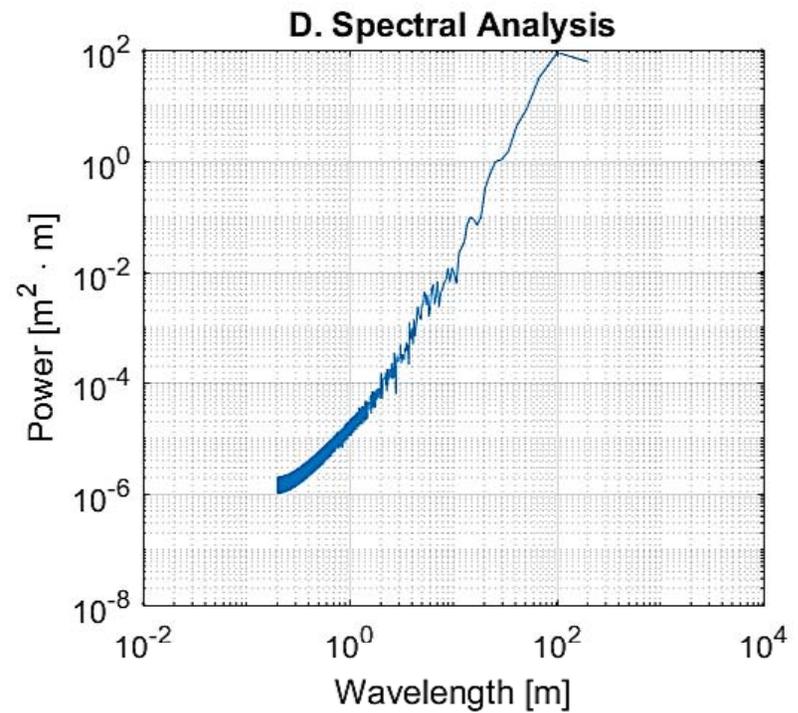
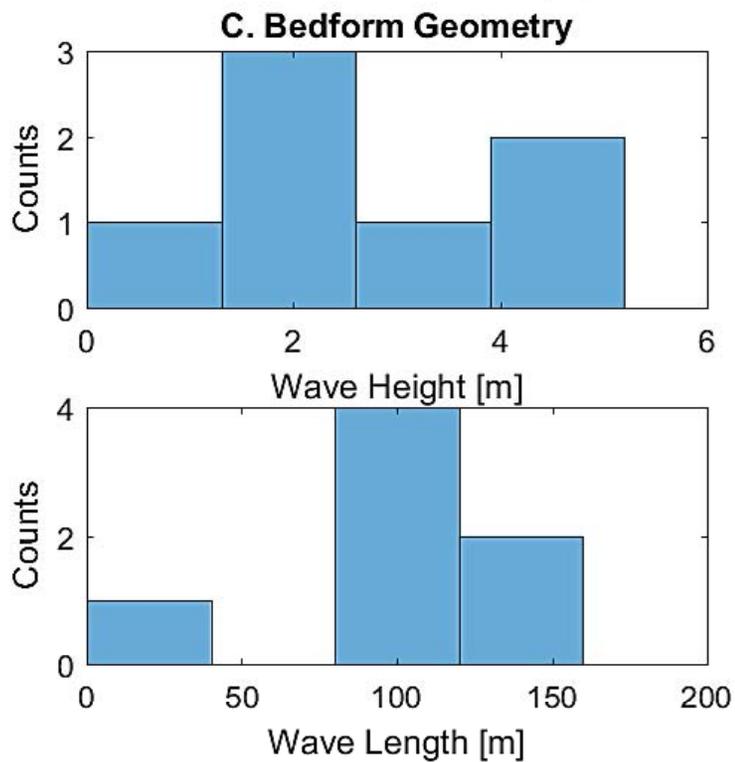
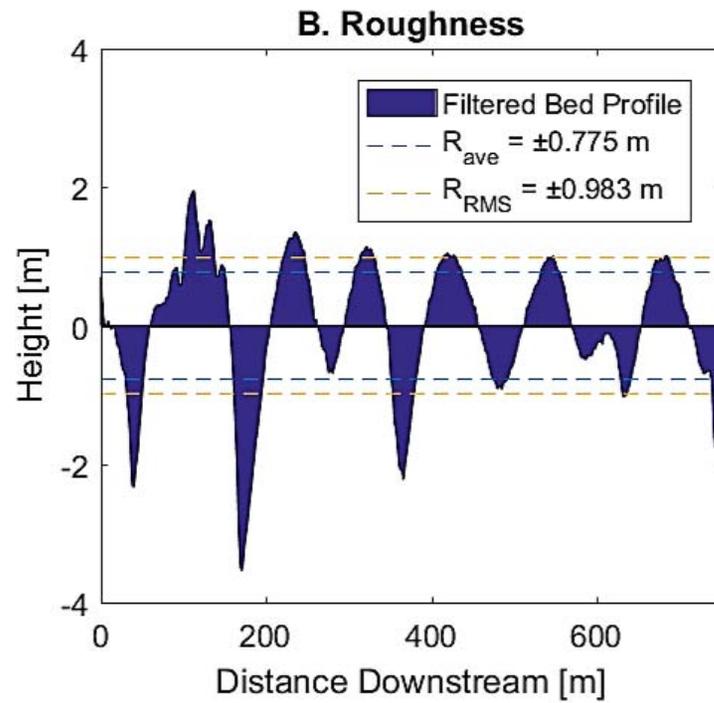
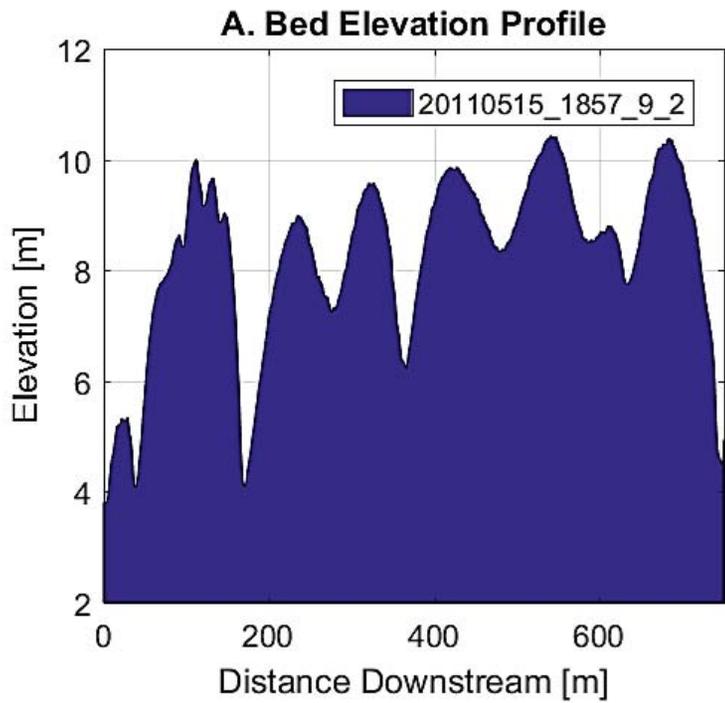


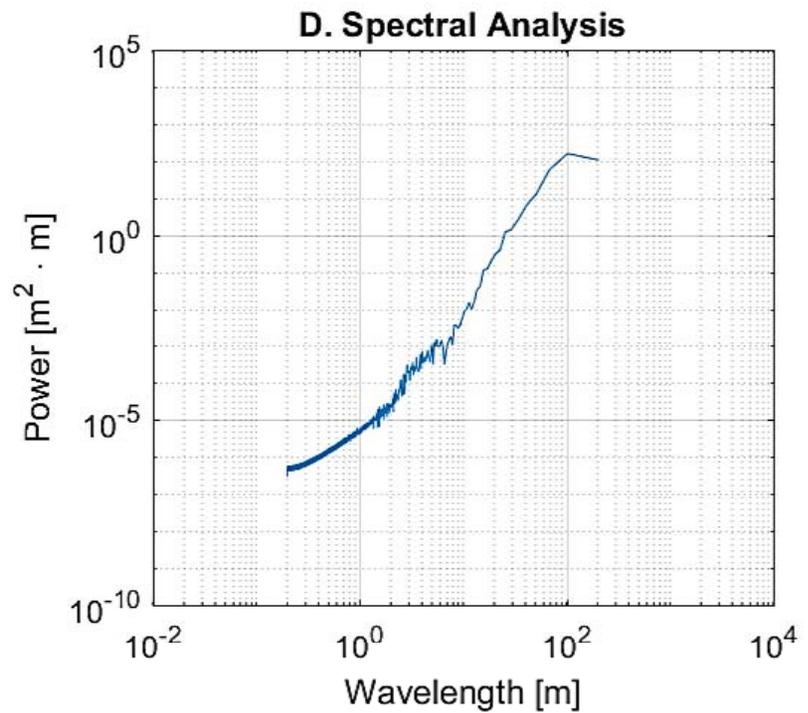
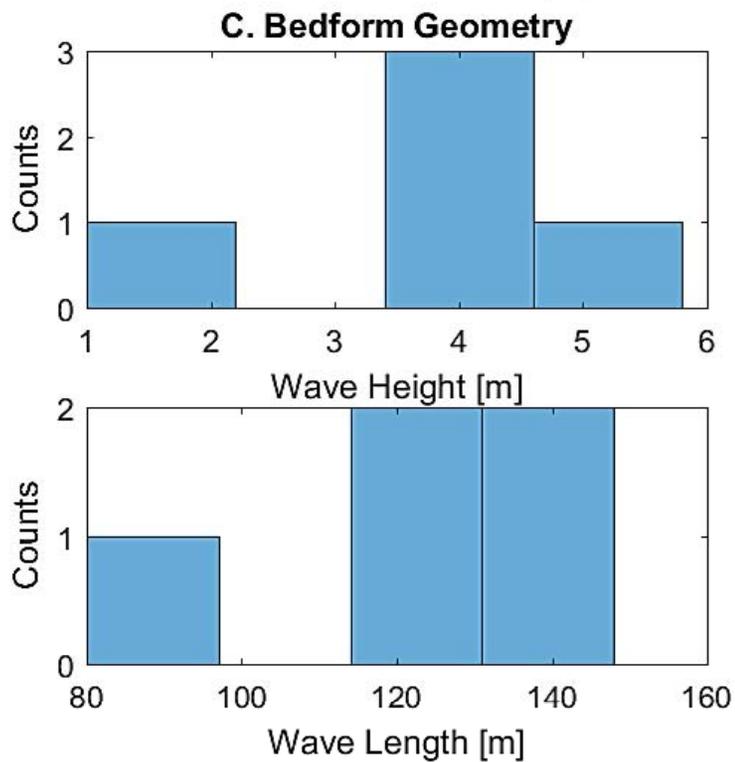
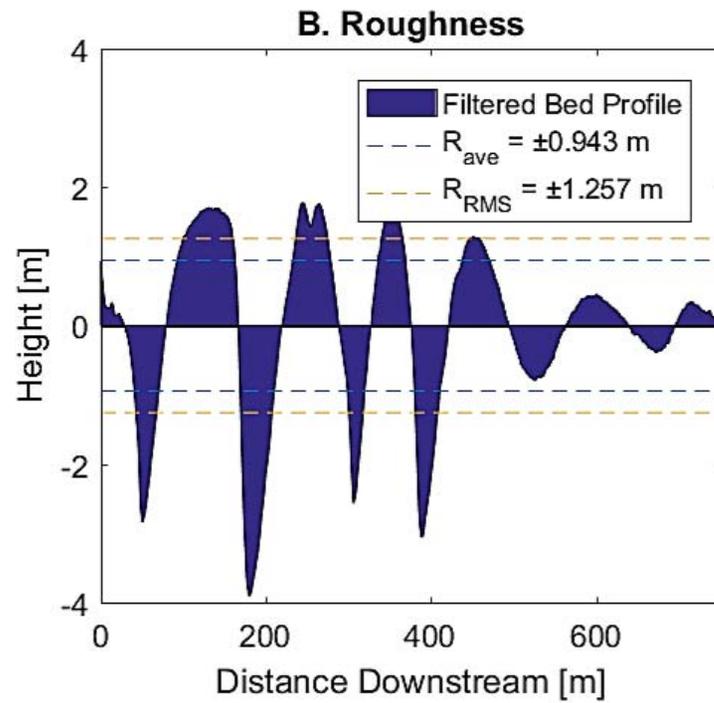
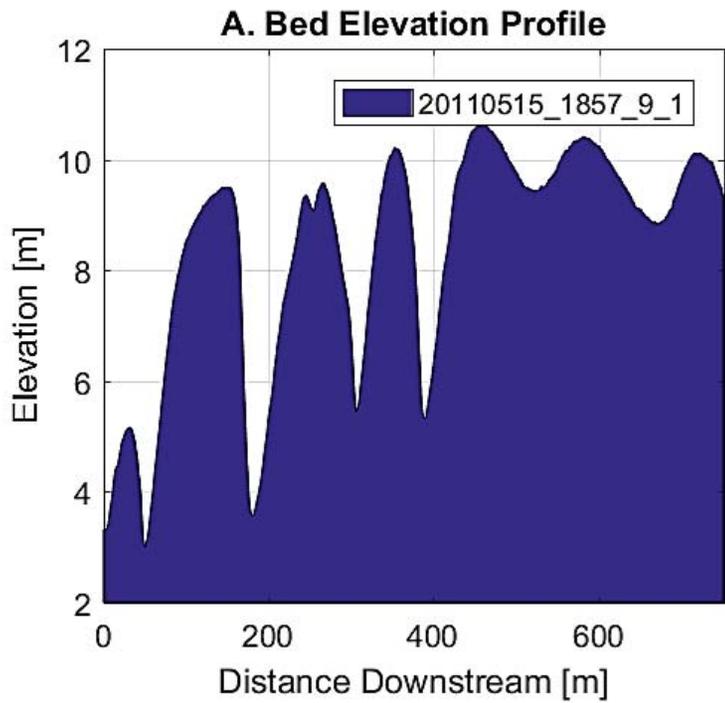


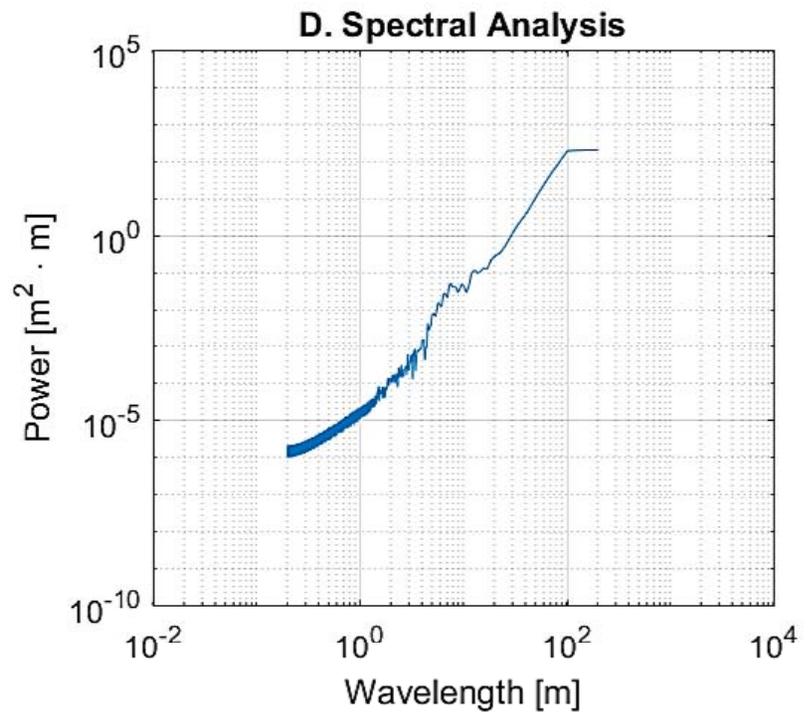
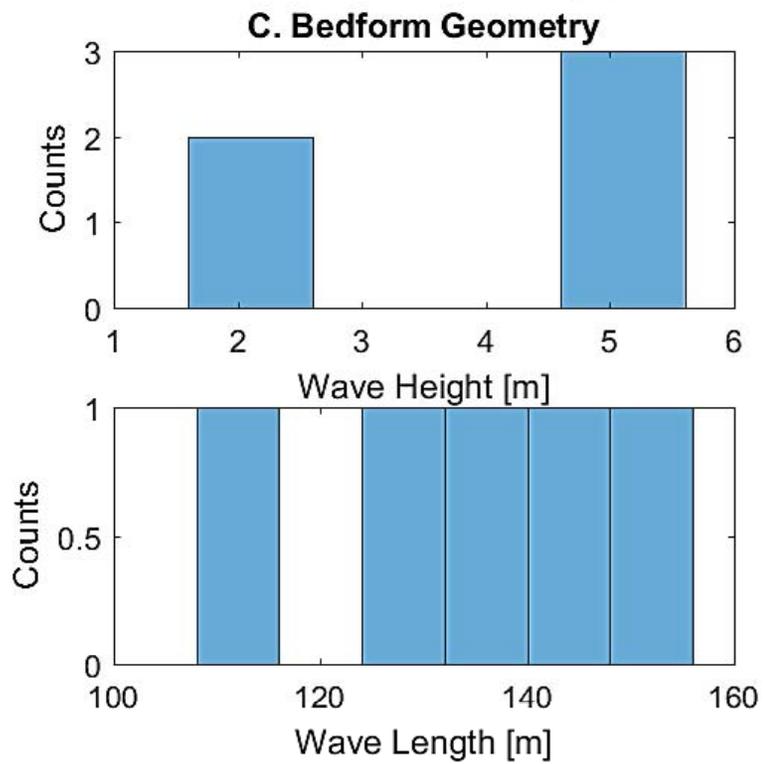
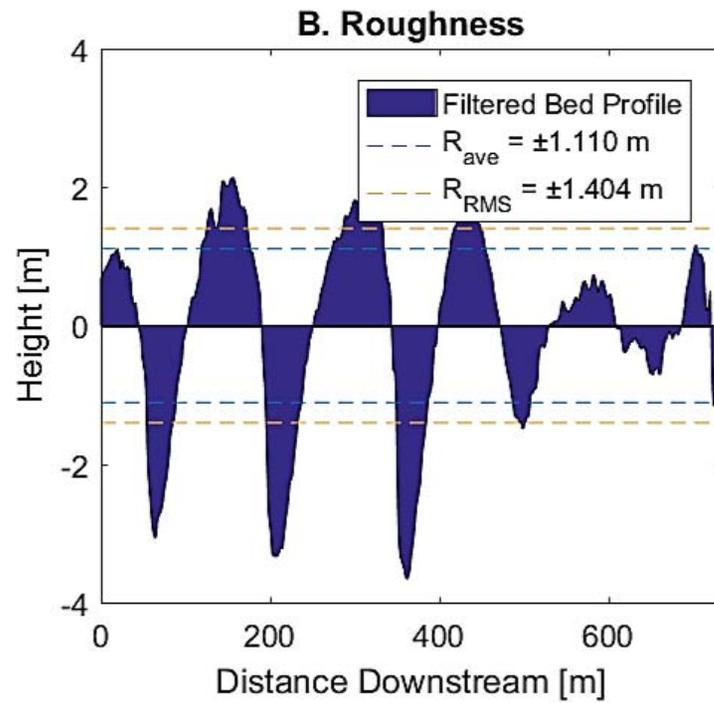
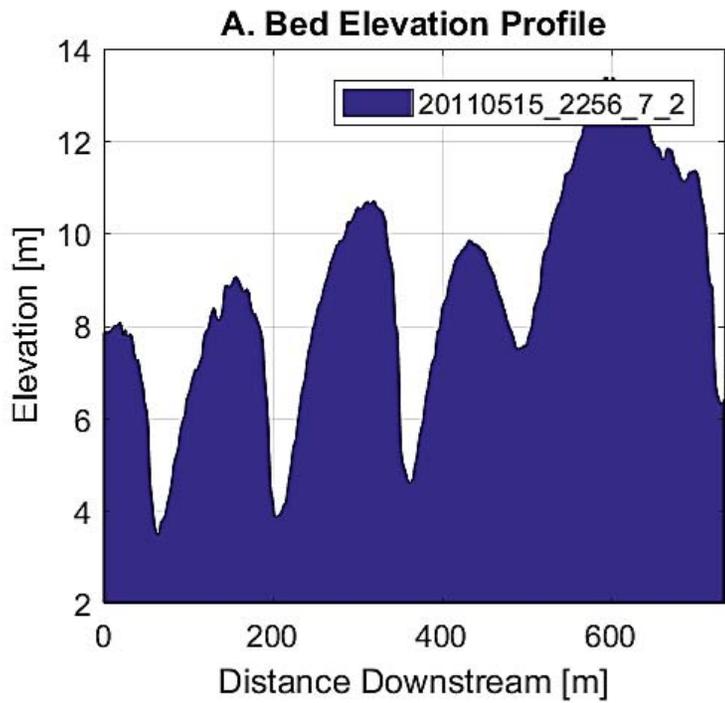


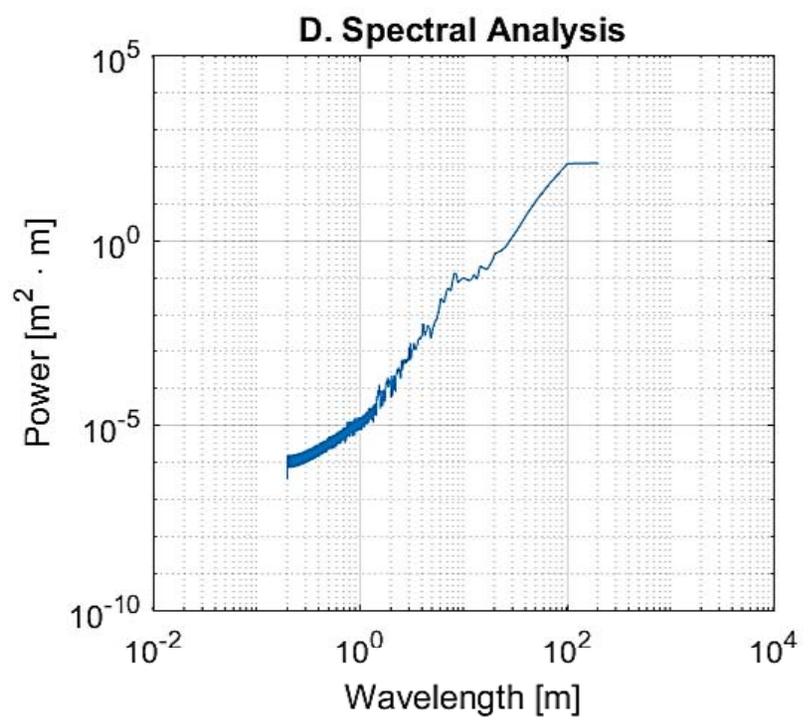
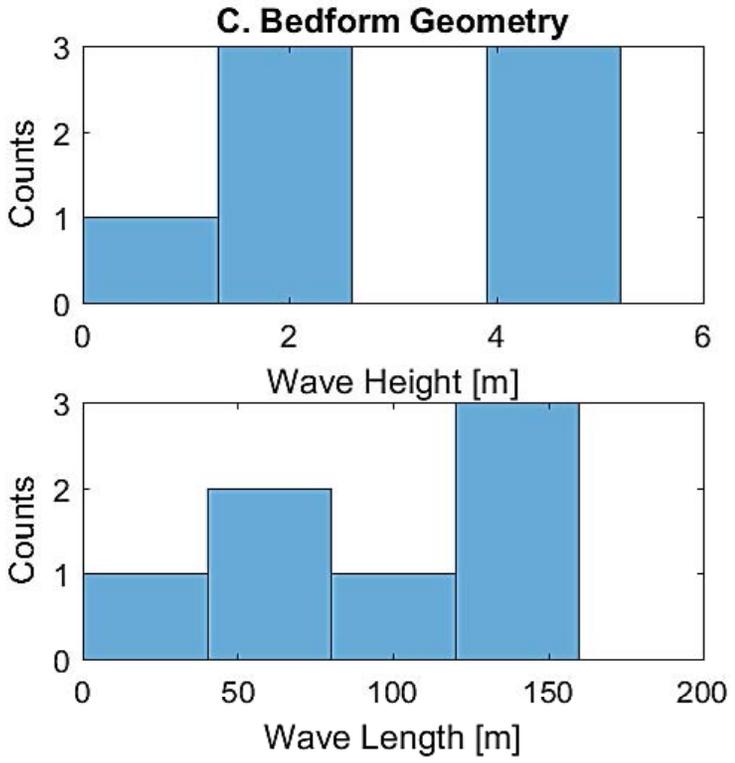
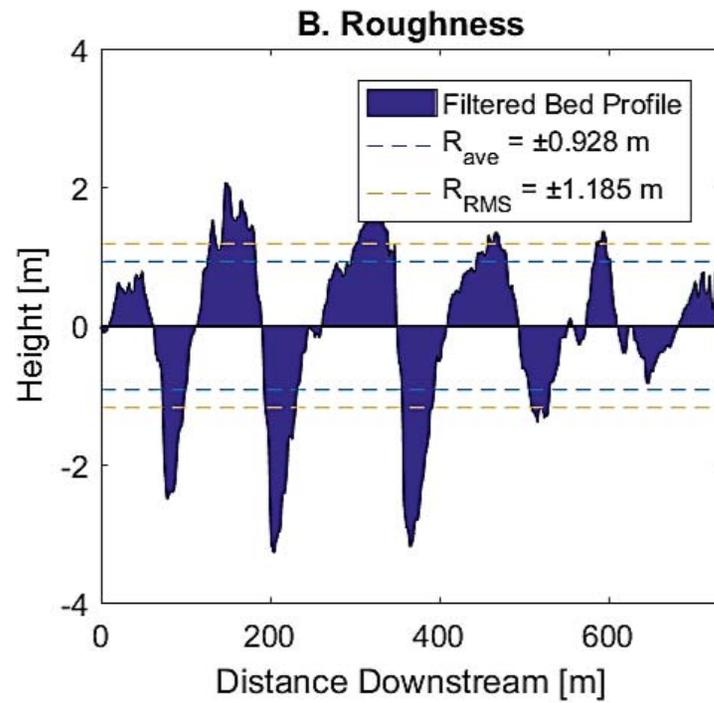
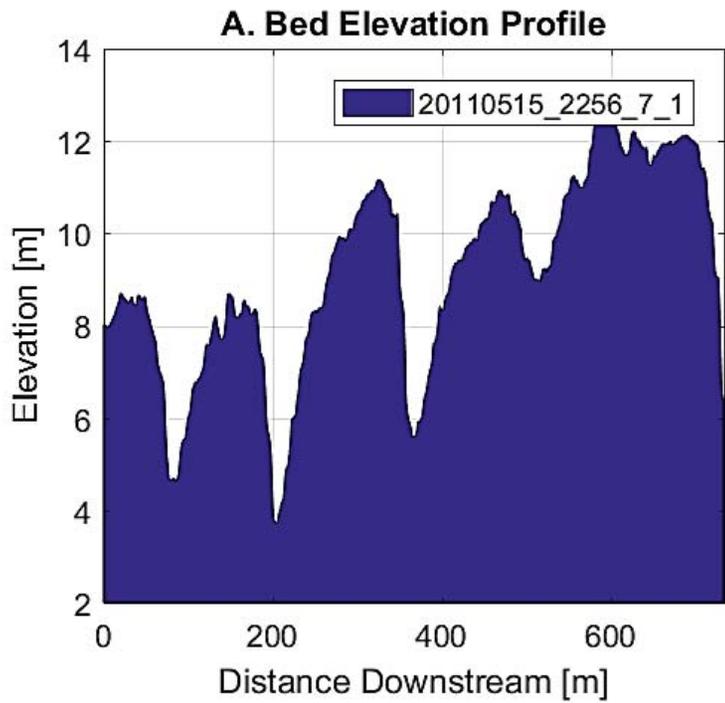


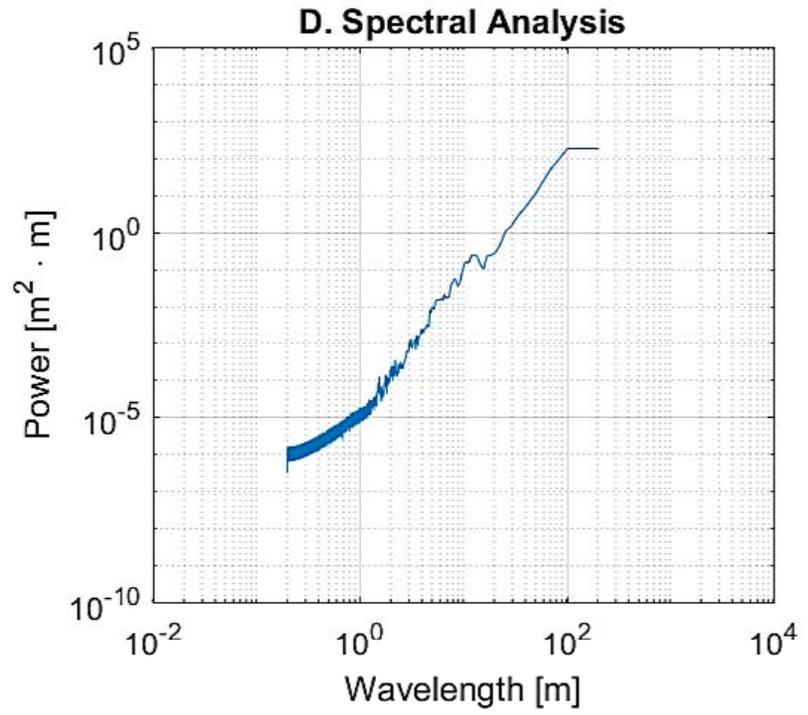
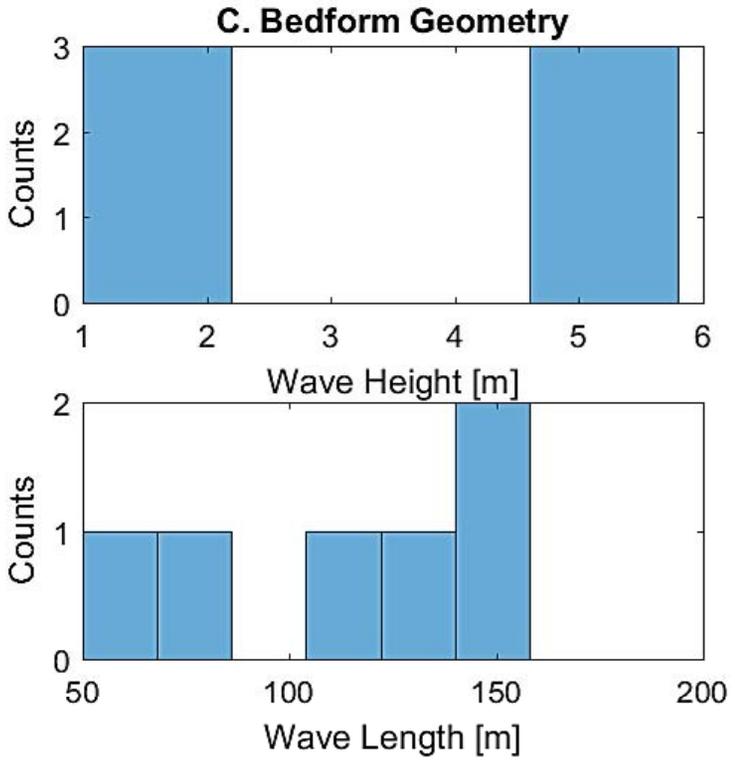
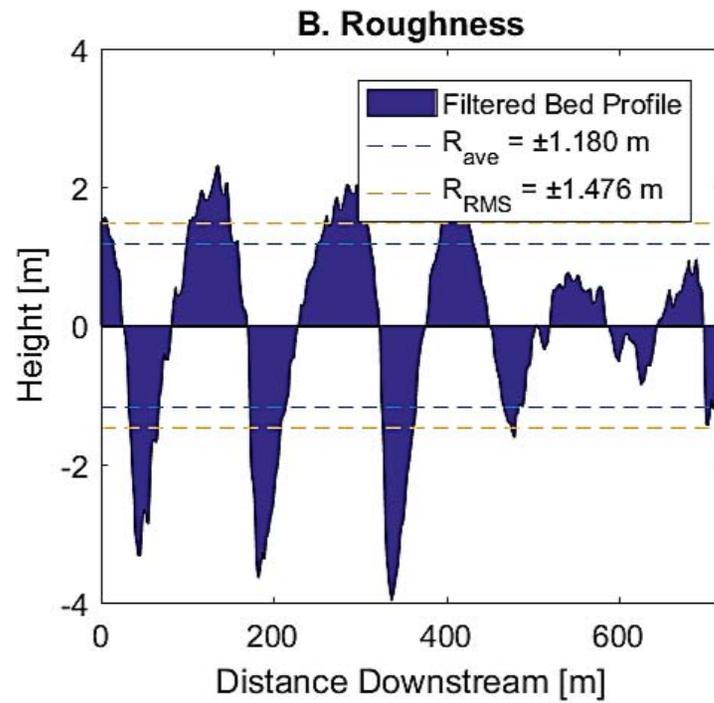
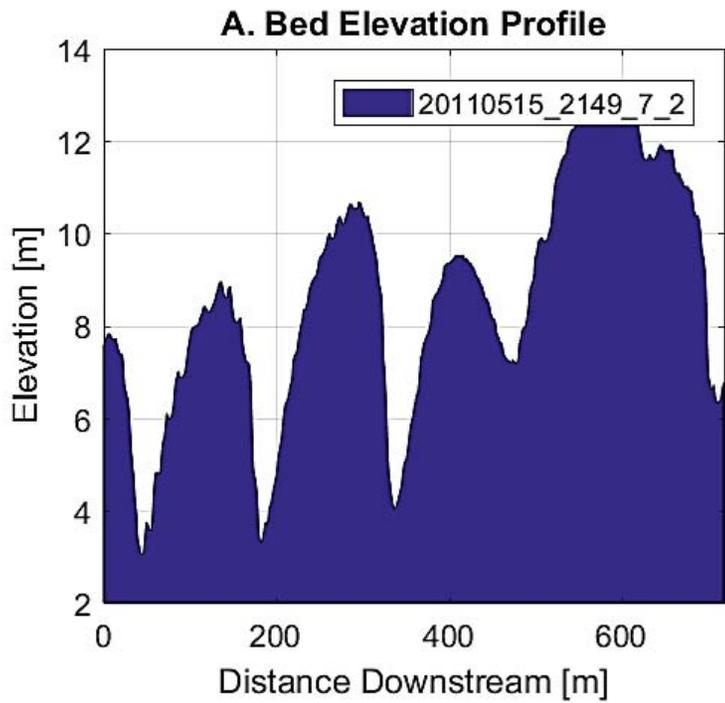


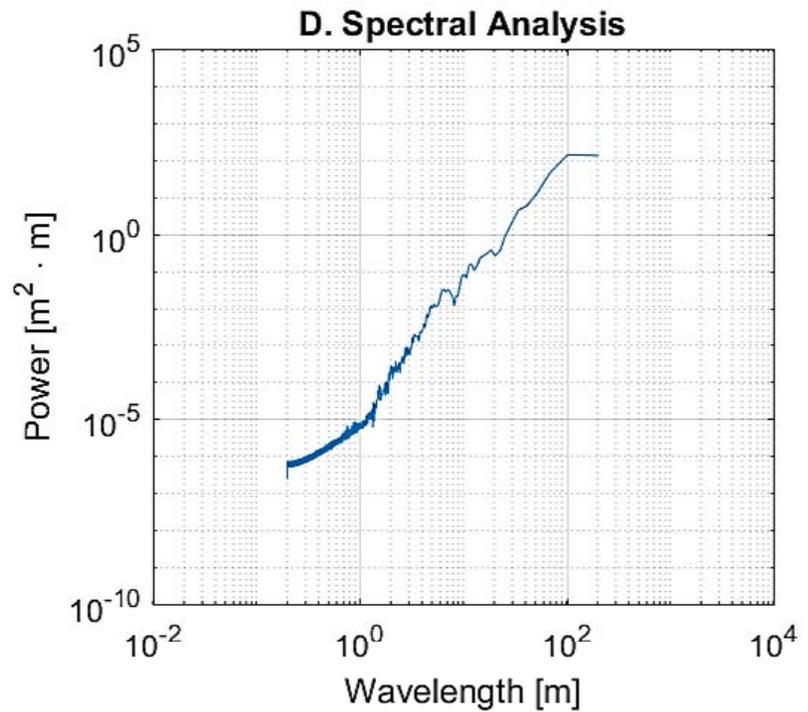
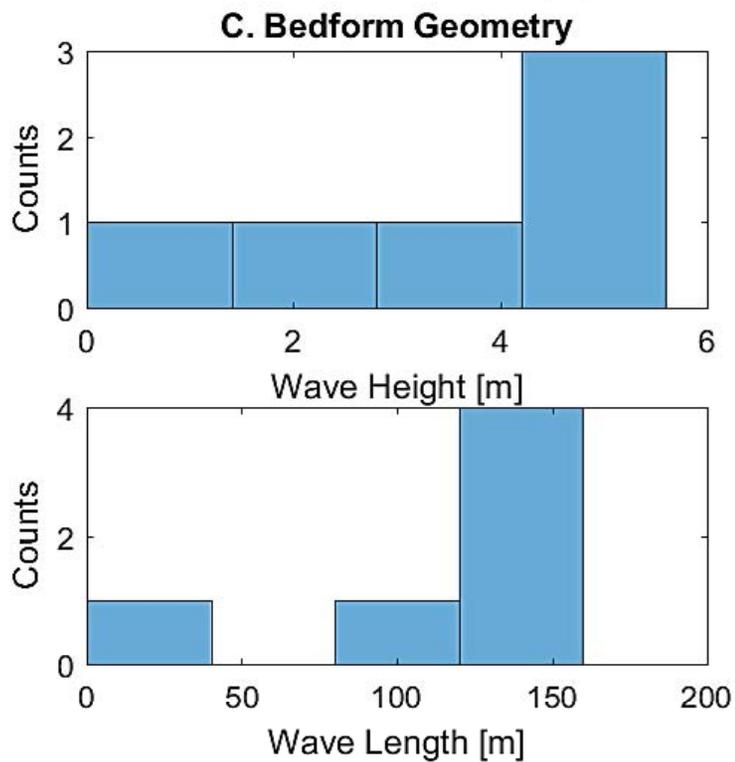
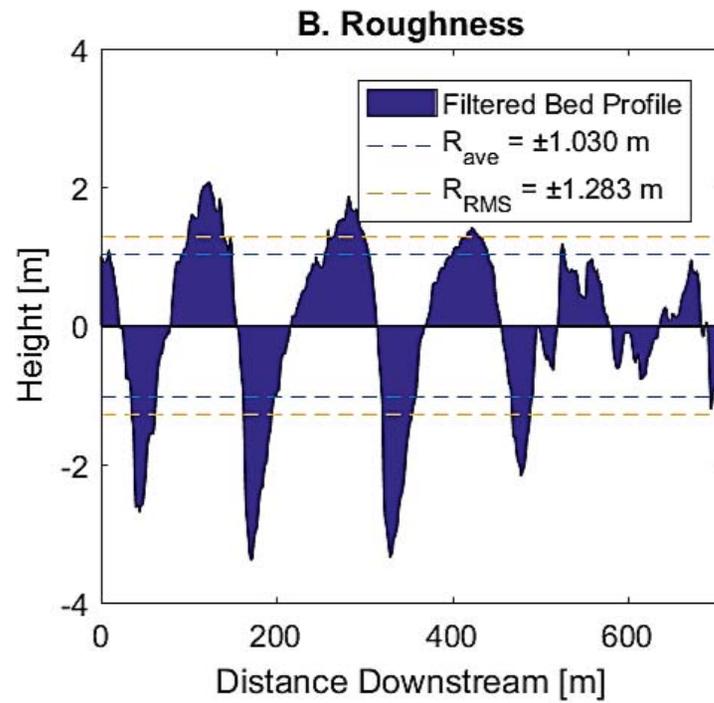
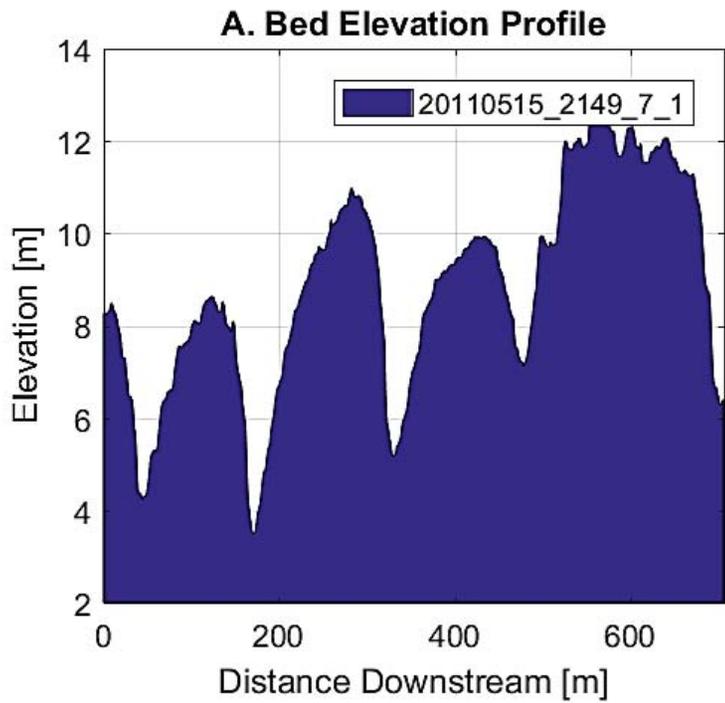


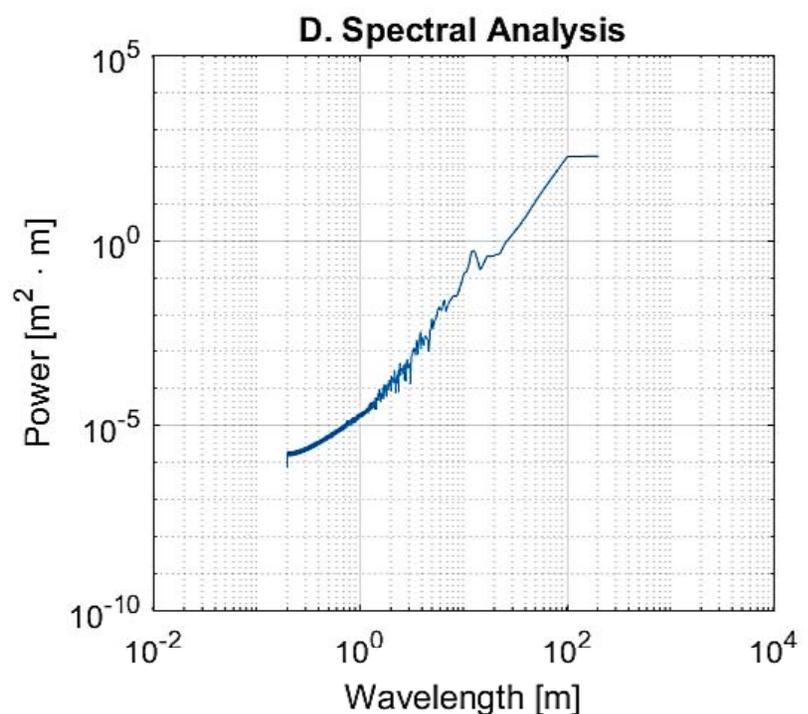
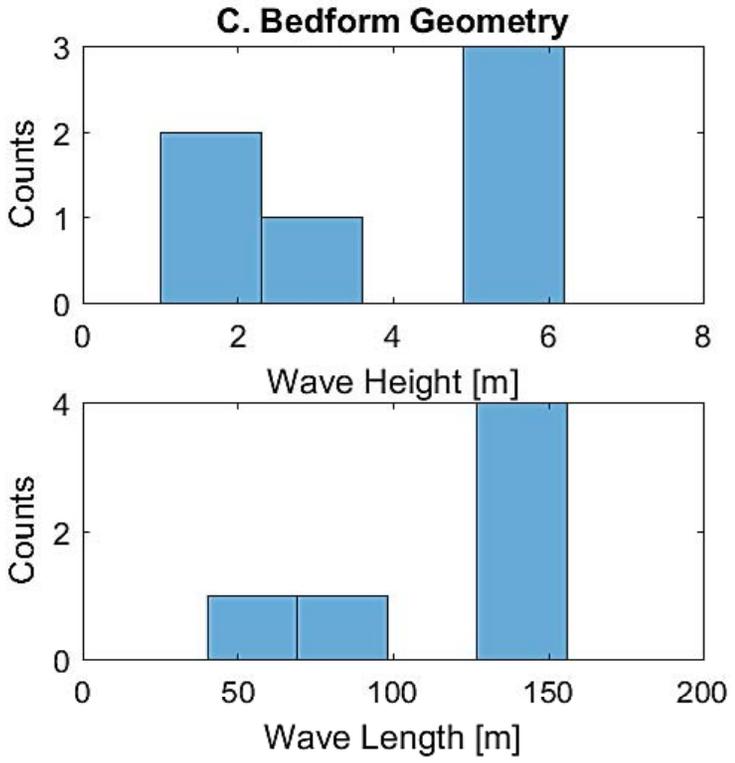
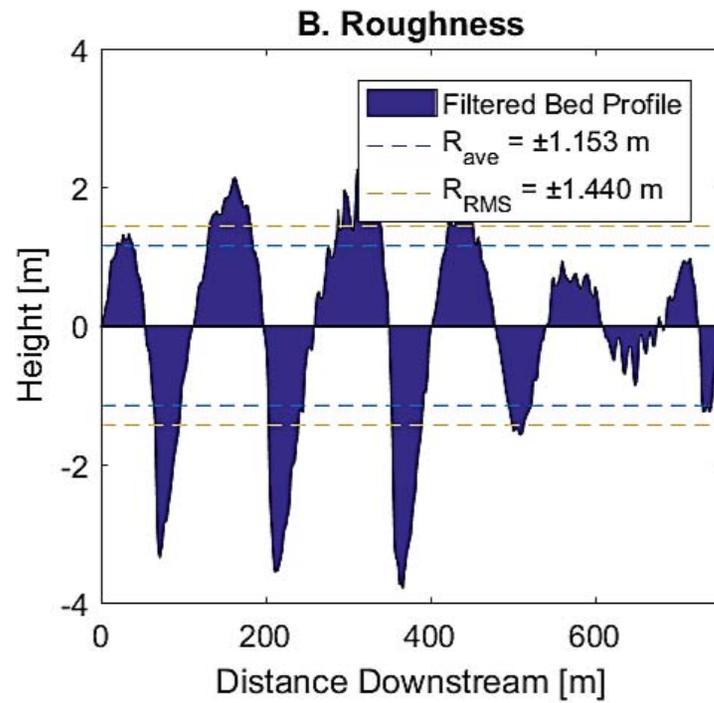
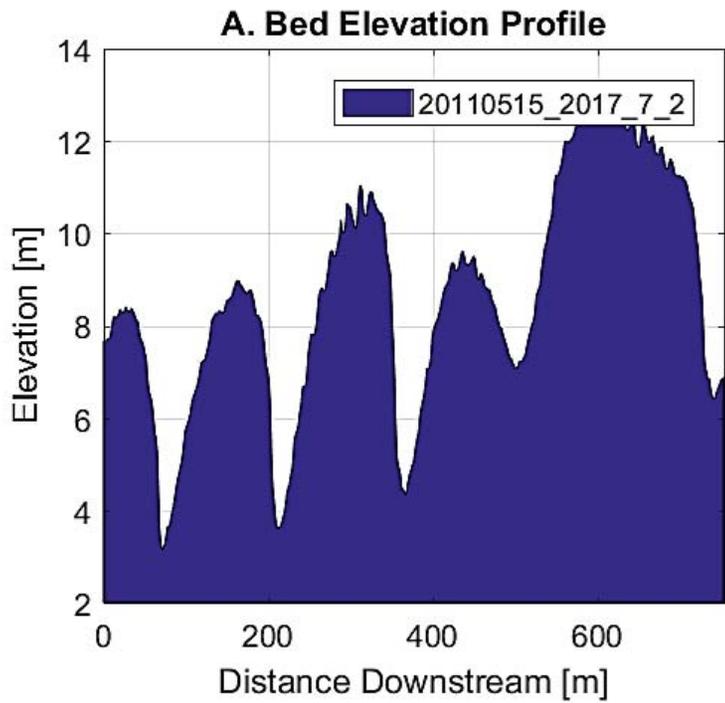




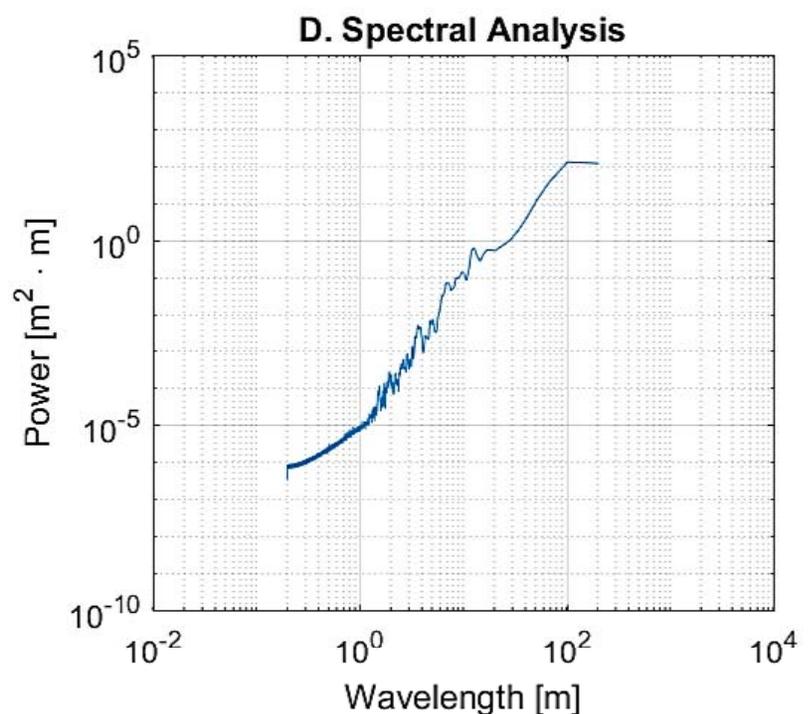
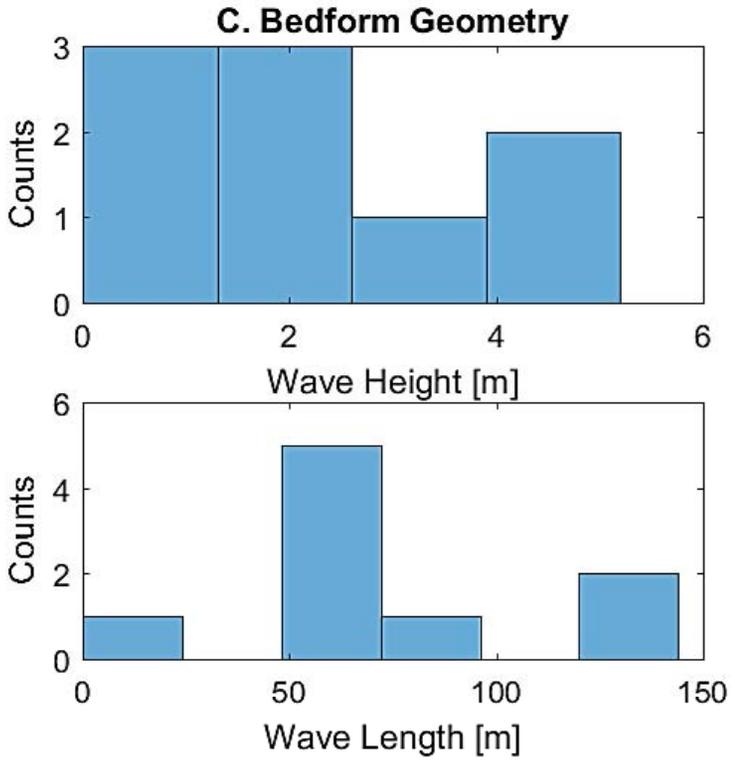
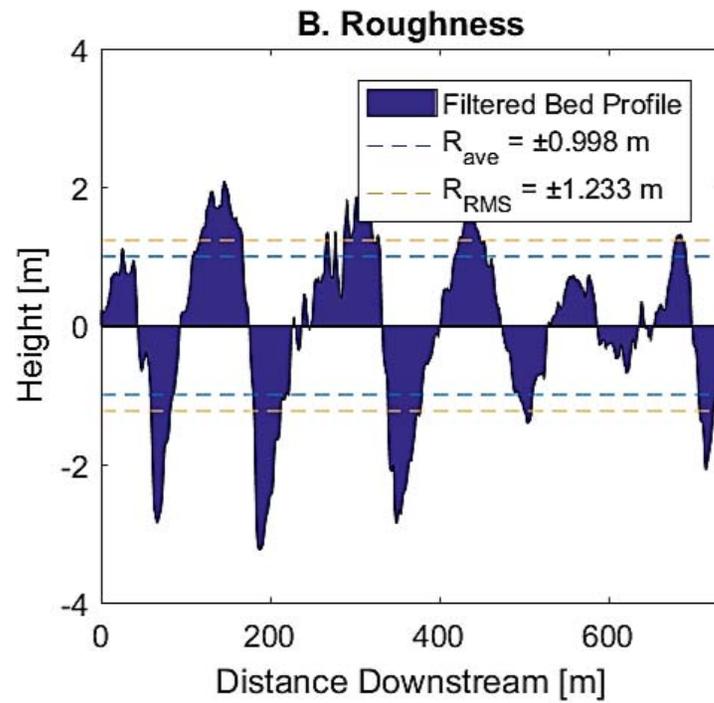
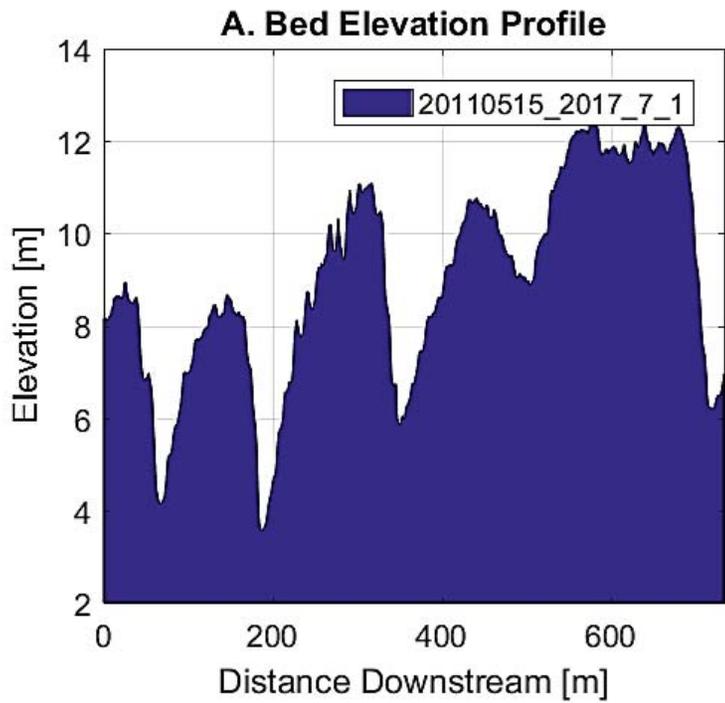


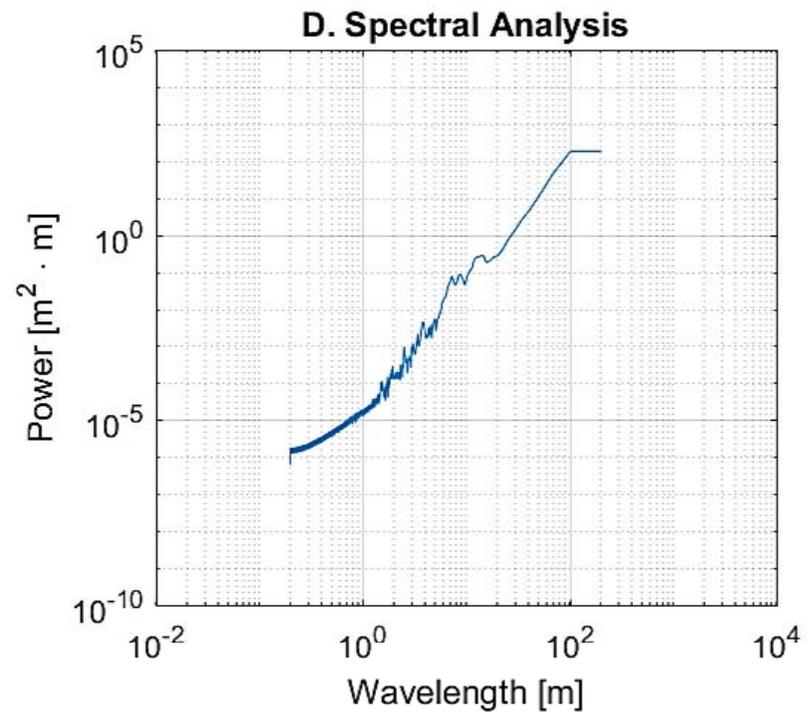
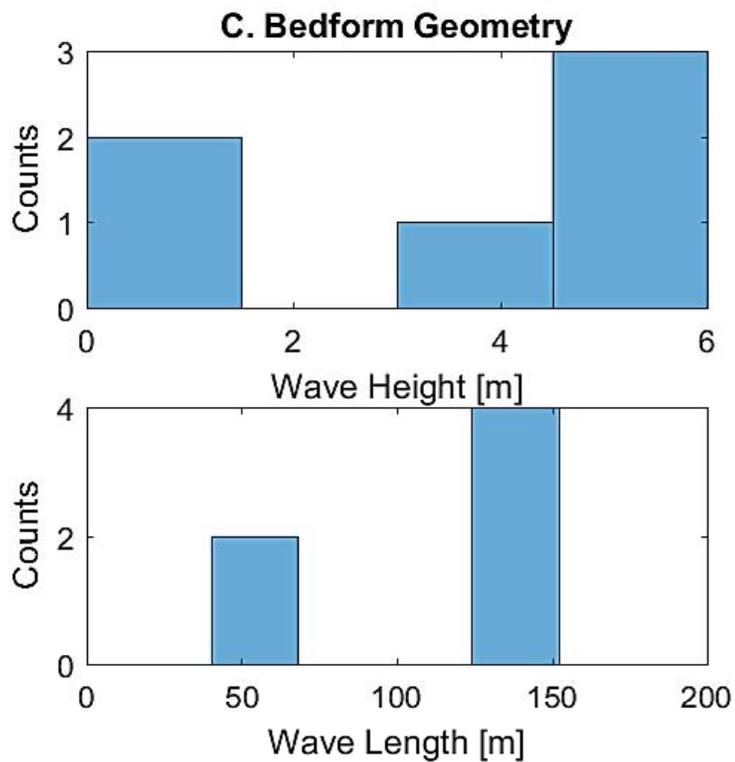
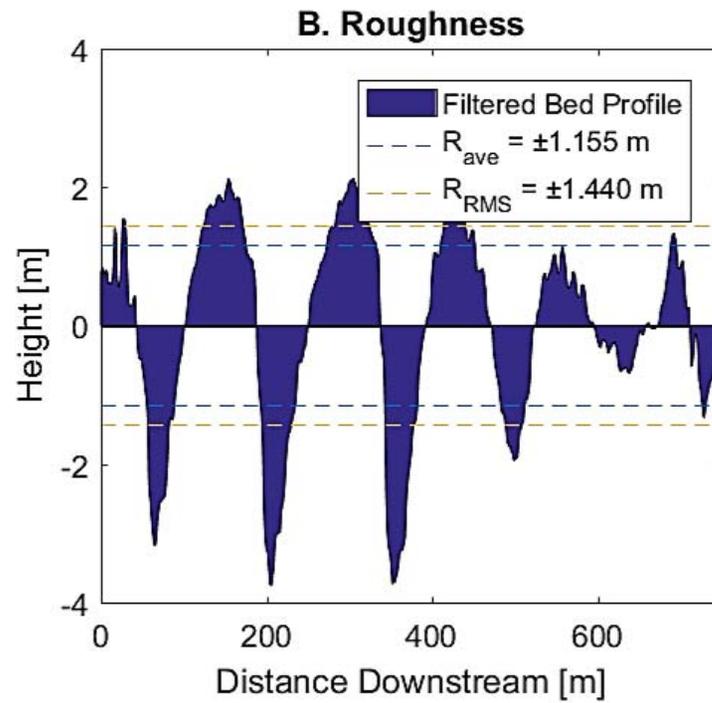
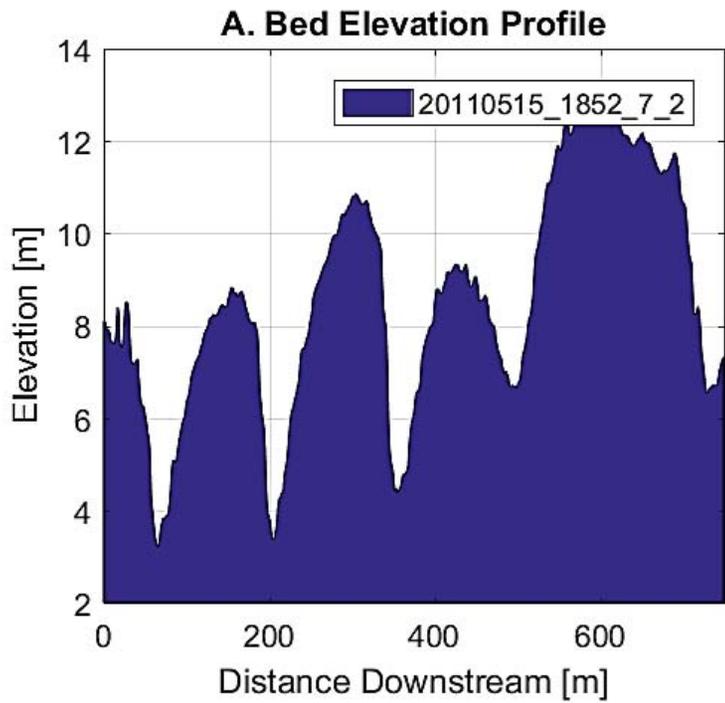


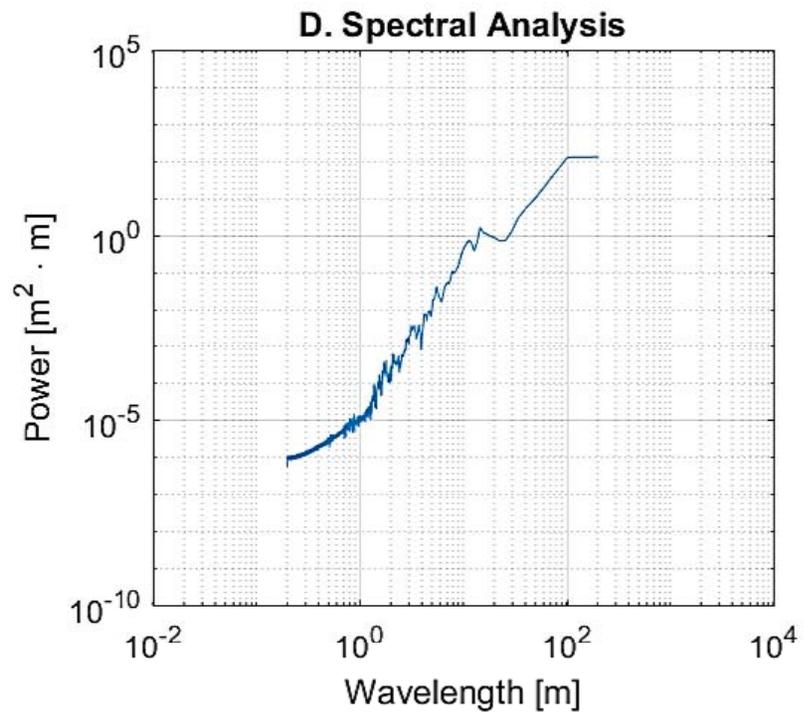
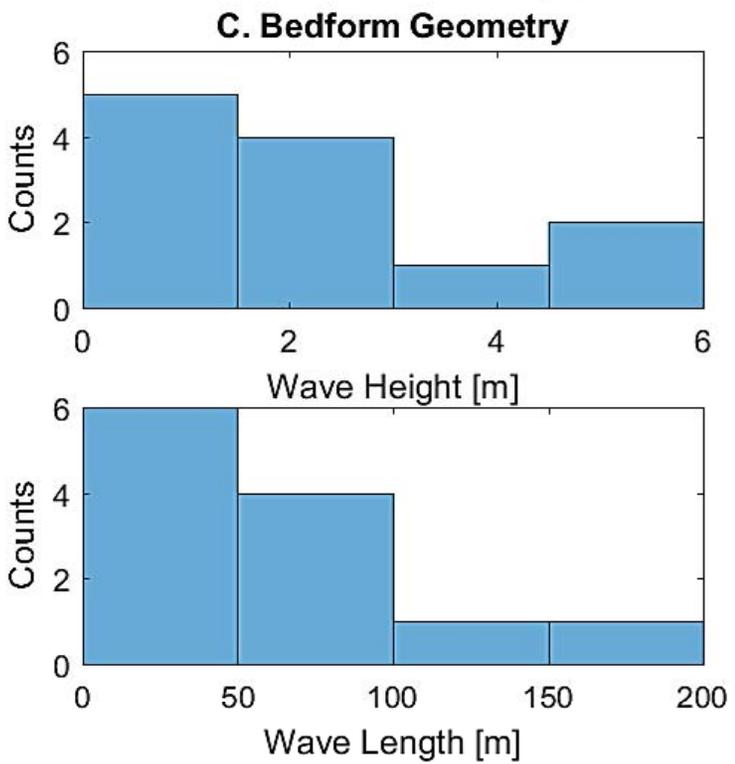
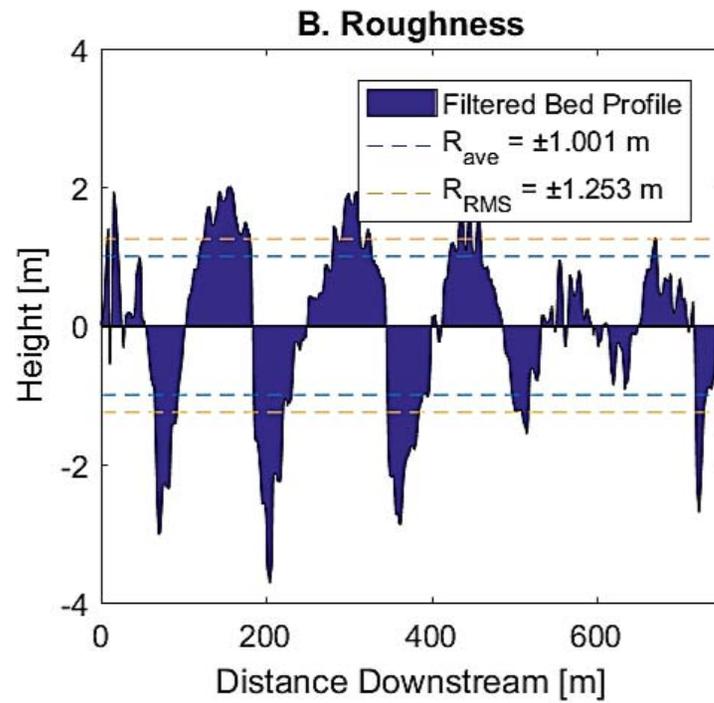
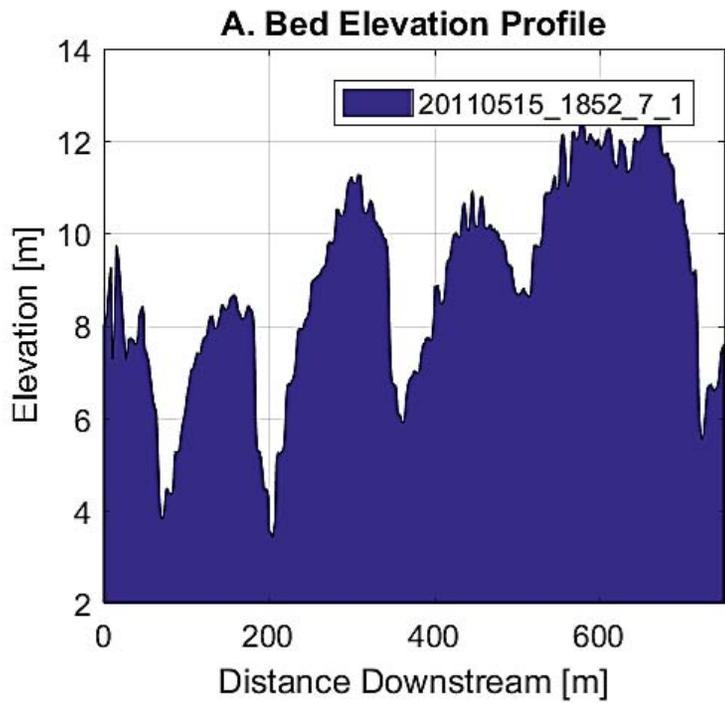


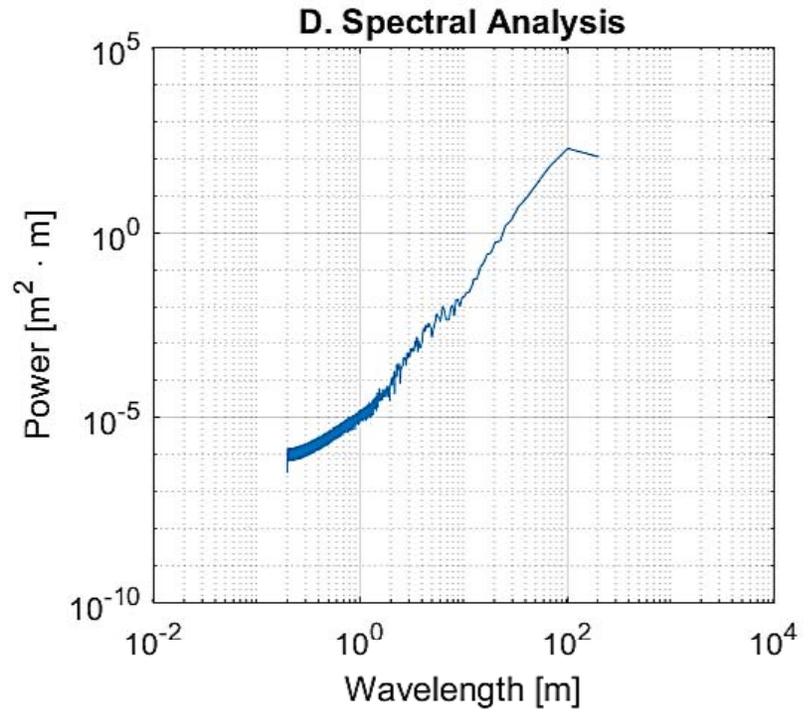
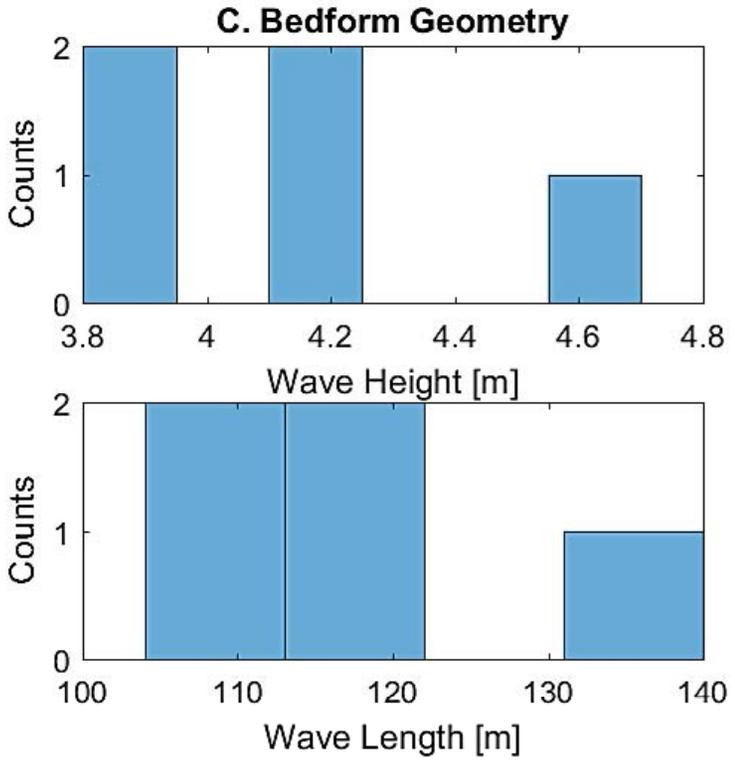
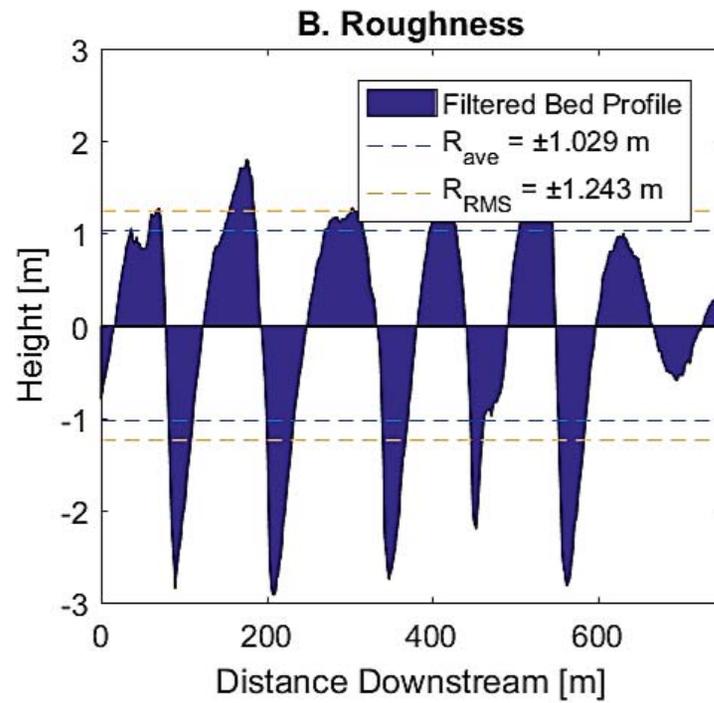
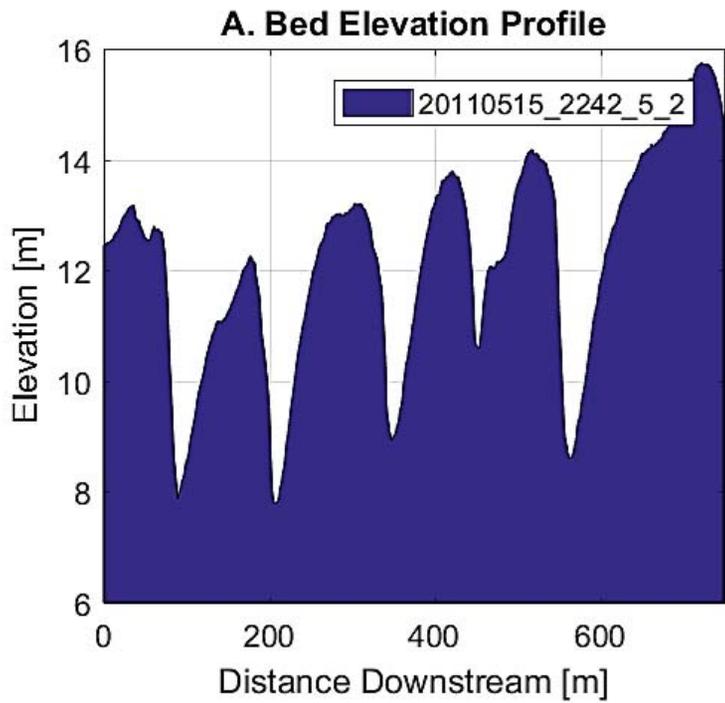












## Appendix C: Bedform Roughness Statistics

Table 3. Calculated roughness statistics.

Date (yyyy mmdd)	Line #	Rough- ness Average ( $R_{ave}$ , m)	Rough- ness RMS ( $R_{RMS}$ , m)	Rugosity ( $R_{rug}$ )	Skew-ness ( $R_{ske}$ )	Kurt- osis ( $R_{kur}$ )	Sig. Wave Height ( $H_{sig}$ , m)	RMS Wave Height ( $H_{RMS}$ , m)	Average Wave- length ( $T_{ave}$ , m)	Steep- ness
20110 515	5.1	0.906	1.172	9.121	-0.568	2.635	4.360	3.055	77.900	0.039
20110 515	5.1	0.991	1.223	9.959	-0.707	2.535	4.653	3.328	86.412	0.039
20110 515	5.1	0.942	1.177	9.471	-0.709	2.747	4.620	3.837	117.350	0.033
20110 515	5.1	0.936	1.192	9.417	-0.660	2.692	4.509	3.465	98.829	0.035
20110 515	5.2	1.030	1.248	10.349	-0.660	2.431	4.363	3.335	96.000	0.035
20110 515	5.2	1.030	1.235	10.347	-0.708	2.475	4.379	3.842	113.517	0.034
20110 515	5.2	0.993	1.229	9.986	-0.771	2.677	4.457	3.862	105.800	0.036
20110 515	5.2	1.029	1.243	10.340	-0.711	2.537	4.656	4.161	117.540	0.035
20110 515	7.1	1.001	1.253	10.058	-0.636	2.822	5.054	2.738	58.975	0.046
20110 515	7.1	0.998	1.233	10.033	-0.605	2.752	4.275	2.725	72.867	0.037
20110 515	7.1	1.030	1.283	10.352	-0.765	2.919	5.017	3.821	111.500	0.034
20110 515	7.1	0.928	1.185	9.334	-0.827	3.276	4.804	3.268	95.243	0.034
20110 515	7.2	1.155	1.440	11.597	-0.752	2.902	5.684	4.181	111.300	0.038
20110 515	7.2	1.153	1.440	11.575	-0.791	2.978	5.749	4.179	111.883	0.037
20110 515	7.2	1.180	1.476	11.844	-0.757	2.932	5.729	4.178	112.033	0.037
20110 515	7.2	1.110	1.404	11.151	-0.784	2.990	5.438	4.298	135.280	0.032
20110 515	9.1	0.943	1.257	9.487	-0.915	3.633	5.677	2.486	122.080	0.035

Date (yyyy mmdd)	Line #	Rough- ness Average ( $R_{ave}$ , m)	Rough- ness RMS ( $R_{RMS}$ , m)	Rugosity ( $R_{rug}$ )	Skew-ness ( $R_{ske}$ )	Kurt- osis ( $R_{kur}$ )	Sig. Wave Height ( $H_{sig}$ , m)	RMS Wave Height ( $H_{RMS}$ , m)	Average Wave- length ( $T_{ave}$ , m)	Steep- ness
20110 515	9.1	0.941	1.260	9.460	-0.886	3.623	5.846	4.386	122.980	0.036
20110 515	9.1	0.919	1.235	9.244	-0.788	3.496	5.342	3.990	109.117	0.037
20110 515	9.1	0.947	1.267	9.522	-0.679	3.473	5.508	4.062	109.000	0.037
20110 515	9.2	0.775	0.893	7.813	-0.873	3.924	4.591	3.032	101.000	0.030
20110 515	9.2	0.810	1.000	8.161	-0.717	3.746	4.648	3.206	118.700	0.027
20110 515	9.2	0.736	0.904	7.433	-0.352	3.720	3.968	2.878	118.117	0.024
20110 515	9.2	0.700	0.884	7.075	-0.752	4.336	4.013	2.595	103.771	0.025
20110 515	11.1	0.245	0.302	2.644	0.403	2.847	1.091	0.765	24.611	0.031
20110 515	11.1	0.235	0.302	2.555	0.648	3.796	1.103	0.744	22.022	0.034
20110 515	11.2	0.200	0.257	2.238	0.143	3.039	0.823	0.551	23.304	0.024
20110 515	11.2	0.200	0.254	2.236	-0.034	2.973	0.807	0.541	25.989	0.021
20110 515	11.2	0.191	0.242	2.154	0.011	3.269	0.735	0.506	26.512	0.019
20110 519	5.1	0.747	0.922	8.541	-0.332	2.654	3.428	2.498	91.683	0.027
20110 519	5.1	0.775	0.933	7.819	-0.397	2.401	3.506	2.860	108.640	0.026
20110 519	5.1	0.763	0.924	7.692	-0.389	2.310	3.232	2.107	69.011	0.031
20110 519	5.1	0.806	0.953	8.123	-0.394	2.304	3.531	2.823	110.720	0.025
20110 519	5.2	0.754	0.946	7.605	-0.927	3.778	4.319	2.997	135.000	0.022
20110 519	5.2	0.770	0.962	7.764	-0.798	3.439	4.210	3.082	136.220	0.023
20110 519	5.2	0.720	0.917	7.269	-0.817	3.612	3.860	2.577	97.729	0.026
20110 519	5.2	0.763	0.953	7.700	-0.818	3.351	3.968	2.866	111.933	0.026

Date (yyyy mmdd)	Line #	Rough- ness Average ( $R_{ave}$ , m)	Rough- ness RMS ( $R_{RMS}$ , m)	Rugosity ( $R_{rug}$ )	Skew-ness ( $R_{ske}$ )	Kurt- osis ( $R_{kur}$ )	Sig. Wave Height ( $H_{sig}$ , m)	RMS Wave Height ( $H_{RMS}$ , m)	Average Wave- length ( $T_{ave}$ , m)	Steep- ness
20110 519	7.1	0.741	0.952	7.476	-0.847	3.662	3.302	2.213	78.867	0.028
20110 519	7.1	0.713	0.939	7.201	-0.814	4.403	3.999	2.593	75.522	0.034
20110 519	7.1	0.769	0.986	7.757	-0.728	3.461	3.542	2.221	58.425	0.038
20110 519	7.1	0.708	0.921	7.156	-0.862	3.585	3.116	1.942	66.670	0.029
20110 519	7.2	0.545	0.686	5.542	-0.763	3.680	2.984	2.163	101.450	0.021
20110 519	7.2	0.547	0.691	5.560	-0.714	3.611	3.021	2.006	67.263	0.024
20110 519	7.2	0.549	0.686	5.585	-0.813	3.815	3.183	2.032	85.325	0.024
20110 519	7.2	0.581	0.719	5.893	-0.720	3.625	3.259	1.921	73.488	0.026
20110 519	9.1	0.791	1.069	7.972	-0.753	3.850	4.626	3.278	96.800	0.034
20110 519	9.1	0.812	1.111	8.180	-0.836	4.205	4.648	3.228	95.267	0.034
20110 519	9.1	0.794	1.091	8.007	-0.781	4.166	4.698	3.010	80.957	0.037
20110 519	9.2	0.817	1.052	8.232	-0.812	3.538	4.367	3.281	80.657	0.041
20110 519	9.2	0.823	1.048	8.292	-0.720	3.370	4.503	3.065	70.000	0.044
20110 519	9.2	0.794	1.006	8.007	-0.594	3.412	4.463	3.116	85.250	0.037
20110 519	11.1	0.212	0.258	2.348	-0.013	2.518	0.842	0.596	21.150	0.028
20110 519	11.1	0.215	0.265	2.368	0.041	2.591	0.934	0.648	21.727	0.030
20110 519	11.1	0.233	0.292	2.533	0.105	2.885	1.000	0.695	22.481	0.031
20110 519	11.1	0.218	0.265	2.397	0.029	2.515	0.876	0.633	27.742	0.023
20110 519	11.2	0.175	0.224	2.014	0.190	3.326	0.829	0.532	29.623	0.018
20110 519	11.2	0.176	0.223	2.026	0.196	3.164	0.758	0.544	30.692	0.018

Date (yyyy mmdd)	Line #	Rough- ness Average ( $R_{ave}$ , m)	Rough- ness RMS ( $R_{RMS}$ , m)	Rugosity ( $R_{rug}$ )	Skew-ness ( $R_{ske}$ )	Kurt- osis ( $R_{kur}$ )	Sig. Wave Height ( $H_{sig}$ , m)	RMS Wave Height ( $H_{RMS}$ , m)	Average Wave- length ( $T_{ave}$ , m)	Steep- ness
20110 519	11.2	0.177	0.227	2.030	-0.015	3.388	0.719	0.494	22.288	0.022
20110 519	11.2	0.186	0.232	2.109	-0.145	3.233	0.753	0.509	27.160	0.019
20121 002	5.1	0.192	0.244	2.163	-0.472	2.873	0.824	0.571	28.652	0.020
20121 002	5.2	0.210	0.266	2.326	-0.134	3.352	0.884	0.593	27.556	0.022
20121 002	7.1	0.324	0.395	3.391	-0.219	2.411	1.333	0.881	40.517	0.022
20121 002	7.2	0.426	0.511	4.377	-0.030	2.361	1.819	1.435	80.789	0.018
20121 002	9.1	0.522	0.605	5.314	-0.330	1.981	1.969	1.612	75.750	0.021
20121 002	9.2	0.515	0.638	5.248	-0.064	2.498	1.824	1.273	42.173	0.030
20121 002	11.1	0.308	0.370	3.240	-0.011	2.476	1.409	0.973	42.018	0.023
20121 002	11.2	0.388	0.500	4.008	1.449	4.011	1.936	1.424	79.533	0.018
20121 003	5.1	0.172	0.215	1.992	-0.227	2.613	0.748	0.555	37.742	0.015
20121 003	5.1	0.185	0.235	2.104	-0.441	2.850	0.789	0.551	29.933	0.018
20121 003	5.1	0.191	0.239	2.158	-0.360	2.704	0.796	0.543	27.612	0.020
20121 003	5.1	0.190	0.240	2.144	-0.358	2.809	0.771	0.532	26.581	0.020
20121 003	5.1	0.190	0.239	2.151	-0.436	2.804	0.846	0.600	29.883	0.020
20121 003	5.1	0.489	0.616	4.996	-0.483	2.795	2.395	1.637	94.120	0.017
20121 003	5.2	0.205	0.253	2.277	-0.088	2.844	0.863	0.619	32.659	0.019
20121 003	5.2	0.211	0.264	2.332	-0.125	3.038	0.997	0.662	39.224	0.017
20121 003	5.2	0.209	0.264	2.315	-0.070	3.083	0.948	0.622	36.045	0.017
20121 003	5.2	0.210	0.264	2.322	-0.099	3.051	0.997	0.657	39.206	0.017



Date (yyyy mmdd)	Line #	Rough- ness Average ( $R_{ave}$ , m)	Rough- ness RMS ( $R_{RMS}$ , m)	Rugosity ( $R_{rug}$ )	Skew-ness ( $R_{ske}$ )	Kurt- osis ( $R_{kur}$ )	Sig. Wave Height ( $H_{sig}$ , m)	RMS Wave Height ( $H_{RMS}$ , m)	Average Wave- length ( $T_{ave}$ , m)	Steep- ness
20121 003	5.2	0.209	0.264	2.321	-0.120	3.060	0.954	0.651	38.883	0.017
20121 003	5.2	0.495	0.626	5.048	0.064	2.941	2.318	1.613	85.300	0.019
20121 003	7.1	0.314	0.380	3.297	-0.079	2.265	1.337	0.985	60.708	0.016
20121 003	7.1	0.315	0.382	3.308	-0.105	2.287	1.348	0.906	52.029	0.017
20121 003	7.1	0.313	0.378	3.284	-0.064	2.251	1.358	0.942	56.046	0.017
20121 003	7.1	0.313	0.379	3.291	-0.072	2.260	1.317	0.910	52.043	0.017
20121 003	7.1	0.315	0.381	3.305	-0.066	2.247	1.358	0.915	52.086	0.018
20121 003	7.1	0.617	0.782	6.251	-0.342	2.764	2.837	1.938	99.830	0.019
20121 003	7.2	0.413	0.497	4.246	-0.013	2.359	1.760	1.331	72.800	0.018
20121 003	7.2	0.408	0.491	4.200	0.013	2.368	1.752	1.314	71.770	0.018
20121 003	7.2	0.410	0.494	4.221	-0.017	2.376	1.750	1.316	72.720	0.018
20121 003	7.2	0.401	0.484	4.130	-0.036	2.402	1.715	1.358	80.789	0.017
20121 003	7.2	0.409	0.494	4.214	-0.012	2.383	1.776	1.259	66.164	0.019
20121 003	7.2	0.781	0.987	7.871	-0.267	2.916	3.681	2.535	119.570	0.021
20121 003	9.1	0.508	0.589	5.178	-0.324	2.014	2.023	1.584	75.725	0.021
20121 003	9.1	0.509	0.590	5.185	-0.322	2.013	1.998	1.582	75.775	0.021
20121 003	9.1	0.510	0.591	5.193	-0.319	2.009	2.114	1.549	75.825	0.020
20121 003	9.1	0.809	1.072	8.147	-0.198	3.299	4.125	2.599	109.009	0.024
20121 003	9.1	0.804	1.063	8.101	-0.204	3.265	3.794	2.508	103.533	0.024
20121 003	9.2	0.500	0.630	5.100	-0.570	2.671	1.871	1.402	57.800	0.024

Date (yyyy mmd)	Line #	Rough- ness Average ( $R_{ave}$ , m)	Rough- ness RMS ( $R_{RMS}$ , m)	Rugosity ( $R_{rug}$ )	Skew-ness ( $R_{ske}$ )	Kurt- osis ( $R_{kur}$ )	Sig. Wave Height ( $H_{sig}$ , m)	RMS Wave Height ( $H_{RMS}$ , m)	Average Wave- length ( $T_{ave}$ , m)	Steep- ness
20121 003	9.2	0.499	0.629	5.085	-0.050	2.687	1.993	1.419	57.864	0.025
20121 003	9.2	0.503	0.633	5.128	-0.053	2.665	2.018	1.525	63.510	0.024
20121 003	9.2	0.798	1.047	8.040	-0.443	3.178	3.838	2.593	107.870	0.024
20121 003	9.2	0.798	1.044	8.043	-0.441	3.189	3.718	2.342	85.800	0.027
20121 003	11.1	0.300	0.357	3.166	0.064	2.416	1.293	0.959	43.820	0.022
20121 003	11.1	0.292	0.351	3.084	0.050	2.498	1.268	0.909	40.072	0.023
20121 003	11.1	0.295	0.351	3.113	0.062	2.402	1.282	0.985	47.147	0.021
20121 003	11.1	0.288	0.345	3.051	0.067	2.437	1.269	0.962	47.067	0.020
20121 003	11.1	0.808	0.954	8.139	-0.020	2.106	3.431	2.695	130.789	0.021
20121 003	11.1	0.831	0.981	8.368	-0.027	2.081	3.562	2.784	127.922	0.022
20121 003	11.2	0.368	0.479	3.815	1.463	4.086	1.809	1.288	71.340	0.018
20121 003	11.2	0.368	0.479	3.818	1.454	4.053	1.819	1.285	71.350	0.018
20121 003	11.2	0.368	0.477	3.816	1.436	3.986	1.876	1.435	87.662	0.016
20121 003	11.2	0.370	0.483	3.832	1.473	4.109	1.823	1.312	74.170	0.018
20121 003	11.2	0.760	0.978	7.667	0.190	3.232	3.775	2.689	137.618	0.020
20121 003	11.2	0.750	0.970	7.568	0.193	3.203	3.781	2.681	137.571	0.019
20130 429	3.1	0.105	0.127	1.447	0.013	2.670	0.405	0.289	13.222	0.022
20130 429	3.1	0.104	0.129	1.444	0.061	2.925	0.402	0.290	13.004	0.022
20130 429	3.1	0.106	0.130	1.454	-0.002	2.677	0.407	0.294	12.753	0.023
20130 429	3.1	0.106	0.132	1.457	0.100	2.840	0.417	0.305	12.773	0.024

Date (yyyy mmdd)	Line #	Rough- ness Average ( $R_{ave}$ , m)	Rough- ness RMS ( $R_{RMS}$ , m)	Rugosity ( $R_{rug}$ )	Skew-ness ( $R_{ske}$ )	Kurt- osis ( $R_{kur}$ )	Sig. Wave Height ( $H_{sig}$ , m)	RMS Wave Height ( $H_{RMS}$ , m)	Average Wave- length ( $T_{ave}$ , m)	Steep- ness
20130 429	3.2	0.130	0.161	1.644	-0.130	2.908	0.517	0.376	12.307	0.031
20130 429	3.2	0.139	0.172	1.715	-0.080	2.877	0.595	0.435	12.529	0.035
20130 429	3.2	0.147	0.182	1.782	-0.164	2.723	0.615	0.453	12.761	0.036
20130 429	3.2	0.146	0.179	1.773	-0.096	2.736	0.618	0.471	13.633	0.035
20130 429	5.1	0.443	0.524	4.542	-0.357	2.339	1.819	1.390	36.375	0.038
20130 429	5.1	0.443	0.531	4.544	-0.330	2.365	1.892	1.521	38.268	0.040
20130 429	5.1	0.452	0.536	4.630	-0.340	2.267	1.819	1.505	38.558	0.039
20130 429	5.1	0.464	0.560	4.750	-0.380	2.475	1.905	1.556	38.000	0.041
20130 429	5.2	0.547	0.678	5.566	-0.062	2.681	2.563	1.868	43.265	0.043
20130 429	5.2	0.539	0.681	5.481	-0.110	2.768	2.560	1.819	41.094	0.044
20130 429	5.2	0.542	0.674	5.509	-0.154	2.666	2.468	1.933	48.973	0.039
20130 429	5.2	0.551	0.688	5.597	-0.028	2.539	2.392	1.868	48.936	0.038
20130 429	7.1	0.555	0.699	5.640	-0.300	2.936	2.453	1.652	42.906	0.039
20130 429	7.1	0.565	0.698	5.743	-0.141	2.892	2.501	1.815	47.973	0.038
20130 429	7.1	0.571	0.690	5.796	-0.264	2.578	2.525	1.909	52.900	0.036
20130 429	7.1	0.565	0.693	5.740	-0.220	2.668	2.634	1.956	53.646	0.036
20130 429	7.2	0.706	0.847	7.134	-0.315	2.343	3.158	2.281	65.036	0.035
20130 429	7.2	0.716	0.855	7.228	-0.342	2.387	3.209	2.322	64.845	0.036
20130 429	7.2	0.705	0.855	7.126	-0.475	2.591	3.308	2.304	64.936	0.035
20130 429	7.2	0.710	0.858	7.170	-0.481	2.580	2.813	2.178	63.100	0.035

Date (yyyy mmdd)	Line #	Rough- ness Average ( $R_{ave}$ , m)	Rough- ness RMS ( $R_{RMS}$ , m)	Rugosity ( $R_{rug}$ )	Skew-ness ( $R_{ske}$ )	Kurt- osis ( $R_{kur}$ )	Sig. Wave Height ( $H_{sig}$ , m)	RMS Wave Height ( $H_{RMS}$ , m)	Average Wave- length ( $T_{ave}$ , m)	Steep- ness
20130 429	9.1	0.595	0.710	6.034	-0.121	2.326	2.740	2.055	45.880	0.045
20130 429	9.1	0.585	0.707	5.939	-0.098	2.425	2.632	1.874	40.612	0.046
20130 429	9.1	0.600	0.726	6.081	-0.104	2.385	2.593	1.844	36.250	0.051
20130 429	9.1	0.572	0.708	5.806	-0.049	2.558	2.565	1.838	37.884	0.049
20130 429	9.2	0.486	0.616	4.964	-0.354	2.998	2.088	1.478	31.664	0.047
20130 429	9.2	0.460	0.589	4.703	-0.303	3.074	2.093	1.488	34.655	0.043
20130 429	9.2	0.466	0.590	4.762	-0.161	2.890	1.815	1.329	30.692	0.043
20130 429	9.2	0.476	0.606	4.862	0.005	2.945	1.960	1.442	30.725	0.047
20130 429	11	0.246	0.304	2.656	-0.204	2.708	1.021	0.766	15.704	0.049
20130 429	11	0.247	0.304	2.662	-0.282	2.647	0.984	0.758	15.388	0.049
20130 429	11	0.238	0.294	2.583	-0.297	2.638	0.992	0.723	14.820	0.049
20130 429	11	0.233	0.293	2.534	-0.291	2.921	0.936	0.681	14.763	0.046
20130 429	11.1	0.173	0.215	1.997	0.125	2.982	0.670	0.507	13.004	0.039
20130 429	11.1	0.162	0.199	1.905	-0.116	2.654	0.642	0.478	12.080	0.040
20130 429	11.1	0.174	0.219	2.004	-0.033	3.074	0.710	0.515	12.331	0.042
20130 429	11.1	0.172	0.216	1.988	0.193	2.903	0.705	0.517	11.514	0.045
20150 319	5.1	0.467	0.577	4.774	-0.475	2.632	1.686	1.054	13.140	0.080
20150 319	5.1	0.463	0.569	4.731	-0.499	2.683	1.569	0.984	11.357	0.087
20150 319	5.1	0.477	0.592	4.873	-0.506	2.767	1.604	1.020	11.550	0.088
20150 319	5.1	0.476	0.580	4.863	-0.471	2.592	1.711	1.092	14.182	0.077

Date (yyyy mmdd)	Line #	Rough- ness Average ( $R_{ave}$ , m)	Rough- ness RMS ( $R_{RMS}$ , m)	Rugosity ( $R_{rug}$ )	Skew-ness ( $R_{ske}$ )	Kurt- osis ( $R_{kur}$ )	Sig. Wave Height ( $H_{sig}$ , m)	RMS Wave Height ( $H_{RMS}$ , m)	Average Wave- length ( $T_{ave}$ , m)	Steep- ness
20150 319	5.2	0.622	0.765	6.301	-0.540	2.670	2.217	1.384	13.663	0.101
20150 319	5.2	0.630	0.779	6.381	-0.597	2.697	1.980	1.227	12.956	0.095
20150 319	5.2	0.642	0.794	6.499	-0.546	2.689	2.177	1.316	14.082	0.093
20150 319	5.2	0.654	0.796	6.612	-0.486	2.553	2.009	1.264	12.086	0.105
20150 319	7.1	0.644	0.769	6.515	-0.429	2.400	2.101	1.334	11.760	0.113
20150 319	7.1	0.658	0.788	6.654	-0.341	2.320	2.065	1.297	11.531	0.112
20150 319	7.1	0.662	0.797	6.695	-0.317	2.527	2.231	1.457	13.607	0.107
20150 319	7.1	0.661	0.794	6.686	-0.289	2.434	2.156	1.359	14.261	0.095
20150 319	7.2	0.581	0.714	5.899	-0.707	2.737	1.888	1.182	11.119	0.106
20150 319	7.2	0.597	0.738	6.051	-0.650	2.797	2.013	1.247	12.182	0.102
20150 319	7.2	0.583	0.720	5.912	-0.628	2.700	1.663	1.057	10.620	0.100
20150 319	7.2	0.585	0.721	5.931	-0.619	2.805	1.639	1.048	10.792	0.097
20150 319	9.1	0.756	0.926	7.620	0.110	2.574	2.232	1.441	12.173	0.118
20150 319	9.1	0.735	0.911	7.410	0.063	2.447	2.026	1.336	11.086	0.121
20150 319	9.1	0.754	0.924	7.601	0.009	2.563	2.048	1.296	12.375	0.105
20150 319	9.1	0.767	0.935	7.731	-0.047	2.387	2.071	1.289	11.538	0.112
20150 319	9.2	0.604	0.755	6.120	-0.133	2.722	1.830	1.159	8.518	0.136
20150 319	9.2	0.611	0.769	6.186	-0.250	2.707	1.768	1.122	7.973	0.141
20150 319	9.2	0.622	0.758	6.294	-0.386	2.489	2.032	1.292	9.644	0.134
20150 319	9.2	0.601	0.738	6.090	-0.371	2.633	1.907	1.210	11.108	0.109

Date (yyyy mmdd)	Line #	Rough- ness Average ( $R_{ave}$ , m)	Rough- ness RMS ( $R_{RMS}$ , m)	Rugosity ( $R_{rug}$ )	Skew-ness ( $R_{ske}$ )	Kurt- osis ( $R_{kur}$ )	Sig. Wave Height ( $H_{sig}$ , m)	RMS Wave Height ( $H_{RMS}$ , m)	Average Wave- length ( $T_{ave}$ , m)	Steep- ness
20150 319	11.1	0.329	0.425	3.437	-0.373	3.201	1.156	0.767	5.973	0.128
20150 319	11.1	0.327	0.417	3.417	-0.312	3.314	1.152	0.759	5.852	0.130
20150 319	11.1	0.330	0.424	3.445	-0.254	3.304	1.187	0.776	5.863	0.132
20150 319	11.1	0.324	0.414	3.395	-0.203	2.981	1.253	0.816	6.545	0.125
20150 319	11.2	0.256	0.321	2.749	-0.244	2.886	0.971	0.648	6.320	0.103
20150 319	11.2	0.255	0.319	2.734	-0.226	2.804	0.996	0.644	5.712	0.113
20150 319	11.2	0.263	0.335	2.814	-0.068	3.258	1.062	0.695	6.066	0.115
20150 319	11.2	0.272	0.344	2.896	-0.116	2.905	1.067	0.707	6.155	0.115
20150 430	5.1	0.478	0.607	4.882	-0.137	2.899	1.540	0.979	13.926	0.070
20150 430	5.1	0.492	0.618	5.021	-0.105	2.813	1.551	0.968	11.966	0.081
20150 430	5.1	0.491	0.623	5.014	-0.052	2.738	1.471	0.922	10.881	0.085
20150 430	5.1	0.495	0.630	5.053	-0.021	2.833	1.667	1.061	13.512	0.079
20150 430	5.2	0.685	0.834	6.925	-0.174	2.436	2.065	1.293	14.350	0.090
20150 430	5.2	0.697	0.838	7.043	-0.207	2.316	2.552	1.556	18.235	0.085
20150 430	5.2	0.690	0.843	6.974	-0.376	2.571	1.792	1.189	12.800	0.093
20150 430	5.2	0.690	0.838	6.969	-0.355	2.604	2.343	1.524	20.282	0.075
20150 430	7.1	0.797	0.984	8.025	-0.647	2.772	1.950	1.270	14.136	0.090
20150 430	7.1	0.785	0.964	7.916	-0.725	2.902	2.044	1.338	15.494	0.086
20150 430	7.1	0.768	0.958	7.744	-0.660	2.992	2.261	1.464	17.931	0.082
20150 430	7.1	0.776	0.964	7.808	-0.627	2.939	2.103	1.374	14.877	0.092

Date (yyyy mmdd)	Line #	Rough- ness Average ( $R_{ave}$ , m)	Rough- ness RMS ( $R_{RMS}$ , m)	Rugosity ( $R_{rug}$ )	Skew-ness ( $R_{ske}$ )	Kurt- osis ( $R_{kur}$ )	Sig. Wave Height ( $H_{sig}$ , m)	RMS Wave Height ( $H_{RMS}$ , m)	Average Wave- length ( $T_{ave}$ , m)	Steep- ness
20150 430	7.2	0.936	1.130	9.394	-0.599	2.749	3.042	1.983	21.686	0.091
20150 430	7.2	0.926	1.107	9.301	-0.548	2.520	2.652	1.679	19.555	0.086
20150 430	7.2	0.956	1.128	9.607	-0.567	2.443	2.653	1.717	19.995	0.086
20150 430	7.2	0.960	1.123	9.646	-0.548	2.270	2.921	1.826	25.589	0.071
20150 430	9.1	0.622	0.772	6.300	-0.334	2.823	1.875	1.183	12.353	0.096
20150 430	9.1	0.621	0.773	6.287	-0.253	2.896	1.794	1.143	11.424	0.100
20150 430	9.1	0.642	0.795	6.495	-0.091	2.783	1.876	1.199	10.937	0.110
20150 430	9.1	0.637	0.777	6.448	-0.098	2.636	2.026	1.283	12.600	0.102
20150 430	9.2	0.486	0.606	4.960	-0.466	2.998	1.626	1.029	7.686	0.134
20150 430	9.2	0.503	0.628	5.131	-0.373	3.006	1.631	1.038	7.756	0.134
20150 430	9.2	0.497	0.613	5.065	-0.413	2.757	1.618	1.030	7.661	0.134
20150 430	9.2	0.523	0.648	5.325	-0.488	3.003	1.762	1.130	8.173	0.138
20150 430	11.1	0.199	0.253	2.227	0.033	3.131	0.697	0.467	4.980	0.094
20150 430	11.1	0.188	0.239	2.126	-0.176	3.098	0.659	0.436	4.353	0.100
20150 430	11.1	0.191	0.240	2.154	0.000	3.158	0.693	0.461	4.832	0.095
20150 430	11.1	0.194	0.245	2.186	-0.109	2.858	0.717	0.474	4.954	0.096
20150 430	11.2	0.187	0.235	2.124	-0.198	3.014	0.738	0.495	4.544	0.109
20150 430	11.2	0.196	0.240	2.201	-0.161	2.698	0.794	0.537	4.874	0.110
20150 430	11.2	0.185	0.231	2.101	-0.173	2.906	0.725	0.477	4.425	0.108
20150 430	11.2	0.189	0.236	2.140	0.081	2.890	0.735	0.500	4.602	0.109

Date (yyyy mmdd)	Line #	Rough- ness Average ( $R_{ave}$ , m)	Rough- ness RMS ( $R_{RMS}$ , m)	Rugosity ( $R_{rug}$ )	Skew-ness ( $R_{ske}$ )	Kurt- osis ( $R_{kur}$ )	Sig. Wave Height ( $H_{sig}$ , m)	RMS Wave Height ( $H_{RMS}$ , m)	Average Wave- length ( $T_{ave}$ , m)	Steep- ness
20150 519	5.1	0.216	0.276	2.381	-0.226	3.413	0.717	0.488	5.263	0.093
20150 519	5.1	0.210	0.272	2.321	-0.207	3.712	0.702	0.481	4.802	0.100
20150 519	5.1	0.216	0.280	2.382	-0.202	3.963	0.714	0.490	4.397	0.111
20150 519	5.1	0.212	0.273	2.339	-0.148	3.848	0.715	0.490	5.321	0.092
20150 519	5.2	0.280	0.354	2.975	-0.330	3.053	0.957	0.651	6.546	0.099
20150 519	5.2	0.288	0.365	3.046	-0.393	3.203	1.011	0.685	6.569	0.104
20150 519	5.2	0.295	0.373	3.112	-0.282	3.131	0.972	0.646	5.887	0.110
20150 519	5.2	0.296	0.372	3.123	-0.329	3.050	0.956	0.638	6.526	0.098
20150 519	7.1	0.292	0.366	3.083	-0.007	2.977	1.014	0.671	7.006	0.096
20150 519	7.1	0.284	0.359	3.014	0.062	2.978	0.935	0.612	6.360	0.096
20150 519	7.1	0.290	0.365	3.071	0.072	2.929	0.988	0.658	5.978	0.110
20150 519	7.1	0.284	0.361	3.012	0.102	3.197	0.923	0.607	6.193	0.098
20150 519	7.2	0.296	0.378	3.120	-0.377	3.215	1.048	0.709	6.179	0.115
20150 519	7.2	0.299	0.376	3.150	-0.433	3.025	0.998	0.647	5.807	0.111
20150 519	7.2	0.306	0.388	3.223	-0.379	3.049	1.035	0.688	5.672	0.121
20150 519	7.2	0.300	0.383	3.162	-0.382	3.311	1.086	0.709	6.423	0.110
20150 519	9.1	0.253	0.317	2.721	-0.253	2.936	0.889	0.604	6.458	0.094
20150 519	9.1	0.251	0.314	2.700	-0.275	3.007	0.873	0.588	6.178	0.095
20150 519	9.1	0.253	0.321	2.717	-0.330	3.224	0.841	0.561	5.041	0.111
20150 519	9.1	0.256	0.324	2.745	-0.326	3.214	0.841	0.568	5.646	0.101



Date (yyyy mmdd)	Line #	Rough- ness Average ( $R_{ave}$ , m)	Rough- ness RMS ( $R_{RMS}$ , m)	Rugosity ( $R_{rug}$ )	Skew-ness ( $R_{ske}$ )	Kurt- osis ( $R_{kur}$ )	Sig. Wave Height ( $H_{sig}$ , m)	RMS Wave Height ( $H_{RMS}$ , m)	Average Wave- length ( $T_{ave}$ , m)	Steep- ness
20150 519	9.2	0.240	0.295	2.596	-0.206	2.735	0.789	0.542	5.464	0.099
20150 519	9.2	0.230	0.286	2.503	-0.160	2.772	0.802	0.558	5.425	0.103
20150 519	9.2	0.239	0.295	2.587	-0.171	2.714	0.806	0.552	4.400	0.125
20150 519	9.2	0.224	0.278	2.455	-0.126	2.930	0.775	0.531	4.883	0.109
20150 519	11.1	0.243	0.317	2.627	-0.099	3.298	0.613	0.421	6.157	0.068
20150 519	11.1	0.247	0.319	2.666	-0.070	3.217	0.605	0.424	6.773	0.063
20150 519	11.1	0.249	0.320	2.687	-0.151	3.169	0.615	0.425	6.123	0.069
20150 519	11.1	0.249	0.319	2.685	-0.055	3.109	0.620	0.440	7.638	0.058
20150 519	11.2	0.165	0.213	1.932	-0.208	3.541	0.523	0.357	4.299	0.083
20150 519	11.2	0.163	0.211	1.909	-0.192	3.492	0.543	0.370	4.434	0.083
20150 519	11.2	0.175	0.227	2.018	-0.268	3.468	0.541	0.366	3.719	0.098
20150 519	11.2	0.171	0.217	1.978	-0.169	3.145	0.566	0.381	4.364	0.087
20160 112	5.1	0.887	1.096	8.866	-0.752	2.793	3.496	2.164	35.357	0.061
20160 112	5.2	1.114	1.332	11.081	-0.703	2.311	4.159	2.591	51.360	0.050
20160 112	7.1	0.900	1.105	9.045	-0.735	2.853	4.178	2.835	75.730	0.037
20160 112	7.2	0.933	1.102	9.384	-0.544	2.423	4.318	3.161	76.410	0.041
20160 112	9.1	1.223	1.401	12.259	-0.301	1.854	4.486	3.422	57.915	0.059
20160 112	9.2	0.834	1.016	8.382	-0.416	2.691	2.977	2.013	33.923	0.059
20160 112	11.1	0.259	0.331	2.769	-0.388	3.274	1.117	0.737	10.640	0.069
20160 112	11.2	0.220	0.272	2.416	-0.044	2.824	0.860	0.572	11.376	0.050

Date (yyyy mmdd)	Line #	Rough- ness Average ( $R_{ave}$ , m)	Rough- ness RMS ( $R_{RMS}$ , m)	Rugosity ( $R_{rug}$ )	Skew-ness ( $R_{ske}$ )	Kurt- osis ( $R_{kur}$ )	Sig. Wave Height ( $H_{sig}$ , m)	RMS Wave Height ( $H_{RMS}$ , m)	Average Wave- length ( $T_{ave}$ , m)	Steep- ness
20160 115	3.1	0.595	0.721	6.030	-0.421	2.486	2.464	1.921	51.407	0.037
20160 115	3.1	0.584	0.714	5.927	-0.486	2.696	2.758	2.107	55.462	0.038
20160 115	3.1	0.566	0.690	5.746	-0.520	2.598	2.393	1.931	54.458	0.035
20160 115	3.2	0.480	0.633	4.902	-0.732	3.487	2.709	1.855	59.017	0.031
20160 115	3.2	0.460	0.609	4.707	-0.699	3.498	2.746	1.906	62.618	0.030
20160 115	3.2	0.470	0.624	4.805	-0.701	3.439	2.749	1.879	57.242	0.033
20160 115	5.1	1.111	1.302	11.159	-0.686	2.186	4.619	3.920	110.640	0.035
20160 115	5.1	1.117	1.309	11.218	-0.698	2.197	4.425	3.914	110.900	0.035
20160 115	5.1	1.099	1.283	11.032	-0.741	2.256	4.514	3.809	110.340	0.035
20160 115	5.2	0.930	1.125	9.359	-0.917	2.729	4.005	3.654	109.333	0.033
20160 115	5.2	0.915	1.114	9.206	-0.950	2.808	4.071	3.643	110.420	0.033
20160 115	5.2	0.913	1.095	9.182	-0.947	2.767	4.110	3.543	110.360	0.032
20160 115	7.1	0.818	1.084	8.237	-0.541	3.319	4.786	3.121	126.540	0.025
20160 115	7.1	0.834	1.105	8.404	-0.542	3.296	4.211	3.245	124.700	0.026
20160 115	7.1	0.829	1.099	8.354	-0.551	3.284	4.212	3.041	105.657	0.029
20160 115	7.2	0.944	1.193	9.492	-0.410	2.825	4.453	3.257	105.750	0.031
20160 115	7.2	0.942	1.192	9.473	-0.371	2.775	4.410	3.621	117.517	0.031
20160 115	7.2	0.947	1.219	9.523	-0.304	2.898	4.696	3.301	90.175	0.037
20160 115	9.1	0.923	1.135	9.285	-0.645	2.737	4.416	3.290	85.229	0.039
20160 115	9.1	0.916	1.116	9.214	-0.605	2.668	4.639	3.066	74.787	0.041

Date (yyyy mmdd)	Line #	Rough- ness Average (R <sub>ave</sub> , m)	Rough- ness RMS (R <sub>RMS</sub> , m)	Rugosity (R <sub>rug</sub> )	Skew-ness (R <sub>skw</sub> )	Kurt- osis (R <sub>kur</sub> )	Sig. Wave Height (H <sub>sig</sub> , m)	RMS Wave Height (H <sub>RMS</sub> , m)	Average Wave- length (T <sub>ave</sub> , m)	Steep- ness
20160 115	9.1	0.888	1.082	8.935	-0.550	2.574	3.868	2.848	72.178	0.039
20160 115	9.2	0.999	1.196	10.043	-0.520	2.379	4.653	3.607	79.438	0.045
20160 115	9.2	1.003	1.190	10.080	-0.552	2.392	4.690	3.454	78.500	0.044
20160 115	9.2	0.990	1.185	9.947	-0.560	2.438	4.780	3.530	78.825	0.045
20160 115	11.1	0.212	0.265	2.341	-0.074	2.885	0.866	0.622	15.874	0.039
20160 115	11.1	0.226	0.281	2.473	0.078	2.792	0.896	0.677	17.300	0.039
20160 115	11.1	0.229	0.292	2.495	0.278	3.564	0.999	0.711	16.362	0.043
20160 115	11.2	0.172	0.214	1.990	-0.223	2.657	0.659	0.490	15.645	0.031
20160 115	11.2	0.178	0.224	2.041	-0.006	2.796	0.735	0.538	15.598	0.035
20160 115	11.2	0.172	0.215	1.991	-0.121	2.904	0.699	0.525	16.611	0.032
20160 125	5.1	0.909	1.130	9.073	-0.674	2.531	4.052	2.356	50.614	0.047
20160 125	5.2	0.616	0.766	6.182	-0.646	3.077	3.066	1.904	43.418	0.044
20160 125	7.1	0.916	1.143	9.205	-0.824	3.030	4.080	2.961	85.425	0.035
20160 125	7.2	1.041	1.231	10.436	-0.539	2.301	4.305	2.830	52.450	0.054
20160 125	9.1	0.824	0.980	8.293	-0.294	2.257	3.623	2.309	42.341	0.055
20160 125	9.2	0.561	0.704	5.699	-0.431	2.803	2.731	1.807	36.400	0.050
20160 125	11.1	0.186	0.230	2.110	0.033	2.710	0.738	0.506	13.012	0.039
20160 125	11.2	0.192	0.241	2.160	0.065	3.057	0.785	0.537	12.234	0.044
20160 129	5.1	0.556	0.680	5.612	-0.472	2.766	2.183	1.372	26.852	0.051
20160 129	5.2	0.526	0.664	5.309	-0.045	2.678	1.856	1.132	15.208	0.074

Date (yyyy mddd)	Line #	Rough- ness Average ( $R_{ave}$ , m)	Rough- ness RMS ( $R_{RMS}$ , m)	Rugosity ( $R_{rug}$ )	Skew-ness ( $R_{ske}$ )	Kurt- osis ( $R_{kur}$ )	Sig. Wave Height ( $H_{sig}$ , m)	RMS Wave Height ( $H_{RMS}$ , m)	Average Wave- length ( $T_{ave}$ , m)	Steep- ness
20160 129	7.1	0.641	0.816	6.487	-0.737	3.136	2.370	1.474	25.279	0.058
20160 129	7.2	0.682	0.891	6.891	-0.668	3.410	2.580	1.715	22.166	0.077
20160 129	9.1	0.546	0.705	5.545	0.146	3.298	2.239	1.524	23.043	0.066
20160 129	9.2	0.521	0.649	5.308	-0.357	2.823	1.995	1.406	21.547	0.065
20160 129	11.1	0.158	0.200	1.865	-0.213	3.311	0.676	0.455	8.690	0.052
20160 129	11.2	0.172	0.222	1.993	-0.262	3.370	0.659	0.431	8.143	0.053

# REPORT DOCUMENTATION PAGE

*Form Approved*  
OMB No. 0704-0188

The public reporting burden for this collection of information is estimated to average 1 hour per response, including the time for reviewing instructions, searching existing data sources, gathering and maintaining the data needed, and completing and reviewing the collection of information. Send comments regarding this burden estimate or any other aspect of this collection of information, including suggestions for reducing the burden, to Department of Defense, Washington Headquarters Services, Directorate for Information Operations and Reports (0704-0188), 1215 Jefferson Davis Highway, Suite 1204, Arlington, VA 22202-4302. Respondents should be aware that notwithstanding any other provision of law, no person shall be subject to any penalty for failing to comply with a collection of information if it does not display a currently valid OMB control number.

**PLEASE DO NOT RETURN YOUR FORM TO THE ABOVE ADDRESS.**

<b>1. REPORT DATE</b> October 2018		<b>2. REPORT TYPE</b> Final Report		<b>3. DATES COVERED (From - To)</b>	
<b>4. TITLE AND SUBTITLE</b> Mississippi River Bedform Roughness and Streamflow Conditions near Vicksburg, Mississippi: Data Collection Summary and Analysis				<b>5a. CONTRACT NUMBER</b>	
				<b>5b. GRANT NUMBER</b>	
				<b>5c. PROGRAM ELEMENT NUMBER</b>	
<b>6. AUTHOR(S)</b> Michael T. Ramirez, S. Jarrell Smith, James W. Lewis, and Thad C. Pratt				<b>5d. PROJECT NUMBER</b> 127672	
				<b>5e. TASK NUMBER</b>	
				<b>5f. WORK UNIT NUMBER</b>	
<b>7. PERFORMING ORGANIZATION NAME(S) AND ADDRESS(ES) (see reverse)</b> Coastal and Hydraulics Laboratory U.S. Army Engineer Research and Development Center 3909 Halls Ferry Road Vicksburg, MS 39180-6199				<b>8. PERFORMING ORGANIZATION REPORT NUMBER</b> MRG&P Report No. 22	
<b>9. SPONSORING/MONITORING AGENCY NAME(S) AND ADDRESS(ES)</b> U.S. Army Corps of Engineers, Mississippi Valley Division Mississippi River Geomorphology & Potamology Program 1400 Walnut Street Vicksburg, MS 39180				<b>10. SPONSOR/MONITOR'S ACRONYM(S)</b> USACE MVD	
				<b>11. SPONSOR/MONITOR'S REPORT NUMBER(S)</b>	
<b>12. DISTRIBUTION/AVAILABILITY STATEMENT</b> Approved for public release; distribution is unlimited.					
<b>13. SUPPLEMENTARY NOTES</b>					
<b>14. ABSTRACT</b> Bedforms are a consequence of flow of sufficient magnitude over a mobile sediment bed. They are a primary component of the drag acting upon a moving stream, yet are infrequently explicitly treated in numerical models of fluvial sediment transport. This study aims to document the collection of bathymetric data in the Mississippi River in an area of persistent and dynamic bedforms over a range of flow conditions, statistically examine bedform geometry, and parameterize results for inclusion in numerical models. Bathymetric data were collected several times to measure rates of bedform transport. Linear profiles of the bedforms were extracted from the bathymetry and analyzed for roughness and dune population statistics. These statistics are compared with the flow conditions under which the bedforms were observed. Bedforms increase in size with discharge and decrease in steepness (height:length ratio). At extremely high discharges, bedforms begin to decrease in size. In comparing results with methods for calculating form drag coefficients, it was observed that the dunes at higher river stages, despite their greater size, may present less resistance to flow due to their reduced steepness and reduced relative heights (dune height:flow depth).					
<b>15. SUBJECT TERMS</b> Mississippi River, River channels—Measurement, Sedimentation and deposition, Sediment transport, Stream measurements, Vicksburg (Miss.)					
<b>16. SECURITY CLASSIFICATION OF:</b>			<b>17. LIMITATION OF ABSTRACT</b>	<b>18. NUMBER OF PAGES</b>	<b>19a. NAME OF RESPONSIBLE PERSON</b>
<b>a. REPORT</b>	<b>b. ABSTRACT</b>	<b>c. THIS PAGE</b>			Ty. V. Wamsley
Unclassified	Unclassified	Unclassified	SAR	343	<b>19b. TELEPHONE NUMBER (Include area code)</b> 601-634-5062